AIC 2025 TAIPEI

Color for Future

Proceedings

of the 16th Congress of the International Colour Association (AIC)

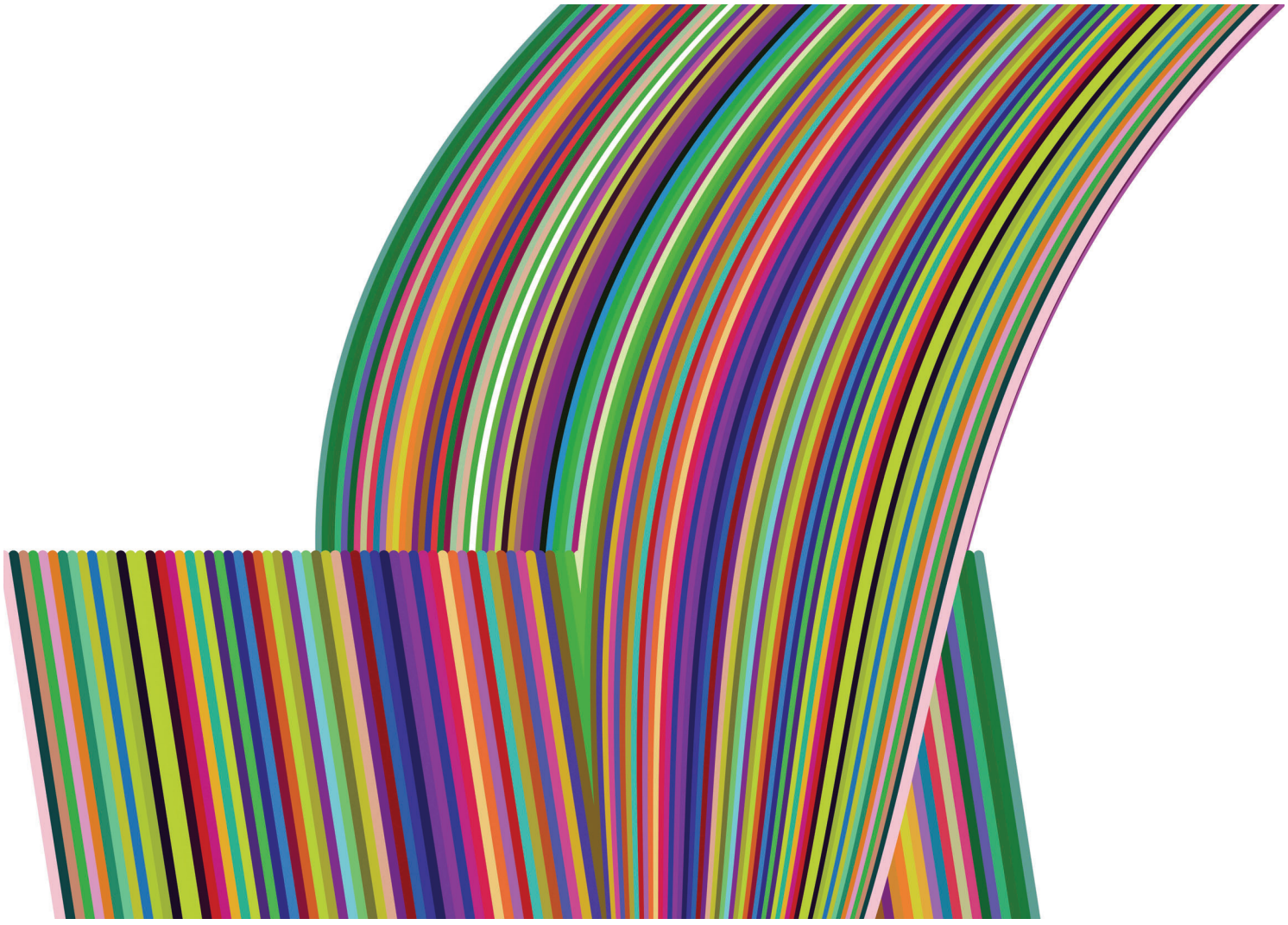

© Petronio Bendito

Taipei, Taiwan

19-24 October 2025

This publication includes invited, oral, and poster papers presented at the 16th Congress of the International Colour Association 2025. The congress was organized by the Color Association of Taiwan (CAT) and held in Taipei, Taiwan, from October 19 to 24, 2025.

More information at www.aic2025.org

2025 International Colour Association - Multidisciplinary Association in the field of Colour

www.aic-color.org

All rights reserved.

Disclaimer

Matters of copyright for all images and text associated with the papers within the Proceedings of the 16th Congress of the International Colour Association 2025 are the responsibility of the authors. The AIC and the Color Association of Taiwan do not accept responsibility for any liabilities arising from the publication of any of the submissions.

Copyright

Reproduction of this document or parts thereof by any means whatsoever is prohibited without the written permission of the International Colour Association - Multidisciplinary Association in the field of Colour.

All copies of the individual articles remain the intellectual property of the individual authors and/or their affiliated institutions.

ISSN: 2617-2410
eISBN: 2617-2429
ISBN: 978-0-6484724-7-6

How to cite this book

AIC (International Colour Association – Multidisciplinary Association in the field of Colour). 2025. Proceedings of the 16th Congress of the International Colour Association 2025. Taipei, Taiwan.

How to cite an article included in this book

Author's name. 2025. Title of the article. In: Proceedings of the 16th Congress of the International Colour Association 2025. Taipei, Taiwan, page numbers of the article.

Organized by the Color Association of Taiwan (CAT)
Published by the International Colour Association - Multidisciplinary Association in the field of Colour (AIC)

Table of Contents

AIC 2025 Committees 1

AIC Members 3

Welcome from the AIC 2025 Organizing Chair 5

Welcome from the AIC President 6

Judd Award 7

CADE Award 19

Technical Program 23

List of Invited Lectures 26

Study Groups 27

List of Oral Presentations 30

List of Poster Presentations 37

Invited Lectures

The Future of AI in the Colour Industries
Stephen Westland 43

A Comprehensive Colour System Across Industries
Ming Ronnier Luo 44

Algorithmic & Digital Color Expressions
Petronio Bendito 51

Investigating Sleep Enhancement via Intelligent Color-Varying Light
Chien-Yu Chen 53

Color Characteristics of Virtual Images in MR/AR Systems
Tsung-Hsun Yang 54

Soviet Spacecraft Design: Architect Galina Balashova's Colours
Maria João Durão 55

The Practice of Color Design: Where Engineering Challenges Meet Market Strategy
Meng-Han Yu 57

Oral Papers

Comparison of AI Based Machine Learning Methods with Basic Polynomial Regression for Cross Media Color Reproduction 59
Muhammad Hamza Zafar, Phil Green*

Dynamic Color Shift Compensation in OLED Displays Using Artificial Intelligence 65
*Ching-Hsiang Hsu, and Mang Ou-Yang**

Cityscape Color Analysis Using Deep Learning-Based Image Segmentation and Color Adjustment for Weather Conditions 71
Motonori Doi, Ryuto Ono, Shun Kuboki*

LCH-Based Deep Learning for Skin Cancer Diagnosis 76
Tzu Hao Kuan, Mei Chun Lo, and Chih Shun Hsu*

Enhancing Image Color Harmony Through Content-Aware Recoloring 84
Yu-Shan Chou and Pei-Li Sun

A Perceptually Neutral White Locus Integrating a Warm-Cool Scale 90
*Jung-En Chang and Li-Chen Ou**

Controlled Dissonance in Contemporary Design: Exploring Chromatic Tension for Emotional Impact and Perceived Quality in Enclosed Spaces 96
Sandhiya Jayaprakash Brindha , Pankaj Daultrao Surve*

An Investigation of the Emotional Perception of Scarf Colors on Different Skin Tones Based on the Color-Emotion Models and Color-Harmony Models 103
Chia-I Liao, Wen-Yuan Lee*

Taste Impressions of Snack Packs and Impression Estimation in Machine Learning of Images 109
*Masato Sakurai**

Testing Spectral-Based Characterization Models for Wide-Color-Gamut Display 114
Ruili He, Kaida Xiao, Xinyi Zhao, and Michael Pointer*

Statistical Analysis of Differences of Spectral Reflectance Values Determined by Colour-Measuring Instruments 119
Erkki Ikonen, Yasaman Rezazadeh, Anders Nilsson, John Seymour, and Juha Peltoniemi*

Enhanced Portrait Auto White Balance in Backlight Environments via Skin Reflectance
Sicong Zhou, Changjun Li, Jinxing Liang, Peihua Lai, Wenjun Sun,Hesong Li Hong Luo and Kaida Xiao**
125

A Comprehensive Investigation on the Taxonomic Classification of Recycled Dark Rubber Materials Using Multiple Spectroscopic Analytical Techniques
Yung-Fou Chen, Raymond Jui-Chang Chiang, and Chun-Ting Yueh*
131

Spectrally-Aware perceptual Image and Video Filtering Using Color Transfer
*Aiman Raza, Marie Dubail, Dominique Dumortier, and Sophie Jost**
138

A Comparative Study: Assessing Image Quality for the Jacobi and Gauss-Seidel Retinex Algorithms
Afsaneh Karami, Graham Finlayson*
143

Characterising Head-Mounted Displays Based on Visual Assessment
Chia-An Lee and Li-Chen Ou*
149

Evaluating Preference for Images Enhanced with Simple Tone Curves
James Bennett, Graham Finlayson*
154

Evaluating the Just Noticeable Difference Threshold of ΔEITP in SDR Displays for Color Experts and Non-Experts
Kuo Mu-Tzu, Chris Yi-Ho Bai*
160

Colour Saliency Effects on Pre-attentive Processes
Katsuaki Sakata, Yasuki Yamauchia*
166

Quantifying Inter-Reflection Effects on Colored Shadows
Ruiquan Mao, Alain Tremeau, Pichayada Katemake*
172

The Color of Roses Was Painted by Protan and Deutan
Yasuyo G. Ichihara, Takashi Sakamoto, Shoji Sunaga*
178

An Appraisal of 'Colour-Music: The Art of Mobile Colour' (1912) by Rimington: A Design History View
*Kyoko Hidaka**
184

Decoding Colour Communication: A Cross-Cultural Study of Colour Associations in Germany and India 188
Lina Schmidt and Melissa Lindemeyer*

Cross-Cultural Study About the Effect of Color on the Perception of Grammatical Gender 195
Alexander Raevskiy, Itsuki Kyoto, Kitirochna Rattanakasamsuk, and Rumi Tokunaga*

An Investigation of Selected Chinese Paintings Colour Theories and How It Differs from the Practical Colour Application Used in Western Paintings 201
Woon Lam Ng and Huiying Goh*

Effects of Colour Vision Deficiency on Educational Experiences in Elementary Schools: A Systematic Review 207
Sánchez Izurieta Juan Francisco, Sunaga Shoji*

Colour Selection Frameworks for Global Colour Education 213
Wenxian Qian, Chaoran Wang*

Mapping of Colors of Master Images with Munsell Color Space – A Mathematical Tool to Assist Color Design 219
Woon Lam Ng, Zhongjian Wang*

Color Education in Schools for Students with Color Vision Deficiency: Important Elements Identified Through In-Depth Interviews with Designers and Artists 226
Tsukasa Muraya, Yunoka Taniguchi, Yasuyo Ichihara and Shoji Sunaga*

Biophilic Colour Schemes (BCS) A Catalogue of Biophilic Colour Schemes Based on Emotional Colour Impact Principles and Natural Analogies from Landscape Prototypes for Evidence-Based Sustainable Design 232
Markus Schlegel, Konstantin Haensch and Claudia Goméz Mejia*

Estimation Method of Rice Fluorescence Emission Spectra from the Image Data and Its Application 240
Shoji Tominaga, Shogo Nishi, and Ryo Ohtera*

Preferable Lighting Conditions for Cooking Hamburger Steak 246
Akari Kagimoto, Yuu Kodama, Shino Okuda, Katsunori Okajima*

Achievements and Issues Demonstrated by Citizen-Lead Community Development - A Case Study of Citizen-Academia Collaboration
Akiyo Makino, Kanako Murakami 250

Measurement Comparison of Black Tea Color Testing Between Tea Testers and Analytical Instruments
Irwan Fathoni, Adi Djoko Guritno, Anggoro Cahyo Sukartiko, Megita Ryanjani Tanuputri* 256

Analysis of Fresh Organic Vegetable Quality at the Farmer and Distributor Levels Based on Color and Texture Measurements
*Dionisius Marlon Ayofi, Anggoro Cahyo Sukartiko, Megita Ryanjani Tanuputri** 262

Employment of Coloring on Clothing-Style Drawings for Understanding Behavior and Personality
Chie Muraki Asano, Sonoka Ikebe, and Akira Asano* 268

Facial Color Perception and Facial Impressions Across Diverse Color Vision Types
Yoko Mizokami, Shun Kurosawa, and Hiromi Sato* 273

Evaluating Fabric Colour Appearance Perception Using LED Simulator
Qinyuan Li, Arsaika Widasati, Yichi Zhang, Ming Ronnier Luo, and Kaida Xiao* 279

The Moral Perception of Scarf Colors on Different Skin Colors
Chia-I Liao, Wen-Yuan Lee* 285

Regarding Racism in Color Theory
Edward R. Charbonneau 291

Human Perspectives on the Role of AI-Enabled Tools for Colour Trend Analysis
Sally Angharad, Stephen Westland, and Peihua Lai* 297

CMF Design: Towards Narrative Development from User-Referencing Visual Texts
Nijoo Dubey, Sudhakar Damodaraswamy* 304

Colour and Memory: Consistency of Memory Colours
Stine Marie Kvist and Phil Green* 310

What Explanations for Color Naming and Categorization Explain
*Don Dedrick** 316

Colour and Memory: Colour as an Aid to Memorization
Mathias Sætersdal and Phil Green* 324

A Comparative Study on Human and AI Interpretation of Traditional Chinese Red Color Names
*Hsueh-Fen, Lin** 329

A Deep Learning-Based Footwear Prediction and Recommendation Model
*Li-Yun Liu, Yi-Ting Luo, and Hung-Chung Li** 335

Restoring Mobile App-Filtered Photos Using CNN-Based Deep Learning
*Ya-Hsuan Lin, Yu-Chieh Chang, Jie-Sen Wang and Pei-Li Sun** 341

Perceived Color Differences for Color-Deficient Observers
*Hsiu-Ying Hsiao, Yi-Yun Chen, Hung-Shing Chen** 347

Color Simulation Strategy of Reflective E-papers
Hung-Shing Chen, Yu-Hsuan Kao* 353

Effects of Ultra-Fast Light-Adaptive Lenses on Perception of Natural Scenes
Sophie Jost, Elisa Dessenne, Pascale Avouac, Aiman Raza, Anne-Catherine Scherlen, Coralie Barrau* 359

The Surface Optical Characteristics of Interior Components in the Japanese Traditional Tea Ceremony Room TENGO-AN
Masayuki Osumi 366

Beyond the Surface: Exploring Dichroic Filters in Folded Geometries
Elvira Jönsson 372

How to Characterize Augmented Reality Glasses for Color Reproduction – Taking the Birdbath Optical Structure as an Example 378
Ya-Chi Chao, Li-Chen Ou*

Fitting SSVEP Hue Selectivity Profile with Individual Data of Color Perception 384
Ichiro Kuriki, Ryota Miyatsuka, Naoto Umeda, Sakura Fukushima, Hiroaki Kiyokawa*

From Pixels to Perception: Reverse-Engineering RGB Images to Simulate Moth Responses to Artificial Light 390
*Aiman Raza, Adrien Lucca**

A Study on a Plant Disease Symptom Recognition System Based on the Fusion of Color Space and Deep Feature Representations 397
Chih-Shun Hsu, Mei-Chun Lo, and Zheng-Hao Liu*

Testing Colour Harmony Model for Personal Colour Analysis 403
Punnaphat Sirisayan, Suchitra Sueeprasan*

An Investigation of Memory Skin Colour in Chinese and Indonesian Observers 409
Yan Lu, Kaida Xiao, and Arsaika Widasati*

A Comparative Study of Seasonal Color Associations in Nature and Personal Color Theory 415
YungKyung Park

Evaluating the Effectiveness and Utility of Fabric Draping-Based Personal Color Diagnosis 421
Jisu Park , Gyoungsil, Choi, YungKyung Park*

Based on Deep Learning: A Regional Analysis of the Facade Color Schemes of Public Housing in HongKong 427
Yixuan Li, Changying Xiang*

Colour Conservation of the Dilworth Building, Auckland, New Zealand 433
Julian Rennie and Alessandro Premier*

Thoughts on The Use of Close-Range Photogrammetry in Chromatic-Spatial Investigations: The Case of Gaudí's Expiatory Temple of The Sagrada Família 439
Leonardo Pestana Collalto Toni, João Carlos de Oliveira Cesar*

Heritage in Color: Challenging the Neutrality of Globalized Urban Landscapes via Chromatic Ambiances

Zeinab Chehata and Faten Hussein*

Poster Papers

Color and Emotions in the Public Space 452
Anna Kmita

Glazed Tiles - Between Art and Architecture. Andreas Stöcklein's Case Study 458
Ana Paula Pinheiro, Rui Duarte*

Experience and Vocabulary in the Study and Use of Color 464
Alfonso de Lucas Tron

Analysis of Scene Illumination Factors Affecting Perceptual Colour Inferences in Images 469
Yuki Tanaka, Midori Tanaka, and Takahiko Horiuchi*

Color Standards in City Planning and Changes in Store Facade Design: The Effects of Facade Design Change Methods on Harmony with the Street, Corporate Identity, and Visibility 475
Takashi Hanari, Masayuki Harada, Toshiharu Terashima, and Tomoka Ono*

From Intuition to Intentionality: Understanding Color Decision-Making Through Reflective Design Practice in Graphic Design Education 481
Gyeonghwa Lee, Jie Yang, and Yun Chen*

Prediction of Watercolor Mixing L*a*b* Values Based on Kolmogorov–Arnold Networks 488
*Xiang-En Sun, Chen-Yu Yuan, Tzung-Han Lin**

Extracting Regional Colors from History: A Case Study on Tsukuba, Kasama, Tsuchiura, and Mito in Japan 494
Meiqing Xin, Sari Yamamoto*

Preference and Emotional Responses to Planterior Design According to the Index of Greenness 500
*SaetByul Kim, YounJin Lee**

Research on the Evaluation of Children's Color Education Effect Based on Cognitive Development Theory 504
Qian Huang, Anni Li, Shang Lan*

A Proposal for a Unified Design for Store Signs in Shopping Streets and Its Effects 509
Nagisa Kishimoto, Shushi Doi, and Hideki Sakai*

The Color of Sour and Salty Tastes 514
Nagisa Kishimoto, Shushi Doi, and Hideki Sakai*

Associative Colors Related to Grief from Pet Loss 520
YeJee Lim, YounJin Lee*

The Influence of Art Material Experience on Basic Color Terms and Color Category Perception 526
*Hyejin Han**

Contrasting Perceptions of Dark Colours Among Designers and Non-Designers: An Empirical Analysis 530
Qi Xiang, Xu Han, Chengliang Ping and Luwen Yu*

Color Measurement of Translucent Liquid Materials Using a Noncontact 2D Colorimetric System with Dome Illumination 536
Hiroyuki Iyota, Mei Higuchi, Ayumu Kinugawa, Hayato Masuda, and Hideki Sakai*

Exploring Word–Colour Associations Among Koreans and Foreign Residents in Korea 542
Junglim Lee, and YungKyung Park**

Reevaluating Brightness Perception: An Empirical Examination of Melanopsin's Influence 548
*Nozomu Mori, Mizuki Takikawa, Marina Saito, Sei-ichi Tsujimura**

From Fabric to Fingertips: Nail Polish as a Tool for Personal Colour Analysis 552
Suchitra Sueeprasan, and Phithunisara Chaimongkol*

A Study on Color Perception on Surfaces Composed of Two Colors: The Effect of Color Difference Between Two Colors in a Checkerboard Pattern on the Perception of Color Unevenness of One of the Colors 557
Naoya Hara, Masami Kono*

Physical Light Field Perception Using Color-Enhanced Photon Flow Visualization 562
Sho Nakadate, Asuka Momiyama, Kazuto Takase, Roland Schregle, and Nozomu Yosizawa*

Fashion Color Preferences and Cultural Capital: An Empirical Study Based on Bourdieu's Theory 568
Jiang Jiani

Color Appearance of Waterlilies 573
Chanprapha Phuangsuwan, Kitirochna Rattanakasamsuk, Mitsuo Ikeda, and Mikiko Kawasumi*

Examining the Degrees of Smoke Emissions Using the Calibrated Camera Technology 578
*Chun-Kung Cheng, Bao-Jen Pong, Yu-Cheng Shih, Yu-Zhi Ou, and Hung-Shing Chen**

Perceptual Associations Between Classical Music and Colour in Mozart's "Twinkle, Twinkle, Little Star" Variations 584
Yu Ting Lee, Fei Man Chang*

Gender and Age-Related Differences in the Contributions of Color to the Recognition of Cultural Landscapes 590
*Olga A. Lavrenova, Yulia A. Griber**

The Effect of Wearing Personal Colors on Attractiveness Rating 596
Aki Kondo, Mami Ogino, Yuto Nonaka, Aoi Togasaki, and Katsumi Watanabe*

The Influence of Food Appearance Color Tone on Eating Behavior and Appetite in a Virtual Reality Environment 602
Tsuyoshi Moriyama, and Aki Matsumoto*

Application of Non-Contact Color Measurement Techniques in Heritage Conservation: A Case Study of the Wufeng Lin Family's "Gongbaodi" Residence 607
Ying-Tsung Lin, Cheng-Min Tsai*

Optimization of Image Colorization for Crime Scene Based on Generative Adversarial Networks 613
*Tzu-Ming Liu, Ming-Chih Cheng, Po-Hsin Yang, and Hung-Chung Li**

The Effects of Typeface and Color Combinations on Perceived Trust, Professionalism, Aesthetics, and Usability in Traditional Chinese (Taiwan Standard) and English GUI Design 619
Fu-Shao Lu, Wen-Yuan Lee*

Perceptual Calibration of Meta Headset: Investigating Luminance Accuracy Through 2D and 3D Senses by Unity 625
Jinbi Jiang, Stephen Westland, Caroline Hemingray, and Kaida Xiao*

Develop the Chinese Hue-Tone Colour System by Utilising the Chinese Adjective Word System (ANCWS) 631
*Wenwen Song, Yifei Chen and Shiyang Zhu**

The Upper Limit of Lightness to Which the Color Name “Black” Can Be Applied 637
Ichiro Katayama

Evaluating Perceptual Color Matching Between Different Backlight Displays and Color-Managed Prints 642
Hong Yu-Kai, Chris Yi-Ho Bai*

Color Reproduction Under Non-Standard Lighting Conditions 648
Eric Kirchner, Lan Njo, Ivo van der Lans, Esther Perales and Aurora Navarro Larrosa*

Influencing Factors of Clothing Colour Preference: A Comparative Study of Beijing and Shanghai Cities 653
Shuang He, Vien Cheung, Liting Li*

Meanings of Spiritual Experiences Arising from Chromotherapy: A Perspective from Semiotics and Subjectivity as an Alternative Path to Well-Being for the Future 659
Hernán Felipe Monsalve Ospina

Color and Gender in Young Children's Free Drawings: Gender Judgments by Childcare College Students and General College Students 665
Yukiko Shimada

Towards a New Lighting Method in Museums Considering the Optimal Brightness of Paintings: Practical Classification Process Based on Oil Painting Characteristics 670
Miyu Aoyama, Yuki Oe, Yoko Mizokami, Miho Takashima and Nozomu Yoshizawa*

Differences in the Diversity of Color Names and Evaluation of Darkness and Lightness of Colors in Surface and Aperture Color Modes 676
Yanan Qiao, Yasuhiro Kawabata*

Investigation of the Colour Design: Follow the User Data or Designer's Intuition to Build a Colour Scheme for the Beer Label 682
Chunxi Nan, Mengmeng Wang, Jinwen Li*

A Study of Lip Color and Social Signalling of Z-generation 686
Jinwen Li, Mengmeng Wang, Chunxi Nan*

Effect of Appearance of Damascus Steel Knives on Visual Impression - Comparative Analyses of Observer Nationality 690
Rino Nomoto, Mikiko Kawasumi, Toshihiko Tsukada, Chanprapha Phuangsuwan, Kitirochna Rattanakasamsuk, and Uravis Tangkijviwat*

Observation of Color and Gloss Change during Drying of Particulate Suspension in Polymer Solution Using a Noncontact 2D Colorimetric System with Dome Illumination 695
Mei Higuchi, Shoki Yamamoto, Ayumu Kinugawa, Hiroyuki Iyota, Hayato Masuda, Hironobu Imakoma, and Hideki Sakai

Effect of ipRGC Response on Contrast Sensitivity in Central Vision 701
Haruka Matsumoto, Masatoshi Ishigane, Hiroshi Takahashi, Masahiro Suzuki, and Keiji Uchikawa*

Differential Perceptions of Colour and Material in Fashion: A Multisensory Analysis of Designer and Consumer Responses 707
Xu Han, Liting Li, Qi Xiang, Kaida Xiao, and Luwen Yu*

Effects of Mixed Color Temperatures on Spatial Perception in Office Lighting Environments 713
Mika Kato, Kokoro Kikuchi*

A Study of Fluorescent Effect on Ink Jet Paper by Spectral Analysis 719
M. James Shyu

Improving RGB Camera-Based Spectral Reflectance Estimation Through a Machine-Learning Approach 725
Shogo Nishi

Research on the Colors and Color Temperatures Unpopular in Home Kitchen Cabinets 730
Chia-Hua Tsai, Cheng-Min Tsai*

Electrochemical Polymerization of Conductive Polymer Thin Films to Obtain Metallic Luster with High Reflectance 736
Katsumi Yamada,Shota Tsuneyasu, and Fukuro Koshiji*

The Impact of Dynamic Lighting Conditions on the Color Perception and Texture Impression of Fabric 742
*Shuilan He**

Elderly Users' Color Emotions and Preferences Toward the Appearance of Differently Designed Care Robots 748
Ching-Chih Liao, Shi-Min Gong, Ya-Han Hsu*

Colours for the Future : Achrome Photographs In Archaeology Maraghiannis of Candie Publishing House 754
*Annie-Dominique Denhez**

The Effects of Positive and Negative Emotional States on Memory Colors 760
*MinSeon Yun, YounJin Lee**

Color Embodiment in Semantics of Abstract Concepts: Correlating Semantic Similarities with Visual Color Proximity in Metaphorical Lexemes Derived from the Chinese Color Term: Huáng, 黃, 'Yellow' 766
Yufeng Wu

A Suggestion on Local Colour Guidelines to Build Inner Mongolia's City Brand 772
Huang Jing, Yoosun Kim, and Yoomi Kim*

The Power of Nature in Art: Exploring Biomorphic Abstraction with Colour and Design 778
*Diana Sena Avoke**

Relationship Between Stability of Color Preference and Personality Traits 789
*Shinji Nakamura**

The Effect of Chroma Contrast in Infographic Color Design on the Viewer's Reading Experience 794
Chen-Pang Tsan, Chun-Po Wang*

Color Standards in City Planning and Store Facade Design Changes Relationship Between the Content of the Landscape Formation Standards and the Adopted Design Change Methods 800
Chun-Ting Shen, Chao-Hua Wen, Bao-Jen Pong*

Colorimetric Characterization of Transparent OLED Displays under Various Backlighting Conditions 806
Chun-Ting Shen, Chao-Hua Wen, Bao-Jen Pong*

Application of Kubelka-Munk Theory in Jadeite Colour Evaluation 812
Jinbi Jiang, Qinxin He, and Stephen Westland*

Beyond Averages: Individual Differences in How Wall Colour Influences Affective Responses and Room Impressions 818
Arsaika Widasati, Stephen Westland, Caroline Hemingray, Soojin Lee*

Linked Hybrid: Color, Light and Perception in the Architecture of Steven Holl 824
Camila Pinheiro Consani, and João Carlos de Oliveira Cesar*

Color Yoga: A Semiotic and Subjective Perspective on Wellbeing for the Future 830
Milton David Henao Jiménez and Hernán Felipe Monsalve Ospina*

Analysis of the Color and Object Characteristics of Seasonal Natural Landscape Images in Japan 836
Hanui Yu, Takeshi Akita, Kotaroh Hirate, and Risa Fujii*

Study on 3D Digital Preservation of Orchids using Photogrammetry Method 842
*Tzu-Hsuan Liu, Chen-Yu Yuan, Chi-Pin Tsai, Shih-Chen Chang, and Tzung-Han Lin**

On the Narrative Function of Costume Color in Chinese Cinema 848
Peitong Li, Dan Han

From Tang Sancai to Ink Painting: Cheng Shifa's Reinterpretation of Ceramic Glaze Aesthetics in Modern Chinese Art 853
Shan-Shan Wang, Keqiang Wang, and Yinghe Xue*

The Influence of Similarity on Color Harmony and Preference 863
*Hyemi Rho, YungKyung Park**

Color as Ingredients: A Material-Driven Design Approach to Natural Pigments in Sustainable Baked Goods 869
Tzu-Jung Wang, Tsuei-Ju Hsieh

Color System Conversion from RGB to L*a*b* Using Four-Layer Neural Network for a Novel Colorimeter Independent of Light Sources 875
Kaito Miyazawa, and Masashi Ohkawa*

Survey on the Empowerment Initiatives for Students with Color Vision Deficiencies 880
Shion Maruyama, Tsukasa Muraya, Shoji Sunaga*

Creation of Educational Materials Designed for a Game About Color Vision Diversity Education 886
Toshiki Fujii, Tsukasa Muraya, Shoji Sunaga*

Colour Accuracy of Low-Cost Spectrophotometers 892
Anders Nilsson, Eric Kirchner, and John Seymuor*

Colour Heritage of Chinese Painting Through Dynastic and Stylistic Change 904
Wenan Li, Ming-Xuan Chen, Xingkai Wang, David Yip, and Luwen Yu*

From Cobalt Blue to Iron Brown: Color Semiotics in Joseon 910
Wona Lhi, YungKyung Park*

A Study on Prompting the In-Depth Exploration of Environmental Color Imagery Using Generative AI 915
Yuh-Chang Wei, Monica Kuo, Ya-Ping Kuo, Zhe Liu

Film Color Grading Model Based on Computer Vision: Construction of Personalized Color Libraries 922
Ming-Xuan Chen, Shijunyan Luo*

From Glaze Color to Perception: A Study on the Color Changes of Opaque Glaze and Human Perceptual Associations 928
Hsuan-Hsuan, Su, Yan-Jun, Lin, Fu-Chi, Shin , Tsuei-Ju, Hsieh*

The Use of Color on the Expiatory Temple of The Sagrada Família by Antoni Gaudi: Nature, Life and Symbolism 934
Leonardo Pestana Collalto Toni, João Carlos de Oliveira Cesar*

Exploring the Emotional Impact of Color Design in Children's Picture Book Covers 940
Yixuan Wang, Wenfei Geng*

A Cost-Effective Method for Measuring and Simulating the Color Appearance of Transparent Plastic Samples 946
*Yung-Chen Hsu and Pei-Li Sun**

A Corpus-Linguistic Study of Context-Dependent Color Naming in Japanese 952
Hiromasa Mita

An Investigation About the Influence of Color Contrast on Binocular Fusion 958
Chia-Chun Liu, Vincent C. Sun, Ming-Chuan Fu*

Individual Cone Spectral Sensitivities and Colour Matching Functions 964
Andrew Stockman, Ming Ronnier Luo, Siyuan Song, Keyu Shi, and Andrew Rider*

Perception–Language Conflict in Color Vision Minorities: A Study of Miscommunication in Naming and Color Term Usage in Japan and China 965
Meiyan Lei, Tsukasa Muraya, Shoji Sunaga*

Sponsors' Ads 971

NCS Colour https://ncscolour.com/
DCH Color YP http://www.ypcolor.com/
Thouslite (Thousand Lights Lighting) https://www.thouslite.com/
BenQ Professional Displays https://www.benq.com/zh-tw/monitor.html
Lighting Recipe Studio https://lightingrecipe.com/

Supporting Partners 976

AIC 2025 Committees

General Chairs

Lee, Tien-Rein, Hwafan University, Taiwan (Chair)

Sun, Pei-Li, National Taiwan University of Science and Technology, Taiwan (Co-chair)

Tsai, Chen-Min, National Taiwan University of Arts, Taiwan (Secretary)

Local Organizing Committees

Program

Lee, Wen-Yuan, Tatung University

Sun, Pei-Li, Nat. Taiwan Univ. of Sci. & Tech.

Social Events

Lee, Tien-Rein, Huafan University

Tung, Po-Shou, Huafan University

Chen, Wen-Yin, , Huafan University

Liu, Yao, Huafan University

Fundraising

Lee, Tien-Rein, Huafan University

Sun, Pei-Li, Nat. Taiwan Univ. of Sci. & Tech.

Tsai, Chen-Min, National Taiwan University of Arts

Registration

Tsai, Chen-Min, National Taiwan University of Arts

Lin, Heng-Li, Huafan University

Website

Tsai, Chen-Min, National Taiwan University of Arts

Publicity

Wei, Yuh-Chang, Chinese Culture University

Hsieh, Tsuei-Ju, National Tsing Hua University

Lee, Wen-Yuan, Tatung University

Chen, Sandy, Huafan University

Publication

Wen-Yuan Lee, Tatung University

Sun, Pei-Li, Nat. Taiwan Univ. of Sci. & Tech.

Logistics & Venue

Lee, Tien-Rein, Huafan University

Chen, Maio-Feng, Huafan University

Huang, Joy, Huafan University

Lui, Vanetta, Huafan University

Hung, Shao-Lun, Huafan University

Documentation & Media

Liu, Yao, Huafan University

International Advisory Boards

Adi Djoko Guritno, Gadjah Mada University, Indonesia

Alessandro Rizzi, University of Milan, Italy

Berit Bergström, Colour Consultant, Sweden

Chanprapha Phuangsuwan, Rajamangala University of Technology, Thailand

Dimitris Mylonas, University College of London, UK

Eva-Lena Bäckström, Umeå Institute of Design, Sweden

Haisong Xu, Zhejiang University, China

Hirohisa Yaguchi, Chiba University, Japan

Javier Romero, University of Granada, Spain

Jon Yngve Hardeberg, Norwegian University of Science and Technology, Norway

José Luis Caivano, University of Buenos Aires, Argentina

Leslie Harrington, Color Association of the United Sates, USA

Maria João Durão, The University of Lisbon, Portugal

Maurizio Rossi, Polytechnic of Milan, Italy

Nick Harkness, NHPL & Colour Made Simple, Australia

Paula Csillag, ESPM University and ProCor, Brazil

Robert Hirschler, Leeds University, Hungary

Shoji Sunaga, Kyushu University, Japan

Stephen Westland, University of Leeds, UK

Valérie Bonnardel, University of Winchester, France

Verena M. Schindler, AIC Study Group on Environmental Colour Design, Switzerland

Vien Cheung, University of Leeds, UK

Yuh-Chang Wei, Chinese Culture University, Taiwan

Scientific Committee

Alain Tremeau, University Jean Monnet, FR

Alessandro Rizzi, University of Milano, IT

Andrew Stockman, UCL Institute of Opthalmology, UK

Chen-Min Tsai, National Taiwan University of Arts, TW

Chien-Yu Chen, National Taiwan University of Science and Technology, TW

Ching-Chih Liao, Ming Chuan University, TW

Dimitris Mylonas, Northeastern University London, UK

Donald Dedrick, University of Guelph, CA

Hirohisa Yaguchi, Chiba University, JP

Hung-Shing Chen, National Taiwan University of Science and Technology, TW

Ichiro Kuriki, Saitama University, JP

Ingrid Calvo Ivanovic, University of Chile, CL

Jan Morovic, HP Inc., ES

Javier Hernandez-Andres, University of Granada, ES

Juan Luis Nieves, University of Granada, ES

Kaida Xiao, University of Leeds, UK

Katsunori Okajima, Yokohama National University, JP

Kitirochna Rattanakasamsuk, Rajamangala University of Technology Thanyaburi, TH

Li-Chen Ou, National Taiwan University of Science and Technology, TW

M. James Shyu, Chinese Culture University, TW

Mang Ou-Yang, National Yang Ming Chiao Tung University, TW

Manuel Melgosa, University of Granada, ES

Maria João Durão, School of Architecture, Lisbon University, PT

Mei-Chun Lo, Shih Hsin University, TW

Mikiko Kawasumi, Meijo University, JP

Minchen Wei, The Hong Kong Polytechnic University, HK

Ming Ronnier Luo, Zhejiang University, CN

Miyoshi Ayama, Utsunomiya University, JP

Pei-Li Sun, National Taiwan University of Science and Technology, TW

Phil Green, Norwegian University of Science and Technology, NO

Pichayada Katemake, Chulalongkorn University, TH

Robert Hirschler, Colour Consultant, HU

Robin Kingsburgh, York University, UK

Saori Kitaguchi, Kyoto Institute of Technology, JP

Shi-Min Gong, Ming Chuan University, TW

Shoji Sunaga, Kyushu University, JP

Silvia Elvira Maria Piardi, Politecnico di Milano, IT

Stephen Westland, University of Leeds, UK

Suchitra Sueeprasan, Chulalongkorn University, TH

Supawadee Theerathammakorn, Sukhothai Thammathirat Open University, TH

Taiichiro Ishida, Kyoto University, JP

Takahiko Horiuchi, Chiba University, JP

Tsung-Xian Lee, National Taiwan University of Science and Technology, TW

Tsuei-Ju Hsieh, Tsing Hua University, TW

Tzung-Han Lin, National Taiwan University of Science and Technology, TW

Valerie Bonnardel, University of Winchester, UK

Verena M. Schindler, AIC Study Group on Environmental Colour Design, CH

Vien Cheung, University of Leeds, UK

Vincent Sun, Chinese Culture University, TW

Wen-Yuan Lee, Department of Media Design, Tatung University, TW

Yoko Mizokami, Chiba University, JP

Youngshin Kwak, Ulsan National Institute of Science and Technology, KR

Yuh-Chang Wei, Chinese Culture University, TW

Yulia A. Griber, Smolensk State University, RU

YungKyung Park, Ewha Womans University, KR

AIC Executive Committee 2024-2025

EC voting members

President ..... Maurizio Rossi (Italy)
Vice President ..... Maria João Durão (Portugal)
Secretary/Treasurer Pichayada Katemake (Thailand)
Ordinary Member ..... Eva-Lena Bäckström (Sweden)
Ordinary Member ..... Valérie Bonnardel (France)
Ordinary Member ..... Ingrid Calvo Ivanovic (Chile)
Ordinary Member (AIC 2025 Congress Representative)..... Pei-Li Sun (Taiwan)

EC consultant members

Auditor ..... Tien-Rein Lee (Tai wan)
Auditor ..... Javier Romero (Spa in)
Immediate Past President..... Leslie Harrington (USA)
JAIC Editor ..... Vien Cheung (UK)

AIC Members

Regular Members

Grupo Argentino del Color ..... Argentina
Colour Society of Australia ..... Australia
Interdisciplinary Colour Association – Belgium ..... Belgium
Associação Pró-Cor do Brasil ..... Brazil
Colour Research Society of Canada ..... Canada
Color Association of China ..... China
Centre Français de la Couleur..... France
Deutscher Verband Farbe..... Germany
The Colour Group (Great Britain) ..... Great Britain
Gruppo del Colore – Associazione Italiana Colore..... Italy
Color Science Association of Japan ..... Japan
Forum Farge ..... Norway
Associação Portuguesa da Cor..... Portugal
Comité Español del Color ..... Spain
Stiftelsen Svenskt Färgcentrum ..... Sweden
Pro/Color…. .....Switzerland
Color Association of Taiwan .....Taiwan
Color Society of Thailand .....Thailand
Stichting Kleurenvisie: Het Nederlands Platform Voor Kleur .....The Netherlands
Inter-Society Color Council ..... United States

AIC Associate Members

International Association of Color Consultants/Designers.....United States

AIC Individual Members

Yuila Griber – Russia

Kazim Himi Or - Turkey

AIC Affiliate Members

Asociatioon Chilena de Color..... Chile - Facebook Instagram

Hungarian National Colour Committeee .....Hungary - aic.kee.hu

Suomen Variyhdistys Svy Ry .....Finland - www.svy.fi

Welcome from the AIC 2025 Organizing Chair

Dear Esteemed AIC Colleagues and Friends,

On behalf of the organizing committee, it is my great honor to invite you to the **AIC 2025 Congress in Taipei, Taiwan**. As the General Chair, I extend my warmest welcome to all researchers, professionals, and enthusiasts in the field of color science, design, and technology.

We are delighted to announce that **AIC 2025 TAIPEI has received 210 paper submissions from 24 countries**, and we are expecting **over 200 registered participants** to join us in this exciting global exchange of ideas and innovations in color.

Taipei, a city where tradition meets modernity, offers an inspiring backdrop for our exploration of color's role in art, science, culture, and industry. Our conference venue, **Songshan Cultural and Creative Park**, lies in the heart of the city—a dynamic hub that seamlessly blends historical architecture with contemporary creative energy. Once an industrial complex, this beautifully restored space now serves as a center for innovation, art, and design—making it an ideal setting for discussions on color's transformative power.

Beyond the conference, Taipei's vibrant streets invite you to wander through historic alleys lined with centuries-old temples, while just around the corner, you'll find cutting-edge architecture, contemporary art galleries, and stylish boutiques. The city's rich culinary landscape blends the old and the new—from traditional tea houses and bustling night markets to sleek, Michelin-starred restaurants.

This October, we also invite all participants to enjoy the **warm hospitality of our city's seasonal festivals**, featuring **art and sports events, live performances, and local gourmet food** that celebrate the creativity and diversity of Taipei. Whether you are enjoying the sights of the city, indulging in local delicacies, or engaging in thought-provoking discussions, **AIC 2025 promises to be an unforgettable experience**.

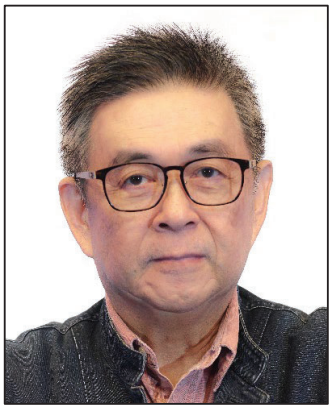

We are curating an enriching program featuring insightful keynote speeches, engaging technical sessions, and cultural experiences that highlight the intersection of color and life. Whether you are presenting your latest research, networking with global experts, or immersing yourself in Taiwan's vibrant aesthetic landscape, we believe AIC 2025 will leave you inspired.

We sincerely welcome you to Taipei for this wonderful AIC event—**and wish you a joyful and memorable stay during our colorful October festival**.

Warmest regards,

Tien-Rein Lee
General Chair, AIC 2025 Taipei
President, Huafan University, Taiwan

Welcome from the AIC President

Dear Researchers, Designers, and Professionals of Color,

Welcome to the AIC 2025 Congress in Taipei, a city where tradition and innovation meet in harmony. Here, the international community gathers once again to share knowledge, creativity, and passion for color in all its meanings — from science to art, from perception to design. May these days together inspire new ideas and collaborations across cultures and disciplines. The AIC 2025 Congress in Taipei will bring together scientists, designers, and professionals from all over the world to present the most recent advances in color research and practice.

The scientific program includes keynote and invited lectures, oral and poster sessions, and meetings of the AIC Study Groups on a four-day program. Sessions and social events will offer opportunities for dialogue and cooperation among academia, industry, and cultural institutions. Special attention is given to emerging topics such as artificial intelligence, lighting and perception, color in virtual and augmented reality, and sustainable color design. The event also celebrates excellence through the AIC Judd, CADE, and Service Awards, honoring significant contributions to the advancement of color science and culture.

The work of consolidating the new AIC structure in Europe is almost complete. A new online platform has been created to host all AIC publications — the Journal of the AIC, the Proceedings of the International Colour Association, the Annual Review, and the Newsletter — making access and management easier for authors and readers. A special thanks goes to Vien Cheung, Chair of the AIC Editorial Committee, and Gianluca Guarini and Alessandro Bortolotti for their invaluable contribution. The AIC legal address has been updated, and financial operations can now also be managed via PayPal.

On November 18th, the AIC General Assembly will be held online to approve the Internal Regulation required by the AIC Statute and to elect the new Executive Committee for the 2026–27 term.

I sincerely thank the organizing committee of AIC 2025, the Color Association of Taiwan, and all volunteers for their remarkable commitment. My gratitude goes to the sponsors and institutional partners whose support made this Congress possible, and to the speakers and authors who enrich our community with their research and creativity. Finally, my warmest thanks to all participants for being here in Taipei — your presence embodies the spirit of collaboration and openness that defines the AIC.

Enjoy the AIC 2025 Congress in Taipei, Taiwan.

The AIC President
Prof. Maurizio Rossi.

JUDD AWARD

2025 AIC Deane B. Judd Award

JOSÉ LUIS CAIVANO

JUDD AWARD

AIC JUDD AWARD CITATION FOR PROFESSOR JOSÉ LUIS CAIVANO

Susana Geat

Argentine Color Group

Corresponding Author: gac@fadu.uba.ar

BIOGRAPHY

José Luis Caivano graduated from the University of Buenos Aires (architect and PhD). Principal Research fellow at the National Council for Research, Argentina. Researcher and professor at the Faculty of Architecture of Buenos Aires University, where he is the director of the Research Program on Color and Visual Semiotics. He holds the highest category (level 1) in the national research system of Argentina. He has been a research associate at the Research Center for Language and Semiotic Studies of Indiana University, USA, in 1989 and 1994.

Caivano was the president of the International Color Association (AIC) for the term 2006- 2009, and president of the International Association for Visual Semiotics (2012-2015). Honorary member of the French association Ad Chroma, the Portuguese Color Association, and the Mexican Association of Color Researchers. He was president of the Argentine Color Group (1994-2004), vice-president of the AIC (2004-2005), and chairman of the AIC Study Group on Environmental Color Design (1997-2005). From 2001 to 2012 he was one of the vice-presidents of the International Association for Visual Semiotics. He was also a member of the advisory board of the International Association for the Interdisciplinary Study of Symmetry. Current or past membership in other scientific associations include: New York Academy of Sciences, International Association for Semiotic Studies, Semiotic Society of America, International Association for the Semiotics of Space, among others.

Caivano has participated in 133 national and international congresses in 29 countries. He was invited lecturer in meetings and taught courses in Argentina and abroad: China, Taiwan, Thailand, Finland, France, Germany, Italy, Portugal, Russia, Spain, Turkey, Bolivia, Brazil, Canada, Chile, Colombia, Ecuador, Mexico, Paraguay, Peru, and Uruguay. He is author of 4 books, editor of other 19 books, and has published 176 articles in books, proceedings of congresses and international journals such as Color Research and Application (New York, Wiley), Die Farbe (Berlin, Muster-Schmidt), Colour: Design & Creativity (UK, Society of Dyers and Colourists), Optica Pura y Aplicada (Spain), Colore (Italy), Languages of Design (Amsterdam, Elsevier), Leonardo (USA, MIT Press), Semiotica (Berlin, Mouton de Gruyter), Visio (Canada, Journal of the International Association for Visual Semiotics), Cruzeiro Semiotico (Portuguese Association of Semiotics), DeSignis (Barcelona, Gedisa), Symmetry: Art and Science (journal of the Society for the Interdisciplinary Study of Symmetry), and others.

Caivano is senior editor of the journal Color Research and Application, associate editor of the journal Color Culture and Science (Italy), member of the editorial committee of the Journal of the International Color Association, JAIC (formerly Colour: Design & Creativity). He was for 10 years editor of the journal AREA, agenda of reflection on architecture, design and urbanism, and the monograph series Serie Difusión, published by the Faculty of Architecture of Buenos Aires University. He was the main editor of the Proceedings of the Argentine Color Congresses (10 volumes published). He has been member of the editorial committee and the advisory board of the journals Visio (Canada), Web Architecture Magazine (Spain), Languages of Design (USA), and The Story of Life (India).

CONTRIBUTIONS TO THE FIELD OF COLOR SCIENCE

The Argentine Color Group would like to nominate José Luis Caivano for the 2025 AIC Judd Award by virtue of a lifelong dedication to color and appearance research and education. In support of this nomination, we have taken into account his contributions to color theory in general, and color in relation to semiotics, architecture and design.

Caivano's rigorous multidisciplinary approach has been particularly useful to build bridges between color science, color language, and environmental color design. He has published papers in prestigious journals, such as *Color Research and Application* (New York), *Die Farbe* (Berlin), *Colour: Design & Creativity* (UK, Society of Dyers and Colourists), *Optica Pura y Aplicada* (Spain), *Colore* (Italy), *Leonardo* (USA, MIT Press), among others. The dissemination of his publications encompass not only English and Spanish languages; we can also find some papers in Italian, French, and Russian. In addition, some of his papers have recently started to be translated into Arabic.

Caivano has also been instrumental at the highest academic level, instigating research programs that have had a deep impact on color discourses, understanding and implementations. In addition to this, the Argentine Color Group would like to emphasize his genuine generosity and enthusiasm for sharing his findings, and his willingness to give his time both to colleagues and in support and encouragement to younger researchers.

I think he needs no further introduction into the AIC community, because he has already participated in 20 AIC conferences since 1993, and has been the AIC president during the term 2006-2009. Caivano's interdisciplinary approach to color research makes it difficult to frame his production either in color science or color design. Instead, it seems to span over both fields; that's why the Argentine Color Group has decided in this opportunity to nominate him for the Judd Award.

1975 Dorothy Nickerson
USA

1977 W. David Wright
Great Britain

1979 Günter Wyszecki
Germany, USA, Canada

1981 Manfred Richter
Germany

1983 David L. MacAdam
USA

1985 Leo Hurvich & Dorothea Jameson
USA

1987 Robert W. G. Hunt
Great Britain

1989 Tarow Indow
Japan, USA

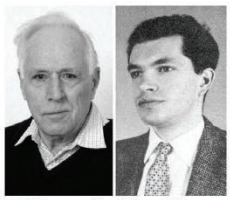
1991 Johannes Vos & Pieter Walraven
The Netherlands

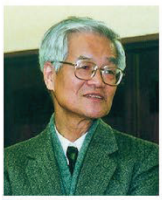
1993 Yoshinobu Nayatani
Japan

1995 Heinz Terstiege
Germany

1997 Anders Hård, Gunnar Tonnquist & Lars Sivik
Sweden

1999 Fred W. Billmeyer
USA

2001 Roberto D. Lozano
Argentina

2003 Mitsuo Ikeda
Japan

2005 John B. Hutchings
Great Britain

2007 Alan Robertson
Canada

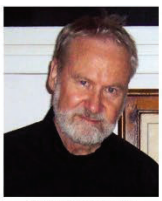
2009 Arne Valberg
Norway

2011 Lucia Ronchi
Italy

2013 Roy S. Berns
USA

2015 Françoise Viénot
France

2017 Ronnier Luo
Great Britain

2019 Hirohisa Yaguchi
Japan

2021 John McCann
USA

2023 Rolf G. Kuehni
USA

2025 José L. Caivano
Argentina

50 years
1975-2025

JUDD AWARD - AIC (International Colour Association)

A science of classification: Personal journey through research on color and visual appearance, within a semiotic framework

José Luis Caivano

Universidad de Buenos Aires, and National Council for Research, *Buenos Aires, Argentina*
caivano@fadu.uba.ar

ABSTRACT

This article is a review of my research work on color and visual appearance, which I generally approached from a semiotic perspective, over a period of 36 years. The paper is divided into five main themes: 1) The developments about cesia (visual appearance other than color), which refers to the visual sensations produced by different spatial distributions of light that is incident upon objects and elicit the perception of transparency, opacity, gloss, translucency, matte appearance, specular appearance, and other intermediate cases. 2) The research on color and visual appearance meanings, signification, rhetoric, synesthetic and cross-modal associations, where color and appearance are protagonists of visual semiosis. 3) The compilation of a chronological bibliography of books on color. 4) The work made in relation to color and appearance in architecture and environmental design. 5) The study of color order systems and chromatic mixtures. These investigations have been generally carried out from the standpoint of taking color and appearance as the signs through which we have the main contact with our visual world. As such, they can be studied within an interdisciplinary semiotic framework, considering that semiotics is a general discipline, a kind of "science of sciences", that seeks to understand how signs function to mediate communication and the construction of knowledge, through different processes of interpretation.

Keywords: visual appearance, color order systems, color in architecture and design, color and semiotics

INTRODUCTION

When preparing this Judd lecture, my first dilemma was whether I should focus on a specific issue,[1] or rather outline a survey of my research and the topics I consider most important. I began searching for other previous Judd lectures, published in the proceedings of AIC conferences, and found examples of both, but the ones reviewing the contributions made throughout the awardee's career predominate. So I ultimately decided on this latter option.

It is a happy coincidence that the AIC gives me the Judd prize at the 50th anniversary of the award. The first recipient was Dorothy Nickerson in 1975, followed in 1977 by W. David Wright, the "father of colorimetry," and 24 other recipients. In some cases, the awards went to teams of two people (Hurvich & Jameson, Vos & Walraven) and to three people (Hård, Tonnquist, & Sivik).

[1] In that case, I thought I would present hypotheses, examples, and some evidences of the gradual transitions observed in various aspects of color and visual appearance, offering a gradualist view that helps relate certain issues that are often interpreted as if they were separate categories. The idea was to continue and expand on what I presented in my invited talk at AIC 2018, Lisbon [1]. For example, to explore intermediate stages or gradations between photopic, mesopic, and scotopic vision; between achromats, dichromats, trichromats, and tetrachromats (with anomalous trichromats as intermediate cases). And also, intermediate stages or gradual transitions between modes of appearance: between surface color and film color, between primary sources (illuminating mode) and secondary sources (surface mode), passing through luminescent translucent objects as intermediate situations.

It is a great honor that the Judd committee considered that I could be on a par with these experts in color science and research. Particularly because my academic background does not come from the physical sciences or mathematics, although throughout my life I have tried to build bridges and promote a common language or a fruitful exchange between what is classically considered "color science" and color in art, architecture, and design. Very often, at the AIC conferences in which I participated, when the program went to parallel sessions, I chose to attend the sessions on color vision, color technology, or colorimetry, rather than listen to the presentations on art, design, and architecture. Partly because I always wanted to learn more about what was foreign or difficult to me, but also because I believe that, given the study of color is eminently interdisciplinary, an effort to connect the different disciplines is needed. In a brief report written in 1986, Wright reminded of "the great divide that still exists between the art and science of color" [2]. Incidentally, 1986 was the year when I began my full-time research activity.

Now, if I have to explain why I became interested in doing color research, the answer is probably simple. I was always drawn to what was most difficult for me, and being a dichromat, the use of color was always a challenge, both in general drawing and in architectural projects. Since childhood, I was very good at drawing, but using color was not easy to me. When I was seven, my parents thought that I had not learned colors well enough, and thus hired an art teacher to give me practical color lessons. At that early age, I started painting saturation scales, monochromatic series with varying lightness and saturation, with mixtures toward white, black, as well as mixtures between chromatic colors. I found that practice fascinating, but it is clear that I never stopped confusing colors, simply because I have the typical deficiency in discriminating shades on the red-green axis that most dichromats suffer from. Thus, perhaps unconsciously, I was drawn to studying color from a more theoretical perspective.

Among other aspects, something that has always caught my attention is the enormous number of color order systems that exist, and the efforts made throughout history to produce these logical and perceptual color classifications. The first time I saw an actual color order system was in 1980, during my first years of architecture school, when professor César Jannello devoted half a year to the theory and practice of color within the annual "Visual Systems" courses. Jannello mainly used Arthur Pope's system, but also Munsell and Ostwald.

Soon after graduating in architecture, I got a research grant from the University of Buenos Aires, and since I was also interested in semiotics, I decided to travel for a semester to stay as a research associate in the Center for Semiotics at Indiana University in Bloomington, directed by Thomas Sebeok. In the library of the university, I had access to countless books on color, and saw the journal *Color Research and Application* for the first time. Upon returning from that trip in mid-1989, I learned that the AIC 1989 conference had been held in Buenos Aires, organized by Roberto Daniel Lozano and the Argentine Color Group. I immediately joined the group and began participating in its courses and meetings. I must thank Lozano for much of my knowledge about color science.

RESEARCH TOPICS

Cesia and visual appearance

Since early 1988, I had already been engaged in an aspect related to color, but somewhat collateral to it: the modes of color appearance and the issues of transparency, opacity, gloss, etc., for which César Jannello had coined the word "cesia". The issue of cesia continues to be at the top of my interests. Concurring with my obsession for order systems, and as part of my research grant, I had set out to create an order system for cesias, which would include the variables of regular and diffuse transmittance and reflectance, on the one hand, and light absorption, on the other [3]. Initially, the model considered the stimulus' physical variables, but soon I realized that it should rather focus on visual sensations (conversations with Osvaldo da Pos were influential on this change).

I thought that if all color sensations can be arranged in color order systems, any other sensorial continuum could have its own system as well.[2] It is just a matter of thinking about it, selecting the variables, looking for the possible

[2] Continuing Jannello's efforts to build a model for visual textures, in 1990 I also published a paper attempting to produce an order system of textures, and a few years later I arrived at a result that seemed satisfactory to me [4-6].

poles of opposition, building the gradations, defining the notations, and making a three-dimensional representation of it. Thus, the construction of the space of cesias resulted from considering the spatial distribution of light on a surface or object, and the four main sensations elicited (transparent, translucent, specular, and opaque matte appearances), plus the sensation of darkness. The three axes or dimensions of the model, with which those sensations can vary, are transparent versus opaque, diffuse versus regular (sharp or specular), and light versus dark.

After some elaboration and adjustments, my first article on the subject appeared in 1991 in the journal *Color Research and Application* [7]. By then, I was already influenced by the books of David Katz, the Optical Society of America, Sven Hesselgren, Ralph Evans, and others [8-11]. And I remember Lozano advising me on terminological issues.

Shortly after that publication, I received a letter from Paul Green-Armytage. In his own words, he was "dismayed" at reading my article, because it turned out he had been working on something very similar [12]. We continued corresponding and agreed to meet at an upcoming AIC conference to discuss the topic further. This happened at AIC 1993 in Budapest. There, I personally met Paul, Osvaldo da Pos (whom Paul introduced to me as the "king of transparency"), Lars Sivik, Antal Nemcsics, John Hutchings, and several other color researchers. It was also the first time I saw the Judd award ceremony, when Yoshinobu Nayatani was given the Judd medal.

In 1993, Paul used the term "tincture", borrowed from heraldry, to refer to various aspects of visual appearance, and included sections on cesia in his papers [13, 14]. In AIC 1993 I delivered an oral presentation about the construction of scales of cesia using spinning discs, somewhat in the manner of Maxwell's discs, or those that Ostwald used to determine the colors of his color system, mixing portions of white, black, and a full color in proportions following logarithmic scales, according to the Weber-Fechner law. On my discs, I mixed five types of surfaces (black, transparent, translucent, specular, and matte white) combined in pairs. By testing Stanley Stevens' power law (which establishes the relationship between the increase in intensity of a physical stimulus and the increase in the magnitude of the perceived sensation),[3] I obtained scales of transparency, gloss, translucency, darkness, etc. The purpose was to cover the sensations of cesia located at the edges of the 3D model. The work was soon published in the journals *Die Farbe* and *Color Research and Application* [15, 16]. On that occasion, I discussed the experimental procedures with María Luisa Mattiello, who had a solid background in visual psychophysics, having worked in the Sensory Research Laboratory headed by Miguelina Guirao, a disciple of Stanley Stevens.

Now, scales of cesia can be obtained in many ways; they can also be achieved by mixing liquids, with surfaces placed in different geometries with respect to illumination, viewing angle, and distance from a contrasting background, etc. In other words, there are countless possible scales of cesia. From there, atlas of cesia (more modest than color atlas in terms of the number of samples) can be assembled using different materials. At AIC 1997 in Kyoto, I presented the construction of the prototype of an atlas materialized with glass samples, produced at the Optics Laboratory of the National Institute of Industrial Technology in Buenos Aires [17].

Two years later, at AIC 1999 in Warsaw, I delivered a summary of the fundamentals for making visual appearance assessments, taking into account sample characteristics (mainly whether transmittance or reflectance is important), illumination and observation geometries, as well as the use of additional devices such as light diffusers or grids to assess contrast and sharpness [18]. I based my work on the methods by the American Society for Testing and Materials for assessing gloss, on the procedures by Richard Hunter, as well as on Karin Fridell Anter's concepts of inherent and perceived color, applied in this case to cesia [19-21].

At AIC 2004 in Porto Alegre, Brazil, I showed the development of a prototype for an atlas of cesia with paint mixtures, made at the Sherwin-Williams laboratory [22]. The same year, Lucia Ronchi and I published an article on how to describe the visual appearance of complex patterns in textiles, a work presented two years earlier at an Argentine color conference [23]. With Paul Green-Armytage, we continued a fruitful exchange of ideas and publications. A

[3] Stevens' power law states that the perceived intensity of a sensation (S) is proportional to the physical intensity of a stimulus (I) raised to a specific power (^{a}), that is, $S = kI^a$, where (k) is a constant and the exponent (^{a}) varies according to the type of sensation. This law describes the nonlinear relationship between physical stimuli and sensations, and it overcomes in some aspects the Weber-Fechner law, since it covers a wider range of perceptions.

culmination of this collaboration was the entry on "Appearance", published in the *Encyclopedia of Color Science and Technology*, both in the 2016 and 2022 editions [24].

More recently, the idea arose to make a chronological compilation of everything published on cesia (including also the most direct antecedents). Many researchers have become involved in the subject, developing some aspects or applications. Lozano integrated the concept of cesia into a more general model of visual appearance, and the CIE Technical Committee 1-65 included a section on cesia in its report on the measurement of visual appearance [25, 26]. In addition, there are already doctoral theses on this topic, and recently two members of the Group μ (referents in visual semiotics, authors of the famous *Treatise on the visual sign*) published an article entirely devoted to cesia [27, 28]. Then, with some members of my research group, we decided to create a website to update information and upload content and new publications on the subject: https://cesiapage.wordpress.com. The site includes a chronology of publications and unpublished documents, and features the people involved in these developments with their contributions over approximately four decades. There is also a selection of antecedents previous to 1990 that refer to similar phenomena without using the name "cesia", which was coined by Jannello somewhere in the 1980s [29]. These authors include Philipp Otto Runge, David Katz, Ludwig Wittgenstein, the Committee on Colorimetry of the Optical Society of America, Sven Hesselgren, Richard Hunter, Ralph Evans, John Hutchings, Paul Green-Armytage, and others; see the details in my invited lecture to AIC 2023 in Thailand [30].

Color, appearance, and visual semiotics: rhetoric, meanings, synesthesia, and cross-modal associations

One of the areas of research that has always interested me is color in relation to visual semiotics, that is, how color functions as a sign, the ways in which color is involved in semiosis, in the everyday use of signs. Already at AIC 1996 in Gothenburg, Sweden, I had presented two papers: one on semiotics and cesia, and another that consisted of replicating in Argentina a survey on color meanings designed by Lars Sivik and Charles Taft in Sweden, using semantic differential scales [31, 32]. Another study, carried out by an international collaborative group headed by Li-Chen Ou and Ronnier Luo, and replicated in eight countries, dealt with the intercultural comparison of color preferences and associations with emotions [33].

In collaboration with Mabel López, I presented and published works on color as a sign of identity in brands and institutions, on the semiotic relationship between color and food, and on the rhetoric of color [34-37]. In the latter case, we addressed the use of color as an argument in visual statements, for example in photography, video, advertising posters, or graphic design in general. Rhetoric is commonly thought of in terms of verbal language, i.e., to convince someone through words and arguments of verbal discourse. This is classical rhetoric. However, there is also a visual rhetoric, and color is a very important part of this type of use of visual languages: arguing and convincing through visual images and color.

At the end of the nineties, I published an article in *Color Research and Application* where I addressed several aspects of color theory from a semiotic framework [38]. Also, my opening lecture at the 2014 AIC conference in Oaxaca, Mexico, focused on the indexical aspects of color, i.e., color working as an index in various modalities: a *signal* that precedes the object to which it refers, a *clue* that remains after the fact or object that caused it, or a *symptom* that appears simultaneously with its object [39]. I have always approached this topic from the perspective of Peircean semiotics, referring to the late 19th and early 20th-century philosopher, logician, mathematician, and polymath Charles Sanders Peirce. The "father of modern semiotics" was influenced by the thought of Kant and by his contemporary William James, with whom he founded the pragmatist movement, and arguably also to a lesser extent by the empiricism of John Locke. He covered several fields of knowledge —mathematics, logic, physics, thermodynamics, optics, photometry, chemistry, metrology, etc.—, but he considered that all of them subsume within a single discipline that encompassed all the processes of human knowledge: semiotics.[4] Peirce had an interesting and deep relationship with color. His

[4] In a letter to Lady Welby from 1908, Peirce wrote: "… it has never been in my power to study anything —mathematics, ethics, metaphysics, gravitation, thermodynamics, optics, chemistry, comparative anatomy, astronomy, psychology, phonetics, economics, the history of science, whist, men and women, wine, metrology— except as a study of semeiotic" [40].

research on stellar photometry deserves to be better known [41]. It is also noteworthy that Christine Ladd-Franklin, author of the book *Colour and colour theories*, was a disciple of Peirce at Johns Hopkins University.

In an article published in 2015, I argued that semiosis is not an exclusively human activity but something that all living beings experience, particularly the semiosis produced by vision systems, which react to light stimuli with the purpose of obtaining information from the environment, in order to live and evolve [42].

As part of the relationship between color and semiotics, one aspect is the issue of chromatic synesthesia, that is, the associations of color —a visual sign— with sensations produced in other sensory channels: touch, smell, taste [43]. Other visual categories also appear in these associations, for example, color and size, or color and shape, something that Kandinsky and other artists were very concerned about. And, of course, we cannot forget about color and music. I had a musical training; before studying architecture, I graduated from the National Conservatory of Music in Argentina, where, among other subjects, I studied acoustics, harmony, and composition. I was always interested in looking for the connections between color and sound. Incidentally, like color, sound is also described in terms of three dimensions or variables [44]. One of the most common types of synesthesia consists of hearing sounds and perceiving colors, or vice versa, seeing colors that elicit sound sensations fired by the color stimuli.

In any case, it is important to clarify that there are two types of synesthesia: *genuine synesthesia* (an innate neurological condition that produces involuntary, consistent, and unique sensorial crossovers for each individual), and *pseudo-synesthesia* (more general, variable, and non-automatic associations between senses, influenced by learning, mood, or cultural factors, and not involving actual perceptual experiences). The latter is sometimes termed cross-modal associations, so as not to confuse it with genuine synesthesia. I say this is part of semiotics because it is a process of semiosis or signification, where one thing works as a sign to represent another: associations between one type of sign and another.

Among these specific aspects, with Pilar Buera (PhD in chemistry and expert in color and appearance in food technology) and a group at the Department of Industries of the Natural Sciences Faculty at the University of Buenos Aires, we conducted experiments and surveys about associations between taste and color. We had the students taste food samples and, at the same time, observe colors with which they should establish associations. The specimens to taste were transparent, colorless liquids and jellies, as well as achromatic cookies, with four tastes (salty, sweet, sour, and bitter). The subjects had no previous information about how the specimens tasted (no descriptive labels were assigned, just random numbers). They simply had to try them and compare or associate with colors in several different tests. One experiment used samples of four elementary colors, another displayed a random list of 12 color names, and a third one involved the whole atlas of the Natural Color System. Some of the strongest associations we found are: red with sweet, orange with sour/sweet, yellow with sour, white and blue-green with salty [45].

Color bibliography

At AIC 2001 in Rochester, Daniel Lozano granted me the honor of delivering the citation for his Judd award.[5] I also presented the compilation of a chronological bibliography of books on color, written or published throughout the ages, a task that I had begun in the early 1990s and continue to do from time to time [46, 47]. My starting point was Michel Indergand's *Bibliographie de la couleur* [48]. At AIC 2003 in Bangkok, I presented some information and statistical data extracted from the bibliographic compilation, since it was based on the Microsoft Access database software [49]. A few years later, I learned that Roy Osborne had also begun compiling a bibliography of books on color, published in print [50]. Currently, my bibliography has around 4,000 records. It has been available online for several years, and I am now looking for a suitable format to put it back online.

[5] At the 2001 AIC assembly in Rochester, I was elected member of the executive committee for the next quadrennium. In August 2003, I replaced Paul Green-Armytage as vice-president, and at AIC 2005 in Granada, I became the AIC president for the quadrennium from January 2006 to December 2009.

Color in architecture and design

In 2001, together with Leo Oberascher, I began coordinating the AIC Study Group on Environmental Color Design. At AIC 2002 in Slovenia, I presented a history of the origins and development of this study group [51]. At AIC 2005 in Granada, I delivered the closing lecture. In this case, I chose to provide a historical overview of color research related to architecture. The work was later published in *Color Research and Application* [52]. In an invited lecture at the Spanish Color Conference in 2010, I addressed the topic of color order systems developed by architects or in relation to architecture along different periods in history [53].

Between 2016 and 2022, Springer published two editions of the *Encyclopedia of Color Science and Technology*, the first one edited by Ronnier Luo and the second one by Renzo Shamey as general editors. For both editions, I was responsible of the "Art and Design" section, which includes more than 30 articles. Among them, I also authored the entries on "Color combination" and "Polychromy" [54, 55].

Color order systems

As mentioned at the beginning, color order systems attracted my interest since my early years as an architecture student, when I began to learn something about color theory through the influence of César Jannello. The question of how all perceptible colors are arranged using variables and logical criteria, seemed intriguing to me. I am always looking for historical examples of them, from the oldest to the most modern ones. In 1995, I published a little book in Spanish, providing a historical overview of color order systems [56]. In Kyoto 1997, coauthored with María Mattiello, I presented a comparison between the Munsell and NCS systems based on psychophysical evaluations, later published in *Color Research and Application* [57].

In 2016, I published the entry on "Color order systems" in the *Encyclopedia of Color Science and Technology* (both the first and second editions), in collaboration with Antal Nemcsics [58]. A year later, Nemcsics would become the first person to receive the CADE (Color in Art, Design and Environment) award from the AIC.

One of the last things I did was trying to classify many color order systems on the basis of schemes that represent where the color wheel is located in relation to the grayscale, to white and black. The outcomes are different when one makes additive, subtractive, or partitive color mixtures. I realized that these different mixtures produce an almost continuous series with gradual variations among them, rather than being "packed" in entirely separate categories. Then, I intended to ascertain how different color systems fit into some basic schemes or models, in a way that is more akin to them. This is related to the issue of cesia (as we see, a recurring topic), since it depends on the degree of transparency or opacity of the mixtures with dyes and pigments. In the case of light mixtures, they follow, of course, additive principles. However, in all the other cases, depending on the degree of transparency or opacity of the colorant used, a wide range of mixture types can be obtained, in a gradual series. This results in color order systems having different characteristic shapes. Hence, we can explain why some systems have the shape of a simple cone (or tetrahedron, pyramid, or hemisphere) with a black vertex, a double cone or sphere with two vertices or poles, or a simple conic shape (or tetrahedron, pyramid, or hemisphere) with a white vertex [59, 60].

CONCLUSION

Throughout my academic life, I have worked on topics of color theory and visual appearance related to architecture and design, order systems, and visual perception. I conducted some research in collaboration with specialists in optics and colorimetry, chemistry and food technology, coating technology, vision and psychophysics, psychology, mathematics, linguistics, music and the arts, without being an expert in any of these fields. Paraphrasing Peirce, I could say that, ultimately, everything I did was semiotics. Anyway, as Wright would say, I find it embarrassing to be considered an expert on color, given all the fields and areas that color studies encompass.

If science is the human activity whose aim is to understand and explain aspects of the world through systematic observation, experimentation, and logical reasoning, in order to get reliable and verifiable knowledge, then I can consider that yes, I have been doing science, and that activity is practically the same as doing semiotics. Because

semiotics is the general science of signs, the study of the processes of signification: how we know things through sign systems that human civilization build to understand different aspects of the world. That is to say, the entire scaffolding of science is an intricate system of languages and sign systems, more or less sophisticated, general or specific, with which we make representations or models of the world that are apprehensible to our mind. *Semiotics* is, then, the science that studies semiosis (obviously, this is a human activity). *Semiosis*, in turn, encompasses the processes of signification that all living beings, of any species whatsoever, carry out in order to live, reproduce, and interact with the world around them. In this sense, color and visual appearance are signs of utmost importance, as Hutchings reminds in a phrase also quoted by Wright in one of his famous reviews published in *Color Research and Application:* "Color and design are vital ... to the life and perpetuation of different biological systems" [61, 62]. Now, what kind of science is color science? For Peirce, "it is … a classificatory, not a cause-seeking science" [63]. Perhaps, this idea has unconsciously guided most of my research interests.

REFERENCES

[1] Caivano, J. (2018) Color from a gradualist perspective. In: *AIC 2018 Proceedings*, 31-38.
[2] Wright, W. D. (1986) Talking about color… *Color Research and Application* 11(4), 293-294.
[3] Caivano, J. (1988) Cesía. In*: Trabajo de investigación…*, research report, dir. C. Guerri. Buenos Aires University.
[4] Jannello, C. V. (1963) Texture as a visual phenomenon. *Architectural Design* 33 (August), 394-396.
[5] Caivano, J. (1990) Visual texture as a semiotic system. *Semiotica* 80(3-4), 239-252.
[6] Caivano, J. (1994) Towards an order system for visual texture. *Languages of Design* 2(1), 59-84.
[7] Caivano, J. (1991) Cesia: a system of visual signs complementing color. *Color Research and Application* 16(4), 258-268.
[8] Katz, D. (1911) *Der Aufbau der Farbwelt*. English translation, *The world of colour*. Kegan, Paul, Trench, Trubner, 1935.
[9] OSA (Optical Society of America), Committee on Colorimetry. (1953) *The science of color*. Crowell.
[10] Hesselgren, S. (1967) *The language of architecture*. Studentlitteratur, Lund, Sweden.
[11] Evans, R. M. (1974) *The perception of color*. Wiley.
[12] Green-Armytage, P. (1989) Colour and other aspects of appearance. Paper to the 2nd National Conference of the Colour Society of Australia, October 1989, manuscript. Published in *Spectrum* (Colour Society of Australia) 6(3), 1992, 1-11.
[13] Green-Armytage, P. (1993) Beyond colour. In: *Color 93, Proceedings*, 155-162.
[14] Green-Armytage, P. (1993) Tincture – A new/old word for the appearance of things. *Journal of the School of Design* 2, 16-23.
[15] Caivano, J. (1993) Appearance (cesia): variables, scales, solid. *Die Farbe* 39(1-6), 115-125.
[16] Caivano, J. (1994) Appearance (cesia): construction of scales by means of spinning disks. *Color Res. Appl.* 19(5), 351-362.
[17] Caivano, J., & Doria, P. (1997) An atlas of cesia with physical samples. In: *AIC Color 97, Proceedings*, 499-502.
[18] Caivano, J. (1999) Evaluation of appearance by means of color and cesia... In: *AIC 1999, Proceedings*, 85-92.
[19] American Society for Testing and Materials. (1990) Standard test method for visual evaluation of gloss differences between surfaces of similar appearance, Standard D 4449.
[20] Hunter, R., & Burns, M. (1970) Geometric and color attributes of object appearance. In: *AIC Color 69, Proceedings*, 525-529.
[21] Fridell Anter, K. (1997) Inherent and perceived colour in exterior architecture. In: *AIC Color 97, Proceedings*, 897-900.
[22] Caivano, J., Menghi, I., & Iadisernia, N. (2004) Cesia and paints: an atlas of cesia with painted samples. In: *AIC 2004, Proceedings*, 113-117.
[23] Ronchi, L., & Caivano, J. (2004) Naming the appearance of patterned complex displays. In: *ArgenColor 2002, Actas del Sexto Congreso*. Grupo Argentino del Color, 499-506.
[24] Caivano, J., & Green-Armytage, P. (2016) Appearance. In: *Encyclopedia of Color Science and Technology*. Springer, 40-47. (2nd ed. 2022).
[25] Lozano, R. D. (2006) A new approach to appearance characterization. *Color Research and Application* 31(3), 164-167.
[26] CIE TC1-65. (2006) *A framework for the measurement of visual appearance*, draft 5 (final), pp. 23, 91.
[27] Jofré, V. (2017) *Aspectos de la cesía en la imagen artística.* Universidad Nacional de Córdoba, Argentina, doctoral thesis.
[28] Groupe μ (F. Édeline, J. M. Klinkenberg). (2023) Un paramètre ignoré des énoncés plastiques : la césie. Systématique et rhétorique de la césie. *Signata* 14.
[29] Jannello, C. V. (c.1980) La cesía como materia conceptual, manuscript. Posthumous publication in: G. Carvajal, *Diseño como poética*. Academia Nacional de Bellas Artes, Buenos Aires, 2005, 112-115.
[30] Caivano, J. (2023) The concept of cesia (visual appearance other than color). In: *AIC 2023, Proceedings*, 85-92.

[31] Caivano, J. (1997) Semiotics and cesia: meanings of the spatial distribution of light. In: *Colour and psychology. From AIC Interim Meeting 96*, 136-140.
[32] Caivano, J., & Rimoldi, L. (1997) The meanings of color in Argentina (Buenos Aires). In: *Colour and psychology. From AIC Interim Meeting 96*, 161-163.
[33] Ou, L. C., Luo, M. R., Caivano, J., et al. (2012) A cross-cultural comparison of colour emotion for two-colour combinations. *Color Research and Application* 37(1), 23-43.
[34] Caivano, J., & López, M. (2007) Chromatic identity in global and local markets: analysis of colours in branding. *Colour: Design & Creativity* 1(1), 1-14.
[35] Caivano, J., & López, M. (2010) Color and feeding, a compromise between necessity and desire: biological and cultural semiotic processes. In: *AIC 2010, Proceedings*, 334-336.
[36] Caivano, J., & López, M. (2003) The rethoric of black, white and red... In: *AIC Color 2003, Proceedings*, 341-346.
[37]Caivano, J., & López, M. (2010) How colour rhetoric is used to persuade: chromatic argumentation in visual statements. *Colour: Design & Creativity* 5(11), 1-11.
[38] Caivano, J. (1998) Color and semiotics: a two-way street. *Color Research and Application* 23(6), 390-401.
[39] Caivano, J. (2014) Color and cesia as signs: Indexical use of color and cesia... In: *AIC 2014, Proceedings*, 19-28.
[40] Peirce, C. S. (1908) Letter to Lady Welby, Dec. 23, 1908. In: P. Wiener (ed.), *Charles S. Peirce: selected writings*. Dover, 1958.
[41] Peirce, C. S. (1878) Photometric researches by C. S. Peirce, made in the years 1872-1875. *Annals of the Astronomical Observatory of Harvad College*, vol. IX.
[42] Caivano, J. (2015) Cognition and semiotic processing of luminous stimuli in various orders of the natural word. *Cognitive Semiotics* 8(2), 129-140.
[43] Caivano, J. (2009) La couleur et la saveur : synesthésies chromo-gustatives. *Primaires* (Centre Francais de la Couleur) 169, 9-10.
[44] Caivano, J. (1994) Color and sound: physical and psychophysical relations. *Color Research and Application* 19(2), 126-133.
[45] Caivano, J., Buera, P., & Schebor, C. (2012) Interaction of color and taste: color synesthesia in the food environment. In: *AIC 2012, Proceedings*, 96-99.
[46] Caivano, J. (2002) Interactive bibliographical database on color. In: *AIC 2001, Proceedings*, 967-970.
[47] Caivano, J. (1997) Chronological bibliography of colour theory. *Spectrum* (Colour Society of Australia) 11(3), 22-27, and 12(1), 20-27. Previous version, in collab. with B. Galeyev and R. Lauzzana, *Languages of Design* 2(4), 1994, 353-364.
[48] Indergand, M. (1984) *Bibliographie de la couleur*. Société des Amis de la Bibliothèque Forney, Paris.
[49] Caivano, J. (2003) Bibliographical database on color: information and statistics... In: *AIC Color 2003, Proceedings*, 319-323.
[50] Osborne, R. (2013) *Books on colour since 1500*. Universal-Publishers, Boca Raton, Florida.
[51] Caivano, J. (2003) A history of the International Color Association study group on Environmental Color Design, from 1982 to 2002. In: *AIC Color 2002, Proceedings*, 187-195.
[52] Caivano, J. (2006) Research on color in architecture and environmental design... *Color Res. Appl.* 31(4), 350-363.
[53] Caivano, J. (2010) Historia de los sistemas de ordenamiento del color desarrollados en relación con la arquitectura. In: *IX Congreso Nacional del Color, Libro de Actas*. Comité Español del Color, 5-11.
[54] Caivano, J. (2016) Color combination. In: *Encyclopedia of Color Science and Technology*. Springer, 275-281. (2nd ed. 2022).
[55] Caivano, J. (2016) Polychromy. In: *Encyclopedia of Color Science and Technology*. Springer, 1058-1063. (2nd ed. 2022).
[56] Caivano, J. (1995) *Sistemas de orden del color*. Buenos Aires: FADU-UBA, Serie Difusión 12.
[57] Caivano, J., & Mattiello, M. (2003) Fixed range scales applied to the evaluation of color: comparative analysis between the Munsell System and the Natural Color System. *Color Research and Application* 28(2), 103-112.
[58] Nemcsics, A., & Caivano, J. (2016) Color order systems. In: *Encyclopedia of Color Science and Technology*. Springer, 329-343. (2nd ed. 2022).
[59] Caivano, J. (2021) Color order systems, color mixtures and the role of cesia. *Color Research and Application* 46(6), 1169-1179.
[60] Caivano, J. (2023) The shape of colour order systems and the evolution of colour theory. In: *Ordering colours in 18th and early 19th century Europe*, ed. T. Kleinwächter, S. Lowengard & F. Steinle. Springer, 15-37.
[61] Hutchings, J. B. (1986) Colour and appearance in nature. *Color Research and Application* 11(2), 107-124.
[62] Wright, W. D. (1989) Talking about color… *Color Research and Application* 14(2), 57-58.
[63] Peirce, C. S. (1879) Rood's Chromatics. *Nation* 29 (Oct. 16), 260. Reprinted in Peirce's *Chronological edition,* vol.4, 47-49.

CADE AWARD

2025 AIC Colour Award in Art, Design and Environment

Berit Bergström

CADE AWARD

AIC CADE AWARD CITATION FOR BERIT BERGSTRÖM

Kennet Vrågård[1], Berit Bergström[1*]
[1]*Swedish Colour Centre Foundation*
[1*]*Corresponding Author: eva-lena@wrd.se*

BIOGRAPHY

Berit Bergström is a Colour Specialist & Educator in colour theory and colour scheme working in her own business, Berit ColourTalks, since 2016. She was employed by NCS Colour AB from 1990 to 2016. She was the Managing Director for NCS Colour Academy between 1991 and 2012. She has long experience of giving international colour design courses and presentations and has conducted colour studies at university level worldwide for more than 30 years. This has newly resulted her new book “Colour Choices. A practitioner's guide to designing colour schemes” in both English and Swedish. She was the secretary of the Colour Science Foundation (1991-1997) and was responsible for granting funding for different colour reseach projects within the field of colour. She is the secretary of the Swedish Colour Centre Foundation since 1991. She has been a member of the AIC Executive Committee between 2006 – 2021. She was the President of AIC 2010 to 2013 and the chairperson of the AIC Study Group on Colour Education between 1998 and 2009.

A GLOBAL MENTOR IN COLOUR FOR ART, DESIGN & ARCHITECTURE

With a career spanning more than 30 years, Berit has dedicated herself to bridging the gap between colour theory and practical application. She has been at the forefront of initiatives that highlight the importance of colour in the fields of art, architecture, and design, while also advancing research in colour perception, communication, and environmental design.

Her leadership in key organizations, including the Swedish Colour Centre Foundation and the International Colour Association (AIC), has elevated the status of colour as a fundamental element in design and the built environment.

Among her most notable contributions:

- Advancing Colour Education – Through her leadership at the Swedish Colour Centre Foundation (1992-2023), Berit has worked tirelessly to incorporate colour education into design and architecture programs, ensuring that future generations of designers understand the impact of colour in spatial and environmental contexts.
- Bridging Research & Practice – As CEO of NCS Colour Academy (1993-2012), she developed the Certified Colour Designer and NCS Certified Teacher programs, ensuring that colour education was not just theoretical but deeply embedded in practical design and architectural applications.
- Encouraging Innovation in Colour Design – She co-founded Awarded Colour (2012), a competition in Sweden that encourages emerging designers, architects, and artists to explore the creative potential of colour in design and the built environment.
- International Colour Advocacy – As President of AIC (2010-2013), she played a critical role in establishing International Colour Day (ICD), ensuring that the cultural and artistic significance of colour was recognized worldwide.
- Shaping Global Colour Discourse – Through numerous international lectures, conferences, and workshops, she has contributed to discussions on colour aesthetics, perception, and its role in architecture, urban design, and cultural identity.

IMPACT ON ART, DESIGN & THE BUILT ENVIRONMENT

Berit's work has directly influenced colour application in architectural and urban spaces, ensuring that colour is not merely decorative but a crucial component of human-centered design. Her research and teachings emphasize how colour affects perception, mood, and spatial experience, making her contributions essential for architects and designers striving to create meaningful, functional, and aesthetically rich environments.

Her book "Colour Choices" distills her decades of experience, offering designers and architects a guide to using colour as a tool for communication, composition, and emotional impact. Her methods integrate scientific research, artistic exploration, and hands-on practice, making her one of the most influential figures in contemporary colour education and application.

Through her teachings and advocacy, Berit has transformed the way colour is perceived in the built environment, ensuring that it is recognized as an essential element of human experience, sustainability, and cultural expression.

MOTIVATION

Berit Bergström is honored with the Colour Award in Art, Design, and Environment (CADE) for her exceptional contributions to the integration of colour within design and the built environment. Through her dedication to education, research, and leadership, she has profoundly advanced the global discourse on colour.

Her work has enriched colour education and research while elevating the importance of colour in shaping the spaces where we live, work, and interact. As a mentor and global ambassador for colour in art, design, and architecture, Berit has inspired countless designers, educators, and practitioners.

Berit's enduring legacy in colour education, research, and practical application continues to influence and inspire worldwide, making her a truly outstanding recipient of this prestigious award.

From Scientific Research to Practical Colour Application

Berit Bergström

Swedish Colour Centre Foundation/Berit ColourTalks*, Sweden*
bergstrom.berit@gmail.com

ABSTRACT

Choosing the right colour is of course an important attribute in colour design. The right colour can make a product a success and the wrong colour a failure. A colour image attracts and grabs a reader of a magazine or catches the eye on a website. When choosing colour in environment design, there are many aspects to consider, such as culture and tradition, the colour identity in the surroundings, the relationship between colour and architecture, will the colour strengthen or weaken the architecture, enlarge or reduce the scale. You also have historical aspects, original colours and access of material. The choice of colour is an important feature in colour applications.

There are of course no roles given. The term "colour research" means different things to different people. The artists naturally often work with colour research from a more emotional perspective and have then no scientific foundation. There is clear evidence that colours and illumination can affect human brain activity. Man is affected by no-visual effects of light and colour. It should be noted that there are ideas of how colours affect us, but many do not hold up for a scientific review. There is a lot of knowledge to be gained from our colour research. It has always been important to me to spread the knowledge that exists in color research so that it is passed on to students and practitioners.

The colour education needs to be more practical and hands-on. Colour education is about perception, communications, associations, colour changes and a lot of practical colour exercises and training. Training in colour analysis of different objects, historical and new buildings and nature's colour palette is a good way of learning where to use different colour scales. How does a colour scale from the 18th century look like? Which are the typical colour areas and which are not? Investigations of nature's colour palette and the heritage colours of different periods provide knowledge for the colour designer of today.

It is important to deepen the knowledge about colour and show the values of colour awareness. Colour is a valuable design factor that affects spatiality, function and aesthetics. Knowledge and experience from colour teaching for 35 years have resulted in my book Colour Choices - A guide to colour schemes.

Unexpected opportunities open for the treatment of colour in education context and can create so much involvement from the students. The whole education program should be completed with an overall colour project where they can use the new colour knowledge and understand how it can be used in their future professional colour applications

Technical Program

Overview

<table>
<tr><th>Date</th><th>19 Oct.
(Sun)</th><th>20 Oct.
Day 1 (Mon)</th><th>21 Oct.
Day 2 (Tue)</th><th>22 Oct.
Day 3 (Wed)</th><th>23 Oct.
Day 4 (Thu)</th><th>24 Oct.
Day 5 (Fri)</th></tr>
<tr><td>9:00 - 9:30</td><td rowspan="5"></td><td>Registration
(8:30-9:30)</td><td rowspan="2">Invited
Lectures</td><td></td><td rowspan="2">Invited
Lectures</td><td rowspan="10">Taipei City
Excursion</td></tr>
<tr><td>9:30 - 10:00</td><td rowspan="2">Opening
Ceremony
& Group Photo</td><td>Morning Tea</td></tr>
<tr><td>10:00 - 10:30</td><td>Coffee Break</td><td rowspan="3">Oral
Presentation
5</td><td>Coffee Break</td></tr>
<tr><td>10:30 - 11:00</td><td>Invited Lecture</td><td rowspan="2">Oral
Presentation
3</td><td rowspan="2">Oral
Presentation
6</td></tr>
<tr><td>11:00 - 12:00</td><td>Oral
Presentation
1</td></tr>
<tr><td>12:00 - 13:00</td><td>Lunch</td><td>Lunch, ACA Meeting</td><td colspan="2">Lunch</td></tr>
<tr><td>13:00 - 14:30</td><td rowspan="4">Workshop
(14:00-
17:00)</td><td>Poster
Session
1</td><td>Poster
Session
2</td><td>Poster
Session
3</td><td>Oral
Presentation
7</td></tr>
<tr><td>14:30 – 15:00</td><td colspan="4">Coffee Break</td></tr>
<tr><td>15:00 – 16:15</td><td>Oral
Presentation
2</td><td>Oral
Presentation
4</td><td>Judd/CADE/
Sphere Award
Ceremonies
& Lectures</td><td>Oral
Presentation
8
(15:00-16:00)</td></tr>
<tr><td>16:15 – 17:30</td><td>SG 1:
Arts and Design
(AD)</td><td>SG 2:
Environmental
Color Design
(ECD)</td><td>SG 3:
Color Vision &
Psychophysics
(CVP)</td><td>Closing
Ceremony
(16:00-16:30)</td></tr>
<tr><td></td><td>Welcome
Reception
(17:00-19:30)</td><td></td><td></td><td>AIC Gala
Banquet
(18:00-21:00)</td><td>VIP Visit
Art-Taipei
(19:00-20:30)</td><td></td></tr>
</table>

1 track
2 tracks
Poster session
Events (optional)

Main Venue: Multi-Purpose Hall (2F), Songshan Cultural and Creative Park, Taipei, Taiwan

Day 1 and Day 2

<table>
<tr><th>Date</th><th>19 Oct.
(Sun)</th><th colspan="2">20 Oct.
Day 1 (Mon)</th><th colspan="2">21 Oct.
Day 2 (Tue)</th></tr>
<tr><td>Time</td><td rowspan="8"></td><td>Hall A</td><td>Hall B</td><td>Hall A</td><td>Hall B</td></tr>
<tr><td>8:30-9:00</td><td colspan="2" rowspan="2">Registration</td><td colspan="2">Registration</td></tr>
<tr><td>9:00 - 9:30</td><td colspan="2" rowspan="3">Invited Lectures
A Comprehensive Colour Solution across Industries, Luo, Ming Ronnier
Algorithmic & Digital Color Expressions
Bendito, Petronio</td></tr>
<tr><td>9:30 - 10:00</td><td colspan="2" rowspan="2">Opening Ceremony
& Group Photo</td></tr>
<tr><td>10:00 - 10:30</td><td colspan="2">Coffee Break</td></tr>
<tr><td>10:30 - 11:00</td><td colspan="2">Invited Lecture
The Future of AI in the Colour Industries
Westland, Stephen</td><td colspan="2" rowspan="2">Oral 3
Color in Display and Imaging</td></tr>
<tr><td>11:00 - 12:00</td><td colspan="2">Oral 1
Color and AI</td></tr>
<tr><td>12:00 - 13:00</td><td colspan="2">Lunch</td><td>Lunch</td><td>ACA Meeting</td></tr>
<tr><td>13:00 - 14:30</td><td rowspan="5">Workshops
(14:00-17:00)
At the venue
Hall C/D</td><td colspan="2">Poster
Session 1</td><td colspan="2">Poster
Session 2</td></tr>
<tr><td>14:30 – 15:00</td><td colspan="4">Coffee Break</td></tr>
<tr><td>15:00 – 16:15</td><td>Oral 2A
Color Emotion, Harmony & Preference</td><td>Oral 2B
Spectral Analysis and Image Enhancement</td><td>Oral 4A
Color in Arts and Culture</td><td>Oral 4B
Color Education</td></tr>
<tr><td>16:15 – 17:30</td><td></td><td>SG 1
Arts and Design (AD)</td><td></td><td>SG 2
Environmental Color Design (ECD)</td></tr>
<tr><td></td><td>Welcome Reception
(17:00 - 19:30)</td><td colspan="2"></td><td colspan="2"></td></tr>
</table>

Day 3 and Day 4

<table>
<tr><th>Date</th><th colspan="2">22 Oct.
Day 3 (Wed)</th><th colspan="2">23 Oct.
Day 4 (Thu)</th><th>24 Oct.
Day 5 (Fri)</th></tr>
<tr><td>Time</td><td>Hall A</td><td>Hall B</td><td>Hall A</td><td>Hall B</td><td rowspan="2"></td></tr>
<tr><td>8:30-9:00</td><td colspan="2" rowspan="2"></td><td colspan="2">Registration</td></tr>
<tr><td>9:00 - 9:30</td><td colspan="2" rowspan="2">Invited Lectures
Investigating Sleep Enhancement via Intelligent Color-Varying Light
Chen, Chien-Yu
Color Characteristics of Virtual Images in MR/AR Systems, Yang, Tsung-Hsun</td><td rowspan="11">Taipei City Excursion</td></tr>
<tr><td>9:30 - 10:00</td><td colspan="2">Registration</td></tr>
<tr><td>10:00 - 10:30</td><td rowspan="2">Oral 5A
Color Application & Marketing</td><td rowspan="2">Oral 5B
Skin Color & Fashion</td><td colspan="2">Coffee Break</td></tr>
<tr><td>10:30 - 12:00</td><td>Oral 6A
Color Category & Memory</td><td>Oral 6B
Colorimetry & Applications</td></tr>
<tr><td>12:00 - 13:00</td><td colspan="4">Lunch</td></tr>
<tr><td>13:00 - 14:30</td><td colspan="2">Poster
Session 3</td><td colspan="2">Oral 7
Color, Lighting, Vision & Perception</td></tr>
<tr><td>14:30 – 15:00</td><td colspan="4">Coffee Break</td></tr>
<tr><td>15:00 – 16:15</td><td colspan="2">Judd / CADE / Sphere Award Ceremonies & Lectures
A Science of Classification: Personal Journey through Research on Color and Visual Appearance, within a Semiotic Framework
Caivano, José Luis
From Scientific Research to Practical Colour Application
Bergström, Berit</td><td>Oral 8A
Personal Color
(15:00-16:00)</td><td>Oral 8B
Color in Urban Environment
(15:00-16:00)</td></tr>
<tr><td>16:15 – 17:30</td><td></td><td>SG 3
Color Vision & Psychophysics
(CVP)</td><td colspan="2">Closing Ceremony
(16:00-16:30)</td></tr>
<tr><td></td><td colspan="4"></td></tr>
<tr><td></td><td colspan="2">AIC Gala Banquet
(18:00-21:00)</td><td colspan="2">VIP Visit
Art-Taipei
(19:00-21:00)</td></tr>
</table>

Invited Lectures (Hall A)

No.	Date	Time	Title / Speaker
1	20 Oct. (Mon)	10:00 10:30	**The Future of AI in the Colour Industries** Westland, Stephen *Professor, School of Design, University of Leeds (UK)*
2	21 Oct. (Tue)	9:00 9:30	**A Comprehensive Colour Solution across Industries** Luo, Ming Ronnier *Chair Professor, College of Optical Science and Engineering, Zhejiang University (China)*
3	21 Oct. (Tue)	9:30 10:00	**Algorithmic & Digital Color Expressions** Bendito, Petronio *Professor, Department of Art and Design, Purdue University (United States)*
4	22 Oct. (Wed)	15:30 16:00	**Plenary Lecture by the 2025 Recipient of the AIC Judd Award: A Science of Classification: Personal Journey through Research on Color and Visual Appearance, within a Semiotic Framework** Caivano, José Luis *Former AIC President (Argentina)*
5	22 Oct. (Wed)	16:00 16:30	**Plenary Lecture by the 2025 Recipient of the AIC CADE Award: From Scientific Research to Practical Colour Application** Bergström, Berit *Swedish Colour Centre Foundation/ Berit ColourTalks (Sweden)*
6	23 Oct. (Thu)	9:00 9:30	**Investigating Sleep Enhancement via Intelligent Color-Varying Light** Chen, Chien-Yu *Professor/Director, Graduate Institute of Color and Illumination Technology, National Taiwan University of Science and Technology (Taiwan)*
7	23 Oct. (Thu)	9:30 10:00	**Color Characteristics of Virtual Images in MR/AR System** Yang, Tsung-Hsun *Professor, Department of Optics and Photonics, National Central University (Taiwan)*
8	22 Oct. (Wed)	11:00 11:15	**Soviet Spacecraft Design: Architect Galina Balashova's Colours** Durão, Maria João **Cancelled due to health issues with a family member** *Profoessor, Faculdade de Arquitectura da Universidade de Lisboa (Portugal)*
9	22 Oct. (Wed)	10:00 10:15	**The Practice of Color Design: Where Engineering Challenges Meet Market** Yu, Meng-Han *Advanced CMF Designer at Garmin Cooperation (Taiwan)*

AIC Study Groups Events (Hall B)

No.	Date	Time	Study Group
SG1	20 Oct. (Mon)	16:15 17:30	**Arts and Design (AD)** Hosted by Maria João Durão
SG2	21 Oct. (Tue)	16:15 17:30	**Environmental Color Design (ECD)** Hosted by Verena M. Schindler and Juan Serra
SG3	22 Oct. (Wed)	16:15 17:30	**Color Vision & Psychophysics (CVP)** Hosted by Shoji Sunaga

Day 1

SG1: AIC Study Group on Arts and Design AIC2025 Meeting (AD)

Chair: Maria João Durão, School of Architecture,
The University of Lisbon, Portugal
Co-chair: David J.C. Briggs, National Art School, Sydney, Australia
sg-ad@aic-color.org

Date: Monday, 20 October 2025, 4:15pm - 5:30pm

The AIC Study Group on Arts and Design-SGAD meeting is chaired by Maria João Durão. The activities developed by the Study Group is the focal point of the discussion, bringing together theory and practice in the Arts and Design.

Disciplines and fields included in the scope of the Study Group on Arts and Design: painting; sculpture; drawing; illustration, and printing; photography, cinema, theatre, audiovisuals, and virtual reality; jewelry design, fashion design, textile design; communication design; product and industrial design; furniture design, automotive and aeronautic design, among other related expressions.

We welcome all the AIC2025 Congress participants to join us.

Day 1

SG2: AIC Study Group on Environmental Color Design (ECD)

The Study Group on Environmental Colour Design (SG ECD) will hold a meeting at the AIC 2025 Congress in Taipei on Tuesday, 21 October 2025, from 16:15 to 17:30. The SG ECD co-chairs are Verena M. Schindler (Switzerland) and Juan Serra (Spain). José Luis Caivano (Argentina), the former SG chair, will present the projects and publications of the study group, and lead the discussion.

Previous projects in 2025 consisted of a symposium, a special issue, and articles for a special collection on environmental colour design research. Recent publications feature the work of SG ECD members in the form of books, journals and articles.

The discussion will focus on the future of environmental colour design.

1. Colour in evidence-based design (EBD) and evidence-informed design (EID).

2. Colour in human-centred design (HCD).

3. Colour and sustainability: What does sustainability mean in environmental colour design today?

4. Biophilic colour design. The focus is on exploring emerging nature-based design for health and well-being in the built environment. Will handcrafted colour design remain relevant in the future?

5. AI-powered colour design. Integrating cutting-edge technologies, such as artificial intelligence (AI), is paramount. What relevant questions does it address? Which current AI tools are used in the design process? How do computational tools manage screen colours? What are the advantages of using AI? What are the disadvantages? Is AI replacing human creativity?

The SD ECD is an international, informal, multidisciplinary study group. Its members are professionals, ranging from architects and designers to scientists and other experts, who are interested in the role of colour in natural, built and sociocultural environments. Research in this field also encompasses the investigation of the impact of colour on human behaviour, cognition and emotion.

The aims of the SG ECD include: 1) Disseminating knowledge among its members. 2) Facilitating the exchange of experience gained in integrating colour into the planning, design and realisation of built and natural environments. 3) Propagating knowledge and evaluative experience through congresses, seminars, workshops, publications and exhibitions. 4) Stimulating research and teaching.

The SG ECD was established in 1982 and has been active for 43 years. It currently has around 350 members from 50 countries. The SG ECD welcomes anyone who is interested in colour. Join us!

The website is www.aicecd.org and the email address is ecd.studygroup@yahoo.com. Day2

SG3: AIC Study Group on Color Vision & Psychophysics (CVP)

The Colour Vision and Psychophysic is an AIC Study Group and was founded to discuss basic and practical studies on colour perception of the elderly, such as colour appearance, colour discrimination, brightness perception of colours, colour preference and application tools for planning and testing universal colour designs, and to share useful information among the members concerning colour perception of the elderly. At the SG meeting in AIC2012, however, we decided that we would change the SG's name to 'Colour Vision and Psychophysics' to expand our domain. In 2013, discuss a broader range of topics from colour vision models to universal colour design, while still including colour perception of the elderly.

This study group, previously called “Color Perception of the Elderly” (CPE), is active since 2001.

The study group on color vision and psychophysics will hold a brief meeting. The meeting agenda is as follows (note that there is no scientific program).

1. Announcement: The chair and secretary positions have been transferred from Prof. Okajima (Yokohama National University, Japan) and Prof. MeLgosa (Universidad de Granada, Spain) to Prof. Sunaga (Kyushu University, Japan) and Chanprapha Phuangsuwan (Rajamangala University of Technology Thanyaburi, Thailand), respectively, effective October 2023.
2. Announcement: The Asia Color Association Conference will be held in New Zealand in 2026 (9^{th}) and Japan in 2027 (10^{th}).
3. Request for the CVP group.

Day 3

Oral Sessions

Monday, 20 October 2025

Oral 1: Color and AI

No.	Presentation Time (Start)	Paper ID	Paper Title / Authors
1	11:00	218	**Comparison of AI Based Machine Learning Methods with Basic Polynomial Regression for Cross Media Color Reproduction** Zafar, Muhammad Hamza*; Green, Phil
2	11:15	153	**Dynamic Color Shift Compensation in OLED Displays Using Artificial Intelligence** Hsu, Ching Hsiang*; Ou-Yang, Mang
3	11:30	67	**Cityscape Color Analysis Using Deep Learning-Based Image Segmentation and Color Adjustment for Weather Conditions** Doi, Motonori*; Ono, Ryuto; Kuboki, Shun
4	11:45	55	**LCH-Based Deep Learning for Skin Cancer Diagnosis** Kuan, Zhu-Hao*; Lo, Mei-Chun; Hsu, Chih-Shun

Day 1

Monday, 20 October 2025

Oral 2A: Color Emotion, Harmony & Preference

No.	Time	Paper ID	Paper Title / Authors
1	15:00	184	**Enhancing Image Color Harmony Through Content-Aware Recoloring** Chou, Yu-Shan; Sun, Pei-Li*
2	15:15	141	**A Perceptually Neutral White Locus Integrating a Warm-Cool Scale** Chang, Jung-En; Ou, Li-Chen*
3	15:30	136	**Controlled Dissonance in Contemporary Design: Exploring Chromatic Tension for Emotional Impact and Perceived Quality in Enclosed Spaces** Jayaprakash Brindha, Sandhiya*; Surve, Pankaj Daulatrao
4	15:45	12	**An Investigation of the Emotional Perception of Scarf Colors on Different Skin Tones Based on the Color-Emotion Models and Color-Harmony Models** Liao, Chia-I*; Lee, Wen-Yuan
5	16:00	95	**Taste Impressions of Snack Packs and Impression Estimation in Machine Learning of Images** Sakurai, Masato

Day 1

Monday, 20 October 2025

Oral 2B: Spectral Analysis and Image Enhancement

No.	Time	Paper ID	Paper Title / Authors
1	15:00	173	**Testing Spectral-Based Characterisation Models for Wide-Colour-Gamut Display** He, Ruili*; Xiao, Kaida; Zhao, Xinyi; Pointer, Michael
2	15:15	186	**Statistical Analysis of Differences of Spectral Reflectance Values Determined by Color-Measuring Instruments** Ikonen, Erkki*; Rezazadeh, Yasaman; Nilsson, Anders; Seymour, John; Peltoniemi, Juha
3	15:30	27	**Enhanced Portrait Auto White Balance in Backlight Environments via Skin Reflectance** Zhou, Sicong*; Li, Changjun; Liang, Jinxing; Lai, Peihua; Sun, Wenjun; Li, Hesong; Luo, Hong; Xiao, Kaida
4	15:45	170	**A Comprehensive Investigation on the Taxonomic Classification of Recycled Dark Rubber Materials Using Multiple Spectroscopic Analytical Technique** Chen, Yung-Fou*; Chiang, Raymond Jui-Chang; Yueh Chun-Ting
5	16:00	32	**Spectrally-Aware Perceptual Image and Video Filtering Using Color Transfer** Raza, Aiman; Dubail, Marie; Dumortier, Dominique; Jost, Sophie*

Day 1

Tuesday, 21 October 2025

Oral 3: Color in Display and Imaging

No.	Time	Paper ID	Paper Title / Authors
1	10:30	155	**A Comparative Study: Assessing Image Quality for the Jacobi and Gauss-Seidel Retinex Algorithms** Karami, Afsaneh*; Finlayson, Graham
2	10:45	96	**Characterising Head-Mounted Displays Based on Visual Assessment** Lee, Chia-An*; Ou, Li-Chen
3	11:00	92	**Evaluating Preference for Images Enhanced with Simple Tone Curves** Bennett, James*; Finlayson, Graham
4	11:15	111	**Evaluating the Just Noticeable Difference Threshold of ΔEITP in SDR Displays for Color Experts and Non-Experts** Kuo, Mu-Tzu*; Bai, Chris Yi-Ho
5	11:30	133	**Colour Saliency Effects on Pre-attentive Processes** Sakata, Katsuaki*; Yamauchia, Yasuki
6	11:45	158	**Quantifying Inter-Reflection Effects on Colored Shadows** Mao, Ruiquan*; Tremeau, Alain; Katemake, Pichayada

Day 2

Tuesday, 21 October 2025

Oral 4A: Color in Arts and Culture

No.	Time	Paper ID	Paper Title / Authors
1	15:00	80	**The Colors of Roses Was Painted by Protan and Deutan** Ichihara, Yasuyo G.*; Sakamoto, Takashi; Sunaga, Shoji
2	15:15	39	**An Appraisal of "Colour-Music: The Art of Mobile Colour" (1912) by Rimington: A Design History View** Hidaka, Kyoko
3	15:30	47	**Decoding Colour Communication: A Cross-Cultural Study of Colour Associations in Germany and India** Schmidt, Lina*; Lindemeyer, Melissa
4	15:45	83	**Cross-cultural Study About the Effect of Color on the Perception of Grammatical Gender** Raevskiy, Alexander*; Kyoto, Itsuki; Rattanakasamsuk, Kitirochna; Tokunaga, Rumi
5	16:00	46	**An Investigation of Selected Chinese Paintings Colour Theories and How it Differs from the Practical Colour Application Used in Western Paintings** Ng, Woon Lam*; Goh, Huiying

Day 2

Tuesday, 21 October 2025

Oral 4B: Color Education

No.	Time	Paper ID	Paper Title / Authors
1	15:00	180	**Effects of Colour Vision Deficiency on Educational Experiences in Elementary Schools: A Systematic Review** Sánchez Izurieta, Juan Francisco*; Sunaga, Shoji
2	15:15	205	**Colour Selection Frameworks for Global Colour Education** Qian, Wenxian*; Wang, Chaoran
3	15:30	7	**Mapping of Colors of Master Images with Munsell Color Space – A Mathematical Tool to Assist Color Design** Ng, Woon Lam*; Wang, Zhongjian
4	15:45	106	**Color Education in Schools for Students with Color Vision Deficiency: Important Elements Identified Through In-Depth Interviews with Designers and Artists** Muraya, Tsukasa*; Taniguchi, Yunoka; Ichihara, Yasuyo; Sunaga, Shoji
5	16:00	193	**Biophilic Colour Schemes (BCS): A Catalogue of Biophilic Colour Schemes based on Emotional Colour Impact Principles and Natural Analogies from Landscape Prototypes for Evidence-based Sustainable Design** Schlegel, Markus*; Haensch, Konstantin; Goméz Mejia, Claudia

Day 2

Wednesday, 22 October 2025

Oral 5A: Color Application & Marketing

No.	Time	Paper ID	Paper Title / Authors
1	10:00	invited	**The Practice of Color Design: Where Engineering Challenges Meet Market Strategy** Yu, Meng-Han
2	10:15	75	**Estimation Method of Rice Fluorescence Emission Spectra from the Image Data and its Application** Tominaga, Shoji*; Nishi, Shogo; Ohtera, Ryo
3	10:30	99	**Preferable Lighting Conditions for Cooking Hamburger Steak** Kagimoto, Akari*; Kodama, Yuu; Okuda, Shino; Okajima, Katsunori
4	10:45	14	**Achievements and Issues Demonstrated by Citizen-lead Community Development — A Case Study of Citizen-Academia Collaboration** Makino, Akiyo*; Murakami, Kanako
5	11:00	Invited	**Soviet Spacecraft Design: Architect Galina Balashova's Colours** Durão, Maria João **Cancelled due to health issues with a family member**
6	11:15	225	**Measurement Comparison of Black Tea Color Testing between Tea Testers and Analytical Instruments** Irwan Fathoni**,** Adi Djoko Guritno, Anggoro Cahyo Sukartiko*, Megita Ryanjani Tanuputri
7	11:30	224	**Analysis of Fresh Organic Vegetable Quality at the Farmer and Distributor Levels based on Color and Texture Measurements** Dionisius Marlon Ayofi, Anggoro Cahyo Sukartiko, Megita Ryanjani Tanuputri*

Day 3

Wednesday, 22 October 2025

Oral 5B: Skin Color & Fashion

No.	Time	Paper ID	Paper Title / Authors
1	10:00	45	**Employment of Coloring on Clothing-style Drawings for Understanding Behavior and Personality** Muraki Asano, Chie*, Ikebe, Sonoka; Asano, Akira
2	10:15	201	**Facial Color Perception and Facial Impressions across Diverse Color Vision Types** Mizokami, Yoko*; Kurosawa, Shun; Sato, Hiromi
3	10:30	174	**Evaluating Fabric Colour Perception using LED Simulator** Li, Qinyuan*; Widasati, Arsaika; Zhang, Yichi; Luo, Ming Ronnier; Xiao, Kaida
4	10:45	13	**The Moral Perception of Scarf Colors on Different Skin Colors** Liao, Chia-I*; Lee, Wen-Yuan
5	11:00	161	**Regarding Racism in Color Theory** Charbonneau, Edward R.
6	11:15	33	**Human Perspectives on the Role of AI-enhanced Tools for Colour Trend Analysis** Angharad, Sally*; Westland, Stephen; Lai Peihua
7	11:30	143	**Colour Design: Developing Narratives from Use Generated Visual Texts** Dubey, Nijoo*; Damodaraswamy, Sudhakar

Day 3

Thursday, 23 October 2025

Oral 6A: Color Category & Memory

No.	Time	Paper ID	Paper Title / Authors
1	10:30	214	**Colour and Memory: Consistency of Memory Colours** Kvist, Stine Marie*; Green, Phil
2	10:45	217	**What Explanations for Color Naming and Categorization Explain?** Dedrick, Donald
3	11:00	215	**Colour and Memory: Colour as an Aid to Memorization** Sætersdal, Mathias*; Green, Phil
4	11:15	90	**A Comparative Study on Human and AI Interpretation of Traditional Chinese Red Color Names** Lin, Hsueh-Fen
5	11:30	57	**A Deep Learning-Based Footwear Prediction and Recommendation Model** Liu, Li-Yun; Luo, Yi-Ting; Li, Hung-Chung*

Day 4

Thursday, 23 October 2025

Oral 6B: Colorimetry & Color Application

No.	Time	Paper ID	Paper Title / Authors
1	10:30	156	**Individual Cone Spectral Sensitivities and Colour Matching Functions** Stockman, Andrew*; Luo, Ming Ronnier; Song, Siyuan; Shi, Keyu; Rider, Andrew
2	10:45	211	**Restoring Mobile APP-Filtered Photos Using CNN-Based Deep Learning** Lin, Ya-Hsuan; Chang, Yu-Chieh; Wang, Jie-Sen; Sun, Pei-Li*
3	11:00	160	**Perceived Color Differences for Color-deficient Observers** Hsiao, Hsiu-Ying; Chen, Yi-Yun; Chen, Hung-Shing*
4	11:15	164	**Color Simulation Strategy of Reflective E-papers** Chen, Hung-Shing*; Kao, Yu-Hsuan
5	11:30	200	**Effects of Ultra-Fast Light-Adaptive Lenses on Perception of Natural Scenes** Jost, Sohie*; Dessenne, Elisa; Avouac, Pascale; Scherlen, Anne-Catherine; Barrau, Coralie

Day 4

Thursday, 23 October 2025

Oral 7: Color,Lighting, Vision & Perception

No.	Time	Paper ID	Paper Title / Authors
1	13:00	66	**The Surface Optical Characteristics of Interior Components in the Japanese Traditional Tea Ceremony Room TENGO-AN** Osumi, Masayuki
2	13:15	77	**Beyond the Surface: Exploring Dichroic Filters in Folded Geometries** Jönsson, Elvira
3	13:30	120	**How to Characterize Augmented Reality Glasses for Color Reproduction – Taking the Birdbath Optical Structure as an Example** Chao, Ya-Chi*; Ou, Li-Chen
4	13:45	196	**Fitting SSVEP Hue Selectivity Profile with Individual Data of Color Perception** Kuriki, Ichiro*; Miyatsuka, Ryota; Umeda, Naoto; Fukushima, Sakura; Kiyokawa, Hiroaki
5	14:00	48	**From Pixels to Perception: Reverse-Engineering RGB Images to Simulate Moth Responses to Artificial Light** Raza, Aiman*; Lucca, Adrien
6	14:15	86	**Enhancing Classification Accuracy of Plant Rust Disease Symptom by Integrating Color Space Transformation and Deep Learning** Liu, Zheng-Hao*; Lo, Mei-Chun; Hsu, Chih-Shun

Day 4

Thursday, 23 October 2025

Oral 8A: Personal Color

No.	Time	Paper ID	Paper Title / Authors
1	15:00	41	**Testing Colour Harmony Model for Personal Colour Analysis** Sirisayan, Punnaphat*; Sueeprasan, Suchitra
2	15:15	91	**An Investigation on Memory Skin Colour and its Acceptable Boundaries** Lu, Yan*; Xiao, Kaida; Widasati, Arsaika
3	15:30	116	**A Comparative Study of Seasonal Color Associations in Nature and Personal Color Theory** Park, YungKyung
4	15:45	110	**Evaluating the Effectiveness and Utility of Fabric Draping-Based Personal Color Diagnosis** Park, Jisu*; Choi, Gyoungsil, Park, YungKyung

Day 4

Thursday, 23 October 2025

Oral 8B: Color in Urban Environment

No.	Time	Paper ID	Paper Title / Authors
1	15:00	171	**Based on Deep Learning: A Regional Analysis of the Facade Color Schemes of Public Housing in Hong Kong** Li, Yixuan*; Xiang, Changying
2	15:15	25	**Colour Conservation of the Dilworth Building, Auckland, New Zealand** Rennie, Julian*; Premier, Alessandro
3	15:30	194	**Thoughts on The Use of Close-Range Photogrammetry in Chromatic-Spatial Investigations: The Case of Gaudí's Expiatory Temple of The Sagrada Família** Toni, Leonardo*; Cesar, João Carlos de Oliveira
4	15:45	150	**Heritage in Color: Challenging the Neutrality of Globalized Urban Landscapes Via Chromatic Ambiances** Chehata, Zeïnab*; Hussein, Faten; Doherty, Gareth

Day 4

Monday, 20 October 2025

Poster Session 1

13:00~14:30

Paper ID	Paper Title / Authors
4	**Color and Emotions in the Public Space** Kmita, Anna
18	**Glazed Tiles - Between Art and Architecture. Andreas Stöcklein's Case Study** Pinheiro, Ana Paula*; Duarte, Rui
22	**Experience and Vocabulary in the Study of Color** de Lucas Tron, Alfonso
31	**Analysis of Scene Illumination Factors Affecting Perceptual Color Inferences in Images** Tanaka, Yuki*; Tanaka, Midori; Horiuchi, Takahiko
36	**Color Standards in City Planning and Changes in Store Facade Design: The Effects of Facade Design Change Methods on Harmony with the Street, Corporate Identity, and Visibility** Hanari, Takashi*; Harada, Masayuki; Terashima, Toshiharu; Ono, Tomoka
42	**From Intuition to Intentionality: Understanding Colour Decision-Making through Reflective Design Practice in Graphic Design Education** Lee, Gyeonghwa*; Yang, Jie; Chen, Yun
51	**Prediction of Watercolor Mixing $L^*a^*b^*$ Values Based on Kolmogorov – Arnold Networks** Sun, Xiang-En; Yuan, Chen-Yu; Lin, Tzung-Han*
54	**Extracting Regional Colors from History: A Case Study on Tsukuba, Kasama, Tsuchiura, and Mito in Japan** Xin, Meiqing*; Yamamoto, Sari
62	**Preference and Emotional Responses to Planterior Design According to the Index of Greenness** Kim, SaetByul*; Lee, YounJin
69	**Research on the Evaluation of Children's Color Education Effect Based on Cognitive Development Theory** Hung, Qian*; Li, Anni; Lan, Shang
72	**A Proposal for a Unified Design for Store Signs in Shopping Districts and its Effects** Kishimoto, Nagisa*; Doi, Shushi; Sakai, Hideki
78	**The Color of Sour and Salty Tastes** Ngamsaard, Thachapong*; Longbutsri, Jitlada; Tangkijviwat, Uravis
84	**Associative Colors Related to Grief from Pet Loss** Lim, YeJee*; Lee, YounJin
94	**The Influence of Art Material Experience on Basic Color Terms and Color Category Perception** Han, Hyejin
103	**Contrasting Perceptions of Dark Colours Among Designers and Non-Designers: An Empirical Analysis** Xiang, Qi*; Han, Xu; Ping, Chengliang; Yu, Luwen
113	**Color Measurement of Translucent Liquid Materials Using a Noncontact 2D Colorimetric System with Dome Illumination** Iyota, Hiroyuki*; Higuchi, Mei; Kinugawa, Ayumu; Masuda, Hayato; Sakai, Hideki
117	**Exploring Word–Colour Associations among Koreans and Foreign Residents in Korea** Lee, Junglim*; Park, YungKyung

Paper ID	Paper Title / Authors
125	**Reevaluating Brightness Perception: An Empirical Examination of Melanopsin's Influence** Mori, Nozomu*; Takikawa, Mizuki; Saito, Marina; Tsujimura, Sei-ichi
131	**From Fabric to Fingertips: Nail Polish as a Tool for Personal Colour Analysis** Sueeprasan, Suchitra*; Chaimongkol, Phithunisara
135	**A Study on Color Perception on Surfaces Composed of Two Colors — The Effect of Color Difference between Two Colors in a Checkerboard Pattern on the Perception of Color Unevenness of One of the Colors** Hara, Naoya*; Kono, Masami
146	**Physical Light Field Perception Using Color-Enhanced Photon Flow Visualization** Nakadate, Sho; Momiyama, Asuka; Takase, Kazuto; Schregle, Roland; Yosizawa, Nozomu
167	**Fashion Color Preferences and Cultural Capital: An Empirical Study Based on Bourdieu's Theory** Jiang, Jiani
179	**Color Appearance of Waterlilies** Phuangsuwan, Chanprapha*; Rattanakasamsuk, Kitirochna; Ikeda, Mitsuo; Kawasumi, Mikiko
185	**Examining the Degrees of Smoke Emissions Using the Calibrated Camera Technology** Cheng, Chun-Kung; Pong, Bao-Jen; Shih, Yu-Cheng; Ou, Yu-Zhi; Chen, Hung-Shing*
191	**Perceptual Associations Between Classical Music and Colour in Mozart's "Twinkle, Twinkle, Little Star" Variations** Lee, Yu-Ting*; Chang, Fei-Man
197	**Gender and Age-Related Differences in the Contributions of Color to the Recognition of Cultural Landscapes** Lavrenova, Olga A.; Griber, Yulia A.*
203	**The Effect of Wearing Personal Colors on Attractiveness Rating** Kondo, Aki*; Ogino, Mami; Nonaka, Yuto; Togasaki, Aoi; Watanabe, Katsumi
209	**The Influence of Food Appearance Color Tone on Eating Behavior and Appetite in a Virtual Reality Environment** Moriyama, Tsuyoshi*; Matsumoto, Aki
220	**Application of Non-Contact Color Measurement Techniques in Heritage Conservation: A Case Study of the Wufeng Lin Family's "Gongbaodi" Residence** Lin, Ying-Tsung*; Tsai, Cheng-Min

Day 1

Tuesday, 21 October 2025

Poster Session 2

13:00~14:30

Paper ID	Paper Title / Authors
5	**Optimization of Image Colorization for Crime Scene Based on Generative Adversarial Network** Liu, Tzu-Ming; Cheng, Ming-Chih; Yang, Po-Hsin; Li, Hung-Chung*
19	**The Effects of Typeface and Color Combinations on Perceived Trust, Professionalism, Aesthetics, and Usability in Traditional Chinese (Taiwan Standard) and English GUI Design** Lu, Fu-Shao*; Lee, Wen-Yuan
24	**Perceptual Calibration of MR Displays: Investigating Colour Accuracy and Memory Hue Representation through 2D and 3D Perception** Jiang, Jinbi*; Westland, Stephen; Hemingray, Caroline; Xiao, Kaida
34	**Develop the Chinese Hue-Tone Colour System by Utilising the Chinese Adjective Word System (ANCWS)** Song, Wenwen; Chen, Yifei*; Zhu, Shiyang
37	**The Upper Limit of Lightness to Which the Color Name "Black" Can Be Applied** Katayama, Ichiro*
43	**Evaluating Perceptual Color Matching Between Different Backlight Displays and Color-Managed Prints** Hong, Yu Kai*; Bai, Chris Yi-Ho
52	**Color Reproduction under Non-standard Lighting Conditions** Kirchner, Eric*; Njo, Lan; van der Lans, Ivo; Perales, Esther; Larrosa, Aurora
60	**Influencing Factors of Clothing Colour Preference: A Comparative Study of Beijing and Shanghai Cities** He, Shuang*; Cheung, Vien; Li, Liting
63	**Meanings of Spiritual Experiences in the Practice of Chromotherapy: A Perspective from Semiotics as an Alternative for Well-being in the Future** Monsalve Ospina, Hernán Felipe
70	**Color and Gender in Young Children's Free Drawings — Gender Judgments by Childcare College Students and General College Students** Shimada, Yukiko
73	**Towards a New Lighting Method in Museums Considering the Optimal Brightness of Paintings - Practical Classification Process Based on Oil Painting Characteristics** Aoyama, Miyu*; Yoshizawa, Nozomu; Oe, Yuki; Mizokami, Yoko; Takashima, Miho
79	**Differences in the Diversity of Color Names and Evaluation of Darkness and Lightness of Colors in Surface and Aperture Color Modes** Qiao, Yanan*; Kawabata, Yasuhiro
85	**Investigation of the Colour Design: Follow the User Data or Designer's Intuition to Build a Colour Scheme for the Beer Label** Nan, Chunxi; Wang, Mengmeng*; Li, Jinwen
97	**A Study of Lip Colour and Social Signalling of Z-generation** Li, Jinwen; Wang, Mengmeng*; Nan, Chunxi

Paper ID	Paper Title / Authors
107	**Effect of Appearance of Damascus Steel Knives on Visual Impression — Comparative Analyses of Observer Nationality** Nomoto, Rino*; Kawasumi, Mikiko; Tsukada, Toshihiko; Phuangsuwan, Chanprapha; Rattanakasamsuk, Kitirochna; Tangkijviwat, Uravis
114	**Observation of Color and Gloss Change during Drying of Particulate Suspension in Polymer Solution Using a Noncontact 2D Colorimetric System with Dome illumination** Higuchi, Mei*; Yamamoto, Shoki; Kinugawa, Ayumu; Iyota, Hiroyuki; Imakoma, Hironobu; Sakai, Hideki
119	**Effect of ipRGC Response on Contrast Sensitivity in Central Vision** Matsumoto, Haruka; Ishigane, Masatoshi; Takahashi*, Hiroshi; Suzuki, Masahiro; Uchikawa, Keiji
126	**Differential Perceptions of Colour and Material in Fashion: A Multisensory Analysis of Designer and Consumer Responses** Han, Xu*; Li, Liting; Xiang, Qi; Xiao, Kaida; Yu, Luwen
132	**Effects of Mixed Color Temperatures on Spatial Perception in Office Lighting Environments** Kato, Mika*; Kikuchi, Kokoro
139	**A Study of Fluorescent Effect on Ink Jet Paper by Spectral Analysis** Shyu, Ming-Ching James
147	**Improving RGB Camera-Based Spectral Reflectance Estimation through a Machine-Learning Approach** Nishi, Shogo
165	**Integrating Color and Lighting Design: An Empirical Study on Disliked Kitchen Cabinet Colors and Ambient Light Color Temperatures in Home Interiors** Tsai, Chia-Hua*; Tsai, Cheng-Min
168	**Electrochemical Polymerization of Conductive Polymer Thin Films to Obtain Metallic Luster with High Reflectance** Yamada, Katsumi*; Tsuneyasu, Shota; Koshiji, Fukuro
181	**The Impact of Dynamic Lighting Conditions on the Color Perception and Texture Impression of Fabric** He, Shuilan
188	**Elderly Users' Color Emotions and Preferences Toward the Appearance of Differently Designed Care Robots** Liao, Ching-Chih*; Gong, Shi-Min; Hsu, Ya-Han
192	**Colours for the Future: Achrome Photographs in Archaeology: Maraghiannis Publishing House in Candia** Denhez, Annie-Dominique
207	**The Effects of Positive and Negative Emotional States on Memory Colors** Yun, Minseon*; Lee, YounJin
210	**Color Embodiment in Semantics of Abstract Concepts: Correlating Semantic Similarities with Visual Color Proximity in Metaphorical Lexemes Derived from the Chinese Color Term huáng, 黃 'Yellow'** Wu, Yufeng
221	**A Suggestion on Local Colour Guidelines to Build Inner Mongolia's City Brand** Huang, Jinga; Kim, Yoosun; Kim, Yoomi

Day 2

Wednesday, 22 October 2025

Poster Session 3

13:00~14:30

Paper ID	Paper Title / Author
11	**The Power of Nature in Art: Exploring Biomorphic Abstraction with Colour and Design** Avoke, Diana
21	**Relationship between Stability of Color Preference and Personality Traits** Nakamura, Shinji
30	**The Effect of Chroma Contrast in Infographic Color Design on the Viewer's Reading Experience** Tsan, Chen-Pang*; Wang, Chun-Po
35	**Color Standards in City Planning and Store Facade Design Changes: Relationship between the Content of the Landscape Formation Standards and the Adopted Design Change Methods** Terashima, Toshiharu*; Harada, Makayuki; Hanari, Takashi
40	**Colorimetric Characterization of Transparent OLED Displays under Various Backlighting Conditions** Shen, Chun-Ting*; Wen, Chao-Hua; Pong, Bao-Jen
50	**Application of Kubelka-Munk Theory in Jadeite Colour Evaluation** Jiang, Jinbi; He, Qinxin*; Westland, Stephen
53	**Beyond Averages: Individual Differences in How Wall Colour Influence Affective Responses and Room Impressions** Widasati, Arsaika*; Westland, Stephen; Hemingray, Caroline; Lee, Soojin
61	**Linked Hybrid: Color, Light and Perception in the Architecture of Steven Holl** Pinheiro Consani, Camila*; de Oliveira Cesar, João Carlos
64	**Color Yoga: A Semiotic and Subjective Perspective on Wellbeing for the Future** Monsalve Ospina, Hernán Felipe; Henao Jiménez, Milton David*
71	**Analysis of the Color and Object Characteristics of Seasonal Natural Landscape Images in Japan** Yu, Hanui*; Akita, Takeshi; Hirate, Kotaroh; Fujii, Risa
76	**Study on 3D Digital Preservation of Orchids using Photogrammetry Method** Liu, Tzu-Hsuan; Yuan, Chen-Yu; Tsai, Chi-Pin; Chang, Shih-Chen; Lin, Tzung-Han*
81	**On the Narrative Function of Costume Color in Chinese Cinema** Li, Peitong*; Han Dan
89	**From Tang Sancai to Ink Painting: Cheng Shifa's Reinterpretation of Ceramic Glaze Aesthetics in Modern Chinese Art** Wang, Shanshan*; Wang, Keqiang; Xue, Yinghe
102	**The Influence of Similarity on Color Harmony and Preference** Rho, Hye Mi; Park, Yung Kyung*
109	**Color as Ingredients: A Material-Driven Design Approach to Natural Pigments in Sustainable Baked Goods** Wang, Tzu-Jung*; Hsieh, Tsuei-Ju
115	**Color System Conversion from RGB to L*a*b* Using Four-Layer Neural Network for a Novel Colorimeter Independent of Light Sources** Miyazawa, Kaito*; Ohkawa, Masashi

Paper ID	Paper Title / Author
121	**Survey on Empowerment Initiatives for Students with Color Deficiencies** Maruyama, Shion*; Muraya, Tsukasa; Sunaga, Shoji
127	**The Conflict between Perception and Language among Color Vision Minorities: A Comparative Study of Naming and Color Terminology in Japan and China** Meiyan, Lei*; Shoji, Sunaga; Tsukasa, Muraya
134	**Creation of Educational Materials Designed for a Game about Color Vision Diversity Education** Fujii, Toshiki*; Muraya, Tukasa; Sunaga, Shoji
142	**Colour Accuracy of Low-cost, Pocket-size Spectrophotometers** Nilsson, Anders*; Kirchner, Eric; Seymour, John
159	**Colour Heritage of Chinese Painting Through Dynastic and Stylistic Change** Li, Wenan*; Chen, Ming-Xuan; Wang, Xingkai; Yip, David; Yu, Luwen
162	**An Investigation about the Influence of Color Contrast on Binocular Fusion** Liu, Chia-Chun*, Sun, Vincent C.; Fu, Ming-Chuan
166	**From Cobalt to Iron: The Semiotic Shift in Joseon Porcelain** Lhi, Wona*; Park YungKyung
169	**A Study on Prompting the In-Depth Exploration of Environmental Color Imagery Using Generative AI** Wei, Yuh-Chang*; Kuo, Monica; Kuo, Ya-Ping
183	**Film Color Grading Model Based on Computer Vision: Construction of Personalized Color libraries** Chen, Ming-Xuan*; Luo, Shijunyan
189	**From Glaze Color to Perception: A Study on the Color Variation of Opaque Glaze and Perceptual Evaluations** Su, Hsuan-Hsuan*; Lin, Yan-Jun; Shin, Fu-Chi; Hsieh, Tsuei-Ju
195	**The Use of Color on the Expiatory Temple of The Sagrada Família by Antoni Gaudi: Nature, Life and Symbolism** Toni, Leonardo*; Cesar, João Carlos de Oliveira
208	**Exploring the Emotional Impact of Color Design in Children's Picture Book Covers** Wang, Yixuan*; Geng, Wenfei
213	**A Cost-effective Method for Measuring and Simulating the Color Appearance of Transparent Plastic Samples** Hsu, Yung-Chen; Sun, Pei-Li*
222	**A Corpus-Linguistic Study of Context-Dependent Color Naming in Japanese** Mita, Hiromasa

Day 3

INVITED LECTURES

.

The Future of AI in the Colour Industries

Stephen Westland

ABSTRACT

Since the introduction of the term artificial intelligence in 1956, the last 70 years have seen increasing sophistication and speed for machine-learning algorithms. This presentation will review the main advances that have been made by describing several applications of AI in the colour-using industries. The talk will discuss the possibility of software achieving artificial general intelligence and what impact this might have on computational practice in colour, colorimetry and colour imaging. The reasons for the current interest in AI will be discussed and some possible outcomes for the next 5-10 years will be presented.

BIOGRAPHY

Stephen Westland is Professor of Colour Science and Technology at the University of Leeds (UK), a position he has held since 2003. During his academic career, Westland has published over 275 refereed books, book chapters, journal papers and conference papers in areas of colour measurement, colour vision and colour design. He holds visiting professorships at University of East Anglia (UK), University of Texas (USA) and Huazhong University of Science and Technology (China).

He has made a notable contribution to the use of computational methods in various areas of colour application. He was first author of Computational Methods in Colour Science (Wiley) that was first published in 2004 with a second edition published in 2012. He was one of the first people to use artificial neural networks in colour science during the first AT era when he showed that multi-layer per- ceptrons could be used to map between colorant recipe data and spectral or colorimetric data. He has since continued to use machine learning to predict colour from recipe data for textile fibre blends using neural networks and to automatically extract key colours from images. He also applied computational methods for colorimetry in dentistry where he developed an optimised whiteness index for dentistry that has been widely used worldwide in clinical trials to develop whitening products. Recently he explored the relationship between whiteness and yellowness in dentistry and developed a yellowness index for use in dentistry.

Westland has also made a sustained contribution to colour education, particularly through his long involvement with the Society of Dyers and Colourists (SDC) since 1983 where he served for many years on the colour measurement committee and, more recently, chairs the Society's Examinations, Qualifications and Examinations Board. He also held the honour of being President of the Society of Dyers and Colourists in 2019/2020. At the universities of Derby and Leeds, he has supervised 66 PhD students (40 as first supervisor). He founded a new journal with the SDC entitled Colour: Design and Creativity which later became the Journal of the International Colour Association (JAIC) of which he continues to be chief academic editor. He is a member of the Colour Literacy Project (supported by ISCC and AIC)

and publishes on issues of colour education. He is co-author of the textbook 100 Princi- ples of Color in Art and Design which addresses many contemporary issues in colour theory.

A Comprehensive Colour System Across Industries

Ming Ronnier Luo

ABSTRACT

This paper describes a comprehensive colour system designed for colour difference evaluation, colour appearance prediction, and colour specification. The sUCS/sCAM model forms the core of the system, which comprises four parts: 1) lightness/chroma/hue angle, 2) a binary hue composition, 3) a depth scale, and 4) colour name categories. The system integrates the best features of existing colour specification systems such as CIELAB, Munsell, and NCS. ICONS (Innovative Colour Naming System), is also derived from this framework. It is designed to be intuitively interconnected among engineers, designers, and ordinary computer users.

BIOGRAPHY

Ming Ronnier Luo is a Qiushi Distinguished Professor at the College of Optical Science and Engineering, Zhejiang University (China). He received his PhD from the Bradford University (UK) on colour science in 1986. He has published over 800 peer reviewed papers in the fields of colour science, imaging science and illumination engineering. He is a Fellow of Society of Dyers and Colouists (SDC) and of Imaging Science and Technology (IS&T). He has been an active member of International Commission on Illumination (CIE), ex-Vice President, ex-Division Director on Colour and Vision, Technical chairs, etc. He has received various research medals from different learn societies including 2003 Davis Medal from the Royal Photographic Society, 2009 Gold Medal from SDC, the Judd 2017 Award from the International Colour Association (AIC), and the Newton 2020 Award from the Colour Group of the Great Britain for his contribution in colour science research.

A Comprehensive Colour System Across Industries

Ming Ronnier Luo

State Key Laboratory of Extreme Photonics and Instrumentation, Zhejiang University, *Hangzhou, Chin*a
M.R.Luo@zju.edu.cn

Abstract

This paper describes a comprehensive colour system designed for colour difference evaluation, colour appearance prediction, and colour specification. The sUCS/sCAM model [1] forms the core of the system, which comprises four parts: 1) lightness/chroma/hue angle, 2) a binary hue composition, 3) a depth scale, and 4) colour name categories. The system integrates the best features of existing colour specification systems such as CIELAB, Munsell, and NCS. ICONS (Innovative Colour Naming System), is also derived from this framework. It is designed to be intuitively interconnected among engineers, designers, and ordinary computer users.

Keywords: Innovative Color Naming System (ICONS), Uniform colour space, colour appearance model, depth scale, colour name categories

Introduction

Numerous colour models serve diverse applications. Imaging engineers typically use device-independent (DI) systems like CIE XYZ [2], CIELAB [2], CIEDE2000 [3], CMC, and CIECAM16/CAM16-UCS [4], and device-dependent (DD) systems (e.g., RGB, HSL, YUV, YCbCr [5]). DI systems, rooted in color science, enable accurate cross-media colour reproduction, while DD systems are primarily used for colour manipulation for a particular display and software such as Microsoft Word and PowerPoint. Colour management technology [5] bridge these two categories. Surface engineers mainly used the colour models in DI category. Conversely, designers often adopt systems using physical samples, such as NCS [6], Munsell [6], and commercial specifiers including Coloro, Pantone, and Achroma. The latter systems are also fundamental in colour education for art and design students.

An ideal colour system would achieve two main goals: first, to provide a universal framework for colour difference evaluation, appearance prediction, and specification, fulfilling the objectives of colorimetry; second, to serve the needs of surface and imaging engineers, designers, and computer users across virtually all applications.

With these goals in mind, a comprehensive colour system has been developed. This system includes four integral parts: a uniform colour space, a colour appearance model, two-dimensional colour appearance scales, and a colour naming system. Each part and its performance are described below. A software has been written to demonstrate the system.

PART I. UNIFORM COLOUR SPACE: sUCS

The current CIE standard uniform colour spaces (UCS) are CIE 1976 L*a*b* and CIEL*u*v* [2]. The CIE is recommending CAM16-UCS based on the CIECAM16 colour appearance model [4]. Although CAM16-UCS performs most accurate in predicting data [7], It suffers from structural complexity, making it difficult to use for computationally intensive tasks like mobile image processing. In 2024, sUCS [1] was successfully derived with the following features:

- **Simple Structure:** It requires approximately five computational steps, significantly reducing overhead.
- **Familiar Attributes:** It includes basic perceptual attributes like lightness (I), chroma (C), hue angle (h), hue composition (H), and opponent channels (a, b), mirroring the widely adopted CIELAB system.
- **Optimal Uniformity:** Its performance matches that of CAM16-UCS when tested against three major colour difference datasets (Large and Small Surface, and Small Display Color Differences), which include 11,273 sample pairs collected over 35 years [7].
- **Hue Linearity:** In gamut mapping and image compression, sUCS matches IPT [8] in hue preservation, particularly in blue regions, and substantially outperforms CIELAB and CAM16-UCS.

Overall, sUCS is a user-friendly colour space that combines operational simplicity with enhanced visual uniformity. It forms the basis of our universal colour model, and its I, C, h, and H values are used in our Innovative Color Naming System (ICONS) (see Part V).

PART II. COLOUR APPEARANCE MODEL: sCAM

Colour appearance models (CAMs) predict how colours are perceived under various viewing conditions, including changes in correlated colour temperature (CCT), luminance levels, background colours, and surround environments. They are indispensable for achieving cross-media colour consistency in imaging, photography, surface colour matching, lighting design, and cultural heritage preservation.

A CAM takes XYZ colorimetric data and viewing conditions as input and processes them through three key stages: 1) chromatic and luminance adaptation transformations to account for lighting variations, 2) computation of chromatic responses to isolate brightness and colour signals, and 3) formulation of perceptual scales like lightness, brightness, chroma, colourfulness, hue angle, and hue composition. The CIE has standardized CAM development through iterative refinements from CIECAM97s [9] to CIECAM02 [10] and finally CIECAM16 [4]. Each iteration improves predictive accuracy, simplifies inverse calculations, and enhances computational efficiency. Validation relies on the LUTCHI dataset [11], a benchmark containing ~5,000 stimuli evaluated by 6 to 10 observers for lightness, brightness, colourfulness, and hue under diverse conditions. While CIECAMs are accurate, their complexity hinders real-time applications like image signal processing. The sCAM [1] addresses this with a minimalist architecture focused on three core perceptual scales: lightness appearance (I_a), brightness (Q), and colourfulness (M).

The sCAM's brightness scale (Q) achieves superior predictive accuracy, while its lightness and colourfulness metrics match or exceed CIECAM16's benchmarks. Each scale can be computed with a single line of code, ensuring unparalleled efficiency for real-time workflows. This streamlined design makes sCAM a transformative tool for industries requiring rapid, perceptually accurate colour adjustments.

PART III. TWO-DIMENSIONAL SCALE: WHITENESS AND DEPTH

The two-dimensional scales of Vividness (V) and Depth (D) have been identified as universal perceptual attributes [12]. These intuitive descriptors transcend cultural and industrial boundaries. Vividness with terms like bright, vibrant, bold, fresh, clean, dirty, and dull, reflecting a colour's intensity. Depth relates to concentrated, saturated, strong, pale, and pastel, encapsulating richness modulated by lightness and saturation. Crucially, these 2D scales resolve a problem in traditional 1D models, which cannot encode the holistic, interdependent way humans perceive colour.

Our recent results [13] confirm this superiority. Participants scaled 2D attributes (Vividness and Depth) 50% more consistently than 1D ones (Brightness, Colourfulness), underscoring their alignment with perceptual reality.

This framework aligns with the Natural Colour System (NCS) [14], which uses Whiteness (W) and Blackness (K) to model human perception on pigment interactions. Adding white increases brightness but reduces chroma (increasing Whiteness), while adding black diminishes both brightness and chroma (increasing Blackness). We identify inverse relationships between these NCS scales and perceptual attributes: W vs. D, and K vs. V [13]. This duality bridges practical design processes (e.g., pigment mixing) with perceptual theory. Finally, depth and vividness scales based on sCAM were derived to fit the NCS whiteness (W) and blackness (K) data, i.e., D=1-W and V=1-K, respectively. The depth scale is employed in our ICONS (see Part V).

Furthermore, a colour system named the Sino Color Book (SCB) [15], was included in the data analysis. It is presented as a colour solid containing approximately 18,200 polyester samples, as shown in Figure 1. It was invented by Yunpeng Xu and published in 1999 by the Taiwan Textile Institute. In this study, data was obtained by measuring a subset of 2,948 samples. It has the unique feature of including Depth, Chroma, and Hue (DCH) attributes. Its Depth data were used to test different depth scales. The sUCS Depth scale performed the best.:

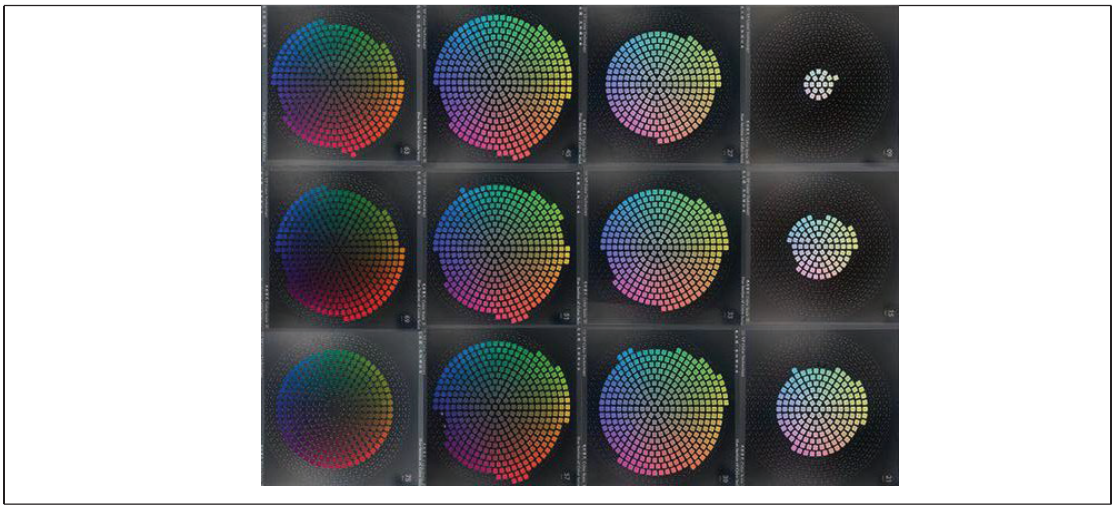

Figure 1: SCB Atlas, showing 12 constant depth samples in the Chroma and Hue plane.

PART IV: COLOUR NAMING CATEGORIES

Our group conducted two experiments to study colour naming. Experiment 1 [16] gathered 50 British and 40 Chinese subjects to assign colour names to 200 ISCC-NBS colour samples using an unconstrained method. The results were analyzed to identify three categories of names: basic names, modifiers, and secondary names. The results showed some cultural and gender differences. However, the results from the basic names agreed well between the two subject groups and the 11 basic colour names identified by Berlin and Kay [17]. Experiment 2 [18] was then conducted by 20 British and 20 Chinese subjects, who assigned basic names to approximately 1500 NCS samples to map them in the NCS colour space; the centroid and spread of the volume occupied by each colour name were determined from the analysis of observer data. An overall good agreement was found between the two subject groups. Finally, a model was constructed based on the basic names to define the boundaries of these colour names [19]. The model is used here to provide colour name categories with an enhancement: grey is divided into light grey and dark grey, and turquoise is introduced. In total, 13 basic categories are used in ICONS (see Part V).

PART V: INNOVATIVE COLOUR NAMING SYSTEM (ICONS)

Another contribution of this study is the Innovative Colour Naming System (ICONS). It is divided into two parts. The first part includes LCh values to precisely specify a colour, facilitating communication among engineers. The second part is planned for designers and ordinary users, incorporating a binary hue, a whiteness-depth scale, and a colour category.

An example is provided here. The ICONS name `080018020Y95RMiddleDepthPink` represents a middle-depth pink colour with a hue composition of 95% red and 5% yellow, and its corresponding lightness, chroma, and hue angle are 80, 18, and 20°, respectively. The first 9 digits represent sUCS Lightness (I), Chroma (C), and Hue angle

(h) [080018020], with 3 digits each, followed by the hue composition (H) [Y95R], the depth (D) expressed by a descriptor [Middle Depth], and finally, a colour name category [Pink]. Note Depth is reported in five intensity levels: Very pale, pale, middle depth, deep and very deep. For an engineer, this translates to a colour with LCh values of 80, 18, and 20°. For a designer, it corresponds to an NCS-like hue composition of 95% red and 5% yellow with a depth descriptor (the inverse of NCS whiteness). For an ordinary user, they should understand the term of a middle- depth pink colour.

This section describes the spacing of the colour system. Software was written to display the system by combining individual dimensions. Figure 2a shows a Color Picker function for coarse colour selection via sUCS hue angle (h) circle and Lightness-Chroma (IC) plane (top left and bottom right), and for fine selection using the ab or Ch plane on the right. The corresponding ICON is shown at the top: `059030013R3BDeepPink`. Figure 2b shows the colour distribution of a set of samples from a dye house (~4500 historical samples) plotted in sUCS ab plane at constant lightness (I), controlled by the grey scale bar on the right. Figure 2c presents the same samples plotted in sUCS's Lightness-Chroma (IC) plane at a constant hue angle (h), controlled by the rainbow hue scale bar on the right. Figures 2b and 2c exhibit the same geographical structure as Munsell spacing [13]. Figure 2d presents the same samples plotted in sUCS Depth-Chroma (DC) plane at a constant hue angle (h). The Depth scale is divided into 5 steps: Very Pale, Pale, Mid Depth, Deep, and Very Deep. Data points at the bottom of Fig. 2c appear darker than those at the top. The apex corresponds to the white colour of the substrate.

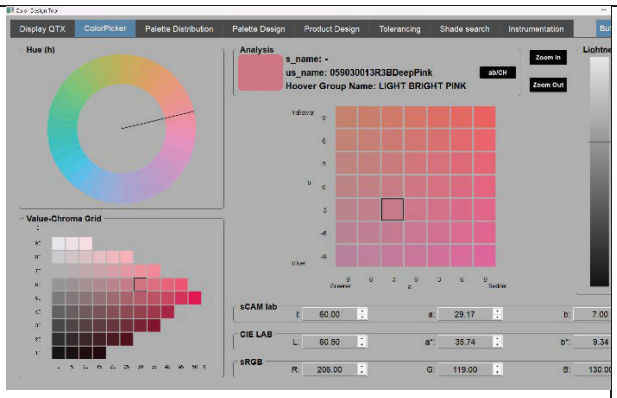

Fig. 2a. Color Picker

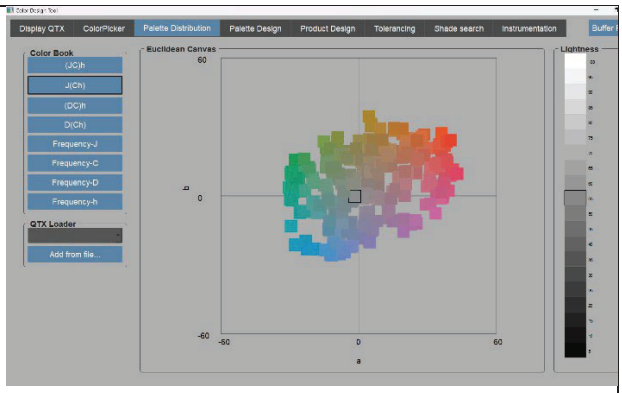

Fig. 2b. Colour distribution of a set of samples from a dye house plotted in sUCS ab or Ch plane with a constant lightness (I).

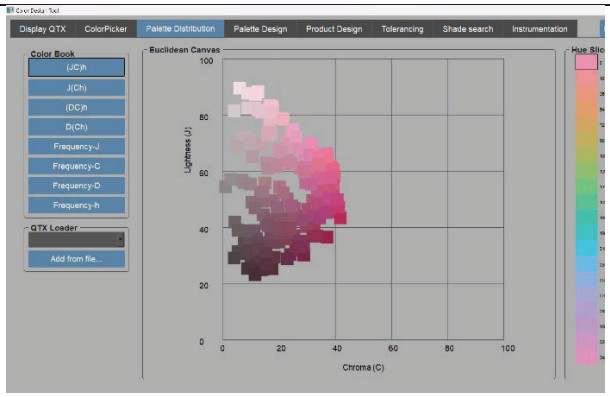

Fig. 2c. Colour distribution of the same sample set plotted in sUCS Lightness-Chroma (IC) plane with a constant hue angle (h).

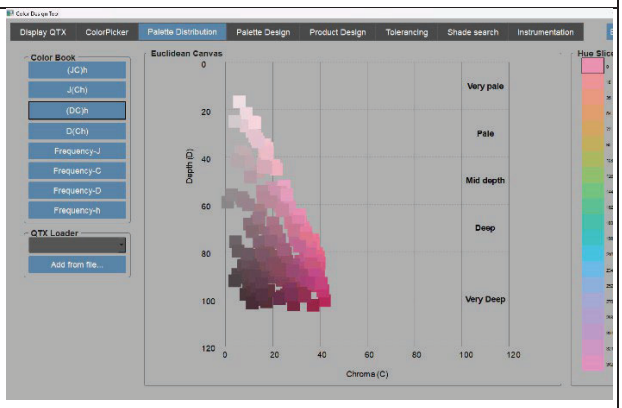

Fig. 2d. Colour distribution of the same sample set plotted in sUCS Depth-Chroma (DC) plane with a constant hue angle (h). The five depth intensity levels are also marked.

Figure 2: The proposed model including the sUCS/sCAM attributes: I, a, b, C, h, D

CONCLUSIONS

This paper describes a complete colour system for accurate colour communication, which includes a colour naming system, ICONS. The entire system is based on the state-of-the-art sUCS uniform colour space and encompasses three parts: lightness/chroma/hue angle, a binary hue composition, a depth scale; and colour name categories. ICONS is designed to be intuitively interconnected among engineers, designers, and ordinary computer users.

REFERENCES

[1]. Li, M., & Luo, M. R. (2024). Simple Colour Appearance Model (sCAM) Based on Simple Uniform Colour Space (sUCS). *Optics Express*, 32(3), 3100-3122.

[2] CIE 015:2018. *Colorimetry, 4th Edition*. Vienna: CIE Central Bureau.

[3] Luo, M. R., Cui, G., & Rigg, B. (2001). The development of the CIE 2000 colour difference formula. *Color Research & Application*, 26(5), 340-350.

[4] Li, C., Li, Z., Wang, Z., ... [et al.]... (2017). Comprehensive color solutions: CAM16, CAT16, and CAM16-UCS. *Color Research & Application*, 42(6), 703-718.

[5] Green, P. (2024). *Fundamentals and Applications of Colour Engineering*. Wiley.

[6]. Hunt, R. W. G., & Pointer, M. R. (2011). *Measuring Colour, 4th Edition*. Wiley.

[7]. Luo, M. R., Xu, Q., ... [et al.]... (2022). A comprehensive test of colour-difference formulae and uniform colour spaces using available visual datasets. *Color Research & Application*, 48(3), 267–282.

[8]. Ebner, F., & Fairchild, M. D. (1998). Development and testing of a color space (IPT) with improved hue uniformity. In Color and Imaging Conference (Vol. 1998, No. 1, pp. 8-13). Society for Imaging Science and Technology.

[9]. Luo, M. R., & Hunt, R. W. G. (1998). The structures of the CIE 1997 colour appearance model (CIECAM97s). *Color Research & Application*, 23(3), 138-146.

[10]. Luo, M. R., Cui, G., & Li, C. (2006). Uniform colour spaces based on CIECAM02 colour appearance model. *Color Research & Application*, 31(4), 320-330.

[11]. Luo, M. R., Clarke, A. A., Rhodes, P. A., ... [et al.]... (1991). Quantifying colour appearance: Part I – LUTCHI colour appearance data. *Color Research & Application*, 16(3), 166-180.

[12]. Berns, R. S. (2014). Extending CIELAB: Vividness, Vab*, depth, Dab*, and clarity, Tab*. *Color Research & Application*, 39(4), 322-330.

[13]. Li, M., & Luo, M. R. (2025). Development of vividness, blackness, depth, and whiteness scales under a high range of luminance levels. *Color Research & Application*, 50(3), 221-239.

[14]. Hård, A., Sivik, L., & Tonnquist, G. (1996). NCS, natural color system—From concept to research and applications. Part I. *Color Research & Application*, 21(3), 180–205.

[15]. Yang, H., Xie, W., Yang, Z., ... [et al.]... (2019). Investigation on color depth formulas. *Color Research & Application*, 44(1), 25-34.

[16]. Lin, H., Luo, M. R., Tarrant, A., & MacDonald, L. W. (2001a). A cross-culture colour-naming study. Part I: Using an unconstrained method. *Color Research & Application*, 26(1), 40-60.

[17]. Berlin, B., & Kay, P. (1969). *Basic Color Terms: Their Universality and Evolution*. University of California Press.

[18]. Lin, H., Luo, M. R., Tarrant, A., & MacDonald, L. W. (2001b). A cross-culture colour-naming study. Part II: Using a constrained method. *Color Research & Application*, 26(3), 193-208.

[19]. Lin, H., Luo, M. R., Tarrant, A., & MacDonald, L. W. (2001c). A cross-culture colour-naming study. Part III: A colour- naming model. *Color Research & Application*, 26(4), 270-277

Algorithmic & Digital Color Expressions

Petronio Bendito

NOTE: *This presentation was scheduled as a keynote address at the "AIC 2024 Midterm Meeting: Color Design, Communication, and Marketing" (aic2024.org/home/program). It was canceled due to unforeseen circumstances.*

EXPANDED ABSTRACT

Computer technology has inspired new approaches to artistic expression and design communication. With the advent of digital technology, colorists have expanded their toolsets, and new methods of creation have emerged. While media arts are defined by artistic expressions that integrate technology into the creative process (National Core Arts Standards, USA), their implications are broad, fostering multidisciplinary thinking that is fundamental to 21st-century art, design, and science education.

In this presentation, I will present two case studies and discuss concepts, methodologies, and applications of the media arts framework in two of my color series: "Color Code" and "Natural Disaster Colors," which span over a decade of practice. The "Color Code" series (https://www.colorcodeart.net) was introduced at the 14th Congress of the International Color Association (AIC), organized by the *Gruppo del Colore – Associazione Italiana Colore*. It was one of three selected papers for submission to the *ACM Journal on Computing and Cultural Heritage* (JOCCH) from the 280 presentations at the conference. The paper was accepted and published with significant additional content in 2023. Central to the paper is a color design methodology that explores the RGB color model as a cognitive tool to generate "objective" color palettes based on six algorithmic methods devised by the author, categorized into two groups: Primitive and Derivative methods. It also investigates concepts of digital color aesthetics, historical and natural associations, and "subjective" color taste.

The second case study will discuss the methodology of the "Natural Disaster Color" series (https://www.naturaldisastercolor.net). The series celebrated its 10th anniversary in 2024, and a retrospective was presented at the *Usina Cultural Energisa* in João Pessoa, Brazil. The works in the "Natural Disaster Color" series incorporate digital color sampling and algorithmic color methods, representing concepts of global citizenship, global humanitarian initiatives, resilience, and a wide range of kinds of natural disasters worldwide. The exhibition was part of Usina Cultural Energisa's annual schedule, where artists are invited to submit exhibition proposals. However, my invited exhibition, titled *Cores Digitais, Formas & Resiliência* [Digital Colors, Forms & Resilience], presented in 2024, was granted to me as one of three invited artists in the "Hors Concours" category. The color palette in this series dialogues with digital images of natural disasters disseminated through social media platforms, personal photography, Creative Commons, and the public domain. The project explores digital printmaking, A.I. integration, and projection mapping. The *Natural Disaster Color* series has been supported by grants from the Instituto Energisa (Brazil), the Indiana Arts Commission, and Purdue Liberal Arts (both USA).

This presentation will introduce the art series as two case studies, exploring the relationship between color, art, technology, science, society, and the environment.

BIOGRAPHY

Petronio Bendito, Ed.D., is a media artist, designer, and professor in the Patti and Rusty Rueff School of Design, Art, and Performance at Purdue University. As a faculty member in the Department of Art and Design, he teaches in the Visual Communication Design program, focusing on digital media design and digital color. His curriculum covers topics such as digital color methods, visual storytelling, web and mobile user interfaces (UI), as well as augmented reality (AR) and virtual reality (VR) design applications.

Bendito's creative and scholarly work investigates digital color literacy and the intersection of art, science, and technology. He is the author of the upcoming *RGB/CMY Digital Color Wheel* program for Davis Publishing Inc., aimed at teaching digital color literacy (Spring 2025). Additionally, he has contributed to *The Bloomsbury Encyclopedia of Design* (UK) and serves on the editorial board for the *Journal of Visual Literacy*, published by the Taylor & Francis Group. Through his artistic and design practice, Bendito examines digital color aesthetics and methods in media arts education, collaborating extensively with professionals from diverse fields including music, dance, theater, light design, mathematics, neuroscience, and computer science. He also co-curates the *Intersection of Art and Science* exhibits in the Department of Computer Science at Purdue University and co-edits the accompanying catalog.

A former member of the International Visual Literacy Association's Board of Directors, Bendito has also served as a contributing editor for *Media-N* and is a founding member of the New Media Caucus. He continues to contribute as a reviewer and board member for the *Journal of Visual Literacy*. His work has been cited in interdisciplinary publications such as *Image and Imagery* (Peter Lang International Academic Publishers), *Les Entreprises Critiques* (Cité du Design, Paris), and *Consortium* (COMAP, Inc.). Additionally, a monograph by the Art Museum of Greater Lafayette, Indiana, titled *Petronio Bendito: Digital Color, Algorithm, and Expression* (2014), includes essays by art historians Catherine Dossin and Elizabeth Mix, highlighting his contributions to digital color and algorithmic expression.

Among his many accolades, Bendito has received the International Visual Literacy Association Creative Achievement Award (2007), the Best of Show/Digital Printmaking Award (2013), and the Indiana Arts Commission Grant (2013). Other honors include the Bank One Purchase Award (2004), the VPA/Purdue Excellence in Teaching Award (2005), the Puffin Foundation Artist Grant Award (2003), and the WIRED magazine's Contest Winner award (2002). His paper, "Algorithmic Color Methods of Media Arts" (2023), published in the *ACM Journal on Computing and Cultural Heritage*, was recognized by the Publication Committee of the International Colour Association (AIC) 14th Congress in Milan as a significant contribution to color studies.

Investigating Sleep Enhancement via Intelligent Color-Varying Light

Chien-Yu Chen

ABSTRACT

Intelligent lighting systems that dynamically adjust color play a crucial role in regulating human circadian rhythms. This presentation explores how variations in color temperature can induce steady-state visual evoked potentials (SSVEP) via the visual pathway to stimulate delta wave production in the brain. Our findings provide neurophysiological evidence that such lighting interventions promote faster sleep onset and enhance deep sleep duration. These results suggest promising applications of smart lighting technology for improving sleep quality and overall well-being.

BIOGRAPHY

Chien-Yu Chen is a Professor and Head of the Graduate Institute of Color and Illumination Technology at National Taiwan University of Science and Technology (NTUST). He also serves as the Director of the Color, Imaging & Illumination Center. He earned his Ph.D. in Optics and Photonics from National Central University. His research includes 3D holographic display, 3D floating projection, medical lighting based on human factors, visual optics for wearable devices, and the design and processing of ultra-precision optical components.

Prof. Chen has actively contributed to international professional organizations. Since 2022, he has served as the Honored Chairperson of the 3D Interaction & Display Association (3DIDA). He has also been a Committee Member of the Society for Information Display (SID) – Applied Vision and has been the Convener of Division 6 of the International Commission on Illumination–Taiwan (CIE-Taiwan) since 2014. With more than 95 SCI journal papers, 160 international conference papers, and over 30 patents, research combines optical system innovation with AI-driven computational holography and 3D floating display optics, advancing next-generation display systems. He is particularly focused on human-centered health lighting technologies and continues to foster collaboration between academia and industry to explore innovative applications and expand future possibilities.

Color Characteristics of Virtual Images in MR/AR System

Tsung-Hsun Yang

ABSTRACT

We delve into the distinctive color gamut characteristics resulting from the color dispersion of surface relief grating (SRG) and wavelength degeneracy of volume holographic optical element (VHOE) in a diffractive light guide. While a laser-like spectrum achieves an impressive 194% sRGB color gamut for both cases, it proves unsuitable for VHOE light guides due to limitations in breaking the field of view (FOV) of the display. Conversely, a broadband light source, such as LEDs, offers continuous FOV but reduces the common color gamut to 50% sRGB. We then present a newly designed VHOE light guide capable of achieving the common color gamut of 130% sRGB using two multiplexed holograms of each color, closely matching the 133% sRGB achieved by an SRG light guide. This work presents the first theoretical methodology to elucidate the color performance of diffractive light guides utilizing VHOEs with holographic multiplexing, affirming their suitability for crafting high-quality near-eye displays.

BIOGRAPHY

Tsung-Hsun Yang is a Professor and Vice Dean of the School of Science at National Central University, Taiwan. He received his Ph.D. degree in Electro-optical Engineering from National Chiao Tung University in 1998. Since 2002, he has been a faculty member of the Department of Optics and Photonics at National Central University. Now, his research interests are color management for LED lighting and display, precision colorimetry, micro-optics, optical MEMS for biosensors, and nonlinear chaotic dynamics. His expertise is focused on the phenomenon of human color vision and its related applications. Based on the existing color science, he further explores research topics including color measurement, color mixing analysis and optimization, color management, LED color control, LED drivers, and color-related specifications and standards. Currently, the main application platforms include lighting, displays, and mixed reality, providing color-related optimization solutions.

Soviet Spacecraft Design: Architect Galina Balashova's Colours

Maria João Durão

ABSTRACT

This talk deals with the use of colour in very particular settings: the interior spaces of the manned spacecraft for Soviet Space Programme No. 1 OKB-1, under the responsibility of Architect Galina Balashova (b. 1931). For more than twenty years, Balashova designed the interiors for all major Soviet spacecraft and space stations, that included the living and working environments for cosmonauts from 1963 to 1986 - until the end of the USSR.

The growing prospects of long-term space flights to the Moon and Mars, require that future space habitats become increasingly more conducive to the well-being of its users. Although in these enclosed and highly technological habitats, variation of colour palettes is constrained by processes of space certifications and stringent flight safety requirements, colour has proven to be fundamental for the improvement of human psychological and physiological effects.

The author considers it timely to revisit Galina Balashova’s unique and pioneer contributions, and sets out to do so in this paper. Hence, the interiors of the orbital modules of the Soyuz spacecrafts, the interiors of Salyut 6, Salyut 7, and the Mir space stations were studied adopting a methodology based on the analysis of Galina Balashova’s views on colour and their application, her sketches, full drawings, dimension plans, full - size model produced for the first habitation module she created, colour materials, colour schemes for interiors, as well as their components such as sleeping capsules, furniture, control panels, and seats, her testimonies and interviews. Galina Balashova’s work is very broad. It ranges from architectural design in general, pieces of furniture, stationery, logos on spaceships, on to medals. The field of concern within the scope of this paper is narrowed down to spatial aspects of habitability.

Results were drawn from the following spatial requirements: 1. Design for zero-gravity conditions; 2. Contrast, differentiation of space activities and functions; 3. Areas, edges, corners, hardware, coding items and level of colour brightness /saturation; 4. Visual environment of spacecrafts 5. Localization, spaciousness, spatial orientation, safety, contrast and recognition of flying objects; 6. Psycho-physiological reaction to stress in confined environment; 7. Arrangement of spaces and scaling interiors; 8. Harmony, dimensions, spatial proportions, distribution of spaces, bodies and material functions, ergonomics in weightlessness; 9. Organisation of visual information and communication in weightlessness; 10. Emotional and aesthetic states in confined habitats.

BIOGRAPHY

Maria João is a Fine Arts graduate (FBAL-UL), holds a PhD Degree with a thesis on Colour and Space and a Doctoral Degree awarded by Lisbon Technical University, with a PRODEP grant. She holds an FCT funded Postdoctoral fellowship from The University of Salford, Manchester and Technion University Haifa in Art, Science and Technology–Drawings of Santiago Calatrava.

Professor at the Lisbon School of Architecture, University of Lisbon since 2001, she founded and directed pioneer Master Degree 'Colour in Architecture' for architects and designers; Founder and Head of the LabCor–Colour Laboratory since 2004; she supervises national and international projects and master, doctoral, post-doctoral research on the culture of drawing, colour and light. She directs 'Colour and Light Research Group–CIAUD/ Faculty of Architecture' since 2016.

Maria João was founder-president of the Portuguese Colour Association (AIC member since 2005) and presently its Honorary President. She is Scientific Council member of first Doctoral Course in Design in Portugal since 2006; lecturer at Doctoral Course in Architecture, as well as Master Degree Programmes in Design, Lighting Design (FA) and Masters for Built Environment Evaluation for Sustainability (U. Salford). In 1994 the Portuguese Ministry of Education approved her curriculum proposal for undergraduate Diploma Degrees in Design and in Art that are still running. She is International Association of Colour Consultants-North America (IACC-NA) honorary member.

Executive Committee member of the International Colour Association (AIC) from 2013 to 2017, Maria João is presently its Vice-President (President in 2026). For the AIC she coordinated the 'International Colour Day' from 2009 to 2024 and is presently the Chair of AIC 'Study Group on Arts and Design'.

She is senior member of American Institute of Aeronautics and Astronautics (AIAA); Member of AIAA Space Architecture Subcommittee of Design Engineering Technical Committee (2004-2007). Co-founder of AIAA Space Architecture Technical Committee-SATC (2008). Presently, she is member of AIAA Space Architecture Technical Committee-SATC, and Chair of the Exhibitions Subcommittee. She wrote for 'Aerospace America' and co-founded Space Architecture–'Team 11' formed in Houston, Texas, in 2003.

Maria João is author, speaker, editor, scientific and editorial committee member, juror, in the fields of art, design, terrestrial architecture and aerospace architecture. Her activities extend to the practice of painting, whose work belongs to national and international public and private collections from England, Japan, Portugal and South Korea.

The Practice of Color Design: Where Engineering Challenges Meet Market Strategy

Meng-Han Yu

ABSTRACT

This presentation aims to demystify the everyday practice of CMF (Color, Material, Finish) Design by providing an in-depth look into the skills and interdisciplinary knowledge required for this profession. Through a series of practical examples, it will explore how CMF Design functions as a bridge between creativity and technical execution within the product development process. The talk will further examine the role of CMF designers in addressing cross-functional challenges across Marketing, Regional Sales, and Engineering, highlighting the strategies employed to balance aesthetic intent, market relevance, and manufacturability. By illustrating how CMF Design contributes to both brand identity and consumer perception, the session will conclude by redefining the mission and value of CMF designers in today's dynamic and competitive design landscape.

BIOGRAPHY

Meng-Han Yu is an Advanced CMF Designer at Garmin Corporation, where she has worked since 2019. Specializing in Color, Material, and Finish (CMF) design and strategy, trend forecasting, and design-to-manufacturing processes, her work focuses on translating design trends into practical and manufacturable solutions while balancing cost, material constraints, and brand identity.

She holds an MA in Industrial Design from Central Saint Martins, University of the Arts London (UAL). Proficient in both English and Japanese, she has gained extensive international experience through working and living in the United States, the United Kingdom, and Japan. Her multicultural perspective enables her to integrate diverse aesthetic sensibilities and emerging design technologies from Europe, Japan, and the U.S. into her creative practice.

Over her six-year CMF career, Meng-Han has received several international design recognitions, including the Red Dot Design Award (2023) for Instinct Crossover and the IDEA Bronze Award (2024) for Descent G1 Ocean. She also contributes to design education as an industry mentor for student thesis projects at Ming Chi University of Technology.

Oral Papers

Comparison of AI Based Machine Learning Methods with Basic Polynomial Regression for Cross Media Color Reproduction

Muhammad Hamza Zafar*, Phil Green

Colourlab, Department of Computer Science, Norwegian University of Science and Technology (NTNU), Gjøvik, Norway

**Corresponding author: Muhammad Hamza Zafar, muhamhz@stud.ntnu.no*

ABSTRACT

Accurate cross-media color reproduction is critical for maintaining visual consistency across devices such as cameras, displays, and printers, which rely on different color generation mechanisms. This work investigates the effectiveness of various machine learning models in predicting XYZ color values from CMY inputs compared to traditional polynomial regression methods. Standardized datasets (FOGRA51 and APTEC PC10/PC11) comprising 1,617 color patches each were used. Models were trained to predict tristimulus values in the XYZ space from cyan–magenta–yellow (CMY) inputs; predicted XYZ values were converted to CIE L*a*b* for evaluation with the CIEDE2000 color-difference metric. To ensure fair comparison, all data were normalized to [0,1], a 90/10 train–test split was used, and mean, median, and maximum color-difference statistics were reported. The results demonstrate that while these advanced models offer some improvements in color prediction accuracy, the gains are relatively modest when compared to polynomial regression. The study reveals that the benefits of machine learning in this context must be carefully balanced against their complexity and implementation challenges.

Keywords: *cross-media color reproduction; AI; machine learning; polynomial regression.*

INTRODUCTION

Accurate color reproduction across different devices and media is a longstanding challenge in color science. Converting printer input values (typically in a CMYK or CMY colorant space) into device independent color coordinates (such as CIE XYZ or L*a*b* values) requires an effective characterization model. Traditionally, relatively simple empirical models like polynomial regression have been used for printer characterization, owing to their ease of implementation and adequate accuracy in practice [1]. Early research in the field demonstrated that a third-order polynomial transform could achieve reasonable color mapping accuracy for limited datasets of printed color patches. At the same time, neural network approaches were explored as a potential improvement [10]. For example, Tominaga [16] employed one of the first neural networks for printer color prediction, and later Cheung et al. [3] compared neural networks against polynomial transforms for camera characterization. These studies found that neural networks could model the color mapping with slightly better accuracy, but the gains were modest, especially given the small size of datasets (often <1000 samples) available at the time.

In recent years, machine learning has advanced significantly, with new algorithms that might better capture the nonlinear relationships between device inputs and color outputs. Moreover, more data has been accumulated for printer characterization, potentially providing the statistical power needed to exploit more complex models. This work aims to systematically compare a wide range of modern machine learning algorithms against polynomial regression. By including methods such as ensemble tree models, support vector machines, Gaussian processes, and deep neural networks, we investigate whether these AI-based approaches can outperform polynomial regression in predicting XYZ coordinates from given CMY values. We focus on three datasets representing offset and digital printing. The objective is to determine if the increased model complexity yields a

tangible improvement in color accuracy, and whether such improvements justify the additional computational and implementation effort.

METHODOLOGY

Experiments were conducted on three printer calibration datasets: FOGRA51 (an offset print dataset) [6] and two inkjet printer datasets APTEC (PC10) and APTEC (PC11) [12]. Each dataset consists of printed color patches with known CMY input values (cyan, magenta, yellow percentages) and measured output color coordinates in the CIE XYZ space. All three datasets were uniform in size, each comprising 1617 sets of data (further filtered by K = 0). This uniformity in dataset size ensured a consistent basis for comparison across different machine learning models and the polynomial regression approach, allowing for a more accurate evaluation of color mapping capabilities in various printing contexts. Prior to modeling, all data were preprocessed by normalizing input and output values to [0,1] ranges, and the data were split into training and testing subsets (typically a 90%–10% split) for performance evaluation. The color prediction error for a given sample was computed as the CIEDE2000 color difference (ΔE_{00}) between the predicted and actual color, after converting predicted and measured XYZ values to CIELAB. This ΔE_{00} metric is the standard for color error assessment [14].

A total of 13 machine learning models were implemented and compared with polynomial regression. These include:

- Linear/Regression Models: Ridge Regression [9], Lasso Regression [15] and Elastic Net [17]:linear models with regularization to prevent overfitting; Principal Component Regression (PCR) [11] and Partial Least Squares Regression (PLSR) [8]: regression models that reduce input dimensionality by extracting latent components.
- Instance-Based and Kernel Model: k-Nearest Neighbors (k-NN) regression [5], which predicts color by interpolating the nearest neighbors in the training data; and Support Vector Machine (SVM) regression [4] using RBF kernels for nonlinear mapping.
- Tree-Based Ensemble Models: Decision Tree regression, a single regression tree with limited depth [2], Random Forest, an ensemble of trees [2], and Gradient Boosting regression, boosted ensemble of trees [7]. These can capture nonlinear interactions and often handle data variability well.
- Bayesian Learning: A Gaussian Process Regressor, a Bayesian non-parametric model [13] is included (referred to as "Bayesian" model in results) which provides probabilistic predictions and can model complex functions given enough data.
- Neural Networks: Two configurations of multilayer perceptron neural networks were used. A "Simple Neural Network" refers to a shallow network (single hidden layer), and a "Deep Learning" model refers to a deeper neural network with multiple hidden layers.

In addition to these AI models, polynomial regression was implemented as a baseline. Polynomial models of degree 1 through 10 were fitted, expanding the CMY inputs into polynomial feature terms up to the given degree. For example, a third-degree polynomial model includes not only linear terms (C, M, Y) but also quadratic and cubic terms:

$$\phi\,(C, M, Y) = [\ 1, C, M, Y, C^2, M^2, Y^2, CM, CY, MY, C^3, M^3, Y^3, C^2M, C^2Y, M^2C, M^2Y, Y^2C, Y^2M, CMY\ ]^T$$

then

$$X=\alpha^T \phi(C, M, Y) \qquad Y=\beta^T \phi(C, M, Y) \qquad Z=\gamma^T \phi(C, M, Y),$$

where the "*T*" means transpose, $\phi(C, M, Y)$ is a column vector of all the polynomial terms (length 20 if cubic), $\alpha, \beta, \gamma \in R^{20}$ are the coefficients to learn. These polynomial models have been the traditional choice for device characterization and provide a benchmark for judging the effectiveness of newer methods.

All models were trained on each dataset's training split and then used to predict XYZ values for the test split. The predictions were converted to CIELAB and compared to the measured LAB values to calculate ΔE_{00} errors for each sample. From these, summary error statistics – mean ΔE_{00}, median ΔE_{00}, and maximum ΔE_{00} – were computed for each model on each dataset. These metrics together provide insight into both typical performance (mean, median)

and worst-case errors (max). Model hyperparameters were either chosen based on default values or simple tuning (for instance, the number of neighbors in k-NN, the depth of trees, regularization strengths, etc.), with an emphasis on using reasonable settings rather than exhaustive optimization. This approach simulates a practical scenario where a practitioner tries standard configurations of various algorithms to see which works best for a given problem.

RESULTS AND DISCUSSION

The APTEC(PC10) dataset was used as a primary case study to compare all models' performance. Table 1 summarizes the mean, maximum, and 95th-percentile (P95) ΔE_{00} errors achieved by each model on the PC10 test set. Lower values indicate better color prediction accuracy. Notably, several machine learning models (e.g., Gradient Boosting, k-NN, Bayesian) achieved slightly lower mean errors than the best polynomial regression model, but the differences are small. The third-order polynomial regression achieved a mean ΔE_{00} of 1.336 with a median of 1.159, which is only marginally higher in mean error than the very best model (Gradient Boosting, mean ΔE_{00} = 1.266). Median errors for top models were around 1.000 (e.g., Bayesian 0.980, Gradient Boosting 1.008, Random Forest 0.995), indicating that half of the color patches were predicted with very low ΔE_{00} error (on the order of 0.9–1.1, near the threshold of perceptible difference). The maximum errors show more variation: most models kept the worst-case error below ΔE_{00} = 5, but some had higher outliers (SVM 6.10; k-NN 5.50; MLP 5.22), and Elastic Net/Lasso were clear outliers with Max = 8.69. Polynomial regression's maximum error was 4.96, suggesting that while its overall performance is good, it performed less well on one or two extreme colors. Gradient Boosting's maximum error was about 4.71 ΔE_{00} with a P95 of 3.345, while the 3rd-order polynomial's P95 was a competitive 3.152. Overall, the consistency of Gradient Boosting and the low overall errors of the Bayesian and k-NN models made them top performers on this dataset, albeit by a slim margin.

Table 1: Summary of Mean, Median, and 95th Percentile (P95) ΔE_{00} errors for each model on the APTEC(PC10) dataset

Algorithm	Mean	Median	95th Percentile
Bayesian (Gaussian Process)	1.272	0.980	3.220
Decision Tree	1.540	1.375	3.611
Deep Learning	1.712	1.513	3.600
Elastic Net	3.892	3.735	7.284
Gradient Boosting	1.266	1.008	3.345
k-NN	1.266	1.048	3.401
Lasso Regression	3.892	3.735	7.284
PCR	1.891	1.681	3.886
PLSR	1.888	1.677	3.873
Random Forest	1.328	0.995	3.573
Ridge Regression	1.890	1.675	3.879
SVM (RBF Kernel)	1.442	0.954	4.016
MLP (Shallow Network)	1.497	1.321	3.244
Polynomial Regression (3rd)	1.336	1.159	3.152

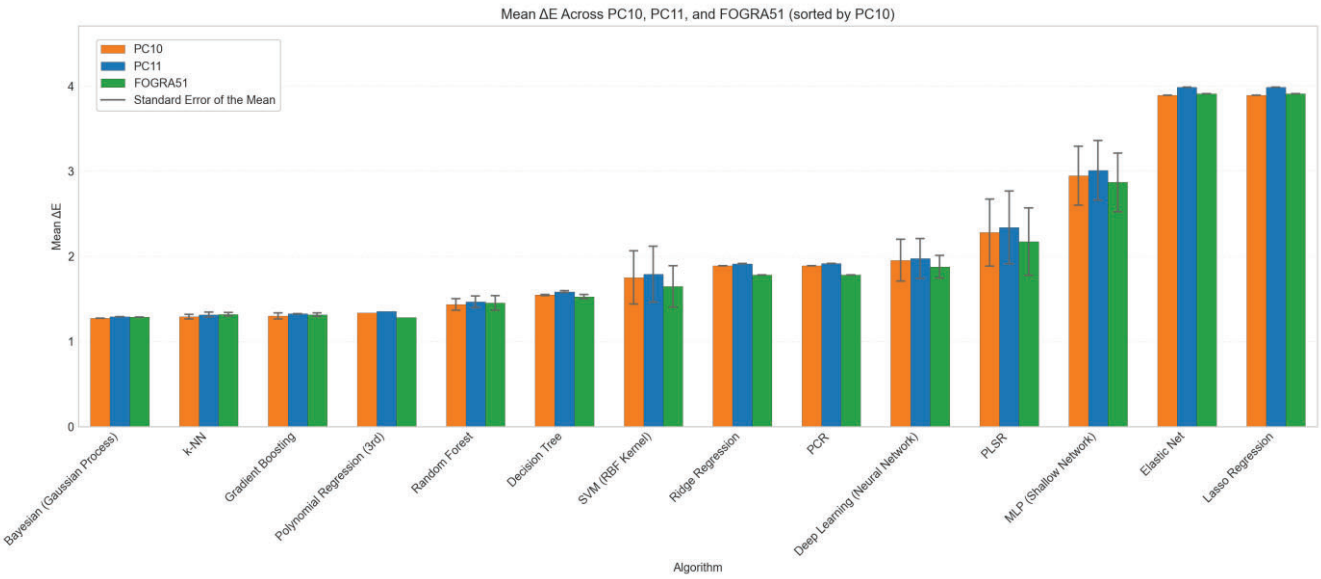

Figure 1: Comparison of Mean ΔE_{00} of all Machine Learning Models Across PC11, PC10, and FOGRA51 Datasets

A similar pattern was observed on the APTEC PC11 and FOGRA51 datasets (Figure 1). Overall error levels on those datasets were on par with PC10, with mean ΔE_{00} errors for the best models in the ~1.2–1.4 range. There were some differences in ranking; for example, on FOGRA51 (a standard offset print profile dataset), Gradient Boosting and Bayesian were among the top performers, with k-NN close behind, while Random Forest was competitive but generally a bit higher in mean error. No single model dominated across all three datasets. The polynomial regression (degree 3) continued to serve as a very strong baseline; in fact, on FOGRA51 its mean error (≈1.284) effectively tied with the best ML model (≈1.285–1.297). This indicates that the advantage of advanced machine learning methods in this application is not consistent; it can vary with the data characteristics of each dataset. Figure 1 includes error bars representing the Standard Error of the Mean (SEM). SEM quantifies the uncertainty in the estimated mean (SEM = SD/√n) across runs/configurations. Smaller SEM indicates more stable performance; overlapping SEM bars imply that apparent differences in mean ΔE_{00} may not be practically or statistically meaningful.

Quantitatively, the mean ΔE_{00} differences between the best machine learning model and the polynomial model were often on the order of ~0.05–0.07 or less (Figure 2). Such a difference is not perceptible in practice and can even be within the margin of experimental error for color measurements. Median errors for the high-performing models were very similar and frequently around ~1.0–1.2 ΔE_{00}, indicating that at least half of the colors in each test set were predicted with very high accuracy regardless of model used. Differences appeared more clearly in the maximum errors, where model choice matters for outliers: several ML models (e.g., Gradient Boosting or Random Forest) often kept worst-case errors lower than models like SVM or the sparsity-regularized linear baselines (Elastic/Lasso), whereas polynomial regression occasionally had a few larger-error outliers. This suggests that while average performance is comparable, using an advanced model can reduce the risk of a very poor prediction for an unusual color sample.

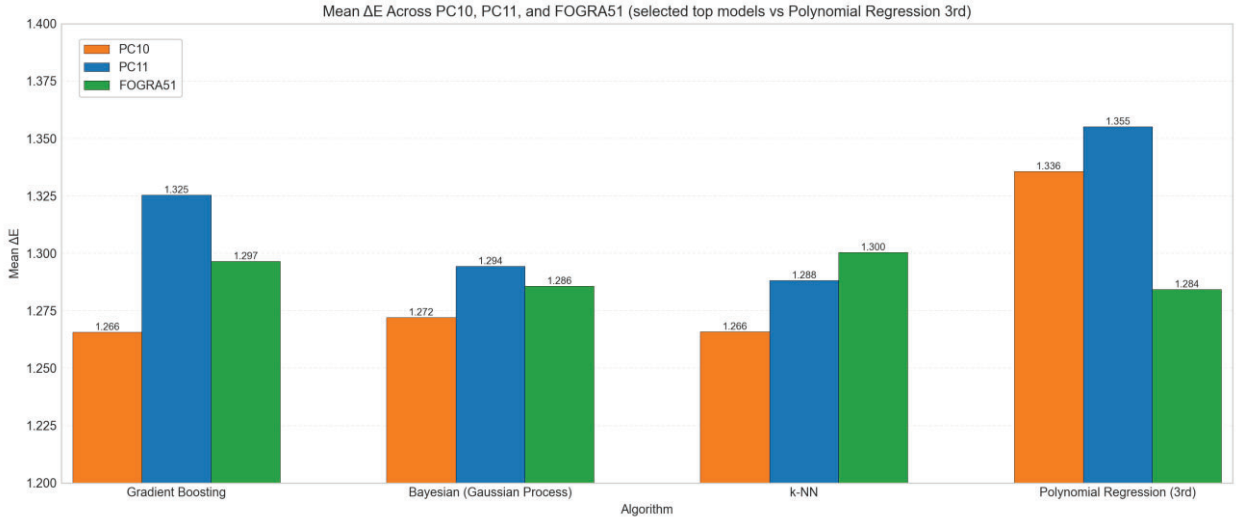

Figure 2: Mean ΔE_{00} of Selected Top Models (Gradient Boosting, Bayesian GP, k-NN) vs. Third-Order Polynomial Regression Across APTEC PC10, APTEC PC11, and FOGRA51 Datasets

CONCLUSION

A comprehensive comparison between a suite of AI-based machine learning models and traditional polynomial regression for predicting XYZ color coordinates from CMY inputs. Using three substantial datasets (FOGRA51, APTEC PC10, PC11) from printer characterization, we evaluated 13 different learning algorithms alongside polynomial fits of degree 1–10. The findings reveal that the differences in prediction accuracy are generally small. These results reinforce the idea that polynomial regression remains a competitive and pragmatic choice for 3-colorant printer calibration, given its simplicity and the negligible loss in accuracy. None of the advanced models consistently outperformed the others across all datasets, suggesting that there is no one-size-fits-all superior model for color prediction in this domain. Future work will investigate whether expanding to four-colorant systems (CMYK) or incorporating much larger training sets can bring benefit. Additionally, examining hybrid approaches (combining polynomial bases with machine learning, or applying feature engineering informed by color science) could provide new insights into improving color characterization models. Ultimately, the goal is to achieve accurate, efficient, and robust color predictions for complex printing systems, ensuring consistent color reproduction in an increasingly digital and data-driven print workflow.

CODE AND DATA AVAILABILITY

Code and data are available through the following link https://github.com/hamzafer/Evaluating-Machine-Learning-Methods.

REFERENCES

[1] Bala, R. (2003). Device characterization. In G. Sharma (Ed.), Digital Color Imaging Handbook (pp. 289– 384). Boca Raton, FL: CRC Press.

[2] Breiman, L., Friedman, J. H., Olshen, R. A., & Stone, C. J. (1984). Classification and Regression Trees. Monterey, CA: Wadsworth. Breiman, L. (2001). Random forests. Machine Learning, 45(1), 5–32.

[3] Cheung, V., Westland, S., Connah, D., & Ripamonti, C. (2004). A comparative study of the characterization of colour cameras by means of neural networks and polynomial transforms. Coloration Technology, 120(1), 19–25.

[4] Cortes, C., & Vapnik, V. (1995). Support-vector networks. Machine Learning, 20(3), 273–297.

[5] Cover, T. M., & Hart, P. E. (1967). Nearest neighbor pattern classification. IEEE Transactions on Information Theory, 13(1), 21–27.

[6] Fogra. (2020). FOGRA51 and FOGRA52 Characterization Data (Version 1.0) [Data set]. Fogra Research Institute. Retrieved from https://fogra.org/en/downloads/work-tools/characterisation-data

[7] Friedman, J. H. (2001). Greedy function approximation: A gradient boosting machine. Annals of Statistics, 29(5), 1189–1232.

[8] Geladi, P., & Kowalski, B. R. (1986). Partial least-squares regression: A tutorial. Analytica Chimica Acta, 185, 1–17.

[9] Hoerl, A. E., & Kennard, R. W. (1970). Ridge regression: Biased estimation for nonorthogonal problems. Technometrics, 12(1), 55–67.

[10] Kang, H. R., & Anderson, P. G. (1992). Neural network applications to the color scanner and printer calibrations. Journal of Electronic Imaging, 1(2), 125–135.

[11] Massy, W. F. (1965). Principal components regression in exploratory statistical research. Journal of the American Statistical Association, 60(309), 234–256.

[12] Pang, B. (2024, September 2). How to adopt printing standardization. ISO/TC 130 Case Study. Retrieved from https://committee.iso.org/sites/tc130/home/resources/case-studies/

[13] Rasmussen, C. E., & Williams, C. K. I. (2006). Gaussian Processes for Machine Learning. Cambridge, MA: MIT Press.

[14] Sharma, G., Wu, W., & Dalal, E. N. (2005). The CIEDE2000 color-difference formula: Implementation notes, supplementary test data, and mathematical observations. Color Research & Application, 30(1), 21– 30.

[15] Tibshirani, R. (1996). Regression shrinkage and selection via the lasso. Journal of the Royal Statistical Society: Series B (Methodological), 58(1), 267–288.

[16] Tominaga, S. (1993). A neural network approach to color reproduction in color printers. In Proceedings of the IS&T/SID Color Imaging Conference (Vol. 1993, No. 1, pp. 173–177). Springfield, VA: Society for Imaging Science and Technology.

[17] Zou, H., & Hastie, T. (2005). Regularization and variable selection via the elastic net. Journal of the Royal Statistical Society: Series B (Statistical Methodology), 67(2), 301–320.

Dynamic Color Shift Compensation in OLED Displays Using Artificial Intelligence

Ching-Hsiang Hsu, and Mang Ou-Yang*

Institute of Electrical and Control Engineering, National Chiao Tung University, Hsinchu, Taiwan

*dirac.ee06@nycu.edu.tw

ABSTRACT

Organic light-emitting diode (OLED) displays have become increasingly prevalent due to their unique advantages, such as high contrast ratio, wide color gamut, vivid color reproduction, fast response time, and mechanical flexibility [1]. Despite these merits, a major obstacle to stable image quality in mass production is temperature-induced brightness and color shift. Since it is impractical to perform per-panel calibration during mass production, efficient and generalizable compensation strategies are required to reduce adjustment time on the production line. This paper presents a systematic comparison between 3D lookup tables (3D-LUT), representing the conventional model-based compensation approach, and a neural network (NN), representing a modern AI-based strategy. Both methods are trained and validated on extensive measurement datasets covering multiple brightness and temperature conditions. The performance of each compensation model is quantitatively evaluated using a single key indicator: the CIEDE2000 color difference formula (ΔE_{00}). A compensation result is deemed successful if the color difference between the corrected output and the target color is $\Delta E_{00} \leq 2$, which typically represents a just-noticeable-difference (JND) to the human eye.". Experimental results demonstrate the trade-offs between the interpretability and stability of the 3D-LUT method and the adaptability and prediction power of the NN method. The findings provide clear insights into the feasibility of adopting AI-based solutions for OLED mass production, highlighting their potential to achieve robust, real-time compensation without increasing manufacturing complexity.

Keywords: OLED display, temperature-induced color shift, 3D-LUT, neural network (NN), AI compensation, ΔE_{00}, γ tracking, chromaticity stability

INTRODUCTION

A key challenge in OLED mass production is panel-to-panel variation, requiring extensive γ adjustment to ensure consistent performance[2]. The complexity of OLED dimming systems necessitates On-line calibration of at least eleven distinct γ curves per panel, tailored for various luminance and usage conditions. This process creates a significant manufacturing bottleneck. Furthermore, performing individual panel calibration to mitigate temperature-dependent color shifts is commercially impractical, as it would drastically escalate production time and cost. The measurement burden is underscored by instruments like the Konica Minolta CA-410, whose speed is luminance-dependent (e.g., 20 Hz >2 cd/m²)[3]. At a standard 28 °C, calibrating just 17 measurement points already requires 236 seconds as shown as Table 1. This inefficiency highlights the urgent need for a novel methodology to enhance production throughput while maintaining color accuracy across all condition.

Table 1. Measurement time for 17-point mass production test using CA-410

Display Mode	L_max (cd/m²)	>12cd/m² (0.05s/pt)	1–12cd/m² (0.20s/pt)	≤ 0.9cd/m² (1.00s/pt)	Each Time (s)
APL20%	2,500.0	13 (0.65s)	1 (0.20s)	3 (3.00s)	11.55
HBM	1,600.0	13 (0.65s)	0 (0.00s)	4 (4.00s)	13.95
Normal (500–2 cd/m²)	–	43 (2.15s)	39 (7.80s)	54 (54.00s)	191.85
AOD	60.0	7 (0.35s)	5 (1.00s)	5 (5.00s)	19.05
Total	–	–	–	–	236.40

Note: L_max denotes the maximum luminance of each display mode. Values are presented as "scans (total time)." For example, 13 (0.65s) means 13 scans in 0.65 seconds.

Temperature-induced brightness and color shift is a critical challenge in current OLED mass production: the electroluminescent response is strongly temperature dependent, so identical drive signals can yield different chromaticities across operating points, degrading visual consistency. On production lines, conventional 3D-LUTs require separate R/G/B calibration and interpolate the white point, which scales poorly with temperature. Using the Konica Minolta CA-410 (AUTO), extending the test from 28 °C to also cover 32 °C and 36 °C increases 3D-LUT measurement time by +472.8 s (total 709.2 s ≈ 11.8 min). By contrast, our NN—trained on 17-point white-only measurements—adds only +157.6 s (total 394.0 s ≈ 6.57 min) for the same grid, reducing calibration overhead while delivering full RGB compensation across brightness and temperature conditions.

Table 2. Measurement time with extra temperature (28°C, 32 °C, 36 °C).

Method	Measurement item	Time (min)
3D-LUT	R/G/B	11.82
NN	W	6.57

METHODOLOGY

All experiments in this study are conducted using production-like measurement data collected from OLED panels under three brightness levels (L1, L2, L3) and three temperature conditions (28 °C, 32 °C, 36 °C). A total of 33 groups are used for model development (training), and an entirely disjoint validation set of 32 groups—drawn from different panels/conditions that never appear in training—is reserved for final testing. For each condition, a standardized 17-point white-only measurement framework is adopted to ensure consistency. Measurements are taken using a Konica Minolta CA-410 color analyzer in AUTO mode, with luminance-dependent measurement speeds. Both methods—3D-LUT and NN—are evaluated under the same 17-point structure to guarantee fair comparison. Unless otherwise stated, cross-validation and hyper-parameter selection are performed exclusively on the 33 training groups (grouped by data source to avoid leakage); all headline results are reported on the held-out validation set.

We use eight input features per gray level—gray_norm, Y_ref, $\hat{\gamma}$, Δx, Δy, ΔE_{00}(origW↔D65), LUT, and temperature (°C); formal definitions are summarized in Table 3. The predictor is a four-layer fully connected neural network with hidden sizes 224→192→160→128 as shown in Figure 1. Each hidden layer uses SiLU activation, followed by layer normalization and dropout (p = 0.05); The network outputs compensated R, G, and B drive values for each gray level.

Table 3. Input features used by the neural network (NN).

Feature	Symbol / Definition	Notes
Normalized gray level	gray_norm = g/255	Per-gray input
Reference luminance	Y_ref = Y(255)	Per-brightness input
Estimated γ	$\hat{\gamma}$ = ln[Y(g)/Y(255)] / ln(g/255)	Per-γ input
D65 chromaticity offset (x)	Δx = x_origW − 0.3127	Per-condition input
D65 chromaticity offset (y)	Δy = y_origW − 0.3290	Per-condition input
ΔE_{00} (origW vs D65)	ΔE_{00}_origW_vs_D65 @ Y_target	Per-gray calibration input
ΔE_{00}(LUT↔D65)	Pre-calibration LUT for target (D65, $\hat{\gamma}$ = 2.2)	Per-LUT input
Temperature	T (°C)	Per-condition {28, 32, 36}

Training uses the Adam optimizer (learning rate = 0.001, batch size = 256), and hyper-parameter selection is performed using GroupKFold cross-validation (5-fold) on the 33 training groups, with the grouping key defined by panel/lot (panel_id) or, when unavailable, by the measurement file tag (source_file), to prevent leakage across folds. To formalize the learning objective, we minimize the average perceptual white-point error across gray levels, measured by the CIEDE2000 color difference (ΔE_{00}) at matched luminance (see Eq. (1)).:

$$L = (1/N) \cdot \Sigma_g \Delta E_{00}^2((x,y,Y)_pred(g), (x,y,Y)_meas(g)) \quad (1)$$

where N is the number of evaluated gray levels; ΔE_{00} is computed at matched luminance Y_target(g); and (x,y,Y)_pred(g) and (x,y,Y)_meas(g) denote the predicted and measured white points at gray level g. For each gray level g, we obtain the NN-predicted RGB drives and pass them through the device forward color pipeline to produce (x,y,Y)_pred(g); we then compute ΔE_{00} against (x,y,Y)_meas(g), square the result, and average over all N gray levels.

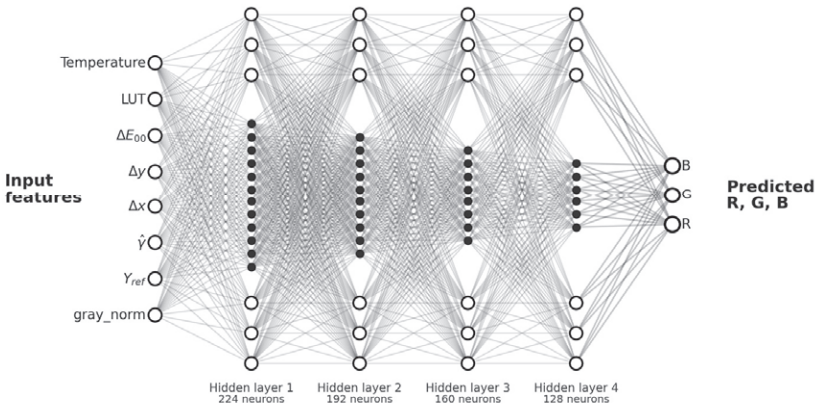

Figure 1. Architecture of the neural network (NN) with 8 input features.

The On-line/Off-line workflow is depicted in Figure 2. Off-line we curate 9,801 samples (33 groups; L1–L3; 28/32/36 °C; 33 whites/condition) and, via GroupKFold (5-fold), train a four-layer neural network (SiLU, LayerNorm, dropout); weights/config are exported. On-line, each condition measures only the 17-point white grid

(CA-410, AUTO), computes eight features (gray_norm, Y_ref, $\hat{\gamma}$, Δx, Δy, ΔE_{00}(origW↔D65), ΔE_{00}(LUT↔D65), Temperature), and runs NN inference for gray-wise RGB compensation. A device-forward check evaluates ΔE_{00} at matched luminance Y_target; the drives are applied to the panel and may be exported as a LUT. This split keeps On-line fast and off-loads learning Off-line, yielding the time savings as shown as Table 2.

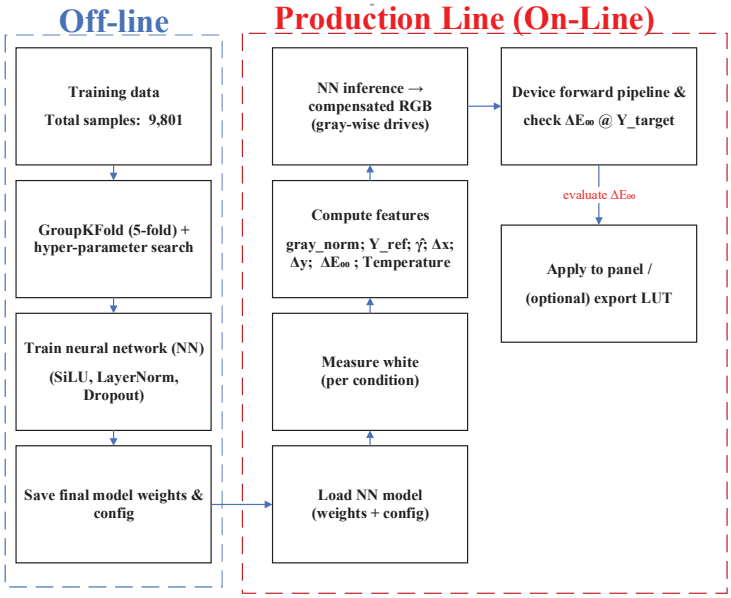

Figure 2. On-line and Off-line flow

RESULTS AND DISCUSSION

We evaluate perceptual color accuracy with CIEDE2000 (ΔE_{00}), reporting OK-rates at $\Delta E_{00} \leq 1$ (stricter) and $\Delta E_{00} \leq 2$ (default). Equal-luminance evaluation is used to isolate chromaticity error from brightness variation along the tone scale. Across all analyses (overall, by temperature, by brightness), the proposed NN surpasses the 3D-LUT in both average performance and worst-case behavior.

Overall accuracy.

On the 32 held-out groups (9,504 points per method), the NN attains 97.63% at $\Delta E_{00} \leq 1$ versus 93.16% for 3D-LUT (+4.47 pp (percentage points)), and 99.66% at $\Delta E_{00} \leq 2$ versus 98.52% (+1.14 pp). Decomposed by error band, the NN shrinks both the mid-band (1–2) from 5.36% → 2.03% and the ≥ 2 tail from 1.48% → 0.34%, indicating fewer perceptually salient outliers.

Temperature robustness (28/32/36 °C).

Under the CIEDE2000 criterion ($\Delta E_{00} \leq 1$), the proposed NN achieves average OK-rates of 96.94%, 99.02%, and 96.94% across the three brightness settings (L1/L2/L3), exceeding the 3D-LUT baseline (91.24%, 94.47%, 93.78%) by 5.70, 4.55, and 3.16 percentage points, respectively. When the threshold is relaxed to $\Delta E_{00} \leq 2$, the NN attains 99.12%, 100.00%, and 99.87%, again outperforming 3D-LUT (98.60%, 98.21%, 98.76%) by 0.52, 1.79, and 1.11 percentage points. A worst-case analysis (minimum OK-rate under $\Delta E_{00} \leq 2$) further indicates that NN performance never falls below 96.97% (96.97/100.00/96.97% for L1/L2/L3), whereas 3D-LUT drops to 93.94% at 32 °C and 36 °C. Error-band decomposition corroborates these findings: at 32 °C the NN eliminates the ≥ 2 bin (0.00% vs. 1.79%) and compresses the 1–2 band (0.98% vs. 3.74%); at 28 °C and 36 °C, the heavy-error tail is

likewise reduced (0.88%/0.13% for NN vs. 1.40%/1.24% for 3D-LUT). Collectively, these results show that the NN improves mean accuracy while tightening the error distribution by suppressing large-error outliers.

Brightness dependence (L1/L2/L3).

Both methods saturate at low/mid luminance: at $\Delta E_{00} \leq 1$, NN is 100.00% for L1/L2, while 3D-LUT reaches 96.88/94.56%. At high luminance (L3), the NN retains a decisive edge—92.90% vs. 88.05% ($\Delta E_{00} \leq 1$) and 98.99% vs. 97.04% ($\Delta E_{00} \leq 2$)—with a lower tail (1.01% vs. 2.96%) and smaller 1–2 band (6.09% vs. 8.99%). Worst-case OK-rates at $\Delta E_{00} \leq 2$ are 100/100/96.97% (NN, L1/L2/L3) versus 100/96.97/93.94% (3D-LUT), underscoring improved robustness where nonlinearity and temperature interaction are strongest.

Interpretation and implications.

The consistent reductions in both the 1–2 band and ≥ 2 tail suggest that the NN's learned mapping—augmented with Temperature and the ΔE_{00}(LUT↔D65) prior—better regularizes difficult regimes than tabular interpolation. Although isolated cases may show larger $\Delta x/\Delta y$ excursions, chromaticity displacement is not perceptually uniform; evaluating ΔE_{00} at matched luminance provides a truer measure of visual quality. Taken together with the measurement-efficiency advantage (Table 2)—R/G/B-based 3D-LUT scaling versus white-only NN—the proposed approach delivers both higher perceptual accuracy and lower calibration overhead for OLED mass production.

Failure analysis and practical implication.

Inspection of the error distribution shows that the NN's rare failures are almost exclusively at gray 255, whereas the 3D-LUT exhibits misses at gray 255, 248, and 200 as well. This concentration at the top end is consistent with panel-to-panel peak-luminance headroom: when a panel's maximum luminance is below the training reference, the desired target at the highest gray may be unattainable (or extremely sensitive to small chromaticity deviations), which can push ΔE_{00} marginally above threshold even after compensation. By contrast, the NN maintains near-100% pass rates across the remaining gray levels, whereas 3D-LUT failures spread into mid-high tones (e.g., 248/200), indicating weaker stability away from the extremes. Taken together with the measurement-efficiency advantage—white-only NN versus per-temperature R/G/B for 3D-LUT—this yields an On-line station time of 394.0 s versus 709.2 s for the same grid (Table 2), i.e., ~ 44% faster, while delivering superior perceptual accuracy

Table 4. Overall OK-rate ($\Delta E_{00} \leq 1, \leq 2$)

Method	Total points	$\Delta E_{00} \leq 1$ OK-rate (%)	$\Delta E_{00} \leq 2$ OK-rate (%)
NN	9504	97.63	99.66
3D-LUT	9504	93.16	98.52

Table 5. OK-rate by temperature set point ($\Delta E_{00} \leq 1, \leq 2$)

Method	Temperature	$\Delta E_{00} \leq 1$ ok-rate (ave)	$\Delta E_{00} \leq 2$ ok-rate (ave)	$\Delta E_{00} \leq 2$ ok-rate (min)
NN	28**°C**	96.94%	99.12%	96.97%
NN	32**°C**	99.02%	100.00%	100.00%
NN	36**°C**	96.94%	99.87%	96.97%
3D-LUT	28**°C**	91.24%	98.60%	96.97%
3D-LUT	32**°C**	94.47%	98.21%	93.94%
3D-LUT	36**°C**	93.78%	98.76%	93.94%

Table 6. OK-rate by brightness level ($\Delta E_{00} \leq 1, \leq 2$)

Method	Brightness	$\Delta E_{00} \leq 1$ok-rate(ave)	$\Delta E_{00} \leq 2$ ok-rate(ave)	$\Delta E_{00} \leq 2$ok-rate(min)
NN	L1	100.00%	100.00%	100.00%
NN	L2	100.00%	100.00%	100.00%
NN	L3	92.90%	98.99%	96.97%
3D-LUT	L1	96.88%	100.00%	100.00%
3D-LUT	L2	94.56%	98.54%	96.97%
3D-LUT	L3	88.05%	97.04%	93.94%

Note: All percentages are reported with two decimal places. $\Delta E_{00} \leq 1$ denotes a stricter perceptual bound; $\Delta E_{00} \leq 2$ is the default OK threshold.

CONCLUSION

This work demonstrates that a compact neural network, trained solely on a standardized 17-point white-only protocol, delivers perceptually superior and production-ready color compensation for OLED panels across temperature (28/32/36 °C) and brightness (L1–L3) conditions. Relative to a table-based 3D-LUT, the proposed method consistently raises OK-rates at both $\Delta E_{00} \leq 1$ and $\Delta E_{00} \leq 2$, compresses the 1–2 band, and suppresses the ≥ 2 tail, yielding fewer visually salient outliers while cutting On-line station time from 709.2 s to 394.0 s per condition (~ 44% reduction). The On-line/Off-line split enables fast deployment: inference on the line uses only the 17-point white grid and eight compact features, whereas learning and model selection are performed Off-line under GroupKFold control to prevent leakage. Failure analysis indicates that the rare NN misses concentrate at gray 255 and stem from panel peak-luminance headroom rather than model instability, with near-perfect pass rates elsewhere—underscoring robustness where 3D-LUT exhibits mid-high-tone fragility. Taken together, these results establish an AI-based, white-only compensation pipeline that is both more accurate perceptually and more efficient operationally, offering a practical blueprint for scaling color consistency in OLED mass production. Looking ahead, integrating adaptive headroom modeling, uncertainty-aware screening, and physics-informed or multi-task objectives (e.g., power/aging co-optimization) may further harden generalization, extend lifetime stability, and broaden applicability to diverse OLED stacks and operating environments

REFERENCES

[1]. J. Kim et al., "35-4: A Compensation Algorithm for Degradation in AMOLED Displays," *SID Symposium Digest of Technical Papers*, 2018, vol. 49, no. 1: Wiley On-line Library, pp. 445-448.

[2]. Pan, T. L., Chao, P. C. P., Nguyen, D. H., Lin, C. C., Pai, F. T., Tsai, Y. C., Tsung, W. N., & Chang, Y. J. (2024). A Novel On-line, Fast Color Correction by Machine Learnings. *Digest of Technical Papers - SID International Symposium, 55*(1), 793-796. https://doi.org/10.1002/sdtp.17647

[3]. K. Lange and E. Lee, "Konica Minolta Sensing Americas, Inc.: Evaluating the latest technological displays using progressive Display Color Analyzer CA-410," *SPIE Exhibition Product Demonstrations*, 2021, vol. 11716: SPIE, p. 1171614.

Cityscape Color Analysis Using Deep Learning-Based Image Segmentation and Color Adjustment for Weather Conditions

Motonori Doi*, Ryuto Ono, Shun Kuboki

Osaka Electro-Communication University, Neyagawa, Japan
**Corresponding author: Motonori Doi, doi@oecu.jp*

ABSTRACT

Many cities have characteristic building colors that reflect their cultures and histories. Analyzing these color features from cityscape photographs is essential for various applications, such as designing colors for new buildings. We propose a method for cityscape color analysis that utilizes deep learning-based image segmentation and adjusts building colors based on weather conditions. When performing automatic color analysis of buildings in cityscape images, it is important to exclude the colors of non-building regions, such as the sky, street trees, and vehicles. Recent advances in deep learning technology have enabled the segmentation of outdoor images into categories such as buildings, sky, trees, cars, and people. The proposed method applies panoptic segmentation, a deep learning-based technique, to segment and classify objects in input images. However, fine regions, such as the boundaries between buildings and the sky, often contain errors, requiring correction after segmentation. In our method, these errors are corrected using the color distributions in the building and sky regions. The RGB values in these regions are coarsely quantized to analyze the color distributions, and color histograms are generated. If a dominant color in the sky region is minor in the building regions, it is excluded from the building analysis. After segmentation, the proposed method adjusts the building colors to account for weather conditions. First, the weather is predicted based on the colors in the sky region. If the weather is predicted to be cloudy, the contrast and saturation of the building regions are adjusted to approximate the color tones observed under clear skies. Finally, the colors of the building regions are visualized using various types of graphs, such as stacked graphs, along with their respective area ratios. We conducted experiments to validate the proposed method. Validation with sunny and cloudy images of a building confirmed that the method achieves favorable analysis results.

Keywords: Cityscape Color Analysis, Image segmentation, Color Adjustment

INTRODUCTION

Many cities have characteristic building colors that reflect their cultures and histories. Analyzing these color features from cityscape photographs is essential for various applications, such as designing colors for new buildings. Automatic color analysis of buildings is particularly useful when processing large amounts of image data. However, when performing automatic color analysis of buildings in cityscape images, it is important to exclude the colors of non-building regions, such as the sky, street trees, and vehicles. Recent advances in deep learning technology have enabled the segmentation of outdoor images into categories such as buildings, sky, trees, cars, and people. In this study, we utilize deep learning-based segmentation to extract building regions in images. Nevertheless, two issues remain. First, fine regions such as the boundaries between buildings and the sky often contain segmentation errors. Second, the detected building colors are influenced by weather conditions.

In this paper, we propose a method for cityscape color analysis that incorporates deep learning-based image segmentation, correction of errors in fine regions, and adjustment of building colors according to weather conditions.

SEGMENTATION AND COLOR ADJUSTMENT OF BULDINGS REGIONS

The schema of the proposed method is shown in Figure 1. The steps are as follows. First, image segmentation is applied to the target image. Next, the sky-colored pixels mistakenly included in the building regions are excluded based on color analysis of the building and sky regions. Then, the weather condition is predicted from the colors in the sky region. If the weather is predicted to be cloudy, color adjustment is applied to the building regions. Finally, color distribution of the building regions is visualized.

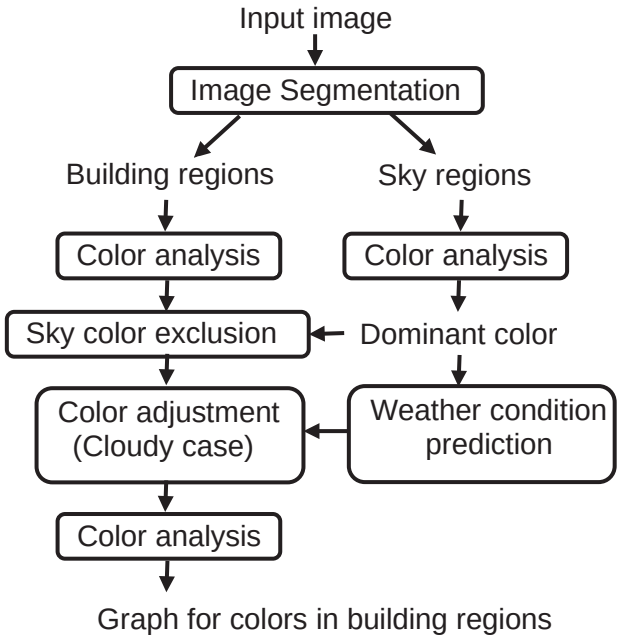

Figure 1: Schema of proposed method

The primary image segmentation methods are semantic segmentation and instance segmentation. The semantic segmentation assigns a class label to each pixel in an image, and the instance segmentation detects each object and delineates it with a bounding box or segmentation mask [1]. In the proposed method, semantic segmentation with a deep learning-based technique is applied to separate and classify regions including buildings, sky, and other elements. After segmentation, errors in fine regions, such as the boundaries between buildings and the sky, are corrected using the color distributions of the building and sky regions. The RGB values in these regions are coarsely quantized to analyze the color distributions, and color histograms are generated. If a dominant color in the sky region is minor in the building regions, it is excluded from the building analysis.

For color adjustment, the weather is predicted based on the colors in the sky region. We use the dominant color in the sky region for the prediction. When the saturation value of the dominant sky color is low, the weather is predicted as cloudy. In such cases, the contrast and saturation of the building region are adjusted to approximate the color tones observed under clear skies.

For visualization of building colors, various types of graphs can be effective. In this study, we use stacked graphs to show colors and their ratios.

EXPERIMENTS

We conducted experiments to validate the proposed method. For image segmentation, we used Detectron2 [2], a tool for the panoptic segmentation. A pretrained model with the COCO-Stuff dataset was used, which includes 80 objects and 91 “stuff” categories, such as buildings, sky, and trees [3]. Panoptic segmentation is a unified framework that combines semantic and instance segmentation [1]. We adopted this tool in considering future scalability.

The image processing programs, including color analysis, sky color exclusion, and color adjustment, were implemented in Python [4] using libraries such as OpenCV [5] and Matplotlib [6]. In color analysis, RGB values were coarsely quantized with an interval of 16. For color adjustment, the RGB values of the image were converted to the HSV color space. Then, the contrast of the image was enhanced in the V (brightness) channel, and the saturation was enhanced in the S (saturation) channel. Finally, the HSV values were converted back to RGB after enhancement.

RESULTS AND DISCUSSION

The effectiveness of the correction of fine-region errors is demonstrated in Figure 2 with an extreme example. The input image (Figure 2(a)) shows a Ferris wheel, and the initial result of building-region extraction (Figure 2(b)) incorrectly includes sky regions between the spokes of the Ferris wheel. Figure 2(c) shows the corrected result, where most of the sky-colored pixels in the building region are successfully excluded.

Figure 3 shows an example of building color analysis on a sunny day. The input image (Figure 3(a)) of a building with a brick-like facade was separated into building and sky regions. The coarsely quantized RGB value of the dominant color in the sky region was (208, 224, 240). Based on this value, the weather was classified as sunny. Sky color removal was applied to the building region (Figure 3(b)), and the resulting color distribution was visualized as a stacked graph (Figure 3(c)).

Figure 4 shows the case of a cloudy sky. The input image (Figure 4(a)) is the same building from Figure 3, captured under cloudy conditions. The coarsely quantized RGB value of the dominant sky color was (240, 240, 240), leading to the weather being classified as cloudy. The contrast and saturation of the building region (Figure 4(b)) were enhanced by factors of 1.5 and 1.2, respectively. These parameters were determined heuristically. The adjusted result is shown in Figure 4(c), where the building colors are close to those in the sunny-day image. Figures 4(d) and 4(e) show the building color distributions before and after adjustment, respectively. After adjustment, the dominant color of the building matches that observed on the sunny day.

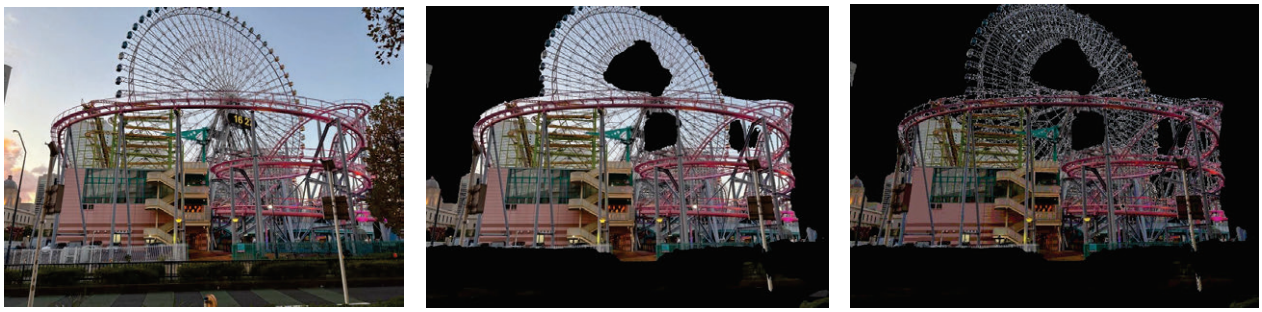

(a) Input image of Ferris wheel (b) Result of semantic segmentation (c) Result of correction

Figure 2: Correction of errors in fine regions by excluding sky-colored pixels in the building region

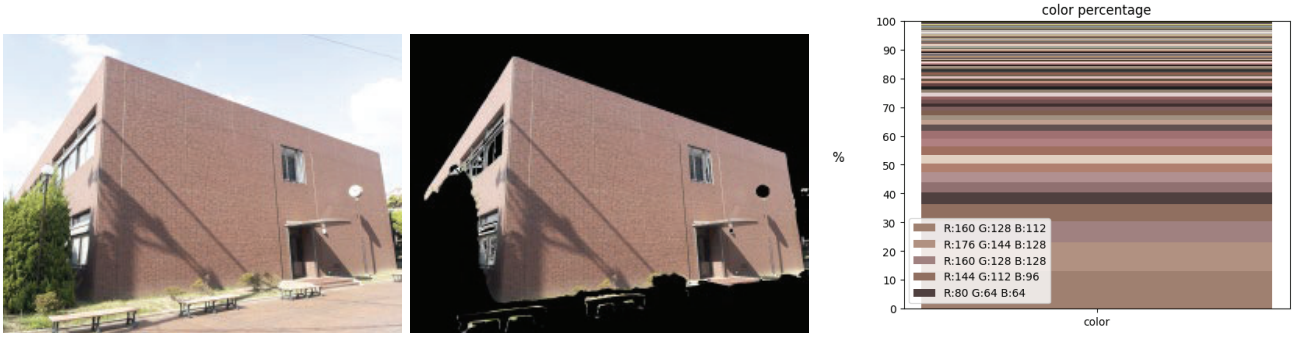

(a) Input image (b) Building region (c) Graph of color in building region

Figure 3: Color analysis of building colors under sunny condition

(a) Input image (b) Building region (c) Color adjustment result

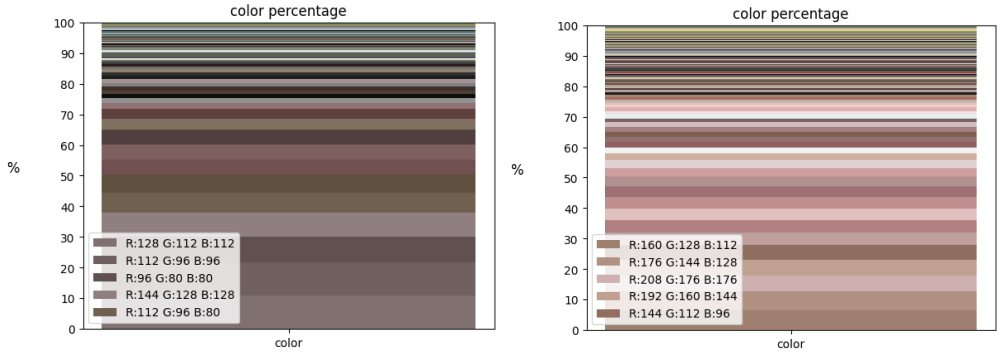

(d) Graph of color before color adjustment (e) Graph of color after color adjustment

Figure 4: Color analysis of building colors under cloudy condition

Validation with sunny and cloudy images of a building confirmed that the proposed method yields favorable analysis results. However, there remain several issues regarding segmentation accuracy and the determination of color adjustment parameters.

The problem of sky-colored pixels mistakenly included in the building regions was addressed. However, in the sunny case, windows reflecting the sky were also removed from the building region, as shown in Figure 3. Whether window color should be considered part of the building's color is a difficult question. n Figure 2, the center of the Ferris wheel was lost due to incorrect segmentation, indicating that the extraction of building regions requires further improvement. Moreover, building images captured under sunny conditions often include shadows. Removing shadow colors from the building colors is also necessary.

In this study, the color adjustment parameters were determined heuristically. Since common cameras apply auto white balance and auto gain control, it is not straightforward to map cloudy images to sunny images. Developing a method for this mapping remains an important direction for future work.

CONCLUSION

This study presented a framework for cityscape color analysis that integrates deep learning-based segmentation, correction of fine-region errors, and color adjustment for weather condition. The results indicate that consistent and reliable building color distributions can be obtained under varying conditions, providing a useful basis for applications in urban design and cultural studies.

REFERENCES

[1]. Kirillov, A., He, K., Girshick, R., Rother, C., and Dollar, P. (2019). Panoptic Segmentation. *CVPR2019*, 9404-9413.

[2]. Wu, Y., Kirillov, A., Massa, F., Lo, W.Y., and Girshick, R. (2019). Detectron2 https://github.com/facebookresearch/detectron2 Accessed July 24, 2024.

[3]. Caesar, H., Uijlings, J., Ferrari, V., (2018). COCO-Stuff: Thing and Stuff Classes in Context, *CVPR2018*, 1209-1218.

[4]. Welcome to pyhon.org. https://www.python.org/. Accessed September 1, 2025.

[5]. OpenCV - Open Computer Vision Library, https://opencv.org/. Accessed September 1, 2025.

[6]. Matplotlib - Visualization with Python. https://matplotlib.org/. Accessed September 1, 2025.

LCH-Based Deep Learning for Skin Cancer Diagnosis

Tzu-Hao Kuan[a*], Me-Chun Lo[b], and Chih-Shun Hsu[c]

[a]*Shih Hsin University, Taipei, Taiwan*
[b]*Shih Hsin University, Taipei, Taiwan*
[c]*Shih Hsin University, Taipei,Taiwan*
[*]*Corresponding author: Tzu Hao Kuan, kuankris021210192126@gmail.com*

ABSTRACT

This paper presents a dermoscopic image–classification pipeline that integrates LCH color–space conversion, targeted preprocessing, and deep learning to improve skin-cancer diagnosis. To reduce the illumination sensitivity of RGB images, we convert inputs to LCH so that lightness, chroma, and hue can be handled independently, yielding more stable color cues and better lesion separability. The pipeline further applies hair removal to suppress linear occlusions and a dark-corner artifact (DCA) enhancement that improves peripheral contrast while preserving central content. We benchmark three representative architectures—YOLOv9, Inception-ResNetV2, and EfficientNetb0—under controlled ablations of the preprocessing steps. Across experiments, the full configuration (LCH + hair removal + DCA) consistently improves accuracy, recall, and F1-score over baseline inputs, with EfficientNetb0 showing the most robust gains among tested models. To strengthen clinical interpretability, we add an ABCD analysis module that automatically quantifies asymmetry, border irregularity, color diversity, and diameter and aggregates them into a Total Dermoscopy Score for decision support. The results indicate that combining color-space transformation with task-specific preprocessing enhances both diagnostic performance and explainability, suggesting a practical path for deploying reliable, interpretable computer-aided diagnosis on dermoscopic images and a foundation for extension to other medical-imaging tasks.

Keywords: LCH color space; hair removal; dark-corner artifact (DCA); EfficientNetb0; Inception-ResNetV2; YOLOv9; ABCD rule; skin cancer diagnosis

INTRODUCTION

Dermoscopy enables non-invasive inspection of pigmented skin lesions, yet automatic diagnosis remains challenging due to color/illumination variability across devices and acquisition sites, and due to artifacts such as occluding hairs that distort borders and texture. When features are extracted directly in RGB, color cues can be unstable under cross-domain shifts, undermining generalization in real-world screening. Converting images to the perceptually organized LCH space separates lightness, chroma, and hue, providing more stable descriptors for lesion structure and color heterogeneity.

Motivated by these issues, this work integrates LCH conversion with targeted preprocessing to strengthen lesion separability and robustness. We remove linear occlusions using a Dull Razor–based pipeline and introduce a dark-corner artifact (DCA) enhancement that increases peripheral attenuation while preserving central content, encouraging models to focus on diagnostically relevant regions. We also incorporate an ABCD module that quantifies asymmetry, border irregularity, color diversity (computed in LCH), and diameter to improve clinical interpretability.

The objectives of this paper are threefold: (1) to verify whether LCH conversion, hair removal, and DCA—individually and in combination—improve classification performance on dermoscopic images; (2) to benchmark representative CNN families (YOLOv9, Inception/Inception-ResNet, and EfficientNet-B0) under controlled

ablations of the preprocessing steps; and (3) to demonstrate that an ABCD-based analysis can complement deep models by adding transparent, human-readable cues for decision support. These goals directly reflect the system we implemented and evaluated in our thesis framework.

METHODOLOGY

1. Dataset and Split

We use the public dermoscopic dataset from ISIC (Kaggle) and randomly split images into training and validation sets with a 70/30 ratio while preserving the benign/malignant folder structure. A Python script automates the split to avoid leakage between sets.

2. Color–Space Conversion (RGB→XYZ→CIELAB→LCH)

To stabilize color cues, inputs are converted from sRGB to CIE XYZ under D65 and then to CIELAB using standard κ and ε thresholds; finally, chroma and hue are computed as:

$$C^* = \sqrt{a^{*2} + b^{*2}} \quad (1)$$

$$h^\circ = atan2(b^*, a^*) \quad (2)$$

This yields independent lightness, chroma, and hue channels (L, C, H) for subsequent processing and model input.

3. Hair Removal (Dull Razor)

We adopt a Dull Razor–style pipeline to suppress linear hair occlusions: (1) convert to grayscale; (2) apply black-hat morphology to enhance dark, thin structures; (3) smooth with Gaussian blur; (4) threshold to obtain a binary hair mask; and (5) inpaint masked regions using the Telea method. Parameters follow our thesis implementation: 9×9 structuring element for black-hat, 3×3 Gaussian blur, mask threshold 10, Telea inpaint radius 6.

4. Dark-Corner Artifact (DCA) Enhancement

To mimic common peripheral attenuation and reduce background distraction, we generate a circular peripheral mask only when an image lacks existing DCA (edge–center brightness difference < threshold 50, measured in grayscale). The mask is Gaussian-blurred (kernel 5×5) and applied to darken the periphery while preserving central content. We varied the mask coverage and set it to 0.6 based on ablation, as 0.3 or 0.8 degraded convergence.

5. Model Architectures and Training

We benchmark three representative CNN families—YOLOv9, Inception-ResNetV2, and EfficientNet-B0—under the same training protocol. Unless stated otherwise, all inputs are resized to 288×288, and models are trained with Adam (initial learning rate 1e-4) plus CosineAnnealingLR, AMP acceleration, and early stopping after 10 non-improving validation epochs. To ensure fairness, image size, epochs, and data-loader threads are unified across runs. Experiments are executed on a workstation with an RTX 4090 GPU.

6. Ablation Settings

We evaluate five input conditions to isolate contributions of each component: (i) RGB only; (ii) RGB+LCH; (iii) Hair-Removal; (iv) DCA; and (v) Full preprocessing (LCH + hair removal + DCA). Each condition is trained for all model families to compare their sensitivity to preprocessing.

7. Evaluation Metrics and ABCD Analysis

Performance is reported using Accuracy, Recall, Specificity, Precision, and F1-score. For interpretability, we compute the Total Dermoscopy Score (TDS) from the ABCD rule using:

$$TDS = A * 1.3 + B * 0.1 + C * 0.5 + D * 0.5 \quad (3)$$

and report benign/suspicious/malignant thresholds following standard practice. This provides human-readable cues alongside model predictions.

RESULTS AND DISCUSSION

1. Overall performance

Table 1 shows that the full preprocessing (LCH + hair removal + DCA) improves both sensitivity and specificity over the RGB baseline across all model families. For YOLOv9, sensitivity increases from 0.752 to 0.812 (+0.060, ~8%), and specificity from 0.835 to 0.880 (+0.045, ~5.4%). Inception improves from 0.728 to 0.757 (+0.029, ~4.0%) in sensitivity and from 0.822 to 0.853 (+0.031, ~3.8%) in specificity. EfficientNet-b0 achieves the best overall results, rising from 0.904/0.931 to 0.936/0.964 (+0.032/+0.033, ~3.5%). These gains indicate that stabilizing color cues in LCH and suppressing artifacts are beneficial for both malignant detection (sensitivity) and benign exclusion (specificity).

2. Convergence behavior

Figure 2 (EfficientNet-b0, Inception) and Figure 3 (YOLOv9) visualize training dynamics. In all cases, the RGB+LCH+preprocessing curves for Precision/Recall/F1 lie consistently above the RGB curves across epochs. The gap widens as training proceeds, and the improved trends are accompanied by earlier and higher

validation peaks (see markers), suggesting more data-efficient learning once color instability and hair occlusions are mitigated.

3. Interpretability with ABCD

Table 2 summarizes ABCD statistics on the test set. Malignant lesions exhibit larger means in all four attributes—A (0.29 vs. 0.12), B (0.26 vs. 0.09), C (4.6 vs. 2.1), and D (8.2 mm vs. 5.8 mm)—with reasonable dispersion (SD shown). These separations corroborate the model trends and provide human-readable cues that complement black-box predictions: higher asymmetry, border irregularity, color diversity, and diameter align with malignant risk and thus support decision-making alongside the classifier outputs.

4. Discussion and limitations

The consistent improvements across three diverse architectures suggest that the proposed preprocessing is complementary rather than model-specific. Gains are most pronounced in sensitivity (especially for YOLOv9), indicating better capture of diagnostically important patterns that are often masked by illumination shifts or linear occlusions. Remaining limitations include evaluation on a single public dataset and a single split; future work will extend to cross-site validation and explore test-time color normalization or lightweight attention that explicitly leverages ABCD features.

5. Limitations and future work

Our evaluation uses a single public dataset and a 70/30 split; although ablations are comprehensive, cross-site validation and calibration on additional cohorts are needed to fully establish generalization. Future work will explore test-time color normalization, self-supervised pretraining in LCH, and lightweight attention modules designed to explicitly leverage ABCD features.

Table 1: Comparison of Sensitivity and Specificity of Each Model in Classification Tasks

Model	Sensitivity	Specificity
YOLOv9 RGB	0.752	0.835
YOLOv9 RGB + LCH + preprocessing	0.812	0.880
Inception RGB	0.728	0.822
Inception RGB + LCH + preprocessing	0.757	0.853
EfficientNetb0 RGB	0.904	0.931

EfficientNetb0 RGB + LCH + preprocessing	0.936	0.964

Table 2 : Test-Set ABCD Feature Statistics: Benign vs. Malignant

Category	A(mean±SD)	B	C	D (mm)
Benign	0.12 ± 0.05	0.09 ± 0.04	2.1 ± 1.0	5.8 ± 1.3
Malignant	0.29 ± 0.08	0.26 ± 0.07	4.6 ± 1.4	8.2 ± 2.1

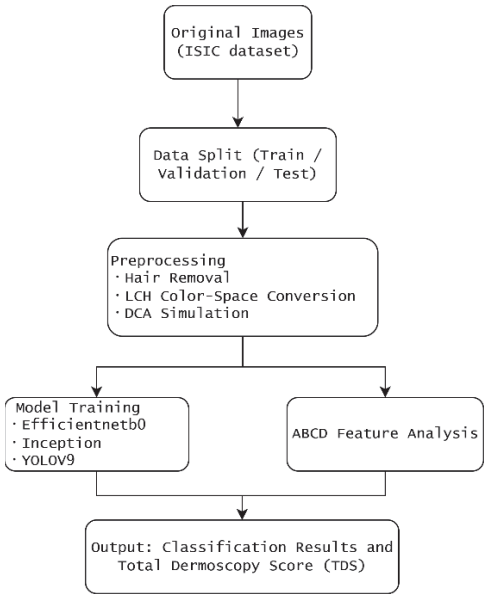

Figure 1: Overall workflow

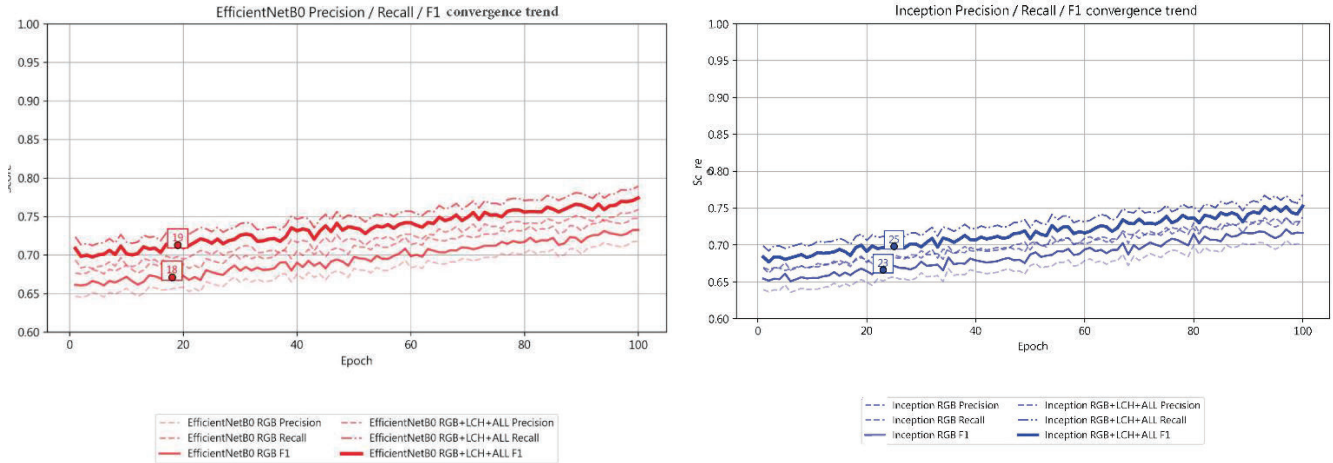

Figure 2 : EfficientB0 and Inception Precision/Recall/F1 convergence trend

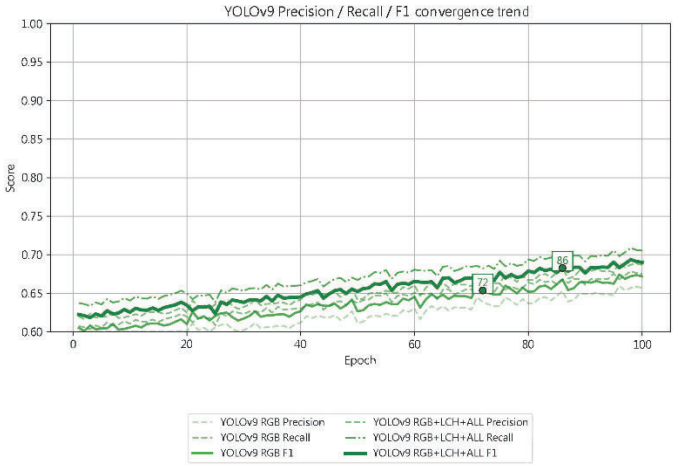

Figure 3 : YOLOv9 Precision/Recall/F1 convergence trend

CONCLUSION

This study shows that combining LCH color-space conversion with hair removal and dark-corner artifact (DCA) enhancement consistently improves dermoscopic image classification across three model families. The full pipeline stabilizes color cues, suppresses linear occlusions and peripheral distractions, and leads to faster, higher validation peaks, culminating in the best test performance—up to 0.936 sensitivity and 0.964 specificity with EfficientNet-b0—while maintaining strong benign exclusion. Beyond accuracy, an ABCD-based module quantifies asymmetry, border irregularity, color diversity, and diameter, providing transparent cues that corroborate the model predictions and facilitate case review. Overall, a small set of physics- and clinic-aware preprocessing steps coupled with modern CNNs yields reliable and interpretable decision support. Future work will validate the approach across sites and devices and explore test-time color normalization and lightweight attention that more tightly couples ABCD features with learned representations for robust deployment.

ACKNOWLEDGEMENTS

The completion of this paper would not have been possible without the support and encouragement of many advisors, classmates, and family members. I am deeply grateful to my advisors, Prof. Mei Chun Lo and Prof. Chih Shun Hsu, for their patient guidance and insightful suggestions throughout the research—from the design of deep-learning models and improvements in image preprocessing to the analysis and interpretation of experimental results. Their rigorous scholarship and broad research vision not only enhanced the quality of this study but also set an example for my future learning and work. I also thank the faculty and classmates of the Department of Information Management for stimulating coursework and constructive feedback, and my laboratory colleagues for sharing valuable experience and resources that made the research process productive and rewarding. I am grateful to Shih Hsin University for providing an excellent research environment and access to library and research facilities, which

facilitated literature review and data analysis. Finally, I offer my heartfelt thanks to my family for their constant support and encouragement; their care has been the driving force that sustained me, and this achievement belongs to them as much as it does to me.

REFERENCES

[1] Akter, M., Khatun, R., Talukder, M. A., Islam, M., Uddin, M. A., Ahamed, M. K., and Khraisat, A. (2025). An integrated deep learning model for skin cancer detection using hybrid feature fusion technique. Biomedical Materials and Devices, 3.
[2] CIE (1976). Colorimetry – Official Recommendations of the International Commission on Illumination. CIE Publication No. 15, Vienna, Austria.
[3] CIE (2004). CIE 15:2004 Colorimetry. CIE Central Bureau, Vienna, Austria, 3rd edition. LAB to LCH conversion in Section 8.2.1.3.
[4] Das, K., Cockerell, C. J., Patil, A., Pietkiewicz, P., Giulini, M., Grabbe, S., and Goldust, M. (2021). Machine learning and its application in skin cancer. International Journal of Environmental Research and Public Health, 18(24).
[5] Delibasis, K., Moutselos, K., Vorgiazidou, E., and Maglogiannis, I. (2023). Automated hair removal in dermoscopy images using shallow and deep learning neural architectures. Computer Methods and Programs in Biomedicine Update, 4:100109.
[6] Fathel, W. R., Al-Obaidi, A. S. I., Qasim, M. A., and Al-Hatab, M. M. M. (2023). Skin cancer detection using k-means clustering-based color segmentation. Texas Journal of Engineering and Technology, 18:46–52.
[7] Gonzalez, R. C. and Woods, R. E. (2018). Digital Image Processing. Pearson, Harlow, Essex, England, 4th edition. Chapter 9: Morphological Image Processing.
[8] Gupta, A., Bharadwaj, M., and Mehrotra, R. (2016). Skin cancer concerns in people of color: Risk factors and prevention. Asian Pacific Journal of Cancer Prevention: APJCP, 17:5257–5264.
[9] Gururaj, H. L., Manju, N., Nagarjun, A., Aradhya, V. N. M., and Flammini, F. (2023). Deepskin: A deep learning approach for skin cancer classification. IEEE Access, 11:50205–50214.
[10] IEC (1999). IEC 61966-2-1:1999: Multimedia Systems and Equipment – Colour Management –Default RGB Colour Space –sRGB. International Electrotechnical Commission, Geneva, Switzerland. Standard IEC 61966-2-1:1999.
[11] Jamil, U., Akram, M. U., Khalid, S., Abbas, S., and Saleem, K. (2016). Computer based melanocytic and nevus image enhancement and segmentation. BioMed Research International, 2016(1):2082589.
[12] Mahbod, A., Schaefer, G., Wang, C., Ecker, R., and Ellinge, I. (2019). Skin lesion classification using hybrid deep neural networks. ICASSP 2019 - IEEE Int. Conf. on Acoustics, Speech and Signal Processing, pages 1229–1233.
[13] Pewton, S. W., Cassidy, B., Kendrick, C., and Yap, M. H. (2024). Dermoscopic dark corner artifacts removal: Friend or foe? Computer Methods and Programs in Biomedicine, 244:107986.
[14] Saeed, J. and Zeebaree, S. (2021). Skin lesion classification based on deep convolutional neural networks architectures. Journal of Applied Science and Technology Trends, 2:41–51.
[15] Saputri, D. U. E., Khasanah, N., Aziz, F., and Hidayat, T. (2023). Enhancing skin cancer classification using optimized inceptionv3 model. Journal Medical Informatics Technology, pages 65–69.
[16] Senan, E. M. and Jadhav, M. E. (2021). Analysis of dermoscopy images by using abcd rule for early detection of skin cancer. Global Transitions Proceedings, 2:1–7.

[17] Serra, J. (1982). Image Analysis and Mathematical Morphology. Academic Press, London, England. Chapter 6: Morphological Filters.
[18] Szegedy, C., Ioffe, S., Vanhoucke, V., and Alemi, A. A. (2017). Inception-v4, inceptionresnet and the impact of residual connections on learning. In Proceedings of the Thirty-First AAAI Conference on Artificial Intelligence, pages 4278–4284. AAAI Press.
[19] Szegedy, C., Vanhoucke, V., Ioffe, S., Shlens, J., and Wojna, Z. (2016). Rethinking the inception architecture for computer vision. In 2016 IEEE Conference on Computer Vision and Pattern Recognition (CVPR), pages 2818–2826.
[20] Tan, M. and Le, Q. V. (2020). Efficientnet: Rethinking model scaling for convolutional neural networks.
[21] Wang, C.-Y., Yeh, I.-H., and Liao, H.-Y. M. (2024). Yolov9: Learning what you want to learn using programmable gradient information.
[22] Wilhelm, K.-P., Elsner, P., Berardesca, E., and Maibach, H. I. (2006). Bioengineering of the Skin: Skin Imaging and Analysis, 2nd Edition. Dermatology: Clinical and Basic Science. CRC Press.
[23] Zhou, Y., Chen, M., and Wang, H. (2025). Gs-transunet: Unified lesion segmentation and classification using gaussian splatting and transformers. arXiv preprint arXiv:2502.16748.
[24] Zhu, J.-Y., Park, T., Isola, P., and Efros, A. A. (2020). Unpaired image-to-image translation using cycle-consistent adversarial networks.
[25] Zunair, H. and Ben Hamza, A. (2020). Melanoma detection using adversarial training and deep transfer learning. Physics in Medicine and Biology, 65(13):135005.

Enhancing Image Color Harmony Through Content-Aware Recoloring

Yu-Shan Chou and Pei-Li Sun

National Taiwan University of Science and Technology, Taipei, Taiwan
Corresponding author: Pei-Li Sun, plsun@mail.ntust.edu.tw

ABSTRACT

Color harmony plays a crucial role in visual aesthetics and communication. However, real-world photographs often contain disharmonious regions, such as strong hue conflicts, chroma inconsistencies, or lightness imbalances, which reduce overall coherence and naturalness. Existing color harmony models mainly focus on abstract color palettes, using geometric rules, regression-based formulas, or generative models, but they are limited in handling images with semantic content. Inspired by prior work on hue-histogram-based template matching for color harmonization, we propose an automatic framework for detecting and optimizing disharmonious regions while preserving semantic content.

The pipeline begins with semantic segmentation using SegFormer to protect critical objects, followed by mean shift clustering on the remaining pixels to form perceptually coherent color regions. A hue histogram is constructed, and the best-fitting Itten template is selected to identify clusters with insufficient template coverage. For optimization, a region adjacency graph (RAG) is built, and disharmonious clusters are recolored by generating candidate colors within the harmonic template range. The final replacement is determined by computing color harmony scores with neighboring clusters using the universal color harmony model, and the scores are further aggregated through an edge-length-weighted scheme proposed in this work.

Experimental results from a perceptual study with 30 participants showed that the optimized images were judged as more harmonious in 83% of trials, with nearly half of the items exceeding 90%. However, attractiveness judgments were more variable, averaging only 57%, indicating that improvements in harmony do not always translate into higher aesthetic preference. These findings confirm the effectiveness of the proposed framework in enhancing perceived color harmony while highlighting the distinction between harmony and attractiveness. The method is particularly suited for applications requiring consistent and balanced color presentation, such as design and media.

Keywords: color harmony, image retouching, image enhancement, instance segmentation

INTRODUCTION

With the rapid development of visual communication and digital media, increasing attention has been devoted to the aesthetic quality of images. Color harmony is a critical factor in shaping visual appeal, influencing emotional response, and enhancing communicative effectiveness. However, real-world photographs often contain disharmonious regions caused by hue conflicts, chroma imbalance, or lightness inconsistencies. These issues not only reduce the attractiveness of images but also diminish their communicative value.

Research on color harmony has evolved from geometric rules in color wheels (e.g., Matsuda [1]; Moon and Spencer [2]) to psychophysical models that quantify harmony through differences in hue, chroma, and lightness. Ou and Luo [3] introduced a regression-based model for two-color combinations, later extended to multi-color and universal frameworks [4,5]. More recently, data-driven methods such as Yang et al. [6] have predicted harmony directly from color datasets, while Xu et al. [7] employed generative adversarial networks to produce harmonious palettes. Although effective for palette-level analysis, these approaches remain limited in addressing contextual and semantic relationships within photographic content.

Li et al. [8] proposed an image recoloring method using geodesic-distance-based color harmonization, where hue histograms were compared against Itten color harmonic templates to find the best global match. While their approach ensures spatially coherent adjustments, it does not differentiate semantically important regions (e.g., human faces, sky) and lacks mechanisms to handle local disharmony between adjacent regions. In other words, although their hue-histogram-based scheme is efficient, it operates at the global template level without considering regional adjacency or semantic constraints.

To address these gaps, this study presents a content-aware color harmony optimization framework. Our method first employs semantic segmentation (SegFormer) [9] to preserve critical regions such as faces and sky. For non-protected areas, mean shift clustering [10] extracts perceptually coherent color regions. A hue histogram is then built to select the most suitable Itten template following Li et al.'s strategy [8], but disharmonious regions are identified not only by template coverage but also by regional adjacency analysis. A region adjacency graph (RAG) is constructed, and Ou's universal color harmony model [5] is applied to compute harmony scores between neighboring clusters. To better reflect spatial importance, we aggregate pairwise harmony scores using an edge-length-weighted scheme proposed in this work. For each disharmonious cluster, candidate colors are generated by sampling hues within the selected Itten template range and slightly adjusting chroma and lightness. The replacement color is chosen as the candidate that yields the highest edge-length-weighted harmony score with its neighbors.

By combining semantic protection, global template guidance, and local adjacency-based optimization, the proposed framework effectively corrects disharmonious regions while preserving naturalness. This work contributes a practical solution for advancing image color harmony optimization and supports applications in photography, design, and digital media.

METHODOLOGY

The overall framework of the proposed image color harmony optimization method is illustrated in Figure 1. The pipeline integrates semantic segmentation, color clustering, hue histogram analysis, harmony evaluation, and adaptive recoloring. The key steps are described in detail as follows.

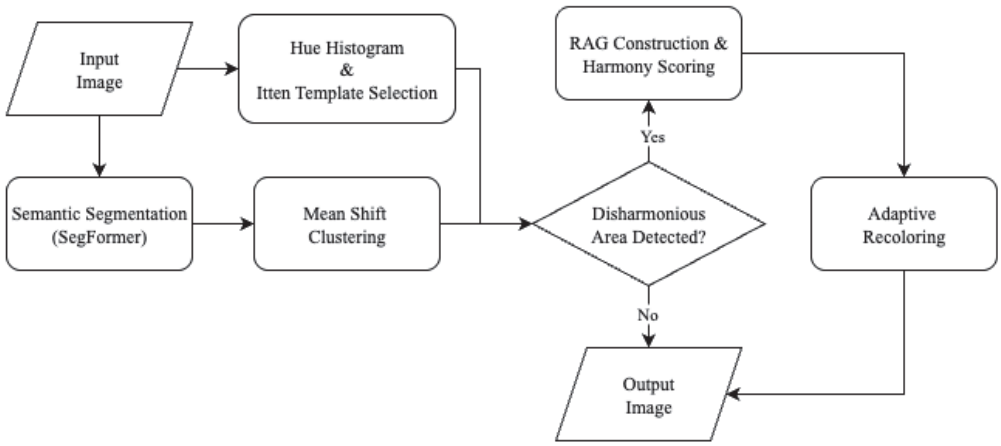

Figure 1. Flowchart of the proposed content-aware color harmony optimization framework.

1. Semantic Segmentation

To preserve semantically important content, SegFormer (pretrained on ADE20K image dataset) [9] is used to generate a pixel-wise label map and construct a binary mask M, marking important regions such as faces and sky as protected to avoid recoloring. Since the *Person* class in ADE20K typically includes clothing, we further refine this mask by intersecting the SegFormer *Person* region with an HSV-based skin prior, resulting in a mask that only preserves skin areas. This ensures that facial and skin regions remain

protected, while apparel pixels can still be adjusted during recoloring. All other non-protected pixels proceed to the subsequent steps.

2. Mean Shift Clustering

Mean Shift Clustering [10] is applied to segment the remaining image regions, using a feature vector that combines lightness-weighted color information (L^*_{wt}, a^*, b^*) with spatial coordinates (x, y). After clustering, each cluster is represented by the average CIELAB color of its pixels, which serves as the cluster's representative color.

3. Hue Histogram and Harmonic Template Selection

Following clustering, a hue histogram is constructed from the entire image to characterize the global hue distribution. To assess global harmony, we adopt the strategy introduced by Li et al. [8], which matches the histogram against Itten's set of harmonic templates (*i*, *V*, *L*, *I*, *T*, *Y*, *X*). The template that maximizes coverage of the histogram is selected as the global reference. Unlike Li et al.'s approach, which directly relocates out-of-template hues using geodesic distances, we retain the selected template as a global constraint while further incorporating local relational analysis at the regional level.

Figure 2. Example images (top) and their corresponding hue histograms with fitted Itten color harmonic templates (bottom). The histograms illustrate the hue distribution of each image, and the gray areas denote the template sectors used to evaluate global color harmony.

4. Disharmonious Region Detection

After mean shift clustering, each cluster is evaluated against the selected Itten template. Specifically, we compute the proportion of pixels within each cluster whose hue values fall inside the template's harmonic sectors. If this coverage ratio is below a predefined threshold (e.g., 60%), the cluster is marked as a disharmonious region. This procedure ensures that clusters dominated by hues outside the harmonic template are identified for subsequent optimization.

This cluster-level detection, combined with the global histogram-based template selection, distinguishes our method from that of Li et al. [8], which operates only at the global image level. By localizing disharmony to specific clusters, our approach preserves global harmonic consistency while enabling targeted adjustments to regions that disrupt harmony. The clusters marked as disharmonious are then passed to the subsequent RAG construction and harmony scoring stage, where the most suitable harmonious replacement color is determined.

5. Harmony Scoring and Adaptive Recoloring

To optimize disharmonious regions, we integrate regional adjacency analysis with adaptive recoloring. A region adjacency graph (RAG) is first constructed from the mean shift clustering result, where each node represents a color region and edges denote spatial adjacency. This representation enables us to consider not only individual clusters but also their contextual relationships. For each edge, harmony is quantified using Ou's universal color harmony model [5], which evaluates differences in hue, chroma, and lightness between adjacent regions. To better reflect perceptual importance, we introduce an edge-length-weighted scheme that aggregates pairwise harmony scores by giving stronger influence to longer shared boundaries.

Clusters previously identified as disharmonious are then recolored in an adaptive manner. For each target cluster, candidate colors are generated by sampling hues within the allowable sectors of the selected Itten template and applying controlled adjustments to chroma and lightness. Each candidate is assessed by recalculating its edge-length-weighted harmony score with all neighboring regions, and the candidate that maximizes the overall weighted score is chosen as the replacement color.

At the core of this evaluation, Ou's universal color harmony model [5] defines the pairwise harmony score between two regions with CIELAB coordinates (L_1, a_1, b_1) and (L_2, a_2, b_2) as

$$CH_U = CH_{\Delta H} + CH_{\Delta C} + CH_{\Delta L} + CH_{L_{sum}} \quad (1)$$

where $CH_{\Delta H}$, $CH_{\Delta C}$, $CH_{\Delta L}$ represent the contributions from hue, chroma, and lightness differences, respectively, and $CH_{L_{sum}}$ accounts for the combined lightness of the two regions.
Each component is approximated using hyperbolic tangent functions to reflect the nonlinear response of human visual perception.
For example,

$$CH_{\Delta H} = -0.7tanh(-0.7 + 0.04\Delta H^*_{ab}) \quad (2)$$

and similar forms are used for $CH_{\Delta C}$, $CH_{\Delta L}$, $CH_{L_{sum}}$.

By combining RAG-based evaluation with adaptive recoloring, the method corrects local disharmony while maintaining global template consistency and semantic naturalness. Unlike previous approaches such as Li et al. [9], which only relocate hues globally based on histogram–template matching, our framework explicitly incorporates spatial adjacency, edge-length weighting, and candidate color search, enabling more precise and content-aware harmony optimization.

RESULTS AND DISCUSSION

We collected judgments from 30 young participants (19 male, 11 female), including 14 with design/art backgrounds, on 11 image pairs. For each pair, participants viewed the original image and the algorithm output and answered two forced-choice questions: which version looked more harmonious, and which looked more attractive.

Across all responses, the algorithm output was selected as more harmonious in 83% of trials. At the per-item level, nearly half of the images (5 out of 11) exceeded 90% preference, and most remaining items exceeded 70% (Fig. 3a). These results indicate a strong and consistent improvement in perceived color harmony.

By contrast, the algorithm output was judged as more attractive in an average of only 57% of trials, with higher variability across items (Fig. 3b). Although some items reached above 70–80%, several were close to or below chance level, indicating cases where the original was aesthetically preferred.

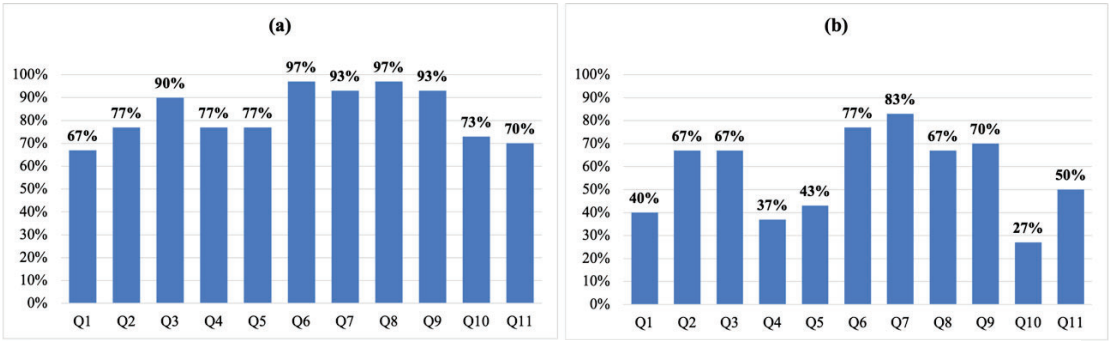

Figure 3. Proportion of 11 optimized images judged as (a) more harmonious, and (b) more attractive.

Plotting per-item harmony (x-axis) vs. attractiveness (y-axis) reveals the relationship between the two judgments (Fig.4). Most items fall to the right of 50% on the x-axis (harmony improved), but several points lie below 50% on the y-axis (attractiveness not improved to the same extent). A subset lies in the upper-right quadrant (both harmony and attractiveness improved), representing the most favorable cases of the algorithm.

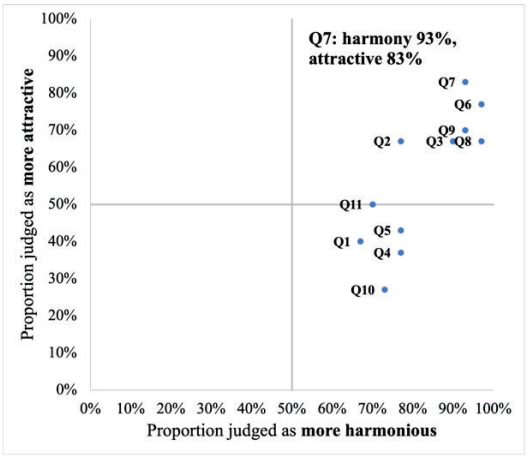

Figure 4. Proportion judged as more harmonious vs. more attractive (per image pair)

Before **After** **Before** **After**

Figure 5. The left image pair (Q7) is located in the first quadrant in Fig. 4, representing image pairs where both harmony and attractiveness improved after recoloring. The right image pair (Q2), where 77% of participants judged the recolored image as more harmonious, only 67% considered it more attractive.

CONCLUSION

This study proposed a color harmony optimization method that integrates semantic segmentation, mean-shift clustering, Itten's color harmony templates, and Ou's universal color harmony model to detect and recolor disharmonious regions in images. Results from a perceptual experiment with 30 participants showed that the optimized images were judged as more harmonious in 83% of trials, with nearly half of the items (5 out of 11) exceeding 90%. These findings confirm the effectiveness of the proposed method in consistently enhancing perceived color harmony.

However, the experiment also revealed that improvements in harmony do not always translate into higher attractiveness, with an average attractiveness preference of only 57%. This indicates that color harmony represents just one dimension of aesthetic preference, and that visual appeal may also depend on factors such as vividness, contrast, and semantic content.

The proposed approach is particularly beneficial for applications requiring balanced and consistent visual presentation, such as graphic design, branding, and user interface imaging. In contrast, artistic or photographic domains may sometimes favor intentional dissonance to create visual impact. Future work will explore multi-objective optimization strategies that jointly consider harmony and attractiveness, and develop content-aware adjustments that adapt to different image contexts.

REFERENCES

[1] Matsuda, Y. (1995). *Color design*, Asakura Shoten, 10.

[2] Moon, P. and Spencer, D. E. (1944). Geometric formulation of classical color harmony, *Journal of the Optical Society of America*, 34(1), 46–59.

[3] Ou, L. C., & Luo, M. R. (2006). A colour harmony model for two-colour combinations. *Color Research & Application*, 31(3), 191–204. https://doi.org/10.1002/col.20208

[4] Ou, L. C., Chong, P., Luo, M. R., & Minchew, C. (2011). Additivity of colour harmony. *Color Research & Application*, 36(5), 355–372. https://doi.org/10.1002/col.20624

[5] Ou, L. C., Yuan, Y., Sato, T., et al. (2018). Universal models of colour emotion and colour harmony. *Color Research & Application*, 43(5), 736–748. https://doi.org/10.1002/col.22243

[6] Yang, B., Wei, T., Fang, X., et al. (2019). A color-pair based approach for accurate color harmony estimation. *Computer Graphics Forum*, 38(7), 481–490. https://doi.org/10.1111/cgf.13854

[7] Xu, L., Liu, D., Park, S.J. and Lee, S. (2025). Unified color harmony model. *Color Research & Application*, 50: 346-371. https://doi.org/10.1002/col.22977

[8] Li, X., Zhao, H., Nie, G. *et al.* (2015). Image recoloring using geodesic distance based color harmonization. *Comp. Visual Media* 1, 143–155. https://doi.org/10.1007/s41095-015-0013-5

[9] Xie, E., Wang, W., Yu, Z., Anandkumar, A., Alvarez, J. M., and Luo, P. (2021). SegFormer: Simple and efficient design for semantic segmentation with transformers. *Advances in Neural Information Processing Systems,* 34, 12077-12090. https://doi.org/10.48550/arXiv.2105.15203

[10] Cheng, Y. (1995). Mean shift, mode seeking, and clustering. *IEEE Transactions on Pattern Analysis and Machine Intelligence*,.17(8), 790-799. https://ieeexplore.ieee.org/document/400568

A Perceptually Neutral White Locus Integrating A Warm-Cool Scale

Jung-En Chang and Li-Chen Ou *

National Taiwan University of Science and Technology, Taipei, Taiwan
**Corresponding author: Li-Chen Ou, lichenou@mail.ntust.edu.tw*

ABSTRACT

This study conducted four psychophysical experiments in a dark room to investigate the perceived neutrality of white stimuli across a range of CCT and Duv values. A calibrated 22.5-inch LCD was used to present colour patches of equal luminance against a black background for paired comparisons throughout the study. A panel of 30 observers with normal colour vision participated in each experimental session. Results of Experiments 1 and 2 suggest that the most neutral white corresponds to CIE Illuminant D75, specified at 7504K with a Duv of 0.0031. A predictive model of perceived neutrality was developed in the form as a neutral white locus extending from 3000K to 10000K. Based on results of Experiment 3 and 4, a new warm-cool model was developed as a linear function of the CIE 1976 u′ and v′ chromaticity coordinates, allowing warm-cool predictions without the need for perceptual attributes such as hue angle. In this model, the warmth perception is defined by the signed distance to a "reference line" in the u′v′ chromaticity diagram, which passes through D75, identified in Experiments 1 and 2 as the most neutral white. Building on this, the study introduces a warm-cool scale (W_n), offering significantly improved perceptual uniformity over CCT. The integration of the W_n scale with the neutral white locus offers a perceptual alternative to the Planckian locus and CCT.

Keywords: neutral white, warm-cool, Planckian locus, correlated colour temperature

INTRODUCTION

The characteristics of white light, whether serving as a light source in lighting applications or as the white point for displays, are typically represented by the correlated colour temperature (CCT) to indicate the warm-cool tint, and the distance to the Planckian locus (Duv) to indicate the yellow-pink tint. Nevertheless, CCT lacks psychophysical relevance and perceptual uniformity. Defining neutral white using Duv at a specified CCT remains inconclusive, as the existing studies have yielded inconsistent results. These issues complicate the colour selection for neutral white based on the Planckian locus and CCT. This study conducted four psychophysical experiments in a dark room to investigate the perceived neutrality of white stimuli across a wide range of CCT and Duv values, and the perceived warmth across a broad range of chromaticities. The objective was to develop a neutral white locus and to integrate this locus with a warm-cool scale in the CIE 1976 u′v′ chromaticity diagram.

METHODS

Four psychophysical experiments were conducted in this study. A calibrated 22.5-inch LCD screen (EIZO CG232W) was used as the presentation medium. During the experiments, colour patches of equal luminance were presented on the LCD for paired comparisons, conducted in a dark room. Figs. 1 (a) and (b) illustrate the presentation of the stimuli used in the four experiments. The two test patches, each measuring 80 mm by 80 mm, were presented side by side with a 0.25 mm-wide gap between them. Both the gap and the background were black.

The viewing distance from the observer was 500 mm. To mitigate the typical light-leakage issue in LCDs, a black cardboard with a rectangular opening exposing the two test patches was placed over the display.

(a) (b)

Figure 1: Schematic illustration of visual presentations in (a) Experiments 1, 2 and 3, and (b) Experiment 4

The aim of Experiment 1 was to investigate the effect of Duv on the perceived neutrality. Two “white” patches were displayed side by side on a black background per trial. The observer selected the patch that appeared "less tinted". The stimuli included 25 “white” colours with 5 CCT levels (3000K, 4000K, 5000K, 6500K and 9500K) and 5 Duv levels (0.010, 0.005, 0, -0.005 and -0.010). The luminance value of all stimuli was 70 cd/m². Each trial compared patches with the same CCT but different Duv values, resulting in C(5, 2) x 5 = 50 pairs for each observer to complete. Experiment 2 examined how CCT affected the perceived neutrality. The experiment employed similar methods to Experiment 1 but had 25 stimuli with a different set of CCT levels: 5000K, 5700K, 6500K, 7700K and 9500K, while maintaining the same set of Duv level. The luminance value of all stimuli was 70 cd/m². Observers were tasked with selecting the patch that appeared "less tinted" from a pair that had the same Duv but different CCT values. Like in Experiment 1, each observer completed 50 paired comparisons. The aim of Experiment 3 was to investigate the relationship between “white” stimuli and the warm-cool perception. It used similar methods to Experiment 1, including the same set of “white” patches, but the observers were tasked with selecting the patch that appeared "warmer". Each observer completed all possible pair combinations of the 25 stimuli, resulting in 300 pairs for comparison. Experiment 4 studied the connection between chromatic colours and warm-cool perception. The methods used were similar to Experiment 3, involving 15 chromatic stimuli selected to provide a broad range of chromaticities. The luminance value of all stimuli was 26 cd/m². Each observer completed comparisons of all possible pair combinations of the 15 stimuli, totaling 105 pairs.

A panel of 30 observers (15 males and 15 females) with normal colour vision participated in each experiment. The observers were aged 19 to 29 years (M = 22). Prior to the experiment, each observer spent 10 minutes adapting to dark condition in the experimental room. Each pair of test patches was then presented on the LCD for 5 seconds, followed by a full black screen, during which the observer was prompted to use the arrow keys on a computer keyboard to select the patch that appeared “less tinted” for Experiments 1 and 2, and “warmer” for Experiments 3 and 4. After pressing the space key to confirm the selection, a full black screen was shown for 2 seconds before the next pair of test patches appeared. All stimulus pairs were presented in a random order.

RESULTS

Effect of Duv on perceived neutrality

The aim of Experiment 1 was to examine the effect of Duv on perceived neutrality using the paired comparison method. In each trial, white patches with the same CCT but different Duv values were compared. Accordingly, the 25 white stimuli were grouped into 5 CCT levels, each containing 5 Duv levels. Scale values of perceived neutrality were calculated within each CCT group and incomparable across different CCT groups. Therefore, the results of Experiment 1 illustrated how Duv affected the perceived neutrality of white stimuli, independent of CCT. Fig. 2

shows the fitted curve plotted on the CIE 1976 u′v′ chromaticity diagram, illustrating its relationship with CIE Illuminant D series. The curve closely aligns with the positions of the D series, particularly D75 and D65.

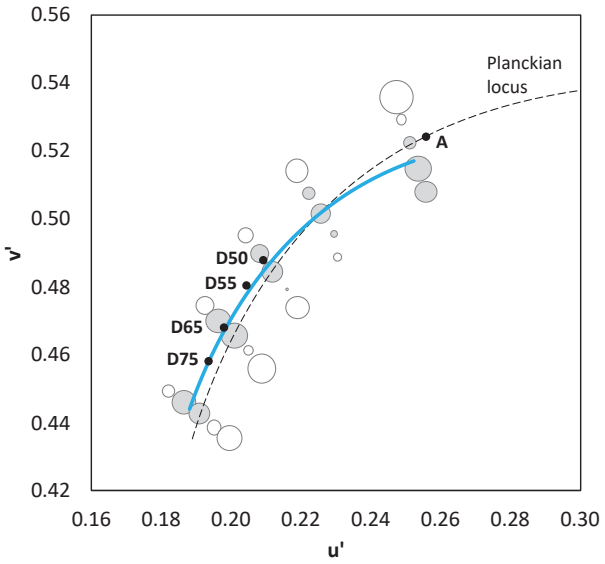

Figure 2: Bubble chart from Experiment 1 displaying scale values of perceived neutrality, with CIE Standard Illuminants and a fitted curve overlaid in the CIE 1976 u'v' chromaticity diagram

Effect of CCT on perceived neutrality

Based on the u′v′ chromaticity coordinates of each stimulus, a bivariate Gaussian function was fitted to the scale values of perceived neutrality from Experiment 2, with central coordinates ($\mu_{u'}$, $\mu_{v'}$) = (0.1938, 0.4593), standard deviations ($\sigma_{u'}$, $\sigma_{v'}$) = (0.0154, 0.0213), and a correlation parameter $\rho_{u'v'}$ = -0.0112, as shown in Fig. 3. The bivariate Gaussian function shows a correlation coefficient of 0.97 with the scale values.

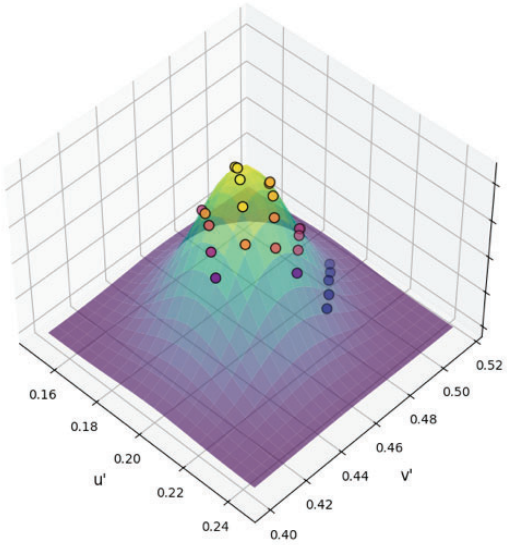

Figure 3: The fitted bivariate Gaussian function for estimating scale values of perceived neutrality based on the results of Experiment 2

The CCT values associated with maximum perceived neutrality were estimated: (1) the highest value of perceived neutrality occur at 7700K across all Duv groups, and (2) the fitted bivariate Gaussian function (in the u′v′ chromaticity diagram) peaks at 7424K. According to the combined results of Experiments 1 and 2, it seems reasonable to assume that the most neutral white corresponds to CIE Illuminant D75, specified at 7504K with a Duv of 0.0031. Thus, a model of perceived neutrality in white stimuli was developed, in the form as a neutral white locus spanning from 3000K to 10000K and passing through D75. The model is defined by the Duv value, denoted as Duv_w, expressed as a function of CCT:

$$Duv_w = 0.00343 \times \left(1 - 13 \times 0.5^{\frac{T-209}{1021}}\right) \quad (1)$$

where *T* is the CCT value. The model is represented by the cyan solid line in Fig. 4.

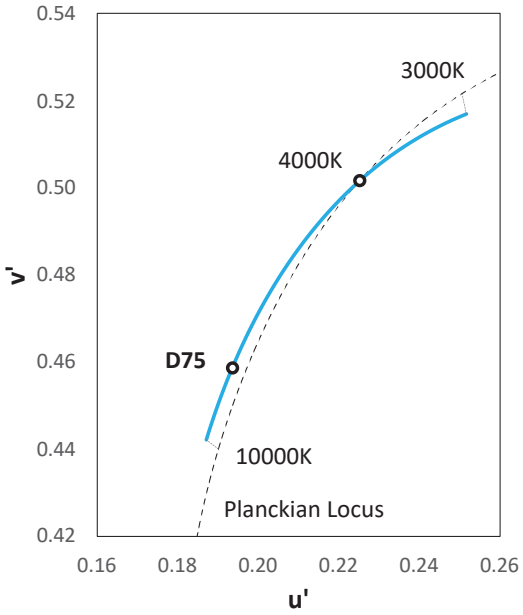

Figure 4: The proposed neutral white locus (cyan solid line)

Correlation between chromaticity and perceived warmth

Experiments 3 and 4 show that increasing u′ and v′ values leads to a higher perceived warmth. By combining these results with the authors' previous colour emotion data [1], a new warm-cool model based on the u′v′ chromaticity diagram was derived, represented as a linear function of u′ and v′, as described in Eq. (2):

$$\text{Warmth} = k \times \frac{a\,u' + b\,v' + c}{\sqrt{a^2 + b^2}} \quad (2)$$

where u' and v' represent the CIE 1976 u'v' chromaticity coordinates. Values of parameters *k*, *a*, *b* and *c* are listed in Table 1.

Table 1: Parameter values in Eq. (2)

Parameter	k	a	b	c
Value	1298.3	2.2175	1	-0.8877

This function calculates the signed distance from any point in the u′v′ chromaticity diagram to a "reference line", defined by $au' + bv' + c = 0$. Colours located on this line are perceived as neither warm nor cool. The reference line passes through D75, which was identified as the most neutral white from Experiments 1 and 2.

Fig. 5 shows the NCS unique hues under D75. Unique reds and unique yellows are located on the right side of the "reference line," while unique greens and unique blues on the left. This distribution appears to support the locational validity of the reference line. The model shows strong agreement with the visual results of the present study, with correlation coefficients of 0.958 for data from Experiment 3, and 0.963 for Experiment 4.

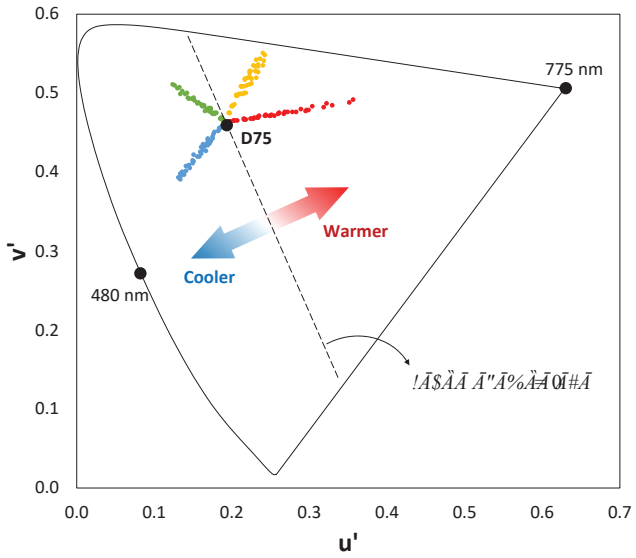

Figure 5: Schematic illustration of the new warm-cool model described by Eq. (2)

A warm-cool model integrated with the neutral white locus

Based on Eq. (1), the chromaticity coordinates of the neutral white locus were determined for each corresponding CCT. These coordinates were used in Eq. (2) to calculate the warmth values along the locus. The relationship between the warmth value (W_n) and the corresponding CCT is expressed by:

$$W_n = -31.18 \times \left(1 - 19.75 \times 0.04^{\frac{T^{0.71}}{610}}\right) \quad (3)$$

where W_n represents the warmth value for colours located on the neutral white locus. T represents CCT value.

By combining these results, the relationship between the chromaticity coordinates of a colour on the neutral white locus and the associated warmth value (W_n) was established, as expressed by:

$$u'_n = 0.1249 \times \left(1 + 0.5525 \times 1.8524^{\frac{W_n}{101.34}}\right) \quad (4)$$

$$v'_n = 0.5465 \times \left(1 - 0.1612 \times 0.4787^{\frac{W_n}{66.16}}\right) \quad (5)$$

where u'_n and v'_n represent the u'v' chromaticity coordinates for any colour on the neutral white locus at a given W_n. Fig. 6 shows the resulting integration of the warm-cool scale (W_n) with the neutral white locus.

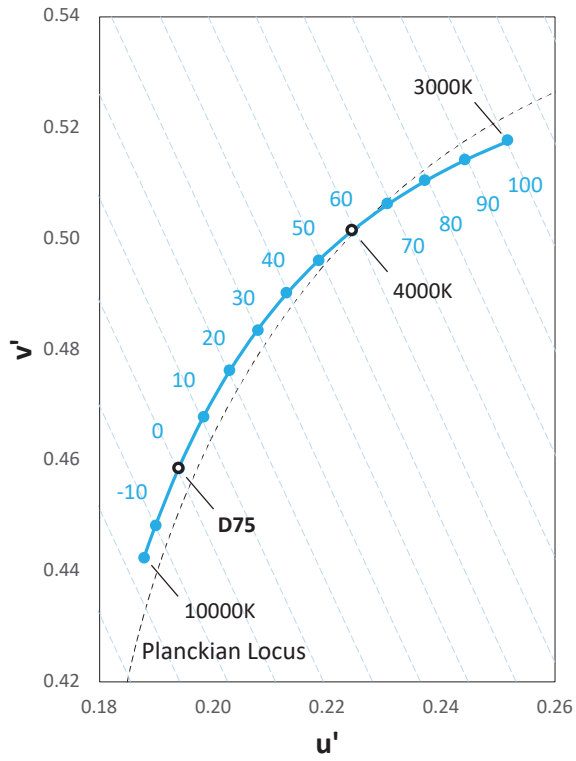

Figure 6: The warm-cool scale (W_n), as indicated by the cyan numbers, is integrated with the neutral white locus (cyan solid line). The pale-cyan dashed lines represent equal perceived warmth.

CONCLUSION

A new neutral white locus was developed in this study, as defined by Eq. (1) and shown in Figs. 4 and 6. Note that this new locus is valid only within the CCT range of 3000K to 10000K. The most neutral white identified in this study closely aligns with the results reported by Vogels and Heynderickx [2], Choi and Suk [3] and Huang et al. [4], all of which are located close to D75. The proposed neutral white locus incorporates the warm-cool scale, as defined by Eqs. (3)-(5), making it a useful tool for applications in related areas. Note that the present study employed an LCD as the medium for presenting white stimuli. The extent to which the findings of this study generalize to interior lighting remains uncertain and will require empirical verification in future research.

REFERENCES

[1]. Ou, L.-C., Yuan, Y., Sato, T., Lee, W. Y., Szabó, F., Sueeprasan, S., & Huertas, R. (2018). Universal models of colour emotion and colour harmony. Color Research & Application, 43(5), 736-748.

[2]. Vogels, I. M., & Heynderickx, I. E. J. (2004). Optimal and acceptable white-point settings of a display. Proceedings of the 12th Color and Imaging Conference, 233-238.

[3]. Choi, K., & Suk, H. J. (2016). Assessment of white for displays under dark- and chromatic-adapted conditions. Optics Express, 24(25), 28945-28957.

[4]. Huang, H. P., Wei, M., & Ou, L.-C. (2018). White appearance of a tablet display under different ambient lighting conditions. Optics Express, 26(4), 5018-5030.

Controlled Dissonance in Contemporary Design: Exploring Chromatic Tension for Emotional Impact and Perceived Quality in Enclosed Spaces

Sandhiya Jayaprakash Brindha[a*], Pankaj Daultrao Surve[b]

[a]*Tata Technologies, Pune, India*
[b]*Tata Motors, Pune, India*
[*]*Corresponding author: Sandhiya Jayaprakash Brindha, sandhiyajb@gmail.com*

ABSTRACT

While classical color theory often equates harmony with quality and comfort, contemporary design practice increasingly leverages calibrated tension to create focus, memorability, and brand distinction. This narrative review synthesizes evidence relevant to controlled dissonance in enclosed spaces (e.g., automotive cabins, compact interiors) across four streams: harmony models and critiques, affective/cognitive responses, cultural/brand/lighting moderators, and cross-industry Color Material Finish (CMF) precedents [1–10,16–23]. We organize findings into a tension spectrum from flat harmony to visual chaos, with a middle zone of controlled dissonance that can heighten engagement without degrading comfort. As context, we report brief online appraisals: experts rated case images; consumers rated palettes. In this convenience sample, perceived value tended to increase with harmony, while mid-tension palettes scored relatively higher on engagement. We provide design guidance on proportion, placement, value structure, finish pairing, and an Environmental Envelope moderator (Equatorial/Temperate/Overcast). The discussion concludes with a proposed design vocabulary for controlled dissonance.
Ethics/Compliance: Secondary sources only; online appraisals were anonymous and non-identifiable.

Keywords: controlled dissonance, perceived quality, visual comfort, enclosed spaces, automotive interiors

INTRODUCTION

Classic harmony ‘recipes’ (analogous, complementary, triadic) were widely taught as routes to quality and ease of viewing [1–3]. Recent empirical work shows that harmony depends less on wheel geometry and more on value structure, chroma balance, and proportion—particularly in multi-hue, real-material contexts [4–7]. Design practice demonstrates that intentionally dissonant accents (small area, high contrast) can sharpen focus and distinctiveness without undermining comfort [8–10].

Enclosed spaces amplify color decisions: surfaces are near, exposure is prolonged, and lighting is constrained. The question is not whether harmony is ‘good,’ but where on a spectrum of tension designers should position a palette to maximize perceived value and engagement, given brand and context. Evidence is scattered across psychophysics, consumer research, CMF case studies, and neuroaesthetics; a consolidated, practice-oriented synthesis is needed. We aim to: (i) Synthesize multidisciplinary findings bearing on chromatic tension. (ii) Articulate a tension spectrum with designable parameters and propose a design vocabulary for controlled dissonance.

METHODOLOGY

This paper is a narrative literature review and design-led synthesis. We surveyed peer-reviewed studies and books on harmony theories and critiques, affective/cognitive responses, cultural/brand/lighting moderators, and cross-industry CMF precedents [1–10,11–15,16–23]. No hypothesis-testing experiments were conducted. Online appraisals: Experts (n = 5) from various industries rated 10 case images on harmony/tension, perceived value, comfort in enclosed space, engagement, and brand fit; consumers (n = 22) rated 12 palettes on liking and perceived value. These snapshots are illustrative: viewing was on uncontrolled, non-calibrated screens, and stimuli were screen renderings rather than physical CMF boards.

RESULTS AND DISCUSSION

Across the literature, harmony rises with coherent luminance relations, moderated chroma, and restricted hue count; categorical wheel relations are neither necessary nor sufficient [4–7]. Perceived quality often increases with order when large areas are involved [5–6,12]. Conversely, small-area high-contrast cues can add focus and memorability without undermining comfort when value hierarchy and finish pairing are calibrated to the base [8–10,21–23]. From vision science, moderate novelty/contrast increases attention and arousal, whereas extremes fragment or fatigue [11,13–15]. Consumer/retail evidence similarly shows that sparing contrast improves distinctiveness if overall order is preserved [9,18–19].

Psychology and neuroaesthetics of tension: Human affect tracks chromatic relationships: harmonious pairings tend to be rated more pleasant, while strong clashes raise arousal and can provoke aversive responses [6]. fMRI data show disharmonious pairs selectively recruit the amygdala, whereas harmonious pairs recruit medial orbitofrontal cortex (mOFC) associated with reward and aesthetic pleasure [28]. Behavioral results separate preference from harmony: people may prefer a figure color that strongly contrasts its background even as overall "harmony" ratings decrease [5]. Harmony can also support visual short-term memory capacity, whereas dissonance can increase salience and memorability of focal elements [5,30].

Cross-cultural calibration: Baseline color meanings and acceptable contrast vary across cultures [24-27]. Some audiences prefer cohesive, analogous sets (e.g., Japanese samples), while others more readily choose contrast for uniqueness (e.g., European Americans) [26]. Consequently, the threshold at which dissonance becomes "too much" differs by context [13,16].

Design precedents: Jaglarz documents architecture where high-contrast facades are judged aggressive yet also serve as memorable signposts [31]. The VW Golf Harlequin's patchwork color-blocking became a cult icon because of its audacious dissonance [32]. Memphis furniture leveraged purposeful clashes to signal play and anti-establishment energy [33]. CMF practice in vehicles uses bright accents to energize muted cabins [34].

Implications for enclosed spaces. Aim for controlled dissonance via: (a) accent proportion ≈5–20% of visible area; (b) clear lightness (value) contrast to maintain legibility; (c) purposeful hue contrast; and (d) complementary finishes to manage glare and harsh edges. Preferences are moderated by brand codes, culture, and lighting; validate palettes under intended illuminants and illuminance levels [16–20,22].

Experts' appraisal positioned 10 cross-industry cases on the tension spectrum. High harmony with strong value hierarchy scored highest on perceived value. Experts endorsed controlled dissonance when accent area was small, value contrast was legible, and finishes were complementary (e.g., contrast stitching, instrument bezels). Equal-area multi-hue clashes fell toward chaos with lower quality signals. Brand fit moderated tolerance

(performance/tech > heritage-luxury). To operationalize the spectrum, Figure 1 summarizes expert placements across cases.

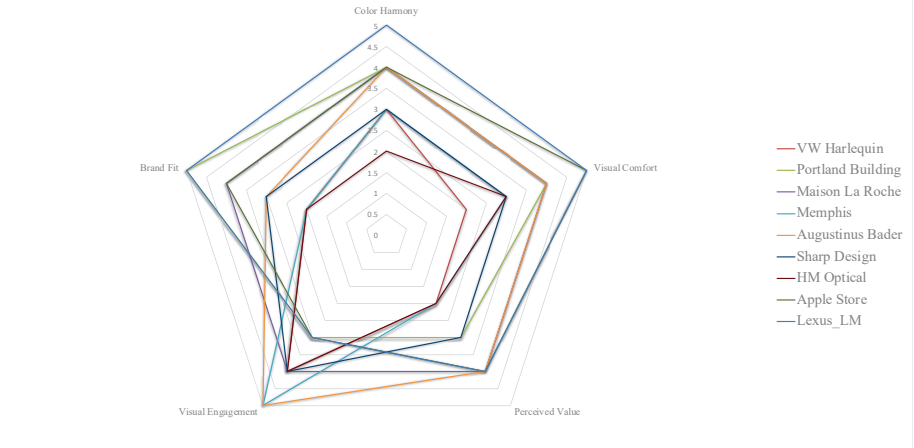

Figure 1: Expert review of case studies

Table 1 lists designable parameter bands (area, ΔL*, Δh°, ΔC*, hue count, finish, placement, lighting) for the controlled-dissonance window.

Table 1: Tension spectrum with designable parameters

Parameter	Definition / units	Target band	Below band (Flat Harmony)	Above band (Chaos)	Practical notes
Accent area (A)	Share of visible surfaces assigned to accent color(s)	5–20%	Under-differentiated, flat harmony	Busy/fragmented; fatigue/chaos risk	Start 10–15% for performance/tech; ≤10% for overcast envelopes; keep driver sightlines calm
ΔL* (lightness contrast)	L* difference between base and accent (CIE L*C*h°)	25–40	Low legibility; dull	"Cut-out"/harsh; glare if glossy	Judge under intended illuminance; raise contrast if both finishes are matte
Δh° (Hue separation)	Shortest hue-angle difference (degrees, CIE L*C*h°)	30°–80°	Near-harmony; low focus	Opponent clash; vibrating boundaries at high chroma	Prefer categorical distance without pushing to complementary at high chroma
ΔC* (chroma difference)	C* difference between base and accent	15–35	Too similar; low salience	Garish unless area is tiny	Pair higher chroma with smaller area and softer sheen

Parameter	Definition / units	Target band	Below band (Flat Harmony)	Above band (Chaos)	Practical notes
Main hues (N)	Count of dominant hues (excl. neutrals)	≤3 (1–2 base + 1 accent)	N=1: calm, low distinctiveness	Clutter; chaos risk	Aim ~70/25/5 dominance split
Finish contrast	Gloss/texture delta	Moderate (matte /satin base; restrained gloss/brushed accent)	Mushy boundaries	Specular glare; perceived "cheapness"	Avoid high gloss on large fields; use sheen to support hierarchy
Placement	Where accent appears	Focal/interaction points, bezels/edges (not large diffuse fields)	Accent unseen/irrelevant	Visual noise, unstable field	Keep accents out of reflective windscreen zones; ensure tactile congruence
Lighting validation	Illuminants & lux	Verify under 2700/4000/6500 K at intended lux	Unverified; color/finish shifts	—	Recheck in Equatorial / Temperate / Overcast envelopes as applicable

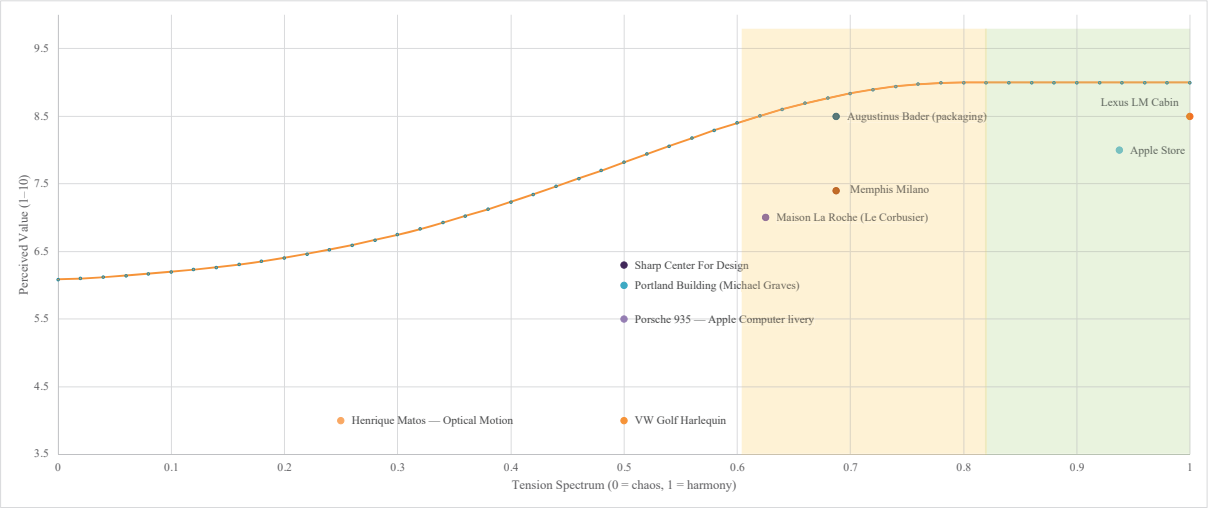

Figure 2: Tension Spectrum (conceptual; enclosed spaces)

X: Chaos (0) → Harmony (1); Y: Perceived Value (1–10).

High Value Zone, Amber 0.60–0.82: controlled dissonance—coherent base + small, well-placed high-contrast accents. Green ≥ 0.82: high-harmony luxury. Curve is conceptual (not a fit).

Expert ratings show an inverse association between harmony and visual engagement across cases—indicating a tunable trade-off for palettes as shown in Figure 3.

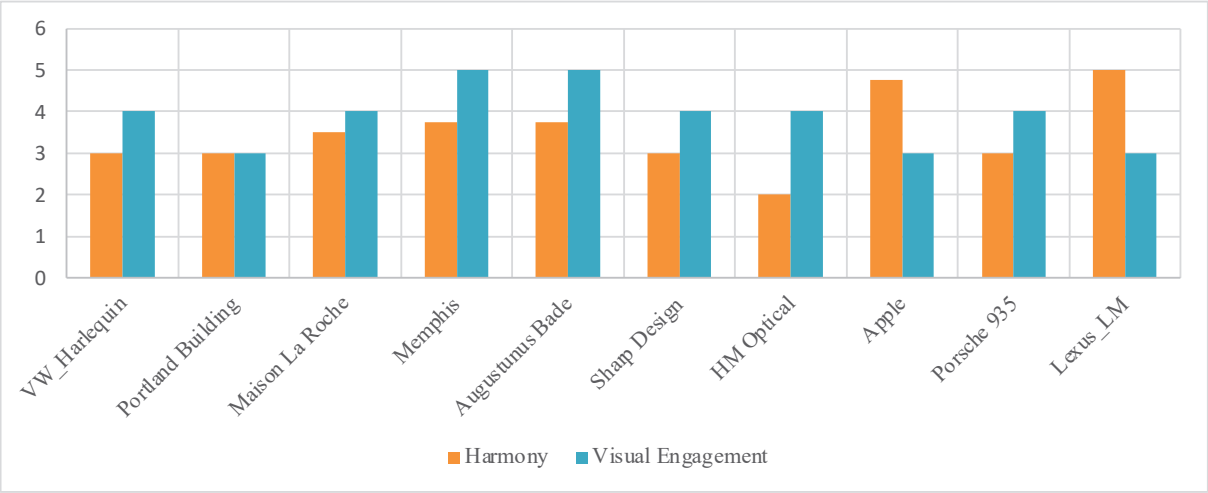

Figure 3: Harmony vs Visual Engagement

Online appraisals by Consumers tended to associate higher perceived value equally with higher harmony and controlled dissonance, while mid-tension palettes were relatively more engaging. However, the likability of the palette did not have a direct relation with the color harmony.

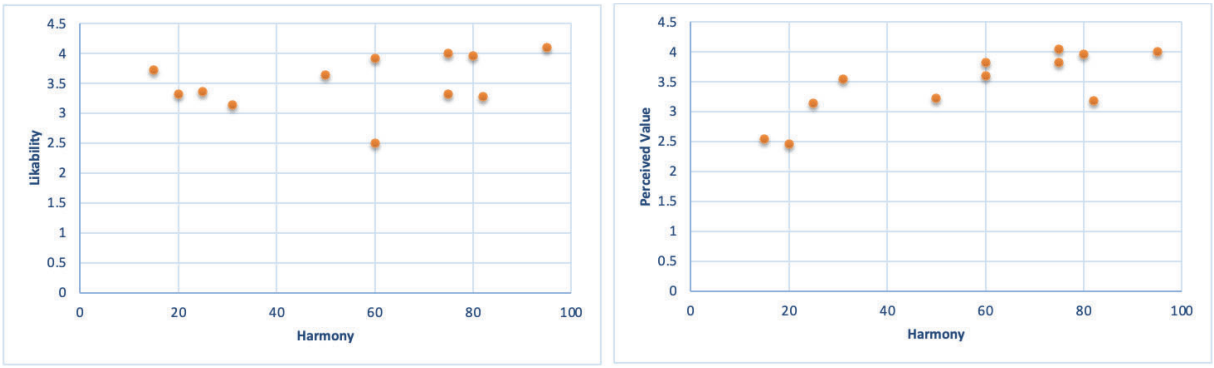

Figure 4: Left – Likability vs Harmony, right – Perceived Value vs Harmony

CONCLUSION

Controlled color dissonance should be treated as an extension of harmony for enclosed spaces. The review indicates that harmony and perceived quality align when large areas dominate, yet calibrated accents (~5–20%) can raise engagement and distinctiveness when value structure and finish pairing are respected. Our online snapshots echo this: consumers (on screens) equate premium with harmony, while experts accept dissonance in small, well-placed cues. Practically, the optimal point on the spectrum is context-bound—shaped by lighting envelope, brand semantics, and material expressivity. Next steps include materials-in-hand studies varying accent proportion, placement, hue vs value contrast, and finish under calibrated lighting (e.g., 2700/4000/6500 K), with cross-cultural sampling to define actionable tolerances.

Design vocabulary for controlled dissonance,

Field / Accent / Trim: Dominant base(s), focal high-chroma elements, and connective darks/metals that mediate between them.

Anchor neutral: Low-chroma base that stabilizes the composition and absorbs contrast.

Tension vector: The combined effect of hue distance, chroma difference, and luminance contrast between elements.

Chroma gate: Context-dependent ceiling on accent chroma to avoid glare/fatigue in long-dwell spaces.

Area ratio: Relative proportion of accent vs. field; small-area bright against larger calm fields signal intent.

Finish modulation: Use of matte/satin/translucent finishes and micro-texture to soften intense pairings.

Dwell-time factor: Expected exposure duration (e.g., cabin vs. transient retail) that shifts acceptable tension.

Cultural tolerance band: Local norms that push the comfort window up/down for saturation and clash.

Functional hierarchy: Priority for legibility and affordance cues (controls, warnings, wayfinding).

Resolution move: A balancing gesture that "answers" a clash elsewhere.

REFERENCES

[1] Itten, J. (1961). The Art of Color. *New York: Van Nostrand*.

[2] Chevreul, M.-E. (1839/1967). The Principles of Harmony and Contrast of Colors. *New York: Reinhold*.

[3] Munsell, A. H. (1915). A Color Notation. *Boston: Munsell*.

[4] Ou, L.-C., & Luo, M. R. (2006). A color harmony model for two-color combinations. *Color Research & Application*, 31(3), 191–204.

[5] Schloss, K. B., & Palmer, S. E. (2011). Aesthetic response to color combinations: Preference, harmony, and similarity. *Attention, Perception, & Psychophysics*, 73(2), 551–571.

[6] Palmer, S. E., & Schloss, K. B. (2010). An ecological valence theory of human color preference. *PNAS*, 107(19), 8877–8882.

[7] Jonauskaite, D., et al. (2020). Color–emotion associations in individuals and cultures. *Journal of Cross-Cultural Psychology*, 51(7–8), 1–23.

[8] Hagtvedt, H., & Patrick, V. M. (2008). Art infusion and luxury perceptions. *Journal of Marketing Research*, 45(3), 379–389.

[9] Labrecque, L. I., & Milne, G. R. (2012). Exciting red and competent blue: The importance of color in marketing. *Journal of the Academy of Marketing Science*, 40(5), 711–727.

[10] Reimann, M., Zaichkowsky, J., Neuhaus, C., Bender, T., & Weber, B. (2010). Aesthetic package design: An fMRI study. *Journal of Consumer Psychology*, 20(4), 431–441.

[11] Leder, H., Belke, B., Oeberst, A., & Augustin, D. (2004). A model of aesthetic appreciation and judgments. *British Journal of Psychology*, 95(4), 489–508.

[12] Bar, M., & Neta, M. (2006). Humans prefer curved visual objects. *Psychological Science*, 17(8), 645–648.

[13] Zeki, S. (1999). Inner Vision: An Exploration of Art and the Brain. *Oxford: Oxford University Press*.

[14] Chatterjee, A. (2014). The Aesthetic Brain. *Oxford: Oxford University Press*.

[15] Biederman, I., & Vessel, E. A. (2006). Perceptual pleasure and the brain. *American Scientist*, 94, 247–253.

[16] Boyce, P. (2014). Human Factors in Lighting (3rd ed.). *Boca Raton: CRC Press*.

[17] CIE (2018). Colorimetry (CIE 015:2018*). Vienna: CIE*.

[18] Orth, U., & Malkewitz, K. (2008). Holistic package design and consumer brand impressions. *Journal of Marketing*, 72(3), 64–81.

[19] Bloch, P., Brunel, F., & Arnold, T. (2003). Individual differences in sensitivity to design. *Journal of Consumer Research*, 29(4), 551–565.

[20] Ou, L.-C., Luo, M. R., Sun, P. L., Hu, N. C., & Chen, H. S. (2012). A cross-cultural comparison of color emotion for two-colored combinations. *Color Research & Application*, 37(1), 23–43.

[21] Ashby, M., & Johnson, K. (2014). Materials and Design (3rd ed.). *Oxford: Butterworth-Heinemann*.

[22] Karana, E., Barati, B., Rognoli, V., & Zeeuw van der Laan, A. (2015). Material experiences framework. *International Journal of Design*, 9(2), 35–54.

[23] Norman, D. A. (2004). Emotional Design. *New York: Basic Books*.

[24] Madden, T. J., Hewett, K., & Roth, M. S. (2000). Managing images in different cultures: A cross-national study of color meanings and preferences. *Journal of International Marketing, 8*(4), 90–107.

[25] Saito, M. (2015). Comparative (cross-cultural) color preference and its structure. In R. Luo (Ed.), *Encyclopedia of Color Science and Technology*. Springer.

[26] Ishii, K., et al. (2014). Cultural differences in color associations and preferences: Comparing Asian and Western responses. *Journal of Cross-Cultural Psychology, 45*(4), 568–590.

[27] Mikuni, J., Spee, B. T., Forlani, G., Leder, H., & Steyrl, D. (2024). Cross-cultural comparison of beauty judgments in visual art using machine-learning analysis. *Empirical Studies of the Arts, 42*(1), 3–25.

[28] Ikeda, T., Matsuyoshi, D., Sawamoto, N., Fukuyama, H., & Osaka, N. (2015). Color harmony represented by activity in the medial orbitofrontal cortex and amygdala. *Frontiers in Human Neuroscience, 9*, 382.

[29] Szabó, F., Bodrogi, P., & Schanda, J. (2010). Experimental modeling of color harmony. *Color Research & Application, 35*(1), 34–49.

[30] Sanocki, T., & Sulman, N. (2009). Color harmony increases the capacity of visual short-term memory. *Journal of Vision, 9*(8), 1–13.

[31] Jaglarz, A. (2023). Perception of colour in architecture and urban space. *Buildings, 13*(8), 2000.

[32] Nosowitz, D. (2017, March 9). What makes this special-edition VW from the ’90s look so cool? *Atlas Obscura*.

[33] Design Museum. (2014). *Memphis Group: Awful or Awesome?* Exhibit notes.

[34] Core77 Editors. (2019). A look at six car design specialties, Part 6: The CMF (Color, Material, Finish) designers. *Core77*.

An Investigation of the Emotional Perception of Scarf Colors on Different Skin Tones Based on The Color-Emotion Models and Color-Harmony Models

Chia-I Liao[a*], Wen-Yuan Lee[b]

[a] *The Graduate Institute of Design Science, Tatung University, Taiwan*
[b] *Department of Media Design, Tatung University, Taiwan*
**Corresponding author: Chia-I Liao d11317005@o365.ttu.edu.tw*

ABSTRACT

The combination of scarf color and skin tone has a significant influence on visual perception and emotional response, shaping overall impressions of women. A well-matched scarf and skin color combination can enhance natural beauty, create a balanced aesthetic, and reinforce personal identity. Conversely, unsuitable pairing may disrupt visual harmony and affect the emotional impact of an appearance. Understanding these is essential for individual styling, color psychology, and design applications, offering insights into how color choices can be optimized for self-expression and perception. However, previous studies on color emotion and harmony have only focused on those evoked by color chips or specific color configurations. There is limited research on the impact of different skin tones and scarf color combinations on emotional responses to color.

This study conducted a psychophysical experiment to investigate the emotional perception of scarf-skin color combinations. Forty-nine observers were invited to evaluate 44 scarf-skin color combinations on five scales. Each color combination was displayed individually on the monitor for the observer to assess on five scales. The scales used included "active-passive," "heavy-light," "warm-cool," "harmonious-disharmonious," and "like-dislike."

The emotional perception of scarf–skin color combinations was used to compare with existing models of color emotion and color harmony. The findings showed that universal color emotion models related to Color Activity and Color Weight can reasonably predict emotional responses to scarf–skin color combinations. However, the Color Heat and existing color harmony models demonstrated limited predictive power in this context. The results also suggested that skin color has a minimal impact on the ranking of scarf–skin color combinations across emotion, harmony, and preference scales.

Keywords: Color emotion, Color harmony, Skin tone, fashion design

INTRODUCTION

In recent years, an increasing number of studies have investigated the emotional perception of outfit colors concerning social and interpersonal evaluations. Studies [1,5] have demonstrated that workplace attire can influence public employees' self-perceptions, and appearance plays a critical role in first-impression contexts such as job interviews or client interactions. Garment color, in particular, has been shown to affect perceived attractiveness, especially in cross-gender situations. [1,9,11,16] When clothing becomes an extension of one's professional identity, the colors of garments and accessories inevitably shape others' impressions of them.

Scarves, a standard accessory in women's fashion, significantly contribute to overall appearance. They not only enhance and balance visual harmony but also reinforce a woman's identity. However, an unsuitable color combination may disrupt visual harmony and undermine the emotional perception conveyed by one's appearance. Luo and Shamey[9] have shown that identical clothing colors can elicit markedly different attractiveness ratings when worn by women of various ethnic backgrounds, suggesting that skin tone may influence emotion perception in fashion contexts.

Despite growing interest in color emotion and color harmony, previous studies have primarily relied on color chips or abstract color configurations. There remains a lack of empirical investigation into how combinations of skin tone and garment color influence emotional perception. Moreover, Ou *et al.*[15] have suggested that the emotional response to multicolor combinations can be estimated by averaging the color emotion values of individual component colors. This provides a basis for predicting the perceived emotion of scarf–skin color pairings using existing models of color emotion and harmony.

To address this gap, the present study examines how scarf–skin color combinations affect emotional perception and compares the empirical findings with predictions derived from established models of color emotion proposed by Ou *et al.*[14], and models of color harmony developed by Ou *et al.*[14], Wei *et al.*[17], Chuang and Ou[3], Gong and Lee[4], and Ou *et al.*[12,13]

EXPERIMENTAL PLAN

To explore the emotional perception of the combination of scarf color and skin tone, this study invited 49 observers to evaluate 44 combinations, consisting of 11 scarf colors on four skin tones. The 49 observers comprised 23 males and 26 females, with an average age of 27.73 years (SD = 9.85). Each observer was asked to make judgments on five emotion scales, including "active-passive," "heavy-light," "warm-cool," "harmonious-disharmonious," and "like-dislike." Data were collected by using a 7-step categorical judgement, as shown in Figure 1.

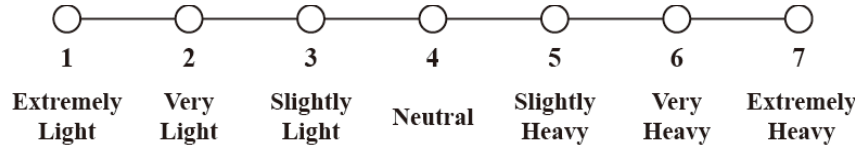

Figure 1: A 7-step categorical judgement, taking "heavy-light" as an example

A total of 44 scarf–skin color combinations were produced using eleven scarf colors and four skin tones. The scarf colors corresponded to the 11 basic color terms proposed by Berlin and Kay[2], including white, grey, black, red, green, yellow, blue, brown, pink, orange, and purple. These colors were further specified by the foci color boundaries defined by Lin *et al.*[6-8]. In terms of skin tone, four skin tones were selected according to the ITA classification system defined by Ly *et al.*[10], including very light, intermediate, brown, and dark skin tones. The scarf-skin color combinations were created by using Adobe Photoshop, as shown in Figure 2.

Figure 2: The 44 scarf–skin color combinations used in the experiment.

Forty-nine observers were invited to participate in the experiment conducted in a dark room. Before the evaluation, each observer wore a large black cloth covering the upper body to minimize visual distractions and completed the Ishihara color blindness test to ensure normal color vision. Observers were seated approximately 70 cm from a 15.3-inch MacBook Air screen, positioned inside a viewing cabinet illuminated by a D65 simulator. The screen was calibrated before the experiment to ensure accurate color representation. They were instructed to assess 44 scarf–skin color combinations presented on the screen. The presentation order was randomized. Each observer made a total of 220 judgments (i.e., 11 scarf colors × 4 skin tones × 5 scales = 220). To examine intra-observer consistency, one of the combinations was repeated during the session.

The CIELAB color values of the scarf and skin tones were measured using an X-Rite i1 Pro 2 in the screen. Measurements were taken from three blurred square regions in Adobe Photoshop, as illustrated in Figure 3(a), and the resulting values were averaged. The averaged color values are plotted in the CIELAB color space, as shown in Figure 3 (b) and (c).

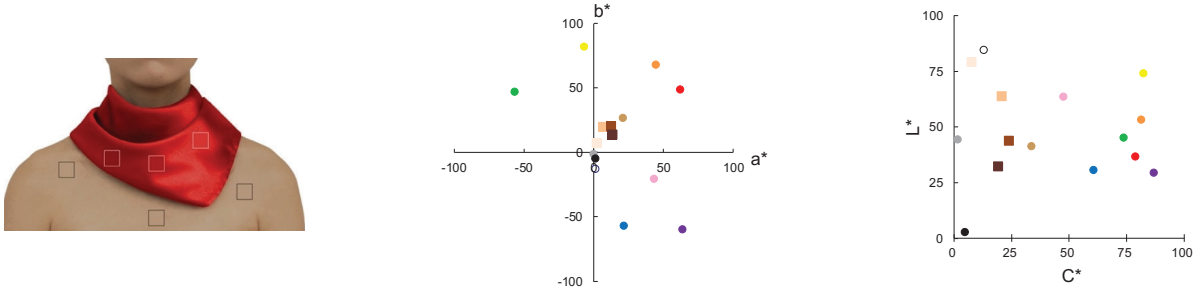

(a) The measured regions (b) CIELAB a*-b* diagram (c) CIELAB L*-C*diagram

Figure 3: (a) The measured regions, (b) The color distribution in CIELAB a*-b* diagram, and (c) CIELAB L*-C* diagram. Circle indicates scarf color, squares skin tones.

INTRA- AND INTER-OBSERVER VARIATION

The data collected from the seven-step categorical judgments on each scale were converted into numerical values. Intra- and inter-observer variations were analyzed using root mean square (RMS) values. Intra-observer variation assessed the consistency of repeated judgments by the same observer, while inter-observer variation evaluated the degree of agreement between individual observers and the overall mean results. The RMS equation is given below.

$$RMS = \sqrt{\frac{\sum(X_i - Y_i)^2}{n}}$$

For intra-observer variation, Xi and Yi represent the initial and replicated judgments, respectively. For inter-observer variation, Xi represents the individual data, and Yi represents the corresponding average across all observers. An RMS value of 0 indicates perfect agreement between two data arrays.

As illustrated in Figure 4, intra-observer RMS values ranged from 0.45 to 2.72, whereas inter-observer values ranged from 1.03 to 1.77. These findings indicate relatively large intra-observer variation but low inter-observer variation, suggesting good consistency across observers. A possible explanation for the higher intra-observer variation is that the repeated sample was presented as the first item, during which observers may have still been adapting to the experimental procedure and calibrating their use of the emotional scale. Therefore, the following analysis used the judgments of all observers, but for the replicates, the second judgment was used.

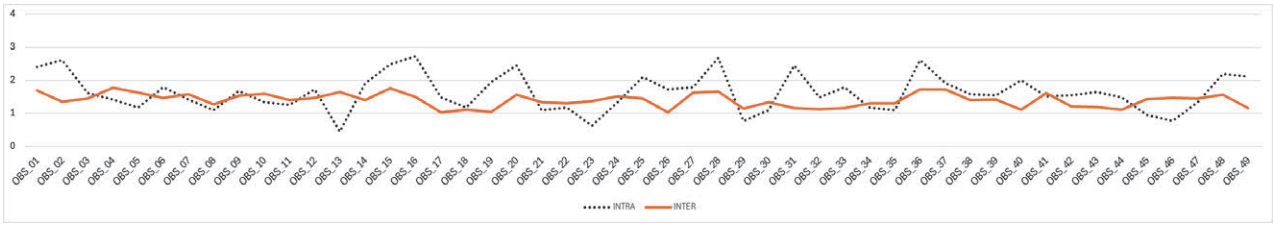

Figure 4: Intra-observer and inter-observer variations

RESULTS

To see whether the emotions perceived from scarf-skin color combinations are consistent with those perceived from color chips, the data obtained from the current studies were used to compare with the model proposed by Ou *et al*.[12,13]. The results are given in Figure 5. In Figure 5, the vertical axis represents the mean results obtained from the current experiment, and the horizontal axis represents the predictions generated from the established models.[12,13] The 45° line and the coefficient of correlation (r) are shown in the diagram to illustrate how well the data distribution aligns.

The results showed that the universal color emotion models of "active-passive" and "heavy-light" predict the emotion perceived from scarf-skin color combinations fairly well, indicated by the r values of 0.60 and 0.76, respectively. However, the universal color emotion model of "warm-cool" is not; the r value is 0.04.

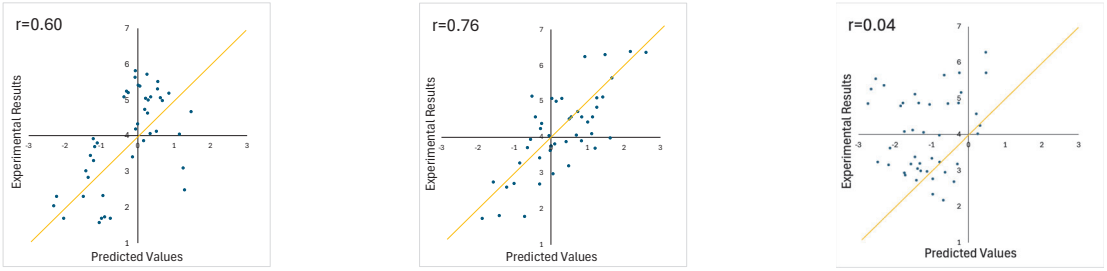

(a) Active-Passive (b) Heavy-light (c) Warm-Cool

Figure 5: Comparison between predictions and mean results.

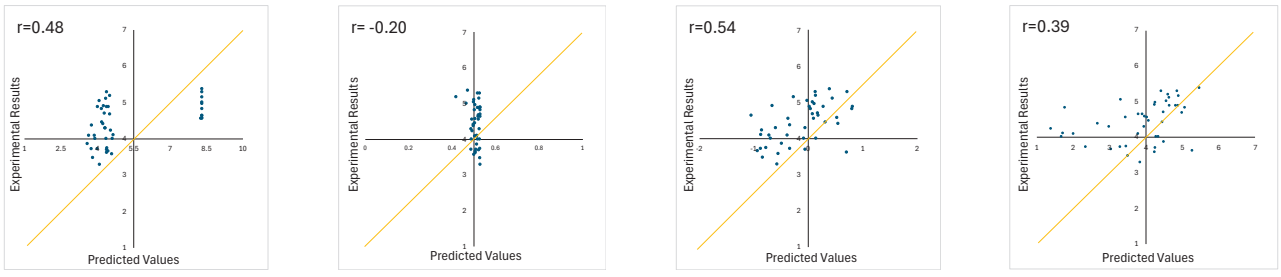

(a) Wei *et al*.[17] (b) Chuang and Ou[3] (b) Gong and Lee[4] (d) Ou *et al*.[12,13]

Figure 6: Compare the mean results with the predictions obtained from color harmony models [3,4,12,13,17].

The same method was applied to examine the color harmony perceived from scarf-skin color combinations, the data obtained from the current studies were used to compare with the models established by Wei *et al.*[17], Chuang and Ou[3], Gong and Lee[4], and Ou *et al.*[12,13]. The results are given in Figure 6.

The results showed that the correlation coefficients of the color harmony models established in previous literature for predicting the color harmony of scarf-skin combinations range from -0.20 to 0.54, which means that the models in previous literature cannot fully predict the color harmony of scarf-skin combinations.

These findings suggest that while color emotions, i.e., "active–passive" and "heavy–light," can be reliably extended from color chip–based models to more complex scarf–skin color combinations, "warm–cool" and color harmony do not generalize as well. This discrepancy may be due to additional factors not accounted for in models based solely on color chips, such as variations in skin tone.

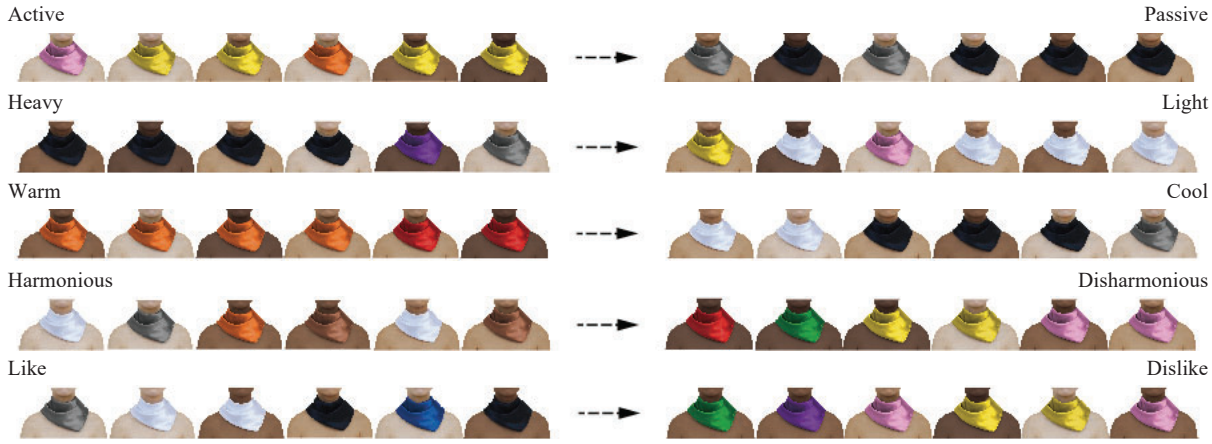

Figure 7. The scarf-skin color combinations were sorted along each scale.

To observe the phenomenon of emotional perception and color harmony in scarf-skin color combinations, the color harmony of these combinations was sorted along each scale. The results are given in Figure 7. It can be seen that:

1. The presence of various skin tones at both extremes of the color emotion, color harmony, and preference scales indicates that skin color has little impact on the ranking of scarf–skin color combinations.
2. In the “Active–Passive” emotion, scarves in pink, yellow, and orange colors were seen as active emotion due to their high chroma, while grey, white, and black were perceived as passive emotion.
3. In the “Heavy–Light” emotion, darker scarf colors such as black, grey, and purple appeared heavier emotion, whereas white, pink, and yellow color were seen as lighter emotion.
4. For “Warm–Cool” emotion, scarves in orange and red colors were perceived as warm emotion, while black, white, and grey were perceived as cool emotion, deviating from typical associations with blue and green colors. The coolness perception of achromatic colors may relate to their low saturation and contrast with skin tones.
5. The ranking on the color harmony and color preference scale is consistent, white, grey, orange, brown, and low-chroma scarf colors were rated as more harmonious and preferred, while pink, yellow, and other colorful colors were seen as disharmonious and disliked.

SUMMARY AND CONCLUSION

This study investigated the emotional perception of scarf–skin color combinations and compared the results with existing models of color emotion and color harmony. The findings showed that universal color emotion models

related to Color Activity and Color Weight can reasonably predict emotional responses to scarf–skin color combinations. However, the Color Heat and existing color harmony models demonstrated limited predictive power in this context. The results also suggested that skin color has a minimal impact on the ranking of scarf–skin color combinations across emotion, harmony, and preference scales.

Nevertheless, several limitations should be acknowledged. This study did not explicitly analyze the interaction effects between skin tone and scarf color, which may influence perception in more complex ways. In addition, the CIELAB values of skin tones and scarf colors were not incorporated into the predictive analysis. Future study should consider integrating quantitative color attributes and modeling the interplay between skin tone and garment color to enhance the accuracy and applicability of emotional and aesthetic predictions in real-world contexts.

REFERENCES

1. Amhorst MLD, Reed JAP. Clothing Color Value and Facial Expression: Effects on Evaluations of Female Job Applicants. Social Behavior and Personality: an international journal 1986;14(1):89-98.
2. Berlin B, Kay P. Basic Color Terms: Their Universality and Evolution. Berkeley, California, USA: University of California Press; 1969.
3. Chuang M-C, Ou L-C. Influence of a holistic color interval on color harmony. Color Research & Application 2001;26(1):29-39.
4. Gong S-M, Lee W-Y. Colour harmony of two-colour combinations using a 3D colour configuration. Coloration Technology 2019;135:292-304.
5. Karl KA, Hall LM, Peluchette JV. City employee perceptions of the impact of dress and appearance: You are what you wear. Public Personnel Management 2013;42(3):452-470.
6. Lin H, Luo MR, MacDonald LW, Tarrant AWS. A cross-cultural colour-naming study. Part I—Using an unconstrained method. Color Res Appl. 2001;26(1):40-60.
7. Lin H, Luo MR, MacDonald LW, Tarrant AWS. A cross-cultural colour-naming study. Part II—Using a Constrained Method. Color Res Appl. 2001;26(3):193-208.
8. Lin H, Luo MR, MacDonald LW, Tarrant AWS. A cross-cultural colour-naming study. Part III—A colour-naming model. Color Res Appl. 2001;26(4):270-277.
9. Luo Z, Shamey R. Cross-ethnic comparison of the effect of garment color on male perception of female attractiveness. Color Research & Application 2023;48(4):355-367.
10. Ly BCK, Dyer EB, Feig JL, Chien AL, Bino SD. Research Techniques Made Simple: Cutaneous Colorimetry: A Reliable Technique for Objective Skin Color Measurement. J Invest Dermatol 2020;140(1):3-12 e1.
11. Lynn M, Giebelhausen M, Garcia S, Li Y, Patumanon I. Clothing Color and Tipping. Journal of Hospitality & Tourism Research 2013;40(4):516-524.
12. Ou L-C, Yuan Y, Sato T, Lee W-Y, Szabó F, Sueeprasan S, Huertas R. Universal models of colour emotion and colour harmony. Color Research & Application 2018;43(5):736-748.
13. Ou L-C, Yuan Y, Sato T, Lee W-Y, Szabó F, Sueeprasan S, Huertas R. 【correction】Universal models of colour emotion and colour harmony. Color Research & Application 2019;44(1):153-153.
14. Ou LC, Luo MR, Woodcock A, Wright A. A study of colour emotion and colour preference. Part I: Colour emotions for single colours. Color Research & Application 2004;29(3):232-240.
15. Ou LC, Luo MR, Woodcock A, Wright A. A study of colour emotion and colour preference. Part II: Colour emotions for two-colour combinations. Color Research & Application 2004;29(4):292-298.
16. Roberts SC, Owen RC, Havlicek J. Distinguishing between perceiver and wearer effects in clothing color-associated attributions. Evolutionary Psychology 2010;8(3):350-364.
17. Wei S-T, Ou LC, Ronnier Luo M, Hutchings J. Psychophysical models of consumer expectations and colour harmony in the context of juice packaging. Color Research & Application 2013;40(2):157-168.

Taste Impressions of Snack Packs and Impression Estimation in Machine Learning of Images

Masato Sakurai[a*]

[a]Tokyo Denki University, Tokyo, Japan
[*]Corresponding author: Masato Sakurai, sakurai.m@mail.dendai.ac.jp

ABSTRACT

The influence of color on taste impressions, such as red makes a sweet impression, has been reported. To clarify the influence of food packages on taste impressions and examine whether taste impressions can be estimated using a model that derives taste impressions from package images, a subjective evaluation experiment was carried out presenting the image of snack packages from foreign-made then estimate to those results. According to the previous studies and survey, thirty images were selected from snack packages made in foreign country as the stimuli in this experiment. The stimuli were presented at the display placed in front of the participant. The participants were asked to evaluate the impression of basic tastes in stimuli presented, to each taste on a five-point scale. Also, based on the results of the previous study of Sakurai & Yamamoto (2021), a high occupancy color is extracted from each of the 99 stimulus images and combined with the taste impression results obtained in a subjective rating experiment and trained with a linear regression model. Using the model, colors with high occupancy are extracted from the stimulus images in this experiment and input into the model to estimate taste impressions. The top one to three occupied colors were selected and the top one to three colors were used for this estimation. A linear regression model trained using taste impression evaluation results and highly occupied colors extracted from images demonstrated that the taste impressions of certain images could be estimated to a degree. However, some estimated results showed trends differing from the evaluation results, suggesting potential for model improvement.

Keywords: color scheme, taste impression, package design, machine learning, subjective evaluation

INTRODUCTION

Previous studies have reported that color influences taste impressions [1-3]. For example, red is associated with sweetness. Therefore, it is not surprising that consumers' willingness to purchase is influenced by the appearance of food packages. Previous studies investigating the taste impressions of food packages have reported strong taste impressions associated with the color occupying the largest area of the package [3]. It would be valuable in the design field if it were possible to create a package based on its taste impression. A system that can derive taste impressions from a package image would be useful for designing packages. According to the results of a previous study, colors with high occupancy were extracted from package images and combined with the taste impression evaluation results. Machine learning was then performed. It is believed that this model can output taste impressions from food package images as input. The usefulness of the model can be verified by comparing taste impressions estimated from a package image by the above model with the results of a subjective evaluation of the taste of the same package. Therefore, this study aimed to clarify the influence of food packages on taste impressions and examine whether taste impressions can be estimated using a model that derives taste impressions from package images.

METHODOLOGY

Stimuli

Based on previous study [3] and preliminary investigations, 30 types of foreign snack packages were prepared as stimuli. These images have edited the square of 1000 x 1000 px (270 x 270 mm) to consistently size each stimulus. The displayed characters were mosaicked to remove the influence of the product name. Figure 1 shows the sample image of stimuli in this experiment. The stimuli were presented by 24-inch display (Color Edge CS240, EIZO) placed in front of the observer and the viewing distance was 600 mm. They were displayed into the square at a visual angle of 25 deg in the center of the screen and set a gray as the background color.

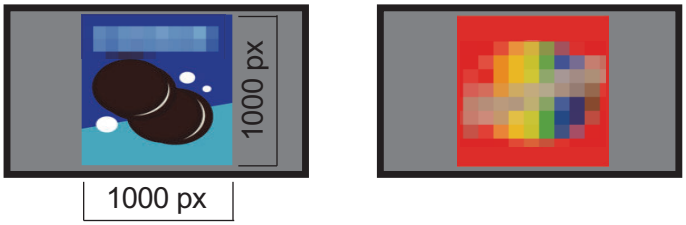

Figure 1: Sample image of stimuli

Procedure

After three minutes light adaption by the D_{65} fluorescent lamps in the experimental booth, the participants were asked to evaluate the impression of basic tastes (i.e., sweetness, sourness, saltiness, bitterness, and umami) in stimuli presented to each taste on a five-point scale (1: feel hardly, 2: feel slightly, 3: feel somewhat, 4: feel, 5: feel very much). The stimuli were presented randomly, and the duration time was 3 s. Then, the evaluation panel was displayed on the screen with a gray background, and the participants input the value of its scale for basic tastes by the numerical keypad. In one session, the participants performed the evaluation of 30 times of all the stimuli, and three sessions were carried out for one participant. It was 90 times in total. Prior to the experiment, the participants had an enough time to practice for the evaluation.

Apparatus

Figure 2 shows the apparatus in this experiment. The experimental booth was covered with a black curtain. It was illuminated by the D_{65} fluorescent lamps of the light booth and the illumination of screen in the display was around 570 lx. The display was placed in front of the participant, and the viewing distance was 600 mm. The participants were asked to respond with the numerical keypad when they evaluate the stimulus.

Participants

Twenty Japanese students participated in this experiment. They were ten female and ten male students and were twenties age. It is same cultural context because they live in Japan so far. And they have the normal color vision.

Estimation method

Figure 3 shows the estimation method with the model to output the taste impression from snack package images. In the previous study of ref. [3], to reveal the relationship between taste impressions and colors of snack packages, a subjective evaluation experiment was carried out presenting the image of 99 types of snack package images commercially available. It is suggested that the highest occupancy color of snack packages strongly affects its taste impression visually. Regarding to the results of the that study, a high occupancy color is extracted from each of the 99 stimulus images and combined with the taste impression results obtained in the subjective rating experiment and trained with a linear regression model. Using the model, colors with high occupancy are extracted

from specific images (stimulus images in this experiment) and input into the model to estimate taste impressions. The top one to three occupied colors were selected and the top one to three colors were used for this estimation.

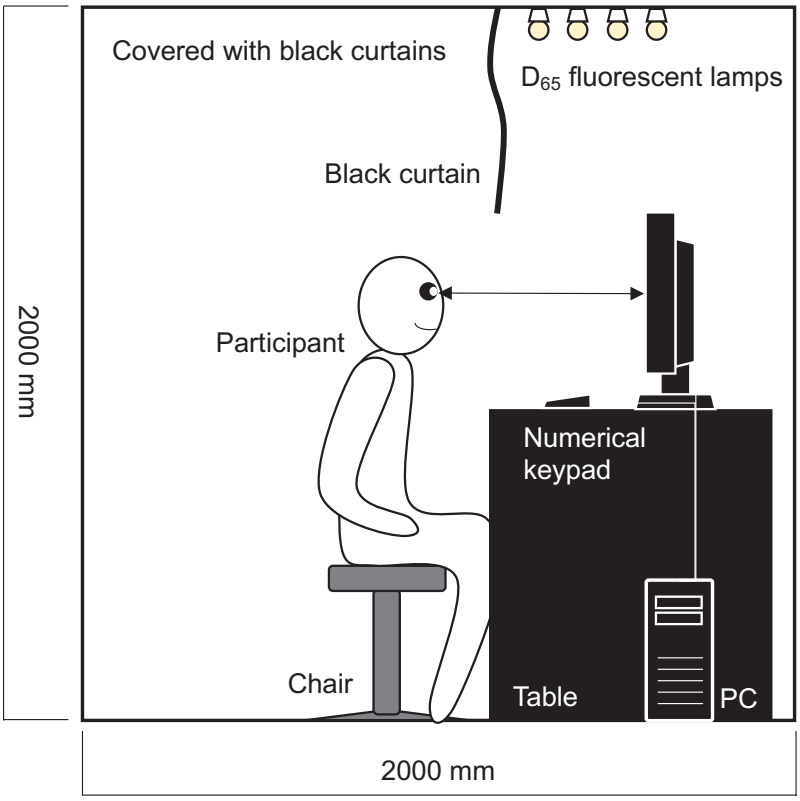

Figure 2: Apparatus

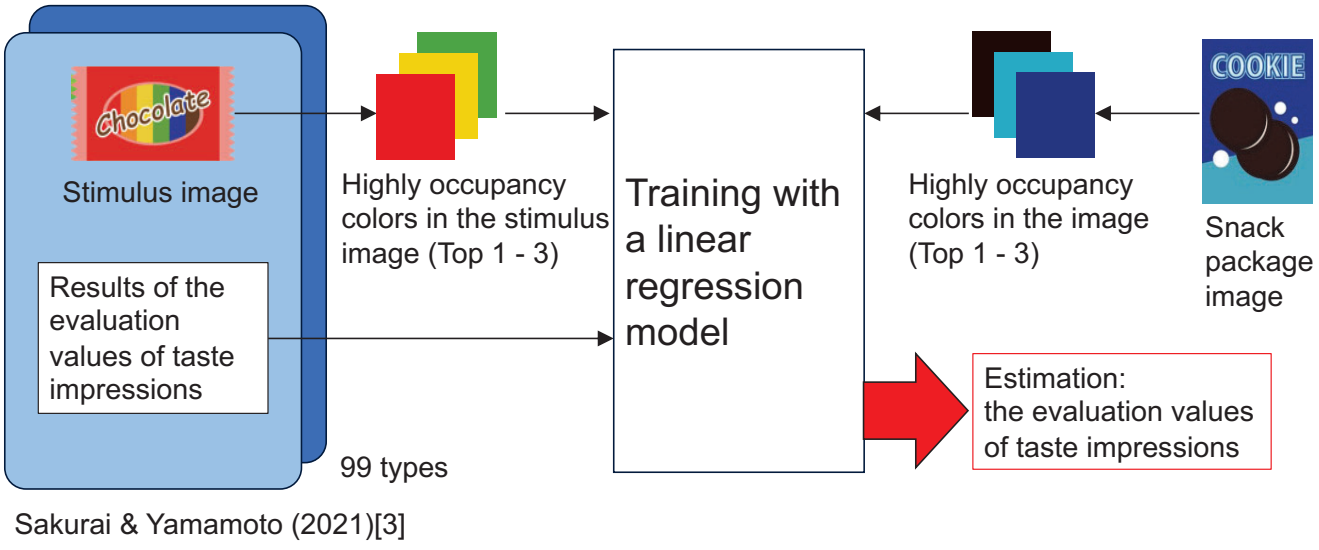

Figure 3: Estimation of the evaluation values of taste impressions from snack package images

RESULTS AND DISCUSSION

Figure 4 shows the typical average results of taste impression for the stimuli based on all the participants evaluations and estimation results of top one to three occupied colors, respectively. In each plot, each vertex of the pentagonal radar chart shows the subjective evaluation values of each of five basic tastes (i.e., Sw: sweetness, So: sourness, Sa: saltiness, Bi: bitterness, and Um: umami), with the further from the center, the higher values. Figure 4 (a) – (b) correspond to the results for the stimuli of each snack package shown in the left-top in each plot. In each plot the tables of the top of figure indicate the values of RGB, HSV, and color appearance of those colors, respectively.

As shown in Figure 4 (a), the results estimated using the top three colors with the highest occupancy rates most closely match the evaluation results, showing a tendency for sweetness to increase, saltiness to decrease, and the shape of the results to align. In Figure 4 (b), even though there is a difference between the subjective evaluation value and estimation with the top one to three colors in sourness evaluation, the results estimated using the top three colors with the highest occupancy rates most closely match the evaluation results as well as Figure 4 (a). Therefore, this estimation using top three colors is considered optimal in this experiment. Also, the result of this study corresponds to the result of previous study that the strong taste impressions associated with the color occupying the largest area of the package [3]. On the other hand, some stimuli elicited estimations differing from the evaluation results or displayed different outcome patterns. For instance, the package with highly occupancy in red color was sometimes imagined to be spicy, differing from the tendency observed in previous studies [1-3] where red was associated with sweetness. Furthermore, the training data was from a Japanese-made package, and differences from the foreign-made package used in this study may also be considered.

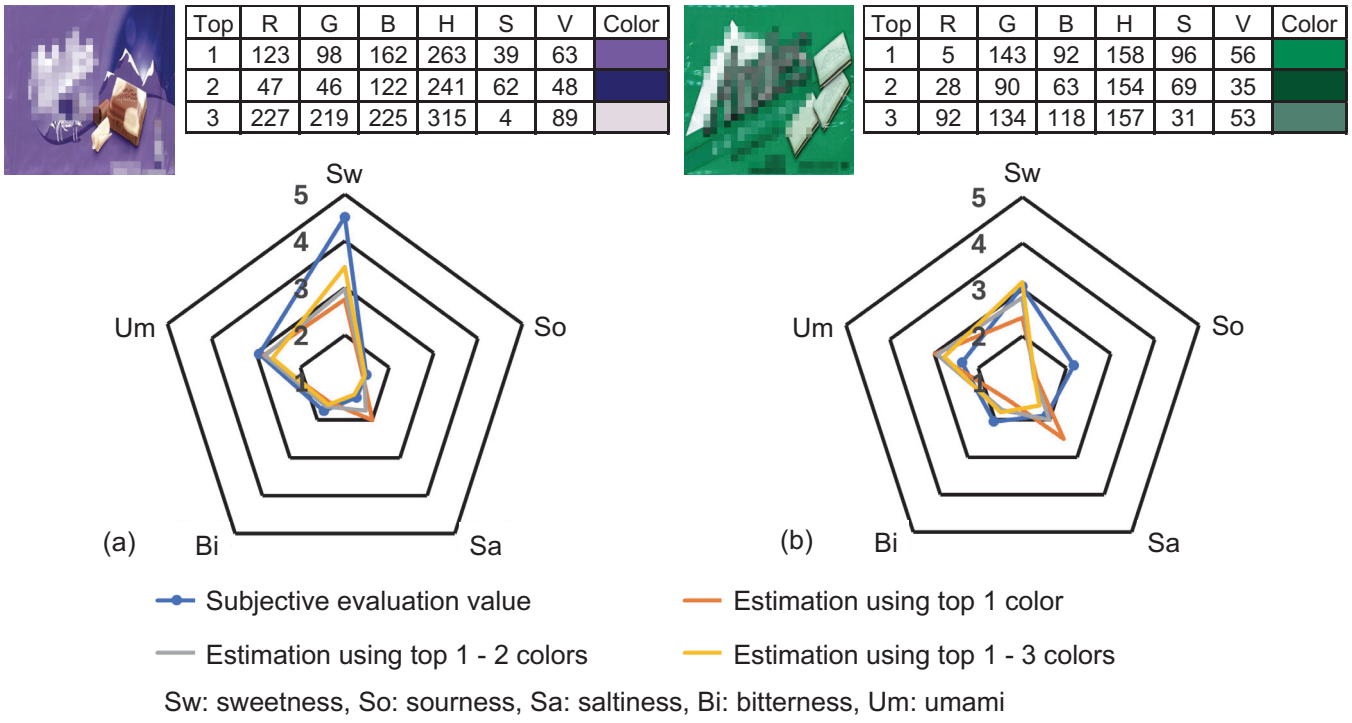

Figure 4: Typical average results of taste impression for the stimuli

CONCLUSION

To clarify the influence of food packages on taste impressions and examine whether taste impressions can be estimated using a model that derives taste impressions from package images, a subjective evaluation experiment was carried out presenting the image of snack packages from foreign-made then estimate to those results. According to the previous studies and survey, thirty images were selected from snack packages made in foreign country as the stimuli in this experiment. The stimuli were presented at the display placed in front of the participant. The participants were asked to evaluate the impression of basic tastes in stimuli presented, to each taste on a five-point scale. Also, based on the results of the previous study [3], a high occupancy color is extracted from each of the 99 stimulus images and combined with the taste impression results obtained in a subjective rating experiment and trained with a linear regression model. Using the model, colors with high occupancy are extracted from the stimulus images in this experiment and input into the model to estimate taste impressions. The top one to three occupied colors were selected and the top one to three colors were used for this estimation. In the results, several stimuli were estimated using the top three colors with the highest occupancy tend to be closest to the evaluation results, with sweetness increasing, saltiness decreasing, and the shape of the results matching. Therefore, this estimation is considered reasonable. On the other hand, there were some stimuli that showed different estimations and different shapes of results from the evaluation results. Some red packages were imagined as spicy, which was different from the tendency to perceive red as sweet in previous studies [1-3]. In addition, it is also possible that the difference between the Japanese packages and the foreign packages used in this study is due to the fact that the training data were from a Japanese package.

ACKNOWLEDGEMENTS

I would like to thank Ms. Mizuki Tsuchida and Mr. Kyotaro Hashiguchi for conducting the experiment of this study.

REFERENCES

[1]. Kinoshita, T., Matsuda, K., and Abe, K. (2010). Effects of Taste Image by Three Attributes of Color, *Design Research*, 54, 107-112 (in Japanese).

[2]. Sakurai, M., Michinaka, Y., and Yoshikawa, T. (2015). Effects on Impression of Taste in Color Stimuli, AIC2015 Tokyo, 348-353.

[3]. Sakurai, M. and Yamamoto, R. (2021). Relationship Between Taste Impression and Color in Snack Packages, AIC2021 Milano, 807-812.

Testing Spectral-Based Characterization Models for Wide-Color-Gamut Display

Ruili He[a*,b], Kaida Xiao[a,b], Xinyi Zhao[a], and Michael Pointer[a]

[a]*School of Design, University of Leeds, Leeds, UK*
[b]*Leeds Institute of Textiles and Colour (LITAC), University of Leeds, Leeds, UK*
[*]*Corresponding author: Ruili, He, r.he1@leeds.ac.uk*

ABSTRACT

Accurate color characterization is critical for consistent cross-media reproduction, especially in wide-color-gamut (WCG) displays with narrow-band primaries. Traditional tristimulus-based models, such as Gain-Offset-Gamma (GOG) and Piecewise Linear Color Correction (PLCC), are widely used due to their simplicity but may suffer from observer metamerism in WCG displays. Spectral-based approaches, including SRPM, SRPPM, and singular value decomposition (SVD), model the spectral power distribution of color stimuli for improved fidelity. In this study, a professional 27-inch LCD in Adobe RGB mode was used to evaluate five models (GOG, PLCC, SRPM, SRPPM, SVD) across 216 test colors. Performance was quantified using mean and maximum CIEDE2000 color differences (ΔE_{00}) and spectral mean square root error (SMSRE). Results show that GOG achieved the best average performance, particularly in spectral reconstruction, while PLCC and SVD provided more stable worst-case colorimetric accuracy. SRPM and SRPPM showed limited improvement over traditional models. These findings provide guidance for selecting characterization methods for next-generation WCG displays, highlighting trade-offs between average accuracy and worst-case robustness.

Keywords: spectral characterization, color reproduction, WCG displays, metamerism reduction

INTRODUCTION

Accurate color characterization of display devices is fundamental for achieving consistent and reliable cross-media color reproduction, particularly in critical applications such as image quality assessment and soft proofing workflows. Traditionally, this characterization has been performed by establishing the transformation between device-dependent RGB color spaces and device-independent CIE XYZ tristimulus values using models such as Gain-Offset-Gamma (GOG) [1] and Piecewise Linear Color Correction (PLCC) [2]. These tristimulus-based approaches remain widely adopted for CRT and LCD displays due to their computational simplicity and ease of implementation.

With the advancement of display technologies, however, devices have been designed with narrower-band primaries to achieve wide color gamut (WCG) and high dynamic range (HDR) reproduction. While these innovations significantly enhance visual performance, they also exacerbate the phenomenon of observer metamerism, where two stimuli with identical tristimulus values may be perceived differently across devices [3-4]. To overcome such limitations, increasing attention has been directed toward spectral-based characterization approaches, which model the full spectral power distribution (SPD) of emitted light rather than relying solely on integrated tristimulus values. By capturing the spectral information of the stimulus, these methods provide richer information and thus enable more accurate characterization.

Several spectral-based models have been proposed in recent years. Liu et al. [5] introduced a spectral radiance partition model (SRPM) based on the spectral additive property of LCD, offering reduced measurement

requirements while maintaining good accuracy. Building on this, Tian et al. [6] developed the spectral radiance piecewise partition model (SRPPM), which establishes a finer mapping between RGB inputs and spectral radiance. Yao et al. [7] further employed singular value decomposition (SVD) on single-channel spectral radiance, demonstrating performance improvements over GOG, PLCC, SRPM and SRPPM. More recently, Hu et al. [8] proposed an adaptive spectral characterization model incorporating a tone reproduction fitting module and a crosstalk compensation module, and an average spectral root mean square error of less than 10^{-4} and an average CIEDE2000 color difference of less than 1.2 were achieved from five types of displays.

Despite these advances, most spectral characterization studies have been conducted on conventional LCDs, while their applicability to next-generation WCG displays remains under-explored. Wider gamut, achieved through narrower-band primaries, presents new challenges for accurate spectral modeling due to their increased sensitivity to spectral mismatches and observer variations.

The aim of this study is therefore to systematically evaluate the performance of representative spectral-based characterization models, namely GOG, PLCC, SRPM, SRPPM, and SVD, on a professional WCG LCD display with narrow-band primaries. For consistency and comparability, the adaptive model of Hu et al. [8] was excluded in this study due to its distinct training requirements and will be considered in future investigations. By testing and comparing these models under WCG conditions, this study aims to provide new insights into the robustness and practical suitability of spectral characterization methods for emerging display technologies.

METHODOLOGY

A 27-inch BenQ 272U display (3840 × 2160 pixels) was employed in this study. The device was set to 6500 K color temperature and Adobe RGB color mode to ensure a wider color gamut compared to the standard sRGB setting and was allowed to warm up for 30 minutes prior to measurement to ensure luminance stability. Spectral measurements were taken using a Konica Minolta CS-2000 spectroradiometer across the 380-780 nm range at 1 nm intervals, including both one-channel and multi-channel RGB digital inputs:

- Single-channel ramps: red, green, blue channels varied independently from 0 to 255 in steps of 15.
- Two-channel ramps: cyan (green + blue), magenta (red + blue), and yellow (red + green) channels varied simultaneously from 0 to 255 in steps of 15.
- Greyscale ramp: equal values across all three channels, incremented by 15.
- RGB combinations: each channel fixed at one of six levels: 10, 50, 100, 150, 200, 250.

These measurements were used to examine the display's channel independence and chromaticity constancy, which are fundamental assumptions for spectral characterization. Channel independence refers to the condition where the three primary channels are driven and controlled independently, allowing the spectrum of any RGB combination to be expressed as the addition of the single-channel spectra. Chromaticity constancy refers to the property that the chromaticity coordinates remain unchanged as the drive level of a single channel varies.

Since previous studies [9, 10] showed that the GOG and PLCC models achieved higher accuracy when trained on grayscale ramps than single-channel data, greyscale measurements were used as the training data for GOG and PLCC in this study, while single-channel RGB measurements were used for SRPM, SRPPM, and SVD.

Model performance was assessed by comparing the predicted and measured spectral radiance of testing colors using two metrics: CIEDE2000 color difference formula (ΔE_{00}) for perceptual color accuracy and Spectral Mean Square Root Error (SMSRE) for spectral reconstruction accuracy. Eq. (1) shows the formula for calculating the SMSRE:

$$SMSRE = \sqrt{\frac{\sum_{i=1}^{n}(S_{mi} - S_{pi})^2}{N}} \quad (1)$$

where S_{mi} and S_{pi} denote the measured and predicted spectral radiance at wavelength i, and N is the total number of sampled wavelengths, N=401.

RESULTS AND DISCUSSION

Figure 1 presents the spectral power distributions (SPDs) of the display's red, green and blue primaries, exhibiting relatively narrow spectral bandwidths, particularly for red. This is consistent with the design strategy for achieving a wider color gamut. To evaluate the display's channel independence, the measured SPDs of two-channel and three-channel ramps (cyan, magenta, yellow, greyscale) were compared with the additive sum of the corresponding single-channel primaries, applying black correction. Table 1 lists the average CIEDE2000 color differences and SMSRE values ($\times 10^{-4}$). The grayscale ramp showed the largest deviation (ΔE_{00}: 1.13 and SMSRE: 0.1958 $\times 10^{-4}$), suggesting minor cross-channel interactions when the three primaries are equally driven. Across all test colors, the mean ΔE_{00} values is 0.69, indicating strong channel independence.

For chromaticity constancy, the black-corrected SPDs of single-channel measurements were used to calculate xy chromaticity coordinates, shown in Figure 2. The green and blue primaries exhibit high stability, whereas the red primary shows slightly poorer constancy, likely due to its higher intensity, narrower spectral bandwidth and the presence of three distinct spectral peaks (Figure 1). Overall, the display demonstrates acceptable and satisfactory chromaticity constancy suitable for spectral characterization.

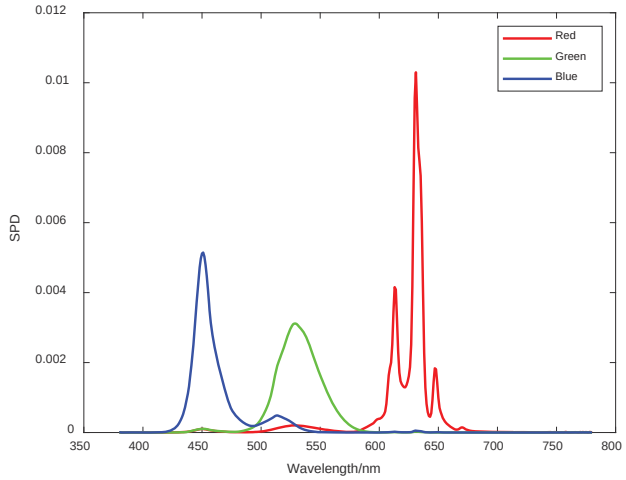

Figure 1: Spectral power distributions of RGB primiries

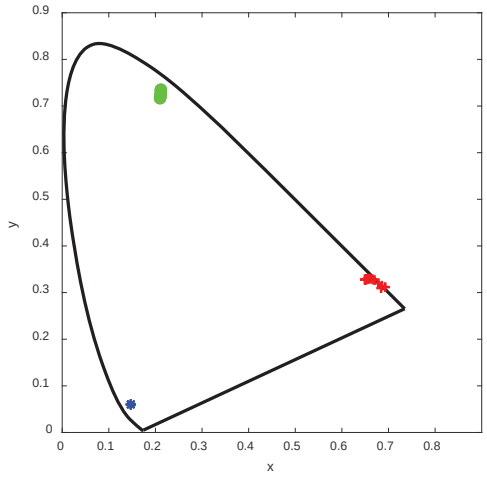

Figure 2: The chromaticity coordinates of the RGB channels black correction

Table 1: Channel independence of the device in terms of CIEDE2000 and SMSRE

	Cyan ramp	Magenta ramp	Yellow ramp	Greyscale ramp	All ramps
ΔE_{00}	0.38	0.40	0.84	1.13	0.69
SMSRE /10^{-4}	0.0802	0.1036	0.0902	0.1958	0.1174

The performance of the five characterization models - GOG, PLCC, SRPM, SRPPM, and SVD- was evaluated using 216 RGB test combinations, with mean and maximum CIEDE2000 color differences and SMSRE values ($\times 10^{-4}$) summarized in Table 2. The GOG model achieved the best overall performance, with the lowest mean ΔE_{00}

(0.33) and SMSRE (0.0643). However, its maximum ΔE_{00} (1.69) was the highest among all models, indicating that although GOG performs vert well on average, it may occasionally produce larger perceptual errors.

The PLCC and SVD models showed comparable accuracy, with mean ΔE_{00} values of approximately 0.73 and mean SMSRE values around 0.18. Notably, both produced lower maximum ΔE_{00} values (1.35) than GOG, but their maximum SMSRE values (≈ 0.48) were substantially higher. This suggests that PLCC and SVD offer more stable worst-case colorimetric accuracy, though at the cost of reduced spectral reconstruction fidelity. The SRPM and SRPPM models demonstrated similar performance, with mean ΔE_{00} values of about 0.80 and mean SMSRE values around 0.19. Both also delivered the highest maximum SMSRE values (>0.48), indicating limited benefit of spectral partitioning for this WCG display.

In summary, GOG remains the most accurate on average, particularly for spectral fidelity, while PLCC and SVD provide better worst-case colorimetric stability, making them suitable alternatives for applications where minimizing outliers is critical.

Table 2: Prediction accuracy of different characterization models

	Mean ΔE_{00}	**Max ΔE_{00}**	**Mean SMSRE /10^{-4}**	**Max SMSRE /10^{-4}**
GOG	0.33	1.69	0.0643	0.1631
PLCC	0.74	1.35	0.1825	0.4836
SRPM	0.81	1.46	0.1910	0.4793
SRPPM	0.80	1.48	0.1934	0.5044
SVD	0.73	1.35	0.1819	0.4813

CONCLUSION

This study evaluated the performance of five characterization models: GOG, PLCC, SRPM, SRPPM, and SVD, on a professional wide-color-gamut LCD display. Channel independence and chromaticity constancy of the display were confirmed, validating the assumptions underlying spectral characterization. Based on 216 RGB test combinations, GOG achieved the lowest mean ΔE_{00} and SMSRE, demonstrating the best overall average performance. However, its maximum ΔE_{00} was higher than that of PLCC and SVD, indicating potential outliers in perceptual accuracy. PLCC and SVD offered more robust worst-case colorimetric performance, while SRPM and SRPPM showed limited improvement over traditional models. Overall, GOG remains highly effective for spectral fidelity, whereas PLCC and SVD provide reliable alternatives where minimizing perceptual outliers is critical. These results highlight the trade-offs between average accuracy and worst-case stability, providing guidance for selecting characterization models for next-generation WCG display.

REFERENCES

[1]. Berns, R. S. (1996). Methods for characterizing CRT displays. *Displays*, 16(4), 173-182.

[2]. D. H. Brainard. (1989) Calibration of a computer controlled color monitor. *Color Res. Appl.*, 14, 23–34.

[3]. Fairchild, M. D., and Wyble, D. R. (2007). Mean observer metamerism and the selection of display primaries. In *Color and Imaging Conference* (Vol. 15, pp. 151-156). Society of Imaging Science and Technology.

[4]. Huang, M., Gao, X., Wei, M., Wang, Y., Li, Y., and Li, X. (2024). Effect of primary peak wavelength and stimulus size on metameric failure through color difference evaluations. *Color Res. Appl.*, 49(2), 222-233.

[5]. Liu, H., Cui, G., Huang, M., Wu, B., Xu, Y., and Luo, M. (2013). Colorimetric characterization of LCD based on wavelength partition spectral model. *Spectroscopy and Spectral Analysis*, 33(10), 2751-2757.

[6]. Tian, Q., Liu, Z., Yu, H., Zhao, D., and Liu, S. (2015). The spectral radiance piecewise partition model for characterizing liquid crystal displays. *Displays*, 39, 133-138.

[7]. Yao, J., Zhang, X., and Li, C. (2021). Spectral characterization of liquid crystal displays based on singular value decomposition. *Acta Opt. Sin.*, 41, 1633002.

[8]. Hu, B., Xu, H., Zhang, Y., Deng, J., Yao, K., and Li, L. (2025). Adaptive spectral characterization model for various types of displays. *Applied Optics*, 64(15), 4276-4283.

[9]. Post, D. L., and Calhoun, C. S. (2000). Further evaluation of methods for producing desired colors on CRT monitors. *Color Res. Appl.*, 25(2), 90-104.

[10]. Zhang, X., Li, X., Gao, C., Wang, Z., Xu, Y., and Li, C. (2020). Spectral characterization for liquid crystal display (LCD). *Spectroscopy and Spectral Analysis*, 40(8), 2392-2396.

Statistical Analysis of Differences of Spectral Reflectance Values Determined by Colour-Measuring Instruments

Erkki Ikonen[a,b*], Yasaman Rezazadeh[a], Anders Nilsson[c], John Seymour[d], and Juha Peltoniemi[a]

[a]*Aalto University, Espoo, Finland*
[b]*VTT MIKES, Espoo, Finland*
[c]*NCS Colour AB, Stockholm, Sweden*
[d]*Clemson University, USA*

[*]*Corresponding author: erkki.ikonen@aalto.fi*

ABSTRACT

Spectral reflectance measurement is a key contribution to quantifying the colour of physical objects. The purpose of this work is to understand the remaining biases in measured spectral reflectance values after all known corrections due to the measurement setup are applied. Although such information is necessary for reliable uncertainty evaluation of spectrally integrated colour quantities, systematic methods to obtain the needed information have not been earlier described in detail. To address the problem, two independent and equally reliable colour-measuring instruments at NCS Colour were used. The instruments have their own calibration procedures defined by the manufacturers. We measured with both instruments in d:8° geometry the reflectance spectra of 707 colour reference samples covering the whole colour space. The amount of data over the wavelength range from 400 nm to 700 nm is sufficient to carry out an extended statistical analysis of the relative differences of spectral reflectance values determined by the two instruments. The analysis reveals a numerical value for the spectral reflectance uncertainty component, which describes the contribution of unknown spectral biases after all known corrections, such as those for the wavelength scale and monochromator bandwidth, have been applied. Information on the quality of those corrections is also obtained. Furthermore, the analysis gives sufficient data on the correlation properties of the unknown spectral biases, which is needed for reliable uncertainty evaluation of colour quantities defined in terms of spectral integrals of measured reflectance. The correlation of spectral biases describes how similar the measurement errors of two reflectance values are when the wavelength difference between them increases. At nearest neighbour wavelengths the errors are probably almost the same, but at the opposite ends of the wavelength range the error at one wavelength cannot be predicted by the knowledge of the error at the other wavelength. Our statistical analysis gives sufficient average information for the uncertainty evaluation of spectral integrals, although it cannot give detailed information on the correlation between values at any two specific wavelengths. Finally, the results of the statistical analysis are applied for evaluating numerical values of the uncertainties of chromaticity coordinates of the 707 reference samples.

Keywords: Colour, spectral reflectance, correlation, uncertainty

INTRODUCTION

It is stated in the standard E2214-20 that “the exact methods for propagating the uncertainty in a reflectance factor measurement into the colour coordinates is still a matter of some dispute” [1]. Our aim here is to describe

such an exact method. The novel method is related to the recent experimental observation that the spectral deviations of participants from the reference value (i.e. true value) in all radiometric key comparisons have a specific spectral structure: On the average, the amplitude of each harmonic component of spectral deviations is inversely proportional to the harmonic order, corresponding to a power-law exponent $b = -1$ [2]. The participants of the key comparisons are National Metrology Institutes, such as NIST in the United States or PTB in Germany, and the key comparison reference value is expected to be the best available estimate for the true value of the comparison artefact characteristic. One of the studied radiometric key comparisons involves measurement of spectral diffuse reflectance. As reflectance reference samples of main manufacturers of colour-measuring instruments are traceable to the National Metrology Institutes, it is reasonable to assume that carefully characterized instruments measure similar deviations from the true reflectance values as observed in the key comparisons, but possibly with a different power-law exponent [3, 4].

Our key innovation here is that we can use the model of the deviations observed in key comparisons to simulate the differences of spectral reflectance values determined by two independent colour-measuring instruments. Simulated distributions of relative differences and of power-law exponents related to the differences are then compared with the corresponding experimental distributions. This procedure allows to adjust the reflectance uncertainties and power-law exponents related to the deviations from the true reflectance values in such a way that best matching is obtained between simulated and experimental distributions.

We used two independent instruments of NCS Colour to measure in d:8° geometry the reflectance spectra of 707 colour reference samples covering the whole colour space. Distributions of relative differences and of power-law exponents related to the differences were then formed from the measured data. The high number of samples is advantageous for comparison with corresponding simulated distributions. The method provides the necessary information on the correlation between measured reflectance values to evaluate the uncertainties of spectrally integrated colour quantities of the different samples. Chromaticity coordinates are used here as example quantities for uncertainty evaluation.

METHODOLOGY

Our study was conducted using reflectance colour samples manufactured by NCS Colour. The 707 samples provide a representative collection of all colours. The spectral reflectance of all samples was measured in d:8° geometry using two independent instruments, Konica-Minolta CM-3700A and X-Rite Color i7, assumed to be equally reliable. Both instruments are carefully calibrated by the manufacturers and corrections are applied for all known error sources, but uncertainties in their measured reflectance values still remain because of unknown residual spectral corrections relative to the true reflectance. Such contributions were revealed and analyzed in Ref. [2].

Analysis of reflectance deviations in colour measurements

Figure 1(a) displays two reflectance spectra $R_1(\lambda)$ and $R_2(\lambda)$ of a yellow colour sample measured by instruments 1 and 2 over the selected wavelength range from $\lambda_1 = 400$ nm to $\lambda_2 = 700$ nm. The relative differences

$$\Delta(\lambda) = [R_2(\lambda) - R_1(\lambda)]/R_1(\lambda) \quad (1)$$

between the reflectance values are shown magnified in Figure 1(b) as open circles. The value of $\Delta(\lambda)^2$ averaged over the measured wavelengths describes the variance between the measurement results of instruments 1 and 2 for the yellow sample. The square root of the variance is related to the spectral reflectance uncertainty bands $\pm u_1 R_1(\lambda)$ and $\pm u_2 R_2(\lambda)$, where u_1 and u_2 describe the relative combined standard uncertainty of unknown spectral biases after all known corrections have been applied. The uncertainty band related to $\Delta(\lambda)$ is $\pm\sqrt{u_1^2 + u_2^2}$.

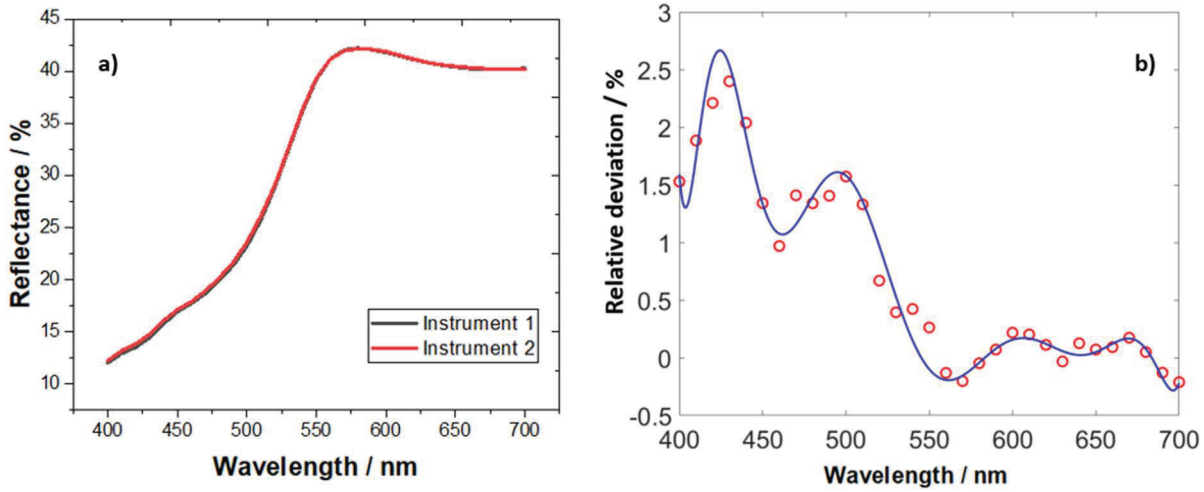

Figure 1: (a) Reflectance spectra of a yellow sample measured with two independent instruments. (b) Relative reflectance differences of the yellow sample and the fitted curve used for spectral analysis. The yellow sample is used as a representative example of all 707 samples used for the measurements and statistical analysis.

The solid line in Figure 1(b) is a fit by equation

$$\Delta(\lambda) = \sum_{i=0}^{N} A_i f_i(\lambda), \tag{2}$$

where $\Delta(\lambda)$ is the relative difference, A_i is the fitted amplitude of the i-th harmonic deviation function, and $N + 1$ is the number of functions used. The harmonic basis functions $f_i(\lambda)$ are orthogonal with respect to each other, i.e. when integrated over the selected wavelength range, their product $f_i(\lambda)f_j(\lambda)$ is nonzero only if $i = j$. The zeroth-order function is $f_0(\lambda) = 1$ and the functions are normalized so that their integral over the selected wavelength range is $\lambda_2 - \lambda_1$. A Fourier series consisting of sinusoidal functions is a special case of Equation (2), but here appropriately normalized Legendre polynomials are used as basis functions. With polynomials, better fits as compared with sinusoidal functions are obtained to slope-like features, where an example is shown in Figure 1(b).

A set of fitted amplitudes A_i, $i = 0, 1, \ldots, 6$, is obtained for each of the 707 difference curves, similar as shown in Figure 1(b) for the yellow sample. A linear fit $\ln A_i = C + B \ln i$ is made to the amplitudes with $i \geq 1$ on a log-log scale. The fit gives a power-law exponent $B = -1.01$ for the data of Figure 1(b), corresponding to the relation $A_i = e^C \cdot i^B$, where constant C is the intercept of the fit at $i = 1$. The power-law exponent characterizes the correlations of measurement errors at different wavelengths, where a high value of $|B|$ indicates enhanced correlation and a low value at around zero means reduced correlation, corresponding to independent errors at all wavelengths, i.e., random noise.

Distributions of relative differences and power-law exponents

Results of a statistical analysis of differences in reflectance values measured by instruments 1 and 2 for all 707 samples are shown in Figure 2. The blue histogram bars in Figure 2(a) show the distribution of the square root of average variance calculated on the basis of measured reflectance values in Equation (1). The distribution extends up to relative deviations of about 0.04. The blue histogram bars in Figure 2(b) show the distribution of power-law exponents B as obtained from the fits of amplitudes A_i by $A_i = e^C \cdot i^B$. The mean is $\langle B \rangle = -0.39$ and the standard deviation of the measured distribution is 0.43.

The distribution of power-law exponents B is obtained from differences in reflectance spectra measured with two independent instruments. However, the power-law exponent b of deviations relative to the unknown true value

of reflectance is of interest for uncertainty analysis of colour quantities. Such deviations for instrument 1 can be simulated by

$$R_1(\lambda) = [1 + \delta(\lambda)u_1]R_0(\lambda), \tag{3}$$

where $R_0(\lambda)$ is the (unknown) true reflectance, u_1 is the relative combined standard uncertainty due to unknown spectral biases after all known corrections have been applied, and the deviation function

$$\delta(\lambda) = \gamma_0 + \sum_{i=1}^{N} i^{b_1}\gamma_i f_i(\lambda) \tag{4}$$

resembles the fitting function of Equation (2), taking into account the power-law exponent b_1 describing the amplitudes when $i \geq 1$. In Equation (4), parameters γ_i are obtained as

$$\gamma_i = \frac{Y_i}{\sqrt{Y_0^2 + \sum_{j=1}^{N} j^{2b_1} Y_j^2}}, \tag{5}$$

where Y_i is a random number from a zero-mean Gaussian distribution with unity variance. Furthermore, the basis functions $f_i(\lambda)$ contain random weights of their odd and even parts. For instrument 2, similar Equations (3-5) for calculation of $R_2(\lambda)$ are used with u_1 and b_1 replaced by u_2 and b_2. Then Equations (1) and (2) can be used to produce the simulated distribution of relative differences of reflectance values and of power-law exponents measured by instruments 1 and 2. Because the instruments are assumed to be equally reliable, further simplifications $u_1 = u_2 = u$ and $b_1 = b_2 = b$ are used in practical Monte Carlo simulations. When $b_1 = 0$, Equations (4) and (5) get the same form as used initially by Kärhä et al [3].

Red histogram bars in Figure 2 display the simulated results, where fitted parameter values $u = 0.0066$ and $b = -0.75$ give the best fit with experimental data. To reduce statistical fluctuations, the simulation of 707 samples was carried out four times and the results averaged. The nonzero histogram bars of the simulated distribution extend to about 0.02 in Figure 2(a). There is a clear deviation in the experimental and simulated distributions between relative differences of 0.02 and 0.04. This deviation may be caused by an error in the applied corrections of one of the instruments or of both instruments. However, the simulation model explains a large majority of the measured relative differences. The simulated distribution of power-law exponents in Figure 2(b) is in good agreement with the experimental distribution. Changing b to −0.85 or to −0.65, resulted in clear weakening of the match between simulated and experimental distributions as compared with the optimal case of $b = -0.75$ in Figure 2(b). The simulated distribution has the mean of $\langle B \rangle = -0.42$ and standard deviation of 0.48, in close agreement with the experimental distribution.

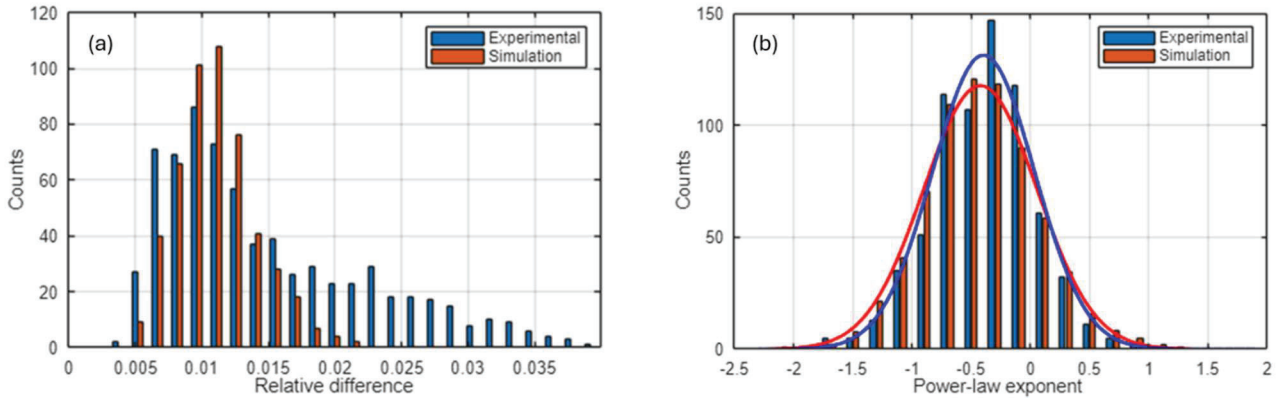

Figure 2: Measured (blue) and simulated (red) distributions of relative reflectance differences (a) and power-law exponents (b). Solid lines in (b) indicate Gaussian fits to the histograms. See text for details.

RESULTS AND DISCUSSION

Uncertainty estimates are calculated from the measured reflectance spectra $R_1(\lambda)$ and $R_2(\lambda)$, such as those of Figure 1(a), for chromaticity coordinates x and y. Monte Carlo method is used to generate the distributions of colour quantities with reflectance spectra deviated analogously to Equation (3) by

$$R_{dev,1}(\lambda) = [1 + \delta(\lambda)u_1]R_1(\lambda), \quad (6)$$

where $u_1 = 0.0066$ is the relative standard uncertainty of all spectral reflectance values and $\delta(\lambda)$ is calculated by Equations (4) and (5) with $b_1 = -0.75$. This uncertainty evaluation assumes that any error in the applied corrections is related to instrument 2.

As an example, the obtained distributions of chromaticity coordinates x and y for the yellow sample of Figure 1(a) are used to evaluate the expanded uncertainties at 95% confidence level shown in Figure 3 as a function of the number N of used non-constant basis functions. The expanded uncertainty at large N becomes independent on N and provides the uncertainty estimate of each quantity. Similar uncertainty evaluation can be carried out for all samples and for other colour quantities, such as L^*, a^* and b^*.

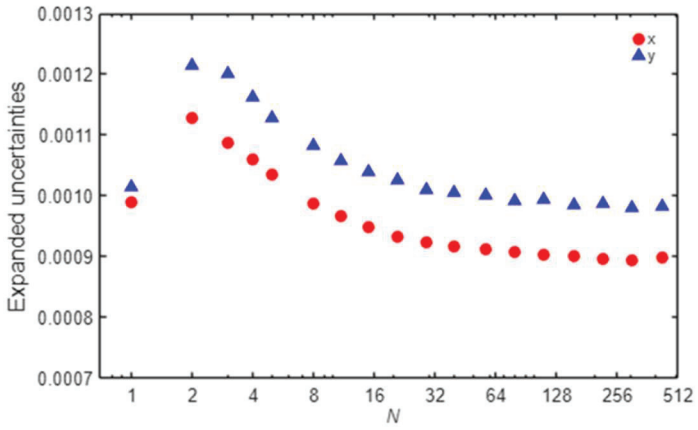

Figure 3: Expanded uncertainty of chromaticity coordinates for the sample with spectral reflectance displayed in Figure 1(a). The expanded uncertainties of 0.0009 and 0.0010 are obtained in the limit of large N for x and y, respectively. The mean values are $x = 0.3831$ and $y = 0.4048$.

The deviation between experimental and simulated distributions in Figure 2(a) would need development of an improved model, because the possibility that both instruments have inadequacies in their spectral corrections cannot be ruled out. In the absence of such an improved model, the ~200 colour samples with large relative differences could be excluded from the initial statistical analysis. Then the described uncertainty evaluation for the group of ~500 samples with regular characteristics can be carried out without the assumption that the error in the applied corrections is related only to one instrument. For the remaining ~200 samples, the model with different values of parameters u and b could be tested. That would probably result in increase of uncertainties by roughly a factor of two as compared to the samples with regular characteristics.

We have also used a strong assumption that the two independent colour-measuring instruments are equally reliable and that the characteristic parameters related to the instruments are equal. This assumption can be relaxed if a third independent instrument is available. Then three sets of differences of spectral reflectance values can be formed, which may give access to determination of specific uncertainty and power-law parameters for each of the three instruments. The third instrument would also give better information on the quality of the spectral corrections of each instrument.

CONCLUSION

The novel method for evaluating the uncertainty of colour quantities is expected to enhance the reliability of colour measurements. Additionally, it addresses the challenge described by ASTM International on propagating the uncertainty of spectral reflectance to colour quantities [1]. Application of the method still has some practical limitations but approaches to overcome those limitations are described.

ACKNOWLEDGEMENTS

The work is part of the Research Council of Finland Flagship Programme, Photonics Research and Innovation (PREIN), decision number 346529, Aalto University.

REFERENCES

[1]. ASTM International E2214 – 20. (2020). Specifying and Verifying the Performance of Colour-Measuring Instruments.

[2]. Maham, K., Kosonen, V., Peltoniemi, J., Kärhä, P. and Ikonen, E. (2024). Spectral analysis of deviations from key comparison reference values. *Metrologia*, 61, 015002. https://doi.org/10.1088/1681-7575/ad0c9e

[3]. Kärhä, P., Vaskuri, A., Mäntynen, H., Mikkonen, N. and Ikonen, E. (2017). Method for estimating effects of unknown correlations in spectral irradiance data on uncertainties of spectrally integrated colorimetric quantities. *Metrologia*, 54, 524 – 534.

[4]. Kärhä, P. Vaskuri, A., Pulli, T. and Ikonen, E. (2018). Key comparison CCPR-K1.a as an interlaboratory comparison of correlated color temperature. *J. Physics: Conf. Ser.* 972, 012012.

Enhanced Portrait Auto White Balance in Backlight Environments via Skin Reflectance

Sicong Zhou[a*], Changjun Li[a], Jinxing Liang[a,b], Peihua Lai[a], Wenjun Sun[c],Hesong Li[c] Hong Luo[c] and Kaida Xiao[a*]

[a]*School of Design, University of Leeds, Leeds, LS2 9JT, West Yorkshire, UK*

[b]*School of Computer Science and Artificial Intelligence, Wuhan Textile University, Wuhan, China*

[c]*Shenzhen Transsion Holdings Co. Ltd., Shenzhen, China*

**Corresponding author: k.xiao1@leeds.ac.uk*

ABSTRACT

Accurately reproducing skin color under varying correlated color temperatures (CCT) and sunlight angles remains a critical challenge in imaging, as it directly affects face recognition, photographic aesthetics, and human–computer interaction. A major difficulty lies in predicting lighting information in backlight conditions while minimizing color distortion and CCT shifts in shadowed regions, which is essential for achieving consistent and natural color reproduction. Conventional automatic white balance (AWB) algorithms, such as the gray-world and brightest white-point assumptions, often fail in backlight scenes due to the influence of indirect lighting and bright backgrounds, leading to inaccurate light source estimation and color deviations. To address these limitations, this paper introduces an improved AWB algorithm specifically designed for backlight environments, extending the skin color reflectance-based AWB (SCR-AWB) framework for predicting spectral power distribution (SPD) and CCT. Daylight spectra were collected across varying angles, times, and locations using the Konica Minolta C-700 spectrophotometer, forming a database covering both front-light and backlight conditions. Based on this analysis, an adaptive proportional function was developed to refine SCR-AWB predictions in backlight scenes. Unlike traditional approaches, the proposed method does not depend on statistical assumptions, enabling robust adaptation to complex lighting. Compared with AI-based AWB algorithms, it also offers lower computational complexity, making it suitable for real-time mobile applications. Experimental results show a 32.7% improvement in CCT prediction accuracy under outdoor backlight and 41.8% under indoor backlight, while preserving natural skin tones and white references across diverse conditions. These findings validate the effectiveness of the proposed approach in enhancing skin color reproduction under challenging backlight. Future work will extend its applicability beyond portrait imaging and incorporate user-driven preferences for more flexible white balance adjustment.

Keywords: Skin Reflectance, Auto White Balance, Color Reproduction

INTRODUCTION

Accurately reproducing color under unknown lighting conditions is a fundamental problem in image processing. In real-world scenarios, variations in the correlated CCT and angle of the light source significantly affect human skin color[1-2], directly impacting applications such as facial recognition[3], photographic aesthetics[4], and human-computer interaction. Backlit environments with daylight are particularly challenging, as shadowed areas and indirect lighting often result in noticeable color shifts and inconsistent rendering between

front-lit and backlit areas[5-6]. Achieving stable and reliable skin color reproduction under these conditions remains an urgent problem for both academic research and mobile camera applications[7].

Traditional AWB algorithms, including those using the grayscale world assumption[8] and the brightest white point assumption[9], perform poorly in backlit scenes[10]. The presence of scattered or reflected light can skew global statistics, and bright backgrounds are often misinterpreted as light sources, resulting in color distortion across the entire image[6]. While AI-based AWB methods have recently demonstrated strong adaptability, they typically require high computational costs and large training datasets. The computational power and time required to perform these methods also limit their deployment in resource-constrained devices such as smartphones[11-12].

To address these limitations, this study proposes an improved AWB algorithm specifically designed for backlighting conditions. Based on the skin color reflectance-based AWB (SCR-AWB) framework[13], this method utilizes daylight spectrum measurements collected at various locations, sun angles, and times to construct a comprehensive database of front and back light daylight spectra refer to the measurement method in [5]. An adaptive scaling function is then introduced to optimize SPD and CCT predictions under complex lighting conditions. Compared to traditional AWB algorithms, this method achieves more accurate illuminant estimation without relying on the image's white point or overall grayscale. Furthermore, it maintains lower computational complexity than AI-based methods, making it suitable for real-time imaging applications.

Experiments on real-world images demonstrate the effectiveness of the proposed algorithm, significantly improving both CCT prediction accuracy and skin color restoration in both indoor and outdoor backlit environments. These results highlight the practical potential of this method for enhancing portrait imaging and lay the foundation for future expansion to a wider range of imaging scenarios.

METHODOLOGY

This section describes an AWB algorithm for backlit scenes based on the SPD prediction algorithm based on past SCR-AWB. For the system workflow and underlying principles of SCR-AWB in practical applications, please refer to our previous research.

Similar to front light scenes, this method first performs preliminary processing (black field compensation and demosaicing interpolation) on the raw sensor data before applying AWB. This preprocessing yields separate RGB color channels , which serve as one of the algorithm's inputs. The algorithm then segments the skin-tone regions and extracts nonlinear RGB values representative of the skin tones of the people in the image. Basis vectors matching the illuminant type are then selected from a database and combined with the estimated skin reflectance data and the sensor sensitivity function to calculate the SPD. Finally, the backlight ratio function is used to calculate the SPD under backlight conditions. The CCT and image white point will be estimated by this predicted SPD to obtain the image's AWB gain, which will be applied to the entire image to achieve accurate white balance correction in backlight situations. For the obtained skin area pixel points, we can list the following basic equations based on the skin color reflectance R(λ), the camera sensor sensitivity function Sr,g,b(λ) and the light source spectrum E(λ):

$$p = \kappa \int E(\lambda) r(\lambda) S_p(\lambda) d\lambda \quad p = R, G, B \tag{1}$$

In the above equation, the scaling factor κ is independent of color and only depends on the light intensity. Since this algorithm does not involve light intensity prediction, κ can be directly set to a constant. In addition, we assume that E(λ) can be a combination of three basis vectors. In direct light or uniform ambient light, E(λ) can be considered the light source of the scene. However, in backlit scenes, the three-channel values corresponding to the skin tone are not actually the light source, but the light reflected from the scene onto the skin tone. Therefore, an adaptive proportional function φ(λ) is required to correct the spectrum caused by this indirect light. Therefore, the actual light source E(λ) of the backlit scene can be described as follows:

$$E(\lambda) = E_S(\lambda)\varphi(\lambda) = (E_1(\lambda) + \alpha_2 E_2(\lambda) + \alpha_3 E_3(\lambda))\varphi(\lambda) \quad (2)$$

Therefore, let λ_i be the wavelength value uniformly sampled at $\Delta\lambda$ intervals within the wavelength range, and convert the equation into the form of numerical integration, we have:

$$m_{j,p} = \kappa \sum_{i=1}^{n} E_p(\lambda_i)\varphi(\lambda_i)r(\lambda_i)S_j(\lambda_i)\Delta\lambda_i \quad j = r, g, b, \ p = 1,2,3 \quad (3)$$

Finally, we solve the α value through the three discretized algebraic equations of the three channels and substitute it into Formula 2 to obtain the actual light source spectrum. Therefore, the key to the algorithm lies in determining the parameters of these quantities to ensure accurate SPD prediction. For skin reflectance, our research group has established a database of skin colors across gender, age, ethnicity, and body part: the International Skin Spectra Archive (ISSA)[14]. The sensor's sensitivity function and the captured and preprocessed three-channel data are provided by the device itself. Finally, the crucial light source data comes from two sources: 1. Light source basis vectors are obtained by performing singular value decomposition on a large-scale database of sunlight and artificial light. 2. An adaptive proportional function is obtained by analyzing sunlight spectra collected at different locations, times, and angles under both direct and reverse lighting conditions.

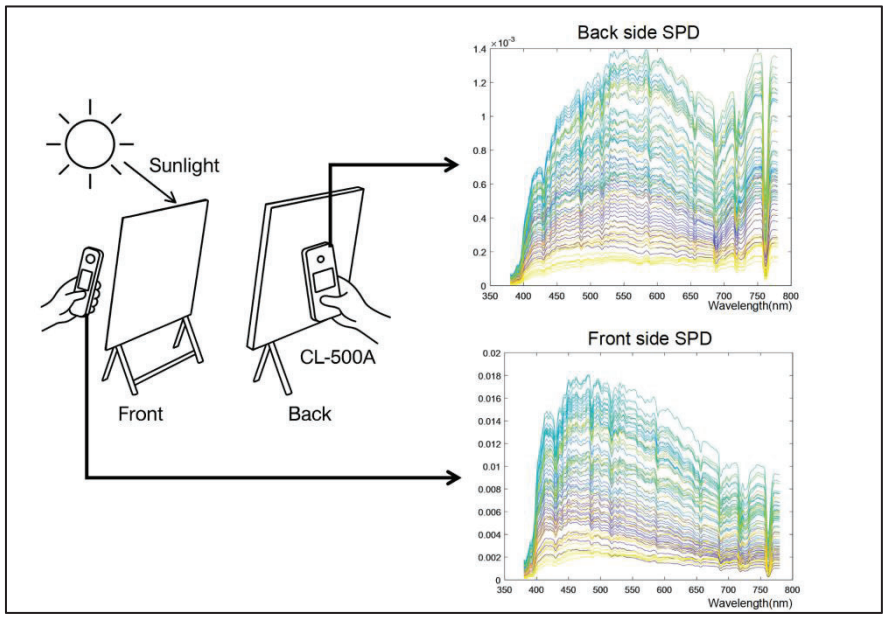

Figure 1: Schematic of sunlight spectral data acquisition using Konica Monica CL-500A(left) and measured SPDs from front and back sides of the white board (right). Measurements were taken on both the front and back sides of a white board. Data were collected continuously from sunrise to sunset at three locations: Leeds (UK), Wuhan (China), and Anshan (China).

In this study, the conventional daylight spectral database was refined by incorporating additional metadata, including front/back light conditions, time of day, geographic location, and solar elevation angle. The experimental procedure and database construction workflow are illustrated in Fig. 1. For daylight measurements, a white board was used as the reflective medium. By positioning the spectroradiometer at different orientations with respect to the white board, SPDs were recorded under both front-light and back-light conditions. Each measurement cycle involved acquiring the front-side SPD followed immediately by the back-side SPD, thereby ensuring near-simultaneous bidirectional sampling. The process was repeated at 10 – 15 minute intervals

throughout the day. Spectral data were collected either with a portable Jeti spectroradiometer at a longer distance or with a CL-500A spectroradiometer at a closer distance.

For data processing, at each time point, we divide the SPD obtained under backlight conditions by the SPD obtained under front lighting conditions, generating an adaptive scaling function. This function will be used to characterize the difference between back light and front light. In the actual application of the algorithm, we will select an appropriate adaptive scaling function based on image information combined with database information elements. To further validate the proposed method, an image-based experiment was conducted in Shanghai under clear-sky conditions in 2025. The image acquisition device is a Transsion CL9 mobile phone with parameter: aperture f/1.8, ISO 203, exposure time 1/100 second, focal length 7mm, and the sensor sensitivity function used in the experiment matches the mobile phone model. Images were captured at three different times of day: morning, afternoon, and dusk across both outdoor and indoor scenarios. The experimental dataset includes: (i)18 outdoor backlit images taken on May 29 (afternoon), (ii)16 outdoor backlit images on June 3 (morning), (iii)16 outdoor backlit images on June 4 (dusk), and (iv)12 indoor backlit images near a window (4 in the afternoon, 4 in daytime, and 4 at dusk). To evaluate the most challenging case for skin color reproduction, subjects with dark skin tones were selected. In addition, a standard 64-color checker was included in each scene to provide a visual reference for algorithmic performance. These images were used to verify that incorporating the adaptive proportional function improved SPD prediction under backlit conditions, thereby enhancing AWB performance.

RESULTS

Experiments were conducted to verify the impact of the adaptive proportional function on SPD prediction in backlit scenes. ΔCCT was used to evaluate the difference between the predicted SPD and the actual scene SPD, where the groundtruth CCT of the scene was measured by a illuminance meter. The SCR-AWB algorithm was used to process backlit portrait images containing skin tones, where w $\varphi(\lambda)$ represent the application of the adaptive proportional function. Table 1 highlights the differences between the CCT predictions of the SCR-AWB algorithm and the actual calibrated scene CCT for different time periods. Generally speaking, smaller ΔCCT values indicate more accurate SPD predictions and, consequently, better color reproduction.

Table 1: Study on the Effect of the Adaptive Proportional Function in Backlit Scenes: ΔCCT Evaluation of GreyWorld vs. Predicted Scene CCTs Using SCR-AWB

Scene	Time	Image Number	SCR-AWB w $\varphi(\lambda)$	GreyWorld
Outdoor Sunlight	Morning	18	565K	227K
	Afternoon	16	245K	283K
	Evening	16	189K	987K
Indoor Nearby Window	Morning	4	167K	950K
	Afternoon	4	1141K	881K
	Evening	4	411K	1122K

Across all tested scenarios, the avg ΔCCT values of SCR-AWB with the adaptive proportional function were consistently lower than those of the GreyWorld method. This indicates that the proposed approach achieves more reliable SPD predictions in backlit scenes, where conventional statistics-based methods often fail. In particular, GreyWorld exhibited large fluctuations at different times of day (e.g., 987 K in the evening outdoor case), while SCR-AWB maintained relatively stable and smaller errors (e.g., 189 K).

The improved performance can be attributed to the adaptive proportional function, which dynamically adjusts the spectral balance according to the scene illumination. By leveraging prior knowledge of skin reflectance, the algorithm effectively suppresses the bias introduced by strong directional light and scattered components in

backlit conditions. Figure 2 shows a visual comparison of the SCR-AWB with φ(λ) and GreyWorld algorithms in different scenes. The images differ only in the AWB parameter settings; the subsequent CCM and gamma correction parameters remain the same.

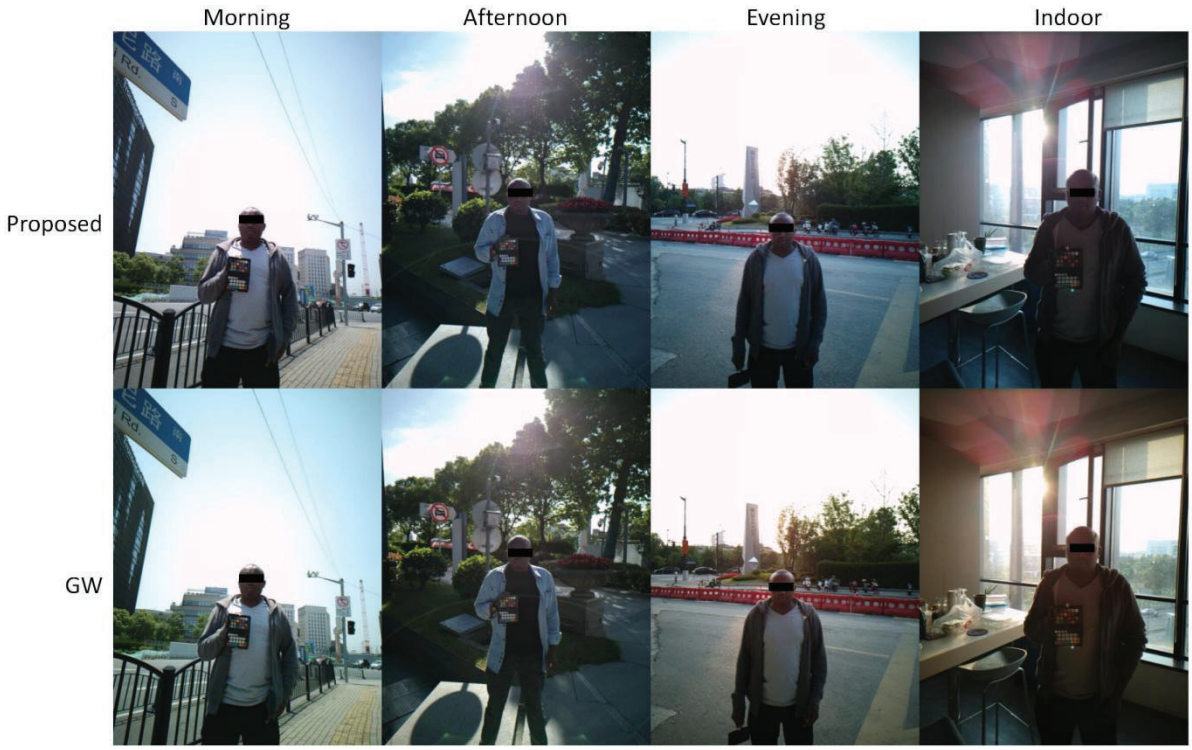

Figure 2: Visual comparison between SCR-AWB (top row) and GreyWorld (bottom row) under different backlit scenes. The images differ only in AWB parameters, while the subsequent CCM and gamma correction remain unchanged.

In summary, these results confirm the robustness of SCR-AWB under challenging illumination, demonstrating that the adaptive proportional function significantly enhances SPD prediction accuracy and, consequently, color reproduction quality in portrait imaging.

DISCUSSION

The experimental results demonstrate that incorporating the adaptive proportional function into SCR-AWB significantly improves SPD prediction accuracy under backlit conditions. Compared with GreyWorld, which exhibited large ΔCCT fluctuations and perceptual color shifts, SCR-AWB maintained more consistent predictions across different times of day and lighting environments. This stability translated into better color reproduction in portrait images, especially for skin tones. The superiority of SCR-AWB arises from its reliance on skin reflectance priors and spectral modeling rather than global RGB statistics. The adaptive proportional function plays a crucial role by dynamically balancing the contributions of direct and scattered light, thereby mitigating the overcompensation often observed in backlit scenes. In contrast, GreyWorld is highly sensitive to illumination imbalance, leading to substantial errors in such conditions.

Although these results confirm the robustness of SCR-AWB, the current evaluation is limited to backlit portrait scenarios. Broader validation across diverse environments, skin tones, and mixed illumination settings is required to fully establish its generalizability. Furthermore, the method depends on accurate skin region detection, which may limit its performance in challenging cases. Future work will focus on extending the approach to multi-

spectral sensors and integrating learning-based strategies under physical priors, thereby enhancing both accuracy and adaptability in real-world imaging pipelines.

CONCLUSION

This study demonstrated that the proposed SCR-AWB algorithm with an adaptive proportional function effectively improves SPD prediction and color reproduction in backlit portrait scenes. Compared with GreyWorld, the method achieved lower ΔCCT errors and produced more consistent visual results across varying illumination conditions. These findings highlight the importance of incorporating skin reflectance priors and adaptive spectral modeling for robust AWB. Future work will extend this framework to broader environments and multi-spectral imaging systems to further enhance generalization.

REFERENCES

[1].Donner, C., & Jensen, H. W. (2006). A Spectral BSSRDF for Shading Human Skin. Rendering techniques, 2006, 409-418.

[2].Sohaib, A., Broadbent, L., Farooq, A. R., Smith, L. N., & Smith, M. L. (2017). BRDF of human skin in the visible spectrum. Sensor review, 37(4), 390-395.

[3].Beveridge, J. R., Bolme, D. S., Draper, B. A., Givens, G. H., Lui, Y. M., & Phillips, P. J. (2010, June). Quantifying how lighting and focus affect face recognition performance. In 2010 IEEE Computer Society Conference on Computer Vision and Pattern Recognition-Workshops (pp. 74-81). IEEE.

[4].Cao, M., & Luo, M. R. (2022). Preferred skin tones on mobile displays under illuminants having different correlated colour temperatures. Vision Research, 198, 108060.

[5].Spitschan, M., Aguirre, G. K., Brainard, D. H., & Sweeney, A. M. (2016). Variation of outdoor illumination as a function of solar elevation and light pollution. Scientific reports, 6(1), 26756.

[6].Morimoto, T., Sato, M., Sunaga, S., & Uchikawa, K. (2025). Human color constancy in cast shadows. i-Perception, 16(4), 20416695251349737.

[7].Afifi, M., & Brown, M. S. (2020). Deep white-balance editing. In Proceedings of the IEEE/CVF Conference on computer vision and pattern recognition (pp. 1397-1406).

[8].Buchsbaum, G. (1980). A spatial processor model for object colour perception. Journal of the Franklin institute, 310(1), 1-26.

[9].Land, E. H. (1977). The retinex theory of color vision. Scientific american, 237(6), 108-129.

[10].Gijsenij, A., & Gevers, T. (2007, June). Color constancy using natural image statistics. In 2007 IEEE Conference on Computer Vision and Pattern Recognition (pp. 1-8). IEEE.

[11].Hu, Y., Wang, B., & Lin, S. (2017). Fc4: Fully convolutional color constancy with confidence-weighted pooling. In Proceedings of the IEEE conference on computer vision and pattern recognition (pp. 4085-4094).

[12].Kim, D., Kim, J., Yu, J., & Kim, S. J. (2024). Attentive illumination decomposition model for multi-illuminant white balancing. In Proceedings of the IEEE/CVF Conference on Computer Vision and Pattern Recognition (pp. 25512-25521).

[13].Zhou, S., Xiao, K., Li, C., Lai, P., Luo, H., & Sun, W. (2025). A New Method for Camera Auto White Balance for Portrait. Technologies, 13(6), 232.

[14].Lu, Y., Xiao, K., Pointer, M., He, R., Zhou, S., Nasseraldin, A., ... & Wuerger, S. (2025). The International Skin Spectra Archive (ISSA): a multicultural human skin phenotype and colour spectra collection. Scientific Data, 12(1), 487.

A Comprehensive Investigation on The Taxonomic Classification of Recycled Dark Rubber Materials Using Multiple Spectroscopic Analytical Techniques

Yung-Fou Chen[a*], Raymond Jui-Chang Chiang[b], and Chun-Ting Yueh[b]

[a] *Department of Forensic Science, Central Police University, Taoyuan, Taiwan, R.O.C*
[b] *Printing Technology Research Institute, New Taipei City, Taiwan, R.O.C.*

[*] *Corresponding author: nanoforensics@mail.cpu.edu.tw*

ABSTRACT

The abstract should be one paragraph long, summarizing the article's main points in 200-400 words. To ensure that your entire paper is correctly indexed in the conference database, the book of abstracts, and the e-proceedings, we strongly recommend updating your full paper title, abstract, and author information in Microsoft's CMT system to match the information of this full paper. Do not include graphs, symbols, or equations in the abstract. Abstract should be typed in Times New Roman 11-point font, justified with a first-line indent in single-line spacing, on A4-sized paper (21.0 × 29.7 cm, portrait format), and must fit within a box measuring 16.5 cm in width by 24.1 cm in height. Please center the "abstract" title on top of this paragraph (in Times New Roman, 14-point font, using capitals).

Keywords: keyword1, keyword2, keyword3, keyword4, keyword5

INTRODUCTION

A standard printing press is equipped with approximately ten rubber rollers per color unit. When these rollers require replacement due to wear, aging, surface degradation, vitrification, or deformation, they enter the rubber recycling stream to be processed into reclaimed rubber. A critical step in this recycling process is the sorting of natural rubber (NR) from butyl rubber (IIR). This separation is necessary because the two elastomers possess distinct properties and applications that influence both the recycling process and the quality of the final recycled product. The primary reason for this is their differing chemical compositions: natural rubber, derived from the latex of rubber trees, is primarily polyisoprene, whereas butyl rubber is a synthetic copolymer of isobutylene and a small amount of isoprene. These chemical and mechanical differences, particularly IIR's superior gas impermeability and resistance to heat and aging, necessitate different processing requirements. The vulcanization and devulcanization processes vary for each rubber type; mixing them can lead to inefficient processing or incomplete recovery of material properties. Proper sorting is therefore essential to ensure that the recycled rubber retains the specific characteristics required for its intended application, thereby maintaining high product quality and preventing the waste that would result from mixing incompatible materials. This study evaluates several non-contact spectroscopic techniques to develop a rapid and reliable method for distinguishing these two rubber types in a recycling environment.

METHODOLOGY

The experimental materials consisted of forty discarded dark rubber rollers harvested from four-color printing press systems, comprising approximately twenty natural rubber (NR) and twenty butyl rubber (IIR) specimens. Each roller was sectioned into standardized 2 × 2 cm squares to accommodate the sample chambers of various analytical instruments. Prior to spectroscopic analysis, all samples underwent surface cleaning using isopropyl alcohol to remove superficial contaminants while preserving the intrinsic material properties.

This experiment focused on non-contact measurement techniques using five distinct instruments to analyze dark rubber samples. The equipment included: a Specim FX10 visible light hyperspectral imaging system (400–1000 nm), a Specim FX17 near-infrared hyperspectral imaging system (900–1700 nm) [1], a Bruker ALPHA II Fourier Transform Infrared (FTIR) Spectrometer (2500–25000 nm, or 4000–400 cm^{-1}) [2], a Pendar handheld Shifted Excitation Raman Difference Spectroscopy (SERDS) [3,4]system, and a Thermo Fisher SCIENTIFIC Niton XL3t 900 X-ray Fluorescence (XRF) Spectrometer. The primary objective was to assess the feasibility of these non-contact spectroscopic methods for classifying and differentiating natural rubber and butyl rubber, specifically targeting the dark-colored rubber rollers common in printing equipment. For the analysis, rubber samples were cut to appropriate sizes compatible with each instrument's optical system and sample chamber to ensure measurement accuracy and data reliability. By leveraging the complementary nature of these multiple spectroscopic techniques, this study aims to establish a high-efficiency, non-destructive methodology for rubber material classification.

RESULTS AND DISCUSSION

Visible Range Imaging Spectroscopy (400–1000 nm)

The spectral analysis conducted using the FX10 visible-range imaging spectrometer revealed limited discriminatory capability between natural rubber (NR) and butyl rubber (IIR) samples. As shown in Figure 1, although the spectral curves demonstrated slight separation between the two material types, the observed reflectance difference was merely 0.04 units. This minimal contrast is insufficient for reliable classification, particularly considering that industrial recycling processes involve washing procedures that may further diminish already subtle spectral differences. The fundamental limitation of this technique stems from its sensitivity primarily to surface coloration characteristics rather than molecular composition, rendering it inadequate for robust rubber classification applications.

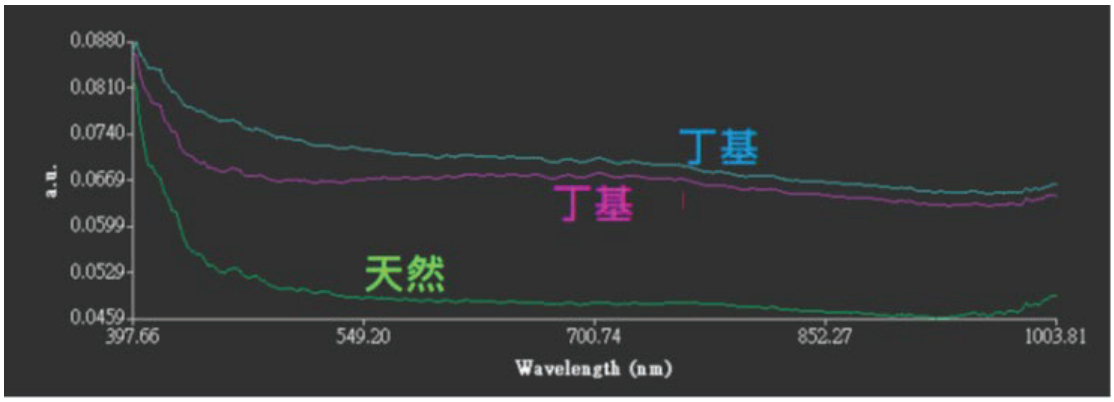

Figure 1: Spectral profiles of NR and IIR samples obtained using visible-range imaging spectroscopy

Short-Wave Infrared Imaging Spectroscopy (900–1700 nm)

The FX17 short-wave infrared imaging spectrometer provided improved discrimination compared to visible-range spectroscopy. As presented in Figure 2, the reflectance curves obtained from three distinct shades of both NR and IIR samples demonstrated measurable separation. The systematic analytical approach employed involved

establishing a reference spectral database followed by implementation of a classification pipeline wherein test samples were compared against reference spectra using similarity algorithms. The spectral angle mapper (SAM) algorithm served as the primary similarity metric, with weighted voting among top-n matches determining final classification outcomes.

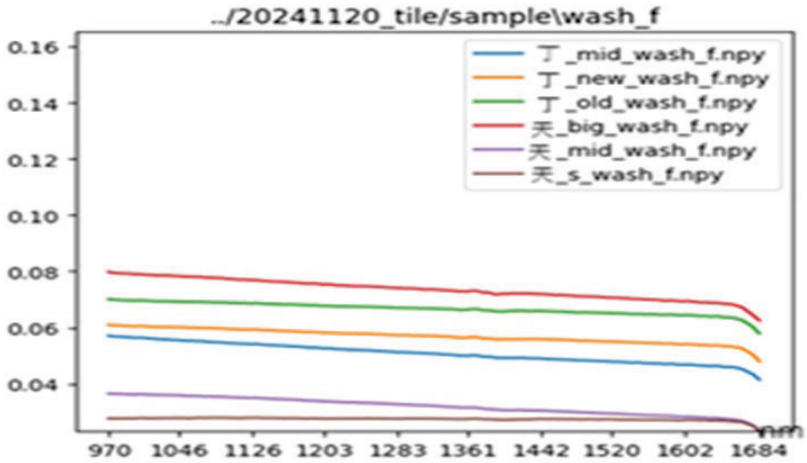

Figure 2: Reflectance spectra of three different shades of natural and butyl rubber were measured using an FX17 spectrometer (900–1700 nm).)

Validation experiments utilizing randomly selected samples (2 IIR and 6 NR specimens) with triplicate sub-region measurements yielded the classification performance summarized in Figure 3. The SAM algorithm achieved remarkable matching accuracy, with most samples reaching 100% concordance. One IIR sample (Sample 2) exhibited a single misclassification in three measurements, resulting in 66.7% confidence. Overall classification accuracy reached 95.7%, with IIR and NR identification rates of 83.3% and 100%, respectively.

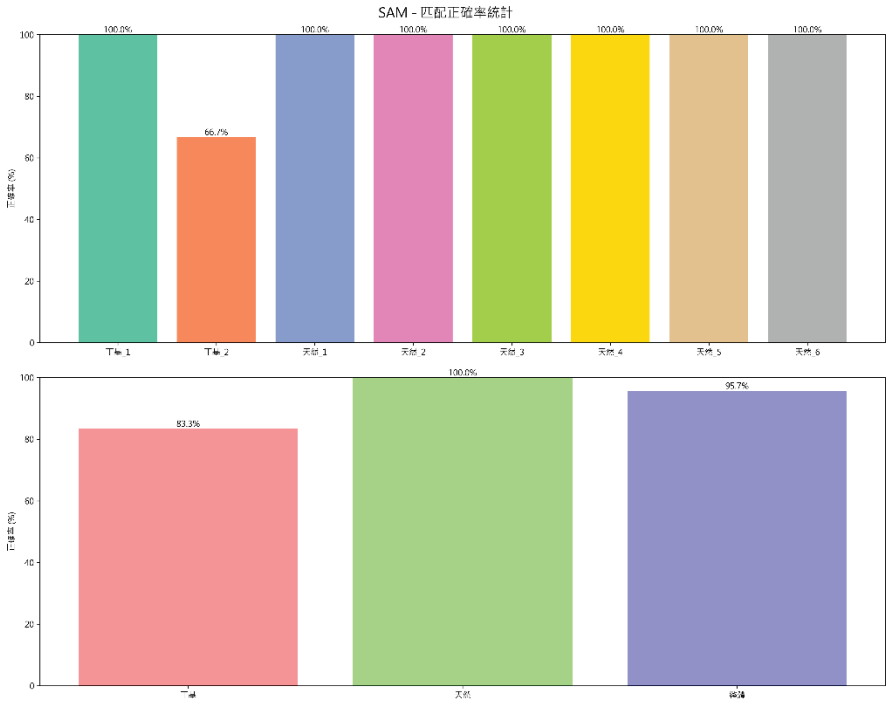

Figure 3: Statistical analysis of SAM matching accuracy across test samples

Extended Short-Wave Infrared Spectroscopy (1000–2500 nm)

Extension into the broader short-wave infrared spectrum provided enhanced spectral separation, as demonstrated in Figure 4. NR samples consistently exhibited lower reflectance values (0.02–0.04 units difference) compared to IIR specimens. However, these modest differences combined with the absence of characteristic spectral features necessitate caution in interpretation. The stability and generalizability of these patterns require verification through expanded sample sizes before industrial implementation.

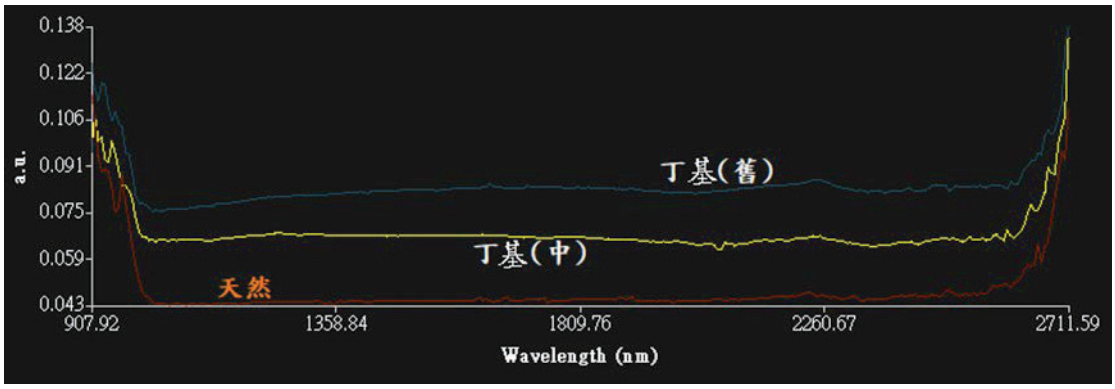

Figure 4: Reflectance spectra of natural and butyl rubber were acquired in the short-wave infrared (SWIR) region (1000–2500 nm).

Fourier Transform Infrared Spectroscopy (FTIR)

FTIR spectroscopy clearly distinguished between natural and butyl rubber based on characteristic absorption bands associated with molecular functional groups. The spectral profiles of the two materials formed two distinct clusters, enabling unambiguous classification. Key features such as C–H stretching, C=C bending, and C–O vibrations differed significantly between NR and IIR, making FTIR the most reliable single-modality technique for material identification in this study.

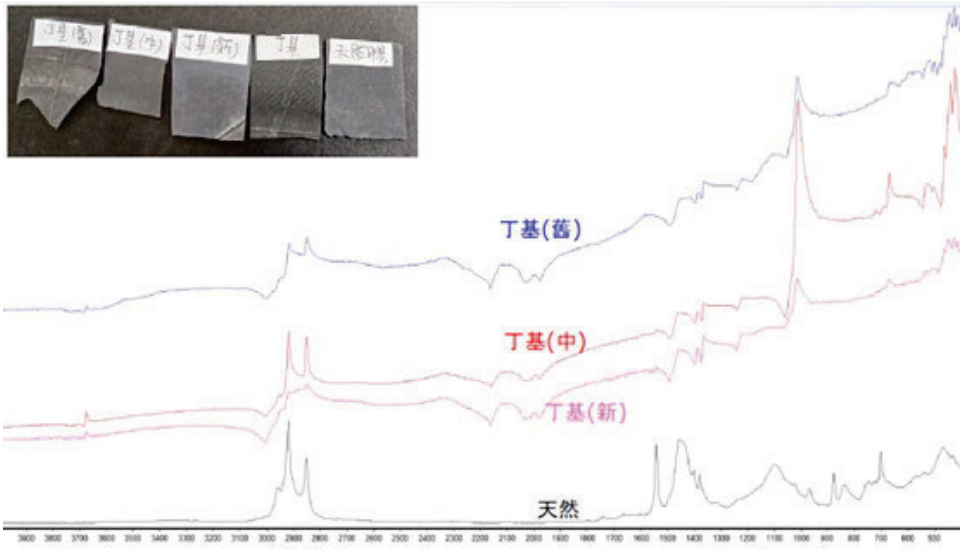

Figure 5: Fourier transform infrared (FTIR) spectroscopy measurements of natural and butyl rubber spectra.

X-Ray Fluorescence Spectroscopy

XRF spectrometry provided complementary elemental analysis, revealing distinctive signatures associated with each rubber type. As shown in Figures 6 and 7, NR samples exhibited characteristic signals for calcium (Ca) and titanium (Ti), while IIR samples showed prominent bromine (Br) emissions. The origins of these elemental signatures—whether inherent to natural composition or introduced during manufacturing—require further investigation to establish reliability as classification markers.

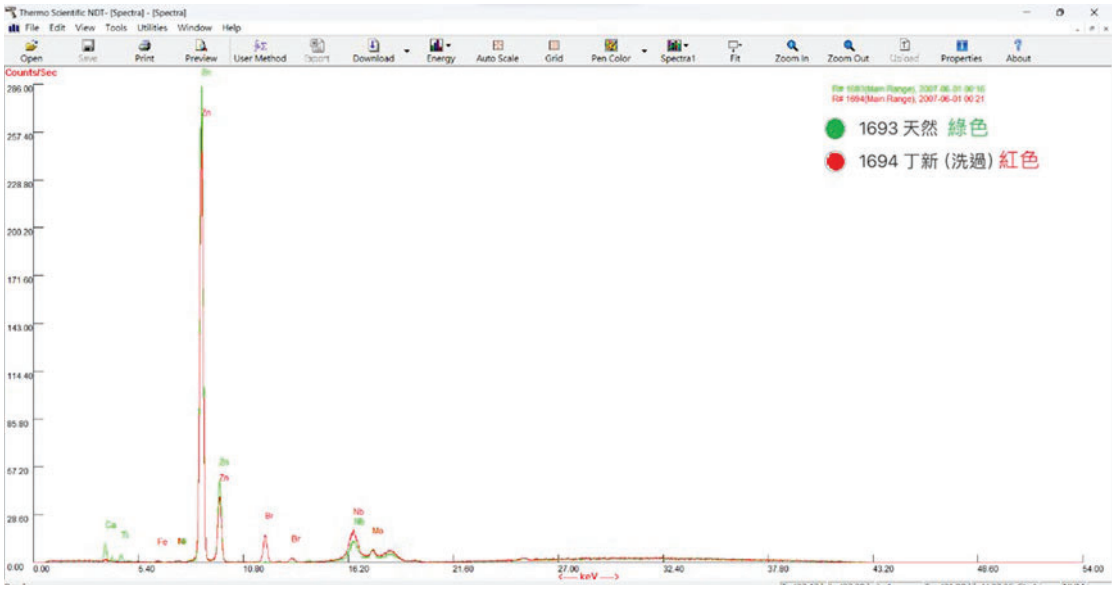

Figure 6: XRF spectral analysis of NR and IIR samples

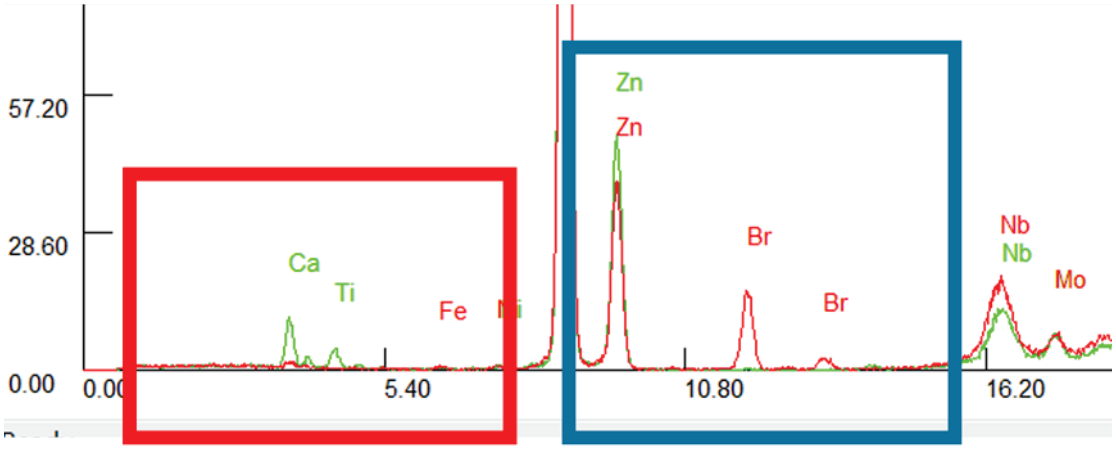

Figure 7: Magnified view of characteristic spectral regions showing elemental differences

Shifted Excitation Raman Difference Spectroscopy (SERDS)

SERDS analysis presented variable performance depending on sample coloration. As shown in Figures 8 and 9, black rubber samples yielded featureless spectra with minimal characteristic signals, while colored specimens

produced distinct Raman spectra with multiple sharp peaks. This discrepancy is attributed to strong absorption of laser excitation by carbon black fillers, resulting in fluorescence interference that obscures Raman signals.

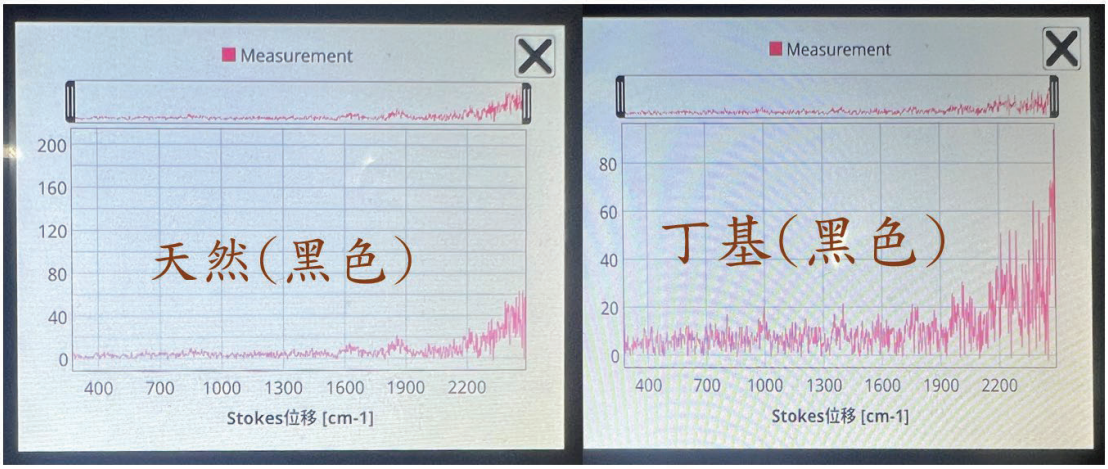

Figure 8: SERDS spectra of black NR and IIR samples showing minimal features

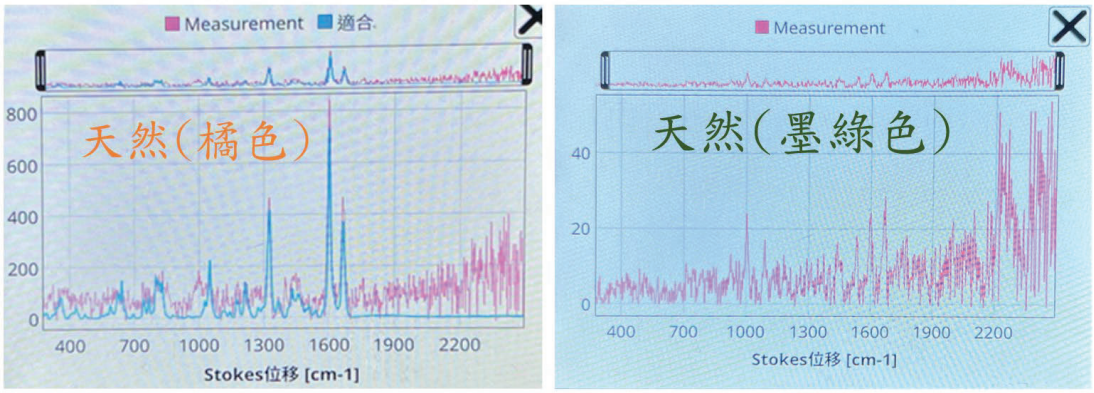

Figure 9: Enhanced spectral features observed in colored rubber samples

CONCLUSION

The compositional differences between natural rubber (NR) and butyl rubber (IIR)—driven by molecular structure—directly govern their performance in critical applications such as seals, tires, vibration dampers, and printing rollers, particularly in mechanical strength, gas barrier properties, and aging resistance. Accurate, non-contact discrimination of these materials is thus vital for advancing recycling efficiency, material purity, and circular economy outcomes. We evaluate five non-contact spectral methods: Vis–NIR (400–1000 nm), SWIR (900–1700 nm), FTIR (4000–400 cm^{-1}), SERDS, and XRF. FTIR delivers the strongest discrimination by resolving distinct functional group vibrations in NR and IIR. However, high carbon black content severely attenuates IR signals, degrading signal-to-noise ratios. To overcome this, we advocate a curated spectral database paired with machine learning (CNN/SVM) to boost classification accuracy. While SERDS is ideal for low-concentration analysis, carbon black induces laser absorption, thermal noise, and fluorescence in black rubber—obscuring Raman features. Crucially, pigmented samples show markedly improved signal clarity, revealing a viable route for Raman-based sorting in colored rubber waste.

ACKNOWLEDGEMENTS

The authors thank Kai-Ber Technology Co., Ltd., Jida Scientific Instruments Co., Ltd., and Sheng-Hsing Instruments Co., Ltd. for technical support and equipment access. This work was partially supported by research grants from the Ministry of Science and Technology, Taiwan.

REFERENCES

[1]. Kruse, F. A., Lefkoff, A. B., Boardman, J. W., Heidebrecht, K. B., Shapiro, A. T., Barloon, P. J., & Goetz, A. F. H. (1993). The spectral image processing system (SIPS)—Interactive visualization and analysis of imaging spectrometer data. *Remote Sensing of Environment*, 44(2), 145–163. https://doi.org/10.1016/0034-4257(93)90013-6

[2]. Grdadolnik, J. (2003). Infrared difference spectroscopy: Part I. Interpretation of the difference spectrum. *Vibrational Spectroscopy*, 31(2), 279–288. https://doi.org/10.1016/S0924-2031(02)00135-5

[3]. Wolf, S., Domes, R., Merian, A., Domes, C., & Frosch, T. (2022). Parallelized Raman difference spectroscopy for the investigation of chemical interactions. *Analytical Chemistry*, 94(29), 10346–10354. https://doi.org/10.1021/acs.analchem.2c01437

[4]. Nan, X., Zeng, S., Chen, L., & Xie, S. (2003). Vibrational imaging of lipid droplets in live fibroblast cells with coherent anti-Stokes Raman scattering microscopy. *Journal of Lipid Research,* 44(11), 2202–2208. https://doi.org/10.1194/jlr.M300225-JLR200

[5]. Hattori, T., Yamamoto, M., & Saito, K. (2001). Application of X-ray fluorescence spectrometry in multielement analysis of rubber samples. Applied Radiation and Isotopes, 54(6), 881–885. https://doi.org/10.1016/S0969-8043(00)00320-1

Spectrally-Aware Perceptual Image and Video Filtering Using Color Transfer

Aiman Raza[a], Marie Dubail[b], Dominique Dumortier[a] and Sophie Jost[a*]

[a] *Ecole Nationale des Travaux Publics de l'Etat, Université de Lyon, Vaulx en Vélin, France*
[b] *EssilorLuxottica, Paris, France*
**Corresponding author: Sophie JOST, sophie.jost@entpe.fr*

ABSTRACT

Simulating colored filters accurately on RGB images currently requires application of spectral transmittances on hyperspectral images of the scene, which is a cumbersome, lengthy and a resource hungry process. Further, under certain circumstances, the capture of accurate hyperspectral data is not possible due to physical constraints of the technology (extreme weather, low-lit scenes, fast moving objects etc.). This study makes use of a simpler Color Transfer (CT) method to overlay the color tones and hue shifts produced by a sunglass filter on an RGB image. Objective analysis using image Color Difference (iCID) metric established the use of the Monge-Kokaram CT method based on the theory of mass transportation as the appropriate candidate for this particular task. Predefined spectral color tones and hues were then transferred to the unfiltered RGB image to create a filtered RGB image. The process was then streamlined for still video creation by applying the filtered color tones on individual frames of unfiltered RGB videos. The final algorithm gave way to a fast, efficient and accurate methodology for creating filtered RGB images and videos in a fraction of time as compared to the reference method of hyperspectral images. The process can be applied on RGB images obtained from any data source or under any illuminant, thus eliminating a major deterrent for filtered image creation. The study also quantified CT methods based on color reproduction accuracy instead of only aesthetic appeal, which was not considered so far in literature as no reference images were available.

Keywords: color transfer, filtered color vision, dominant colors

INTRODUCTION

Traditionally sunglasses have gray or brown tints, but with the advent of sunglasses optimized for sports and outdoor recreational activities, highly chromatic sunglasses are increasingly present in the market. The strong color shifts induced by such sunglasses require analysis of their color fidelity or possible color enhancements. Currently, the most accurate method to portray the impact of a sunglass on human vision is via hyperspectral imaging [1]. Though hyperspectral imaging is a cumbersome, lengthy and a resource hungry process. Further, under certain circumstances, the capture of accurate hyperspectral data is not possible due to physical constraints of the technology (extreme weather, low-lit scenes, fast moving objects etc.). To create filtered still videos, this would be even less practical as one would have to capture spectral data per frame of the video and then apply the filter following the methodology described in Raza 2021. Machine learning techniques to simulate spectral data from RGB images (or RGB frames of a still video) could further add a layer of complexity to the already complicated task. We propose a novel solution to overlay the color tones and hue shifts produced by a sunglass on an RGB image using Image Color Transfer. Color transfer (CT) is the process of transferring the color tones of one image (or a color palette) to another image by statistical manipulations on the associated color data of the original image. For example, in the Figure 1, the color tone of the target color palette (b) is transferred on the original image (a).

We propose to compute dominant colors of the target image [2] and assign spectral reflectance to each dominant color from a database of >7 million colors [3] by calculate CIELAB ΔEab* between the dominant colors and the colors from the spectral database under D65. Then we apply the sunglass transmittances to each spectra [1], convert the filtered spectra into RGB and transfer the filtered RGB color palette to the target image using a Color Transfer algorithm. Since this process is relatively fast, this technique can be applied to each frame of unfiltered still videos and create sunglass filtered still videos.

Figure 1, Color Transfer: The image (B) serves as the target color palette to be transferred on the image (A) to obtain a color transferred image (C)

METHODOLOGY

After an empirical and subjective testing of ten CT methods with publicly available code in MATLAB or Python, three candidate CT methods were shortlisted. The CT methods which introduced artifacts (created a negative image, desaturated the image or lost details) in the transferred images were not taken in account. The three selected CT methods were Erik Reinhard's Ruderman-lαβ linear transformation method [4], Adrian Ilie's polynomial transformation method [5], and Francois Pitie's MK theory of mass transport method [6].

To be able to identify the most appropriate CT method among the three, a selection of five outdoor scenes was compiled and shown in Figure 2 (A1-A5). These images were created using hyperspectral imaging and image color appearance modelling [1]. The hyperspectral data was also used to create sunglass filtered images for three sunglass filter transmittance shown in Figure 2 (B), thus creating reference images for comparison with CT methods [1].

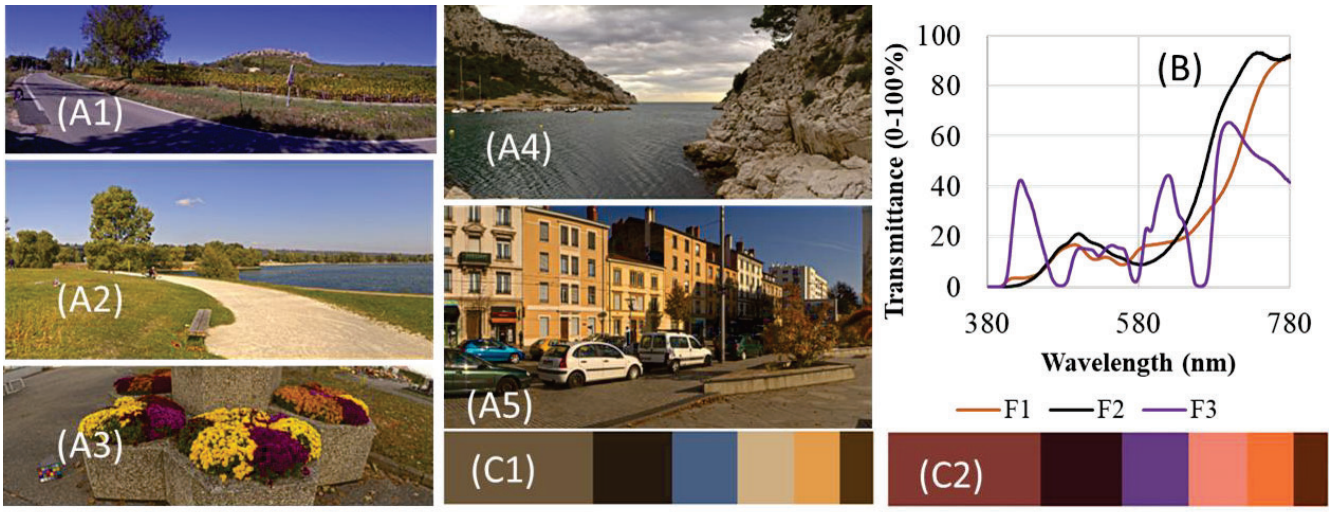

Figure 2, (A1-A6) Test unfiltered images, (B) Test spectral filters, (C1) color palette of the image A5 and filtered color palette of image A5 under filter F2.

The selected CT methods were used to create filtered images from the unfiltered RGB images and the three sunglass filter transmittances (Figure 2 (B)). The dominant colors from the unfiltered image were identified and converted into CIELAB [2].

Separately, a spectral reflectance database (wavelength range of 400 nm -10 nm- 700 nm, [3]) was combined with the D65 illuminant to obtain spectral radiance values, which were used to calculate their CIELAB values under D65. With the help of the CIELAB Delta E*2000 color difference formula, the colors of the spectral data closest to the dominant colors of the unfiltered image were identified. Further, the spectral transmittance of the selected sunglass was applied to the identified spectral radiances and converted to CIE XYZ followed by Adobe RGB to obtain filtered dominant colors or the target color palette. The dominant colors for the Figure 2 (A5) and the filtered dominant colors for the same image under the filter F3 are shown in Figure 2 (C1-C2 respectively).

RESULTS AND DISCUSSION

The three identified filters were thus used to create target color palettes for each image and applied to the unfiltered images using the three CT methods to create filtered Adobe RGB images. The unfiltered images, their color transferred images and reference images, under the filter F2 are shown in Figure 3.

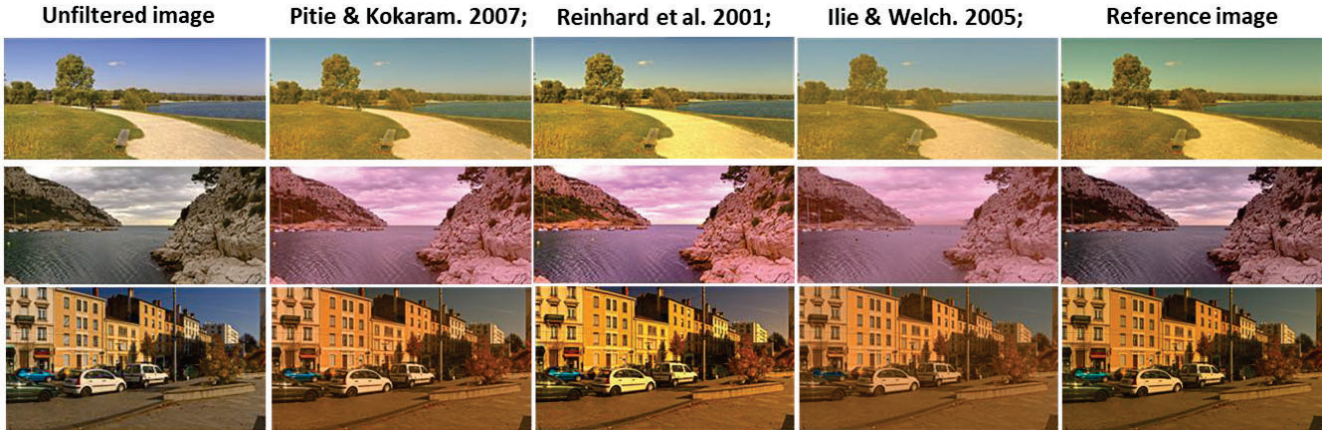

Figure 3, Three unfiltered images, their filtered version under the filter F1-F2-F3 (respectively row wise), using the three tested CT methods and their reference filtered image generated using spectral imaging.

The improved Color Image Difference (iCID) metric proposed by Preiss et al. was used to objectively identify color transferred images closest to the reference filtered image through a single score for each image [7]. The iCID scores lie between 0-1 where a lower score is associated with a lower perceptual difference between two images. Statistical analyses were conducted on the iCID scores obtained, the independent variable was the CT Method, while the iCID score was the dependent variable. As per a Shapiro Wilk normality test, the data was found to be non-parametric, thus the iCID scores were ranked from smallest to largest and an ANOVA was performed on the ranks. The ANOVA test revealed a significant impact ($p<0.05$) of the choice of CT method ($F(2)=29.93$, $p<0.0001$*). The non-parametric ANOVA was followed by a Tukey's post-hoc test. The CT method of Pitie & Kokaram (MK) (mean iCID = 0.31, CL: 0.28-0.33) significantly outperformed both, the Reinhard et al. (mean iCID = 0.39, CL: 0.37-0.42) and Ilie & Welch (Polynomial) method (mean iCID = 0.41, CL: 0.39-0.44).

The CT algorithm developed by Pitie & Kokaram (MK method) produces color transferred images of sunglass filters that are significantly closer to the reference filtered images (hyperspectral imaging) as compared to either Reinhard et al's model or that of Ilie & Welch. The Ist, IInd and IIIrd quartile values of iCID scores for only MK method are: 0.1095, 0.1938 and 0.3385, respectively. This suggests that, in general, an acceptable accuracy of filter color simulation is obtained for the majority of images with the MK color transfer method (Pitie & Kokaram method).

With the CT method finalized, filtered still videos were created by extracting the dominant colors of the N/25 frame (out of N frames) and the same methodology as described for images was applied on every frame of the video. Since the video content across frames doesn't change much for still videos, a single target palette of the N/25th frame was sufficient for video filtering.

CONCLUSION

Wearers chose sunglasses largely on the basis of the sunglass frame and its aesthetic qualities. Visual tools that simulate sunglass filtered vision provide necessary information to the wearers so that they can also include the choice of filter tint in their selection criteria. Color transfer techniques offer an acceptably accurate and fast alternative to illustrate a filter's color qualities without relying on difficult to obtain hyperspectral images. Since color transfer is performed on 2D RGB images, any image can be used to simulate a filtered vision. The color transfer technique and the algorithm for filter simulation identified in this study are fast enough to be applied on still videos as well, thus further improving the information wearers can obtain in order to make an informed choice. The color transfer method, based on Monge-Kantorovitch's mass transportation problem, was identified as the most accurate method for filter simulation after objective tests and statistical analyses.

Even if the visual quality of the filtered images and videos is adequate; certain problems still remain. Very dark or very clear regions have a strong chromatic cast, though applying any chromatic adaptation transform virtually undoes the color transfer. Perhaps a selective chromatic adaptation per region could further improve the color appearance of the filtered images. Various bright regions are sometimes saturated though applying any luminance tone compression also undoes chromatic tone shifts. Perhaps a luminance correction or normalization as per the source image WP and filter transmittance could improve the tone fidelity. Despite these shortcomings, the algorithm is robust enough for preview purposes, and produces filters simulations on images and videos with acceptable accuracy. The algorithm developed in this study can also be applied in other domains, for example in lighting engineering, to accurately and promptly simulate images under light sources (or window glazing) different to that of the acquisition.

REFERENCES

[1] Raza A 2021 *Color Vision Simulation through Ophthalmic Filters* (Lyon, France: Université de Lyon)

[2] Raza A, Jost S and Dubail M 2020 Dominant color and Image color composition retrieval from complex images AIC 2020 (Avignon, France)

[3] Qiu J, Xu H and Xu P 2017 Comparison of Object-Color and Illuminant Metamerism for Digital Image Color Correction

[4] Reinhard E, Adhikhmin M, Gooch B and Shirley P 2001 Color transfer between images *IEEE Comput. Graph. Appl.* **21** 34–41

[5] Ilie A and Welch G 2005 Ensuring color consistency across multiple cameras *Tenth IEEE Int. Conf. Comput. Vis. ICCV05 Vol. 1* **2** 1268-1275 Vol. 2

[6] Pitie F and Kokaram A 2007 The linear Monge-Kantorovitch linear colour mapping for example-based colour transfer *IET 4th European Conference on Visual Media Production (CVMP 2007)* IET 4th European Conference on Visual Media Production (CVMP 2007) vol 2007 (London, UK: IEE) pp 23–23

[7] Preiss J, Fernandes F and Urban P 2014 Color-Image Quality Assessment: From Prediction to Optimization *IEEE Trans. Image Process.* **23** 1366–78

A Comparative Study: Assessing Image Quality for The Jacobi and Gauss-Seidel Retinex Algorithms

Afsaneh Karami[a*], Graham Finlayson[a]

[a]*Computing Science, University of East Anglia, Norwich, England*

[*]*Corresponding author: Afsaneh Karami, A.Karami@uea.ac.uk*

ABSTRACT

We present a comparative image quality experiment for the Jacobi and Gauss-Seidel Retinex, which are, from an algorithmic perspective, improved versions of the McCann99. In previous work, we reformulated the path-based McCann99 into an iterative convolutional center-surround framework, which offers advantages. First, it aligns with the human visual receptive field and unifies three common Retinex categories—path-based method, lightness processing, and center-surround mechanisms—into a coherent framework. Furthermore, from a computational standpoint, it demonstrates faster convergence rates and better rendition of images with fewer artefacts compared to McCann99. The Gauss-Seidel algorithm further reduces Retinex's computational costs. While our earlier research focused on the mathematical formulation and convergence behaviour of the Jacobi and Gauss-Seidel Retinex methods, the current work emphasises image quality assessment and halo artefact evaluation. We compared our methods with McCann99 and TMO-Net, a deep learning tone mapper algorithm. We conducted our experiment on the LVZ-HDR dataset using objective quality metrics, including TMQI, FSITM, and LOE, as well as subjective preference experiments. Our objective results demonstrate that the Jacobi and Gauss-Seidel variants outperform the original McCann99 algorithm in terms of visual quality. The lower LOE scores of our methods compared to McCann99 indicate better preservation of lightness order and reduction of halo artefacts. The preference experiment shows that user preferences remain similar across all three Retinex methods. Notably, our methods also perform competitively against TMO-Net in both objective metrics (TMQI and FSITM) and subjective assessments, all while requiring no training on large datasets.

Keywords: Retinex, image quality, halo artefacts, HDR tone mapper

INTRODUCTION

High Dynamic Range (HDR) imaging has become increasingly important in visual media due to its ability to capture and reproduce a broader range of luminance levels [13]. HDR capture is a requirement to understand how the human visual system (HVS) sees the world [13]. HDR images are used in some multimedia applications [3] (where capturing and conveying all the available scene data is important). HDR image capture is particularly useful when the lighting conditions are not a priori known [8]. However, due to the limited dynamic range of most display devices, HDR images must be converted into a low dynamic range (LDR) for practical viewing. A tone mapper compresses the dynamic range while preserving essential visual attributes such as contrast and colour fidelity. Among various tone mapping strategies, Retinex-based methods stand out as biologically inspired approaches that emulate the human eye's ability [10] to adapt to local illumination and perceive reflectance. Retinex compresses the dynamic range by removing the illumination component and produces LDR renditions of an HDR image.

McCann99 Retinex [11] is a common path-based approach that we reformulated into center-surround framework using Jacobi [5] and Gauss-Seidel [6] methods. These new formulations enhance the original algorithm by aligning more closely with HVS receptive fields, unifying the three main categories of Retinex algorithms, achieving faster convergence, and reducing halo artefacts. Halo artefacts are a well-known limitation of many Retinex-based methods that degrade image quality. The Gauss-Seidel variant further improves convergence speed over the Jacobi version by employing sequential updates. While our earlier focus was on theoretical formulation and convergence analysis of our methods, their perceptual image quality had not yet been comprehensively assessed. This paper addresses this IQ question by evaluating the visual quality and halo suppression capabilities of our Jacobi and Gauss-Seidel Retinex methods in comparison with the classical McCann99 and TMO-Net [14], a modern deep learning-based tone mapping method.

Image quality assessment can be performed using either subjective or objective methods. Subjective evaluations, which involve human observers, are considered more reliable as they directly reflect human perceptual experience. However, they are time-consuming, resource-intensive, and difficult to scale. On the other hand, objective metrics provide efficient and repeatable evaluations, though they may not always correlate perfectly with human perception [7]. We conduct a comprehensive comparison of image quality using TMQI [22], FSITM [23], and LOE [21] as objective metrics and a pairwise preference experiment as a subjective evaluation. Thurstone Case V scaling [15] is used to scale the result of the preference experiment. Taken together, our experiments indicate that the Jacobi and Gauss-Seidel Retinexes deliver leading objective and subjective image quality.

BACKGROUND

The Retinex algorithm aims to achieve colour constancy by separating reflectance from illumination, which better corresponds to the perceived colour of an object. Numerous algorithms have been developed within the Retinex framework, which can broadly be classified into three main categories: path-based methods [11], center-surround mechanisms [9, 1], and lightness-based methods [4].

McCann99 Retinex [12] is a path-based approach that has three operators: (1) the ratio operator, which computes the product of luminance values along a path; (2) the reset operator, which constrains overly bright values; and (3) the average operator, which blends the current estimate with prior results. The algorithm processes the logarithms of the image hierarchically across multiple resolutions, from coarse to fine scales. At each resolution level, the algorithm first calculates the intensity difference between each pixel and its neighbours (ratio operation), followed by the reset operation to clamp values exceeding a predefined intensity threshold. Finally, the average operator updates each pixel by combining the current estimate with the upsampled result from the coarser resolution level. This iterative procedure is applied across eight neighbouring directions, with the number of iterations defined by the user.

Jacobi Retinex [5] is a new version of McCann99 that uses an iterative convolutional center-surround structure. It operates in a multiscale, coarse-to-fine order: at each resolution, the Laplacian extracts derivative information, then Jacobi iteration [2] applies to reconstruct the reflectance image, followed by a reset operation to suppress excessive brightness. The integrated image at this level is upsampled and used as an initial guess for the Jacobi iteration at the next finer resolution level. This formulation improves convergence and reduces halo artefacts compared to McCann99.

Gauss-Seidel Retinex [6] replaces the Jacobi iteration with the Gauss-Seidel [2], further improving convergence speed through an immediate update strategy. Unlike the Jacobi approach, which updates all pixels' values at the end of the convolution process in each iteration, Gauss-Seidel rewrites each pixel as soon as its new value is computed. This reuse of freshly updated information within the same iteration accelerates convergence.

Numerous tone mapping operators (TMOs) that map HDR to LDR images rely on extensive training and hyperparameter tuning. Among them, **TMO-Net** [14] stands out as a deep learning parameter-free method trained on a diverse dataset of 4548 low-light image pairs. It adopts a U-Net–like architecture, enhanced with attention-guided modules and cascaded residual dense blocks, to effectively preserve both local details and global contrast. TMO-Net was evaluated on the LVZ-HDR dataset [14] against 19 state-of-the-art TMOs using quality metrics (TMQI, FSITM, NIQE), and it demonstrated strong generalisability and superior visual quality.

For illustration, Fig. 1 presents an example output from all methods, including TMO-Net, McCann99, Jacobi, and Gauss-Seidel. Notably, when zooming in around the window region, visible halo artefacts appear in the McCann99 output, whereas these artefacts are significantly reduced in the Jacobi and Gauss-Seidel Retinexes.

Figure 1: Left to right, HDR image rendered with TMO-Net, McCann99, Jacobi, and Gauss-Seidel.

METHOD

In this study, we benchmark our methods against McCann99 and TMO-Net to evaluate their performance in terms of image quality and halo artefact, using both objective and subjective assessments. We utilise the LVZ-HDR dataset [14], which provides a diverse and extensive collection of 457 HDR images captured under various conditions. The dataset captures different times of day, environments, and locations, and offers a rich variety of scenes. The dataset is categorised into four main groups: Indoors (71), Nature (173), Nighttime (80), and River-side-sunset (133), enabling a comprehensive evaluation across a wide range of visual contexts.

The metric for objective evaluation includes: (1) The Tone Mapping Quality Index (TMQI) [22], which assesses image quality by combining multiscale structural similarity and statistical naturalness. The structural fidelity component calculates how accurately the output image preserves details from the original scene, and statistical naturalness measures how realistic the image appears based on natural intensity distributions. A higher TMQI score corresponds to better perceptual quality. (2) The Feature Similarity Index for Tone Mapped images (FSITM) [23] measures perceptual feature similarity between the output image and its HDR reference by analysing local phase information. It compares locally weighted mean phase angle maps of the original HDR and the tone mapped LDR image. Higher FSITM scores indicate superior structural and perceptual fidelity. FSITM provides scores for each colour channel (R, G, and B), and this study uses the average of all three channels. (3) Lightness Order Error (LOE) [21] evaluates how well the relative lightness relationships between pixels in the HDR image are preserved after mapping to an LDR. A lower value indicates better preservation of these relationships, contributing to a more natural and visually consistent image. LOE is particularly useful for detecting halo artefacts, as such artefacts often disrupt local lightness order near sharp edges and high-contrast regions by creating unnatural bright or dark outlines.

An important detail for McCann-type Retinex algorithms is that the rendition quality of the output image is related to the number of iterations used as the input to the algorithm. As the number goes from 1 to many iterations, the image is initially too bright and eventually iterates back to the input image. Somewhere in between these bounds is a ‘good-looking image’. In our first experiment, we manually selected an optimal number of iterations for the McCann99 algorithm and adjusted the iteration counts for the Jacobi and Gauss-Seidel versions to generate visually equivalent images to McCann99. We iterated our methods until the mean CIELAB delta E (CIE76) [17] difference from the McCann99 output fell below 3, a threshold generally considered imperceptible to the human eye for complex images [18]. This criterion led to 32 iterations for McCann99, 16 for Gauss-Seidel, and 24 for Jacobi.

In the second experiment, we observed that the Retinex outputs had a different colour rendition compared to TMO-Net. To make the comparison more perceptually fair, we applied colour transfer (excluding tone) from the Retinex outputs of the first experiment to match the colour style of TMO-Net, using the Reinhard method [16].

Finally, in the third experiment, we used the TMQI as a stopping criterion. We selected the iteration count that yielded the highest TMQI score for each method and image and compared their outputs under this optimised setting.

To more accurately assess the visual quality of Retinex, we conducted a preference experiment using colour-transformed outputs from the second experiment. Preference experiments evaluate image quality based on human perception by asking participants to compare pairs of images produced by different methods and choose the one they prefer. In our study, four methods were evaluated: TMO-Net, Jacobi Retinex, Gauss-Seidel Retinex, and McCann99. We employed pairwise comparisons, where observers are shown two images side-by-side and asked to select the preferred one. With four methods, there are $\binom{4}{2} = 6$ unique image pairs. Each observer evaluated 16 scenes, with each pair presented twice (left-right positions swapped), resulting in 192 comparisons per participant. After collecting the data, we estimated the preference probabilities between methods and used Thurstone's Case V model to scale the results [19]. Outliers were identified and removed following the procedure in [15], and final scores were reported in just-objectionable-difference (JOD) units with confidence intervals using bootstrapping [20, 15] with 1000 samples. These JOD scores quantify image quality difference relative to a reference of perfect quality, providing a perceptually meaningful basis for comparison across all methods.

EXPERIMENTS AND RESULTS

The results of the objective evaluation are summarised in Table 1. In the first experiment, the TMQI scores were 0.870 for McCann99 and 0.875 for Jacobi, Gauss-Seidel, and TMO-Net. For FSITM, the scores were 0.840 for TMO-Net, 0.889 for McCann99, 0.897 for Jacobi, and 0.896 for Gauss-Seidel. In terms of the LOE, McCann99 scored 286, while Jacobi and Gauss-Seidel achieved improved scores of 257 and 263, respectively. TMO-Net recorded the lowest LOE score at 170, indicating superior preservation of lightness order. Following colour transfer in the second experiment, TMQI improved slightly to 0.881 for McCann99 and 0.885 for our methods. However, this enhancement came at the cost of degraded FSITM and LOE scores. In the third experiment, TMQI scores reached 0.879 for McCann99, 0.888 for Jacobi, and 0.887 for Gauss-Seidel. The corresponding FSITM scores were 0.890, 0.896, and 0.897, while LOE values were 287 for McCann99, 264 for Jacobi, and 273 for Gauss-Seidel.

Table 1: Results of objective metrics of TMO-Net, McCann99, Jacobi, and Gauss-Seidel on LVZ-HDR dataset.

Experiment	Method	TMQI	FSITM	LOE
	TMO-Net	0.875	0.840	170
1: Iteration-matched(ΔE)	McCann99	0.870	0.889	286
	Jacobi	**0.875**	**0.897**	**257**
	Gauss-Seidel	**0.875**	0.896	263
2: Colour-transferred	McCann99	0.881	0.870	330
	Jacobi	**0.885**	**0.876**	**305**
	Gauss-Seidel	**0.885**	**0.876**	320
3: TMQI-optimised	McCann99	0.879	0.890	287
	Jacobi	**0.888**	0.896	**264**
	Gauss-Seidel	0.887	**0.897**	273

Across all experiments, our Retinex methods consistently outperformed McCann99, with objective metrics—particularly the lower LOE values—highlighting their effectiveness in mitigating halo artefacts. Compared to TMO-Net, they performed comparably in the first experiment and exceeded it in TMQI and FSITM in subsequent tests. The results of the preference experiment are shown in Fig. 2. We recruited 10 observers, and one was excluded due to being identified as an outlier.

The results of the pairwise preference experiment show that the three Retinex methods—Jacobi, Gauss-Seidel, and McCann99—are consistently preferred over TMO-Net. All three achieved positive JOD scores around 0.17, with overlapping confidence intervals, indicating no statistically significant difference in preference among them. In contrast, TMO-Net received a negative JOD score, reflecting its lower perceived image quality. This supports the effectiveness of Retinex-based tone mapping approaches in delivering more visually pleasing results.

Most deep learning approaches are driven by loss-functions that attempt to maximise an objective measure of image quality. Our preference experiment, however, teaches that one of the best deep learning tone mappers delivers images that are much less preferred than Retinex (a classical algorithm that is 50 years old).

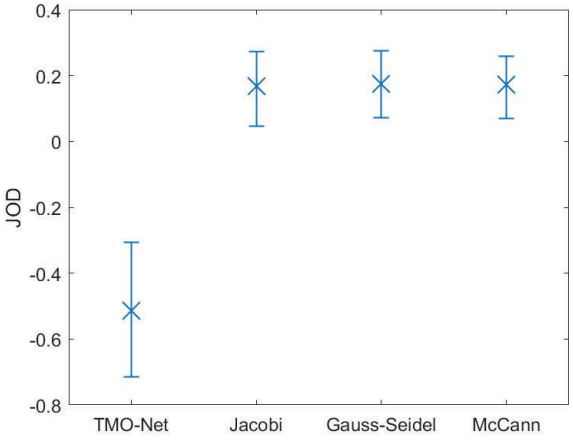

Figure 2: JOD scores comparing TMO-Net, McCann99, Jacobi, and Gauss-Seidel

CONCLUSION

In this paper, we evaluated the Jacobi and Gauss-Seidel Retinex methods in terms of image quality and halo artefacts, using both objective metrics and a subjective preference experiment. To provide a comprehensive comparison, we included the original McCann99 algorithm as well as a recent deep learning-based method, TMO-Net. Our results show that the Jacobi and Gauss-Seidel methods outperform McCann99 and TMO-Net in objective image quality metrics, TMQI and FSITM. Moreover, the subjective preference study confirmed that Retinex-based methods are consistently favoured over TMO-Net by human observers. The objective metrics, particularly the LOE, indicate that our Retinexes are more effective than McCann99 at suppressing halo artefacts; however, the preference experiment does not show this advantage. The results of objective and subjective tests suggest that Jacobi and Gauss-Seidel Retinex algorithms offer the best overall performance, without requiring any training data. Their simplicity, generalisability, and high performance make them promising candidates for practical tone mapping applications.

ACKNOWLEDGEMENTS

This work was supported by the Engineering and Physical Sciences Research Council and AgriFoRwArdS CDT, grants EP/S023917/1. and EP/S028730.

REFERENCES

[1]. Frankle, J. A. and McCann, J. J. (1983), Method and apparatus for lightness imaging. Patent US 4,384,336.

[2]. Golub, G. H. and Van Loan, C. F. (2013), Matrix computations, Johns Hopkins University Press.

[3]. Hanhart, P., Korshunov, P. and Ebrahimi, T. (2014), Subjective evaluation of higher dynamic range video, Applications of Digital Image Processing XXXVII, 9217, 162–174.

[4]. Horn, B. K. (1974), Determining lightness from an image, Computer Graphics and Image Processing 3(4), 277–299.

[5]. Karami, A. and Finlayson, G. (2024), Unifying path and center-surround Retinex algorithms, London Imaging Meeting, Society for Imaging Science and Technology, 17–21.

[6]. Karami, A. and Finlayson, G. (2025), Gauss-seidel Retinex, London Imaging Meeting, Society for Imaging Science and Technology. Accepted, to appear.

[7]. Khan, I. R., Alotaibi, T. A., Siddiq, A. and Bourennani, F. (2022), Evaluating quantitative metrics of tone-mapped images, IEEE Transactions on Image Processing, 31, 1751–1760.

[8]. Korshunov, P., Nemoto, H., Skodras, A. and Ebrahimi, T. (2014), Crowdsourcing-based evaluation of privacy in HDR images, Optics, Photonics, and Digital Technologies for Multimedia Applications III, SPIE.

[9]. Land, E. H. (1986), An alternative technique for the computation of the designator in the retinex theory of colour vision, Proceedings of the National Academy of Sciences, 83(10), 3078–3080.

[10]. Land, E. H. and McCann, J. J. (1971), Lightness and retinex theory, Journal of the Optical Society of America, 61(1), 1–11.

[11]. McCann, J. J. (1999), Lessons learned from Mondrians applied to real images and colour gamuts, Color and Imaging Conference, Society for Imaging Science and Technology, 1–8.

[12]. McCann, J. J., McKee, S. P. and Taylor, T. H. (1976), Quantitative studies in retinex theory a comparison between theoretical predictions and observer responses to the “color mondrian” experiments, Vision Research, 16(5), 445–453.

[13]. Narwaria, M., Da Silva, M. P. and Le Callet, P. (2015), HDR-VQM: An objective quality measure for high dynamic range video, Signal Processing: Image Communication, 35, 46–60.

[14]. Panetta, K., Kezebou, L., Oludare, V., Agaian, S. and Xia, Z. (2021), TMO-Net: A parameter-free tone mapping operator using generative adversarial network, and performance benchmarking on large scale HDR dataset, IEEE Access, 9, 39500–39517.

[15]. Perez-Ortiz, M. and Mantiuk, R. K. (2017), A practical guide and software for analysing pairwise comparison experiments, arXiv preprint arXiv:1712.03686 .

[16]. Reinhard, E., Adhikhmin, M., Gooch, B. and Shirley, P. (2002), Color transfer between images, IEEE Computer Graphics and Applications, 21(5), 34–41.

[17]. Robertson, A. R. (1977), CIE recommendations on uniform color spaces, color-difference equations, and metric color terms, Color Research & Application, 2(1), 7–11.

[18]. Stokes, M., Fairchild, M. D. and Berns, R. S. (1992), Precision requirements for digital color reproduction, ACM Transactions on Graphics, 11(4), 406—422.

[19]. Thurstone, L. L. (2017), A law of comparative judgment, in ‘Scaling’, Routledge, 81–92.

[20]. Tibshirani, R. J. and Efron, B. (1993), An introduction to the bootstrap, Monographs on Statistics and Applied Probability 57(1), 1–436.

[21]. Wang, S., Zheng, J., Hu, H. and Li, B. (2013), Naturalness preserved enhancement algorithm for non-uniform illumination images, IEEE Transactions on Image Processing, 22(9), 3538–3548.

[22]. Yeganeh, H. and Wang, Z. (2012), Objective quality assessment of Tone-Mapped images, IEEE Transactions on Image Processing, 22(2), 657–667.

[23]. Ziaei Nafchi, H., Shahkolaei, A., Farrahi Moghaddam, R. and Cheriet, M. (2014), FSITM: a feature similarity index for Tone-Mapped images, IEEE Signal Processing Letters, 22(8), 1026–1029.

Characterising Head-Mounted Displays Based on Visual Assessment

Chia-An Lee* and Li-Chen Ou

National Taiwan University of Science and Technology, Taipei, Taiwan
**Corresponding author: Chia-An Lee, D11322501@mail.ntust.edu.tw*

ABSTRACT

The study used the gain–offset–gamma (GOG) model while replacing traditional instrumental RGB measurements with three psychophysical approaches: partition scaling for estimating perceived lightness across RGB channels and establishing opto-electronic transfer functions, unique hue assessment for improving hue accuracy, and color matching between the test HMD and a reference LCD for estimating the maximum red, green, and blue RGB values, determining linear transformation parameters. Two psychophysical experiments were carried out to validate this visual-assessment-based GOG model. The findings reveal good predictive accuracy for hue quadrature and satisfactory performance for both colourfulness and lightness scales. This research demonstrates that visual assessment methods can serve as an alternative approach when traditional measurement equipment is either impractical or inaccessible, offering researchers practical tools for advancing virtual reality applications and development.

Keywords Visual Assessment, Colorimetric Characterisation, Head-Mounted Display, Virtual Reality, Psychophysics

INTRODUCTION

With the proliferation of virtual reality (VR) applications, accurate colorimetric characterization of head-mounted displays (HMDs) has become critical for advancing research in colour science, imaging, visual perception, and immersive interface design. Conventional instrumental measurement approaches pose substantial challenges for HMD characterisation, making it difficult for researchers to conduct research in colorimetric investigations. While specialized colour measurement instruments for HMDs are available, their high cost remains a significant barrier for many researchers. To overcome these constraints, this study introduces a new method that enables HMD characterization without direct instrumental colour measurement but employs an approach based on visual assessment techniques.

METHODS

The proposed method employs the gain–offset–gamma (GOG) model [1] as the foundation while substituting instrumental RGB measurements with visual assessment techniques. The GOG model is a two-stage model that involves nonlinear and linear transformations, each represented by a 3×3 matrix. Traditionally, the nonlinear stage needs measurement data of CIE tristimulus values for the RGB channel colours to establish opto-electronic transfer functions (OETFs) with the gain, offset, and gamma parameters. The OETFs transform display digital values for any specified colour into corresponding RGB values, which are then converted to CIE tristimulus values during the linear stage. This conversion matrix also requires the tristimulus value measurement for the display's peak white

and the maximum RGB colours. The fundamental concept of the proposed approach involves substituting conventional instrumental measurements required for GOG model development with three visual assessment methods: partition scaling, unique hue judgment, and colour matching.

Two psychophysical experiments were conducted in this study. Experiment 1 included 24 observers assessing colour stimuli on an HTC Vive HMD, using partition scaling, unique hue judgement, and colour matching to derive the GOG model. Experiment 2 involved 20 observers in a colour appearance experiment for testing the model's predictive performance.

Partition Scaling

The partition scaling method [2] was adopted in this study to estimate lightness values of colours across RGB channels for determining gain, offset, and gamma parameters in the OETFs. Partition scaling represents a psychophysical procedure utilizing bisection tasks that can derive interval scales of psychological attributes from observers' visual evaluations of presented stimuli. In each trial, observers viewed three coloured discs, all selected from one of the three RGB channels or from the achromatic scale, arranged horizontally on the display, as shown in Figure 1. The coloured discs positioned at the two sides exhibit the a high and a low lightness within a selected lightness range. Observers were instructed to adjust the lightness of the central disc until it appeared to possess intermediate lightness between the discs on the two sides. Each RGB channel was segmented into eight lightness divisions, creating seven lightness boundaries whose values were estimated through partition scaling results. These lightness values subsequently determined the OETFs in the GOG model. In addition to the RGB channels, the achromatic channel was also included into the partition scaling to enhance the accuracy of the characterisation model.

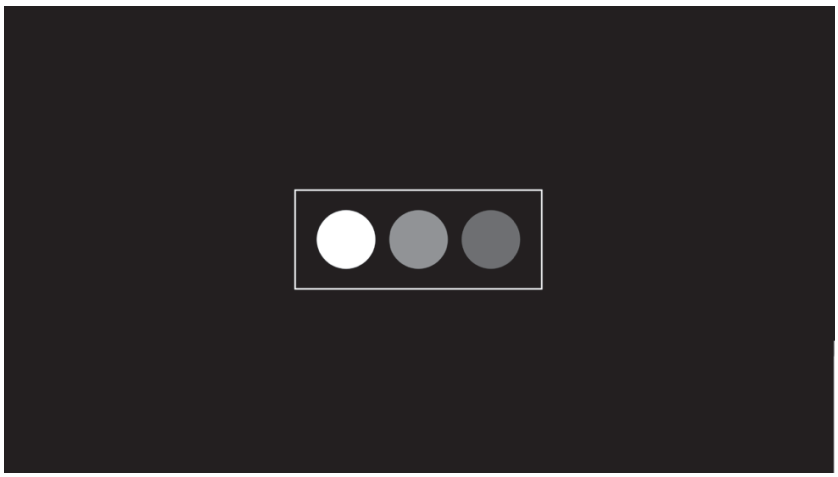

Figure 1: Schematic layout of partition scaling in this study for the achromatic channel

Unique Hue Judgement

The unique hue judgment method [3] was used for hue correction in the GOG model. All the four unique hues were assessed: red, yellow, green, and blue. Hue indicators and hue-related differences obtained from these sessions were then applied to refine the GOG model. Figure 2 presents the experimental layout design for the unique green session. Each unique hue comprised four sets of colour stimuli, each containing ten colour stimuli with identical chroma and lightness but varying hue.

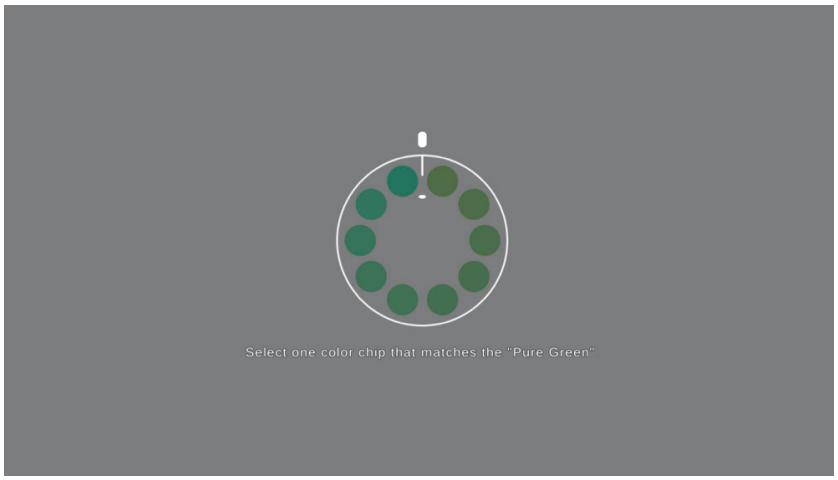

Figure 2: Schematic layout of unique hue judgement in this study for the unique green session

Colour matching

The colour matching technique was used to compare colours displayed on a 27-inch BenQ LCD with the HMD's peak white and maximum RGB colours. The observer was asked to adjust the hue, lightness and chroma of the colour on the LCD until it appeared to match the target colour shown on the HMD. This resulted in the visual estimation of the tristimulus values of the maximal RGB colours on the HMD, thus determining the 3×3 matrix for the linear stage of the GOG model.

Figure 3 displays the experimental set-up for the colour matching sessions. The actual setup is operated in a dark room. The HMD was secured on a mounting system to prevent unwanted movement and reduce observer discomfort while wearing the device.

Figure 3: The experimental set-up for the colour matching experiment. The actual set-up was a dim environment with all lights off in the room.

Due to colour gamut differences between the LCD and the HMD, colour stimuli used in partition scaling and colour matching sessions were selected within a reduced HMD gamut. This limitation means that while the GOG characterisation model for the HMD demonstrates accurate predictions within this reduced gamut, its predictive accuracy for colours beyond this gamut remains uncertain. A potential solution involves utilizing an LCD with a colour gamut exceeding that of the HMD.

RESULTS

Figures 4 (a)-(c) present comparisons between perceived lightness, colourfulness, and hue quadrature, respectively, with values predicted by CIECAM02 and CIECAM16 utilizing the GOG model developed from Experiment 1. The results demonstrate high predictive performance for hue quadrature (CV = 5.5, r = 0.995), and moderate performance for both colourfulness (CV = 33.9, r = 0.958) and lightness (CV = 22.7, r = 0.870). According to Figures 4 (a) and (b), the model appears to underestimate the perceived colourfulness and lightness. This was likely attributed to the HMD's high display luminance while the experiment was conducted in the dark room.

Table 1 displays the correlation coefficient (r) and coefficient of variation (CV) between model predictions and experimental observations. The visual-assessment-based GOG model demonstrates excellent performance in predicting hue quadrature, showing the highest r and lowest CV among the three scales, as illustrated in Figure 4 (c). The model's lightness predictions and the visual results show the weakest r value among the three scales, with their relationship displaying subtle non-linearity, as presented in Figure 4 (a). The model's colourfulness predictions consistently underestimate observers' visual results, as demonstrated in Figure 4 (b).

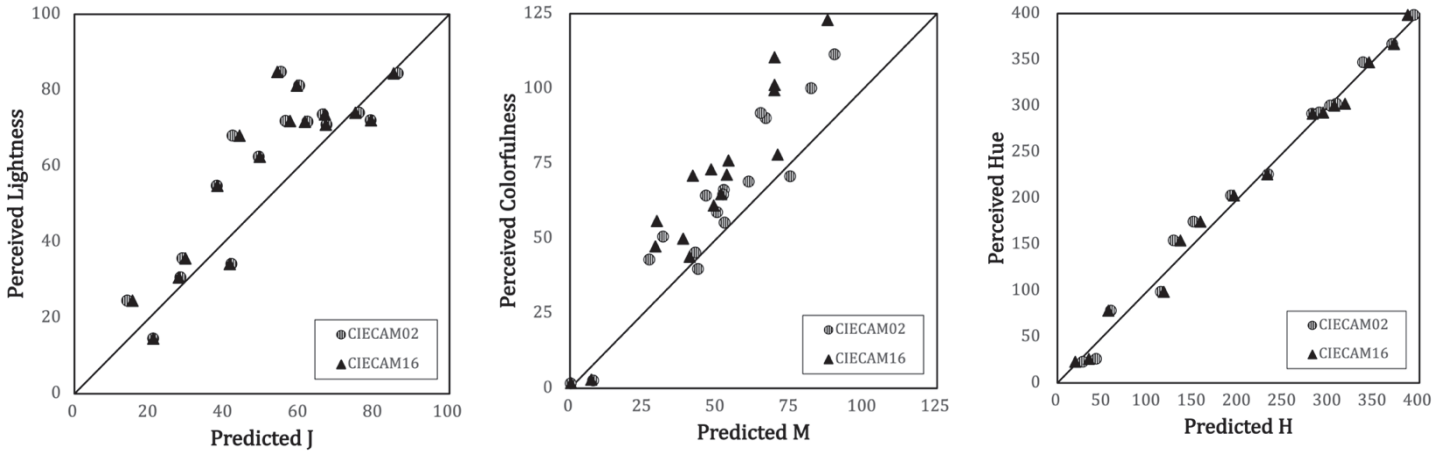

(a) **(b)** **(c)**

Figure 4: Comparisons in (a) lightness, (b) colourfulness and (c) hue quadrature between the visual results and the predicted values by CIECAM02 and CIECAM16

Table 1: Correlation coefficient (r) and coefficient of variation (CV) between predicted values and visual results.

	CIECAM02			CIECAM16		
	J	M	H	J	M	H
r	0.866	0.951	0.994	0.870	0.958	0.995
CV	23.0	23.9	6.0	22.7	33.9	5.5

CONCLUSION

Visual assessing techniques, including partition scaling, unique hue judgment, and colour matching, were used in this research to establish a GOG model for the VR HMD. The experimental results demonstrate strong predictive performances of the visual-assessment-based model. This model exhibits best performance in hue prediction among the three perceptual attributes. The slight underestimation of lightness and colourfulness values may be attributed to the high display luminance of the HMD when the experiment was conducted in a dark room. The proposed new method can be a useful tool for HMD characterisation when constraints exist in utilizing measurement instruments.

ACKNOWLEDGEMENT

This research was sponsored in part by the National Science and Technology Council, Taiwan (NSTC 113-2410-H-011-006 MY2).

REFERENCES

[1]. Berns, R. S. (1996). Methods for characterizing CRT displays. Displays,16(4), 173–182.

[2]. Van De Perre, L., Ryckaert, W. R., Dujardin, M., Hanselaer, P., Smet, K. A. 2019. Derivation of brightness scales using partition scaling. LEUKOS, 17(2), 125–139.

[3]. Xiao, K., Wuerger, S., Fu, C., Karatzas, D. 2011. Unique hue data for colour appearance models. Part I: Loci of unique hues and hue uniformity. Color Research & Application, 36(5), 316–323.

Evaluating Preference for Images Enhanced with Simple Tone Curves

James Bennett[a*], Graham Finlayson[a]

[a]*University of East Anglia, Norwich, United Kingdom*
[*]*Corresponding author: James Bennett, james.r.bennett@uea.ac.uk*

ABSTRACT

Tone curves are central to camera pipelines and image editing workflows, describing how tonal values are mapped to produce visually appealing images. While tone curves can be arbitrarily complex, recent work has suggested that simple tone curves – defined as monotonic functions with at most one inflexion point – are sufficient to approximate expert adjustments. This raises an important perceptual question of whether human observers prefer images enhanced with simple tone curves. We address this by conducting a psychophysical study on the MIT-Adobe FiveK dataset. Expert tone curves were approximated using a constrained optimisation method from the prior art to derive the best simple curve in the primal domain, and additionally in a logarithmic domain. For each of 24 selected images (drawn from well-, less-well- and poorest-fitted simple curves), we compared four renditions: the unenhanced input, the expert output, the primal-domain simple rendition, and the log-domain simple rendition. Eight naïve observers completed pairwise preference tests under controlled viewing conditions. Our results show that both primal and log-domain simple tone curves produce images with perceptual quality comparable to expert renditions. Observers did not show a significant preference between expert and simple renditions, indicating that simplified curves provide a suitable approximation, with the log-domain simple renditions being marginally favoured. These findings demonstrate that simple tone curves are not only objectively similar but also perceptually competitive to expert renderings, offering a practical alternative to complex expert adjustments in image enhancement.

Keywords: Tone mapping, Tone curves, Image enhancement, Psychophysical experiment, Pairwise preference

INTRODUCTION

Tone mapping is widely used in camera pipelines and image editing workflows to manipulate brightnesses and enhance the perception of images. When applied to real world luminance, tone maps describe camera response functions and the conversion from high dynamic range [1,2]. Tone mapping can also be applied within post processing [3,4] to enhance the perception of an image according to one's preference [5]. A tone curve describes the function that maps input tonal values to output tonal values. When the same function is applied to every pixel in the image, the tone mapping is said to be global. Tone curves may have a fixed shape, be custom-defined per image, or be computed algorithmically. They can take specific functional forms, such as power laws or sigmoids, or be free-form curves created by interpolating control points. While tone curves are continuous and usually increasing, their shape is typically unconstrained.

Previous work [6] has argued that tone curves should be simple – that is, they have at most one inflexion point, in contrast to complex, "wiggly" curves. This gives rise to four possible cases, depicted in Figure 1. Case 1 and Case 2 have zero inflexion points: in Case 1 the gradient increases monotonically, while in Case 2 it decreases monotonically. Case 2 corresponds to common tone curve shapes, such as gamma encoding. Case 3 and Case 4 each have one inflexion point, the position of which can vary across the domain. Case 3 is the commonly seen "S-

shaped" curve, where the gradient increases to the inflexion point and then decreases, boosting midtone contrast. Case 4 is the opposite, with the gradient decreasing to the inflexion point and then increasing.

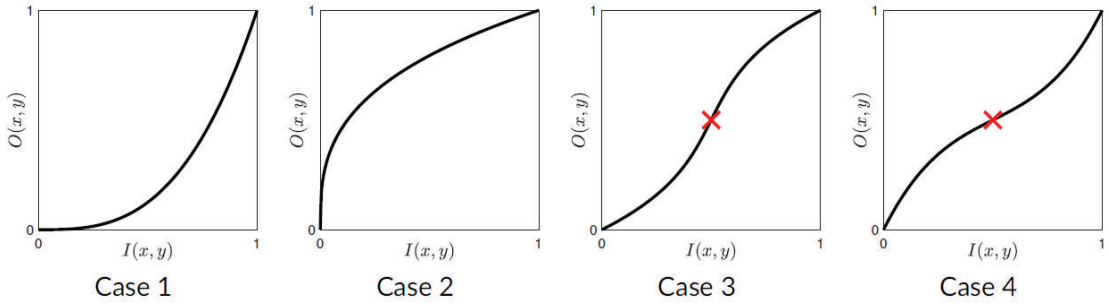

Figure 1: Depiction of four simple cases

In [6], a mathematical optimisation method was proposed to derive a simple curve that approximates a more complex tone curve. The objective function seeks a simple tone curve that closely matches a target curve, subject to constraints enforcing monotonicity and the allowed inflexion case. The problem is formulated as a quadratic program with linear constraints and can be solved efficiently and a global minimum is found [7]. For the MIT-Adobe FiveK dataset, expert tone curves were found to be either inherently simple or well approximated with a simple curve.

In this work, we investigate whether human observers prefer images enhanced with simple versus complex tone curves. We conduct a psychophysical experiment to evaluate preference between the ground-truth expert images and their simplified counterparts. The remainder of this paper details the creation of images for the subjective experiment using the optimisation method, describes the experimental setup, and presents the results. Our findings indicate that the simplification method produces images that are as preferred as expert renditions, with a marginal perceptual advantage when the simple curves are solved in log space.

METHODOLOGY

Generating the images

This study uses the MIT-Adobe FiveK dataset [8], provided as an Adobe Lightroom catalogue from which pairs of input–output images can be extracted. Following the procedure of [6], adopted from [9], we export input images from the collection Input minus 1.5 in ProPhoto 16-bit TIFF format, with the long edge scaled to 640 px. Because the Lightroom adjustments are numerous and undisclosed, the images are not strictly related by a single global tone curve. The expert images are generated according to [6] ensuring a global mapping. Informally, the most global fit was found by mapping the L* channel of CIELAB. The input, expert and simple images, per (x, y) pixel, are respectively $\mathcal{I}(x, y)$ and $\mathcal{P}(x, y)$:

$$\mathcal{I}(x, y) = [L_I^* \; a_I^* \; b_I^*]^\top$$

$$\mathcal{P}(x, y) = [L_P^* \; a_P^* \; b_P^*]^\top = [T(L_I^*) \; a_P^* \; b_P^*]^\top$$

$$\hat{\mathcal{P}}(x, y) = \left[\hat{T}(L_I^*) \; a_P^* \; b_P^*\right]^\top$$

Function T is the expert's global tone curve mapping L_I^* to L_P^*. For each input-expert pair, we use the prior optimisation to solve for a simple tone curve $\hat{T}$ (constrained to be increasing with at most one inflexion point) that best approximates the expert tone curve, generating $\hat{\mathcal{P}}(x, y)$. Simple tone-mapped images are generated by applying $\hat{T}$ to the input L^*. We also solve for the simple tone curve in logarithmic space. Applying a logarithmic transformation to the L^* channel emphasises darker values in the optimisation. The simple tone curve is then solved in this transformed space, and subsequently mapped back to the original domain. For each image, then, we have: (1) the input version, (2) the expert rendition (where the expert tone curve may be complex), (3) an image tone

mapped with a simple approximation of the expert curve, (4) a simple tone mapped rendition where the simple curve is solved for in log-space. These are exported from MATLAB in the sRGB colour space for display.

Conducting the preference experiments

We conducted a pairwise psychophysical experiment using a subset of 24 images from the MIT-Adobe FiveK dataset. The selection comprised the 8 images with the highest ΔE colour difference between simple and expert renditions, 8 chosen randomly from above the 99th percentile, and 8 chosen randomly from below it.

The experiment compared four image renditions: input, expert, simple, and log-space simple. A pair of renditions were shown side by side at a time. The observer was asked to choose which image they preferred by clicking a button. For four renditions there are six unique pairings. Each pair was shown twice with reversed display order, giving 12 comparisons per image and 288 comparisons per observer.

Eight naïve observers with normal colour vision (verified using Ishihara plates) participated in the study. Experiments were conducted in a grey room with controlled lighting and a calibrated monitor, following ISO 3664:2009. Images were displayed in random order (with the restriction that the same image was not shown simultaneously). Observers viewed the images and recorded preferences through a MATLAB graphical user interface, with colour profiles matched to the monitor.

RESULTS AND DISCUSSION

Table 1 lists the images used in the psychophysical experiment by their expert and input number. For each image we report the objective ΔE colour difference between the expert rendition and the simple renditions (solved in both primal and logarithmic domains), along with the ΔE rank out of 25,000 images. The table also shows the number of times each rendition was voted as preferred. Each row (of preference votes) sums to 96, corresponding to 12 comparisons per image for each of the eight observers.

Table 1: Psychophysical experiment statistics and preference votes.

	Primal solved		Log solved		Preference votes			
Image	ΔE	**Rank**	ΔE	**Rank**	**Input**	**Expert**	**Simple**	**Log simple**
C2704	< 0.01	29	0.0658	18479	0	39	30	27
B3531	< 0.01	7982	< 0.01	9079	16	27	20	33
A286	< 0.01	10503	0.0176	13091	1	31	29	35
A2485	< 0.01	11408	< 0.01	2738	0	31	29	36
E3626	< 0.01	11446	< 0.01	7141	0	30	27	39
A2213	0.0503	19062	< 0.01	3335	12	26	23	35
B2473	0.0551	19423	0.274	22666	0	32	32	32
B1373	0.151	22671	0.180	21634	3	28	28	37
A707	0.827	24780	2.64	24982	0	28	31	37
C1620	0.848	24800	1.54	24896	0	37	34	25
B2079	0.890	24815	1.00	24709	12	23	27	34
C823	1.00	24858	1.33	24863	0	32	30	34
A1543	1.06	24869	1.11	24772	1	28	36	31
E604	1.12	24887	0.610	24176	0	31	32	33
C4215	1.62	24957	2.01	24949	6	29	29	32
C374	1.68	24962	1.63	24905	0	30	33	33

A21	2.68	24993	0.630	24228	3	32	27	34
A596	2.69	24994	0.357	23268	31	29	16	20
A1692	2.72	24995	2.75	24984	0	25	37	34
A2628	2.86	24996	0.840	24576	0	33	28	35
B1999	2.88	24997	2.60	24978	0	30	33	33
A2049	3.12	24998	2.14	24957	10	28	34	24
A2823	3.13	24999	1.92	24942	0	37	27	32
A2673	3.22	25000	1.52	24893	1	38	29	28

From Table 1 we see that the selected images span a wide range of objective ΔE values, in line with the selection methodology. To illustrate the renditions and their tone curves, we display image A2823 in Figure 2, one of the most challenging cases. The top images compares the input (left) with the expert rendition (right). The expert is an enhanced version of the input produced through a complex tone curve. The bottom row shows two simplified alternatives: the left image is generated by applying the best primal-domain simple curve, while the right image applies the best simple curve solved in log-space. Visually, the log-domain solution more closely resembles the expert rendition due to closer similarity of the dark tones.

(a) Input rendition

(b) Expert rendition

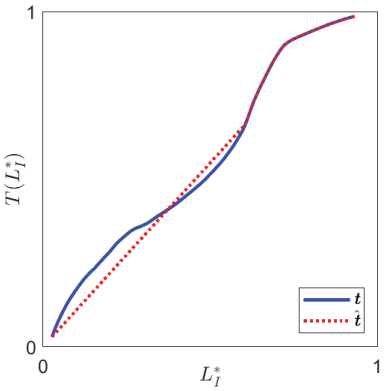

(c) Curves in primal domain

(d) Simple rendition

(e) Log simple rendition

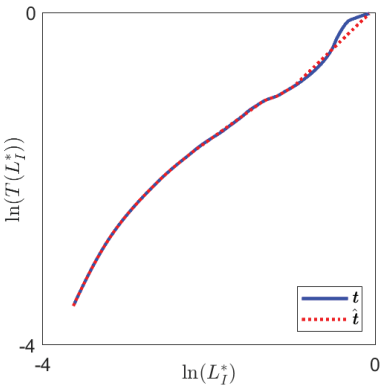

(f) Curves in log domain

Figure 2: Results for image 2823 showing image renditions and expert and solved for simple curves.

To better understand this behaviour, we plot the corresponding tone curves for $L^*$and for $log(L^*)$. In both cases, the non-simple expert curve is shown in solid blue and the best simple approximation in dotted red. Consistent with the visual results, the simple curve solved in the log domain more faithfully follows the expert curve, especially in the dark tones, suggesting that the logarithmic transformation improves the approximation for this image.

For most images, Table 1 shows that the expert, primal, and log-simple renditions were preferred more often than the unenhanced input. Nevertheless, in some cases the input rendition still attracted votes, indicating that observers do not universally reject unenhanced images. Preferences among the expert, primal, and log-simple renditions varied by image, making it difficult to draw strong conclusions from raw vote counts alone.

To aggregate and compare preferences across all images, we applied Thurstone's Case V model [10] using a pairwise comparison toolbox [11]. This method psychometrically scales the pairwise votes into *Just Objectionable Difference* (JOD) units, where higher scores indicate stronger preference and 1 JOD unit corresponds to a 75% discrimination threshold. Although the units are arbitrary and not comparable across experiments, they provide a consistent scale for analysing relative differences. Figure 3 shows the scaled results, with 95% confidence intervals computed via bootstrapping (1,000 samples).

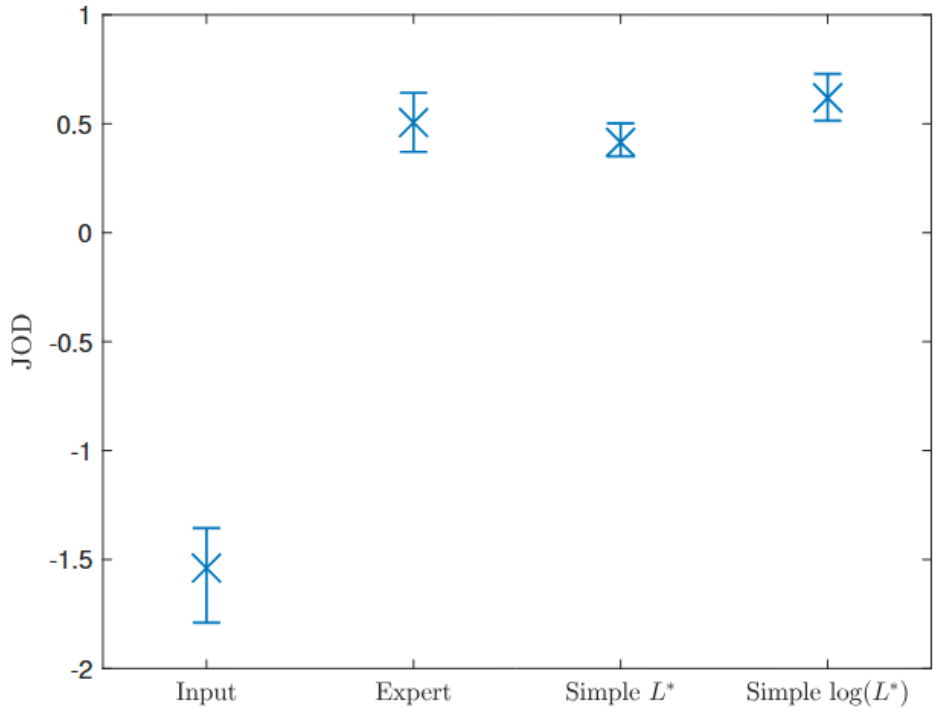

Figure 3: Scaled preference scores, input (-1.54), expert (0.51), simple (0.42), and log-space simple (0.62).

As expected, observers preferred the expert and simple renditions over the input, confirming that the enhancements provide a perceptual benefit. The differences among expert, primal, and log-simple renditions were within the margin of uncertainty, with overlapping confidence intervals. This suggests that observers do not exhibit a strong preference between these three methods, and that the simplified tone curves approximate the expert adjustments effectively.

A point of interest is the slightly higher preference for log-space simple curves. While we must be cautious about over-interpreting results with overlapping confidence intervals, the data suggest that observers may favour log-space solutions. Whilst the primal-domain simple renditions scored just below the expert renditions, the log-domain renditions scored slightly above. This indicates that observers may even prefer a simple tone enhancement to the expert-designed one.

CONCLUSION

Simple tone curves – defined as monotonic increasing functions with at most one inflexion point – can effectively enhance images while preserving visual quality comparable to more complex expert-designed curves. Our study shows that human observers do not exhibit a significant preference for expert tone curves over simple ones. Moreover, solving for the simple tone curve in log space appears to provide a slight perceptual advantage. These results support the use of simple tone curves as a practical tool for image enhancement. By reducing complexity without sacrificing perceptual quality, simple curves offer a compelling alternative to expert adjustments and may, in some cases, even be preferred.

ACKNOWLEDGEMENTS

This work was supported by the Engineering and Physical Sciences Research Council, grants EP/S023917/1 and EP/S028730/1.

REFERENCES

[1] Grossberg, M., & Nayar, S. K. (2003). Determining the camera response from images: What is knowable? IEEE Transactions on Pattern Analysis and Machine Intelligence, 25(11), 1455–1467. https://doi.org/10.1109/tpami.2003.1240119

[2] Salih, Y., bt. Md-Esa, W., Malik, A. S., & Saad, N. (2012). Tone mapping of HDR images: A review. 2012 4th International Conference on Intelligent and Advanced Systems (ICIAS2012), 1, 368–373. https://doi.org/10.1109/ICIAS.2012.6306220

[3] Qi, Y., Yang, Z., Sun, W., Lou, M., Lian, J., Zhao, W., Deng, X., & Ma, Y. (2021). A Comprehensive Overview of Image Enhancement Techniques. Archives of Computational Methods in Engineering, 29(1), 583–607. https://doi.org/10.1007/s11831-021-09587-6

[4] Wang, D. C. C., Vagnucci, A. H., & Li, C. C. (1983). Digital image enhancement: A survey. Computer Vision, Graphics, and Image Processing, 24(3), 363–381. https://doi.org/10.1016/0734-189x(83)90061-0

[5] Sing Bing Kang, Kapoor, A., & Lischinski, D. (2010, June 1). Personalization of image enhancement. IEEE Conference on Computer Vision and Pattern Recognition. https://doi.org/10.1109/cvpr.2010.5539850

[6] Bennett, J., & Finlayson, G. (2023). Simplifying Tone Curves for Image Enhancement. Color and Imaging Conference, 31(1), 108–114. https://doi.org/10.2352/cic.2023.31.1.21

[7] Lawson, C. L., & Hanson, R. J. (1974). Solving Least Squares Problems. Prentice-Hall.

[8] Vladimir Bychkovsky, Paris, S., Chun, E., & Durand, F. (2011, June 1). Learning photographic global tonal adjustment with a database of input/output image pairs. CVPR 2011. IEEE Conference on Computer Vision and Pattern Recognition. https://doi.org/10.1109/cvpr.2011.5995413

[9] Hu, Y., He, H., Xu, C., Wang, B., & Lin, S. (2018). Exposure: A White-Box Photo Post-Processing Framework. ACM Transactions on Graphics, 37(2), 1–17. https://doi.org/10.1145/3181974

[10] Thurstone, L. L. (1927). A law of comparative judgment. Psychological Review, 34(4), 273–286. https://doi.org/10.1037/h0070288

[11] Perez-Ortiz, M., & Mantiuk, Rafal K. (2017). A practical guide and software for analysing pairwise comparison experiments. ArXiv.org. https://arxiv.org/abs/1712.03686

Evaluating The Just Noticeable Difference Threshold of ΔE_{ITP} in SDR Displays for Color Experts and Non-Experts

Mu-Tzu Kuo[a*], Chris Yi-Ho Bai[a]

[a]*Color Technology Lab, BenQ Corp., Taipei, Taiwan.*

**Melody.MT.Kuo@BenQ.com*

ABSTRACT

This study examines the Just Noticeable Difference (JND) threshold of ΔE_{ITP} in SDR displays to evaluate its suitability as a perceptual color difference metric outside its typical HDR context. While IC_TC_P and ΔE_{ITP} are widely used in HDR due to PQ or HLG encoding, their performance in SDR remains unclear. A psychophysical experiment was conducted on a 32-inch professional SDR display with 29 observers (14 experts, 15 non-experts). The QUEST adaptive procedure was used to efficiently determine JND thresholds across four luminance levels (25, 80, 160, 300 cd/m²). Test stimuli included RGB primaries, CMY secondaries, and neutral white. Results show ΔE_{2000} thresholds remain stable (~1.0), consistent with prior research. ΔE_{ITP} thresholds, however, vary widely (1.0–21.0), with red and blue producing the largest values, indicating visually non-uniformity in IC_TC_P space. White and black exhibited stable thresholds. Luminance had minimal effect on JND for both ΔE_{2000} and ΔE_{ITP} under SDR conditions. Recommended ΔE_{ITP} JND thresholds in SDR are 6.3 for experts and 7.6 for non-experts. Further scaling adjustments are needed for perceptual consistency.

Keywords: IC_TC_P, Just-Noticeable Difference (JND), DCI-P3, Standard Dynamic Range (SDR)

INTRODUCTION

Color difference metric is an important indicator for display evaluation. For Standard Dynamic Range (SDR) displays, ΔE_{2000} [1] is the international standard method for display evaluation. Although it was originally developed based on reflective paint samples, but ΔE_{2000} has been adopted for the display industry. For High Dynamic Range (HDR) displays, industry has proposed to use IC_TC_P as the standard metric for display evaluation [2]. The IC_TC_P color difference metric, developed by Dolby Laboratories, is characterized by its ability to simulate the human visual system and incorporate PQ ST 2084 or HLG EOTF, making IC_TC_P more suitable than ΔE_{2000} for HDR displays with higher contrast and a wider color gamut [3].

However, SDR displays still dominate the market due to the affordable price and greater accessibility. Hence, the study of color difference metric is mainly focused on $\Delta E_{2000.}$ Therefore, this study primarily investigates the feasibility of adopting ΔE_{ITP} in SDR displays, with the aim of determining the perceptible color difference threshold for ΔE_{ITP} in SDR conditions. A psychophysical experiment was conducted on BenQ SW321C display and calibrated to four different luminance levels (25, 80, 160, and 300 cd/m²). The goal was to determine the Just Noticeable Difference (JND) thresholds [4]. A total of 29 participants took part in the experiment, including 14 color experts and 15 non-experts. The experiment combined the QUEST method and the Alternative Forced Choice (4-AFC) method, asking participants to select the color patch they perceived as different. Finally, the ΔE_{2000} and ΔE_{ITP} values were calculated separately, with the ultimate goal of establishing a ΔE_{ITP} threshold standard for SDR displays.

METHODOLOGY

This section will introduce the experimental methodology of this study.

IC_TC_P and ΔE_{ITP} calculation

The experiment aims to determine IC_TC_P JND thresholds at various display luminance levels. RGB signals are first converted to LMS (Eq. 1) before computing ΔE_{ITP}.

$$\begin{bmatrix} L \\ M \\ S \end{bmatrix} = \begin{bmatrix} 0.3346 & 0.5763 & 0.0891 \\ 0.1585 & 0.7135 & 0.1279 \\ 0.0205 & 0.0917 & 0.8872 \end{bmatrix} \begin{bmatrix} R \\ G \\ B \end{bmatrix} \tag{1}$$

The experiment aims to determine IC_TC_P JND thresholds at different display luminance levels. Since RGB must first be converted to LMS for ΔE_{ITP} computation, this study derives a DCI-P3–based RGB-to-LMS transform. Unlike Dolby's BT.2020 approach, DCI-P3 is adopted due to display limitations. To reduce errors, a 4% cross-talk correction is applied to the Hunt-Pointer-Estevez (HPE) LMS transform. The resulting DCI-P3 to LMS conversion is expressed in Eq. 2 - Eq .3:

$$\begin{bmatrix} L \\ M \\ S \end{bmatrix} = Crosstalk \times \begin{bmatrix} L \\ M \\ S \end{bmatrix}_{HPE} = \begin{bmatrix} 0.3592 & 0.6976 & -0.0358 \\ -0.1922 & 1.1004 & 0.0755 \\ 0.0070 & 0.0749 & 0.8434 \end{bmatrix} \times \begin{bmatrix} X \\ Y \\ Z \end{bmatrix} \tag{2}$$

$$\begin{aligned} \begin{bmatrix} L \\ M \\ S \end{bmatrix} &= \begin{bmatrix} 0.3592 & 0.6976 & -0.0358 \\ -0.1922 & 1.1004 & 0.0755 \\ 0.0070 & 0.0749 & 0.8434 \end{bmatrix} \times \begin{bmatrix} 2.4928 & -0.9311 & -0.4026 \\ -0.8295 & 1.7627 & 0.0236 \\ 0.0359 & -0.0762 & 0.9574 \end{bmatrix}^{-1} \times \begin{bmatrix} R \\ G \\ B \end{bmatrix} \\ &= \begin{bmatrix} 0.3346 & 0.5763 & 0.0891 \\ 0.1585 & 0.7135 & 0.1279 \\ 0.0205 & 0.0917 & 0.8872 \end{bmatrix} \times \begin{bmatrix} R \\ G \\ B \end{bmatrix} \end{aligned} \tag{3}$$

Then, applying the non-linearity. In this study, the Hybrid Log-Gamma (HLG) Optical-Electro Transfer Function (OETF) is applied in this step (Eq. 4):

$$E' = OETF[E] = \begin{cases} \sqrt{3E} & 0 \le E \le {}^{1}/_{12} \\ a \times ln(12E - b) + c & {}^{1}/_{12} < E \le 1 \end{cases} \tag{4}$$

Where, E represents the signal of each component corresponding to the human eye's peak sensitivity wavelengths {L, M, S}, normalized to the range [0:1]. E' is the resulting nonlinear signal {L', M', S'}, also within the range [0:1].

The parameters are defined as: $a = 0.17883277,\ b = 1 - 4a\ ,\ c = 0.5 - a \times \ln(4a)$.

Finally, the HLG L'M'S' signal is applied to the IC_TC_P matrix (Eq. 5):

$$\begin{bmatrix} I \\ C_T \\ C_P \end{bmatrix} = \begin{bmatrix} 0.5 & 0.5 & 0 \\ 0.885009766 & -1.822509766 & 0.9375 \\ 2.319335938 & -2.249023438 & -0.0703125 \end{bmatrix} \begin{bmatrix} L' \\ M' \\ S' \end{bmatrix} \tag{5}$$

After converting to IC_TC_P, ΔE_{ITP} is calculated with a correction factor of 0.25 on the C_P axis. To enable comparison with ΔE_{2000} on SDR displays, Pytlarz et al. [5] showed that multiplying by 720 approximates one JND, yielding Eq. 6:

$$\Delta E_{ITP\ JND} = 720 \times \sqrt{(\Delta I)^2 + 0.25 \times (\Delta C_T)^2 + (\Delta C_P)^2} \quad (6)$$

Observers and Material

A total of 29 observers participated in this experiment. Among them, 14 observers were color experts, while the remaining observers had limited or no knowledge of the field. The experiment was conducted in a darkroom, using a 32-inch IPS display to present the stimuli. The distance between the observers' eyes and the display was approximately 50 cm, with their line of sight directed toward the center of the display. Observers used a mouse to click on the target color patch that differed from the other three patches, and the software automatically recorded their responses. The experimental setup is shown in Figure 1.

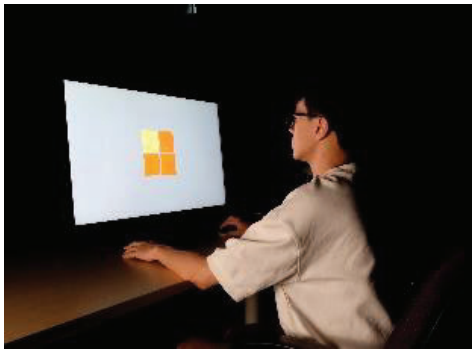

Figure 1: Experiment setup.

Test and Reference Stimuli

In the psychophysical experiment, an X-rite i1 Display Pro colorimeter was used to calibrate the display to D65 white point, DCI-P3 color gamut, and sRGB gamma curve. Four different luminance levels were selected: 25, 80, 160, and 300 cd/m². This study measured JND values in 12 different directions, as shown in Table 1.

The experimental pattern is illustrated in Figure 2: four square color patches were displayed at the center of the screen, with one patch having RGB values different from the other three. The background was medium gray with Lab* values of (50, 0, 0), and the experimental screen was presented in full-screen mode. The QUEST method [6] was employed to adaptively adjust the difficulty in each trial. In addition, both a forward and an inverse characterization model were constructed to predict the required RGB values [7].

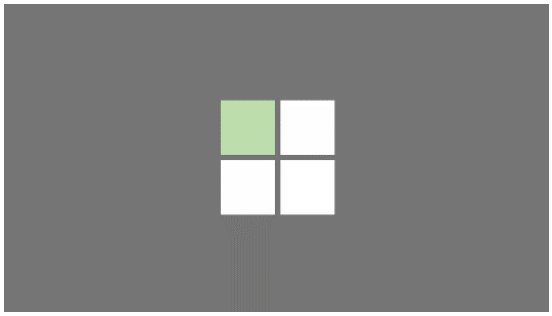

Figure 2: Test pattern. Each color patch has an approximate viewing angle of 5.7 degrees

Table 1: Reference and test color

	Ref. color	Test color
RW	□	■
GW	□	■
BW	□	■
WR	■	□
GR	■	■
BR	■	■
WG	■	□
RG	■	■
BG	■	■

	Ref. color	Test color
WB	■	□
RB	■	■
GB	■	■
WC	■	□
GC	■	■
BC	■	■
WM	■	□
RM	■	■
BM	■	■

	Ref. color	Test color
WY	■	□
RY	■	■
GY	■	■
WK	■	□
RK	■	■
GK	■	■
BK	■	■

Experimental Procedure

Before the experiment and calibration, the display was warmed up for at least 30 minutes. The entire procedure consisted of the five steps shown in Figure 3:

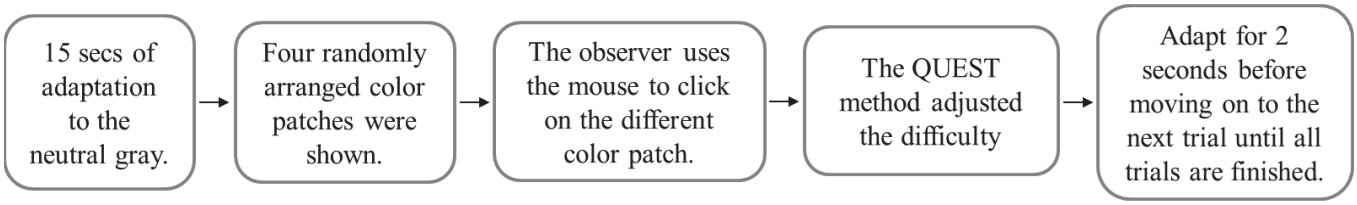

Figure 3: Experiment procedure.

In the experiment, each test group was presented randomly. Furthermore, in every trial, the correct test color patch appeared randomly in one of the four positions.

RESULTS AND DISCUSSION

This section presents the JND results. Test groups are labeled by the direction from reference to test color (e.g., "RW" = red toward white) and analyzed in CIE $L^*a^*b^*$. ΔE_{2000} and ΔE_{ITP} JND ellipses are calculated to establish SDR standards for experts and non-experts. For illustration purpose, the results of 160 cd/m² are presented in both the CIE $L^*a^*b^*$ space (Fig. 4) and the IC_TC_P color space (Fig. 5). In Figs. 4 and 5, the center point of each ellipse represents the reference point. The solid circles and solid triangles near the reference point indicate the JND values obtained from the experimental results for color experts and non-experts, respectively. The solid and dashed circles surrounding the experimental JND values represent the MAE values. The ellipses around the reference point show the recommended JND values derived from the experimental results: the blue solid line represents the recommended JND values for color experts, while the orange dashed line represents those for non-experts. The calculated mean JND values across all luminance levels are summarized in Table 2

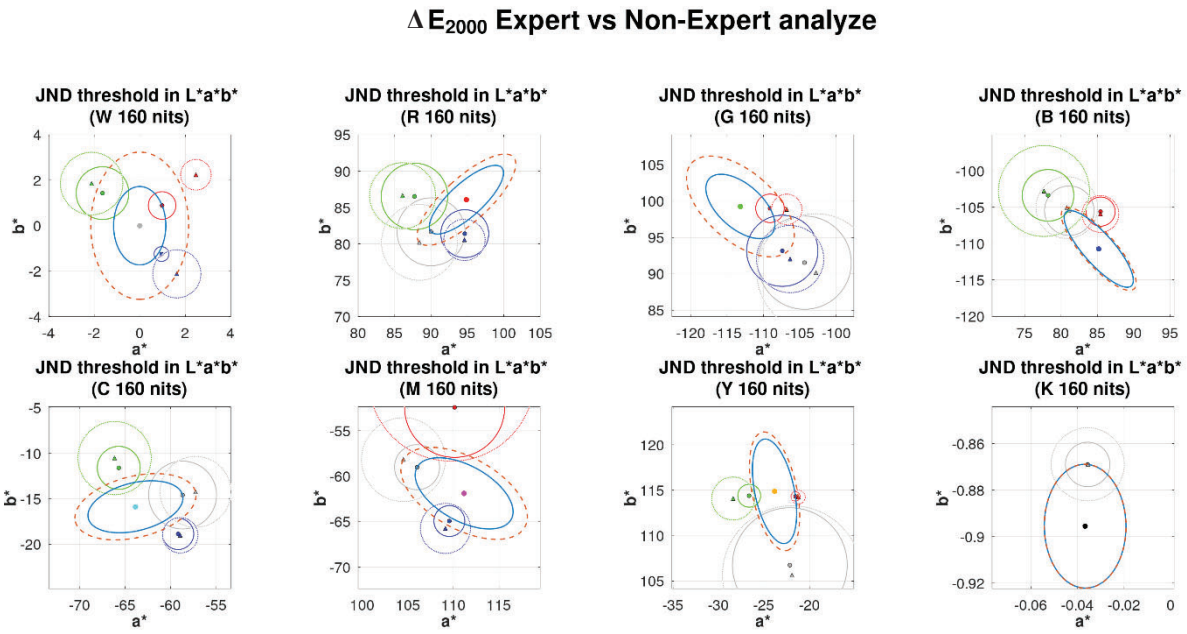

Figure 4: Results of ΔE_{2000} JND values in the CIE L*a*b* color space

Table 2: The calculated mean JND values of all luminance levels

		25 nits		80 nits		160 nits		300 nits		Average
		JND	CV	JND	CV	JND	CV	JND	CV	
ΔE_{2000}	Expert	0.98	58.84	0.97	51.90	0.94	47.68	1.40	88.42	1.07
	Non-Expert	1.22	59.42	1.20	57.96	1.34	61.07	1.72	88.14	1.37
ΔE_{ITP}	Expert	6.61	110.10	5.72	69.30	6.09	75.31	6.62	70.30	6.26
	Non-Expert	7.41	93.86	8.42	82.60	7.77	67.66	6.98	69.35	7.65

In the psychophysical experiment, the SDR display was calibrated to four different luminance levels in order to observe the relationship between JND thresholds under varying luminance conditions and to determine the corresponding thresholds. As shown in Table 2, the average expert's JND threshold of ΔE_{2000} is approximately equal to 1, which is consistent with previous studies [1]. In most cases, the JND values of color experts are significantly smaller than those of non-experts, indicating that color experts possess better color discrimination ability. For color experts, ΔE_{ITP} threshold was found to be 6.3 under SDR conditions, whereas for non-experts, ΔE_{ITP} threshold was found to be 7.6.

CONCLUSION

The aim of this experiment was to determine the JND thresholds of ΔE_{ITP} on SDR displays for both color experts and non-experts. The calculation of ΔE_{ITP} incorporates the HLG curve, which is considered to better align with human visual perception and to make color difference calculations more objective. The JND threshold for ΔE_{ITP} was determined for both color experts and non-experts under SDR condition. The same procedure will be replicated in HDR condition to determine the ΔE_{ITP} threshold for HDR condition.

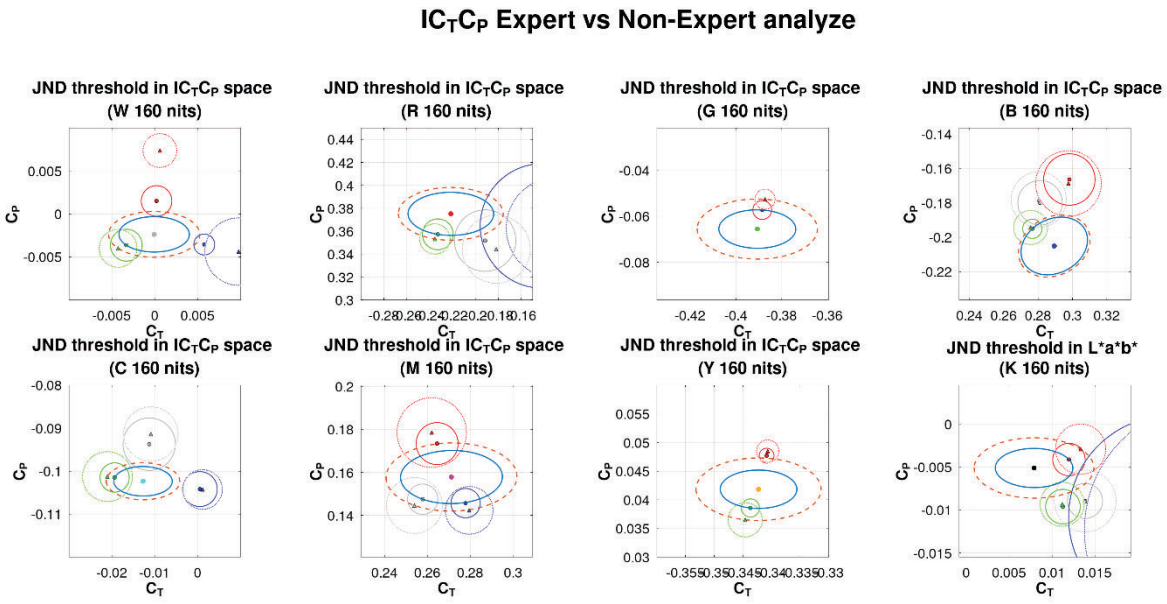

Figure 5: Results of ΔE_{ITP} JND values in the IC_TC_P color space

ACKNOWLEDGEMENTS

The authors would like to thank Dr. Chris Bai and the colleagues at the Color Technology Lab of BenQ Corp. for providing technical resources, calibration equipment, and experimental facilities, as well as for their continued guidance and valuable suggestions throughout the development of this research. Their expertise greatly contributed to the successful progress and direction of this project. The authors also sincerely thank the participating observers, whose involvement and support made the successful completion of this study possible.

REFERENCE

[1] Luo, M. R., Cui, G., & Rigg, B. (2001). *The Development of the CIE 2000 Colour-Difference Formula: CIE DE2000*. Color Research & Application, 26(5), 340–350.

[2] ICtCp *Dolby White Paper*, Dolby (2017) https://www.dolby.com/us/en/technologies/dolby-vision/ictcp-white paper.pdf

[3] Recommendation ITU-R BT.2100-2 (2018). I*mage parameter values for high dynamic range television for u se in production and international programme exchange.*

[4] Macadam, D. L. (1942). *Visual Sensitivities to Color Differences in Daylight. Journal of the Optical Society of America*, 32(5), 247–274.

[5] Pytlarz, J., & Pieri, E. (2018). *HOW CLOSE IS CLOSE ENOUGH? SPECIFYING COLOUR TOLERANCES FOR HDR AND WCG DISPLAYS*.

[6] Watson, A. B., & Pelli, D. G. (1942). *Quest: A Bayesian Adaptive Psychometric Method*. Perception & Psych ophysics, 33, 247–274.

[7] Berns, R. S. (1996). Methods for Characterizing CRT Displays. Displays, 16(4), 155–229.

Colour Saliency Effects on Pre-attentive Processes

Katsuaki Sakata*, Yasuki Yamauchi

Yamagata University Graduate School of Science and Engineering, Yonezawa, Japan
** Katsuaki Sakata: chromatica.katz@gmail.com*

ABSTRACT

Introduction: Recent research on visual attention suggests that the colour saliency effect is processed by pre-attentive processes, and that this effect differs depending on the colour. Based on this assumption, the colour saliency effect should affect the Stroop effect differently if the degree of interference is controlled in the Stroop effect, in which language processing processes related to colour are interfered with by language processing of word meanings. In this study, we used a two-stimulus presentation task to investigate whether the reaction time of the 2AFC, in which participants judge whether the preceding Stroop stimulus matches the subsequently presented test stimulus, is affected by differences in colour when ISI is varied to change the degree of Stroop interference.

Experiment: Stimuli consisted of a Stroop stimulus and a test stimulus: after 500 ms of fixation point presentation, one of the three words 'Red', 'Blue' and 'XXX' were presented as Stroop stimuli for 500 ms in iso-luminant and iso-saturated red, blue or green, After a certain ISI duration (0, 200, 400, 600 ms), a black letter colour name or colour patch was presented as test stimuli. The participants' task was a 2AFC task in which they had to judge as quickly and as accurately as possible whether the colour of the Stroop stimulus matched the test stimulus. The stimuli were presented on an LCD 57 cm away from the observer. A two-factor analysis of variance was conducted to examine the main effects of colour differences and ISI. The results showed that there was a main effect of ISI, with reaction times decreasing as ISI increased, but there were no significant differences in colour differences. Significant differences were also found in the word and colour patch conditions, but no significant differences were found in the colour-meaning congruent or in congruent of the Stroop stimuli.

Discussion: Reaction times decreased when the test stimulus was a colour patch compared to a word because the colour patch condition did not require verbalisation of the colour perception results, which is consistent with the results of previous studies. The fact that there was no difference between the congruent and incongruent conditions suggests that this same-different judgement is processed in the pre-attentive process. If the Stroop effect is a phenomenon caused by the allocation of attention between colour perception and language processing, the fact that no difference in reaction time was observed for different colours suggests that colour saliency has no influence on the pre-attentive process related to colour processing.

Keywords: Colour saliency, Attention, Stroop effect

INTRODUCTION

From observing embedded figures and ambiguous figures (figure-ground reversal), we can see that we cannot perceive the outside world simply by obtaining its image on our retinas; rather, perception is realised by directing our attention to it. It is well known that colours such as red and white have the effect of attracting our attention [2], but what is noteworthy is that we do not know what colour something is before we see it. Namely, it is not because fire hydrants are bright red that they are easy to find, but because we find them that we know they are bright red.

However, as you know from experience, bright red and orange colours clearly attract our attention more than brown and dark blue. It has been shown that salience and novelty compete in bottom-up attention supplementation [2]. How is it that we can distinguish between colours that attract our attention and those that do not, even before we see the object, that is, before our brain recognises the colour?

It is known that the focus of our attention does not necessarily correspond to eye movements, and the mechanism by which it is captured by the saliency of objects in the field of vision has been thought to be realised in extremely low-level visual processing mechanisms, based on the speed of reaction times in many psychophysical experiments. Since colour salience is affected by contrast, it can be inferred that this mechanism exists not only in the retina but also in areas that realise retinotopic mapping, such as the lateral geniculate body and primary visual cortex. The salience of the colour of the visual object is thought to greatly influence the perceptual organisation that forms the visual object image from stimuli on the retina. It has been reported that input from L, M, and S cone cells, which are in the early stages of colour vision, strongly contributes to perceptual organisation [3] and that S contrast which is the ancient mammalian subsystem of colour vision is stronger than L and M contrast in normal trichromats [4].

However, the mechanism of colour salience in the early stages of visual information processing shown by these psychophysical studies may only represent one aspect of a phenomenon that involves not only bottom-up but also top-down information processing. A number of psychophysical studies concerning the detection, organisation and localisation of visual objects have suggested that two stages are necessary: first, the 'pre-attentive' mode in which simple features are processed quickly and in parallel across the entire visual field; and second, the 'attentive' mode in which attention is directed to a particular locations in the visual field for detailed information processing. The influence of colour saliency in the latter “attentive” mode has been studied relatively extensively, but there are still many aspects of colour saliency in the former “pre-attentive” mode that remain unclear. Many studies indicate that colour perception processing time is less than 500 ms, so it can be considered that the processing time is too short for colour saliency to function in “pre-attentive” mode. However, considering the influence of top-down processing, this hypothesis cannot be easily rejected. There are also many studies introducing the concept of saliency maps that enable colour information selection in the pre-attentive process [6,7]. Several electrophysiological studies have shown that multiple neural maps exist in the thalamus, superior colliculus, and parietal sulcus, which are thought to specifically encode the salience of visual stimuli [8, 9, 10, 11].

Therefore, in this study, we used the Stroop effect, in which information selection of colour and language information processing is important, to examine the effect of the saliency of colours before they are affected by language information processing on reaction times. The Stroop effect is a phenomenon in which, when the meaning of a colour word does not match the colour in which it is displayed (e.g., “Blue” printed in red), the time taken to read the word is the same as when it is printed in black, but the time taken to colour name the displayed colour (the printed colour) is significantly delayed compared to the time taken to name the colour of the square. The hypothesis proposed by Stroop to explain this phenomenon is that the more familiar and practised reading response competes with the less familiar colour naming response [12]. However, a more plausible explanation currently is that interference between perceptual attributes is smaller than interference within perceptual processing attributes [13]. If colour salience functions even at the “pre-attentive” stage of information processing, the influence of colour salience should appear in the experimental results regardless of the attributes of perceptual processing. In other words, not only does language perception affect colour naming through the Stroop effect, but the reverse Stroop effect, in which colour perception affects word reading, may also occur. In addition, Treisman et al. presented standard stimuli and test stimuli simultaneously [13], whereas in this study, they were presented sequentially, and ISI was controlled to examine at what point interference occurs in the Stroop effect. If the saliency of colours is affected by an increase in ISI, it can be considered that Stroop interference has already begun at the presentation of the Stroop stimulus as the standard stimulus and that processing has progressed until the presentation of the test stimulus. On the other hand, if reaction times remain constant regardless of changes in ISI, this indicates that Stroop interference occurs only when the test stimulus is presented and the task is determined.

EXPERIMENTAL

- **Procedure:** In all trials, the cross for fixation was presented first for 500 ms, followed by the Stroop stimulus for 500 ms, and then a 500 ms test stimulus was presented after an ISI of 0–600 ms.
- **Stimuli**: The standard stimulus was the Japanese hiragana (phonogram) word 'Red,' 'Blue,' and 'Green,' as well as XXX, all of which were adjusted in size so that the number of pixels was the same. The colour was one of three colours of equiluminance red, blue, and green selected so that they were equidistant from the achromatic chromaticity of the adapted background in the cone excitation chromaticity diagram according to MacLeod & Boynton [14]. On the other hand, test stimulus was red, blue, or green colour name word in black, or patch of the same colour as the standard stimuli, presented at a size such that the number of pixels was approximately the same as that of the colour name words. All stimuli were presented on an LCD monitor controlled by a PC installed in a dark room. To avoid the influence of retinal afterimages, standard stimuli and test stimuli were presented at different random positions on a virtual circle with a radius of 4 degrees from the centre of the screen.
- **Condition**: There were three experimental conditions. In the Word condition, participants were asked to determine whether the colour of the colour name word presented as the Stroop stimulus matched the meaning of the colour name word presented as the test stimulus. In the Colour condition, participants were asked to determine whether the colour of the Stroop stimulus matched the colour of the colour patch presented as the test stimulus. Under neutral conditions, participants responded to whether the colour of the "XXX" presented in the standard stimulus matched the meaning of the colour name in black or the colour of the colour disk presented, presented in the test stimulus (Figure 1). In addition, there were congruent conditions where the meaning of colour words of Stroop stimulus matched the displayed colours, and incongruent conditions where they did not match, for both Word conditions and Colour conditions.
- **Task:** The experimental task was a 2-AFC (2 alternative forced choice) task, in which participants were asked to respond as quickly and accurately as possible to indicate whether the presented colour of the standard stimulus was the same or different from that of the test stimulus.

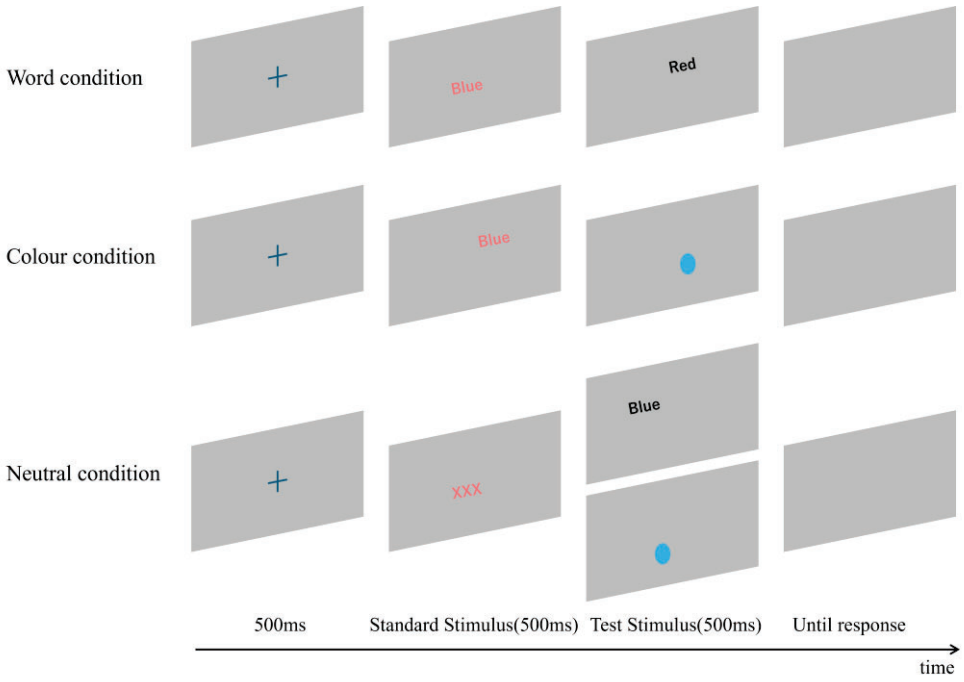

Figure 1: Experimental design

- **Participants:** 55 students and staff with major trichromatic colour vision and normal acuity.
- **Statistical analysis:** Data was analyzed using Microsoft Excel and used the statistical method programed by VBA. One- and two-way analyses of variance (ANOVA) were applied to determine significant differences between conditions, and where significant differences were observed, a t-test was applied to determine where the differences lay. The resulting p values were Bonferroni corrected for multiple comparisons.

The study protocol was approved by the ethics committees of Yamagata University. Experiments adhered to the tenets of the Declaration of Helsinki and were performed after providing each participant with a thorough explanation of the study protocol, its underlying principles, and additional pertinent information regarding color vision testing. All participants provided written informed consent.

RESULTS

In neutral conditions, where there was no effect of congruent or incongruent conditions on standard stimuli, reaction times are shown in Figure 1 for each stimulus colour. The results of a one-way ANOVA showed no difference in reaction times due to differences in stimulus colour (F [2, 1797] =0.68, p = .505, η^2=0.00076).

Figure 3 shows the reaction times for each Stroop condition in the Word condition and Colour condition. The results of a two-factor ANOVA showed that the reaction times were faster in the Colour condition than in the Word condition (F (1, 10771) = 802.54, p = 2.4E-170, η^2 = .0694） , but there was no difference in the reaction times for each Stroop condition compared to those in the Neutral condition (F (1, 10771) = 0.875, p=.466, η^2 = .0002).

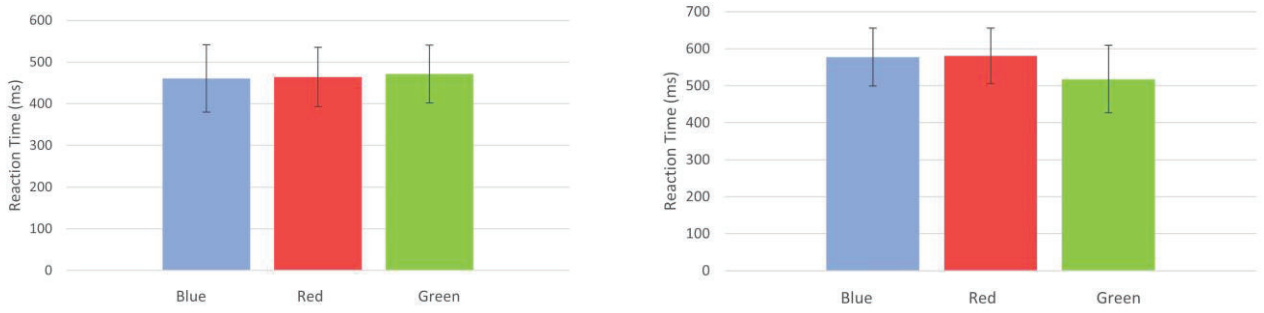

(a) Word condition **(b) Colour condition**

Figure2: Reaction time on each standard stimulus colour

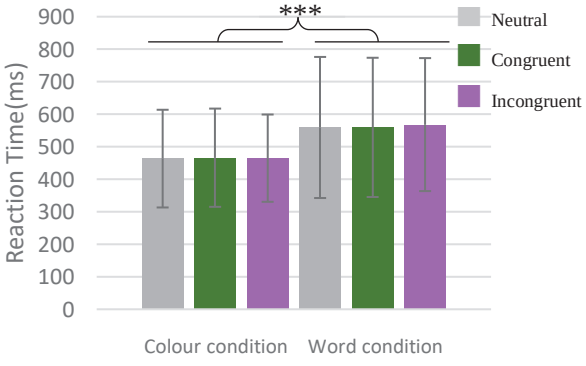

Figure3: Reaction time on each Stroop condition

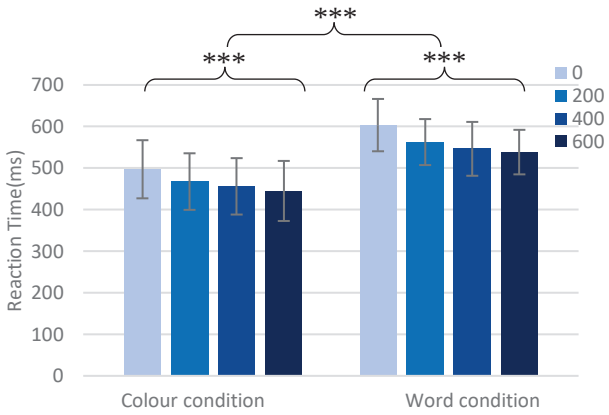

Figure4: Reaction time on each ISI condition

Figure 4 shows the effects of ISI separated into colour conditions and word conditions. The results of the two-factor ANOVA showed that reaction time decreased as ISI increased in both conditions($F(1, 10743) = 912.454$, p=1.88E-192, $\eta^2 = .0772$), and an interaction effect was observed between the effects of colour conditions and word conditions and the main effect of ISI ($F(3, 10743) = 55.240$, p=.2E-35, $\eta^2 = .0140$).

DISCUSSION

As shown in Figure 2, there was no difference in reaction time between the three stimulus colours used in the experiment, whether comparing colours with text or colours with colours. This suggests that in the pre-attentive processing of colours, which occurs in a very short time, the saliency of colours does not appear, but rather their influence appears after they come to consciousness. The theory that humans are instinctively attracted to the colour red has been frequently heard in the past, but this phenomenon does not exist before attention is directed towards it, but rather suggests that it is due to higher-order colour processing that attracts attention after colours are recognised.

In the Stroop condition, no significant difference in reaction times was observed between congruent and incongruent stimuli. This suggests that when viewing standard stimuli, participants were not reading the words. Thus, the hypothesis that the Stroop effect arises from interference between language processing of auto-reading and colour perception, leading to delayed responses when recalling colour names, was not supported in this study.On the other hand, when comparing words with words and colours with colours, the latter was significantly faster, indicating that colour perception prior to colour name utterance occurs more rapidly than the linguistic processing involved in determining the similarity or difference between words.

Finally, it was inferred from the ISI effect that perceptual processing had already begun even though the subject did not yet know whether to respond to colour or text when the standard stimulus was presented. This suggests that colour perception and language processing through colour naming and word reading do not necessarily begin simultaneously, but that mutual interference may occur during the parallel processing stages.

CONCLUSION

Our perception mechanisms perform multiple information processing tasks simultaneously, and interference often occurs between these processes. This interference cannot be perceived directly and is thought to occur during a very transient, widespread, shallow information processing process called the ’pre-attentive' process. After this process, effects that attract our attention, such as the salience of colours, are thought to appear in the subsequent 'attentive' process.

LIMITATION

In this study, the Stroop effect was verified using reaction times as an indicator of judgment, employing a different method of sequential presentation compared to the original study.This could be interpreted as the Stroop effect occurring in memory rather than perception, and it might be criticised as differing from the original phenomenon. However, in many vision science studies, researchers often modify stimulus presentation or measurement methods to obtain clearer evidence, and sequential presentation has been used in previous studies to examine the Stroop effect. In this study, rather than focusing on the Stroop effect, it might be more appropriate to consider it as an investigation into the mechanisms of attention and perception in humans.

ACKNOWLEDGEMENTS

This study was partially supported by JSPS KAKENHI Grant Number 23K11142.

DECLARATION OF CONFLICTING INTERESTS

The authors declare that There is no conflicts of interest to report.

REFERENCES

[1]. Wang, Y., Li, T., Wu, J., & Ding, C. H. Q. (2022). Bio-driven visual saliency detection with color factor. Frontiers in bioengineering and biotechnology, 10, 946084. https://doi.org/10.3389/fbioe.2022.946084

[2]. Ernst, D., Becker, S., & Horstmann, G. (2020). Novelty competes with saliency for attention. Vision research, 168, 42 - 52. https://doi.org/10.1016/j.visres.2020.01.004

[3]. Regan, B.C., Mollon, J.D. (1997). The relative salience of the cardinal axes of colour space in normal and anomalous trichromats. In: Cavonius, C.R. (eds) Colour Vision Deficiencies XIII. Documenta Ophthalmologica Proceedings Series, vol 59. Springer, Dordrecht. https://doi.org/10.1007/978-94-011-5408-6_27

[4]. Kingdom, F. A., Kardous, N., Curran, L., Gheorghiu, E., & Bell, J. (2014). Saliency interactions between the 'L-M' and 'S' cardinal colour directions. Vision research, 95, 36-42. https://doi.org/10.1016/j.visres.2013.12.004

[5]. Koch, C., Ullman, S. (1987). Shifts in Selective Visual Attention: Towards the Underlying Neural Circuitry. In: Vaina, L.M. (eds) Matters of Intelligence. Synthese Library, vol 188. Springer, Dordrecht. https://doi.org/10.1007/978-94-009-3833-5_5

[6]. Itti, L., & Koch, C. (2000). A saliency-based search mechanism for overt and covert shifts of visual attention. Vision research, 40(10-12), 1489-1506. https://doi.org/10.1016/s0042-6989(99)00163-7

[7]. Treisman A. (1988). Features and objects: the fourteenth Bartlett memorial lecture. *The Quarterly journal of experimental psychology. A, Human experimental psychology*, *40*(2), 201–237. https://doi.org/10.1080/02724988843000104

[8]. Robinson, D. L., & Petersen, S. E. (1992). The pulvinar and visual salience. *Trends in neurosciences*, *15*(4), 127–132. https://doi.org/10.1016/0166-2236(92)90354-b

[9]. Gottlieb, J. P., Kusunoki, M., & Goldberg, M. E. (1998). The representation of visual salience in monkey parietal cortex. *Nature*, *391*(6666), 481–484. https://doi.org/10.1038/35135

[10]. Colby, C. L., & Goldberg, M. E. (1999). Space and attention in parietal cortex. *Annual review of neuroscience*, *22*, 319–349. https://doi.org/10.1146/annurev.neuro.22.1.319

[11]. Rockland, K. S., Andresen, J., Cowie, R. J., & Robinson, D. L. (1999). Single axon analysis of pulvinocortical connections to several visual areas in the macaque. *The Journal of comparative neurology*, *406*(2), 221–250. https://doi.org/10.1002/(sici)1096-9861(19990405)406:2<221::aid-cne7>3.0.co;2-k

[12]. Stroop, J. R. (1935). Studies of interference in serial verbal reactions. *Journal of Experimental Psychology, 18*(6), 643–662. https://doi.org/10.1037/h0054651

[13]. Treisman, A., & Fearnley, S. (1969). The Stroop test: selective attention to colours and words. *Nature*, *222*(5192), 437–439. https://doi.org/10.1038/222437a0

[14]. MacLeod, D. I., & Boynton, R. M. (1979). Chromaticity diagram showing cone excitation by stimuli of equal luminance. Journal of the Optical Society of America, 69(8), 1183–1186. https://doi.org/10.1364/josa.69. 001183

Quantifying Inter-Reflection Effects on Colored Shadows

Ruiquan Mao[a*], Alain Tremeau[b], Pichayada Katemake[c]

[a]*QiZha Information Technology Co., Ltd, Lianyungang, China*
[b]*Laboratoire Hubert Curien, University Jean Monnet, Saint-Étienne, France*
[c]*Chulalongkorn University, Bangkok, Thailand*
[*]*Corresponding author: Ruiquan Mao, mao.rq.21@qizhatech.com*

Abstract

Shadows are integral to visual perception, conveying depth and spatial context. Yet their potential to reflect color through inter-reflection remains underexplored. This study addresses this gap by developing a comprehensive synthetic database comprising 19,440 configurations to investigate how inter-reflections between opaque and glossy objects, such as colored spheres, generate colored shadows. Unlike traditional grayscale shadow models, our research highlights the role of indirect light in modifying shadow appearance, induced by reflections between surfaces, and assesses the impact of variations in material properties and lighting conditions. The proposed methodology uses a path-tracing technique with controlled ray bounce limits (0–4), allowing a detailed analysis of how incremental bounces transform shadow intensity and hue. Experimental results reveal that initial bounces significantly improve shadow realism, while incremental bounces contribute little due to energy loss, thus providing new insights into dynamics of light interactions. The generated database, accessible online (http://gofile.me/7pQBr/eccdoMIa0), constitutes a resource for the color science and rendering communities, supporting the development of advanced visual technologies. Additionally, this study explores the application of machine learning methods to simulate these shadow effects, thereby improving the accuracy of Virtual Reality (VR) and Augmented Reality (AR) environments. By manipulating shadow characteristics—such as color and distribution—this work paves the way for tailored visual designs for digital media. Future efforts will extend this database to include transparent materials, broadening its scope of application. This research bridges theoretical understanding and practical implementation, advancing the field of digital color perception and its interdisciplinary applications.

Keywords: Inter-reflections, mutual illumination, ray bounces model, shadow perception, shadow rendering

Introduction

Shadows play a pivotal role in human visual perception, providing cues about depth, shape, and spatial relationships. Traditionally perceived as grayscale, shadows can exhibit subtle color variations due to inter-reflection, where light bounces between surfaces, as noted by Forsyth and Zisserman [4]. This phenomenon, also known as mutual illumination, affects the appearance of shadows, especially in scenes with bright and colorful objects at close distances. Early research, such as the analysis of shape from shading by Forsyth and Zisserman's [5], highlighted its complexity, while later studies by Funt and Drew [6], and Tominaga et al. [10], extended it to color and fluorescent materials. Pichayda et al. [8] investigated whether accounting for

inter-reflections could improve color constancy models. Despite these advances, the overall understanding of color shadows induced by inter-reflection remains limited, especially in practical contexts.

The main reason for conducting this research stems from the lack of a systematic database capturing colored shadow effects, a gap identified in previous works [4, 9]. Existing models, such as the infinite-bounce approach by Deeb et al. [1-3], focus on global illumination but neglect the specific dynamics of shadows. Our interest lies in everyday objects such as shiny spheres, where inter-reflections create noticeable areas of color. Yet no studies quantify these effects under controlled conditions. The advent of Virtual Reality (VR) and Augmented Reality (AR) requires accurate shadow rendering, motivating new investigations of light propagation rules. This research addresses these needs by leveraging a controlled rendering pipeline.

The primary objective of this study was to develop a synthetic database of 19,440 configurations to analyze inter-reflection effects on colored shadows, focusing on two glossy spheres. We aimed to quantify the impact of limited ray bounces (0–4) on shadow appearance, using a path-tracing model to isolate direct and indirect light contributions. Our study investigates inter-reflection effects through a novel methodology. By decomposing the number of bounces into distinct increments (0–4) and simulating them independently, we can directly evaluate the visual appearance resulting from each bounce. This approach allows us to verify the relevance of the bounce model and identify light translation rules, which align with the principle of energy preservation. Unlike previous methods that aggregate multiple bounces or focus on infinite iterations, our technique isolates individual contributions, providing a detailed understanding of how light propagates and interacts with materials to form colored shadows, especially in regions dependent on indirect illumination.

Methodology

We created a synthetic database comprising 19,440 distinct configurations to study the inter-reflection effects on the resulting colored-shadows, using a commercial high-performance graphics rendering engine designed by QiZha Information Technology Co., Ltd (https://www.qizhatech.com/). The scene features two 9 cm diameter spheres positioned at (-13, 12, 0) cm and (13, 12, 0) cm on a table centered at (0, 0, 0) cm, coated with six plastic materials from the vMaterials library version 2.4 written in MDL [7], selected for their various color and reflectivity properties.

A textured surface beneath the spheres enhances realism, while a virtual perspective spherical camera model having FOV as 15 degree, θ as 0.7, and φ within the set (0.65, 0.75, 0.85), positioned at a distance of 20 cm from its center of interest, with its center of interest location defined at coordinates (0, 0, -5) cm in the 3D coordinate system, allows a comprehensive view to capture spatial relationships and lighting distribution, recorded using a standard imaging device.

The illumination setup integrates a directional light source and an ambient white light (255, 255, 255), ensuring uniform ambient lighting in all configurations. The material reflectivity ranges from 0.0 to 1.0 in increments of 0.2; the rendering process adjusts parameters including lighting conditions (white, red, green, blue) and camera angles (0.65, 0.75, 0.85) in radians.

The generation of colored shadows through inter-reflection effects relies on the simulation of light propagation, where rays interact in a controlled manner with object surfaces. When a ray strikes a surface, its trajectory is governed by the material's bidirectional reflectance distribution function (BRDF) and the surface normal, which determine the reflection direction and strength. The rendering pipeline provided by QiZha Information Technology Co., Ltd uses Russian Roulette, a Monte Carlo technique [11] that assigns a random probability to the continuation or termination of a ray's trajectory, simplifying the physical simulation by reducing the number of traced paths. To manage computational complexity further, the path length—defined as the number of ray bounces—was limited in this study. Unlike real-world scenarios where ray paths are theoretically infinite,

this method approximates energy loss and convergence. We limited the maximum ray bounce number in the path-tracing pipeline from 0 to 4, which defines the path length as the number of interactions. Part of the results can be seen in Figure 1.

The total number of configurations is calculated as the product of the following variables: 4 (illumination color) × 3 (left sphere material instance) × 6 (left sphere material's roughness level) × 3 (right sphere material instance) × 6 (right sphere material's roughness level) × 5 (bouncing number) × 3 (camera viewing angle), yielding 19,440 configurations. The database, accessible at http://gofile.me/7pQBr/eccdoMIa0, supports applications in color science, machine learning, and VR/AR development.

Results and Discussion

The maximum number of bounces is limited from 0 to 4, with a minimum path length of 0, to systematically analyze the incremental contribution of indirect light to shadow appearance. A path length of 0 limits the simulation to direct illumination only, thus canceling out reflection effects. Higher values improve realism by incorporating multiple inter-reflections, but with diminishing returns due to energy attenuation.

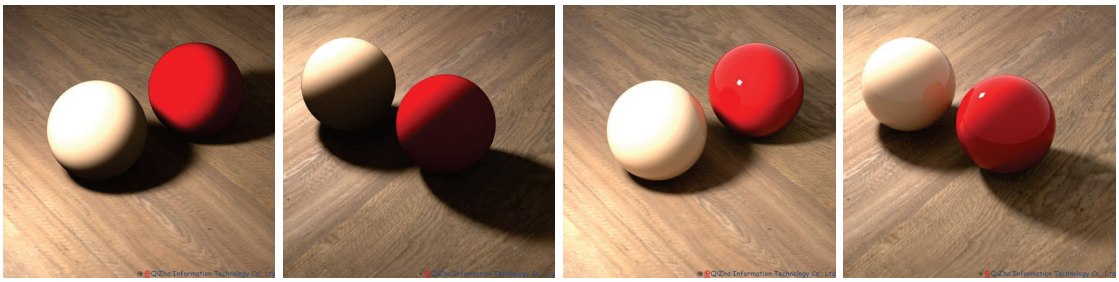

(a) Only direct light (b) Only direct light (c) after 1st bouncing (d) after 1st bouncing

(e) after 2nd bouncing (f) after 2nd bouncing (g) after 3rd bouncing (h) after 3rd bouncing

Figure 1: Changes in shadow rendering due to different bounce counts

In the absence of ray bounces (path length = 0), only direct light from the illumination sources—comprising area and ambient light—reaches the scene surfaces, as depicted in Figures 1.a and 1.b. This configuration produces dark black shadows on both spheres, particularly noticeable on ROI-A (the right upper region of the left sphere, Figure 2.a), where no indirect light mitigates the direct light occlusion. The lack of reflected light prevents

the perception of material properties, such as reflectance, making it indistinguishable in terms of texture or color. This benchmark case highlights the predominance of direct illumination, providing a benchmark for assessing the impact of subsequent bounces on shadow brightness and color.

With the addition of the first ray bounce (optical path length = 1), indirect light impacts the color of the shadow area, as illustrated in Figures 1.c and 1.d. The overall brightness of the scene increases, and shadow regions, including that of the right sphere, change from black to gray under the combined effect of ambient and inter-reflected illumination. A distinct color patch emerges in ROI-A, reflecting the hue of ROI-B (the left upper region of the right sphere, Figure 2.b), oriented toward the directional light. This effect results from the high reflectance of the bright right sphere, where light bounces back to illuminate the left sphere. The initial bounce significantly alters the visual perception of shadow areas, introducing color and mitigating darkness.

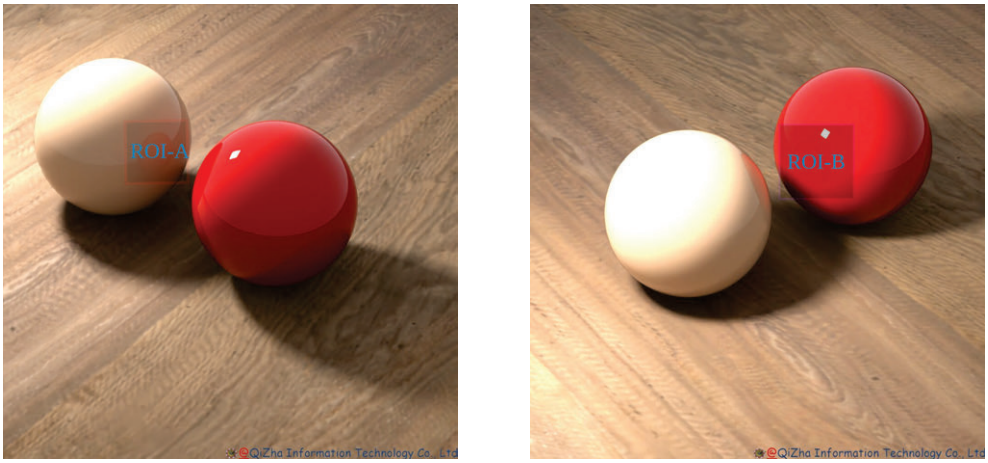

(a) ROI-A (b) ROI-B

Figure 2: Two ROI (regions of interest) on different spheres

As the bounce number increases to 2 (Figure 1.e and 1.f), next 3 (Figure 1.g and 1.h), the visual perception of the scene stabilizes with minimal brightness variations. For ROI-A, the color patch softens compared to the 1st bounce, with light bouncing from the left sphere to the right sphere, bringing energy and modulating the reflected hue through the left sphere's material spectrum. Beyond the second bounce, visual changes become negligible due to the rapid attenuation of ray energy.

The first bounce induces significant changes in shadow brightness and material appearance perceptibility, while the second bounce refines realism by completing inter-reflection effects. Subsequent bounces contribute to convergence, fine-tuning the simulation but having only a limited impact on the overall result. This suggests that the main perceptual improvement occurs during the first two bounces.

Conclusion

This study provides a detailed analysis of colored shadows generated by inter-reflections between two opaque and shiny spheres, bringing new insights to color science and shadow rendering. The analysis focuses on ROI-A (right side of the left sphere), which receives no direct light, and relies on reflections from ROI-B (left side of the right sphere), thus highlighting the critical role of indirect illumination in the visual appearance of shadows.

The first bounce induces significant changes in shadow brightness and material appearance perception, while the second bounce refines realism by completing inter-reflection effects. Subsequent bounces contribute to convergence, fine-tuning the simulation but having only a limited impact on the overall result. This suggests that the main perceptual improvements occur during the first two bounces. Afterwards, the visual appearance of the scene stabilizes with minimal brightness variations. For the ROI-A, the color patch softens relative to the first bounce, as light bounces from the left sphere to the right sphere, modulating the reflected hue across the spectrum of the left sphere material. This inter-reflection enhances the brightness on ROI-B, introducing a color shadow area derived from the left sphere. Beyond the second bounce, visual appearance changes become negligible due to the rapid attenuation of ray energy.

A key limitation arises from the optical setup, ROI-A's reliance on reflections from ROI-B, enhanced by iridescence, limits the energy to indirect sources. The assumption of non-transparent materials limits applicability, as transparent spheres with varying Indices of Refraction (IOR) could alter light scattering and shadow intensity. The scope of this study is further restricted to shadows attached to ROI-A, with shadows cast on the table and other regions, as well as the effects of point or mesh illumination, remaining underexplored.

QiZha Information Technology Co., Ltd. plans to expand this research by creating databases with transparent and semi-transparent sphere configurations, which will be made freely available online for the research community. The study will incorporate various types of illumination (e.g., point, mesh) and conduct spectral analyses to evaluate color modulation. Online psychophysical experiments will link color perception to objective parameters such as reflectance and bounce number, improving machine learning models for real-time VR/AR rendering. These efforts will support dynamic shadow adjustments in architectural and automotive design.

Acknowledgements

Ruiquan Mao expresses his sincere gratitude to Roland Fleming at Justus Liebig University Giessen for his insightful guidance on shadow perception, which significantly influenced Ruiquan Mao during his tenure as a Marie Curie Fellow. Additionally, Ruiquan Mao extends thanks to Alain Tremeau at the University of Jean Monnet for providing valuable research resources that have supported this study and will facilitate future investigations. This work was funded by QiZha Information Technology Co., Ltd. under the VISO (Vision and Shadow) project, with project number VISO-P3Y7AWB92.

References

[1]. Rada Deeb, Damien Muselet, Mathieu Hebert, and Alain Tremeau. 2018. Interreflections in Computer Vision: A Survey and an Introduction to Spectral Infinite-Bounce Model. Journal of Mathematical Imaging and Vision 60, 5 (June 2018), 661–680. doi:10.1007/s10851-017-0781-x

[2]. Rada Deeb, Damien Muselet, Mathieu Hebert, and Alain Trémeau. 2018. Spectral reflectance estimation from one RGB image using self-interreflections in a concave object. Applied Optics 57, 17 (June 2018), 4918. doi:10.1364/AO.57.004918

[3]. Rada Deeb, Joost Van De Weijer, Damien Muselet, Mathieu Hebert, and Alain Tremeau. 2019. Deep Spectral Reflectance and Illuminant Estimation from Self-Interreflections. Journal of the Optical Society of America A 36, 1 (Jan. 2019), 105. doi:10.1364/JOSAA.36.000105 arXiv:1812.03559 [cs].

[4]. D. Forsyth and A. Zisserman. 1989. Mutual illumination. IEEE. https://ora.ox.ac.uk/objects/uuid:97a4a4a6-5add-41ab-a9ef-82d5b0f48e42 ISSN: 1063-6919.

[5]. D. Forsyth and A. Zisserman. 1989. Shape from Shading in the Light of Mutual Illumination. In Proceedings of the Alvey Vision Conference 1989. Alvey Vision Club, Reading, 33.1–33.6. doi:10.5244/C.3.33

[6]. B.V. Funt and M.S. Drew. 1993. Color space analysis of mutual illumination. IEEE Transactions on Pattern Analysis and Machine Intelligence 15, 12 (Dec. 1993), 1319–1326. doi:10.1109/34.250838

[7]. L. Kettner, M. Raab, D. Seibert, J. Jordan, and A. Keller. 2015. The material definition language. In Proceedings of the Third Workshop on Material Appearance Modeling: Issues and Acquisition (MAM ’15). Eurographics Association, Goslar, DEU, 1–4.

[8]. Katemake Pichayda, Rada Deeb, Damien Muselet, Mathieu Hebert, and Alain Trémeau. 2017. Mutual Illumination and Color Constancy. AIC 2017 Jeju (Oct. 2017), 67–70. https://www.dbpia.co.kr/journal/articleDetail?nodeId=NODE07993837

[9]. Shoji Tominaga and Giuseppe Claudio Guarnera. 2022. Appearance synthesis of fluorescent objects with mutual illumination effects. Color Research & Application 47, 3 (June 2022), 615–629. doi:10.1002/col.22747

[10]. Shoji Tominaga, Keiji Kato, Keita Hirai, and Takahiko Horiuchi. 2016. Spectral Image Analysis of Fluorescent Objects with Mutual Illumination. Color and Imaging Conference 24, 1 (Nov. 2016), 59–64. doi:10.2352/ISSN.2169-2629.2017.32.59

[11]. Veach, Eric. Robust Monte Carlo Methods for Light Transport Simulation. Ph.D. dissertation, Stanford University, 1998.

The Color of Roses Was Painted by Protan and Deutan

Yasuyo G. Ichihara[a*], Takashi Sakamoto[b], Shoji Sunaga [c]

[a*]*Kogakuin University, CUDO Color Universal design Organization, Tokyo, Japan*
[b] *Faculty of Science and Engineering, Chuo University, Tokyo, Japan*
[c] *Faculty of Design, Kyusyu University, Fukuoka, Japan*
[*]*Corresponding author: ichihara@cc.kogkauin.ac.jp*

ABSTRACT

We know that it is a very painful experience for anyone to be forced to act against their own senses. It is the imposition of other people's senses when one is forced to say that something bitter is sweet or to smile in times of distress. It would be a very painful art class if you were told that you absolutely had to paint with a certain color and you had to use that color which is against your own senses. Until a certain time in the past, in art classes, the identification of color categories between certain reds and greens, certain yellow-greens, ochres and oranges, and certain light blues, grays, and pinks wes deemed a "color mistake," and students were forced to make corrections. Before sketching, students were made to check the names of paint colors, and they were forced to paint skin in a certain skin color (“hada-iro = surface orange color, fresh”)_, tree trunks in brown, and leaves in green. It is not possible for such an art class to be enjoyable when your sensibilities are corrected by others who have different sensibilities. This research aims to create a new culture of color perception. We will exhibit paintings created by individuals with red-green confusion (CUDO) using only their sense of color, with the names of the paints hidden.

Keywords: human color vision, congenital red-green color deficiency, color picture, color universal design

INTRODUCTION

The background: The background to this paper is the prejudice specific to Japanese society against the diversity of congenital red-green color vision. Until the 1980s, this was actually done in art and craft classes for children and students with congenital red-green color deficiency, commonly known as color blindness or color weakness. Those who attended art and craft classes during this period were forced to correct the assimilation of color categories between certain types of red and green, between certain types of yellow-green, ochre, and orange, and between certain types of light blue, gray, and pink, calling them "color mistakes" during art class. People with red-green color blindness are in the minority, but it is impossible to enjoy art class when the colors to be used are forced upon you by the majority (in this study, people with red-green color blindness are called minority color vision, and those with other color vision are called majority color vision).

It is now known that congenital red-green color deficiency is a genetic variation that occurs in 1 in 20 males and 1 in 500 females in Japan. In the past, test results for the Ishihara color vision test for schools were divided into two categories: "normal" and "abnormal." However, it is now pointed out that color vision is caused by gradual genetic polymorphisms, and that there is a continuum with the normal group, making it impossible to draw a line between "normal" and "abnormal."

The significance of this study: One of the roles of art is the liberation of the soul. The soul is something that

exists within humans, but it is difficult to get a glimpse into the human psyche. This presents a vast and profound problem. One of the reasons this problem is so profound is the diversity of individual senses. The diversity of senses is not just an issue within humans; in recent years, it has been analyzed in various academic fields, such as molecular biology, and new discoveries are being made. A prime example of the type of sense that has been discovered in this way is color vision. The physical properties of color as light have been scientifically explained to a large extent.

However, there are many unknown aspects of the mental representations that emerge as colors after capturing light. Colors can be seen in dreams, and they contain imaginary elements that can be depicted through memory reconstruction. Such imaginary colors have been a difficult field for scientific research. For example, it has been difficult to ask what the nature of such internal colors is, such as when something like "warm," an imaginative quality inherent in humans, is associated in most people with a color range centered on red, and something like "loneliness" is associated with a color range centered on blue.

A series of studies by Ichihara et al. have reported that the "warm" and "loneliness" of color vision minorities fall into different color name ranges from those of color vision majority individuals[1-2]).

This suggests that by freeing minority color vision from social notions created by the majority color names, such as "warm" = red and "loneliness" = blue, it may be possible to create a new culture of color sensation based on the world of colors represented by minority color vision.

The purpose: The purpose of this study is to liberate the consciousness of older individuals with red-green color deficiency who once believed that only their own color vision was abnormal, and to encourage younger individuals with red-green color deficiency, once they are no longer subject to coercion by the majority, to work with minority peers who share their senses to create a creative culture of color vision, such as by creating individual color names based on their own color vision. As one such effort, this study reports on the experience of having 12 individuals with congenital red-green color deficiency paint pictures using only their own color sense, without revealing the names of the paints. The subjects they painted were roses of various colors.

METHODOLOGY

1. All the color names of the 108 watercolor paints were covered with a black marker to make them unreadable (to prevent people from using color names to paint).
2. About 20 varieties and 20 colors of roses were used as motifs. The roses had a wide variety of colors, including white, red, pink, orange, yellow, purple, and brown, and the leaves had various colors of green. The shape of the roses was easy to draw, and even beginners could easily create the shape.
3. The artist with type deutan of dichromat color vision (Yu Kurosaka) was the art instructor, and I outlined the composition and shapes and colored them according to his instructions.
4. The overall work was reviewed, and a critique session was held.
5. A color analysis was conducted.

The color analysis of the drawings was carried out using a CM-700D spectrophotometer (Konica Minolta), and the results were used for discussion.

RESULTS AND DISCUSSION

Figure 1 is shows roses painted by a protan and their motif. When a person with majority color vision looks at a photograph of a rose, they can see that the green rose depicted in the picture is a rose of a color that a person with majority color vision would call red. Area 1in Figure 1 shows that protan perceives red and green as being in the same color category, resulting in the appearance of a beautiful green rose.

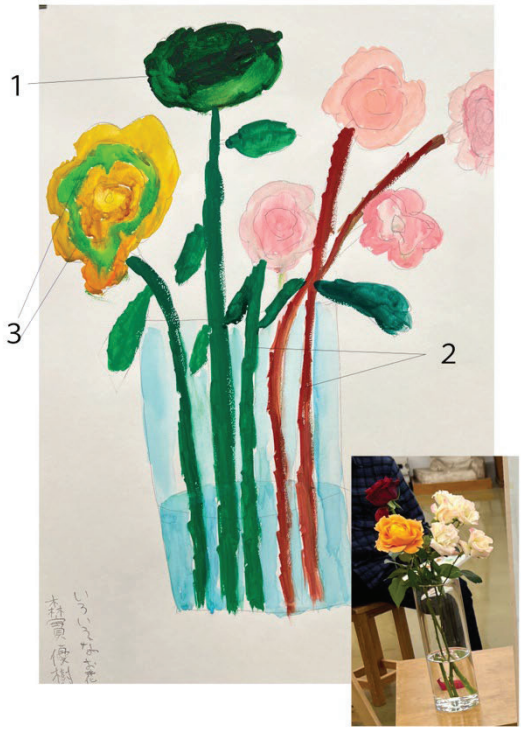

Figure 1: The green rose (Reprinted with permission of the author)

Looking at Figure 1 and Figure 2 , we can see that the stems of the green rose and the red rose drawn by a Protan are indeed on the pseudoisochromatic line. These colors belong to the same color category, so it is thought that a beautiful green rose appeared in the painting. (see part 2 of Figure 1）

Also, the shadow of a yellow rose that is close to orange is yellow-green (see part 3 of Figure 1). Figure 3 shows that these two colors are also on the pseudoisochromatic line, meaning they are in the same color category. Yellow-orange and yellow-green are in the same color category.

Figure 4 depicts a gray rose with a pink border. When people with the majority of color vision see a photograph of the rose motif, they will percerve it as a reddish-gray rose. It may be a surprising color to many people, but here exists a beautiful world of harmony.

Area 1 in Figure 4 is a mixture of gray, light blue, and pink, and the center of the flower appears to be gray with a hint of yellow. The important thing to note here is that, since people with majority color vision are sensitive to red, pink is rarely used in shadow areas.

People with majority color vision can also become aware of the peculiarities of their own color vision through the eyes of people with minority color vision. In Figure 5, the gray roses outlined in pink are drawn in different colors because the pseudoisochromatic lines do not match. In Figure 4, part 2 shows the shadow color and pink, which are similar colors. In part 3, various leaf colors are depicted. Color vision minorities do not live in a world of few colors, but in their own world of many colors.

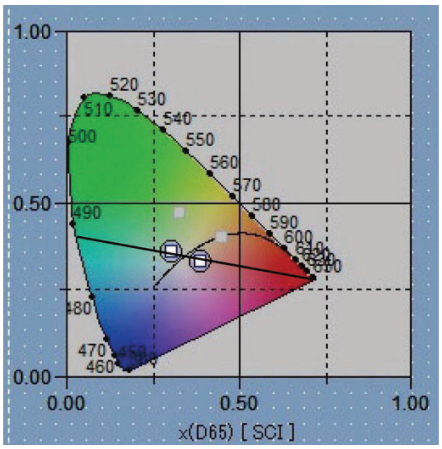

Figure 2: The green rose color and the red stem color are on the pseudoisochromatic line.

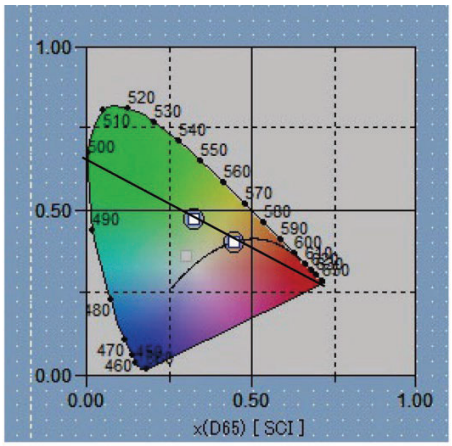

The yellow-orange flowers have a yellow-green shadow.
(They're on the pseudoisochromatic line,
so they're in the same category.)

Figure 3: The chromaticity of the yellow-orange rose and its shadow color

Figure 6 shows that the leaves are depicted in a variety of colors, spanning a wide range from green to brown. The minority color category is different that of from the majority. The appearance of such colors spans a wide range of pseudoisochromatic colors, which is why a variety of colors were available. For example, pink, light blue, and gray all fall into the same category, suggesting that pink could be used as a shadow color. The majority of people believe that reddish colors are difficult to use for shadows. It was also considered that the range of colors used for leaf colors is very wide.

The problems with color vision simulation also became clear through this experiment. In simulations of dichromats, colors are concentrated at one point on the pseudoisochromatic line, but it is thought that this is not actually the case. For example, “a protan or deutan. sees a red apple as ochre" is incorrect, because the red in a red apple is merely the name of the majority color, which corresponds to many points on pseudoisochromat line in protan or deutan. It is not possible to point to a single corresponding point and say that it corresponds to the majority ochre color.

This experiment also revealed that Ōta's statement in the 1990s that "color-blind people tend to draw pictures with dark, murky colors"[3] is not true. In fact, the paintings were very bright and clear in color.

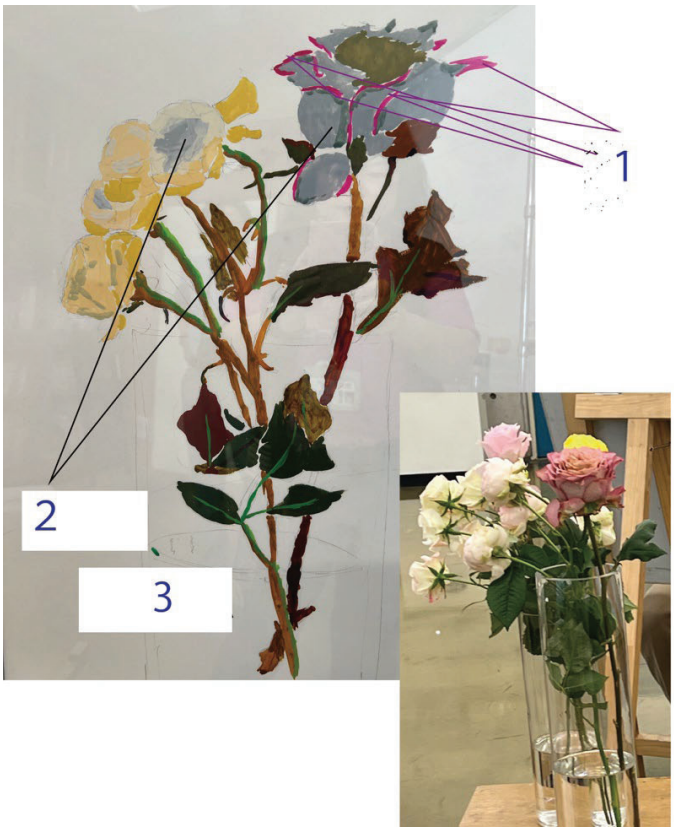

Figure 4: The gray rose (Reprinted with permission of the author)

There was once a misconception that the colors drawn by color-blind people are dark and muddy, but it has been suggested that this may be a misinterpretation that arose from the majority evaluating colors that were forced on minority color vision individuals.

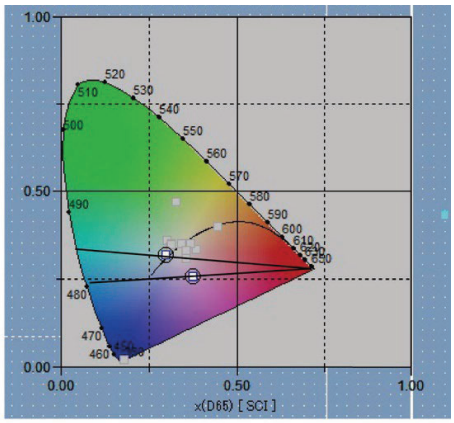

The pink and gray Rose The pseudoisochromatic lines do not match = he is not painting the same color

Figure 5: The chromaticity of pink and gray of the rose.

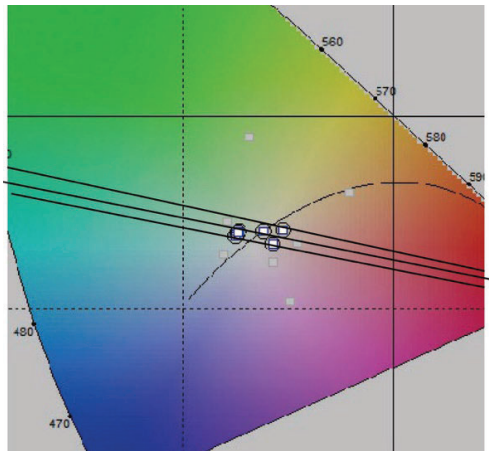

Figure 6: There are many different leaf colors. The leaf color category is broad, ranging from green to brown.

CONCLUSION

In this study, the names of the colors were hidden, and people with red-green color blindness, a minority color vision condition, were asked to choose paints and paint a rose using only their own color sense. The painting does not use colors that would be used by someone with majority color vision, and when viewed by someone with color vision that is majority, the colors of the motif and the painting will be not matching.
However, the color sensations of minority color vision are expressed, which brings a new "awareness" to those with majority color vision. This "awareness" is brought about by the uniqueness of minority color vision and can be said to express a new world of colors that is possible through the color sensations of minority color vision.

ACKNOWLEDGEMENTS

This research was supported by grants from the Japan Society for the Promotion of Science (JSPS) JP25K00431, JP 21H03534, JP 21H04342, and JP 24H00167. We would also like to thank the artist Yu Kurosaka for his art instruction, and the other artists from CUDO who participated in the sketching and provided their paintings.

REFERENCES

[1]. Kojima, N., Ichihara, Y. G., Ikeda, T., Kamachi, M. G., Ito, K.: Color Universal Design: Analysis of Color Dependency on Color Vision Type (3), Proc. SPIE 8292, Color Imaging XVII: Displaying, Processing, Hardcopy, and Applications, 82920, 2012.
https://doi.org/10.1117/12.907669

[2]. Ikeda, T., Ichihara, Y. G., Kojima, N., Tanaka, H., Ito, K.: Color Universal Design: Analysis of Color Dependency on Color Vision Type, Proc. SPIE 8652, Color Imaging XVIII: Displaying, Processing, Hardcopy, and Applications, 86520G, 2013. https://doi.org/10.1117/12.2001582

[3]. At the 28th Annual Meeting of the Color Science Association of Japan (Joshibi University of Art and Design) or Color Forum 97 (Kogakuin University) in 1997, Professor Emeritus Ōta Yasuo of Tokyo Medical University told me, "I also have several paintings by people with color vision deficiencies, and many of them have dark, muddy colors.

An Appraisal of "Colour-Music: The Art of Mobile Colour" (1912) by Rimington: A Design History View

Kyoko Hidaka[a*]

[a]*Joshibi University of Art and Design, Tokyo, Japan*

[*]*Corresponding author: Kyoko Hidaka, hidaka25028@venus.joshibi.jp*

ABSTRACT

Alexander Wallace Rimington's *Colour-Music: The Art of Mobile Colour* (1912) represents a landmark in the history of design and color theory. By introducing the Colour-Organ, Rimington pioneered a medium that synchronizes color and music in a dynamic, performative format, redefining color as an active counterpart to sound rather than a secondary visual element. This paper reexamines his work from a design historical perspective, situating it within early 20th-century contexts of scientific inquiry, technological innovation, and artistic experimentation. It explores key influences, including Louis-Bertrand Castel's *ocular harpsichord* (1725), George Field's *Chromatics* (1817/1845), Albert Munsell's *A Color Notation* (1905), Thomas Wilfred's *Lumia*, and Mary Hallock-Greenewalt's *Nourathar*, alongside the luminiferous ether theory that conceptualized color and sound as vibrational phenomena. The author further connects *Colour-Music* to Japanese media art, notably Toshio Iwai's *Piano – As Image Media* (1995), emphasizing the interplay between sound and image. By bridging static color systems with performative aesthetics, this study highlights *Colour-Music*'s role in expanding the expressive potential of visual design and foreshadowing developments in kinetic and multimedia art.

Keywords: Colour-Music, Colour-Organ, mobile color, color scheme, colored light

INTRODUCTION

In the early 20th century, the intersection of scientific inquiry, technological advancement, and artistic experimentation gave rise to new conceptions of color as an expressive medium. In this context, British painter and Queen's College professor A. Wallace Rimington published *Colour-Music: The Art of Mobile Colour* (1912), introducing the Colour-Organ as a novel instrument that synchronized color and music in a dynamic, performative format. By projecting fluid sequences of colored light through optical filters, Rimington challenged the traditional, subordinate role of color in the visual arts, positioning it as an active analogue to sound.

Rooted in Newtonian optics, psychological theories of color perception, and the luminiferous ether hypothesis, Rimington's work reflects the era's fascination with synesthetic experience. This paper reappraises *Colour-Music* from a design historical perspective, analyzing its theoretical foundations, color-music analogies, and the technical design of the Colour-Organ. It also traces key influences, including Louis-Bertrand Castel's *ocular harpsichord*, George Field's *Chromatics*, Albert Munsell's *A Color Notation*, Thomas Wilfred's *Lumia*, and Mary Hallock-Greenewalt's *Nourathar*.

The study draws connections to Toshio Iwai's *Piano – As Image Media* (1995), highlighting the enduring legacy of color-music in audiovisual art. Ultimately, this paper positions Rimington's work as a critical bridge between static color theory and performative aesthetics, anticipating developments in kinetic, multimedia, and light-based art.

METHODOLOGY

This study employs a tripartite methodological framework: (1) analysis of the design and operation of Rimington's 1895 Colour-Organ, a device projecting dynamic color sequences via electric light and optical filters, controlled by a keyboard-like interface to synchronize colors with musical scores; (2) examination of Rimington's synchronization framework in *Colour-Music*, particularly his correlation of hues (e.g., C/red, G/blue) with musical scales and their emotional effects, through close reading of key chapters like "Points of Analogy between Sound and Colour"; and (3) contextualization of Rimington's work within the historical and theoretical lineage of color-music theory, from Castel's 18th-century ocular harpsichord to Wilfred and Hallock-Greenewalt's 20th-century innovations. The analysis integrates primary sources, including *Colour-Music* and contemporaneous scientific literature on luminiferous ether, with textual analysis, historical comparison, and technological evaluation to elucidate Rimington's pioneering conceptualization of color as a performative medium.

HISTORICAL PRECURSORS AND CONTEMPORARIES

Rimington's *Colour-Music* draws on a lineage of color-music explorations, from 18th-century experiments to early 20th-century innovations.

Louis-Bertrand Castel's Ocular Harpsichord (1725)

Louis-Bertrand Castel, a French Jesuit mathematician, introduced the ocular harpsichord in 1725 to create "visual music" by linking color and sound. Inspired by Newton's Opticks, he matched seven spectral colors to musical notes. His early model used candle-lit colored paper; later versions featured 60 glass panels for richer hues. Castel saw light and sound as vibrations, possibly connected by an ether-like medium, aiming to evoke musical beauty through visuals. Although criticized by Voltaire, his idea influenced Telemann, Diderot, and later color-music theorists. Rimington's Colour-Organ, using electric light and filters, brought Castel's vision to life, showing a strong conceptual link.

George Field's %+*(#-&$, (1817/1845)

George Field's *Chromatics: or, The Analogy, Harmony, and Philosophy of Colours* (1817, revised 1845) integrated scientific, artistic, and philosophical perspectives. Influenced by Newton, Field developed a color wheel and harmony theories, proposing analogies between hues and musical scales to evoke emotional responses. Widely read in 19th-century British art circles, Chromatics shaped Rimington's milieu. His hue-to-note mappings and emphasis on color harmony echo Field's ideas, though Rimington's performative framework surpassed Field's static applications in painting and dyeing. The prevalence of color-music analogies suggests Field's indirect influence, despite no direct citations.

Albert Henry Munsell's ÀĀ *'*+Ā''*-#-&*(1905)

Albert Henry Munsell's *A Color Notation* (1905) introduced an alphabetical-numeric notation defined by hue, value, and chroma for art education and industry. Unlike Rimington's performative approach, Munsell's system was static and scientific. Published shortly before *Colour-Music*, it had limited influence in Britain by 1912. *Colour-Music* does not reference Munsell, and their differing aims suggest minimal influence, though the trend of systematizing color may have informed Rimington's structured scales.

Thomas Wilfred's !.(&#Ā(1919)

Thomas Wilfred (1889-1968) developed *Lumia*, an "eighth art" of light, performed on his Clavilux (developed from 1919, debuted in 1922). Unlike Rimington's music-synchronized Colour-Organ, *Lumia* was typically silent, projecting abstract light forms using rotating disks, mirrors, and prisms, as seen in *Lumia Suite, Opus 158* (MoMA, 1964-1980). Wilfred's Clavilux emphasized light's autonomy, contrasting with Rimington's

music-driven approach. While postdating *Colour-Music*, *Lumia* shares its commitment to dynamic light, and Rimington's work likely shaped the intellectual climate for Wilfred's innovations.

Mary Hallock-Greenewalt's ″*.+#-%#+(1920)

Mary Hallock-Greenewalt (1871-1950) developed *Nourathar*, a visual music form performed on her Sarabet color organ (patented 1920). Named "essence of light" in Arabic, *Nourathar* synchronized colored lighting with music, as detailed in her 1946 book *Nourathar: The Fine Art of Light-Color Playing*. Her Sarabet's non-linear rheostat enabled precise light control, allowing flexible colour-music interpretations, unlike Rimington's fixed mappings. Contemporaneous with *Colour-Music*, *Nourathar*'s interpretive approach contrasts with Rimington's structured analogy, though both used electric light. Rimington likely influenced the broader color-music movement.

Figure 1: Illustration of Rimington's Colour-Organ from *À$#$'%Ã '&″!*(1912), showing its keyboard interface and light projection system

THE ROLE OF ETHER THEORY

The luminiferous ether theory, which posited an invisible medium for the transmission of light waves, played a foundational role in Rimington's color-music analogy. In the late 19th and early 20th centuries, ether was widely accepted as the medium through which both light and sound vibrations propagated, offering a scientific rationale for their perceived correspondence. Drawing on optical theories, particularly those of Helmholtz, Rimington used this framework to justify his mappings between hues and musical notes, conceptualizing both as vibrational phenomena. Although the ether theory was later invalidated by Einstein's theory of relativity (1905), it remained influential during the period in which *Colour-Music* was developed. From a design historical perspective, the theory enabled Rimington to reconceptualize color as a temporal, performative medium, bridging scientific thought and artistic innovation.

DISCUSSION: DESIGN HISTORY SIGNIFICANCE

Unlike Castel's ocular harpsichord or Field's chromatic theories, Rimington's Colour-Organ was a functional instrument using electric light and filters for immersive audiovisuals. Its tech prefigured later innovations like Wilfred's Lumia and Hallock-Greenewalt's *Nourathar*, aligning with Bauhaus ideals of blending art and technology. Toshio Iwai's *Piano – As Image Media* (1995) transforms a grand piano into an interactive audiovisual interface, projecting computer-generated visuals in response to musical input—an approach that mirrors Rimington's *Colour-Music* synchronization.

Figure 2: A caricature of Louis-Bertrand Castel's Ocular Harpsichord

CONCLUSION

Colour-Music: The Art of Mobile Colour (1912) reimagines color as a dynamic, performative medium analogous to sound. Building on Castel's ocular harpsichord and Field's harmonic theories, Rimington diverged from static models like Munsell's, integrating science, technology, and art. His Colour-Organ, framed by luminiferous ether theory, anticipated kinetic and multimedia art, influencing contemporaries such as Wilfred, Hallock-Greenewalt, and later Japanese artists like Iwai. The work reshaped visual culture and laid the foundations for modern color-music discourse.

ACKNOWLEDGEMENTS

This work was supported by JSPS KAKENHI Grant Number 23K11775.

REFERENCES.

[1]. Castel, L.-B. (1725). "L'Optique des Couleurs." *Mercure de France*, November 1725.

[2]. Field, G. (1845). *Chromatics; or, The Analogy, Harmony, and Philosophy of Colours* (2nd ed.). London: David Bogue.

[3]. Greenewalt, M. H. (1946). *Nourathar: The Fine Art of Light-Color Playing*. Philadelphia: Westbrook Publishing.

[4]. Rimington, A. W. (1912). *Colour-Music: The Art of Mobile Colour*. London: Hutchinson & Co.

[5]. Wilfred, T. (2006). *Thomas Wilfred's Clavilux* (M. Betancourt, Ed.). Borgo Press.

Decoding Colour Communication: A Cross-Cultural Study of Colour Associations in Germany and India

Lina Schmidt[a]* and Melissa Lindemeyer[b]

[a]*RAL Colours, Bonn, Germany*
[b]*Farbkultur.design, Hildesheim, Germany*
**Corresponding author: Lina Schmidt, lina.schmidt@ral.de*

ABSTRACT

Colour functions both as a sensory stimulus and a cultural symbol, shaping perception, emotion, and communication. This study compares colour-adjective associations in Germany and India, exploring universal patterns and culture-specific nuances. A quantitative survey invited 147 participants (76 Germany, 71 India) to select from 52 standardised RAL Design System *plus* swatches in response to word pairs spanning five conceptual dimensions: functional, emotional, sensual-sensory, symbolic-cultural, and proportional-spatial.

Across both cultures, the single most chosen colour for most adjectives was the same, indicating a strong shared perceptual-semantic core, with only a few notable exceptions (e.g., *calm*, *familiar*, *eye-catching*). However, when looking beyond the top choice to full selection profiles, clear cultural patterns emerged: While vivid colours dominated in both cultures, Germany showed a preference for lighter, muted tones with greater agreement, while India embraced darker shades and more varied hues. These findings show that while many colour-association links are universally recognised, their expression is shaped by cultural preferences in hue, character, and proportion.

By integrating hue, lightness, and chroma, the study advances understanding of colour as both a universal language and a culturally inflected code. The results have direct implications for culturally responsive design and marketing, moving beyond generic colour-emotion mappings toward nuanced, context-specific palette strategies.

Keywords: colour culture, cross-cultural communication, colour association, colour perception, colour psychology

INTRODUCTION

Colour plays a crucial role in human perception and communication. It operates not only as a sensory stimulus but also as a symbolic-cultural medium that conveys function, evokes emotions, sets sensory expectations, and shapes spatial experiences [1]. Across disciplines ranging from design and marketing to psychology and cultural studies, colour is recognised as a powerful tool for defining visual narratives and influencing behaviour. While some colour responses are rooted in biology and perceptual psychology, cultural norms and social constructs influence how colours are interpreted.

Former research in the field of psychology has demonstrated both universal and culture-specific patterns in colour associations. Jonauskaite and colleagues found strong alignment between colour patches and basic emotions, suggesting an interplay between *perceptual* and *conceptual* processing [2]. Their earlier machine learning study confirmed that while certain associations are universal, cultural differences remain significant, a pattern also observed by Hupka and colleagues [3,4]. Clarke and Costall highlighted, through a qualitative approach, that colour meanings are shaped by everyday experiences, metaphors, and language [5]. In this sense, culture, understood as the shared ways of life, beliefs, and values within a society, provides the contextual framework that guides how

such meanings are formed [6]. Mohr and colleagues called for unified cross-cultural frameworks in colour research, emphasising the need to distinguish between *linguistic* and *perceptual* stimuli, an important methodological concern also noted by Jonauskaite and contributors [7,2]. Our study responds directly to this call by using a standardised, cross-cultural design and presenting participants in Germany and India with *perceptual* colour stimuli from the RAL Design System *plus*. At the same time, the stimuli were paired with *linguistic* prompts, i.e., adjectives, allowing us to capture the intersection between visual perception and semantic association. This dual approach not only enables direct perceptual comparison but also surfaces the influence of culture on colour association.

In applied contexts, especially marketing and design, colour serves as a strategic cue. Aslam warned against assuming universal meanings, advocating for culture-specific strategies [8]. Bradfield supported this, documenting symbolic colour variation in contexts such as weddings and funerals. Such cultural distinctions have direct implications for designers working in visual communication, product development, interface design, architecture, and fashion [9]. Together, these studies underline the importance of empirical, comparative research on colour communication that accounts for multiple dimensions. However, most studies focus on basic colour terms, i.e., hue, and overlook other key dimensions, such as lightness and chroma. Our study addresses this gap by incorporating all three parameters, providing a more nuanced understanding of colour perception with direct applicability for designers and marketers.

While research on colour symbolism and perception is extensive, direct empirical comparisons between specific cultural contexts remain limited. Germany and India represent two culturally distinct contexts with contrasting historical, aesthetic, and symbolic uses of colour. German colour application tends to be more restrained and functional, whereas India often embraces bolder, high-chroma combinations. These are broad tendencies, shaped by regional variation, urban-rural differences, and contemporary design trends within both countries. Nevertheless, such cultural contrasts provide a compelling opportunity to examine how individuals from each culture associate colour with specific meanings and concepts. Understanding these associations is not only academically valuable but also practically relevant for professionals in design, marketing, and cross-cultural communication.

METHODOLOGY

The aim of this study was to examine and compare colour associations among participants from Germany and India, identifying both universal and culture-specific interpretations. A quantitative, cross-cultural survey design was employed, in which participants selected colour patches they most associated with specific adjectives.

Building on the research of Rieke, these adjectives span five conceptual dimensions of colour communication [10], capturing the multi-faceted ways in which colour conveys meaning and enabling nuanced cross-cultural analysis. This framework is particularly well suited for design and marketing because it translates directly into practical applications: aligning with brand personality and atmosphere creation, connecting to multisensory cues and material perception for packaging, interiors, and products, embedding cultural meaning and narrative potential for targeted messaging, and shaping visual weight, composition, and spatial perception in branding, architecture, and interface design. These dimensions offer a versatile vocabulary for turning colour research into targeted, context-sensitive design strategies:

- **Functional** (eye-catching vs. unobtrusive; playful vs. technological)
- **Emotional** (happy vs. sad; calm vs. dynamic)
- **Sensual-sensory** (warm vs. cold; hard vs. soft)
- **Symbolic-cultural** (natural vs. artificial; unusual vs. familiar)
- **Proportional-spatial** (heavy vs. light; open vs. closed)

The colour stimuli were based on the RAL Design System *plus*, a meta-system comprising 1.825 colours defined by a 7-digit code that encodes three parameters: **Hue** (first three digits, degrees on the colour wheel), **Lightness** (middle two, higher values indicate lighter tones), and **Chroma** (last two, higher values indicate greater

saturation). From the RAL Design System *plus*, 52 swatches were chosen to evenly cover the hue circle while varying lightness and chroma, i.e., character. In addition to the Neutrals (L 15-90, C 0) with no chroma, each of the twelve hues was represented across the remaining four characters, Dark (L 30-40, C 10-30), Muted (L 60-80, C 10-25), Pale (L 85-90, C 5-30), and Vivid (L 40-80, C 40-75), ensuring balanced variation in lightness and saturation. **Figure 1** shows the full set with descriptive colour terms which were added to improve readability.

Figure 1: *$%--* RAL colour samples with hue labels and character group classifications. *!(&'-* - Systematic sortation of the 52 colours into the RAL Design System *+).,* , illustrating the three dimensions.

The survey was administered via *Typeform*, with participants recruited through online invitations. Each adjective was shown individually, and participants selected the single colour they most associated with it from a fixed 52-swatch palette, presented in a constant order for comparability. German and English versions of each adjective were displayed side by side. A total of 147 participants completed the survey: 76 from Germany (51.7%) and 71 from India (48.3%). Ages ranged from 18 to 65+, with the largest group aged 25-34 (45.6%). Slightly more participants identified as male (53.1%) than female (45.6%), and 1.4% identified as diverse.

Descriptive comparisons between Germany and India were conducted to identify overlaps and divergences in hue and character preferences. Responses were analysed using both absolute counts and percentages, with visualisations illustrating selection patterns for individual adjectives and aggregated categories. **Figure 2** demonstrates the analytical approach, using *eye-catching* as an example for both countries:

- **Hue wheel**: Depicts the distribution of selected colours across the hue spectrum, highlighting only those hue ranges chosen by at least five participants. This view emphasises dominant hue tendencies and reveals cross-cultural differences or overlaps in hue preference.
- **Character groupings**: Plots all selected colours on a lightness-chroma grid, overlaid with "character zones" (neutral, dark, muted, pale, vivid). The size of each plotted point reflects its selection frequency, making it easy to see which character category an adjective is most strongly associated with.
- **Circular colour profile**: Arranges all selected hues along the 360° colour circle, with each segment proportional to its selection frequency. Individual RAL codes are labelled for colours chosen by at least five participants, enabling a precise identification of the most representative colours within each adjective.
- **Sorted colour profile**: Displays the most selected hues as a horizontal bar, sorted by frequency of selection. This format facilitates direct proportional comparison of dominant colours between cultures.

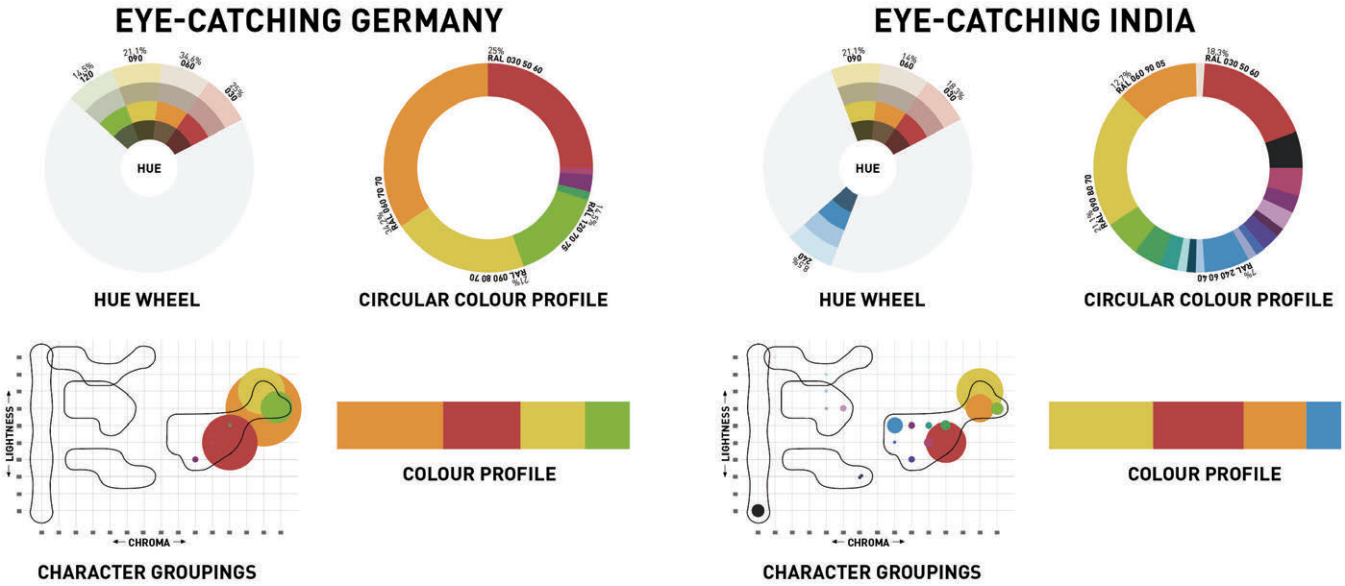

Figure 2: Visual analysis graphics created for each adjective and country, here exemplified with *$/$À#"-#'(*&* for Germany and India.

RESULTS AND DISCUSSION

Findings reveal both universal tendencies and cultural nuances. For most adjectives, the most frequently chosen colour was identical across cultures, indicating shared perceptual and semantic associations (see **Figure 3**). Exceptions included *eye-catching*, *unobtrusive*, *playful*, *familiar*, and *calm*. In the first four, differences were more subtle - for example, for *unobtrusive*, Germans favoured a light beige while Indians chose a neutral white, two closely related tones. For *familiar*, both profiles included a considerable amount of red, even though Germany's top choice was black, suggesting partial consensus. The starkest contrast appeared in *calm*: India's surprisingly vivid selections echoed their choices for *familiar* and *natural*, whereas Germany's leaned toward muted tones consistent with their *cool*, *light*, and *open* profiles.

Expanded analysis, including all hues chosen by at least five participants, reveals distinct cultural nuances beyond the top choices. Taking *eye-catching* as an example (**Figure 2**), Germany favoured vivid orange, India vivid yellow. Both linked the adjective to vivid hues (30°, 60°, 90°), but distributions differed. Additionally, Germany leaned toward vivid lime, while India chose vivid blue. German choices showed stronger consensus and a narrower range; Indian selections, though vivid-dominated, spanned more characters, showing more diversity. This points to a shared warm and vivid preference for *eye-catching* alongside distinct secondary tendencies. When analysing and decoding the emerging colour palettes according to the same analytical strategy, multiple clusters emerged that are summarised in **Table 1**.

The clusters suggest a shared semantic core of concepts, where positive and negative connotations can be clearly distinguished through colour profiles. Consistent with Jonauskaite's findings, some colours, such as vivid red or neutral white, appear across different adjectives, carrying both positive and negative meanings depending on context [2]. Even though colours share a semantic core, their communicative impact depends on cultural context, proportional balance, and character. Moving beyond generic colour-emotion links, these findings highlight the value of nuanced, data-driven palettes that reflect specific audience sensibilities, empowering designers and marketers to craft colour strategies that are both culturally resonant and contextually precise.

Table 1: Clusters of colour-adjective associations, showing shared semantic cores and cultural nuances.

Neutral & Dark profiles - typically carrying negative, neutral, or serious connotations	
1. Only neutrals	*sad, unobtrusive* (India); *hard* (Germany)
2. Neutrals + dark profiles	*closed, heavy* (both); *hard* (India)*; sad* (Germany)
Pale & slightly muted profiles - smallest cluster, more diverse in hue	
3. Profiles	*soft, light, cool* (both); *open, unobtrusive, calm* (Germany)
Vivid profiles - largest cluster, often linked to positive or energised connotations	
4. Darker, less chromatic vivid profiles	*unusual, artificial (both); technological* (India)
5. Mid-range vivid profiles	*familiar*, *dynamic* (both); *natural* (India); *warm* (Germany)
6. Lightest, most chromatic vivid profiles	*eye-catching*, *happy, playful* (both); *warm* (India)
Hue-driven profiles - typically move across several character groups but are anchored in specific hue planes	
7. Transitional profiles	*cool, warm, natural, unusual, artificial* (both); *calm, open* (India); *technological* (Germany) - anchored here despite dispersion

Across the five conceptual groups of adjectives, distinct links to colour contrasts emerge. **Functional terms** reflect contrasts of hue and quality, with saturation marking profiles of higher valence and arousal against more subdued opposites. **Emotional terms** such as *happy* and *sad* align with light-dark contrasts anchored in universal pairings like yellow-joy and black-grief, while *calm* reveals a cross-cultural contrast of quality, with Germany favouring pale-muted tones and India selecting vivids and neutral white. **Sensory-sensual terms** oppose *warm* and *cool* through complementary contrast, while *soft* and *hard* derive from light-dark dynamics. **Symbolic-cultural terms** set *natural* and *artificial* in complementary contrast, while *familiar* and *unusual* prove less opposed than expected, though *unusual* and *artificial* show parallel patterns within each culture. Finally, the **proportional-spatial group** underscores how black-white relationships universally structure spatial perception. Taken together, these patterns show how colour semantics weave universal contrast principles with culturally nuanced variation.

In both cultures, vivid and neutral colours dominated selections, with India showing an even greater share of vivid characters. Pales ranked next, slightly favoured by Germans, followed by darks, chosen a bit more often by Indians. Muted colours were rare overall. These patterns support the view that vivid colours are globally more familiar and easier to name, while muted palettes are harder to describe and less perceptually emphasised [11]. While vivid colours dominated across both cultural groups, their direct applicability to many design contexts, such as interiors, products, and architecture, is limited, as high-chroma tones may not align with desired atmospheres or functional requirements. Exploring other atmospheric descriptors, such as *focused, communicative,* or *regenerative*, could open new avenues for creating context-specific colour schemes. Future studies would benefit from a more task-, context-, and needs-oriented approach, examining how associations shift in specific applications to enhance the practical relevance of findings for design and marketing.

While these shared tendencies underscore robust cross-cultural patterns, several contextual factors also shaped responses. Methodologically, while the RAL Design System *plus* provided standardised colour definitions, participants viewed swatches on personal devices, where variations in display calibration could subtly alter perception. Language may have also played a role: German participants responded in their native language, while Indian participants used English, which may not fully capture nuances from their first languages. Finally, neither Germany nor India is culturally homogeneous; regional, linguistic, and urban-rural differences likely influenced individual responses, suggesting that intra-cultural variation is a valuable area for deeper investigation.

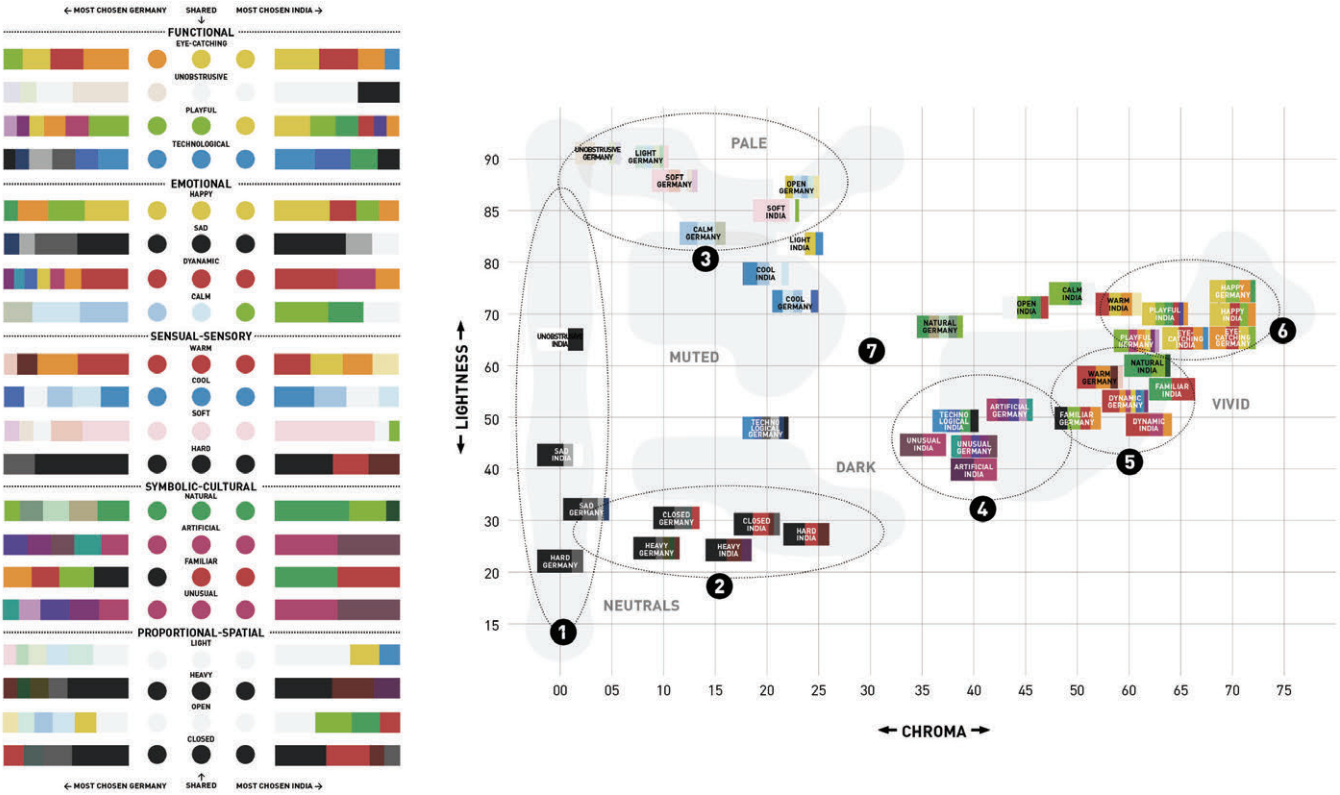

Figure 3: *$%*-- Most frequently chosen colour and shared consensus alongside the full selection profile for each adjective. *!(&'-* - Distribution of colour-adjective associations mapped onto a lightness-chroma grid, averaged per adjective, with superimposed character zones (neutral, dark, muted, pale, vivid). Groupings reveal shared perceptual patterns and culturally specific profiles, corresponding to the clusters summarised in Table 1.*Ā*

CONCLUSION

This study demonstrates that while Germany and India share certain colour-adjective associations, cultural differences emerge in hue and character preferences, as well as proportional balance. By decoding the intersection of hue, lightness, and chroma, and considering full selection profiles rather than single dominant colours, the findings reveal both a shared semantic core and meaningful divergences. These nuances show that even when colours carry similar meanings in associations, their communicative effect depends on cultural context and secondary choices, making universalist palette strategies insufficient for design and marketing.

Methodological factors such as screen-based viewing, language differences, and intra-cultural diversity highlight the complexity of cross-cultural colour research and the importance of refining experimental controls. Future work should explore colour combinations, additional atmospheric descriptors and link results to specific contexts and needs, ensuring direct applicability to real-world contexts.

Decoding colour communication reveals that we have shared hues, but different accents: colour is a universal language with cultural dialects.

REFERENCES

[1]. Elliot, A. J., & Maier, M. A. (2014). Color psychology: Effects of perceiving color on psychological functioning in humans. *Annual Review of Psychology, 65,* 95-120. https://doi.org/10.1146/annurev-psych-010213-115035

[2]. Jonauskaite, D., Parraga, C. A., Quiblier, M., & Mohr, C. (2020). Feeling blue or seeing red? Similar patterns of emotion associations with colour patches and colour terms. *i-Perception*, 11(1), 1-24. https://doi.org/10.1177/2041669520902484

[3]. Jonauskaite, D., Wicker, J., Mohr, C., Dael, N., Havelka, J., Papadatou-Pastou, M., Zhang, M., & Oberfeld, D. (2019). A machine learning approach to quantify the specificity of colour-emotion associations and their cultural differences. *Royal Society Open Science*, 6(9), 190741. https://doi.org/10.1098/rsos.190741

[4]. Hupka, R. B., Zaleski, Z., Otto, J., Reidl, L., & Tarabrina, N. V. (1997). The colors of anger, envy, fear, and jealousy: A cross-cultural study. *Journal of Cross-Cultural Psychology*, 28(2), 156-171. https://doi.org/10.1177/0022022197282002

[5]. Clarke, T., & Costall, A. (2008). The emotional connotations of color: A qualitative investigation. *Color Research & Application*, 33(5), 406-410. https://doi.org/10.1002/col.20435

[6]. Williams, R. (1958). *Culture is ordinary*. In N. McKenzie (Ed.), *Conviction* (pp. 74–92). MacGibbon & Kee. Retrieved from https://www.giarts.org/article/culture-ordinary

[7]. Mohr, C., Jonauskaite, D., Dan-Glauser, E. S., Uusküla, M., & Dael, N. (2018). Unifying research on colour and emotion: Time for a cross-cultural survey on emotion associations with colour terms. In L. W. MacDonald, C. P. Biggam, & G. V. Paramei (Eds.), *Progress in Colour Studies: Cognition, Language and Beyond* (pp. 209-222). John Benjamins Publishing Company. https://doi.org/10.1075/z.217.11moh

[8]. Aslam, M. M. (2005). *Are you selling the right colour? A cross-cultural review of colour as a marketing cue*. In I. Papasolomou (Ed.), *Developments and Trends in Corporate and Marketing Communications: Plotting the Mindscape of the 21st Century* (pp. 1-14). InterCollege, School of Business Administration. https://ro.uow.edu.au/commpapers/1043

[9]. Bradfield, E. L. (2014). *The diversity of color: An analysis of cross-cultural color symbolism* (Honors thesis, Andrews University). https://dx.doi.org/10.32597/honors/90/

[10]. Rieke, T. (2008). *Haptic visuals - Oberfläche und Struktur: Farbe und ihre Beziehung zur Tastwahrnehmung* [Haptic visuals - Surface and structure: Colour and its relationship to tactile perception]. Verlag Farbe und Gesundheit.

[11]. Lindsey, D. T., & Brown, A. M. (2009). World Color Survey color naming reveals universal motifs and their within-language diversity. *Proceedings of the National Academy of Sciences, 106*(47), 19785-19790. https://doi.org/10.1073/pnas.0910981106

Cross-Cultural Study About The Effect of Color on The Perception of Grammatical Gender

Alexander Raevskiy[a*], Itsuki Kyoto[b], Kitirochna Rattanakasamsuk[c], and Rumi Tokunaga[b]

[a]*Tohoku University, Sendai, Japan*
[b]*Chiba University, Chiba, Japan*
[c] *Rajamangala University of Technology Thanyaburi, Thanyaburi, Thailand*

[*]*Corresponding author: Raevskiy Alexander, raevskiy.alexander.d4@tohoku.ac.jp*

ABSTRACT

Grammatical gender is one of the most difficult and challenging categories for learners of a new foreign language (that possesses this category), as it cannot be understood by logic and should be only remembered. In this case color can be a mnemonic hint, as it provides some cross-modal associations with gender, as previous studies have demonstrated. The aims of the current study were 1) to find out whether color can be used as a mechanism for effective memorizing of a gender category in an unfamiliar language, and 2) to explore cross-cultural differences in gender/color perception. Participants from Japan and Thailand took part in the experimental study which consisted of 3 parts. In all three experiments, the task was the same: they were asked to select which grammatical gender (male, female or neutral) the image/color appearing on the screen should be attributed. In Experiment 1, participants were presented with 24 images of different objects (table, flower, train, etc.) drawn with black lines. In Experiment 2, they were presented with a homogenous screen of one of nine colors (black, red, green, blue, purple, pale red, pale green, pale blue and pale purple). In Experiment 3, they were presented with 24 images, drawn with lines of the 9 colors listed above. Images were presented in a random order, and the procedure was repeated four times. Results showed significant differences between Japanese and Thai participants. First, Japanese participants showed more consistency in responses: many answers were selected by 70% of respondents or more (in several cases – 100%), while in Thai responses this percentage was much lower. Second, Japanese participants demonstrated lower exposure to the color impact, than the Thai. Thus, it can be suggested that color-gender associations are influenced by culture and language.

Keywords: impression of color, cross-cultural differences, grammatical gender, language acquisition

INTRODUCTION

Discussions and speculations upon the grammatical category of gender in linguistics are not new; from ancient times philosophers and scientists explored this concept. First theories upon grammatical gender can be found among Greek philosophers. Different reasons for the origin of gender in language have been suggested, but the answer is still not found (1).

Claims were made that grammatical gender is the result of the tendency of primitive people to individualize and personify inanimate objects and to associate them with physical gender (i.e., some objects were perceived by members of a certain language group as males, and other – as females). This view was long-lived for many

generations of linguists; however, it is based on a presumption about primitive peoples' cognition and, thus, is hard to find supporting evidence for that. Since the origins of grammatical gender are unclear, we should think of this category as of a classification principle which is run by lexical properties of the words, rather than by implicit associations. Greenberg (2) proposes that grammatical gender is a combination of classification and agreement.

What we can say for sure is that this category is not vital for the proper functioning of language (as there are languages that don't have it) and adds nothing to the meaning of the word; this is why it is often considered to be a secondary grammatical category. Furthermore, it is hard to find common features in the languages which possess this category (as well, as in those that don't), because grammatical gender can be found in very different languages, both agglutinative and inflected (1).

Whatever the nature of this grammatical category could be, gender is one of the most difficult and challenging categories for learners of a new foreign language (that possesses this category), as it cannot be understood by logic or analysis, thus, should be only remembered. Studies showed that learning gender requires more time than acquiring other grammatical categories; especially when learners have to get used to a different gender system from their native language (3,4).

In the current study, we aimed to investigate whether a color can serve as a hint for the grammatical gender distinction. First, it should be noted that there are some common gendered associations with pink and blue, where the former is associated with girls, and the latter – with boys (5). It is claimed that this distinction is rather late, emerging from the second half of 20th century, and it cannot be found earlier (6); however, even if this association is a late phenomenon, we should agree upon its strong role in modern human perception. Second, it has been reported (7) that not only pink and blue, but other basic colors can provide certain associations with genders and emotions. More specifically, a recent study using Stroop task (8) demonstrated that some colors reflect masculine traits (black, gray, green), while some are associated with females (white, purple, red).

The aims of the current study were 1) to find out whether color can be used as a mechanism for effective memorizing of a gender category in an unfamiliar language, and 2) to explore cross-cultural differences in gender/color perception.

METHODOLOGY

In all experiments the procedure was the same: participants were presented with visual stimuli (image or color) on the PC monitor and asked to select (basing on their first impression) to which grammatical gender (male, female or neutral) the appearing items should be attributed. The stimuli in all 3 experimental tasks were different. Experiments were conducted with PsychoPy. Images were presented on a monitor in a dark room.

In Experiment 1, participants were presented with 24 images of different objects (table, flower, train, etc.) drawn with black lines. In Experiment 2, they were presented with a homogenous screen of one of nine colors (black, red, green, blue, purple, pale red, pale green, pale blue and pale purple). In Experiment 3, they were presented with the same 24 images as in Experiment 1, drawn with lines of the 9 colors listed above. The image/color was presented randomly, and the procedure was repeated four times.

Images were selected to include different categories (foods, geometrical objects, transport, nature, clothes, etc.; each category consisted of 3 items) and were drawn by hand in simple lines, as shown in Fig. 1. Colors were selected to include those with higher (blue, red, pale blue and pale red) and low (green, purple) levels of color-gender association. Experiment 1 with the Black-line condition was considered to be a neutral condition.

After completing the experiments, participants were provided with a questionnaire and were asked to answer some questions about the reasons for their selection of gender.

Participants from Thailand (N = 20) and Japan (N = 20) took part in the experiments. All participants had a n ormal color vision tested by the Ishihara color plate.

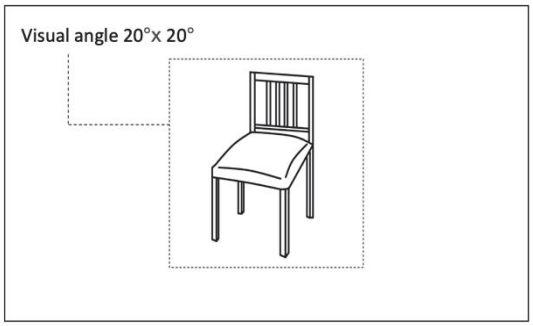

Figure 1: Example of image used in Experiments 1 and 3

Table 1: Color specification for Experiment 2

Color	Y (cd/m^2)	Chromaticity	
		u'	v'
Red	13.1	0.43	0.52
Green	14.2	0.13	0.55
Blue	9.3	0.16	0.30
Purple	12.5	0.22	0.32
Pale Red	31.9	0.24	0.48
Pale Green	34.5	0.17	0.50
Pale Blue	30.1	0.19	0.43
Pale Purple	31.6	0.22	0.32

RESULTS AND DISCUSSION

In Experiment 1, the most selected gender for most images was the neutral gender, both for Thai and Japanese participants. This tendency can be explained by the lack of specific associations: as no participants possess a category of gender in their languages, the most natural answer for them is probably a neutral gender. However, there were objects that were mostly attributed by both groups of participants either to masculine (a mountain, a leg and a train), or to feminine gender (a scarf, a ring, a flower, and an eye). It should also be noted that certain categories tend to be attributed to a certain gender. Specifically, transport was associated more with masculine gender, while clothes – with the feminine.

The results of Experiment 2 revealed some cross-cultural differences between the two groups. Specifically, Japanese participants showed a tendency to associate colors either with masculine or feminine gender: 8 colors out of 9 were attributed to these two genders by more than 50% of respondents, whereas among Thai participants such division was not distinctive, and neutral gender was selected often.

However, basic associations were similar: blue color was predominantly associated with masculine gender, while pale purple and pale red were linked to feminine gender, which is consistent with previous research findings (7, 8). Interestingly, gender associations with red color didn't reveal a specific connection to the feminine.

Black and green were also commonly associated with masculinity among participants. Notably, the color that exhibited the greatest divergence in gender associations between the two cultural groups was purple: it was perceived as neutral gender by 60% of Thai participants, whereas the majority of Japanese participants (65%) tended to associate it with feminine gender. Furthermore, it was demonstrated by the results of Experiment 2, that pale colors (especially pale red and pale purple) were associated with feminine gender.

The results of Experiment 3, in which participants responded to images drawn with colored lines, revealed notable differences between Japanese and Thai respondents. Most significantly, Japanese participants demonstrated a higher degree of response consistency for images with different colors: many choices were selected in the same way by 70% or more of respondents. In some cases, complete agreement was reached: for example, train in Blue condition was perceived as masculine, while ring and flower in Pale Red condition - as feminine by 100% of respondents. While this marked disparity is difficult to account for definitively, similar patterns have been observed in previous studies, including research on color–taste associations (9). In contrast, Thai participants exhibited considerably lower levels of consensus, and 70% agreement was reached in Blue and Pale Red conditions (masculine and feminine genders, respectively).

Another remarkable feature is that Japanese participants demonstrated lower exposure to the color impact, than the Thai. Their gender selection was mostly the same, independent of the color of the lines. On the contrary, Thai participants demonstrated a high level of exposure to color. Among them, all items in the Blue condition were attributed to male gender, and in the Pale red condition – to female, while among Japanese participants, the difference between gender associations between Black and other conditions was not so significant.

Some cross-cultural differences were also revealed, although not so distinctively. Thus, Green condition showed a tendency to be associated with masculine gender among Thai participants, and neutral gender – among the Japanese. Percentage of images attributed to a certain gender by over 50% of respondents is shown on Figure 2.

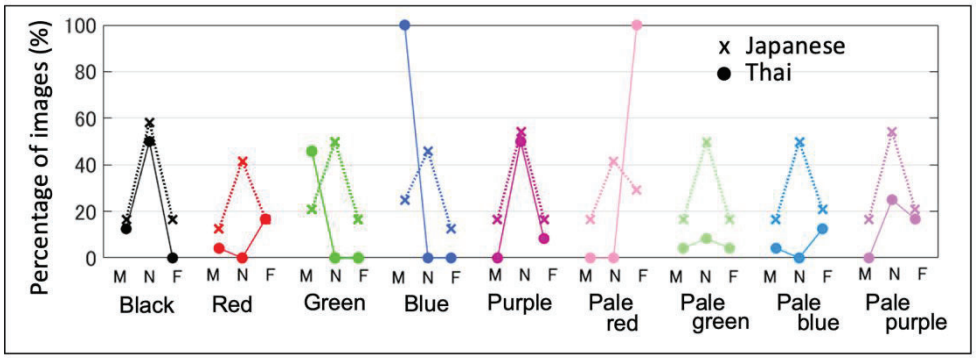

Figure 2: Results of Experiment 3. Percent of images that were attributed to a certain gender by more than 50 % of respondents in each color condition

It should be also noted that color selection was dependent on object, i.e. some items had a stronger association with gender (independently of the color), while gender associations for other items were more influenced by color. However, few patterns were the same among the two groups, which suggests that color-gender associations are influenced by culture and language. For example, a train in most color conditions was attributed to masculine gender, while a ring – to the feminine. This example shows that certain objects already have some association with gender,

and color does not play a significant role in these cases.

In a questionnaire, participants were asked to rate from 1 to 10 which factor - the color or the object itself (1 - meaning the strongest color influence, and 10 – the strongest object influence) was more important for their decision about gender. Both Thai and Japanese participants reported about stronger impact of color: for the Japanese the average was 4.8 (SD = 2.48), for Thai – 3.4 (SD = 2.83). However, the results of the experiments showed more differences between the two groups.

CONCLUSION

Current study showed that color can reflect some gender traits and provide impact on perception of gender of certain objects. Thus, it can be used as a mnemonic mechanism for remembering grammatical category of gender in unfamiliar languages, especially blue and pink colors.

However, cross-cultural differences should also be mentioned. Although basic associations between objects and gender (Blue for masculine; Pink for feminine) are generally similar, some associations are suggested to be cultural-specific. Another remarkable point is the impact of color on the grammatical gender perception: we should admit that exposure to color demonstrates significant distinction between Japanese and Thai participants.

As a limitation of study, it should be noted that it was conducted only on two groups of respondents (both representatives of Asian culture), thus, it seems promising to include European countries in further research, to explore cross-cultural differences on a wider scale.

REFERENCES

[1]. Greenberg, Joseph H. (1978): How does a language acquire gender markers? In: Greenberg, Joseph H./Ferguson, Charles A./Moravcsik, Edith (eds.): Universals of human language. Stanford, CA: Stanford University Press. 47–82

[2]. Ibrahim, M.H. (1973). Grammatical gender: Its origin and development. Paris.: Mouton.

[3]. Denhovska, N, Serratrice, L. (2017). Incidental Learning of Gender Agreement in L2. Journal of Psycholinguistic Research, 46(5):1187-1211

[4]. Kirova, A. & Camacho, J., (2021) “Failed gender agreement in L1 English L2 Spanish: Syntactic or lexical problem?”, *Glossa: a journal of general linguistics* 6(1): 129

[5]. Cunningham, S.J., Macrae, C.N. (2011). The colour of gender stereotyping. British Journal of Psychology. 102(3): 598-614.

[6]. Del Giudice M. (2012): The twentieth century reversal of pink-blue gender coding: A scientific urban legend? Archives of Sexual Behavior. 41: 1321–1323.

[7]. Jonauskaite, D., Sutton, A., Cristianini, N., Mohr, C. (2021). English colour terms carry gender and valence biases: A corpus study using word embeddings. PLoS One. Jun 1;16(6):e0251559.

[8]. Wang, C., Zhu, C., & Zuo, B. (2025). If colors have gender: Color-gender stereotype and the impact on impression evaluation and interpersonal interaction. *The Journal of General Psychology*, 1–40.

[9]. Raevskiy, A., Bubnov, I., Chen, Y.C., Sakai, N. (2022). Differences in Color Representations of Tastes: Cross-cultural Study Among Japanese, Russian and Taiwanese. In: Rau, PL.P. (eds) Cross-Cultural Design. Interaction Design Across Cultures. HCII 2022. Lecture Notes in Computer Science, vol 13311. Springer, Cham.

An Investigation of Selected Chinese Paintings Colour Theories and How It Differs from The Practical Colour Application Used in Western Paintings

Woon Lam Ng[a*] and Huiying Goh[a]

[a]*Nanyang Technological University, Singapore, Singapore*
[*]*Corresponding author: Woon Lam Ng, ngwoonlam@ntu.edu.sg*

ABSTRACT

Western colour theories have been well researched and established since Newton's discovery of light in the 18th century. Western painters such as the Impressionists were known for reading books written by the colour scientists and used their principles of colours on their artwork. On the other hand, little was discussed about colours by the Chinese painters. This paper seeks to investigate how the Chinese understood colours, compare and contrast with how the painters from the West used colour theories in their paintings. Western colour theories is heavily based off modern science concepts in physics, neuroscience and psychology. Before the start of Western influences in China in the 20th century, Chinese painters did not use colours based off modern science. Instead, the Chinese painters understood and used colours based off the Chinese philosophies which is a blend of Confucianism, Taoism and Buddhism. As well as the concept of Five Elements and Five Colours (五行五色 *wu xing wu se*). Ten paintings by Chinese and Western artists are used for the comparison studies, with a selection criterion based on the colour proficiency of the artwork. The selected painting is fed into the 3D software model of the Munsell colour space which generates the painting's 3D Munsell colour space through a mapping algorithm and allows colour analysis comparison. The colour analysis of these paintings provides a comprehensive view of the different directions and objectives of Chinese painting art. Discussions of the results reflect the strong scholarly connections of Chinese ink paintings and therefore there are additional factors that would not be considered in Western visual art but are regarded as critical parameters in Chinese ink paintings. The color schemes are therefore bound by these factors.

Keywords: Western Colour Theories, Chinese Philosophies, Paintings, Munsell 3D Colour Space Generator

INTRODUCTION

The origins of Western colour theory can be traced back to ancient Greece, when Aristotle (384 – 322 BCE) studied the rainbow and suggested that red, green, and violet were the only "true colours" that could not be created by mixing other hues. The important development in colour science was in 1709 when Isaac Newton published *Opticks: A Treatise of the Reflections, Refractions, Inflections and Colors of Light*. Newton discovered that when white light passed through a glass prism, it decomposed into seven visible colours namely red, orange, yellow, green, blue, indigo and violet. Newton also implied the existence of colour harmony in nature, introduced a circular colour arrangement and related colours to the seven musical tones. In 1810, Johann Wolfgang Von Goethe published *Theory of Color* which opposed Newton's theory that darkness was an absent of light. Goethe explored the physiological experience and perception phenomenon of human, which marked the start of colour psychology research. Goethe also rejected Newton's theory on white light being the synthesis of colours, and proposed that colours recomposed into grey. In current day understanding, Newton's theory was based off additive mixing in coloured light, whereas Goethe was referring to subtractive mixing in pigments. While colour scientists were

publishing and debating theories about colours, painters of the time, such as J.M.W. Turner, were also studying and applying both ideas combining results of additive and subtractive color mixing in his paintings. Turner has influenced Impressionists especially Monet and Pissarro.

The development of colour science in the West in the 19th century was in parallel with the Realist and Impressionist art movements. The theory of simultaneous contrast from Michael Eugene Chevreul's *The Principles of Harmony and Contrast of Colours, and Their Applications to the Arts* served as a basis of optical colour mixing by Impressionists. Impressionists painters such as Monet, George Seurat and Paul Signac placed opposite (or complimentary) colours beside each other to make the colours more chromatic or create a sense of movement. The discoveries of colour theories continued and colour scientists such as Lambert, Runge, Chevreul and Ostwald developed the concept of a 3D colour model. In 1905, Albert Henry Munsell introduced an asymmetrical 3D colour model and proved that the practical range of colours were not equal. Munsell redefined the three qualities of colour as hue, value and chroma. Till today, Western colour theories which were based off colour science continued to impact the way artists understood and use colours in their paintings.

In contrast to the Western counterpart, the Chinese painters understood and used colours very differently. Similar to the unbroken civilization in China, the principles and concept behind Chinese painting remained relatively unchanged over the past 1,500 years. Unlike the Western colours which was based on science, the Chinese idea of colours was based on philosophies from Taoism, Confucianism and Buddhism. "The Dao produced One; One produced Two; Two produced Three; Three produced All things." (道生一，一生二，二生三，三生万物 *dao sheng yi yi sheng er er sheng san san sheng wan wu*) originated from Laozi's (老子 *laozi*) *The Classic of the Way's Virtues* (道德经 *daode jing*) [7]. Tao, as the originator of the undivided universe (one), gave rise to yin-yang (two), heaven, earth and human (three) and all worldly things. Zhuangzi (庄子 *zhuangzi*), another Taoism philosopher, said that the vibrancy of colours disturbed the peaceful thoughts of human and disrupted the pursue of the Way (道 *dao*), "(their fondness for) the five colours disorder the eye" (五色乱目 *wuse luanmu*) [7]. Confucius (孔子 *kongzi*) said in *The Analect* (论语 *lunyu*), "perfect is the virtue which is according to the constant mean" (中庸之为德也 *zhongyong zhiwei deye*) [7]. It refers to the Doctrine of the Mean where it is important for a person to maintain balance and avoid extremes in his actions and thoughts. The Buddha said in Heart Sutra (般罗波罗蜜多心经 *banluo boluomiduo xinjing*) that "form is emptiness, emptiness is form" (色即是空，空即是色 *se jishi kong, kong jishi se*).

The history of colours in Chinese paintings can be viewed in the following four phases: Pre-Tang (before 618 AD), Tang-Song (618 - 1279 AD), Yuan-Ming-Qing (1271-1912 AD) and 20th century onwards [9]. Before the start of Western influences in China in the 20th century, Chinese painters did not use colours based off modern science. Western colour theories, on the other hand, is heavily based off modern science concepts in physics, neuroscience and psychology. Colour is light. My red is not your red. Colour is in the mind. The early writings of Western colour theories were a mix and opposing theories based off subtractive and additive colours; 2-dimensional and 3-dimensional colour wheels; symmetrical and asymmetrical colour space. Whereas the Chinese painters were guided by Chinese philosophies, which is a blend of Taoism, Confucianism and Buddhism. This mixed beliefs and philosophies led to the common principles used in Chinese ink painting such as spirit vitality (气韵 *qiyun*), emptiness-fullness (虚与实 *xuyushi*) and brush ink (笔墨 *bimo*). In some periods, different dynasties also claimed a specific colour as their element colour for the dynasty. For example, Qin dynasty was known to adopt black as the dynasty colour as Qin was considered the element of water in Five Elements and Five Colours (五行五色 *wu xing wu se*) [5]. Although the Chinese scholars also warned on the limitation and over usage of Five Elements Five Colours in explaining how Chinese painters use their colours [8]. As it often had a human bias and political reason in it. These concepts will be referred and explained further in the painting comparison segment.

The aim of this paper is to investigate how Chinese painters used colours in their artwork and how it differed from its Western counterpart. In order to be able to identify the similarities and differences between the West and the Chinese, the research methodology designed for the study is defined in the following segment.

METHODOLOGY

The introduction segment reviewed on how colour theories were developed in both the West and in China. This study predominantly adopted qualitative research methods, where content analysis is used for comparison studies on the selected paintings. The Munsell 3D colour space generator software is used to create individual 3D colour space diagrams and colour data to aid in the visual comparison.

Ten paintings by ten Western and Chinese painters are selected for comparison studies (refer to Table 1). The selection criteria are based on general audience familiarity and the visual proficiency of the artwork. The selection is across a spread of timeline, encompassing important milestones made by both Western and Chinese painters in their respective art history. The selected painting is fed into the 3D software model of the Munsell colour space which generates the painting's 3D Munsell colour space through a mapping algorithm [4]. Some of the Chinese ink paintings darkened over the years due to the ageing of the material, but it will not affect the result of the comparison as colour is relative, and not absolute. The Appendix contains details of the ten selected artwork and the generated 3D colourspace diagrams. The results of the comparisons will be discussed in the next section.

Table 1. Details of the ten selected artworks for comparison studies

s/n	Artist name	Medium	Title of artwork	Period
1	Titian	Oil on canvas	*Bacchus and Ariadne*	Renaissance
2	Leonardo da Vinci	Oil on wood	*The Virgin of the Rocks*	Renaissance
3	Yan Li Ben (阎立本)	Chinese pigments on silk	*The Imperial Sedan Chair - Emperor Taizong Receiving the Tibetan Envoy*	Tang dynasty
4	Zhang Xuan (张萱)	Ink, colour and gold on silk	*Court Ladies Preparing Newly Woven Silk*	Norther Song
5	J.M.W. Turner	Oil on canvas	*The Fighting Temeraire*	Romanticism
6	Claude Monet	Oil on canvas	*Poppy Field Near Argenteuil*	Impressionism
7	Ju Ran (巨然)	Chinese ink on silk	*Seeking the Tao in Autumn Mountains*	Five Dynasties
8	Fan Kuan (范宽)	Chinese ink on silk	*Travelers Among Mountains and Streams*	Northern Song
9	Mi Fu (米芾)	Chinese ink on silk	*Cloudy Mountain*	Northern Song
10	Georges Seurat	Oil on canvas	*A Sunday on La Grande Jatte*	Neo-impressionism

RESULTS AND DISCUSSION

The first set of painting comparison are by Turner, Monet, Seurat, Ju Ran, Fan Kuan and Mifu. The commonality between these two groups of Western early 20th century painters and Chinese Northern Song dynasty landscape painters is that they are chronologically aligned, and are pivotal figures on their way of discovering new painting techniques. It is also important to note that although all six painters' artwork are of landscape sceneries,

but the Chinese mountain-water painting (山水画 *shangshui hua*) are not landscapes. Shanshui appeared a thousand years earlier than Western landscape and does not seek record the extreme natural events, but to depict the Taoist doctrine of life [3].

As reflected in the generated 3D Munsell colourspace diagrams, Ju Ran, Fan Kuan and Mifu's paintings have very limited colour data. The literati painters did not make use of the tonal range in ink or the practical colour mixing capacity that pigments had provided. Instead, the paintings were driven by the Chinese philosophies that the Northern Song literati painters adopted, which were heavily influenced by the Taoist philosophies. Firstly, spirit vitality (气韵神通 *qiyun shentong*) is the first law in Xie He's *Six Principles of Chinese Painting* (谢赫六法 *xiehe liufa*) [1]. The Chinese phrase has different transcriptions including "spiritual rhythm expressed in the movement of life", "rhythmic vitality or "resonance of spirit; movement of life". Breath (气 *qi*), the driving force behind all life forms, dictates the sequential formation of a picture composition. Next, the concept of emptiness-fullness (虚与实 *xu yu shi*) came from both the Taoist and Buddhist ontologies. In Taoist term, "empty" (无 *wu*) could be understood as nothingness, which is the opposite of "being" (有 *you*). "Empty" (虚 *xu*) could also be interpreted as hollowness, which is the opposite of "fullness" (实 *shi*) [2]. In Buddhism, "empty" (空 *kong*) means non-existence (非有 *fei you*). This idea of polarity leads to Chinese painting techniques such as open-and-shut (开合 *kaihe*) and the use of dark and light (阴阳 *yinyang*). Lastly, the concept of brush-ink (笔墨 *bimo*). The tool (brush) is termed together with ink because ink is just a material on its own [2]. Only when paired with a brush, ink is given with life. "The brush to give birth to substance and form, and the ink to capture colour and light". The rendering of values with light and dark ink often represent the word "colour" (色 *se*). In *Notes of Past Famous Paintings* (历代名画记 *lidai minghua ji*), Zhang Yanyuan (张彦远) wrote that ink provided all five colours (运墨而五色具 *yunmo er wuse ju*), namely: dry, wet, concentrated, diluted, black (干湿浓淡黑 *gan shi nong dan hei*). In Qing dynasty, Tang Dai (唐岱) said that ink consist of six colours (墨色之中，分为六彩 *mose zhizhong, fenwei liucai*), which includes the empty white space (留白 *liubai*) as the sixth colour. Taoist philosopher Zhuang Zi (庄子) said (五色乱目，使目不明 *wuse luanmu shimu buming*) [7]. As self-cultivation is an important way of life for the literati painters, colours disappeared from the Chinese palette and was replaced by a strong use of brush strokes and attentive planning in the pictorial composition.

Although pictorial composition also played an important role in Western art, the painters active during the age of industry revolution such as Turner, Monet and Seurat focused more on colour theories and how the mind perceived colours. Turner's *The Fighting Temeraire* was painted in 1838 and was seen to be precursor in capturing light on paintings. The Impressionists, which was led by Monet, were influenced by the way Turner used colours. Monet's *Poppy Field Near Argenteuil* made use of colour theory of how opposite colours appeared to be more chromatic beside each other, and how human brain could not locate and differentiate hues of similar value to mimic movements at the poppy field on a windy day. Neo-impressionist Seurat painted *A Sunday on La Grande Jatte* with tiny colourful dots which were closely spaced to create an optical mixing effect to make the green tree shimmer.

The second set of comparison consist of four paintings on human portraiture and figurative paintings by Titian, Da Vinci, Yan Li Ben and Zhang Xuan. This set of comparison is between the Renaissance painters engaged by the religious institutions and Tang dynasty court painters engaged by the Chinese imperial family. Similar to mountain-water painting, the human portrait painting in Western art is different from the human (人物 *renwu*) painting in Chinese painting. Among these four paintings, Zhang Xuan's *Court Ladies Preparing Newly Woven* Silk has the widest colour range. This result is aligned with the historical development of Chinese paintings in Tang dynasty where vibrant coloured Buddhist art was introduced along with Buddhism. Figure 1 (d) showed the diagram of Yan Li Ben's painting, which colours on silk painting had deteriorated over the years. It is probably one of the reasons why practical colour application studies could not be conducted on most Chinese paintings.

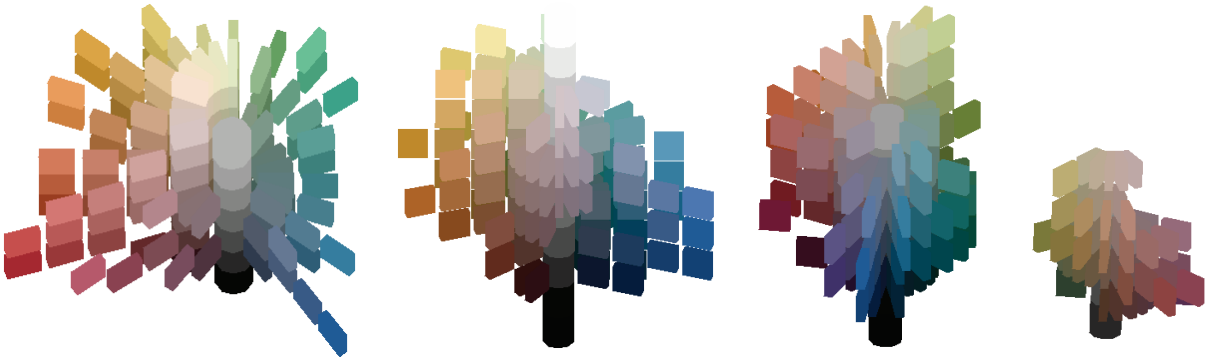

1 (a) 1 (b) 1 (c) 1 (d)

Figure 1 (a) to (d) are 3D colourspace models generated by inputting paintings of (4) Zhang Xuan, (2) Da Vinci, (1) Titian, and (3) Yan Li Ben respectively.

Lastly, it is important to note that both the Western and Chinese painters have access to very different painting materials of their time. For Western art, canvas, wooden board and wall surfaces were commonly used for painting. In Chinese paintings, rice paper, bamboo paper and silk are the commonly used painting surfaces. Pigments in general are quite similar for both Western and Chinese. For the majority part of art and painting history, the colour pigments came from natural minerals such as earth, gems or insects. But that was before synthetic dye was invented during the industrial revolution by the textile industry. Not only were the Impressionists exposed to the latest colour science findings written by the scientists, they also had access to new inventions such as synthetic paints which are more chromatic in colour. With this piece of information in mind, we will look at the last set of comparison within Western art itself.

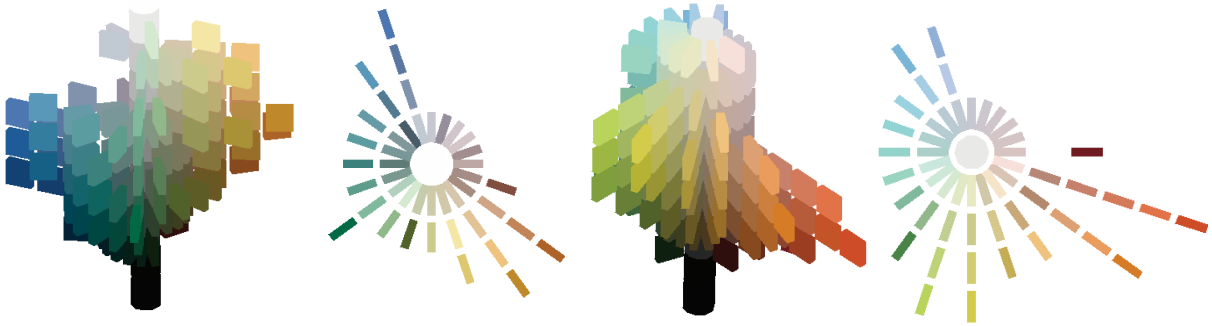

2 (a) 2 (b) 2 (c) 2 (d)

Figure 2 (a) to (d) are various views of 3D colourspace diagrams generated by inputting paintings of (2) Leonardo da Vinci and (6) Claude Monet respectively.

Renaissance painter Leonardo da Vinci's *Virgin of the Rocks* (2) was painted between 1483 and 1486. Impressionist Claude Monet's *Poppy Field Near Argenteuil* (6) was painted in 1873. There two paintings were almost 400 years apart. With industry revolution happening in the 20th century, Monet had access to better mode of transport (train and car instead of horse carriages), tubed paints (instead of hand grinded and blended paints) and synthetic colours (expanding the range of hue and chroma), which allowed him to capture light with colours. Figure 2 (a) to (d) reflected the top view of the 3D colourspace diagrams of the two paintings. Monet's painting had more intensified colours as compared to Da Vinci's painting. The hue range for green and red are a lot wider in Monet's 3d colourspace diagram. Da Vinci did not have access to green pigments but used different values of blues in this painting.

CONCLUSION

In conclusion, the Western painters used colours (three qualities of colours: hue, value, chroma) to depict the form (chiaroscuro during Renaissance) and capture light (colour theories during Impressionism). The Chinese painters on the other hand, created art based on philosophies which are a mix of Taoism, Confucianism and Buddhism. Hence the use of spirt-vitality, emptiness-fullness and brush-ink in Chinese paintings. As explained by Chinese scholar Song Jian Ming, Chinese painting is based on "concept" (意 *yi*) and not "appearance" (象 *xiang*) [6].

This study covers a large spectrum of Western and Chinese paintings in the limited length of a journal article. It is a rough attempt on a broad topic, where more research and discussions can to be done further. For instance, we did not get to look at how various painting surfaces absorb pigments differently. Rice paper, for example, absorbs the pigments more than a canvas used for oil painting. Another observation that was made during this study, but not part of the research question and not addressed is – Buddhist art paintings and wall murals which are painted and dated before Renaissance paintings, has more chromatic colours despite using organic minerals. How did the Chinese painters achieve the chroma?

ACKNOWLEDGEMENTS

The research is funded by Ministry of Education (MOE), Singapore, Tier 1 grant: **#024366-00001:Developing 3D Interactive Color Theory Model based on the Munsell Color System.** The research team would like to thank both Nanyang Technological University and MOE Singapore for supporting the whole research activities with funding and all other resources.

REFERENCES

[1]. Cahill, J. F. (1961). The Six Laws and How to Read Them. Ars Orientalis, 4, 372–381. Retrieved from http://www.jstor.org.ezlibproxy1.ntu.edu.sg/stable/4629151

[2]. Cheng, F. (1994). *Empty and full: the language of Chinese painting.* Shambhala.

[3]. Law, S. S.-m., & Blishen, T. (2016). *Reading Chinese painting: beyond forms and colors: a comparative approach to art appreciation*. Shanghai Press.

[4]. Ng, W. L., & Xiao, Y. (2017). Development of 3D Color Space to Improve Learning of Color Theory. Paper presented at the 2nd International Conference on Modern Management, Education Technology, and Social Science (MMETSS 2017).

[5]. Peng, D., 彭德. (2008). *Chinese Five Colours 中华五色*. Fine Arts Publishing House 江苏美术出版社.

[6]. Song, J. M., 宋建明. (2016). A Discussion on the Relationship between "Appearance" and "Concept" in Traditional Chinese Color Theory 试论传统中国色彩之"象"与"意"的关系. In *The Seminar of 2016 Chinese Traditional Color Theory 2016 中国传统色彩理论研讨会论文集* (pp. 1–13). Culture and Art Publishing House 文化艺术出版社.

[7]. Sturgeon D. (n.d.). *Chinese Text Project*. https://ctext.org

[8]. Wang, X. Y., 王兴业. (2024). Comprehensive Interpretation of Yin-Yang, Five Elements, and Colors – Traditional Color Research Should Adopt a "Holistic" Perspective 阴阳五行与色彩通解 – 传统色彩研究应树立"全观"视野. In *The Seminar of 2024 Chinese Traditional Color Theory 2024 中国传统色彩理论研讨会论文集* (pp. 99–107). Culture and Art Publishing House 文化艺术出版社.

[9]. Wang, W. J., 王文娟. (2006). *An Aesthetic Exploration of Colours in Chinese Painting 墨韵色章— 中国画色彩的美学探渊*. Central Compilation & Translation Press 中央编译出版社.

Effects of Colour Vision Deficiency on Educational Experiences in Elementary Schools: A Systematic Review

Sánchez Izurieta Juan Francisco[a*], Sunaga Shoji[b]

[a]*Graduate School of Design, Kyushu University, Fukuoka, Japan*
[b]*Faculty of Design, Kyushu University, Fukuoka, Japan*
[*]*Corresponding author: Sánchez Izurieta Juan Francisco, sanchez.juan.francisco.426@s.kyushu-u.ac.jp*

ABSTRACT

Background: Colour Vision Deficiency (CVD) affects a significant portion of the population globally, with studies reporting prevalence rates ranging from 2.2–8% of males in school-aged populations [1–4]. This condition limits the interpretation of colour-coded information, impacting academic performance, engagement, and self-esteem, despite student coping strategies [5]. Interventions within elementary education remain inconsistent, vague, and heavily reliant on teachers' awareness and students' self-accommodation. This systematic review synthesises global evidence on CVD to evaluate existing strategies and policies. **Objectives:** To review the educational impact of CVD and assess interventions, frameworks, and strategies in elementary schools. **Methods:** Guided by PRISMA guidelines [6], a systematic review was conducted across seven databases and grey literature. Following PICO-based screening, 13 studies were included for thematic synthesis on prevalence, interventions, and inclusive practices. **Results:** Analysis identified four key themes: 1) the significant psycho-educational impact of unaddressed CVD; 2) teacher knowledge gaps as a primary barrier to support; 3) the availability of effective yet inconsistently applied adaptations; and 4) a prevailing lack of policy frameworks hindering consistent implementation. **Conclusions:** While evidence supports the efficacy of specific strategies, significant gaps persist in standardising inclusive practices. Concerted action is needed to develop universal design frameworks, mandate teacher training, and establish robust policy support. Future research must prioritise institutionally led, long-term, and universally applicable interventions.

Keywords: Colour vision · Colour blindness · Inclusive education · Educational experiences · Systematic review

INTRODUCTION

Colour Vision Deficiency (CVD) is an often-overlooked sensory difference with profound implications for learning in elementary education, where colour is a fundamental tool for instruction, organisation, and assessment. Globally, CVD affects approximately 1 in 12 boys (8%) and 1 in 200 girls (0.5%) [2,3]. This high prevalence means that in any given classroom, it is highly likely that at least one student will experience the nowadays highly colour-coded, screen-dependent curriculum differently, which can lead to disadvantage, frustration, and diminished educational outcomes [1,3,7,8]. This is especially true when their condition is not considered a special need and they are faced with textbooks and educational materials that are not designed or adapted to meet their needs.

The impact of unaddressed CVD extends beyond the classroom, affecting safety, career prospects, and is recognised under equality legislation [9]. Despite this, a critical policy and practice gap exists. In many countries, routine colour vision screening has been removed from national child health programmes (e.g., the UK's Healthy

Child Programme in 2009), creating systemic confusion and an assumption that identification occurs elsewhere, which it often does not. This has resulted in an estimated 80% of affected students arriving at secondary school undiagnosed, underscoring a significant failure in the educational and health systems to support this population [3]. These students have completed primary education, forced to adapt to the curriculum and face the complications presented by their condition without adequate support.

This review addresses this critical gap by moving beyond the established literature on CVD prevalence and diagnosis to synthesise the global evidence on practical educational interventions and systemic frameworks for inclusion. The primary objectives are to: (i) assess the psycho-educational impact of CVD on elementary school students, (ii) identify and evaluate effective interventions and strategies, and (iii) propose key components for a standardised framework to promote inclusivity and improve outcomes.

METHODOLOGY

This systematic review followed PRISMA guidelines with an a priori PICO-based protocol.

Employing the PICO framework, eligibility criteria focused on elementary students (ages 5–11) with colour vision deficiency (CVD), their educators, librarians, designers and other professionals of the learning ecosystem. Interventions of interest included any inclusivity strategy, such as teacher training, awareness campaigns, or universal design tools like the ColorAdd system, contrasted with existing fragmented approaches. Primary outcomes were student engagement, academic performance, and self-esteem; secondary outcomes were improvements in educator knowledge, awareness, and practice [3,9]. Studies were excluded if focused solely on medical diagnosis, involved non-elementary populations, or were unavailable in the six specified languages.

A systematic search of seven databases and grey literature used Boolean and semantic terms for CVD, elementary education, and inclusivity. The search string combined variants of these concepts and was limited to publications from January 2001 to May 2024 in the six languages. Database filters were applied to target the relevant population and academic fields (e.g., education, psychology) while excluding clinical fields like medicine, yielding 1,824 initial references.

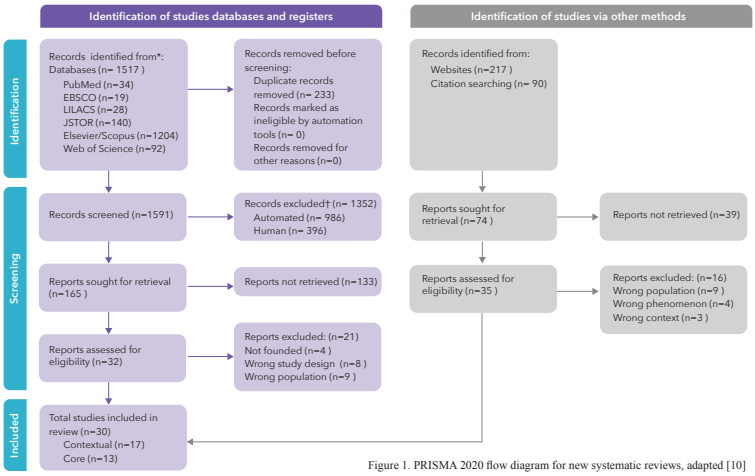

Figure 1. PRISMA 2020 flow diagram for new systematic reviews, adapted [10]

Figure 1: PRISMA Flow Diagram.

The study selection process followed the PRISMA flow diagram (Figure 1). After removing 233 duplicates, 1,591 unique records were screened by title/abstract, excluding 1,352. Full-text review of 239 records led to the exclusion of 172 for not contributing to analytical themes. Of 67 studies assessed in-depth, 37 were excluded, leaving 137 for data extraction. A qualitative synthesis was performed on 13 studies addressing interventions; an

additional 17 served as contextual references for prevalence and impact [3,9]. Of the 13 included studies, data were extracted via a pilot-tested form. Thematic synthesis was conducted through line-by-line coding, developing descriptive themes, and generating analytical themes.

Table 1: Characteristics of Studies Included in the Systematic Review

Ref.	Study Design	Key Focus
[1]	Cross-sectional	Impact of CVD on daily & academic tasks
[4]	Position Paper	Advocacy for policy change to mandate support
[5]	Practical Guide	Practical strategies for teachers and policy advocacy
[7]	Survey	Knowledge gaps and beliefs of school librarians
[11]	Descriptive study.	Game-based strategies for inclusive color education
[12]	Mixed-Methods	Impact of UDL training on library practices
[13]	Theoretical Proposal	Proposal for integrating ColorAdd system into curriculum
[14]	Action Research	Use of simulation glasses for teacher training
[15]	Design Proposal	Design of a symbolic framework for art education
[16]	Narrative Review	Review of challenges and inclusive practices
[17]	Cross-sectional	Impact of CVD on learning areas and teacher perception
[18]	Survey	Knowledge and practices of art teachers regarding CVD
[19]	Content Analysis	Textbook accessibility analysis

The table summarises the included studies, design type and focus. Primary studies provide empirical evidence based on psychoeducational, pedagogical, and behavioural impacts, while contextual studies offer legal, theoretical, and policy perspectives. These references are illustrative, not exhaustive, situating findings within broader frameworks.

RESULTS

Findings are synthesised across four analytical themes (T1-T4), detailing the evidence strength and impact of each study.

Theme 1: The Profound Psycho-educational Impact of Unaddressed CVD

CVD is a significant physical non-visible disability, a "hidden disability" [3], creating a measurable handicap for over 95% of individuals in daily and professional tasks [1,9]. Children report considerable difficulty with colour-dependent tasks in computers (63.2%), arts (60-72.7%), and selecting clothing (61.5%), among others [1], leading to frustration, anxiety, and a negative academic self-concept [16]. This can result in long-term psychosocial harm and misclassification [4]. Paradoxically, one study found no significant differences in early academic performance, hypothesising that children develop compensatory strategies [17]. A qualitative study confirmed difficulties but noted resilience and self-help strategies mitigated severe impacts on final grades [5]. The impact is primarily psychosocial, but it can be mitigated by implementing compensatory strategies and creating supportive environments.

Theme 2: Awareness and Knowledge Gaps as the Primary Barrier

A profound lack of CVD awareness among educators and other professionals of the learning ecosystem is the fundamental barrier [3]. The removal of routine screening erroneously assumes teachers will naturally identify and accommodate CVD students, leaving students undiagnosed [3,7]. Surveys reveal significant knowledge gaps; only 32.5% of art teachers had university-level learning on CVD [18], and 62.4% reported no school initiatives for it [14]. This ignorance forces students to self-advocate, with teachers often becoming impatient until the condition is explained [18]. Training alone may be insufficient without institutional support to overcome resistance [20]. The barrier to accommodating CVD is not a simple unwillingness to help but a deep-rooted, systemic lack of awareness at both the policy and practitioner levels, creating an environment where students are forced to compensate for the system's failure.

Theme 3: Effective Adaptations in Pedagogy and Materials

Effective adaptations in pedagogy and materials, grounded in Universal Design for Learning (UDL), encompass material, pedagogical, and systemic strategies. Material and design-based strategies include using high-contrast colour pairs, avoiding problematic combinations like red/green, and augmenting information with patterns, textures, or labels [8], an approach so effective that colourimetric analysis of textbooks has prompted commitments from publishers to redesign their materials [19]. Pedagogical and attitudinal adaptations involve implementing practical rules like the "6x6 rule," verifying accessibility by checking materials in greyscale [12], and fostering a supportive environment that avoids criticising a student's "wrong" colour use [8,15]. Furthermore, systemic training through experiential methods like simulation glasses has been reported to be highly effective [13], with UDL-based programs having significantly increased knowledge and awareness among professionals such as librarians [12]. These recommendations, which are often aligned between expert guidelines and lived experience, ultimately benefit all learners [5].

Theme 4: The Policy Vacuum and the Imperative for Systemic Change

A disconnection exists due to the removal of routine colour vision screening, rendering students invisible [3,4]. This creates inequitable, teacher-dependent support [4,20]. National curricula often lack any mention of CVD accommodations [18]. This vacuum forces students into burdensome self-advocacy [5]. Formal recognition of CVD as a Special Educational Need (SEN) is proposed to mandate consistent support and resources [4,9].

DISCUSSION

The educational experience for students with CVD is defined by inconsistency, stemming from educator awareness gaps and a policy vacuum caused by the deprioritisation of CVD (e.g., removal of routine screening) [3,4]. A key paradox exists between the significant psycho-educational challenges these students face [16] and a common lack of measurable academic deficits in early childhood [17], which is explained by unconscious compensatory strategies that mask difficulties, negative impacts, such as increased cognitive load, frustration, anxiety, and negative self-concept, that are not captured by standardized tests, and the escalating academic consequences that emerge in later grades with increasingly complex, colour-coded curricula [19]. Consequently, a successful framework must leverage these existing adaptive strategies by formalising tools (e.g., ColorAdd) and peer support into structured inclusive practice [5].

A proposed standardised framework: Training must move beyond theoretical knowledge to include experiential components (e.g., simulation tools, VR) integrated into both initial teacher education and continuous professional development to overcome misconceptions and provide subject-specific guidance [12,15,18]. This is complemented by the system-wide adoption of Universal Design for Learning (UDL), applying principles of redundant signalling [4,16] and multiple means of representation to create a proactively inclusive environment [8,12,19]. Furthermore, policy reform and formal recognition are essential to mandate the acknowledgement of CVD, thereby triggering necessary screening, resource allocation, and concrete action to bridge the gap between voluntary initiatives and universal standards [3,4,20], including the revision of national curricula to include

accommodations. Finally, the framework calls for the development of practical, subject-specific guidelines that translate these principles into actionable checklists for lessons and digital content [8], as well as specialised frameworks for subjects like art education [18].

Limitations: The review is limited by the available literature, including small-scale, qualitative, or theoretical studies and grey literature [11,13], lacking long-term empirical evaluation, and a geographic distribution that may affect generalizability.

CONCLUSION

This review establishes that colour vision deficiency (CVD) significantly impacts elementary students' psycho-emotional well-being and academic engagement. Although compensatory strategies can mask early academic deficits, substantial barriers, including frustration, anxiety, and educator misperception, persist and increase due to the technological shift that includes colour and screens as a base media to deliver information to the learners. While effective adaptations do exist, their implementation is hindered by a systemic failure to prioritise CVD, a problem rooted in defunct screening policies and gaps in teacher knowledge. Consequently, a shift from awareness to action is required. Future research must empirically evaluate interventions such as symbolic coding systems and pedagogical games, develop subject-specific strategies for expressive subjects like art, science, math and physical education, where colour has a particular role and perception that is different in each subject. As well as conduct longitudinal studies on long-term outcomes and the efficacy of compensatory strategies, and analyse policy barriers to formal CVD recognition and the reintegration of screening. Ultimately, an equitable learning environment depends on a standardised framework built on mandated teacher training, universal design, and supportive policy to transform colour from a persistent barrier into an effective tool for learning

REFERENCES

[1] Mashige, K. P. (2019). Impact of congenital color vision defect on color-related tasks among schoolchildren in Durban, South Africa. *Clinical Optometry*, *11*, 97–102. https://doi.org/10.2147/OPTO.S204332

[2] Harrington, S., Davison, P. A., & O'Dwyer, V. (2021). Prevalence of colour vision deficiency in the Republic of Ireland schoolchildren and associated socio-demographic factors. *Clinical and Experimental Optometry*, *104*(1), 48–55. https://doi.org/10.1111/cxo.13072

[3] Albany-Ward, K., & Sobande, M. (2015). What do you really know about colour blindness? *British Journal of School Nursing*, *10*(4), 123–125.

[4] Kvitle, A. K. (2018). Should colour vision deficiency be a recognized special education need (SEN)? *Studies in Health Technology and Informatics*, *256*, 832–838. https://doi.org/10.3233/978-1-61499-923-2-832

[5] Louw, A. (2022). *Strategies for teachers in support of learners with colour vision deficiency* (Order No. 30699927) [Doctoral dissertation, North-West University]. ProQuest Dissertations & Theses Global.

[6] Page, M. J., McKenzie, J. E., Bossuyt, P. M., Boutron, I., Hoffmann, T. C., Mulrow, C. D., & Moher, D. (2021). The PRISMA 2020 statement: An updated guideline for reporting systematic reviews. *BMJ*, *372*, n71. https://doi.org/10.1136/bmj.n71

[7] Collins, K. B. (2015). What do elementary school librarians know and believe about students with color vision deficiencies? *Education & Human Services Faculty Publications*, *1*. https://digitalcommons.longwood.edu/cehs_facpubs/1

[8] Prieto, L. R., Siegel, Z. D., & Kaiser, D. J. (2020). One fish, two fish; red fish (or green fish?): Assisting students with color vision deficiency. *Teaching of Psychology*, *48*(1), 90–94. https://doi.org/10.1177/0098628320959946

[9] Cole, B. L. (2004). The handicap of abnormal colour vision. *Clinical and Experimental Optometry*, *87*(4-5), 258–275. https://doi.org/10.1111/j.1444-0938.2004.tb05056.x

[10] PRISMA. (2021). PRISMA 2020 flow diagram for new systematic reviews, which included searches of databases, registers and other sources. http://www.prisma-statement.org/

[11] Carvalho de Oliveira, J., Westphal, A. B., & Pinheiro, K. y Sa, K. (2021). Daltonismo Infantil: Abordagem de uma prática pedagógica com jogos [Childhood color blindness: Approach to a pedagogical practice with games]. *Anais do EVINCI – UniBrasil*, *7*(1), 478. https://portaldeperiodicos.unibrasil.com.br/index.php/anaisevinci/article/view/6267

[12] Collins, K. B. (2013). *Addressing the needs of students with color vision deficiencies in the elementary school library* (Order No. 3574569) [Doctoral dissertation, Longwood University]. ProQuest Dissertations & Theses Global.

[13] Cunha, A. K., & Santos Cruz, J. A. (2016). Inclusão Pedagógico Cultural: daltonismo e o ensino de cores na educação infantil [Cultural pedagogical inclusion: Color blindness and color teaching in early childhood education]. *Revista on line de Política e Gestão Educacional*, *20*(3), 729–738. http://dx.doi.org/10.22633/rpge.v20.n3.728-737

[14] Henriques, K. M. T. C., & Abões Vercelli, L. de C. (2019). A Interdisciplinaridade na Gestão da Saúde e Educação: A Sensibilização dos Professores da Primeira Infância para o Daltonismo [Interdisciplinarity in health and education management: Raising awareness of early childhood teachers about color blindness]. *Revista De Gestão Em Sistemas De Saúde*, *8*(1), 36–53. https://doi.org/10.5585/rgss.v8i1.13677

[15] Hui, Z. (2021). Color identification: Guiding children with color vision deficiency to learn art. In *Proceedings of the 6th International Conference on Education, Language, Art and Inter-cultural Communication (ICELAIC 2021)* (pp. 543-547). Atlantis Press. https://doi.org/10.2991/assehr.k.210813.111

[16] Klooster, S. (2016). *The inclusion of individuals with colour vision deficiencies* [Master's dissertation, Nipissing University]. Scholaris. https://utoronto.scholaris.ca/server/api/core/bitstreams/209f3b59-94eb-47b0-9d6c-26df861bd6dc/content

[17] Montanero, M., González, M., Pardo, P., Palomino, M., Gil, J., Rodríguez, á., & López, M. (2003). *Daltonismo y rendimiento escolar en la educación infantil* [Color blindness and school performance in early childhood education]. https://www.researchgate.net/publication/39208094_Daltonismo_y_rendimiento_escolar_en_la_educacion_infantil

[18] Muraya, T., Chikara, R., & Sunaga, S. (2024). 色覚多様性を基盤とした図画工作・美術の教育環境構築に向けた研究[Study on constructing the color education basis on the color vision diversity]. *Color Science Research*, *2*(2), 55–68. https://doi.org/10.15048/csr.00011

[19] Torrents, A., Bofill, F., & Cardona, G. (2011). Suitability of school textbooks for 5 to 7 year old children with colour vision deficiencies. *Learning and Individual Differences*, *21*(5), 607–612. https://doi.org/10.1016/j.lindif.2011.07.004

[20] Pinner, M. H. (2021). *The effect of training upon faculty stages of concern about making color vision deficiency adaptations* (Publication No. 2877) [Doctoral dissertation, Liberty University]. Liberty University Digital Commons. https://digitalcommons.liberty.edu/doctoral/2877

Colour Selection Frameworks for Global Colour Education

Wenxian Qian[a*], Chaoran Wang[b]

[a]Lancaster University, Lancaster, United Kingdom
[b]Lancaster University, Lancaster, United Kingdom
[*]Corresponding author: Wenxian Qian, w.qian2@lancaster.ac.uk

ABSTRACT

This paper reports on the common challenges that design students face in colour selection and the design support offered within higher education. The objective is to help students to transform the conceptual meanings of personal preferences, emotions, culture, and style into a colour palette that can be applied to packaging design tasks, through a Colour Selection Framework. Data on colour preference, colour use and colour teaching were collected from mainland China and the United Kingdom. 90 design students participated in a three-stage workshop: 1) Exploring personal colour preferences. 2) Using digital tools to extract colours from existing designs to generate new colour palettes. 3) Applying generated colour palettes to poster design tasks. Additionally, through semi-structured interviews with colour educators from China and the UK, the study further identified key challenges in colour education, particularly the disconnect between theoretical knowledge and practical application. This study provides a novel and practice-oriented framework tool for developing colour education, bridging the gap between personal preferences and colour application. The findings will inform the building of a Colour Selection Framework which has potential as a student-centered design support tool. Future research will expand cross-cultural comparisons and continue to refine the framework for broader educational applications.

Keywords: Colour teaching and learning1, colour selection2, framework3, preference4, palette5

INTRODUCTION

Colour is a complex and interdisciplinary field of knowledge and an important form of communication between humans and their surroundings. As Goethe [1] observed, colour is the result of the interaction between the eye, light, shadows, media and the subjective experience of the observer and can evoke emotional responses and inner imagination. Due to its ability to convey information and symbolic meaning, colour is widely used in various fields . In the field of design, colour is considered a key yet complex element. Especially in visual communication design, colour has gradually shifted from a secondary or decorative supporting role to a strategically significant element [2]. Research indicates that colour plays a significant role in guiding visual attention [3], enhancing the readability and legibility of information [4], and conveying emotional and symbolic associations [5].

Colour selection is the process of choosing colours for a specific design task and constructing a colour palette, which often influences the outcome of the design. Despite the abundance of colour theory and design process research, designers' colour selection behaviour in practice exhibits non-standardised trends, with few designers adhering to standard procedures or rules [6]. Conversely, the methods used by designers during the design process and the creation of colour palettes are more dependent on personal preferences [7], intuition [8] and cultural context [9]. Although colour research has been conducted for centuries, most of it has focused on the normative aspects of colour design, such as colour systems and models (e.g., Munsell, CIE Lab, RGB, CMYK), harmony rules [10], perceptual and psychophysical studies of hue, lightness, and saturation, and standardisation

and has not adequately addressed the application of colour theory knowledge in creative design practice [11]. This gap between theory and practice is particularly evident among novice designers and design students.

The disconnect between theory and practice highlights the structural issues within the current colour education system. Mottram [12] pointed out that art and design programmes in British higher education rarely systematically address colour. Despite being a fundamental element of visual disciplines, colour use is not listed as a core skill in the teaching standards documents for British art and design higher education [13], which instead emphasise skills such as drawing. Current colour education lacks effective support for students in making colour decisions, often relying on intuition and unconscious judgments in design tasks [14].These issues are prevalent worldwide, as reflected in Calvo Ivanovic's [11] systematic review of 103 higher education colour courses in design programmes across Latin America, North America, Europe, and Oceania. She noted three major challenges in global colour education: fragmented curriculum content, outdated course materials, and the absence of teaching methods and strategies to support colour selection. This lack of structured guidance limits students' ability to translate colour knowledge into practical design skills.

Research on colour education in Asia, especially in China, is still relatively scarce. Although China's design education system is increasingly sophisticated, colour teaching has not yet received attention. In the proceedings of international design conferences such as DRS and IASDR, studies specifically addressing colour education in China are scarcely encountered. Publicly available information on institutional curricula further corroborates this marginalisation. For example, the Tsinghua University undergraduate curriculum only includes two 3-credit courses, ‘Colour’ and ‘Colour Sketching,’ in the first-year foundational module, with no further expansion of colour education in subsequent years [15]. The course description of the China Academy of Art also does not explicitly list independent colour courses [16]. This situation is not unique; Studies on Chinese design education reform have highlighted that the curriculum structure remains fragmented [17]. To further understand the practical manifestations of colour education in a cross-cultural context and its impact on students' learning pathways, the challenges, strategies, and teaching support needs for the colour selection process have been investigated in a study of design students from the UK and China.

METHODOLOGY

This research aims to explore the challenges students encounter during the colour selection process and to provide a platform for proposing a Colour Selection Framework as a pedagogical support tool. A phased mixed-methods strategy, combining student workshops with tutor interviews, gathered multi-perspective data and had three main phases: 1) student colour workshops; 2) visual analysis and data extraction; and 3) semi-structured tutor interviews. The ultimate goal is to propose a cross-culturally adaptable, student-centred colour selection support framework for future teaching practices and curriculum development in colour education.

The colour preferences and the colour palettes used in a specific poster design task by students from both countries forms the phase 1 and 2 data. Poster design assignments prompt students to make colour selection decisions within authentic visual contexts, enabling comparison of discrepancies between students' colour preferences and their practical application while controlling variables. As a common teaching task in design education, posters possess strong pedagogical representativeness and facilitate cross-cultural comparisons. Phase 3 primarily employed qualitative methods to explore perception of colour selection behaviours and pedagogical support within design education. The research questions considered are: What teaching challenges do colour tutors face in helping design students apply colour theory to practical tasks? And: Do design students' colour preferences influence their choices when developing colour palettes for graphic design tasks?

Semi-structured interviews were conducted with design tutors to explore their teaching methods, observations, and experiences in daily colour teaching practices. Six tutors from China, the UK, and Italy were interviewed, representing different design fields, teaching experiences, age groups, and cultural backgrounds. The aim was to reveal commonalities and differences in colour teaching practices within current design education. As

Leedy and Ormrod [18] pointed out, qualitative research is particularly suitable when the research objective is to explore the nature of processes, systems, or human behaviour in the real world. This method enables researchers to gain in-depth insights, identify the challenges faced by practitioners, and help identify challenges in educational practice, as well as reveal conceptual patterns that quantitative methods may not be able to capture. Although the sample size is small, the interviews and workshops were viewed as an exploratory method. By combining interview data with visual materials from the workshop phase, data triangulation enhances the reliability and interpretability of the research findings.

RESULTS AND DISCUSSION

The outcomes of the workshop elements of the research design suggest that there are some patterns in the sorts of palettes of colours preferred by students. Analysis revealed several phenomena: A discrepancy existed between preferred colour schemes and actual usage. Although 72% of students preferred highly saturated colours (e.g. red and orange), 61% opted for predominantly lighter, soft-toned schemes in their specific designs. Black appeared in 33% of palettes in both stages. This phenomenon may reflect uncertainty or a ‘preference for safety’ in colour application during real design scenarios. Despite preferring vivid hues, students tended towards secure, neutral colour combinations in execution, particularly when balancing brand expression or compositional considerations (see Figure1). The colour palettes used for the design task had narrower colour ranges than in the preference palettes.

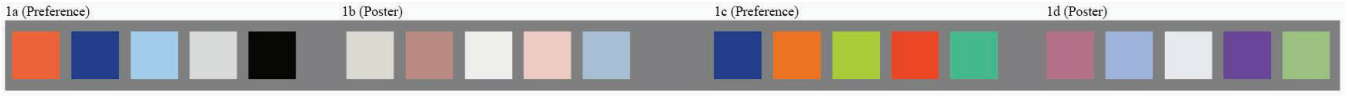

Figure1: Examples of participant preferred palettes (1a, 1c) and poster palettes (1b, 1d)

The poster outputs from Chinese and British students revealed distinct differences in visual language: British posters had more brand-oriented visual styles with restrained colour palettes; Chinese students favoured more figurative or emotive compositions, with decorative colour schemes (see Figure2).

Figure2: Examples of poster designs by UK and Chinese workshop participants

These observations resonate with challenges faced by students as identified in the interviews conducted with design tutors, who commented on insufficient confidence in colour application, colour intuition dominating decisions, and delayed engagement of colour-related cognition. The contrast between preferences and actual usage highlights a critical issue in colour education: the lack of confidence or strategic awareness when integrating vivid or unconventional colours into design contexts.

The interviews with tutors teaching colour in design education revealed shared concerns about the recurring challenges students face when learning and applying colour. Although the tutors adopted different teaching approaches, with some emphasising exploratory and research-led methods and others preferring structured and theoretical styles, most of them focused on the difficulties students encounter in colour Learning rather than on specific teaching strategies. An analysis of these interviews provides insight into the nature of these challenges and how tutors can better support students in applied design contexts.

Students' colour learning challenges are seen as a lack of confidence in colour decision-making, an over-reliance on intuition and habitual preferences, a lack of vocabulary and conceptual clarity, and weak integration of colour in design thinking. The lack of confidence in colour decision-making was identified by all six tutors. Tutor 3 stated bluntly: 'Some students hesitate for ages when faced with colour choices, persistently believing their selections are wrong, even when they are perfectly adequate.' Notably, Tutors 1 and 4 emphasised the absence of structured training, while Tutors 3 and 5 focused more on students' emotional volatility and self-doubt when facing criticism. 'Lack of confidence' in colour decision-making is not a singular psychological phenomenon, but rather arises from the interplay of multiple factors: teaching structures, lack of experience, and insufficient cultural understanding. Teachers may address this issue through structured, constructive feedback and guided reflection, encouraging students to view colour selection as a skill that can be practised and refined, rather than a final, fixed judgement.

A second set of significant factors commonly observed by the design tutors was students' excessive reliance on intuitive judgements or long-established habitual preferences when making colour decisions, without conducting thorough analysis. Tutor 2 observed that many students 'always select colours they personally favour,' seldom considering whether these choices genuinely align with project objectives or usage contexts. Tutor 4 shared a similar perspective: 'They often don't know how to step outside their comfort zone.' When questioned about their choices, the tutor reported many students simply replied, 'I just like it'. While such emotionally driven responses are genuine, they also reveal deficiencies in students' colour vocabulary and theoretical grounding. They are thought to fail to translate intuition into professionally justifiable judgements.

Students frequently mistake 'feeling right' for the basis of selecting appropriate colours, a pattern Tutor 1 found to be both common and concerning. Without supporting tools and linguistic frameworks such as colour associations, cultural coding, or semantic structures, students' intuition and personal experience cannot be translated into professional judgement and decision-making. Tutor 5 added that this issue is particularly pronounced among beginners, who rely on 'habit' to determine colour schemes without thorough analysis and struggle to articulate the rationale behind their choices. Overall, this tendency reveals a pronounced disconnect in colour education: students remain constrained not only by personal preferences but also by the absence of systematic instructional guidance, hindering the development of genuine colour literacy. Without effective intervention, intuition may become an obstacle rather than a bridge to professional expression.

To address this, several tutors employ research-guided approaches, structured questioning, and colour scheme reflection exercises to push students beyond their comfort zones. Tutors unanimously emphasise the need for pedagogical strategies that guide students from 'unconsidered preferences' towards 'informed choices', embedding colour decisions within a conscious, evidence-based design framework. Three colour tutors emphasised that design students commonly lack systematic colour vocabulary and clear conceptual understanding, with this deficiency being particularly evident in colour judgement, attribute comprehension, and theoretical application. Tutor 5 highlighted students' pronounced weaknesses in colour naming and attribute recognition, especially their poor ability to identify and name neutral colours, grey tones, and low-saturation hues. When saturation or brightness varies, students cannot accurately state colour names nor discern suitable contexts for their use. Furthermore, many lack training in observing and identifying colour attributes such as hue, value, and chroma. This results in a disconnect between colour judgement and functional design decisions. Tutor 3 observes that some students, despite studying foundational colour theory, still 'struggle to distinguish colour differences' in practice. Other students, despite possessing theoretical knowledge, struggle to apply it within design tasks. This deficiency in vocabulary and conceptual understanding creates a gap between terminology memorisation, perceptual ability, and practical application. This disconnect limits their deep understanding of colour and professional expression, impacting both the accuracy and creativity of their design judgements.

In common with the UK students, Chinese students are seen to struggle to articulate colour preferences, frequently resorting to vague terms like brighter, normal, or attractive, exposing weaknesses in mastering colour vocabulary and attributes. Concurrently, they face difficulties translating terminology into practical contexts; even

when able to name colours, students ‘find it hard to explain why these colours should be used in design’ (tutor 2). It appears that, despite differing cultural and educational systems, students universally experience a disconnect between structured expression of colour terminology, perceptual ability, and practical application. It suggests a need to re-examine the relationship between language, perception, and application within colour pedagogy.

A critical issue emerging consistently in interviews with all six tutors was that many design students fail to integrate colour as a systematic element into their design thinking process during the early stages of projects. Instead, they defer colour treatment, often treating it as a final “decorative step”. This phenomenon transcends both Chinese and British cultural contexts, with all six tutors highlighting it, reflecting a common disconnect in colour education across curriculum structures and student perceptions. Chinese tutor 2 noted: Many students leave colouring until the very end, which is far too late. She emphasised that this delay weakens colour's role in supporting the subject matter and often leads to stylistic homogeneity or blind imitation. British tutor 4 expressed a similar view: Colour is frequently treated as a superficial matter rather than a tool for stimulating creativity. Tutors 1 and 5 further noted that students frequently finalise colour palettes in initial drafts or neglect exploring colour's expressive potential during research phases. These observations reveal colour's marginalisation within the curriculum, treated more as decorative embellishment than an integral component of conceptual development. Despite the UK tutor's attempt to introduce the “Double Diamond Model” to encourage colour consideration during exploration, its impact proved limited. The potential of colour as a design language remains largely untapped, with its “decorative” status limiting expressive breadth and design depth.

To address these challenges, tutors employed teaching strategies including exploratory learning, continuous feedback, visual tools, and cultural and contextual awareness. Influenced by pedagogical philosophies and curricular contexts, these strategies aim to translate teaching objectives into effective classroom practice [19] while enhancing learning outcomes and design capabilities by supporting students' conscious use of colour [20].

CONCLUSION

This paper has focused on analysing the challenges students face in colour learning. Teaching strategies and other topics arising in the interviews with design tutors, such as colour association and cultural background and future directions in colour education, will be explored in subsequent publications. The interview findings are corroborated by data from the student workshop phase, highlighting issues such as insufficient confidence in colour decisions, colour-matching behaviour prioritising intuition over rationale, and failure to integrate colour thinking early on repeatedly manifested in task performance. This cross-validation process utilising multiple data sources from interviews and workshops will be elaborated upon in subsequent papers. Future research will explore how pedagogical strategies and visual tools can facilitate students' transition from preference to expression in real design contexts, thereby enhancing their colour judgement and strategic development capabilities. Together, the interviews and the colour workshops undertaken in this study paint a picture of achievement despite challenges, suggesting that there is potential to further enhance design outcomes if a framework for supporting colour design decisions were in place.

ACKNOWLEDGEMENTS

With thanks to Professor Judith Mottram and Dr Chaoran Wang for their generous support and thoughtful guidance throughout this research journey. Thanks are due to the design tutors and students from Suzhou University of Science and Technology and Lancaster University for their participation in this study.

REFERENCES

[1] Von Goethe, J. W. (1840). *Theory of colours* (No. 3). MIT Press

[2] Calvo Ivanovic, I. (2021). Colour design training itinerary. A framework for the teaching and learning of colour in the design discipline.

[3] Ware, C. (2019). *Information visualization: perception for design*. Morgan Kaufmann.

[4] Hegemann, L., & Oulasvirta, A. (2024, May). Palette, purpose, prototype: The three ps of color design and how designers navigate them. *In Proceedings of the 2024 CHI Conference on Human Factors in Computing Systems* (pp. 1-19).

[5] Jonauskaite, D., Abu-Akel, A., Dael, N., Oberfeld, D., Abdel-Khalek, A. M., Al-Rasheed, A. S., ... & Mohr, C. (2020). Universal patterns in color-emotion associations are further shaped by linguistic and geographic proximity. *Psychological Science*, 31(10), 1245-1260.

[6] Lunenfeld, P. (2003). *Design research: Methods and perspectives*. MIT press.

[7] Potočnik, J., Košir, M., & Dovjak, M. (2022). Colour preference in relation to personal determinants and implications for indoor circadian luminous environment. *Indoor and Built Environment*, 31(1), 121-138.

[8] Bengtsson, A., & Grahn, P. (2014). Outdoor environments in healthcare settings: A quality evaluation tool for use in designing healthcare gardens. *Urban forestry & urban greening*, 13(4), 878-891.

[9] Mottram, J. (2017). Colour in culture: Shifting values, understanding and functions. *In Colour Design* (pp. 477-490). Woodhead Publishing.

[10] Forni, O., Manzini, F., Pedersini, F., Rossi, M., & Zavagno, D. (2025). Colour harmony revisited: A data-driven approach to hue preference and combinability. *arXiv*. https://arxiv.org/abs/2508.15777

[11] Calvo Ivanovic, I. (2024). Analyzing color training in design education: A review from 2010 to 2022. *Color Research & Application*, 49(5), 498-514.

[12] Mottram, J. (2018). Identifying colour use and knowledge in textile design practice. *In Progress in Colour Studies* (pp. 371-389). John Benjamins Publishing Company

[13] Quality Assurance Agency (QAA). 2018. The UK Quality Code for Higher Education Subject Benchmark Statements, Subject Benchmark Statement: Art and Design. https://www.qaa.ac.uk/the-quality-code/2018

[14] Ural, S. E., Akbay, S., & Altay, B. (2017). Progression of color decision making in introductory design education. *Color Research & Application*, 42(6), 849-860.

[15] Tsinghua University. (n.d.). *Undergraduate curriculum plan: Academy of Arts & Design* [PDF]. Retrieved August 26, 2025, from https://www.tsinghua.edu.cn/jxjywj/bksjywj/62-77meiyuan.pdf

[16] China Academy of Art. (n.d.). *Course construction overview*. Retrieved August 26, 2025, from https://www.caa.edu.cn/jx/kcjs/index.html

[17] Wang, J. (2020). The reform situation of Chinese design education in the 21st century. *Design and Technology Education: An International Journal*, 25(2), 151–164.

[18] Leedy, P. D., & Ormrod, J. E. (2015). *Practical research*. Pearson Education UK.

[19] Borich, G. D. (2016). Observation skills for effective teaching: Research-based practice. Routledge.

[20] Muijs, D., Kyriakides, L., Van der Werf, G., Creemers, B., Timperley, H., & Earl, L. (2014). State of the art–teacher effectiveness and professional learning. School effectiveness and school improvement, 25(2), 231-256.

Mapping of Colors of Master Images with Munsell Color Space – A Mathematical Tool to Assist Color Design

Woon Lam Ng[a]*, Zhongjian Wang[b]

[a]*Nanyang Technological University, Singapore*
[b]*Nanyang Technological University, Singapore*
[*]*Corresponding author:Ng Woon Lam, ngwoonlam@ntu.edu.sg*

ABSTRACT

This research seeks to develop a comprehensive three-dimensional color theory model that enhances analytical capacity of color selection, supporting artists, designers, and students in making informed decisions to meet color design and selection needs. Currently, the two-dimensional color wheel remains the dominant teaching tool in tertiary art education and creative industries such as animation and design. Rooted in Newton's closed-ring concept and later refined into the Itten Color Wheel at the Bauhaus, this model was popularized in the United States by Josef Albers and has since become standard in leading art institutions. While the Itten model continues to be widely used in visual arts, including animation, filmmaking, and design, it lacks the quantifiable accuracy required in industries that demand precise color measurement and repeatability. Addressing this need, Professor Albert Munsell introduced the Munsell Color System in the early 20th century. Though initially overlooked by American art institutions due to the entrenched popularity of the Itten model, Munsell's scientifically grounded three-dimensional system was eventually adopted across various industries for its ability to provide standardized, objective color measurement. Such precision is essential in evaluating color relationships, determining visibility between adjacent hues, and establishing visual hierarchy and rhythm in design. Acknowledging the disconnect between educational color models and industry standards, this research builds upon a pilot model based on Munsell's framework. It expands the model's analytical capacity to include cross-sectional mapping of an image's color space, identifying intermediate hues and the relationships between distant hues of any mapped image. This deeper analysis offers a more nuanced understanding of an image's color design. In addition, the study will build an image library of color schemes drawn from master paintings in Western, Chinese, Japanese, and Korean art history. This resource aims to serve both pedagogical, industrial and research needs. The resulting tool bridges practical usability with analytical rigor, aligning color education more closely with professional and industrial norms to better support color-related practices across art and design disciplines.

Keywords: Color, Munsell, Design, Composition, Art

INTRODUCTION

The project is an expansion of a previously developed three-dimensional color analysis tool based on the Munsell Color System. The current popular pedagogical model depends heavily on the two-dimensional color wheel derived from the Itten Color System, initially developed during the Bauhausian era in the early 20th century (Itten, 1970) . The Itten's system was developed based on Chevreul's concepts of simultaneous contrast and successive contrast treating neutral gray as the equilibrium state in human vision. Color pairing that could arrive at the medium value neutral gray through an optical spinning experiment (Mahyar et al., 2007) is defined as a complementary pair while this equilibrium state is regarded as harmony(Chevreul, 2001). Color harmony is also further categorized by Koenig into 3 different types, namely (i) simple harmony, (ii) contrast harmony and (iii) balanced harmony while

complementary color pairing here belongs to type (ii) (Westland et al., 2007). However, quantitative experiments have not consistently demonstrated supposedly pleasant visual responses from audience. Therefore, the concept of color harmony derived from the Greek living philosophy remains ambiguous (Burchett, 2005; Ng, 2021)

To address practical needs with quantifiable consistency and repeatability in color application processes, our previous research adopted the perceptually uniform Munsell Color System. This formed the basis for a three-dimensional color analysis model that allows users to study color compositions in images, particularly master paintings from various historical periods, to gain deeper insights into their color design strategies(Ng & Xiao, 2017). A small Western art image library was also established as a reference archive. While the three-dimensional model effectively maps the range of colors and their relative abundances in each analyzed image, users may not immediately grasp the underlying structure of the color scheme. In practice, users are often more interested in understanding how prominent colors relate to each other, for example, which intermediate hues are used to bridge dominant colors, or how less abundant but visually critical colors are employed to create contrast and balance in the overall design. These insights can only be uncovered through a comprehensive exploration of the image's full color space. To simplify this complex task for users, this research further developed analytical tools that use basic mathematical models to generate cross-sectional views and vector relationships within the color space. These tools allow users to visualize how major color schemes are distributed and related throughout the image, making it easier to interpret design strategies. By mapping relationships across the full color space, users can quantitatively compare different groups of colors, gaining insight into nuanced design decisions—such as the strategic use of low-abundance accent colors or the management of visual tension created by high-contrast hues. This is especially valuable when working with complex color families like green, which spans the largest portion of the color space. The cross-sectional mapping reveals distinctions between various greens and their transitional tones—such as brownish or grayish greens—offering a measurable understanding of their visual roles. These visual and analytical tools significantly accelerate the study of color design, eliminating the need for time-consuming trial-and-error experimentation to decipher color schemes. To further enhance the software's practical utility, the reference library is currently being expanded to include master paintings from Chinese, Japanese, and Korean art traditions.

METHODOLOGY

The research process covers two major scopes, namely the expansion of the master image library data which is less technical though more time consuming. Image data were obtained from official museums and institutes online sites with licenses. Data are categorized chronologically and regionally for ease of reference. These categories are Western (including oil and watercolor paintings) and ink paintings from China, Japan and Korea. While the decision was made based on the limitation of research resources, comparing Asian ink art colors and Western paintings across more than 500 years of history should cover a comprehensive view of the differences in color selection and design.

The second part of the project is the technical development of the three-dimensional software tool that requires computation of the abundances of colors used based on pre-defined thresholds for which users may define. The Munsell Color Space conversion from its hue, value and chroma to the digital RGB display were obtained from online source(Centore, 2013). The construction of the three-dimensional model was followed by mathematical models developed to enable capturing of the cross-section of the mapped color space. The cross-section has to be decided based on the assumption that the largest cross-sectional area obtained would likely to estimate the furthest color vectors, in visual art terms, representing the highest color tension across the color space. Below are the brief steps in locating the most representative cross-section of the mapped color space.

(i) A user selects the threshold digital value from the program to convert the original RBG images with lower resolution pixels to match the lower numbers of discrete digital points the Munsell Color Space has. Hence the reduced resolution digital data can be converted to the Munsell color coordinates and plotted back as RGB display. The mapped color space in RGB can be displayed and allows users to rotate and have an overall view of all the mapped colors.

(ii) This dataset is then used for the cross-section analysis of the mapped color space of the image.
(iii) A mathematical approach, the Principal Component Analysis (PCA)(Abdi & Williams, 2010) is used to find the largest vector plane for the cross-sectioning to be carried out.

Principal Component Analysis (PCA) is a statistical technique used for dimensionality reduction while preserving as much variance as possible. It transforms the data into a new coordinate system such that the greatest variance by any projection lies on the first coordinate (the first principal component), the second greatest variance on the second coordinate, and so on. Incorporating density estimation allows us to understand the underlying distribution of the data more effectively, especially in the case of discrete data points. The mathematical process is listed below:

Let $X = \{x_1, x_2, \ldots, x_n\}$ be a set of n discrete observations in R^p. The steps involved in PCA can be summarized as follows. First, the density-weighted mean μ is computed. When considering the density $p(x)$ of the discrete data points, the mean vector can be computed as a density-weighted mean:

$$\mu = \frac{1}{N} \sum_{i=1}^{n} p(x_i) x_i$$

where $N = \sum_{i=1}^{n} p(x_i)$ is the normalization factor, ensuring that the weights sum to 1. The covariance matrix C can be computed using the density of the discrete points:

$$C = \frac{1}{N} \sum_{i=1}^{n} p(x_i)\,(x_i - \mu)(x_i - \mu)^T$$

This formulation accounts for the distribution of the data points, providing a more accurate representation of the variance and covariance among the variables. Next, we perform eigenvalue decomposition of the density-weighted covariance matrix, where λ are the eigenvalues and v are the corresponding eigenvectors. The eigenvectors represent the directions of maximum variance, and the eigenvalues indicate the magnitude of variance in those directions.

$$Cv = \lambda v$$

The equation of the plane can be expressed as: $P = \{(x, y, z) \in R^3 \mid N_0 x + N_1 y + N_2 z = 0,$ N is the eigenvector with the smallest eigenvalue$\}$. After using iteration to search for the closest amount of points, we can get a set of position matrix X. The projection is shown in the equation below, and for the 3D space we take $k=2$ to visualize the points on the plane

$$Z = XV_k$$

(iv) While the largest estimates the possible largest cross-section of the plotted color space and predicted the highest color tensions amount different hues used in the image, there are also other important color design related factors to be considered; the abundances of certain hues are equally important. The dominating hues significantly reflect the overall color character of an image while the image may use a wide range of hues. Therefore, the abundances of each hue range can also be presented to complement the cross-sectional map.

RESULTS AND DISCUSSION

To briefly elaborate the software function and showcase its usefulness, multiple master images from the library collection of this software, with vastly different color designs across various eras were selected for the demonstration. While images from the Renaissance and during Impressionism were selected to indicate the typical color design difference, two images with a similar color scheme, painted during the same period by the same artist, John Singer Sargent, were also selected for comparison. The latter comparison allows users to comprehend more in-depth color design difference between artworks even when the color scheme from a first glance may look similar. This process could again explain the weakness of adopting formulated color pairing approach based on the symmetrical Itten Color System without a basic quantitative idea in selecting various hues in color design.

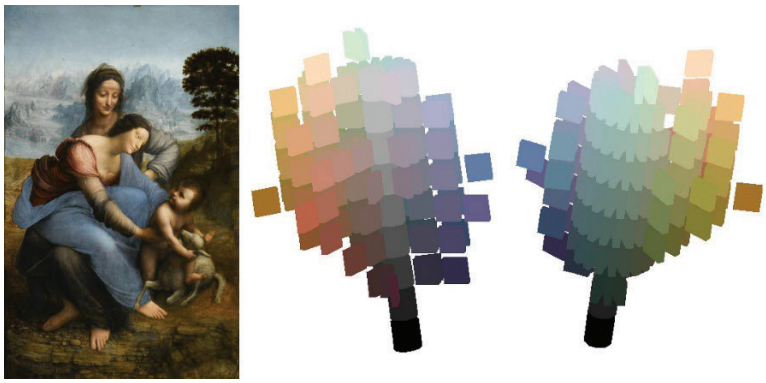

Figure 1: Color analysis of Virgin & Child with St. Anne(Da Vinci, 1503).

Figure 2: Color analysis of Haystacks – Effect of Snow & Sun (Monet, 1891).

Figures 1 and 2 illustrate the core functions of the software by mapping the color usage of two significant periods in art history. By utilizing a perceptually uniform color space, the software effectively highlights the intermediate hues that bridge distant colors in both paintings. In the mapped color space of Virgin and Child with St. Anne, the distribution appears horizontally compressed—reflecting Da Vinci's emphasis on tonal contrast along the vertical axis through a chiaroscuro technique. This effect is further influenced by the limited availability of chromatic pigments during his time (Shapiro, 1994; Shearman, 1962). On the contrary, the plein air painting of haystacks, with easier access to chromatic pigments after industrial revolution, Monet sacrifices some value range and expands differences in hues (Lyon, 1991; Ó Gráda, 2016).

Historically, there have been efforts to mathematically distinguish film color schemes based on genre. However, due to limited data size, the results were constrained. While the models showed some success in identifying color patterns associated with horror and mystery films, they were less effective in predicting the color schemes of light-hearted genres such as comedies and happy movies. (Xue et al., 2013). Horror films are typically shot in low-light settings with minimal variations in hue and chroma, making their color range easier to predict using digital models. In contrast, comedies are often filmed in natural or brightly lit environments where a full spectrum of hues is visible. This introduces a significantly larger number of variables compared to darker scenes, making accurate modeling nearly impossible without access to a large-scale database. Similarly, researchers at Stanford University found that romantic films exhibit a broader range of color dynamics, an observation that aligns with Xue's earlier findings. (Chen et al., 2012). Romantic movies are filmed in a bright environment. Therefore, it has a similar color complexity to comedies and happy movies.

Pursuing quick, formulaic solutions, as mentioned above—is less practical without substantial investment in building a large-scale database. Instead, for the purpose of developing professional expertise in color design, conducting comprehensive color analyses of individual images proves more effective. A detailed study of just a few

master paintings can offer immediate insights into the range of colors used, particularly the intermediate transitions and the proportional distribution of dominant hues. Often, it is the presence of less chromatic transitional colors and the major hues that define the overall mood and atmosphere of an image (Ng, 2020). The intermediate colors further create the required transitions between distant hues and forms the visual rhythm.

Two paintings by master artist John Singer Sargent are used to illustrate the effectiveness of this color analysis approach. Despite their distinct color compositions, both works feature dominant bright hues, offering a strong basis for comparison. These examples highlight how a more comprehensive analysis can reveal key differences in color design—differences that are difficult to capture using conventional modeling techniques due to the multidimensional nature of color. While the three-dimensional color maps in Figures 3(a) and 3(b) show only subtle contrasts, the cross-sectional views in Figures 4(a) and 4(b) clearly show the variations in intermediate transitional colors. Notably, the selection of these transitional hues between distant colors differs significantly across the two paintings when mapped within the Munsell Color Space.

Figure 4(a) reveals a higher presence of purples, greenish purples, and grays as intermediate colors. In the painting shown in Figure 3(a), these hues serve as bridges between the more chromatic reddish-oranges and greens. Since the green and reddish orange occupy distant regions in the Munsell Color Space, a substantial amount of transitional colors, particularly purples and purplish grays, are necessary to create a smooth visual transition, explaining their large proportion in the composition. In contrast, the painting in Figure 3(b) features a dominant use of yellow, yellowish-brown, and orange brown, complemented by selective use of contrasting blues. Figure 4(b) indicates that transitional browns and oranges are primarily used to connect the dominant yellow hues. Additionally, some purples and grays act as intermediaries between the prominent yellows and the limited use of blue. Green appears only minimally and carries a brownish tone to maintain unity with the surrounding browns and yellows. These cross-sectional mappings offer a more nuanced and comprehensive understanding of color design, revealing how transitional hues contribute to the coherence and mood of an image even when the color schemes are completx.

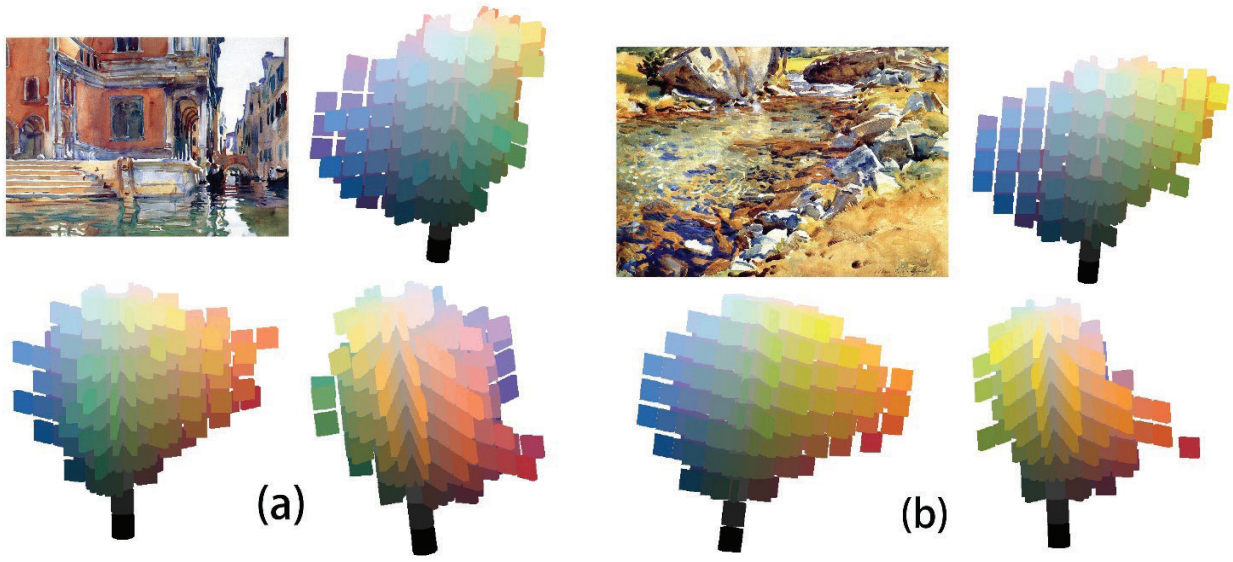

Figure 3(a) & (b): Color analyses of John Singer Sargent's paintings (Sargent, 1903, 1907).

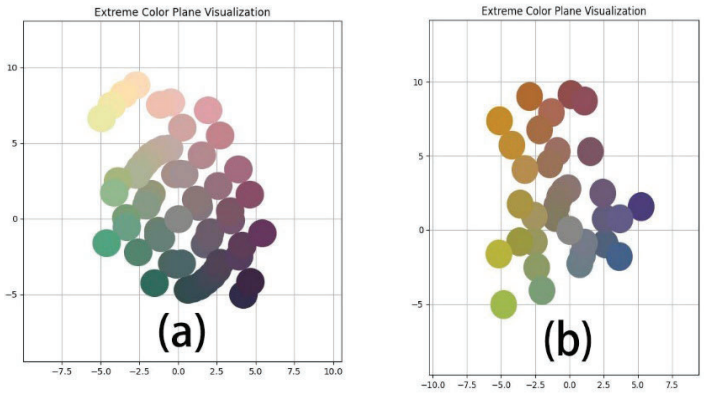

Figure 4(a) & (b): Cross-sectional analyses of Sargent's painting in 3(a) & (b) (Sargent, 1903, 1907)

CONCLUSION

The developed software effectively demonstrates how the use of color across different painting eras can be more deeply understood through uniform color space mapping. The visualizations reveal clear distinctions in the dominant color attributes chosen by Renaissance artists versus Impressionists. Additionally, the software enables detailed analysis of master paintings that employ a wide range of hues, offering valuable insight into the intermediate transitional colors used to bridge distant chromatic tones. With this analytical capability, designers, artists, and students can use the software to study images from its built-in library or analyze external images. During the color design process, the software can identify gaps between widely separated hues, helping users recognize where intermediate colors may be needed to achieve smoother transitions. It also allows for a comprehensive breakdown of the rhythm and dynamics within complex color schemes. Currently, the software displays a representative cross-sectional view of the mapped color space. Future enhancements may include interactive tools that allow users to manually explore cross-sections from various angles, offering even deeper insights into color relationships. In summary, the software provides an efficient and practical method for color analysis, greatly supporting both learning and application in color scheme design.

ACKNOWLEDGEMENTS

The research is funded by Ministry of Education (MOE), Singapore, Tier 1 grant: #024366-00001: Developing 3D Interactive Color Theory Model based on the Munsell Color System. The research team would like to thank both Nanyang Technological University and MOE Singapore for supporting all research activities with funding and all other resources.

REFERENCES

Abdi, H., & Williams, L. J. (2010). Principal component analysis. *Wiley Interdisciplinary Reviews: Computational Statistics*, *2*(4), 433–459. https://doi.org/10.1002/wics.101

Burchett, K. E. (2005). *A Bibliographical History of The Study and Use of Color From Aristotle to Kandinsky*. The Edwin Mellen Press, Ltd.

Centore, P. (2013). *Conversions Between the Munsell and sRGB*.

Chen, I.-P., Wu, F.-Y., & Lin, C.-H. (2012). Characteristic color use in different film genres. *Empirical Studies of the Arts*, *30*(1), Article 1. https://doi.org/10.2190/EM.30.1.e

Chevreul, M. E. (2001). Michel-Eugène Chevreul: From laws and principles to the production of colour plates. *Color Research & Application*, *27*(1), 4–14. https://doi.org/10.1002/col.10000

Da Vinci, L. (1503). *Saint Anne, the Virgin Mary and the Infant Jesus* [Oil on wood]. https://collections.louvre.fr/en/ark:/53355/cl010066107

Itten, J. (1970). *The Elements of Color* (1st ed.). John Wiley & Sons, INC.

Lyon, C. (1991). Unveiling Monet. *MoMa*, *7*, pp14-23.

Mahyar, F., Cheung, V., Westland, S., & Henry, P. (2007). Investigation of complementary colour harmony in CIELAB colour space. *AIC 2007*, 82–85. http://www.aic-color.org/congr_archivos/aic2007proc.pdf

Monet, C. (1891). *Haystacks (Effect of Snow and Sun)* [Oil on canvas]. https://www.metmuseum.org/art/collection/search/437122

Ng, W. L. (2020). Tonal Design: A Mathematical Guide in Constructing Mood and Weather. *The International Journal of Design Education*, *15*(1), 1. https://doi.org/10.18848/2325-128X/CGP/v15i01/1-15

Ng, W. L. (2021). The teaching of the concept of color harmony and its ambiguity. *Asia-Pacific Journal of Humanities and Social Sciences*, *1*(2), Article 2. https://10.53789/j.1653-0465.2021.0102.002

Ng, W. L., & Xiao, Y. (2017). Development of 3D Color Space to Improve Learning of Color Theory. *Proceedings of the 2017 2nd International Conference on Modern Management, Education Technology, and Social Science (MMETSS 2017)*. MMERSS 2017, Singapore. https://10.2991/mmetss-17.2017.6

Ó Gráda, C. (2016). Did science cause the industrial revolution? *Journal of Economic Literature, 54*(1), 224–239. https://10.1257/jel.54.1.224

Sargent, J. S. (1903). *Scuola di San Rocco* [Watercolour on paper]. https://burchfieldpenney.org/about/news/article:05-01-2014-12-00am-john-singer-sargent-the-watercolorist/

Sargent, J. S. (1907). *Brook among Rocks* [Watercolor on paper]. https://www.artrenewal.org/artworks/brook-among-rocks/john-singer-sargent/13686

Shapiro, A. E. (1994). Artists' Colors and Newton's Colors. *The University of Chicago Press on Behalf of The History of Science Society*, *85*(4), Article 4. https://10.1086/356979

Shearman, J. (1962). Leonardo's colour and chiaroscuro. *Zeitschrift Für Kunstgeschichte*, *25*(H. 1), 13–47. http://www.jstor.org/stable/1481484 .

Westland, S., Laycock, K., Cheung, V., Henry, P., & Mahyar, F. (2007). Color Harmony. *Colour Journal - Design and Creativity*, *1*(1), Article 1.

Xue, S., Agarwala, A., Dorsey, J., & Rushmeier, H. (2013). *Learning and applying color styles from feature films*. *32*(7), 255–264. https://doi.org/10.1111/cgf.12233

Color Education in Schools for Students with Color Vision Deficiency: Important Elements Identified Through In-Depth Interviews with Designers and Artists

Tsukasa Muraya[a*], Yunoka Taniguchi[b], Yasuyo Ichihara[c] and Shoji Sunaga[d]

[a] *Faculty of Contemporary Social Studies, Chikushi Jogakuen University, Fukuoka, Japan*
[b]*School of Design, Kyushu University, Fukuoka, Japan*
[c]*Kogakuin University, Tokyo, Japan*
[d]*Faculty of Design, Kyushu University, Fukuoka, Japan*

[*]*Corresponding author: Tsukasa Muraya, t-muraya@chikushi-u.ac.jp*

ABSTRACT

Background: Previous research has shown that individuals with color vision deficiency (CVD) often experience emotional distress and lose interest in art when their color choices are labeled as "wrong" in elementary school art classes. In Japanese society, pursuing a career as a designer or artist has long been considered difficult for people with CVD. Nevertheless, professional designers and artists with CVD do exist in Japan. How do they perceive their own color vision? How have they learned to navigate color usage professionally? Aim: This study aims to explore the lived experiences of professional designers and artists with CVD, focusing on how they overcame various obstacles, their visions for ideal color education, and the key elements needed to create inclusive color education programs that embrace color vision diversity. Methods: We conducted in-depth interviews with eleven individuals with CVD: five designers (including one university student aspiring to become a designer) and six artists. The interviews explored their experiences in school art classes, difficulties and turning points related to their color vision, strategies and sources of resilience, motivations for choosing creative careers, and their ideas for ideal color education in schools. Findings: Most participants reported negative experiences in school art classes that made it feel nearly impossible to pursue careers in art or design. Several had been discouraged by teachers, excluded from entrance exams, or made to feel that their color perception was a limitation. Despite these challenges, all participants emphasized that individuals with CVD can become successful designers and artists. Many had traumatic memories of being told their color choices were "wrong," and they expressed frustration at not being allowed to explore or express their unique perceptual worlds. While art education often encourages students to "enjoy colors," this message can feel disingenuous to students with CVD when their enjoyment is constrained by normative expectations. Conclusion: This study found that participants, despite their strong creative drive, had been deeply affected by educational environments that prioritized color "accuracy" over self-expression. To foster inclusive color education, teachers should move away from rigid standards and instead cultivate environments that encourage diverse ways of seeing and expressing color. Supporting color vision diversity requires both scientific understanding and sensitivity to lived experience.

Keywords: color vision diversity, color vision deficiency, art, inclusion, art education

INTRODUCTION

In Japanese society, individuals with color vision deficiency (CVD) have historically been labeled as having "abnormal" color perception and have faced discrimination in various aspects of life. One of the most significant

impacts has been on their career choices, particularly in the fields of art and design. As recently as 2015, the Japanese Ophthalmologists Association published a poster warning students with CVD about occupations that might be difficult for them to pursue—including careers in design and art [1].Although public awareness has gradually improved in recent years, students with CVD still face substantial barriers when applying to university programs in art and design or pursuing creative professions. These challenges stem from persistent assumptions about their supposed inability to perceive colors accurately. CVD, typically diagnosed by ophthalmologists, refers to atypical color perception compared to the majority population (trichromats). Individuals with CVD often have difficulty distinguishing specific color pairs—such as red and green, or pink and light blue—depending on the function of their eyes and brain [2].

In contrast to this historically restrictive view, the Genetics Society of Japan introduced the term *color vision variation* in 2017 [3]. This concept reframes color perception not as a binary distinction between "normal" and "abnormal," but as a spectrum of human diversity. However, this inclusive perspective has yet to be fully integrated into Japan's educational system. School art classes continue to operate under the assumption that all students are trichromats. Prior studies have shown that students with CVD often feel discouraged when their color choices are labeled as "wrong," which can reduce their interest in art and color [4][5]. Rather than enjoying their unique perception of color, these students may develop a fear of making mistakes—contrary to the goals of art education, which should encourage creative exploration. While Japan's national education policy promotes the cultivation of students' "zest for living" (ikiru chikara) [6], this ideal may be undermined in art education for students with CVD.

These negative experiences can be especially traumatic; however, many teachers remain unaware of color vision diversity, largely due to a lack of formal training [7]. In Japan, elementary school art is typically taught by homeroom teachers, while junior high schools have subject-specific art instructors. Yet, most educators—regardless of specialization—receive little to no instruction on CVD and are often unaware of the presence of students with CVD in their classrooms [7]. Statistically, at least one student with CVD is likely to be present in every class of 40 students (assuming equal gender distribution), indicating that such students are not rare. Nevertheless, teacher training programs and art education textbooks seldom address how to support students with CVD. Instruction on color is generally based exclusively on the trichromatic perspective [7]. Although recent scholarship has advocated for a shift away from "normal color vision–based" instruction toward approaches that embrace color vision diversity, this paradigm shift has yet to be realized in practice [8].

Despite these challenges, professional designers and artists with CVD do exist in Japan. How do they perceive their own color vision? How have they adapted their use of color? What do they envision as ideal color education? This study aims to explore the lived experiences of designers and artists with CVD, the strategies they have developed, and their perspectives on inclusive color education. The goal is to identify essential components for future educational programs that promote understanding and inclusion of color vision diversity.

METHODOLOGY

We conducted in-depth interviews with eleven individuals with color vision deficiency (CVD), comprising five designers (participants a–e in Table 1, including one university student aspiring to become a professional designer) and six artists (participants f–k). Participants were recruited through convenience sampling and referrals facilitated by the Color Universal Design Organization (CUDO), a Japanese nonprofit organization dedicated to promoting inclusive design for people with CVD. Although broadly categorized as either "designers" or "artists," many participants engaged in both client-based design work and independent artistic expression. All participants were male, ranging in age from their late teens to their 60s. They self-reported various types of CVD, including protanomaly, deuteranomaly, protanopia, and deuteranopia; three were diagnosed as having red-green CVD.

Semi-structured interviews were conducted to explore the following topics: participants' experiences in school art classes, emotional setbacks related to their color vision, strategies or events that fostered resilience, turning points in their career paths, and their views on ideal color education in school settings. Data collection took place

between October 2022 and February 2023, with each interview lasting approximately 90 minutes on average. All interviews were transcribed verbatim, and a qualitative thematic analysis was conducted to identify recurring patterns and interpret participants' experiences in depth.

RESULTS AND DISCUSSION

The curse of "wrong color"

All participants recalled being enthusiastic about drawing and enjoying creative activities during childhood. However, they also reported negative experiences related to color use in school art classes—especially during assignments involving the reproduction of famous artworks or landscape sketches. These tasks typically required students to closely observe and accurately replicate shapes, composition, and colors. Yet, some of the participants' color choices were evaluated as "incorrect." They recounted being told their colors were "wrong" when their selections differed from the "normal" hues expected by teachers or peers. Several participants described feeling pressure when using watercolor paints, particularly when mixing pigments and losing track of color names. Consequently, some reported that they relied on knowledge rather than intuition when selecting colors. They trained

Table 1: The basic data of the participants

PART	Birth Year	Types of Color vision	Time of diagnosis	Academic history	Current occupation/ Coloring Techniques
a	2001	Deuteranopia	Middle school	Design in university (current student)	University student/ PC App.
b	1987	Red-green CVD	Elementary school, grade 4	Art University	Filmmaker (live action, Animation)/ PC App.
c	1974	Protanopia	Pre-school child	Art University	Designer (CI), copy writer/ PC App.
d	1958	Protanopia	Elementary school	Art University	Designer (PD)/ Watercolor, acrylic paint
e	1953	Protanomaly	Elementary school, first grade	Architecture in University	Designer (CI, VI)/ PC App.
f	1998	Protanopia	University	Art University	Office worker, Illustrator/ Watercolor, PC App.
g	1991	Deuteranopia	Elementary school, grade 4	Art University	Artist (Painting)/ Oil paint
h	1988	Red-green CVD	High school	Art University	Artist (Contemporary Art)/ PC App.
i	1986	Deuteranopia or Deuteranomaly	High school	Art University	Artist (Paint), Designer (UX)/ Oil paint
j	1968	Red-green CVD	Elementary school and High school	Art University	Artist (Painting)/ Mineral Pigments
k	1954	Deuteranopia	Elementary school	Technical school	Artist (Painting)/ Watercolor

CI: Corporate Identity design, PD: Product design, VI: Visual design, UX: User Experience Design

themselves to avoid making "mistakes" by constantly checking pigment labels and practicing how to mix colors to produce socially accepted shades—such as green for leaves or red for the sun—starting as early as elementary school.

Challenges Related to Color Vision and Factors Promoting Resilience

Most participants described feeling that becoming a designer or artist was an unrealistic goal due to their CVD, and many had considered abandoning these career paths. Older participants recalled being explicitly prohibited from taking entrance exams for university design programs because of regulations that excluded individuals with CVD. Although such discriminatory rules have since been officially abolished, younger participants still encountered significant barriers, particularly during entrance exams that included color composition tasks. Some initially aimed to enter design departments but instead shifted to fine arts programs, while others began their careers in unrelated fields and transitioned into design or art professions later when new opportunities emerged. For example, one participant initially worked in a non-creative job but eventually entered the design field after gaining confidence in his abilities.

One younger participant explained that he had never been discouraged by criticism of his color usage and had maintained a strong determination to become a creator from the outset. Other participants who had temporarily abandoned creative careers continued to hold a sense of confidence and a desire for artistic expression. Positive feedback and external recognition of their work helped reinforce their belief in their creative abilities. As they pursued careers in design and art, many participants actively trained their color perception skills, learning to distinguish subtle color differences that had previously been challenging. Technological advances—such as color identification apps and digital tools—also contributed to their confidence by enabling them to verify color values on screen. While all participants expressed deep fulfillment in their current creative work, they also voiced frustration with the exclusionary educational and professional systems that discouraged children with CVD from freely exploring color. They criticized the tendency of ophthalmologists to impose occupational limitations based solely on color vision differences.

Participants emphasized that while individuals with CVD can certainly become designers and artists, they must make conscious efforts to understand the differences between their own color perception and that of trichromats. In particular, design work often requires meeting client expectations, and since most clients are trichromats, some degree of adaptation is necessary. However, participants noted that with the advancement of digital tools and color-checking apps, designers with CVD are now able to verify color accuracy effectively. They did not view this additional training as a disadvantage but rather as a natural aspect of becoming a professional, arguing that all professionals must cultivate specific skills relevant to their field.

Participants' Perspectives on Ideal Color Education in Schools

Drawing on both their past experiences in school art classes and their current roles as professional creators, participants shared their visions for ideal color education.

First, they emphasized that students' artistic work should not be evaluated based on the "accuracy" of color usage. In Japanese compulsory education, art classes often include assignments such as reproducing famous artworks or creating observational drawings, with the implicit expectation that students will depict colors "as they are seen"—that is, through the lens of trichromatic color vision. However, this assumption excludes the perspectives of students with color vision deficiency (CVD), whose perception of color can differ substantially. Some participants also noted that the commonly held belief that "color is to be enjoyed" in art class can be problematic. While intended to encourage creative exploration, this framing often pressures students with CVD to find enjoyment in a perceptual world that does not reflect their own experiences.

Second, participants reflected on the role of teachers and the potential pitfalls of excessive or misguided accommodations. They criticized practices such as instructing students with CVD to choose colors that conform to trichromatic standards, or advising peers and teachers to refrain from commenting on "strange" color choices. While

such approaches may aim to prevent discrimination, they do little to promote genuine understanding of color vision diversity. Instead, participants advocated for teachers to accept each student's unique use of color and to support self-expression through constructive feedback. They expressed concern that Japanese art education in compulsory schooling often promotes a singular "correct" mode of expression—an approach that contrasts sharply with the openness and diversity embraced in the professional art world.

Third, participants emphasized that understanding color vision diversity can serve as an entry point to broader awareness of human diversity. While it is natural for students with typical color vision to feel confused or surprised by unconventional color choices, such reactions may foster feelings of inferiority among students with CVD—especially if teachers scold them or assign lower evaluations based on "incorrect" colors. Participants argued that teachers must possess accurate scientific knowledge about color perception—namely, that color is not a fixed property of objects, but a subjective experience constructed in the brain. Each person's perception of color is unique and inherently unshareable. From this standpoint, participants proposed that just as diverse modes of expression are celebrated in art history, diversity in color perception and expression should also be embraced in education—particularly in elementary schools, where creative exploration forms a critical foundation. Without this fundamental understanding, teachers are unlikely to recognize the legitimacy of each student's perceptual world or appreciate their distinct forms of artistic expression.

Discussion: Toward a Future Color Education Embracing Color Vision Diversity

A key finding of this study was the participants' repeated use of the phrase "wrong color," even when their choices were subjectively appropriate. Initially, they enjoyed using color intuitively; however, over time, they developed anxiety and discomfort due to reactions from peers and teachers with trichromatic color vision. These reactions—often delivered as corrections or evaluations—fostered feelings of inferiority, despite the participants' perceptual accuracy within their own visual frameworks. This suggests that the difficulties students with color vision deficiency (CVD) face in color expression are not rooted in perceptual limitations, but rather in social and institutional responses that frame their color use as erroneous. Consequently, the notion of "wrong color" should not be viewed as an individual deficiency, but rather as a socially constructed barrier to inclusion within educational environments [9].

The participants' career trajectories further highlight how societal and institutional structures contribute to discouraging creative aspirations among individuals with color vision deficiency (CVD). Many recalled that the diagnosis of CVD was conveyed to them as a fatal limitation—particularly by ophthalmologists and school personnel—causing them to abandon aspirations of becoming artists or designers. Moreover, entrance examinations for design programs often prioritize tasks involving color composition with paint, thereby imposing practical barriers to entry. Despite these challenges, all participants eventually regained confidence through hands-on creative work, external recognition, and the use of supportive technologies such as color-identification applications. These findings suggest that medical classifications should not be conflated with educational or creative potential. The role of ophthalmologists in shaping students' career trajectories should be reconsidered in light of this distinction. [7].

To build a truly inclusive art education framework, participants emphasized the importance of evaluative criteria that value diverse modes of color expression rather than enforcing narrow standards of color "accuracy." Their dual perspectives—as individuals with minoritized visual experiences and as professional creators—offer critical insights into how such an educational model can be realized. Avoiding discrimination in art classrooms is important but insufficient. Teachers must be equipped with both scientific knowledge of color perception and a practical understanding of color vision diversity [10]. The participants advocated for a pedagogical approach that not only prevents exclusion but also actively celebrates perceptual and expressive diversity as a core principle of art education. From this perspective, constructing color education grounded in the concept of color vision diversity is not merely a form of accommodation; it is an essential step toward realizing the broader mission of art education for all learners.

CONCLUSION

The purpose of this study was to explore the lived experiences of designers and artists with color vision deficiency (CVD), the strategies they developed, and their perspectives on inclusive color education. The aim was to identify essential elements for future educational programs that foster understanding and inclusion of color vision diversity. Semi-structured interviews were conducted with eleven professional designers and artists, and qualitative analysis was employed. Findings revealed that most participants had experienced trauma related to color usage during their school years, despite their strong creative motivation. In art classes, teachers should avoid focusing excessively on the "correctness" of color choices and instead foster an environment in which students can express themselves freely—without fear or pressure. Building inclusive color education requires attention to both scientific understanding and the lived experiences of learners. While this study focused on the Japanese context, the findings and proposed approaches hold potential to inform global efforts to rethink art education through the lens of perceptual diversity.

ACKNOWLEDGEMENTS

This work was supported by grants from JSPS KAKENHI (grant numbers: JP 21H04342 and JP 24H00167).

REFERENCES

[1]. Japan Ophthalmologists Association. *Shikikaku kensa no susume* (in Japanese). Retrieved September 14, 2025, from https://www.gankaikai.or.jp/colorvision/20151005_poster.pdf.

[2]. Japan Ophthalmologists Association. *Shikikaku ijou to iwaretara* (in Japanese). Retrieved September 14, 2025, from https://www.gankaikai.or.jp/health/50/index.html

[3]. The Genetics Society of Japan. *Idrngaku yougo kaitei nitsuite* (in Japanese). Retrieved September 14, 2025, from https://gsj3.org/wordpress_v2/wp-content/themes/gsj3/assets/docs/pdf/revisionterm_20170911.pdf

[4]. Miyaura, T., Utsumi, Y., Kashiwai, M., et al. (2012). A follow-up survey on the actual conditions of patients with congenital color vision deficiency in FY 2010 and 2011. *Journal of Japanese Ophthalmology*, 83(11), 1541–1557. (in Japanese)

[5]. Tsuji, S., Sunaga, M., & Katsura, S. (2020). A survey on the degree of interest in art among individuals with color vision deficiency. *Journal of the Color Science Association of Japan*, 44(3), 207–210. (in Japanese)

[6]. Ministry of Education, Culture, Sports, Science and Technology. (n.d.). *Gakushū shidō yōryō "Ikiru chikara"* [Curriculum Guidelines: "Capacity for Living"]. Retrieved September 14, 2025, from https://www.mext.go.jp/a_menu/shotou/new-cs/

[7]. Muraya, T., Chikara, R., & Sunaga, S. (2024). Study on constructing the color education basis on the color vision diversity: Suggesting the subjects for the investigation by assessing the actual situations of art classes through questionnaire survey. *Color Science Research*, 2(2), 55–68..

[8]. Muraya, T., & Sunaga, S. (2023). The components of color vision diversity: A literature review and interview study. *Color Science Research*, 1(1), 45–56.

[9]. World Health Organization. (2002). International Classification of Functioning, Disability and Health (ICF): Japanese Edition (Shōgaisha Fukushi Kenkyūkai, Ed.). Chuohoki Publishing.

[10]. Muraya, T., Nagatomi, M., Inoshita, T., & Sunaga, S. (2024). Enjoy Learning for Wonder of Colors and Color Vision Diversity. In *Proceedings of the Midterm Meeting of the International Colour Association 2024* (pp. 305–308). São Paulo, Brazil, September 16–19.

Biophilic Colour Schemes (BCS) A Catalogue of Biophilic Colour Schemes Based on Emotional Colour Impact Principles and Natural Analogies from Iandscape Prototypes for Evidence-Based Sustainable Design

Markus Schlegel[a]*, Konstantin Haensch[b] and Claudia Goméz Mejia[c]

[a]*University of Applied Sciences HAWK Hildesheim IIT, Hildesheim, Germany*
[b]*University of Applied Sciences HAWK Hildesheim IIT, Hildesheim, Germany*
[c]*Universidad Del Rosario, Bogotá, Colombia*

ABSTRACT

This study develops an evidence-based colour collection as a practical tool for interior design within the framework of evidence-based design (EBD). The catalogue addresses a recurrent gap in planning processes: the absence of a reliable and justified basis for colour selection. Colour atmospheres are key components of spatial perception, experienced immediately and emotionally rather than through deliberate analysis. Building on the assumption that emotional responses arise spontaneously, the study argues that a positive immediate reaction to colour atmospheres significantly increases the likelihood of user acceptance of a space and its ambience. The study anchors its approach in existing research on the emotional effects of colourfulness and supplements this with surveys conducted in a 1:1 room model. With a focus on health-related design, references to salutogenesis and the biophilia hypothesis are combined with principles of emotional impact to establish a new approach to effect-based colour selection. To identify pragmatic colour compositions from millions of possibilities, the method draws on landscape prototypes or image archetypes as natural analogies within the biophilia hypothesis. These are understood as typical landscapes with distinctive topography and vegetation that reveal both a clarity and a depth of image, and they provide the foundation for the colour profiles in the catalogue. The resulting collection consists of 25 natural analogue colour profiles distributed evenly across the colour space from hue H0 to H360, encompassing reddish, yellowish, greenish, blue, and violet tones. For each composition, two closely related profiles were created: one capturing the colourfulness of ground or vegetation in the foreground, and the other the impression of the sky as a colour-light phenomenon with its many shades. Each composition includes six colours, one main colour and five complementary colours. By translating these profiles into standardised colour tones within established systems such as LCH and NCS, the catalogue provides planners with a validated resource for design practice. The study thereby closes a gap in the planning process while also establishing a basis for further research. A future database of landscape archetypes across cultural areas, regions, seasons, and times of day, supported by international partnerships, holds particular promise. Finally, while this study develops evidence-based colour profiles from natural analogies, it also acknowledges that the concept of biophilia and the relationship between colour and territory are culturally situated – a perspective taken up in greater depth in the concluding South-North discussion.

Keywords: evidence-based design concepts, colour-emotion impact, colour profiles as natural analogies health-promoting design, biophilia

INTRODUCTION

The background and motivation for this study are years of practical and research experience on the subject of colour schemes and the effect of colour in rooms. Various studies, see sources in the appendix and in the further explanations, conducted between 1994 and 2018 have examined the emotional effect of colour on observers. The results point in the same direction in many areas, such as the interaction of colour intensity and/or contrast and a

more stimulating effect. Nevertheless, most studies remain stuck in the discussion of basic colours or small colour samples and fail to translate these findings into applications in room design.

In our daily work, it has become increasingly clear that this important topic neither offers a valid basis for justifiable colour schemes nor do planners, operators of educational institutions or healthcare facilities have experience in dealing with colour schemes in spaces. At the same time, megatrends such as health and demographics are developing rapidly and demand function-oriented and people-friendly atmospheres for hospitals, care facilities, educational institutions and work environments. The aim of this study was therefore to create an evidence-based colour collection to be developed as a tool for evidence-based design concepts (EBD) [1] in interior design. With its range of colours, the catalogue is intended to fill a frequently observed gap in the planning process, namely a justifiable colour selection.

METHODOLOGY

The investigation of emotional responses to colour is based on a three-dimensional view of emotion, namely valence, arousal and dominance. In addition, all three dimensions of colour perception, namely hue, chroma (saturation) and brightness, are considered and included in the respective evaluations. The evaluations of colour effects are in a field ranging from rather pleasant and stimulating to pleasantly relaxing to neutral. This initially justifies the decision to use the SAM self-assessment method as a measuring instrument and the LCH system as a colour classification system and colour standard. The SAM questionnaires are used to survey subjective assessments of the participants' well-being during the experiment. These are dependent variables. The background to this survey method is explained below. Russell and Mehrabian (1977) developed three independent emotional dimensions: satisfaction vs. dissatisfaction (‘pleasure’ or “valence”), arousal vs. non-arousal (‘arousal’) and dominance vs. submissiveness (Russell & Mehrabian, 1977, p. 274)[2]. These are bipolar and independent of each other in that they can coexist simultaneously in different magnitudes. According to their theory, emotions such as anger and fear are a mixture of the three dimensions. Based on this theory, Peter Lang developed the Self-Assessment Manikin (SAM) questionnaire method in 1985. According to Morris (1995), it is a promising solution for measuring emotions (Morris, 1995, p. 63) [3]. The degree of satisfaction is referred to as ‘pleasure’ or ‘valence’, the state of arousal as “arousal” and the degree of dominance as ‘dominance’.

Studies on the emotional impact of colour on viewers by Valdez and Mehrabian (1994)[4], Suk and Irtel (2008)[5], Hirschmüller, Irtel and Schlegel (2008)[6] and Wilms and Oberfeld (2018)[7] show out a fundamental fact, namely that colours with high colour saturation or colour intensity are perceived as more stimulating than colours with lower colour saturation. On the other hand, brightness and the logically resulting low colour intensity have a considerable influence on the so-called valence dimension, i.e. they determine whether we perceive the colourfulness or the colour of a room as pleasant or unpleasant. Up to medium brightness and thus intensity values, these increase well-being and positive evaluation (Valdez & Mehrabian, 1994, p. 402)[4]. In this catalogue, the classifications of light colours or medium brightness for the different colour spaces are further classified using different colour classification systems such as NCS (psychological-physiological) or LCH (physical-physiological). While the influence of pure colour tones such as red, green or blue is less decisive, the parameters of brightness and colour saturation take precedence in the emotional response to colour, especially on the dimension of pleasur (valence) and excitement (arousal). Hirschmüller, Irtel and Schlegel (2008)[6] as well as Wilms and Oberfeld (2018)[7] also show the largely universal influence of different colour dimensions, whereby here too it is less about the specific colour tones themselves and more about the differences in brightness and intensity (Wilms & Oberfeld, 2018)[7]. These findings provide a valid initial foundation for developing widely applicable baseline colour collections, which can then serve as the basis for localization. The subjective desire for light and natural shades in private homes, which emerged from further studies by the IIT HAWK, also points to the focus on nature-analogous colour profiles in the catalogue. The various studies on the emotional effect of colour on viewers therefore form the framework for the classification of nature analogies as colour profiles ranging from ‘rather stimulating to rather relaxing’.

Based on previous studies, the BCS catalogue classifies colour tones and colour profiles as light, clear, white-like, light grey to light, clear pastel tones as colour profiles with a rather pleasant, relaxing emotional effect. Based on this thesis, further surveys are currently being conducted in a 1:1 model. As contrasts within a colour composition increase, whether in terms of colourfulness or brightness or colourfulness and brightness, the emotional feeling towards 'stimulation' increases depending on the increase in colour quantity and/or colour quality. Accordingly, these colour profiles, which are increased in colour quantity and/or colour quality, have an increasingly pleasant and stimulating effect. There is no 'mathematical' limit, but rather a visually perceived, colour-qualitative and quantitative limit of approximately +25%, above which the emotional perception of a colour composition shifts completely from a relaxing effect to an increasingly stimulating one.

In our initial study selection of colour tones and colour profiles, a central question was how to pragmatically capture, document, and analyse the seemingly infinite phenomena of "nature" in order to make the results useful and applicable for design. Which natural patterns of human viewing habits are particularly relevant? The savanna hypothesis, first described by Wilson (1984)[8], suggests that humans possess an innate preference for savanna-like landscapes. Studies by Orians and Heerwagen (1992)[10] and Balling and Falk (1982)[11] provide cross-cultural evidence for this claim, showing a recurring preference for acacia-like trees, open green spaces, scattered vegetation, water sources, and expansive views. Research in environmental psychology, landscape preferences, and architecture likewise confirms that people often favour such savanna-associated features. As highlighted above, our study therefore places particular emphasis on "natural" or "nature-like" viewing habits and their significance for health-promoting design. On a physiological and psychological level, the term describes the way in which people perceive visual information and interpret, for example, landscape image prototypes, archetypes or more abstract analogies to nature. Certain patterns of perception are likely particularly deeply rooted, especially in environments that are 'proto- to archetypal' in nature, shaped by evolution and significant for human history. 'Nature-like viewing habits' refer to ways of seeing that have developed in natural or naturalistic contexts and incorporate archetypal motifs such as expansive landscapes, gradations of landscape, earth and stones, vegetation, sky variations, sunrises and sunsets, or water surfaces as formative visual archetypes. The aim is therefore to capture these viewing habits as abstract colour profiles, as analogies to nature, to systematically utilise them for the design of artificial environments. Conceptually, the work is based on Edward O. Wilson's biophilia hypothesis, which assumes that humans have a deep-rooted biological affinity for nature (Wilson, 1984)[8]. These assumptions form the methodological basis for selecting visual prototypes and archetypes from which the colour schemes are generated. In addition to these evolutionary models, the study considers aspects of Antonovsky's salutogenesis-theory[13] and empirical studies by Roger Ulrich, according to which viewing nature can have positive effects on the immune system and healing processes. Methodologically, the implementation initially took the form of an open photographic collection of selected international landscape images that serve as prototypes and archetypes. Our initial selection of landscape archetypes was based on criteria such as country, motif, time of day and weather conditions to ensure comparability in terms of image depth and spatial dimension, for example. The selection was made by individuals from Korea, Taiwan, Germany and Colombia. For the first step of the prototypical collection of approximately 250 landscape images collected worldwide, it was important that they all reflected essential material and light-related colours such as earth tones, sand, stones, vegetation, water, sky, and sunlight. It was also important that there were no artefacts or linguistic-typographical elements in the image.

Processing of image information: The image data was digitally analysed in a multi-stage process. Image depth, proportions and the ratio of ground to sky were examined. In order to guarantee the comparability of colour profiles in the catalogue, the image data was finally adjusted proportionally, then reduced to six colour values in three steps regarding colour and optical appearance, and visually coded according to LCH/NCS. Visually sampled here means that a photo was viewed and compared in print and on different end devices, and then the respective colour tones were determined as a visual average value by colour designers from Colombia, Germany, Korea and Taiwan. This is because neither the sky, light colour, haze nor image depth can be measured metrically. This allowed their essential chromatic information could be determined into nature-analogous colour profiles. We are aware that many textures can alter and distort the actual image and colour state. The images are exemplary snapshots that represent a moment from millions of subtle nuances.

Within this scientific work, methodological steps are defined on the one hand, while on the other hand, visual experience with natural colour nuances and the determination of image and colour reduction were used as a basis. It was essential that the resulting colour profiles and colour reductions reflect the original image as closely as possible and function as natural analogies, decoupled from the semantics of the image. The resulting catalogue, 'Colour Profiles – Natural Analogies Sorted in the RDS-LCH System,' now offers the possibility of selecting comparable brightness or contrast colour profiles from different colour spaces. The practical transfer was tested in a series of smaller application studies in 1:75 models and collages.

Transfer into practice: To test the practicality and principles of action in space, a collaboration took place with the Swiss Centre for Design and Health (SCDH) in Biel. The Swiss space laboratory offers the opportunity to work with full-scale modelling. To test our hypotheses from the Colour & Emotion studies with the newly developed colour profile nature analogies from the BCS catalogue, the first step was to select three colour profiles with comparable contrast and brightness from the H54, H114 and H320 (Figure 2) colour ranges and transfer them to 1:1 room models. Two identical 1:1 room models each show two different types of furnishings, namely a more school-like, relaxed co-working situation and a health application in a patient's room. The aim is to determine differences in the emotional colour effect of the light pastel yellow-orange, green and violet spectrum in two different usage scenarios. In a second test setup, more colour-intensive, high-contrast colour profiles from the same natural analogue colour ranges H54, H114 and H320 will then be transferred to 1:1 room models to determine differences in effect on the activation and pleasure/valence scale in comparison to the light pastel yellow-orange, green and violet spectrums.

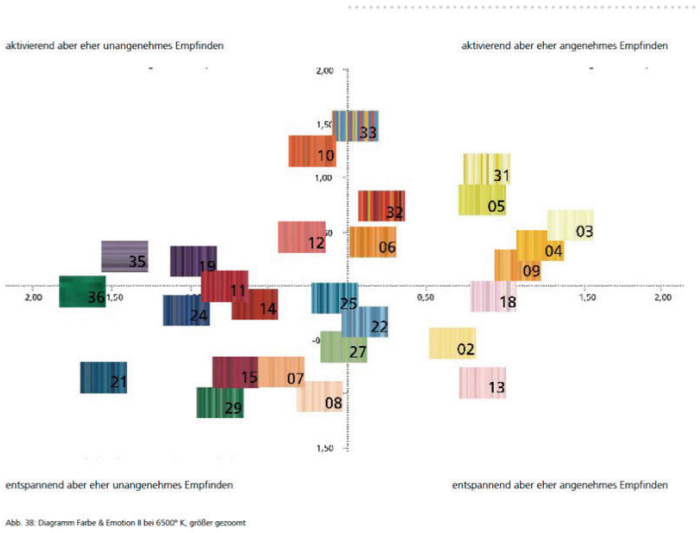

Figure 1: Evaluation of the Colour Emotion Study 2007

RESULTS AND DISCUSSION

The Biophilic Colour Schemes (BCS) catalogue is a nuanced, practical creative tool that provides a sound basis for the use of impact-based colour compositions in spatial environments. The result is based on various surveys on the emotional effects of colour on people and the translation of landscape image archetypes into abstract colour patterns known as nature analogies. Aspects such as form, materiality and acoustics were largely disregarded in the study, but the influence of light as a significant interaction factor on the colour atmosphere was included in the investigations.

The catalogue consists of 25 natural analogue colour profiles sorted equally in the colour space from Hue H0-H360, ranging from reddish to yellowish, greenish, blue and violet. These 25 colour compositions form the individual colour chapters in the catalogue. For each of the 25 colour compositions, two natural analogue colour profiles have been created (Figure 2) that are closely related to each other, as they each form a corresponding

landscape image prototype and archetype in a reduced, abstract representation from two different perspectives. The main colour tone of the first colour profile conveys a visual impression of the colourfulness of the ground or vegetation in the foreground of an image, while the main colour tone of the corresponding second colour profile captures the visual impression of the sky.

These 25 colour compositions, standardised in terms of content, each consist of six colours, one main colour and 5 complementary colours (Figure 3). The main colours thus always represent a balance between a material colour and a colour-light phenomenon, namely the sky with clouds, light colours or in its many shades of blue. It is important to note that none of the colours were sampled digitally from images or analogously from samples or materials. They are always a visual representation of an image impression, an average value of the perceived image. For this reason, care was taken to ensure that the landscape images were not 'over-exposed' or photographed with filters.

Additional colours in the colour profiles: The five additional colours associated with each main colour are natural visual gradations of different colour nuances, depending on the colour space in the landscape image archetype or the atmosphere in the image.

Additional colour profile nuances in the 25 chapters: The two nature-inspired colour profiles created for each landscape image archetype are also offered in four lighter shades, ranging from pale to white, for design purposes. These lightening effects simulate a gradual increase in natural lighting, i.e. a higher lux value, such as a natural increase in brightness when the sun is high in the sky or when a colour tone, material or colour profile is exposed to direct sunlight. In addition, the brightening has practical reasons, as our BCS catalogue is also intended to create bright, soft and naturally strongly lit atmospheres in the room as natural analogies. The aim is to complement natural lighting and daylight planning, light and shadow in the room, materials, nature in the room or visual connections to nature with colour to enable staggered lighting of natural analogies as brightness levels in the room.

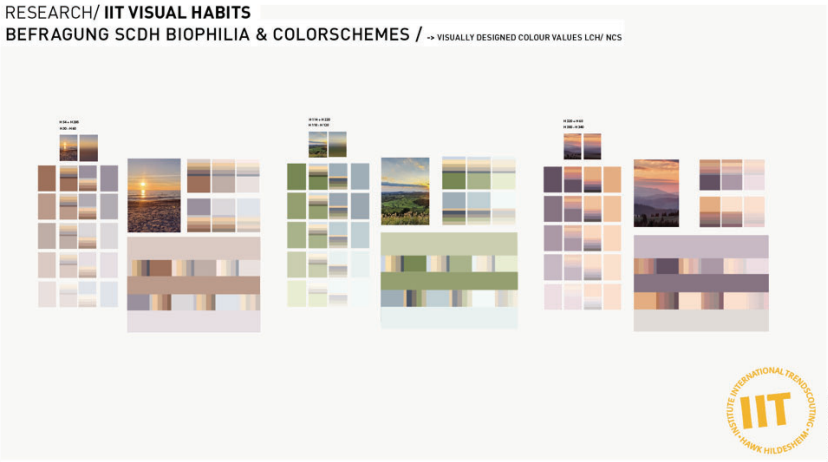

Figure 2: Colour profile H54/ H114/ H320, two natural-analogue colour profiles each

The colour profiles of the landscape image archetypes: According to the studies available, the lightest, white-covered variants of all colour profiles produce very gentle, low-contrast and yet subtly coloured results when applied. With its four graduated lightening effects, the catalogue offers a range of possible effects as a composition of natural analogies, from pleasantly relaxing to pleasantly stimulating. The four graded lightening levels of the colour profile natural analogies can be combined relatively pragmatically, quickly and reliably within a chapter, so that, according to the principle that increasing contrasts have an increasingly stimulating effect, individually contrast-enhancing colour profiles and compositions can also be created (Figure 4).

If the colour profiles are to be combined for different rooms or open room arrangements, this can be done using the same system. Based on previous experience, combining the lightest variants of natural colour profiles usually

creates pleasant, relaxing scenarios and atmospheres. Combining natural colour profiles of varying intensities increases the emotional impact of the resulting colour atmospheres, making them more pleasant and stimulating. The different lightening effects and thus intensities of the colour tones of the colour profiles also simplify the integration of existing building materials into the concepts when renovating existing buildings. This article will not go into the topic of light in depth. However, studies indicate that room atmospheres of all colour ranges tend to be more stimulating with directed light and more relaxing with diffuse light. Light cones and light points in particular tend to have a stimulating effect in a room.

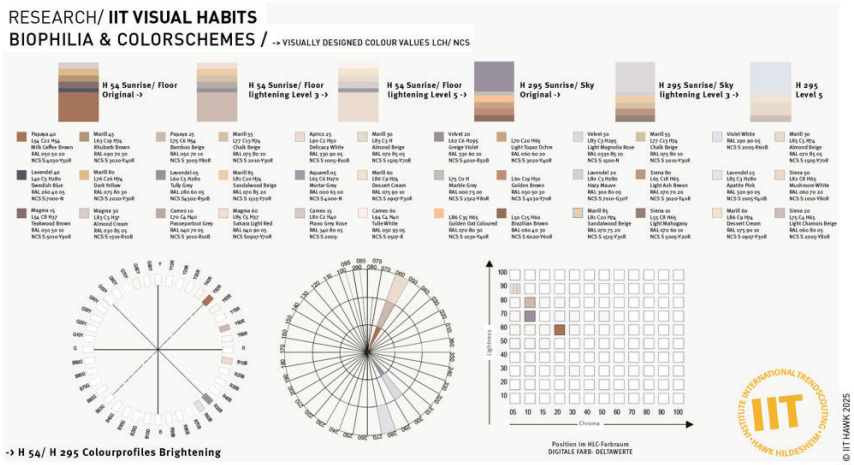

Figure 3: Colour profile H54 with six colours, one main colour and five complementary colours

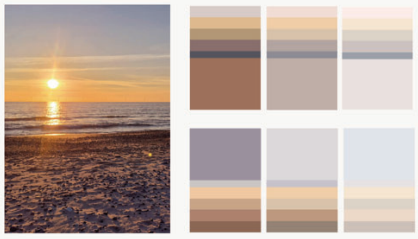

Figure 4: Colour profile H54 with two lightening levels

CONCLUSION

We know that, on the one hand, the idea of biophilic design has become a guiding concept in Western discourse in environmental psychology, architecture, landscape design and, more recently, sustainable urban development. On the other hand, the discourse on biophilic design is hardly or not universally discussed but bears clear traces of Western ideas about nature and humanity. We would therefore like to open a brief discussion on the topic of 'South-North' to contextualise our present study. Western modernity often separates 'nature' and 'culture', "humanity" and 'environment'. Although biophilia is expressed as reconnection (the longing for 'closeness to nature' as a remedy for alienation), it remains stuck in the motif of separation and reconnection (Descola 2013[14]). Relationship instead of separation: Many indigenous cosmologies (e.g. in the Andean region: Pachamama, among the Amazonian peoples, the First Nations in Canada) are based on a relational worldview. Humans, animals, plants, mountains, rivers and spirits are actors in an interdependent network and not separate entities (Viveiros de Castro, 2015[15]; Descola, 2013[14]).

Years of partnerships with Colombia, Peru, Turkey or Korea have shaped the work of the IIT HAWK. Our international perspective and methodology are based on the theory that there is an intrinsic relationship between colour, atmosphere and territory, and that colour is not only a visual phenomenon but can also be an expression of

a place. The relationship between colour and territory is intrinsic, not imposed or decorative, but arises from the interplay between local ecology, materiality and cultural practice. The pigments extracted from a particular landscape are more than just shades of colour; they are substances steeped in history, carrying within them the memory of the soil, water, vegetation and the human communities that have developed alongside them (Escobar, 2018[16]; Cusicanqui, 2010[17]). From the ochre tones of Provence or desert soils to the bright reds of cochineal in the Andean highlands, these chromatic manifestations are inextricably linked to the processes through which they are obtained: in this way, colour becomes a record of territorial interconnections – a form of chromatic cartography that registers the deep connections between landscape and society. These chromatic expressions are not only ecological adaptations, but also deeply emotional and symbolic, anchoring notions of belonging and identity, as is often found in urban spaces through the materials used in construction.

In this context, power is bound up with how colour knowledge is produced and legitimised. Much empirical research on colour and emotion stems from Western traditions that universalise their findings, often at the expense of alternative chromatic epistemologies. As the critique of biophilia shows, such frameworks remain tied to the separation/reconnection logic of Western modernity (Descola, 2013[14]; Viveiros de Castro, 2015[15]), whereas many indigenous cosmologies already situate colour, material and environment in relational networks. The history of pigments – from indigo to cochineal – further reveals how colour has long been entangled with colonial extraction, so that uncritical use risks reproducing asymmetries of power (Escobar, 2018[16]; Cusicanqui, 2010[17]). To operationalise "colour worlds," layered frameworks are needed: universalist, evidence-based profiles alongside registers of local and territorial practices. These can be articulated across four dimensions – perceptual, ecological, symbolic and affective – and explored through comparative cases, such as "sky blue" in environmental psychology versus Andean cosmology. Future research should develop such "chromatic cartographies" collaboratively, ensuring that diverse epistemologies are acknowledged rather than absorbed into universal models.

This integrative understanding of nature, place, and people has long been part of human experience, even if it has often been overlooked. Today, it continues to inform the practices of many communities and regions worldwide. Locally grounded knowledge of materials and colours can give rise to design languages that foster a strong sense of identity and inspire architectural interpretations in interior design. As designers, pursuing such connections remains a central objective, which is why engaging with this field of research and its approaches is essential.

At the same time, the question remains how different user groups emotionally experience such colour atmospheres. A follow-up study with several institutions in Colombia is already underway, and conducting comparable research in Taiwan would be equally valuable. Beyond these contexts, metropolises and large cities worldwide are increasingly shaped by globalized design practices, particularly in spaces such as hospitals, schools, and offices where people spend much of their daily lives. The BCS catalogue is therefore intended above all for these urban settings, offering designers a tool to create meaningful atmospheres in environments that are often detached from direct contact with nature.

Our abstracted nature analogies draw on a broad spectrum of landscape prototypes and image archetypes – topographies, vegetation, earth, stones, and light phenomena – from diverse regions. This process has produced archetypal image clusters that are comparable in vegetation greens, earth and sand tones, sfumato effects (greying into the distance), and depth of field. By reducing and abstracting these archetypes to essential chromatic values, topographical and material details are filtered out, leaving universally legible analogies that recur across cultures. Presented here as colour profiles, they form the basis for further study.

These profiles underpin a set of standardised compositions, validated through methods such as the Self-Assessment Manikin (SAM) and the Semantic Differential Scale (SDS). Organised systematically in the catalogue via LCH and NCS models, the collection offers an open database of nature-analogous colour profiles, evaluated for their emotional impact on joy, happiness, arousal, and activation. It provides a flexible, evidence-based tool for design, accommodating both subjective preferences and objectively verifiable principles of effect, and applicable across varied social contexts and user groups. In this way, the study establishes a foundation for interior and architectural designs that demonstrably promote well-being and health.

By drawing on material-oriented design and geochromatic thinking, contemporary practice can both honour and renew this tradition. Designers who "listen" to a landscape – literally and figuratively – can craft colour palettes or translate them into materials and patterns that respond to ecological conditions while respecting cultural histories.

The result is colour schemes that not only operate through impact and aesthetic richness but also convey an ethical and sustainable sense of place.

ACKNOWLEDGEMENTS

Special thanks go to Dr. Anna Hirschmüller from Karlsruhe University of Applied Sciences, Karlsruhe, Germany. We have been working together on this topic for over 15 years. Her constant conscientious and patient revision of the psychological aspects of the paper compels us to be precise and to correctly classify and assign statements and points of view. The responses and feedback will certainly force us to think and research even more comprehensively and in greater detail.

REFERENCES

[1]. Stichler, J. F., & Hamilton, D. K. (2008). Evidence-based design: What is it? *HERD: Health Environments Research & Design Journal, 1*(2), 3–4. https://doi.org/10.1177/193758670800100201

[2]. Russell, J. A., & Mehrabian, A. (1977). Evidence for a three-factor theory of emotions. *Journal of Research in Personality, 11*(3), 273-29.

[3]. Morris, J. D. (1995). Observations: SAM: The self-assessment manikin: An efficient cross-cultural measurement of emotional response. *Journal of Advertising Research, 35*(6), 63–68. https://doi.org/10.1080/00218499.1995.12466497

[4]. Valdez, P., & Mehrabian, A. (1994). Effects of color on emotions. *Journal of Experimental Psychology: General, 123*(4), 394–409. https://doi.org/10.1037/0096-3445.123.4.394

[5]. Suk, H.-J., & Irtel, H. (2009). Emotional response to color across media. *Color Research & Application, 35*(1), 64–77.

[6]. Hirschmüller, A.K., Irtel, H., & Schlegel, M. (2008). Emotional response to interior room colour attributes in full-scale room modelling. In I. Kortbawl, B. Bergström, K. F. Anter, & Scandinavian Colour Institute AB. *Colour effects & affects. Interim Meeting of the international colour association: Proceedings*

[7]. Wilms, L., & Oberfeld, D. (2018). Color and emotion: Effects of hue, saturation, and brightness. *Psychological Research, 82*(5), 896–914.

[8]. Wilson, E. O. (1984). *Biophilia: The human bond with other species*. Cambridge, MA: Harvard University Press.

[9]. Ulrich, R. S. (1984). View through a window may influence recovery from surgery. *Science, 224*(4647), 420–421. https://doi.org/10.1126/science.6143402

[10]. Orians, G. H., & Heerwagen, J. H. (1992). Evolved Responses to Landscapes. In J.H. Barkow, L. Cosmides, & J. Tooby (eds), *The Adapted Mind: Evolutionary Psychology and the Emergence of Culture* (pp. 555–579). Oxford University Press

[11]. Balling, J. D., & Falk, J. H. (1982). Development of visual preference for natural environments. *Environment and Behavior, 14*(1), 5–28. https://doi.org/10.1177/0013916582141001

[12]. Bennett, K. (2019). Savanna Hypothesis and Landscape Preferences. In T. K. Shackelford & V. A. Weekes-Shackelford (Eds.), *Encyclopedia of Evolutionary Psychological Science* (pp. 1-4). Cham, Switzerland: Springer International Publishing. https://doi.org/10.1007/978-3-319-16999-6_3726-1

[13]. Antonovsky, A. (1979). *Health, stress, and coping: New perspectives on mental and physical well-being*. San Francisco, CA: Jossey-Bass.

[14]. Descola, P. (2013). *Beyond nature and culture*. Chicago, IL: University of Chicago Press.

[15]. Viveiros de Castro, E. (2015). *The relative native: Essays on indigenous conceptual worlds*. London, England: Hau Books.

[16]. Escobar, A. (2018). *Designs for the pluriverse: Radical interdependence, autonomy, and the making of worlds*. Durham, NC: Duke University Press.

[17]. Cusicanqui, S. R. (2010). *Ch'ixinakax utxiwa: A reflection on the practices and discourses of decolonization*. Buenos Aires, Argentina: Tinta Limón.

Estimation Method of Rice Fluorescence Emission Spectra from The Image Data and Its Application

Shoji Tominaga[a*], Shogo Nishi[b], and Ryo Ohtera[c]

[a] *Norwegian University of Science and Technology, 2815 Gjovik, Norway, and Nagano University, Ueda 386-1298, Japan*
[b] *Osaka Electro-Communication University, Neyagawa 572-8530, Japan*
[c] *Kobe Institute of Computing, Chuo-ku, Kobe 650-0001, Japan*
**Corresponding author: shojitominaga12@gmail.com*

ABSTRACT

This study proposes a method for estimating the spectral images of fluorescence spectral distributions emitted from rice and shows the experimental results. A multiband imaging system with six channels is constructed by adding optical filters to a mobile phone camera to detect the fluorescence emission in the visible wavelength region. UV light is used to illuminate rice grains and excite the fluorescence emission from the rice grains. We present a method to obtain a reliable estimate of the fluorescence emission spectral distribution at every pixel point from only the acquired image data. A ridge regression approach is adopted, where the fluorescence emission spectrum is estimated by optimally selecting the ridge parameter. Experiments are performed using rice from different origins and storage conditions. The fluorescence emission spectra are estimated using the proposed method on the image data of the respective rice brands. The estimated spectral distributions are compared with direct measurements using a spectroradiometer. The visual appearance of fluorescence emission from the rice grains is rendered using sRGB images. As the applications, we investigate the dependence of fluorescence spectral distribution of rice on the origin, and the fluorescence spectral intensity distributions in different storage conditions to evaluate the freshness of rice.

Keywords: fluorescence emission spectra, spectral estimation method, multiband imaging system, rice fluorescence

INTRODUCTION

Fluorescent substances are commonly found in everyday products such as paper, paint, plastics, and clothing. While, a variety of natural objects exist in addition to man-made ones that emit fluorescence, such as minerals, deep-sea fish, corals, and plants. Among these, plants have recently attracted significant interest as a research topic owing to the need to increase food production [1-3]. Rice has great significance for agricultural production and food market as one of the globally important plant grains. In this study, we estimate the spectral images of fluorescence spectral distributions emitted from rice. Polished rice grains emit fluorescence in the blue-wavelength range. Fluorescence is emitted from lipids (fat) contained in rice, and the intensity of fluorescence increases as lipids are oxidized. After harvest, as time passes, the oxidation of lipids in rice progresses, the fluorescence intensity increases. Therefore, it is reported that the freshness of rice can be predicted by estimating the fluorescence intensity (see [4-5]). The fluorescence spectral distribution of rice also depends on its origins. It is reported that the origin of rice can be identified by estimating its fluorescence spectral distribution (see [6]). However, the previous studies to estimate the fluorescence spectral distribution were based on using a spectrometer. Although such spectrometers as a spectroradiometer, spectrocolorimeter, and fluorescence spectrometer directly measure the spectral distribution of fluorescent emission, the instruments are expensive and poorly portable, and a major issue is that they can only obtain spectral information of one point in a scene.

In this study, we develop an imaging system and algorithm to estimate the distribution of fluorescence emitted by rice as a spectral image. We construct a multiband imaging system by adding the minimum number of necessary filters to a mobile phone camera. Numerous methods have been proposed in the field of color and imaging science and technology for estimating spectral distributions from camera data. However, most of these methods are based solely on the reflected light from a non-fluorescent object and not on emitted light, such as fluorescence. We propose a method to estimate the fluorescence emission spectral distribution at every pixel point from only the acquired image data. We adopt a ridge regression method [7-8]. This approach does not require statistics such as the mean, variance, and autocorrelation matrix.

In the experiments using rice from different origins and storage conditions, UV light illuminates the rice and the emitted fluorescence images are captured using imaging systems. The fluorescence emission spectra are estimated using the proposed algorithm on the image data. These estimates are compared with direct measurements using a spectroradiometer. The visual appearance of fluorescence emission from the respective objects of the rice grains is rendered using sRGB images. As the applications, we compare the spectral distributions of rice from different producing regions. We also compare the spectral distributions of rice stored in different conditions to evaluate freshness of rice.

MULTIBAND IMAGING SYSTEM

A UV LED light (NCSU276A, NICHIA, Tokushima, Japan) was used to excite fluorescence from rice grains. The peak wavelength of the UV-light was 365 nm. As fluorescence emission from rice grains has the spectral distribution in the visible wavelength range, we used a mobile phone camera with RGB channels (iPhone 6s, Apple Inc, Cupertino, CA, USA) and made it multiband. The bit depth of the camera employed is 12 bits. Figure 1 shows the curves of spectral sensitivity functions of the RGB camera [9]. For multiband image acquisition, we selected two color filters from a set of commercial color filters (Fujifilm Optical Filter, Fujifilm, Tokyo, Japan). Combining the filter transmittances with the original spectral sensitivities leads to different sets of trichromatic spectral sensitivity functions. Figure 2 shows the overall spectral sensitivity functions of the present multiband imaging system with six channels, constructed using an RGB mobile phone camera and two color filters. It is noteworthy that this multiband imaging system is available for fluorescence image acquisition over the entire visible range. Each filter was attached to the front of the mobile phone camera lens. The image of each channel was acquired in Adobe's digital negative (DNG) format.

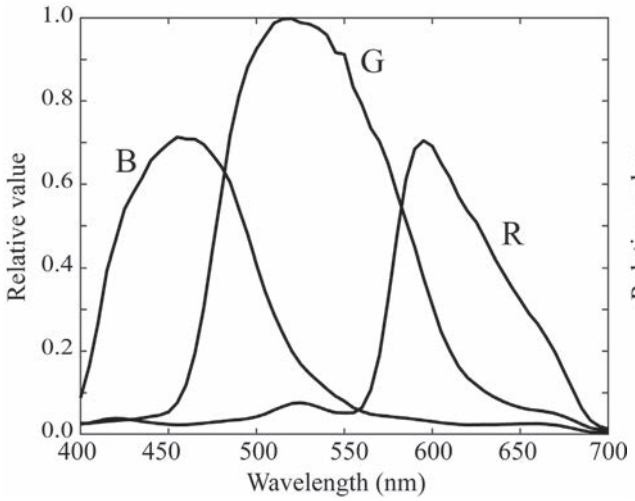

Figure 1: Spectral sensitivity functions of the RGB camera

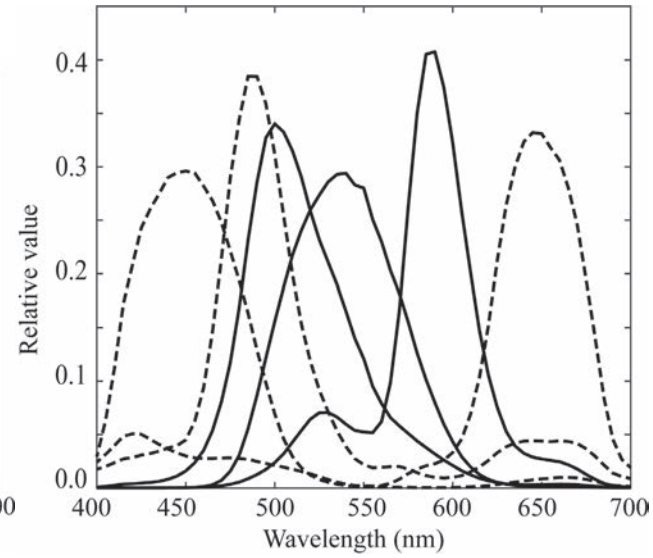

Figure 2: Overall spectral sensitivity functions of the multiband imaging system

SPECTRAL ESTIMATION METHOD

Observation model

We express the six observations y_i (i = 1, 2, …, 6) as

$$y_i = \int x(\lambda) r_i(\lambda) d\lambda + n_i, \tag{1}$$

where $x(\lambda)$ is the spectral-power distribution of fluorescence emitted from the target rice, and $r_i(\lambda)$ (i = 1, 2, …, 6) denote the spectral sensitivity functions of the multiband imaging systems. The wavelength range of integration is in the visible range (400–700 nm). The sensitivity functions $r_i(\lambda)$ are shown in Figure 2, which are defined by the multiplication of the RGB spectral sensitivity functions of the mobile phone camera and spectral transmittance of the additional color filters. Furthermore, n_i denote the noise in the imaging system. We assume that n_i are the white noise with zero mean and the variance a, and are uncorrelated with $x(\lambda)$.

For digital representation, the fluorescence spectra and spectral sensitivities are sampled at N wavelength points at equal intervals, and represented by N-dimensional column vectors as

$$\mathbf{x} = \begin{bmatrix} x(\lambda_1) \\ x(\lambda_2) \\ \vdots \\ x(\lambda_N) \end{bmatrix}, \qquad \mathbf{r}_i = \begin{bmatrix} r_i(\lambda_1) \\ r_i(\lambda_2) \\ \vdots \\ r_i(\lambda_N) \end{bmatrix} (i = 1, 2, ..., 6) \tag{2}$$

The discrete representation of the observation model is then expressed in a matrix form as follows:

$$\mathbf{y} = \mathbf{A}\mathbf{x} + \mathbf{n}, \tag{3}$$

where $\mathbf{A}$ is a (6 × N) matrix defined by the spectral sensitivities and is written as

$$\mathbf{A}^t = \left[\mathbf{r}_1, \mathbf{r}_2, \cdots, \mathbf{r}_6\right] \Delta\lambda \tag{4}$$

and $\mathbf{y}$ and $\mathbf{n}$ are 6-dimensional column vectors written as

$$\mathbf{y} = \begin{bmatrix} y_1 \\ y_2 \\ \vdots \\ y_6 \end{bmatrix}, \quad \mathbf{n} = \begin{bmatrix} n_1 \\ n_2 \\ \vdots \\ n_6 \end{bmatrix} \tag{5}$$

The superscript t and $\Delta\lambda$ in Eq. (4) represent the matrix transposition and wavelength sampling interval, respectively. When the continuous spectra are sampled with $\Delta\lambda$ =5, the discrete spectral functions are represented by 61-dimensional column vectors with N = 61 in 400-700 nm.

Estimation algorithm

We consider a method to estimate the best fluorescence emission spectral distribution from only acquired image data. Let us consider the number of observations p (=6). For $p \geq N$, we have the well-known least-squares solution: Here, we note that $p < N$. In this case, an infinite number of solutions satisfy Eq. (3), and the minimum norm solution among them is often used. However, the minimum norm solution method sometimes has a large estimation error and is not reliable for solving the present problem. In this study, we adopt the ridge regression method [7–8], which estimates the coefficients of multiple regression models in scenarios where the independent variables are highly correlated. Ridge regression can provide a possible solution to the imprecision of minimum norm estimators when linear regression models have highly correlated independent variables. Consequently, the following ridge regression estimator often has a smaller error than the minimum norm estimator.

In the present case, the ridge estimator is expressed as follows:

$$\hat{\mathbf{x}} = \mathbf{A}^t \left(\mathbf{A}\mathbf{A}^t + \alpha \mathbf{I}_p \right)^{-1} \mathbf{y} \tag{6}$$

where $\mathbf{y}$ denotes the p-dimensional observation vector, $\mathbf{A}$ denotes the ($p \times N$) matrix defined in (4), and $\mathbf{I}_p$ denotes the ($p \times p$) identity matrix. The ridge parameter α serves as the constant shifting the diagonals of the matrix $\mathbf{A}\mathbf{A}^t$. Therefore, even if the matrix $\mathbf{A}\mathbf{A}^t$ is nearly singular, the influence of the singularity is alleviated by adding constant elements to the diagonals. To identify the most appropriate ridge parameter α, we can use a cross-validation technique called p-fold cross-validation or leave-one-out [10]. This technique divides the data into p parts, one of which is used as test data, and the remaining p-1 parts are used as training data to evaluate the accuracy rate. Training is performed p times such that all p pieces of data are used as test data once, and then the average accuracy is obtained. The practical algorithm is provided in [11].

EXPERIMENTS

Performance

We examined the performance of the proposed estimation method for rice fluorescence emission spectra using the cultivar “Akitakomachi” harvested in 2023 in Akita Prefecture, Japan. A set of white rice grains was measured after the rice was polished. The rice grains were placed in a transparent box, and while it was illuminated with UV light from the outside, the spectral-power distribution of the fluorescence emitted from the rice grains was measured using a spectroradiometer to validate the estimation results. We captured multiband images of the surface of rice grains using the developed imaging system from the same direction as the spectroradiometer. Observation $\mathbf{y}$ was averaged over an appropriate region of the object’s surface to estimate the spectral distribution of the fluorescence emission. First, the minimum norm estimate was obtained. However, the minimum norm estimate had a large error and was unreliable. Subsequently, the ridge estimation method was applied to the present problem. The optimal value of the ridge parameter α was determined as α =0.106. Figure 3 shows the estimation results, where the estimated spectral curve of $\hat{\mathbf{x}}$ is compared with the direct measurement using the spectroradiometer. Furthermore, we rendered the visual appearance of the fluorescent emission from the entire rice grains as an image. To determine the perceptual color of the fluorescence emission, we first applied the CIE color matching functions to the estimated fluorescence spectrum at each pixel point to obtain the tristimulus values XYZ in the visible wavelength region and then converted them into sRGB values. Figure 4 shows the visual appearance of the fluorescence emission rendered using the sRGB image of the rice grain object.

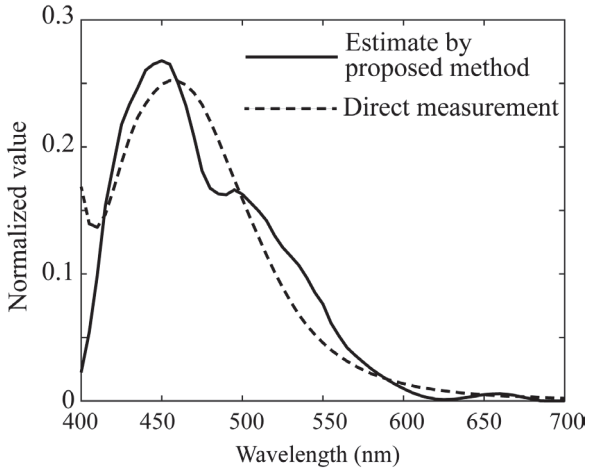

Figure 3: Estimation result for the rice grains of "Akitakomachi."

Figure 4: Visual appearance with an sRGB image.

Applications

We first investigated the dependence of fluorescence spectral distribution of rice on the origin. We collected rice from many different regions, including 10 domestic brands and 3 foreign brands. The spectral curves obtained by the direct measurement using the spectroradiometer were found to be very similar. Therefore, we concluded that it is difficult to estimate the origin of rice based on these spectral distributions of fluorescence emission. Next, we investigated the fluorescence spectral intensity distributions in different storage conditions. The storage conditions were two types of room temperature and frozen in a freezer. Figure 5 shows the spectral intensity distributions in last December estimated by the proposed imaging method under the room temperature and frozen conditions. Note that the spectral intensity distributions under both storage conditions were almost coincident. Figure 6 compares the estimated intensity spectral distributions six months later, in June of this year. The spectral intensity distribution under the room temperature has increased, while the one under the frozen condition was unchanged. Thus, we can see that, as time passes, the oxidation of lipids in rice progresses and the fluorescence intensity increases.

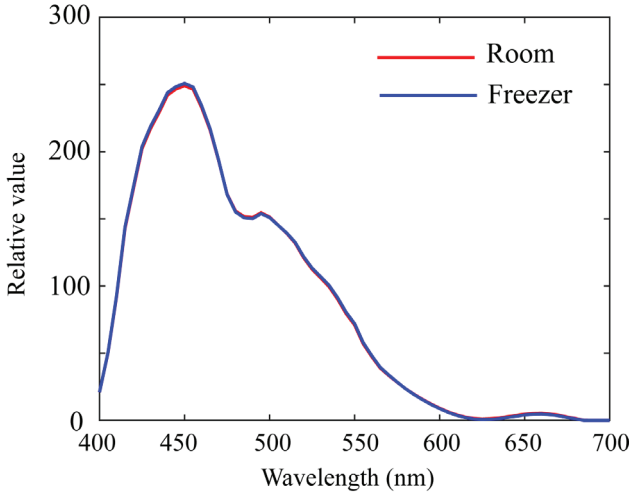

Figure 5: Spectral intensity distributions in last December.

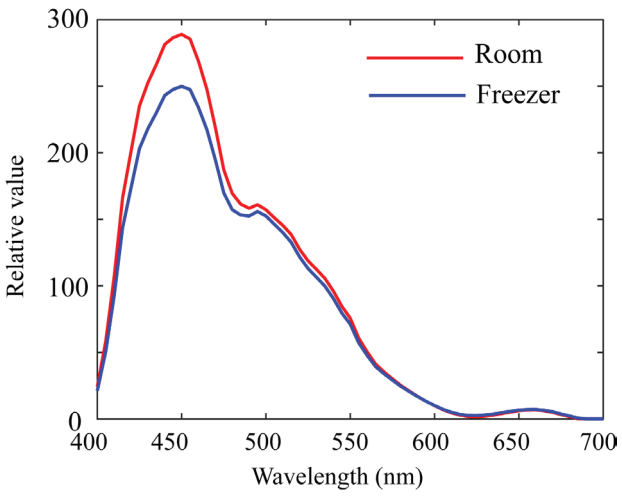

Figure 6: Estimated intensity distributions six months later.

CONCLUSION

We have proposed a method for estimating the spectral images of fluorescence spectral distributions emitted from rice and showed the experimental results. A multiband imaging system with six channels was constructed by adding optical filters to a mobile phone camera. UV light was used to illuminate rice grains and excite the fluorescence emission from the rice grains. A ridge regression approach was adopted to obtain a reliable estimate of the fluorescence emission spectral distribution at every pixel point from only the acquired image data. Experiments were performed using rice from different origins and storage conditions. The estimated fluorescence emission spectra were compared with direct measurements using a spectroradiometer. The visual appearance of fluorescence emission was rendered as sRGB images. As the application results, although it was difficult to estimate the rice origin, we confirmed that as time passes, the fluorescence intensity increased.

REFERENCES

[1]. Hachiya, M., Asanome, N., Goto, T., and Noda, T. (2009). Fluorescence imaging with UV-excitation for evaluating freshness of rice, JARQ 2009, 43 (3), 193–198.

[2]. Mahirah, J. et al. (2019). Rice quality assessment using fluorescence imaging technique, Proc. MSAE 2019, 152–155.

[3]. Tubuxin, B. et al. (2015). Estimating chlorophyll content and photochemical yield of photosystem II (ΦPSII) using solar-induced chlorophyll fluorescence measurements at different growing stages of attached leaves, J. Exp. Bot. 2015, 66 (18), 5595–5603.

[4]. Asanome, N. et al. (2011). Evaluation system for freshness of rice using a fluorescence imaging method with ultraviolet-light excitation, J. Jpn. Soc. Agric. Mach. 2011, 73(4), 263-270.

[5]. Zhou, Y. et al. (2024). Study on the identification of brown rice storage year based on fluorescence spectral fusion technique, Agriculture, 2024, 14, 2041, 1-12.

[6]. Li, C., Tan, Y., Liu, C., and Guo, W. (2024). Rice origin tracing technology based on fluorescence spectroscopy and stoichiometry, Sensors, 24 (2994), 1-10.

[7]. Hoerl, A.E. and Kennard, R.W. (1970). Ridge regression: Biased estimation for nonorthogonal problems, Technometrics 12 (1), 55–67.

[8]. Hoerl, A.E. and Kennard, R.W. (1970), Ridge regression: Applications to nonorthogonal problems, Technometrics, 12 (1), 69–82.

[9]. Tominaga, S., Nishi, S., Ohtera, R. (2021). Measurement and estimation of spectral sensitivity functions for mobile phone cameras, Sensors, 21 (4985), 1-22.

[10]. Kohavi, R. (1995). A study of cross-validation and bootstrap for accuracy estimation and model selection, Proc. 14th Inter. Joint Conf. Artificial Intelligence 1995, 2, 1137–1143.

[11]. Tominaga, S., Nishi, S., Ohtera, R., and Sakai, H. (2025). A method for estimating fluorescence emission spectra from the image data of plant grain and leaves without a spectrometer, Journal of Imaging, 11 (30),1-17.

Preferable Lighting Conditions for Cooking Hamburger Steak

Akari Kagimoto[a*], Yuu Kodama[b], Shino Okuda[b], Katsunori Okajima[c]

[a]*Nara Women's University, Nara, Japan*
[b]*Doshisha Women's College of Liberal Arts, Kyoto, Japan*
[c]*Yokohama National University, Kanagawa, Japan*
[*]*Corresponding author: Akari Kagimoto, kagimoto@cc.nara-wu.ac.jp*

ABSTRACT

Appearances of color and visual texture of objects depend upon spectral power distributions of lighting. Therefore, appropriate lighting conditions for cooking need to be considered to ensure preference or safety to eat. We have revealed that the judgement of the degree of doneness for ground meat is different depending on spectral distributions. However, the desired lighting environment for cooked meat such as hamburger steaks might be different compared to that for just ground meat. In this study, to reveal appropriate lighting conditions for cooking hamburger steaks, we measured *u'*, *v'* chromaticity values of hamburger steaks for some cooked time under some lighting conditions that differ correlated color temperatures (CCTs) and duv values by using two-dimensional luminance colorimeter. Then, we also measured internal temperatures of the hamburger steaks. The obtained chromaticity values were converted to *R*, *G* and *B* values to a display monitor, we conducted a subjective experiment by using the images of hamburger steaks. According to the results, lighting conditions that range from 4000 K to 7000 K in CCTs, and where duv values are close to 0, are preferred for cooking hamburger steaks. It was also shown that lighting conditions of duv value of -0.01 for 4000 K and D65 were less likely to cause misjudgment among the preferred CCTs conditions.

Keywords: color appearance, correlated color temperature, duv, hamburger steak

INTRODUCTION

Recently, LED lighting has been widely popular in homes. We can control spectral distributions more easily by using LED lighting than conventional light sources, so it is possible to provide lighting that is suitable for various daily activities.

One of the daily activities that emphasizes the appearance of objects is cooking. We determine whether the food is cooked based on information about its color and texture. However, appearances of the color and visual texture of the food depend on the spectral distribution of the lighting. In addition, visual palatability [1] and our judgement whether the food is cooked [2] are modulated by the lighting condition. The CIE [3] and Japanese Industrial Standards [4] recommend illuminance and color rendering for various rooms, but do not mention the type of work to be performed in the kitchen.

Minced meat products may cause health problems if they are not fully cooked [5]. Some studies have reported on the color measurement of food during baking [6][7], but these did not cover meat products. Numerous reports have been made on the chemical relationship between meat color and heating [5], but no mention has been made of the relationship with lighting and the appearance of the food. Previously, we have obtained average chromaticity data for 2 cm^2 samples of ground chicken, pork and beef during baking, and showed that how the color changes differ depending on the lighting conditions, and that the judgements whether the minced meats were cooked varied depending on the light color and spectral distributions from the subjective experiments [2].

However, the lighting requirements may differ from those for other types of meat. Thus, to determine the appropriate lighting conditions for cooking hamburger steaks, we measured the surface color and the internal temperature of hamburger steaks during cooking and conducted subjective evaluation experiments using images of the hamburger steaks under different lighting conditions by performing a faithful color conversion method.

METHODOLOGY

We used a white spherical dome to ensure uniform illumination. Figure 1 shows a plan of the apparatus of color measurement. The dome was equipped with two RGB LED lamps [iColor Cove MX Powercore, Philips Color Kinetics] and two white LED lamps [iW Cove MX Powercore, Philips Color Kinetics], each containing three types of LED chips. In addition, two fluorescent lamps of a standard illuminant D65 [FL20s D-EDL-D65, TOSHIBA] were installed in the dome. Table 1 shows all experimental lighting conditions. We prepared 25 lighting conditions which were standard illuminant D65 and 24 conditions by combining different correlated color temperatures (CCTs) and different duv (the distance between the Planckian locus) values. In addition, CIE General Colour Rendering Index (R_a), CIE General Colour Fidelity Index [8] (R_f), and gamut index, IES TM-30 [9] (R_g) were set to be 80 or higher. Each of the three hamburger steaks (A, B and C) of 95 mm in diameter and 15 mm in thickness were cooked in 10 steps (4, 6, 8, 10, 12, 14, 16, 18, 25 and 35 min.) using a microwave toaster oven combination appliance. The internal temperatures of the hamburger steaks were measured every minute using a thermocouple [T35LC, Okazaki Manufacturing Co.]. These hamburger steaks were placed on the stage in the center of the dome. The top surfaces of the hamburger steaks were measured from above by using a two-dimensional luminance colorimeter [UA-1000A, TOPCON Co. Ltd].

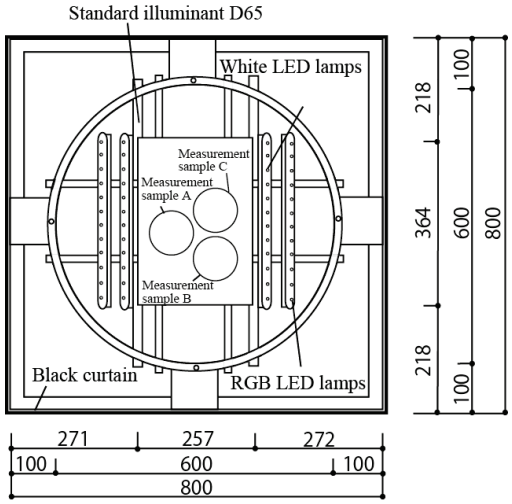

Figure 1: Plan of the measurement apparatus

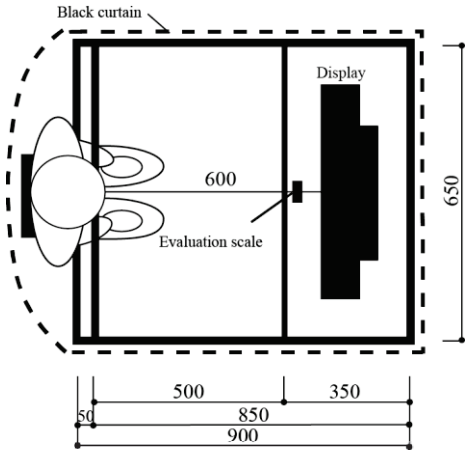

Figure 2: Plan of the experimental space

Table 1: Lighting conditions

CCT	3000, 4000, 5000, 7000, 10000 K (+D65)
Duv	-0.02, -0.01, 0, +0.01, +0.02* (*: except for 3000 K)

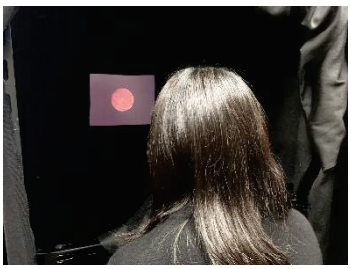

Figure 3: Actual image of the participants

The chromaticity values of each pixel of the hamburger steaks under 25 lighting conditions were transformed into *R*, *G* and *B* values using the calibration data of a display [ColorEdge CG245W, EIZO]. We conducted a subjective experiment using these transformed color data. Figure 2 shows the plan of the experimental space, and Figure 3 shows the actual image of the participants. Twenty-one students in their 20s participated in this experiment from the Department of Food Science and Nutrition at Doshisha Women's College of Liberal Arts who had experience in cooking. They rated "degree of doneness" on a seven-point scale and the "degree of preferable lighting" on a seven-point scale in terms of how easy it was to understand doneness.

RESULTS AND DISCUSSION

The sanitary management of large-scale cooking facilities manual in Japan [10] specifies that food requires cooking must be cooked so that the internal temperature can be held at 75 °C above for at least 1 minute. Table 2 shows the average values of internal temperature in the hamburger steaks while cooking. We measured the internal temperature of each of the three hamburger steaks twice. According to the results, it took approximately 16 minutes for hamburger steak to be cooked.

However, the judgments on the degree of doneness at the same cooking time were different depending on the lighting conditions. Figure 4 shows that 14 minutes was sufficient for the response rate of "cooked" or better. More than 70% of the participants were judged the hamburger steak to be "cooked" or better, even when the cooking time was 14 minutes at duv value of -0.01 for 3000 K, at duv value of 0 for 4000 K, at duv value of -0.02 for 5000 K and at duv value of 0 for 7000 K, suggesting that these lighting conditions are likely to lead to incorrect judgement. On the other hand, less than 50% participants evaluated "cooked" at duv value of -0.01 under 4000 K, duv value of -0.01 under 10000 K and D65.

Table 2: Internal temperature of each three hamburger steaks

Measurements	1st time			2nd time			Average
Hamburger steaks	A	B	C	A	B	C	
Time to reach 75 °C	16.02	14.58	18.46	13.6	20.98	17.44	16.85

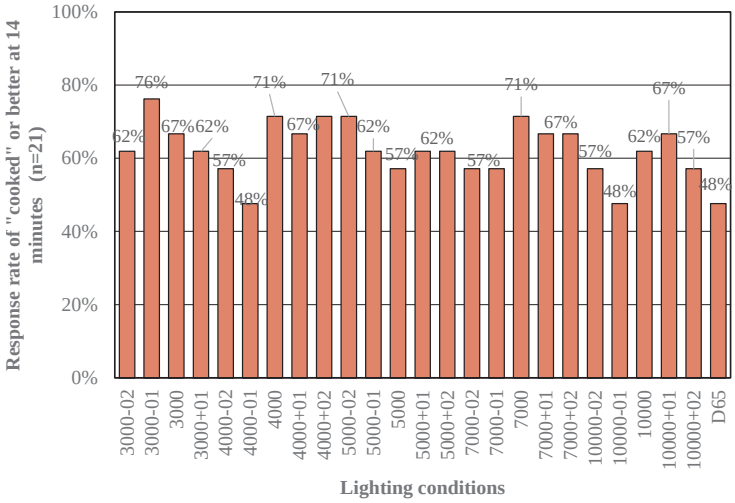

Figure 4: Response rate of "cooked" or better at 14 minutes

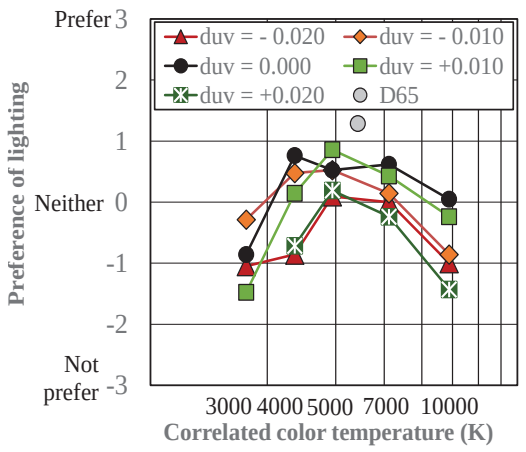

Figure 5: Results of preference of lighting

Figure 5 shows the preference of lighting. The preference depends on the CCTs, it was shown that the range from 4000 K to 7000 K in CCTs is better conditions. It was also shown that duv values of -0.02 and +0.02 conditions were not preferred compared to the other duv value conditions for cooking because the color appearances of the hamburger steaks under these lighting conditions were difficult to understand doneness. According to the results, the lighting conditions of duv value of -0.01 for 4000 K and D65 conditions are better for cooking hamburger steak.

CONCLUSIONS

The perceptual judgment on the degree of doneness of physically identical hamburger steaks depends on the lighting conditions. Duv value of -0.01 for 4000 K and D65 conditions are appropriate for cooking hamburger steak whereas duv values of -0.02 and +0.02 conditions for all CCT conditions, duv value of -0.01 for 3000K, duv value of 0 for 4000 K and 7000 K conditions are inappropriate.

ACKNOWLEDGMENTS

This study is founded by JSPS KAKENHI Grant Number JP17H01947 and JP23K25150 and supported by the Organization for the Promotion of Gender Equality at Nara Women's University.

REFERENCES

[1]. Okuda, S. Okajima, K. and Arce-Lopera, C. (2015). Visual palatability of food dishes in color appearance, glossiness and convexo-concave perception depending on light source. *Journal of Light & Visual Environment*, 39, 8-14.

[2]. Kagimoto, A., Okuda, S., and Okajima, K. (2025). Influence of the illumination on the color and the appearance of meat during baking process. *Journal of Japan Society of Kansei Engneering*, 24(2), 203-209. (in Japanese), doi.org/10.5057/jjske.TJSKE-D-24-00051

[3]. Technical Committee ISO/CIE274. (2025). *Light and lighting – Lighting of work places- Part 1:Indoor*, ISO/CIE 8995-1 1st ed. ISO.

[4]. Japanese Standard Association and the Illuminating Engineering Institute of Japan (2023). *Recommendation for indoor lighting*, JIS Z 9125: 2023. Japanese Standard Association. (in Japanese)

[5]. J. King, N., and Whyte R. (2006). Does it look cooked? A review of factors that influence cooked meat color. *Journal of Food Science*, 71(4), R31-R40.

[6]. Iyota, S., Sakai, H. and Mamiya, Y. (2013). Color measurement methods for optimization of oven operation (baking of sliced bread with superheated steam and hot air). 19(6), 939-947.

[7]. Sakai, H. and Iyota, H. (2013). Sensory evaluation of preference of baked food color. AIC 2013 12th International AIC Congress. Newcatsle Gateshead, United Kingdom.

[8]. TC 1-90. (2017). Colour fidelity index for accurate scientific use. CIE 224:2017. CIE.

[9]. Illuminating Engineering Society. (2020). *ANSI/IES TM-30-20 Method for evaluating light source color rendition*. Lighting Services.

[10]. Ministry of Health, Labor and Welfare. (2017). *Sanitary management of large-scale cooking facilities manual*, Retrieved August 13, 2025, from https://www.mhlw.go.jp/stf/seisakunitsuite/bunya/kenkou_iryou/shokuhin/syokuchu/01.html (in Japanese)

Achievements and Issues Demonstrated by Citizen-Lead Community Development – A Case Study of Citizen-Academia Collaboration

Akiyo Makino[a], Kanako Murakami[b]

[a]*Tokai Gakuen University, Aichi, Japan*
[b]*Kagoshima University, Kagoshima, Japan*

ABSTRACT

This study aims to clarify the achievements and issues of collaboration between universities and a shopping district association in citizen-led community development using local identity colors derived from regional resources. The research area was the Usuki Shopping District in Kagoshima City, Kagoshima Prefecture, Japan. The project was implemented by the Usuki Shopping District Association and led by three members, including the chairman and directors, along with two university researchers. The research period spanned February 2023 to November 2024. This study focuses on the development of "typical Usuki Shopping District colors" derived from local resources. The study consisted of (1) a workshop to identify the local identity colors, (2) impression surveys regarding the shopping district, (3) adjustment of the candidate colors for voting, (4) voting on the local identity colors, and (5) color planning. This study yields several findings. One notable observation is that it took considerable time to reach an agreement within the association; however, once decisions were made, they were rarely overturned. This highlights the importance of dialogue in promoting consensus-building by appropriately using both formal and informal meetings. Moreover, after the candidate colors were selected, the members of the association developed a deeper understanding of the research. Subsequently, they began to suggest concrete ideas and plans that were expected to contribute to community development. This study also identified several important issues. Researchers from universities should provide local residents with clear explanations of the study. Specific goals should be indicated as deliverables. Including a leader who can respond flexibly to carry out the project as well as supportive young board members within the association is crucial.

Keywords: Local identity color, Local resources, Community development, Collaboration

INTRODUCTION

In Japan, following the enactment of the Landscape Act in 2004, a total of 666 landscape plans had been formulated by 816 landscape administration bodies as of March 2024. Approximately 90% of these plans include provisions regarding color schemes. Given the high level of public interest in color, it has become an important element in landscape guidance for residents and local governments. The Environmental Color Research Group at Kagoshima University developed a regional color palette titled Kagonma no Iro® (hereinafter referred to as "Kagonma no Iro"), which aims to visually express the unique identity of Kagoshima Prefecture through colors. This palette was officially announced in 2019 [1]. Since then, Kagoshima University has actively promoted regional revitalization by utilizing Kagonma no Iro in various initiatives, including public relations efforts for the prefecture and the development of local specialty products. Kagonma no Iro was created by surveying the colors of regional resources throughout Kagoshima Prefecture and selecting representative colors through consensus-building with local residents and other stakeholders. Nevertheless, practical knowledge on how to involve residents and manage color-based town development remains limited. Moreover, since the public release of Kagonma no Iro, numerous communities have requested support for the development of palettes that capture the distinctive colors of their areas.

Accordingly, this study aims to elucidate both the achievements and challenges that arise when collaborating with local residents to promote town development based on colors derived from regional resources.

METHODOLOGY

Methodology

The subject of this study is the Usuki Shopping Street, located in Kagoshima City, Kagoshima Prefecture, Japan. The area centers around JR Usuki Station and the Wakida tram stop, spanning across the Usuki 1-chome, 3-chome, and 4-chome districts. It encompasses Usuki Street and the area facing the former national highway. The total length of the shopping street is approximately 550 meters, and the neighboring commercial area has a population of approximately 22,000 as of 2010 [2]. Usuki Shopping Street has actively engaged in community communication by publishing newsletters and disseminating information under the vision of becoming “the most desirable place to live in Kagoshima.” [3]. Consequently, it has gained recognition as a lively shopping district that attracts customers from Japan and abroad. In 2024, it was awarded for the Local Shining Shopping Street Award organized by the Small and Medium Enterprise Agency of Japan, which honors districts that enhance their uniqueness, diversity, and regional value [4]. The study was conducted through a collaborative framework involving the Usuki Shopping Street Promotion Association (hereinafter referred to as “the Association”), led by its chairman and two board members, along with academic experts supporting landscape-based community development. The research period spanned February 2023 to November 2024. This study focuses on the development of colors that represent the unique identity of Usuki Shopping Street, derived from its local resources. The methodology follows the framework of the aforementioned Kagonma no Iro study [1] and includes: (1) a workshop to identify the local identity colors, (2) impression surveys regarding the shopping district, (3) adjustment of candidate colors for voting, (4) voting on the local identity colors, and (5) color planning.

Preparations

As previously reported by Makino and Murakami (2024) [5], initial contact was facilitated by a special research advisor at Kagoshima University who had long been familiar with the initiatives of the Usuki Shopping Street. Through this intermediary, the chairman of the Usuki Shopping Street Promotion Association (hereinafter referred to as “the Chairman”) and the university engaged in discussions on town development using colors derived from local resources and the Kagonma no Iro initiative. These exchanges, held on February 20 and July 7, 2023, led the Chairman to express interest in the project. However, implementing the study required formal approval from the Usuki Shopping Street Promotion Association Board of Directors (hereinafter referred to as “the Board”), comprising ten members. Therefore, a detailed explanation of the proposed study was presented by the university to the Board on September 21 of the same year. The Chairman initiated a motion based on this presentation and officially approved the implementation of the study. In preparation for the study, two individuals with a strong interest in landscape and community development were appointed as key collaborators: one serving concurrently as the vice-chairman and the other as a youth division member and proxy board member. Together with the Chairman, these two representatives formed a core team of three to work collaboratively with the university. A series of planning meetings was held to develop the workshop details, with key discussions taking place on February 29, March 7, and March 28, 2024. Additionally, to ensure the smooth execution of the workshops, the university conducted field surveys in the area surrounding the shopping street on March 28. The Chairman and university representatives visited Usuki Elementary School, provided a briefing on the project, and requested the distribution of promotional flyers to encourage the participation of upper-grade elementary school students deemed suitable for a color-themed workshop. In total, ten preparatory meetings and approximately one year of coordination were required to establish a collaborative framework between the Association and the university. A formal joint research agreement was signed on May 31, 2024.

RESULTS AND DISCUSSION

Workshop

The workshop was conducted on May 19, 2024, with the objective of exploring the distinctive qualities of the shopping district, uncovering their values, and identifying colors that symbolically represent the local character. The participants included four elementary and junior high school students (three boys and one girl; mean age = 10.75 years, *SD* = 1.30), along with board members, parents, and other stakeholders, making up a total of 12 attendees. On the day of the workshop, the university staff served as instructors, providing an overview of the research procedures and guiding all participants in practicing color measurement techniques. The shopping district was pre-divided into two survey areas, designated as Areas A and B (Figure 1). The participants were organized into two groups, and a walking color survey was conducted using a toolkit that included the 2021 L-size Pocket Edition of the Standard Colors for Paints and a semi-structured worksheet developed based on the methodology of Koga et al. (1999) [6] (Figure 2). The weather was clear, and the survey was conducted over a 60-minute period from 11:00 a.m. to 12:00 p.m. The survey identified various locally rooted resources and recorded their corresponding measured color values, including the waiting area of the Wakida tram stop, zelkova, camphor trees, the Tanokami deity statue in Wakida Park, the torii gate of Shinmei Shrine, and the Wakida River (Tables 1 and 2).

Figure 1: Survey areas in the workshop

Figure 2: Survey scenes

Table 1: Color measurement results in survey area A

Items for Investigation (● indicates mandatory items for survey)	Munsell color system	
	Participant 1	Participant 2
● Waiting Room at Wakida Tram Stop (Chairs)	2.5PB5/8	—
● Waiting Room at Wakida Tram Stop (Electronic Display Board)	—	10YR3/2
●Zelkova Tree (Trunk)	2.5Y6/2	—
●Zelkova Tree (Leaves)	—	10Y6/4
●Camphor Tree (Trunk)	10R6/6	—
●Camphor Tree (Leaves)	—	2.5GY8/8
●Tanokami (Rice Field Deity) in Wakita Park	7.5GY8/2	5R5/3
●Sakurajima Eruption Monument in Wakita Park	7.5R4/8	5R5/2
Tanokami (Rice Field Deity) in Usuki 4-chome	10Y6/4	5R4/2

Table 2: Color measurement results in survey area B

Items for Investigation (● indicates mandatory items for survey)	Munsell color system	
	Participant 3	Participant 4
●Streetlights in Usuki Shopping Street	5PB6/8	5PB4/10
●Torii Gate of Shinmei Shrine	8.75R5/12	8.75R5/12
●Wakida river	10YR7/6	10YR5/4
Exterior Wall of the Post Office	2.5G7/2	2.5G5/6
Car Stopper at the Local Bank	1.5Y7.5/14	—
Slide in Wakida Central Park	—	2.5PB4/10

Impression Surveys

As previously reported by Makino and Murakami (2024) [5], an exploratory survey of impression words was conducted among the elementary and junior high school students who participated in the workshop. This was based

on Kobayashi's approach (1997) [7]. Fifteen adjectives written only in hiragana or katakana (to avoid the use of kanji) were prepared: かわいい (cute), エレガントな (elegant), ゴージャスな (gorgeous), ロマンチックな (romantic), シックな (chic), ダイナミックな (dynamic), せいけつな (clean), わかわかしい (youthful), ワイルドな (wild), しぜんな (natural), ダンディな (dandy), じゅうこうな (dignified), カジュアルな (casual), クラシックな (classic), フォーマルな (formal), and モダンな (modern). Participants were asked to select three words that best expressed the qualities of Usuki Shopping Street that they hoped would be preserved in the future. However, some students submitted blank responses because they did not understand the meaning of several terms; consequently, sufficient responses could not be collected from this group. In contrast, responses were successfully obtained from the parents who attended the workshop. Subsequently, the same descriptive word survey was administered between May and July 2024 to a broader group of 20 people, including the board members of the shopping street. The results indicated that the most frequently selected words were "せいけつな (clean)" and "しぜんな (natural)" (both at 20.8%), followed by "カジュアルな (casual)" (18.9%). Using the color analysis software, Image Analyst (Japan Color Design Research Institute), an analysis of the color tendencies associated with these impression words revealed a high affinity for high-lightness, medium- to high-chroma colors spanning from warm to cool hues, and achromatic colors. Simultaneously, an impression survey was conducted in the shopping street. The survey items included "Good qualities of the shopping street," "Things and events characteristic of the shopping street," and "Proposed names for the colors representing the shopping street." Key responses identified "transport convenience," "interpersonal connections," and "the abundance of events" as valued attributes. Typical events cited as characteristics included the Summer Festival, Toka Ebisu, and the Ojyattamonse Market. Regarding color names, "Usuki no Iro" was the most common suggestion, followed by proposals such as "Usuki Wakida Iro," "Usuki Color," and "U-suki Color."

Adjusting the candidate colors

Based on the findings of the workshop and impression surveys, the direction for colors derived from local resources in Usuki Shopping Street was consolidated. For local resources that were not sufficiently identified during the workshop, visual color measurements were conducted using reference materials on the shopping street [3]. When selecting candidate colors, the university referred to Sugiyama's categorization of three landscape color types (natural, social, and cultural) [8] and incorporated locally relevant words and impressions. The visual measurements followed this procedure, and the reference standard colors were selected from the 9th edition of the JIS Standard Color Sample Glossy Series (JIS Z 8721; 2,141 colors). Measurements were taken in accordance with JIS Z8723:2000, using a color comparison booth (byko-spectra mini, BYK-Gardner) illuminated by the standard light source D65. Booth lighting was switched on 30 minutes prior to observation to stabilize illumination. The illuminance across the three points (center and both ends) of the work surface averaged approximately 1,600 lux with a uniformity of 85%. The surface color was a matte achromatic tone with a Munsell value of 7.0. The observer was a certified normal trichromat with demonstrated ability to discriminate between subtle color differences using a color arrangement test device. During the observation, the observer wore a white lab coat to ensure that no strongly colored surfaces were visible in the field of view, other than the samples being tested. The observer took frequent short breaks to maintain visual judgment accuracy. The samples and reference standards were arranged side by side on the same plane, 500 mm from the eyes, and compared at a 45-degree viewing angle under 0-degree illumination. A color-masking frame was used and the viewing angle for each colored area was approximately 2 degrees. From these procedures, the hue, value (lightness), and chroma of each sample were determined using the Munsell color system. They were subsequently categorized using the PCCS system and converted into RGB values using the Color Calc software (Japan Color Research Institute). In subsequent discussions between the shopping street and the university, it was agreed to limit the number of local resources and candidate colors to approximately 30 to facilitate participation by both children and elderly residents. A panel comprising 24 colors grouped into four hue categories was created.

Voting

The community voting event was named the “Usuki no Iro (Provisional) Grand Voting,” an idea proposed by younger board members. It was held on August 31, 2024, during the 41st Usuki Summer Evening Festival (organized by the Usuki Shopping Street) from 3:00 p.m. to 9:00 p.m. under clear weather conditions. A freestanding display board (900 mm high × 1,800 mm wide) featuring the printed color panels was prepared onsite, and visitors were invited to vote. The voters represented a wide range of ages from children to seniors, and 288 ballots were collected. The voting results showed that the camphor tree at Usuki Elementary School ranked first, followed by the city tram and bus and the Shinto priest’s hakama as the top three selections (Table 3).

Table 3: Voting results

rank	Color name ideas	Color images	Number of votes	PCCS
1	Camphor Tree at Usuki Elementary School		47	b10
2	City tram and bus		28	s7
3	Shinto priest’s hakama at Shinmei Shrine		23	lt16
4	Wakida carrots		19	s5
5	Torii gate of Shinmei Shrine		18	s3
6	Lapsana apogonoides		18	lt9
7	Logo color of Usuki Shopping Street		16	v4
8	Kingfisher		15	sf16
9	Ebisu emblem of Usuki Shopping Street		14	v19
10	City bus		13	d12
11	Streetlights in Usuki Shopping Street		11	sf19
12	Zelkova Tree at Usuki Elementary School		10	d10
13	Scutellaria dependens		10	ltg22
14	Silene armeria		10	lt24
15	Wakida River		8	d7
16	Exterior wall of the Post Office		7	ltg12
17	Sakurajima Eruption Monument		5	mGy
18	JR Usuki Station		4	W
19	Tanokami		4	dkg2
20	The traditional stone monument		2	ltGy
21	Waiting Room at Wakida tram stop		2	W
22	Ardea intermedia		2	W
23	The wish-granting stone		1	W
24	Juncus bufonius		1	d4

Color Planning

Based on the results of the grand voting event described above, the high-chroma colors that received the most votes were designated as candidate symbolic colors for the shopping street. On the other hand, although the lower-ranked colors included low-chroma and achromatic tones, shopping street stakeholders expressed the view that they should also be incorporated because of their importance in harmonizing with the surrounding environment and their connection to significant local resources. Consequently, the final color palette, representing the colors derived from local resources in the shopping street, was established by combining both the high-ranking vivid colors and these more subdued tones [9]. Subsequently, members of the shopping district proposed ideas for using these candidate colors to paint the walls of the local elementary school and streetlights. Based on these developments, the members of the association can be said to have developed a deeper understanding of this study through the process from the workshop to the color planning.

CONCLUSION

This study aimed to clarify the achievements and issues of collaboration between universities and a shopping district association in citizen-led community development using local identity colors derived from regional resources. This study had several achievements. One notable observation was that it took approximately one year of preparation, including ten rounds of discussion, to organize the workshop. This highlights that it takes time to reach an agreement within an association, but decisions are rarely overturned. It also underscores the importance of dialogue in promoting consensus building by appropriately using both formal and informal meetings. After the candidate colors were selected, association members developed a deeper understanding of the research. They

subsequently began to propose concrete ideas and plans that were expected to contribute to community development. The study also identified the importance of having a leader who can respond flexibly to carry out such activities, as well as supportive young board members within the association. Several important issues were also identified. In the initial phase, the university may not have fully conveyed to the shopping street community the potential for color development as a means of promoting regional revitalization. Accordingly, it was suggested that the university should make greater efforts to communicate clearly and carefully with local residents, including those in the shopping district, about the impact of color on community building and the specific goals of such initiatives. However, it was inferred that the shopping street required the active participation of key individuals such as leaders who could drive the project forward and younger board members who could work collaboratively to create the color palette, as well as their proactive involvement throughout the process. A remaining challenge identified in this study is how local residents will autonomously consider and implement ways to apply the selected colors to landscape-oriented community development and revitalization of the shopping district.

In conclusion, the collaboration between the university and shopping street successfully yielded meaningful outcomes in developing colors rooted in local resources.

ACKNOWLEDGEMENTS

This study was supported by a grant from the YS City Garden Community Foundation (Grant No. YS City Garden 11–S14). We would like to thank Editage (www.editage.jp) for English language editing.

REFERENCES

[1]. Makino, A., & Kikata, T. (2021). ISSUES RELATED TO COLOR PLANNING FOR LOCAL PLACE BRANDING. AIJ Journal of Technology and Design, 27(66), 991–996. https://doi.org/10.3130/aijt.27.991

[2]. 宇宿商店街振興組合 (2020). PDCA 鹿児島宇宿商店街 2020.

[3]. 宇宿商店街振興組合 (2019).みんなの笑顔が作る商店街 宇宿タウンガイド USUKI TOWN GUIDE.

[4].中小企業庁 (2024). 地域にかがやくわがまち商店街表彰.

https://www.chusho.meti.go.jp/shogyo/shogyo/award/index2024.html (e.g., accessed July 20, 2024)

[5]. Makino, A., & Murakami, K. (2024). Achievements and problems demonstrated by citizen-lead landscape development. SHIKISAIGAKU, 3(3), 139-142.

[6]. Takaaki, K., Akihiko, T., Jun, M., Takaya, K., Kotaroh, H., & Masahito, Y. (1999). PARTCIPATORY RESEARCH OF TOWNSCAPE, USING “CAPTION EVALUATION METHOD” – Studies of the cognition and the evaluation of townscape, Part 1 –. Transactions of AIJ. Journal of architecture, planning and environmental engineering, 64(517), 79-84, https://doi.org/10.3130/aija.64.79_2

[7].小林 重順（1997）. カラーリスト -色彩心理ハンドブック- 講談社.

[8]. Sugiyama, A.（2017）. Report on the municipal government activity of the landscape color education to primary school children. Journal of the Color Science Association of Japan, 41(3), 60-63, https://doi・org/10.15048/jcsaj.41.3__60

[9]. Murakami, K., & Makino, A. (2025). Practical Research of Colors Based upon Local Resources by academia-shopping District Collaboration. Proceedings of the 56th Annual Meeting of the Color Science Association of Japan, 123-126.

Measurement Comparison of Black Tea Color Testing between Tea Testers and Analytical Instruments

Irwan Fathoni[a], Adi Djoko Guritno[b], Anggoro Cahyo Sukartiko[c*], Megita Ryanjani Tanuputri[d]

[a,b,c,d]*Department of Agroindustrial Technology Universitas Gadjah Mada, Yogyakarta, Indonesia*
[*]*Corresponding author: Anggoro Cahyo Sukartiko, cahyos@ugm.ac.id*

ABSTRACT

Black Tea is one of the commodities that is in demand in the world. Some of the main potential risks are poor quality control in handling raw materials and tea quality testing from tea testers, which is prone to deviations compared to quality measuring instruments. This research aims to compare black tea color testing between tea testers and analytical instruments. Black tea color testing involves examining dry tea, brewed tea, and tea dregs using organoleptic methods by four tea testers, as well as utilizing a chromameter and UV-Vis spectrophotometer. The tea sample used was an orthodox tea with variants of *Broken Orange Pekoe* (BOP), *Pekoe Fanning* (PF), *Fanning* II (F II), and Dust. Analysis was used based on the deviation of test data from the average and the gap between subjective testing by tea testers and objective testing with quality analytical instruments. The first two testers yield more consistent results and are nearly equivalent to quality measuring instruments, as they are certified and experienced, compared to the other two. Based on the risk response, deviations and gaps are evaluated in the analysis results. These results will, in the future, enable the development of a risk map matrix, which is used as a risk assessment tool in the risk mitigation process.

Keywords: black tea, chromameter, organoleptic, UV-Vis Spectrophotometer

INTRODUCTION

Black tea (*Camellia sinensis*) is a commodity widely consumed by the world community, especially in Indonesia. The ingestion of black tea is associated with numerous health benefits, including the presence of a complex phenolic compound that is renowned for its antioxidant properties [1], [2], [3]. Apart from that, the unique local taste makes black tea from Indonesia popular even abroad [4]. Black tea has a distinctive color obtained from the manufacturing process. To be able to produce black tea, fresh leaf tea shoots from the garden are served for 12-18 hours at a temperature of 22-28 °C; then the withered leaves are rolled using an automatic rolling machine for 40-50 minutes and continued with wet sorting; tea leaves are transferred to ferment for 20 minutes at 20°C; fermented tea leaves then dried at 50-55°C; then the tea is sorted according to its grade, then packaged and stored [5], [6]. This process will cause redness in black tea [2]. After the production stage, black tea will be divided into several quality grades, such as leafy, broken, small, and mixed. Tea testers will perform organoleptic testing by seeing, smelling, and tasting it [7],[8].

One of tea plantation company in Indonesia is PT Pagilaran, which is one of the largest tea plantation companies in Central Java province. Orthodox black tea produced by PT Pagilaran has its characteristics in color, taste, and aroma, and it is usually used as a central blend by consumer companies. Black tea is susceptible to fungal attacks after fermentation, affecting its quality, especially in terms of taste [9]. The volume of tea exported decreased by 5% between 2015 and 2020, which weakened the competitiveness of Indonesian tea in the global market [10]. The poor quality of the tea leaves also contributed to this situation [11]. At present, the quality control of black tea

is still subject to subjective sensory methods, resulting in test results that vary between tea testers. Testing carried out by tea testers is subjective, while testing using quality measuring instruments is objective. Both testing methods may result in any gap in the value. This research aims to compare black tea color testing between tea testers and analytical instruments. The comparison is based on a quality control process by tea testers and quality measurement instruments.

METHODOLOGY

This study was conducted using a quantitative and qualitative approach. The qualitative approach is carried out by processing data from tea testers' black tea color test results and using quality measuring instruments such as chromameters and spectrophotometers. The tea sample used was an orthodox tea with variants of *Broken Orange Pekoe* (BOP), *Pekoe Fanning* (PF), *Fanning* II (F II), and Dust. In this brewing process, based on SNI 1902:2016, dry tea was weighed with a mass of 5.68 grams and put into a 280 ml trial cup. Bring pure water (with a pH of 7 or usually deionized water (DI)) to a boil, wait 10 seconds, pour it into a test cup containing tea, cover it, and let it stand for 6 minutes. Pour the brewed tea into the trial bowl, fill it, and make sure no tea dregs enter it. The tea dregs are squeezed so that the water content is reduced and transferred from the test glass to the lid of the test glass in an inverted position, or the tea dregs can be moved to a glass plate and pressed with another glass plate to remove the dregs. Based on SNI 1902:2016, color testing is done by smearing a tea sample on a black base and observing the color. The assessment is carried out based on the color of the tea, from good to bad.

Brewed tea samples were tested for color using an Ultraviolet-Visible (UV-Vis) Spectrophotometer (Jenway 6305). The wavelength used for black brewed tea samples is between 380 to 570 nm [12],[13]. Experiments were conducted to find the highest absorbance value by adjusting the wavelength by 10 nm from 380 to 570 nm [14]. The wavelength setting is stopped at the wavelength with the highest absorbance value or after the device has read the absorbance value. The wavelength with the highest absorbance value is the wavelength with a particular color that is most absorbed. From these wavelengths, complementary colors or colors can be seen in the brewed tea sample. The wavelength used must be the highest absorbance value of the solution being tested because it has great sensitivity [15]. The absorbed and complementary colors can be seen in Table 1. The color of the brewed tea can be tested by a tea tester using criteria including the type of color, concentration, clarity, brightness, and life characteristics of the water. The assessment was made based on the color of the brewed tea. Meanwhile, tea dregs were put on the lid of the experimenter's cup in an upside-down position to visually test the color of the tea dregs and the evenness of the tea dregs. The characteristics of dry tea, brewed tea, and tea dregs can be seen in Table 2.

Table 1: Absorbed and complementary colors

Wavelength Color (nm)	Absorbed Color	Complementary Color	Wavelength Color (nm)	Absorbed Color	Complementary Color
400 – 435	Violet	Yellowish green	560 – 580	Yellowish green	Purple
435 – 480	Blue	Yellow	580 – 595	Yellow	Blue
480 – 490	Greenish blue	Orange	595 – 610	Orange	Greenish blue
490 – 500	Bluish green	Red	610 – 800	Red	Bluish green
500 – 560	Green	Violet			

Color measurements were carried out at each test interval on dry tea and tea dregs using a tristimulus chromameter color analyzer (CR-400 Series, Konica, Minolta Optics Inc., Japan) calibrated with a white porcelain reference plate. The chromameter takes three consecutive readings and produces an average number for each sample. Color parameters are quantified using the chromameter's CIELAB parameters (L*, a*, b*) [16]. The brightness level is indicated by the symbol L*. Meanwhile, the chromatic color intensity will be marked by the symbols a* and b*. The symbol a* will represent the chromatic color value, indicating red and green with a +a value for red and a value -a for green. The symbol b* indicates the chromatic color values of blue and yellow, with +b for yellow and -b for blue [17], [18], [19], [20].

RESULTS AND DISCUSSION

In the black tea color test, a score is used to classify the color of the tea from good to bad. The scoring used is based on the color of dry tea with grades A, B, C, D, and E; brewed tea with grades 5, 4, 3, 2, and 1; and tea dregs with scores a, b, c, d, and e. Because the score is ordinal scale data, it cannot be compared with test data from quality measurement instruments on a ratio scale.

In the initial trial, standard tea was used to convert ordinal scale score data into ratio scale data. The conversion table is created by using standard tea with a score which has been agreed upon by tea testers. This standard is then tested using a chromameter for dry tea and tea dregs, then a spectrophotometer for tea brewing water. The value of each tea color score can be used to convert the color test score carried out by a tea tester on an ordinal scale into a ratio scale value, such as the value issued from a quality measurement instrument. This aims to ensure that the test data from the tea tester can be compared with data from the quality measurement instrument. The results of the standard tea conversion can be seen in Table 3. Each grade level has a pattern of increasingly larger values, such as the value at each brewed water grade level. In dry tea and tea dregs, only a few parameters do not have a pattern of increasing values. However, the L*a*b* parameter values in dry tea and tea dregs are one integral component in defining color, so they are not independent. Therefore, this value can be used as a conversion of primary data for color testing carried out by tea testers to compare the data with data from quality measuring instruments later. Similar research has also been conducted to determine the value of the L*a*b* parameters in assessing the freshness level of spinach [21] and to standardize the grade of Aucklandia root according to its color, as used in Traditional Chinese Medicine (TCM) [22]. When compared with previous research, in this initial trial to create tea standards according to color, only tea samples from one location were used, that is, the plantation owned by PT Pagilaran. The tea standard results in this initial trial can only be used in one location, PT Pagilaran.

Table 2: Black Tea Characteristics

Dry Tea			Brewed Tea			Tea Dregs		
Score	**Appearance**	**Characteristic**	**Score**	**Appearance**	**Characteristic**	**Score**	**Appearance**	**Characteristic**
A		blackish	5		very bright and colorful	a	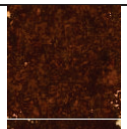	very bright and coppery
B	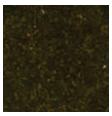	brownish black	4		bright and colorful	b		bright and coppery
C		black, brown to reddish	3		bright	c		fairly bright
D		reddish to grayish	2		light and bright	d		greenish
E		greyish	1		very dull	e		dull

The results of the color test for brewed tea, dry tea, and tea dregs were conducted by four tea testers (T1, T2, T3, and T4) with organoleptic methods and quantitatively tests using chromameter and spectrophotometer. The data from the results of the test by the tea testers was presented in converted form based on the values of quality measuring instrument parameters (wavelength and L* a* b*). The samples used were three samples for each tea

variant; therefore, the data displayed was the average of the results from the three samples. Tea testers' use of organoleptic methods in determining the quality grade of black tea may yield subjective results that correspond to the personal perception of each tea tester. These subjective evaluations lack scientific validation and cannot be standardized. In the tea industry, they can be considered a potential risk to quality and quantity, which may lead to vulnerability in operations [23, 24]. Therefore, electronic alternatives are needed to validate the tea tester's efforts [8] scientifically.

Table 2: Standard Tea Conversion

Score	L*	a*	b*	Score	Wavelength (nm)
Dry Tea				**Brewed Tea**	
A	34.37 ± 0.34	1.63 ± 0.14	4.52 ± 0.14	5	420.67 ± 2.31
B	34.78 ± 0.10	1.52 ± 0.14	4.36 ± 0.15	4	432.00 ± 1.00
C	35.05 ± 0.25	1.53 ± 0.09	4.71 ± 0.19	3	438.67 ± 2.52
D	39.82 ± 0.22	1.54 ± 0.08	8.85 ± 0.15	2	443.33 ± 1.53
E	38.31 ± 0.90	2.14 ± 0.33	8.26 ± 0.67	1	453.00 ± 2.65
Tea dregs					
a	33.86 ± 0.39	2.62 ± 0.16	5.76 ± 0.22		
b	32.68 ± 0.42	2.47 ± 0.13	5.59 ± 0.23		
c	30.94 ± 1.16	4.84 ± 0.17	8.47 ± 0.89		
d	33.80 ± 0.15	3.47 ± 0.33	6.47 ± 0.36		
e	32.75 ± 0.26	3.47 ± 0.15	4.22 ± 0.20		

During the three color tests using organoleptic and color measurement instruments, each deviation analysis was carried out to determine how far the data deviated from the average. This analysis was carried out by separating all color parameters, which were L*, a*, and b*, and wavelength (nm), to compare the results of the tests conducted by the tea testers and the testing device for all tea variants: BOP, PF, F II, and Dust. Furthermore, data from the four tea testers and quality measuring instruments on one of the tea variants and color parameters (L*, a*, b*, and wavelength (nm)) were averaged. An example of a deviation analysis is shown in Figure 1.

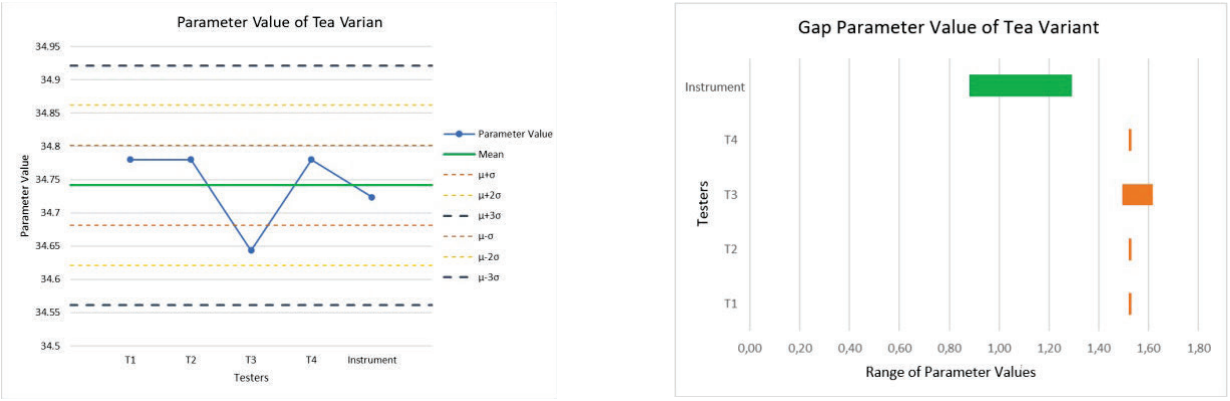

(a) (b)

Figure 1: (a) Deviation analysis diagram of the parameter value of the tea variant, and (b) Gap analysis on the parameter value of the tea variant

Figure 1 (a) shows the graph of the deviation analysis carried out on the parameter value of the tea variant. The upper limit (μ+σ, μ+2σ, μ+3σ) and lower limit (μ-σ, μ-2σ, μ-3σ) were determined, indicating the level of risk of deviation from each data set against the average. Deviations with a low-risk level occurred when the data fell between the limits of μ+σ to μ-σ, deviations with medium risk levels were between the limits of μ+σ to μ+2σ and between the limits of μ-σ to μ-2σ, deviations with a high-risk level were between the limits of μ+2σ to μ+3σ and

between the limits of μ-2σ to μ-3σ, and deviations with a very high-risk level occurred above the limit of μ+3σ and below the limit of μ-3σ. In addition to deviation analysis, a gap evaluation (Figure 1b) was also carried out by comparing the test results of the four tea testers with those of the quality measuring instruments. If the two test results did not match or a gap was observed, it was likely that the test results between the tea testers and the testing equipment were not the same, which could result in a fatal/high-risk. The analysis as a whole was also carried out on all tea variants (BOP, PF, F II, and Dust) and all color parameters (L*, a*, b*, and wavelength (nm)).

CONCLUSION

Color is one of the important components in black tea quality. The tea tester always carries out the quality control process by testing the black tea during the production process to keep the commodity in line with the standard. Since tea testers have a big responsibility in risk management on black tea quality, an assessment was conducted to determine their consistency with the applicable standards. The first two testers yield more consistent results and are nearly equivalent to quality measuring instruments, as they are certified and experienced, compared to the other two.

ACKNOWLEDGEMENTS

The authors would like to thank the Ministry of Education, Research, and Technology for funding this research.

REFERENCES

[1] A. U. P. Djuardi, N. D. Yuliana, M. Ogawa, T. Akazawa, and M. T. Suhartono, “Emulsifying properties and antioxidant activity of soy protein isolate conjugated with tea polyphenol extracts,” *J. Food Sci. Technol.*, vol. 57, no. 10, pp. 3591–3600, 2020, doi: 10.1007/s13197-020-04391-9.

[2] M. Zareef *et al.*, “Rapid screening of phenolic compounds in congou black tea (Camellia sinensis) during in vitro fermentation process using portable spectral analytical system coupled chemometrics,” *J. Food Process. Preserv.*, vol. 43, no. 7, 2019, doi: 10.1111/jfpp.13996.

[3] D. O?neill Rothenberg and L. Zhang, “Mechanisms underlying the anti-depressive effects of regular tea consumption,” *Nutrients*, vol. 11, no. 6, 2019, doi: 10.3390/nu11061361.

[4] D. Ralisnawati, A. C. Sukartiko, A. Suryandono, and K. Triyana, “Detecting aroma changes of local flavored green tea (Camellia sinensis) using electronic nose,” in *IOP Conference Series*, 2018. doi: 10.1088/1755-1315/131/1/012004.

[5] M. K. Lee *et al.*, “Characterization of catechins, theaflavins, and flavonols by leaf processing step in green and black teas (Camellia sinensis) using UPLC-DAD-QToF/MS,” *Eur. Food Res. Technol.*, vol. 245, no. 5, pp. 997–1010, 2019, doi: 10.1007/s00217-018-3201-6.

[6] L. Zhang *et al.*, “Multivariate effects of Chinese keemun black tea grades (Camellia sinensis var. sinensis) on the phenolic composition, antioxidant, antihemolytic and cytotoxic/cytoprotection activities,” *Food Res. Int.*, vol. 125, 2019, doi: 10.1016/j.foodres.2019.108516.

[7] M. Fitzgerald, M. Heinrich, and A. Booker, “Medicinal plant analysis: A historical and regional discussion of emergent complex techniques,” *Front. Pharmacol.*, vol. 10, 2019, doi: 10.3389/fphar.2019.01480.

[8] S. Ghosh, B. Tudu, N. Bhattacharyya, and R. Bandyopadhyay, “A recurrent Elman network in conjunction with an electronic nose for fast prediction of optimum fermentation time of black tea,” *Neural Comput. Appl.*, vol. 31, pp. 1165–1171, 2019, doi: 10.1007/s00521-017-3072-y.

[9] S. Hu *et al.*, “Changes of fungal community and non-volatile metabolites during pile-fermentation of dark green tea,” *Food Res. Int.*, vol. 147, 2021, doi: 10.1016/j.foodres.2021.110472.

[10] D. G. of Estate Crops, *Tree crops estate Statistics of Indonesia 2018-2022*. Jakarta: Directorate General of Estate Crops, 2022.

[11] M. R. Tanuputri and H. Bai, “A framework to build a resilient supply chain: a case study of?Javanese tea in Indonesia,” *Int. J. Logist. Manag.*, vol. 34, no. 6, pp. 1629–1648, 2023, doi: 10.1108/IJLM-11-2021-0558.

[12] C. Liu *et al.*, *Differences in the quality of black tea (Camellia sinensis var. Yinghong No. 9) in different seasons and the underlying factors*. Food Chemistry: X, 20, 2023. doi: 10.1016/j.fochx.2023.100998.

[13] L. T. Meguekam, M. M. Zamfirache, V. D. Taffouo, and C. D. Jit?reanu, “Effect of sodium chloride on physiological, biochemical traits, and mineral nutrition inhibition of peanut varieties in large temperature fluctuations,” *Plant Stress*, vol. 6, 2022, doi: 10.1016/j.stress.2022.100123.

[14] S. Nurmilah, Y. Cahyana, and G. L. Utama, “Metagenomics analysis of the polymeric and monomeric phenolic dynamic changes related to the indigenous bacteria of black tea spontaneous fermentation,” *Biotechnol. Reports*, vol. 36, 2022, doi: 10.1016/j.btre.2022.e00774.

[15] H. Wardiyah, Y. Alioes, and D. Pertiwi, “Perbandingan Reaksi Zat Besi Terhadap Teh Hitam dan Teh Hijau Secara In Vitro dengan Menggunakan Spektrofotometer Uv-Vis,” *J. Kesehat. Andalas*, vol. 3, no. 1, 2014, [Online]. Available: http://jurnal.fk.unand.ac.id

[16] S. G. Nkhata, “Total color change (?E?) is a poor estimator of total carotenoids lost during post-harvest storage of biofortified maize grains,” *Heliyon*, vol. 6, no. 10, 2020, doi: 10.1016/j.heliyon.2020.e05173.

[17] D. Gunasekara, A. Bulathgama, and I. Wickramasinghe, “Comparison of Different Hydrocolloids on the Novel Development of Muffins from ?purple Yam?,” *Dioscorea alata) Flour Sensory, Textural, Nutr. Asp. Int. J. Food Sci.*, vol. 2021, 2021, doi: 10.1155/2021/9970291.

[18] N. P. Mart?n, N. M. Schreurs, S. T. Morris, N. L?pez-Villalobos, J. McDade, and R. E. Hickson, “Meat quality of beef-cross-dairy cattle from Angus or Hereford sires: A case study in a pasture-based system in New Zealand,” *Meat Sci.*, vol. 190, 2022, doi: 10.1016/j.meatsci.2022.108840.

[19] A. Y. Pekel, “al,” *k, A., Alata?, M. S., Kuter, E., Cengiz, Omurtag, G. Z., Ina. G. Eval. Correl. between Nutr. Fat. Acids, Heavy Met. Deoxynivalenol Corn (Zea mays L.). J. Appl. Poult. Res.*, vol. 28, no. 1, pp. 94–107, 2019, doi: 10.3382/japr/pfy023.

[20] G. Sun, Y. Xiong, X. Feng, and Z. Fang, “Effects of incorporation of hempseed meal on the quality attributes of chicken sausage,” *Futur. Foods*, vol. 6, 2022, doi: 10.1016/j.fufo.2022.100169.

[21] K. Koyama, M. Tanaka, B. H. Cho, Y. Yoshikawa, and S. Koseki, “Predicting sensory evaluation of spinach freshness using machine learning model and digital images,” *PLoS One*, vol. 16, no. 3, Mar. 2021, doi: 10.1371/journal.pone.0248769.

[22] J. bo Wang *et al.*, “Colorimetric Grading Scale Can Promote the Standardization of Experiential and Sensory Evaluation in Quality Control of Traditional Chinese Medicines,” *PLoS One*, vol. 7, no. 11, 2012, doi: 10.1371/journal.pone.0048887.

[23] A. D. Guritno, N. N. Aini, M. S. Dharmawati, and E. S. Rahayu, “Development of ready-to-drink tea with Lactobacillus plantarum Dad-13 based on the vulnerability aspects of the production process,” *Food Res.*, vol. 7, no. 2, pp. 143–153, 2023, doi: 10.26656/fr.2017.7(2).957.

[24] A. D. Guritno, “Supply Chain Risk Management: An Approach to Reduce The Agricultural Product's Logistics Costs,” *ICoA Conf. Proc.*, vol. 3, no. 3, p. 6, 2016, doi: 10.18502/kls.v3i3.397.

Analysis of Fresh Organic Vegetable Quality at The Farmer and Distributor Levels based on Color and Texture Measurements

Dionisius Marlon Ayofi[a] , Anggoro Cahyo Sukartiko[a], Megita Ryanjani Tanuputri[a*]

[a]*Department of Agroindustrial Technology, Faculty of Agricultural Technology, Universitas Gadjah Mada, Yogyakarta, Indonesia*
[*]*Corresponding author: Megita Ryanjani Tanuputri, megita.ryanjani@ugm.ac.id*

ABSTRACT

Fresh organic vegetables are increasingly demanded by health-conscious consumers, yet their quality is highly vulnerable to risks across the supply chain. This study analyzes the physical quality parameters of organic tomatoes, carrots, and cabbages at the farmer and distributor levels, with the goal of analyzing risks based on the quality parameters and proposing mitigation strategies. Samples were collected using stratified random sampling and tested based on Indonesian National Standards (SNI). Color analysis was conducted using an RGB model by placing the sample in a photo studio foldable-box LED6000K lamp and photographed using a Nikon D3100 DSLR camera with fixed settings then proceed with ImageJ software, while texture was measured using a Fruit Hardness Tester (FHT200). Results show that tomato samples at the farmer level had an average RGB value of 125±14 and hardness of 8.71±2.02 N/m², compared with 136±14 and 7.22±1.44 N/m² at the distributor level, reflecting both ripening and a decline in firmness. Carrots exhibited consistent color values between farmers (137±10 RGB) and distributors (134±11 RGB), with a slight increase in texture hardness at the distributor stage (78.72±14.09 to 82.30±10.32 N/m²) due to sorting and handling. Cabbages showed relatively stable greenish-white coloration (130±13 vs. 128±5 RGB), though minor cleanliness differences were noted between tiers. Findings highlight that physical quality is strongly influenced by harvesting, handling, and transportation practices, with tomatoes being most susceptible to deterioration. To sustain quality, supply chain actors must strengthen material handling procedures, adopt standardized operating practices, and implement preventive measures against pests and distribution-related damage.

Keywords: Color test, organic vegetables, quality parameter, RGB, supply chain

INTRODUCTION

The agricultural sector in Indonesia is one of the main sectors driving the Indonesian economy. The agricultural sector also promotes job creation and is the cornerstone of national food security. Currently, the agricultural sector in Indonesia is beginning to venture into organic and environmentally friendly farming practices, one of which is for fresh vegetable commodities. The transition to organic vegetable agriculture has become a priority as public awareness of the importance of healthy and sustainable food consumption has grown. Organic food consumption significantly impacts consumer health and environmental sustainability [1]. Organic vegetable production is attracting attention because sustainability is key to healthy food. Organic food can significantly benefit from increased consumer health awareness [2]. According to the Indonesian Organic Alliance (AOI) in 2023, organic vegetables were the top three choices for consumers of organic products: 23% for organic vegetables, 21% for organic rice, and 18% for organic fruit [3]. Organic vegetable products are characterized by being pesticide-free and possessing natural ingredients, which is why consumers strongly consider purchasing organic vegetables. There are several reasons why consumers choose to consume organic vegetables, primarily due to health considerations

and partly due to following trends [4]. Organic agricultural cultivation must be managed professionally by farmers and producers to meet market needs in terms of quality, quantity, and continuity [5].

As with other agro-industrial products, organically grown vegetables are also perishable. They have a very limited shelf life before they can be marketed [6]. Organic vegetable products have a higher antioxidant content, such as polyphenols, flavonoids, and vitamin C. Organic vegetable products are also often chosen by consumers because they do not contain pesticide residues, which can have harmful effects on the human body [7]. Individuals who consume organic foods have lower levels of pesticides in their bodies [8]. There are several challenges in the fresh organic vegetable supply chain in Indonesia. In addition to the risk of organic farming systems being more vulnerable to pest attacks because they do not use pesticides, there are distribution risks because the process of delivering organic vegetables from each tier uses different vehicles. The condition of the product during transport also greatly affects product quality. The risk of damage during distribution using vehicles will directly affect the physical quality of organic vegetables. Quality attributes are specific parameters that can be used to evaluate product quality. Quality attributes are used to ensure that a product meets the standards desired by consumers, regulations, and the market. Quality attributes are important for a product because standards and regulations can ensure product compliance with national regulations, such as the Indonesian National Standard (SNI). Therefore, this study was conducted with the aim of analyzing the quality of fresh organic vegetables at the farmer and distributor levels.

METHODOLOGY

This research was conducted in the Special Region of Yogyakarta during March to June 2025. This study analyzed the quality parameters at each tier of the organic vegetable supply chain. Primary data on organic vegetable quality parameters was obtained from testing samples of tomatoes, carrots, and cabbage. Attribute determination is carried out for further quality testing. The quality attributes determined for testing are physical quality based on SNI (Indonesian National Standard). Physical testing includes color, size, and texture. Physical quality testing requires sample preparation. This testing is conducted to determine the quality of organic vegetables. The organic vegetables selected for physical quality testing are tomatoes, carrots, and cabbage. The organic vegetables selected represent each type of vegetable: tomatoes are fruit vegetables, carrots are root vegetables, and cabbage is leafy vegetables. The selection of these vegetables is also based on the consistent volume of vegetables available to farmers and distributors. Furthermore, the organic vegetables selected are those registered or certified by the Indonesian National Standard (SNI). Tomatoes meet SNI 01-3162-1992, carrots meet SNI 3163-2014, and cabbage meet SNI 01-3174-1998. Based on the sampling guidelines outlined in the SNI for tomatoes, carrots, and cabbage, samples were taken using stratified random sampling. This technique was chosen to ensure that the samples taken represent one basket of harvested produce per tier. Harvested vegetables were placed in one basket, from one basket of harvest, with vegetables taken from the top, middle, and bottom. From each of these strata, samples were taken randomly to obtain at least 10 samples so that the total sample reflected variations that may occur due to stacking and placement in the basket. Testing was conducted at each tier of the supply chain, and the samples obtained from each tier of the supply chain were carried in Styrofoam boxes and ice packs.

Color testing was done by capturing images of organic vegetable products. The images were taken in a foldable-box photostudio measuring 22 x 23 x 24 cm with 6000K LED lights at the front and rear, with a white background. The images were taken using a Nikon D3100 DSLR camera with the same settings, namely a wide angle of 18 mm, aperture of f/5, shutter speed of 1/100 second, ISO 400, exposure of 0, and no flash compulsory. The images were then analyzed for color parameters using the RGB (Red Green Blue) color model with a score of 0-255 using ImageJ software. This color model is the lighting color of the base color, which when combined will produce white. Next, the size of the organic vegetables was measured using scales, and the length was measured using a ruler with an accuracy of 0.1 cm, referring to SNI. The texture of the organic vegetables was tested by analyzing the hardness of the organic vegetables using a Fruit Hardness Tester FHT200 with a basic accuracy of 0.5% and a penetrometer of 3 mm for tomatoes and 66 mm for carrots.

RESULTS AND DISCUSSION

In the Special Region of Yogyakarta, the organic vegetable supply chain involves organic vegetable players such as farmers and farmer groups, distributors, modern markets, and end consumers. The organic vegetable supply chain is also supported by government agencies, including the Yogyakarta Provincial Department of Agriculture and Food Security. The market for organic vegetables is smaller than that of conventional vegetables, and the supply chain is shorter because the organic vegetable market is clearly segmented. In this study, we identified the organic vegetable supply chain in the Special Region of Yogyakarta, as shown in **Table 1.**

Table 1. Supply chain stakeholders

Tier	Process	Notes
Farmer and Farmer Group	1. Planting 2. Maintenance 3. Harvest 4. Selling	Carrying out the organic vegetable production process on the land, carrying out land maintenance, harvesting, and making sales to business units or directly to consumers.
Distributor	1. Packaging 2. Storage 3. Shipping 4. Payment	The process of purchasing vegetables from farmers with an agreed agreement, carrying out the packaging process including labeling, storing before sending, and making deliveries, as well as payments to farmers.
Market	1. Purchasing 2. Selling	Make purchases from distributors then sell to end consumers.
Consumer	1. Purchasing	Purchase organic vegetables from the market.

The physical aspect of organic vegetables is important to consumers. Human perception of color has been used to identify and clarify matured agroindustrial products such as vegetables and fruit [9]. The results of testing the physical parameters of organic vegetables for tomatoes, carrots, and cabbage are presented in terms of color, weight, length, and texture at the farmer and distributor levels. Test results for 20 samples of fresh tomatoes at the farmer level showed good quality based on physical quality parameters. All samples taken had variety uniformity, indicating consistency in variety form. The color of fresh organic tomatoes varied considerably from green, reddish green, to dark red. This color variation indicates different harvest phases, but is still within the range acceptable to agribusiness.

Furthermore, the results of fresh tomato quality specification tests at the distributor tier show variety uniformity, indicating consistency in the round shape variety. The ripeness level of organic tomatoes is also uniform, but there are organic tomatoes that are still reddish green and orange in color. When compared to the farmer tier, reddish green color is not commonly found, as organic tomatoes have undergone a more mature color change. Differences in the handling and storage of tomatoes affect the color intensity of tomatoes, which reflects the level of freshness, ripeness, and potential for physical damage. The results of measuring the color of tomatoes are shown in **Figure 1a**. Each R (red) value is dominant compared to the G (green) and B (blue) values, which means that the red color is dominant in tomatoes, which is also related to the level of ripeness. The dominance of red also increases from the farmer to the distributor, indicating that the tomatoes are riper at the distributor tier. Changes in the color of ripe tomatoes can be identified by an increase in the RGB value [10]. At the distributor tier, some tomatoes show black spots or dirt, which are likely the result of pests or insects on the harvested plants. Some damage to organic tomatoes, such as scratches, bruises, and dents, was also found, one of which was caused by improper material handling and transportation from farmers to distributors. Furthermore, the texture test results on fresh organic tomatoes showed a decrease in the hardness of fresh tomatoes, where the farmer tier had an average texture of 8.71 N/m^2, while the distributor tier had an average texture of 7.22 N/m^2 (**Figure 1b**).

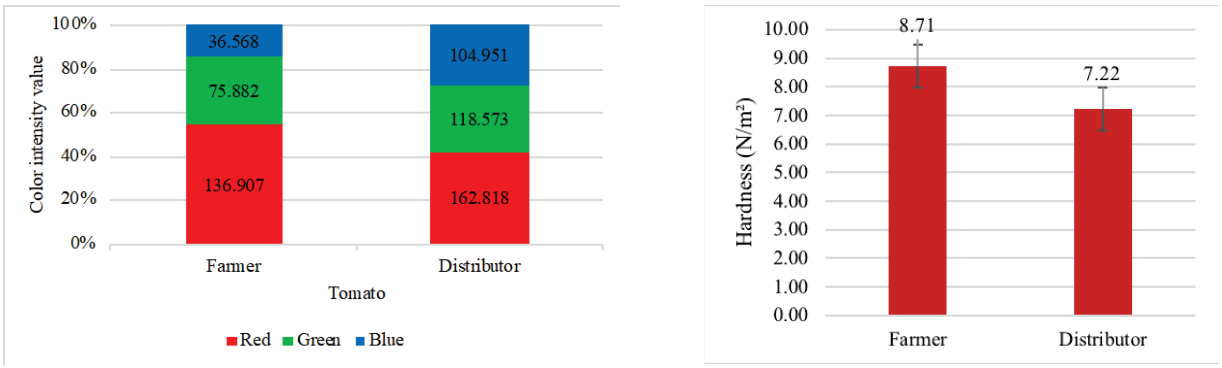

(a) (b)

Figure 1. (a) The RGB color and (b) hardness tester of tomatoes

The same quality parameter testing was also conducted for fresh organic carrots. All carrot samples taken had a uniform color, namely bright orange, and appeared fresh/not wilted at both the farmer and distributor tiers. This was supported by RGB measurements (**Figure 2a**), where the R (red) value at both tiers had an orange color intensity that did not change significantly. Overall, the color freshness of the carrots was consistent. However, the overall RGB value of carrots at the distributor tier increased due to the handling of the product at the distributor, namely the sorting process for packaging. This is in line with previous research which states that changes in the RGB color of samples can be an indication of other conditions [11]. Furthermore, texture testing results using a 6 mm FHT200 penetrometer showed that carrots from the farmer tier had an average texture of 78.72 N/m^2, while those from the distributor tier had an average texture of 82.30 N/m^2 (**Figure 2b**). This increase in carrot hardness is due to the fact that carrots at the distributor have undergone a sorting process, so that carrots that are not in good condition are not accepted by the distributor. Damage to carrots at the farmer tier indicates that the carrot samples at the farmers' premises may have suffered mechanical damage during handling, which is also related to supply chain quality risks. This also indicates that distributors play an important role in sorting vegetables sent from farmers, as only vegetables of good quality will be packaged and sent to the market or consumers.

Color is related to the visual aspect and perception to the human eye in various components [11]. Also in organic vegetables, the color component contributes to the physical quality aspect. The limitation of the human eye to identify a color, which cannot recognize small changes in the RGB value range, but the small changes in the RGB value range have meaning [11]. Color models were developed to make standard representations in digital aspects [12]. In the fresh organic cabbage sample, the physical quality parameters were assessed on 10 fresh cabbages randomly selected from the harvest baskets of farmers and distributors, respectively. At both the farmer and distributor tiers, the cabbages were uniformly greenish-white in color, although some cabbages were still dirty when they were at the farmer's. The blanching process and storage of cabbage affect the intensity of the greenish-white color, which reflects the freshness and cleanliness of the cabbage. Based on **Figure 3**, the G (green) value is slightly higher than the R (red) and B (blue) values, meaning that the color tends to be slightly greenish. The RGB value of cabbage at the farmer tier is 130.312, while at the distributor tier it is 128.481. This change in RGB value can be used to analyze changes in cabbage color, which can be applied to detect microorganism contamination and cabbage contamination [13]. The small difference between the three colors means that the color is not too striking or, in other words, the pale or white color is slightly greener. This is in accordance with the RGB color theory that white is a color that has a combination of red, green, and blue light spectrums [11]. This condition also applies to cabbage at both the farmer and distributor levels, which are uniformly greenish-white in color. The RGB value in cabbage is quite the same for each color. In the RGB model, white is a rich color spectrum because it is a combination of the light spectrum [11]. The color model is digitally used through the intensity levels of red, green, and blue light from 0 to 255 [12]. For cabbages, vegetables with thin or layered leaves, texture testing is not suitable. Cabbage and other leafy vegetables cannot be tested using the FHT200 because they did not provide a stable enough pressure surface for pressure measurement.

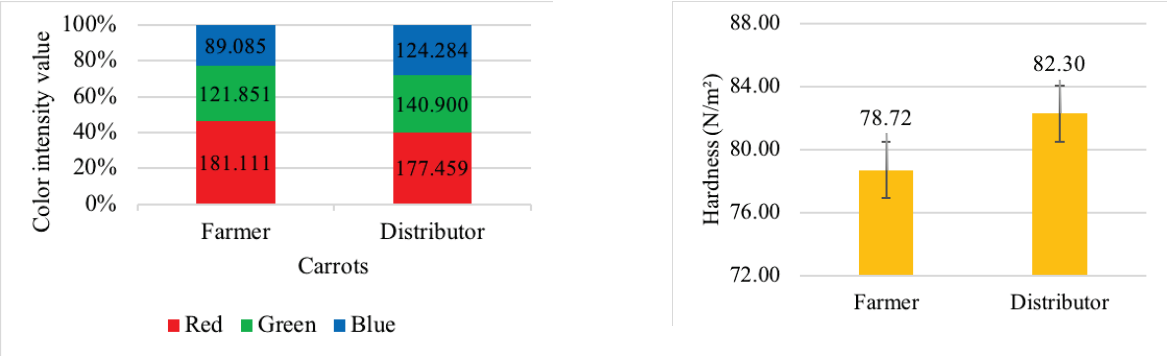

(a) (b)

Figure 2. (a) The RGB color and (b) hardness tester of carrot

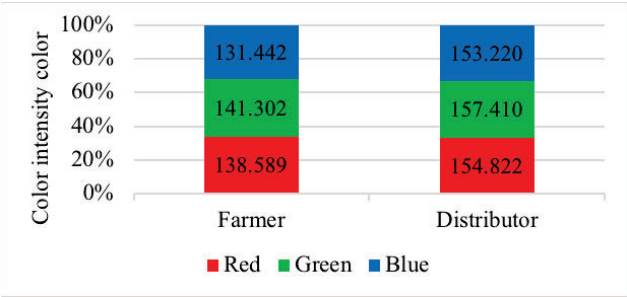

Figure 3. The RGB color of cabbage

The results show that the physical quality of organic vegetables is highly susceptible to pre-harvest and post-harvest activities. The risk of handling materials during the planting period also plays an important role in the quality of organic vegetables produced. Based on field observations, risks related to pests and plant diseases have a significant impact on harvest yields at the farmer level, where the physical quality of vegetables declines and cannot be absorbed by the market. This certainly causes financial losses for farmers and distributors acting as off-takers. In addition, improper material handling during harvest poses a greater risk to the next tier, where the quality of fresh organic vegetables may decline. Improper material handling during harvest can increase the risk of quality deterioration of vegetables during distribution. This study shows that the physical quality of organic vegetables is highly susceptible to the risk of damage due to transportation or distribution and handling of organic vegetables, especially fresh tomatoes. The main supply chain quality risk identified is physical damage due to shocks during transportation, which causes bruising, scratches, or dents on organic tomatoes. Therefore, crop handling during the planting period needs to be improved, such as crop rotation with good scheduling to reduce the impact of pests that can attack crops. Standard operating procedures for material handling and shipping need to be tightened at the farmer and distributor levels to mitigate the decline in the quality of fresh organic vegetables.

CONCLUSION

The quality of the organic vegetable supply chain is determined by several visual parameters, such as color, texture, and physical defects such as holes and bruises caused by pests and mechanical damage, both during harvest and distribution. These parameters are significantly influenced by the handling of the material at each tier of the supply chain and the distribution process. The results of quality parameter testing indicate differences in parameter values between tiers, indicating that quality control is crucial from the production or planting process through to packaging and shipping. Standardization is also crucial in maintaining supply chain quality, ensuring consumer acceptance.

ACKNOWLEDGMENTS

The authors wish to sincerely thank CV Tani Organik Merapi (TOM) for their willingness and cooperation throughout this research. Also to all respondents and risk owners for their significant contribution in collecting relevant data for this research.

REFERENCES

[1]. Hansmann, R., Baur, I., & Binder, C. R. (2020). Increasing organic food consumption: An integrating model of drivers and barriers. Journal of Cleaner Production, 275, 123058. https://doi.org/10.1016/j.jclepro.2020.123058

[2]. Issock, P. B. I., Mpinganjira, M., & Roberts-Lombard, M. (2023). Beyond sustainable consumption practices: Linking organic food consumption to hedonic and eudaimonic well-being. Appetite, 188, 106633. https://doi.org/10.1016/j.appet.2023.106633

[3]. Indonesian Organic Alliance (AOI). (2023). Indonesian organic agriculture statistics 2023. AOI.

[4]. Indonesian Organic Alliance (AOI). (2017). Indonesian organic agriculture statistics 2017. AOI.

[5]. Indonesian Organic Alliance. (2025). PAMOR Indonesia – Organic quality assurance.

[6]. Davies, G. (2012). Organic vegetable production: A complete guide. Crowood.

[7]. Barański, M., Średnicka-Tober, D., Volakakis, N., Seal, C., Sanderson, R., Stewart, G. B., Benbrook, C., Biavati, B., Markellou, E., Giotis, C., & Gromadzka-Ostrowska, J. (2014). Higher antioxidant and lower cadmium concentrations and lower incidence of pesticide residues in organically grown crops: A systematic literature review and meta-analyses. British Journal of Nutrition, 112(5), 794–811. https://doi.org/10.1017/S0007114514001366

[8]. Curl, C. L., Beresford, S. A., Fenske, R. A., Fitzpatrick, A. L., Lu, C., Nettleton, J. A., & Kaufman, J. D. (2015). Estimating pesticide exposure from dietary intake and organic food choices: The Multi-Ethnic Study of Atherosclerosis (MESA). Environmental Health Perspectives, 123(5), 475–483. https://doi.org/10.1289/ehp.1408197

[9]. Yahaya, O. K. M., MatJafri, M. Z., Aziz, A. A., & Omar, A. F. (2014, August). Non-destructive quality evaluation of fruit by color based on RGB LEDs system. In 2014 2nd International Conference on Electronic Design (ICED) (pp. 230–233). IEEE. https://doi.org/10.1109/ICED.2014.7015804

[10]. Ayuningtyas, D., Suryani, E., & Wiharto, W. (2021, June). Identification of tomato maturity based on HIS color space using the K-nearest neighbor method. In 2021 International Conference on Artificial Intelligence and Computer Science Technology (ICAICST) (pp. 73–78). IEEE. https://doi.org/10.1109/ICAICST53116.2021.9497843

[11]. Hermida, I. D. P., Prabowo, B. A., Kurniawan, D., Manurung, R. V., Sulaeman, Y., Riyadi, M. A., & Wahono, M. D. (2018, October). Use of smartphone based on Android as a color sensor. In 2018 Electrical Power, Electronics, Communications, Controls and Informatics Seminar (EECCIS) (pp. 424–429). IEEE. https://doi.org/10.1109/EECCIS.2018.8692848

[12]. Mazur, F., Han, Z., Tjandra, A. D., & Chandrawati, R. (2024). Digitalization of colorimetric sensor technologies for food safety. Advanced Materials, 36(42), 2404274. https://doi.org/10.1002/adma.202404274

[13]. Sezgin, G. C., & Ocsoy, I. (2023). Anthocyanin-rich black carrot (Daucus carota ssp. sativus var. atrorubens Alef.) and red cabbage (Brassica oleracea) extracts incorporated biosensor for colorimetric detection of Helicobacter pylori with color image processing. Brazilian Journal of Microbiology, 54(2), 897–905. https://doi.org/10.1007/s42770-023-00989-1

Employment of Coloring on Clothing-Style Drawings for Understanding Behavior and Personality

Chie Muraki Asano [a*], Sonoka Ikebe [a], and Akira Asano [b]

[a] *Sapporo Campus, Hokkaido University of Education, Sapporo, Japan*
[b] *Faculty of Informatics, Kansai University, Takatsuki, Osaka, Japan*
[*] *Corresponding author: asano.chie@s.hokkyodai.ac.jp*

ABSTRACT

This study investigates the relationship between personality traits and coloring characteristics in clothing-style drawings. Previous research has suggested a connection between individual characteristics and coloring preferences using abstract drawings and human portraits. We employed clothing-style drawings because respondents' internal feelings are projected and compensated through the coloring of daily clothing styles.

Respondents colored four clothing-style drawings and estimated the age of the person depicted in each. They also answered questions to estimate their personality using the Enneagram model. Ward's hierarchical clustering method categorized each respondent's nine-dimensional personality vector into six clusters, with the number of clusters determined through a preliminary experiment. The characteristics of the respondents' coloring in each cluster were analyzed.

Participants included 32 university students in their 20s and 20 individuals over 50. Age estimation results showed that younger respondents tended to estimate the figures as older than their actual age, suggesting a projection of their future selves. In contrast, older respondents estimated younger ages, indicating compensation for their past years.

The six clusters showed distinct coloring characteristics. Clusters 1 and 2, mainly composed of university students, had notable traits: Cluster 1 showed a wide hue range, reflecting each respondent's personality in daily life; Cluster 2 showed a narrower hue range, with vivid (v) tones in the PCCS color system absent. Cluster 3, mainly older respondents, used neutral colors and deep (dp) tones. Minor clusters also had unique features: Cluster 4 showed middle Chroma with individual coloring styles; Cluster 5 used dark (dk) and deep tones; Cluster 6 used dark (dk) and vivid (v) tones.

These results indicate that each cluster categorized by the Enneagram has distinct coloring characteristics, and these characteristics reflect the respondent's personality. The findings have educational applications, especially for schoolchildren who may find it difficult to verbalize their feelings. Coloring may provide an easier and more intuitive way to express emotions. Our research supports this idea, as the relationship between personality traits and coloring characteristics was clearly observed.

Keywords: coloring of clothing-style drawings, personality, personality enneagram

INTRODUCTION

We investigate the relationship between personality traits and coloring characteristics in clothing-style drawings. Previous studies have suggested that individuals project and compensate for their internal feelings

through color choices, particularly in abstract drawings and human portraits [1][2]. However, clothing-style drawings offer a more familiar and contextually grounded medium, as clothing is closely tied to daily life and personal identity. The way individuals color these drawings may reflect not only aesthetic preferences but also deeper psychological tendencies.

To explore this relationship, we employed the Enneagram personality model, a psychological framework that categorizes human personality into nine distinct but interconnected types. The Enneagram is widely used in both clinical and educational settings to understand personality structure, emotional dynamics, and interpersonal relationships. Unlike trait-based models such as the Big Five, the Enneagram emphasizes internal drives and transformation, making it particularly suitable for studies involving expressive and projective tasks like coloring.

In this study, respondents replied to an Enneagram-based personality assessment, which was represented as a nine -dimensional vector. These vectors were then grouped into six clusters using Ward's hierarchical clustering metho d, allowing us to examine how different personality profiles correspond to specific coloring behaviors. Respondent s also colored four clothing-style drawings and estimated the age of the person depicted in each. This task was des igned to reveal psychological projection and compensation mechanisms related to age perception.

METHODOLOGY

To examine differences across age groups, the study recruited 52 participants: 32 university students in their 20s and 20 individuals aged over 50. All participants gave informed consent before taking part in the study.

Figure 1 presents the four clothing-style drawings used in this investigation, depicting different types of daily clothing. These drawings were designed to be gender-neutral and culturally neutral to minimize bias. Participants used colored pencils as the coloring medium. The pencil set was based on a 40-color vinyl set used in previous studies [3], with an additional six shades of brown added to better capture the expressive qualities of clothing. The final set consisted of 46 colors and was organized according to the Practical Color Co-ordinate System (PCCS), which includes a range of chromatic tones—such as vivid (v), deep (dp), and dark (dk)—as well as achromatic colors like black, white, and gray. This ensured that both colorful and neutral expressions could be represented in the drawings.

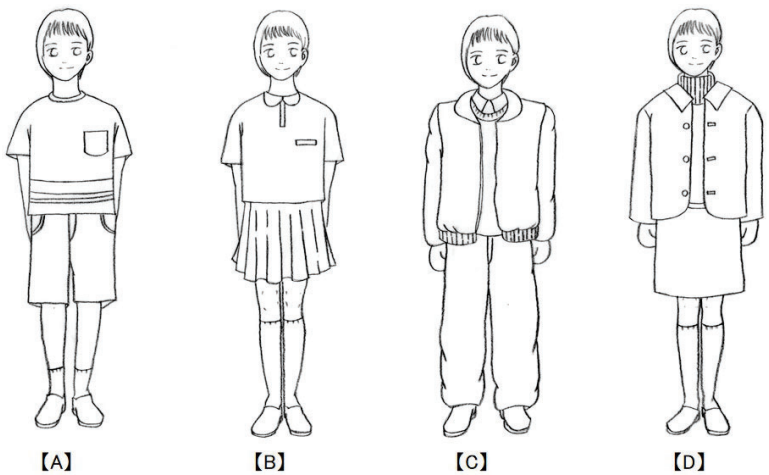

Figure 1: The four clothing-style drawings depicting different types of daily clothing

Participants were asked to color each of the four clothing-style drawings freely, using any combination of colors from the provided color set. After completing the coloring task, they were instructed to estimate the age, sex, and personality of the person depicted in each drawing. These estimations were intended to reveal psychological projection and compensation mechanisms, particularly in relation to age perception, gender attribution, and personality inference. The order of the drawings was randomized to minimize order effects.

Following these tasks, participants completed a personality assessment based on the Enneagram model. The results were recorded as nine-dimensional personality vectors, which were later used for clustering analysis. All tasks were conducted in a quiet environment, and participants were given sufficient time to complete each part of the study without time pressure.

Following the coloring and age estimation tasks, participants completed a personality assessment based on the Enneagram model. The Enneagram categorizes personality into nine types, each associated with specific emotional patterns and motivational structures. The results of the assessment were represented as nine-dimensional personality vectors.

Ward's hierarchical clustering method was applied to the Enneagram vectors to classify participants into six personality clusters. The number of clusters was determined through a preliminary experiment to ensure meaningful differentiation. For each cluster, the coloring characteristics—such as hue range, tone usage, and chroma—were analyzed and compared. Differences between age groups in age estimation and coloring tendencies were also examined to explore patterns of projection and compensation.

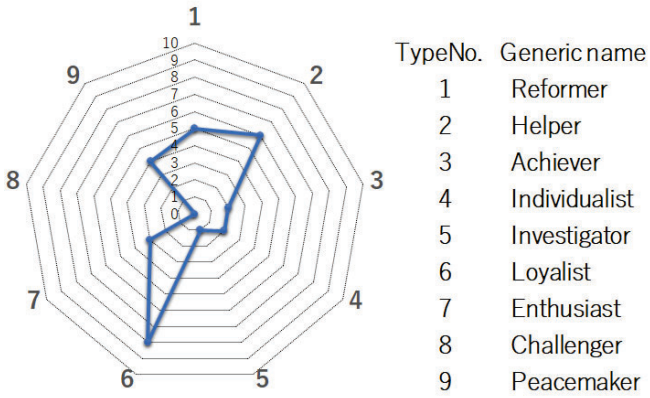

Figure 2: Examples of Enneagram Type 9 Expressions (Left) Genetic Names of each Axis (Right)

RESULTS AND DISCUSSION

Analysis of the coloring results revealed that drawings C and D showed a higher frequency of dark (dk) tones, particularly in brown hues. This suggests the necessity of including dk tones—especially browns—in the color set when evaluating clothing-related color choices.

Regarding age estimation, university students tended to assign higher ages to the figures compared to participants aged 50 and above. This indicates a possible projection of future self-images among younger respondents. In contrast, the older group showed greater variability in age estimation for Drawing D. This may reflect the influence of non-clothing elements such as facial features, hairstyle, makeup, and accessories, which were present in the drawings and may have affected perceived age.

Regarding age estimation, university students tended to assign higher ages to the figures compared to participants aged 50 and above. This indicates a possible projection of future self-images among younger respondents. In contrast, the older group showed greater variability in age estimation for Drawing D. This may reflect the influence of non-clothing elements such as facial features, hairstyle, makeup, and accessories, which were present in the drawings and may have affected perceived age.

The results of the Enneagram personality assessment showed no strong correlations between types; no pairwise correlation exceeded 0.60. Based on this outcome, we conducted a cluster analysis using Ward's hierarchical method. A dendrogram was generated, and six clusters were identified at a distance level that provided meaningful separation of personality profiles in Figure 3.

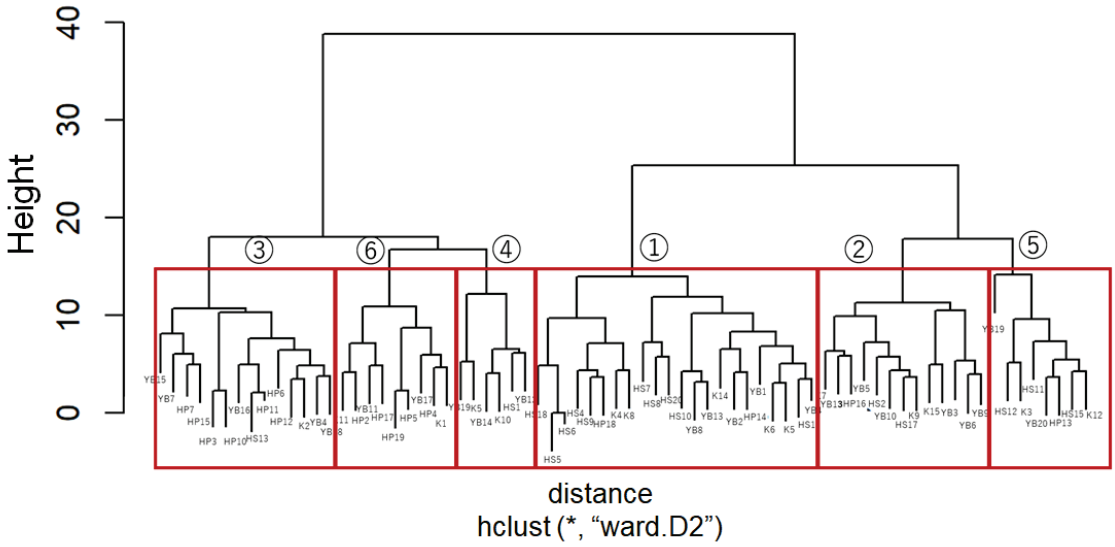

Figure 3: Cluster Analysis of Responses to the Enneagram Questionnaire

Each cluster was then analyzed in terms of age group composition, estimated age of the figures, coloring characteristics, number of colors used, hue range, and tone preferences. These findings provide insight into how personality traits, as categorized by the Enneagram, relate to visual expression in clothing-style drawings.

CONCLUSION

We investigated the relationship between personality traits and coloring characteristics in clothing-style drawings, using the Enneagram model to classify respondents' personalities and analyze their visual expression. The results revealed distinct patterns in color usage, tone preferences, and age estimation across different personality clusters and age groups. Younger participants tended to project future selves by estimating higher ages, while older participants showed signs of compensating for past experiences. The inclusion of dark (dk) tones, particularly browns, proved essential in capturing the expressive qualities of clothing, especially in drawings C and D.

Beyond its psychological implications, this research has potential applications in educational contexts. Children, especially in early developmental stages, often struggle to verbalize their emotions and thoughts. Coloring activities can serve as an intuitive and non-verbal medium for emotional expression. By identifying patterns between personality traits and coloring behavior, educators may gain insights into students' emotional states and

personality tendencies, enabling more personalized and empathetic support. Our study contributes to this perspective by demonstrating how visual expression can reflect internal psychological structures, offering a valuable tool for both psychological assessment and educational practice.

ACKNOWLEDGEMENTS

This research was partly financially supported by JSPS KAKENHI Grant Nos. 19K12692, 21H04342 and 22K03202.

REFERENCES

[1]. Nakamura, S. (2024). *The relationship between color preference and personality traits in clothing selection*. Journal of Child Development Studies, Nihon Fukushi University, 16.

[2]. Nomura, N., et al. (n.d.). *A method for extracting character and affective information from facial expressions*. Mukogawa Women's University.

[3]. Muraki Asano, C., Ohba, Y., Ohyama, Y., Sasaki, T., & Asano, A. (2022, September 6–9). *A study on the relationship between children's developmental stages and sense of color: Analysis of the characteristics of color schemes to coloring book images by iPad*. In Proceedings of the 9th International Conference on Kansei Engineering and Emotion Research (KEER 2022), Barcelona, Spain.

Facial Color Perception and Facial Impressions Across Diverse Color Vision Types

Yoko Mizokami [a*], Shun Kurosawa [a], and Hiromi Sato [a]

[a] *Chiba University, Chiba, Japan*
[*] *Corresponding author: Yoko Mizokami, mizokami@faculty.chiba-u.jp*

ABSTRACT

This study investigates how individuals with different types of color vision perceive facial skin color and how these perceptual differences influence affective evaluations of faces. Human skin color is primarily determined by melanin and hemoglobin. Previous research has shown that individuals with normal trichromatic vision are more sensitive to color changes related to hemoglobin, which contribute to reddish tones, than to changes associated with melanin, which affect skin darkness. In contrast, individuals with color vision deficiencies such as protanopia, deuteranopia, protanomaly, and deuteranomaly show reduced sensitivity to both color changes. However, it remains unclear how these differences in perceptual sensitivity affect higher-level judgments such as preference, naturalness, and perceived healthiness. The present study asked participants to evaluate facial images systematically modified in melanin, hemoglobin, lightness, and chromaticity to address this question. A standard facial image was used as a reference, and participants rated each variation on five attributes: preference, naturalness, hue (yellowish to reddish), brightness, and healthiness, using a seven-point scale. The results showed that evaluations of brightness were relatively consistent across all types of color vision. However, differences were found in hue perception, particularly among dichromats, who were more likely to perceive darker skin as redder. This suggests that they may use different perceptual strategies when interpreting facial color. Across all vision groups, preference ratings were strongly correlated with perceptions of healthiness and naturalness, with these relationships being especially pronounced among those with normal color vision. In addition, individuals with normal trichromatic vision tended to prefer redder facial tones, a pattern not seen in other groups. When examining the relationship between brightness and naturalness, most groups showed a negative correlation, indicating that very bright skin was unnatural, while anomalous trichromats showed the opposite pattern. These findings suggest that individual differences in color vision influence not only basic perceptual processes but also how people form impressions of others. The results highlight the importance of considering perceptual diversity in areas such as visual design, digital imaging, psychology, and healthcare, where facial appearance plays a key role in communication and decision-making.

Keywords: Skin color, Facial impression, Color discrimination, Color deficiency, Hemoglobin, Melanin

INTRODUCTION

Skin color perception is essential in communication as skin and facial color can convey information about a person Skin color perception plays a vital role in communication, as the color of the skin and face can convey important information about a person's emotional and physical state. It is well-established that melanin and hemoglobin are the primary pigments determining skin color. Previous studies by Hamada et al. [1] and Mishima et al. [2] have demonstrated that skin color can be highly discriminative, particularly regarding increased or decreased redness resulting from changes in hemoglobin levels.

Kurosawa et al. [3] clarified the characteristics of skin color change discrimination across different types of color vision by examining both individuals with congenital color vision deficiencies and those with normal color

vision, with and without using color-weakness simulating filters. The results indicate that individuals with normal trichromatic vision are more sensitive to color changes associated with hemoglobin—contributing to reddish tones—than to those related to melanin, which primarily affect skin darkness. In contrast, individuals with color vision deficiencies such as protanopia, deuteranopia, protanomaly, and deuteranomaly, as well as those using simulating filters, exhibited reduced sensitivity to both types of color changes compared to those with normal color vision, with especially diminished sensitivity in the hemoglobin-related direction. These findings suggest that facial skin color discrimination cues vary depending on the type of color vision and the direction of color modulation.

However, it remains unclear how these differences in perceptual sensitivity affect facial impressions—such as preference, naturalness, and perceived healthiness—which involve higher-level judgments and may be influenced by environmental and social factors [4]. To address this question, the present study investigates how facial images systematically modified in melanin, hemoglobin, lightness, and chromaticity influence impressions across five attributes: preference, naturalness, hue (from yellowish to reddish), brightness, and healthiness.

METHODOLOGY

EXPERIMENT 1

Stimuli

As used in previous studies, the average face of Japanese women was employed for the facial images [5]. To generate the stimuli, skin spectral reflectance was simulated using a Monte Carlo method developed by Maeda et al. [6]. Based on the simulated spectral reflectance, CIELAB values corresponding to skin color changes caused by variations in melanin and hemoglobin levels were calculated, and these values were used to create the stimuli. The standard (reference) stimulus was a face image with Japanese women's average skin color values (L^* = 65.6, a^* = 9.0, b^* = 17.8). Test stimuli were generated in each of the four series: increased melanin (M+), decreased melanin (M−), increased hemoglobin (H+), and reduced hemoglobin (H−). We selected both weakly and strongly modified face images in each direction (M--, M-, M+, M++, H--, H-, H+, and H++), as illustrated in Figure 1. Since changes in melanin and hemoglobin levels result in alterations in both chromaticity and lightness, we additionally created two control sets of stimuli: (1) faces with chromaticity changes due to melanin and hemoglobin variations while keeping lightness constant (M--', M-', M+', M++', H--', H-', H+', H++'), and (2) faces with only lightness changes while maintaining constant chromaticity (L--, L-, L+, and L++). These were included to isolate and verify the individual effects of chromaticity and lightness on facial impressions.

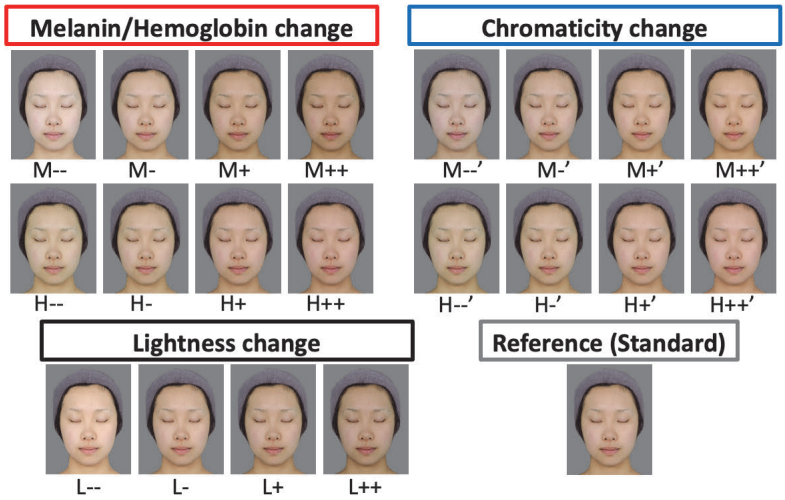

Figure 1. Test stimuli with color modulation applied to melanin, hemoglobin, chromaticity, and lightness.

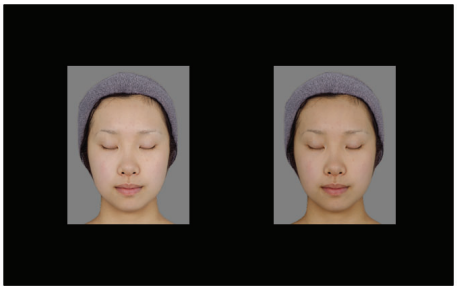

Figure 2. Experimental display setup. The reference stimulus is shown on the left, and the test stimuli with color modulation are presented sequentially on the right.

As shown in Figure 2, the stimuli were presented on a 31.1-inch liquid crystal display (LCD) monitor. The size of each image was about 18×14 degrees. The reference (standard) stimulus was displayed on the left side against a black background, while the test stimuli were presented sequentially on the right for evaluation. Participants assessed each modulated stimulus on the right with reference to the standard stimulus on the left.

Procedure

Participants evaluated the appearance of facial color in each test stimulus using a 7-point scale, where 1 represented the lowest and 7 the highest rating. Ratings could be given in 0.5-point increments. Evaluations were made based on the following five criteria: preference (1 = unfavorable / 7 = favorable), naturalness (1 = unnatural / 7 = natural, hue (1 = yellowish / 7 = reddish), brightness (1 = dark / 7 = bright), healthiness (1 = unhealthy / 7 = healthy)

Participants

The participants in the experiment included eight individuals with normal color vision (N1–N8), two with protanopia (P1, P2), six with deuteranopia (D1–D6), one with protanomaly (PA1), and three with deuteranomaly (DA1–DA3). Given the relative similarity in color perception between protan and deutan types, the results were analyzed by grouping the participants into three categories: normal color vision, dichromacy, and anomalous trichromacy. All participants were young males, approximately 20 years old.

RESULTS AND DISCUSSION

Examples of evaluation results for each image are shown in Figure 3, including the following conditions: melanin variation (M-- and M++), hemoglobin variation (H-- and H++), melanin chromaticity variation (M--' and M++'), hemoglobin chromaticity variation (H--' and H++'), and brightness variation (L-- and L++). The horizontal axis represents the evaluation criteria, while the vertical axis indicates the evaluation scores. The black cross symbols denote the average scores of participants with normal color vision, blue circles represent those with anomalous trichromacy, and red squares indicate those with dichromacy. Error bars represent the standard error. Brightness evaluations were relatively consistent across all types of color vision. However, conditions involving decreased pigment density or increased lightness (M--, H--, M--', H--', and L++) tended to show greater differences among the color vision groups across multiple evaluation criteria.

Transitions in the evaluations of yellowish/reddish hue for the melanin variation, hemoglobin variation, and lightness variation stimuli are shown in Figure 4. The vertical axis represents the evaluation scores, while the horizontal axis indicates the stimulus types. In each graph, the stimuli progress from left to right as follows: in (a), melanin increases (i.e., more yellowish); in (b), hemoglobin increases (i.e., more reddish); and in (c), brightness decreases. The black, blue, and red lines represent the average scores of participants with normal color vision, anomalous trichromacy, and dichromacy, respectively. Notable differences in hue perception were observed,

particularly among dichromats, who tended to perceive darker skin as redder. This suggests that individuals with dichromacy may employ different perceptual strategies when interpreting facial coloration.

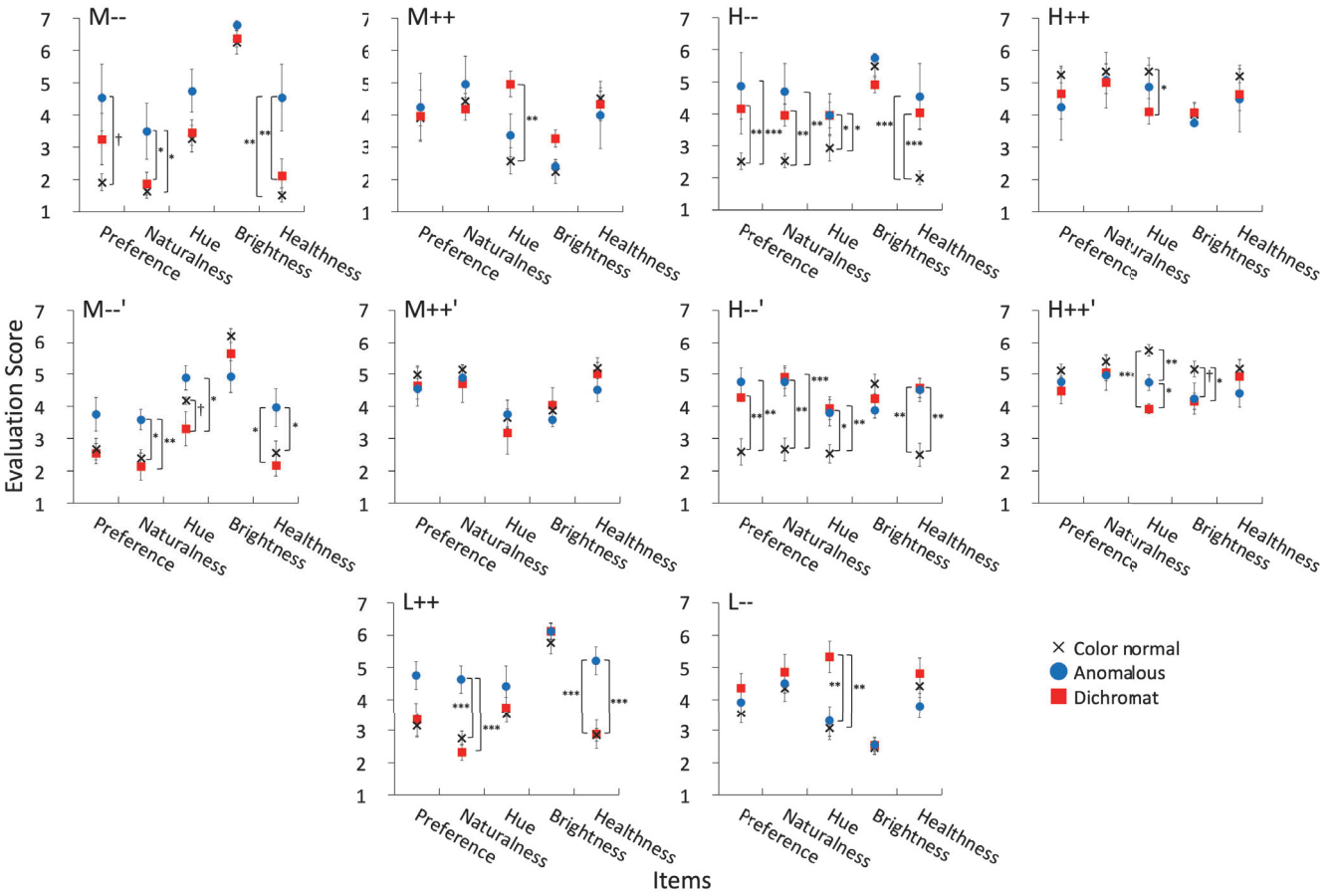

Figure 3. Evaluation scores for each item. The stimuli include melanin variation (M--, M++), hemoglobin variation (H--, H++), melanin chromaticity variation (M--', M++'), hemoglobin chromaticity variation (H--', H++'), and brightness variation (L--, L++). Error bars represent SE. †$\bar{A}$< .10, *$\bar{A}$< .05, **$\bar{A}$< .01, *$\bar{A}$< .001.**

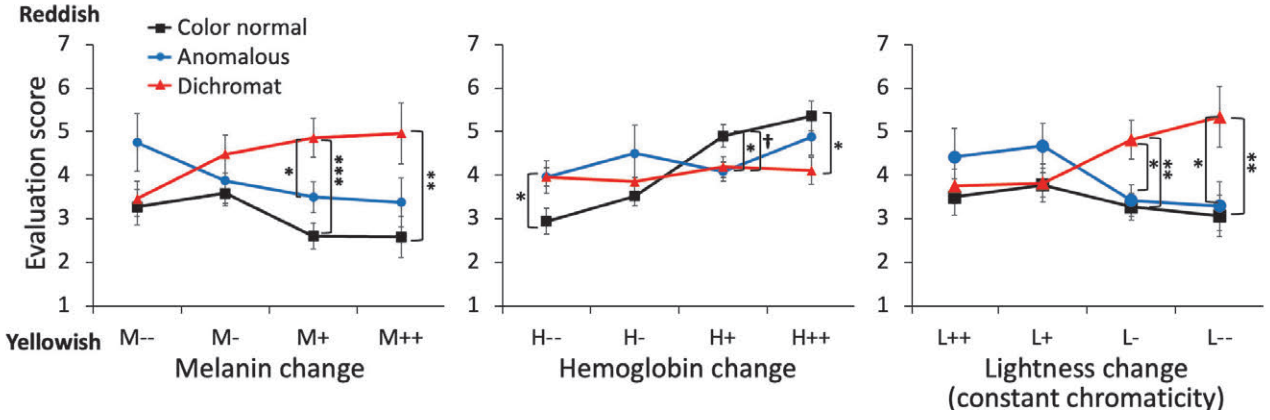

(a) Melanin change (b) Hemoglobin change (c) Lightness change

Figure 4. Variation in yellowish/reddish scores in relation to facial color changes. Error bars represent SE. †$\bar{A}$< .10, *$\bar{A}$< .05, **$\bar{A}$< .01, *$\bar{A}$< .001.**

The correlations among the five evaluation items for the 20 experimental stimuli are presented in Figure 5. Square symbols indicate the average values of the eight participants with normal color vision, circles represent the four participants with anomalous trichromacy, and triangles represent the eight participants with dichromacy. The diagonal cells display histograms of each evaluation item, the upper triangular region shows the correlation coefficients, and the lower triangular region presents scatter plots.

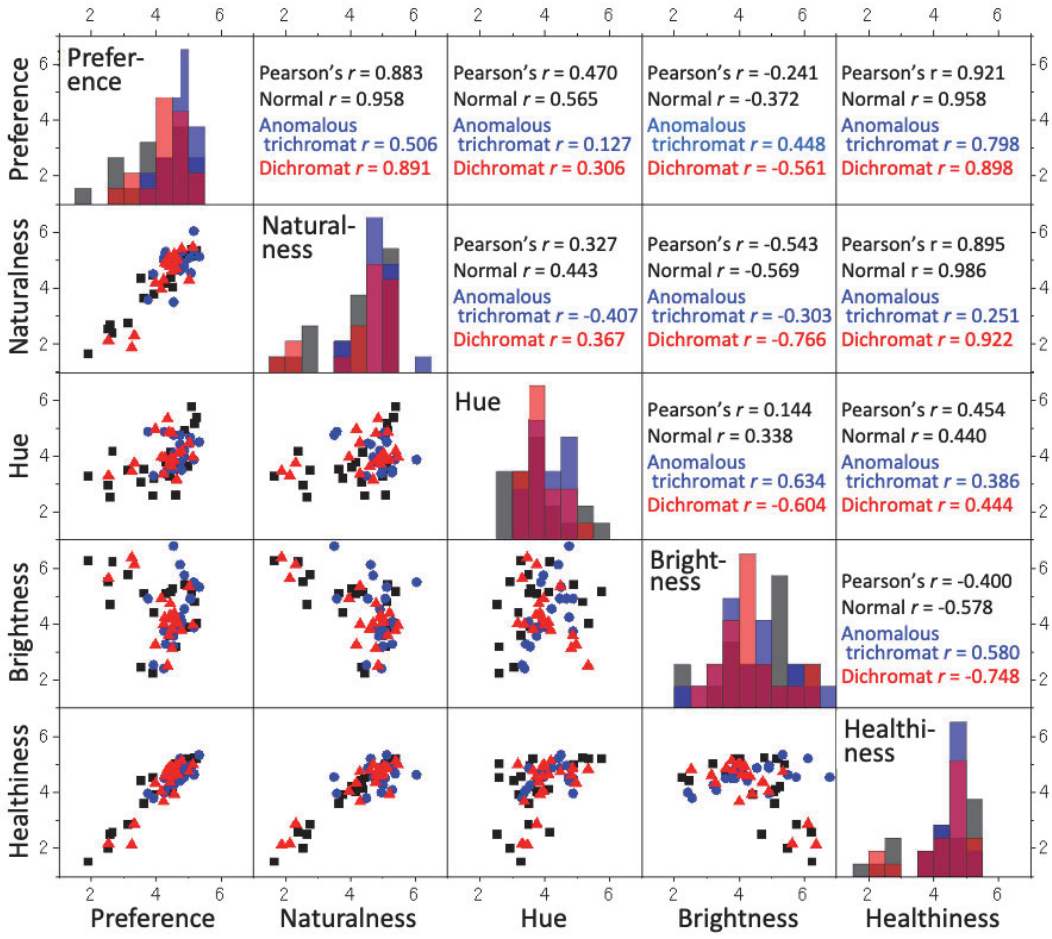

Figure 5. Correlations among evaluation items. Black squares represent participants with normal color vision; blue circles represent anomalous trichromats; and red triangles represent dichromat participants.

Stronger correlations ($r > .50$) were observed across all types of color vision between *preference–healthiness* and *preference–naturalness*. For *preference–hue*, participants with normal color vision tended to rate facial images with more reddish hues as more preferable. In contrast, no such correlation was found for the other color vision groups. In the case of *preference–brightness*, participants with normal color vision and dichromacy showed negative correlations, while anomalous trichromats exhibited a positive correlation, indicating a distinct evaluation trend in the latter group. A strong positive correlation ($r > .90$) between *naturalness–healthiness* was observed for both the normal and dichromatic groups, but not for anomalous trichromats. This suggests that *preference*, *naturalness*, and *healthiness* are closely linked for participants with normal color vision and dichromacy. Additionally, a stronger negative correlation ($r < -.50$) was observed between *naturalness–brightness* in these two groups, indicating that overly bright skin tones were perceived as unnatural. The correlation between *hue–brightness* varied depending on color vision type: participants with normal color vision showed a weak correlation, anomalous trichromats showed a stronger positive correlation ($r > .50$), and dichromats exhibited a stronger negative correlation ($r < -.50$). These differences suggest that the perception of facial redness is

influenced by brightness in a manner that varies across color vision types. Specifically, dichromats tended to perceive stronger redness when skin brightness was low, while anomalous trichromats perceived stronger redness when brightness was high. This implies that hue perception in skin tone may be modulated by brightness information. For *brightness–healthiness*, stronger negative correlations ($r < -.50$) were found among participants with normal color vision and dichromacy, indicating that overly bright skin was perceived as unhealthy. In contrast, anomalous trichromats showed a positive correlation ($r > .50$), associating brighter skin with a healthier appearance.

These differences may be attributed to inherent visual experiences associated with each color vision type and individual variation, as suggested by previous studies [7–8].

CONCLUSION

This study investigates how facial images systematically modified in melanin, hemoglobin, lightness, and chromaticity influence impressions across five attributes: preference, naturalness, hue (yellowish to reddish), brightness, and healthiness. Participants with anomalous trichromacy and dichromacy exhibited evaluation tendencies that differed from those with normal color vision. For example, they were more likely to perceive darker skin as redder and to form distinct overall impressions. Our findings suggest that individual differences in color vision influence not only basic perceptual processes but also how people create social impressions of others. These results highlight the importance of considering perceptual diversity in fields such as visual design, digital imaging, psychology, and healthcare, where facial appearance plays a key role in communication and decision-making.

ACKNOWLEDGEMENTS

This work was supported by JSPS KAKENHI (JP21H05805, JP23H04332, and JP24K03024).

REFERENCES

[1]. Hamada, K., Mizokami, Y., & Yaguchi, H. (2017). Discrimination thresholds for skin image and uniform color stimulus. *Journal of the Color Science Society of Japan*, *41*(3), 48–49. [in Japanese].

[2]. Mishima, N., & Mizokami, Y. (2020). Detectability of skin color difference due to skin pigment in facial images. *Journal of the Color Science Society of Japan*, *44*(6), 284. [in Japanese].

[3]. Kurosawa, S., Sato, H., & Mizokami, Y. (2024). Effect of diverse color vision on the sensitivity to skin color change. The 8th Asia Color Association Conference (ACA 2024). Bangkok, Thailand.

[4]. He, Y., Sato, H., & Mizokami, Y. (2024). Cross-cultural comparison of the influence of skin-color change on facial impressions. *i-Perception,* 15(5), 20416695241288032.

[5]. Yoshikawa, H., Kikuchi, K., Yaguchi, H., Mizokami, Y., & Takata, S. (2012). Effect of chromatic components on facial skin whiteness. *Color Research & Application*, 37(4), 281-291.

[6]. Maeda, T., Arakawa, N., Takahashi, M., & Aizu, Y. (2010). Monte Carlo simulation of spectral reflectance using a multilayered skin tissue model. *Optical Review*, *17*(3), 223–229.

[7]. Baraas, R. C., Foster, D. H., Amano, K., & Nascimento, S. M. (2010). Color constancy of red-green dichromats and anomalous trichromats. *Investigative Ophthalmology & Visual Science*, *51*(4), 2286-2293.

[8]. Emery, K. J., Parthasarathy, M. K., Joyce, D. S., & Webster, M. A. (2021). Color perception and compensation in color deficiencies assessed with hue scaling. *Vision Research*, *183*, 1-15.

Evaluating Fabric Colour Appearance Perception Using LEDsimulator

Qinyuan Li[a], Arsaika Widasati[a], Yichi Zhang[a], Ming Ronnier Luo[a,b,*], and Kaida Xiao[a]

[a]*University of Leeds, Leeds, United Kingdom*
[b]*Zhejiang University, Hangzhou, China*
[*]*Corresponding author: Ming Ronnier Luo, M.R.Luo@leeds.ac.uk*

Abstract

Appearance includes a study of colour, texture, gloss and translucency. The colour and texture could be the most important factors that affects fabric appearance. Although advanced instruments, such as spectrophotometer, were developed to measure spot fabric colours, human perception of fabric colour was less investigated due to four key aspects: (1) fabrics can display varying colours due to the different dyeing properties of fibre materials under the same dyeing process; (2) differences in fabric structures also influence the fabric colour appearance due to the infinite textures of woven and knitted constructions; (3) differences in fabric folding and draping properties lead to infinite shape; (4) the perception of fabric colour vary from individual to individual due to individual colour vision. The present study aims to investigate human perception of fabric colour appearance using a novel device named LEDsimuilator. It is a device to design colour with specific textures and is used in the textile supply chain for appearance communication. It is also a valuable tool to study appearance. It includes a viewing cabinet to illuminate physically coloured samples and a projector formed by the two spectral tunable LED lighting systems to illuminate coloured light to white substrates having different textures. In the present study, three white substrates with different surface textures were used as reference fabrics to be illuminated by the coloured lights generated by the two LED panels. A total of 30 fabric samples, varying in materials, colours, and textures, were used in two colour matching psychophysical experiments. In the first experiment, participants performed colour matching using flat fabric samples, while in the other, draped fabric samples were used.

Keywords: fabric colour appearance, colour perception, colour matching, texture, shape

Introduction

Colour matching experiment is of vital importance in CIE colorimetry, starting with the trichromatic colour matching experiments conducted by John Guild and W.David Wright independently which set the foundation of CIEXYZ tristimulus values and the CIELAB colour space in line with human visual perception [1]. The method has been widely used to collect perceived colour data, obtained through the observation of real objects, e.g., cubes, [2], colour patches displayed on monitors [3, 4], and images of real objects [5, 6]. In [2], a physical colour patch from a book of paint chips was selected to best match the colour of a cube illuminated in the viewing cabinet. In contrast, the other experiments [3-6] required observers to adjust the colour of a patch displayed on the monitor until it visually matched the target stimulus. The target stimulus can be nearly uniform colour patches, textured images of real objects, and real objects with visible shape, while the matching area is typically represented by a textureless colour patch. Although texture and shape are important physical properties of the object, the roles have been overlooked in previous studies applying colour matching.

Fabric is one of the most essential materials in human life, and its appearance strongly affects the evaluation of fabric quality as well as human preference. The fabric appearance is decided by the dyeing properties of various

fibre material, the diversity of woven and knitted structures, and the folding and shaping characteristics of fabrics. Previous studies normally focused on the detection of fabric surface defects to ensure a complete appearance [7], while a few studies investigated the dyeing consistency and colour fastness [8, 9]. In contrast, the human perception of fabric appearance is less investigated, mainly due to the complexity appearance-related factors and the limited availability of evaluation tools. Moreover, the perceived fabric appearance is ultimately decided by consumers, where individual differences in human visual system lead to subjective variation and a lack of standardised criteria.

Give all the above, the aim of the present study is to investigate the human perception of fabric colour appearance, including both flat appearance and draped appearance. A novel evaluation tool, LEDsimulator, was used by allowing the integrated consideration of colour, texture, and shape.

Methodology

In the present study, three white substrates were used as reference fabrics, illuminated by the two LED panels of LEDsimulator. The appearance of white substrates was shown in Figure 1, illustrating the different textures and appearances. A total of 30 fabric samples, varying in material, colour, and textures, were used in two colour matching psychophysical experiments. The fabric samples were shown in Figure 2. The fabrics were selected from Leeds Fabric Tactile Database [10] due to their similar texture coarseness to the three reference substrates shown in Figure 1.

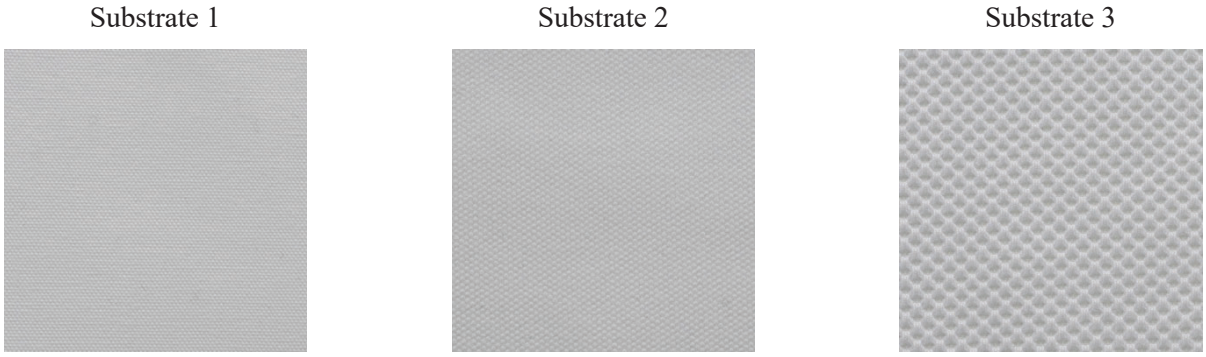

Figure 1: Three reference white substrates. From left to right, the texture exhibited a gradual increase in coarseness.

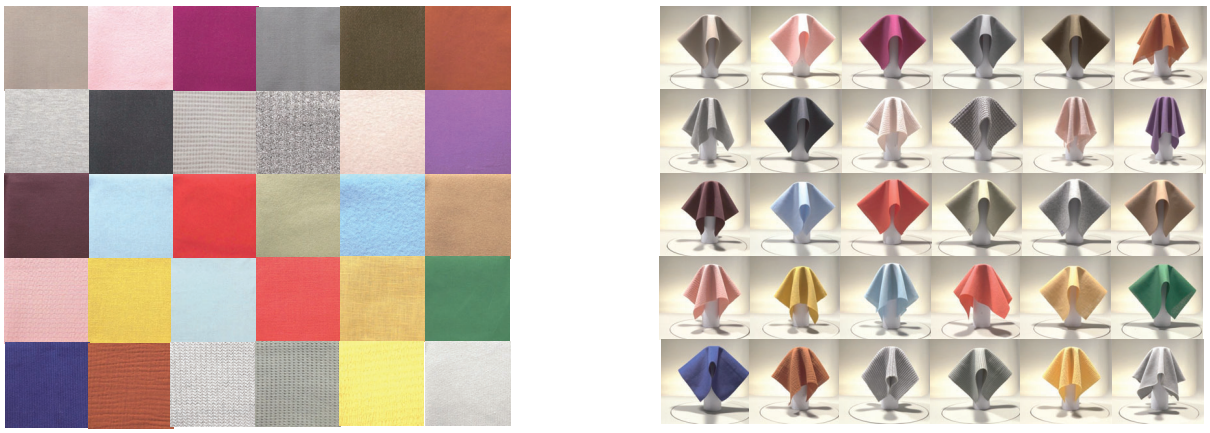

Figure 2: Flat and draped fabric appearance. Left: flat fabric appearance. Right: draped fabric appearance.

By using LEDsimulator, the reference substrate was placed behind the matching window and illuminated by two LED panels. In the first colour matching experiment, fabric samples were placed in flat condition and beside

the matching window, as shown in Figure 3-left. Participants were asked to tune the LED lightings projected on the reference substrates until the colour appearance of the reference and fabric sample matched. The CIELAB values were recorded. Each participant completed 90 fabric colour appearance matching tasks (3 reference substrates, 30 fabric samples). In addition, ten of fabric samples were repeated in the matching task using substrate 1 to assess the intra-observer variability. In the second experiment, the fabric samples were placed in draped condition and beside the matching window, as shown in Figure 3-right. The procedure was the same as in the first experiment. 10 participants, who passed Ishihara test, completed the two experiments, respectively.

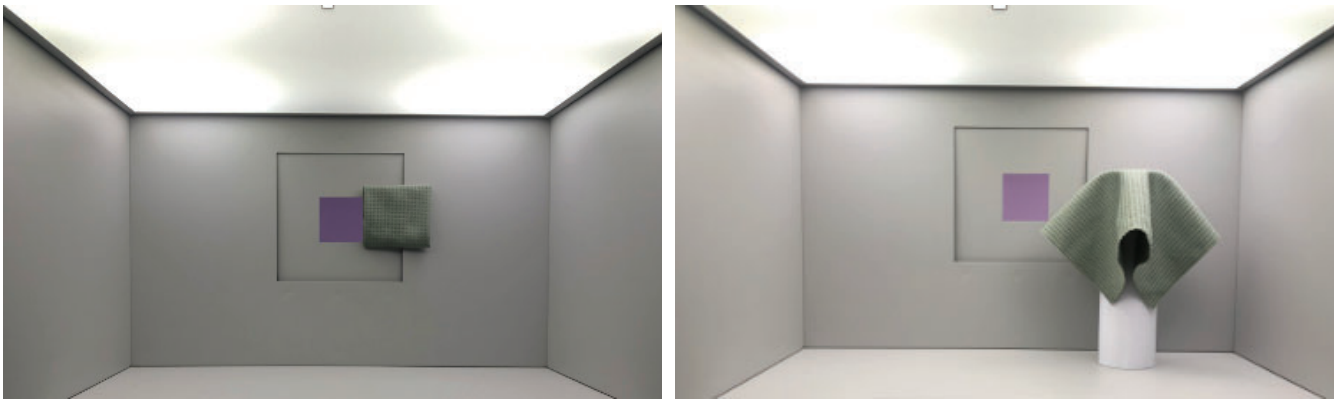

Figure 3: Experiment interface. Left: flat-fabric matching. Right: draped -fabric matching.

Results and Discussion

Observer variability

Observer variability includes intra- and inter-observer variability, indicated by the mean colour difference from the mean (MCDM). The intra-observer variability was calculated for each participant's MCDM for the 10 repeated fabric samples, taking the average over 10 repeated fabric samples and over all participants. Participants showed good repeatability with an MCDM of 3.16 ΔE^*_{00} and 3.00 ΔE^*_{00} in flat-fabric matching and draped-fabric matching, respectively. The inter-observer variability represents the consistency between all participants, assessed for each fabric sample by calculating the ΔE^*_{00} between the matched colour of an individual and the average over all participants. The mean ΔE^*_{00} of all participants for each fabric sample was calculated, and inter-observer variability was indicated by the mean of 30 fabric samples. For substrate 1, 2, and 3, the inter-observer MCDM was 6.32, 5.20, 5.30 ΔE^*_{00} and 5.99, 6.36, 6.70 ΔE^*_{00} in flat-fabric matching and draped-fabric matching, respectively. Table 1 lists the results of observer variability in terms of MCDM.

Table 1: Observer variability (MCDM, ΔE^*_{00})

		substrate 1	substrate 2	substrate 3
Flat fabric colour matching	Intra-observer variability	3.16		
	Inter-observer variability	6.32	5.20	5.30
Draped fabric colour matching	Intra-observer variability	3.00		
	Inter-observer variability	5.99	6.36	6.70

Comparison of colour perception between three substrates

The matched CIE L*, a*, b* and C* values obtained through flat- and draped-fabric matching experiments were compared across three reference substrates. For each substrate, the matched colour was recorded, and pairwise comparisons were conducted between the three sets of data. Figure 4 illustrates the comparison in terms of CIE L*, a*, b*, and C* for experiments matching flat fabrics (left-three) and matching draped fabrics (right-three). A 45-degree line was plotted in each figure to indicate the line of equality, representing cases where the two compared values are equal.

When substrate 1 was used as the reference, the matched fabric lightness (L*) was generally higher than that obtained using substrate 2 and 3 as references in the flat-fabric matching condition (see figures on row 1, column 1 and 2). Moreover, the matched fabric L* using substrate 2 as the reference was generally higher than that using substrate 3 as the reference (see figure on row 1, column 3). A clear trend was found that decreasing substrate coarseness generally leads to higher matched L* in flat-fabric matching condition. A similar trend was also observed in the draped-fabric matching condition, which suggests that the perceptual effect of substrate texture on the matched fabric L* is consistent across different presentation modes of the fabrics. Specifically, in the flat-fabric and draped-fabric matching conditions, the average matched fabric L* using substrate 1 was 1.18 units and 0.65 units higher than that of substrate 2, and the average matched L* using substrate 2 was 1.22 units and 1.11 units higher than that of substrate 3, respectively.

In addition to fabric L*, the matched fabric redness-greenness (a*), yellowness-blueness (b*), and chromaticity (C*) were compared across three reference substrates in Figure 4. The results showed that the matched a*, b*, and C* values were highly consistent among the three reference substrates, suggesting that the substrate texture had little influence on fabric chromatic perception.

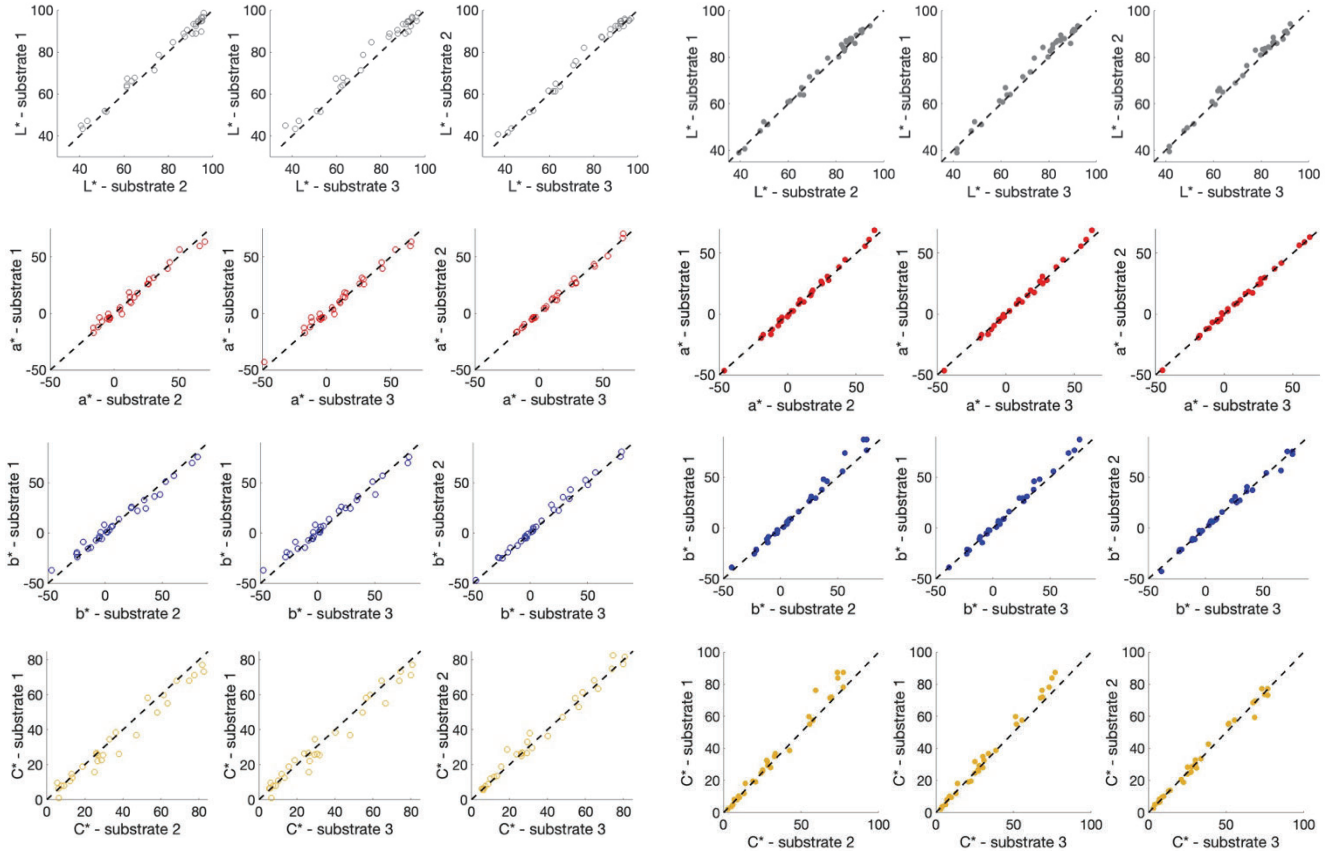

Figure 4: Comparison of the matched L*, a*, b*, and C* between three substrates. Left: flat-fabric matching. Right: draped-fabric matching.

The colour differences of the matched fabric colour among using three reference substrates were calculated in unit of ΔE^*_{00}. The results were listed in Table 2. The largest matched colour difference was observed between the colours matched using substrate 1 and substrate 3 as references, with values of 3.88 ΔE^*_{00} units and 2.47 ΔE^*_{00} units for flat-fabric matching and draped-fabric matching, respectively. Among the three reference substrates, substrate 1 and substrate 3 exhibited a large difference in surface texture and coarseness (see Figure 1). The relatively larger colour difference observed when using them as references suggests that fabric texture played a role in fabric colour perception, regardless of the presentation modes of fabrics (flat or draped).

Table 2: The matched fabric colour difference (ΔE^*_{00}) among using different reference substrates, averaged over 30 fabric samples

	substrate 1 VS substrate 2	substrate 1 VS substrate 3	substrate 2 VS substrate 3
Flat-fabric colour matching	3.33	3.88	2.12
Draped-fabric colour matching	2.00	2.47	1.78

Comparison of colour perception between flat and draped matching

The matched CIE L*, a*, b* and C* values obtained using three reference substrates were also compared between flat-fabric matching and draped-fabric matching, as shown in Figure 5. Regardless of the substrate used, the matched fabric L* obtained from flat-fabric matching was slightly higher than that from draped-fabric matching, especially for fabrics with higher L*. Compared to flat fabrics, the presence of shape, shadow, and folds in draped fabrics leads to a reasonable reduction in the perceived fabric lightness. In contrast, the matched fabric chromaticity (a*, b*, C*) showed little difference between flat-fabric matching and draped-fabric matching. Even though shape, shadow, and folds were visible only for draped fabrics, they had only a limited effect on the perception of fabric chromaticity. In addition, as shown in Table 2, the colour differences among the three reference substrates were consistently larger in flat-fabric matching than in draped-fabric matching. The results indicated that texture played a more important role in flat-fabric matching, while the draped shape reduced the effect of texture when perceiving the fabric colours.

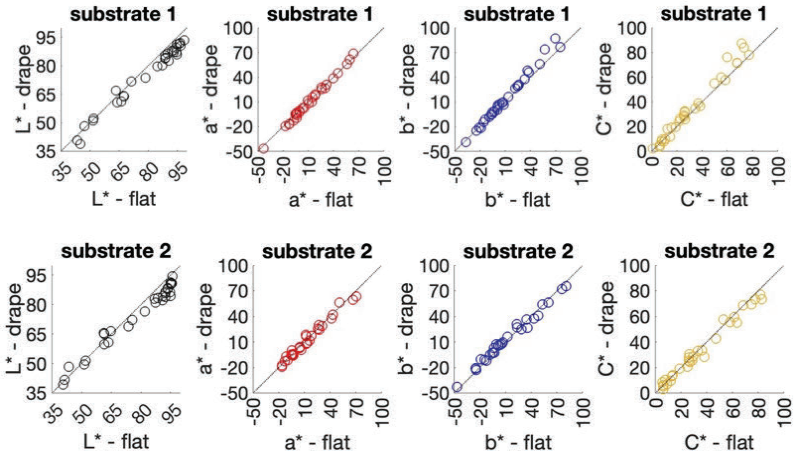

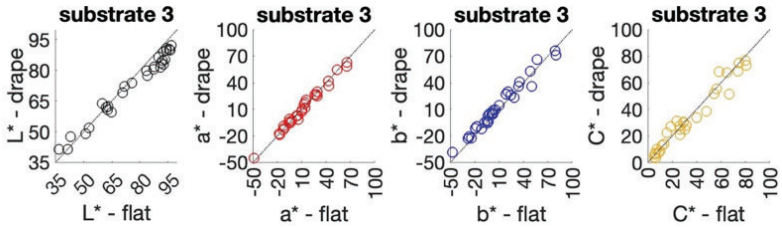

Figure 5: Comparison of the matched L*, a*, b*, and C between flat-fabric and draped-fabric matching.

Conclusion

The present study introduced a colour matching experiment to achieve colour matches between fabric samples in flat and draped states and the projected reference substrates with three different textures. 30 fabrics samples were used, and 90 times flat-fabric matching and draped-fabric matching were conducted by 10 participants. By comparing the matching results among reference substrates, it indicated that higher fabric L* was generally obtained along with the lower substrate coarseness in both flat- and draped-fabric matching. What's more, the matched flat-fabric L* was generally higher than the matched draped-fabric L*, indicating the effect of fabric shape in the fabric colour perception. In contrast, the matched fabric chromaticity (a*, b*, C*) was less affected by the presence of texture and shape. The findings demonstrated the importance of texture and shape in real object's colour perception, which could be recommended for future investigation.

References

[1]. Hunt, R.W.G., and Pointer, M.R. (2011). *Measuring colour*, 4th. Ed., John Wiley & Sons. http://DOI:10.1002/9781119975595

[2]. Allred, S.R. and Olkkonen, M. (2015). The effect of memory and context changes on color matches to real objects. *Attention, Perception, & Psychophysics*, 77(5), 1608-1624.

[3]. Zhu, Y., Zhai, Q., and Luo, M.R. (2018). *Investigating chromatic adaptation via memory colour matching method on a display (CIC)*. Retrieved 31, August 2025, from https://library.imaging.org/cic/articles/26/1/art00052

[4]. Shi, K., Luo, M.R. (2022). Factors affecting colour matching between displays. *Optics Express*, 30(15), 26841-26855.

[5]. Zhang, Y., Motoyoshi, I. (2023). Perceiving the representative surface color of real-world materials. *Scientific Reports,* 13(1), 6300.

[6]. Lu, Y., and Xiao, K. (2021). Quantifying facial colour appearance of Caucasian and Chinese faces (AIC). Retrieved 31 August, 2025, from https://aic-color.org/history

[7]. Arshad, S.R. and Shahzad, M.K. (2024). Deep learning-based fabric defect detection: A review. *Textile Research Journal*, 93(5-6), 1485-1503.

[8]. Pervez, M.N., Yeo, W.S., and Lin, L. (2023). Optimization and prediction of the cotton fabric dyein process using Taguchi design-integrated machine learning approach. *Scientific Reports*, 13(1), 12363.

[9]. Alegbe, E.O., and Uthman, T.O. (2024). A review of history, properties, classification, applications, and challenges of natural and synthetic dyes. Heliyon, 10(13), e33646.

[10]. Li, Q. (2025). *Predicting the tactile properties of fabrics from vision and touch.* Doctoral dissertation, University of Leeds.

The Moral Perception of Scarf Colors on Different Skin Colors

Chia-I Liao[a*], Wen-Yuan Lee[b]

[a] *The Graduate Institute of Design Science, Tatung University, Taiwan*
[b] *Department of Media Design, Tatung University, Taiwan*
**Corresponding author: Chia-I Liao d11317005@o365.ttu.edu.tw*

ABSTRACT

Clothing is a powerful medium through which individuals express their identity and convey their social roles. However, prior research has primarily focused on color chips or abstract color patterns, which leaves an essential gap in our understanding of how the combination of clothing color and skin tone affects people's moral perception. This study examines how scarf color and skin tone combinations affect moral perception, using the Five Foundations of Morality as the conceptual framework.

The experiment conducted a psychophysical experiment to investigate how scarf color influences moral perception when paired with different skin tones. A total of 49 observers were invited to evaluate 44 scarf–skin color combinations across 11 moral perception scales. These combinations were systematically designed by crossing 11 scarf colors with four skin tone levels, corresponding to "very light," "intermediate," "brown," and "dark" skin, based on L*, a*, b* values aligned with four of the six Individual Typology Angle (ITA) skin tone categories. The 11 moral perception scales, which were developed according to five moral foundation dimensions. The scales included adjective pairs such as: kind–cruel, authoritative–submissive, sympathetic–indifferent, fair–partial, honest–deceitful, loyal–hypocritical, polite–rude, arrogant–humble, formal–casual, and cautious–reckless. Participants rated each sample using a seven-point categorical judgment scale.

The major findings are as follows: (1) Two underlying components of moral perception, Perceived Social Formality and Perceived Sincere Character, were identified as independent of gender differences; (2) The moral perception evoked by skin-scarf color combinations was found to be primarily influenced by the scarf color rather than the skin tone. The data obtained from the experiment were used to analyze the connection between scarf color, skin tone, and moral perception, offering new perspectives on color psychology, social cognition, and fashion marketing.

Keywords: Moral Perception, Skin tone, fashion design, Scarf colors

INTRODUCTION

Clothing serves as a powerful means for people to express themselves and showcase their social identities. Individuals often have a great deal of freedom in their clothing choices, allowing them to communicate how they want to present themselves to others.[13] Research shows that what people wear, including the style (like formal or casual) and color of their clothing, plays a significant role in how first impressions are formed and how individuals are evaluated socially. This is because clothing serves as a type of nonverbal communication that can send both intentional and subconscious messages.[3,6,15,16] Formal attire, for instance, is frequently associated with competence and professionalism, which in turn fosters more favorable moral impressions.[4,7,16] Similarly, clothing color has been shown to influence perceived attractiveness and exert profound psychological effects on both the wearer and the observer.[1,11,14] Subtle variations in attire may prompt observers to apply differing moral standards, attributing distinct intentions or motives to the wearer.[4] Moreover, clothing color may interact with other nonverbal cues, such as skin tone, to modulate social and moral perceptions in complex ways.[1]

In previous research, most studies have focused on color chips or abstract color patterns, which leaves an essential gap in our understanding of how the combination of clothing color and skin tone affects people's moral perception. This is important because skin tone is a significant visual cue that can work in conjunction with clothing color to influence how we perceive someone's moral perception, especially in diverse social settings

where these combinations can carry cultural meanings. Filling this gap is essential for enhancing our understanding of how visual signals impact moral perception. This has significant consequences for social interactions, cultural biases, and even in professional environments where how someone dresses can shape perceptions of trustworthiness and ethical behavior.

To address this, the present study investigates how combinations of scarf color and skin tone influence moral perception, drawing on the Five Foundations of Morality framework.[5] This framework posits that moral judgments are grounded in five key dimensions: (1) harm/care, (2) fairness/cheating, (3) loyalty/betrayal, (4) authority/subversion, and (5) sanctity/degradation. Based on these foundations, we developed 11 adjective-pair scales to assess moral perceptions." These scales were used to evaluate moral perception of 44 scarf–skin tone combinations, comprising 11 scarf colors across four distinct skin tones. The significance of this research lies in its potential to uncover how subtle, everyday choices in attire, when combined with inherent physical traits such as skin tone, influence moral perception in social contexts. This study intended to offer novel insights into the nuanced dynamics of nonverbal communication and moral perception.

EXPERIMENTAL PLAN

To examine the impact of scarf color and skin tone on moral perception, this study recruited 49 observers to evaluate 44 unique combinations, consisting of 11 scarf colors paired with four distinct skin tones. The observer group comprised 23 males and 26 females, with a mean age of 27.73 years (SD = 9.85). Each observer evaluated the combinations using 11 moral perception scales, derived from the Five Foundations of Morality framework: "kind-cruel," "compassionate-indifferent," "honest-deceitful," "impartial-biased," "loyal-treacherous," "polite-rude," "arrogant-humble," "formal-casual," "authoritative-submissive," "prudent-reckless," and "sincere-hypocritical." Assessments were conducted using a 7-point categorical judgment scale, as depicted in Figure 1.

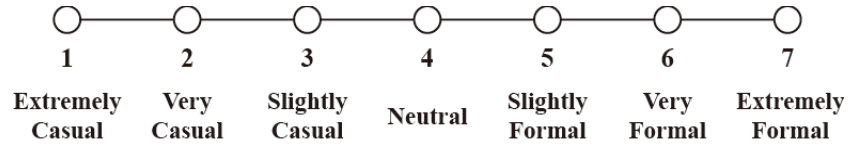

Figure 1. A 7-step categorical judgement, taking "casual-formal" as an example

The study generated a total of 44 scarf-skin color combinations by pairing 11 scarf colors with four different skin tones. The selected skin tones very light, intermediate, brown, and dark were based on the ITA classification system defined by Ly *et al*.[12]. The scarf color corresponded to the 11 basic color terms proposed by Berlin and Kay[2], including red, orange, yellow, green, blue, purple, pink, brown, black, grey, and white. These colors were further refined using the foci color boundaries defined by Lin *et al*.[8-10]. The scarf-skin color combinations shown in Figure 2 were created using Adobe Photoshop.

Forty-nine observers completed the Ishihara color blindness test to ensure accurate color representation. All observers were invited to participate in the experiment, which was conducted in a dark room. Each observer wore a large black cloth covering their upper body to minimize visual distractions. Observers were asked to assess 44 scarf–skin color combinations that were shown on a 15.3-inch MacBook Air screen. The screen was placed inside a viewing cabinet with D65 lighting, and each observer sat about 70 cm away from it. The order of presentation was random. Each observer made a total of 484 judgments (11 scarf colors × 4 skin tones × 11 moral perception scales). To examine intra-observer consistency, one of the combinations was shown twice in the session.

Figure 2.The experimental samples consisted of 44 images combining 11 scarf colours and 4 skin tones.

The CIELAB color values of both the scarf and skin tones were obtained using an X-Rite i1 Pro 2 device from the screen display. As shown in Figure 3(a), measurements were taken from three blurred square areas in Adobe Photoshop, and the average of these values was calculated. The averaged color values were then plotted in the CIELAB color space, as shown in Figure 3(b) and 3(c).

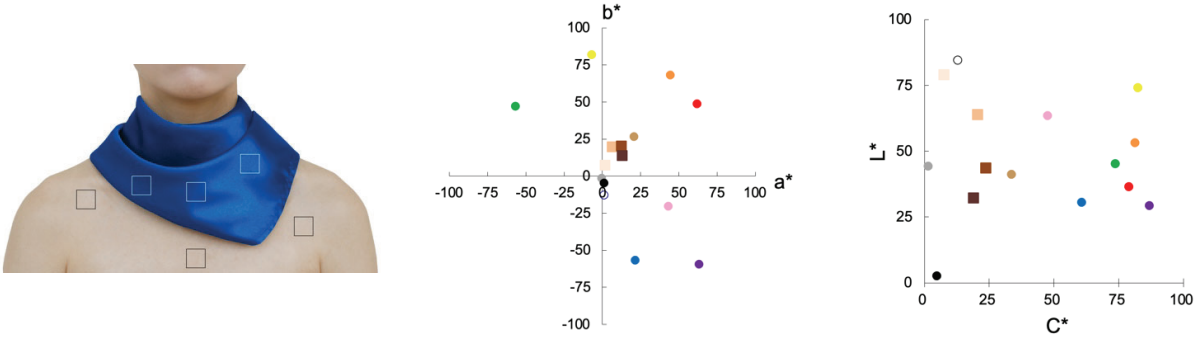

(a) The measured regions (b) CIELAB a*-b* diagram (c) CIELAB L*-C*diagram

Figure 3:(a) The measured regions, (b) The color distribution in CIELAB a*-b* diagram, and (c) CIELAB L*-C* diagram. The circle indicates the scarf color, while the squares represent skin tones.

INTRA-AND INTER-OBSERVER VARIATION

The data collected from the seven-step categorical judgment scales were converted into numerical values for analysis. Variations within and between observers were examined using the root mean square (RMS) method. Intra-observer variation was used to evaluate the consistency of repeated responses from the same observer. In contrast, inter-observer variation measured the degree of agreement between each observer and the group average. The RMS equation is given below.

$$RMS = \sqrt{\frac{\sum(X_i - Y_i)^2}{n}}$$

For intra-observer variation, Xi and Yi represent the initial and replicated judgments, respectively. For inter-observer variation, Xi represents the individual data, and Yi represents the corresponding average across all observers. An RMS value of 0 indicates perfect agreement between two data arrays.

As shown in Figure 4, the RMS values for intra-observer variation range between 0.70 and 3.04, indicating disagreement within individual observers' repeated assessments. In contrast, RMS values for inter-observer variation range from 0.88 to 1.72, indicating high agreement between observers and suggesting consistency across observers. The elevated intra-observer variation may be attributed to the experimental design, wherein the repeated sample was the first item presented. During this initial assessment, observers were likely still adapting to the experimental procedure and calibrating their application of the moral perception scale, which could account for the observed inconsistency in their repeated judgments. Therefore, the following analysis used the judgments of all observers, but for the replicates, the second judgment was used.

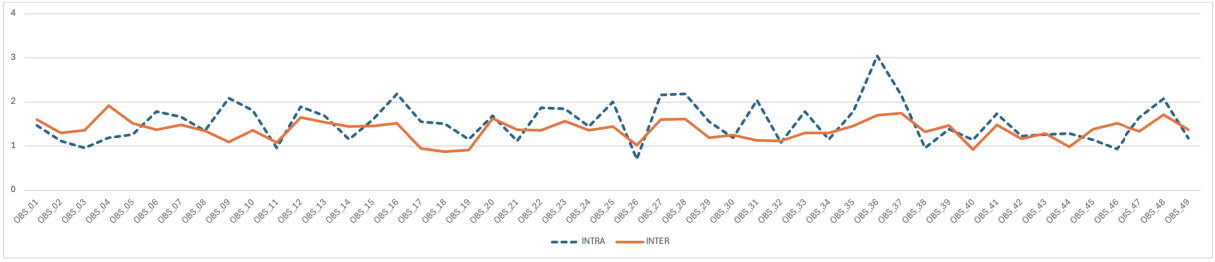

Figure 4: Intra-observer and inter-observer variations

RESULTS

To investigate the existence of gender differences in the evaluation of scarf-skin color combinations on the 11 moral perception scales, the independent-sample T-test was carried out. The gender difference was found on three moral perception scales, including “honest–deceitful,” “kind–cruel,” and “impartial–biased.” This suggests that these scales may reflect gender-specific moral perception rather than universal moral perception.

To extract a generalizable moral perception component and avoid confounding effects in the subsequent principal component analysis (PCA), these three scales were excluded. The remaining eight scales were processed using PCA to reveal shared perceptual components rather than gender-biased tendencies, enhancing the interpretability and cross-gender robustness of the results.

A Principal Component Analysis (PCA) with varimax rotation was performed on the remaining eight moral perception scales, extracting two components with eigenvalues greater than 1.0, which together explained 83% of the total variance, as given in Table 1.

The principal component analysis revealed that Component 1 included the scales of "Formal–casual," "Compassionate–indifferent," "Prudent–reckless," "Authoritative–submissive," and "Polite–rude." These scales appear to reflect a perceived orientation toward behavioral propriety, adherence to social roles, and sensitivity to contextual norms. This component was interpreted as representing Perceived Social Formality, with the two poles characterized as "Dignified" and "Relaxed." Component 2 comprised the scales "Arrogant–humble," "Sincere–hypocritical," and "Loyal–treacherous," which collectively relate to impressions of interpersonal transparency and integrity. This component was interpreted as representing Perceived Sincere Character, with its poles described as "Trustworthy" and "Unreliable."

The component loadings of each scale were used to conduct Cluster analysis. This analysis reveals underlying patterns in how combinations are perceived along the dimensions of Perceived Social Formality and Perceived Sincere Character. Based on their positions in the two-dimensional principal component space, the skin–scarf combinations were classified into five groups. The results are visualized in the principal component space, as shown in Figure 5, which illustrates the five groups of skin–scarf combinations based on their perceptual similarities.

Table 1: The results obtained from the principal component analysis

	Component	
	1	2
Formal-casual	0.95	-0.06
Compassionate-indifferent	-0.93	0.28
Prudent-reckless	0.92	0.31
Authoritative-submissive	0.69	-0.57
Polite-rude	0.69	0.61
Arrogant-humble	-0.02	-0.89
Sincere-hypocritical	-0.29	0.85
Loyal-treacherous	0.13	0.78
Eigenvalue	3.66	2.98
% of Variance	45.78 %	37.30 %
Cumulative %	45.78%	83.08%

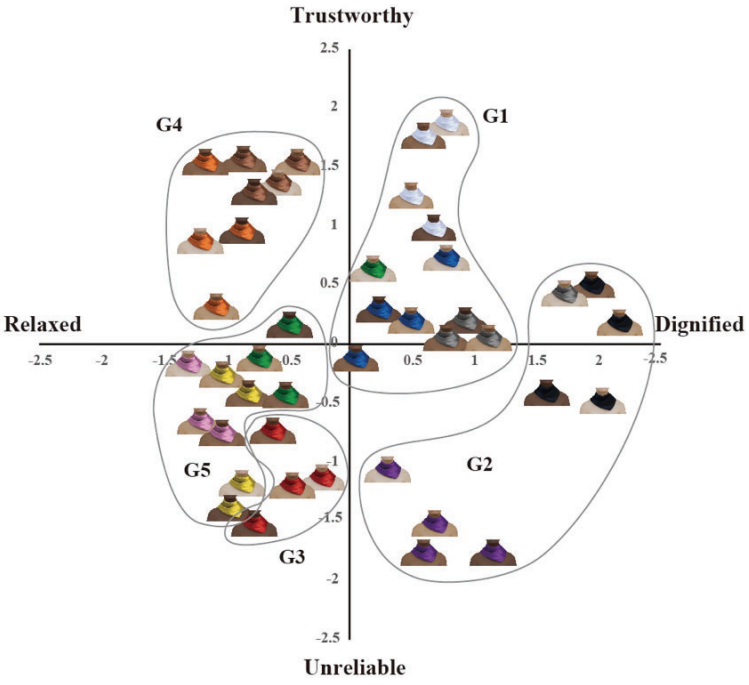

Figure 5: The Principal component space. The horizontal axis is Perceived Social Formality, and the vertical axis is Perceived Sincere Character

In the principal component space, combinations of different skin tones with the same scarf color are grouped in the same cluster. This indicates that, in this context, moral perception is more strongly influenced by the color of the scarf than by skin tone. Also, it can be seen that

1. The scarf colors in Group 1 include white, blue, and gray colors. These scarf colors can convey trustworthiness and moral dignity.
2. In Group 2, the scarf colors include black and purple colors. However, within this group, a subgroup phenomenon can be clearly observed. Black scarves represent dignified moral perceptions, while purple scarves represent unreliable moral perceptions.
3. Red scarves are classified into Group 3. Regardless of skin color, red scarves convey a sense of unreliable and relaxed perceived morality.
4. The orange and brown scarves are classified into Group 4, delivering a sense of trustworthy and relaxed perceived morality.
5. Green, yellow, and pink scarves belong to Group 5, conveying a relaxed moral perception and tending towards unreliable.

SUMMARY AND CONCLUSION

This study investigates how combinations of scarf colors and skin tones influence moral perception. The major findings are as follows: (1) Two underlying components of moral perception, Perceived Social Formality and Perceived Sincere Character, were identified as independent of gender differences; (2) The moral perception

evoked by skin-scarf color combinations was found to be primarily influenced by the scarf color rather than the skin tone.

Future studies are recommended to incorporate more diverse observers in terms of age, cultural background, and ethnicity. Additionally, it would be valuable to investigate how these moral perceptions may shift under real-life or context-specific scenarios. Given that scarf colors were found to evoke moral perceptions, future studies should also explore how these findings relate to well-established concepts in color emotion and color harmony. The subtle variations in color attributes may further affect moral perceptions.

Moreover, these insights may have practical applications in fields such as branding, fashion design, and political image management, where strategic color choices in self-presentation and nonverbal communication could shape perceptions of moral character and social identity.

REFERENCES

1. Amhorst MLD, Reed JAP. Clothing Color Value and Facial Expression: Effects on Evaluations of Female Job Applicants. Social Behavior and Personality: an international journal 1986;14(1):89-98.
2. Berlin B, Kay P. Basic Color Terms: Their Universality and Evolution. Berkeley, California, USA: University of California Press; 1969.
3. Carr D, Davies T, Lavin A. The effect of business faculty attire on student perceptions of the quality of instruction and program quality. College Student Journal 2009;43(1):45-56.
4. Dong M, van Prooijen J-W, van Lange PAM. Status cues and moral judgment: Formal attire induces moral favoritism but not for hypocrites. Current Psychology 2024;43(21):19247-19263.
5. Haidt J, Joseph C. Intuitive ethics: how innately prepared intuitions generate culturally variable virtues. Daedalus 2004;133(4):55-66.
6. Howlett N, Pine K, Orakçıoğlu I, Fletcher B. The influence of clothing on first impressions: Rapid and positive responses to minor changes in male attire. Journal of Fashion Marketing and Management: An International Journal 2013;17(1):38-48.
7. Karl KA, Hall LM, Peluchette JV. City employee perceptions of the impact of dress and appearance: You are what you wear. Public Personnel Management 2013;42(3):452-470.
8. Lin H, Luo MR, MacDonald LW, Tarrant AWS. A cross-cultural colour-naming study. Part I—Using an unconstrained method. Color Res Appl. 2001;26(1):40-60.
9. Lin H, Luo MR, MacDonald LW, Tarrant AWS. A cross-cultural colour-naming study. Part II—Using a Constrained Method. Color Res Appl. 2001;26(3):193-208.
10. Lin H, Luo MR, MacDonald LW, Tarrant AWS. A cross-cultural colour-naming study. Part III—A colour-naming model. Color Res Appl. 2001;26(4):270-277.
11. Luo Z, Shamey R. Cross-ethnic comparison of the effect of garment color on male perception of female attractiveness. Color Research & Application 2023;48(4):355-367.
12. Ly BCK, Dyer EB, Feig JL, Chien AL, Bino SD. Research Techniques Made Simple: Cutaneous Colorimetry: A Reliable Technique for Objective Skin Color Measurement. J Invest Dermatol 2020;140(1):3-12 e1.
13. Nezlek JB, Mochort E, Cypryanska M. Self-presentational motives and public self-consciousness: Why do people dress a certain way? J Pers 2019;87(3):648-660.
14. Roberts SC, Owen RC, Havlicek J. Distinguishing between perceiver and wearer effects in clothing color-associated attributions. Evolutionary Psychology 2010;8(3):350-364.
15. Šakić V, Franc R, Ivičić I, Maričić J. Tie–an Accessory Fashion Detail or a Symbol? Croatian medical journal 2007;48(4):419.
16. Slepian ML, Ferber SN, Gold JM, Rutchick AM. The cognitive consequences of formal clothing. Social Psychological and Personality Science 2015;6(6):661-668.

Regarding Racism in Color Theory

Edward R. Charbonneau
Minneapolis College of Art and Design, Minneapolis, United States

ABSTRACT

This research is intended to place Johannes Itten's color theories into the context of his white supremacist philosophy and beliefs. Itten taught at the Bauhaus school in Weimar, Germany from 1919-1923, while he was a member of an occult religion known as Mazdaznan, a racist belief system masquerading as a health and wellness spiritual movement. Through its doctrines and practices, Mazdaznan promoted a hierarchy of races where the white race was defined as having the highest purity of blood. Through diet, exercise, and other lifestyle choices, devotees to this doctrine, like Itten, sought to bring into existence what they viewed as the next evolution of humanity, a race of transparent beings, predicted to occur in 1960. The main argument of this paper outlines how Itten centered Mazdaznan ideologies to inform his mindset. He theorized that his students' subjective color preferences were situated in the colors of their eyes, hair, and skin, while he sought to establish universal laws of color harmony in art and design education. Since 1961, Itten's deeply flawed methodologies regarding color usage and instruction have become entangled within educational systems and traditions to such degrees that their origins are nearly invisible within the shroud of their authority. Apart from contextualizing Itten's writing through a Mazdaznan lens, the goal of this paper is to ask how we may examine our past traditions, and utilize the insight gleaned when designing new pedagogical approaches to teaching and learning about color theory? Moreover, how can the field open up, expand, and break free from past ideologies and dogmas to respond to contemporary practices?

Keywords: Johannes Itten, Faber Birren, Mazdaznan, Color Harmony, Color Theory

INTRODUCTION

Johannes Itten first gained notoriety as the designer and master instructor of the famous *Preliminary Course* (or *Vorkurs,* the *Foundation Course;* the *Basic Course*) at the Bauhaus School in Weimar, Germany, from its inception in 1919 until he resigned in 1923 [1, 14]. Before, during, and after his tenure on the Bauhaus faculty, Itten was a devout follower of the Mazdaznan religion [13, 15]. The pedagogical practices which Itten played a role in developing spread across the globe as faculty and students fled Germany to take up teaching assignments in other parts of the world after the school was closed by the Nazi regime in 1933 [11, 16].

In 1961, Itten published his ideologies on color theory within the treatise *Kunst der Farbe: Subjektives Erleben und Objektives Erkennen als Wege zur Kunst,* translated into English the same year as, *The Art of Color: The Subjective Experience and Objective Rationale of Color* [6, 7]. Nine years later, in 1970, and three years after Itten's death, *The Art of Color* was abridged and republished as the *Studienausgabe* edition (study edition), edited by Johannes' widow, Anneliese Itten [11]. Itten's text was further abridged and published the same year by Faber Birren as, *The Elements of Color: A treatise on the color system of Johannes Itten based on his book The Art of Color, edited and with a foreword and evaluation by Faber Birren* [2].

Research for this paper was undertaken for several reasons: first, my growing awareness of Itten's published works, or works attributed to him, such as Birren's *Elements of Color*, as well as their prevalence in education; second, a learned knowledge as a painter that Itten's color mixing instruction is not reliably applicable in practice; third, observations of the overwhelming prevalence of Itten's recipes for color harmony appearing in brand and package design, as well as other fields in which color plays a role; and fourth, a deeper knowledge of how

Mazdaznan ideologies played a role in Itten's life, teaching practice, writing, as well as his work as an artist. The objective of this research is to contextualize the writing and instruction of Johannes Itten within the lens of the Mazdaznan religion's white supremacist ideologies so that contemporary and future educators may contemplate these source materials with respect to their pedagogical and studio practices.

METHODOLOGIES

My research was conducted through literature and public media searches of books, periodicals, and databases referencing the texts of Johannes Itten and other sources cited, as well as Itten's original writing. My thirty-five years as a practicing artist and painter has taught me that Itten's guidance pertaining to color mixing does not reliably predict how pigments mix. This knowledge initially led my research and investigation in an attempt to understand why Itten would have promoted such an untenable color mixing system; learning about Itten's faith beliefs in the Mazdaznan religion spurred further research as to whether or not Mazdaznan's white supremacist ideologies had an impact on his teaching and writing practices. Addressing this question became the impetus for writing this paper.

RESULTS AND DISCUSSION

The two primary theses of Itten's color theories, and pedagogical methodologies, reside in the subtitle of his English language publication, *The Art of Color: The Subjective Experience and Objective Rationale of Color.* Itten believed that subjective experience is possible to define and classify, and secondly, color usage requires an objective rationale. Itten proclaimed all colors which mix to an achromatic gray, white, or black color to be objectively harmonious, a position he adopted from prior color theorists and philosophers. Subsequently, he centered his definition of subjective color preferences as relative to a person's skin, hair, and eye colors. Within the pages of the *The Art of Color* (1961)*,* Itten describes "individual aptitudes" and "types" of students in regard to the colors they are drawn to use [7, p. 26]. Within the two 1970 abridged editions, the *Studienausgabe* and *The Elements of Color*, the concept of a person's color aura, or what is termed to be their *Subjecktiven Farbenklange* (Subjective Color Sounds) in the first volume*,* and *Subjective Timbre,* in the latter, is defined more specifically:

> Light blond types with blue eyes and pink skin incline towards very pure colors, often with a great many clearly distinguished color qualities. Contrast of hue is the basic feature. Depending on the forcefulness of the individual, the colors may be more or less luminous.
>
> A very different type is represented by people with black hair, dark skin, and dark eyes, for whom black plays an important part in harmony [2, p. 24].

Itten then proceeds to instruct educators to not assign similar projects, or subjects, to students of differing skin, hair, and eye colors, Itten writes:

> The blond type would be assigned such subjects as Springtime, Kindergarten, Baptism, Festival of Bright Flowers, Garden at Morning. Nature subjects should be vivid, without light/dark contrasts.
>
> Good assignments for the dark type would be Night, Light in a Dark Room, Autumn Storm, Burial, Grief, The Blues, etc. Nature studies can be done in charcoal or black and white pigments.

> In other words, it is wrong to impose the same standard flower or figure studies for all students. Individual, subjectively slanted assignments are necessary so that students will be able to discover correct solutions intuitively. When a student is presented with themes 'alien' to himself, he is forced to deal with them intellectually while as yet lacking the objective knowledge to do so [2, pp. 24-25].

The view that individuals of differing skin, hair, and eye colors lack the intellect to comprehend shared experiences in classroom settings align with the central tenet of the Mazdaznan religion's white supremacist teachings, of which Itten was a devout follower [3, p. 173; 18, p. 113]. The passages stated below appeared in the forward to the publication *Mazdaznan Health and Breath Culture,* written by the religion's founder, are representative of the Mazdaznan worldview:

> ...the change in the blood that made the anthropological developments possible, to the extent of sharp lines of demarcation, separating one race from another not only as to color but as to mental possibilities….
>
> Father Ammann in 'The Coming Race and Race Hygiene' gives to the scientific world the key to life when he says: 'Blood is the original matter which influences all outer manifestations and formations and changes them in the course of development. Blood is the essential race builder. The consistency of the blood determines the infallible sign of racial relation. The purer the blood, the clearer the pigment. The darker the skin, the lower the race. Blood is not only the carrier of the inherited, but also the progenitor to all the attainable spiritual tendencies' [4, p. 199].

In 1923, after departing the Bauhaus faculty, Itten lived for three years at the Mazdaznan temple known as *Aryana*, in Herrliberg, Switzerland [13, p. 12]. In 1955, while attending the opening of the Ulm School of Design, in Ulm, Germany, Itten reflected on this post-Bauhaus period of his life, stating:

> My ideas about a new foundation for culture based on the individual development of each person were not what he [Walter Gropius, the Bauhaus' director] wanted. I, on the other hand, was convinced that a new way of building had to grow out of a new attitude towards life [13, pp. 18-19].

While at Aryana in 1923, Itten delivered the eulogy for David Ammann, the *Father Ammann* cited in the earlier quoted passage from *Mazdaznan Health and Breath Culture* [13, p. 12]. The same year, Itten published an article in the *Mazdaznan Journal of Aryan Wisdom and Art of Living*, which summarized his teaching philosophy. Titled, *Rassenlehre und Kunstenwicklun,* or, *Racial Theory and Artistic Development* (also *Racial Doctrine and Artistic Development*), Itten wrote:

> The white man creates from his centre through the gift of inspiration and revelation. We found that in all earlier races, the basis of creative work was always one-sidedly the material or spiritual or intellectual system or a combination of two such systems. Only in the white race did the union and the balance of the three temperaments come about, in such a way that the centre, the source, the soul was recognized and everything was now derived from this source, this individuality.
>
> Only the white race has been given the opportunity to create perfect, i.e. harmonious, works of art as symbols and models of progress towards human perfection, towards holiness. The visual arts (paintings, sculpture, architecture, the art of sound and the word) only come into their own in the white race. [13, p. 8]

The above passages foreshadow what Itten would later write when introducing the concept of *color contrasts* in *the Art of Color,* and *The Elements of Color*, describing the role of the artist in mediating three aspects of color aesthetics: the *visual, mental*, and *spiritual,* correspondingly, the *constructional, expressional,* and *impressional*. Artworks (and their authors) capable of representing only one, or a combination of two aspects of Itten's color aesthetics, without the presence of the third are deemed failures by Itten within his late mid-century texts [7, p. 16-17; 2, p. 12-13].

Itten developed and published his *twelve-part colour star* in 1921, and began formulating his concept of "subjektiven Farben," (or *subjective colors*) in Berlin between 1926-34 [9, p. 5]. Itten's specific phrasing *subjektiven Farbenklange*, or *subjective color tones*; as well as *Subjective Timbre* in *The Elements of Color*, have many parallels to Mazdaznan literature which repeatedly referenced rhythm (of breath to oxygenate blood as a vehicle of racial transcendence), resonance, and vibration. The below passage published in the monthly periodical, *Mazdaznan*, January 1914, is an early example conflating vibration with race:

> Color of races [sic] is not due to climatic reasons so much, as to the vibratory activities of the Kosmos which correspond to colors and produce them. Kali is black, for black is the color of disintegration. The black color will disappear with the disappearance of the Kali vibration. Black and brown races will disappear from the Earth, not in the sense that those individuals will die, but rather that they will go through a change in their vibration, and color will be changed. Of course this will cause the death of many of them, owing to difficulty in adjustment of themselves to the new vibration. [10, p. 22]

Regarding his *Theory of Color Design,* Itten writes: "Deliberate intellectual construction is the 'conveyance' that carries us to the portals of this new reality" [7, p. 34; 2, p. 28]. Serendipitously, he made a lithographic print of a futuristic structure called, *The House of the White Man* (1921), which, according to Itten vis-à-vis, a Mazdaznan prophecy, would house the forthcoming, seventh race of humanity; a transparent race ascendent through whiteness [13, p. 5; 20, 5]. This evolution in humanity was predicted by Mazdaznan lore to occur in 1960, the year before *The Art of Color* was ultimately first published [13, p. 7-8]. Itten may have had this new iteration of humanity in mind when he celebrated the birth of his first child, whom he painted as a toddler in 1921/22 as a tribute to the infant's whiteness, proclaiming that his "transparent whiteness*"* foreshadowed "the coming of man*"* [12]. He also wrote about individual subjectivity in his 1963 book, *Design and Form: The Basic Course at the Bauhaus*. Itten devotes the final chapter to *Subjective Forms,* where he describes a student within the initial sentences of the first paragraph: "Her eyes were like moonstones, and her pale skin was transparent" [8, p. 177].

Itten's second hypothesis in the various editions of *The Art of Color,* and Birren's *The Elements of Color,* states that all harmonious color palettes mix to a neutral gray color [7, p. 22; 2, p. 20]. He adopted the nineteenth century view that afterimages are proof of the mind's ability to maintain visual stasis (i.e., harmony) by spontaneously producing the complement of an inducer color. The product of the two colors comprise the entire spectrum and therefore *complete each other* by forming an achromatic white, gray, or black color [9, p. 21; 2, p. 20]. Based on that theory, he surmised that any assortment of pigments which mix to a neutral gray or black color inherently form harmonious palettes. In this way, he conflated additive and subtractive color mixing by confusing how subtractive pigments mix with how additive wavelengths are perceived as colors. Itten's stated goal was to remove the subjectivity of personal color preferences and define an "objective principle" [7, p. 21; 2, p. 19]. He claimed that the formula brought a "...heightened degree of order and truth…." to a palette [7, p. 34; 2, p. 30].

Writing in the late mid-century, Itten promoted the red-yellow-blue triad of primary colors as the foundation of his *twelve-part color circle*, and corresponding *twelve-point color star* of 1921. This color star is a flattened spherical, globe-shaped color mixing chart of Itten's design with its north pole (white) at its center and its south pole elongated and spread out along the star's circumference, represented as a series of twelve black colors. The twelve points of the star mirror, in number, the twelve lessons described in the book, *Mazdaznan Health and Breath Culture*, as well as the twelve "Aryan" tribes identified by Mazdaznan lore published in monthly periodicals, such as *Mazdaznan and the Messenger,* and *The Sun-Worshipper* [4, 18, p. 44].

Itten's color theory methodologies have had tremendous impacts on art and design education over the past 64 years [17, 19]. His reliance on the red-yellow-blue primary triad as the foundation for subtractive pigment mixing persists to this day in color education despite modern cyan, magenta, and yellow pigments yielding larger color gamuts. The cyan-magenta-yellow primary color triad produces a subtractive color circle where magenta and green, cyan and red, and yellow and blue are directly across from each other, a notion Itten rejected, due to yellow and blue pigments mixing to a green color and not a neutral gray or black [2, p. 21]. However, magenta and green mix to an achromatic black color, which Itten overlooks and does not define the duo as complementary. Due to the acceptance of Itten's theories as canon, his recipe for color harmony has led to a dominance of complementary color schemes within art and design fields of education and practical usage.

Could Johannes Itten have been naive when developing and publishing his color theories? Throughout his writing, he supported the concepts he presented by providing historical and scientific evidence and precedence, to bring authority to his own conjectures, which indicates that he was well-informed in his field. Could he have been motivated by other factors? After extensive study, and reviewing thousands of pages of Mazdaznan literature, it is my view that Ittten was motivated by a desire to promote an objective order which was consistent with his religious mindset of racial hierarchy. His two theses rest on his definitions of objectivity and subjectivity; defining an objective harmony necessitated him to address the subjectivity of individual preferences. Due to the Mazdaznan religion's obsession with defining race in terms of the purity of one's blood, Itten, in the 1961, *The Art of Color,* used coded language to describe his students as possessing *individual aptitudes*, or of being of *types*; whereas, in the 1970 *Studienaugabe* and *The Elements of Color* publications, the specific classification of his students is defined by their eye, hair, and skin colors. Framing subjective preferences as such, he immediately follows up with written instructions to educators to not assign the same projects to cohorts of students of differing eye, hair, and skin colors, as they are incapable of comprehending each other.

Is Itten's formula for color harmony itself racist? Not necessarily. He was reiterating the formula of color harmony described by others, including 19th century theorists and philosophers, such as Johann Wolfgang von Goethe, Ewald Hering, Arthur Schopenhauer, and Otto Runge, whom Itten references in his writing [7, 2]. Were Itten's motivations, methodologies, and conclusions based on a racist's mindset? Undoubtedly. Itten wrote: "The concept of color harmony should be removed from the realm of subjective attitude into that of objective principle" [2, p 19]. He promoted an objective principle of harmony which worked to remove the value of individuality, and ranked lower in esteem subjective personal preferences, tastes, points of view, and cultural traditions. The insistence that all colors fall into an objective scheme is consistent with Itten's worldview that people would fall into his defined view of their *subjective color tones,* or *subjective timbre*; that the objective system subjugates and dictates personal choice.

CONCLUSION

The teaching and practices of color theories and their many applications need to always welcome and embrace questions, re-examinations, and revisions. It is my view after concerted research and practice with Johannes Itten's methodologies that his principles should not have been embraced and promoted throughout and after his tenure. His books have had enormous, and in my opinion, harmful, impacts on the teaching of color across many fields of study. Over the decades, how many color usage traditions have been devalued, sidelined, dismissed or rejected outright by the mass adoption within educational models of Itten's prescribed color theories? In view of his Mazdaznan mindset, Itten's justifications for an objective color harmony and a subjective color predilection are an anathema to contemporary teaching practices. How is it that after first reading *The Elements of Color* in 1988, and Itten's clearly-written definitions of his students' color preferences, based on their eye, hair, and skin colors, did it take me 37 years to ask these questions myself? How do we challenge what is presented to us as canon in the field of color theory? Who, historically, has not been recognized? What new ideas, concepts, and methodologies regarding color, its usage, and pedagogical approaches have yet to emerge?

REFERENCES

[1]. Aoki, K. (2016). Hölzel Circle as the Proto-Bauhaus: The Situation in the Stuttgart Academy and the Concepts Brought to the Bauhaus. *Asian Conference of Design History and Theory Journal*, 1, 41-52. https://acdht.com/journal_2016.html

[2]. Birren, F. (1970). *The Elements of Color: A Treatise on the Color System of Johannes Itten Based on the Book The Art of Color.* Van Nostrand Reinhold Company.

[3]. Hanish, O. (1920) An Extract, *Mazdaznan,* 19(3). PDF

[4]. Hanish, O. (1914) *Mazdaznan Health and Breath Culture.* Mazdaznan Press.

[5]. Hilton, K. (1914) The Master-Thought. *Mazdaznan (Master Thought) and the Messenger,* 13(8), 242-246. PDF

[6]. Itten, J. (1961) *Kunst der Farbe: Subjektives Erleben und Objektives Erkennen als Wege zur Kunst.* Van Nostrand Reinhold Company.

[7]. Itten, J. (1961). *The Art of Color: The Subjective Experience and Objective Rationale of Color.* Van Nostrand Reinhold Company.

[8]. Itten, J. (1963). *Design and Form: The Basic Course at the Bauhaus.* Reinhold Publishing Corporation.

[9]. Itten, J. (2021). *Kunst der Farbe: Subjektives Erleben und Objektives Erkennen als Wege zur Kunst.* (A. Itten, Ed.). Van Nostrand Reinhold Company. (Original work published 1970).

[10]. Johnson, A. (1914). The Stanzas of Dzyan. *Mazdaznan and the Messenger,* 3(1), 20-24. PDF

[11]. Lerner, F. (2005). Foundations for Design Education: Continuing the Bauhaus Vorkurs Vision. *Studies in Art Education*, 46(3), 211–226. https://www.jstor.org/stable/3497081

[12]. Linse, U. (2019). Johannes Itten and Mazdaznan at the Bauhaus. *Bauhaus Imaginista Journal,* 1. https://www.bauhaus-imaginista.org/articles/4787/johannes-itten-and-mazdaznan-at-the-bauhaus

[13]. Linse, U. The Mazdaznan Pedagogy of Bauhaus Master Johannes Itten. *Bauhaus Vorträge*. PDF

[14]. Moholy, L. (1968). Johannes Itten 1888-1967. *Art Journal*, 27(3), 304–304. https://www.jstor.org/stable/775093

[15]. Moore, P. E., & Whittlesea, I. (2017). *The Egyptian Postures*. The Egyptian Postures. PDF

[16]. Raleigh, H. (1968). Johannes Itten and the Background of Modern Art Education. *Art Journal*, 27(3), 284–302. doi.org/10.1080/00043249.1968.10793830

[17]. Wheelwright, N. (1920). Federation of Nations: Study of Man, *Mazdaznan,* 19(2), 175-180. PDF

[18]. Wheelwright, N. (1922). Federator: Study of Man, *Mazdaznan,* 21(1), 43-44. PDF

[19]. White-Hancock, L. (2022). Insights from Bauhaus innovation for education and workplaces in a post-pandemic world. *International Journal of Technology and Education,* 33, 261–279. https://doi.org/10.1007/s10798-022-09729-2

[20]. Volkmar, G. (1920) Prognosis of the Future of the White Race. *Mazdaznan,* 19(1), 51-54. PDF

Human Perspectives on The Role of AI-Enabled Tools for Colour Trend Analysis

Sally Angharad*, Stephen Westland, and Peihua Lai

Leeds Institute of Textiles and Colour, the University of Leeds, Leeds, United Kingdom
**Sally Angharad: Sally Angharad, sdsab@leeds.ac.uk*

ABSTRACT

Artificial Intelligence (AI) is increasingly being used for tasks traditionally carried out by human experts. Colour forecasting, a practice with over a century of history, involves sub-tasks around colour analysis that can be time consuming. In the past decade, machine learning algorithms have been developed for tasks such as automatic analysis of images and text and the extraction of colour palettes from images and mood boards. These approaches are proving effective, particularly when operating in collaboration with designers and forecasters. However, this paper focuses on the human aspect of such human–machine collaboration. The research questions addressed are: what role do AI technologies currently play in professional colour forecasting practice, and what role do experts envisage AI playing in their industries in the near future? The study also explores expert processes, including how they validate colour decisions and how they communicate with clients to build confidence. The methodology is qualitative, based on open-ended one-to-one interviews with five design professionals, each lasting approximately 90 minutes. The data were analysed using thematic analysis to identify key patterns and perspectives. Findings indicate that while AI is valued for efficiency, human expertise remains essential for creativity, cultural interpretation, and building trust, pointing to a future of hybrid human–AI collaboration in colour forecasting.

Keywords: colour forecasting, colour design, artificial intelligence (AI), co-piloting, human expertise

INTRODUCTION

Colour forecasting has been integral to fashion and textiles for over a century, with forecasters drawing on visual research, cultural signals, and tacit expertise to predict colour directions [1,2]. Traditionally, this combined intuition with systematic analysis, positioning forecasters as interpreters and communicators of aesthetic and cultural trends [3]. Technological change is now reshaping the field, with Artificial Intelligence (AI) emerging as tools for tasks once considered uniquely human [4]. AI is most evident in automated palette extraction, image analysis, and social media "nowcasting" [5,6]. Methods such as k-means clustering and generative networks enable large-scale processing, offering efficiencies over manual approaches [7]. Industry platforms like Heuritech and HueData show how such tools are applied in practice [8]. Yet, while they can identify statistical patterns, their ability to capture dimensions central to human forecasting remains uncertain.

Emerging scholarship often positions AI as a "co-pilot," augmenting rather than replacing creativity. Automated analysis can streamline technical processes while leaving conceptual tasks to human experts [9]. Similarly, emotional resonance and cultural interpretation remain uniquely human contributions [10]. These debates highlight the importance of exploring how AI-enabled tools intersect with traditional practice. Much existing work recognises technological advancements, but often neglects practitioner perspectives [5,6]. Yet, colour and trend forecasting depends as much on tacit knowledge and cultural sensitivity as on systematic processes [1,3]. Neglecting the human dimension risks overlooking critical issues such as trust, creativity, and personalisation.

Forecasters also act as translators, bridging data and culture to create narratives that resonate with clients [2,11]. Their credibility and ability to communicate stories often matter more than the colour palettes themselves [12]. The “black box” nature of AI [13] therefore raises questions about how trust in forecasts will be established and how experts may mediate between machine outputs and cultural interpretation. Sustainability adds further complexity. Forecasting has historically been linked to the acceleration of fashion cycles and associated waste [14]. One viewpoint is that AI could contribute to this by promoting rapid-response processes; however, human experts may position AI as a tool to support longer-term forecasting directions, emphasising palettes with lasting cultural and psychological value [15]. Understanding how professionals navigate these tensions is key to evaluating responsible integration of AI into design practice. This study therefore investigates expert voices in debates on AI and forecasting.

It addresses three questions: (1) How do forecasters validate colour decisions and communicate them to clients? (2) What role do AI technologies currently play in professional colour forecasting? (3) How do industry experts envisage their role changing with the influence of AI?

METHODOLOGY

This study adopted a qualitative research design to explore the perspectives of colour forecasting professionals on the role of AI-enabled tools. Data were collected through semi-structured, one-to-one interviews conducted in 2025 to to allow participants to narrate their experiences and perspectives in depth while providing enough structure to explore key topics. Open-ended questions were used to encourage reflective discussion, and prompts were employed to elicit detail where relevant. All interviews were audio-recorded, transcribed and analysed using thematic analysis [16]. Initial coding involved identifying meaningful units of text related to the research questions. To contextualise the interviews, participants were introduced to outputs from two earlier experiments such as the palette selections shown in Figure 1, investigating automated tools designed to extract palettes from images [9].

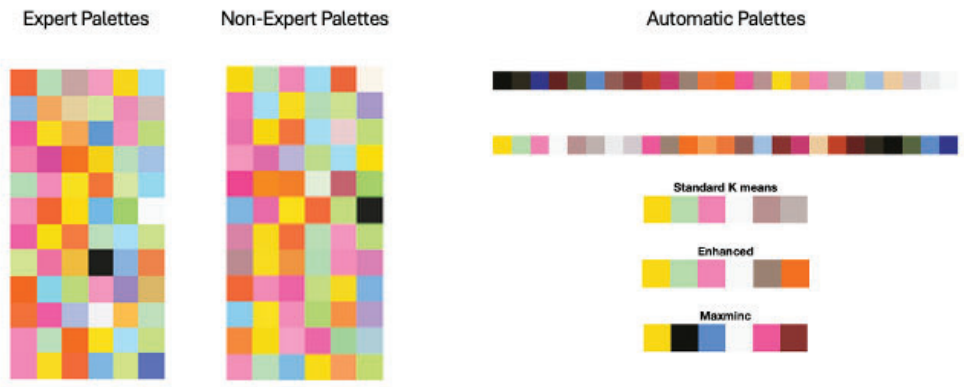

Figure 1: Palette Selections for one of the mood boards across humans and machine models

These examples provided a reference point for discussing the potential role of AI in colour forecasting and analysis. Five professionals (Interviewee A to E) working in the field of colour forecasting and design consultancy participated in the study. These participants were selected for their specialist knowledge of colour trends and their awareness of emerging technological developments within the industry.

Transparency was achieved by maintaining an audit trail linking raw transcripts, codes, and final themes. Transferability was supported by providing detailed descriptions of participant backgrounds and industry contexts.

These measures aimed to ensure that the findings are both rigorous and meaningful for advancing understanding in this emerging area of research.

RESULTS AND DISCUSSION

Figure 2: Word Cloud summarising key words from industry interviews

Taken together, the themes in Table 1 highlight a balance between the opportunities and limitations of AI-enabled tools in colour trend forecasting. The condensed thematic matrix presented here includes two illustrative quotes per themes that serve to represent the broader findings of the full thematic analysis.

AI as a Support Tool

Participants consistently highlighted AI's strengths in speed, scalability, and technical consistency. AI was valued for processing large datasets and streamlining palette extraction. However, participants emphasised that these capabilities were supportive rather than substitutive, aligning with recent scholarship that positions AI as a co-pilot for design rather than a replacement for human expertise [9,10]. As one interviewee noted, AI could act as "an extension of the designer," expanding technical possibilities but remaining dependent on human expertise.

Human Creativity and Intuition

Creativity and intuition were repeatedly described as indispensable to forecasting practice. Forecasters stressed that intuition integrates tacit knowledge, sensory experience, and cultural immersion, which cannot be replicated computationally. This finding is consistent with previous work [1,3] that argued that forecasting is shaped by affective and cultural practices as much as systematic research. This supports beliefs that AI lacks the imaginative and emotional dimensions central to human creativity [9,10]. Participants' framing of forecasting as "part science, part intuition" reinforces the hybrid nature of the practice, where human judgement remains irreplaceable.

Trust and Transparency

Trust emerged as a critical issue across interviews. Participants explained that clients rely on the credibility of the forecaster and the narrative supporting colour choices, echoing research that situates forecasting as a communicative practice [2,11]. While AI can generate outputs rapidly, its "black box" qualities [13] raised concerns about whether such outputs would be accepted without expert mediation. Forecasters stressed that clients "want stories, not just palettes," suggesting that trust is built through interpretation and narrative framing, rather than raw data. These findings extend ongoing debates on human-centred AI by emphasising the value of narrative within design contexts [12,13].

Table 1: Condensed Thematic Matrix with Indicative Quotes

Theme	Summary Insight	Indicative Quotes
AI as a Support Tool	AI valued for efficiency and technical support but not seen as a replacement for expertise.	*"AI can speed up analysing large volumes of images, but it still lacks the feeling associated with human-led choices." (Interviewee B)* *"AI could act as an extension of the designer, pushing creative exploration beyond what can be achieved individually." (Interviewee A)*
Human Creativity and Intuition	Intuition, sensory experience, and cultural knowledge remain central.	*"It is always part science, part intuition - you can't separate them." (Interviewee B)* *"Forecasting is grounded in intuition and lived experience." (Interviewee C)*
Trust and Transparency	Trust depends on expert credibility and narrative; AI's 'black box' raises concerns.	*"Clients want stories, not just palettes." (Interviewee B)* *"AI can scan masses of images, but it doesn't know what feels right." (Interviewee D)*
Cultural and Contextual Nuance	Colour meanings are culturally dependent; AI struggles with symbolic interpretation.	*"Colours carry cultural symbolism, like mourning or celebration." (Interviewee C)* *"Colour choices are tied to politics, lifestyle, and cultural interpretation." (Interviewee D)*
Ethical and Industry Concerns	Sustainability and overproduction risks heightened by AI if unmanaged.	*"Long-lasting palettes are critical to addressing waste." (Interviewee B)* *"AI could lead to fast cycles and superficiality." (Interviewee D)*
Future of Design Practice	Hybrid approaches expected, with AI assisting but humans leading interpretation.	*"Hybrid approaches will shape future practice." (Interviewee D)* *"Remote collaboration and bespoke forecasting are enabled by digital tools." (Interviewee E)*
Experts as Translators	Experts act as translators of data, psychology, and culture into narratives.	*"I see myself as a translator of wellbeing and colour psychology." (Interviewee A)* *"It is about brand story translation." (Interviewee E)*

Cultural and Contextual Nuance

Participants highlighted that colour meanings are culturally situated, shaped by political, social, and lifestyle contexts. They argued that AI, while capable of identifying statistical patterns, is limited in recognising symbolic associations. This supports earlier scholarship emphasising forecasting as a culturally embedded practice [1–3]. One participant described how colours associated with mourning in one culture signify celebration in another. This reinforces arguments that cultural interpretation remains a human responsibility [10].

Ethical and Industry Concerns

Sustainability was a recurring theme, with participants concerned that AI might accelerate fashion cycles and contribute to overproduction. This reflects wider critiques of forecasting's role in unsustainable industry practices [14]. However, participants also recognised AI's potential to support more responsible approaches, for example by identifying palettes with longer-term cultural value. This aligns with arguments that colour psychology and cultural resonance can be leveraged to promote sustainable design choices [15]. Forecasters thus positioned themselves as mediators who could direct AI toward either reinforcing or challenging unsustainable practices.

Future of Design Practice

Interviewees anticipated that forecasting will evolve into a hybrid model in which AI assists with technical efficiency, while humans retain responsibility for interpretation and storytelling. This echoes research that demonstrates how AI can streamline processes without replacing humans [9], as well as the view of design as an adaptive and collaborative practice [11]. Participants noted that AI may enable new forms of remote collaboration and digital co-creation, aligning with broader shifts in colour and trend forecasting [10]. Rather than threatening expertise, participants framed AI as part of the profession's ongoing adaptation to technological change.

Experts as Translators

A strong emergent theme was the forecaster as a "translator" of data, psychology, and culture into meaningful narratives. Participants described their role as converting signals into stories that resonate with clients, reflecting earlier accounts of forecasting as communicative practice [2,11]. Unlike AI, which produces statistical outputs, forecasters contextualise these within emotional and cultural frameworks. This theme underscores the irreplaceable human role in bridging computational analysis with cultural meaning, reinforcing the profession's identity as both analytical and interpretive.

CONCLUSION

This study explored human perspectives on the role of AI-enabled tools in colour trend forecasting, drawing on interviews with five industry experts from consultancy, corporate practice, education, and global forecasting. The findings highlight a nuanced view: participants acknowledged the opportunities of AI in terms of speed, efficiency, and data analysis, but consistently reinforced the irreplaceable value of human creativity, intuition, and cultural sensitivity. Trust, transparency, and ethics emerged as critical concerns, with participants stressing that forecasting is not only a technical process but also a narrative and interpretive practice. The analysis suggests that AI is best positioned as a complementary tool rather than a replacement for human forecasters. By adopting hybrid approaches, forecasting practice can benefit from the scalability of machine learning while retaining the interpretive depth provided by expert translators of cultural and emotional signals. This reframing contributes to ongoing debates in design research, extending scholarship on human–machine collaboration by showing how expert roles may evolve. For industry, the findings highlight both risks and opportunities: while AI may improve efficiency and sustainability, it could also accelerate fast cycles if applied without ethical sensitivity. For research, the study points to the need for empirical testing of hybrid models to better understand the evolving relationship between human expertise and AI-enabled forecasting. Ultimately, the human forecaster remains central, acting not only as a creative decision-maker but as a translator, storyteller, and ethical compass within the complex and culturally embedded practice of colour forecasting.

REFERENCES

[1]. Cassidy, T. D., & Cassidy, T. (2012). Using soft systems methodology to improve the colour forecasting process. *Journal of the International Colour Association*, *7*, 27-50.

[2]. Cassidy, T. (2019). Colour forecasting as communicative practice. *Color Research & Application, 44*(6), 902–913. https://doi.org/10.1002/col.22435

[3]. Blaszczyk, R., & Wubs, B. (2018). *The Fashion Forecasters: A Hidden History of Colour and Trend Prediction*. Bloomsbury.

[4]. Shneiderman, B. (2020). Human-Centered Artificial Intelligence: Reliable, Safe & Trustworthy. *International Journal of Human-Computer Interaction.*, *36*(6), 495–504. https://doi.org/10.1080/10447318.2020.174111

[5]. Joshi, N. (2018, July 22). *Big data is stepping into the fashion world*. BBN Times. https://www.bbntimes.com/technology/big-data-is-stepping-into-the-fashion-world

[6]. Chaudhuri, S. (2018, May 7). H&M Pivots to Big Data to Spot Next Big Fast-Fashion Trends; Instead of cookie-cutter stores, the H&M chain is using granular data to customize the offerings in each one of its 4,200 locations. *Wall Street Journal (Online)*, n/a.

[7]. DuBreuil, M., & Lu, S. (2020). Traditional vs. big-data fashion trend forecasting: An examination using WGSN and EDITED. *International Journal of Fashion Design, Technology and Education*, *13*(1), 68–77. https://doi.org/10.1080/17543266.2020.1732482

[8]. Lechner, A. (2023). On Design Decisions in the Age of Data and Artificial Intelligence. *Design Management Review.*, *34*(1), 54–59. https://doi.org/10.1111/drev.12332

[9]. Angharad, S., Lai, P., & Westland, S. (2025). Automated colour analysis co-piloting tool for design. *Fashion Technology, 1*(1), 42–46.

[10]. Wingström, R., Hautala, J., & Lundman, R. (2022). Redefining Creativity in the Era of AI? Perspectives of Computer Scientists and New Media Artists. *Creativity Research Journal*, *36*(2), 177–193. https://doi.org/10.1080/10400419.2022.2107850.

[11]. Kimbell, L. (2012). Rethinking Design Thinking: Part II. *Design and Culture*, *4*(2), 129–148. https://doi.org/10.2752/175470812X13281948975413

[12]. Raymond, M. (2019). *The trend forecaster's handbook*. Hachette UK.

[13]. Shneiderman, B. (2020). Human-centered artificial intelligence: Reliable, safe & trustworthy. *International Journal of Human–Computer Interaction, 36*(6), 495–504.

[14]. Rousso, C., & Ostroff, N. (2018). *Fashion forward: A guide to fashion forecasting*. Fairchild Books.

[15]. Whitfield, T. W. A., & Whelton, J. (2015). The arcane roots of colour psychology, chromotherapy, and colour forecasting. *Color Research & Application*, *40*(1), 99–106. https://doi.org/10.1002/col.21862

[16]. Braun, V., & Clarke, V. (2006). Using thematic analysis in psychology. *Qualitative Research in Psychology*, *3*(2), 77–101. https://doi.org/10.1191/1478088706qp063oa

CMF Design: Towards Narrative Development from User-referencing Visual Texts

Nijoo Dubey[a*], Sudhakar Damodaraswamy[b]

[a]*National Institute of Design, Bengaluru, India*
[b]*School of Design and Innovation, R V University, Bengaluru, India*
[*]*Nijoo Dubey, nijoo@nid.edu*

ABSTRACT

Colour designers use thematic narratives to develop product colour themes that connect emotionally with users. This process is often intuitive, relying on personal experience, which limits decision traceability and insights into user culture. To address this, we tested the hypothesis that a structured visual research method could strengthen narrative development through methodical experiments in CMF design courses. The paper introduces a three-stage curatorial and extractive process that generates user-attuned themes by employing user-referencing visual texts in place of conventional mood boards. This approach creates a structured avenue for exploring users' contexts, behaviours, and attitudes, enabling seamless integration of research and design. By embedding reflexivity and ensuring strong user correlation, the method demonstrates the potential to significantly enhance the rigor and creative depth of colour theme generation in both educational and professional practice.

Keywords: *colour design process, conceptual narratives, visual research, user-aligned design*

INTRODUCTION

Products communicate function as well as emotion, shaping how users engage with them [1]. CMF—colour, material, and finish—forms a critical dimension of product design, influencing perception, aesthetics, functionality, and brand value [2]. Positioned at the intersection of material culture, sensory experience, and brand strategy, CMF decisions determine how products are recognised, valued, and remembered [3]. Among these elements, colour is often pre-eminent for its immediate impact on perception and acceptance [4]. In practice, CMF strategies are framed through conceptual narratives that translate research insights into coherent and culturally resonant design directions [3].

Current process and scope for improvement

The CMF design process typically involves information gathering, establishing narratives, defining strategy, developing palettes, and design development [3]. Among these, narratives are pivotal in guiding design direction; they must be imaginative, inspirational, and aligned with users' perceptual and aspirational needs.

Personas and moodboards remain the dominant tools for narrative development [3]. Personas represent hypothesised user groups, while moodboards—assemblages of images, text, and materials—offer aesthetic cues. Both rely on visual representations to convey the "synthesised essence" of user attitudes and behaviours, which is central to narrative construction.

However, teaching experience and analysis of student outputs and online portfolios reveal limitations in the process, particularly in information gathering and narrative development. Translating extensive user research into concise, resonant personas and moodboards demands high levels of intuition and experience. In practice, outcomes

are often limited by experience, or shaped by dominant trends, or focused on surface aesthetics rather than narrative depth. These findings, corroborated by prior research [5],[6],[7] as well as the author's experiences, highlight the need for methods that more directly integrate user research with the generation of conceptual narratives.

Proposed enhancement

Visual literacy is a core proficiency cultivated in designers, enabling them to observe, interpret, and critically engage with the world through visual mediation [8]. Building on this capacity, visual research has emerged as a valuable ethnographic method, particularly with the abundance of visual content available online, offering new ways to approach consumer contexts [8], [10]. Since narrative construction in CMF design already relies heavily on visual representation, incorporating visual research holds the potential to strengthen inquiry and enrich narrative development [11].

Drawing from Becerra's established framework, the proposed enhancement introduces **user-referencing visual texts**—photographs capturing users in their lived, everyday contexts—as a structured means to extract nuanced insights into lifestyle, attitudes, and preferences. This integration positions visual research as a potent tool that deepens the rigour and cultural attunement of conceptual narratives in CMF design[1].

METHODOLOGY

This research adopts a Research through Design (RtD) approach [12] to develop and validate the proposed enhancements. RtD, grounded in the design process, employs iterative and reflective cycles to refine solutions and validate emergent outcomes [13]. Among the various methods identified within RtD [14], we selected iterative design experiments as the primary mode of inquiry, using hands-on CMF design activities to test and improve the conceptual narrative generation process.

Experiments

The modified CMF design process presented in this study emerged from eight serial experiments conducted over two years within postgraduate CMF design courses for product and furniture design students (class sizes: 17–24). Each experiment followed a six-stage sequence: (1) image curation, (2) interpretation of selected images through rich descriptive writing, (3) extraction of textual narrative phrases, (4) derivation of key colors, (5) development of the CMF palette, and (6) application and iterative refinement. While guidance was provided for clarity, intermediate outputs—including images and initial narratives—were intentionally insulated from critique to avoid bias, ensuring authentic exploration. Ethical considerations were addressed through informed consent, anonymization of visual data via blurring, and restriction of all materials to academic use.

Assessments

The efficacy of the process was assessed through the textual narrative phrases, which formed the conceptual themes underlying the final color schemes. Each narrative was evaluated against three criteria: (1) alignment with the referenced images, (2) expressiveness of thematic phrasing, and (3) potency in inspiring creative ideas, using a three-point scale (low, medium, high). The evaluation was conducted jointly by the author and an additional expert reviewer, with rankings consensually arrived at to ensure reliability of judgment. Iterative refinement continued across experiments until narrative phrases consistently demonstrated high quality, reflecting improvements in visual curation, narrative articulation, and thematic generation. By focusing evaluation on the narrative phase, the assessment captured the cumulative impact of all preceding steps, validating the robustness of the proposed CMF design methodology. A sample worksheet (Figure: 1) illustrates how the rating was carried out on images and the

[1] The use of visual texts in research necessitates careful ethical consideration, including issues of consent, attribution, modification, and cultural sensitivity, to ensure responsible and respectful representation of users.

themes derived from them making an explicit connection between visual inputs, derived themes, and their subsequent ratings.

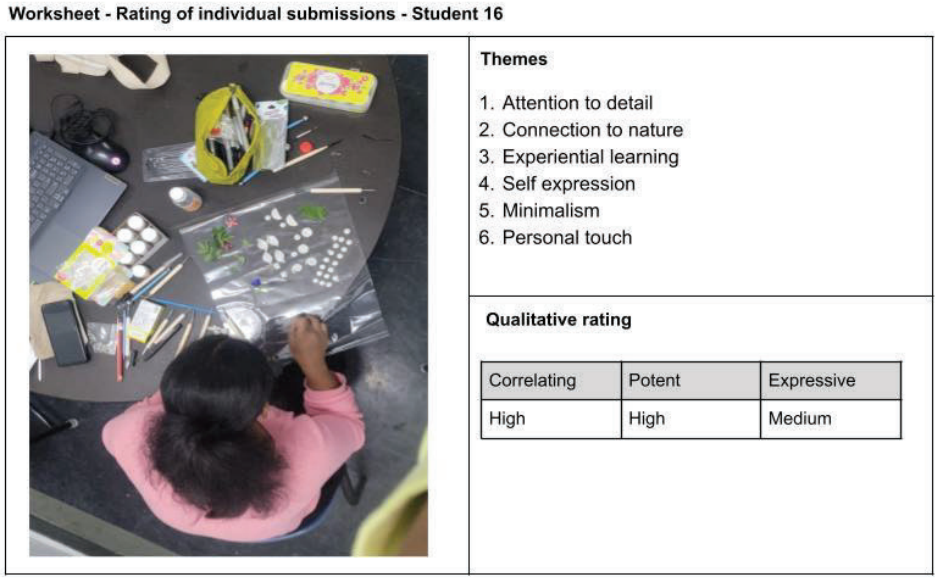

Figure 1: Sample worksheet showing extracted themes and qualitative rating of an individual submission

RESULTS AND DISCUSSION

The research produced several key outcomes, including a refined six-stage CMF design process and practical visual research guidelines tailored to support the first two stages—image curation, and their interpretation through rich descriptive writing—along with quantitative evidence of process efficacy. Particular emphasis was placed on these initial stages, where improvements were most pronounced in shaping the subsequent narrative phrases and color derivation. In the eighth and final experiment, the evaluated textual narrative phrases consistently achieved medium or high scores in at least 70% of cases across all three evaluation criteria, confirming the effectiveness of the methodology. The process was further validated in two additional trials, with novice and expert designers, yielding similarly successful outcomes. Representative visual outcomes illustrate the refined process, while detailed procedural steps are omitted for brevity.

Stage 1: Curation of images

This stage focuses on collecting user-referencing visual texts in accordance with a given CMF design brief. Iteratively developed guidelines emphasize selecting authentic depictions of users in their everyday environments, providing contextual lifestyle cues rather than sterile product shots, advertisements, or close-ups lacking surrounding detail (Figure: 2). This approach ensures the curated images offer strong potential for inferring psychographic details and cultural references relevant to the design brief.

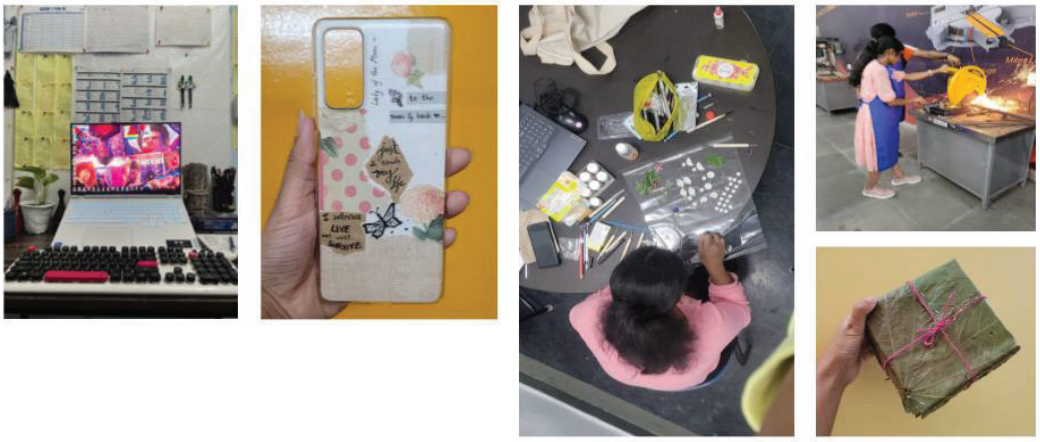

Figure 2: Curated user-referencing images illustrating contextual lifestyle cues

Stage 2: Interpretation of selected images

This stage involves rich descriptive writing to interpret the curated visuals. Iteratively developed guidelines encourage participants to expand their observations into fuller narratives by situating the user in context, capturing thoughts and emotions, inferring motivations and intentions, and articulating the significance of details within the scene (Figure: 3). These refinements ensured that the narratives moved beyond surface description toward accounts that conveyed sensory depth, emotional nuance, and contextual meaning. Such narratives provided a strong foundation for extracting key thematic phrases in Stage 3.

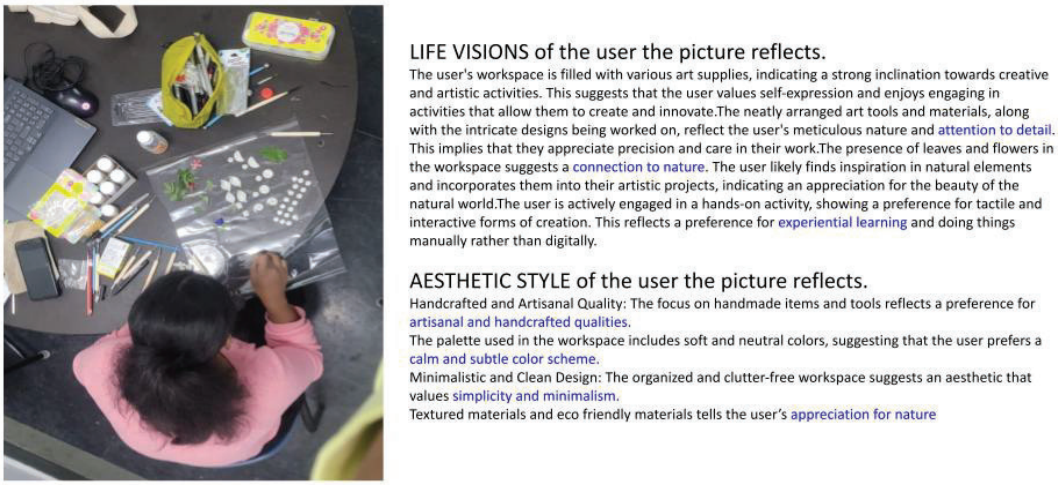

LIFE VISIONS of the user the picture reflects.

The user's workspace is filled with various art supplies, indicating a strong inclination towards creative and artistic activities. This suggests that the user values self-expression and enjoys engaging in activities that allow them to create and innovate.The neatly arranged art tools and materials, along with the intricate designs being worked on, reflect the user's meticulous nature and attention to detail. This implies that they appreciate precision and care in their work.The presence of leaves and flowers in the workspace suggests a connection to nature. The user likely finds inspiration in natural elements and incorporates them into their artistic projects, indicating an appreciation for the beauty of the natural world.The user is actively engaged in a hands-on activity, showing a preference for tactile and interactive forms of creation. This reflects a preference for experiential learning and doing things manually rather than digitally.

AESTHETIC STYLE of the user the picture reflects.

Handcrafted and Artisanal Quality: The focus on handmade items and tools reflects a preference for artisanal and handcrafted qualities.

The palette used in the workspace includes soft and neutral colors, suggesting that the user prefers a calm and subtle color scheme.

Minimalistic and Clean Design: The organized and clutter-free workspace suggests an aesthetic that values simplicity and minimalism.

Textured materials and eco friendly materials tells the user's appreciation for nature

Figure 3: Excerpt from a rich descriptive narrative highlighting interpretive depth

Stage 3-6: Theme extraction and CMF development

From the descriptive narratives, key themes are distilled as succinct words or phrases, encapsulating lifestyle, emotional, and functional insights, and refined to provide potent creative inspiration (Figure: 4). Building on these themes, designers proceed through the more conventional CMF steps: selecting key colors that embody the insights, formulating a comprehensive CMF palette integrating materials and finishes, and applying the palette to models with iterative refinement based on visual assessment and design objectives.

This structure underscores the pivotal role of Stages 1 and 2 in generating deep, culturally attuned insights, while situating Stages 3–6 as extensions of this foundation, ensuring a coherent and actionable design process.

Figure 4: Extracted themes and their translation into a developed CMF palette applied to a conceptual product model.

Discussion

The central enhancement of the modified CMF process lies in embedding systematic reflexivity into narrative development, ensuring that colour themes emerge directly from authentic user contexts rather than intuition or trend-driven cues. Designers reflexively engage with the process at multiple levels: through curation of user-referencing images, evaluation and interpretation of visual cues through rich descriptive writing, and a deliberate review of these narratives to extract key colour themes. These themes, reflective of the emotional, cultural, and contextual dimensions of the user, serve as the conceptual foundation for subsequent CMF palette development.

This reflexive engagement balances designer subjectivity with user objectivity, ensuring that creative interpretation remains anchored in the lived realities of users. By embedding systematic rigour and reflexivity, this research strengthens the CMF design process, enhancing its reliability and the fidelity of conceptual narratives derived from user's lived contexts. The result is a method that produces culturally attuned, emotionally engaging, and practically actionable colour themes, demonstrating how structured and reflexive approaches can significantly elevate the quality and trustworthiness of CMF design outcomes

CONCLUSION

This study presents a modified CMF design process that represents a significant enhancement to current practices, embedding systematic reflexivity into the generation of conceptual narratives and colour themes grounded in user's lived contexts. Central to this enhancement is the use of user-referencing visual texts, which replace traditional personas and moodboards and provide multiple benefits: (1) seamless integration of research into the generative design process, (2) strong correlation with the user's lived context, attitudes, and behaviours, and (3) inbuilt structure and reflexivity through deliberate review and choice-making. Given the limited discourse on CMF design methodologies, this paper aims to stimulate discussion and highlight the potential of visual research as a core component of narrative development. There is further scope for comparative studies with current practices and testing in professional settings to evaluate effectiveness and adaptability. We hope that this study contributes both a practical methodology and a conceptual platform for advancing research and discourse in CMF design.

REFERENCES

[1]. Norman, D. (2004). Emotional design: Why we love (or hate) everyday things. *The Journal of American Culture, 27*(1), 87–92.

[2]. Damodaraswamy, S., & Dubey, N. (2023). A colour value framework for colour design of lifestyle products. In *Proceedings of the 15th Congress of the International Colour Association (AIC 2023)* (pp. 485–490). Chiang Rai, Thailand.

[3]. Becerra, L. (2016). *CMF design: The fundamental principles of colour, material and finish design*. Frame Publishers (pp. 10–62).

[4]. Reddy, S., Chowdhury, A., Chakrabarti, D., & Karmakar, S. (2015). Role of colour and form in product choice and variation of preferences across product categories: A review. In K. S. Soliman (Ed.), *Smart innovation, systems and technologies* (Vol. 35, pp. 631–640). Springer.

[5]. Cassidy, T. (2008). Mood boards: Current practice in learning and teaching strategies and students' understanding of the process. *International Journal of Fashion Design, Technology and Education, 1*(1), 43–54.

[6]. McDonagh, D., & Storer, I. (2004). Mood boards as a design catalyst and resource: Researching an under-researched area. *The Design Journal, 7*(3), 16–31. https://doi.org/10.2752/146069204789338424

[7]. Lingala, A. (2015). *Cultures / of / taking: Exploring cultural exchange in contemporary fashion design practice* [Master's thesis, Royal College of Art / Victoria & Albert Museum History of Design Programme].

[8]. Dondis, D. A. (1974). *A primer of visual literacy*. MIT Press.

[9]. Rose, G. (2001). *Visual methodologies: An introduction to the interpretation of visual materials*. SAGE.

[10]. Banks, M. (2001). *Visual methods in social research*. SAGE.

[11]. Schembri, S., & Boyle, M. V. (2013). Visual ethnography: Achieving rigorous and authentic interpretations. *Journal of Business Research, 66*(9), 1251–1254.

[12]. Frayling, C. (1994). Research in art and design. *Royal College of Art Research Papers, 1*(1), 1–5. Retrieved from https://researchonline.rca.ac.uk/384/

[13]. Godin, D., & Zahedi, M. (n.d.). Aspects of research through design: A literature review. Unpublished manuscript.

[14]. Krogh, P., Markussen, T., & Bang, A. (2015). Ways of drifting – Five methods of experimentation in research through design. *Proceedings of the Nordic Design Research Conference (NORDES 2015)*, 1–10.

Colour and Memory: Consistency of Memory Colours

Stine Marie Kvist[a*] and Phil Green[a]

[a]NTNU, Gjovik, Norway
[*]Corresponding author: Stine Marie Kvist, SmKvist@outlook.com

ABSTRACT

Memory colours are those colours of physical objects for which we hold a prototypical reference in memory. Commonly cited examples are sky, grass and flesh, but in reality these vary widely across the world. This study focused on a single culture using objects that are ubiquitous within that culture and could thus be expected to represent memory colours. 55 observers in Norway were asked to use a colour picker to select colours corresponding to 11 items that are very well-known in the country, including the Norwegian flag, salmon, advent candles and some brand colours. For each item a reference colour was determined in CIELAB, for example by direct measurements or by using the published colour specification for the item. The range of colours selected by the observers varies considerably, and outliers were removed by generating a robust covariance estimate of the CIELAB data.

In many cases the variation in selected colours is primarily on the chroma axis (as might be expected). The results show that in some cases the robust mean was in good agreement with the reference colour, but in other cases there was a significant deviation. The CIEDE2000 colour difference between the robust mean and the reference colour ranged from 6.05 to 34.01. The variation in the colours selected for each object (using the mean colour difference from the mean, or MCDM), ranged from 4.83 to 17.93.

Keywords: memory colour, colour difference, culture, survey,

INTRODUCTION

A memory colour is simply the "typical colour of an object that an observer acquires through their experience with that object" [1]. With reference to colour reproduction, and earlier work by Bartleson, R. W. G. Hunt stated that "the basis of judgement is usually a comparison between the colour sensations aroused by the reproduction and a mental recollection of the sensations similar to the ones being appraised" [2]. Memory colours are often diagnostic, in the sense that they aid in identifying an object through a strongly associated colour; and while there is variation in the colours that people recall, for many objects a particular colour can be said to be representative or ‘canonical’ [1].

Commonly-cited examples of memory colours include sky, grass, skin [3] and bananas [4], but in reality these items vary widely across the world, as well as by season or even time of day, and moreover these examples could be considered to have a Western bias. However, Zhu et al [5] found that cross-cultural variation was smaller than intra-group variation.

The aim of this study was first to identify a small set of well-known colours within a single culture for which there exists reasonably consistent and reproducible references, and then to explore the deviation between these reference colours and those recalled by observers, and finally to explore the degree of variation within the recalled colours by different observers.

METHODOLOGY

An on-line study was performed in which 55 Norwegian observers used a colour picker to select the colours corresponding to 11 objects well-known in Norwegian culture.

The experiment was hosted on the survey platform Paperform, as it includes a built-in colour picker function. The survey included information about the purpose, together with participant consent and demographic questions, in addition to the colour test. Participants were shown black and white photographs of the selected objects and asked to select the colour of each object based on their memory.

Reference colours for these 11 objects were selected as follows:

IKEA: the IKEA blue is defined in the brand identity guide [6]. However, as the actual colour depends on the substrate, it was decided to measure an IKEA bag.

Flag: the red of the Norwegian flag is defined on government websites as PANTONE 186C [7].

Snus: is a Scandinavian tobacco product consisting of ground up tobacco leaves, salt, an alkalizer and flavorings. Its colour was changed to PANTONE 448C in 2017, with the aim of making it visually unappealing [8].

Freia: milk chocolate has a yellow package colour. As no brand ID colour could be found, examples were measured.

Salmon: flesh varies in colour, depending on the food consumed by the fish, and there are sample swatches available. We measured fresh, uncooked salmon to obtain a reference colour.

Blackboard: Although a Blackboard Green RAL colour exists, it was unknown whether this is representative of the blackboards used in Norwegian schools, and hence in-situ measurements were made in a classroom.

Advent Candle: Norwegian advent candles are a blue-violet colour, and are an important part of Christmas preparation and celebration in Norway. It has been stated that the colour is NCS colour S 4550-R70B [9], although light and dark versions are permitted and a red version also occurs.

Gingerbread: also varies in colour depending on ingredients and the baking process. For this study, samples were baked using a Norwegian recipe and measured.

Vest: High-visibility clothing is common in the darker winter months in Norway. A sample was measured; due to the high reflectance the XYZ values were outside the sRGB gamut, and were linearly scaled to the gamut so that the colour could be matched by observers.

Rema1000: is a Norwegian supermarket, found in most towns in the country. No brand ID colour could be found, so the colour was sampled in RGB from graphics appearing on the company website.

Red Cross: the logo is visible in many locations in Norway. A visual profile on the Red Cross website [10] identifies this colour as the RGB triplet [213 43 30].

To obtain the measurements, objects were placed under a diffuse illumination simulating D65 using Thouslite LEDCube overhead luminaires [11] and measured five times with a Minolta CS3000 telespectroradiometer and the data averaged. A calibrated tile was used to obtain D65 XYZ values relative to a perfect diffuser, which were subsequently converted to CIELAB. All values defined in RGB were assumed to be sRGB and D65, and converted to XYZ and CIELAB, while colours defined in the PANTONE and RAL colour order systems were measured from sample books using a spectrophotometer.

The resulting reference CIELAB values for the 11 colours are shown in Table 1. There is a degree of uncertainty in some of the reference colours as in some are not well defined, or are specified in a colour space that is not colorimetric. All items were measured under the same illumination, but their appearance may vary depending on viewing conditions, with some items more likely to viewed under indoor lighting. The colour of the fluorescent yellow high-visibility vest will depend on the amount of UV present in the illumination.

RESULTS AND DISCUSSION

As expected, there was a considerable degree of variability in the colours selected by observers. The experiment was set up as an on-line survey, and the calibration state of the participants' displays is unknown and hence sRGB is just a guess at reconstructing the colorimetry. At least two participants were known to have a colour vision deficiency. As it was an unsupervised experiment, it is also possible that some participants may have exercised less skill or diligence when selecting the memory colours. For these reasons it was necessary to remove outliers from the data set.

The outliers were identified using a fast minimum covariance determinant [12][13], which has been shown to be a robust estimator of multivariate location and scatter [14]. The outlier proportion was set at 0.25. The resulting robust mean for each colour is shown in Table 1, together with the CIEDE2000 deviation of the robust mean from the reference colour. The variation in selections among observers, in terms of the mean colour difference from the mean (MCDM), in CIEDE2000, of the observations, is also shown.

Table 1: CIELAB values for reference and robust mean of test colours, with difference between reference and robust mean, and observer variation

	Reference			Robust mean			Deviation	Variation
Item	**L***	**a***	**b***	**L***	**a***	**b***	**ΔE^*_{00}**	**MCDM**
IKEA	37.16	7.69	-46.61	55.40	7.49	56.88	20.93	15.16
Flag	43.57	67.98	37.76	51.82	70.98	55.45	19.75	5.58
Snus	28.21	2.09	15.71	41.48	-0.96	8.47	15.42	17.93
Freia	88.28	-5.96	77.32	90.01	-7.08	83.01	6.05	6.71
Salmon	67.55	25.28	32.78	64.36	46.70	31.77	21.67	13.27
Blackboard	42.47	-22.95	10.28	34.74	16.21	13.46	10.74	16.85
Advent candle	21.91	20.92	-41.58	34.34	51.92	47.99	34.01	16.90
Gingerbread	57.02	10.17	29.93	43.26	19.18	34.17	16.98	16.20
Hi-vis vest	93.34	-43.62	89.75	92.33	18.96	83.12	25.56	10.33
Rema1000	29.97	26.79	-60.08	48.24	22.92	65.93	19.58	16.91
Red Cross	46.94	63.54	49.42	52.23	73.60	58.61	14.61	4.83

The results are illustrated (in a*/b* projection) in Figure 1. For each item, observations are shown as diamonds, with solid black markers representing the robust values, and red open markers the outliers. The robust mean is shown as a black '+' and the reference colour is shown as a solid green 'o'. A least-squares ellipse with a 95% tolerance was fitted to the a*/b* data. (Note that some outliers appear to fall within the tolerance ellipses due to their difference from the robust mean being primarily in L*).

It can be seen in Figure 1 that some observations are far from the reference. Use of the minimum covariance determinant appears to have successfully identified these outliers and thus yielded a more robust and reproducible central tendency. In the case of the Advent candle, there appears to be a whole sub-population of observers who recalled the red rather than the blue-violet version of the candle, and these have all been identified.

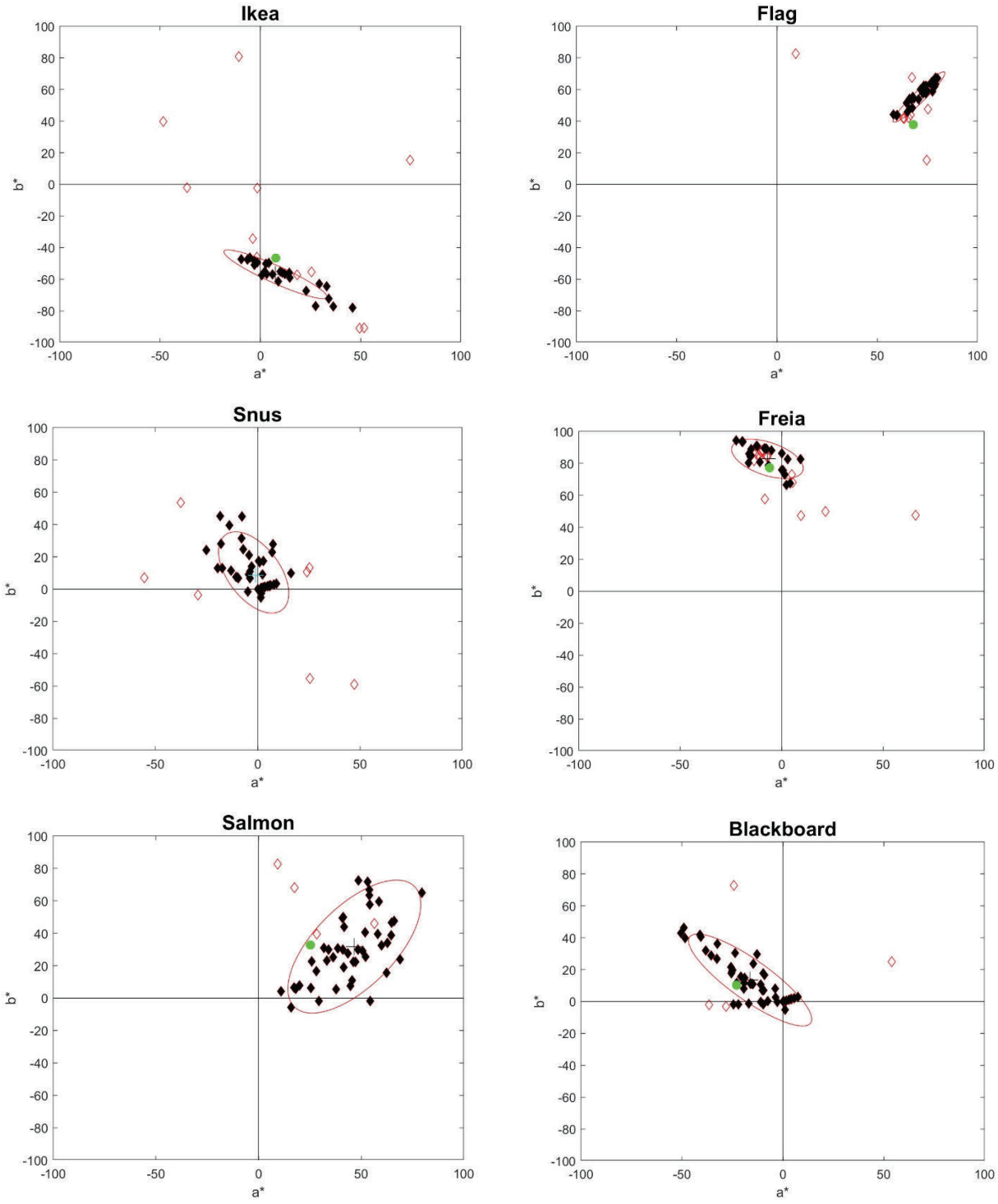
Ikea
Flag
Snus
Freia
Salmon
Blackboard
a*
b*

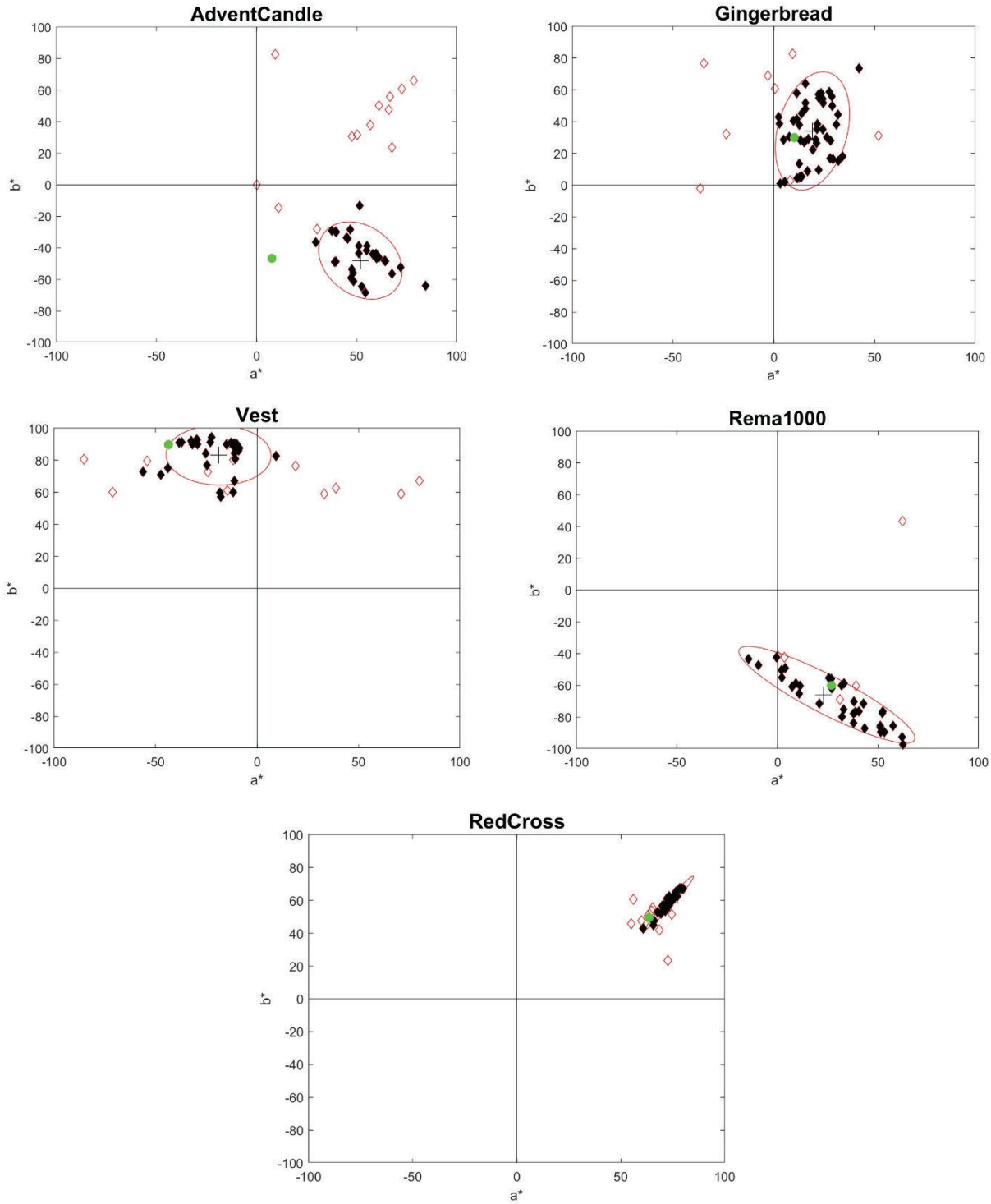

Figure 1: Observer data with outliers, robust mean and reference colour for each item

It can be see that for most colours the observer variation is primarily in the chroma direction, suggesting better agreement on hue. The exception is the fluorescent yellow of the high-visibility vest, where observer variation is mainly in hue. This is likely due to the range of colours used in these items, together with varying amounts of UV in the viewing illumination.

CONCLUSIONS

For some items in this study there was good agreement amongst observers on the prototypical colour for the item, while for others there was much more variation. The main axis of variation tended to be along the C* chroma dimension, suggesting that the hue of a memory colour is more consistently recalled. Whether or not the item had a well-defined reference colour did not seem to determine either the variation in the observations or the difference between reference and robust mean. It would be interesting to explore this issue in other cultures.

A large amount of scatter was seen in the observations, and the use of the minimum covariance determinant to identify outliers has led to an improved estimate of the mean of the observations for each item. The smaller tolerance ellipses that result are also in better agreement with previous work such as [5].

ACKNOWLEDGEMENTS

The authors would like to thank Greg High at Colourlab, NTNU for his assistance in making the measurements.

REFERENCES

[1]. Hunt, R. W. G. (2004) *The reproduction of colour* 6th edn. Wiley

[2]. Witzel, C. and Gegenfurter, K., (2013) Memory color in Luo, M. R. (ed) *Encyclopedia of Color Science and Technology*, Springer

[3]. Bartleson, C.J. and Bray, C.P., (1962) On the preferred reproduction of flesh, blue-sky, and green-grass colors, *J. Phot Sci Eng*, 6, 19-25

[4]. Yendrikhovskij, S.N., Blommaert, F.J. and de Ridder, J.H. (1999) Representation of memory prototype for an object color, *Col. Res. Appl*. 24 393-410

[5]. Zhu, Y.T., Luo, M. R., Xu, L.H., Liu, X.Y., Cui, G.H., Fischer, S., Bodrogi, P. and Khanh, T.Q., (2015) Investigation of Memory Colours across Cultures, *Proc. IS&T Color and Imaging Conf* 133-137.

[6]. IKEA. *Clear and simple* https://cdn.bndlyr.com/nr1dxae7lw/assets/clear-and-simple.pdf [Accessed: 2025-03-31].

[7]. Norwegian Government. *Det norske flagg* https://teststeder.regjeringen.no/standarddesign/det-norske-flagg/ [Accessed: 2025-08-31].

[8]. Helsedirektoratet. (2025). *Statistikk og historikk om røyking, snus og e-sigaretter* https://www.helsedirektoratet.no/forebygging-diagnose-og-behandling/forebygging-og-levevaner/tobakk/statistikk-om-royking-bruk-av-snus-og-e-sigaretter [Accessed:2025-03-31].

[9]. Norwegian Colour Senter (2018). *Hva er riktig adventsfarge*? [Accessed: 2025-03-31]. https://www.facebook.com/ncscolour.no/posts/hva-er-riktig-adventsfarge/2491631247568754/

[10]. Røde Kors *Farger* https://www.rodekors.no/om/visuell-profil/farger/ [Accessed: 2025-04-01].

[11]. Thouslite *LEDCube* https://thouslite.com/product_detail/124.html [Accessed 2025-08-31]

[12]. Rousseeuw, P.J. and Van Driessen, K. (1999.) A fast algorithm for the minimum covariance determinant estimator. *Technometrics*, 41, 212-223

[13]. Maronna, R. A. and Zamar, R.H. (2002) Robust estimates of location and dispersion for high dimensional datasets. *Technometrics*, 44 307-317

[14]. Hubert, M. and Debruyne, M., (2010) Minimum covariance determinant, *Comp Stats* 2 36–43

What Explanations for Color Naming and Categorization Explain

Don Dedrick*
Department of Philosophy, University of Guelph, Guelph, Ontario, Canada
**Corresponding author: ddedrick@uoguelph.ca*

ABSTRACT

Colour naming and categorization is not a singular phenomenon, so that when we talk about "the explanation for basic colour terms (and/or categories)" we are not, or should not be, talking about one thing. At the very least there are three phases in the process of developing a socially robust colour categorical scheme. One: a colour needs to be singled out as worthy of colour naming. Two: colour categories need to be formed. Three: colour categories need to transmitted across generations. This paper argues that these phases are empirically distinct. At some point in a language's history, there are no colour names and the colours that are to be named have to be determined. That's phase one. In phase two, category boundaries and relations to other colour categories, are articulated. Phase three, sees a mature colour categorization scheme (a socially robust set of colour categories) that may be taught and transmitted. This paper does two things: first, it defends the three-phase process; second, it considers how, or rather *where* different explanations for colour naming regularities, are relevant to the three phase process.

Keywords: colour, colour terms, colour categories, basic colour terms, basic colour categories

INTRODUCTION

It is widely if not universally agreed that the concept of a basic colour term and the corresponding notion of basic colour category [1] [14] has robust application across the languages of the world. Not only are their basic colour terms in all languages, but the total number of basic colour terms, the roster of basic terms, as it were, is quite limited. [1] [26] While different researchers count basic terms differently, [2] and there are still disputes and disagreements, [6] basic colour terms (BCT) and the corresponding concept of basic colour categories (BCC) are robust concepts, with universal application. If the existence of basic colour terms and categories seem secure, their explanation is not. [1] [14] A range of possible explanations have been proposed: colour is distributed across the natural environment in a way reflected by basic terms [27] ; basic colour names are derived from socially or culturally significant objects; [18] [6] basic colour naming aims for communicative efficiency; [15] [17] [22] colour naming is a function of visual physiology. [11] It may be the case that one of these explanations, or types of explanation is correct, the others mistaken. It's also possible that multiple explanations are causally effective. This paper takes it that a multiple explanation hypothesis is correct, but for a very particular reason. Colour naming is not a singular phenomenon, so that when we talk about "the explanation for basic colour terms (and/or categories)" we are not, or should not be, talking about one thing. At the very least there are three phases in the process of developing a socially robust colour categorical scheme. One: a colour needs to be singled out as worthy of colour naming. Two: colour categories need to be formed. Three: colour categories need to transmitted across generations. This paper argues that these phases are empirically distinct. At some point in a language's history, there are no colour names and the colours that are to be named have to be determined.

That's phase one. In phase two, category boundaries and relations to other colour categories, are articulated. Phase three, sees a mature colour categorisation scheme (a socially robust set of colour categories) that may be taught and transmitted. This paper does two things: first, it defends the three-phase process; second, it considers how, or rather *where* different explanations types, such as those mentioned above, are relevant to the three phase process.

The constraints

There are universal constraints on basic colour terms and categories—generalizations that hold universally. In the current literature, the constraints are typically described like this: languages are constrained from adding an unlimited number of basic terms, there is a small number that appear universally and in predictable order, though with some variation; languages are constrained when it comes to the best examples of their basic colour categories, colour category centroids are universal, though again, with some variation; basic colour category boundaries are constrained in the sense that the basic category boundaries are relatively predictable, and hence universal—there is variation, and boundaries are "soft" [28], but that variation is not unrestricted.

The constraints are, let us say, *rules* that are derived from the cross-cultural data. What is not clear is the basis for these rules. What makes these rules true? There is no one accepted theory. In this paper I propose that the literature is not always clear about the separable processes that are involved in the development and maintenance of colour categorization schemes, and that clarifying the distinctiveness of the processes point toward different types of explanation for the different processes.

The explanations

A number of different explanations, or explanation types, have been proposed to account for the constraints. They do this in different ways. Here are the four explanations most commonly mentioned:

A. Visual Ecology hypothesis. Colour is distributed across the natural environment in a way reflected in basic terms and the categories they name. [27]
B. Anthropological-historical hypothesis. Basic colour names are derived from socially or culturally significant things or properties. [19] [6]
C. Perceptual salience hypothesis. Basic colour names and/or categories reflect some aspect of underlying human psychology and/or physiology. [5] [9] [11]
D. Communicative efficiency. Basic colour naming aims for communicative efficiency. [21] [17]

One way to think about these explanations for the constraints would go like this. There are universal processes that affect colour naming practices, and then there are cultural drivers that modify the way those universal processes are expressed in a given language. So, to take the ecological distribution hypothesis, colours that get named tend to be the ones most common in the natural world, and when that's not true, there is some cultural effect that is responsible. Or, if we think about perceptual salience, there are certain colours at say a high level of saturation, or certain colour categories that have a biological basis, but culture can override these perceptual, biologically based saliences. Or, there is a scheme of colour categories that is optimal from, say, a communicative perspective (not too many distinctions, not too few), but culture overrides that optimality, leading to less optimal schemes that are nonetheless culturally salient. While its possible this is the right way to understand these explanations, relative to the constraints, and it does seem to be suggested by some researchers, [26] it gives cultural explanation a jack of all trades role: whenever we encounter a counterexample to an explanatory theory, it's culture doing the work, in one way another,

"overriding" some universal dimension of BCTs/BCCs. This is not a principled or illuminating way of explaining the constraints.

The three phases

Phase I: The origin of a colour word in a language is, in the first place, historical. At some point there are no colour words in a language, at a later point there are. We have no direct access to phase I, but there is a great deal of evidence that suggests colour words begin as the names for things and then are generalized to a wider class of objects that share a similar colour. The most obvious case where this is so is in reduplicative languages, where a common noun is uttered twice to indicate that it is being used to specify colour. [4] We can tell such utterances are about colour because the extension or range of the duplicated term is broader than that of the noun itself, and the duplicated term names things (for simplicity, we count properties as things) with a similar colour to that of the thing named by the base word. Reduplicative languages are not common, but evidence from historical semantics often tie colour words to things as well. There is evidence for this in Modern English (ME), with "orange" (the fruit), "purple" (a snail shell), "pink" (a flower) and "green" (as grass—green and grass have the same root). Other ME colour words, "brown" and "yellow", are rooted, as for many European languages, in the adjective, "shiny," though in different ways. The connection to the original word-as-name may become lost over time, with the referent of the now-a-colour-word becoming more abstract—in the sense that it has become the name for a colour in an abstract colour space not a name for a thing. [3] The ME origin of "red" seems like this—already abstract in Proto Indo-European (PIE). What we want to say here is that the process of constructing abstract colour categories based on the names for things is part of phase II not I. Phase I is best explained by B, the anthropological/historical hypothesis. Colour names that are grounded in objectual reference are not the target of BCT/BCC explanations, and Berlin and Kay make a point of ruling them out because they take it that such double-use words are not essentially colour classifiers. The criteria for basicness explicitly say that a basic colour term should not be a word for a thing. [1] Some researchers [2] have pointed out that this is too narrow a view. It should be the way a term functions in a language not its origin that matters and though we agree, the claim here is not that such object related words, in phase I at least, are BCTs. A phase I colour word is transitioning from name-for-the-colour-of-a-thing to name-for-a-colour. In this sense phase I colour terms are proto-BCT (referring to proto BCC), and they are *inputs* to phase II.

We say that B, the anthropological/historical hypothesis, provides the best explanation for phase I because colour words in this phase are the locally specific names for things. B-type explanations are prima facie applicable in phase I, are other explanation types relevant as well? It has been proposed that the environmental distribution of colours, A, explains the basic colour term distribution. The speakers of a language pick their colour exemplars of B, but the exemplars that are picked are chosen from the colours available, as a consequence of environmental distribution. The more a colour is present in an environment, the more likely it is to be the colour of an object culturally worthy of being named. It is worth pointing out that these two types of explanation [i] socio-cultural and [ii] ecological distribution are not in competition. Socio-cultural decisions on colour categorization take place within a larger envelope of ecological distribution. What about accounts of colour category formation that are based on perceptual salience, C? Since the publication of Berlin and Kay [1] a number of candidates for perceptual salience have been proposed: best examples/focal colours, Hering primaries, innate colour categories, colour space geometry, a warm/cool distinction. [15] One of the advantages to distinguishing colour naming and categorizational processes in the way that we have is that it allows us to see that, for example, perceptual salience is not as relevant to phase I as we might think. This might seem surprising, for surely some aspect of colour as perceptually salient is the first thing humans encounter experientially! Red pops out, some

colours are muted while others are vibrant, some colour stimuli are experienced categorically, and so forth. We propose that while the proposed perceptual saliences may form another envelope in which phase I naming activity takes place, they have more to do with the formation of categories in phase II. All the perceptual saliences are comparative: they emerge when we consider some colour or colours in relation to others. Perceptual saliences (or ecological distribution for that matter) seem insufficient to account for all the facts about phase I colour naming. We say "seem" because it is possible that culturally specific colour word choices are determined by perceptual saliences. Yet this is problematical: if a language has a term for red that is rooted in its word for a berry we would need to say that the cultural significance of the berry is not the determining factor for the proto BCT. Rather, it is perceptual salience. But this would make perceptual salience a winner-take-all explanation for colour naming. There are two problems with this view: one, it makes B type anthropological explanations all errors, despite their prima-facie plausibility; two, it makes it difficult to invoke B-type explanations for variation (categories that are incompatible with one's preferred salience) in a non-ad hoc way: they are ruled out as explanatory in the case where they are most plausible, and ruled in to account for inconsistencies with a C-type hypothesis. We do think that perceptual salience may override anthropological-historical significance, but not in phase I. As for the colour naming explanations that focus on communicative optimality or efficiency—the idea that colour term vocabulary's develop and evolved to maximize communicative efficiency and minimize cognitive uncertainty—this form of explanation is properly applied to phase II where categorical schemes that are not simply dual use name-colour words are formed.

One clear advantage to taking B-type explanations as the best explanations for phase I colour words is that it solves a problem articulated by Davidoff [6] which is of general importance. Davidoff writes that "The distinction, in Berinmo [a language spoken in Papua New Guinea] between leaves that are edible (green) and those that are inedible (yellow) makes up two of their terms. Their red term is the name of a berry which, like most berries, is a dark, saturated red when at its best to eat. The red term in other cultures is the word for blood (Rivers, 1905), which is a similar hue to the color of ripe berries. So a physiological explanation for the origin of color terms is not needed for any language, nor is it needed for the similarity of its terms to those in other languages for which there would be similar natural constraints." Davidoff's implication is that the explanatory story is finished for this case (and others like it—many according to the view expressed here). A B-type explanation is sufficient. Our view is that a B-type explanation is sufficient for understanding and predicting phase I proto-BCTs. B type explanations are local explanations [7] and they are not sufficient to explain the more global, universalist constraints, even if there is an object specific root for every colour name in every language.

Phase II. What is happening in this phase is relatively clear in outline: a group of people are constructing, beginning with their use of dual-function colour words (phase I) as inputs, a colour categorizational scheme. This must be difficult because it is hard for children in supervised contexts. [16] [23] It's also worth pointing out that it is fundamentally a cooperative endeavour. The naming data that constitute the World Colour Survey [24] the main database that is the basis colour naming research, can report average and modal responses for a community of language speakers, and it is the data for a community that counts. Claims in the BCT/BCC literature are almost always about languages not individual speakers. Constructing a colour categorical scheme (a system of at least three BCT/BCC) is an instance of unsupervised learning where the features the colour namers are identifying are not given in advance. There is no teacher, correcting error and guiding individuals implicitly or explicitly, toward a socially satisfactory end (as there is in phase III). Colour categories can (and do) have soft boundaries [29] reflecting variation in individual judgments (and perception) of category membership. But this softness must have limits. A

categorical scheme is used to talk about colour in the world, and will collapse if it fails to accomplish that task reliably. From a more abstract point of view, phase II is concerned with the development of a concept of colour as a domain of its own that is distinct from the object exemplars that are so important in phase I. Object related names may be retained in phase II, as they are vestigially for many ME colour words, but in phase II it is the formation of an abstract colour categorizational scheme, where the primary referents of colour terms are colours not things. What will matter is not that this thing looks like that thing (such that the similarity marked in terms of colour) but, rather, this colour looks like that colour (or not). When it comes to hypothetical explanations for phase II, D, communicative efficiency must be given precedence. It is the only hypothesis that is about colour naming as socially embedded with a particular social goal—an interpersonally robust colour categorizational scheme—that really is non-negotiable. It would not be possible to have the naming maps we have unless this desideratum was realized. More importantly, D can deal with variation in a different way than the other hypotheses (excepting B, which we will return to shortly). To see this, consider one version of C, the perceptual salience hypothesis, categorical perception version. On this view, there are prelinguistic colour categories, psychologically salient to prelinguistic children, that correspond to Berlin and Kay BCC. And yet the match is not 1 to 1. The categorical perception of colour research began in 1976 [5] and it has been much refined and improved [8] but there is a problem with it that persists throughout and to this day: a significant number of extant colour categorical schemes, described in WCS naming maps, do not correspond to the prelinguistic categories. [21] This means that there is another mechanism or causal force at work, and that force or mechanism is typically described in terms of cultural interests overriding perceptual salience. Similar versions of this scenario arise for other accounts of perceptual salience, all of which are reductive in character, by which we mean they attempt to explain high level linguistic activity in terms of lower level, non-linguist properties of brains and minds. Failure of fit inevitably leads to the convenience of the anthropological-historical stand-in explanation. Not in any principled way, but because that seems the only response to negative evidence. And thus we are back to the core idea: there are universal constraints on colour naming and variations that are determined by anthropological-historical facts. Type D hypotheses are able to evade this characterization. Type D hypotheses don't aim to align some set of non-linguistic facts with constraints derived from human linguistic behaviour, they aim to *model* that behaviour. In this sense type-D hypotheses don't need to distinguish between universal features of colour naming and variations from a universal scheme. They can treat each naming map, for each language, as a form of solution to a communication problem, and then look to see if those individual solutions constitute a model of colour naming with general application. One communicative model [17] [13] proposes that the judgement of relative similarity is the key to defining category boundaries, an essential function in what we have called phase II. Abstractly, you could begin with two colour exemplars, inputs from phase I, say, and generalize away from that exemplar. If you do this, your decision procedure for category membership will be "is x similar to exemplar?" But suppose you ask: "Is x more like exemplar 1 than it is like exemplar 2? This comparison is more constrained as a decision procedure than the similarity to exemplar model. So, in the real world, if your exemplars are the colours red and the colours green, yellow will be more like red, and blue will be more like green. When D-type theorists talk about cognitive optimality they are saying that if you need to communicate about colour, there will be a maximum number of BCT/BCC that encode an optimal set of categorical distinctions. Adding more categorical distinctions will yield diminishing communicative returns, having less will result in a too imprecise decision procedure: "Is x (orange) more like red than yellow?" for example. It is also the case that D type-theorists need not imagine full optimality (the maximum set of BCC) is realized in all languages, or any given language. Schemes may have an optimality that is relative to the number of categories they possess. And they may change over time, as Berlin and

Kay imagined them to do, in a predictable way. It also seems likely that D-type theories will exploit perceptual facts about colour experience--we have done so here to motivate the advantages to a mechanism such as relative similarity.

D type communicative efficiency hypotheses should do the heavy lifting in phase II. They can treat variation as an integral part of the explanation, rather than as something to be explained away by undefined anthropological effects. That is not to say that the other explanatory hypotheses are not relevant here. If communicative theories focus on a mechanism for generating category boundaries, that mechanism might be too general, capable, if not constrained, of generating colour categories outside those that have been attested in the WCS data. This is where C, perceptual salience explanation has the most bite--as a constraint upon communicative mechanisms. So, perhaps, we need a psychologically salient distinction between warm colours (red, yellow) and cool colours (blue, green) to make appropriate judgments of relative similarity possible. [12] It's also true that red is the first chromatic colour to be named as a BCT. [14] That cannot be explained by the communicative model. There are other examples where perceptual salience may constrain communicative models. Is there a role for B style explanations in phase II? Yes, but relative to communicative models they have a more principled role. So, for instance, one might predict that the particular colour categorizational scheme we find in a language has got something to do with how often people talk about colour and what colours they talk about [21]; we might find that the presence of a BCT/BCC for blue, in particular, is correlated with a linguistic groups proximity to a large body of water. Both of these effects have been observed. More speculatively, we might predict that BCC "centroids," the name for the most selected best examples of a BCT, might be a different shade of colour than the colour that is associated with the input exemplar from phase I. We don't need the salience of object colour to carry over to the category forming mechanisms of phase II. Research that claims focal colours for a categorical scheme emerge after category boundaries do is along these lines. [15]

Phase III. We are not going to say much about phase III. By the time a colour nomenclature is transmissible, it is already a part of the data set to be explained. There is a naming map for it, and its BCT/BCC are in place. There are many interesting results describing how children learn and use colour language, but consistency with the WCS data is not at issue, it's a given. That is not to say that specific developmental research is irrelevant to, in particular, phase II. A current model of children's colour term acquisition, [23] which views colour name learning as a dual stage process where a child first quickly learns a colour name, off the name of a coloured thing, and then spends months or years refining the boundaries of that term to achieve adult competence, might be thought to recapitulate phases I and II. Categorical perception demonstrated in prelinguistic children would seem clearly to be a boost or constraint on colour category formation, but the project of showing that it is seems to have stalled. More directly, free sorting experiments, [18] where experimental participants are not engaged in supervised learning, may be directly relevant to category formation in phase II, as is research that examines the classification of colours by artifical agents [22]. But these examples just scratch the surface of a wide range of experimental results.

CONCLUSION

In this paper we've made a case for three phases in the process of developing a socially robust system of colour names and categories. We have related those phases to four different explanatory strategies that have been proposed for the BCT/BCC universal constraints. In doing so we have singled out anthropological-historical accounts as essential to phase I and communicative efficiency accounts as

essential to phase II. We have made a case for a principled way to think about the universal constraints and their explanations.

REFERENCES

[1] Berlin, B. & Kay, P. 1969. Basic Color Terms: Their Universality and Evolution. Berkeley, Ca: University of California Press.

[2] Biggam, C. P. 2012. The Semantics of Colour. Cambridge, UK: Cambridge University Press.

[3] Biggam, C. P. 2010. The Development Of The Basic Colour Terms Of English. In *Interfaces Between Language and Culture in Medieval England* (Vol. 48, pp. 231–266). BRILL. https://doi.org/10.1163/ej.9789004180116.i-340.68

[4] Blust, R. (2001). Reduplicated colour terms in Oceanic languages, In Pawley, A., Ross, M. and Tryon, D. editors, The boy from Bundaberg: Studies in Melanesian linguistics in honour of Tom Dutton. PL514:23-50. Pacific Linguistics, The Australian National University, 2001. doi.org/10.15144/PL514.23

[5] Bornstein, M., Kessen, W., and Weiskopf, S. 1976. Color vision and hue categorisation in young human infants. Journal of Experimental Psychology: Human Perception and Performance, 2, 115–29.

[6] Davidoff, J. 2015. Color Categorization across Cultures. In Handbook of Color Psychology, Andrew J. Elliot, Mark D. Fairchild, and Anna Franklin (Eds.). Cambridge UK: Cambridge University Press, 259–78.

[7] Dedrick, D. Two kinds of explanation for basic colour terms? 2022. *Proceedings of the International Colour Association (AIC) Conference 2022*, Toronto, ON. 112-118.

[8] Franklin, A. 2015. “Development of Color Categorization.” In Handbook of Color Psychology, edited by A Franklin, Anna. 2015. “Development of Color Categorization.”In Handbook of Color Psychology, edited by An drew J. Elliot, Mark D. Fairchild and Anna Franklin. Cambridge, UK: Cambridge University Press, 279–94.

[9] Franklin, A. and Davies., IRL. (2005). Converging Evidence for Pre-Linguistic Colour Categorizations. In Progress in Colour Studies Volume II: Psychological Aspects, N. J. Pitchford and C.P. Biggam (Eds.) Amsterdam: John Benjamins, 101-20.

[10] Groh, A. 2016. Culture, Language and Thought: Field Studies on Colour Concepts. Journal of Cognition & Culture, 16(1/2), 83–106. doi.org/10.1163/15685373-12342169

[11] Hardin, C. L. 2005. Explaining Basic Color Categories. Cross-Cultural Research 39 (1): 72–87.

[12] Holmes, K. J., & Regier, T. 2017. Categorical perception beyond the basic level: The case of warm and cool colors. *Cognitive science*, *41*(4), 1135-1147.

[13] Jameson, K. and Roy G. D’Andrade. 1997. “It’s Not Really Red, Yellow, Green, and Blue: An Inquiry into Perceptual Color Space.” In Color Categories in Thought and Language, edited by C.L. Hardin and Luissa Maffi. Cambridge, UK: Cambridge University Press, 295–319.

[14] Kay, P. 2015. Universality of color categorization. In Handbook of Color Psychology, A.J. Elliot, A. Franklin, and M.D. Fairchild (Eds.), Cambridge: Cambridge University Press, 243–244.

[15] Lindsay, Delwin T. and Angela M. Brown. 2019. “Recent Progress in Understanding the Origins of Color Universals in Language.” Current Opinion in Behavioral Sciences 30: 122-9. https://doi.org/10.1016/j.cobeha.2019.05.007

[16] Pitchford N.J. Reflections on how color term acquisition is constrained. 2006. J Exp Child Psychol. Aug; 94(4): 328-33. doi: 10.1016/j.jecp.2006.02.004. PMID: 16603178.

[17] Regier, Terry, Paul Kay and Naveen Khetarpal. 2007.“Color Naming Reflects Optimal Partitions of Color Space.” Proceedings of the National Academy of Sciences, 104: 1436–41. https://doi.org/10.1073/pnas.0610341104

[18] Roberson, D., Davies, I., Corbett, G., & Vandervyver, M. 2005. Free-Sorting of Colors Across Cultures: Are there Universal Grounds for Grouping?. Journal of Cognition and Culture, 5(3-4), 349-386. https://doi.org/10.1163/156853705774648536

[19] Roberson, D. and J.R. Hanley. 2010. “Relatively Speaking: An Account of the Relationship between Language and Thought in the Color Domain.” In Words and the Mind: How Words Capture Human Experience, edited by B.C. Malt and P. Wolff. New York: Oxford University Press,183-9.

[20] Skelton A. E., Catchpole G., Abbott J.T., Bosten J.M., Franklin A. 2017. Biological origins of color categorization. Proc Natl Acad Sci U S A. May 23;114(21): 5545-5550, https://www.pnas.org/doi/full/10.1073/pnas.1612881114

[21] Twomey, C.R. , G. Roberts, D.H. Brainard, & J.B. Plotkin. 2021. What we talk about when we talk about colors, Proc. Natl. Acad. Sci. U.S.A. 118 (39) e2109237118, https://doi.org/10.1073/pnas.2109237118

[22] Steels, Luc and Tony Belpaeme. 2005. “Coordinating Perceptually Grounded Categories through Language: A Case Study for Colour.” Behavioral and Brain Sciences 28: 469–89.

[23] Wagner, K., K. Dobkins, & D. Barner. 2013. Slow mapping: Color word learning as a gradual inductive process. Cognition, 127(3), 307–317. doi.org/10.1016/j.cognition.2013.01.010

[24] WCS (World Color Survey). n.d. Data Archive. Accessed Sept. 10, 2025. http://www.icsi.berkeley.edu/wcs/data.html

[25] Wierzbicka, Anna. 2018. “How Much Longer can the Berlin and Kay Paradigm Dominate Visual Semantics?” In Rematerializing Colour, from Concept to Substance, edited by Diana Young. Canyon Pyon, UK: Sean Kingston, 67-89

[26] Witzel, C. 2019. Misconceptions About Colour Categories. Review of Philosophy and Psychology 10: 499–540. https://doi.org/10.1007/s13164-018-0404-5

[27] Yendrikhovskij S.N. 2001. Computing color categories from statistics of natural images. J. Imaging Sci. Technol.;45:409–417

[28] Zaslavsky, N., C. Kemp, T. Regier, & N. Tishby. 2018. Efficient compression in color naming and its evolution, Proc. Natl. Acad. Sci. U.S.A. 115 (31) 7937-7942, https://doi.org/10.1073/pnas.1800521115

[29] Zaslavsky, N., Kemp, C., Tishby, N. & Regier, T. 2020 Communicative need in colour naming. Cognitive Neuropsychology, 37:5-6, 312-324, doi: 10.1080/02643294.2019.1604502

Colour and Memory: Colour as An Aid to Memorization

Mathias Sætersdal[a*] and Phil Green[a]

[a]NTNU, Gjovik, Norway
[*]Corresponding author: Phil Green, philip.green@ntnu.no

ABSTRACT

Can memory enhance recall? It could be anticipated that increased salience due to colour contrast would lead to better short-term memory and object recall. However, previous studies have shown mixed results, with some suggesting that colour enhances attention and strengthens neural encoding, while others finding that the effects are negligible. To test the idea, 20 participants were asked to recall objects from AI-generated images, using semantically unrelated visual stimuli and standardized test conditions. Participants were presented with both greyscale and coloured sets of image, and they recalled on average 45% of items from both colour and grayscale images. Analysis showed that there was no correlation between recall performance and colour attributes; however, relative object size was positively correlated indicating that spatial attributes had a greater influence on the likelihood that an item was correctly identified in the recall phase.

Keywords: memory, colour attributes, salience

INTRODUCTION

Memory is a complex cognitive process influenced by numerous factors, and colour has long been hypothesized to play a significant role. Previous studies have indicated that colour enhances attention, but its effect on recall is contested. The results of previous studies on the impact of colour on memory are mixed, with some research claiming enhanced recall on colour-coded information, while others demonstrate negligible effects [1]. It has been proposed that colour acts as a memory cue, strengthening neural encoding [2]. Others argue that the effects are negligible without meaningful context. Some of the variation in results may stem from differences in experimental design, such as the use of semantically related stimuli, and insufficient control of the time duration of test phases.

This study investigates whether colour enhances recall of everyday objects compared to grayscale stimuli, by using a controlled experiment with randomized, non-associated generated images to eliminate guessing bias. This technique isolates colour as the primary variable.

METHODOLOGY

The study measured observer recall accuracy for sets of colour and grayscale objects using standardized scoring techniques. Participants' replies were categorized as either correct (exact match) or incorrect [3].

Particpants

Twenty young adults (ages 20-28) took part the study, comprising both university students and working young adults. This target group is commonly used in cognitive tests to ensure maturity while minimizing age-related

variability [4]. All participants reported normal vision and successfully completed the Ishihara test of colour vision, which has high sensitivity for red-green colour deficiency [5].

Test design

A test design known as Kim's Game, based on a game described in a novel by Rudyard Kipling [6], was used for the experiment. In a previous version of Kim's Game designed for young children [7] participants recalled items from a visual display featuring two familiar scenes: a vibrant farmers market stall (high recognisability, diverse colours); and an office setting with typical office or school supplies. Pilot testing revealed that participants could logically reconstruct forgotten items based on the remembered ones. This semantic risk inflates recall rates, as both scenes had items related to each other. A modified version of Kim's Game was used: each trial presented an image of unrelated objects, either in full colour or grayscale, on a display for 15 seconds, followed immediately by a 10-second period in which participants counted down backwards before commencing the recall task. This approach aided in isolating pure visual memory, and simulated real-world situations where distractions can affect memory by blocking rehearsal through a cognitive task. This is intended to give more accurate results by minimizing confounding variables.

Stimuli

A colour test images were generated using ChatGPT [8], with the prompt "Generate a photorealistic image containing 20 clearly visible household objects arranged naturally on a table. Include items like a wristwatch, pen, and Post-it notes with varied colours and sizes, ensuring all objects are distinct and non-overlapping." A second image was generated using the same prompt but specifying black and white instead of varied colours. The two images are shown in Figure 1 and Figure 2. This ensured minimal semantic overlap to prevent clustering effects during recall. Each image displayed different items, with some duplication; in the case of the grayscale image there were only 17 unique objects, whereas the colour image had 20 unique objects. This would have placed a slightly lower burden on participants completing the task with the grayscale image. It can also be noted that recall is likely to be highest (for Western participants at least) for objects presented at top left, since observers tend to scan a visual array in a Z pattern and the first objects viewed will be less affected by limits on the capacity of short-term memory [9].

Figure 1: Colour stimulus generated via ChatGPT 4.0, showing 20 household items.

Figure 2: Greyscale stimulus generated via ChatGPT 4.0 (OpenAI, 2023), showing 17 household items.

Experimental

Each trial presented 20 unrelated objects, either in full colour or grayscale, for 15 seconds, followed immediately by a 10-second backward countdown task before recall. This retention recall served a critical purpose. It isolated pure visual memory, and replicated real-world situations where distractions can affect memory by blocking rehearsal through a cognitive task. This yields more accurate results by ensuring that performance differences could be attributed solely to the presence or absence of colour. The order of colour/grayscale trials was randomized across participants to offset any sequence effect. Verbal recall responses were recorded to minimize motor interference, and only exact matches were recorded as correct.

1. Encoding Phase: Participants observed images for 15 seconds per set (colour or grayscale).

2. Retention Interval: To prevent rehearsal, a 10-second countdown task ("count aloud backward from 10") was implemented.

3. Recall Phase: Participants verbally listed all remembered items within 60 seconds. Responses were audio-recorded and manually scored.

RESULTS AND DISCUSSION

Participants correctly recalled between 7 and 11 of the 20 images from Figure 1, and 4-11 images from the black-and-white Figure 2. However, the difference between the average proportion correctly recalled from the two figures was negligible, as shown in Table 1.

Table 1: Proportion of objects correctly recalled from test image

Colour	Grayscale
0.448	0.450

The results for Figure 1 (coloured objects) were further analysed to determine the correlation between image attributes and recall performance. Two colour-related attributes (lightness and chroma) were selected, together with

two spatial attributes (relative size and entropy (or randomness)). Well-lit areas of the images were sampled to extract RGB values, which were then converted to XYZ using an ICC profile for sRGB, and then to CIELCh. The size was found from the number of pixels in the region occupied by each object. The entropy, *H*, of each object was found by converting the image to greyscale and calculating the entropy in Matlab according to Eqn (1), [10] where *p*, the probability of any grayscale intensity value, is the 2D array of normalized frequences of pixel values.

$$H = -\sum p\, log_2(p) \tag{1}$$

Pearson correlation coefficients were calculated between the attribute values and the average recall performance of observers for each image. The results are shown in Table 2. It can be seen that only image size has a significant positive correlation, suggesting that spatial attributes (specifically the relative object size), rather than colour attributes, were the more important factors influencing recall for this set of images.

Table 2: Correlation coefficients between image attributes and proportion recalled for each image

L* lightness	C^*_{ab} chroma	Size	Entropy
-0.032	-0.199	0.531	-0.122

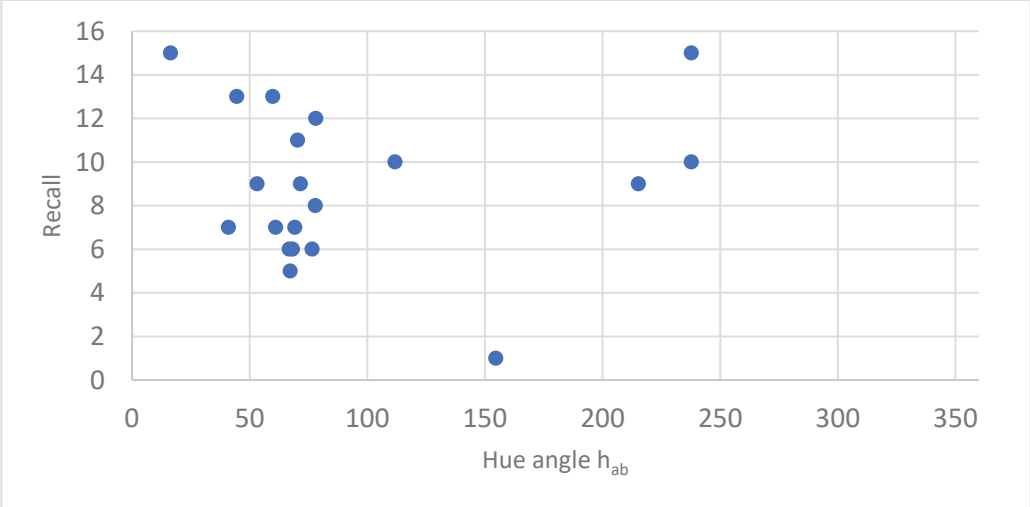

Figure 3: Recall performance by hue angle.

The correlation coefficient for hue angle with recall performance was also calculated, and found to be 0.046. This is also not significant, although somewhat less meaningful since hue angle is not a continuous scale. Object hues were dominated by colours in the red region including browns and pinks, as shown in Figure 3. Categorical colour names (using 10 of the 11 basic English terms identified by Berlin and Kay [11]) were assigned to the objects and again no pattern could be discerned in relation to recall performance.

The outcome of this admittedly small study runs counter to much previous work. It has been proposed that highly salient visual components like colour are processed automatically, even when cognitive restrictions are present [12]. Colour is claimed to be effective in directing attention and improving memory; according to studies on attentional capture: for example, colour is said to automatically focus attention without requiring verbal processing [13]. According to Domain-Specific Attention Theory [14], colour improves memory best when it is diagnostic of item identification. This could be reflected in greater recall of the tomato, for example (65%), where the colour is more strongly associated with the item, in comparison with those items that have arbitrary coloration.

CONCLUSION

Although it could be expected that colour would increase salience and hence aid in object memorization and recall, no such effect was found in this small study. Object identification is mediated by appearance attributes, which include edge contrast, texture, gloss, translucency and colour, and it may be that the familiar objects in this study were readily identifiable by those attributes which contribute to the apparent shape, leaving little or no further improvement to be gained from the dimension of colour. The greater correlation of object size with recall performance points to spatial attributes having greater importance than colour attributes for the task undertaken in this study. A larger study, with more trials and a greater number of observers, might further clarify the role of colour in recall.

REFERENCES

[1]. Dzulkifli, M. A., & Mustafar, M. F. (2013). The influence of colour on memory performance: A review. *The Malaysian Journal of Medical Sciences*, 20(2), 3-9.

[2]. Spence, I., Wong, P., Rusan, M., & Rastegar, N. (2006). How color enhances visual memory for natural scenes. *Psychological Science*, 17(1), 1-6.

[3]. Cowan, N. (2017). The many faces of working memory and short-term storage. *Psychonomic Bulletin & Review*, 24(4), 1158-1170.

[4]. Craik, F. I. M., & Salthouse, T. A. (Eds.). (2008). *The handbook of aging and cognition* (3rd ed.). Psychology Press.

[5]. Birch, J. (1997). Efficiency of the Ishihara test for identifying red-green colour deficiency. *Ophthalmic and Physiological Optics*, 17(5), 403-408

[6]. Kipling, R. (1959) *Kim*, Illustrated by Stuart Tresilian, Macmillan

[7]. Learning and Teaching Scotland (2007) *Study Skills: "Kim's Game"*. Archived from the original on October 15, 2008. https://web.archive.org/web/20081015170130/http://www.ltscotland.org.uk/studyskills/5to9/remember/KimsGame/resources/index.asp

[8]. OpenAI. (2023). *ChatGPT (Version 4)* https://chat.openai.com

[9]. Atkinson, R. C., & Shiffrin, R. M. (1968). Human memory: A proposed system and its control processes. *Psychology of Learning and Motivation*, 2, 89-195

[10]. Gonzalez, R. C., Woods, R. E. and Eddins, S. L. *Digital Image Processing Using MATLAB*. New Jersey, Prentice Hall, 2003, Chapter 11.

[11]. Berlin, B and Kay, P. (1969) *Basic Color Terms: Their Universality and Evolution*, University of California Press

[12]. Lavie, N. (2005). Distracted and confused? Selective attention under load. *Trends in Cognitive Sciences*, 9(2), 75-82.

[13]. Theeuwes, J. (2010). Top-down and bottom-up control of visual selection. *Acta Psychologica,* 135(2), 77-99

[14]. Tanaka, J. W., & Presnell, L. M. (1999). Color diagnosticity in object recognition. *Perception & Psychophysics*, 61(6), 1140-1153.

A Comparative Study on Human and AI Interpretation of Traditional Chinese Red Color Names

Hsueh-Fen Lin[a*]

[a]*Department of visual and communication design, Cheng Shiu University, Kaohsiung, Taiwan*
[*]*Corresponding author: Hsueh-Fen, Lin, linsf0408@gmail.com*

ABSTRACT

This study investigates how humans and large language models (LLMs) interpret traditional Chinese red color terms, aiming to clarify differences in semantic understanding and color association. Fifteen terms were selected from classical and modern dictionaries, representing categories such as symbolism, flora and fauna, minerals, and bodily/metaphorical imagery. A three-stage framework was applied: (1) extraction and categorization of color terms; (2) a human survey with 40 participants evaluating familiarity, semantic associations, and color selections; and (3) prompting four LLMs—GPT-5, GPT-4o, Gemini Pro 2.5, and Claude Sonnet 4—to provide explanations and corresponding HEX codes. Results showed that humans produced more consistent color choices for familiar and concrete terms (e.g., Xuehong, "blood red"; Taohong, "peach blossom pink"), but highly divergent choices for obscure or metaphorical ones (e.g., Quetouse, "sparrow-head color"; Zhenzhuhong, traditionally evoked in classical poetry such as "small vats of wine dripping like pearl-red" (小槽酒滴真珠紅), referring to the deep crimson of fine wine). Notably, none of the AI models aligned with this cultural meaning of Zhenzhuhong, instead generating pinkish or bright red tones. LLMs displayed stronger convergence on terms with tangible origins (e.g., Zhuhong, cinnabar red) but diverged sharply on metaphorical expressions such as Shuihong ("watery pink," a poetic and metaphorical expression) and Zhenzhuhong. Correlation analysis revealed only a minimal relationship between familiarity and color consistency ($r \approx 0.08$), indicating that semantic clarity appears to play a more decisive role than familiarity. The findings highlight both the potential and cultural limitations of LLMs, suggesting future directions for collaborative human–AI semantic color databases and culturally informed design education.

Keywords: Traditional Chinese Color Names, Large Language Models, Color Cognition, Human–AI Comparison

INTRODUCTION

Color, as a visual language element rich in symbolism and cultural meaning, evokes consistent associations even in abstract contexts (Mukherjee et al., 2024) [3]. With the rapid development of large language models (LLMs), researchers have begun to explore whether these models can emulate human associations between language and color. Mukherjee et al. (2024) found that GPT-4 generated stable color associations for concrete concepts [3], while Xu and Benítez-Burraco (2025) showed that LLMs often produce overly convergent and positively biased outputs when dealing with abstract meanings such as emotions [4]. Komatsu et al. (2022) further noted that even advanced models like GPT-4o diverge from human interpretation when processing culturally embedded or semantically ambiguous terms [1]. Similarly, the Foundation Model Color Map proposed by Languénou and Hurter (2025) revealed that LLMs' semantic interpretations of colors are largely constrained by training data distributions rather than cultural semantics [2].

Although these studies establish both the potential and the limitations of LLMs in color–meaning association, they mainly focus on modern, general vocabulary and neglect traditional Chinese color terms. Such terms, found in classical dictionaries, are culturally rich but semantically complex. For example, relatively concrete terms like Xuehong ("blood red") or Taohong ("peach blossom pink") contrast with culturally embedded or metaphorical expressions such as Nanfangse ("southern symbolic red"), Tanse ("sandalwood red"), or Shuihong ("watery pink"). Whether contemporary users still share consistent associations with these terms, and whether LLMs can interpret them meaningfully, remain open questions.

To address this gap, the present study asks three research questions: (1) Do humans show greater consensus for concrete and familiar terms compared to abstract or metaphorical ones? (2) How do LLMs interpret and visualize traditional Chinese color terms, and where do they diverge from human interpretations? (3) Does familiarity with a term predict greater consistency in color selection? By combining human survey data and outputs from four advanced LLMs, this study offers the first systematic comparison of human and AI interpretations of traditional Chinese red color names, contributing to color cognition research, cultural computing, and design education.

METHODOLOGY

This study investigates how humans and large language models (LLMs) interpret traditional Chinese red color terms, focusing on differences in semantic understanding and color association. The methodology consists of three stages: (1) term collection and selection, (2) human participant survey, and (3) prompt-based color generation using four large language models (LLMs).

1. Term Collection and Categorization

In the first stage, traditional red color terms were collected and categorized using content analysis. Twelve representative Chinese dictionaries and lexicons from the Pre-Qin to the modern era were systematically reviewed, including the Cangjie Pian (Qin), Erya (Warring States to early Western Han), Jijiupian (Western Han), Shuowen Jiezi and Shiming (Eastern Han), Guangya (Cao Wei), Yupian (Southern Dynasties), Guangyun (Song), Zhengzitong (Ming), Kangxi Dictionary (Qing), Zhonghua Dictionary (Republic of China), and the Combined Edition of Ciyuan and its Supplements. All red-related color terms were manually extracted in order of appearance by flipping through each entry page-by-page. A total of 26 red color terms were collected.

From these, 15 representative terms were selected for analysis. Selection was based on two criteria: (1) semantic clarity in modern dictionaries, and (2) cultural depth and historical appearance in ancient sources. Given that traditional color terms are often metaphorical, symbolic, or tied to material culture, their interpretation can vary widely across users and systems. To account for this diversity, a representative selection of terms was required. The 15 terms were categorized into four conceptual groups: (1) Natural and cultural symbolism: Huochi (火赤, "fiery red"), Richuzhi Chi (日出赤, "sunrise red"), Nanfangse (南方色, "symbolic red of the South in traditional Chinese cosmology, where the South is associated with the element fire and the color red"), Yangfeise (楊妃色, "a soft pink named after Lady Yang, imperial consort of the Tang dynasty"); (2) Flora and fauna: Quetouse (雀頭色, "sparrow-head red"), Jiguanse (雞冠色, "a vivid red inspired by the rooster's comb"), Zaose (棗色, "jujube red"), Huase (樺色, "birch-bark color"), Tanse (檀色, "deep reddish-brown inspired by sandalwood"), Zonghong (椶色, "palm red"), Taohong (桃紅, "pinkish red from peach blossoms"); (3) Minerals and materials: Zhuhong (硃紅, "cinnabar red"); (4) Bodily and metaphorical imagery: Xuehong (血紅, "blood red"), Shuihong (水紅, "watery pink"), Zhenzhuhong (真珠紅, " wine crimson").

2. Human Participant Survey

A total of 40 adult participants were recruited through random sampling. All participants reported normal color vision and no history of color blindness. The questionnaire included two parts: basic demographic data (gender, age, education level, and whether they had studied color theory), and a color-naming test with 15 items. For each item, participants rated their familiarity with the color term (5-point Likert scale), described their semantic associations (open-ended), and selected a color using Google's online color picker interface. Responses were collected using a 13.3-inch MacBook Air (1280×1024 resolution), ensuring consistency across participants. The tool's intuitive interface and real-time visual feedback enabled participants—even without design background—to accurately and intuitively select a HEX code, improving the reliability and validity of the data.

3. LLM Prompting and Output Collection

In the final stage, the study analyzed how large language models interpret the semantic and visual meaning of red color terms. Four major LLMs were selected: OpenAI's ChatGPT-5 and ChatGPT-4o, Google's Gemini Pro 2.5, and Anthropic's Claude Sonnet 4. These models were chosen based on their public availability, advanced language comprehension, and ability to process Traditional Chinese. A unified prompt was used to ensure consistency across models: "Do you know the color term '○○'? Please describe your understanding of this term, provide the HEX color code that best corresponds to it, and explain the reasoning behind your choice (such as references, meaning, imagery, or color logic)." This prompt combined open-endedness and clarity to elicit both semantic explanations and specific color codes. Responses were collected in August 2025 via the official platforms of each model to ensure consistency. Each model was prompted once per term, and the first response was recorded for analysis. This one-shot approach allowed consistency and comparability across models, but it also represents a limitation. Variability due to prompt phrasing or model randomness was not accounted for. Future studies may expand this method by experimenting with multiple prompt styles, measuring inter-run consistency, or fine-tuning models on culturally specific lexical datasets.

RESULTS AND DISCUSSION

A total of 40 participants (20 female, 20 male) took part in the questionnaire survey examining semantic understanding and color selection of traditional Chinese red color terms. The survey assessed familiarity, semantic associations, and selected HEX color values. Among them, 19 participants (47.5%) were aged 18–24—the largest age group—representing the core demographic of design learners and digital-native users. Educational backgrounds included university (n = 31), graduate level (n = 7), and high school (n = 2). Half of the participants (n = 20) had previously studied color-related subjects.

1. Human Interpretation and Color Association of Traditional Red Color Terms

This study collected participants' semantic associations and color selections for 15 traditional Chinese red color terms via questionnaire. In the open-ended section, participants entered words they associated with each color name. Common responses included "lychee," "wood," "jujube," "peach blossom," "flame," and "sunrise," reflecting a strong tendency toward concrete, natural, and everyday imagery. These associations were categorized into four types: natural entities, cultural and symbolic references, emotional or abstract concepts, and cases of unclear or missing associations. Among these, natural entities were most frequent, followed by emotional/abstract references. Certain terms such as Quetouse (sparrow-head color), Zonghong (palm-red), and Zhenzhuhong (wine crimson) showed highly divergent responses, suggesting a weak link between the lexical meaning and modern-day conceptual understanding.

For the color selection task, participants used the Google online color picker to choose the HEX code that best represented their perception of each color term. These results were converted into color swatches and displayed horizontally for visual comparison (see **Figure 1**). Terms such as Huochi (fiery red), Richuzhi Chi (sunrise red),

Jiguanse (rooster comb red), and Xuehong (blood red) showed high consistency, with most selections falling within the red-orange hue range. In contrast, terms like Quetouse, Zhenzhuhong, Zaose (jujube), and Nanfangse revealed scattered results across blue, green, and brown hues, indicating varied interpretations and weak consensus. In particular, Nanfangse illustrates how a term rooted in traditional cosmology may lack concrete visual reference for contemporary users: although historically linked to the red of the South and the element fire, modern participants no longer share this cultural framework, leading to divergent and uncertain color associations.

A correlation analysis between familiarity ratings and hue standard deviation revealed minimal relationship ($r \approx 0.08$). Even for familiar terms like Xuehong ("blood red") and Taohong ("peach blossom pink"), hue selections were relatively consistent, yet saturation and brightness still varied. Less familiar, metaphorical terms such as Zonghong and Quetouse showed much greater hue dispersion. This suggests that familiarity alone does not ensure visual agreement; semantic clarity and concreteness are more critical.

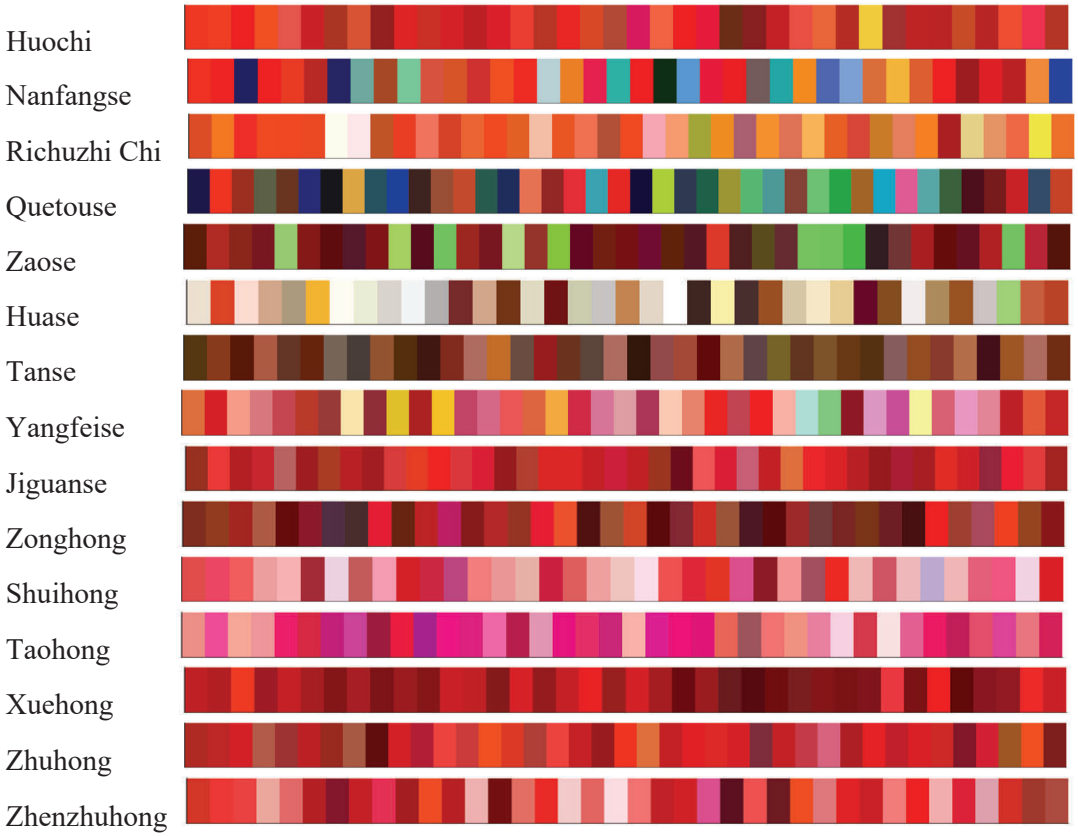

Figure 1: Participants' Color Associations with Traditional Color Names

2. AI Output Comparison and Semantic Analysis of Traditional Red Color Terms

This study analyzed the outputs of four major LLMs in response to 15 traditional Chinese red color terms. For each term, we collected the generated HEX codes, corresponding color representations (hue, saturation, brightness), classification as red-related, and textual descriptions. Comparisons focused on five aspects: (1) conversion of HEX to hue values to detect clustering or deviation; (2) alignment between color codes and descriptions (e.g., whether

"light pink" corresponds to bright pink tones); (3) cross-model consistency in both values and interpretations; (4) semantic understanding of the terms' origins, rhetorical features, and symbolic meanings (e.g., cinnabar, blood, femininity); and (5) whether the models recognized the terms as part of the traditional Chinese color system, referencing classical sources.

Table 1: HEX Codes and Color Outputs from AI Models

color name	gpt-5	gpt-4o	gemini pro 2.5	claude sonnet 4	Degree of Variation
Huochi	#FF3300	#E64028	#E62E00	#DC143C / #E63946	Medium
Nanfangse	#FF0000	#D6001C	#C90016	#FF6B35 #E74C3C	Medium
Richuzhi Chi	#FF4500	#E2553D	#F35B2D	#FF4500 / #FF6347	Medium
Quetouse	#8B5C42	#005E5B	#7B4A3A	#8B4513 / #A0522D	High
Zaose	#701C1C #822020	#7C2629	#6E2C24	#722F37 / #8B0000	Low
Huase	#B35C1E	#C1693C	#B76F4B	#DEB887 #D2B48C	Medium
Tanse	#B36B6B #9C4848	#763C28	#4A2226	#8B4513 #A0522D	Medium
Yangfeise	#E04E75	#E6A49F	#F0B3B3	#F8BBD0 #FFB6C1	Medium
Jiguanse	#E60026	#B11B24	#D81E06	#ED1C24 #FF2D2D	Low
Zonghong	#9B3D3D	#943A36	#A52A2A	#9B4400	Medium
Shuihong	#F5B6B6	#F4C6C6	#F8959D	#F3D3E7	High
Xuehong	#990000	#990000	#990000	#8B0000 #A0001C	Low
Taohong	#FF3399	#F596AA	#FF69B4	#F47983	Medium
Zhuhong	#FF4C00	#E23C28	#E34234	#DD2C00	Low
Zhenzhuhong	#E78EA9	#E7A1A1	#C72539	#CC527A #E8175D	High

(Compiled by this study)

Table 1 shows the compiled HEX codes and their corresponding color samples from each AI model, allowing visual comparison. In general, the models displayed reasonable alignment between cultural meaning and color assignment. Terms such as Zhuhong (cinnabar red), derived from cinnabar pigment, were consistently associated with orange-red tones (Hue 10°–15°), and linked to imperial or ceremonial symbolism. Xuehong (blood red) was interpreted as fresh blood, relating to themes of life and war, and located in dark red hues (Hue 350°–0°). Lighter shades such as Taohong (peach blossom pink), with floral associations, and Shuihong (watery pink), a more poetic and metaphorical term, were generally interpreted within the pink hue range (Hue 330°–350°), often linked to femininity and softness.

However, abstract or metaphorical terms showed greater variation. For example, Quetouse (sparrow-head color) was read as reddish-brown by GPT-5, Gemini, and Claude, while GPT-4o generated a teal (#005E5B), reflecting divergence in interpretation. Zhenzhuhong (wine crimson), appearing in classical poetry such as *"small vats of wine dripping like pearl-red"* (小槽酒滴真珠紅), metaphorically describes the deep crimson of fine wine.None of the AI models captured this historical meaning: GPT-5 and GPT-4o produced light pinks (#E78EA9, #E7A1A1), Gemini a vivid cool red (#C72539), and Claude a bright pink-red (#CC527A). These outputs misinterpreted "zhenzhu" literally as "pearl," leading to associations with contemporary pearl pink tones rather than the traditional wine-red imagery.

In contrast, terms with clear material referents—such as Zhuhong, blood red, or jujube red—produced more convergent results, likely due to their stronger cultural anchors. This highlights both the potential and the limitations of LLMs in interpreting traditional color language, especially when dealing with metaphor-rich or historically nuanced vocabulary.

CONCLUSION

This study compared human responses and AI outputs on 15 traditional Chinese red color terms. Participants chose consistent colors for familiar, concrete terms such as Xuehong ("blood red") and Taohong ("peach blossom pink"), but showed wide variation for metaphorical or obscure terms such as Quetouse ("sparrow-head color"), Zonghong ("palm red"), Shuihong ("watery pink"), and Zhenzhuhong ("wine crimson"). Similarly, AI models could recognize culturally anchored terms like Zhuhong ("cinnabar red") or Yangfeise ("a pink shade named after Lady Yang, Tang Dynasty imperial consort"), yet diverged sharply on metaphorical expressions, sometimes producing colors outside the expected hue range.

Correlation analysis revealed only a minimal relationship between familiarity and color consistency ($r \approx 0.08$), indicating that semantic clarity rather than familiarity is the decisive factor in achieving consistent interpretations.

Overall, the findings highlight both the potential and cultural limitations of LLMs in mapping language to color. While LLMs demonstrate basic reasoning ability, they still fall short of replicating the nuanced cultural knowledge and contextual judgment embedded in human intuition. Future research may focus on developing collaborative human–AI semantic color systems, culturally grounded databases of traditional color terms, and applications in color education and design practice.

REFERENCES

[1]. Komatsu, H., Maeno, A., & Watanabe, E. (2022). Origin of the ease of association of color names: Comparison between humans and AI. i-Perception, 13(5), 20416695221131832. https://doi.org/10.1177/20416695221131832

[2]. Languénou, É., & Hurter, C. (2025). Foundation Model ColorMap: A Framework for Extracting and Visualizing the Foundation Models' Color Knowledge. In Proceedings of CHI 2025, Yokohama, Japan. https://enac.hal.science/hal-05020362v1

[3]. Mukherjee, K., Rogers T. T., & Schloss K. B. (2024). *Large Language Models estimate fine-grained human color-concept associations.* (arXiv:2406.17781) [Preprint]. arXiv. https://doi.org/10.48550/arXiv.2406.17781

[4]. Xu, M., & Benítez-Burraco, A. (2025, February). Do Large Language Models see the world with rose-colored glasses? Prompting ChatGPT-4o to associate colors with emotions in Spanish and Mandarin [Preprint]. OSF. https://doi.org/10.31234/osf.io/pnc3q_v1

A Deep Learning-Based Footwear Prediction and Recommendation Model

Li-Yun Liu[a], Yi-Ting Luo[a], and Hung-Chung Li[a*]

[a]*Bachelor Program in Intellectual Creativity Engineering, National Chung Hsing University, Taichung, Taiwan*
[*]*Corresponding author: Hung-Chung Li, hcli01@nchu.edu.tw*

ABSTRACT

The study aims to design and develop an AI-based footwear recommendation system using deep learning, addressing the common consumer challenge of choosing suitable shoe styles. The system integrates human keypoint detection, image segmentation, computer vision, and deep learning algorithms to extract clothing features from user-submitted outfit photos automatically. By leveraging advanced image processing and Vision Transformer (ViT) models, the system can effectively learn the correlation between upper-body clothing, lower-body clothing, and footwear to recommend suitable shoe styles. The proposed system also analyzes fashion styles and trends to suggest shoe options that match the user's outfit. Background removal and segmentation techniques enable the accurate identification of clothing and footwear features. By analyzing outfit images, the system predicts matching shoes to improve the online shopping experience. Personalized recommendations are generated through an integrated recommendation algorithm, providing users with instant, visualized suggestions along with product purchase links to enhance shopping efficiency and satisfaction. The research encompasses data collection, model design and optimization, system development, and user testing. Feedback from users will be further used to evaluate the accuracy and practicality of the recommendations. Ultimately, the system delivers an intelligent and innovative solution tailored to the needs of users in the footwear e-commerce industry.

Keywords: footwear, recommender system, computer vision, deep learning, vision transformer

INTRODUCTION

As living standards improve, the variety of consumer products continues to grow. In today’s internet-driven society, users face overwhelming choices in clothing. Beyond price and functionality, appearance and aesthetics have become key factors, particularly in the fashion industry. With the rapid rise of e-commerce, shoppers often feel overwhelmed by the abundance of clothing options. Also, constantly shifting fashion trends add to the challenge of making suitable outfit choices.

In deep learning, as a core technology in artificial intelligence, multi-layer Artificial Neural Networks (ANNs) could learn and extract features from large datasets, offering improved efficiency and accuracy over traditional feature engineering [1]. Since the proposal of Deep Belief Networks (DBN) by Hinton et al., models such as Convolutional Neural Networks (CNN) and Long Short-Term Memory (LSTM) have emerged, significantly advancing computer vision applications. Krizhevsky et al. used a CNN model to process the ImageNet dataset, reducing classification error to 16% [3]. The introduction of ResNet [4] addressed gradient vanishing issues, thereby further enhancing network training capabilities. Technologies such as You Only Look Once (YOLO), and Generative Adversarial Network (GAN) have expanded their applications in real-time object recognition and image generation. In fashion applications, deep learning has driven developments such as virtual try-ons, smart outfit

suggestions, and product recognition (e.g., Google Lens), thereby enhancing the consumer experience and accelerating industry digitization.

For recommendation systems, the architecture typically involves data collection, construction of a similarity matrix, computation of recommendations, and display or feedback of results. By analyzing user behavior and preferences, personalized suggestions are generated and widely adopted in e-commerce and media platforms. Woiceshyn et al. developed a personalized clothing recommendation robot capable of learning user preferences [5]. Additionally, Liu et al. introduced a multi-branch deep neural network with a Channel Attention Model (CAM), achieving an accuracy of over 93% in gender and clothing category predictions [6].

Despite these advances, most fashion recommendation systems focus on clothing and offer limited support for footwear. Traditional rule-based systems often fail to capture nuanced style features, resulting in less accurate recommendations [7]. Therefore, this research aims to fill this gap by developing an intelligent system that extracts style, color, and material features to provide personalized shoe recommendations based on outfit aesthetics.

METHODOLOGY

The study proposes a content-based shoe recommendation system that leverages deep learning and image processing techniques to analyze full-body outfit images and automatically recommend appropriate footwear. As shown in Figure 1, the overall framework comprises four key modules: user feature modeling, item feature modeling, training the prediction model using the shoe feature vector, and computing content similarity.

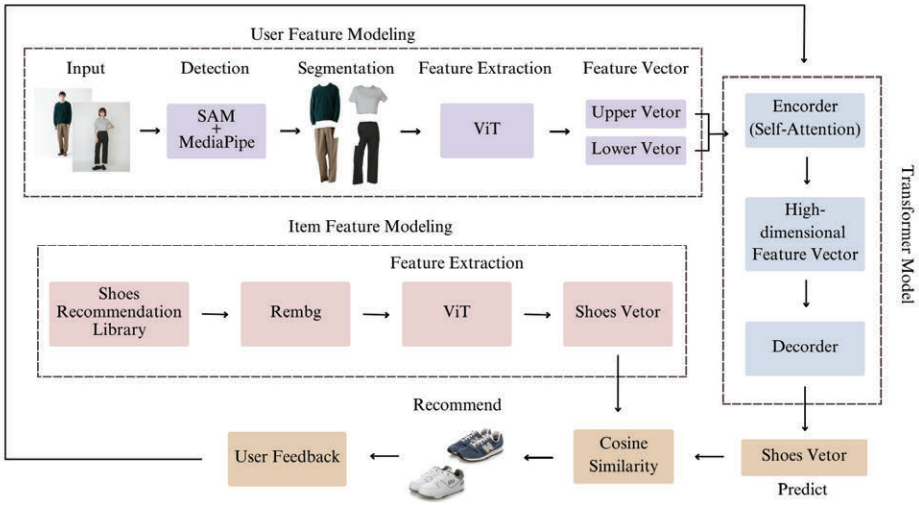

Figure 1: Recommendation system workflow

User Feature Modeling

Full-body images crawling from the D+AF e-commerce platform (2,036 images) and DeepFashion (6,648 images) are utilized as training data to learn the relationship between upper and lower clothing and footwear. First, the Segment Anything Model (SAM) model segments different regions of the image, as shown in Figure 2. Then, MediaPipe extracts human keypoints to identify the upper body, lower body, and shoe regions, as data preprocessing. These regions are used to train the model. The process enables the model to focus on individual clothing and footwear elements in isolation, allowing for a more precise analysis of their features.

Figure 2: Segmentation results of SAM with MediaPipe

Referring to Figure 3, a 768-dimensional image feature vector for the corresponding image region is extracted using Vision Transformer (ViT), which splits images into 16×16 patches and applies a self-attention mechanism to learn global features. Based on the Query (Q), Key (K), and Value (V) relationships, ViT dynamically adjusts its attention to focus on the texture and material of garments. A CLS token is added to each patch, which is then encoded to generate high-dimensional feature representations. RGB and HSV color features are also integrated to enhance the understanding of color harmony in outfits. Therefore, a total of 774 dimensions of features are used, ensuring the model captures both visual and color matching considerations in the footwear recommendation process. The training dataset consists of approximately 5,000 samples of top, bottom, and shoes, with 80% used for training and 20% for testing. Attention maps, as Figure 4, confirm that ViT effectively focuses on clothing and ignores background noise, validating its usefulness for fashion image analysis.

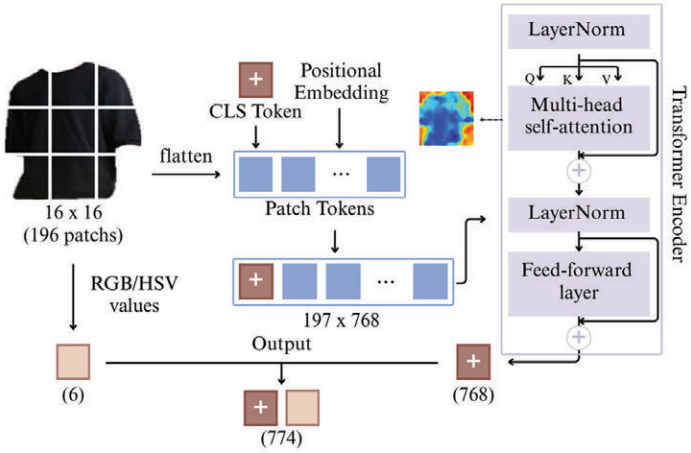

Figure 3: Proposed vision transformer

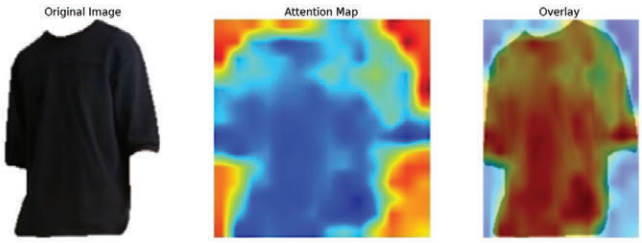

Figure 4: Attention map of clothing

To recommend footwear that aligns with users' outfit styles, this study builds a shoe recommendation database of approximately 20,000 shoe images scraped from the Fasbee e-commerce platform as the data source. A web crawler gathers brand names and URLs of shoes. The Rembg algorithm removes backgrounds to ensure the model focuses solely on shoe features, improving accuracy and matching quality.

A Transformer-based model is used to learn the matching relationships between upper and lower-body clothing and predict suitable shoes. Upper and lower body feature vectors pass through the Transformer encoder, where multi-layer self-attention captures inter-part correlations. The resulting high-dimensional feature vector is then decoded into a shoe feature vector. Feedforward neural networks are added after each attention block to expand feature space and improve prediction accuracy.

Similarity Computation

Cosine similarity, as Eq.1, is used to compare the predicted vector with vectors in the shoe recommendation database. Scores closer to 1 indicate higher similarity. The top 10 most similar shoes are selected as recommendations and presented with images and purchase links.

$$Cosine\ Similarity(V_{pred},\ V_{shoe}) = \frac{V_{pred} \cdot V_{shoe}}{\|V_{pred}\| \cdot \|V_{shoe}\|} \tag{1}$$

RESULTS AND DISCUSSION

To verify the assumption that visually similar images yield similar feature vectors, t-SNE is used for dimensionality reduction and visualization. Figure 5(a) shows that the three categories (upper, lower, and shoes) form distinct clusters, indicating the model's ability to distinguish clothing types effectively, and Figure 5(b) depicts the cosine similarity between clothing objects.

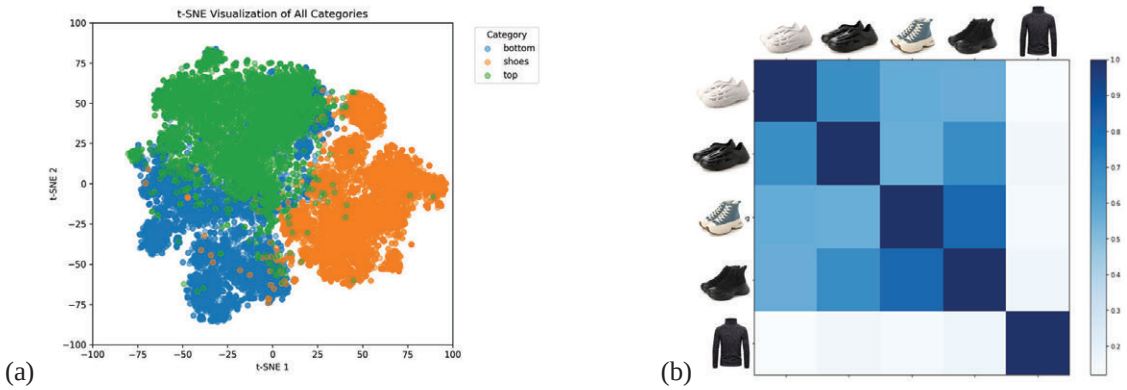

(a) (b)

Figure 5: (a) t-SNE projection; (b) similarity between objects

Mean Squared Error (MSE) is used as the loss function, and the model is trained using the Adam optimizer with 2,000 epochs. Figure 6 shows that training loss steadily decreases, indicating proper model convergence and effective learning of upper and lower body correlations. Figure 7 illustrates the cosine similarity between predictions and actual vectors in the validation set, with most samples concentrated between 0.7 and 0.8. The average similarity

score is approximately 0.73 and 0.68 for males and females, respectively, confirming the model's accuracy in predicting shoe feature vectors.

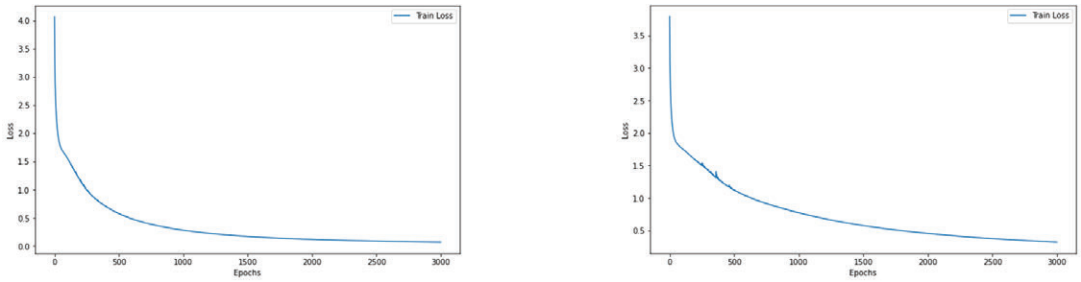

Figure 6: Training loss curves. (Left: male; Right: female)

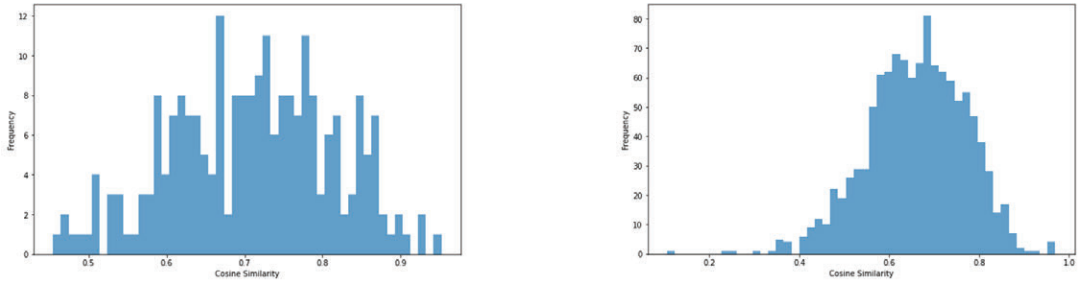

Figure 7: Cosine similarity distribution (Left: male; Right: female)

For recommendation results, consider the outfit shown in Figure 8 as an example, where the user is wearing an off-shoulder tank top and a maxi skirt. The model recommends ballet flats and ankle boots, which complement the outfit's elegant yet casual aesthetic. The recommendation is logical and adaptive to various occasions. Additionally, a user interface has been established for the application, which enables users to input user-submitted outfit photos into a transformer model, predict the corresponding vector, and utilize cosine similarity to identify the top 10 most similar shoes from the recommendation library. The highest-ranked favorited item will be recorded in each recommendation for the user, as shown in Figure 9.

Figure 8: Shoe recommendation results by the model. (Left: test outfit image; Right: recommended shoes)

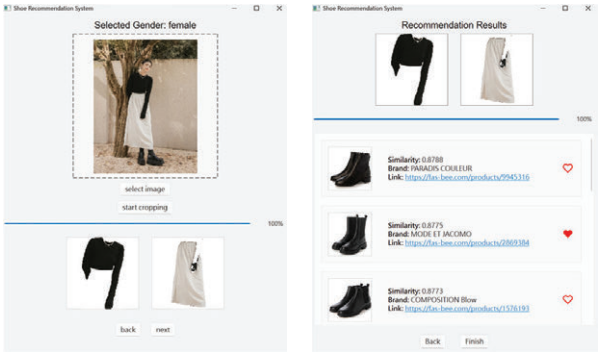

Figure 9: The user interface of shoe recommendation system

CONCLUSION

The study develops a deep learning-based shoe recommendation system that integrates human keypoint detection and ViT with a transformer-based prediction model to analyze outfit features automatically and suggest matching footwear. The results demonstrate that feature vectors exhibit strong discriminative power, and the model effectively predicts accurate shoe vectors with consistent training convergence. Additionally, the recommendations align with real-world fashion logic and offer diverse, context-appropriate options to enhance the user experience. Future improvements include expanding data sources, incorporating user feedback mechanisms, and integrating virtual try-on functionalities to improve the system's practicality and promote innovative e-commerce development.

ACKNOWLEDGEMENTS

This research project is partly supported by the National Science and Technology Council (NSTC-113-2634-F-005-002 and NSTC-114-2221-E-005-024)

REFERENCES

[1]. Bishop, C. M., & Nasrabadi, N. M. (2006). *Pattern recognition and machine learning* (Vol. 4, No. 4, p. 738). New York: springer.

[2]. Hinton, G. E., Osindero, S., & Teh, Y. W. (2006). A fast learning algorithm for deep belief nets. *Neural computation*, *18*(7), 1527-1554.

[3]. Deng, J., Dong, W., Socher, R., Li, L. J., Li, K., & Fei-Fei, L. (2009). ImageNet: A large-scale hierarchical image database. In *Proceedings of the IEEE Conference on Computer Vision and Pattern Recognition (CVPR)* (pp. 248-255). IEEE.

[4]. He, K., Zhang, X., Ren, S., & Sun, J. (2016). Deep residual learning for image recognition. In *Proceedings of the IEEE Conference on Computer Vision and Pattern Recognition (CVPR)* (pp. 770-778). IEEE.

[5]. Woiceshyn, L., Wang, Y., Nejat, G., & Benhabib, B. (2017, October). Personalized clothing recommendation by a social robot. In *2017 IEEE International Symposium on Robotics and Intelligent Sensors (IRIS)* (pp. 179-185). IEEE.

[6]. Liu, K. H., Chuang, H. L., & Liu, T. J. (2022, July). Clothing recommendation based on deep learning. In *2022 IEEE International Conference on Consumer Electronics-Taiwan* (pp. 281-282). IEEE.

Restoring Mobile App-Filtered Photos Using CNN-Based Deep Learning

Ya-Hsuan Lin, Yu-Chieh Chang, Jie-Sen Wang and Pei-Li Sun*

National Taiwan University of Science and Technology, Taipei, Taiwan
**Corresponding author: plsun@mail.ntust.edu.tw*

ABSTRACT

With the widespread use of social media and mobile photo-editing apps, many images are modified with filters, beautification tools, and color adjustments. While these edits enhance aesthetics, they often distort original colors, posing challenges for applications requiring color fidelity, such as visual recognition and cultural heritage archiving. To address this, we propose a deep learning framework to restore original colors from stylized images by modeling and reversing common editing operations.

Our method uses a multi-task ResNet-50 with a shared backbone branching into two sub-networks: one detects whether an image is edited, and the other regresses seven editing parameters—exposure, contrast, saturation, red–blue adjustment, shadows, highlights, and vignetting—using mean squared error loss. Predicted parameters are then inverted via an image restoration pipeline to approximate the unedited image.

Trained on paired datasets of original and artificially edited photos, the model achieved 98% classification accuracy and reduced CIE94 color difference by 80%. Errors in saturation and red–blue adjustment had the greatest impact on perceived quality. Visual inspection confirms recovery of natural color tones even under heavy stylization.

This framework offers high restoration fidelity, interpretability, and efficiency, making it suitable for automated photo correction, batch restoration, and vision-based diagnostics.

Keywords: image color restoration, photo-editing, style filters, CNN-based deep learning

INTRODUCTION

The growing use of mobile photography and real-time editing apps has transformed image capture and sharing, with complex filters and artistic effects often introducing substantial deviations from a scene's original color distribution. While enhancing creative expression, such distortions hinder applications requiring accurate color fidelity, such as digital archiving and cultural heritage preservation. Existing methods rarely account for the parameters and processes involved in multi-functional editing, making it difficult to restore the colors of app-filtered photos.

Recent advances in deep learning—particularly Convolutional Neural Networks (CNNs)[1]—offer a way forward. CNNs extract hierarchical visual features via local receptive fields[3], shared weights, and nonlinear activations, drawing inspiration from the biological visual cortex and providing strong invariance to noise, occlusion, and geometric transformations. Residual learning frameworks like ResNet introduce shortcut connections to stabilize gradients and enable deeper networks[2], while Multi-Task Learning (MTL) improves generalization and efficiency by sharing features across related objectives[4].

Building on these advances, we propose a ResNet-based dual-branch framework for detecting and correcting stylized photographic content. One branch performs binary classification to detect edits; the other regresses seven

editing parameters—exposure, contrast, saturation, red–blue adjustment, shadows, highlights, and vignetting—using mean squared error loss. Trained on a paired dataset of original and synthetically filtered images, the model predicts editing status and parameter values in a single pass. For edited images, inverse transformations with a residual enhancement path approximate the original appearance while preserving fine spatial details. This efficient, interpretable framework supports robust restoration across diverse stylization styles, enabling batch enhancement reversal, mobile deployment, and consistent visual archiving.

METHODOLOGY

To train a model capable of restoring original colors from stylized images, we constructed a paired dataset specifically designed for learning inverse editing transformations. Each data group contains 21 images: one original unedited landscape photograph and twenty corresponding stylized versions generated through different combinations of image editing parameters. These parameters include exposure, shadows, highlights, contrast, saturation, red–blue color adjustment, and vignetting.

Figure 1: Visual demonstration of the seven editing parameters

Figure 1 illustrates the perceptual impact of these editing operations. For each parameter, images were adjusted to extreme values (e.g., exposure −100 or +100), demonstrating the corresponding visual distortions. These examples define the types of transformations that the proposed model is trained to estimate and reverse.

A total of 3,000 such image groups were generated using a custom-built multi-functional image editing program, resulting in 63,000 images in total. The dataset was divided according to an 80:10:10 split ratio for training, validation, and testing, respectively, ensuring sufficient variation across lighting, composition, and style conditions.

The proposed restoration model is based on a ResNet-50 backbone pre-trained on ImageNet, with its final fully connected layer removed to serve as a feature extractor. The extracted features are passed to two parallel output branches: a classification head to detect whether the image has been edited, and a regression head to estimate the seven predefined editing parameters. The predicted parameters are then applied to a customized inverse adjustment pipeline to approximate the original image. The overall network architecture is illustrated in Figure 2.

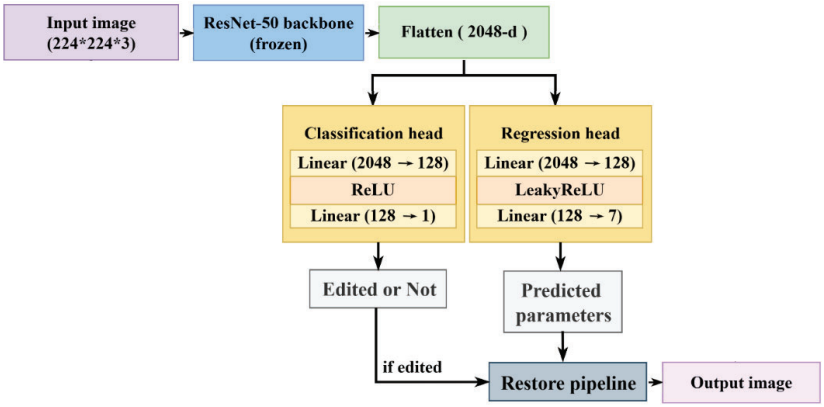

Figure 2: Architecture of the proposed model

During training, the classification branch is optimized using the binary cross-entropy loss with logits, defined in Eq.1, where x_i is the predicted logit, y_i is the ground truth label, and N is the number of samples. The regression branch is trained only on samples labeled as "edited," using a weighted mean squared error to account for differences in parameter scale, as shown in Eq.2, and the total loss function is the sum of the classification and regression losses, as given in Eq.3.

$$L_{cls} = \frac{1}{N}\sum_{i=1}^{N} \max(x_i, 0) - x_i y_i + \log(1 + e^{-|x_i|}) \tag{1}$$

$$L_{reg} = \frac{1}{N}\sum_{i=1}^{N} w_i (y_i^{pred} - y_i^{gt})^2 \tag{2}$$

$$L_{total} = L_{cls} + L_{reg} \tag{3}$$

An early stopping mechanism is employed: if the validation loss does not decrease for 15 of epochs, training is terminated and the best-performing model weights are preserved. The model was trained using the Adam optimizer with a learning rate of 0.0001. Training was conducted for 100 epochs with a batch size of 16, and all experiments were implemented in PyTorch and executed on a workstation equipped with an NVIDIA GeForce RTX 3070 GPU.

To illustrate how editing transformations were applied and subsequently reversed, Figure 3 presents the forward editing pipeline, while Figure 4 shows the inverse restoration pipeline. In the forward process, the original image is converted to float32 format and sequentially adjusted through tone mapping in RGB space, saturation changes in HSL space, red–blue ratio modification, and vignette effects, before being transformed back into 8-bit format. The inverse pipeline mirrors these operations in reverse order, progressively removing vignette, restoring red–blue ratio and saturation, recovering tonal balance, and finally converting the restored image back into 8-bit format.

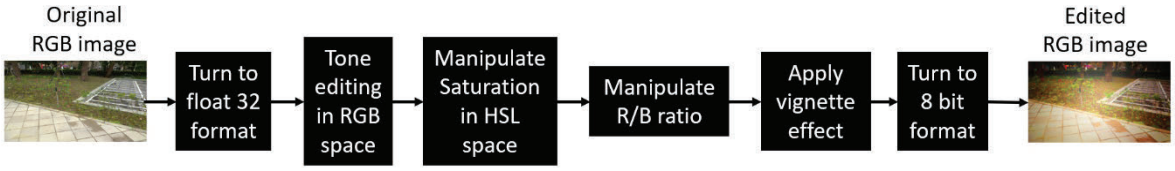

Figure 3: Image editing pipeline

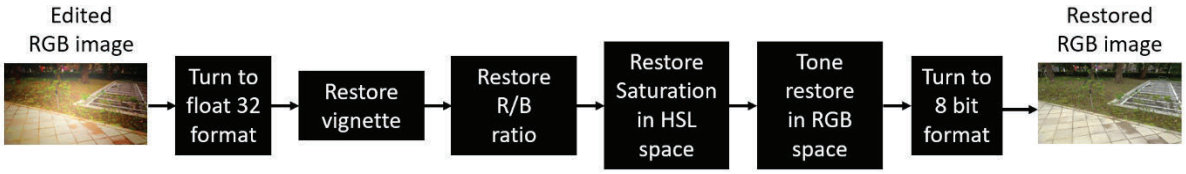

Figure 4: Image restoration pipeline

RESULTS AND DISCUSSION

Classification Accuracy

Before performing color restoration, the system first determines whether an input image has undergone stylization or editing. This is achieved using the binary classification branch of the proposed multi-task network, which outputs a probability value (logit ∈ [0, 1]). A threshold of 0.5 is applied to this probability to classify the input as either Edited (requiring restoration) or Original (no restoration required).

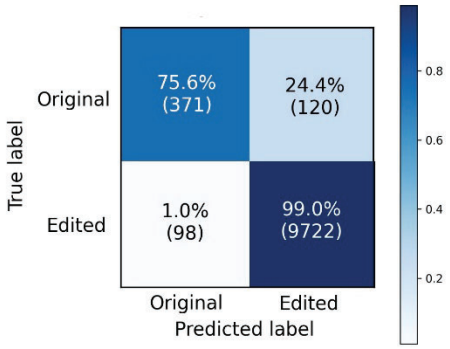

Figure 5: Confusion matrix

The classification performance is illustrated in the confusion matrix shown in Figure 5 , it can be observed that the majority of samples are correctly classified, with the model achieving an overall classification accuracy of 98%.

Parameter Prediction Error

Table 1 summarizes the proposed model's regression accuracy for seven editing parameters. Edited MAE (mean absolute error) denotes the baseline error when assuming no edits (all parameters set to zero), while Restored MAE (mean absolute error) measures the error between predicted and ground-truth parameters after restoration. The Improvement Rate, computed from MAE, reflects the percentage reduction in error relative to the baseline.

Results show that red–blue adjustment and vignette achieve the lowest restored MAE (1.41 and 0.85) with over 94% improvement, reaching 95% for red–blue adjustment, indicating strong recovery for parameters with clear localized cues. Shadows and saturation also exceed 90% improvement but retain higher RMSE, likely due to spatially varying details and intense stylization effects.

Table 1: Parameter error

Parameters	Edited MAE	Restored MAE	Improvement rate
Exposure	18.03	2.06	89%
Shadow	33.61	3.10	91%
Highlight	26.59	2.49	91%
Contrast	35.19	2.78	92%
Saturation	35.10	3.29	91%
Red-blue adjustment	26.88	1.41	95%
Vignette	13.19	0.85	94%

Color Difference Analysis

To assess perceptual quality, the CIE94 color difference ($\Delta \boldsymbol{E}^*_{\boldsymbol{94}}$) was computed between ground-truth original images and both the edited and restored versions [5]. Figure 6 compares the distributions: in the edited images (a), most pixels have a color difference between 10 and 20, with an average of 11.71 and a 95th percentile of 20.54, indicating substantial deviation from the original colors. In the restored images (b), the distribution shifts markedly toward lower values, with most pixels below 5, an average of 2.42, and a 95th percentile of 7.09, confirming that the proposed method greatly reduces color distortion and produces images perceptually closer to the originals.

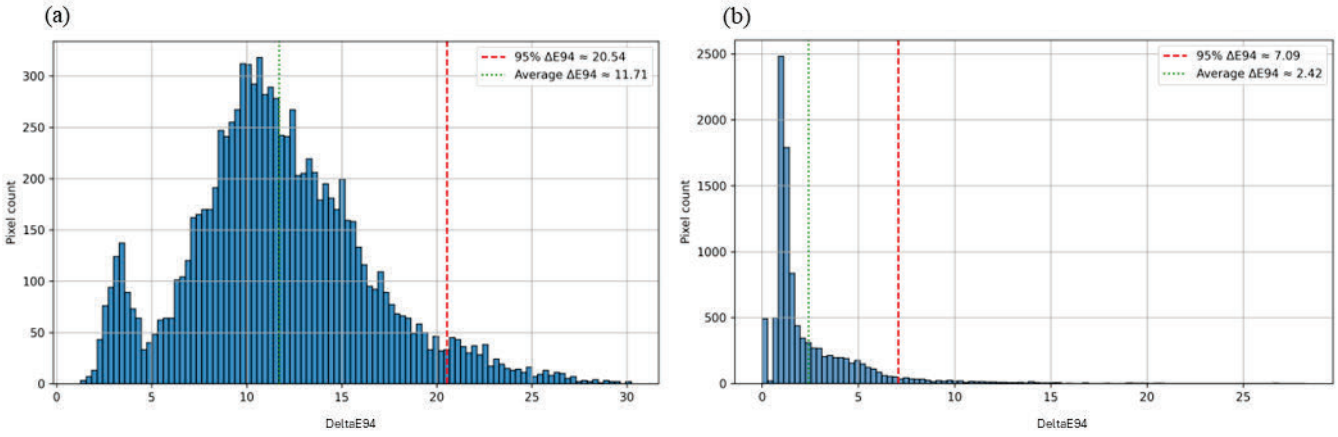

Figure 6: Color difference ($\Delta \boldsymbol{E}^*_{\boldsymbol{94}}$) of (a) edited images and (b) restored images.

CONCLUSION

This study presented a multi-task deep learning framework for detecting and reversing stylized image edits by jointly performing binary classification and multi-parameter regression. Built on a ResNet-50 backbone, the network integrates a classification branch to determine whether restoration is needed and a regression branch to estimate seven common editing parameters—exposure, contrast, saturation, red–blue adjustment, shadows, highlights, and vignetting. Trained on a custom-paired dataset of original and synthetically edited images, the proposed approach achieved a 98% classification accuracy, ensuring that restoration is applied selectively and appropriately. The regression results showed consistent error reduction across all parameters, with improvement rates exceeding 89% and reaching up to 95% for red–blue adjustment.

Quantitative evaluation using the CIE94 color difference metric demonstrated that the method reduced the mean $\Delta \boldsymbol{E}^*_{\boldsymbol{94}}$ from 11.71 in edited images to 2.42 after restoration, while lowering the 95th percentile from 20.54 to 7.09. These results confirm the framework's ability to effectively recover natural color tones and minimize perceptual discrepancies, even under heavy stylization. Given its high restoration fidelity, interpretability, and computational efficiency, the proposed method holds strong potential for applications in automated photo correction, large-scale image restoration, and visual content preservation in domains such as digital archiving and cultural heritage.

REFERENCES

[1]. Alzubaidi, L., et al. (2021). "Review of deep learning: concepts, CNN architectures, challenges, applications, future directions." Journal of big Data **8**: 1-74.

[2]. He, K., et al. (2016). Deep residual learning for image recognition. Proceedings of the IEEE conference on computer vision and pattern recognition.

[3]. LeCun, Y., et al. (2015). "Deep learning." Nature **521**(7553): 436-444.

[4]. Ruder, S. (2017). "An overview of multi-task learning in deep neural networks." arXiv preprint arXiv:1706.05098.

[5]. Berns, R. S. (2019). Principles of Color Technology, 4th ed., p.101, Wiley.

Perceived Color Differences for Color-Deficient Observers

Hsiu-Ying Hsiao [a], Yi-Yun Chen[b], Hung-Shing Chen[b*]

[a] *Graduate Institute of Applied Science and Technology, National Taiwan University of Science and Technology, Taipei, Taiwan*

[b] *Graduate Institute of Electro-Optical Engineering, National Taiwan University of Science and Technology, Taipei, Taiwan*

**Corresponding author: bridge@mail.ntust.edu.tw*

ABSTRACT

This study investigates perceptual differences in color discrimination between individuals with normal vision and those with color vision deficiency (CVD). Addressing the gap in color-difference metrics primarily based on normal observers, this work examines how CVD observers perceive color differences. Fourteen male participants (9 protanopes, 5 deuteranopes) evaluated Munsell samples (Munsell 5G, Munsell V=4, 6, 8) under controlled conditions. Stimuli were displayed on a calibrated Adobe RGB monitor in dim room, and participants rated perceptual differences via a gray scale method. Average scores were plotted onto the CIE a^*b^* plane to generate perceptual color difference maps. Results showed that protanopes and deuteranopes perceived smaller color differences along the red–green (a^*) direction than those along the yellow–blue (b^*) direction. Their perceptual color difference range (0 ~14, ΔE_{ab}^*) was much narrower than that of normal observers (0 ~100, ΔE_{ab}^*). It can be seen that color samples with higher lightness reduced discriminability, and correlations with normal observers were weak ($r \approx 0.25$), while protanopes and deuteranopes were strongly correlated ($r= 0.86$). Comparisons with the dichromatic vision models yielded only moderate agreement ($r= 0.20 \sim 0.45$). These findings highlight the asymmetry of CVD perception and provide empirical evidence to refine CVD color vision models and support inclusive design strategies.

Keywords: color vision deficiency, color difference metric, color vision test, perceived color difference, gray scale method

INTRODUCTION

Color plays a crucial role in our daily lives, influencing not only aesthetic perception but also the efficiency of communication and functionality in various fields such as design, engineering, medicine, and transportation. For individuals with normal color vision, distinguishing subtle differences in hue, lightness, and chroma can be accomplished with relative ease. However, for those with color vision deficiency (CVD), such tasks present significant challenges. CVD, commonly referred to as color blindness or color weakness, affects approximately 5% of the global population, with males representing the majority of cases. The condition arises from anomalies or the absence of cone photoreceptor functions in the retina, leading to altered spectral sensitivities and subsequently impaired color discrimination.

Difficulties in perceiving and discriminating colors can create obstacles in everyday activities such as driving, reading maps, or selecting clothing. More critically, they may restrict access to professions requiring precise color identification, including medicine, graphic design, and electrical engineering. In public spaces, conventional color-coded signals or signage often neglect the needs of individuals with CVD, resulting in reduced accessibility and potential safety hazards. To address these issues, inclusive design strategies—such as enhanced luminance contrast, redundant coding through patterns or text, and the adoption of color-vision-friendly palettes—have been proposed.

Nevertheless, the scientific foundation for these strategies remains incomplete without a thorough understanding of how CVD observers actually perceive and evaluate color differences.

Over the past decades, several color-difference metrics have been developed, such as the CIE1976, CIE94, and CIEDE2000, to quantify perceived color differences. However, these metrics were primarily derived from experiments with observers possessing normal vision. Studies focusing on CVD populations remain relatively scarce. Besides, several color vison models, such as the physiologically based approach of Machado et al. (2009) or the anomalous trichromat model of Yaguchi et al. (2018), provide valuable insights into how images may appear to individuals with CVD. Yet, the predictive validity of these color vison models in representing actual perceptual experiences has not been sufficiently verified through empirical testing.

This study aims to bridge this gap by investigating the perceptual evaluation of color differences among both normal vision and CVD. By means of using Munsell color charts as experimental stimuli, with hue 5G selected as the references (i.e., Munsell 5G, Munsell V=4, 6, 8), participants were asked to assess perceived color differences under controlled lighting conditions. The collected data were visualized on the CIE a^*b^* plane as color difference contour maps to reveal systematic patterns in color-difference perception. Comparisons were then made between normal observers, protanopes (P-type CVD), and deuteranopes (D-type CVD), across 3 layers of Munsell V levels. Furthermore, the relationship between simulated and actual perceptual color differences was further analyzed to evaluate the accuracy of existing color vision models.

By clarifying the characteristics of color-difference perception in CVDs, this research provides empirical evidence that can inform the design of color-vision-friendly environments. The findings are expected to contribute to the development of more inclusive design principles, improve accessibility in public information systems, and inspire future enhancements in color-difference metrics tailored to diverse visual populations.

METHODOLOGY

Participants: Fourteen male participants aged 19–26 years were recruited for the study. Among them, nine were diagnosed as protanopes and five as deuteranopes, which were verified using the Munsell D-15 color arrangement test. All participants had normal or corrected-to-normal visual acuity, and none reported any additional visual impairments.

Experiment design: The experiment was designed to measure perceptual color differences between reference and test colors on the monitor. Munsell color samples with hue 5G at three lightness levels (Munsell V=4, 6, 8) were selected as reference stimuli. A total of 293 test colors were paired with these references. Stimuli were displayed on a well-calibrated LCD monitor (EIZO CG241W), which was calibrated to the Adobe RGB gamut, 6500 K white point, and 2.2 of γ value. Each color patch on the monitor subtended approximately 5.7° × 5.7° of visual angle (5 × 5 cm at a 50 cm viewing distance) and was presented side by side with the reference against a neutral gray background. Observers were seated at a fixed distance of 50 cm in a dimly lit room (<50 lx). During the trials, each participant was asked to visually assess the perceived color differences between the reference and test samples, providing a direct measure of perceptual sensitivity across chromatic directions.

Color difference rating experiment: Following the visual comparison, participants rated perceived color differences via the SDC gray scale method. Ratings were assigned on a nine-point scale, ranging from "no noticeable difference (ΔE^*_{ab}=0.0)" to "very large difference (ΔE^*_{ab}=13.4)". After each pair of reference and test colors was evaluated, the average ratings across participants were calculated. The resulting data were plotted onto the CIE a^*b^* color plane, and perceptual color-difference contour maps were generated. Moreover, Pearson correlation coefficients were computed to show the relationships across observer groups. The descriptive statistics were also applied for group comparisons. These color-difference maps provided a visual representation of discrimination thresholds for both normal-vision and CVDs, allowing comparison of the color sensitivities along the red–green (a^*) and yellow–blue (b^*) directions.

RESULTS AND DISCUSSION

The analytical results revealed that the following clear and systematic patterns in the perceptual evaluation of color differences among CVDs.

Color sensitivity: Both protanopes and deuteranopes demonstrated markedly reduced color differences along the red–green (a^*) direction in comparison with those along the yellow–blue (b^*) direction. This asymmetry highlights the reliance of CVDs on the yellow–blue direction for discriminating colors. As illustrated in Figure 1, the color difference maps for normal-vision and CVD observers clearly differ in color distributions: The normal-vision observers show a balanced distribution along both a^* and b^* axes (Figures (d), (e), (f)). In contrast, the contour maps for protanopes and deuteranopes revealed smaller color differences along a^* direction, while showed larger color differences along b^* direction relatively (Figures (a), (b), (c)).

Perceptual color difference **range:** When compared to normal-vision observers, who exhibited a perceptual color-difference color difference range extending from 0 to 100 of ΔE^*_{ab}, CVD participants' ratings for perceptual color differences were considerably compressed, spanning only 0 to 14 (ΔE^*_{ab}) on the SDC scale. This narrower perceptual bandwidth suggested significant limitations in detecting subtle color differences.

Lightness effect: Results across different lightness levels (Munsell V=4, 6, 8) showed that higher lightness conditions led to lower perceived differences. At Munsell V=8, color distinctions became less evident, indicating that bright samples reduce discriminability for CVD observers. This lightness-dependent trend is visible in the color difference maps of Figure 1, where perceptual boundaries appear more compact at higher Values. This may be related to cone response saturation or to the relative reduction of chromatic contrast for color samples with higher lightness values.

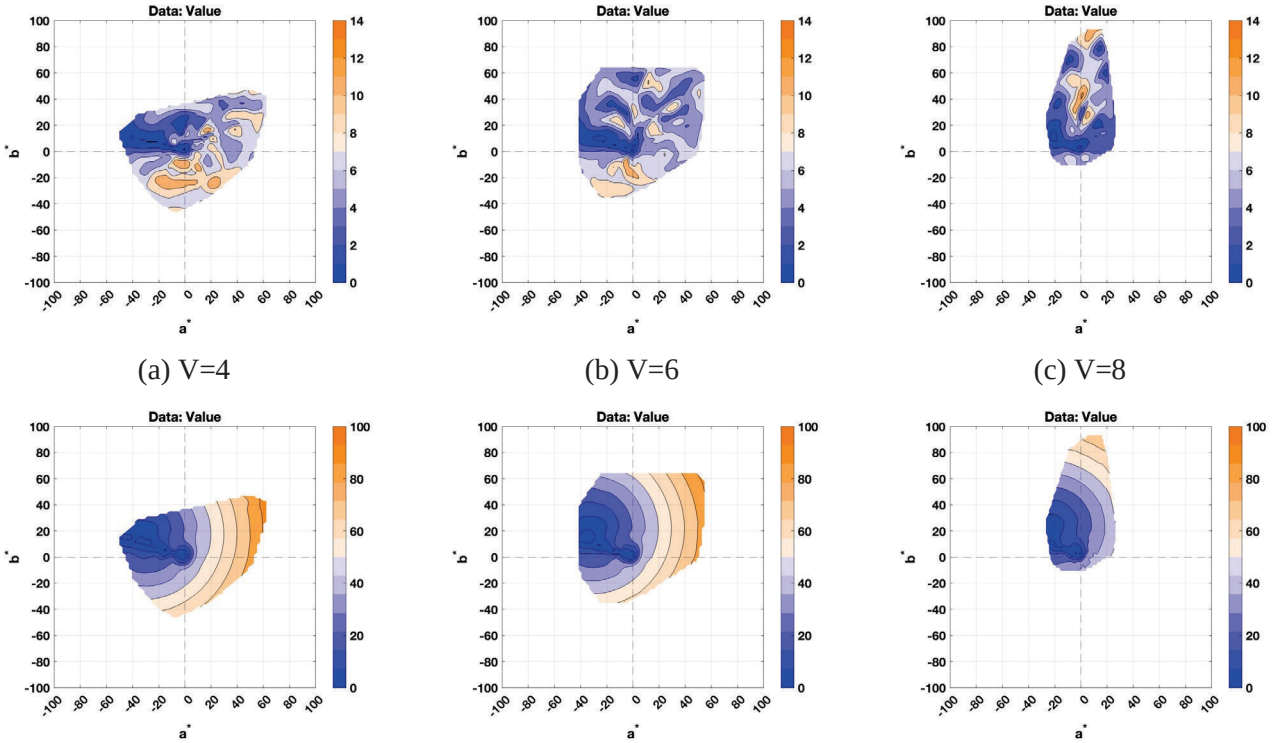

(a) V=4 (b) V=6 (c) V=8

(d) V=4 (e) V=6 (f) V=8

Figure 1. Example of perceptual color difference contour maps on the CIE a^*b^* plane: subfigures (a), (b), (c) represent 4, 6, 8 of Munsell V values for CVD respectively; and subfigures (d), (e), (f) represent, 6, 8 of Munsell V values for normal vision respectively.

Correlation analysis: The correlation between normal vision and CVD was relatively weak ($r \approx 0.25$), suggesting limited alignment between their perceptual frameworks. In contrast, protanopes and deuteranopes shared a strong inter-correlation (r=0.86), reflecting their similar perceptual tendencies despite difference types in color deficiencies. These relationships are summarized in Table 1 and graphically depicted in Figure 2, where scatter plots highlight the weak correlations between normal vision and CVDs (Figure 2(a), and Figure2(b)), but a strong linear trend between protanopes and deuteranopes (Figure 2(c)).

Table 1. Correlation analysis results

Color difference comparison	Correlation (r)	Observation
Normal vision vs. CVD	0.25	Weak correlation
Protan vs. Deutan	0.86	Strong correlation
Simulated CVD vs. experimental CVD	0.20 ~ 0.45	Moderate correlation

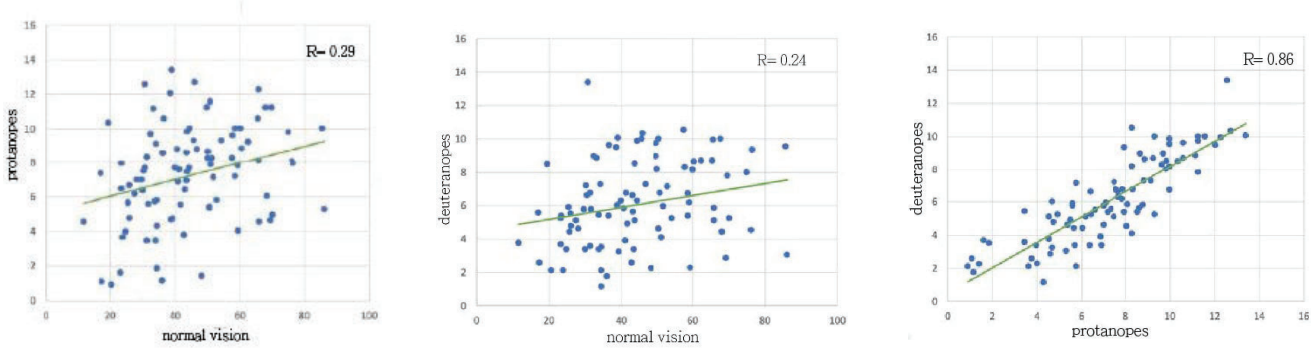

(a) (b) (c)

Figure 2. Color difference correlations between normal vision and red-green color vision deficiencies: (a) Normal vision vs. protanopia, (b) Normal vision vs. deuteranopia, (c) Deuteranopia vs. protanopia.

Model validation: The comparisons between perceived color differences and those predicted by Machado's color vison model (e.g., Machado et al., 2009) revealed only modest agreement, with correlation coefficients ranging from 0.20 to 0.45 depending on lightness. This suggested that Machado model cannot fully replicate the actual perceptual experiences of CVDs. The correlation plots for protanopia (Figure 3(a)) and deuteranopia (Figure 3(b)) both exhibit large variability and relatively flatter slopes, underscoring the discrepancy between simulated and perceived differences. This suggested that Machado model may require non-linear adjustments or the incorporation of individual variability to better approximate actual perceptual data. Such refinements are essential if the color vision models are to be applied reliably in accessibility-oriented design.

Consequently, these results emphasized the asymmetric nature of CVD perception, and reveal lightness-dependent changes in discriminability, and provided empirical data to guide the development of more inclusive color-difference models and visual design strategies for CVDs.

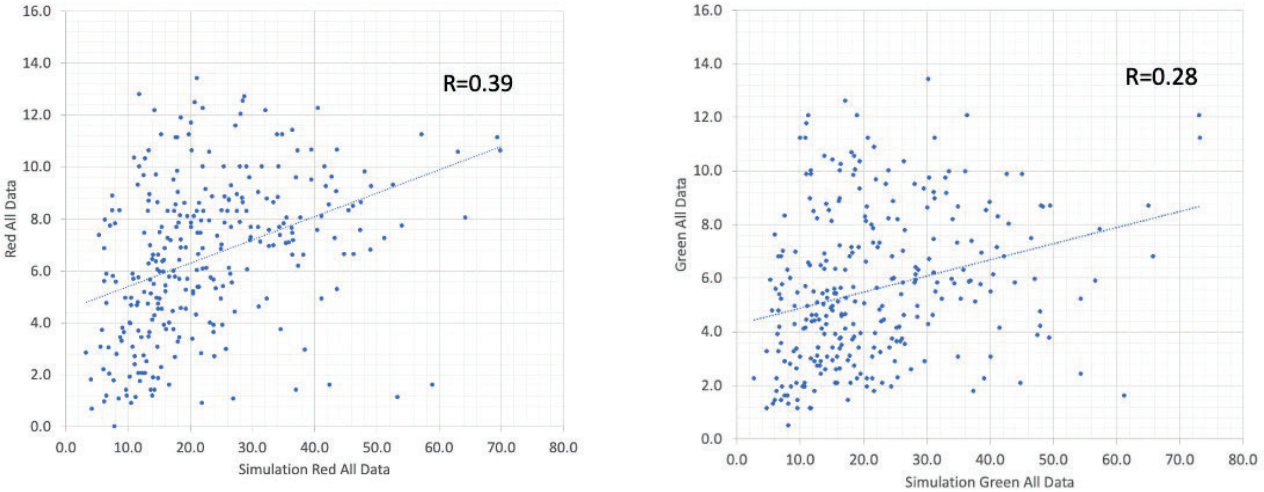

(a) (b)

Figure 3. Correlation between simulated and perceived color differences: (a) protanopia, (b) deuteranopia.

CONCLUSION

This study demonstrates systematic differences in color-difference perception between normal-vision and CVD observers. Protanopes and deuteranopes exhibited compressed color sensitivity on the red–green direction and reduced discriminability at higher lightness level. These results highlight the asymmetry of CVD perception and underscore the limitations of current simulation-based approaches. The study has several limitations, including a relatively small sample size (14 participants) and a narrow age range (19–26 years). Future research should expand the participant pool to include broader demographics, examine additional hues and luminance levels, and integrate more advanced statistical analyses to validate perceptual models.

Despite these limitations, the findings provide valuable empirical data that can inform the development of more accurate color-difference metrics and color simulation tools for CVD populations. Practically, the results emphasize the need for color-inclusive design in public information systems, educational materials, and digital displays. By moving beyond color comparisons between red colors and green colors, designers can improve accessibility and foster more inclusive visual communication for CVD. Overall, this study provides quantitative evidence to guide inclusive color design and to support the refinement of color-difference metrics tailored for CVDs.

REFERENCES

[1] Machado, G., Oliveira, M., & Fernandes, L. (2009). A physiologically-based model for simulation of color vision deficiency. IEEE Transactions on Visualization and Computer Graphics, 15(6), 1291–1298.

[2] Meyer, G. W., & Greenberg, D. P. (1988). Color-defective vision and computer graphics displays. IEEE Computer Graphics and Applications, 8(5), 28–40.

[3] Viénot, F., Brettel, H., & Mollon, J. D. (1999). Digital video colourmaps for checking the legibility of displays by dichromats. Color Research and Application, 24(4), 243–252.

[4] Graham, C. H., & Hsia, Y. (1958). Color defect and color theory: Studies of normal and color-blind persons. Science, 127(3300), 675–682.

[5] Yaguchi, H., Luo, J., Kato, M., & Mizokami, Y. (2018). Computerized simulation of color appearance for anomalous trichromats using the multispectral image. Journal of the Optical Society of America A, 35(4), 278–286.

[6] Fairchild, M. D. (2013). Color appearance models (2nd ed.). Wiley.

[7] Luo, M. R., & Rigg, B. (1986). Chromaticity-discrimination ellipses for surface colours. Color Research and Application, 11(1), 25–42.

Color Simulation Strategy of Reflective E-Papers

Hung-Shing Chen[a*], Yu-Hsuan Kao[b]

[a*] *Graduate Institute of Electro-Optical Engineering,*
National Taiwan University of Science and Technology, Taipei, 106335, Taiwan

[b] *Graduate Institute of Color and Illumination Technology,*
National Taiwan University of Science and Technology, Taipei, 106335, Taiwan

[*]*Corresponding author: bridge@mail.ntust.edu.tw*

ABSTRACT

This study focuses on two types of e-papers as the research object and designs two experiments. Experiment 1 aims to measure color reproduction characteristics of the reflective e-papers (IRIS ChLCD and E ink Spectra 6) and explore color gamuts that the e-papers can reproduce. Experiment 2 aims to establish an LCD simulate platform for assessing color image qualities of the reflective ChLCD images. The analysis of Experiment 1 showed that ChLCD boasts a 36% larger gamut volume in CIE $L^*a^*b^*$ color space than Spectra 6 under standard illuminant D65. Besides, the analytical result of the contrast ratio indicated Spectra 6 outperforms ChLCD, achieving a contrast ratio of 26:1 compared to 10:1. The analytical result of Experiment 2 demonstrated that the closest mode that matches with 'color similarity' of ChLCD is that with 100% reference gamut / 6500 K / LUT.

Keywords: e-paper, ChLCD, E ink, color similarity

INTRODUCTION

Electronic paper (e-paper) is a kind of paper-like reflective display media with a promising technology. Its color reproduction acts as a new media between paper (object color) and display (luminous color). It is providing a novel solution of visual sensation in the display field. Like regular paper media, the texts or images on the e-paper rely primarily on illumination from the ambient light. E-paper owns most advantages combining with display and paper. It has the ability to change the contents like a display instantly, while maintaining paper-like reading experience.

Spectra 6 is the latest product of E ink's microcup® electronic ink technology [1]. Its imaging way involves the placing red, blue, yellow, and white microcup particles in embedded in the inner layer of electronic paper. By changing different voltages to drive the movement of the ink particles, it can generate six primary colors. These primary colors can be further mixed by the algorithm to create the full-color images. In contrast, cholesteric liquid crystal display (ChLCD, IRIS) is constructed using three layers of cholesteric liquid crystal by reflecting red (R), green (G), and blue (B) lights individually [2]. Different inputted electric fields can control the rotations of the liquid crystal molecules, and allow them to maintain a bistable state even though the electric fields are turned off.

The ICC (International Color Consortium) color profile provides a solution that can establish and promote an open cross-media color management system [3]. Table 1 arranges the comparison of ICC color profiles of e-papers (ChLCD, Spectra 6) and printing media (newspaper / web coated paper of Japan Color Standard). Note that the

input color spaces in color profiles of e-papers are RGB colors, while printing media like newspaper and web coated paper are CMYK colors. The output color spaces of them are CIE $L^*a^*b^*$.

Traditionally, ICC color profiles can be applied to displays and printers to build up a color management system. Displays utilize RGB color signals. Digital printers utilize CMY or CMYK color signals. Because color reproduction principles of the e-papers differ from general displays and printers, color rendering pipelines and color processing systems of the e-papers have been not verified until now. Therefore, a hybrid approach mixing display and printer media is attempted to tailor ICC color profile for the usage of e-papers in this study.

METHODOLOGY

This paper focused on two types of e-papers (IRIS ChLCD and E ink Spectra 6) as the research object and designed two experiments below. Experiment 1 (Exp.1), titled 'color gamut analysis of reflective e-papers', aims to analyze color reproduction characteristics of the reflective e-papers and explore color gamuts that the e-papers can reproduce. That is, Exp.1 executed the computation simulation using ICC color profiles to visualize 2-D and 3-D color gamuts of color e-papers. Gamut volume estimations of the e-papers were also discussed. Experiment 2 (Exp.2), titled 'simulation platform of reflective e-paper', aims to establish an LCD simulate platform of the reflective ChLCD images. The simulated images were displayed on a calibrated LCD and evaluated by the subjects in a visual assessment experiment. That is, Exp.2 involved the establishment of well-calibrated LCD platform (ColorEdge, EIZO) [4], which has the ability to simulate color appearances of the displayed images on ChLCD media.

To find which media parameters of LCD that better match reflective ChLCD, the fundamental color characteristics of ChLCD, including color gamut, tone response curves (TRCs), and color temperature, were measured by a spectrophotometer (i1 Pro 2, X-rite). By means of establishing CIE xy triangular gamut area that most closely resemble the ChLCD, we created a 'reference gamut' of the ChLCD and defined it with the reference gamut of 100%. Moreover, another reference gamut of 120% was also created and was tested in Exp.2 (Figure 1).

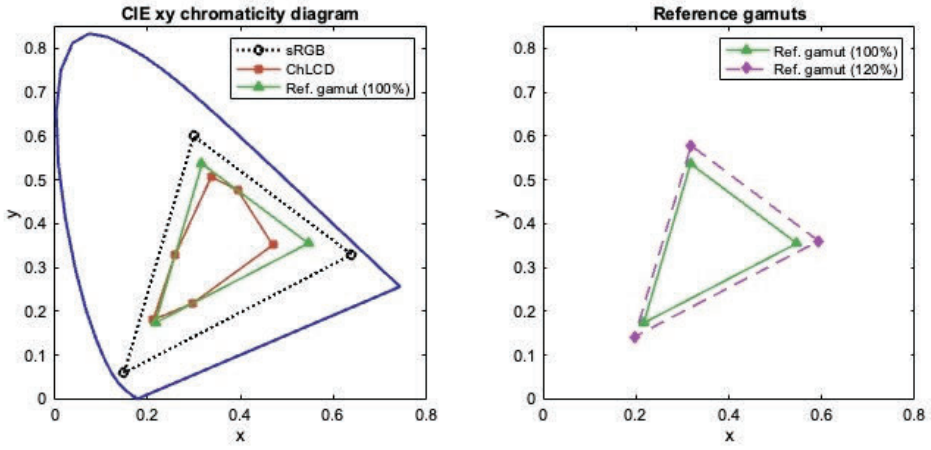

Figure 1: Reference gamuts: (a) ChLCD's gamut and the corresponding reference gamut; (b) Reference gamuts with gamut areas of 100% and 120%

By combining 3 media parameter settings: reference gamut (G), TRC (R), and color temperature (T), totally 12 media modes were created on the LCD platform. Consequently, 2 reference gamuts (G1, G2), 3 color temperatures

(T1, T2, T3), and 2 TRCs (R1, R2) were combined. As a result, 12 media modes (Mode1 ~Mode 12) for simulating the displayed images on the ChLCD were produced on the LCD platform (Table 1 & Table 2). Note that 'LUT' in 'R1' parameter means that the original gray TRC on the ChLCD, which was recorded with the form of 'Lookup Table'.

Table 3 lists 5 color images tested in Exp.2, which featured high-saturated colors ('glass'), large area of white detail ('dog'), natural flowers ('flowers'), large area of dark detail ('train'), and skin-color portraits ('girls'). A total of 12 subjects were invited to attend the psychophysical experiment to assess 'color similarity' of test images rendered by 12 media modes on the LCD. In comparison with two LCD screens, a reference image was displayed on the reflective ChLCD under illuminant D65 in a light cabinet. Then each subject was asked to evaluate the degrees of 'color similarity' of the rendered images displayed on the LCD screens. The subject compared the same image displayed on the pair of LCD screens rendered by pairs of 12 media modes (Mode1 ~Mode 12), and determined which one is more similar in color presentation of the reference image on the reflective ChLCD. After the evaluated scores were collected, the statistical significance test was done for each of three media parameters to analyze the effects of media modes in terms of color similarity.

Table 1: Settings of media parameters

Media parameter	Notation	Setting	Notation	Setting	Notation	Setting
Reference gamut (G)	G1	100 %	G2	120 %		
Color temperature (T)	T1	5000 K	T2	6500 K	T3	7400 K
Tone response curve (R)	R1	γ=2.2	R2	LUT		

Table 2: Media modes

Mode 1	Mode 2	Mode 3	Mode 4
G1/T1/R1	G1/T2/R1	G1/T3/R1	G1/T1/R2
Mode 5	**Mode 6**	**Mode 7**	**Mode 8**
G1/T2/R2	G1/T3/R2	G2/T1/R1	G2/T2/R1
Mode 9	**Mode 10**	**Mode 11**	**Mode 12**
G2/T3/R1	G2/T1/R2	G2/T2/R2	G2/T3/R2

Table 3: Test images

Name	Photo	Name	Photo	Name	Photo
Glass	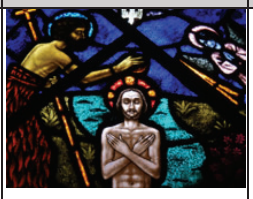	Train	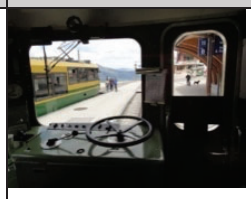	Flower	
Dog	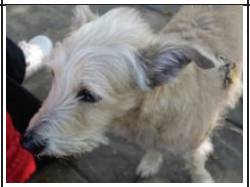	Girls			

RESULTS AND DISCUSSION

In Exp.1, 2-D and 3-D color gamuts of the e-papers (ChLCD and Spectra 6) were drawn by Matlab software, which were set by the color rendering intent of 'Absolute Colorimetric Intent' (i.e., 'AToB3') embedded in the ICC color profiles. Figure 2 shows the CIE u'v' gamuts of two types of e-papers (ChLCD and Spectra 6) and comparative printing medias, including newspaper and web coated paper. It indicated that the CIE u'v' gamuts of two e-papers are larger than newspaper, but smaller than web coated paper. Besides, the analysis of 3-D color gamut showed that ChLCD boasts a 36% larger gamut volume in CIE $L^*a^*b^*$ color space than Spectra 6 under illuminant D65 (Figure 3). Spectra 6 outperforms ChLCD in contrast ratio, achieving a contrast ratio of 26:1 compared to 10:1.

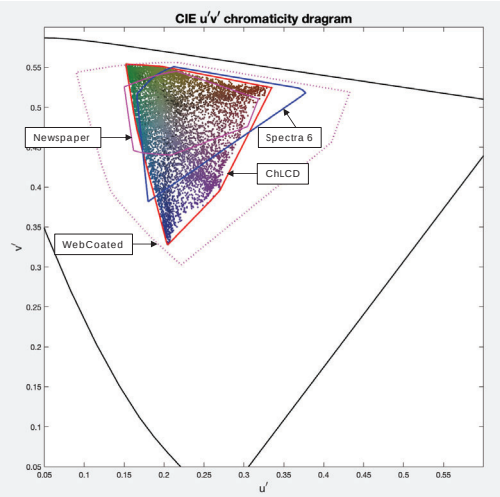

Figure 2: CIE u'v' color gamuts of the e-papers and printing media (ChLCD, Spectra 6, newspaper and web coated paper)

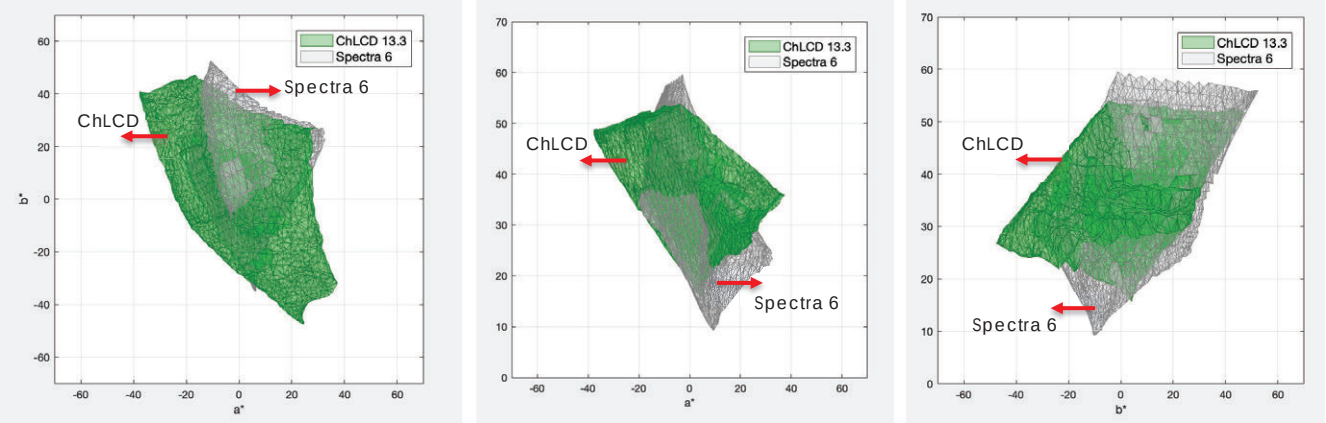

(a) **(b)** **(c)**

Figure 3: 3-D color gamuts of e-papers, including ChLCD and Spectra 6: (a) view of a^*b^* plane; (b) view of a^*L^* plane; and (c) view of b^*L^* plane

The results of Exp.2 showed that larger reference gamut (G) is rated more similarly in color reproduction for most of test images, whereas higher color temperature (T) is evaluated less similarly on color reproduction. In addition, TRC (R) has a less significant impact on color similarity of displayed images. Consequently, all of the three meida parameters have significant effects, where reference gamut (G) has the most significant impact on color similarity (Figure 4).

Moreover, the statistical tests revealed the significant effects of different media parameters. As can be seen in Figure 4(a), G2 parameter significantly outperforms the G1. Statistical analysis revealed that a significant difference between G1 and G2 indicates a significant improvement in reference gamut (G) parameter ('*' means $p=0.000 < 0.01$). Figure 4(b) indicated T1 parameter outperforms both T2 and T3, with significant differences observed between T1 and T3 ('*' means $p=0.023 < 0.01$). It can be seen that T1 performs best, followed by T2, and T3 performs worst. Finally, Figure 4(c) indicated R2 outperforms R1, with significant differences ('* 'means $p=0.025 < 0.01$), indicating that the LUT type of R2 produces a superior result. Ultimately, the evaluation results indicated that variations in all three media parameters have significant effects. Accordingly, the analytical result demonstrated that most closely matches 'color similarity' of ChLCD is G1/T2/R2 (Mode 5 with 100% reference gamut / 6500 K / LUT).

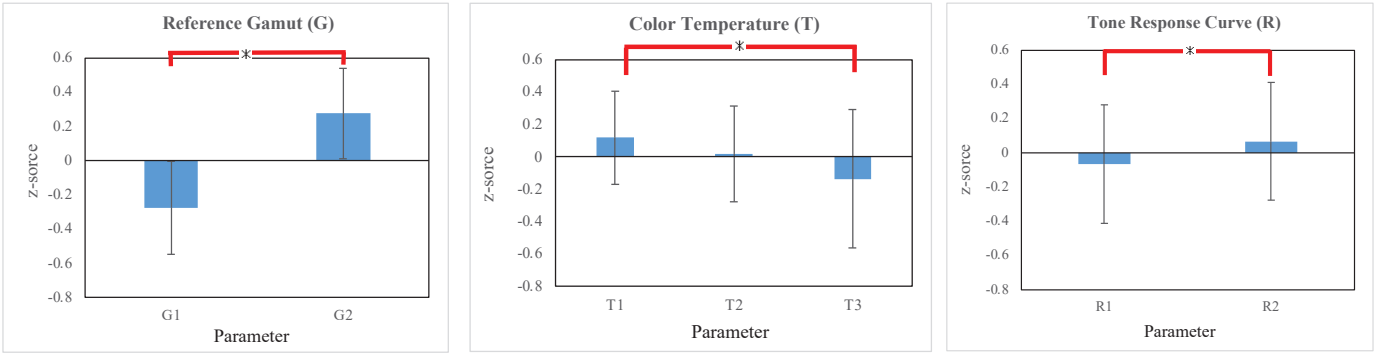

(a) **(b)** **(c)**

Figure 4: Statistical analysis: (a) reference gamut; (b) color temperature; and (c) TRC

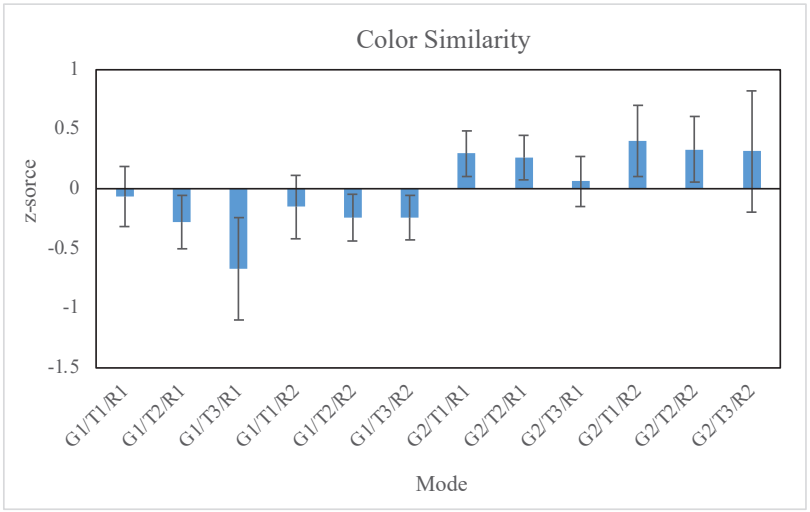

Figure 5: Color similarity evaluation result of the media modes

CONCLUSION

A method consisting of gamut visualization and color simulation of the reflective e-paper media using ICC color profile were proposed. Two kinds of experiments were designed. Experiment 1 aims to analyze the color reproduction characteristics of reflective e-papers and explore 2-D and 3-D color gamuts that e-papers can reproduce. Experiment 2 aims to establish an LCD simulate platform for assessing the color qualities of the reflective ChLCD images. The analysis of Experiment 1 showed that ChLCD boasts a 36% larger gamut volume in CIE $L^*a^*b^*$ color space than Spectra 6 under illuminant D65. Besides, Spectra 6 outperforms the ChLCD in contrast ratio, achieving a contrast ratio of 26:1 compared to 10:1. The analytical result of Experiment 2 demonstrated that most closely matches 'color similarity' of ChLCD is the mode with 100% reference gamut / 6500 K / LUT. We believe that color e-papers will achieve breakthroughs in color quality, with larger sizes, higher color saturation, and higher contrast in the near future.

ACKNOWLEDGEMENTS

We would like to thank IRIS Optoelectronics for providing the valuable industry-university collaboration opportunity, which enabled our team to successfully complete this fruitful and meaningful research.

REFERENCES

[1]. Spectra™ 6, E ink, https://tw.eink.com/brand/detail/Spectra6

[2]. IRIS Optronics, https://iris-opt.com/tw/blog/what-is-chlcd/

[3]. International Color Consortium, https://www.color.org/index.xalter

[4]. EIZO, https://www.eizoglobal.com/products/coloredge/index.html

Effects of Ultra-Fast Light-Adaptive Lenses on Perception of Natural Scenes

Sophie Jost[a*], Elisa Dessenne[a], Pascale Avouac[a], Aiman Raza[a], Anne-Catherine Scherlen[b], Coralie Barrau[b]

[a]ENTPE, Ecole Centrale de Lyon, CNRS, LTDS, UMR 5513, 69518 Vaulx-en-Velin, France
[b]EssilorLuxottica, Paris, France
*Corresponding author: Sophie Jost, sophie.jost@entpe.fr

ABSTRACT

Ultra-fast light-adaptive lenses represent a breakthrough in vision care, offering rapid response to dynamic light conditions to improve comfort, reduce glare, and support optimal visual performance. Beyond these functional benefits, such lenses also alter the way users perceive color in natural scenes—a dimension that remains underexplored. The primary objective of this study was to investigate how the eight full tints of these new lenses influenced perceptual judgments of warmness, colorfulness, and contrast, and to identify objective indices capable of predicting these perceptual changes. Using a robust simulation pipeline based on hyperspectral imaging and the iCAM06 appearance model, real-world outdoor scenes (two urban, two natural) were rendered through each lens tint. The images were displayed on a color-calibrated monitor (Eizo ColorEdge CG277) set with AdobeRGB parameters to ensure accurate color reproduction. A psychophysical experiment was conducted with 40 participants under fully controlled viewing conditions. Each participant performed paired comparisons of nine images of the same scene (eight filtered by the lenses and one original scene) for the four scenes and for three visual descriptors: warmness, colorfulness and color contrast. In total, each participant completed 432 comparisons (36 x 4 x 3). The order of image pairs was randomized for each participant, while the left/right positioning, scene order, and descriptor sequence were counterbalanced across participants to minimize order effects. Eye-tracking data were continuously recorded, and post-task interviews provided qualitative insights. Thurstone modeling revealed that perceived warmness was reliably predicted by two objective metrics: correlated color temperature and the proportion of warm-toned pixels. These findings were confirmed by multivariate regression, independent of age or gender, and supported by consistent eye-tracking patterns. Amber and Brown were rated warmest, while Sapphire was consistently seen as the coldest. For colorfulness, two distinct perceptual strategies emerged, forming two clusters (C1 and C2), validated by both eye-tracking behavior and colorimetric modeling. C1 participants favored local color separations, best predicted by ΔE2000, and rated Sapphire as most colorful. C2 participants judged colorfulness globally, linked to gamut area and warm pixel proportion, consistently ranking Ruby highest. These two strategies were mutually exclusive across individuals. They showed a significant association with gender. Eye tracking strategies further supported the perceptual clusters, showing local vs. global scan paths. In summary, this study highlights that while warmness perception can be simply modeled with a high degree of predictability, colorfulness judgments are more complex and user-dependent. The proposed methodology combining hyperspectral simulation, psychophysics, eye tracking, and advanced color metrics offers a robust framework for future personalized tint designs. It reinforces the need to move beyond universal color filtering strategies toward perceptually informed, individualized lens recommendations.

Keywords: color perception, hyperspectral images, light-adaptive lenses, perceptual strategies, color metrics, predictive model

INTRODUCTION

Ultra-fast light-adaptive lenses represent a disruptive innovation in vision care, designed to respond rapidly to changing illumination conditions. These lenses dynamically tint in bright light to reduce glare and brightness and fade back quickly in moderate light. Light is a fundamental variable influencing vision. Standard measures such as visual acuity do not fully predict real-world visual performance under fluctuating lighting [1]. The constant variation of light in real-world conditions requires continuous photoreceptor adaptation [2]. Both sustained and transient glare are known to degrade visual performance across central and peripheral fields [3], and bright light can cause temporary visual disability [4]. These challenges are further amplified by ametropia, aging eyes, or ocular conditions such as dry eye or age-related macular degeneration [1] [5-7]. Recent clinical evidence demonstrates that Transitions® Gen S™ lenses significantly improve vision and comfort under real-world, variable lighting conditions, outperforming static clear lenses and traditional photochromic tinted lenses. Specifically, compared to static clear lenses, they stabilize light exposure within an optimal range for good vision in 90% of outdoor scenes —compared to just 30% with clear [8]. They also accelerate visual recovery after light transitions, providing up to 2.5 times faster contrast sensitivity recovery and 30 seconds faster return to full vision after re-entering indoor environments [9], along with 2 times less squinting in bright light [10]. Transitions® Gen S™ lenses come in eight engineered tints, each maintaining chromatic consistency throughout their activation and deactivation cycles, and each compliant with all traffic color recognition standards.

Beyond measurable gains in visual performance, a critical yet underexplored dimension is how spectral filtering through tinted lenses modifies color perception in natural environments. Color sensitivity varies significantly across individuals and plays a crucial role in subjective visual experience [11, 12]. The eight engineered tints of Transitions® Gen S™ lenses provide a controlled platform to systematically study these perceptual effects.

We combined hyperspectral scene simulations, psychophysical paired comparisons, advanced colorimetric modeling, and eye tracking to assess how each full tint of Transitions® Gen S™ lenses impacts the perception of warmness, colorfulness, and contrast in natural outdoor scenes—and to evaluate how accurately these perceptions can be predicted using objective color metrics and visual attention patterns.

METHODOLOGY

Population: Forty healthy volunteers (18 male, 22 female; mean age 35.5 ± 15 years) participated. All had normal color vision, confirmed by the Ishihara Color Blind test. None reported any history of ocular disease or neurological conditions that could affect visual performance. Written informed consent was obtained prior to participation, and the study adhered to the Declaration of Helsinki.

Stimuli, Lenses and Image Processing: Four outdoor scenes were acquired using hyperspectral imaging. They provide a representative range of outdoor visual environments, two landscapes and two urban environments (Figure 1A-D). A validated method enabled accurate simulation of color vision as perceived through tinted lenses, using hyperspectral imaging in combination with the iCAM06 image color appearance model, allowing for the simulation of lens transmittance effects on an RGB display [13]. The images were displayed on a color-calibrated monitor (Eizo ColorEdge CG277) set with AdobeRGB parameters to ensure accurate color reproduction. Nine versions of each scene were generated: eight filtered through each of the 8 full tints of Transitions® Gen STM lenses (called Amber, Brown, Emerald, Green, Sapphire, Grey, Amethyst, Ruby) (Figure 1E) and one unfiltered reference.

Experimental procedure: The experiment was conducted in a dedicated laboratory space with controlled lighting conditions. To eliminate uncontrolled light cues, participants were seated in a dark room with no ambient illumination other than the stimulus display. A side-by-side paired-comparison psychophysical design was used (Figure 1F-G). Each participant viewed image pairs while eye movements were continuously

recorded using a Tobii Pro Fusion eye tracker (Tobii, USA). Each participant completed a total of 432 comparisons (36 pairs × 4 scenes × 3 perceptual items). To minimize order and positioning biases, the order of image pairs was randomized for each participant, while left–right positioning, scene order, and descriptor sequence were fully counterbalanced across the sample. For each trial, participants viewed two side-by-side images of the same scene and judged them along one of three perceptual descriptors: warmness, colorfulness and color contrast. Among those 3 perceptual attributes, two are described in the paper: warmness and colorfulness – the third is still being analyzed.

Figure 1: Selected outdoor scenes (A: Miribel, B: Ocres, C: Poste; D: Urban), Lenses Transitions® Gen S™ (E), and side-by-side paired comparisons (F, G)

Data acquisition and analysis: Eye movements were continuously recorded using a Tobii ProFusion eye-tracking system at 120 Hz to monitor gaze behavior, fixation and saccades patterns during the comparisons. Perceptual judgments from the paired-comparison task were analyzed using Thurstone's Law of Comparative Judgments to generate psychometric scales for each descriptor across lens conditions. These perceptual indices were then compared to the physical properties of the lenses to explore potential predictive models of user judgments.

RESULTS AND DISCUSSION

Perceived warmness showed strong and consistent associations with two key objective metrics: correlated color temperature (CCT) and the proportion of warm pixels in the image. Warmness ratings were negatively correlated with CCT ($r = –0.89$) and positively correlated with warm pixel proportion ($r = 0.82$), indicating that lower CCT and higher proportions of red/orange tones reliably predict higher warmness perception. These findings were confirmed through multivariate linear regression ($R^2 = 0.987$, $p < .001$), with CCT ($\beta = –0.25$, $p < .001$) and warm pixels ($\beta = 0.82$, $p < .001$) as the only significant predictors. PCA analysis further identified these variables as key contributors to the principal component associated with warmness. Importantly, this relationship was independent of age, gender, or scene, and further supported by homogeneous eye-tracking patterns across participants during warmness evaluations. Together, these results indicate that warmness is a stable and shared perceptual mechanism. In terms of lens tint rankings, Amber and Brown were consistently perceived as the warmest, Sapphire as the coldest, while Amethyst was unexpectedly judged more neutral than both Grey and the unfiltered baseline.

Colorfulness judgments revealed two distinct perceptual strategies, grouped as Cluster 1 (C1, N=23) and Cluster 2 (C2, N=15) (Figure 3), supported by eye-tracking data. C1 participants consistently rated Sapphire as the most colorful filter across all scenes ($p < .001$ vs. Ruby, Amber, Brown, and Green; $p < .001$ vs. No Filter except in Urban scene) (Figure 4). Amethyst was perceived as more neutral than Grey or the unfiltered baseline in urban

environments, but more colorful in landscape scenes (Figure 4). These participants' ratings were strongly associated with local color differences, supported by eye-tracking data showing targeted fixations, and correlated strongly with ΔE2000 (r = 0.78).

In contrast, C2 participants rated Ruby highest in colorfulness across all scenes, far beyond the unfiltered reference ($p < .001$ vs. Grey, Green, Emerald, Sapphire, and No Filter; $p < .001$ vs. Amber and Brown for Urban and Ocres) (Figure 4). Although Amethyst had lower mean ratings and higher variability, it was the only filter not statistically different from Ruby across all scenes (Figure 4). C2 participants favored a global impression of saturation and vividness, showing more saccades and longer scanning behavior — particularly for Ruby, Amber, and Brown. Their judgments aligned better with gamut area metrics (r = 0.66 with Gamut 2D PT) and the proportion of warm pixels (r = 0.72).

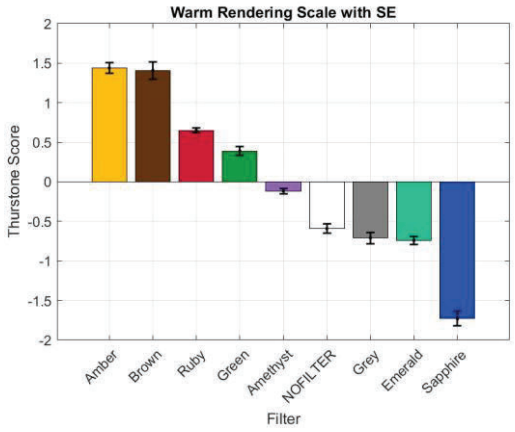

Figure 2: Mean perceptual warmness ratings per filter, expressed as Thurstone scores (± SEM), averaged for all scenes

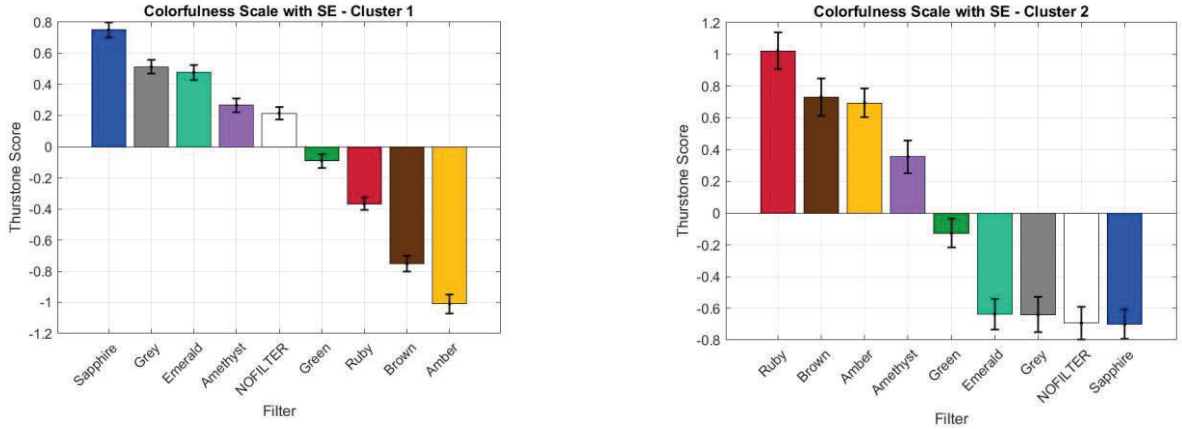

Figure 3: Mean perceptual colorfulness ratings per filter, expressed as Thurstone scores (± SEM), separated by perceptual cluster (Cluster 1 left and Cluster 2 right), and averaged for all scenes

Green was consistently perceived as the most neutral tint in terms of colorfulness across both clusters and for all scenes (Figure 4). The type (urban vs landscape) and the color content of scenes modulated perceptual scores but had limited influence on the ranking of filters (except for Amethyst), suggesting that individual perceptual strategies dominate over contextual scene differences. This reinforces the robustness of the C1/C2 clustering and the role of individual color processing styles.

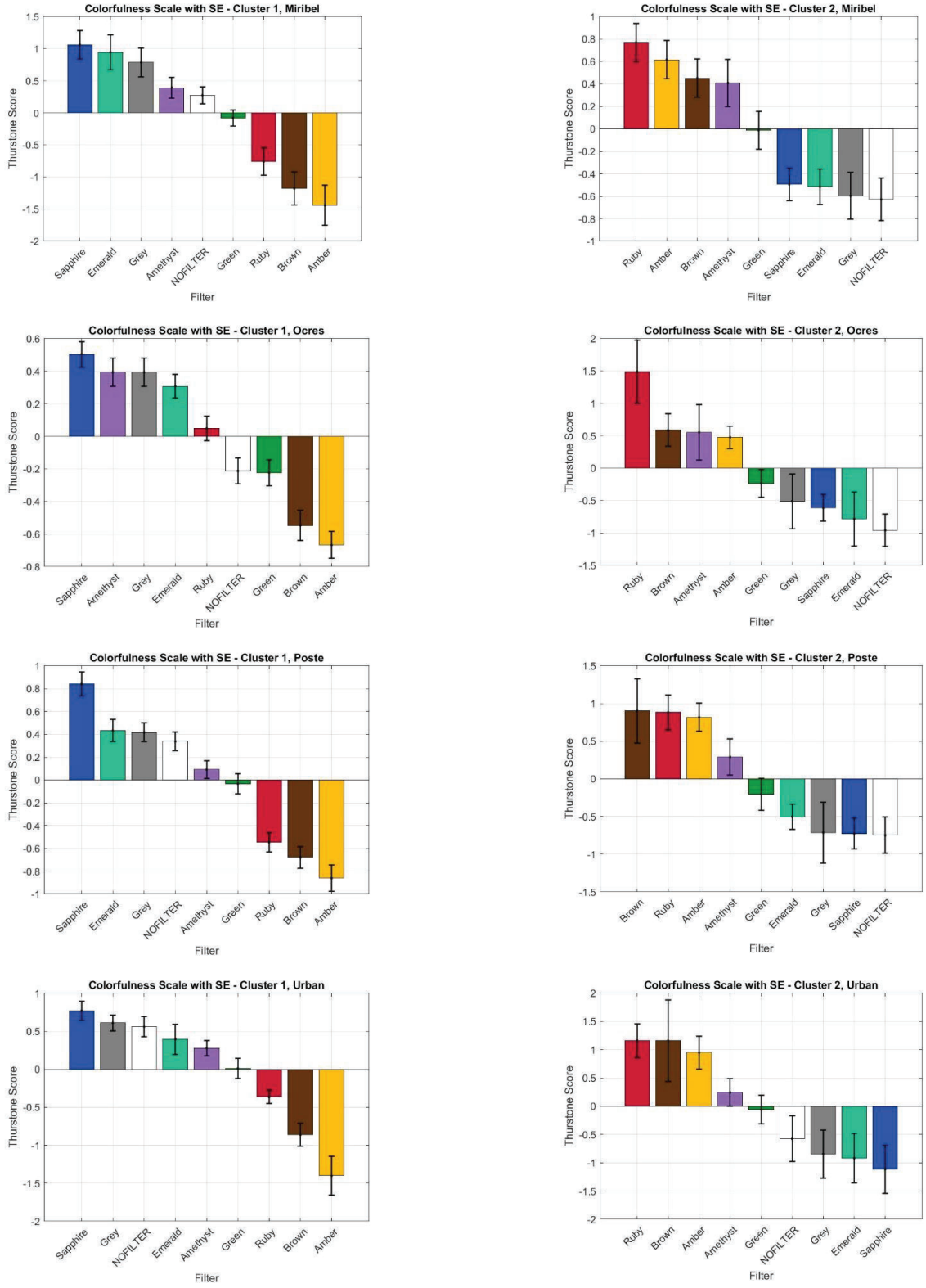

Figure 4: Mean perceptual colorfulness ratings per filter, expressed as Thurstone scores (± SEM), separated by perceptual cluster (Cluster 1 left and 2 right) and scene type (Miribel, Ocres, Poste, Urban).

A significant association between gender and perceptual cluster for colorfulness was observed ($p < .05$): men were overrepresented in C1, while women were overrepresented in C2, suggesting a possible gender-related influence on perceptual strategies, aligned with the findings described by Rodriguez-Carmona and colleagues [14].

Finally, colorfulness strategies were inversely correlated ($r = –0.91$ between C1 and C2 scores), confirming they reflect mutually exclusive perceptual modes (Figure 5). Notably, warmness perception correlated positively with C2 ($r = 0.68$) and negatively with C1 ($r = –0.92$) (Figure 5), suggesting a shared basis between global vividness and warmness perception.

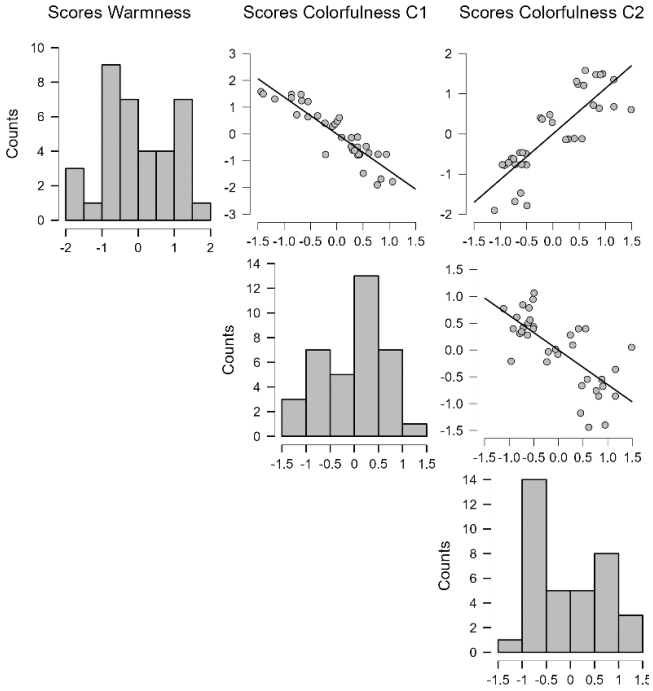

Figure 5: Distributions and Interrelationships of Perceptual Judgments: Warmness, Colorfulness C1 & C2

These findings reinforce that color perception is shaped by individual perceptual and cognitive strategies. The emergence of distinct perceptual clusters suggests that people process visual information using different internal frameworks—some prioritizing local color differences, others global vividness. Furthermore, eye-tracking data proved valuable as a non-verbal marker of perceptual strategy, highlighting its potential as a diagnostic tool in personalized lens design or vision science more broadly.

CONCLUSION

While maintaining excellent color discrimination for everyday use, ultra-fast light-adaptive lenses measurably influence color perception in natural outdoor scenes and offer options suited to diverse perceptual profiles. These effects are partly predictable using objective colorimetric metrics. Perceived warmness, in particular, showed strong and consistent correlations with CCT and the proportion of warm pixels—supporting the development of reliable, model-based predictions. In contrast, colorfulness perception followed two distinct and mutually exclusive strategies: one based on local color differences, the other on global saturation. These strategies were reflected in distinct eye-tracking patterns and showed associations with demographic variables such as gender**.** The methodological framework developed—integrating hyperspectral scene simulations, psychophysical evaluation, colorimetric modeling, and gaze behavior—provides a robust reinforce that color perception is shaped by individual perceptual and cognitive strategies.

REFERENCES

[1]. Brabyn J, Schneck M, Haegerstrom-Portnoy G, Lott L. (2001). The Smith-Kettlewell Institute (SKI) longitudinal study of vision function and its impact among the elderly: an overview. Optom Vis Sci. 78(5):264-9.

[2]. Wang, Shuxiao and Jianping Zhao (2022). New perspectives on light adaptation of visual system research with the emerging knowledge on non-image forming effect. Frontiers in Built Environment.

[3]. Wu D, Liu N, Xu P, Sun K, Xiao W, Li C. (2020). Reduced Contrast Sensitivity Function in Central and Peripheral Vision by Disability Glare. Perception. 49(12):1348-1361.

[4]. Hammond BR, Fletcher LM, Roos F, Wittwer J, Schalch W. (2014). A double-blind, placebo-controlled study on the effects of lutein and zeaxanthin on photostress recovery, glare disability, and chromatic contrast. Invest Ophthalmol Vis Sci. 55(12):8583-9.

[5]. Ávila, F.J.; Casado, P.; Ares, J. (2023). Photostress Recovery Time after Flash-Lighting Is Increased in Myopic Eyes. Photonics. 10, 86.

[6]. Puell, M.C., Benítez-del-Castillo, J.M., Martínez-de-la-Casa, J., Sánchez-Ramos, C., Vico, E., Pérez-Carrasco, M.J., Pedraza, C. and Del-Hierro, A. (2006), Contrast sensitivity and disability glare in patients with dry eye. Acta Ophthalmologica Scandinavica, 84: 527-531.

[7]. Chikezie Grand Ihesiulor., et al. (2022). Photo Stress Recovery Time Variations in Common Posterior Segment Ocular Diseases. Acta Scientific Ophthalmology. 26-33.

[8]. Barrau, C., Prince C., Ehrismann C., Kobia-Acquah E., Coughlan D., Hazle J., Baldy C. (2025) Ultra-Fast Light-Adaptive Lens stabilizes light exposure across a comprehensive real-world light database. Presented at European Academy of Optometry and Optics 2025.

[9]. Duarte-Toledo, R., Mompeán, J., Paniagua-Díaz, A.M., et al. (2024). A new photochromic lens improves contrast sensitivity during fade-back. Invest. Ophthalmol. Vis. Sci.

[10]. Harth, J.B., Hammond, B.R., Renzi-Hammond, L.M. (2025). New photochromic spectacle lenses improve glare discomfort and photostress recovery. Results in Optics.

[11]. Azwar, S., Amin, M., Muzahidul Islam, A., & Mikami, O. (2019). ELECTROENCEPHALOGRAM (EEG) STUDIES ON HUMAN PERCEPTION IN COLOURS. Journal of Advanced Manufacturing Technology. 13(2(1).

[12]. Elliot AJ (2015) Color and psychological functioning: a review of theoretical and empirical work. Front. Psychol. 6:368.

[13]. Raza A, Dubail M., Dumortier D. and Jost, S. (2025). Coloured Sunglass Simulation using Hyperspectral Imaging and ICAM06. Presented at CIE 2025, Midterm Meeting, Vienna, Austria.

[14]. Rodríguez-Carmona M, Sharpe LT, Harlow JA, Barbur JL. (2008). Sex-related differences in chromatic sensitivity. Vis Neurosci. 25(3):433-40.

The Surface Optical Characteristics of Interior Components in The Japanese Traditional Tea Ceremony Room TENGO-AN

Masayuki Osumi[a*]

[a]Office Color Science Co., LTD., Kumamoto, Japan
[*]Masayuki Osumi, maayuki-osumi@nifty.com

ABSTRACT

The spirit of WABI-SABI is important in Japanese tea ceremony. ENSHU KOBORI had built a tea house TENGO-AN in Rokujizo in Fushimi, Kyoto during the EDO period, and it was relocated to the Tokyo National Museum in Ueno, Tokyo. I had the opportunity to conduct optical measurements of color and texture inside this tea room. Objectively optical measurement of cultural heritage is very meaningful in understanding the spirit of WABI-SABI or the texture of SADO objects. For the walls, ceilings, floors, columns, etc., which are the main components that have a visual impact in the tea room, respectively, the parameters related to spectral reflectance, normal reflectance intensity, and surface unevenness were measured by a surface analyzer, and gonio-photometric property was measured by a spectrophotometer that can measure multiple angles. As a result of the measurements, the spectral reflectance of most of the components showed low values on the short-wavelength side and high values on the long-wavelength side. And the TATAMI mat and the AJIRO ceiling exhibited significant gonioapparent property. The color temperature inside had dropped by about 2000 K° compared to the outdoors. In addition, regarding the angle dependence of the AJIRO ceiling materials and TATAMI floors, we clarified the microstructure of similar materials used in tea rooms by digital microscopy, and also confirmed the angle dependence of textures by the gonio-photometric spectral imaging equipment. The surface of both of them has a streak-like structure in a certain direction, and it was found that there was a significant difference in flop properties in the azimuth direction relative to the surface of the member. In particular, the TATAMI floor has changed significantly over time, so we compared it with the one that has been used for about 10 years with the one that has not been used. Inside the TENGO-AN, many members with gonioapparent properties are used. Also, high saturation and brightness are not used for color. It is presumed that along with the spirit of WABI-SABI, consideration was given to directing a once-in-a-lifetime meeting.

Keywords: tea ceremony room, color and texture, gonioapparent property, 2-dimensional Reflective properties, aging

INTRODUCTION

One of the aesthetic consciousnesses of Japan is a concept called WABI and SABI. WABI is to find spiritual peace and beauty in simple and imperfect things. In addition, loneliness means the change and deterioration of time, and the taste felt in old things. The spirit of WABI-SABI is regarded as a pivotal concept in the tea ceremony and is reflected in the tea room and tea utensils. In order to get a glimpse of the ingenuity of our predecessors who built the tea ceremony, it is of great significance to measure cultural heritage with objective physical data, that is, optical physical data, such as reflection characteristics related to color and texture related to visual information, and to evaluate and consider based on them. This study measured the interior of the tea room TENGO-AN, which was relocated to the Tokyo National Museum, using a device that can perform complex measurements of color and

texture. Furthermore, focusing on the constituent components such as the AJIRO ceiling and the TATAMI mat used in the tea room, we measured the fine surface structure to analyze the mechanism of texture expression. In addition, based on the measurement results, tried to interpret it in a way that is consistent with the spirit of WABI-SABI in the tea ceremony.

METHODOLOGY

About TENGO-AN

TENGO-AN is a tea ceremony room built by ENSHU KOBORI in Rokujizo Fushimi Kyoto in EDO period for the occasion of the gift of tea container "ODAIMYO" from imperial prince HACHIJO-NO-MIYA-TOMOHITO-SHINNO. ENSHU KOBORI studied under SEN-NO-RIKYU and ORIBE FURUTA and served as a tea ceremony instructor for the TOKUGAWA shogun family, and was active as a leading tea ceremony expert at the time. The tea container is for a holding green tea powder MACCHA and is one of the most important tools at a tea ceremony. The tea container "ODAIMYO" is considered to be the original of SETO-CHAIRE-MENTORIDE. It is said that ENSHU removed the spout and remade it into its current form, which was originally in the shape of a water droplet with a spout. It is brown and glossy, and has a shape with triangular ears with holes in both shoulders. The floor plan of the tea room is only two tatami mats size and is very small. The interior of the tea ceremony room is roughly configured a floor surface made of TATAMI mats, a wall surface made of clay, a ceiling surface made of wood, and wooden doors and pillars. In particular, the ceiling is partly made of cedar boards called AJIRO. TENGO-AN was relocated to the Tokyo National Museum in Ueno, Tokyo.

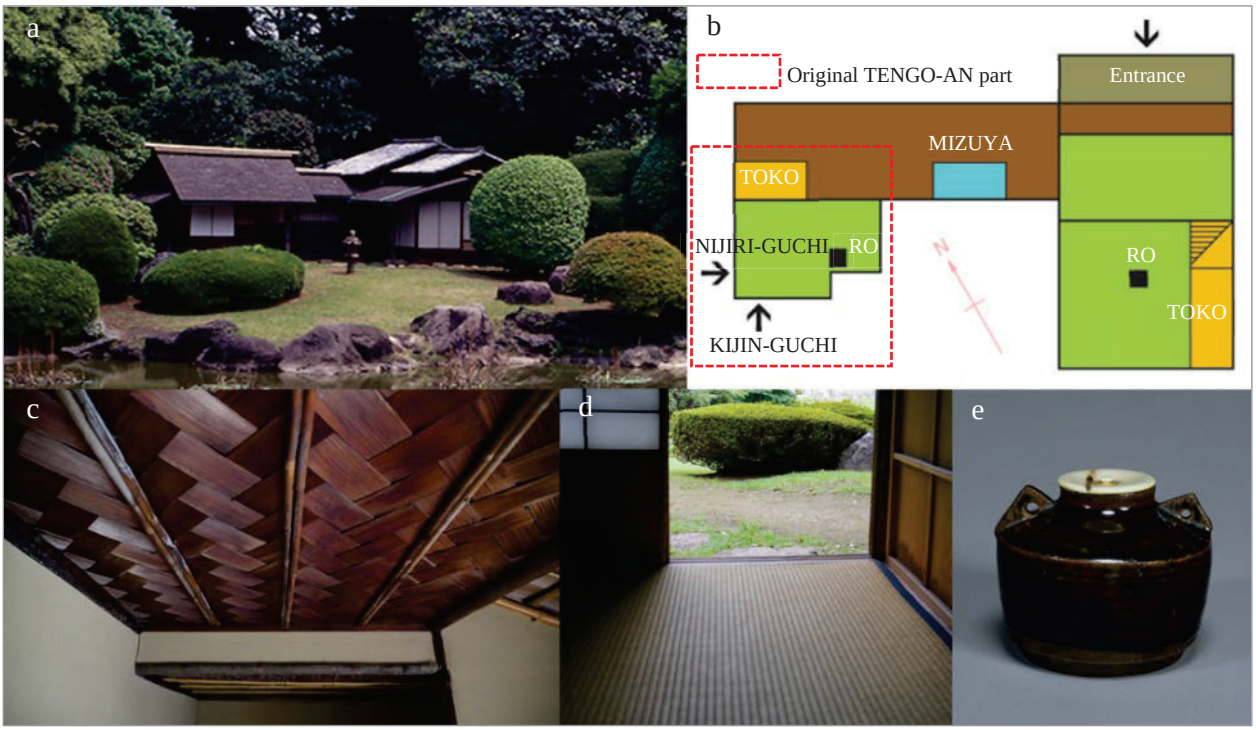

Figure 1: Tea room TENGO-AN

a: TENGO-AN in Tokyo national museum. b: Floor plan (MIZUYA: Kitchen for prepare the tea ceremony, RO: Fire place to boil water, TOKO: Alcove, NIJIRI-GUCHI: Small entrance to a tea ceremony room, KIJIN-GUCHI: Entrance for imperial people). c: AJIRO ceiling and cray wall. d: Tatami mat and NIJIRI-GUCHI entrance. e: The green tea leaf powder ceramic container ODAIMYO.

Measurement Method for inside of the TENGO-AN

The ceiling, walls, pillars, and floor of the tea room were measured. The ceiling is characterized by a AJIRO, which was created by weaving a few centimeters wide of thinly torn cedar boards in a regular manner. The wall is a clay wall, and the surface is not flat, but has fine unevenness, and the lower part is covered with dark green washi paper. The pillars are generally dark-brown wood with a noticeable grain pattern. The same applies to the wood of the TOKO alcoves and wooden doors. Normally, the paper on the tatami mat and shoji is replaced every certain period of time, so these are not from the time of construction. In order to numerically capture the colour and texture of each part, the spectral reflectance and two-dimensional surface reflection characteristics were measured with a surface analyzer (Spectra 2 Profiler, BYK Gardner, shown in Figure 2, a.). And the gonioapparent spectroscopic characteristics were measured with a portable multi-angle spectrophotometer (BYK mac I, BYK Gardner, shown in Figure 2, b.). In addition, the spectral emission intensity of the room and exterior was measured with a spectroradiometer (MK350S Premium, UPRtek, shown in Figure 2, c.).

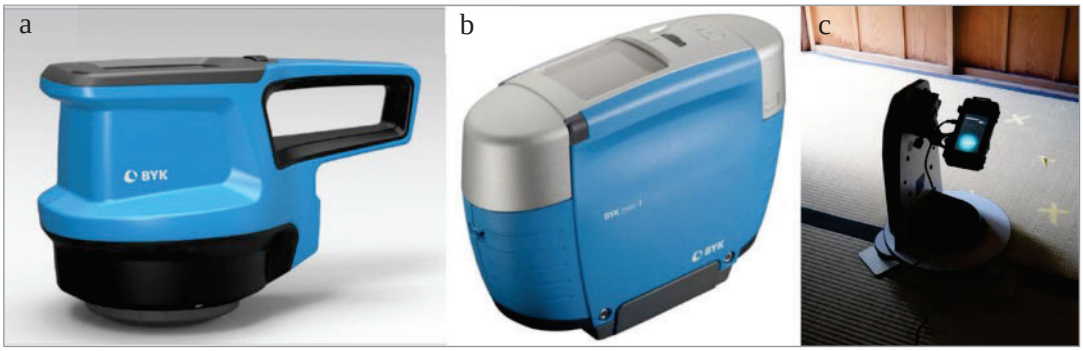

Figure 2: Measurement Devices for inside of the TENGO-AN

Measurement of the surface microstructure of the parts used in the TENGO-AN

The characteristics of gonio-apparent property and reflectivity were found for the AJIRO ceiling and TATAMI floor, but in order to investigate in more detail, the microstructure of similar commercially available members was clarified by digital microscopy (VHX-7000, Keyence, shown in Figure 3, d), laser confocal microscope (VX-1000 Keyence shown in Figure 3, c.), and 3D scanner (VR-5000 Keyence). The gonio-photometric spectral imaging was also used to measure the angular dependence of textures and shown in Figure 3, a and b. In addition, since the change in TATAMI mats over time is remarkable, we compared measurements between unused TATAMI mats and those that have been used for 10 years.

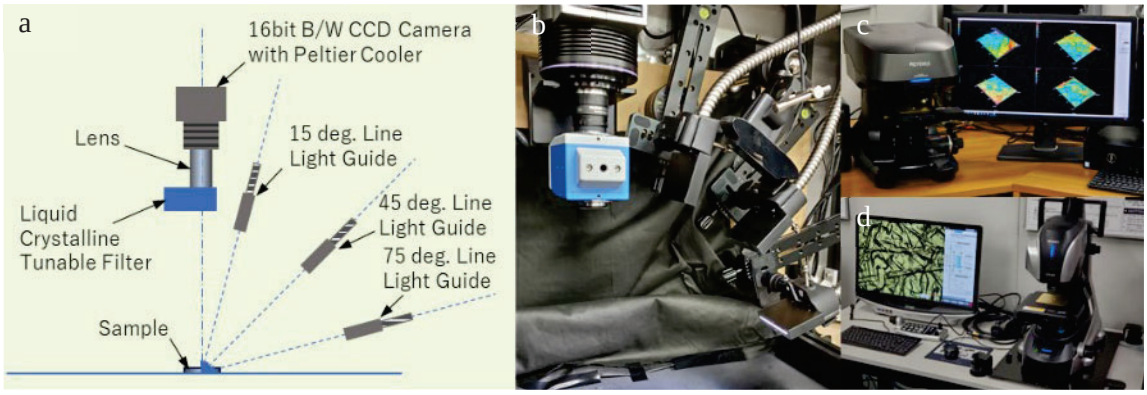

Figure 3: Measurement devices for the surface microstructure

RESULTS AND DISCUSSION

Among the floor, wall, and ceiling surfaces, the average brightness is high on the floor and wall, and the ceiling is relatively low. The ceiling surface is coated with persimmon tannin and colour is dark brown. On the other hand, the reflection intensity was relatively high for TATAMI mat on the floor, followed by the ceiling and low on the walls. The surface reflectivity of the constituent members was slightly lower on the short-wavelength side and higher on the long-wavelength side. In addition, the handheld spectrometer measurement showed that the colour temperature of the internal light is about 4000 K° and decreased about 2000 K° from external light.

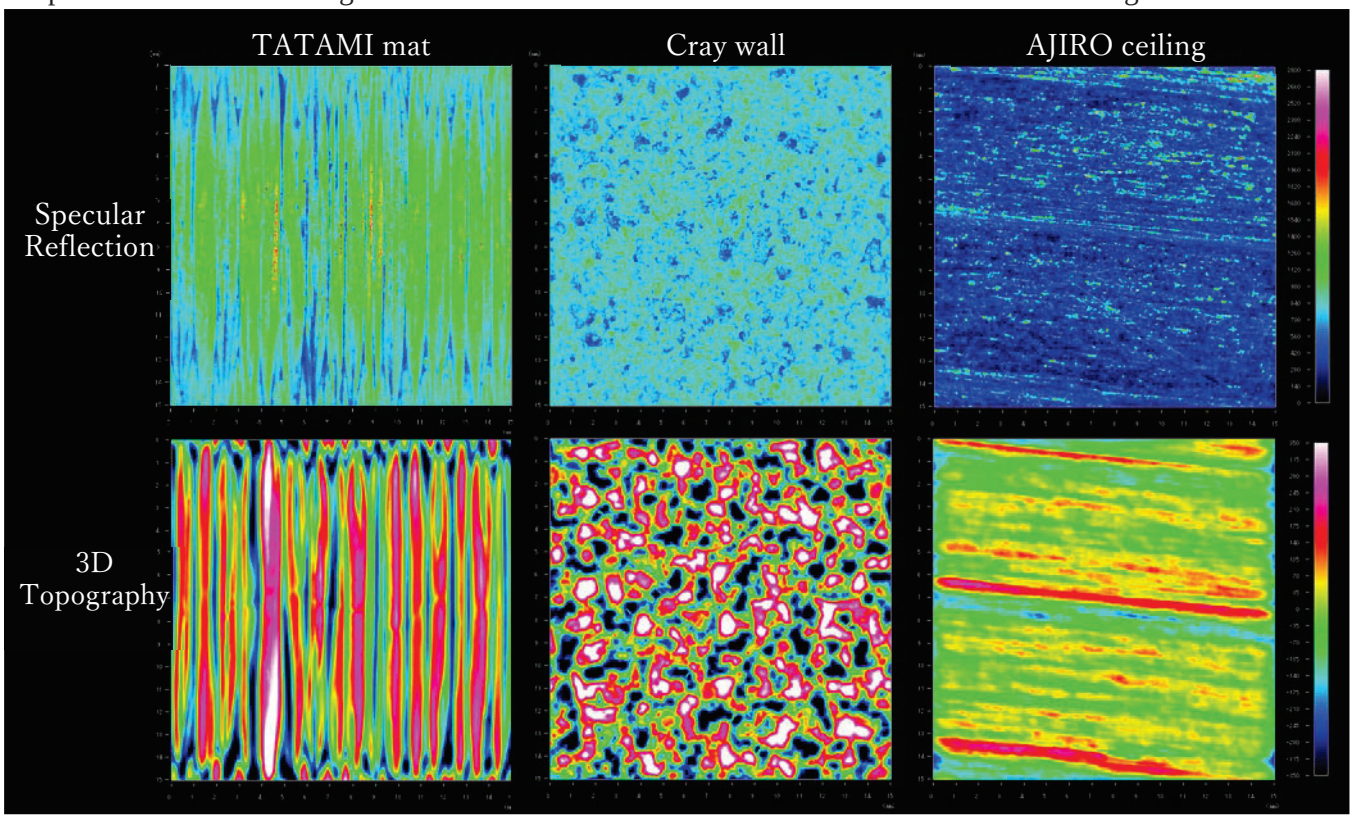

Figure 4: Surface analyzer measurement result

	TATAMI mat	Cray wall	AJIRO ceiling
L*	62.51	56.76	28.12
a*	2.77	6.88	11.21
b*	27.51	21.90	12.46
C*	27.65	22.96	16.76
Gloss	1.63	0.50	1.99
Reflectivity	973.90	798.00	417.50
Cs(Deviation)	0.71	0.50	0.53

Table 1: Surface analyzer measurement result

Furthermore, a comparison of gonioapparent characteristics using a multi-angle spectrophotometer showed that the AJIRO ceiling and the TATAMI mat were relatively high, and the wall surface was remarkably low. The flop properties of the TATAMI mat change from positive flop values to negative flop values depending on the direction. In addition, the flop value of the earthen wall is small, but it shows a tendency to negative flop.

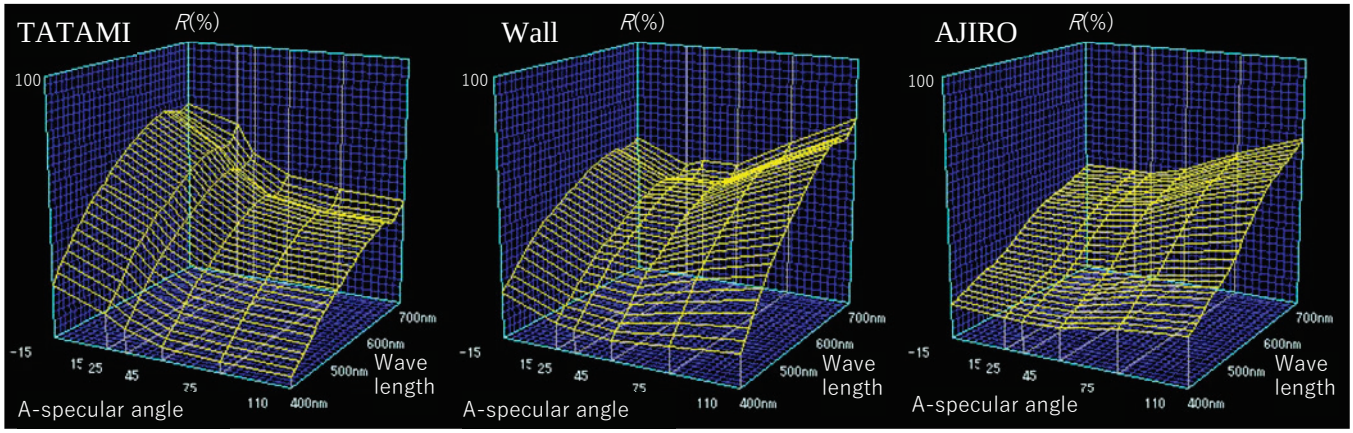

Figure 5: Multi-angle spectrophotometer measurement result

It was found that the cedar boards used for the AJIRO ceiling are thinly peeled boards along the wooden conduits, and have a fine and linear streak-like undulating structure, which expresses gonioapparent property. As a result of microscopic observation of the TATAMI mats, it is presumed that the surface of the rush (Juncus decipiens), which is the constituent material of the TATAMI mats, has streak-like undulations, which together with the weaving structure contributes to the expression of gonioapparent property. Measurements by multi-angle spectroscopic imaging also confirmed the angle-dependent characteristics related to texture of both the AJIRO ceiling material and the TATAMI mats. As for the TATAMI mats, it is interesting to note that the glossy component was observed more strongly with the change in colour than the new one that had been used for about 10 years. Also, the one that was used for 10 years had a higher gloss value.

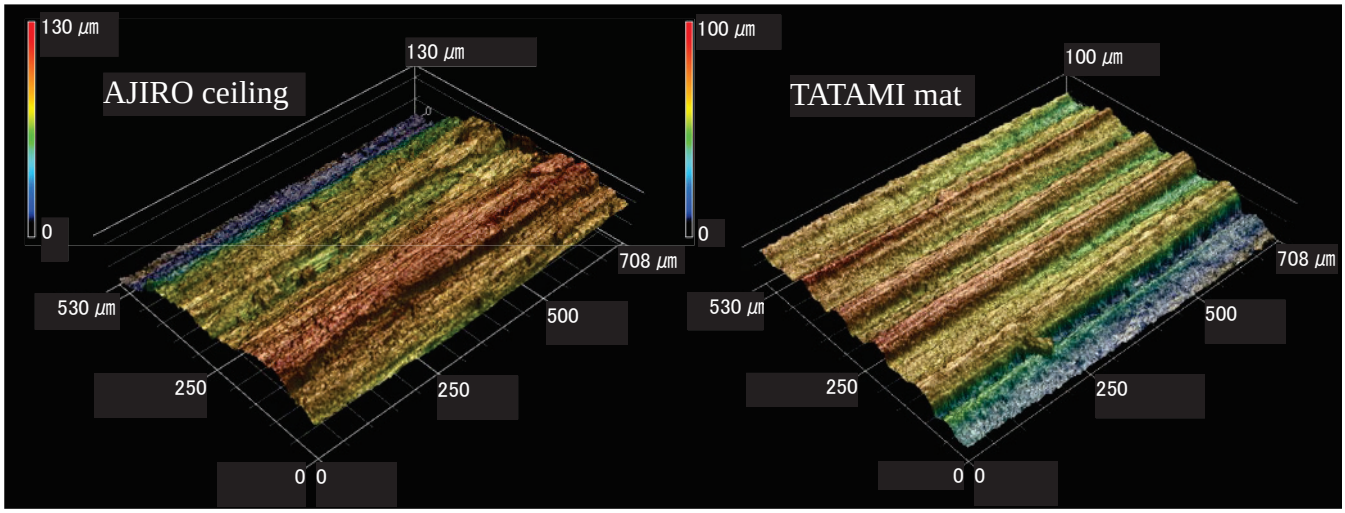

Figure 6: Laser confocal microscope measurement result

In the measurement by gonio-photometric spectral imaging, a similar trend was observed in the angle dependence of tatami mats and net ceiling materials. As the illumination angle from the vertical direction of the sample surface increases, the amplitude of the L* value in the image increases. Tatami mats with a greater degree of surface irregularity will have a more noticeable increase in amplitude. (Shown in Figure 7)

The small space tea ceremony room TENGO-AN was conceived with the intention of being a place to show the tea container ODAIMYO. And from the measurement results, the following can be inferred. The SHOJI which is paper screen in a specific direction in the room illuminates the room with a certain degree of diffusion, and the

microscopic irregularities on the walls further diffuse the soft light, as is common to many traditional Japanese tea ceremony rooms. The light reflected from the TATAMI mats on the floor illuminates the tea utensils from below, but the brightness and texture of the background change with the seasons, time, and weather. On the other hand, although there is relatively weak light reflected from the ceiling, the pattern of the AJIRO has remarkable changes in facial expressions from moment to moment in response to slight changes in lighting conditions, creating a once-in-a-lifetime situation that is valued in the tea ceremony.

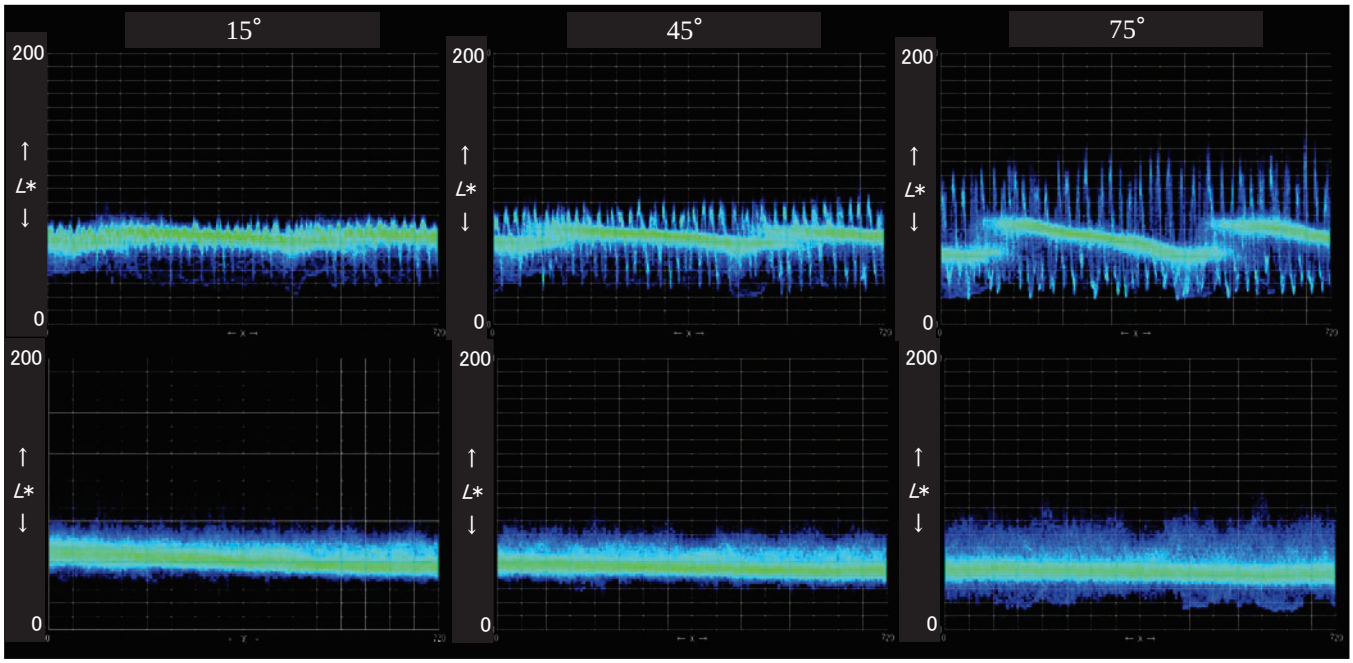

Figure 7: Gonio-photometric spectral imaging measurement result

CONCLUSION

As mentioned above, the tea ceremony room is a lighting space that uses natural light, and there is a two-sided mechanism. One is homeostasis or constancy, and the other is the effect of bringing about subtle changes incorporating aging that leads to ICHIGO-ICHIE that meaning is the once-in-a-lifetime meetings.

REFERENCES

[1]. Bhimani, S. An Inquiry into the making of Japanese architecture through the study of tea houses, The University of Arizona

[2]. Saito, Y. (2007) The Moral Dimension of Japanese Aesthetics, The Journal of Aesthetics and Art Criticism, Volume 65, Issue 1, 85–97, https://doi.org/10.1111/j.1540-594X.2007.00240.x

[3]. Stanford Encyclopedia of Philosophy (2005) Japanese Aesthetics

[4]. Avdulov, A. (2022) Understanding Wabi and Sabi in the Context of Japanese Aesthetics, The Asian Conference on Cultural Studies 2022 Official Conference Proceedings

[5]. Jian, Y. (2021) The Meaning and Expression of Wabi-Sabi in Environmental Art Design, Pacific International Journal, Vol. 4(2), 45-48, DOI: 10.55014/pij.v4i2.15, https://rclss.com/index.php/pij

Beyond The Surface: Exploring Dichroic Filters in Folded Geometries

Elvira Jönsson
University of Borås – The Swedish School of Textiles, Borås, Sweden
elvira.jonsson@hb.se

ABSTRACT

This research addresses the limited exploration of dichroic filters on non-planar or flexible surfaces. It investigates their optical behavior when applied to folded paper geometries, forming a basis for future integration into textile and flexible design contexts. Through systematic variations in fold geometry, filter placement, and light angle, the study explores how three-dimensional form influences both the surface color of dichroic filters and the behavior of reflected colored light. Findings show that fold direction, angle, filter scale, and angle of light source strongly impact surface coloration and spatial light effects. The project positions the dichroic filter not merely as a surface treatment, but as a responsive material that interacts dynamically with form, light, and motion.

Keywords: dichroic filter, three-dimensional geometries, dynamic colors

INTRODUCTION

Light and color captivate us instantly with their vibrant, shifting qualities, often commanding attention in design. Yet without the tangible role of material in giving them form, they remain intangible—mere phenomena without substance [1]. It is material that lends light and color structure, depth, and presence. When designers engage with all three—material, light, and color—they open up the potential for immersive experiences that evolve with time, movement, and perception [2].

Material also has the power to transcend disciplinary boundaries, continually redefined through new processes, combinations, and contexts. For this reason, the designer's role is to recognize and harness this potential by identifying the design possibilities a material offers through experimental exploration and actively applying them to create something new or valuable [3].

This research focuses on one such material: the dichroic filter—a surface treatment that responds dynamically to light, offering rich possibilities for optical exploration. Also known as interference filters, dichroic materials consist of multi-layered polymer films protected by a hard-coated polyester layer [4]. When exposed to strong sunlight or focused artificial light [4, 5], they reflect and transmit different wavelengths of colored light depending on the angle of light source.

Unlike traditional pigments or colored coatings, dichroic materials offer a dynamic color experience driven by light and motion. Their behavior introduces temporal and spatial complexity, making them especially compelling for use in architecture, installations, and material driven design research [6].

In architecture and artistic applications, designers use the color-shifting properties of dichroic materials to highlight both aesthetic and performative qualities [7,8,9]. A notable example is 90 Pairs of Hands [7] by Chris Wood Light Studio, a site-specific installation mounted on a white wall. The work features hundreds of small, rectangular dichroic glass elements, each tilted at 90 degrees to form a radiating, wave-like pattern. As natural light shifts throughout the day, the dichroic glass reflects, transmits, and refracts vivid colors, transforming the wall into a dynamic optical display.

While previous works succeed in illustrating the aesthetic and performative qualities of dichroic filters—focusing on shimmer, color shifts, and light interactions in site-specific installations or kinetic sculptures—

they typically apply the filters to flat, rigid substrates such as glass or acrylic. Even when introducing movement through rotation, kinetic modulation, or shifting daylight, these works remain within a planar framework where the dichroic layer functions as a surface treatment rather than as an integrated structural element. This leaves little exploration of how the material behaves when the supporting form is non-planar, folded, or flexible.

This research aims to establish foundational knowledge of dichroic filter behavior in three-dimensional geometries. By treating the filter as a dynamic material rather than a surface coating, the project aims to extend its design potential and uncover new interactions between light, color, and form. In doing so, it lays the groundwork for future applications where dichroic filters can be integrated into flexible or textile-based contexts.

METHODS

Experimental setup

This research explores the optical and structural behavior of dichroic filters using folded paper models, building on earlier findings [10] to inform future 3D textile applications. Samples were folded from 150 × 150 mm, 80 g/m² paper, with longer sheets (210 × 120 mm) for unidirectional pleats. The Blaze variant of 3M's Dichroic Glass Finish DF-PA [4] was used; adhesive-backed film strips (3–50 mm) were applied in various positions to test scale and placement effects on reflectivity and color. Optical behavior was tested by varying light angle, viewing angle, and sample orientation. Rotating the light source or sample caused stronger color shifts than changing viewing angle alone, confirming that light movement is the main trigger. Samples were lit by a focused 2700 K LED lamp rotating 360° in 10° steps around a fixed sample at a 55° angle and 25 cm distance, with the camera fixed overhead (0° view) for consistent documentation.

Experiment 1: Simple Pleats

The first set of examples used a simple pleated folding method, with the dichroic filter applied in various positions: (a) fully covering the fold, (b) as a slim strip at the center, (c) in the valley, and (d) on the peak. Each position was tested with both single-sided (as shown in the technical drawing, Fig. 1, Image 1) and double-sided filter placement to investigate how positioning affects reflected colored light. When illuminated by a moving light source (LS) in a 360° arc, each sample revealed its full visible color-shifting range between 0° and 180°, depending on fold angle (FA) and filter placement. Beyond 180°, no new behaviors appeared—the color transitions simply mirrored those from the first half of the rotation.

When comparing positions b, c, and d at, for example, at 60° FA, b and d show similar behavior: both produce slim highlights on the opposite side of the fold that shift from saturated orange at 0° LS to faint green glints, disappearing as the LS moves toward 180°. Placement d, at the highest position toward the peak, the reflected colored light travels further—from bottom to top—creating a more dramatic movement, while in b, it stops lower on the fold. In contrast, position c produces reflected light that remains attached to the filter surface, extending upward from the valley. The surface of the dichroic filter and the reflected colored light blend into a smooth gradient.

When cut into slim strips (e.g., 5 mm), the filter adhered unevenly and created wavy surfaces, distorting the reflected colored light—partly due to the paper's flexible, uneven surface during handling (Fig. 1, Images 2–3). In contrast, covering the full fold (e.g., 2 cm) allowed for smoother adhesion and produced clean, rectangular reflections (Fig. 1, Image 4). The narrow strips produced highly localized, intense reflections, while full coverage created broader, smoother color washes. Filters placed along peaks generated wave-like highlights extending outward, whereas those in valley folds cast longer, upward reflections on the opposite side, forming gradual gradients.

Fold angles were manually adjusted between ~20° and 100° (Fig. 1, Images 4–6). Narrow folds (~20°) exposed less filter surface, producing weaker light reflections and faint wall projections (Image 4). Wider folds

(~100°) enhanced color shifts, increased surface reflections (Image 5), and cast larger, more saturated patterns in space (Image 6). Outside this range, the effect weakened, as folds became too compressed or open to reflect light effectively.

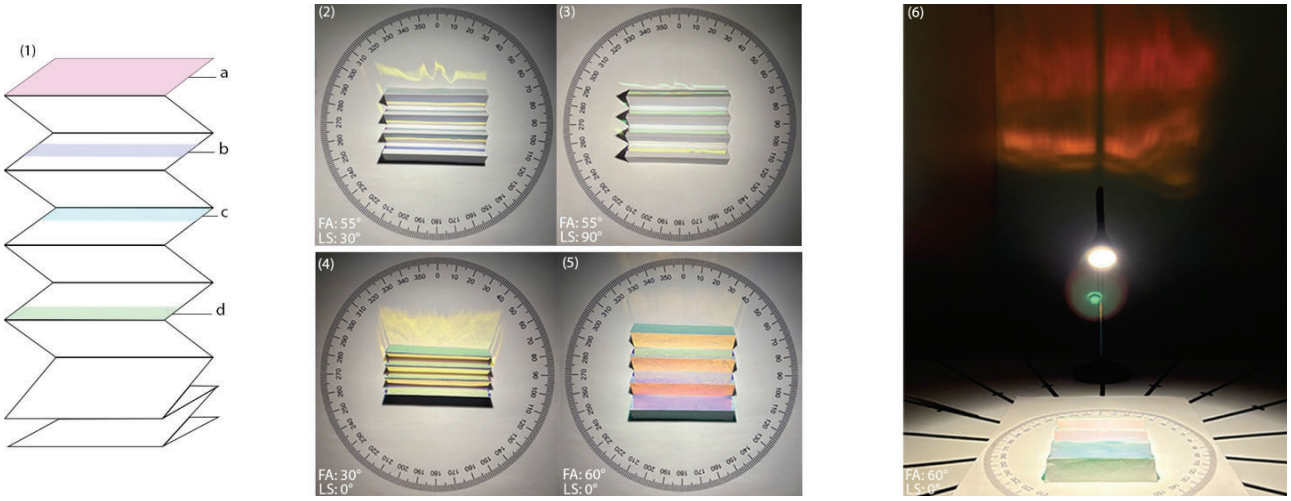

Figure 1: Image 1 shows filter placements (a–d). Images 2 and 3 show 5 mm filters in position b, single-sided, highlight irregular reflected colored light. Images 4 and 5 (position a) show how fold angles affect reflected light on the opposite side and surrounding space. Image 6 (also position a) displays reflected light on surrounding space resembling a sunrise.

Experiment 2: V-pleats

The second examples are symmetrical V-pleats with folds angled toward a central line, forming a shallow V-shape. Based on results of experiment 1, narrow 5 mm dichroic strips were used to balance the filter, paper, and folds, avoiding any element dominating. The central fold introduced a directional change, causing reflected colored light to bend with the V-shape. Filters were placed in positions (a) valley center fold, (b) peak center fold, (c) peak sides, and (d) valley sides—both single- and double-sided (see Fig. 2, Image 1).

Based on surface color of the dichroic filter, reflected light, and spatial effects, certain filter positions stood out (Fig. 2, Images 2–4). Single-sided filters at position c produced long, saturated orange reflections along the V-shape, contrasting with the purple-blue surface (Image 2). Double-sided filters at position b created a distinct green–orange split between 300° and 60°, with surface shifts from light green to purple-gray (Image 3). Combinations of positions a, b, and c revealed overlapping effects, with merged hues—like teal green—and wave-like yellow reflections extending across the table (Image 4).

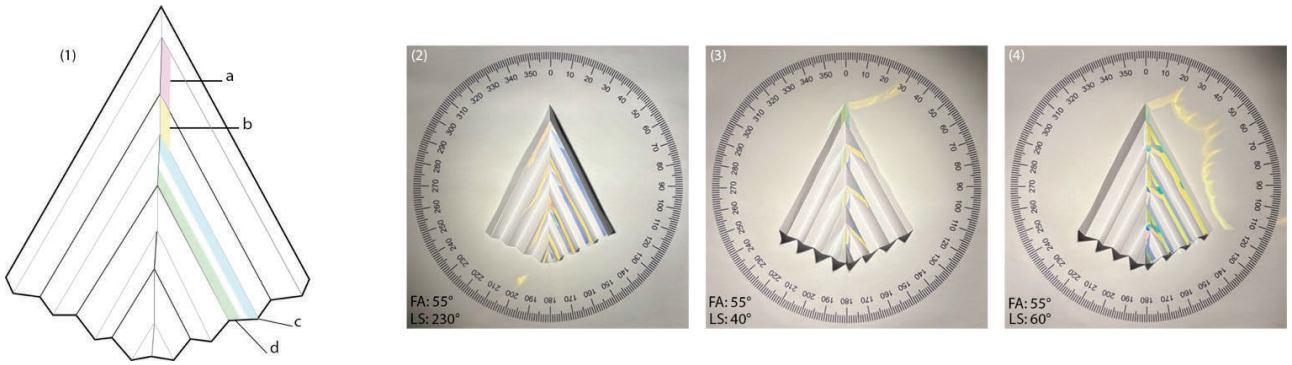

Figure 2: Image 1 shows filter placements at positions a–d. Image 2 shows filters at position c, producing the longest reflected colored light, bending along the fold. Image 3 shows filters at position b, double-

sided, with a clear split in the reflected light. Image 4 shows filters at positions a and b (single-sided) and c (double-sided), creating overlapping reflections that extend into the surrounding space.

Experiment 3: Herringbone

Building on the V-pleat's ability to direct reflected colored light, the herringbone fold was introduced to explore how repetition and alternating directionality affect optical behavior. This fold creates a zigzag geometry composed of repeated V-shapes. It applied the same filter positions as the V-pleat (a–d, see Fig. 2), but with 3.5 mm dichroic strips on both sides of each V (all positions in one example are shown in Fig. 3 image 1).

The angled, alternating segments—about 13 mm from peak to valley—created shifting patterns of surface hues and reflected light, with certain filter placements appearing more prominent (Fig. 3, Images 2–4). In position b (Image 2), reflected colored light formed repeating rectangular shapes in orange, yellow, and green, which split and merge in a circular rhythm as the light moves. The filter surface showed mostly green and gray tones, becoming most saturated in turquoise blue around LS 90° and 270°, where light hit the surface at the most direct angle. Position c (Image 3) produced vibrant green and yellow wavy reflections that overlapped across the folds, generating a multicolored effect on the surface. In position a (Image 4), reflected colored light created a soft gradient—casting saturated orange-yellow hues onto the non-filtered side and blending with purple-gray tones across the filter surface.

Positions c and d produced the strongest overall spatial effects. Position d generated the most consistent reflected colored light throughout the 360° rotation, casting zigzag orange patterns onto the ceiling. Similarly, position c projected dynamic reflections onto the surrounding walls.

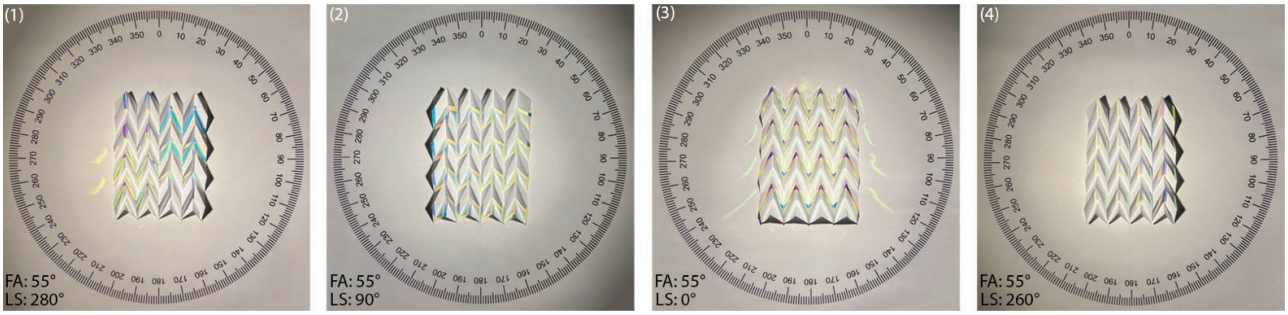

Figure 3: Image 1 shows all filter positions (a–d) in one folded form. Image 2 filters position b, double-sided, shows reflected colored light in alternating repeat. Image 3, filters position c, double-sided, shows wavy reflections extended to the surrounding space. Image 4 filters position a, single-sided, shows a softer gradient of hues.

Experiment 4: Contrasting Folded Squares

The fourth series of experiments, Contrasting Folded Squares, builds on the V-pleat by introducing diagonal folds that create opposing directions in the inner and outer squares, resulting in strong visual and structural contrast. The fold angles also differ: the inner square features wider pleats (~100°), while the outer square varies between 50° and 100°. As in the V-pleat and herringbone setups, filter positions a–d were used (see Fig. 2, Image 1), still with 3.5 mm stripes. However, instead of following a single central line (as in earlier drawings), the filters were aligned with the fold lines of the inner square.

This shift affected the visual outcome. For example, in one case using both positions a and b (see Fig. 4, Image 1), b produced sharp, saturated reflected colored light splits in yellow and orange across multiple areas, while the filter surface displayed intense blue and purple hues throughout the 360° rotation. Meanwhile, position a contributed the strongest spatial effect: the wide fold angles and placement along the inner square's outline caused reflections to scatter in several directions, appearing as orange dots on nearby walls and ceiling.

Two particularly strong optical behavior came from filters placed in positions d and c (Fig. 4, Images 2-3), where the visual focus shifted between inner and outer squares depending on the angel of the light. In position d (Image 2), the inner square reflected vibrant orange light, while the filter surface showed blue and purple tones. The outer square, by contrast, remained more subdued, with minimal reflected light on its folds and a turquoise hue on the filter surface. In position c (Image 3), the outer square reflected wavelike yellow light from a blue-toned filter surface, while the inner square maintained a blue appearance.

Finally, combining filter positions b and c (Fig. 4, Image 4) activated both inner and outer folds at once, producing multiple dynamic effects. Yellow, wave-like reflections appeared on the outer square, while the inner square showed saturated yellow and orange highlights. Both areas also displayed blue and purple tones on the filter surface.

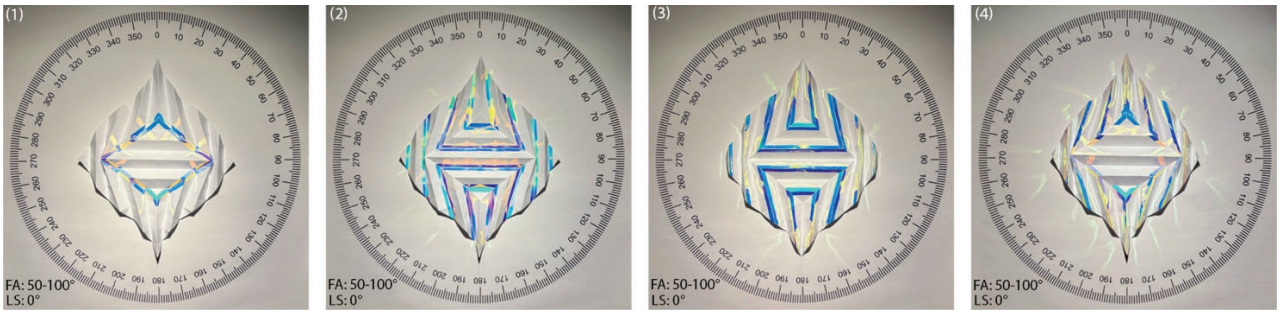

Figure 4: Image 1 shows filter positions a and b, double-sided, highlighting a split in the reflected pattern. Image 2 shows position d, and Image 3 shows position c, both double-sided, illustrating the contrast between inner and outer squares. Image 4 combines positions b and c, double-sided, activating both the inner and outer squares simultaneously.

DISCUSSION

The experiments demonstrate that the optical behavior of dichroic filters can be choreographed through folding, repetition, surface angle, and movement—both through material flexibility and changes in the angle of the light source—creating directional patterns of reflected colored light. When applied to folded paper geometries, the dichroic filter produces effects that transcend shimmering surface treatments, as the three-dimensional folds influence both the intensity and direction of light.

For example, V-pleats and herringbone folds guide light along predetermined paths, creating dynamic patterns responsive to moving light sources. Contrasting folded squares demonstrate how opposing fold directions create visual contrast, with reflected color alternating between saturation and subtlety depending on orientation and filter placement. Simple pleats show that wider fold angles increase both the intensity and spread of reflected light, while narrow folds limit expressive potential. These findings reinforce fold geometry as a key design parameter for dynamic light interactions.

As light interacts with flexible folds, color effects become choreographed, casting shifting hues across surfaces and space. Reflected patterns split and merge; at times, saturated orange tones appear on distant walls, resembling a sunrise in a darkened room. These phenomena reveal the dramatic yet temporal nature of a material shaped—and reshaped—through flexible design. Such qualities suggest potential for immersive, responsive experiences that evolve with time, movement, and perception [2]. Further development could invite direct user engagement—through touch to reshape folds or movement to alter perception and guide spatial experiences, potentially transforming how users perceive and relate to material surfaces.

Future exploration could involve flexible substrates such as textiles, where drape and fold geometry introduce further complexity to light interaction. Integrating kinetic or interactive lighting systems could enhance their performative character, enabling real-time shifts in color and pattern. These directions may

expand applications from static installations to wearable, responsive, or environmental designs, aligning with Solanki's [3] call for experimental material exploration to generate new design value.

CONCLUSION

In Conclusion, this research demonstrates that the optical potential of dichroic filters is intimately linked to the geometry of their supporting substrate. By considering fold angles, directional arrangements, and filter placement, designers can use dichroic materials to create dynamic, spatially and temporally complex color experiences—opening new avenues for material-driven design in textile and fashion design, architecture, installation art, and beyond.

REFERENCES

[1]. Praun, S., & Stratimirovic, A. (Eds.). (2015). You say light I think shadow: One hundred and nine perspectives collected & visualized. Art and Theory Publishing.

[2]. Jongeriuslab. (n.d.). Breathing Colour exhibition at the Design Museum, London. Retrieved August 21, 2025, from https://jongeriuslab.com/product/breathing-colour-exhibition-at-the-design-museum-london/

[3]. Solanki, S. (2018) Why Materials Matter: Responsible Design for a Better World. Munich: Prestel Publishing.

[4]. 3M Science Applied to Life. (n.d). 3M TM Dichroic Films for Architectural Laminated Glass. Retrived July 22 2025. http://coolsunlight.com/pdf/Dichroic%20DF-PA%20Technical%20Data%20Sheet.pdf

[5]. Winnewisser, C., Lewen, F. T., Schall, M., Walther, M., & Helm, H. (2000). Characterization and application of dichroic filters in the 0.1–3 THz region. IEEE Transactions on Microwave Theory and Techniques, 48(4), 744–749.

[6]. 2025). Karana, E., Barati, B., Rognoli, V., & Zeeuw van der Laan, A. (2015). Material driven design (MDD): A method to design for material experiences. International Journal of Design, 9(2), 35–54. Retrieved July 24, 2025, from https://www.ijdesign.org/index.php/IJDesign/article/view/1965

[7]. Chris Wood Light. (2024). 90 Pairs of Hands [Installation]. Retrieved August 14, 2025, from https://www.chriswoodlight.art/90pairsofhands

[8]. KUFstudios. (n.d.). Curved Twist [Design]. Retrieved August 14, 2025, from https://www.kufstudios.com/kuftwist

[9]. Seyama, Y. (2022–2023). Saiyah #2.8 [Kinetic light installation]. Yoko Seyama. Retrieved August 14, 2025, from https://yokoseyama.com/works/saiyah-2/

[10]. Jönsson, E., & Kooroshnia, M. (2023). Creating sensuous experiences: Combining dichroic filters and textile weaving to create aesthetic spatial installations. Color Research & Application, 48(5), 484–496. https://doi.org/10.1002/col.22830

How to Characterize Augmented Reality Glasses for Color Reproduction – Taking The Birdbath Optical Structure as An Example

Ya-Chi Chao*, Li-Chen Ou

Graduate Institute of Color and Illumination Technology, National Taiwan University of Science and Technology, Taipei, Taiwan

*Corresponding author: Ya-Chi Chao, ades96026@gmail.com

ABSTRACT

Accurate colorimetric characterization is essential for augmented reality (AR) glasses, where perceived colors result from the mixture of virtual images and real-world scenes. This study proposes a new characterization model for birdbath-based AR glasses, featuring both forward and inverse directions. The forward model predicts the perceived color (CIE XYZ) from background color and AR content, while the inverse model determines the AR content RGB values required for a target perceived color. To address the difficulty of measuring real-world spectral power distribution (SPD), we introduce a single-value transmittance estimation method, enabling direct conversion of background XYZ values into their transmitted form. An s-curve approach is further applied to model the AR display's RGB-to-XYZ conversion. Experiments verify the model in both directions: results show extremely high accuracy with coefficients of determination (R^2) above 0.99 for CIELAB L*, a*, b* in the forward model and above 0.97 for RGB channels in the inverse model. The proposed method provides a reliable framework for AR color characterization, with future work focusing on incorporating simultaneous contrast effects to further improve perceptual accuracy.

Keywords: colorimetric characterization, augmented reality, head-mounted displays, optical see-through

1. INTRODUCTION

Colorimetric characterization establishes the mapping between device-dependent (RGB) and device-independent (CIE XYZ) color spaces, ensuring consistent reproduction across devices [1]. Unlike conventional displays, optical see-through AR glasses pose additional challenges because perceived colors result from additive mixing of real-world backgrounds and virtual imagery, making traditional display models inadequate [2]. Among various AR designs, the birdbath architecture is widely adopted for its optical efficiency but complicates colorimetric modeling due to the interaction of optical structures and transmitted light [3]. To address this gap, this study proposes a birdbath-based characterization model that combines a simplified single-value transmittance estimation with an s-curve display model, enabling accurate prediction of perceived colors (forward model) and inverse computation of AR input values for target appearances [4].

2. METHODS

A pair of optical see-through AR glasses (XReal Pro 2 Air) was selected for characterization. The device adopts birdbath optics with electrochromic dimmable lenses, and features a Micro-OLED display with a resolution

of 1920×1080 pixels per eye, refresh rate of 120 Hz, and a peak luminance of 500 cd/m². To simulate real-world backgrounds, a 27-inch BenQ LCD monitor was positioned behind the AR glasses and controlled by a computer. All measurements were conducted in a darkened room to minimize ambient light interference. A TOPCON SR-UL1R tele-spectroradiometer was used for data acquisition, measuring both the colors displayed on the LCD (background) and the colors perceived through the AR glasses (combined view).

2.1 AR-Content Characterization

To characterize the AR display's response, a total of 84 color samples were measured against a black background, including reference primaries, single-channel gradients (18 levels each), application-related tones (skin, vegetation, sky), and grayscale patches. For each sample, XYZ values and SPDs were recorded.

A two-stage S-Curve model was then established. The first stage applies hyperbolic tangent functions to describe the nonlinear optoelectronic transfer functions of each channel, capturing saturation tendencies not addressed by conventional gamma functions, as shown in Equation Set (1):

$$\begin{aligned} \mathbf{R}' &= \boldsymbol{k_{0,r}} + \boldsymbol{k_{1,r}} \cdot \tanh\left(\boldsymbol{k_{2,r}} \cdot \boldsymbol{R_V} - \boldsymbol{k_{3,r}}\right) \\ \mathbf{G}' &= \boldsymbol{k_{0,g}} + \boldsymbol{k_{1,g}} \cdot \tanh\left(\boldsymbol{k_{2,g}} \cdot \boldsymbol{G_V} - \boldsymbol{k_{3,g}}\right) \\ \mathbf{B}' &= \boldsymbol{k_{0,b}} + \boldsymbol{k_{1,b}} \cdot \tanh\left(\boldsymbol{k_{2,b}} \cdot \boldsymbol{B_V} - \boldsymbol{k_{3,b}}\right) \end{aligned} \quad (1)$$

where $(\mathbf{R}'\ \mathbf{G}'\ \mathbf{B}')$ are the output values for the three channels; $(\boldsymbol{R_V}\ \boldsymbol{G_V}\ \boldsymbol{B_V})$ are the normalized digital inputs of the three channels for the AR content only; $\boldsymbol{k_0}$, $\boldsymbol{k_1}$, $\boldsymbol{k_2}$, $\boldsymbol{k_3}$ are the constant and coefficients in the hyperbolic function of each channel.

The second stage employs a 3×3 linear transformation to map intermediate values into CIE XYZ tristimulus space, as shown in Equation Set (2):

$$\begin{bmatrix} \boldsymbol{X_V} \\ \boldsymbol{Y_V} \\ \boldsymbol{Z_V} \end{bmatrix} = \begin{bmatrix} \boldsymbol{X_{r,max}} & \boldsymbol{X_{g,max}} & \boldsymbol{X_{b,max}} \\ \boldsymbol{Y_{r,max}} & \boldsymbol{Y_{g,max}} & \boldsymbol{Y_{b,max}} \\ \boldsymbol{Z_{r,max}} & \boldsymbol{Z_{g,max}} & \boldsymbol{Z_{b,max}} \end{bmatrix} \begin{bmatrix} \boldsymbol{R'} \\ \boldsymbol{G'} \\ \boldsymbol{B'} \end{bmatrix} \quad (2)$$

where the "max" subscript defines each channel's maximum output after black correction.

2.2 Single-Value Transmittance Estimation

This study introduces a simplified single-value transmittance method. Instead of requiring full spectral power distribution (SPD) data of background colors and detailed transmittance curves, each tristimulus component is assigned an average transmittance factor. Ideally, CIE tristimulus values of any color on an LCD $(\boldsymbol{X_R}\ \boldsymbol{Y_R}\ \boldsymbol{Z_R})$ for absolute colorimetry (in the unit of cd/m2) can be determined using Equation Set (3) when the SPD of the LCD color is available:

$$\begin{aligned} \boldsymbol{X_R} &= \mathbf{683} \int \boldsymbol{S}(\boldsymbol{\lambda})\, \bar{\boldsymbol{x}}(\boldsymbol{\lambda}) \boldsymbol{d\lambda} \\ \boldsymbol{Y_R} &= \mathbf{683} \int \boldsymbol{S}(\boldsymbol{\lambda})\, \bar{\boldsymbol{y}}(\boldsymbol{\lambda}) \boldsymbol{d\lambda} \\ \boldsymbol{Z_R} &= \mathbf{683} \int \boldsymbol{S}(\boldsymbol{\lambda})\, \bar{\boldsymbol{z}}(\boldsymbol{\lambda}) \boldsymbol{d\lambda} \end{aligned} \quad (3)$$

where $\boldsymbol{S}(\boldsymbol{\lambda})$ is the SPD of the color shown on the LCD; $\bar{\boldsymbol{x}}(\boldsymbol{\lambda})$, $\bar{\boldsymbol{y}}(\boldsymbol{\lambda})$, and $\bar{\boldsymbol{z}}(\boldsymbol{\lambda})$ are CIE 1931 color matching functions.

The transmitted tristimulus values $(\boldsymbol{X_T}\ \boldsymbol{Y_T}\ \boldsymbol{Z_T})$ are then determined using Equation Set (4) when the spectral transmittance of the AR glasses is known:

$$\begin{aligned} X_T &= 683 \int S(\lambda)T(\lambda)\,\bar{x}(\lambda)d\lambda \\ Y_T &= 683 \int S(\lambda)T(\lambda)\,\bar{y}(\lambda)d\lambda \\ Z_T &= 683 \int S(\lambda)\,T(\lambda)\bar{z}(\lambda)d\lambda \end{aligned} \quad (4)$$

where T(λ) is the spectral transmittance of the AR glasses.

In practice, particularly for applications of AR devices, a single-value transmittance for each tristimulus value is desirable. This can be done by calculating the integral of a product of a color matching function and the spectral transmittance, divided by the integral of the same color matching function, as described in Equation Set (5):

$$\begin{aligned} T_X(\%) &= \frac{\int \bar{x}(\lambda)T(\lambda)d\lambda}{\int \bar{x}(\lambda)d\lambda} \\ T_y(\%) &= \frac{\int \bar{y}(\lambda)T(\lambda)d\lambda}{\int \bar{y}(\lambda)d\lambda} \\ T_z(\%) &= \frac{\int \bar{z}(\lambda)T(\lambda)d\lambda}{\int \bar{z}(\lambda)d\lambda} \end{aligned} \quad (5)$$

where $T_X(\%)$, $T_Y(\%)$, and $T_Z(\%)$ are the single-value transmittance for the CIE tristimulus values X, Y and Z, respectively.

The transmitted tristimulus values ($X_T\ Y_T\ Z_T$) can then be estimated approximately by Equation Set (6):

$$\begin{aligned} X_T &\approx X_R \times T_X(\%) \\ Y_T &\approx Y_R \times T_Y(\%) \\ Z_T &\approx Z_R \times T_Z(\%) \end{aligned} \quad (6)$$

To test the single-value transmittance, as described above, we measured nine colors with and without the AR glasses placed between the LCD and the measuring instrument. The nine colors were selected randomly from CIELAB space.

3. RESULTS

3.1 Verification of the AR content characterization

The s-curve model for AR content characterization was established using the measurement data described in Section 2.1. The fitted functions for the nonlinear transformation and the subsequent linear mapping are presented in Equations (7) and (8).

$$\begin{aligned} \mathrm{R}' &= 0.66 + 0.68 \cdot \tanh(2.74 \cdot R - 2.25) \\ \mathrm{G}' &= 0.71 + 0.73 \cdot \tanh(2.71 \cdot G - 2.35) \\ \mathrm{B}' &= 0.69 + 0.71 \cdot \tanh(2.69 \cdot B - 2.22) \end{aligned} \quad (7)$$

$$\begin{bmatrix} X \\ Y \\ Z \end{bmatrix} = \begin{bmatrix} 267.08 & 201.33 & 102.02 \\ 131.67 & 412.90 & 51.53 \\ 4.55 & 72.06 & 563.39 \end{bmatrix} \begin{bmatrix} R' \\ G' \\ B' \end{bmatrix} \quad (8)$$

To validate the model, colors defined by RGB input values were compared with the corresponding outputs predicted by the s-curve formulation. As depicted in Figures 1(a)–(c), the predicted and measured results show an

excellent match, with coefficients of correlation (r) exceeding 0.99 across all channels. These findings confirm the high fidelity of the proposed s-curve model.

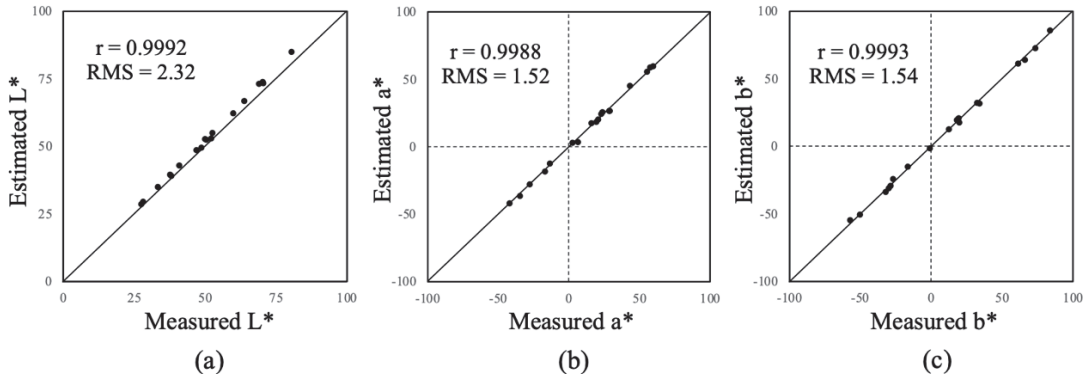

Fig. 1 Predicted vs. measured values for the s-curve model: (a) L*, (b) a* and (c) b* values in the right lens of the AR glasses

3.2 Verification of the single-value transmittance

To evaluate the effectiveness of the proposed single-value transmittance algorithm, the estimated tristimulus values derived from Section 2.2 were compared with those directly measured when the AR glasses were positioned in front of the LCD. For consistency, all results were transformed into the CIELAB color space prior to comparison. As illustrated in Figures 2(a)–(c), the estimated and measured values exhibited an exceptionally strong agreement, with coefficients of correlation (r) exceeding 0.99 in all cases. These results confirm the high accuracy and reliability of the algorithm.

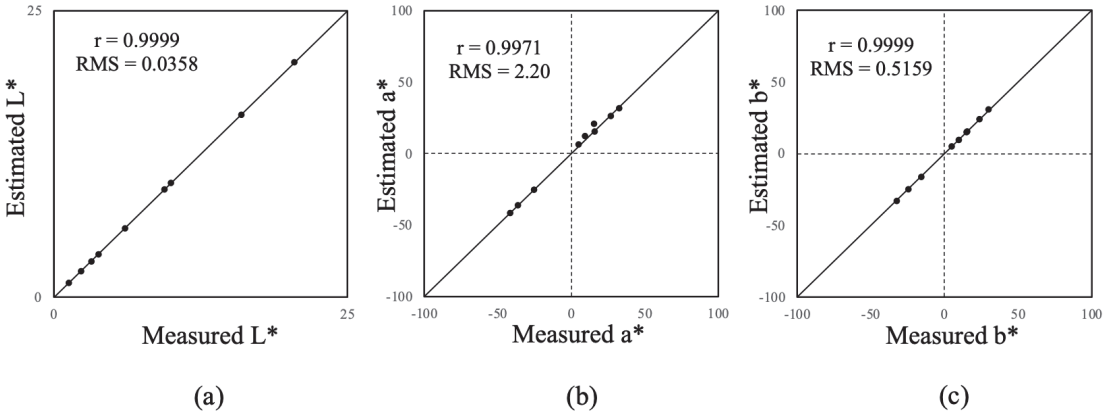

Fig. 2 Estimated vs. measured values for single-value transmittance: (a) L*, (b) a* and (c) b* values in the right lens of the AR glasses

3.3 Predictive performance of the entire model for colorimetric characterization of AR glasses

The forward direction of the model predicts the color to be viewed by the AR user, in terms of tristimulus values. This requires the following input data:

(1) CIE tristimulus values of the real-world background color ($X_R\ Y_R\ Z_R$).
(2) Digital inputs for AR content ($R_V\ G_V\ B_V$).

To test the predictive performance of the model, we compared target colors defined in RGB inputs with those estimated by the model, which integrates both the single-value transmittance and the AR-content characterization. As shown in Figures 3(a)–(c), the agreement between measured and predicted values was remarkably strong, with all correlation coefficients (r) exceeding 0.99. These results demonstrate that the forward model achieves highly reliable accuracy.

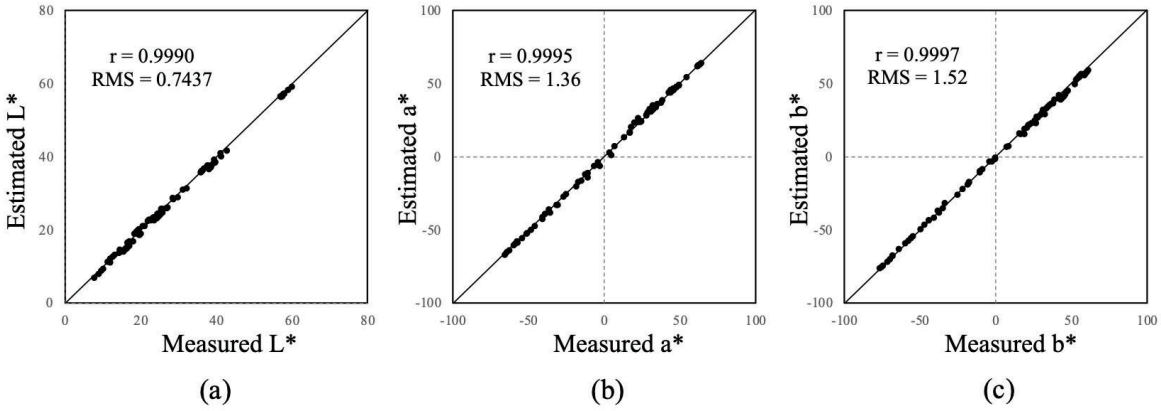

Fig. 3 Estimated vs. measured values for the forward direction of the model: (a) L*, (b) a* and (c) b* values in the right lens of the AR glasses

The inverse direction of the model predicts the digital inputs for AR content. This requires the following input data for the model:

(1) CIE tristimulus values of the real-world background color ($X_R\ Y_R\ Z_R$).
(2) CIE tristimulus values of the color to be viewed by the AR user (X Y Z).

To validate the model in the inverse direction, we compared the RGB values estimated by the model—based on the single-value transmittance and AR-content characterization—with the original RGB inputs. As shown in Figures 4(a)–(c), the predicted results closely matched the measurements, with all coefficients of correlation (r) above 0.98. These findings confirm that the inverse model provides reliable and accurate performance.

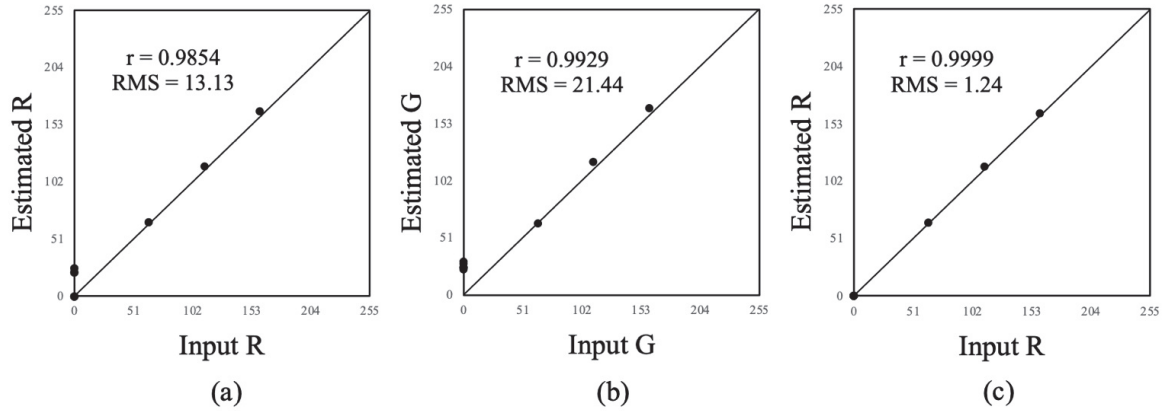

Fig. 4 Specified vs. estimated RGB values for the inverse direction of the model in the right lens of the AR glasses

4. CONCLUSION

This study proposed a colorimetric characterization framework for birdbath-based AR head-mounted displays (HMDs), addressing the challenge of color reproduction under virtual–real fusion conditions. By integrating an s-curve display characterization model with a simplified single-value transmittance estimation of the optical components, a dual-direction model was developed.

The forward direction models the AR viewing process by applying lens transmittance to background tristimulus values and adding the virtual display's contribution from the characterization model, yielding the final perceived color. Conversely, the inverse direction starts from a target perceptual color, subtracts the transmitted background, and converts the required virtual contribution back into RGB inputs, thus determining the display settings needed to reproduce the desired appearance.

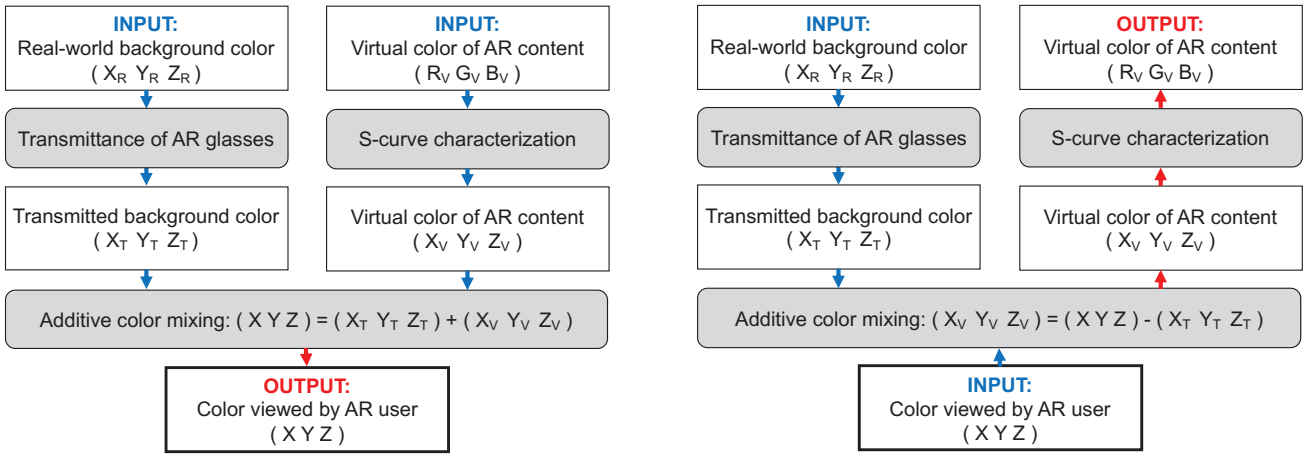

Fig. 5 Framework of the model for the forward direction and inverse direction

REFERENCES

[1]. Berns, R. S. (1996). Methods for characterizing CRT displays. Displays, 16(4), 173–182.

[2]. Sridharan, S. K., Hincapié-Ramos, J. D., Flatla, D. R., & Irani, P. (2013). Color correction for optical see-through displays using display color profiles. Proceedings of the 19th ACM Symposium on Virtual Reality Software and Technology, 231–240.

[3]. Rolland, J. P., Holloway, R. L., & Fuchs, H. (2000). A comparison of optical and video see-through head-mounted displays. Presence: Teleoperators & Virtual Environments, 9(3), 287–309.

[4]. Weiland, C., Braun, A. K., & Heiden, W. (2009). Colorimetric and photometric compensation for optical see-through displays. International Conference on Universal Access in Human-Computer Interaction, 603–612.

Fitting SSVEP Hue Selectivity Profile with Individual Data of Color Perception

Ichiro Kuriki*, Ryota Miyatsuka, Naoto Umeda, Sakura Fukushima, Hiroaki Kiyokawa

Graduate School of Science and Engineering, Saitama University, Saitama, Japan
*Corresponding author: Ichiro Kuriki, ikuriki@mail.saitama-u.ac.jp

ABSTRACT

Individual variability in the hue selectivity of EEG (SSVEP) amplitude was analyzed using individual perceptual profiles (N = 11), such as flicker saliency, brightness, and chromatic saturation. Multiple regression analysis assessed the contribution of these three perceptual profiles and the cone-opponent model, where most participants showing a greater weight for brightness perception. The findings also identified two participant groups: one group displayed higher weights for the perceptual model and S-cone model; the other group showed higher weights for the cone-opponent models in addition to the brightness model. These results indicate that differences in SSVEP amplitude profiles related to hue selectivity are influenced by the relative contribution of perceptual components, with brightness accounting for the largest weight among perceptual properties.

Keywords: Color vision, EEG, perception, saturation, brightness

INTRODUCTION

We perceive colors almost effortlessly, but it is not well known how the color signal is processed in the brain. In particular, the neural basis for the sensation of colors that we subjectively experience, so called color appearance, is not clearly understood. Several studies have pointed out that the cone-opponent signal from retina, conveyed through LGN, is not the neural basis of color appearance; responses of cone-opponent channels (i.e., L-M and S-(L+M)) do not represent the purest landmark colors in the Hering's opponent color theory, i.e., unique hues [1, 2].

Our group measured EEG (electro-encephalography) responses to isoluminant colors using a steady-state visually evoked potential (SSVEP) technique, while the color of flickering visual stimulus swept along a hue circle [3]. The SSVEP is a spectral component of EEG that appears at a temporal frequency corresponding to the visual stimulus. We measured the amplitude and phase profile of the SSVEP and found asymmetric changes in the SSVEP amplitude with stimulus hue whose grand mean is shown in Figure 3 [3]. We reported the presence of hue selective mechanisms in addition to the cone-opponent channels by fitting numerical models of cone opponent mechanisms and iso-Chroma contour of Munsell color chips. This study also found reliable and non-negligible individual differences in its hue selectivity profile [4]. On the other hand, several aspects of color appearance are known to exhibit individual differences, but links between the SSVEP response and perception has never been studied. In the present study, we investigated relationships between individual differences in color perception and the hue selectivity profile of SSVEP amplitudes.

METHODOLOGY

We collected a new set of SSVEP data of 11 participants, based on the same experimental procedure as Kaneko et al [3]. The method of experiment was approved by the ethics committee of Saitama University (R3-E-11). Healthy graduate / undergraduate students participated the experiment, and they gave written consent before the EEG and psychophysical experiments. The visual stimulus in the EEG experiment was presented with a CRT display GDM-2000CT (SONY, Tokyo, Japan) and the EEG recording was conducted by using a 32ch active electrode system BrainAmp actiCHamp+ (Brain Products, Germany). Electrodes around the occipital pole Oz, O1, and O2 in

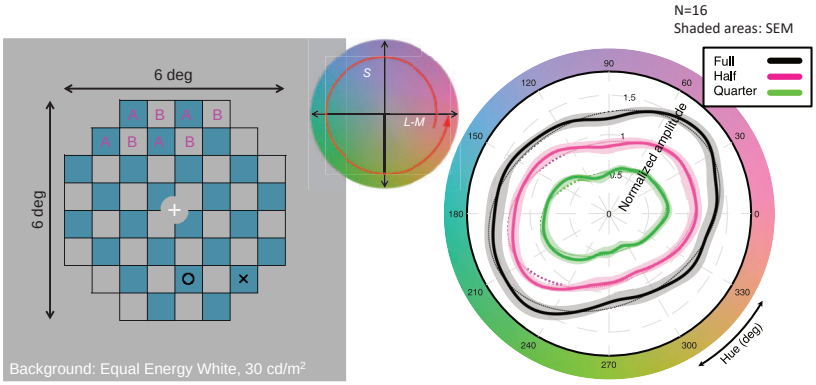

Figure 1. Visual stimulus (left) and main result (right) of our previous study [3]. The horizontal and vertical axis of the result represent cone opponent (L-M, S-(L+M)) axes, respectively. Different line colors represent different chromatic contrast. Shaded areas indicate variability across participants (N=16).

international 10-20 method were used in the main analysis. Reference electrode was placed at a parietal area: Cz. Eye movements and blinks were also monitored by two electrodes attached around the right eye; one placed at the corner and another under the eye.

The visual stimulus was same as a previous study; it was a flickering checkerboard that subtended approx. 6 deg in diameter and the pattern reversed at 5 Hz between a hue and the background gray, the metamer of equal-energy white at 30 cd/m2 (Figure 1; see [3] for details). The hue of visual stimulus was defined in a cone-opponent space, in which the difference of L- and M-cone responses and S-cone responses define the chromatic plane [3,4]. The chromaticity of the highest ("full") saturation condition was defined by the maximum available radius around the background gray, while the scale of L/M and S-axes are equated roughly by chromatic detection threshold; delta-L/L_{bkgnd} = 0.07 and delta-S/S_{bkgnd} = 0.70 in cone contrast [5]. The middle and low contrast conditions used half and quarter of the radii of the full contrast. The hue of color stimulus changed progressively along a hue circle by taking 24 s/cycle, and the data of SSVEP amplitude for each participant was obtained during the hue cycle presentations (each 24+1 s /run) at full, middle, or quarter color contrast. Starting hue of the hue cycle and the direction of hue change was randomized across runs in the EEG experiment, and 24 repetitions for both clockwise (CW) and counterclockwise (CCW) hue changes were conducted.

Table 1. Differences in stimulus conditions and criteria among perceptual experiments.

Conditions	A. Flicker saliency	B. Chromatic saturation	C. Brightness
Stimuli	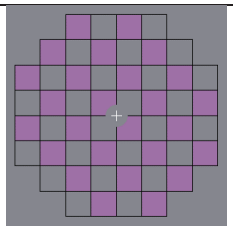	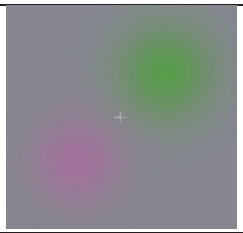	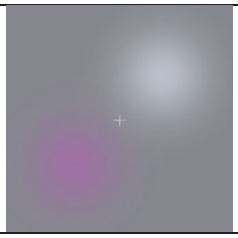
Spatio-temporal profiles	Check pattern (same as EEG) reversed at 5 Hz	Gaussian blob (σ = 1º) steady presentation	Gaussian blob (σ = 1º) steady presentation
Participant's tasks	Adjust saturation of standard stimulus to match saliency.	Adjust saturation of standard stimulus to match chromatic contrast.	Adjust luminance of achromatic patch to match brightness.

A high pass filter (above 0.05 Hz) and the rejection of trials with eye-movements and/or blinks were applied to all data. Data of participants with low behavioral performance of Go-NoGo task and the EEG data with low SNR (< 8.0) were not included in the formal analyses. After reorganizing and gathering 24 sectors of EEG data by splitting each cycle (24 s) by 1 s after discarding the first 1 s, summation was taken across runs to derive an average data. FFT was applied with a moving Gaussian window (sigma = 0.5 s) to obtain the time course of SSVEP responses to the flickering stimulus during the hue changes. The datasets for CW and CCW hue changes were initially analyzed separately, and merged after SSVEP amplitudes were obtained. We confirmed that the correlations between CW and CCW SSVEP amplitude profiles within each participant were significantly higher than that across participants.

SSVEP amplitude at 5 Hz under the highest chromatic-contrast condition was used for the fitting analysis. All participants performed psychophysical experiments for flicker saliency, brightness, and chromatic saturation for 24 hues along the hue circle. Chromaticity of stimuli used in these psychophysical measurements were sampled at 24 points with an equal step (15º) along the hue circle under the highest saturation condition of EEG. The spatio-temporal arrangements of the stimuli were slightly different (Table 1).

In the flicker-saliency matching, the participants were asked to match apparent saliency of the check pattern that reversed at 5 Hz between a test hue and a pre-defined standard hue (Table 1, column A.). The luminance of achromatic stimulus was adjusted to match apparent brightness (Table 1, column C.) with a test hue or to match apparent chromatic contrast (Table 1, column B.) of test hue with a standard hue at 30 cd/m2. More than 10 repetitions were averaged. The SSVEP profile in each participant was first converted to 24 points on the hue circle by averaging within each 15 deg bin and fit with perceptual data (saliency, brightness, and saturation). After then, we added a set of cone-opponent models (+L-M, -L+M, +S, and -S channels) consists of rectified cosine curves to perform multiple regression analysis. The optimality of the models was evaluated by Akaike's Information Criterion (AIC [6]).

RESULTS AND DISCUSSION

The results of SSVEP recording are shown in Figure 3. The hue selectivity curves show a similar hue-selectivity profile as the one by Kaneko et al. (2020) [3] with asymmetric selectivity across cone-opponent axes and showed higher responses to magenta-lime direction. The individual data (Figure 3B) show remarkable individual

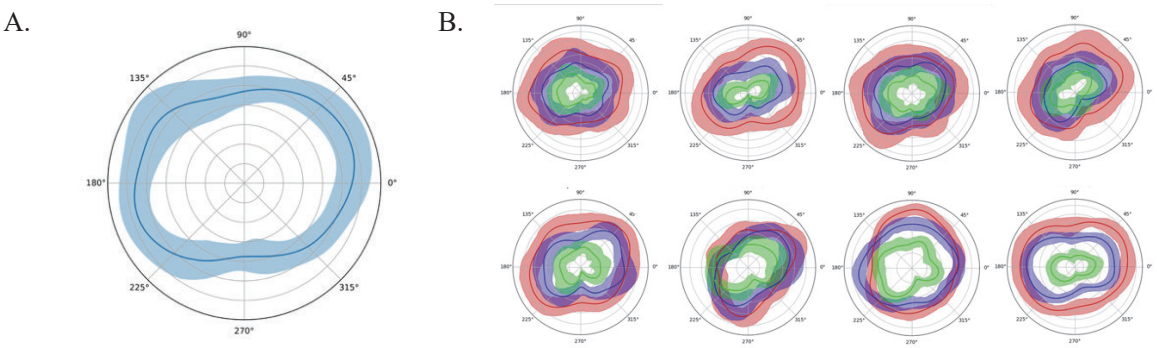

Figure 3. SSVEP amplitude profiles. A. Grand mean data (N = 11) of the full contrast condition, averaged after normalizing to each participant's mean SSVEP amplitude. The horizontal and vertical axes represent L-M and S-axes of cone-opponent space. Distance from the origin represent relative magnitude of the average SSVEP amplitude-response. It shows elongation in 45-225º direction [3]. Shaded area represents SEM across participants. B. Individual differences in SSVEP amplitude in 8 example participants. Axes are the same as panel A. Red, blue, and green lines indicate difference in chromatic contrast conditions. Shaded area shows 95% confidence interval by bootstrap analysis.

differences in its shape, as it was observed in the previous study [3]. The results of full condition were used in the fitting analysis.

The results of perceptual data are shown in Figure 4. The results for saliency have sharp dip in 90º and 270º, which corresponds to the direction of S-cone selective axis. Since the saliency stimulus was flickered at 5 Hz, the responses to L- and M-cones were more prominent than the S-cone. This tendency was commonly found in all participants result. The saturation results show a small dip at 115º (Fig.4B) and brightness results show a dip around 300º (Fig.4C). as the distribution of thin lines represent, the brightness profile showed slightly larger individual differences than other perceptual profiles.

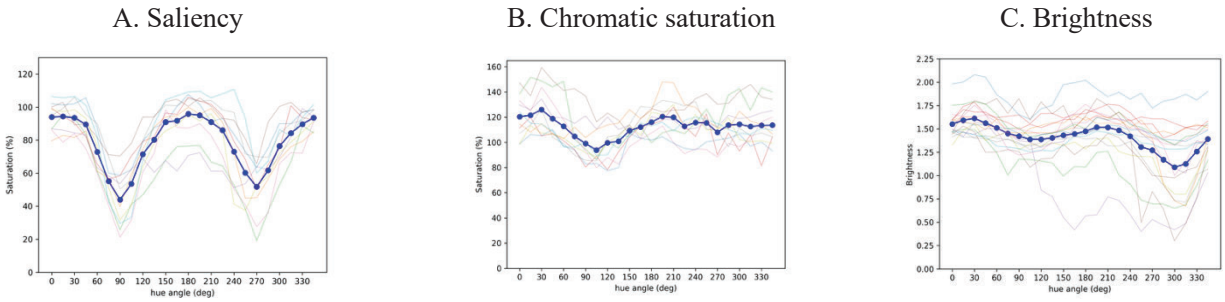

Figure 4. Results of perceptual experiments. The horizontal and vertical axes indicate hue angle and relative intensity, respectively. A-C. Thick lines with symbol indicate mean, and thin lines indicate individual data.

The result of fitting mean SSVEP curve with a linear combination of mean perceptual data alone was not bad, but not remarkable $R^2 = 0.78$ (not shown). The fitting with perceptual data alone was conducted in each participant and the goodness of fit was drastically different across participants; R^2 values ranged between 0.07 to 0.89 (horizontal axis in Figure 5B). Although SSVEP hue selectivity is known to include cone-opponent responses [3], our perceptual data did not include cone-opponent factors, in particular corresponding to S-cone responses. Therefore, we added cone-opponent models using rectified cosine function, each of which was centered at the L-M or S axis. The R^2 value improved to 0.97 for the average data (Figure 5A), and individual data also showed remarkable improvement: the R^2 value ranged between 0.21 to 0.89 (vertical axis in Figure 5B). The participants

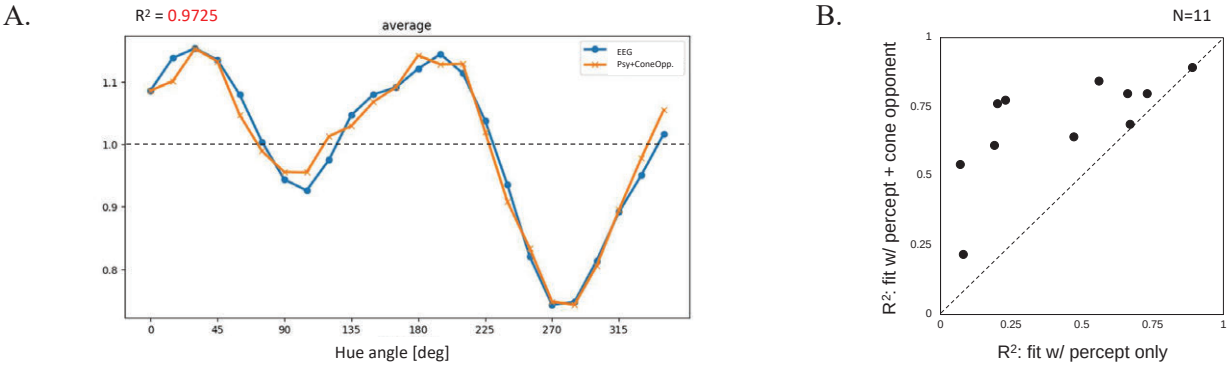

Figure 5. Curve fits improved by combining perception data and cone-opponent models. A. Grand mean curve of SSVEP amplitude (N=11) fit with perceptual data (Fig.4) and cone-opponent models. Horizontal and vertical axis represent hue angle and relative intensity, respectively. Blue circle symbols represent SSVEP amplitude profile. B. Improvement of R^2 values in each participant (N=11). Horizontal and vertical axes represent R^2 for fitting with perception only and that with perception and cone-opponent models (panel A), respectively. Each symbol represents individual R^2 value.

with best R^2 values did not improve much, indicating that this participants SSVEP profile was mostly accounted for by the linear combination of perceptual data alone.

Next, we applied multiple regression analysis to avoid the collinearity among the models used for fitting. After the variance inflation factor (VIF) was evaluated, the perceptual flicker-saliency profile (Fig.4A) had high correlation with cosine-based cone-opponent channels (+L-M and -L+M) in most participant. We tested the models by changing the combinations of three perceptual models, +L-M, -L+M, +S and -S models. We also tested the model by fixing the relative contributions of positive and negative part of the cone opponent channels or by treating them independently. The optimal model was evaluated with AIC. Finally, the most compact model with reasonable R^2 value comprised two perceptual models (brightness and saturation; Figs.4B & 4C) with two cone-opponent models, L–M and +S, where L–M implies a bipolar model with symmetric weight of +L–M and –L+M models. The weight for brightness model was the highest, on average (Table 2).

The principal component analysis (PCA) was applied on the fitting results of optimal model, and it revealed the presence of two types of participant groups. One group showed higher weight on brightness and +S models, while another group showed highest weight on brightness and L/M model (Table 2), but both groups showed high positive weight on the brightness model.

Table 2. Optimal model parameters

	Perception models		Cone-opponent models	
	Saturation	Brightness	+S	L/M
Grand mean (N=11)	**-0.204**	**0.564**	**-0.115**	**0.192**
"Percept" group mean	0.189	0.559	1.05	-0.425
"Cone-opponent" group mean	-0.754	0.529	-0.804	0.579

The results of SSVEP amplitude profile exhibited larger error ranges (95% confidence intervals after bootstrap) in our data. This was possibly because the recording environment was noisier than the previous study [3]. The recordings in our previous study [3] were conducted in an electromagnetic shielded room, while data for this study was obtained in a tiny shield by covering the recording booth with a radio-frequency-shielding cloth.

Among the participants, there were two groups in the relative contribution of the two models (perceptual and cone-opponent models), whether the relative contribution of cone-opponent model was higher or lower. The mixed contribution of the cone-opponent (approx. 40%) and perceptual (approx. 60%) mechanisms was found in the study of Kaneko et al. [3] and our result is in line the previous study. The analysis of fitting parameter revealed that the brightness was commonly significant as a factor that possibly contributed to the hue selectivity profile of the SSVEP. The causes of difference between the two groups are not clear. In future study, we would like to clarify the cause of these individual differences by increasing the number of participants.

CONCLUSION

To conclude, we have successfully replicated the measurement of hue selectivity profile in SSVEP responses. The perceptual profile of hue selectivity was also measured from the same participants (N=11) and the curve fitting was applied together with cone-opponent models. The fitting results showed high R^2 values with the highest weight for the brightness perception, on average. Individual differences in the contribution of these factors should be studied in future by adding a greater number of participants.

ACKNOWLEDGEMENTS

This study was supported by JSPS Grant-in-Aid for Scientific Research (KAKENHI) Nos.20H00597 and 24H00702 to IK.

REFERENCES

[1] De Valois, R. L., De Valois, K. K., Switkes, E., & Mahon, L. (1997). Hue scaling of isoluminant and cone-specific lights. Vision Research, 37(7), 885-897.

[2] Webster, M. A., Miyahara, E., Malkoc, G., & Raker, V. E. (2000). Variations in normal color vision. II. Unique hues. Journal of the Optical Society of America A, 17(9), 1545-1555.

[3] Kaneko, S., Kuriki, I., & Andersen, S. K. (2020). Steady-state visual evoked potentials elicited from early visual cortex reflect both perceptual color space and cone-opponent mechanisms. Cerebral Cortex Communications, 1(1), tgaa059.

[4] Kaneko, S., Kuriki, I., Andersen, S.K., & Peterzell, D.H. Individual variability in steady-state VEP responses for hues sweeping around cardinal color axes: clues to cortical color coding? Journal of Vision (in press)

[5] Kuriki, I., Sun, P., Ueno, K., Tanaka, K., & Cheng, K. (2015). Hue selectivity in human visual cortex revealed by functional magnetic resonance imaging. Cerebral Cortex, 25(12), 4869-4884.

[6] Akaike, H. (1974), "A new look at the statistical model identification", IEEE Transactions on Automatic Control, 19 (6): 716–723,

From Pixels to Perception: Reverse-Engineering RGB Images to Simulate Moth Responses to Artificial Light

Aiman Raza[a], Adrien Lucca[b]*

[a]Lyon Neuroscience Research Center, Waking Team, Inserm UMRS 1028, CNRS UMR 5292, France

[b]Studio Adrien Lucca, LMNO, Brussels, Belgium

*Corresponding author: Adrien LUCCA, projects@adrienlucca.net

ABSTRACT

Artificial light at night (ALAN) from LED installations is a major source of light pollution, with adverse consequences for human health and biodiversity. Nocturnal Elephant hawkmoths, depend on the UV information present in natural twilight to navigate, pollinate and feed. This study proposes a model to simulate moth color vision to visualize the impact of ALAN using UV spectral imaging and colorimetry. Firstly, using a UV reflectance database of 3000+ samples, arranged as a KD Tree structure, we map reflectance spectra under twilight to CIELAB colors of human RGB images. Secondly, we combine UV spectral irradiances of twilight and moth photoreceptor sensitivities to create 3D UV-Blue-Green (UVBG) images. Finally, with the help of a customized UVBG to CIE XYZ transformation matrix, we create corresponding moth CIE XYZ images and sRGB images. These steps are repeated for twilight polluted with LED to compare the color appearance of the same space under different illuminants. Resulting images reveal that LED-polluted twilight scenes cause significant loss of UV-based contrast at floral edges and petal centers, reduce chromatic richness, and oversaturate non-UV regions, potentially impeding flower detection, landing, and navigation in dim light. Our findings highlight the magnitude of perceptual changes introduced by LED light pollution for moths, underscoring the ecological risks of ALAN and motivating future research incorporating moth-specific visual ecology.

Keywords: insect color vison, UV spectral reconstruction, LED light pollution, art-science symbiosis

INTRODUCTION

Lighting installations have been part of human life for ages, from the era of oil lamps to the present LED era. The presence of artificial light in dimly lit situations enhances human color vision and allows us to continue our activities in conditions where the under-activation of our cone photoreceptors would otherwise hinder task execution. With the advent of cost-effective LED lamps, more and more dim spaces are brightly illuminated for longer hours. Energy savings continue to motivate various public entities to retrofit older lamps with energy-efficient LED alternatives.

This phenomenon has also led to a rapid increase in Artificial Light at Night (ALAN). An estimated 80% of the world's population now lives under a light-polluted sky [1]. It has become a significant scientific and environmental concern closely tied to rapid technological growth. This is not only limited to urban areas, as rural regions are also affected by light pollution from road networks among other installations. Light pollution

deteriorates the natural dark sky essential for astronomical research, has direct consequences on human health, and further alters reproductive cycles and migratory patterns in animals [2].

This has (fortunately) led to a significant increase in scientific interest in studying the evolution of light pollution, characterizing it, and identifying its impact on humans, animals, and biodiversity. The StudioTopia 2.0 How to Look at Looking is a European project focused on the effects of light pollution on insect species, specifically the vision of Deilephila elpenor, commonly known as the elephant hawk moth. It is part of the larger StudioTopia 2.0 initiative, which brings together scientists and artists from across Europe to create artworks based on scientific research. The consortium's objective is to raise public awareness and propose possible solutions to global challenges facing the planet. For clarity, in this article, the "elephant hawk moth" will be referred to simply as "moth."

This study aims to simulate moth vision using adapted radiometry and colorimetry functions. The objective is to shift the human-centric perspective of visualizing spaces toward a moth's viewpoint, in order to assess the impact of LED light pollution on their vision. Moths are nocturnal insects, mainly active during twilight hours (sunset to sunrise), with highly developed low-light color vision that contrasts with human vision [3]. They inhabit a wide range of environments, from grasslands and forests to countryside and urban gardens, which also increases their exposure to ALAN during crucial feeding hours. Like humans, moths are trichromats, but their sensitivity is shifted toward shorter wavelengths: Ultra-Violet (UV, peak at 340 nm), Blue (peak at 440 nm), and Green (peak at 520 nm) [3].

To mimic moth color vision, our approach uses simulated UV–Visual hyperspectral images under various light sources to model moth spectral sensitivities and render them in an adapted UV–Blue–Green color space. The goal is to re-visualize human spaces from a moth's perspective by substituting human photoreceptors with moth photoreceptors, thereby generating moth-adapted images of these environments.

METHODOLOGY

Color imaging is a useful tool for capturing human color perception under real light sources while considering spatial context. To accurately simulate human vision of the same scene under different lighting conditions, a hyperspectral reflectance image of the scene in the range of human vision (~380–780 nm) is required. Using light source spectra (in spectral radiance/irradiance) together with CIE color matching functions, one can efficiently reproduce how the same scene would appear under different lighting.

Using the same principle, moth vision can be simulated with a hyperspectral reflectance image of the scene in the moths' visual range (300–700 nm), combined with moth photoreceptor spectral sensitivities and the desired light source in spectral irradiance/radiance. Moth photoreceptor sensitivities have been established through spectrophotometric analysis of their eyes [4]. Point measurements of light sources are also widely available across a broad spectrum, including UV content.

Unlike for humans, however, spectral images of moth-relevant environments within their detectable range are scarce, since most datasets cover only the visible or near-infrared spectra. Creating new UV hyperspectral images presents further challenges due to bulky equipment, high costs, and poor nighttime fidelity. While point-based spectral measurements of object colors are publicly available, full spectral image sets are not.

Although moths are trichromats, they are not sensitive to red (long) wavelengths, just as humans are not sensitive to UV. This makes creating UV-inclusive images that remain interpretable for humans especially difficult. Still, moths and humans do share green and blue channels, even if their ordering and amplitudes differ.

We propose the following 10-point methodology to address the challenges of simulating human images adapted to moth vision:

1. Compile RGB images of moth-relevant scenes under both daytime and twilight conditions.
2. Assemble a database of single-point reflectance measurements of flowers, leaves, and other objects.

3. Cross-reference the RGB image colors with the reflectance database (under a chosen light source) using efficient data-structuring methods.
4. Generate a spectral image of the scene by substituting the corresponding spectral data for each RGB pixel.
5. Multiply the spectral reflectance image by target illuminant irradiances (daylight/twilight) to obtain a spectral irradiance image.
6. Multiply and integrate this spectral irradiance image with moth photoreceptor sensitivities to form a three-dimensional image in UV, Blue, and Green components.
7. Construct a transformation matrix that maps moth UV-Blue-Green components to CIE XYZ under a white daylight source.
8. Apply this matrix to create the moth-equivalent XYZ image.
9. Perform a chromatic adaptation transform on the XYZ image and convert it into sRGB for visualization.
10. Repeat steps 5–9 with artificial light sources to compare moth color vision under natural light versus ALAN-polluted conditions.

RGB image compilation

An RGB image database of over 40 late-evening and nighttime scenes containing flowers, leaves, vegetation, and other objects was compiled from publicly available datasets and supplemented with images from the authors. Care was taken to exclude direct artificial light sources, allowing the simulation of natural light images with the possibility of later superposing artificial light. A selection of five such images is shown in Figure 3 (top row). The first column depicts a scene under sunlight, while the others are under twilight.

Reflectance and light source database compilation

The publicly available FReD (Floral Reflectance Database), containing 2,162 flower reflectance samples in the 300–700 nm range, was used for this study [5]. To complement this dataset with other objects (leaves, stones, clay, etc.), the authors measured and compiled about 1,025 additional reflectance samples within the same spectral range. The reflectances of theses samples with corresponding RGB colors (under daylight) are shown in Figure 1.

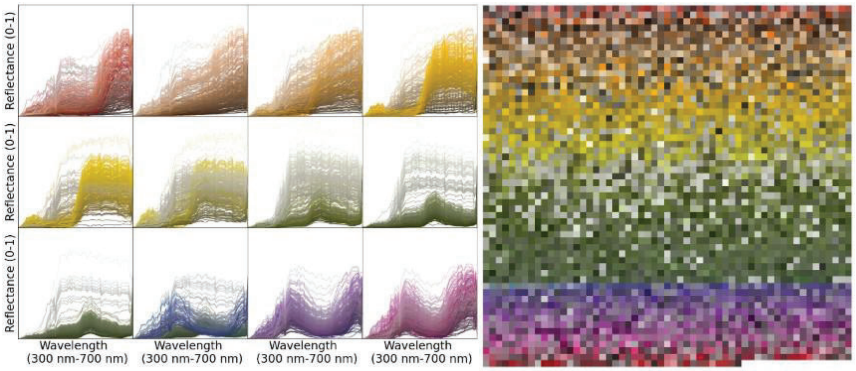

Figure 1, Reflectances of 3187 samples and the corresponding RGB color palette (under daylight)

The authors also collected spectral irradiance data for three light sources: sunlight, twilight [6], and LED. These spectra were measured in the 300–700 nm range and are shown in Figure 2, along with their corresponding colorimetric values calculated using the CIE 2-degree CMFs.

UV-hyperspectral image creation using the spectral dataset and the test RGB image

The spectral database was converted into a spectral irradiance dataset by multiplying it with the source illuminant (sunlight or twilight). These spectra were then transformed into CIELAB colors, and entries with identical values (due to metamerism) were removed to reduce redundant calculations. The resulting CIELAB dataset was organized into a K-Dimensional Tree (KD-Tree) structure to enable fast and accurate spatial searches. The KD-Tree partitions CIELAB data in Euclidean space by recursively splitting along alternating axes, arranging the data hierarchically into sub-trees and thereby minimizing computational time for nearest-neighbor searches. All processes in this work were implemented in Python on a Dell Precision 5480 with 32 GB RAM and a 13th Gen Intel Core i7-13800H 2.50 GHz processor, without GPU support.

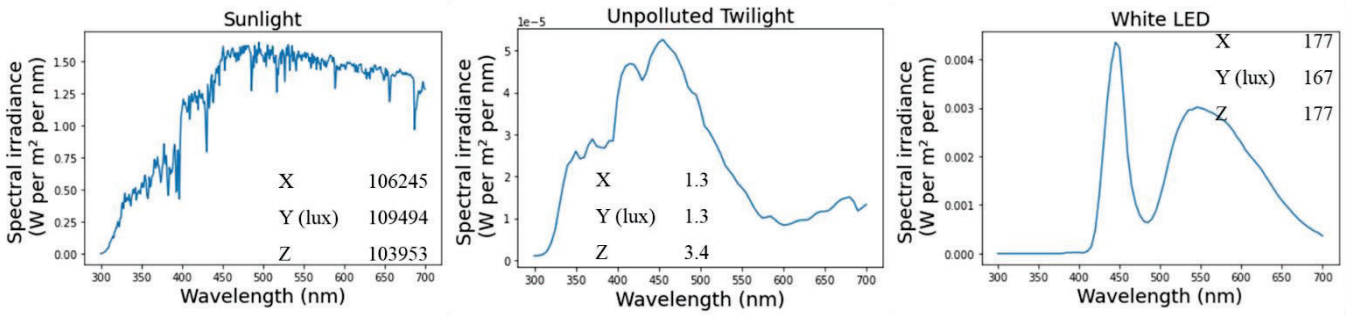

Figure 2, Spectral irradiances of the three tested light sources with their colorimetric coordinates

The test RGB image was converted into CIELAB colors, and only unique values were retained. Each unique CIELAB color was then matched to an irradiance spectrum through a CIE ΔEab* space search on the KD-Tree. The corresponding reflectance spectrum for each pixel was used to reconstruct a spectral reflectance image, while preserving the original pixel organization. This spectral image was further used to generate a reflectance irradiance image under with the desired light source.

Moth photoreceptor and adapted human color simulation

The resulting spectral images for the source and target illuminants were converted into a UV-Blue-Green (UVBG) 3D image by multiplying and integrating the moth spectral sensitivities with the irradiance data, analogous to the process used for humans with CIE LMS sensitivities.

To simulate a corresponding human CIE XYZ image from the moth UVBG image, a color transformation matrix was implemented using the CIE XYZ (10-degree) color matching functions and moth spectral sensitivities under sunlight. The procedure followed the same steps as those used to construct a matrix for transforming a human LMS image into a CIE XYZ image under D65 illumination.

To achieve this, the moth spectral sensitivities were first scaled to the CIE XYZ CMFs so that both moth and human had the same total energy. The transformation matrix was then calculated by mapping the moth Blue channel to CIE Z, the Green channel to CIE Y, and the UV channel to CIE X. This mapping was obtained by computing the inner product of the respective channels using the trapezoidal rule. Finally, the matrix was normalized to ensure identical color responses for humans and moths when viewing a perfect diffuser illuminated by sunlight. The resulting 3×3 color transformation matrix, which maps the moth UVBG image to the human XYZ image, is presented in Eq. 1.

$$\begin{bmatrix} X^{human_adapted} \\ Y^{human_adapted} \\ Z^{human_adapted} \end{bmatrix} = \begin{bmatrix} 1.1839 & 0.0757 & 0.6412 \\ 0 & -0.3438 & 1.2731 \\ 0 & 1.4212 & -0.0216 \end{bmatrix} * \begin{bmatrix} UV_{moth} \\ G_{moth} \\ B_{moth} \end{bmatrix} \quad (1)$$

Moth RGB image creation adapted to humans

Finally, the color transformation matrix was applied to the UVBG image, generated from the spectral irradiance data (source and target illuminants) and moth spectral sensitivities. The resulting XYZ image was then chromatically adapted to D65 and converted into sRGB for human visualization.

RESULTS AND DISCUSSION

Figure 3 shows the tested human RGB images (top row) and their corresponding simulated moth vision under natural light (middle row). The bottom row presents the equivalent moth images under natural light polluted with an LED source. Figure 3-1A, taken under sunlight, is included for reference only. Because the energy of the LED illuminant is much lower than that of sunlight, no perceptible difference is observed between the sunlight-only moth image (1B) and the sunlight-plus-LED image (1C).

For the other cases, however, clear differences emerge when comparing the twilight-only moth images with those under twilight polluted by LED light. Since twilight (1.3 lux) has far lower energy than LED (167 lux), the UV portion of the spectrum is effectively overshadowed by the non-UV components. Although UV information is still theoretically present, the much higher intensity of the non-UV spectra renders it imperceptible, as the LED's spectral energy distribution strongly favors the human-visible range. In image 2B, the purple flowers, which contained both UV and Blue components, appear only bluish, having lost their UV information and thus altering their color appearance for moths. In image 3B, the dark red flowers that reflected UV lose all UV information; since moths cannot perceive red, the flowers now appear black. The smaller pink-violet flowers with leaves also lose contrast along their UV-reflecting edges and become largely monochromatic (blue).

In image 4B, the UV-reflecting edges of the flower similarly become monochromatic due to UV loss, which may hinder moths' ability to detect or land on the petals. Images 5B and 6B appear very dark but still contain significant UV information mixed with non-UV regions. However, the amplification of the non-UV areas reduces chromatic contrast across the scene. Additionally, the approximately 120-fold increase in total energy under polluted lighting makes these scenes appear much brighter and more saturated than under twilight alone, potentially disturbing the high sensitivity of moths in dim environments.

Figure 3, (top) Human RGB images, (middle) corresponding moth images in natural light, (bottom) corresponding moth images in polluted natural light

CONCLUSION

The rapid increase in the installation and use of artificial LED lighting has significantly raised light-pollution levels, disrupting not only human health but also biodiversity. Most insects, including moths, are highly sensitive to the UV range of the spectrum. They rely on UV photoreceptors for navigation in the dark and for locating UV-rich floral regions. The strong amplification of non-UV light from LEDs may suppress essential UV information.

This study presents a model to simulate moth UV-Blue-Green vision by substituting human LMS photoreceptors and recreating human scenes under different light sources, in order to visualize the impact of ALAN—particularly LEDs—on moth vision. Under polluted twilight, moth images show significant loss of contrast at petal edges (important for landing) and centers (important for pollination), making their color appearance markedly different from that under natural twilight. Increased saturation of achromatic content may also disturb moth navigation.

Despite the model's usefulness, it retains human bias, particularly in the derivation of the UVBG-to-XYZ transformation matrix, the use of chromatic adaptation, and the reliance on human spatial acuity. Addressing these issues was beyond the scope of this study, which aimed instead to explore how human spaces might appear if viewed through moth photoreceptors. Future research incorporating moth-specific chromatic adaptation, color acuity, and field of view could yield deeper insights into the impact of light pollution on moth vision. The results nevertheless demonstrate that polluted twilight severely alters visual information for moths: UV content and color contrast are diminished, while achromatic saturation is exaggerated.

ACKNOWLEDGEMENTS

We would like to thanks StudioTopia 2.0 and GLUON art Gallery, Brussels, Belgium for the financial and material support provided to the authors.

REFERENCES

[1] Falchi F, Cinzano P, Duriscoe D, Kyba C C M, Elvidge C D, Baugh K, Portnov B A, Rybnikova N A and Furgoni R 2016 The new world atlas of artificial night sky brightness Sci. Adv. **2** e1600377

[2] Linares Arroyo H, Abascal A, Degen T, Aubé M, Espey B R, Gyuk G, Hölker F, Jechow A, Kuffer M, Sánchez De Miguel A, Simoneau A, Walczak K and Kyba C C M 2024 Monitoring, trends and impacts of light pollution Nat. Rev. Earth Environ. **5** 417–30

[3] Kelber A, Balkenius A and Warrant E J 2002 Scotopic colour vision in nocturnal hawkmoths Nature **419** 922–5

[4] Schwemer J and Paulsen R 1973 Three visual pigments inDeilephila elpenor (Lepidoptera, Sphingidae) J. Comp. Physiol. **86** 215–29

[5] Arnold S E J, Faruq S, Savolainen V, McOwan P W and Chittka L 2010 FReD: The Floral Reflectance Database — A Web Portal for Analyses of Flower Colour ed M Giurfa PLoS ONE **5** e14287

[6] Spitschan M, Aguirre G K, Brainard D H and Sweeney A M 2016 Variation of outdoor illumination as a function of solar elevation and light pollution Sci. Rep. **6** 26756

A Study on A Plant Disease Symptom Recognition System Based on The Fusion of Color Space and Deep Feature Representations

Chih-Shun Hsu[a*], Mei-Chun Lo[b], and Zheng-Hao Liu[c]

[a]Shih Hsin University, Taipei, Taiwan
[b]Shih Hsin University, Taipei, Taiwan
[c]Shih Hsin University, Taipei, Taiwan
[*]Corresponding author: Chih-Shun Hsu, cshsu@mail.shu.edu.tw

ABSTRACT

With the rapid growth of machine learning, early plant disease detection has shown strong potential. While hyperspectral imaging provides rich information, its cost and complexity limit field applications. This study explores whether consumer-grade RGB images can achieve accurate disease recognition and proposes a framework combining LCH color space transformation and deep learning. To reduce illumination and background interference, LCH conversion and background removal (Rembg) were applied. Using the Plant Pathology 2020-FGVC7 and 2021-FGVC8 datasets, models such as EfficientNetV2 and Swin ViT were evaluated with color space and augmentation strategies. Results indicate that the proposed framework enhances accuracy and stability, offering a low-cost, non-invasive solution for plant disease monitoring and valuable insights for smart agriculture.

Keywords: Deep Learning, Plant Disease, LCH Color Space, CNN Models, Image Preprocessing

INTRODUCTION

Research Background: Plant diseases cause an estimated 20% to 40% reduction in global crop yields each year[1][2], posing a serious threat to food security and agricultural economies. Traditional diagnostic approaches rely heavily on expert knowledge or laboratory testing, which, although accurate, are costly, time-consuming, and impractical for large-scale applications. With the rapid advancement of artificial intelligence (AI) and image recognition technologies, automated plant disease diagnosis has emerged as a promising alternative, offering new solutions for timely and efficient disease management.

Research Motivation: AI-powered image recognition combined with deep learning has demonstrated diagnostic capabilities that match or even surpass human experts, enabling rapid and precise detection of symptoms such as leaf spots, discoloration, and texture changes[6]. This is particularly valuable in agricultural scenarios requiring large-scale, real-time analysis. However, existing approaches still face challenges, including sensitivity to illumination, visual similarity between different diseases, and limited model generalization. Addressing these issues is critical to developing fast, cost-effective, and accurate diagnostic tools that can advance the practice of smart agriculture.

Research Objectives: This study focuses on overcoming the limitations of consumer-grade RGB imagery in plant disease identification. By introducing CIE LCH color space transformation[4], background removal, and image augmentation techniques, and integrating them into deep learning frameworks, the study aims to mitigate problems such as lighting variations, disease feature similarity, and environmental noise. The ultimate goal is to

establish a low-cost yet accurate plant disease recognition system that can provide practical and reliable support in real-world agricultural settings, thereby contributing to the advancement of smart farming practices.

METHODOLOGY

This study aims to establish a plant disease symptom recognition system through the integration of image preprocessing and deep learning models. The overall workflow consists of data preprocessing, model construction, evaluation design, and experimental environment setup, which are described as follows.

Image quality plays a critical role in the performance of deep learning models. To minimize the effects of illumination variation and background interference, and to enhance disease-related features, three preprocessing techniques were applied:

- **CIE LCH Color Space Transformation:** RGB images were linearized, converted into the XYZ and Lab color spaces, and subsequently mapped into the LCH (Lightness, Chroma, Hue) representation. The perceptual uniformity of LCH allows more accurate reflection of human sensitivity to color differences, thereby improving the distinction between diseased and healthy leaf regions (Eq. 1, 2, 3, 4, 5).

$$\begin{bmatrix} X \\ Y \\ Z \end{bmatrix} = \begin{bmatrix} 0.4124 & 0.3576 & 0.1805 \\ 0.2126 & 0.7152 & 0.0722 \\ 0.0193 & 0.1192 & 0.9505 \end{bmatrix} \cdot \begin{bmatrix} R_{\text{lin}} \\ G_{\text{lin}} \\ B_{\text{lin}} \end{bmatrix} \tag{1}$$

$$f(t) = \begin{cases} t^{1/3}, & \text{若} t > \left(\frac{6}{29}\right)^3 \\ \frac{1}{3}\left(\frac{29}{6}\right)^2 t + \frac{4}{29}, & \text{若} t \le \left(\frac{6}{29}\right)^3 \end{cases} \tag{2}$$

$$L^* = 116 \cdot f\left(\frac{Y}{Y_n}\right) - 16 \tag{3}$$

$$a^* = 500 \cdot \left[f\left(\frac{X}{X_n}\right) - f\left(\frac{Y}{Y_n}\right) \right]$$

$$b^* = 200 \cdot \left[f\left(\frac{Y}{Y_n}\right) - f\left(\frac{Z}{Z_n}\right) \right]$$

$$C^* = \sqrt{a^{*2} + b^{*2}} \tag{4}$$

$$h^{\circ} = \begin{cases} \arctan\left(\frac{b^*}{a^*}\right), & \text{if } \arctan\left(\frac{b^*}{a^*}\right) \geq 0 \\ \arctan\left(\frac{b^*}{a^*}\right) + 360^{\circ}, & \text{otherwise} \end{cases} \quad (5)$$

- **Rembg Background Removal:** A deep learning–based tool (Rembg)[3] was employed to remove non-leaf regions from images. This process reduces background interference and focuses the analysis on leaf symptoms.
- **HSV Color Space Transformation**: Images were transformed into the Hue, Saturation, and Value (HSV) space. By applying Hue-based thresholding, diseased and healthy regions were effectively contrasted, enabling candidate lesion extraction for subsequent analysis (Eq. 6, 7).

$$V = C_{\max}, \qquad S = \begin{cases} 0, & C_{\max} = 0, \\ \frac{\Delta}{C_{\max}}, & C_{\max} > 0. \end{cases} \quad (6)$$

$$H = \begin{cases} 0, & \Delta = 0, \\ 60^{\circ} \times \mathrm{mod}\left(\frac{g-b}{\Delta}, 6\right), & C_{\max} = r, \\ 60^{\circ} \times \left(\frac{b-r}{\Delta} + 2\right), & C_{\max} = g, \\ 60^{\circ} \times \left(\frac{r-g}{\Delta} + 4\right), & C_{\max} = b, \end{cases} \quad H \in [0, 360). \quad (7)$$

Two state-of-the-art models were adopted for classification: **EfficientNetV2**[8] and **Swin Transformer (ViT)**[5]. EfficientNetV2 leverages compound scaling and progressive data augmentation to improve convergence efficiency, while Swin Transformer applies Shifted Window Attention to enhance long-range dependency modeling. Both models were evaluated using raw RGB inputs and color-transformed inputs for comparative analysis.

The evaluation methodology and experimental design consist of the following:

- **Dataset Partitioning:** The experiments employed the **Plant Pathology 2020-FGVC7** and **2021-FGVC8** datasets. Data were partitioned into training, validation, and test sets at fixed ratios to ensure fair evaluation.
- **Evaluation Metrics:** The performance of the models was assessed using **Accuracy, Precision, Recall, F1-Score**, and **AUROC**. A confusion matrix was additionally applied to verify classification outcomes.
- **Experimental Design:** A comparative study was conducted on preprocessing variations (RGB, LCH, Rembg, and All). The influence of data augmentation strategies and class imbalance handling on model robustness was further investigated.

All experiments were executed on a workstation equipped with an **Intel i9 CPU, NVIDIA RTX 4070 Ti GPU, and 32GB RAM**. The software environment comprised **Python 3.11, PyTorch 2.x**, and related deep learning libraries (timm, torchvision, pytorch-lightning).

RESULTS AND DISCUSSION

A comparative evaluation was conducted across different input color spaces (RGB and CIELCH) and model architectures (Swin ViT and EfficientNetV2), and the specific experimental group results are summarized as follows:

- **Convergence Evaluation of Training With and Without LCH Color Space Transformation (Experimental Group 1) :**

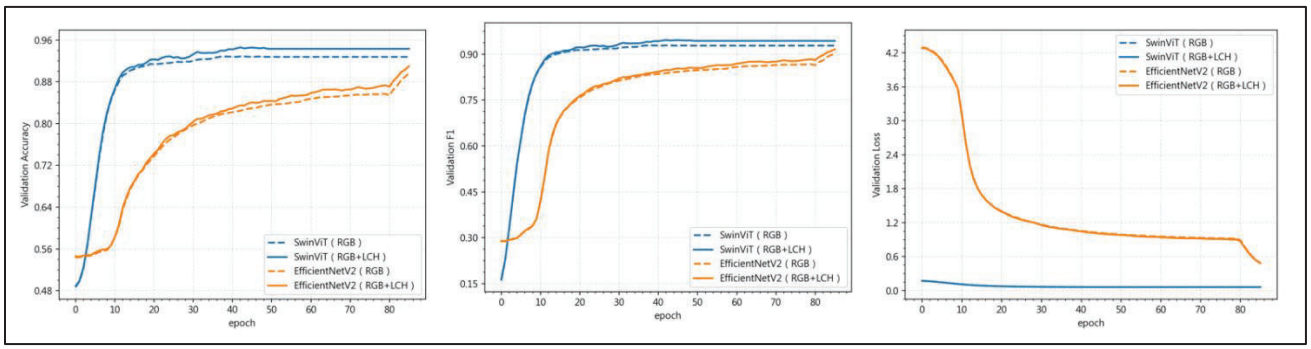

Figure 1: RGB vs. with LCH Integration

- **Convergence Evaluation of Training With and Without Background Removal (Experimental Group 2) :**

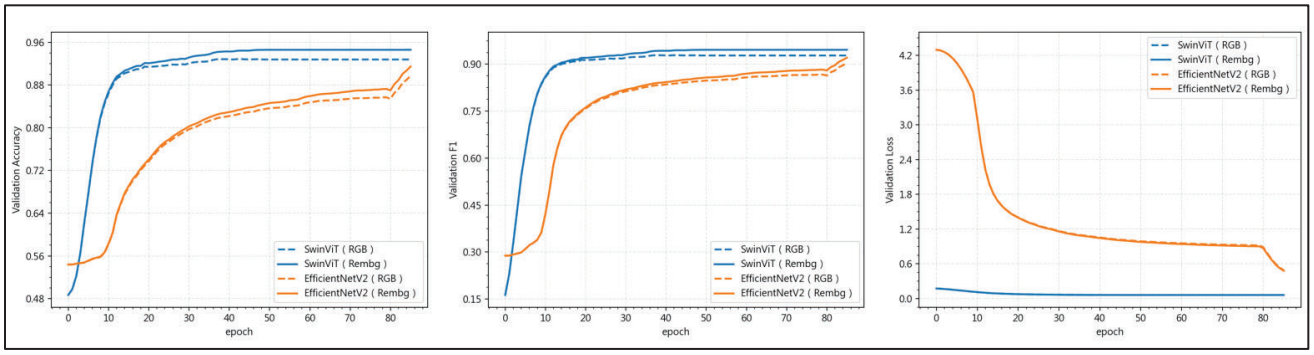

Figure 2: RGB vs. After Rembg Processing

- **Convergence Analysis of Training Incorporating LCH and Background Removal (Experimental Group 3) :**

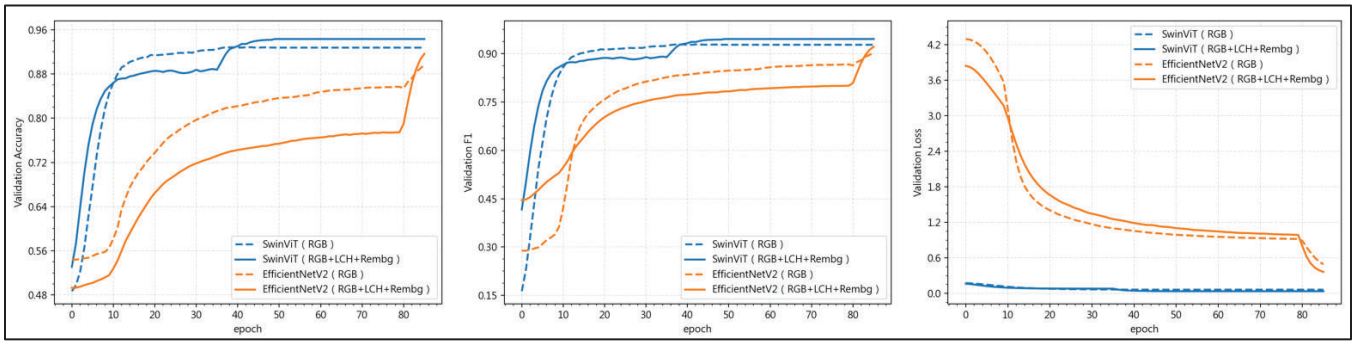

Figure 3: RGB vs. All Processing Methods

Although the HSV color space–based calculation of symptom severity is not used as the primary criterion for classification decisions, it can serve as a supplementary descriptor and quantitative representation of symptom color characteristics within the diagnostic system.

Symptom feature extraction was conducted using the HSV color space, which enables effective quantification of color types and distribution differences. Compared with the traditional RGB color space, HSV provides a more intuitive representation of color and is more consistent with human visual perception, thereby offering greater interpretability in diagnostic applications. The analysis results indicate that, as shown in Figure 4, plant diseases exhibit more pronounced variations in the Hue and Value dimensions of the HSV color space.

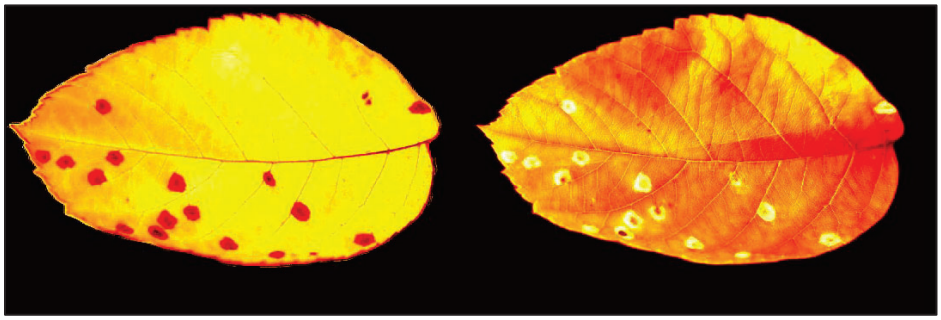

Figure 4: Hue(Left), Value(Right)

The current threshold settings for HSV-based symptom extraction were determined through sampling and analysis of images from the Rocole dataset[7] across different severity levels. Figure 5 illustrates an example of RGB, HSV, and binarized feature extraction images.

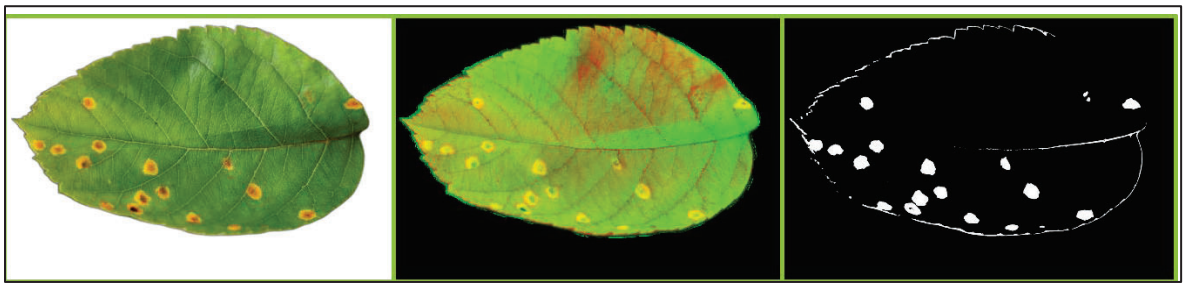

Figure 5: RGB(Left), HSV(Middle), Feature Extraction Binarization(Right)

CONCLUSION

This study proposed a plant disease recognition framework that integrates LCH color space transformation with deep learning models, complemented by Rembg-based background removal and color enhancement techniques. The approach effectively mitigates the sensitivity of RGB images to illumination and background variations, leading to improved convergence speed, classification accuracy, and generalization capability. Experimental results demonstrated that both EfficientNetV2 and Swin Transformer achieved significant performance gains when combined with color space conversion and preprocessing, confirming the feasibility of using consumer-grade imagery for reliable plant disease detection. Furthermore, the incorporation of HSV-based feature extraction enabled quantitative analysis of disease severity, establishing a unified framework for both recognition and severity assessment. Overall, the findings highlight the potential of combining color space fusion and deep feature

representations for smart agriculture, providing a foundation for the development of low-cost and automated plant disease monitoring systems.

REFERENCES

[1]. FAO (2019). Moving Forward on Food Loss and Waste Reduction. Food and Agriculture Organization.

[2]. FAO (2023). Annual Report 2022- Plant Production and Protection. Food and Agriculture Organization.

[3]. Gatis, D. (2025). Rembg Is a Tool to Remove Images Background. https://github.com/danielgatis/rembg

[4]. Internationale Beleuchtungskommission (2004). Colorimetry. International Commission on Illumination

[5]. Liu, Z., Lin, Y., Cao, Y., Hu, H., Wei, Y., Zhang, Z., Lin, S., and Guo, B. (2021). Swin Transformer: Hierarchical Vision Transformer Using Shifted Windows. https://doi.org/10.48550/arXiv.2103.14030

[6]. Mohanty, S. P., Hughes, D. P., and Salathé, M. (2016). Using Deep Learning for Image-Based Plant Disease Detection. Front. Plant Sci., 7, 1419.

[7]. Parraga-Alava, J., Cusme, K., Loor, A., and Santander, E. (2019). RoCoLe: A Robusta Coffee Leaf Images Dataset for Evaluation of Machine Learning Based Methods in Plant Diseases Recognition. Data in Brief , 25, 104414.

[8]. Tan, M. and Le, Q. V. (2021). EfficientNetV2: Smaller Models and Faster Training. https://doi.org/10.48550/arXiv.2104.00298

Testing Colour Harmony Model for Personal Colour Analysis

Punnaphat Sirisayan*, Suchitra Sueeprasan

Department of Imaging and Printing Technology, Faculty of Science, Chulalongkorn University, Bangkok, Thailand
*Corresponding author: Punnaphat, pok.punnaphat@gmail.com

ABSTRACT

In today's society, where first impressions are formed within seven seconds, clothing plays a crucial role alongside physical appearance and body shape in creating favourable judgements. Whilst dressing well can enhance one's appearance and confidence, the suitability of attire varies considerably between individuals, with skin colour serving as a key determinant of whether clothing colours complement the wearer. This complex relationship between skin colour and clothing colour has led to the emergence of "Personal Colour" analysis, an increasingly popular field that aims to identify appropriate colour choices to enhance appearance, reduce blemishes and dark circles, and boost confidence. Traditional personal colour analysis categorises individuals into four seasonal colour groups (spring, summer, autumn, or winter), each associated with specific colour palettes, and relies on expert analysis involving fabric draping and subjective observation. However, this method is time-consuming, costly, and lacks scientific rigour due to its dependence on individual expert judgement, raising concerns about consistency, accuracy, and reliability. The concept aligns closely with colour harmony theory, which involves combining colours to create balance, visual appeal, and aesthetic pleasure. Whilst a universal colour harmony model has been developed and performed well for general colour samples, it had not been tested specifically for skin tone-colour combinations. To address this gap, an experimental study was designed using fifteen skin tone samples from the Pantone SkinTone Guide, representing both warm and cool undertones, paired with 128 seasonal colour samples (32 per season), creating 1,920 colour pairs in total. Thirty Thai observers (15 male, 15 female) aged between 20 and 40 years evaluated each colour pair's harmony level using a scale from -5 (disharmonious) to 5 (most harmonious) under controlled laboratory conditions. The averaged experimental results were compared with predictions from the universal colour harmony model, revealing poor correlation coefficients when applied to skin colour and seasonal colour combinations. This finding indicates that existing colour harmony models are inadequate for personal colour analysis applications and highlights the need for developing more specific colour harmony models tailored to accurately predict harmonious relationships between skin tones and clothing colours.

Keywords: personal colour, colour harmony model, skin tone, skin undertone, skin colour.

INTRODUCTION

What role does colour play in our daily experiences? Colour serves as a pervasive and informative element in human perception[1]. Research demonstrates that individuals form judgments within 7 seconds[2] to 90 seconds[3] of initial exposure to people or objects, with 62 to 90 percent of these assessments being influenced primarily by colour alone.

Colour harmony and Universal Colour Harmony Model

The interaction of multiple colours generates artistic visual appeal, which relates to psychophysical principles and can be categorized along various emotional dimensions including warm-cool, heavy-light, modern-classical, clean-

dirty, active-passive, and hard-soft spectrums [4]. Colour harmony refers to the extent to which an observer perceives that colours within a combination complement each other and belong together, regardless of whether the observer finds the combination aesthetically pleasing, or alternatively, it can be understood as the viewer's perception of how a foreground colour relates to its background colour. Colour combinations and harmonious colour relationships are ubiquitous in contemporary environments, manifesting in fashion, cosmetics, interior design, advertising, consumer products, and food presentation, with particular prominence in clothing and costume design. Research conducted by Jiang and Cai examined four distinct levels of colour contrast applied to two-piece suit combinations, revealing an inverse relationship between clothing attractiveness and colour contrast intensity [5]. Finally, a universal color harmony model [6] has been developed that incorporates color characteristics such as hue, saturation, and brightness into an equation to predict the color harmony of two colors.

Skin Colour

The question arises: how can we determine whether the clothing colours we wear achieve harmonious compatibility with our individual characteristics according to colour harmony principles? The critical variable in this assessment is skin tone. Human skin colour has garnered increasing research attention in recent years. For instance, the CIE TC1-92 committee, led by Dr. Xiao's research [7], has investigated methodologies for measuring skin colour and elucidating variations in human skin colour measurements obtained through different instrumental approaches. This work has also established appropriate protocols for such measurements, acknowledging that human skin possesses complex physical structural properties.

Personal Colour

The science of predicting which colours will be most suitable for individuals is termed personal colour, providing the foundation for determining which clothing colours truly complement an individual's appearance. The process of identifying these optimal colours is referred to as personal colour analysis, which serves as a methodology for selecting clothing colours that harmony an individual's natural characteristics and enhance facial luminosity and overall aesthetic appeal by placing them into one of four seasonal colour groups: Spring (high lightness, high chroma), Autumn (low lightness, low chroma), Summer (high lightness, low chroma), and Winter (low lightness, high chroma). Each with an appropriate colour palette that aligns with the concept of colour harmony to create balance, visual appeal, and aesthetic pleasure. Nevertheless, achieving optimal colour selection for individuals presents significant challenges. The prevailing analytical approach involves draping colour fabric samples against the client's body for assessment. This methodology faces several constraints, including the requirement for specialised expertise, substantial time investment, and considerable financial cost. Furthermore, personal colour analysis outcomes rely heavily upon expert judgement, which may vary between practitioners or diverge from broader aesthetic consensus, potentially raising questions regarding the consistency, precision, and effectiveness of colour recommendations [8].

This research seeks to develop an alternative approach to personal colour analysis by investigating the relationship between skin tone compatibility and colour harmony principles through evaluating colour harmony for skin tones paired with colours varying in hue, lightness, and chroma, proposing that personal colour selection can be effectively analysed through systematic harmony evaluation that examines how specific colours achieve visual coherence with individual skin tones using collective observer assessments rather than individual expert opinions which lack scientific validation and consistency, with visual assessment results subsequently compared against established colour harmony theoretical frameworks[6] to determine whether specialized colour harmony frameworks specifically designed for personal colour analysis applications are necessary should the empirical findings diverge from predictions based on universal colour harmony models.

METHODOLOGY

Selection of Colour Samples

This research investigated the relationship between between skin tone and colour harmony to define personalised colour. Accordingly, two sets of colour samples were created: one representing various skin tones and the other illustrating customised colour palettes.

1. Skin tone samples: The study employed skin tone specimens from the Pantone SkinTone Guide, which comprises 110 distinct skin colour variations. Spectrophotometric analysis was carried out on all 110 specimens to obtain their CIELAB colour coordinates (D65/2, SCI MAV configuration). Each Pantone SkinTone sample is identified by a four-character alphanumeric code indicating both the undertone and depth of the skin colour. Undertones are categorised into two types: yellow-based (warm undertone) and red-based(cool undertone). Analysis of the ab colour plot revealed that a 60-degree hue angle effectively separates these two undertone categories [9]. In line with personal colour principles, an individual's most flattering clothing and cosmetic shades are determined by their skin undertone. Fifteen representative skin tone samples were chosen (Figure 1), comprising eight with warm undertones and seven with cool undertones.

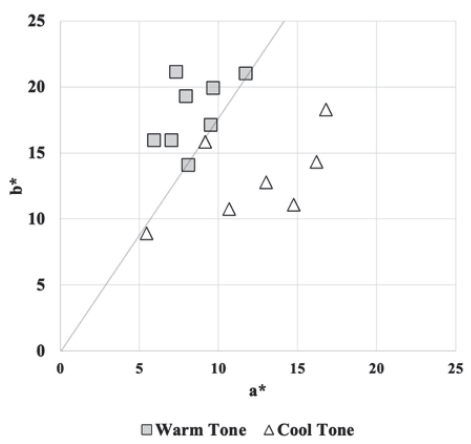

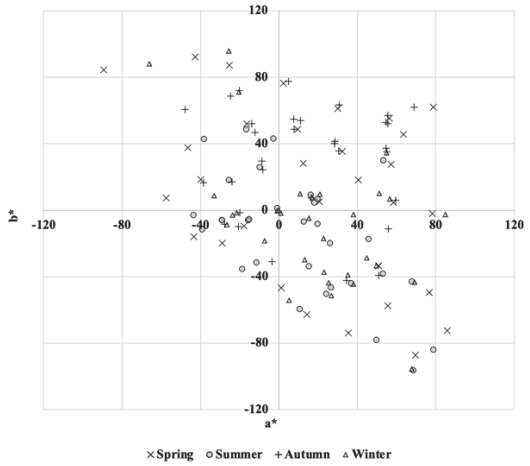

Figure 1: (left) Selected fifteen representative skin tone samples.
Figure 2: (right) Distribution of 128 seasonal colour variations.

2. Colour samples: To examine whether colour harmony assessments could reliably determine individual colour profiles, the colour specimens paired with the skin tone samples needed to represent personal colour categories accurately. According to established personal colour theories, warm hues complement warm undertones, whereas cool hues are more suited to cool undertones. This study adopted the personal colour specimens identified in the research of Kim and Kim [10], which classified personal colours into four seasonal groups: spring, summer, autumn, and winter. Each seasonal group comprised 32 colour variations, giving a total of 128 colours. Figure 2 illustrates the colourimetric distribution of these specimens, hereafter referred to as "seasonal colours."

Visual Experiment

Seasonal colours were paired with corresponding skin tones using single-colour patches measuring 2" × 2.3". Observers viewed the paired samples from 80 cm away, producing a visual angle of approximately 3.58 degrees. The patches were displayed adjacent to one another on a uniform grey background centred on the monitor.

Thirty Thai observers (15 female and 15 male), aged between 21 and 40 years, took part in the visual experiments. All had normal colour vision. Prior to testing, they were introduced to the concept of colour harmony, defined as the degree to which a colour is liked when viewed against a background colour. Observers were instructed to evaluate combinations of human skin tones with other colours using a scale from -5 to -1 for disharmony and 1 to 5 for harmony, with ±5 representing the extremes. Training was provided on how to use the custom software interface designed for displaying colour pairs and recording harmony ratings.

The experimental setup involved observers positioned 80cm from an LCD screen in a darkened room, with a 10-second grey background adaptation period before colour pair presentation. Observers selected the appropriate button to assign a colour harmony rating to each displayed colour pair. Score adjustments were permitted through

alternative button presses provided the "Confirm" button remained unpressed. Subsequently, observers viewed a grey background for 2 seconds to eliminate potential after-image interference before the following colour pair appeared. This procedure (Figure 3) continued systematically until observers had assessed all colour pairs within the session. Each observer encountered the colour pairs in randomised sequence. All observers evaluated 1,920 colour pairs across 6 sessions (320 pairs each), taking 20-40 minutes per session with breaks between sessions. Fifteen observers completed an additional 15-minute repeatability test with 108 pairs.

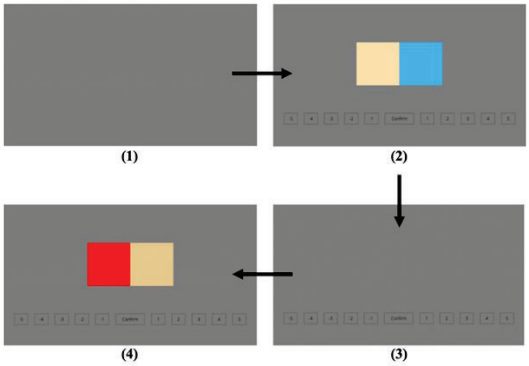

Figure 3: Order of colour pair presentation sequence.

Universial Color Harmony Model

This equation predicts the harmony between two colour pairs by considering the following four factors: hue similarity, chroma similarity, lightness difference, and high lightness [6]. The predicted scores range from negative to positive values. A positive score indicates that the two colour pairs are harmonious, whilst negative values suggest that these colour pairs do not harmonise well together.

This method can determine the correspondence between scores obtained from the assessment termed "Visual result" and the predicted values from the Universal Colour Harmony model (referred to as "Predict value") by plotting a graph of the score values. Through analysis of the r-value or correlation coefficient, the resulting figures indicate the accuracy and consistency between the two datasets. For instance, if r = 1, the assessment score corresponds perfectly with the score predicted by the Universal Colour Harmony Model (100% consistency). Alternatively, if r = 0.5, this indicates that the assessment score corresponds with the Universal Colour Harmony Model's prediction by only 50%.

RESULTS AND DISCUSSION

To examine whether existing colour harmony models possess the capability to predict outcomes for skin tone combinations and subsequently be applied to personal colour analysis applications, comprehensive colour harmony scores for all 1,920 colour pairs were systematically calculated using the Universal Colour Harmony model [6]. Following this calculation process, the correlation coefficient (r-value) was determined to establish and quantify the level of agreement between the model's predicted values and the visual assessment results obtained through this empirical study.

Figure 4 presents the graphical representation plotting the relationship between the predicted values and the visual results, alongside the corresponding r-value measurement. The analysis revealed an r-value of 0.53, indicating that merely 53% of the dataset demonstrated concordance between predicted and observed outcomes. Expressed differently, the Universal Colour Harmony model demonstrated accurate predictive capability for only 53% of colours when paired with various skin tones, leaving nearly half of the predictions unreliable.

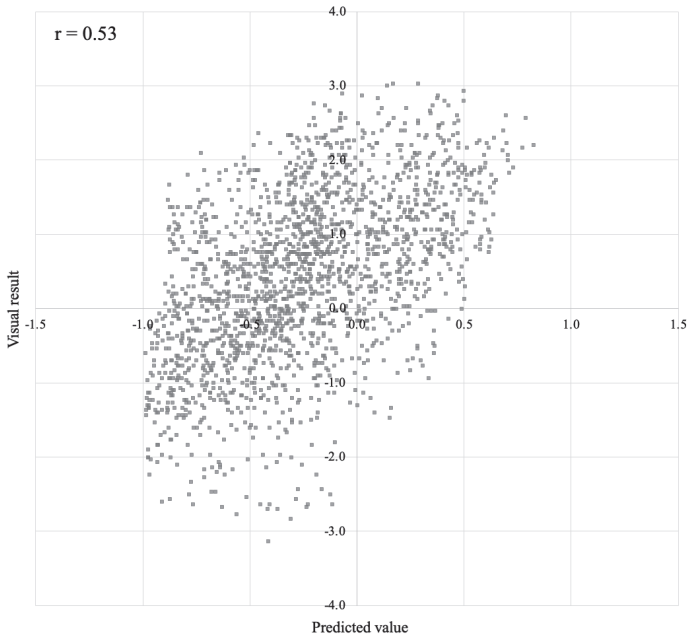

Figure 4: Perceived colour harmony values plotted against predicted values.

From the experimental results, the low r-squared value may be attributable to the following factors: Firstly, human skin colour possesses a complex and three-dimensional structure. In the analysis employing the universal colour harmony equation, only a single colour plate is utilised. Due to the differing properties of the independent variables used in the equation, the obtained r-squared values may be inconsistent. Secondly, observers evaluating colour harmony may perceive the simulated skin colour on the screen as a conventional, single-colour plate. This may result from the observer's tendency to overlook that it represents skin colour. Finally, this may be due to fatigue arising from performing the colour harmony assessment, which requires a considerable amount of time.

This level of predictive accuracy must be regarded as substantially inadequate for practical applications, particularly considering that approximately 50% probability exists for incorrect predictions. Such findings constitute compelling evidence that currently available colour harmony models remain fundamentally unsuitable for personal colour analysis purposes. The results strongly suggest that there exists a critical need for developing a specialised model designed specifically for personal colour analysis applications, one that accounts for the unique characteristics and complexities inherent in skin tone colour harmony relationships.

CONCLUSION

From the correlation coefficient or r-value, which describes the relationship between two datasets in this study, the visual assessment results (Visual result) and the Universal Colour Harmony model's predicted values (Predict value) it was found that the value stood at 0.53, which is considered low. This indicates that the relationship between the datasets can only be explained by 53%. Based on the study results obtained, one can confidently conclude that there should be a specific model designed to predict colour harmony between skin tones and sample colours, in order to achieve greater accuracy in colour harmony prediction.

REFERENCES

[1]. Singh, S. (2006). Impact of color on marketing. Management decision, 44(6), 783-789.

[2]. Wargo, E. (2006). How many seconds to a first impression?. APS Observer, 19(7). https://www.psychologicalscience.org/observer/how-many-seconds-to-a-first-impression (accessed 30 July 2025).

[3]. Ulrich, P. V., Jo Anderson-Connell, L., & Wu, W. (2003). Consumer co-design of apparel for mass customization. Journal of Fashion Marketing and Management: An International Journal, 7(4), 398-412.

[4]. Ou, L. C., Luo, M. R., Woodcock, A., & Wright, A. (2004). A study of colour emotion and colour preference. Part I: Colour emotions for single colours. Color Research & Application, 29(3), 232-240.

[5]. Jiang, X., & Cai, L. (2013). Evaluation of aesthetic response to clothing color combination: A behavioral and electrophysiological study. Journal of Fiber Bioengineering and Informatics, 6(4), 405-414.

[6]. Ou, L. C., Yuan, Y., Sato, T., Lee, W. Y., Szabó, F., Sueeprasan, S., & Huertas, R. (2018). Universal models of colour emotion and colour harmony. Color Research & Application, 43(5), 736-748.

[7]. Xiao, K., Yates, J. M., Zardawi, F., Sueeprasan, S., Liao, N., Gill, L., ... & Wuerger, S. (2017). Characterising the variations in ethnic skin colours: a new calibrated data base for human skin. Skin Research and Technology, 23(1), 21-29.

[8]. Hong, H. R., & Kim, Y. I. (2019). A mobile application for personal colour analysis. Cogent Business & Management. 6(1), 1-11.

[9]. Iranmanesh, B., Gholamianpour, A., Kandi, S. G., Ansari, K., & Asl, M. A. (2017, December 19-21). Brief overview of PANTONE SkinTone Guide chart in CIEL*a*b* color space [Paper presentation]. The 7th International Color & Coating Congress (ICCC2017), Tehran, Iran. https://www.researchgate.net/publication/325286809_Brief_overview_of_PANTONE_SkinTone_Guide_chart_in_CIELab_color (accessed 30 July 2025).

[10]. Kim, M. K., & Kim, M. K. (2016). Correlation between the factors of personal color diagnosis guide and brain wave analysis. Asian Journal of Beauty and Cosmetology, 14(4), 407-416.

An Investigation of Memory Skin Colour in Chinese and Indonesian Observers

Yan Lu[a,b*], Kaida Xiao[a,b], and Arsaika Widasati[a,b]

[a]*University of Leeds, Leeds, UK*
[b]*Leeds Institute of Textiles and Colour, Leeds, UK*
[*]*Corresponding author: Yan Lu, y.lu3@leeds.ac.uk*

ABSTRACT

Memory colour, the phenomenon where familiar objects are recalled with typical colours, has been widely studied for fruits and natural scenes but remains underexplored for human skin. Unlike other objects with relatively stable chromatic properties, skin spans a wide gamut and carries strong perceptual, cultural, and social significance. This study investigated memory skin colour among Chinese (CN) and Indonesian (ID) observers using psychophysical experiments with a memory-matching technique. Twenty-five participants (12 CN, 13 ID) completed two sessions. In Session 1, each observer's cheek skin was measured with a spectrophotometer and compared with their memory-matched reproduction. In Session 2, observers recalled the typical skin colour of four target ethnic groups—Caucasian (East European, CA), Chinese (CN), Southeast Asian (SA), and African (AF)—by adjusting colour patches in CIELAB space. Results of Session 1 showed that both CN and ID observers overestimated lightness; CN observers under-represented redness, while ID observers over-represented yellowness. For the target ethnic groups, memory colour centres deviated more strongly across groups compared to International Skin Spectra Archive (ISSA) averages. The greatest inter-observer variability was found when recalling one's own ethnic group, suggesting that familiarity may increase sensitivity to natural variation. Two-way ANOVA confirmed significant effects of cultural background and target ethnicity on lightness and yellowness perception, but not redness. In conclusion, memory skin colour is systematically biased, with cultural background shaping lightness and yellowness, highlighting distinct perceptual patterns that differ from other familiar objects. The findings provide a valuable dataset across CN and ID populations and have implications for skin tone reproduction in applications such as cosmetics, photography, colour rendering, and face recognition.

Keywords: memory skin colour, chromatic tolerance ellipses, cultural differences, colour perception

INTRODUCTION

Human colour perception is not only determined by the physical properties of stimuli but is also strongly shaped by prior knowledge and memory. This phenomenon, referred to as *memory colour*, describes the tendency for observers to recall familiar objects with diagnostically typical colours, such as bananas being remembered as yellow and foliage as green. Previous research has extensively examined memory colour for familiar objects such as fruits, vegetables, and natural scenes, showing that memory colour often differs systematically from physical measurements, tending toward higher saturation or prototypical hues [1], [2]. Moreover, memory colour has been shown to interact with geographical region and culture, although the effect size is relatively small [3]. This perceptual bias is deeply embedded in the visual system and shapes evaluations of realism, quality, and colour accuracy in images [4], [5].

Skin colour, as a unique and complex target, has not been thoroughly explored in this context. Existing studies on memory skin colour have often relied on one or two simplified skin or facial images as stimuli [3], [6]. Unlike other familiar objects with relatively consistent chromatic attributes, skin colour spans a wide gamut, ranging from

dark to light with varied hues, and within-group variation can often exceed between-group differences [7]. Such simplified approaches fail to capture the full diversity of human skin tone or to account for the unique perceptual and social processing of skin as a biological and cultural feature. These factors may lead to a distinct perceptual gamut for skin colour across populations, distinguishing it from other familiar objects.

Skin colour perception is further complicated by its social, aesthetic, and cultural significance. Observers' internal criteria for "ideal" or "acceptable" skin tones can influence judgments of naturalness and attractiveness, shaping preferences in contexts such as cosmetics, photography, lighting, and virtual rendering [8]. In imaging applications, accurate reproduction of skin tones is considered critical, as small deviations may affect perceived realism and viewer satisfaction [9]. Consequently, understanding the perceptual boundaries of memory skin colour is important for applications in image quality assessment, lighting design, cosmetics research, face recognition algorithms, etc.

Given the diversity of human skin tones and the cultural and geographical variations in perception, investigating memory skin colour across populations is essential. The present study explores memory skin colour in Chinese (CN) and Indonesian (ID) observers. Specifically, we examine how individuals recall and perceive their own skin colour as well as the skin colours of four different ethnic groups: Caucasian (East European, CA), Chinese (CN), Southeast Asian (SA), and African (AF). By doing so, we aim to establish the memory skin colour ranges for CN and ID observers and investigate how cultural background and familiarity shape their perception of skin colour.

METHODOLOGY

A psychophysical experiment on memory skin colour was conducted in a dark room with observers from CN and IN backgrounds. A well-calibrated and characterised BenQ display was used to ensure accurate colour reproduction. The experiment consisted of two sessions. Session 1 examined the accuracy of one's own skin colour in memory. The cheek colour of each observer was measured using a Konica Minolta CM700d spectrophotometer. Observers were then asked to reproduce their own cheek skin colour using the memory matching technique. Session 2 investigated memory skin colour for four target ethnic groups: CN, CA, SA, and AF. In this session, reference facial images were provided to observers to ensure consistency in the target identity. These reference images were the average faces of each target group created for the *World of Averages* project [10]. In both sessions, observers were instructed to adjust the colour of a patch on display along the three CIELAB dimensions, lightness (L*), redness (a*), and yellowness (b*), until they reached what they perceived as the best match for the skin colour in their memory. No time limits were imposed.

A total of 25 observers with normal colour vision participated in this experiment, including 12 CN observers (9 females, age = 28.9 ± 3.1 years) and 13 ID observers (9 females, age = 35.7 ± 3.7 years). Results were analysed in CIELAB colour space as it is a relatively uniform colour space, and the colour appearance attributes are easy to understand and manipulate after basic training in experiments. For Session 1, the actual measured skin colour and the recalled skin colour were compared. For Session 2, the inter-observer variability of long-term memory skin colour was quantified using the Mean Colour Difference from the Mean (MCDM). Group-level results were represented by memory colour centres plotted in CIELAB space, and average results were compared with the corresponding group means from the International Skin Spectra Archive (ISSA) database [7]. The ISSA is the most comprehensive human skin dataset to date, including over 15,256 spectroradiometric measurements from 2,113 subjects of diverse ethnicities, genders, and age groups. The scatter of responses was expressed as tolerance ellipses in both a^*b^* plane and L^*C_{ab} plane, fitted at a 95% confidence level. Finally, the effects of observer group (CN vs. ID) and target ethnicity (CN, CA, SA, AF) on memory skin colour were statistically evaluated using two-way ANOVA.

RESULTS AND DISCUSSION

Table 1 summarises the mean and standard deviation of measured and self-matched skin colours in CIELAB space for CN and ID observers. For both groups, recalled skin colours deviated systematically from the actual measured values. Specifically, CN observers recalled their skin as lighter and less chromatic (less reddish, less yellowish) compared to the spectrophotometric measurements. In contrast, ID observers also recalled their skin as lighter and less reddish, but more yellowish. As expected, memory-matched values exhibit greater variability than measured values.

Table 1: Mean and standard deviation of measured and self-matched skin colours in CIELAB space

Observer	Measured L*	Measured a*	Measured b*	Matched L*	Matched a*	Matched b*
CN	65.9 (3.1)	15.5 (1.7)	19.0 (2.5)	75.1 (10.1)	11.8 (3.5)	17.8 (5.6)
ID	61.0 (3.9)	17.4 (2.0)	22.1 (1.3)	72.8 (9.6)	16.5 (4.1)	24.0 (3.6)

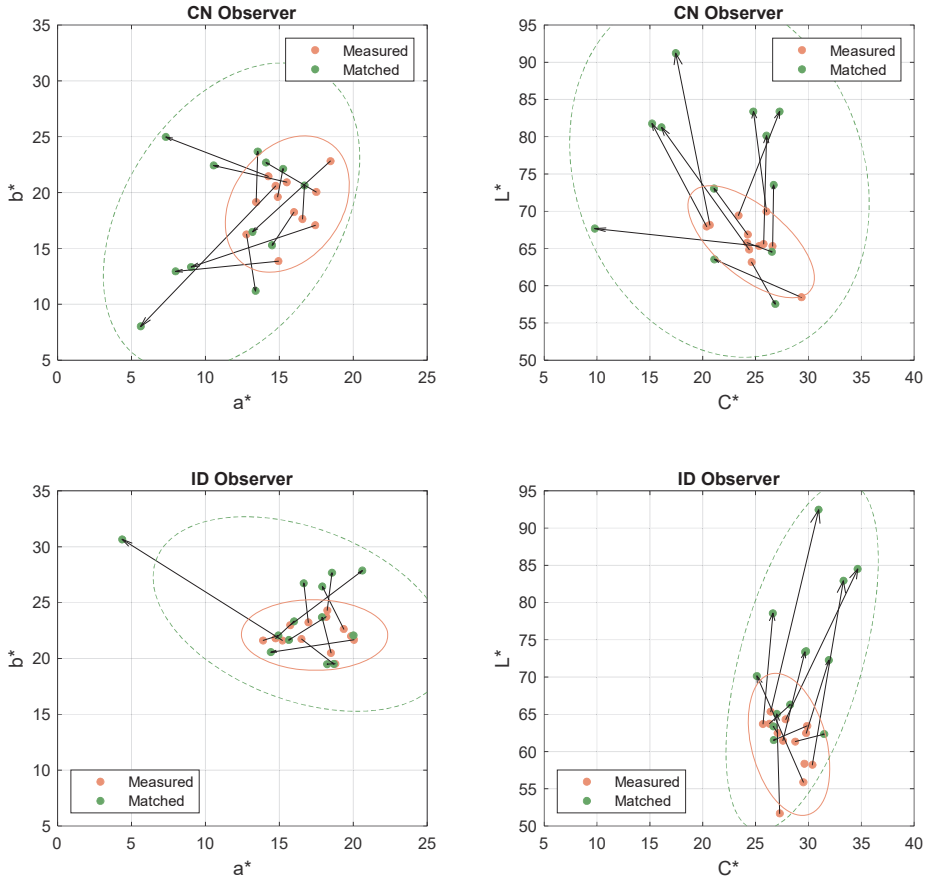

Figure 1: Measured and self-matched skin colour for CN and ID observers in the CIELAB a^*b^* plane and L^*C_{ab} plane. Arrows represent the direction from measured to memory-matched values. Ellipses represent 95% confidence intervals of the distribution.

The scatter plots in Figure 1 illustrate individual observer differences. The arrows, showing the direction from measured to memory-matched values, indicate a universal bias toward overestimating lightness. CN observers tended to under-represent chromaticity, particularly redness, whereas ID observers primarily over-represented yellowness. The confidence ellipses confirm that the variability of memory-matched colours for both observer groups was much higher than that of measured skin colour.

Table 2 presents the mean memory colour centres in CIELAB space for the four target ethnic groups (CA, CN, SA, AF) recalled by CN and ID observers. Systematic differences were observed across groups and target ethnicities. Variability across observers, quantified by the MCDM, ranged from 6.8 to 9.1. Interestingly, both CN and ID observers showed higher observer variability when recalling the skin of their own ethnic groups (CN: 9.1; ID: 8.9). This suggests that familiarity may increase awareness of nature variance and individual differences.

Table 2: Mean memory colour centres (with standard deviation) and inter-observer variability (MCDM) in CIELAB space

Observer	Target Group	Matched L*	Matched a*	Matched b*	MCDM
CN	CA	82.1 (9.1)	8.3 (3.1)	9.8 (2.4)	9.0
	CN	73.3 (9.9)	9.5 (1.9)	17.2 (2.7)	9.1
	SA	60.2 (6.4)	10.4 (2.8)	20.3 (3.7)	6.8
	AF	24.4 (8.0)	7.2 (4.0)	10.4 (3.1)	8.7
ID	CA	86.8 (7.0)	9.7 (5.1)	16.3 (3.4)	8.2
	CN	87.7 (4.8)	5.9 (3.0)	16.5 (6.4)	7.6
	SA	66.2 (8.5)	11.5 (3.8)	22.4 (3.7)	8.9
	AF	28.2 (7.3)	8.5 (4.0)	11.8 (3.7)	8.2

Figure 2 illustrates these distributions in CIELAB space, with ellipses representing 95% confidence intervals. Note that the Southeast Asian (SA) reference corresponds to the Thai (TH) group in the ISSA database. The scatter patterns confirm that memory skin colour centres (crosses) are broadly aligned with the corresponding ISSA database averages (stars), though with notably larger deviations across groups. Both CN and ID observers recalled SA skin as lighter and more chromatic than the measured SA skin colour centre, consistent with previous findings on natural objects, where memory colour is often more saturated and lighter than reality [2]. However, this pattern did not hold for the recalled skin colour of other ethnic groups. For example, both CN and ID observers recalled AF skin as darker and less chromatic than the ISSA average. This suggests that memory skin colour may follow different perceptual rules compared with other familiar objects, and the cultural background of familiarity could be an influential factor.

Two-way ANOVA was conducted to assess the effects of observer ethnicity (CN vs. ID) and target ethnicity (CA, CN, SA, AF) on recalled skin colour. For L* (lightness), both observer ethnicity ($F = 10.64$, $p < 0.001$) and target ethnicity ($F = 61.07$, $p < 0.001$) showed significant main effects, along with a significant interaction ($F = 3.85$, $p = 0.002$). This confirms that both cultural background and target group strongly influenced the memory of skin lightness. For a* (redness), neither observer ethnicity ($F = 0.50$, $p = 0.61$) nor target ethnicity ($F = 2.16$, $p = 0.098$) reached significance. This suggests relatively small group-level differences in redness perception. For b* (yellowness), both observer ethnicity ($F = 4.98$, $p = 0.009$) and target ethnicity ($F = 10.83$, $p < 0.001$) were significant, with interaction approaching significance ($p = 0.052$). These findings indicate that observers' cultural background significantly influences memory for lightness and yellowness but has less effect on redness.

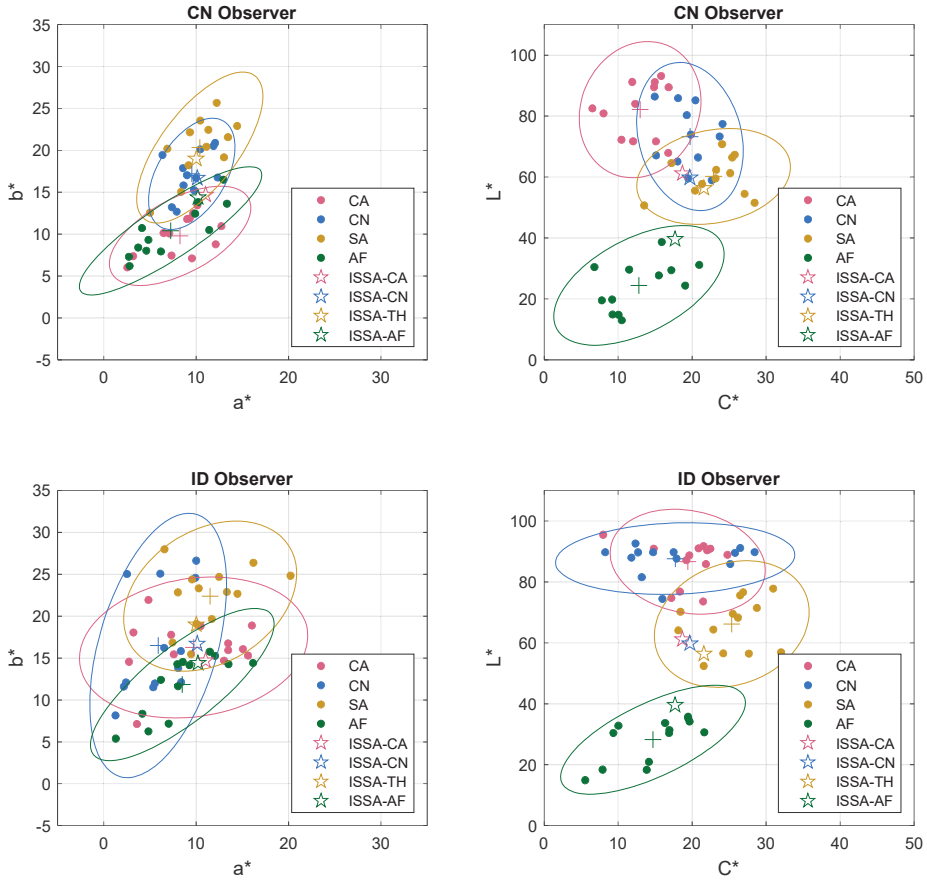

Figure 2: Memory skin colour distributions for four target ethnic groups (CA, CN, SA, AF) for CN and ID observers. Ellipses represent the 95% confidence intervals for each ethnic target group. Crosses denote the memory-matched skin colour centres; stars denote mean measured colour centres in the ISSA database.

These findings provide initial insights into how cultural background and familiarity influence memory of skin colour. Future studies should expand the scope to include more ethnic groups, gender and age differences, and acceptable boundaries of memory skin colour to build a more comprehensive understanding.

CONCLUSION

In this study, psychophysical experiments using a memory-matching technique were employed to examine memory skin colour among Chinese (CN) and Indonesian (ID) observers and to investigate the influence of cultural background and familiarity on perception. When comparing memory-matched with measured cheek skin colour, both groups overestimated lightness; CN observers under-represented redness, while ID observers over-represented yellowness. For the four target ethnic groups (CA, CN, SA, AF), memory skin colour centres across groups showed greater variation than the ISSA database averages and were not universally more saturated or lighter than their measured counterparts. Observers also showed greater variability when recalling the skin colour of their own ethnic group, suggesting that familiarity may increase sensitivity to natural variation. Overall, memory skin colour was

systematically biased, with cultural background and familiarity shaping lightness and yellowness but not redness, revealing distinct perceptual patterns that differ from other familiar objects. This research provides a valuable dataset of memory skin colour for CN and ID populations and offers insights into the perceptual and cultural factors underlying skin colour perception, with practical implications for imaging applications.

REFERENCES

[1]. Bartleson, C. J. (1960). Memory Colors of Familiar Objects*. *Journal of the Optical Society of America*, *50*(1), 73. https://doi.org/10.1364/JOSA.50.000073

[2]. Cao, M., Luo, M. R., Lu, Y., & Xaio, K. (2023). A study of preferred and natural memory colours across different ethnic groups. *Color Research & Application*, *48*(2), 178–200. https://doi.org/10.1002/col.22841

[3]. Hansen, T., Olkkonen, M., & Walter, S. (2006). Memory modulates color appearance. *Nature Neuroscience*, *9*(11), 1367–1368. https://doi.org/10.1038/nn1794

[4]. Ling, Y., & Hurlbert, A. (2009). Role of color memory in successive color constancy: erratum. *Journal of the Optical Society of America A*, *26*(7), 1544. https://doi.org/10.1364/JOSAA.26.001544

[5]. Lu, Y., Xiao, K., Pointer, M., He, R., Zhou, S., Nasseraldin, A., Sueeprasan, S., Gao, C., Li, C., Sohaib, A., He, Y., Mizokami, Y., Wang, M., Romero, E. P., Zardawi, F., Gill, L., Liao, N., & Wuerger, S. (2025). The International Skin Spectra Archive (ISSA): a multicultural human skin phenotype and colour spectra collection. *Scientific Data*, *12*(1), 487. https://doi.org/10.1038/s41597-025-04857-5

[6]. Lu, Y., Xiao, K., Yang, J., Pointer, M., Li, C., & Wuerger, S. (2022). Different colour predictions of facial preference by Caucasian and Chinese observers. *Scientific Reports*, *12*(1), 12194. https://doi.org/10.1038/s41598-022-15951-8

[7]. Smet, K. A. G., Lin, Y., Nagy, B. V., Németh, Z., Duque-Chica, G. L., Quintero, J. M., Chen, H.-S., Luo, R. M., Safi, M., & Hanselaer, P. (2014). Cross-cultural variation of memory colors of familiar objects. *Optics Express*, *22*(26), 32308. https://doi.org/10.1364/oe.22.032308

[8]. *"The world of averages."* (2011). Http://Pmsol3.Wordpress.Com.

[9]. Zeng, H., & Luo, R. (2013). Colour and tolerance of preferred skin colours on digital photographic images. *Color Research and Application*, *38*(1), 30–45. https://doi.org/10.1002/col.20696

[10]. Zhu, Y., Luo, M. R., Fischer, S., Bodrogi, P., & Khanh, T. Q. (2017). Long-term memory color investigation: culture effect and experimental setting factors. *Journal of the Optical Society of America A*, *34*(10), 1757. https://doi.org/10.1364/JOSAA.34.001757

A Comparative Study of Seasonal Color Associations in Nature and Personal Color Theory

YungKyung Park[a*]

[a]Ewha Womans University, Seoul, Korea
[*]Corresponding author: YungKyung Park, yungkyung.park@ewha.ac.kr

ABSTRACT

This study investigates the relationship between natural seasonal color associations and standardized personal color palettes to evaluate how faithfully personal color theory reflects seasonal phenomena. While seasonal associations are often derived from salient objects observable in each season, personal color palettes represent a more abstract synthesis of seasonal imagery optimized for harmony with skin undertones. This divergence raises important questions about how much these systems differ and why such differences occur. Participants were asked to freely associate colors with the four seasons—Spring, Summer, Autumn, and Winter—resulting in a dataset reflecting intuitive connections to natural seasonal objects. These associations were compared with Carole Jackson's well-known seasonal palettes[1], which were digitized and analyzed in CIELAB space. Distributions of hue, lightness, and chroma were examined, and color differences (ΔE*) were calculated between representative seasonal skin tones and both sets of palettes. The results revealed systematic discrepancies. Natural associations displayed broader variability, with certain hues (e.g., purple in Autumn, yellow in Winter) more prominent than in personal palettes. Personal color palettes, by contrast, simplified distributions and consistently reduced ΔE values relative to skin tones, particularly in Summer and Winter. This suggests that personal palettes stylize seasonal imagery to achieve perceptual harmony, potentially at the expense of ecological fidelity. These findings suggest that seasonal associations and personal palettes are inherently different yet meaningfully comparable: one reflects immediate perceptual impressions of seasonal objects, while the other reflects an abstract, macro-level construction for aesthetic and perceptual alignment. By quantifying the extent and causes of these differences, the study contributes to a more comprehensive understanding of seasonal color semiotics, with implications for design, fashion, and cosmetics.

Keywords: Seasonal Color, Skin Color, Harmony

INTRODUCTION

Seasonal color theory, widely applied in fashion, cosmetics, and personal styling, classifies colors into four categories—Spring, Summer, Autumn, and Winter—based on skin undertones, lightness, and chroma. While this framework has gained popularity in practice, its foundations are largely aesthetic and heuristic rather than empirical. The classification often relies on symbolic or cultural associations of seasons rather than on systematic comparisons with the actual colors observed in nature. The four-season framework owes much of its popularity to Carole Jackson's influential book Color Me Beautiful [1], which introduced personal color analysis to a broad audience. Jackson adopted the metaphor of the four seasons not as a scientific taxonomy but as an intuitive and accessible way for laypeople to understand complex dimensions of colors such as warm versus cool, light versus dark, and clear versus muted. By linking these abstract attributes to familiar seasonal imagery, her system offered both cognitive simplicity and emotional resonance. However, relatively few studies have investigated whether the personal color system, which links individual skin tones to seasonal palettes, faithfully reflects the visual and

emotional characteristics of natural seasonal environments. This raises the question of whether the seasonal classification in personal color analysis is arbitrary or whether it embodies a meaningful correspondence with the hue, lightness, and chroma features of seasonal phenomena. The present study addresses this gap by comparing natural seasonal color associations, which reflect salient objects observed in each season, with personal color palettes, which represent a more abstract synthesis of seasonal imagery interpreted from a broader perspective. By doing so, the study aims to clarify not only the extent of their differences but also the reasons underlying these differences.

METHODOLOGY

This study employed a comparative approach to investigate the alignment between natural seasonal color associations and the standardized palettes commonly used in personal color theory. First, data on seasonal color associations were collected through a survey in which participants were asked to freely associate colors with each of the four seasons—Spring, Summer, Autumn, and Winter. To ensure sufficient coverage, participants were instructed to identify 30 representative colors for each season, selected from a broad range of natural imagery. Seasonal images were drawn from multiple categories (over 100 images per season), including flowers, foliage, landscapes, and weather phenomena. From these images, colors were systematically extracted, allowing both chromatic and neutral tones to be represented. These associations were then compiled and analyzed to identify representative hues, lightness levels, and chroma ranges for each season. Second, these empirically derived seasonal color associations were compared with the seasonal palettes described in Carole Jackson's book [1], which form the basis of the four-season personal color classification system. Following the procedure described in Park [2], 30 representative colors for each season were selected from Jackson's book using the original color names provided. These palettes were then digitized and analyzed using CIELAB color coordinates to enable systematic comparison with the collected data. The comparative analysis focused on two aspects:

Color aspects – examining the degree of overlap or divergence between participant-associated seasonal hues and Jackson's seasonal palettes.

Color Differences with Skin Tones – calculating ΔE* values between representative seasonal skin tones and both types of palettes, in order to assess whether personal color classifications optimize visual harmony with skin undertones.

RESULTS

Seasonal Palette Comparisons

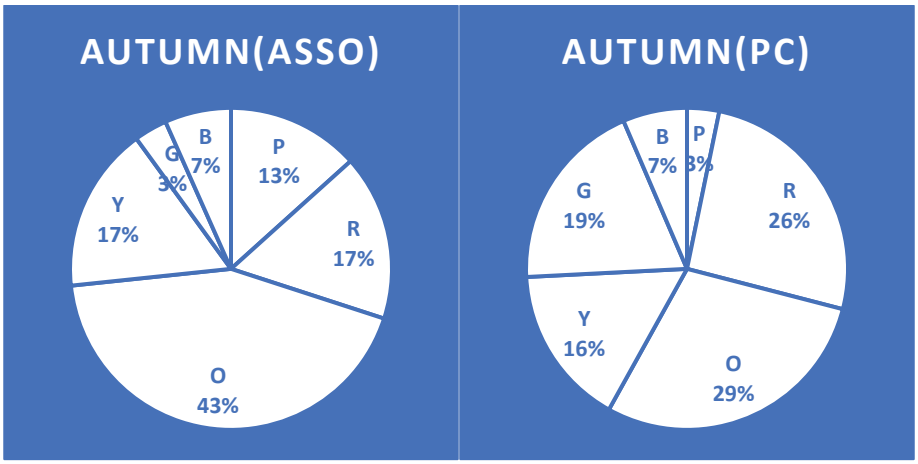

Figure 1: Selected Hues for Autumn associated and personal color in percentage

- **Autumn**: Participants strongly associated Autumn with **Orange (43%)**, while the personal color palette emphasized **Red (26%)** and **Green (19%)**, reducing the role of purple (3% vs. 13% in associations). This suggests that PC palettes stylize Autumn by elevating green and minimizing purple.

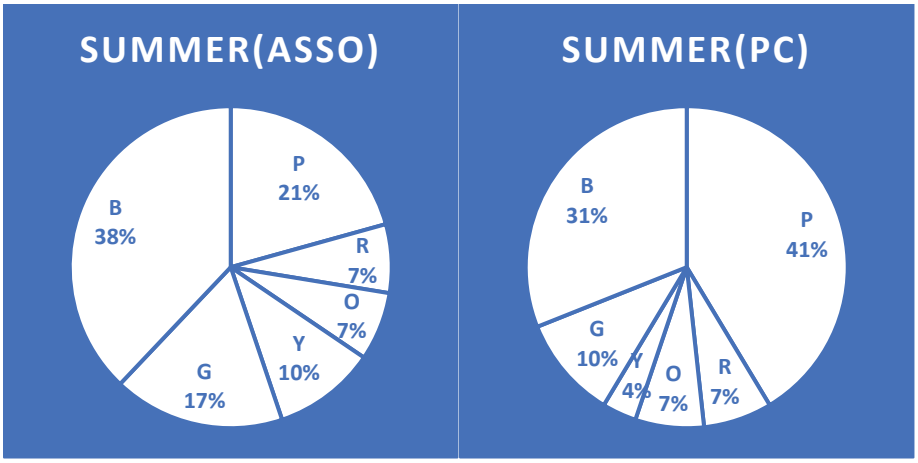

Figure 2: Selected Hues for Summer associated and personal color in percentage

- **Summer**: Participants perceived Summer mainly as **Blue (38%)** and **Purple (21%)**, while the PC palette reversed this emphasis with **Purple (41%)** dominant. Yellow was moderately present in associations (10%) but minimized in PC palettes (4%).

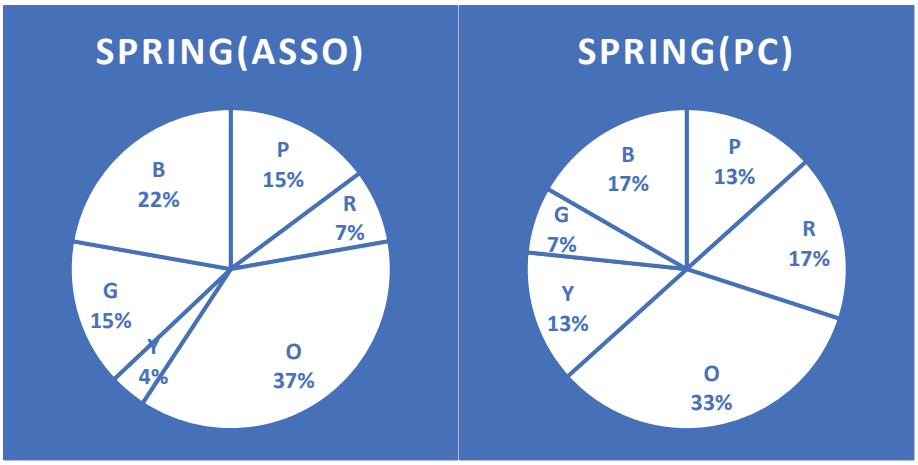

Figure 3: Selected Hues for Spring associated and personal color in percentage

- **Spring**: Associations highlighted **Orange (37%)** and **Blue (22%)**, whereas the PC palette increased the share of **Red (17%)** and **Yellow (13%)**, reducing Blue and Green. This indicates stylization toward orangish hues.

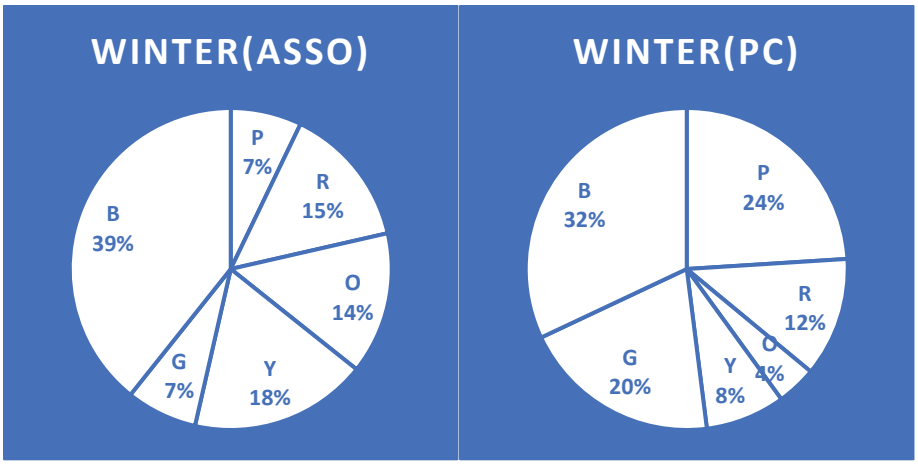

Figure 4: Selected Hues for Winter associated and personal color in percentage

- **Winter**: Participants associated Winter strongly with **Blue (39%)** and **Yellow (18%)**, but the PC palette emphasized **Purple (24%)** and **Green (20%)**, while suppressing Yellow (8%) and Orange (4%).

Overall, participants' natural associations revealed broader hue variability, while personal color palettes showed simplified distributions of more various hues.

Tone Analysis

In terms of tone, no significant differences were observed across the four seasons. Both participants' associations and the standardized personal color palettes displayed comparable distributions of lightness and chroma. This suggests that while hue categories varied considerably between natural associations and personal palettes, tone remained relatively stable across both systems.

Color Differences with Skin Tones

Table 1: Representative skin ccolors

	L*	a*	b*
Autumn	50.7	16.30	20.10
Spring	72.4	5.95	13.99
Summer	69.8	17.14	18.78
Winter	61.4	10.88	10.45

Representative skin colors for each season were also included in the analysis. As summarized in **Table 1**, a mid-level lightness value was selected for each seasonal skin tone to provide a consistent basis for calculating ΔE_{00} values between skin and palette colors. Figure 5 represents ΔE_{00} values between representative seasonal skin colors and both associated colors and personal color palettes.

- **Associated Colors**: Larger color differences were observed in Summer and Winter, indicating greater divergence between participants' associations and skin tones.
- **Personal Colors**: Across all seasons, PC palettes consistently reduced ΔE values relative to associated colors, with particularly strong improvements in Summer and Winter.

This pattern shows that personal color palettes intentionally minimize perceptual differences, thereby enhancing harmony between skin tones and seasonal palettes.

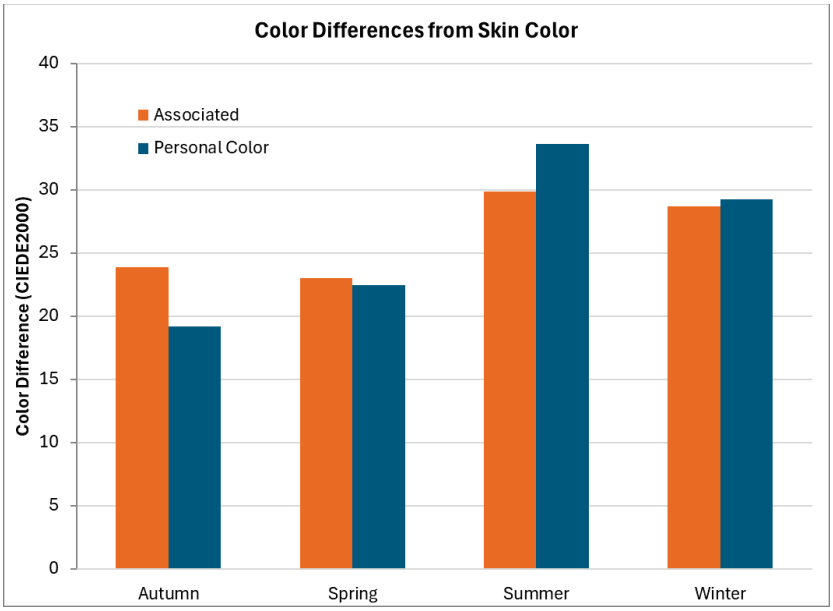

Figure 5: ΔE_{00} values between representative seasonal skin colors and both associated colors and personal color palettes.

DISCUSSION

The results demonstrate that while personal color theory broadly reflects seasonal distinctions, it systematically simplifies and stylizes natural seasonal associations. For example, Autumn palettes increase the role of green while suppressing purple, Summer palettes highlight purple over blue, Spring palettes shift toward warmer hues, and Winter palettes reduce yellow and orange. These modifications create cleaner, more uniform seasonal palettes but diverge from the more complex distributions found in participants' natural associations. The inclusion of skin tone analysis reveals the underlying rationale for these differences. Personal color palettes are not designed solely to replicate seasonal ecology; rather, they are constructed to optimize skin-tone harmony. By reducing ΔE_{00} values, especially in Summer and Winter, personal color palettes achieve closer alignment with representative skin tones. This functional optimization explains why certain naturally salient hues (e.g., purple in Autumn, yellow in Winter) are minimized. These findings highlight a fundamental trade-off between natural seasonal associations and standardized personal color palettes. On the one hand, natural associations capture the ecological and symbolic richness of seasonal environments, reflecting the diverse hues and cultural meanings attached to seasonal objects. However, this ecological fidelity often results in conflicts with skin undertones, leading to less harmonious visual integration. On the other hand, personal color palettes are constructed to enhance harmony with skin tones by simplifying and stylizing seasonal colors, but this comes at the cost of ecological validity, reducing the complexity and variability found in actual seasonal imagery.

In addition, the role of tone—defined by lightness and chroma—proved more stable across both natural associations and personal palettes. This finding resonates with recent research on achromatic color sensitivity and visual attention [2], which demonstrated that perceptual thresholds for detecting differences in neutral tones are closely linked to attentional mechanisms. From this perspective, the relative consistency of tonal structures across systems may reflect a perceptual baseline that supports both ecological recognition and aesthetic harmony. However,

the simplification of neutral tones in personal color palettes may overlook their role in perceptual stability, suggesting an avenue for further investigation.

Finally, it should be noted that seasonal color associations are not culturally universal. Environmental conditions, symbolic traditions, and linguistic categories shape how individuals perceive and recall seasonal colors [3]. For instance, Spring may be associated with cherry blossoms (pale pink) in East Asia, but with fresh green fields or bright tropical flowers in other regions. Similarly, Winter is often linked to snowy whites and blues in northern cultures, whereas in regions without snow, it may evoke earthy browns or muted landscapes. These cultural variations suggest that the ecological basis of seasonal colors interacts with cultural semiotics, highlighting the need for cross-cultural studies to refine or expand personal color systems beyond their Western origins.

CONCLUSION

This study demonstrates that seasonal associations, grounded in the perceptual experience of seasonal objects, naturally diverge from personal color palettes, which represent an abstract synthesis of seasonal imagery optimized for skin-tone harmony. The differences are therefore unsurprising, but their magnitude and underlying causes are revealing. Natural associations capture ecological richness and cultural diversity, while personal palettes standardize seasonal imagery to create visual harmony with human skin. The present study contributes by quantifying how different these two systems are and exploring why they diverge, situating the analysis within both color science and perceptual psychology. Future research should extend this approach by incorporating cross-cultural and developmental perspectives, examining how geography, culture, and age influence seasonal associations, and how personal color frameworks might adapt to integrate ecological fidelity, skin-tone harmony, and perceptual mechanisms.

REFERENCE

[1]. Jackson, C. (1980). Color Me Beautiful. Ballantine Books.

[2]. Park, Y. (2025). Sensitivity of achromatic color considering visual attention. Journal of Korea Color Research, 39(3), 83–91.

[3]. Schloss, K. B., & Palmer, S. E. (2011). Aesthetic response to color combinations: Preference, harmony, and similarity. Attention, Perception, & Psychophysics, 73(2), 551–571.

Evaluating The Effectiveness and Utility of Fabric Draping-Based Personal Color Diagnosis

Jisu Park[1*] , Gyoungsil Choi[2] and Yungkyung Park[3]

[1]*Department of Color Design, Ewha womans University, Seoul, Korea. kgod6930@ewhain.net*
[2]*Department of Color Design, Ewha womans University, Seoul, Korea. gschoi@ewha.ac.kr*
[3]*Department of Color Design, Ewha womans University, Seoul,* Korea*. yungkyung.park@ewha.ac.kr*
[*]*Corresponding author: Park, Yungkyung, yungkyung.park@ewha.ac.kr*

ABSTRACT

The demand for personal color, which enhances attractiveness through colors suited to one's skin tone and facial features, continues to grow. While professional diagnoses using draping fabrics have been the mainstream, limitations such as lack of consistency, environmental constraints, and the burden of time and cost have led to the emergence of alternative methods, including self-diagnosis, mobile applications, and AI-based virtual assessments. Nevertheless, the demand for fabric-based expert diagnosis persists. To examine the effectiveness and utility of fabric diagnosis, surveys were conducted to measure preferred hues and tones before and after the diagnosis, and the results were compared. Findings revealed that preferred colors shifted according to the seasonal palettes suggested during diagnosis. This indicates that the immediate visual impression of fabric in direct contact with the body influences psychological factors such as color preference. Although fabric diagnosis by experts is experiential and intuitive, this very characteristic appears to provide greater satisfaction to consumers who seek clarity amid ambiguous beauty standards.

Keywords: : Personal Color Diagnosis, Fabric Draping, Color Preference, Four Seasonal Color Type, Professional diagnoses

INTRODUCTION

Elliot and Niesta (2008) argued that "men perceive women wearing red clothing as more attractive" based on the perceptual and cognitive effects of the color red. However, does this mean that all women appear equally attractive and beautiful when wearing red? The answer is no, since women differ in skin tone, facial features, and overall image. A single absolute color cannot universally enhance attractiveness across such individual differences. Jackson(1989), who popularized the concept of personal color, suggested that one way to improve physical attractiveness is by wearing clothing colors that harmonize with one's skin tone. Since the rise of the personal color concept, individuals have continually sought hue and tones that enhance their image and features, often through personal color diagnosis. Traditionally, such diagnoses have been conducted by experts who drape colored fabrics close to the face to determine which hues and tones best suit or conflict with the individual's skin tone and appearance. While this is the oldest and most fundamental method, it presents limitations: expert judgments may vary, results can differ depending on fabric condition and diagnostic environment, and the process demands significant time and cost. Furthermore, diagnostic fabrics are not standardized across providers, and diagnostic frameworks lack consistency. Despite these limitations, demand for personal color diagnosis remains strong, leading to the emergence of alternatives such as self-diagnosis (Kim, H.M., 2018), mobile applications (Hong, H.R. & Kim, Y.I., 2019), and AI-based virtual assessments (Park, J.S., 2018). These methods are characterized by quantitative, data-driven approaches that compute diagnoses, classify results automatically, and propose

applications in fashion and beauty. They significantly reduce time and cost, making diagnosis more accessible to non-experts without requiring fabric draping. However, studies show that 53% of mobile app users still prefer fabric-based diagnosis (Hong, H.R. & Kim, Y.I., 2019), and results from self-diagnostic tools have shown large discrepancies compared to expert assessments (Eun, K.H. et al., 2021), highlighting the limitations of these alternatives. Although the limitations of consistency and objectivity of expert diagnosis continue to be raised, it is said that they are interested and satisfied with the immediate changes in the face during the diagnosis process through draping cloth (Park, Y.S. et al. 2019). Despite the limitations of the diagnosis method using draping cloth, there is a continuous demand, and we would like to conduct research on the effectiveness and usefulness of the diagnosis method using fabric.

METHODOLOGY

To examine the effectiveness and utility of personal color diagnosis using draping fabrics, a survey and interview experiment was conducted to investigate how color preferences change before and after the diagnosis. In this study, questionnaires were administered both prior to and following the diagnostic process. The questionnaire included demographic information as well as items that asked participants to rank 15 hues and 12 tones. Surveys were conducted five minutes before and after the diagnosis. Following the survey, participants underwent a personal color diagnosis, which lasted approximately 50 to 60 minutes.

Experimental Conditions The experiment was conducted under standardized daylight-colored lighting (5500K) in a classroom environment. Given the nature of personal color diagnosis, clear daylight was necessary to ensure more accurate assessments; therefore, the experiment was carried out between 12:00 p.m. and 5:00 p.m., and no sessions were conducted on rainy days.

Observer Training All data collection through surveys and personal color diagnosis was conducted by a single researcher. To ensure consistency and reliability of the diagnosis, the researcher completed professional training in personal color analysis and obtained relevant certification from a specialized institution ([VSTlab], 2025). Prior to this study, the researcher underwent three months of systematic training, which included theoretical understanding of color systems, draping practice, and skin tone analysis.

Operational Definition Jonauskaite et al. (2016) demonstrated that general color preference may differ from color preferences for specific objects, and that preferred attributes of color vary depending on the context of the target. In line with this, the present study defines color preference not as an abstract, personal liking of color, but rather as the preference for colors perceived to harmonize well when applied to accessories, fashion, or beauty products actually worn or used by the individual.

Stimulus For the survey, the color stimuli were based on the KS (Korea Industrial Standard) system, which is derived from the Munsell system. The KS system consists of 15 hues (12 chromatic colors and 3 achromatic colors: Red, Yellow Red, Yellow, Green Yellow, Green, Blue Green, Blue, Purple Blue, Purple, Red Purple, Pink, Brown, White, Gray, and Black) and 12 tones (whitish, pale, light, vivid, light grayish, grayish, dark grayish, soft, dull, deep, dark, and blackish). Using these 15 hues and 12 tones, the survey stimuli were developed and presented for evaluation through a display.

Subjects A total of 27 Korean women in their 20s to 50s participated in the survey and personal color diagnosis. The study was conducted over a 16-day period, from August 19 to September 3, 2025.

Procedures Following the survey, participants underwent a personal color diagnosis using 160 draping fabrics produced based on the KS system. The diagnostic criteria were derived from Jackson's (1980) four-season personal color typology, which categorizes image, hue, and tone into seasonal palettes:

- **Spring**: bright and clear image / tones: vivid, light, pale

- **Summer**: cool and soft image / tones: pale, soft, light grayish
- **Autumn**: rich and deep image / tones: vivid, dull, deep, dark
- **Winter**: cool and intense image / tones: vivid, pale, light, dark

In this study, a "well-suited" color was defined as one that made the participant's skin tone, facial features, or overall image appear more positively enhanced. Once the seasonal type was determined through diagnosis, the corresponding seasonal palette was presented to the participant. The palettes used to propose hues and tones are shown in <Table 1>.

Table 1 : Seasonal Proposal Palette

SPRING	SUMMER	AUTUMN	WINTER
HUE : R, YR, Y, GY, G . Pk TONE: vv, pl, lt	HUE : Pk, Y, G, B, P, Wh TONE: pl, lt, sf, ltgy	HUE : Y, YR, Br, G, B TONE: dl, dp, dk, vv, ltgy, gy	HUE: RP, P, Pk, BG, G, Gy, Bk TONE: vv, dp, dk, bk, wh~pl

RESULTS AND DISCUSSION

Among the 27 participants, 9 were classified as 'Spring' type, 6 as 'Summer' type, 6 as 'Autumn' type, and 6 as 'Winter' type. The data obtained from the experiment were analyzed using graphs modified and supplemented from Lind (1994), who compared abstract color preferences with clothing color preferences, and Stephen (2012), who examined changes in color preference according to tone variation.

For the 'Spring' type, the color 'Pink' (M_{Diff} = 2.33) showed the greatest increase in preference after diagnosis. In addition to 'Pink', preference for 'Red' (M_{Diff}= 1.78), 'Yellow Red' (M_{Diff}= 2), and 'Green Yellow' (M_{Diff}= 2.67) also increased. Overall, except for 'Green' (M_{Diff}= -0.89), most of the colors proposed in the seasonal palette showed higher preference after the diagnosis compared to before. With regard to tone preference, increases were observed in 'pale' (M_{Diff}= 1.33), 'vivid' (M_{Diff}= 0.56), 'light' (M_{Diff}= 0.33), and 'soft' (M_{Diff}= 0.33). In contrast, lower-lightness and lower-chroma tones, which were inconsistent with the proposed palette, such as 'deep' (M_{Diff}= -0.33), 'dark' (M_{Diff}= -1.67), and 'blackish' (M_{Diff}= -1.56), decreased in preference after the diagnosis. The results for the spring types are illustrated in <Figure 1>.

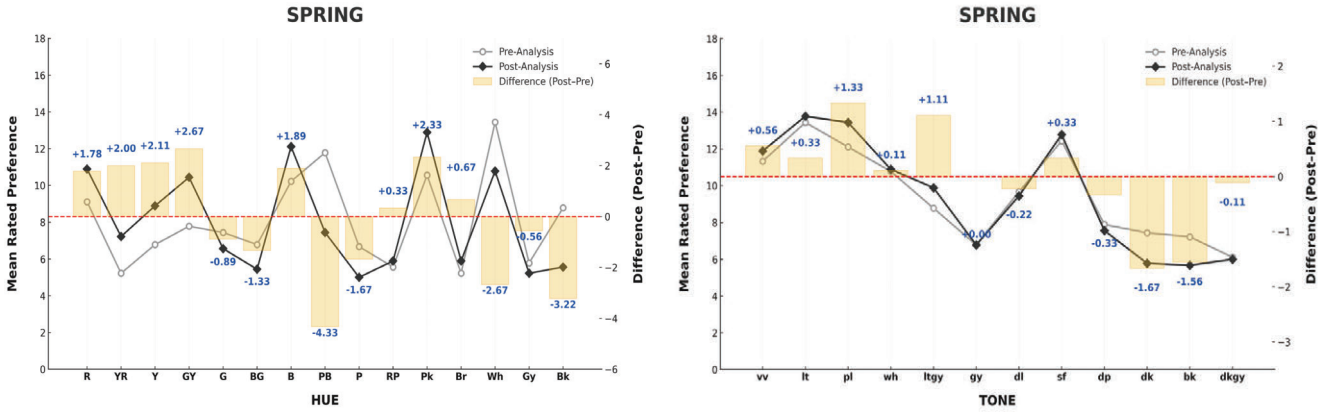

Figure 1. Spring — HUE (left) and TONE (right)

For the 'Summer' type, the greatest increase in color preference was observed for 'Pink' (M_{Diff} = 5.83), similar to the 'Spring type'. In addition to 'Pink', preference also increased for the representative palette colors 'Yellow' (M_{Diff}= 1.5), 'Green' (M_{Diff}= 1.67), and 'Blue' (M_{Diff}= 0.83). In contrast, hue with inherently lower lightness, such as 'Purple Bule' (M_{Diff}= -3.83) and 'Black' (M_{Diff}= -3.17), showed a decrease in preference after diagnosis. With regard to tone preference, the 'whitish' tone (M_{Diff}= 4.17) showed the largest increase. Other tones suggested in the seasonal palette, including 'lightgrayish' (M_{Diff}= 2.83), 'pale' (M_{Diff}= 2), and 'light' (M_{Diff}= 1.17), also showed increased preference. Conversely, lower-lightness and lower-chroma tones such as 'dark' (M_{Diff}= -2.33) and 'blackish' (M_{Diff}= -4.67) showed substantial decreases in preference, along with the high-chroma tone 'vivid' (M_{Diff}= -3.33), which also decreased markedly. The results for the Summer type are illustrated in <Figure 2>.

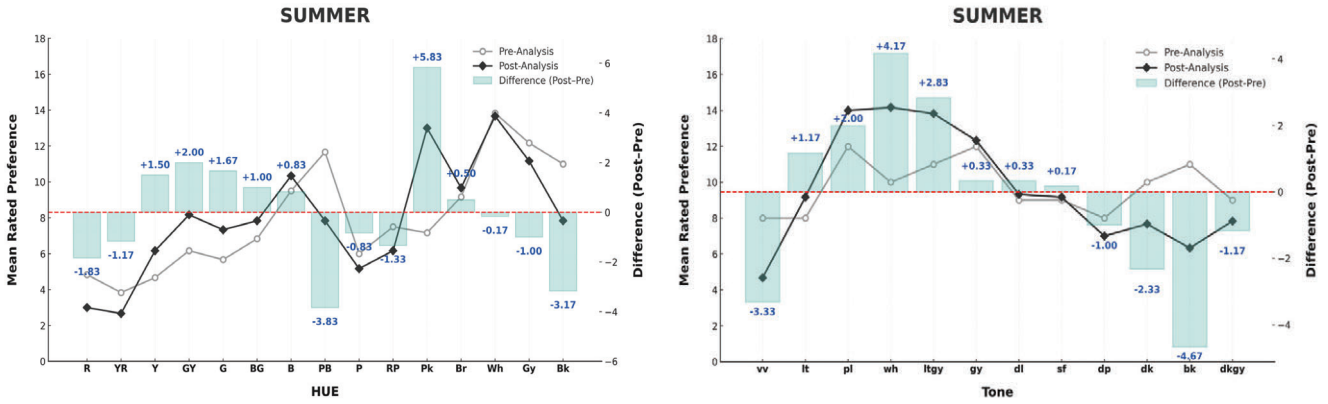

Figure 2. Summer — HUE (left) and TONE (right)

For the 'Autumn' type, the representative palette color 'Brown' (M_{Diff}3.33) showed the greatest increase in preference. This was followed by 'Yellow Red' (M_{Diff}= 2.50), 'Blue' (M_{Diff}= 2.50), and 'Green' (M_{Diff}= 0.67). In addition, preference for the achromatic colors 'Gray' (M_{Diff} = 1.00) and 'Black' (M_{Diff}= 1.00) also increased. In contrast, 'Yellow' (M_{Diff}= -2.33), despite being a palette-recommended color, showed a decrease in preference after the diagnosis. With regard to tone preference, the 'deep' tone (M_{Diff} = 3.17) showed the largest increase, followed by 'dark' (M_{Diff}= 2.17), 'black' (M_{Diff}= 2), 'lightgrayish' (M_{Diff}= 2.33), 'grayish' (M_{Diff}= 1.33), and 'dull' (M_{Diff}= 0.5). Conversely, higher-lightness and lower-chroma tones such as 'light' (M_{Diff}= -2.67), 'pale' (M_{Diff}= -1), 'whitish' (M_{Diff}= -2.33), and 'soft' (M_{Diff}= -2.50) decreased in preference for the 'Autumn' type after diagnosis. Notably, the representative Autumn tone 'vivid' (M_{Diff}= -3) showed a substantial decrease in

preference. This suggests that participants in the Autumn group were likely subtypes for whom muted mid-chroma and low-lightness tones were more suitable, leading to relatively lower evaluations of the high-chroma 'vivid' tone. The results for the Autumn type are illustrated in <Figure 3>.

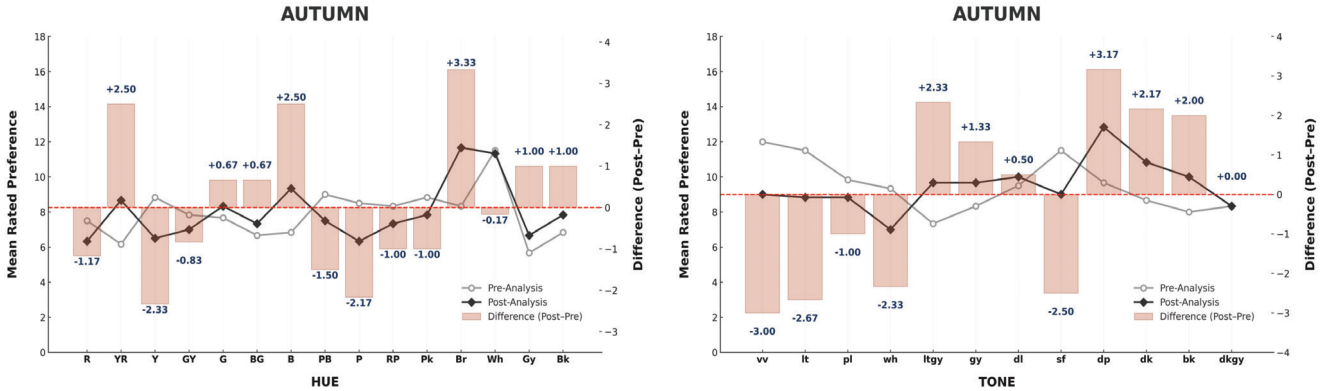

Figure 3. Autumn — HUE (left) and TONE (right)

For the 'Winter' type, the representative palette colors 'Purple' (M_{Diff} = 3.67) and 'Red Purple' (M_{Diff} = 3.5) showed the greatest increase in preference. This was followed by 'Blue Green' (M_{Diff} = 3.17) and 'Red' (M_{Diff} = 3.17), which increased by the same margin. Overall, the results aligned with the colors suggested in the Winter palette. In contrast, preference for 'Yellow' (M_{Diff} = -1.50), 'Green Yellow' (M_{Diff} = -1.83), and 'Brown' (M_{Diff} = -0.33), which were representative colors for the Spring and Autumn palettes, decreased after diagnosis. With regard to tone preference, the representative Winter tone 'vivid' (M_{Diff} = 2.5) showed the largest increase, followed by 'blackish' (M_{Diff} = 2.33), 'deep' (M_{Diff} = 2.17), and 'dark' (M_{Diff} = 1.5). In contrast, higher-lightness and mid-chroma tones such as 'lightgrayish' (M_{Diff} = -3.83), 'grayish' (M_{Diff} = -2.33), 'dull' (M_{Diff} = -0.5), and 'soff' (M_{Diff} = -0.67) decreased in preference. The results for the 'Winter' type are illustrated in <Figure 4>.

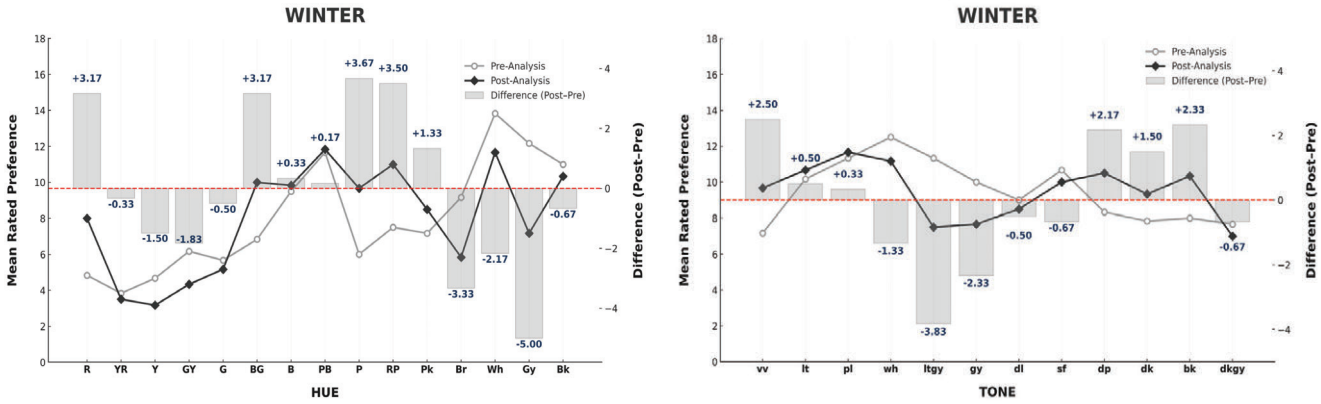

Figure 4. Winter — HUE (left) and TONE (right)

As observed in the results by seasonal type, with the exception of 'Green' in the 'Spring' type, 'Yellow' in the 'Autumn' type, and the 'vivid' tone, preferences for colors and tones generally increased after diagnosis when they aligned with the palettes suggested during personal color analysis. This indicates that fabric-based diagnosis exerts a noticeable effect on preference change. When draping fabrics are placed directly against the body during diagnosis,

individuals immediately perceive the transformation, and this impact is often experienced as highly significant (Byun & Lee, 2019). Such perceptual changes can also trigger psychological shifts, as demonstrated by the changes in color preference found in this study. Moreover, in the study by Park et al. (2019) on the motivations and effects of personal color consulting, interviewees expressed dissatisfaction with rigid and overly theoretical consulting approaches. This suggests that what is valued in personal color consulting is not merely the diagnostic result identifying one's type. Rather, through the experiential process of fabric draping, individuals directly perceive changes and are convinced of the outcome, which in turn fosters greater trust and satisfaction with the consultant's recommendations for specific hues and tones.

A limitation of this study is that the effectiveness of fabric-based diagnosis was not directly compared with self-diagnosis or app-based methods, making it difficult to draw firm conclusions about their relative differences and effects. Future research should conduct direct comparisons across diagnostic approaches to examine their unique characteristics and effectiveness in greater detail.

CONCLUSION

The ultimate purpose of personal color is the pursuit of beauty. However, aesthetic perception is inherently subjective, as there are no fixed standards for determining what is beautiful or unattractive (Adilova, 2024). Consequently, the criteria of personal color, which centers on the pursuit of beauty, remain ambiguous and difficult to define with precision. To address this ambiguity, personal color has developed through efforts to establish quantification and objectivity. Although future diagnostic methods and criteria will continue to emerge through the integration of various scientific technologies, neglecting the experiential and expert-driven aspects of diagnosis in favor of rigid standardization may reduce consumer satisfaction, leading to consultations that feel less personalized and more formulaic. Although a quantified approach grounded in logic and systematic theory is essential, the combination of experiential judgment and intuitive insight provides a more effective diagnosis for those striving to discover the form of beauty that best highlights their individuality.

REFERENCES

[1]. Adilova, A., & Shamoi, P (2024). Personalized Aesthetic Assessment : Integrating Fuzzy Logic and Color Preferences. IEEE Access.

[2]. Byun,J.Y & Lee,Y.J (2019). A study on the Evaluation Characteristics of Personal Color Diagnosis and Result : for Job preparation student. J. Korea Soc. Beauty Art. 20(4), p.97-110.

[3]. Eun,G.H & Choi, M.L & Mun,Y.K (2021). A Study on the Difference Between Personal Color Self-diagnosis and Sensory Evaluation. . J. Korea Soc. Beauty Art. 22(4), p.41-54

[4]. Hong, H. R & Kim, Y. I (2019). A Mobile Application for Personal Colour Analysis. Cogent Business & Management. 6(1)

[5]. JACKSON, C. (1980) Color me beautiful. Washington, DC: Acropolis

[6]. Jonauskaite et al., (2020) Most and Least Preferred Colours According to object context : New Insights from an unrestricted colour range. PLOS ONE. 11(3).

[7]. Park,J.S & Kim,H.J & Ji,S.M & Hwang,E.J(2018). An Automatic Virtual Makeup Scheme Based on Personal Color Analysis. IMCOM '18. ACM

[8]. Park,Y.S & Kyung, C.H & Hyuk, Y.E.(2019). Qualitative Research on Motivations, Decision-Makers, and Effect of Personal Color Consulting. Journal of Fashion Design. 19(2), p.37-56

[9]. Radeloff, D.J. (1990). Role of color in perception of attractiveness. Perceptual and Motor Skills, 71(1), 151–160. doi:10.2466/PMS.71.5.151-160

Based on Deep Learning: A Regional Analysis of The Facade Color Schemes of Public Housing in Hong Kong

Yixuan Li*, Changying Xiang

Hong Kong University of Science and Technology, Hong Kong, China

**Corresponding author: ylita@connect.ust.hk*

ABSTRACT

Due to the large number of residents, public housing has always attracted widespread attention as a unique category of residential building in Hong Kong. Residents want to enhance the functionality and design of the housing units and the facade of their public housing. Most of the current study focused on monochromatic analyses of individual buildings. Research on the matching schemes and proportions of multiple colors remains notably scarce. Moreover, the process of analyzing colors relies heavily on manual operations performed by researchers, which may not yield quantitative results regarding different color ratios. We selected 16 public housing estates built after 2000 as the analysis objects and collected the main facade photos of them from Google Maps. The process of color analysis mainly consists of three steps. Primarily, we use Deep White Balance (DWB) to perform color correction on the collected photos. Subsequently, a deep learning-based object detection framework (Mask2Former) is employed to conduct batch semantic segmentation of the architectural part of the photos. Ultimately, we extracted the color types and proportions of these photos by K-means, followed by statistical analysis. Through the analysis, we observed that the predominant colors in most public housing are low-saturation grayish-white, characterized by high-saturation colors. Among these, the high-saturation colors primarily consist of green, blue, and orange hues, while purple appears less frequently. Decorative colors, as a more prominent part of architecture, tend to have high saturation and moderate lightness. This color scheme trend can provide a reference for the color design of public housing renewal and new public housing construction in Hong Kong and offer new solutions for the research on the color design of residential buildings.

Keywords: color in art and design, deep learning, architectural facade color, color identity

INTRODUCTION

As a typical residential building in high-density urban areas, public housing in Hong Kong has garnered significant attention. The public is not only concerned with the updates to building typologies but also places considerable emphasis on the visual effects of building facades. Residents navigate through public housing communities daily, and the facades of these buildings occupy a substantial portion of their visual field. Therefore, it is essential to conduct research on the color design of public housing facades.

At present, research on architectural color mainly focuses on two aspects: urban planning and individual buildings. Urban color planning emphasizes quality analysis based on regional cultural aesthetics[1]. Individual buildings color research focus on analyzing a single main color[2]. Therefore, there is still a significant gap in the quantitative analysis of multi-color facade color matching in architectural discourse.

Research on building facade colors often starts with collecting street view images or conducting on-site photography to gather image data[3]. On this basis, color correction and analysis are carried out on the building facade. Color correction in this process relies heavily on the personal experience of professionals, while

segmentation of the architectural components necessitates repetitive operations conducted by specialists. As the number of architectural samples increases, the workload associated with these two stages will consequently grow exponentially.With the popularization of machine learning, architectural color research has also attempted to embed deep learning models. Researchers can specifically train these deep learning models to meet their needs. The trained models are capable of effectively replacing labor-intensive and repetitive experimental procedures.
The primary objectives of this study are as follows:1) To design a research workflow for architectural facade color schemes by referencing traditional color analysis processes and integrating deep learning models; 2) To enhance the efficiency and accuracy of color research by substituting labor-intensive tasks with deep learning models during the quantitative analysis; 3) To identify trends in facade color combinations of public housing in Hong Kong through this research.

METHODOLOGY

The initial stage of the research conducted a survey on the quantity and distribution of public housing in Hong Kong. According to statistics from public sources such as the Hong Kong Housing Authority, there are currently approximately 264 public housing communities still in operation. After randomly selecting 20 public housing estates and excluding 4 public housing communities with overly old facade colors, 16 public housing estates were finally selected for the preference questionnaire survey (link:https://www.wjx.cn/vm/h4NUg6y.aspx). A total of 60 people participated in the questionnaire survey, among whom the ratio of male to female was approximately 1:1, and the ratio of design majors to non-design majors was also about 1:1. The proportion of Hong Kong residents among the participants is approximately 30%. Based on the results of the questionnaire statistics, the top 10 public housing estates in terms of popularity, including Cho Yiu Chuen , were selected as the important sample basis for color analysis.Given the timeliness of Street View images on Google Maps, real images of public housing were collected for this study. During this process, we also included eight adjacent public housing units of different colors in the sample and ultimately obtained 18 public housing buildings.

The traditional process for analyzing the color of building facades includes the following steps: obtaining street view images online, performing image color correction, segmenting parts of the building images, extracting colors, and conducting color analysis. This paper proposes a novel workflow of color analysis that involves capturing field images of buildings, applying deep white balance (DWB) for color correction, utilizing Mask2Former for image segmentation, employing the K-means algorithm for color extraction, and leveraging Python libraries such as Matplotlib for comprehensive color analysis（**Figure 1: Color Analysis Workflow**）.

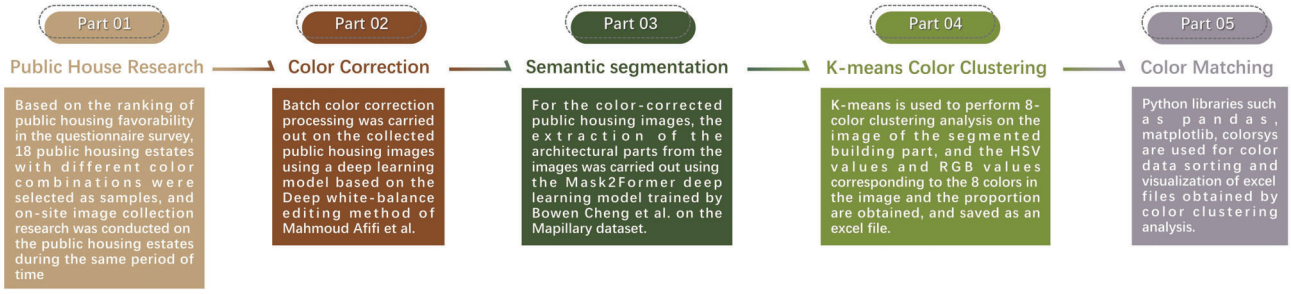

Figure 1: Color Analysis Workflow

Field research on public housing images is an important link to ensure the timeliness of images. To avoid color differences due to weather factors, image data collection was set between 12 am and 2:30 pm on a sunny day in June. Color correction is the second step in color analysis. The main purpose of this step is to correct color distortion caused by outdoor light. This study employs a deep learning model based on the Deep White-Balance Editing method[4]. This model specifically uses a DNN architecture to process images in sRGB format. Research

indicates that this model outperforms other models such as FC4, Quasi-U CC, and KNN-WB in terms of color correction effectiveness. The third stage is semantic segmentation of building images. In this study, the Mask2Former deep learning model trained by the Mapillary dataset was used for image segmentation [5] .The model has been proved to be superior to the currently widely used MaskFormer, Mask R-CNN and other models in segmentation effect, and its semantic model has the best performance in Mean Intersection over Union (mIoU). Notably, the Mask2Former model retains all the buildings during segmentation. To ensure the accuracy of the color analysis results, we manually removed the surrounding buildings from the images using Photoshop software.Next step after image segmentation is the color extraction of the image. In this study, the K-means algorithm is selected to cluster and extract colors, and the relationship between the main colors and decorative colors is analyzed[6]. After professional analysis, the maximum number of color types in the sample buildings was 8. Therefore, the K value for color extraction is set to 8 clusters (**Figure 2: Color Extraction Result**). The color extraction results include the HSV value, the RGB value of the color, and the corresponding proportion. During the color extraction process, dark colors with a brightness threshold lower than 0.3 are filtered out to eliminate the interference of reflection from the glass surface.The last step is data visualization. This study uses open-source Python libraries such as pandas, colorsys, and matplotlib to implement data visualization. The color data of this research is firstly read through pandas， then converted from RGB to HSV color systems by colorsys and finally visualized using matplotlib.

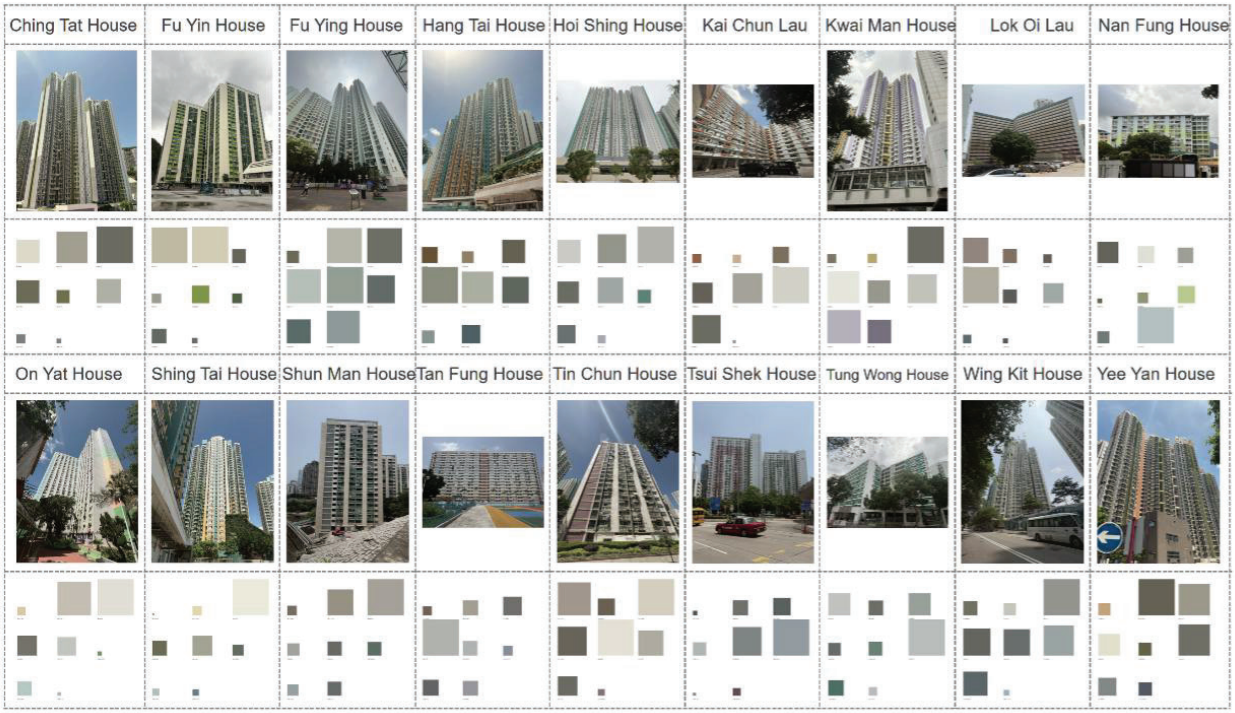

Figure 2: Color Extraction Result

Traditional color analysis typically employs three dimensions—hue, saturation, and value (HSV). In this study's data analysis, the values for three dimensions are uniformly set within a range of 0 to 1. Specifically, in the hue dimension (H), a value of 0 corresponds to red, approximately 1/3 (or 0.333) corresponds to green, and approximately 2/3 (or 0.667) corresponds to blue; in the saturation dimension (S), a value of 0 indicates complete desaturation (grayscale), while a value of 1 signifies full saturation (the most vivid colors); finally, in the value dimension (V), a value of 0 represents black (complete absence of light), whereas a value of 1 denotes maximum brightness for that color. Overall data is presented through bar charts (the x-axis represents RGB values and the y-axis indicates proportions) and 3D scatter plots. In the bar chart, each column's color directly illustrates its

corresponding hue and is grouped with dashed lines that indicate associated buildings. The 3D scatter plots include HVP diagrams (with hue on the x-axis, brightness on the y-axis, and proportion on the z-axis) as well as SVP diagrams (with saturation on the x-axis, brightness on the y-axis, and proportion on the z-axis). Additionally, 2D scatter plots are utilized to display primary colors and decorative colors in public housing facades[7].

RESULTS AND DISCUSSION

All color data statistics are plotted in a bar chart and two 3D scatter plots. As can be seen from the bar chart, the color scheme of each building is mainly composed of low-saturation grayish white as the main color and one or two high-saturation colors as decorative colors (**Figure 3: Overall Colors Bar Chart**). The main colors are divided into two types: cool colors and warm colors. In terms of color proportion, the proportion of decorative colors is mostly less than 10%, while the proportion of main colors is mostly higher than 15%. Meanwhile, there are low-saturation dark colors in few building's color scheme.

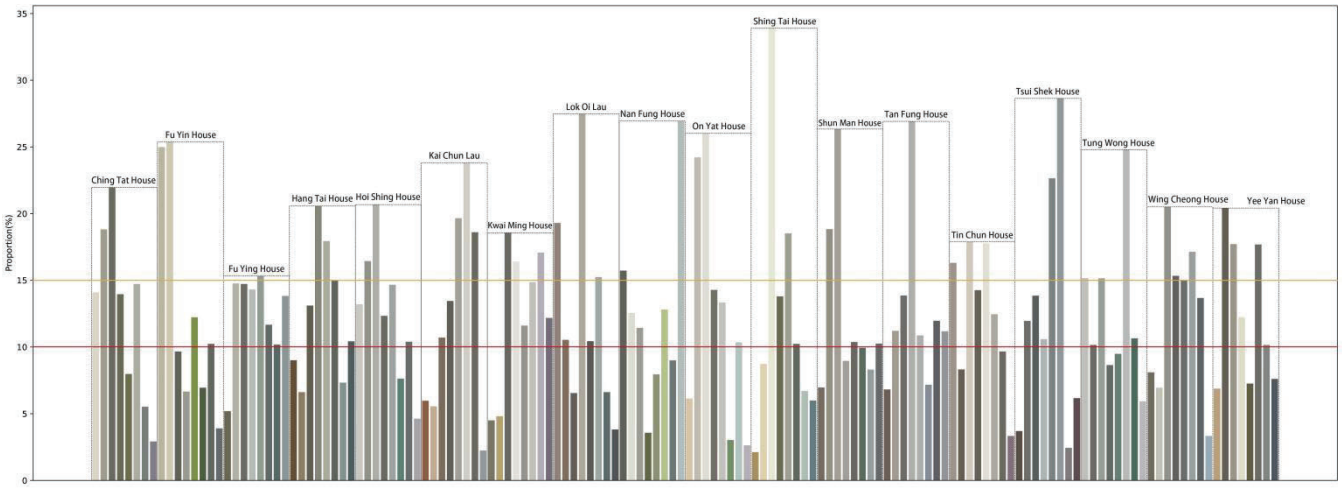

Figure 3: Overall Colors Bar Chart

From the 3D scatter plot, it can be seen that the HSV distribution of the overall color of the public housing facade is as follows:1) The S values are mostly concentrated between 0 and 0.3; 2) The H values are mostly concentrated in the orange range of 0 to 0.25, followed by the green and blue-green ranges of 0.35 to 0.55 with few above 0.8. 3) The V values are mostly uniformly dispersed above 0.45, with only a small amount of aggregation between 0.35 and 0.45(**Figure 4: Overall Colors 3D Scatter Plot**).

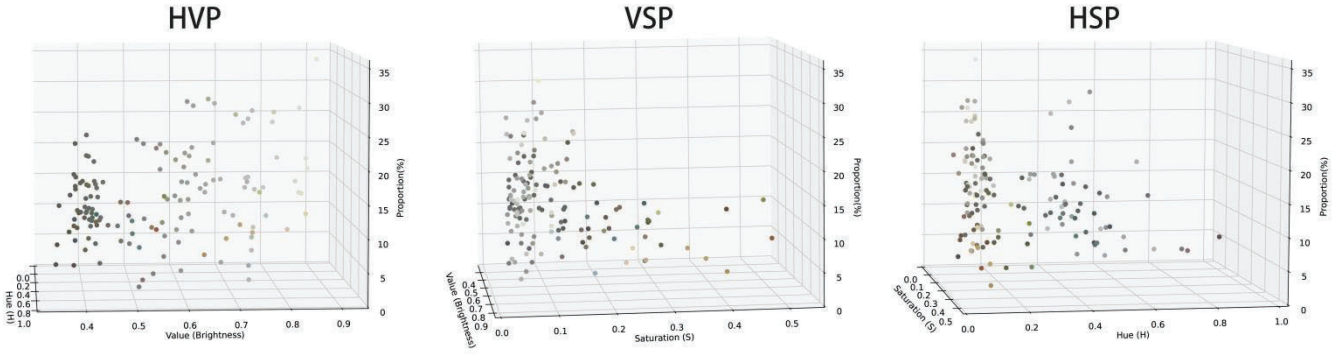

Figure 4: Overall Colors 3D Scatter Plot

The primary colors (with a proportion greater than 15%) and decorative colors (with a proportion less than 10%) are analyzed separately. From the figure, it can be observed that the S values of the primary colors are relatively evenly distributed between 0.02 and 0.16; the H values range from 0 to 0.75, with most concentrated between 0 and 0.23 (grayish hue); and the V values fall within the range of 0.35 to 0.9, predominantly above 0.5 (brighter color), while a small portion is found between 0.45 and 0.55(**Figure 5: Main Color 2D Scatter Plot**).

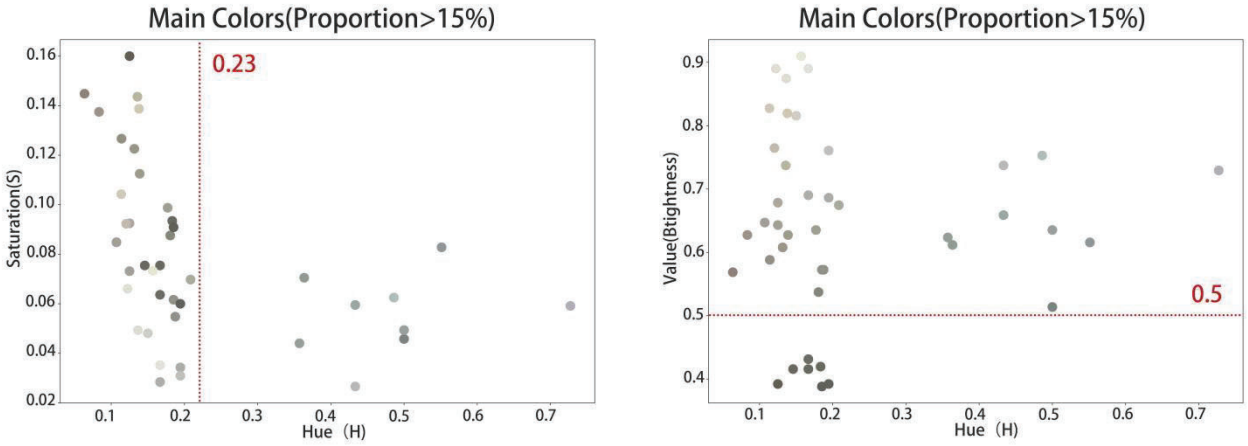

Figure 5: Main Color 2D Scatter Plot

The trend of decorative color is as follows: The S value ranges from 0 to 0.55, with the majority concentrated between 0 and 0.35. The V value spans from 0.3 to 0.9, exhibiting a relatively even distribution, although a small portion is concentrated between 0.35 and 0.55. The H value is relatively evenly distributed throughout the range of 0 to 1, with the majority falling within the range of 0 to 0.6. This range corresponds to yellow, green and blue (**Figure 6: Decorative Color 2D Scatter Plot**).

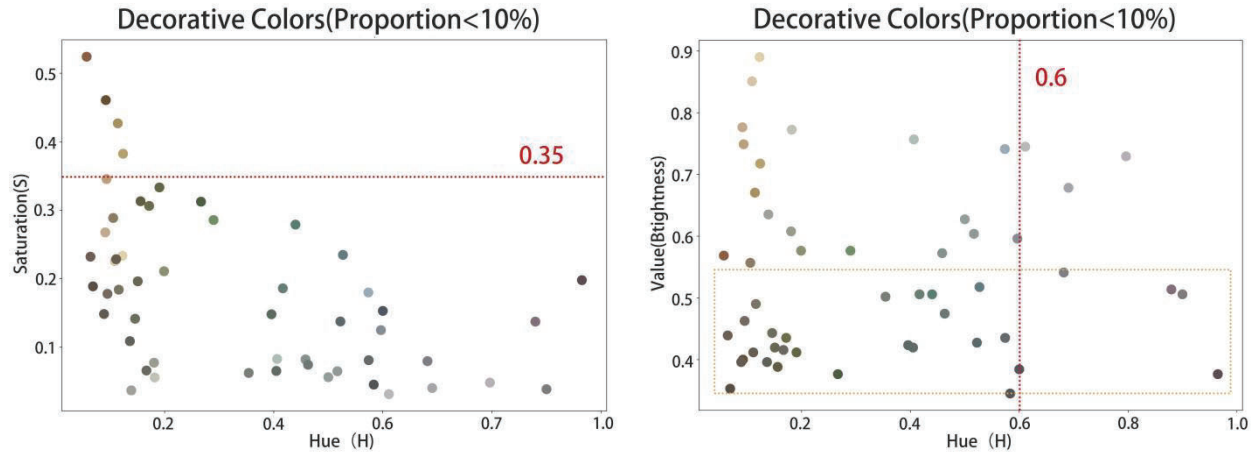

Figure 6: Decorative Color 2D Scatter Plot

From a quantitative perspective, this paper uses DL models to analyze the color schemes of public housing facades in Hong Kong:1) The DWB model is used for color correction; 2) the Mask2Former model segments the building components in the image; 3) K-means clustering is adopted to extract the facade color of public residential buildings; 4) Python libraries such as matplotlib were used to analyze overall color trends and HSV distributions of primary and decorative colors. These deep learning models have effectively replaced repetitive

tasks that were traditionally performed by professionals. This method not only saves human resources and shortens processing time but also reduces the impact of individual aesthetic differences on color results.

There are limitations in this research workflow. The image segmentation model used in this research can only identify the entire building but cannot remove the reflection from the window glass. Therefore, the clustering results still contain a certain proportion of dark colors even when colors with a brightness threshold lower than 0.3 are excluded. Moreover, shadows may cause one color to be wrongly identified as two or more different colors, which may affect the accuracy of results. Future research can enhance image segmentation models to extract building walls and remove building components like windows and pipes. In addition, the color clustering method needs to be improved in reducing the shadow's effect on color judgment, thereby enhancing the accuracy of the clustering results.

CONCLUSION

This article studies the tendency toward color matching on the facades of public housing buildings. Research has found that the facade color schemes of most public housing estates are composed of low-saturation grayish-white and high-saturation colors. Most high-saturation colors are orange, green, and blue, with less purple. The research results fill the gap in the study of facade color matching for public housing in Hong Kong and have great reference significance for the future facade color design of public housing. This study proposes a color analysis workflow combined with deep learning models. This workflow shortens the research time and avoids the influence of personal aesthetics on the research results. This workflow provides new ideas and inspirations for future research on the color of building facades.

REFERENCES

[1]. Xu, J. (2023). A linguistic approach to urban color design and research—Exploring jianming song’s methodologies. Color Research & Application, 48(5), 612–621. https://doi.org/10.1002/col.22849

[2]. Li, K.-R., Yang, Y.-Q., & Zheng, Z.-Q. (2020). Research on color harmony of building façades. Color Research & Application, 45(1), 105–119. https://doi.org/10.1002/col.22448

[3]. Gou, A., & Wang, J. (2017). A comparison between wishes and status: Gray is not the preference for residents while the city shows neutral colors. Color Research & Application, 42(5), 650–663. https://doi.org/10.1002/col.22122

[4]. Afifi, M., & Brown, M. S. (2020). Deep white-balance editing. 2020 IEEE/CVF Conference on Computer Vision and Pattern Recognition (CVPR), 1394–1403. https://doi.org/10.1109/CVPR42600.2020.00147

[5]. Cheng, B., Misra, I., Schwing, A. G., Kirillov, A., & Girdhar, R. (2022). Masked-attention mask transformer for universal image segmentation (No. arXiv:2112.01527). arXiv. https://doi.org/10.48550/arXiv.2112.01527

[6]. Molada-Tebar, A., Marqués-Mateu, Á., Lerma, J. L., & Westland, S. (2020). Dominant color extraction with K-means for camera characterization in cultural heritage documentation. Remote Sensing, 12(3), Article 3. https://doi.org/10.3390/rs12030520

[7]. Hunter, J. D. (2007). Matplotlib: A 2D graphics environment. Computing in Science & Engineering, 9(3), 90–95. https://doi.org/10.1109/MCSE.2007.55

Colour Conservation of The Dilworth Building, Auckland, New Zealand

Julian Rennie[a]* and Alessandro Premier[b]

[a]School of Architecture, Unitec, New Zealand.
[b]Future Cities Research Centre, School of Architecture and Planning, The University of Auckland, New Zealand.
*Corresponding author: Julian Rennie, jrennie@unitec.ac.nz

ABSTRACT

Architect William Gummer (1884–1966) was born in Auckland, New Zealand. In 1908, he travelled to the United Kingdom to study at the Royal Academy of Arts in London and later qualified as an Associate of the Royal Institute of British Architects. He notably worked for Sir Edwin Lutyens and Daniel Burnham of Chicago. Upon his return to New Zealand, he established the architectural practice Gummer Ford in 1923 with Englishman C.R. Ford, who had earlier travelled as the youngest member of Scott's Antarctica 1901–04 expedition. The practice went on to design several notable Auckland buildings, initially in the Beaux-Arts style and later in Modernist idioms. The Dilworth Building, constructed between 1925 and 1927, was commissioned to provide rental income for a school for disadvantaged boys. Built with a reinforced concrete structure and clad in Portland Stone, it occupies a prominent corner site at Queen Street and Customs Street in Auckland's CBD, facing the waterfront and the Ferry Building just 100 metres to the north. Its distinctive corner turret established it as one of the most recognisable buildings in the city. The Dilworth Trust office and boardroom occupied the top and most prestigious of its nine storeys, while the remaining floors were leased to tenants. Today, the building continues to house a mix of offices, apartments, and street-level shops. Although sold by the Dilworth Trust in the 1980s, it retains some original interiors. It commemorates a prominent early settler and member of the Provincial Council and contributes significantly to Auckland's early twentieth-century urban streetscape. This paper contextualises the colours used in the Dilworth Building alongside other works by Gummer Ford. The methodology combines a literature review, archival research (historic photographs and drawings), and on-site surveys. The latter includes identification of the building's interior and lightwell colour palette using the NCS Colourpin SE tool. The recorded colour codes are mapped to the NCS 1950 chart with equivalent RGB values. The resulting palette provides a basis for developing preliminary guidelines for the building's colour conservation. The aim of this research is to build upon the widely recognised significance of this important example of urban architecture in New Zealand.

Keywords: Colour conservation, Cultural heritage, New Zealand Heritage, Gummer Ford Architects.

INTRODUCTION

The current Dilworth Building is sited on the corner of Queen Street and Customs Street, Auckland, New Zealand, just 100 metres from the commercial waterfront of the Waitematā Harbour. This downtown building was commissioned to provide regular rental income for a school for disadvantaged boys, in the name of Irishman James Dilworth, and provides an example of the role played by philanthropy in the development of colonial New Zealand education. The school itself, Dilworth College, is still standing in the Auckland suburb of Epsom at 2 Erin Street, Epsom [1].

The CBD Dilworth Building was constructed between 1925 and 1927, with a steel-reinforced concrete frame and reinforced concrete floor slabs. The exterior cladding was Portland Stone, punctuated with steel-framed windows (generally casement sashes and fixed glazing). These stone claddings were sourced from quarries in Dorset,

England. Figure 1 illustrates the honey-toned warmth that Portland Stone offers. The title of Gummer and Ford's watercolour Urbis Porta (Latin for "City Gateway") clearly conveys the intent of creating an urban portal at the base of Queen Street, representing the view that a newly arrived colonial immigrant would encounter upon stepping off a ship at the Ferry Building had the mirrored double of the Dilworth Building been realised.

	NCS 1950	RGB	CIE L*a*b*	ELEMENTS
ENTRY (CUSTOM STREET)	S 4005-Y50R	158, 145, 134	lab (60.99, 2.9, 7.58)	TERRAZZO FLOOR
	S 3020-Y30R	190, 153, 115	lab (65.72, 8.57, 25.2)	TERRAZO FLOOR
	S 3020-R20B	178, 139, 150	lab (61.77, 16.56, -0.15)	TERRAZZO FLOOR
	S 6502-Y	105, 101, 94	lab (42.94, 0.21, 4.52)	TERRAZZO FLOOR: LETTERING
	S 8000-N	65, 63, 62	lab (26.81, 0.63, 0.91)	BRASS DOOR: NON OXIDISED
	S 5010-B30G	107, 125, 127	lab (51.07, -6.11, -3.3)	BRASS DOOR: OXIDISED
	S 8500-N	48, 46, 44	lab (19.07, 0.44, 1.61)	WALL CLADDING: MARBLE

Figure 1 (left): Gummer and Ford's %"#&ĀÀ$%1926), watercolour render looking south up Queen Street, Auckland, NZ of the proposed Dilworth Building (LHS), and the proposed mirror image building (never realized to the RHS). (Dilworth Building, Gummer & Ford Collection, GF33, Architecture Archive, UoA, accessed 14.07.2025) [2]. Figure 2 (right): colour palette of the entry (by the authors).

As cited in Heritage New Zealand, the Dilworth Building was built in memory of James Dilworth (1815–1894). Born in County Tyrone, Northern Ireland, he was educated at The Royal School, Dungannon, and later employed at the Northern Bank in Dungannon. He emigrated to New South Wales, Australia, in 1831 and travelled on to Auckland, New Zealand, in 1841. He purchased land around Mt Hobson, where Dilworth School (a school for boys) still operates today. Dilworth was also a prominent citizen, involved in establishing the Auckland Savings Bank (ASB). He served as a member of the Auckland Provincial Council and later on the University College Council [1].

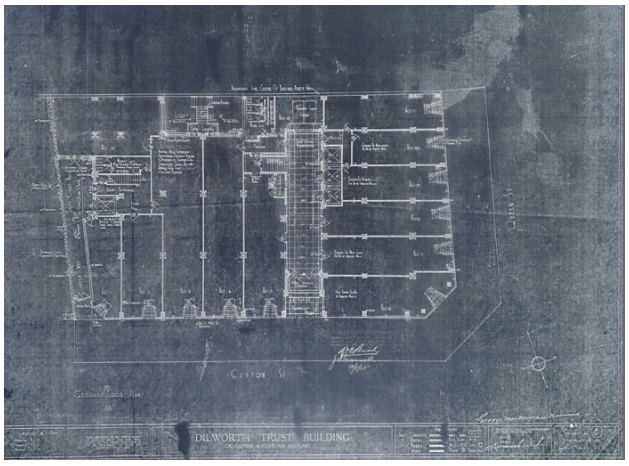

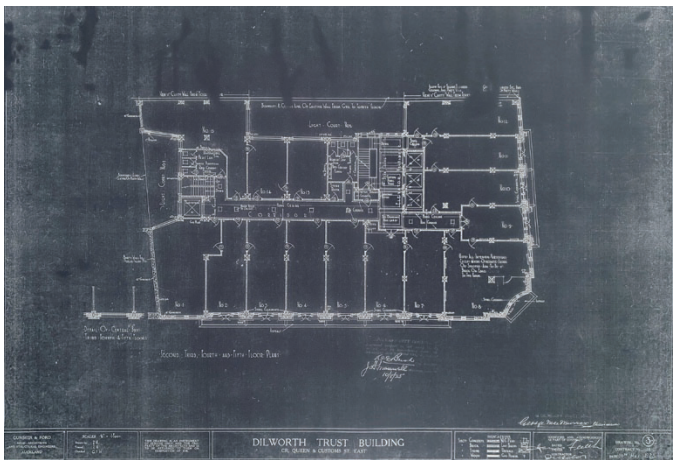

Figure 3 (left). Gummer and Ford's Blueprint of the Dilworth Building Ground Floor Plan, DWG #1, of Contract 12B, (14 May 1925). Figure 4 (right). Gummer and Ford's Blueprint of the Dilworth Building Second, Third , Fourth & Fifth Floor Plans, DWG #3, of Contract 12B, 14 May 1925. (Dilworth Building, Gummer & Ford Collection, GF33, Architecture Archive, UoA, accessed 14.07.2025). [2].

James Dilworth died in 1894, aged 79, without children of his own. He left most of his considerable estate to fund a school for boys from good families whose circumstances might otherwise prevent them from fulfilling their potential. Under the direction of his wife, Isabella Dilworth, the Dilworth Ulster Institute [known today as "Dilworth College"] was opened on 12 March 1906 [3].

The terms of Dilworth's will also stipulated that the school required an additional stream of annual income. Consequently, the CBD Dilworth Building was commissioned and built between 1925 and 1927 [3]. This new commercial downtown building provided rental income from "offices, shops and a ground floor restaurant. It had eleven shops… as well as the restaurant which was on the Customs Street frontage" [4]. However, the 1925 blueprints show twelve shops (see Figure 3). Today, there are currently eight shops, possibly reflecting the impact of online retail. The seven floors above the ground level were originally divided into twelve spaces per floor, separated by brick-on-edge interior walls (see Figure 4), which could accommodate offices. At present, the Building Directory beside the ground floor lobby lifts lists offices only on Levels 2 and 3, while Levels 4 to 8 are occupied by apartments. These inner-city apartments highlight the ongoing appeal of this high-quality building and its sought-after CBD location. Level 8 was originally designed as a type of "penthouse level," containing a loggia, two lightwells, a Building Manager's flat, and the Dilworth Trust Boardroom, an octagonal-shaped room with windows on all four sides, forming the "crown" of the corner tower massing above the two flanking street frontages (see Figure 4: Level 8 and Tower Floor Plans). Customs Street Elevation shows the contractual drawing of the proposed roof form above the rooftop Boardroom, which differs slightly from what is depicted in the watercolour of Figure 1. Finally, note the clusters of driven hardwood piles (essentially sharpened tree trunks) that were sunk into the seabed to support the reclamation foundation for this steel, concrete, and stone-clad building.

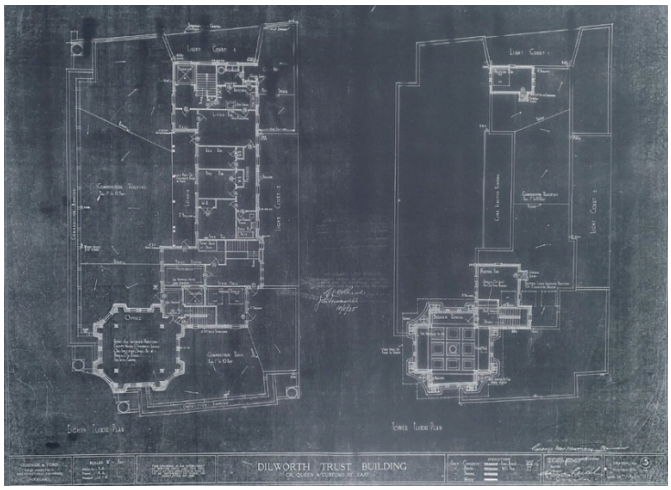

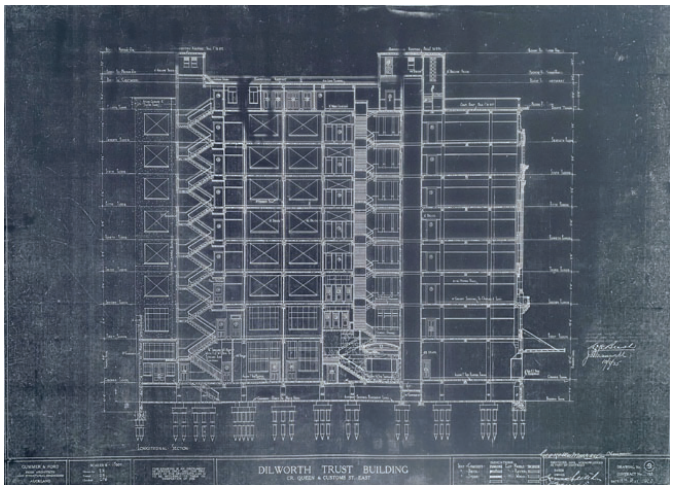

Figure 5 (left). Gummer and Ford's Blueprint of the Dilworth Building Eighth and Tower Floor Plans, DWG #5, of Contract 12B, (14 May 1925). Figure 6 (right). Gummer and Ford's Blueprint of the Dilworth Building Eighth and Tower Floor Plans, DWG #9, of Contract 12B, (14 May 1925). [2].

The Dilworth Trust Board sold the CBD building in 1984, although many of the longstanding tenants remained [3]. It is still a much sought-after address for inner-city apartments, with its staircase, balustrades, and handrails largely intact. Entry to the upper floors was originally from Customs Street, via a 20.300 m deep by 3.770 m wide entry lobby (see East–West Section in Figure 6). The original shallow vaulted ceiling of the lobby has since been modernised, but the marble wall linings remain largely as they were. The three lifts at the back right-hand side of the lobby also survive. The current lobby floor is terrazzo, which does not appear to be original.

Shanahan described the original entry elements as follows:

"a set of large metal folding doors… above there is a wrought iron grill incorporating a glass plate, stretching across the width of the entrance, with the name of the building in gold letters. On either side of the entrance vestibule, directly behind the first set of doors, are the large wooden framed directories" [4].

These original entry elements have since been removed. Today, the entry consists of a set of side-hung bronze-framed toughened glass doors (with swipe card access for after-hours), set between similar fixed sidelight glazed panels. The name of the building (via Bronze letters) is now set terrazzo paving at the entry threshold. This lobby from Customs Street runs north to south to the three lifts, which from the first floor (and above) the circulation corridor runs in a west to east direction to provide access to the current apartments (previously offices).

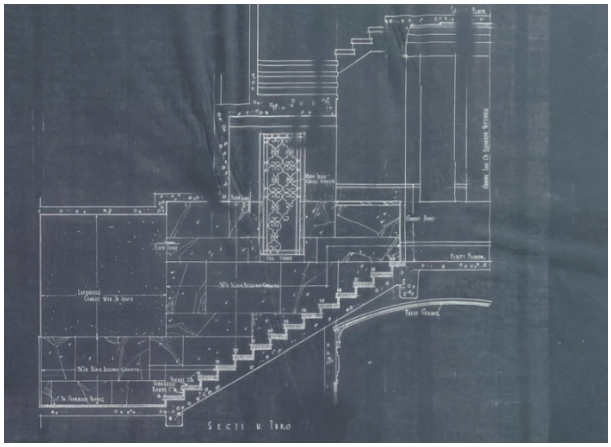

Figure 7 (left) Authors own photo (LHS). Figure 8 (right) Gummer and Ford's Blueprint of part Details of the Dilworth Lobby Stair, DWG #26, of Contract 12B, (14 May 1925). [2].

METHODOLOGY

The research employed a mixed-methods approach comprising desktop study, archival investigation, and field analysis using the NCS Colourpin SE tool. The desktop study focused on literature relating to the architects' work, including theses available at the University of Auckland Library, research reports, journal articles, and relevant online resources. The archival investigation examined the original architectural drawings held in the University of Auckland's Measured Drawing Collection (see Figures 1, 3, 4, 5, 6 & 8). The building's colour palette was established through a field study using the Natural Colour System (NCS). Surface colours were recorded by applying the NCS Colourpin SE device directly to building surfaces, with matches captured via the Colourpin mobile application. Identified colours were tabulated against the NCS 1950 chart, with corresponding RGB values generated by the software as well as CIELAB codes to better suit contemporary colour management and applications. Given the building's history of modifications, the analysis focused primarily on existing surface colours. The resulting palette was critically analysed using NCS+ software. Colour spaces were examined to identify recurring hues and material groupings. Their position within the colour space provided insights into the rationale underlying the designers' chromatic choices.

RESULTS AND DISCUSSION

The colour palettes of the building (Figures 2 and 9) reveal the wide range of materials that have been used, as well as the consistency in the material selection within the building and with other relevant work of the same practice. By looking at the terrazzo flooring of the entry one may immediately connect this building with the NZI Building

(1918) in Queen Street, (now called the New Zealand Guardian Trust Building). However, in Shanahan's [4] thesis there is no mention of such flooring. Similarly to that building, iron balustrades with polished wooden handrails (S 5040-Y40R) characterize the staircase [5]. Doors are also solid timber. There is a wide use of marble. Differently from the NZI Building, at the entry black Nelson marble is used on walls (S 8502-Y), on the main staircase (S 8000-N) and on skirting (S 7500-N). On the upper floors (e.g., level 7) grey-coloured marble is used on lift lobby wall linings (S 3502-Y). Wall paint is currently almost always in whitish hues, as noted in the NZI Building, while concrete staircase steps are painted grey. The marble hues range from beige to grey and black in the entry lobby. The terrazzo flooring at the entry along Customs Street is identical to the entry lobby and it clearly recalls that of the NZI Building entry hall. However, it is not clear whether this is a recent addition inspired by previous work of the same architects. From Shanahan's thesis (1983) [4] it seems that the entry lobby, while maintaining the brass doors, has been modified with the removal of significant woodwork. The multi-coloured terrazzo flooring is in three main hues (earthy natural colours). Inside the fire riser ducts it was possible to identify different wall paint in whitish colours. Overall, we may affirm that the colour palette of the Dilworth Building is less rich than that of the antecedent NZI Building, indicating an overall lower budget for surface materials and finishes.

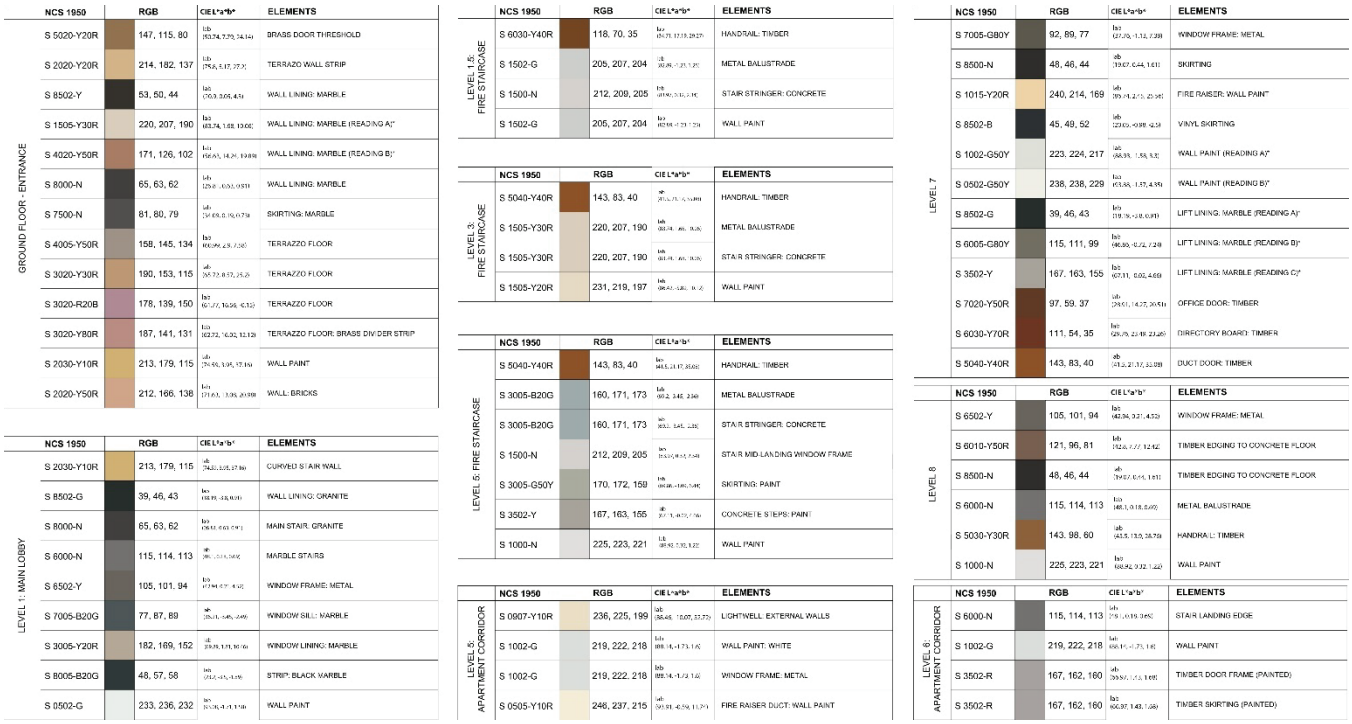

Figure 9. Colour palette of the Interior spaces of the building (by the authors)

Overall, the colour palette, similarly to the Gummer's NZI Building [5], highlights the use of natural materials: marble and timber with their contrasting colours, and the 'earthy', 'warm' hues of the terrazzo flooring. It should be noted that the building has apparently been modified over the years, although a specific analysis of the property files has not been carried out in this case. The analysis of part of the NCS colour space (Figure 10) indicates at least six different materials with the same hue Y50R – 50% yellow and 50% red – and Y30R – 70% yellow and 30% red – and different nuances (blackness and chroma). This, once again, highlights the selection of key materials that are in the same colour space and are recurring in the building: terrazzo flooring, timber doors, bricks, and marble lining. It is noteworthy that four of these colours are darker (closer to pure black – S) and three of them are lighter (closer to pure white – W), hence equally distributed within that space. All of them are clearly very far from the maximum chromaticness (C), which indicates the choice of low-saturated colours, typical of natural materials and paints

produced with natural pigments. This is perfectly aligned with the analysis of the NZI Building previously carried out by the same authors [5].

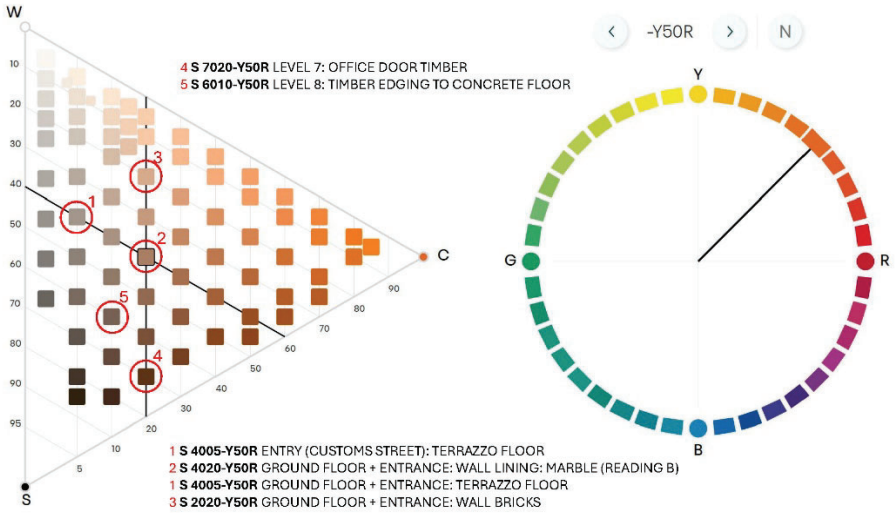

Figure 10. NCS Colour-space of Y50R

CONCLUSIONS AND RECOMMENDATIONS

As always, conservation interventions should tend towards a rigorous preservation of existing original materials, with a critical reflection that could be applied to the colour of materials that are clearly replacements of the original ones (for example, the vinyl skirting). Our research, which combined desktop analyses and field survey using the Colourpin device and the NCS Navigator to study colour combinations, led us to formulate the following recommendations for the colour conservation of this building: remove the existing vinyl skirting where present (e.g., on level 7) and replace it with a suitable plaster finish; we also suggest harmonising the indoor wall paints with a common white, for which S 1002-G seems appropriate. Our on-site research and Colourpin analysis of final colour palettes are intended to serve as a reference for practitioners in regard to any future conservation, without resorting to damaging the building via 'paint scrapings' or other intrusive methods of investigation.

REFERENCES

[1]. Dilworth Trust Board. (2024). The Story of Dilworth. Dilworth. https://www.dilworth.school.nz/about-us/the-story-of-dilworth/

[2]. Gummer & Ford. (n.d.). Dilworth Building, Gummer & Ford Collection, GF33, Architecture Archive, University of Auckland.

[3]. Heritage New Zealand. (2023). Dilworth Building: Historic Place Category 1 (List No. 4600). Heritage New Zealand Pouhere Taonga. https://www.heritage.org.nz/list-details/4600/4600

[4]. Shanahan, K.J. (1983). The Work of William H. Gummer, Architect [B.Arch. Thesis]. School of Architecture, University of Auckland.

[5]. Premier A., Rennie J. (2024). Colour conservation of the New Zealand Guardian Trust building, 48th Asian Color Association Conference (ACA2024). Proceedings of 8th Asian Color Association Conference: Harmony in Hue: Bridging Colors and Code. Chulalongkorn University.

Thoughts on The Use of Close-Range Photogrammetry in Chromatic-Spatial Investigations: The Case of Gaudí's Expiatory Temple of The Sagrada Família

Leonardo Pestana Collalto Toni[a*], João Carlos de Oliveira Cesar[a]

[a] Faculty of Architecture, Urbanism, and Design of the University of São Paulo – FAUUSP, São Paulo, Brazil

[*]Corresponding author: Leonardo Pestana Collalto Toni, leocollalto@usp.br

ABSTRACT

The study of chromatic compositions in architecture is an important way to understand the various possibilities of thinking about color in the creation of architectural spaces. These studies often rely on methodologies involving the digital reading of color samples using devices like Colorpin or Nix chromatic sensors, or by comparing the samples with color charts. However, these tools do not allow the reading of the colors projected by lights or shadows, which can change over time and significantly alter the perception of an environment's chromatic context. A building that exemplifies this issue is Antoni Gaudí's Expiatory Temple of the Sagrada Família, whose interior is bathed in a dynamic variety of colors projected by the light filtered through its multicolored stained-glass windows. These windows imbue the space with cooler tones in the morning and warmer tones in the afternoon, mimicking the natural hues of the sunlight throughout the day. This is a key component on the concept of the interior of the basilica, which seeks to represent a lush forest, not only in its form, but with its ambience built by the play of lights, shadows and colors. How, then, can we perform a truthful chromatic reading of those colors that are not embedded in the construction materials themselves but are instead conferred upon them by the ambient light? Close-range photogrammetry can serve as a useful tool for chromatic mapping in such cases. These surveys, based on a methodical photographic record, generate data such as georeferenced colored point clouds, from which the colorimetry of each point can be extracted, allowing for analyses of the environment's chromaticity not only at one time, but even comparing the colors on the studied spaces between different hours of the day. Additionally, this type of chromatic survey can be conducted with accessible devices, such as smartphones or digital cameras, as opposed to the up mentioned costly colorimeters. This presentation seeks to investigate the possibilities of using the close-range photogrammetry survey in the chromatic study of built environments with colors projected by lights, using the interior of Gaudi's Basilica of the Sagrada Familia as a case study. For the proposed analysis, a photogrammetric survey was conducted using over 2,600 images captured on site in 2023. This process resulted in a three-dimensional point cloud comprising more than 790,000 georeferenced points, from which chromatic information was individually extracted and then analyzed.

Keywords: close-range photogrammetry, chromatic survey, Expiatory Temple of the Sagrada Familia, Antoni Gaudí

INTRODUCTION

Designed by Antoni Gaudí i Cornet, the Expiatory Temple of the Sagrada Família in Spain is a monumental architectural work, remarkable not only for its physical scale but also for its formal complexity and its symbolic and chromatic richness. Construction began in 1882 and continues to this day, even 99 years after Gaudí's death, following the project he developed over more than 40 years of his life. The temple was conceived as a physical and

symbolic representation of the life of Christ, with each element, color, and façade intentionally designed as a vehicle for meaning and symbolism, always drawing inspiration from nature [1].

Gaudí's chromatic conception for the Sagrada Família sought to endow the building with life—not a static life, but one that changes in accordance with the passing of days, months, and years after its construction [2]. One of the most striking examples of this is the temple's interior, bathed in the colors of multicolored stained-glass windows designed to mimic the hues of sunlight throughout the day. Cooler tones dominate in the morning, while warmer tones appear in the afternoon, transforming the chromatic atmosphere of the temple's interior in response to the sun's shifting position.

Figure 1: Naves of the Sagrada Família colored by sunlight filtered through its stained-glass windows.

This type of chromaticism in space, defined by incident light rather than by the inherent properties of construction materials, poses significant challenges for conducting chromatic analyses of such environments. In addition to being in constant flux, it cannot be measured using conventional chromatic readers such as Colorpin or Nix, which isolate the sample from external light in order to record it [3]. These devices, based on the registration of samples illuminated by their own standardized light source, can only capture the chromatic information of the materials themselves. Other methods of chromatic assessment, such as visual color pallets, also encounter limitations, as they require consistent illumination and physical access to the surface being analyzed.

To overcome these challenges, close-range photogrammetry has been proposed as an alternative tool for chromatic assessment and analysis in environments where color is defined primarily by light. This method, based on the systematic photographic recording of the object of study followed by digital processing, makes it possible to generate georeferenced and colorized point clouds. The resulting datasets can then be exported and analyzed either individually or through spatial and quantitative subsets. The present article seeks to explore the potential of this tool for chromatic surveying, focusing on the analysis of the interior of the Sagrada Família.

METHODOLOGY

To carry out this investigation, a methodology was defined consisting of four sequential procedural stages:

1 - A systematic photographic survey of the interior of the Expiatory Temple of the Sagrada Família, using a Redmi Note 10 Pro (Xiaomi) smartphone camera, with 64 megapixels;

2 - Photogrammetric processing of the photographs in Agisoft Metashape to generate a georeferenced and colorized point cloud;

3 - Export of the positional and chromatic data of the model's points into a Microsoft Excel spreadsheet;

4 - Analysis of the exported data based on chromatic–spatial relationships.

RESULTS AND DISCUSSION

Close Range Photogrammetry of the Expiatory Temple of the Sagrada Família

Since it is based on photographic recording, close-range photogrammetry enables the capture of chromatic information of spaces in a way that more closely reflects human visual perception. It also accounts for contextual factors and does not restrict the reading of colors projected by light. On this basis, the analysis began with a systematic photographic survey of the interior of the Expiatory Temple of the Sagrada Família, carried out on March 21 and 22, 2023, at different times of day, in order to document the full range of luminous variations that occur within the space throughout a day. A total of 2,643 images were captured, with the aim of recording every detail and element of the temple's interior. The large number of photographs was crucial, as the reliability and accuracy of the point cloud depend on the cross-referencing of visual information from multiple recorded angles [4].

The images were processed using Agisoft Metashape, a software that compares them in pairs, identifies common points, and triangulates them with corresponding points from other images, positioning them within the three-dimensional space reconstructed by the program. The full workflow of procedures, calculations, and outputs performed by Metashape is detailed in Pepe & Domenica [5].

The processing resulted in a georeferenced and colorized point cloud (Figure 2) with more than 1,500,000 points, each containing three positional attributes (X, Y, Z) and three chromatic attributes (R, G, B). After filtering and refinement, this dataset was reduced to 796,350 points. The point cloud and its attributes were then exported to a .txt file containing 796,350 lines, each representing a point with its positional data in meters, and its chromatic data in RGB values. This text file was subsequently imported into a Microsoft Excel spreadsheet, where the data were organized into rows and columns. In this structure, each row corresponds to a point and each column to one of its attributes: columns A, B, and C containing the positional data in meters, while columns D, E, and F containing the chromatic information in RGB.

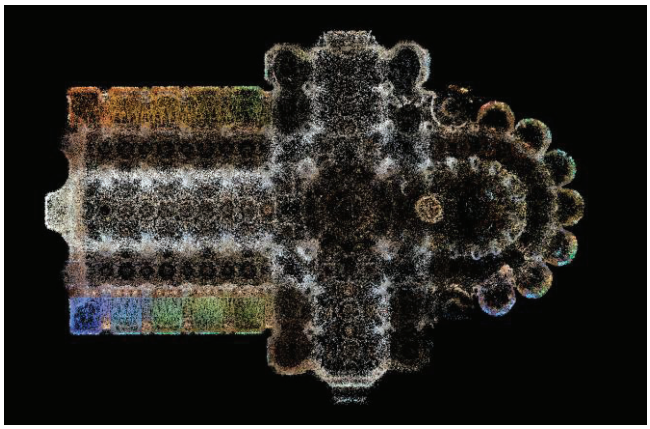

Figure 2: Top view of the point cloud generated from the interior of the Sagrada Família.

Chromatic/Spatial analysis of the point cloud

The first step undertaken in the analysis was the extraction of additional color properties from the points of the cloud, using Excel function macros. Seven different macros were created to derive, from each row, the color represented by the exported RGB code, its corresponding hexadecimal code, the numerical chromatic hue (ranging

axes) and a 15 m module in height section. Thus, the choir positioned along the sides of the temple is at 15 m in height, the lower vaults are at 30 m, the central nave vaults reach 45 m, the central vault at the crossing is at 60 m, and the top of the Maria vault, above the altar, reaches 75 m [1]. Each of these "slices" exhibits distinct chromatic treatment in the stained-glass windows and construction materials, affecting the dispersion of light and hue within the church, as shown in Table 2.

Table 2: Average color by vertical module of the temple and overall average color.

AVERAGE COLOR PER HEIGHT				
HEIGHT	R	G	B	COLOR
0-15 m	116	106	95	
15-30 m	109	103	90	
30-45 m	147	142	135	
45-60 m	122	108	91	
60-75 m	110	85	60	
GLOBAL	119	110	99	

Although the temple presents different chromatic treatments on its two sides—with cooler-toned stained glass on the east and warmer tones on the west—these differences neutralize each other, creating a more balanced, grayish mid-range color, visible in the sections between 0 and 30 m in Table 2. The region between 30 and 45 m contains colorless stained glass windows, which Gaudí intended to bring in pure white light, symbolizing Christ according to Christian belief [1]. The region from 45 to 60 m includes vaults covered with reddish ceramic pieces, edged in concrete, resulting in a warm yet still grayish tone. The region between 60 and 75 m encompasses only the vault dedicated to Mary, fully clad in ceramic tiles with golden edges, producing a reddish tone with higher saturation.

Finally, two global analyses of the colors within the Sagrada Família's interior were conducted. The first, shown in the chart in Figure 4, displays the overall quantitative distribution of points according to their hue range. The second, shown in Figure 5, presents the quantitative distribution of points based on their value properties (percentage of white and black) and saturation. For the first analysis, 12 chromatic sections were defined, each representing 30° of the 360° color wheel. This reading highlights the predominance of reddish and orange tones within the interior, followed by a much smaller secondary peak of bluish tones. This pattern is explained by the dominance of reddish and orange construction materials, such as sandstone and porphyry, as well as the large western-side stained-glass windows. Blue tones are primarily found in the east-side and apse stained glass windows, and in pieces of Blue Bahia marble used in portions of the floor.

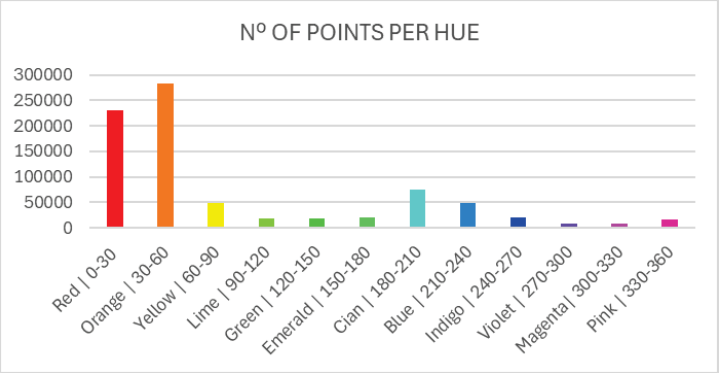

Figure 4: Global quantitative distribution of points according to their hue.

In the second global analysis, presented in the chart in Figure 5, a large concentration of points with a low percentage of white is evident, peaking between 20% and 30%, a medium concentration of black, peaking between 50% and 60%, and low saturation, peaking between 0% and 10%. This analysis allows us to identify that, although there are points with high saturation—such as in the stained-glass windows—the overall chromatic composition of the temple's interior is predominantly desaturated and dark.

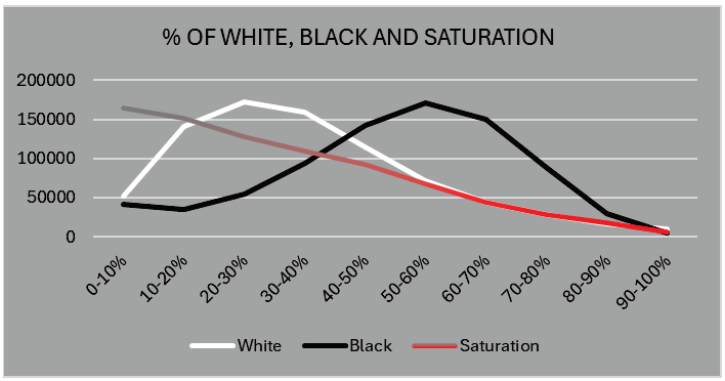

Figure 5: Global distribution of points based on the percentage of white, black, and saturation in their chromatic composition.

CONCLUSION

Although chromatic survey through close-range photogrammetry does not guarantee an extremely precise reading of colors—since such capture may vary according to the settings and quality of the camera employed—its use nonetheless enabled the analysis of the ephemeral chromaticism of the interior of the Sagrada Família, produced by the projection of colored light through its large stained-glass windows. This method produced over 790,000 individual chromatic readings, which could be analyzed both individually and collectively, considering not only the composition of color but also its spatial distribution. The study demonstrates that, once variables are controlled and based on a homogeneous and extensive photographic survey, close-range photogrammetry can serve as an important alternative for chromatic analysis of environments whose colors are defined by variations in lighting, in addition to the inherent properties of the materials used in their construction.

REFERENCES

[1]. Faulí i Oller, J. (2021). The Basilica of the Sagrada Familia. Barcelona, ALDEASA.

[2]. Brunet, C. M. (2007). Conversas com Gaudi (1ª edition). São Paulo, Perspectiva.

[3]. Mancini, M., Weindorf, D. C., Monteiro, M. E. C., de Faria, Á. J. G., dos Santos Teixeira, A. F., de Lima, W., de Lima, F. R. D., Dijair, T. S. B., Marques, F. D., Ribeiro, D., Silva, S. H. G., Chakraborty, S., & Curi, N. (2020). From sensor data to Munsell color system: Machine learning algorithm applied to tropical soil color classification via Nix^{TM} Pro sensor. Geoderma, 375, 114471. https://doi.org/10.1016/j.geoderma.2020.114471

[4]. Moyano, J., Nieto-Julián, J. E., Bienvenido-Huertas, D., & Marín-García, D. (2020). Validation of Close-Range Photogrammetry for Architectural and Archaeological Heritage: Analysis of Point Density and 3D Mesh Geometry. Remote Sensing, 12(21), Article 21. https://doi.org/10.3390/rs12213571

[5]. Pepe, M., & Domenica, C. (2020). Techniques, tools, platforms and algorithms in close range photogrammetry in building 3D model and 2D representation of objects and complex architectures. https://doi.org/10.14733/cadaps.2021.42-65

[6]. Lluch, J. S. (2019). Color for Architects. Princeton Architectural Press.

[7]. Brandi, M. F. P. (2025). Sutilezas cromáticas na arquitetura de Frank Lloyd Wright. [Dissertação, Universidade de São Paulo]. https://doi.org/10.11606/D.16.2025.tde-26052025-162817

Heritage in Color: Challenging The Neutrality of Globalized Urban Landscapes via Chromatic Ambiances

Zeinab Chehata[a*] and Faten Hussein[b]

[a] PhD student, ERA, LARPAA, National School of Architecture and Urbanism, University of Carthage,Tunisia

[b] Associate Professor, ERA, LARPAA, National School of Architecture and Urbanism, University of Carthage, Tunisia

ABSTRACT

Colonialism has long been erasing indigenous cultures; not always through destruction, occupation and exploitation, but through slow, calculated suppression. While direct violence is easy to condemn, globalization has introduced a quieter form of cultural erasure under the pretense of "modernization". Nowhere is it more evident than in architecture and urban spaces, where local and traditional chromatic ambiances and practices are being overwritten by neutral, standardized palettes dictated by economic and political intentions rather than cultural narratives. In post-colonial regions like the Middle East and North Africa (MENA region), this is more than just an aesthetic shift; it is the loss of a sensory heritage deeply embedded in cultural identity. The ideological deployment of white façades in modernist and post-war contexts similarly illustrates how color suppression served both political and economic agendas. This research investigates the reclamation of chromatic identity as an act of cultural resistance, using the Medina of Sousse as a case study. Once rich in color and ambiance, the medina has suffered a gradual erasure of its indigenous palettes due to anarchic urban expansion after independence and haphazard restoration policies that disregard autochthonous representation. To address this, the study employs a methodological protocol based on multiple "color walks" along the same path, carried out by different profiles of users: a local resident, a local non-resident visitor, a foreign visitor, and an expert observer. Each participant documents chromatic ambiances through photographs and narratives, allowing the comparison of individual perception with expert analysis. These observations are then processed with digital tools, including colorimeter applications, to scientifically identify palettes, hues, and concentrations. A key aspect of this research is the role of Artificial Intelligence (AI), which, while majorly complicit in spreading mass-produced aesthetics, is here redirected toward cultural preservation. Color data gathered from fieldwork and historical records will be used to train AI models to recognize and reconstruct chromatic identities, generating predictive palettes that can be compared against community recollections. This dual analysis allows the evaluation of whether AI can act as a reliable tool for safeguarding collective chromatic memory or risks reinforcing homogenization. Beyond cultural resistance, the study highlights sustainability: traditional palettes are tied to locally sourced materials and climate-adaptive design, making their revival both an ecological and cultural necessity. By combining ethnographic engagement with technological innovation, this research positions chromatic identity as an essential yet neglected dimension of heritage conservation, advocating for restoration practices that revive and reclaim rather than neutralize and erase.

Keywords: Chromatic Identity, Cultural Resistance, Heritage Preservation, Artificial Intelligence, Indigenous Sensory Ambiances

INTRODUCTION

Globalization and post-colonial urban development have reshaped the sensory landscapes of cities, often erasing indigenous chromatic ambiances that encode cultural memory and identity. In architecture and urban spaces, traditional palettes are increasingly replaced by neutral, standardized colors dictated by economic, political, or aesthetic agendas, resulting in the gradual disappearance of culturally embedded sensory heritage [1]. The Medina of Sousse exemplifies this transformation, where uncontrolled urban expansion and inconsistent restoration policies have fragmented its traditional color patterns and disrupted collective memory [2].

Despite growing interest in architectural and urban heritage, few studies systematically reclaim color as a medium of resistance. The limited use of emerging technologies, such as AI, in heritage color analysis further motivates this research. Color remains a powerful vector against homogenization, reaffirming urban identity and sustaining ambiances that anchor communities in their historical continuum. Reframing it as a tool of cultural agency is thus essential for rethinking heritage practices.

This study aims to document the Medina of Sousse's chromatic ambiances through participatory "Color Walks," apply AI-assisted analysis to identify and model heritage palettes, and evaluate the alignment between algorithmic predictions and community recollections, positioning color as both a cultural and environmental heritage.

METHODOLOGY

Case Study

The research focuses on the Medina of Sousse; a UNESCO World Heritage Site selected for its layered chromatic identity and its exposure to pressures of globalization. Four participant profiles were included in the Color Walks: a local resident, a local non-resident visitor, a foreign visitor (tourist), and an expert observer.

Participants followed a 15mns walking route across the medina, designed after Petit's methodological precedent [3, p. 282] to ensure immersion without fatigue. They carried out three parallel tasks: (1) Colorimetric sampling with smartphone applications to quantify hue, saturation, and intensity, (2) Photographic documentation at scales significant to each participant, and (3) Spontaneous verbal commentary, audio-recorded during the walk. This protocol integrated measurable chromatic data with perceptual memory and narrative interpretation [4].

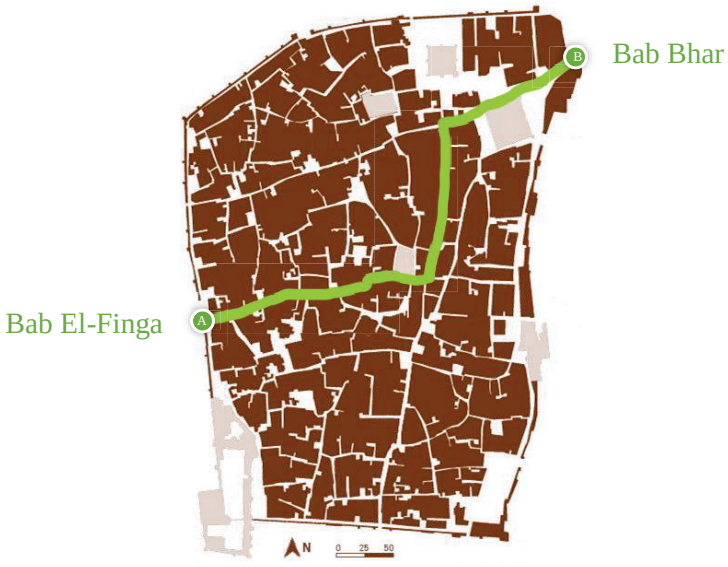

Figure 1: Orientation map provided to participants with the chosen "parcours" in green. Source: Author

Analytical Framework

Two smartphone applications were used: Color Picker & Generator (Appsvek) for palette extraction and Color Picker (Mikhail Gribanov) for precise RGB, LAB, and HSV sampling, with white-balance calibrated via a neutral grey card. Compared to traditional colorimeters, this lightweight, app-based approach enabled accessible façade-level surveys [3, pp. 139, 143–144].

Chromatic extraction and clustering: Photographs were processed with Color Thief for dominant pixel clusters, complemented by point-based swatches. Each participant dataset combined app palettes, clusters, swatches, and coded commentary (e.g., residents emphasized identity and material, tourists emphasized atmosphere and views).

Archival, policy and oral-memory layer: Historical photographs, municipal records, and semi-structured interviews with older residents and artisans reconstructed past palettes and distinguished top-down from grassroots color changes [5]. AI-colorized archival images were analyzed alongside contemporary data to track diachronic shifts.

AI-assisted analysis (pilot): AI was introduced as an exploratory, human-guided layer rather than a replacement for interpretation [3, p. 147]. Workflows included clustering and predictive palette generation, weighted by participant-identified cultural significance [6], and validated against participant feedback and historical reconstructions to avoid homogenization.

Triangulation and validation strategy: Five layers were triangulated: app-derived colorimetry, image-based clustering, ethnographic coding, AI-generated predictive palettes, and AI-colorized archival palettes. Validation combined internal cross-checking with participant evaluation of generated palettes.

Contribution: This protocol integrates participatory fieldwork, calibrated digital sampling, archival and oral memory, and AI-assisted analysis, offering a robust framework for reconstructing and preserving heritage chromatic identity.

RESULTS AND DISCUSSION

Distinct patterns emerged across participant types, reflecting how chromatic identity is filtered by cultural position and experience:

1. **Local resident:** Photographs centered on pale limewashed walls, muted whites, and blue-painted woodwork. Commentary emphasized continuity: "This is how the houses always looked; these colors feel like home even when they fade."
2. **Local non-resident visitor:** Balanced between architectural fragments and vibrant public spaces, capturing blues and ochres but also painted signs. "It is familiar, but the colors are more mixed now, some original, some newer."
3. **Foreign visitor (tourist):** Focused heavily on markets, fabrics, and merchandise. Palettes extracted were dominated by saturated reds, greens, and bright textiles. "This is what I will remember of the medina; all the colors of the shops."
4. **Expert observer:** Targeted architectural materials (stone, plaster, ceramics), avoiding commercial intrusions; palettes leaned toward ochres, beige, and weathered blue. "The nuisances disappear if you look at the materials; the chromatic identity lies in these layers."

Coding participant narratives via Pyykkö's seven categories highlighted differing emphases: tourists prioritized views and atmosphere, residents' identity and material, experts' architectural detail, and local non-residents contrasts [7].

from 0 to 360), the chromatic sector of the hue, and the levels of black, white, and saturation (ranging from 0% to 100%). These properties enable a comprehensive understanding of the analyzed colors, as they are determined by their hue, brightness, and saturation [6], as presented by Brandi [7, p. 49]:

> "Saturation is the intensity of the purity of the perceived color. It ranges from gray (minimum saturation) to pure hue (maximum saturation). The term vividness is often used to describe saturation. Brightness refers to the amount of black or white in the color. It depends on the amount of radiant energy of the stimulus and the structure of the retina. Hue corresponds to the dominant wavelength of the received stimulus. It is the chromatic attribute that distinguishes colors such as yellow from orange and green."

The outcome was a dataset (Table 1) containing more than 10,350,000 individual entries, which enabled analyses not only of the colors themselves but also of their spatial distribution throughout the temple.

Table 1: First 15 rows of the dataset containing over 796,000 rows in total, each representing the data of a specific point in the point cloud.

POINT CLOUD CHROMATIC DATA | EXPIATORY TEMPLE OF THE SAGRADA FAMÍLIA														
POINT	SPATIAL POSITION			COLOR PROPERTIES										
	X (m)	Y (m)	Z (m)	R	G	B	COLOR	HEX	HUE	HUE INTERVAL	BLACK (%)	WHITE (%)	SATURATION (%)	
1	22,248	7,151	0,074	77	60	47		#4D3C2F	26,00	Red	69,8	18,43	38,96	
2	50,514	8,504	0,091	132	120	91		#84785B	42,44	Orange	48,24	35,69	31,06	
3	63,860	23,732	0,110	171	132	86		#AB8456	32,47	Orange	32,94	33,73	49,71	
4	50,226	8,582	0,143	121	106	96		#796A60	24,00	Red	52,55	37,65	20,66	
5	17,984	25,269	0,152	119	90	63		#775A3F	28,93	Red	53,33	24,71	47,06	
6	32,159	30,613	0,169	79	53	31		#4F351F	27,50	Red	69,02	12,16	60,76	
7	67,051	39,360	0,198	103	113	122		#67717A	208,42	Cian	52,16	40,39	15,57	
8	25,875	5,906	0,202	86	89	83		#565953	90,00	Lime	65,1	32,55	6,74	
9	17,852	25,631	0,205	120	86	54		#785636	29,09	Red	52,94	21,18	55	
10	50,914	29,257	0,206	179	164	153		#B3A499	25,38	Red	29,8	60	14,53	
11	32,341	30,571	0,210	109	87	67		#6D5743	28,57	Red	57,25	26,27	38,53	
12	17,220	12,801	0,211	38	40	34		#262822	80,00	Yellow	84,31	13,33	15	
13	32,469	30,646	0,231	70	45	25		#462D19	26,67	Red	72,55	9,8	64,29	
14	19,079	12,819	0,234	61	56	44		#3D382C	42,35	Orange	76,08	17,25	27,87	
15	17,874	13,362	0,237	27	27	24		#1B1B18	60,00	Yellow	89,41	9,41	11,11	

The first analysis focused on the spatial distribution of points within the temple. Since the data collection was based on photographic records from the ground level, and depended on the overlap of information, it was anticipated that the lower areas which were closest to the photographic captures would contain a higher density of points, resulting in a non-homogeneous data cloud—a condition confirmed by the chart shown in Figure 3. This limitation could be addressed by conducting a photographic survey with drones, allowing the environment to be recorded from different heights and with a greater variety of viewpoints.

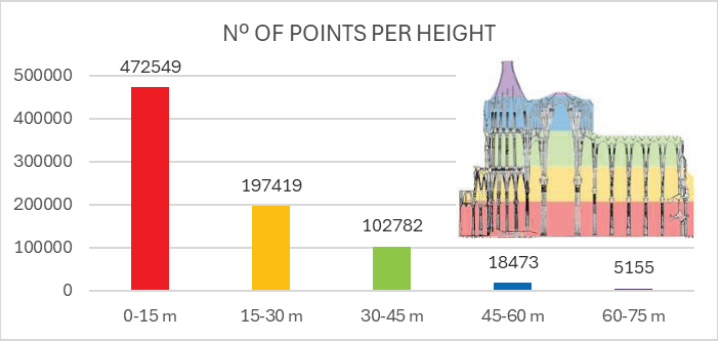

Figure 3: Chart with the spatial distribution of the points, with cross-section for reference.

The second analysis focused on chromatic variation across the different vertical regions of the temple. Gaudí organized the interior according to dimensional modules, with a 7.5 m module in plan (distance between structural

Cross-comparison of app data and clustering outputs revealed a core heritage palette (lime white, sky blue, ochre, and muted earth tones) while secondary palettes diverged: tourists favored ephemeral spectacle, occasionally bordering on kitsch, whereas experts and residents emphasized enduring material tones. AI-generated palettes generally matched dominant colors but sometimes missed subtle, context-specific shades, reflecting Petit's observation that chromatic perception includes both permanent and impermanent impressions [3, p. 370].

Table 1: Algorithmic vs Human-determined dominant colors (sampled spots)

	Photograph	Algorithmic generation	Human perception
Local resident			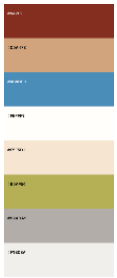
Local non-resident visitor			
Foreign visitor (tourist)			
Expert observer			

Historic–contemporary comparisons using AI-colorized archival images confirmed persistent core material tones and recurring accents (ochres, maroons, teal/sky-blue), though algorithmic extractions frequently produced grey-dominated "dominant" colors, underrepresenting culturally salient hues.

Table 2: Historic palette vs. Contemporary palette

Historic palette			Contemporary palette		
Archive photograph	**Algorithmic generation**	**Human perception**	**Participant photograph**	**Algorithmic generation**	**Human perception**
		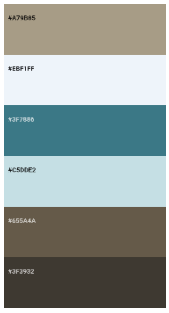			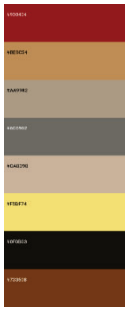

Key Findings

1. Subjective vs. Objective Chromatic Identity: Participant commentaries demonstrated that chromatic identity is not a fixed attribute but a negotiated perception. Tourists defined "identity" through saturated spectacle, while residents emphasized memory-laden tones tied to continuity (faded limewash, blue carpentry). Algorithmic clustering validated recurrent palettes (lime, ochre, blue), yet ignored symbolic resonance. This echoes Adamante's observation in Curitiba: colors in heritage sites function as mnemonic anchors, persisting in cultural memory even when physically faded [5]. Objective tools alone risk flattening this meaning, reinforcing the need for triangulation between perception, materiality, and measurement.

2. Movement, Permanence, and Impermanence: Chromatic ambiances are experienced as sequences in movement, where permanent structures coexist with impermanent interventions. Interventions in historical landscapes often privilege surface spectacle at the expense of continuity, producing fragmented identities. Our results confirm that they are not opposites but overlapping registers of urban memory, each emphasized differently depending on observer position. For heritage practice, recognizing both dimensions is essential.

3. AI as Amplification, Not Substitution: AI proved useful in accentuating recurrent clusters and making patterns legible, but its outputs risked homogenization, missing subtle, context-specific shades highlighted in participant narratives. This reflects Hinterthür's observation [3, p. 196] that chromatic representations must often be "exaggerated" to reveal contrast. Left without interpretive guidance, AI-generated palettes can become sterile and standardized, diminishing the very cultural continuity they aim to preserve. Historic–contemporary comparisons further exposed a recurring grey-bias in automated extractions. This limitation highlights the necessity of human-in-the-loop calibration [8]: participant-flagged colors must inform predictive outputs to maintain culturally significant, low-frequency hues. AI thus functions as an amplification tool, not a substitute for embodied perception.

Synthesis

Chromatic identity in Sousse is both perceptual and material, scientific and cultural. Integrating participatory walks, ethnographic coding, and AI-assisted analysis provides an interdisciplinary framework where digital tools validate patterns, human memory anchors meaning, and heritage continuity is safeguarded [9].

CONCLUSION

Color in urban spaces functions as a vessel of heritage, resistance, and environmental adaptation. This pilot study demonstrates a methodology combining Pyykkö's multi-user Color Walks [7], Adamante's ethnographic observation [5], and AI-assisted analysis to identify and begin reclaiming the Medina of Sousse's chromatic identity. Findings reveal persistent core palettes alongside divergent perceptions, showing that participatory methods and technological tools together can safeguard both perceptual richness and cultural memory. Notably, diachronic comparisons using AI-colorized archival images revealed modest overall chromatic change but highlighted a recurring grey-bias in algorithmic extractions, emphasizing that AI must be human-guided to reliably support heritage applications. By adapting Petit's methodological framework [3] to a historical context, this research demonstrates that approaches originally developed for contemporary urban studies can also protect historical identity. The Medina of Sousse thus becomes a proving ground where chromatic ambiances are reclaimed not only as perceptual effects but as vessels of memory, identity, and resistance. As an exploratory study, it relies on mobile applications which, although already proven reliable in previous research, will be reinforced by more precise colorimetric measurements in future investigations. This study positions itself as a pilot for broader applications in urban heritage conservation, with future work aiming to expand participant diversity, refine AI predictive models, and develop tools for heritage-led urban design, ensuring color remains an active component of urban identity.

ACKNOWLEDGEMENTS

The authors thank the four participants of the Color Walks for generously sharing their time and perspectives. Special thanks are extended to Assoc. Prof. Gareth Doherty (Harvard University) and Assoc. Prof. Faten Hussein (ENAU), whose guidance and supervision were invaluable throughout this research.

REFERENCES

[1]. Cao, X., Yun, Y., & Ren, L. (2025). Research on the Assessment of Architectural Colors in Cultural Heritage Blocks Based on Computer Vision: A Case Study of Tianjin. Land, 14(6), 1159. https://doi.org/10.3390/land14061159

[2]. Conservation of cultural heritage in the Arab Region: Issues in the conservation and management of heritage sites. (2017). ICCROM-ATHAR.

[3]. Petit, A. (2015). Effets chromatiques et méthodes d'approche de la couleur dans la démarche de projet architectural et urbain [Phdthesis, Ministere de la Recherche et de l'Enseignement Superieur]. https://hal.science/tel-01248894

[4]. Ke, Z., & Mustafa, M. (2024). Promoting Public Engagement in Urban Heritage Preservation through Participatory Art Case Studies of Practices and Approaches. Archives of Design Research, 37(5), 221–243. https://doi.org/10.15187/adr.2024.11.37.5.221

[5]. Adamante, A. C. (2024). MEMÓRIA E COR: INTERVENÇÕES CROMÁTICAS NA PAISAGEM HISTÓRICA CURITIBANA. Seven Editora, 1–19.

[6]. Tan, K., Wu, Y., Liu, Y., & Zeng, H. (2025). A Multidimensional AI-powered Framework for Analyzing Tourist Perception in Historic Urban Quarters: A Case Study in Shanghai (No. arXiv:2509.03830). arXiv. https://doi.org/10.48550/arXiv.2509.03830

[7]. Pyykkö, S. (2023). Conceptualizing the chromatic experience of environment: Two case studies using the Color Walk method. Color Research & Application, 48(5), 585–598. https://doi.org/10.1002/col.22878

[8]. Colace, F., Gaeta, R., Lorusso, A., Pellegrino, M., & Santaniello, D. (2025). New AI challenges for cultural heritage protection: A general overview. Journal of Cultural Heritage, 75, 168–193. https://doi.org/10.1016/j.culher.2025.07.019

[9]. Li, X., Qin, J., & Long, Y. (2024). Urban Architectural Color Evaluation: A Cognitive Framework Combining Machine Learning and Human Perception. Buildings, 14(12), 3901. https://doi.org/10.3390/buildings14123901

Poster Papers

Color and Emotions in The Public Space

Anna Kmita

Academy of Fine Arts & Design Katowice, Katowice, Poland
Anna Kmita, akmita@asp.katowice.pl

Keywords: color education, color emotion and preference, color design, landscape and urban design, CMF design.

ABSTRACT

The paper describes projects in public space created as a result of color research and design at the Academy of Fine Arts & Design in Katowice, Poland. In the course of lectures, case studies and practical assignments students acquire basic knowledge and skills at parametrization and design of color. For over a decade, the designer, together with her students, has been creating projects presenting the role of color in the immediate environment. She deals with micro-interventions in the space of buildings and cities, showing the importance of color and how you can distinguish and differentiate seemingly ordinary places in your surroundings. Together with local institutions and companies, she tries to make them more friendly and teach the effect of color on the environment. A few such projects include the complex colors set for functional spaces, interior guidelines, furniture and lighting of the Municipal Hospital in Siemianowice in the Silesia region, the design of the stairs and parking space of the University building, several projects in the Katowice city center, and interior designs for a selected facilities in Katowice. The author prepares color pallets (present hues, saturation and brightness) which are proposals to be used as color code in visual information, systems of public spaces, a color pallet in architecture as well as for decorative structures. As a result of the research, designated projects along with books of patterns and colors are created, which are then used for didactic and popularizing purposes for young designers.

INTRODUCTION

Color scheme design is a subject in the second year of BA studies at the Academy of Fine Arts and Design in Katowice, design major, the program of which was formulated by the Author when there was a need for a new subject to support students in the area of theory of color and applying this knowledge to design.

Along with her own professional development in the discipline of color scheme design, together with her students, she came up with the optimum scope of competencies and skills of recognizing design needs, as well as gathering, analyzing, systematizing and interpreting knowledge regarding the color scheme of a design.

Matters related to color scheme design are a very important component of industrial design education. Johannes Itten was of the same opinion, as he claimed that “contrast effects and their classification are a proper starting point in the study of color aesthetics. The problems of subjectively conditioned color perception are especially pertinent to art education and scholarship, architecture and commercial design (...) [we can speak] of three different points of view for purposes of studying color – constructional, expressional and impressional (...)

emotional effect without constructive symbolic content or visual strength would be limited to the plane of sentimental expression.[1].

METHODOLOGY

The division of substantive notions in the subject of color scheme design could be presented as follows:

- knowledge in the scope of history, theory and models of color,
- basic knowledge and application of systems regarding classification and record of color along with parametrization tools in design work,
- principles of forming color schemes, matters of color effect on the recipient, defining a design problem concerning issues of color,
- skills connected with color design and development of color scheme documentation of a design of selected products, objects, spaces, elements of visual identity.

Assignments in the theory of color, contrast and composition, carried out during classes, usually have a workshop form connected with manually making or matching color pallets and working with color charts available in the studio. Students gain important experience of physically mixing color, observing the color of light and different reception of color related to the change of lighting of a product. Together with her students, the author develops and discusses collected color samples, systematizing them into selected categories and their potential use in design. Such work is often conducted in teams and includes a group presentation, which encourages students to discuss color perception, advocate their personal preferences, breaking clichés to the benefit of noticing nuances in color schemes, materials and surfaces. Students come up with their own catalogue of references in the area of semantics and symbolic of color, based on the chart of psychological character of color developed by means of experiments by Prof. Adam Zausznica and described in his coursebook “Nauka o barwie” [The Study of Colour].[2].

Figure 1: workshops on color symbolism

The observation of students work and diagnosis of their educational needs resulted in developing a set of design assignments based on CMF (Color, Material, Finish) methodology. It is a design discipline and a way of thinking about design assuming the integration of knowledge from many areas in order to develop a particular creative model. The model involves a process of product color scheme design parallel in psycho-physiological, physical and technical aspects.[3] It is successfully used for design and marketing studies in the world, such as Color Marketing Group and MLAb, and diversified in many areas (color design, color development, material design, surface design, finish design, CMF strategy, trend tracking and forecasting). In color scheme design classes, students attempt to apply this system in various areas, of which this article discusses product design, interior design, and public space design.

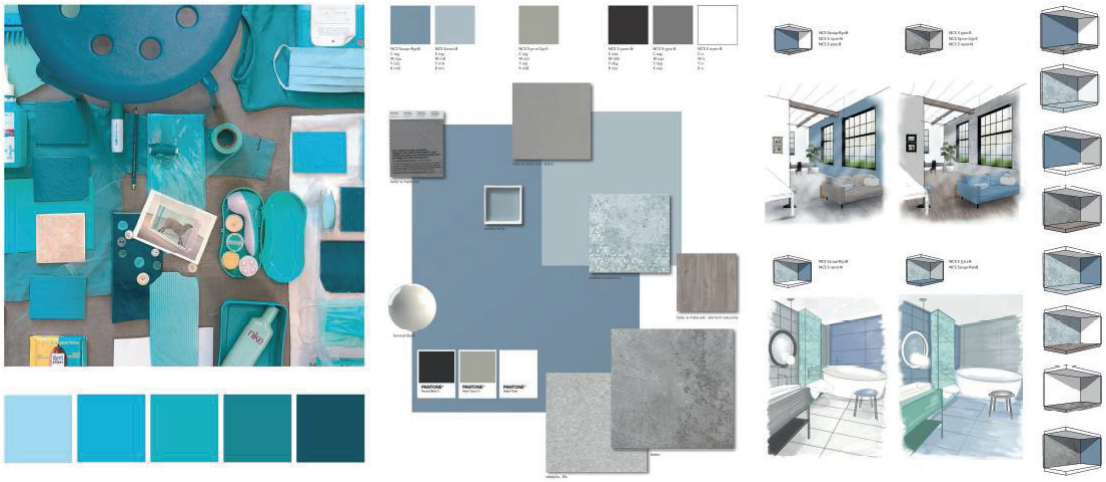

Figure 2: color mooadbords

RESULTS AND DISCUSSION

The ambition of the color scheme design studio is for students of the second year of BA program to be able to design, in a given scope, according to a real market brief, in collaboration with external client, therefore didactic assignments in the second semester are always carried out in cooperation with external stakeholders. We collaborate with the distributor of Sigma and Tikkurila paints, which enabled us to create a colorful space of the stairs in one of the Academy's buildings, as well as to design the color scheme for the Municipal Hospital in Siemianowice Śląskie. Another partner significant to our didactic course is the furniture textile company, Lech Fabrics, which provided sponsoring and mentoring for students to design and produce complete interior decoration of a play and relaxation room for underprivileged children in the "Gniazdo" Community Centre in Katowice, for which they were awarded with a visit to the Salone del Mobile fairs in Milan. Recently, our studio has completed, with the City of Katowice, a year-long project of designing "color micro-interventions" in the space of city center in order to improve its visual quality and attract attention to its creative potential hidden in ordinary elements of urban infrastructure. Students developed a set of works promoting the surroundings of academies (both the Academy of Fine Arts and Design and the University of Economics are located in the very center of Katowice), which emphasize the attractiveness of the area and indicate the visible presence of young designers in the city. The project included unconventional canopies of circulation areas (tunnels, passages, walkways), graffiti localized within pedestrian crossings, and colorful elements of the urban wayfinding system, presenting the most iconic buildings of Katowice.

The studio also had an opportunity to collaborate with many product design enterprises, i.a. Lecce Pen, the manufacturer of writing materials, and Merida, the producer of bicycles. Such operations in the form of closed competitions with professional consulting for the Academy's students in their didactic course resulted in implemented products, which is always satisfactory to enterprises, the Academy, and mainly to young designers.

This year, a student of color scheme design also won the national competition of the automotive company Spline for a design of a car freshener bottle, the form of which effected from a didactic assignment carried out in the studio in reference to color synesthesia and senses.

The most important component of the works we carry out together is the ability of applying the acquired knowledge on color in practice, since each of the above-mentioned projects required careful documentation, selection of materials and development of technical specification, as well as working in interdisciplinary teams responsible for its implementation.

Figure 3: the color scheme for the Municipal Hospital in Siemianowice Śląskie.

Figure 4: interior decoration in the "Gniazdo" Community Centre in Katowice.

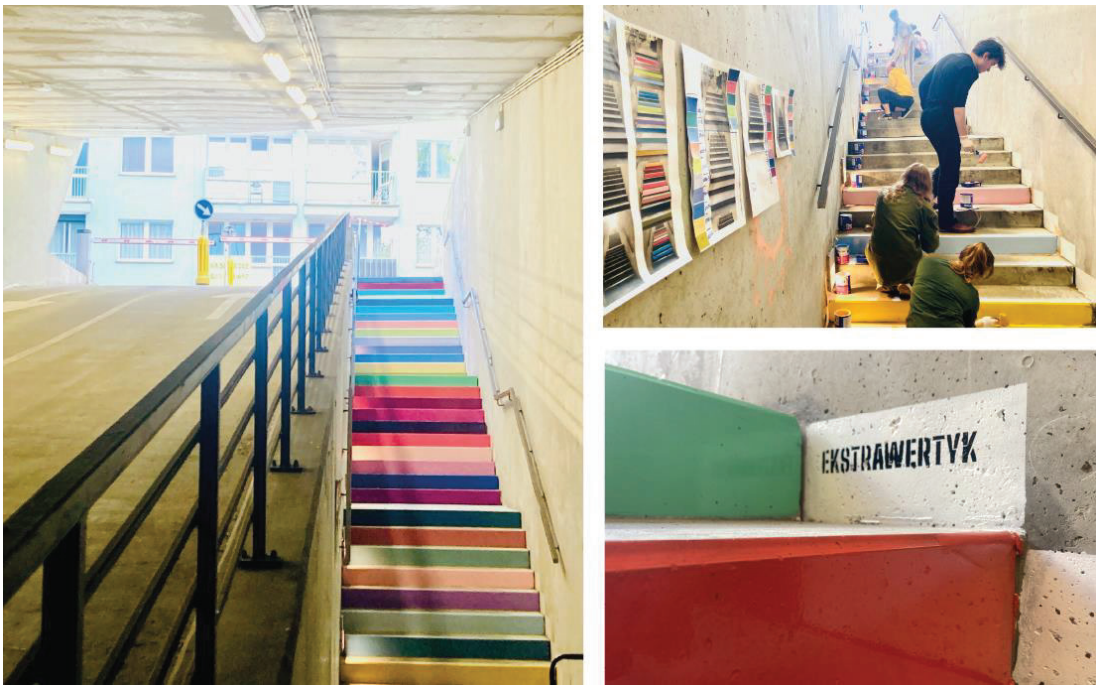

Figure 5: the colorful space of the stairs in one of the Academy of Fine Arts.

Figure 6: a set of works promoting the surroundings of Katowice centre.

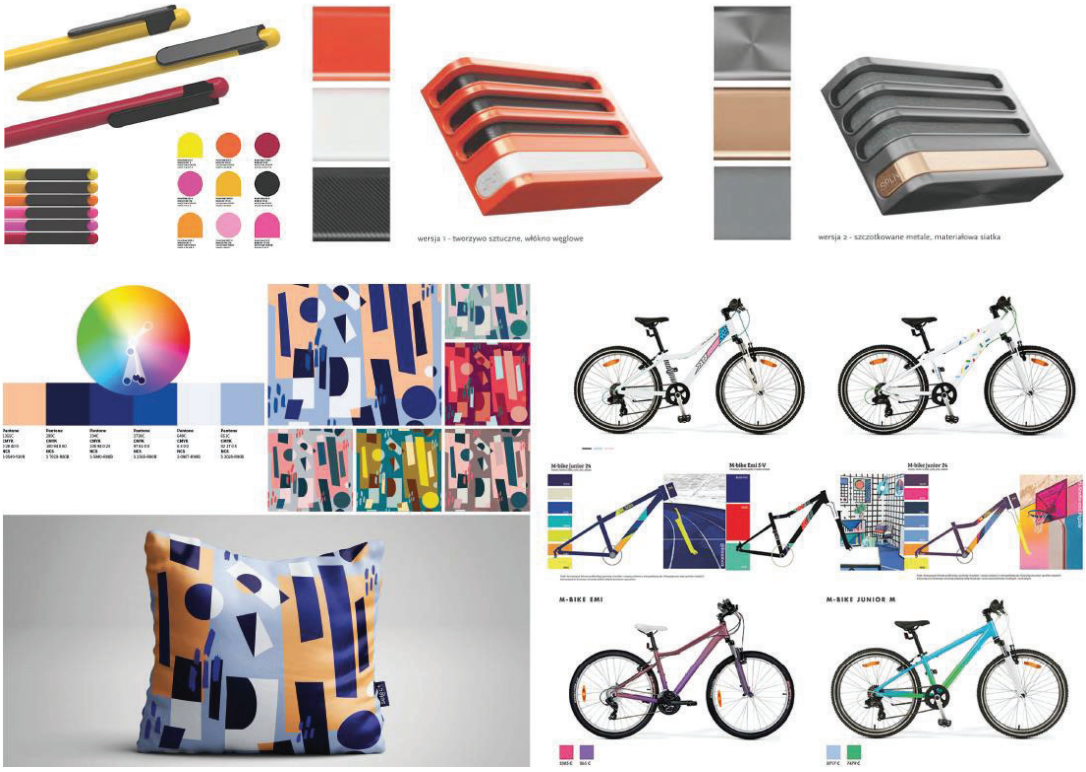

Figure 7: the color scheme in design competitions.

CONCLUSION

The Academy of Fine Arts and Design in Katowice conducts research and education in the area of color scheme design and its operations have a considerable influence on shaping the appearance of public space in the region. The collaboration with external stakeholders allows students to gain skills in the area of color parametrization and design. Within particular projects, supported with lectures, case studies, and practice, students acquire knowledge regarding the use of color in design and are able to implement it in their immediate surroundings. Operations focused on product implementation and interior design as well as creating public space have been noticeable in the city for over two decades. Due to this collaboration, both partners (design students and authorities of the city and public buildings) consider themselves co-creators of the environment where they study and live.

REFERENCES

[1]. Itten, J. (1973). The Art of Color. The subjective experience and objective rationel of color. Translated by Ernst van Haagen. Van Nostrand Reinhold Company. New York. 17

[2]. Zausznica, A. (1959). Nauka o barwie. Państwowe Wydawnictwa Naukowe. Warszawa. 468

[3]. Becerra, L. (2016). The fundamental principles of CMF design. Frame Publisher. Amsterdam.12

Glazed Tiles - Between Art and Architecture. Andreas Stöcklein's Case Study

Ana Paula Pinheiro[a*], Rui Duarte[b]

[a]Colour and Light Research Group, Lisbon School of Architecture, Universidade de Lisboa, Lisbon, Portugal

[b]Universidade de Lisboa, Lisbon School of Architecture, Lisbon, Portugal

ABSTRACT

This article explores the relationship between art and architecture through Andreas Stöcklein's glazed tiles. It will analyze significant examples of this interaction. The use of glazed tiles in Portuguese and Spanish architecture has deep roots stemming from Islamic influence, and tiles are a vital part of the visual and architectural heritage. Islamic tiles feature geometric patterns, but in Portugal, compositions with different patterns and figurative tiles dominate. By referencing Stöcklein's work, we emphasize a path where the artist creatively develops an innovative aesthetic concept by creating pieces that play a relevant role in spatial visuality, interacting symbiotically with architecture. He employs glazed tiles to convey contemporary and universal themes that sometimes include myths, in a poetics that proposes a reflection on cultural identity, space, and time. It is a reinterpretation that broadens the contemporary art discourse, anchored in the material's historical roots. The color of the tiles—which varies according to the theme explored—is chosen from a selection of previously cataloged pigments, with a palette showing the correspondence with the color obtained after firing, which is always different. Stöcklein deconstructs or distorts the traditional function of tiles, exploring their geometric, abstract, or figurative shapes in a play of colors, patterns, and textures. In transitioning from paper painting to tile, the artist becomes a craftsman, expanding the pictorial experience with an architectural and urban sensibility. The handmade glazed tiles in the Faculty of Law are a paradigmatic example of how this material can be utilized in new and innovative expressions within a contemporary context, bringing a fresh artistic vision. The glazed tiles explore the relationship between the past and the present, between tradition and innovation, creating a unique, reflective experience for those who interact with this space. They celebrate the renewed cultural and aesthetic continuity that enriches the academic and architectural environment. Andreas Stöcklein's handmade glazed tiles represent a striking example of the fusion between contemporary art and the tradition of Portuguese tiles, a material that significantly marks Portugal's architectural culture.

Keywords: glazed tiles, art, architecture, sustainability, Andreas Stöcklein

INTRODUCTION

The use of glazed tiles in Portuguese and Spanish architecture has deep roots in Islamic influence, with tiles being a vital part of the visual and architectural heritage of these regions. Islamic tiles feature geometric patterns, but in Portugal, compositions with different types of patterns and figurative tiles dominate.

Azulejos (glazed tiles) originated from the word "azul" (blue) and "zellig" (meaning small polished stone in Arabic), and were introduced in Portugal in 1584 [1].

When German artist Andreas Stöcklein came to Portugal, he knew tiles, which came as a shock to him because they had such a strong traditional connotation, and he was more of a conceptual artist [2]. He began by working in restoration, and it was during this phase that he came into contact with tiles. When he adopted Baroque themes, specifically cherubs and borders, the conceptualization process involved decontextualizing and fragmenting the

theme. In addition, the circular shapes of the medallions also influenced his design. There are two pure shapes—the circles and squares of the tiles. Another form he uses is the ellipse, a reflection on themes he finds in gardens. It was the first starting point he found at the Ratton Gallery (Galeria Ratton). He also uses charcoal, Indian ink, and red—which does not refer to fires—but to the energy that this color conveys. Energy is a determining factor in his compositions, where he also draws on relationships with the underground and connects humanity with the Earth. This symbolic dimension combines with the more rational part.

The tiles allow for a composition with degrees of freedom, which enables him to bring together parts that he calls an exotic space—a space of illusion. The tile material has a significant impact on communication, which is further enhanced by glazing and firing, allowing for the exploration of textures and colors.

In his experimental journey, he questions the transposition of the painting technique from paper to ceramics—a different medium that allows him to explore the potential of the new material, as well as to examine the tile as a modular unit. This morpheme—the smallest meaningful unit—constitutes a discursive potential for artistic exploration, allowing the creation of compositional sequences as a work open to thematic innovation.

When referring to Stöcklein's work, we emphasize a path where the artist creatively develops an innovative aesthetic concept by creating pieces that play a relevant role as spatial visuality, interacting symbiotically with architecture. This article aims to explore the relationships between art and architecture through the use of handmade glazed tiles (azulejos) by Andreas Stöcklein.

METHODOLOGY

The methodology involves considering the support as a transposition of painting onto tiles. This material can be removed and placed on another support, which differentiates it from the fixity of painting, such as fresco.

However, there are other aspects to explore: the joints between modules constitute a discursive potential for suturing gaps and deepening new systems of relationships. Thus, support, matrix, and joints are factors that contribute to broadening the artistic vision, which in turn affects the scale of the theme.

But there is another point: Gödel's 'Incompleteness Theorem' enabled us to deviate from the standard outline. Stöcklein notes that "since mathematician Kurt Gödel developed the 'Incompleteness Theorem' in 1931, no closed system can fully define itself without resorting to external elements. Research in this area may lead to breaking the regular outline of a panel, requiring it to ‘spill over’ from its strict containment within the grid in order to preserve the coherence of its internal logic” [3]. Metaphorically speaking, it is yet another way of breaking boundaries.

Being seen from afar and up close are communicative potentials that also exist in architecture. For the ancients, good architecture seen from afar reflected its proportion and rhythm, the balance of the whole. Seen up close, it revealed the constructive rigor of the details, the materiality, and the changing play of light and shadows.

The color of the tiles—which varies according to the theme explored—is chosen from a selection of previously cataloged pigments, with a palette showing the correspondence with the color obtained after firing, which is always different. “The materials used as dyes are heat-resistant oxides: chromium oxide for green, iron oxide for yellow, orange, and brown, manganese oxide for browns and purples, cobalt oxide for blue, antimony for yellow, copper for green, tin for white” [4].

According to Ratton Gallery, he was compulsive when he started working and utilized all the available techniques. The tiles they prepared for him were typically 14 cm x 14 cm in size, with a thickness of approximately 1cm. Andreas coated the tile with glass powder and painted it with a brush or paintbrush using a pigment that was previously soaked in water. He had a vast number of samples that decode the various pigments, as the raw color almost always differs from the color after firing. Alternatively, he sometimes used the raw, colored glass directly on the tile, using various spatulas. If he wanted to cut out some elements after firing, he would weaken the cutting area by removing the glass, making it easier and ensuring that it would not break.

Figure 1: Faculty of Law of the University of Lisbon. Municipal Prize "Jorge Colaço" Tile Work 2000

Figure 2: Faculty of Law of the University of Lisbon – Patio and terrace. Photos: RBD.APP 2023 (left); Sérgio Mah 2001 (right)

At the Faculty of Law, the use of tiles was decided at the outset of the architectural project, allowing for genuine cooperation between the artist and the architects. The question raised here, of art enhancing an architectural space, becomes obsolete when there is a symbiosis between the two, in which each enriches the other [5].

Of particular note is the effect obtained by the pearlescent color on the justice panel at the Faculty of Law of the University of Lisbon, as well as the color of the golden curved line (Figure 1).

Thus, the application of the same principle in tile composition enables a deeper dialogue with the architecture, making it both communicative and aesthetically appealing through the vibration of the composition articulated with the architectural support (Figure 2).

This type of integration into interventions in public and private spaces, along with a commitment to cultural preservation and the creation of harmony with the environment, continues the "modernist tradition," while also promoting environmental sustainability.

RESULTS AND DISCUSSION

Figure 3: Palm Tree Manor, Portugal. Indoor pool with handmade glazed tiles by Andreas Stöcklein. Photos: RBD.APP, 2006

In revisiting the aesthetics of tiles, Andreas Stöcklein employs them as a means of communication, incorporating contemporary and universal themes that sometimes draw on myths, in a poetic style that invites reflection on cultural identity, space, and time. It is a reinterpretation that broadens the discourse of contemporary art, anchored in the historical roots of the material.

The use of tiles in the pool area creates an environment that vibrates under the zenithal light, capturing reflections on the glazed surface of the tiles. The colors refer to contextual values of granite and blue, with cosmic geometric lines in shades of red and gold, and a poem about Narcissus inside the pool [6].

By distancing itself from ornamentation and the tradition of decorative ceramics, working with tiles places them in the context of contemporary art. Used to question the relationship between art and architectural and urban space, it controls sequences of movement and different scales of vision, sometimes explored in the relationships between each tile unit.

Known for creating tile pieces that incorporate geometric shapes, abstract and figurative patterns, he expresses philosophical and spatial concepts through compositional themes, offering an innovative interpretation that broadens the traditional references of tile use.

The chromatic variations change with the support, the type of pigment, and the firing temperature, aiming to achieve the shine and texture that complement the color. As mentioned earlier, the Artist also used glass powder to achieve the desired density of the material and the corresponding expression that produces the effect he imagined. Combined with natural or artificial light, the variations obtained accentuate particular aspects of shine or matte.

The expression of Stöcklein's innovative artistic work gives tiles a dimension that goes beyond that of a cultural artifact. The tile panels combined with the architecture create a symbiosis that transforms the perception of space, and their integration is a form of sensory interaction that contributes to the humanization of the architectural space.

The discussion focuses on two distinct and symbiotic aspects: in the first phase, of conception and discussion of ideas, there was always teamwork that resulted from the cultural framework with the gallery he worked with, and with the architects with whom he interacted for 34 years, but also with the clients with whom essential concepts were debated, poetically assimilated, and transmuted by the author's creativity [7].

A rewarding experience that consistently exceeded expectations, an attribute of the artist in the transposition of themes and in the richness of the chromatic palette that unfolds with the proximity of vision.

The other aspect of the discussion stems from the contribution to redefining the principles of intervention in tiles: using painting and drawing techniques directly on the tile's surface; in the way of looking at the 14 cm x 14 cm tile module as potential for new compositions by altering sequences; in the way of exploring tile joints – like sutures – as an element that generates new compositions; in the way of fragmenting compositions.

His creative irreverence constitutes a profound shift in the rules of composition, creating new articulations of the modules, artistic expression, and texture use, thereby enriching the chromatic palette.

Thus, by exploring the geometric, abstract, or figurative forms of tiles in a play of colors, patterns, and textures, Stöcklein's contemporary gaze deconstructs or distorts their traditional function.

Seen from the side, the well is an ellipse that constitutes an anamorphosis —a distortion in perspective —a principle that Malevich explored in his painting "Rectangle in Perspective" and in architecture by Rafael Moneo in the Juan Miró Museum in Mallorca, as well as by Frank Gehry in the Guggenheim in Bilbao.

Combining anamorphosis and the illusion of the Baroque, they create a "mixture of imagination, observation, logic, and, eventually, measurements to deduce the essential features of how the eye might work" [8].

One of the aspects underlying the traditional use of tiles is that they are easy to maintain, a key condition for achieving green building certification.

CONCLUSION

Andreas Stöcklein (1957-2024), a German artist based in Portugal, has distinguished himself through his innovative exploration of tile work aesthetics.

Due to its modular flexibility and ability to evoke cultural memories, tile work can serve as a point of convergence between different approaches, creating contemporary works rooted in Portuguese tradition. This principle emphasizes the importance of the craftsman, whose work is not repetitive but exploratory in its application of a creative technique. It underscores the significance of tradition in linking culture with the ability to add, innovate, and surpass through art.

Andreas controlled the issue of colors, selecting them from a catalog of previously chosen pigments, comparing them with a palette that showed the correspondence with the color obtained after firing, which is always

different. By moving from painting on paper to tiles, the artist also becomes a craftsman, expanding the pictorial experience with an architectural and urban spatial sense.

The Faculty of Law of the University of Lisbon is a historic and emblematic building, a National Monument, which combines classical architectural codes with modernist and contemporary influences, providing a perfect setting for integrating modern art within an academic and institutional context. The use of tiles in Portuguese architecture is a symbol of cultural and historical identity.

The presence of contemporary handmade tiles in the academic space adds a touch of renewal and reflection on cultural heritage and contemporary art. Thus, in addition to preserving tradition, it also questions and expands it, raising a broad discussion about the cultural identity of architecture combined with art in today's society.

ACKNOWLEDGEMENTS

We want to thank the Ratton Gallery (Galeria Ratton) for providing information about Andreas Stocklein's work.

We also thank RBD.APP - Architects for the availability of the photographs.

REFERENCES

[1]. Lenclos, J. P., and Lenclos, D. (2016). Couleurs de la Méditerranée Géographie de la couleur, Editions Le Moniteur, Antony, 51.

[2]. Interview with Andreas Stöcklein (2005). Conducted by Raquel Santos, June 21, 2005, from https://arquivos.rtp.pt/conteudos/andreas-stocklein/

[3]. Araújo, M. A., and Stöcklein, A. (2023). Between Here and There – Other Places, Ratton Gallery Exhibition, 15 March 2012. In: Exhibition Catalog. Over the Horizon - Andreas Stöcklein in the Ratton Collection, National Tile Museum Exhibition, Lisbon, Portugal, 69.

[4]. Lenclos, J. P., and Lenclos, D. (2016). Couleurs de la Méditerranée Géographie de la couleur, Editions Le Moniteur, Antony, 51.

[5]. Exhibition Catalog (2023). Over the Horizon - Andreas Stöcklein in the Ratton Collection, National Tile Museum Exhibition, Lisbon, Portugal 57-58.

[6]. Duarte, R., and Pinheiro, A. P. (2012). Materialities and Immanence of Color in Architecture, Faculdade de Direito da Universidade de Lisboa | Solar da Palmeira. archi NEWS. Special Edition, 28-29.

[7]. Interview with Andreas Stocklein (2024). Over the Horizon, National Tile Museum, March 12, 2024, from https://www.youtube.com/watch?v=Ljc9BXKARzg

[8]. Groh, J. (2014). Making Space, 8.

Experience and Vocabulary in The Study and Use of Color

Alfonso de Lucas Tron
Facultad de Estudios Superiores Acatlán
Universidad Nacional Autónoma de México
Mexico City
109849@pcpuma.acatlan.unam.mx

ABSTRACT

Color poses a paradox that ensures that perception cannot be communicated because chromatic impressions cannot be explained to individuals who are sightless from birth, this contradicting that there are color dictionaries and glossaries. There exists a very limited vocabulary of color for everyday usage; however, doubt arises as to whether this serves in specialized circles in the sciences and industry. Thus, it was that the following inquiries were formulated: Do the specialists need to increase their vocabulary? Can one and the same vocabulary serve different trades? Can experience render increased understanding of the terms? This is an essay based on a phenomenological analysis that has as its **objective** to show that the understanding of the word color and all that related to it increases with the experience that an individual has in the study and use of that sensory impression, deriving from the premise of Richard Müeller-Freienfels: that more that is seen the more that is known, given that the field of perception increases with knowledge and culture. The assertion sustains the **thesis** that specialists increase the understanding of the words to the extent that they study and employ color. The vocabularies have their origin in the sensory impression, observing that people who have never perceived color will not be able to associate it with words and therefore will not be able to communicate these sensory impressions. White light and its eventual absorption in opaque bodies generate such an immense chromatic mosaic that it is impossible to assign names to all of the chromatic sensations that the eye can capture. This situation promoted enormous efforts to approximate verbal expression to visual sensation. A significant advance in the color vocabulary was furnished by Albert Henry Munsell, who associated three words with the perception of color: Hue, Value, and Chroma. This proposal led to the development of a taxonomy known as the Munsell Color System. Munsell's book was the basis for creating The ISCC–NBS System of Color Designation, the purpose of which was to systematize and standardize color definitions for application in many trades and activities. Despite that effort, the vocabularies cannot incorporate what the eye is capable of, if it is borne in mind that there are hundreds and thousands of colors that the human eye can perceive, thus the “lexicon” is more precise when the impression of a nuance is related to a code. This was the success of Pantone, which is a standardized system with a more extensive gamut in that each sample is numbered to recreate the color exactly. Pantone allows to observe that eye contact provides the precise idea of the hue. From this, we can conclude that we can talk about color because there is a sensory experience that allows communication between interlocutors. Without experience, color could not communicate in any way, since it draws on all kinds of elements in a holistic knowledge that allows color to communicate in two ways: through the definition of words in dictionaries (concepts) and through direct visual impressions (precepts). The paradox, then, is clarified on observing that there exist two mental functions that intervene in the communication of color: the concepts, which are related with the word, and the precepts, which are related with the sensations, both made up of the holistic quality of the experience.

Keywords: color, experience, vocabulary, words, perception.

INTRODUCTION

Color poses an interesting paradox that ensures that perception cannot be communicated (Wolff, 1979, p. 51) if one departs from that the impressions of color cannot be explained to people who are sightless from birth and, in fact, from that Gestalt psychologists utilize figures for describing perceptive processes that solely can be understood by means of the direct impression (Mueller F.-L., 1991, p. 414) such as simultaneous contrast (Figure 1). This contradicts that in fact there are dictionaries and glossaries of color. Despite this discrepancy, it can be ensured that color can be communicated in two ways: that of the word and that of the sensation. In this respect, Ian Paterson (A Dictionary of Colour, 2003) says that "The best way of indicating the "meaning" of a particular color word, is to display its actual color." (2003)

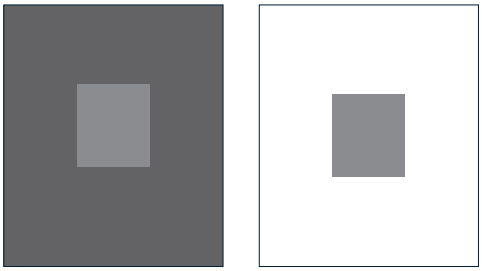

Figure 1. Simultaneous contrast cannot be explained by means of the word; only the direct impression affords the understanding that two similar colors modify their aspect of agreement with the fields into which they are inserted.

Most individuals employ an elementary vocabulary for naming the colors of objects. Brent Berlin and Paul Kay (1991) found a pattern of seven stages that describes how the basic terms of color come to appear in different languages, such that the first of these only has black (dark-cold) and white (clear-warm) and that the languages of Stage VII possess eight or more basic color terms, although to the extent that the languages evolve acquiring new terms in an ordered sequence. According to the authors, eleven is the number of basic universal terms. It is thus clear that the number of color terms for daily usage is restricted; however, the doubt arises as to whether this "basic" vocabulary serves in specialized circles in the study and application of color, such as the textile industry, graphic arts, the production of dyes and paints, etc. It is precisely the use of words for skilled trades that gave rise to the following three inquiries: Do specialists need to increase their vocabulary in order to make themselves understood in their trade? Can the same vocabulary serve different trades and activities? Can experience render compression of the terms?

This work comprises an essay based on a phenomenological analysis that has as its objective to expose that the understanding of the word color, and that way that is related with it increases with the experience that the individual has in the study and use of this sensory impression despite the limits of the vocabulary. This derives from the premise of Richard Müeller-Freienfels (1991, p. 286), in that the more that is seen the more that is known given that the field of perception increases with knowledge and culture. Based on this argument, the thesis is sustained that specialists increase their understanding of the words to the degree that they study and employ color for their own purposes; however, they need the direct impression to refer to specific color nuances.

1. Sensation and nomenclature of color

The words related to color have their origin in this sensory impression from which it forms an alliance in the sense that, if a person never has perceived the colors, they will not be able to associate them with words, therefore they will not be able to communicate these sensory perceptions. Different from animals, humans can designate perceptions through words ((Müeller-Freienfels, 1966, p. 282). It is noteworthy that the wavelengths in white light and their eventual absorption in opaque bodies generate such an immense chromatic mosaic that Josef Cohen (1989, p.41) observes that, in theory, the number of values and shades is infinite. Regarding this point, Ian Paterson

observes that "…there is an infinite number of colours and shades, hues and tints (some suggest as many as 16 million) so that it would obviously not be possible to provide each of them with a distinct name. Furthermore, those colour descriptions which do exist do not have a sufficiently exact meaning to enable any colour to be determined with precision."

From this we deduce that it is impossible to name all of the chromatic sensations that the eye can capture. This situation has driven enormous efforts to approximate verbal expression to the visual sensation, observing that the words must be standardized for them to be understandable for all people without their trade or activity mattering. For example, for centuries, the nomenclature for the production of paint was confusing and negligibly systemic due to the abundant denominations that the manufacturers assigned to their products. This situation made obligatory, in the United States, the regulation of the nomenclature of the production of dyes and paints in the so-called <Paint Standard> (Mayer, 1985, p. 30). On the other hand, despite there, existing glossaries, the case may present of there being, in the translation of one language to another, terms varying in meaning from that assigned by the author. For example, the glossary of Robert Chung (2008) is in English, Spanish, and Portuguese.

A meaning advances in the vocabulary that provides it. Albert Henry Munsell (1858-1931). In his book A Color Notation (2022, p. 1) the author ensures that "Clear mental images make clear speech. Vague thoughts find vague utterance." Munsell was successful in uniting three words with the perception of color, in such a manner that "Hue is the quality by which we distinguish one color from another"; "Value is the quality by which we distinguish a light color from a dark one." And "Chroma is the quality by which we distinguish a strong color from a weak one." This definition was the basis for elaborating a taxonomy that is known as the Munsell System of Color.

This System was the base for creating the ISCC-NBS [The Inter-Society Color Council (ISCC)–National Bureau of Standards (NBS) System of Color Designation], which served to name colors based on thirteen basic color terms and a small set of modifying adjectives. Its purpose was to systematize and standardize the definitions of color with diverse degrees of precision, from generic to precise, obtained through spectrophotometric measurements. The dictionary was designed for its application in many trades and activities such as industry, the sciences, printing, fashion, botanics, and geology, etc., in such a way that specialists would be able to share the same lexicon. This work came to fruition in the publication of Color: Universal Language and Dictionary of Names, the definitive source on the ISCC–NBS system.

Despite the massive effort to increase the vocabulary it fell far from including what the eye is capable of perceiving. Ian Paterson (2003) ensures that "Any attempt to define any particular colour merely by means of words is doomed to failure." The lexicon is more precise when it links a specific nuance with a code [or name]. In this regard, the success of Pantone is that it is a standardized system with a very extensive range [color gamut] that employs industry in order for the color to not vary from design to production. This system is based on a palette that is frequently obtained by means of mixtures of determined tints. The color is described by enumerated samples that allow the recreation of the color exactly. Pantone allows us to observe that eye contact provides the precise idea of the hue.

2. Experience and the vocabulary of color

This work departs from the premise that the sensory impression is the starting point for verbal or visual communication. People can speak about color because these are sensations associated with concepts (Cohen, 1989, p. 11). From this we can deduce that **we can talk about color because there is a sensory experience that allows communication between interlocutors. Without experience, color could not be communicated**. [Infrared rays, like visible light, are part of the electromagnetic spectrum; however, infrared rays are invisible to the human eye; therefore, there is no sensory experience in infrared rays].

El Diccionario de la Lengua Española (Española, 2001, p. 691) states that "experience" is "The prolonged practice that provides the knowledge or skill for doing something." Experience constantly feeds and strengthens itself with elements of all sorts such as intellectual, cultural, social, sensory, experiential, etc. It integrates, additionally, experiences from the past with those of the present, thus demonstrating holistic knowledge. From this

point of view, **experience determines that there are two ways to conduct the communication of color: by means of the definition of the words in dictionaries [concepts] and by direct visual impression [precepts]**, although both forms mutually complement each other. Departing, then, from that vocabulary cannot name what the human eye is capable of perceiving, our thesis asserts that experience broadens the understanding of words to the extent that an individual studies and employs color, although the specificity of a hue is only obtained from a direct impression.

Although attempts have been made to standardize vocabulary, it cannot be ruled out that certain professions may have their own jargon. This is exemplified in artists who, given their experience, develop sensitivity and exquisite color calibration ranging from paint emerging from the tubes, the mixture on the palette, and the polychromal effects appearing on the painting itself. Their experience makes them realize that each blue color has its own hue; they know that there are different types of blues, such as cobalt, cerulean, ultramarine, indigo, phthalocyanine, etc., and that each has its own hue. Similarly, each blue emits a different effect on being mixed with other colors. The jargon of painters may seem strange to other guilds when they use terms such as “bright”, “gray”, “soft”, “dull” or “dirty” colors. Artists also use words with synesthetic properties such as warm, cold, sweet, sour, etc. (Kandinsky, 1981). Müeller-Freienfels observes: “If the world is a reality, it also is a diversely known reality.” (1966, p. 261).

In conclusion, we cite a reflection of Vasily Kandinsky (1973, p. 92) “Words are and always will be mere indicators, external labels for colors. The possibility of monumental art lies in the impossibility of replacing the essence of color with words or any other means.”

CONCLUSIONS

This work proposed the paradox of that color cannot be communicated and, at the same time, there are glossaries and dictionaries that define color and that with which it is related. The paradox becomes clear on proposing that there are two mental functions that intervene in the communication of color: the concepts, related with the words, and the precepts, with the sensations. Both are integrated by experience through their holistic qualities. Deriving from then, that the word and the sensation can be communicated, it is undeniable that each possesses its own radius of action: the word is more general, which allows for a glossary for daily uses and specialized for trades, while sensation is more exact because it provides the direct impression of the color. Thus, it is clear that words express generalities and sensations express particularities.

Deriving from the reflection of Richard Müeller-Freienfels (1991, p. 286) which sustains the thesis of this work, comprising that the more is seen the more is known, given that the field of perception increases with knowledge and culture, we can ensure that the prolonged experience which each specialist possesses in their work area will convey with it understanding of the words in spite of their limits, something that permits fluidity in communication. From this it is deduced that the vocabulary can be overrun and, on passing its limits, there will be no words to express the idea that the specialist has in mind: there are experiences of color that cannot be expressed by means of words. It remains clear, in addition, that words are flexible: they can entertain different levels of understanding according to the experience of everyone.

To conclude, the theme is observed as far from being exhausted. Therefore, this work only provides a panoramic view of two focuses of color communication: that of the word and that of the sensory impression, both necessary for understanding the language of color. This throws open the doors to explore a semantics that can and that cannot be expressed by means of words.

REFERENCES

Bartley, S. H. (1978). *Principios de percepción.* México: Trillas.

Berlin, B., & Kay, P. (1991). Basic Color Terms. Their Universality and Evolution. Los Angeles: University of California Press.

Chung, R. (2008). Glossary of Terms: Color, Imaging Technology & Color Management Systems. New York State: Rochester Institute of Technology.

Cohen, J. (1989). Sensación y percepción visuales. México: Trillas.

Diccionario Larousse de la Pintura. (1987). Barcelona: Planeta--De Agostini.

Dondis, D. (1982). La sintaxis de la imagen. Introducción al alfabeto visual. Barcelona: Gustavo Gili.

Española, R. A. (2001). Diccionario de la lengua española. Buenos Aires: Grupo Editorial Planeta.

Kandinsky, V. (1981). De lo espiritual en el arte. México, D. F.: Premiá, Editora.

Kandisnki, V. V. (1973). De lo espiritual en el arte. Barcelona: Barral.

Mayer, R. (1985). Materiales y Técnicas del Arte. Madrid: Hermann Blume.

Mueller, C. G., & Mae, R. (1974). Luz y visión. Estados Unidos de Norteamérica: Time, Inc.

Mueller, F.-L. (1991). Historia de la Psicología. De la antigüedad a nuestros días. México: Fondo de Cultura Económica.

Müeller-Freienfels, R. (1966). Tu alma y la ajena. Una psicología práctica para todos. Barcelona: Labor.

Munsell, A. H. (2022). A Color Notation. North Haven, CT.

Paterson, I. (2003). A Dictionary of Colour. London: Thorogood Publishing.

Wolff, W. (1979). Introducción a la psicología. México: Fondo de Cultura Económica.

Analysis of Scene Illumination Factors Affecting Perceptual Colour Inferences in Images

Yuki Tanaka[a*], Midori Tanaka[b], and Takahiko Horiuchi[b]

[a]Graduate School of Science and Engineering, Chiba University, Chiba, Japan
[b]Graduate School of Informatics, Chiba University, Chiba, Japan

[*]Corresponding author: Yuki Tanaka, 25wm3213@student.gs.chiba-u.jp

ABSTRACT

The image known as #theDress phenomenon shows a stark individual difference in colour perception—some see it as blue and black (BK), others as white and gold (WG), even under identical display conditions. This study investigated how object characteristics, lighting direction, and background colour affect colour inference through two experiments. In Experiment A, 14 images of materials with varying properties (e.g., glossiness) were shown on black backgrounds. In Experiment B, 38 images with altered lighting (front or back) and coloured illumination (blue or yellow) were presented after perceptual type classification. Participants chose among 14 colours. The chromaticity of images was modified using Witzel et al.'s method, and natural backgrounds were AI-generated. Among 100 Japanese participants, 23% of WG viewers changed their perceived colour depending on lighting direction, compared to only 7% of BK viewers. Glossy surfaces and familiar object colours remained stable across conditions. Compared to Witzel et al.'s 60% shift rate, only up to 20% changed colour with background illumination shifts, suggesting lower perceptual sensitivity to lighting in composite scenes. These results support the hypothesis that lighting estimation and prior experience affect colour perception but also reveal that not all lighting manipulations are perceptually salient.

Keywords: #theDress, colour perception, colour constancy, illumination estimation, individual difference

INTRODUCTION

In 2015, a photograph of a dress (#theDress) posted on Tumblr sparked a global debate, drawing attention to the strong dependence of human colour perception on scene illumination, particularly in the context of colour constancy and illumination estimation. Remarkably, despite identical pixel information, objects were divided into those who perceived the dress as "blue and black (BK)" and those who saw it as "white and gold (WG)," demonstrating that colour perception can vary significantly even under standardized viewing conditions. Since then, other images—such as #theShoe and #theJacket—have elicited similar perceptual discrepancies, further supporting the illumination estimation hypothesis as a leading explanation for these individual differences. However, it remains unclear which specific cues within an image are used by objects to estimate illumination.

Previous research has examined various contributing factors, including physiological traits (e.g., pupil size, genetic and twin studies) [1–3], low-level image features (e.g., principal component analysis of chromaticity distributions) [4, 5], and luminance cues (e.g., the brightest colour hypothesis) [6]. Yet, none of these factors alone fully account for the observed individual variation. In particular, the role of higher-order scene information—such as background context, object glossiness, and shape—has not been systematically explored. This study seeks to

advance the illumination estimation hypothesis by empirically evaluating how combinations of background and object characteristics influence colour perception.

METHODOLOGY

Experiment A：Perceptual changes with object type

Experiment A was conducted to investigate whether perceptual outcomes differ depending on the visual characteristics of objects, such as glossiness. Thirteen distinct objects (ball, bird, butterfly, cocktail, fish, flower, frog, ice cream, leaf, watermelon, parrot, tie, vase) were presented against a uniform black background, with no concrete background elements included. The image stimuli used in this experiment are shown in Figure 1.

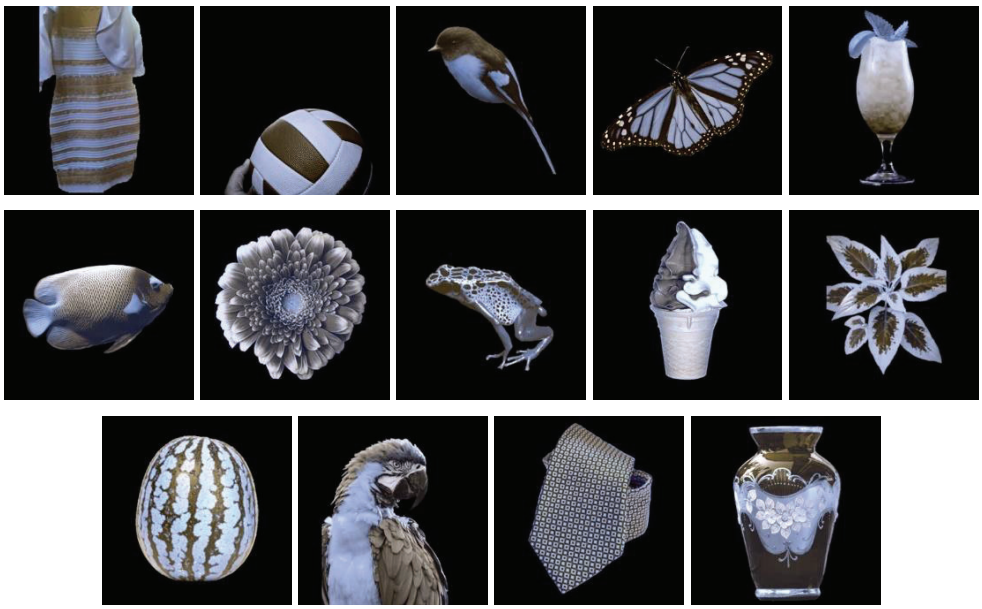

Figure 1: Stimuli used in Experiment A

Experiment B: Perceptual Changes Based on Concrete Background

Building on the concept of unconscious scene illumination estimation, Witzel et al. demonstrated that colour perception can be influenced by manipulating the direction of illumination—specifically, through forward versus backlighting [7]. Under forward illumination, objects tend to appear blue and black (BK), consistent with daylight lighting. In contrast, under backlighting, they are more likely perceived as white and gold (WG), due to the presence of shadows. Werner et al. further confirmed, using a real dress under ambiguous lighting, that individual differences persist even in real-world settings when visual lighting cues are withheld from the observer [8].

Werner et al. also proposed the Segmentation Hypothesis, which posits that WG viewers perceptually separate the object from the background illumination, while BK viewers perceive both as being illuminated by the same light source. BK viewers thus interpret the object and background as a unified scene, focusing on relative colour contrasts. WG viewers, by contrast, interpret the object as being in shadow and process the object and background separately. Based on this framework, we hypothesized that WG viewers would be more likely to shift toward BK perception when the background lighting direction is altered (e.g., from backlit to front-lit), and conversely, BK

viewers would be more likely to shift their perception when the chromaticity of the background is manipulated (e.g., blue vs. yellow).

As in Experiment A, image stimuli were created by combining objects (generated using the chromaticity transformation method of Witzel et al.) with specific background images. The final stimuli consisted of 9 objects (ball, bird, butterfly, chair, leaf, watermelon, parrot, necktie, and vase) each paired with four background types: forward light, backlight, blue illumination, and yellow illumination. Partial stimuli are shown in Fig. 2. The backgrounds were generated using proprietary web-based tools, which allow image synthesis that preserves the pixel values of the object area while adapting the background to suit illumination prompts. Images were selected by the authors from multiple generated results, based on suitability for representing intended lighting direction or chromaticity. Although prompt control allowed some customization of illumination characteristics, the generated background quality varied, and in some cases, the lighting direction was ambiguous. In total, the stimuli set included 36 newly generated images (9 objects × 4 backgrounds), along with #theDress, #theShoe, and the forward- and backlit dress stimuli from Witzel et al. [7]. The purpose of including these existing stimuli was to compare their influence on colour perception with that of the newly created images.

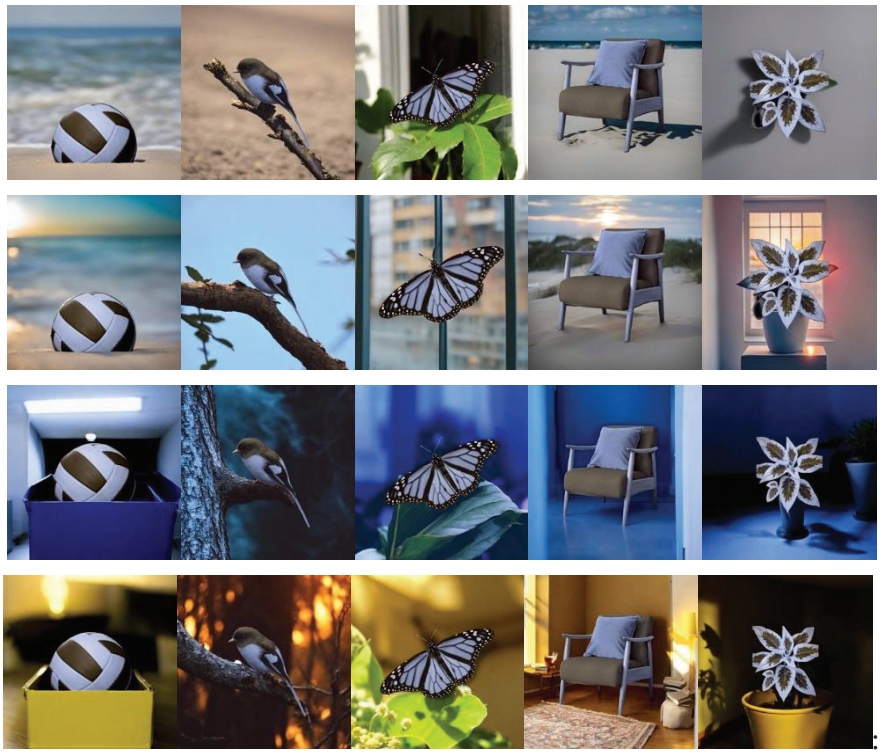

Figure 2: Partial stimuli used in Experiment B

Participants and Procedure

Two experiments were conducted using the PsyToolkit platform [9, 10], involving a total of 200 native Japanese speakers (Experiment A: mean age = 41.5 ± 8.3 years; Experiment B: mean age = 42.3 ± 8.5 years), with 100 participants in each experiment. Participants were first asked to report their perceived colour of the original #theDress image. Following this, they proceeded to evaluate a series of newly created image stimuli. For each stimulus, a monochromatic mask was initially presented to clearly delineate the area of interest, followed by the

full-colour image stimulus, which was displayed for 10 seconds. All image stimuli were presented in randomized order to minimize sequence effects. Participants responded by selecting from Berlin and Kay's 11 basic colour terms, with the addition of "gold," "silver," and "other." If "other" was selected, participants were prompted to provide a free-text description of the perceived colour.

RESULTS AND DISCUSSION

Figure 3 presents the distribution of responses for each image stimulus in Experiment A. In this experiment, most participants directly reported the perceived pixel colours—predominantly blue and gold (BG)—when the stimuli were shown against a black background. Compared to the original #theDress stimulus (WG: 15, BK: 31, BG: 41), the proportions of WG and BK responses decreased, suggesting that the absence of a contextual background reduced the influence of colour constancy mechanisms. Glossy objects such as the vase, watermelon, and butterfly elicited a relatively higher proportion of BK responses (approximately 50%), indicating a greater influence of inferred lighting conditions. These findings imply that, when background information is absent, participants tend to rely more on raw pixel chromaticity rather than on illumination correction.

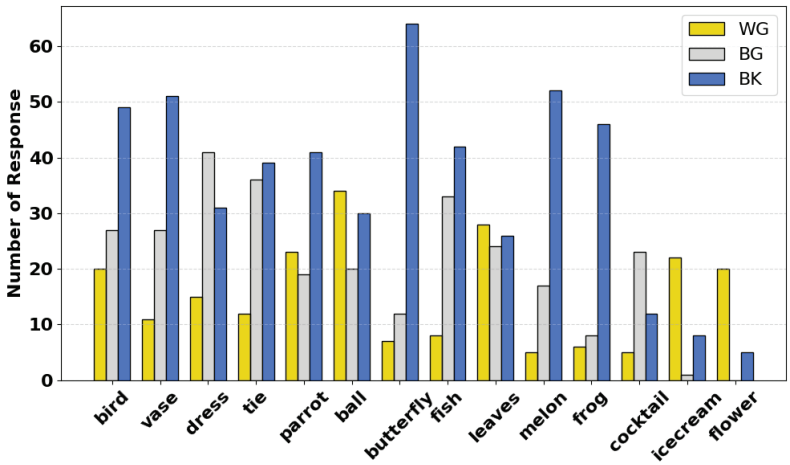

Figure 3: Result of Experiment A

Figure 4 shows the proportion of participants who switched their colour perception from their initial #theDress classification when the direction of background-derived illumination was altered in Experiment B. Among WG viewers, a notable percentage (approximately 15–23%) changed their responses in stimuli such as the parrot, bird, and leaf, indicating sensitivity to lighting direction. In contrast, BK viewers exhibited a lower rate of perceptual change (7–9%), suggesting a relatively stable interpretation of scene lighting.

Figure 5 illustrates the percentage of perceptual switching in response to changes in background chromaticity (blue vs. yellow backgrounds) for each perceptual group in #theDress, based on Experiment B. Across both groups, switching rates ranged from approximately 8% to 31%, with no significant difference between the WG and BK groups. This suggests that background chromaticity-induced contrast may influence colour perception independently of individual baseline differences in lighting estimation strategies.

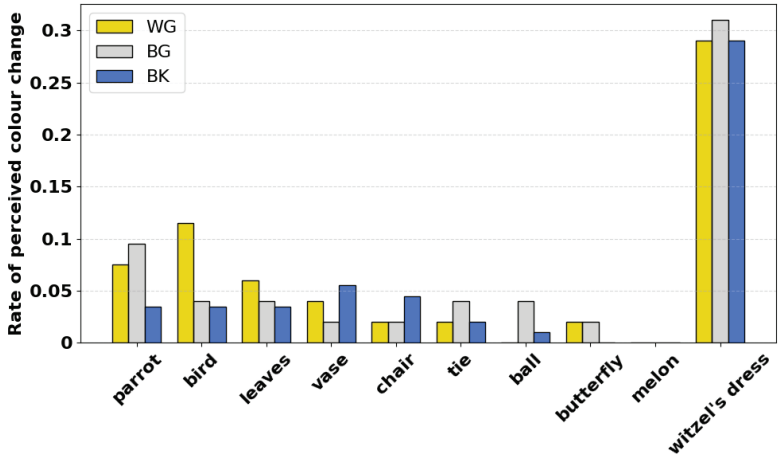

Figure 4: Percentage of participants who changed perceived colour in response to changes in lighting direction

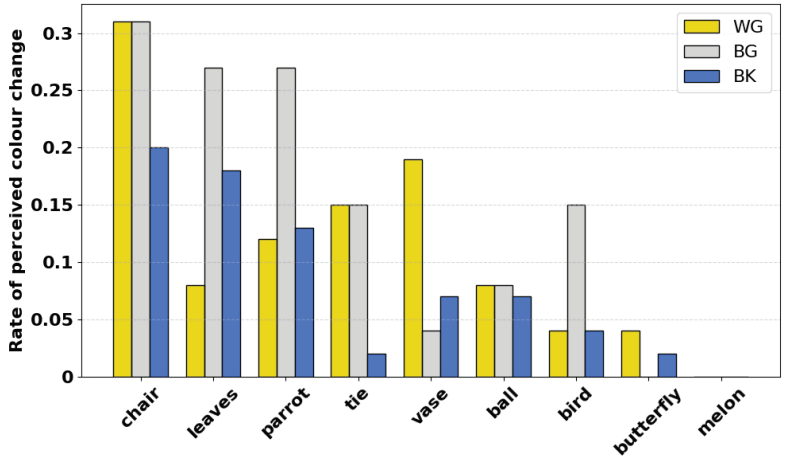

Figure 5: Percentage of participants who changed perceived colour in response to background chromaticity changes

DISCUSSION

Experiment A demonstrated that when background information was absent (i.e., with a uniform black background), a larger proportion of participants perceived the subject's colours as blue and gold (BG)—the actual pixel values. In contrast, the original #theDress image elicited fewer BG responses, with stronger polarization between the white/gold (WG) and blue/black (BK) interpretations. This suggests that background context plays a key role in triggering individual differences, possibly by enabling or constraining illumination-based perceptual corrections. When scene cues are ambiguous or lacking, observers tend to rely more on raw chromaticity rather than inferred lighting conditions.

The image known as #theDress is notable for its ambiguous background, which can be interpreted as either front-lit or backlit. Prior studies have attributed individual differences in perception to this ambiguity, proposing that viewers resolve the scene by unconsciously estimating illumination. Our findings support this idea, but also

suggest it is not the sole factor. Witzel et al. reported that about 60% of participants shifted their colour perception when lighting direction was manipulated in the original dress image, reinforcing the role of illumination ambiguity. However, our custom image stimuli produced far lower switching rates (approximately 10%), indicating that manipulating lighting direction alone is insufficient to replicate the #theDress effect. Notably, Witzel's stimuli also differed in lower-level features such as luminance contrast and background chromaticity, which may have contributed to the perceptual shifts. When background chromaticity (e.g., blue vs. yellow) was manipulated in Experiment B, both WG and BK participants showed similar switching rates (8–31%), regardless of their original perceptual classification. This suggests that colour contrast or chromatic induction effects operate independently of the individual difference mechanisms associated with illumination estimation.

In summary, while lighting direction is a contributing factor, other background-related features—particularly spatial structure and luminance contrast—appear to be equally or more influential. Future research should systematically isolate and test these features to better understand their specific roles in colour constancy and inter-individual variation in perception.

REFERENCES

[1] Xiao, F., Cai, G., and Zhang, H. (2016). Segregation analysis suggests that a genetic reason may contribute to "the dress" colour perception, PLoS One, 11(10), e0165095.

[2] Mahroo, O. A., Williams, K. M., Hossain, I. T., Yonova-Doing, E., Kozareva, D., Yusuf, A., Sheriff, I., Oomerjee, M., Soorma, T., and Hammond, C. J. (2017). Do twins share the same dress code? Quantifying relative genetic and environmental contributions to subjective perceptions of "the dress" in a classical twin study, J Vis, 17(1), 29.

[3] Vemuri, K., Bisla, K., Mulpuru, S. and Varadharajan, S. (2016). Do normal pupil diameter differences in the population underlie the colour selection of #thedress? J. Opt. Soc. Am. A, 33(3), A137−A142.

[4] Lafer-Sousa, R., Hermann, K. L., and Conway, B. R. (2015). Striking individual differences in colour perception uncovered by "the dress" photograph, Curr Biol, 25(13), R545−R546.

[5] Winkler, D., Spillmann, L., Werner, J. S., and Webster, M. A. (2015). Asymmetries in blue-yellow colour perception and in the colour of 'the dress'. Curr Biol, 25(13), R547−R548.

[6] Uchikawa, K., Morimoto, T., and Matsumoto, T. (2017). Understanding individual differences in colour appearance of "#thedress" based on the optimal colour hypothesis, J Vis, 17(8), 10.

[7] Witzel, C., Racey, C., and O'Regan, J. K. (2017). The most reasonable explanation of "the dress": Implicit assumptions about illumination, J Vis, 17(2), 1.

[8] Werner, A., Schmidt, A., Hilmers, J., Boborzi, L., and Weigold, M. (2021). Colour ambiguity in real scenes and the role of perceptual organisation, bioRxiv. https://doi.org/10.1101/2021.01.03.423255

[9] Stoet, G. (2010). Psytoolkit: A software package for programming psychological experiments using linux, Behavior Research Methods, 42(4), 1096–1104.

[10] ——, (2017), Psytoolkit: A novel web-based method for running online questionnaires and reaction-time experiments, Teaching of Psychology, 44(1), 24–31.

Color Standards in City Planning and Changes in Store Facade Design: The Effects of Facade Design Change Methods on Harmony with The Street Corporate Identity and Visibility

Takashi Hanari[a*], Masayuki Harada[b], Toshiharu Terashima[c], and Tomoka Ono[d]

[a]Sugiyama Jogakuen University, Nagoya, Japan
[b]Nagoya City University, Nagoya, Japan
[c]Aichi Sangyo University, Okazaki, Japan
[d]Nagoya City Hall, Nagoya, Japan
*Takashi Hanari: hanari@sugiyama-u.ac.jp

ABSTRACT

In Japan, many local governments are implementing landscape plans, including color standards, to maintain the aesthetic appeal of streets. The color standards require chain stores, which generally have their own standard facade designs, to change their designs so as not to ruin the street's aesthetics. However, it is not easy for chain stores to change their facade designs because many have their own unique designs to maintain their corporate identity. This study examines how each method of changing designs affects harmony with the street or building, corporate identity, corporate image, and visibility of the store. In the experiment, we presented participants with photo images on two high-precision color displays, showing the facade design of each chain store and the street on which the store was located. One display showed a photo image of the facade design changed by using the methods being studied. The other display repeatedly showed a photo image of the standard design facade of each chain store and street. We found the following results. Low chroma and Low lightness, Use corporate color as a line, Cut lettering design, and Replace signs position from outdoor to indoor were effective in many cases. These methods could harmonize stores with the streets, or the buildings where the stores were tenants, maintain the corporate identity, and improve the corporate image. On the other hand, these change methods were less effective for visibility of the store.

Keywords: color standards, facade design, change method, harmony with the street, corporate identity

INTRODUCTION

In Japan, more than 660 local governments are implementing landscape plans, including color standards, to maintain the aesthetic appeal of streets. Most local governments formulate their plans independently, although prefectures and major urban cities are required to maintain landscapes by the Japanese Landscape Act. The specific landscape formation standards formulated on each plan are generally limited to specific areas within the city. In particular, color standards require chain stores, which generally have their own standard facade designs, to change their designs so as not to ruin the street's aesthetics. However, it is not easy for chain stores to change their facade designs because many have their own unique designs to maintain their corporate identity.

In our previous research [1], we conducted a field survey of chain stores to find out methods of changing facade designs. We identified about 15 change methods and categorized them as Achromatization, Material colorization, Low chroma and Low lightness, Color number reduction, Color inversion of figure-ground, Reduction in regulated color area ratio, Use corporate color as a line, Cut lettering design, Sign size reduction, Replace signs

position from outdoor to indoor, etc. Moreover, these change methods could be classified roughly into 3 groups: group A involves changing colors of the signage; group B involves changing the signage elements (e. g. sizes or lettering); and group C involves changing the position or location of the signage.

We aimed to clarify the effects of the change methods on harmony with the street on which the store was located or the building in which the stores were tenants, maintenance of corporate identity, and visibility of the store adopting any of the change methods. Preliminary analysis [2] suggested that Low chroma and Low lightness, Use corporate color as a line, Cut lettering design, and Replace signs position from outdoor to indoor were effective in achieving harmony between the store and the street/building, and could contribute to improvement of the corporate image, although they were slightly disadvantageous in terms of visibility. This study examines in more detail how change methods affect harmony between stores and streets/buildings, maintenance of corporate identity, corporate image, and visibility of the store.

METHODOLOGY

Participants

Thirty-two Japanese graduate and undergraduate students participated in the experiment (24 females, 8 males, 20–24 years old). All participants were confirmed as normal trichromats by Ishihara's tests for color deficiency, concise edition.

Materials

We used 21 changed design facades selected from 17 chain stores, which had their own standard facade designs. Most of the 17 chain stores were well known in Japan. Four kinds of the same chain stores were involved in the 21 changed design facades. The 21 stores with changed design facades were located in 6 areas selected from major urban cities in Japan. Two streets (Karasuma and Oike) were in Kyoto, 2 streets (Midosuji and Route 2) were in Osaka, 1 street (Aoyama) was in Tokyo, and 1 district (the vicinity of Odawara Station) was in Odawara. Photo images were prepared of 21 changed design facades, the 6 streets around them, and the 17 standard design facades. Figure 1 shows examples of photo images taken of changed design facades and standard designs used in the experiment.

Questionnaire

The questionnaire consisted of 17 questions related to harmony between the changed design facade and the street/building where the store was located, maintenance of the corporate identity, visibility/conspicuity of the store, effectiveness in improving corporate image, and other factors. Some specific examples were:

Q. 01 To what degree do you think that the store is in harmony with the street?
Q. 02 To what degree do you think that the store contributes to the attractiveness of the street?
Q. 16 To what degree do you think that the store is superior to the standard design in harmony with the street?
Q. 12 To what degree do you think that the store maintains the corporate identity?
Q. 05 To what degree do you think that the store is attractive in the street?
Q. 08 To what degree do you think that the store is easy to find for people walking down the street?

Participants were asked to answer on a 5-level scale from 2 to −2. For example, 2 means "extremely in harmony with the street". 1 means "in harmony with the street". 0 means "not sure or no opinion". −1 means "not in harmony with the street". −2 means "not at all in harmony with the street". Three other questions were also included. These questions asked whether participants had already known the chain store or not, known the standard design of the chain store or not, and had used the chain store somewhere or not. The data for these 3 questions are not mentioned in this paper.

Procedures

In the experiment, we presented participants with photo images, on two high-precision color displays manufactured by Eizo, showing the facade design of each chain store and the street on which the store is located. One display showed a photo image of the changed design facade which adopted any change methods we had

classified. The other display repeatedly showed a photo image of the standard design facade of each chain store and the streets. The participants rated 17 questions on the facade design of each chain store, observing the photo images on both displays. The experiment was conducted from November 2024 to March 2025.

Ethics

This study was approved by the Ethical Committee at the Nagoya City University.

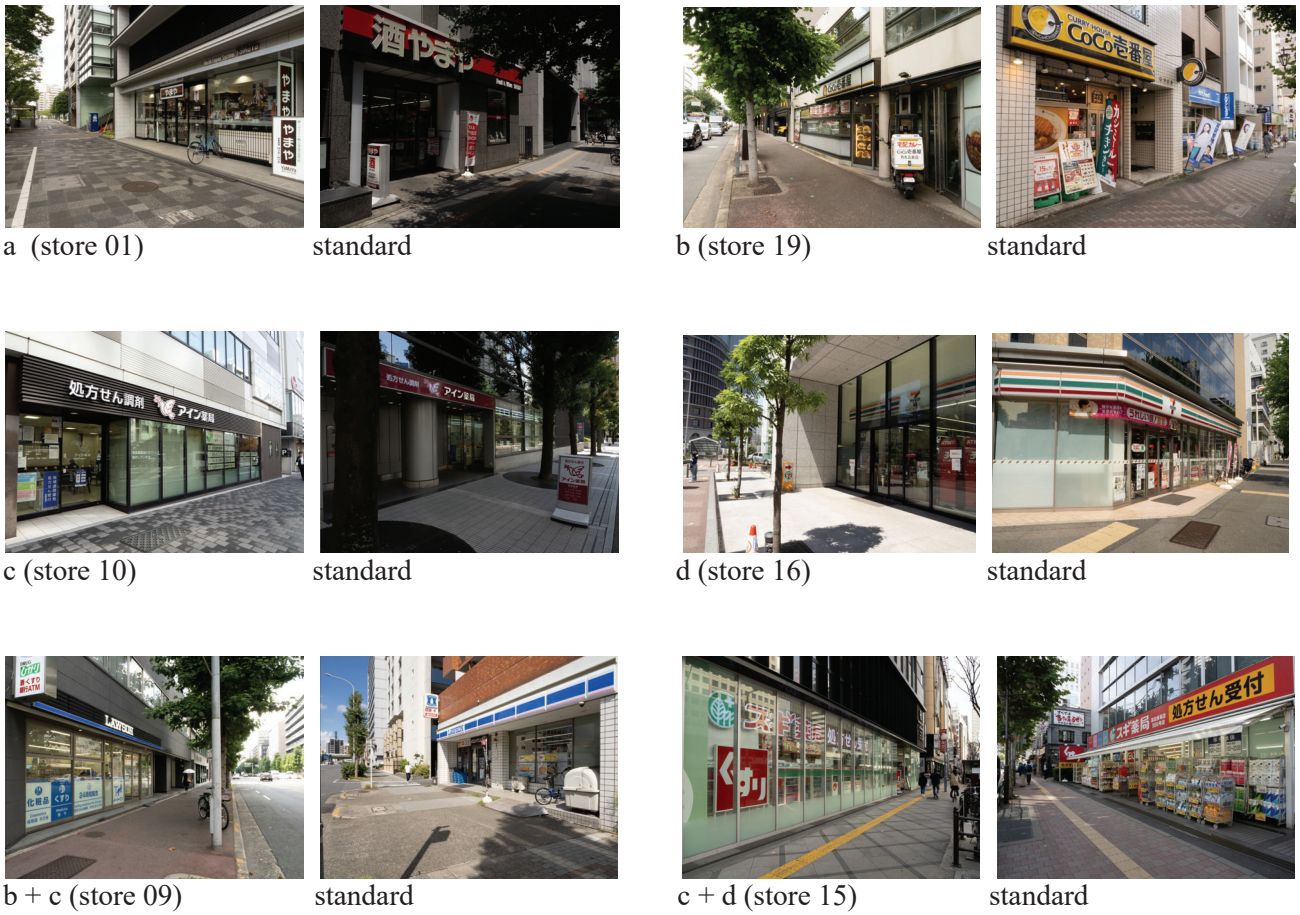

a (store 01) standard b (store 19) standard

c (store 10) standard d (store 16) standard

b + c (store 09) standard c + d (store 15) standard

Figure 1: Examples of changed facades designs (left) and standard facade designs (right)

Changed method a: Low chroma and Low lightness b: Use corporate color as a line
c: Cut lettering design d: Replace signs position from outdoor to indoor

RESULTS AND DISCUSSION

Table 1 shows the average evaluation for each of the 14 questions for all 21 changed design facades. Positive numbers indicate a positive evaluation, while negative numbers indicate a negative evaluation. Overall, it was suggested that the changed design facades were effective in terms of harmony with the street/building (Q. 01, 02, 16/Q. 03, 04, 17), maintenance of corporate identity (Q. 12). In particular, superiority to the standard design was very clear (see green-marked value). However, they were slightly disadvantageous in terms of visibility of the store (Q. 05, 08, 15) (see yellow-marked value) and were generally well received in terms of improvement in corporate image (Q. 06, 13, 14 [see green-marked value]), except Q. 07 (see yellow-marked value).

Table 1: Evaluation of the 21 facades in harmony with the street/building, maintenance of corporate identity, visibility of the store, and improvement in corporate image.

	Harmony with the street			Harmony with the building			Maintenance of CI	Visibility of the store			Improvement in corporate image			
	Q. 01	Q. 02	Q. 16	Q. 03	Q. 04	Q. 17	Q. 12	Q. 05	Q. 08	Q. 15	Q. 06	Q. 07	Q. 13	Q. 14
	Harmony with the street	Contribution to the street	Superiority to the standard design	Harmony with the building	Contribution to the building	Superiority to the standard design	Maintenance of CI	Conspicuity	Visibility	Superiority to the standard design	Good impression for the store	Intention of spreading the changed design	Increase of intention use the store	Good impression for the corporation
mean	0.7	0.5	1.3	0.8	0.5	1.3	0.8	0.1	0.2	-0.4	0.4	-1.3	0.4	1.0
SD	1.2	1.1	0.9	1.1	1.0	0.9	1.3	1.1	1.3	1.2	1.0	1.0	1.0	0.9

Next, we focused on the change methods used in several cases: Use corporate color as a line (5 cases), Low chroma and Low lightness (4 cases), Cut lettering design (7 cases), and Replace signs position from outdoor to indoor (4 cases). Of the above 20 cases, 3 cases adopted the combination of Use corporate color as a line and Cut lettering design, and 2 cases adopted Cut lettering design and Replace signs position from outdoor to indoor. Table 2 shows the average evaluations for the 25 cases (15 stores) according to the change method adopted. Green-marked values indicate very positive evaluations (1.0 or above), while yellow-marked values indicate negative evaluations (below 0.0).

[Harmony with the street and the building] Q. 01, 02, 16/Q03, 04, 17

It was suggested that all the change methods were effective in terms of harmony with the street and the building. Of the change methods, Cutletteringdesign seemed to be most effective. For example, store 09 (Figure 1) and store 17 (Figure 2) were highly evaluated in all 6 questions. Both stores adopted Cut lettering design and another change method: store 09 adopted Use corporate color as a line, and store 17 adopted Replace signs position from outdoor to indoor. Adding another method to Cut lettering design could be very effective. On the other hand, Low chroma and Low lightness appears to be less effective than the other methods. For example, store 02 received negative evaluations at Q. 01, 02, 03, and 04. This may be because many products with high chroma colored price tags were displayed in front of the store, as shown in Figure 2. Additionally, the large white background of the signboard may be too conspicuous. Conversely, that may explain why store 02's visibility and conspicuity were not significantly impaired (Q. 05, 08).

[Maintenance of corporate identity] Q. 12

It seems that Replace signs position from outdoor to indoor is the most effective method of maintaining corporate identity, followed by Cut lettering design. However, the other change methods did not severely decrease corporate identity. Naturally, Replace signs position from outdoor to indoor leaves the standard facade designs almost unchanged, making it easy to maintain corporate identity. As mentioned above, store 09 and store 17 were highly evaluated in terms of harmony. However, of these two stores, store 17 was also highly evaluated in terms of maintenance of corporate identity. The store adopted both Cut lettering design and Replace signs position from outdoor to indoor. Therefore, the combination of Cut lettering design and Replace signs position from outdoor to indoor could be a good example of balancing aesthetic appeal and corporate identity. Store 01 (Figure 1), which adopted Low chroma and Low lightness, had the lowest score. When the standard facade design included high chroma and advancing colors, as with store 01, Low chroma and Low lightness could be disadvantageous for maintaining corporate identity.

[Visibility of the store] Q. 05, 08, 15

As might be expected, all change methods were disadvantageous to the visibility of the store compared to the standard design facades. In particular, Replace signs position from outdoor to indoor was advantageous for maintenance of corporate identity, as mentioned above, but it made the store difficult to see. In addition, a very negative case of under −1.0 was found at store 01 which adopted Low chroma and Low lightness. This could be an example of reducing visibility and conspicuity by decreasing chroma and/or value too much.

Table 2: Evaluation for the facades adopting each changed method in harmony with the street/building, maintenance of corporate identity, visibility of the store, and improvement in corporate image.

Change Method	Store No.		Harmony with the street			Harmony with the building			Maintenance of CI	Visibility of the store			Improvement in corporate image			
			Q. 01	Q. 02	Q. 16	Q. 03	Q. 04	Q. 17	Q. 12	Q. 05	Q. 08	Q. 15	Q. 06	Q. 07	Q. 13	Q. 14
			Harmony with the street	Contribution to the street	Superiority to the standard design	Harmony with the building	Contribution to the building	Superiority to the standard design	Maintenance of CI	Conspicuity	Visibility	Superiority to the standard design	Good impression for the store	Intention of spreading the changed design	Increase of intention use the store	Good impression for the corporation
Use corporate color as a line	store 06	mean	0.2	0.1	1.4	0.6	0.2	1.2	1.7	0.8	1.1	0.2	0.1	-1.7	0.4	0.9
		SD	1.2	0.9	0.7	1.0	0.8	0.9	0.5	0.9	1.0	1.2	0.9	0.6	0.8	0.9
	store 07	mean	1.1	0.8	1.5	1.0	0.9	1.3	0.9	0.2	0.3	-0.5	0.7	-1.1	0.4	1.2
		SD	0.9	0.9	0.8	1.0	0.9	1.1	1.1	1.1	1.1	1.2	0.8	1.2	1.0	0.8
	store08	mean	1.3	0.8	1.7	1.7	1.1	1.9	-0.2	-0.3	-0.3	-0.5	0.6	-1.2	1.0	1.3
		SD	1.0	0.9	0.9	0.5	0.9	0.4	1.2	0.8	1.2	1.2	0.9	1.0	0.8	0.6
	store09	mean	1.3	1.2	1.5	1.4	1.2	1.6	0.7	0.1	0.1	-0.6	0.9	-0.6	0.8	1.3
		SD	1.0	0.8	0.9	`	0.9	0.9	1.3	1.1	1.2	1.1	0.9	1.4	1.1	0.9
	store19	mean	1.0	0.4	1.4	0.9	0.6	1.3	1.1	-0.1	0.3	-0.3	0.6	-1.5	0.5	1.1
		SD	0.7	0.8	0.7	0.9	0.8	0.9	0.8	0.8	1.0	1.0	0.8	0.8	0.8	0.6
	Total	mean	1.0	0.7	1.5	1.1	0.8	1.5	0.8	0.2	0.3	-0.3	0.6	-1.2	0.6	1.2
		SD	1.0	0.9	0.8	1.0	0.9	0.9	1.2	1.0	1.2	1.1	0.9	1.1	0.9	0.8
Low chroma and Low lightness	store01	mean	1.2	0.6	1.7	1.3	0.6	1.5	-1.1	-0.7	-0.6	-1.3	0.5	-1.5	0.3	1.1
		SD	0.8	1.0	0.8	0.9	1.0	0.8	1.0	0.9	1.1	0.9	1.0	0.9	1.1	1.1
	store02	mean	-0.3	-0.2	1.1	-0.1	-0.2	1.1	0.4	0.8	0.8	-0.5	-0.1	-1.7	0.3	0.6
		SD	1.1	0.9	0.9	1.2	0.8	0.8	1.2	1.0	1.3	1.1	0.9	0.7	0.8	0.8
	store03	mean	0.8	0.6	1.2	0.8	0.5	1.1	1.1	-0.2	0.0	-0.3	0.7	-1.3	0.2	1.0
		SD	1.0	0.9	0.9	1.2	1.0	1.0	1.1	1.0	1.1	1.0	0.9	1.0	0.9	0.8
	store04	mean	1.0	0.9	1.8	1.1	0.8	1.5	0.9	0.0	0.1	-0.3	0.8	-1.1	0.7	1.5
		SD	0.8	1.0	0.4	1.0	1.1	0.8	1.1	1.0	1.1	1.1	0.8	1.3	0.9	0.6
	Total	mean	0.7	0.5	1.4	0.8	0.4	1.3	0.3	0.0	0.1	-0.6	0.5	-1.4	0.4	1.0
		SD	1.1	1.0	0.8	1.2	1.0	0.9	1.4	1.1	1.3	1.1	0.9	1.0	1.0	0.9
Cut lettering design	store07	mean	1.1	0.8	1.5	1.0	0.9	1.3	0.9	0.2	0.3	-0.5	0.7	-1.1	0.4	1.2
		SD	0.9	0.9	0.8	1.0	0.9	1.1	1.1	1.1	1.1	1.2	0.8	1.2	1.0	0.8
	store08	mean	1.3	0.8	1.7	1.7	1.1	1.9	-0.2	-0.3	-0.3	-0.5	0.6	-1.2	1.0	1.3
		SD	1.0	0.9	0.9	0.5	0.9	0.4	1.2	0.8	1.2	1.2	0.9	1.0	0.8	0.6
	store09	mean	1.3	1.2	1.5	1.4	1.2	1.6	0.7	0.1	0.1	-0.6	0.9	-0.6	0.8	1.3
		SD	1.0	0.8	0.9	0.9	0.9	0.9	1.3	1.1	1.2	1.1	0.9	1.4	1.1	0.9
	store10	mean	1.6	1.0	1.9	1.1	0.7	1.7	-0.2	-0.7	-0.6	-0.8	0.6	-1.5	0.6	1.4
		SD	0.7	0.9	0.4	1.0	1.0	0.7	1.3	1.0	1.1	1.3	1.0	0.8	0.9	0.7
	store11	mean	1.0	0.8	1.5	0.9	0.9	1.5	1.4	0.5	0.5	-0.2	0.9	-1.0	1.0	1.6
		SD	1.1	1.0	0.8	1.0	0.8	0.9	0.9	1.0	1.2	1.1	0.7	1.3	0.7	0.6
	store15	mean	1.2	0.9	1.7	0.9	0.9	1.8	1.6	0.8	0.9	0.3	0.7	-1.0	1.1	1.3
		SD	1.0	0.9	0.6	1.1	1.1	0.6	0.7	0.8	1.0	1.3	1.0	1.3	1.0	0.8
	store17	mean	1.4	1.5	1.8	1.6	1.4	1.8	1.3	0.3	0.0	-0.6	1.5	-0.3	1.6	1.6
		SD	0.9	0.6	0.7	0.6	0.7	0.6	0.9	1.2	1.3	1.2	0.6	1.5	0.7	0.7
	Total	mean	1.3	1.0	1.6	1.2	1.0	1.6	0.8	0.1	0.1	-0.4	0.8	-1.0	0.9	1.4
		SD	0.9	0.9	0.8	0.9	0.9	0.8	1.3	1.1	1.2	1.2	0.9	1.3	0.9	0.7
Replace signs position from outdoor to indoor	store15	mean	1.2	0.9	1.7	0.9	0.9	1.8	1.6	0.8	0.9	0.3	0.7	-1.0	1.1	1.3
		SD	1.0	0.9	0.6	1.1	1.1	0.6	0.7	0.8	1.0	1.3	1.0	1.3	1.0	0.8
	store16	mean	1.2	0.6	1.4	1.0	0.7	1.5	1.6	-0.9	-0.8	-0.8	0.5	-1.6	0.5	0.9
		SD	1.0	1.0	0.9	1.1	1.1	0.8	0.8	0.9	1.2	1.1	0.9	0.7	0.9	1.0
	store17	mean	1.4	1.5	1.8	1.6	1.4	1.8	1.3	0.3	0.0	-0.6	1.5	-0.3	1.6	1.6
		SD	0.9	0.6	0.7	0.6	0.7	0.6	0.9	1.2	1.3	1.2	0.6	1.5	0.7	0.7
	store18	mean	1.4	0.5	1.0	1.2	0.7	1.4	0.9	-0.8	-0.6	-0.9	0.4	-1.5	0.0	0.5
		SD	0.9	0.9	1.1	1.1	1.2	0.9	1.4	1.1	1.3	0.9	1.1	0.7	0.9	1.2
	Total	mean	1.3	0.9	1.5	1.2	0.9	1.6	1.4	-0.2	-0.1	-0.5	0.8	-1.1	0.8	1.1
		SD	0.9	1.0	0.9	1.0	1.1	0.8	1.0	1.2	1.4	1.2	1.0	1.2	1.0	1.0
Use corporate color as a line + Cut lettering design	store07	mean	1.1	0.8	1.5	1.0	0.9	1.3	0.9	0.2	0.3	-0.5	0.7	-1.1	0.4	1.2
		SD	0.9	0.9	0.8	1.0	0.9	1.1	1.1	1.1	1.1	1.2	0.8	1.2	1.0	0.8
	store08	mean	1.3	0.8	1.7	1.7	1.1	1.9	-0.2	-0.3	-0.3	-0.5	0.6	-1.2	1.0	1.3
		SD	1.0	0.9	0.9	0.5	0.9	0.4	1.2	0.8	1.2	1.2	0.9	1.0	0.8	0.6
	store09	mean	1.3	1.2	1.5	1.4	1.2	1.6	0.7	0.1	0.1	-0.6	0.9	-0.6	0.8	1.3
		SD	1.0	0.8	0.9	0.9	0.9	0.9	1.3	1.1	1.2	1.1	0.9	1.4	1.1	0.9
	Total	mean	1.2	0.9	1.5	1.4	1.1	1.6	0.5	0.0	0.1	-0.5	0.7	-1.0	0.7	1.3
		SD	1.0	0.9	0.9	0.9	0.9	0.9	1.3	1.0	1.2	1.1	0.8	1.2	1.0	0.8
Cut lettering design + Replace signs position from outdoor to indoor	store15	mean	1.2	0.9	1.7	0.9	0.9	1.8	1.6	0.8	0.9	0.3	0.7	-1.0	1.1	1.3
		SD	1.0	0.9	0.6	1.1	1.1	0.6	0.7	0.8	1.0	1.3	1.0	1.3	1.0	0.8
	store17	mean	1.4	1.5	1.8	1.6	1.4	1.8	1.3	0.3	0.0	-0.6	1.5	-0.3	1.6	1.6
		SD	0.9	0.6	0.7	0.6	0.7	0.6	0.9	1.2	1.3	1.2	0.6	1.5	0.7	0.7
	Total	mean	1.3	1.2	1.8	1.2	1.2	1.8	1.5	0.5	0.4	-0.2	1.0	-0.7	1.3	1.4
		SD	0.9	0.9	0.7	0.9	1.0	0.6	0.8	1.0	1.3	1.3	0.9	1.4	0.9	0.8

store 17 Standard store 02 Standard

Figure 2: Store 17 changed by *Cut lettering design + Replace signs position from outdoor to indoor* and store 02 changed by *Low chroma and Low lightness.*

[Improvement in corporate image] Q. 06, 07, 13, 14

All the change methods were particularly effective in creating a good impression of the corporation (Q. 14). Several cases could encourage customers to make purchases at the stores which adopted Cut lettering design (Q. 13). On the other hand, there was little motivation to spread the changed design via social media or word of mouth (Q. 07). Regardless of the change method, it was not expected to be spread by customers, even if it was unique or attractive.

CONCLUSION

It was confirmed that introducing the following change methods was a useful approach to the aesthetic appeal of streets or buildings, and improving corporation image: Low chroma and Low lightness, Use corporate color as a line, Cut lettering design, and Replace signs position from outdoor to indoor. Additionally, none of the change methods significantly impaired corporate identity. However, they were slightly disadvantageous to store visibility. Of the change methods, Cut lettering design seemed to be most effective in terms of harmony with the street and building. Combining Cut lettering design with another method could be very effective. Meanwhile, Replace signs position from outdoor to indoor seemed to be more effective in terms of maintenance of corporate identity. Combining Cut lettering design with Replace signs position from outdoor to indoor could be an effective way of balancing aesthetic appeal and corporate identity.

ACKNOWLEDGEMENTS

This study was supported by JSPS KAKENHI (23H03682/23K28371).

REFERENCES

[1]. Shibahara, K., Ono, T., Takeuchi, A., Terashima, T., Harada, M., Mukaiguchi, T. & Hanari, T. (2024). Color standards in city planning and store facade design changes: Part 2 Field survey on priority landscape districts in Osaka city, Kyoto City, Kanazawa City and classification of methods for changing CI elements of stores. AIJ Journal Architectural Institute of Japan Tokai Branch, Research Report, 61, 429-432.

[2]. Harada, M., Ono, T., Terashima, T., & Hanari, T. (2024). Color standards in city planning and store facade design changes: Part 7 Preliminary analysis of the effects of facade change methods through psychological evaluation experiment. AIJ Journal Architectural Institute of Japan Kanto Branch, Research Report, 95, 367-370.

From Intuition to Intentionality: Understanding Color Decision-Making through Reflective Design Practice in Graphic Design Education

Gyeonghwa Lee[a*], Jie Yang[b], and Yun Chen[c]

[a]Birmingham City University, Birmingham, United Kingdom
[b]Beijing Institute of Graphic Communication, Beijing, China
[c] Beijing Institute of Technology, Beijing, China
[*]Corresponding author: Gyeonghwa Lee, gyeonghwa.lee2@bcu.ac.uk

ABSTRACT

This study examines how first-year graphic design students select colors across varied themes during a month-long project. It also identifies cognitive and psychological factors that shape those choices to inform evidence-based teaching and practice. Fifty first-year students created an eight-page magazine after choosing one of nine themed media articles. Students then created a cover using a photo to represent the theme. Five colors were extracted from each cover with Adobe Color and converted to NCS codes. Four-section email interviews (involving twelve students) were coded using NVivo. They revealed initial thinking, intuitive color, strategic color, and self-assessment with future shift. Interviews showed two motivation profiles: form-led and meaning-led. Students judged whether to keep or modify selected colors using three stable criteria: theme fit, legibility control, and image harmony. Strategies followed multiple routes: plan-first, source-led, and layout-first. Self-reports showed strategic fit, intuitive fit, and balanced fit. Future intentions were four balanced, four intuitive, and two strategic. Cover colors revealed category-based patterns that remained consistent across themes. Culture had the highest mean chroma and used both warm and cool axes. Politics clustered on the Y to R axis with higher S and mid-level chroma. Art was neutral-dominant with the lowest mean chroma and relatively low S. Psychology showed a high neutral share with the widest S-C coverage and mid chroma. Future studies could track the same students to see how strategies evolve, how the weighting of criteria shifts with experience, and how practice changes under real task constraints. The analysis offers a foundation for ongoing evaluation of color decision-making in design education.

Keywords: Color decision-making, Intuition and strategy, Color design education, Reflective practice

INTRODUCTION

Designers' knowledge and behavior have long been central research topics across diverse design fields. Understanding behavior is critical not only for informing curriculum design but also for improving efficiency in professional design practice. Previous studies [1-6] have compared student, novice, and expert designers, as well as designers and non-designers. However, much of this research has concentrated on how expert designers think and act in task contexts, while the characteristics of less experienced or student designers have been comparatively under examined. As a result, student and novice designers are often positioned mainly as contrasts that emphasize expert performance. Color, meanwhile, is a core design element applied not only in most design domains but also in related disciplines such as psychology and architecture. Yet studies of design behavior that focus specifically on color remain scarce. Color functions through aesthetic selection, shaping legibility, meaning, identity, and user experience, and these effects are highly contextual. Nevertheless, compared with other areas, there is still a lack of behavior focused research tracing how student designers select and apply color in contextual design settings.

Taken together, these gaps underline the need to understand how student designers choose and use color in real task contexts. Understanding student behavior is central to curriculum design, and grasping the specifics of color selection is essential. Color choice directly affects not only aesthetics but also readability, communication of meaning, and user experience, making it a key determinant of successful design outcomes. In this sense, effective color education can provide students with skills, understanding, and confidence in color use, supporting their development into capable designers. Therefore, this study begins from that problem space. It systematically documents student designers color choices within a real project context, traces how their thinking and behavior evolve during the process and draws out education focused implications grounded in data analysis.

METHODOLOGY

In this study, data collection was conducted in three stages: (1) magazine creation (by students) (2) identification of color use (by researchers), and (3) reflection on the design process (by students). In the first stage, fifty first-year undergraduate graphic design students were given nine online media articles, each with a distinct theme (Table 1). Participants selected one themed article each and created an eight-page magazine with it. They used Adobe InDesign to transform the textual content into a visual composition and layout. Students then placed a photograph on the cover of the magazine to represent their chosen theme. The image was treated as a condensed expression of project identity.

Table 1: Nine themes provided

Article No.	Main Category	Topic	Title
1	Culture	Originality & Trend	Can You Ever Really Own an Aesthetic?
2	Art	Minimalism	Graphic Designers Have Always Loved Minimalism, but at What Cost?
3	Politics	Racial Diversity	Where Are All the Black Designers?
4	Culture	Cultural Branding	Bitter Aftertaste: The Fraught World of Branding Cultural Food Products
5	Politics	Arabic Typography	Who Gets to Design Arabic Typography?
6	Society	Gender Bias in AI Interfaces	What Would a Feminist Alexa Look, or Rather Sound, Like?
7	Society	Performative Activism	Real Activism or Clicks without a Cause?
8	Politics	Modernism & Whiteness	Helvetica, Modernism and the Status Quo of Design
9	Psychology	Perfectionism	When Perfectionism Makes You a Better Creative, and When It Doesn’t

For the second stage of the study, it was hypothesized by the researchers that color choice on the cover would provide a standardized, representative proxy for color use in the whole-document. Therefore in this stage, five colors were extracted from each cover using Adobe Color. This enabled identification of overall color trends for each theme. A total of two hundred colors were collected at this stage and analyzed using the NCS color system. The Society category was excluded from the quantitative NCS analysis due to insufficient cases (fewer than ten cover palettes), whereas all other categories provided at least ten. In the final stage of the study, participants reflected on

the rationale for their color choices. To allow this, qualitative data were collected via email interviews. Participants (n=12) were anonymized by assigning alphabetic codes. The interview had four sections (Table 2). Data from this stage were qualitatively coded using NVivo 15. Codes are presented in italics to distinguish them clearly from descriptive text.

RESULTS AND DISCUSSION

In the first section of the interviews (initial thinking), there were three questions asked: (1) why participants selected one theme from the nine article options, (2) the first five design elements or principles they prioritized while designing their magazine, and (3) five elements or principles they considered later in the process.

The analysis indicates two main motivation orientations: Form-led Preference and Meaning-led Preference. Motivation seems to be closely tied to element and principle choices across the design process. For example, the form-led group typically begin with color and typography. Meaning-led preference is divided into three subtypes: Personal Relevance, Societal or Industry Relevance, and Learning or Skill Goals. However, the meaning-led group diverge by subtype: those guided by personal relevance later prioritize audience needs, message consistency, and user experience. On the other hand, the participants from this group motivated by learning or skill goals maintain the salience of typography and layout in response to questions 2 and 3. They cited societal or industry relevance shift at the end of the process toward user-experience and content-structure assessments. Beyond the two primary motivations, a minority of participants displayed a desire for differentiation (3 in 12, Participants O5, D1, and D7), a pattern that seems to link to originality and creative risk-taking. Differentiation, although expressed by only a minority (3 in 12), should still be considered in teaching and assessment as it is linked to originality and creative risk-taking, qualities valued in design education. Overall, early choices concentrated on visible form - color, typography, images, layout, later choices shifted to how the work is read, emphasizing visual hierarchy, audience, and conceptual consistency.

Table 2: Structure of the four-section color reflection email interview

Section	Description
1	Initial Thinking
2	Basis of Color Choice (Intuitive)
3	Basis of Color Choice (Strategic)
4	Self-Assessment and Future Shift

In the second section of interviews, questions focused on the topic Basis of Color Choice (Intuitive). Two main parent codes, Immediate Color Recall and Retrospective Evaluation of Intuitive Color Choices, were found to be the most theoretically informative for color decision-making. In terms of Immediate Color Recall, there was an even split between two first-child codes: Recall-Present and Recall-Absent (6/12 and 6/12). Participants in the Recall-Present group first recalled a specific color, then extended reasoning via stable semantic links (e.g., minimalism, activism, and modernism). However, the Recall-Absent group did not recall a specific color. They stated a tonal direction, mentioned an image, or contrast, or gave no answer.

In Retrospective Evaluation of Intuitive Color Choices, responses indicated that most selections of color would be retained. Responses were satisfaction (7/10), dissatisfaction (2/10), and wish for improvement (1/10) (valid responses=10). Retention was supported by participant statements about holding attention or visual hierarchy and page unity (Participants T1, D7, and O5). Notably, statements of satisfaction were found to fall within three operative criteria: Theme Fit, Legibility Control, and Image Harmony. Participants fitted these criteria as follows: Theme fit (D17 and T1), Legibility control (O18, O5, and O4), and Image harmony (D3 and D1). Also, it seems

that participants progressed from an intuition trigger to a named criterion to a decision. For example, pastel purple felt right, the fit to the minimalism theme was confirmed, and the choice was kept (T1). Regret was linked to a safe selection or systemic misfit (T3) and concerns about insufficient palette coherence across pages (O21). Together, these patterns indicate that design participants judge intuitive color decisions against a small set of stable standards (theme fit, legibility control, and image harmony) and that prompting a look-back makes those standards explicit. Also, minimal starting cues are advisable for students who do not recall a specific color. Tone (light or dark), temperature (warm or cool), or contrast can guide an initial choice while keeping creative options open.

In the third section of the interviews, Basis of Color Choice (Strategic), the findings fall under five main codes: Planned Palette, Color Sketches and Notes, Color Meanings and Psychological Effects, External Inspiration, and Readability and Inclusivity. Firstly, in terms of Planned Palette, some participants planned palettes before design. Participant T1 experimented with palettes to test what range best served the idea of minimalism. Participant D17 limited the set to black, white, and red to deliver a strong impression aligned with modernist aesthetics. Others deferred the palette decision: prioritized imagery (O18) and structure or layout (D18). A few combined colors without a fixed palette (O4). Secondly, under Color Sketches and Notes, there were two groups. One group produced notes or hand sketches before application (D7 and O5). Another group explored directly in software (O4). Thirdly, regarding Color Meanings and Psychological Effects, three groups were identified. A research-led group sought psychological or semantic references and integrated them into choices (T1, O5, and D9). A targeted group conducted narrow, keyword-based searches tied to a single concept. For example, D18 searched for a color that symbolizes ‘perfectionism’ and identified white, yet this did not drive the final palette. A third group did not engage in meaning research. Some participants also reported aesthetic precedent reviews or technical study of color spaces. Regarding External Inspiration, sources were wide-ranging. Participants cited well-known editorial references, social platforms, brands, curated websites, public environments, and course reading lists. Lastly, Readability and Inclusivity showed both practice and gaps. Participant O21 explicitly considered type size so that key information could be read. Participant O5 reported adjustments after a lecture that shifted their awareness. Only a minority addressed specific user groups. Participant O18 checked legibility for readers with neurological conditions. Participant D7 simplified color distinctions to support color-vision diversity. Non-inclusive patterns were also present. Stated reasons included aesthetic priority over accessibility, early stage of learning plus lack of explicit instruction, limited awareness, and assumptions about audience ability.

The findings for the five main codes indicate that, among the participants, no single route for color strategy was observed. Three identifiable entry routes coexisted: plan-first (D17), source-led (O5 and D9), and layout-first (D18), some students used mixed routes (T1 and D18). What mattered was not just whether planning or research was present. The key was how evidence was applied. Students who analyzed sources (T1, O5, D9, D18) or linked psychological reasons (T1, O5) to design constraints gave clearer grounds for decisions. In several cases this link extended to concrete inclusive practices (O18, D7). Taken together, the patterns suggest high-impact intervention points. Integrating explicit prompts to students, structured source analysis, and easy-to-implement readability and color-accessibility checks can shift cognition and translate into action.

So far, the focus has been on color choice (selection). The next paragraph summarizes the value logics used to judge those choices. In terms of color choice, there are two codes under the umbrella of value logics. The first is justification and message fit, where a color is chosen to serve a communicative aim. For example, Participant O21 mentioned “Sometimes you need to make a strategic decision to choose a color that communicates a specific idea, mood, or intention”. The second is authenticity and expression, where a color is chosen to convey a personal voice and an honest feel. For example, O4 stated, “Trusting my instincts makes the design more original and authentic”. This quotation evidence authenticity through reliance on instinct and expression and an emphasis on originality.

The focus now shifts from color choice (selection) to color use (application) under task constraints, framed by Self-Assessment and Future Shift. For the final section of the interviews related to the magazine design task, codes or integration rules were identified also for how participants described their strategies for using color (self-assessment), and how they might do so in future (future shift). First, Strategic fit (a planned decision) was

predominant (7/11, D17, D18, D7, D3, O18, O5, and T3). Then, intuitive fit appeared (3/11, D9, T1, and O4) where an initial affective frame guided action. Also, balanced fit arose for one (O21) indicating both approaches. In terms of future color strategies (Future Shift), four participants reported that they would adopt a balanced fit strategy (O21, D9, D18, and D7). Another four would prefer an intuitive fit strategy for a future design task (D17, O18, O4, and T1). Two remained strategic.

There were clear patterns for integrating strategic and intuitive approaches in both the task and future intentions. First, a research-first sequence was described. This can be seen from Participant D18: “Do your research. Once you have this base of information and knowledge, trust your gut and intuition”. Second, an intuition-first route was described, where intuition was coupled with reasons for communication: “Intuition needs to be backed up by reasoning to support a message” (Participant O21). A combined stance also appears from Participant D7, who stated, “Both as they offer slightly different insights which I think are equally as useful”. In addition to these approaches, task constraints also shaped decisions resulting in compromise. For example, Participant D18 stated “I was struggling to decide what color palette to use. I went with the color palette that was the easiest and quickest to save time”. Retrospective reflections on learning and alignment with assessment informed the responses. For instance, T3 stated “I feel my original strategy would have worked better than my intuition did. Results could be much better if more thought out”. Participant O18 stated “I wanted a good mark. I needed an informed strategy to back up my design”.

To sum up, color choice decisions were shaped by two value logics-justification and message fit versus authenticity and expression, and by approaches or integration rules for color use operating under real task constraints, namely research-first and intuition-first. In teaching, the requirement for a brief post-project memo that states the value logic used for color choice and the approach to color use or integration rule applied would align reflection with assessment and make the quality of students’ color decision-making more transparent.

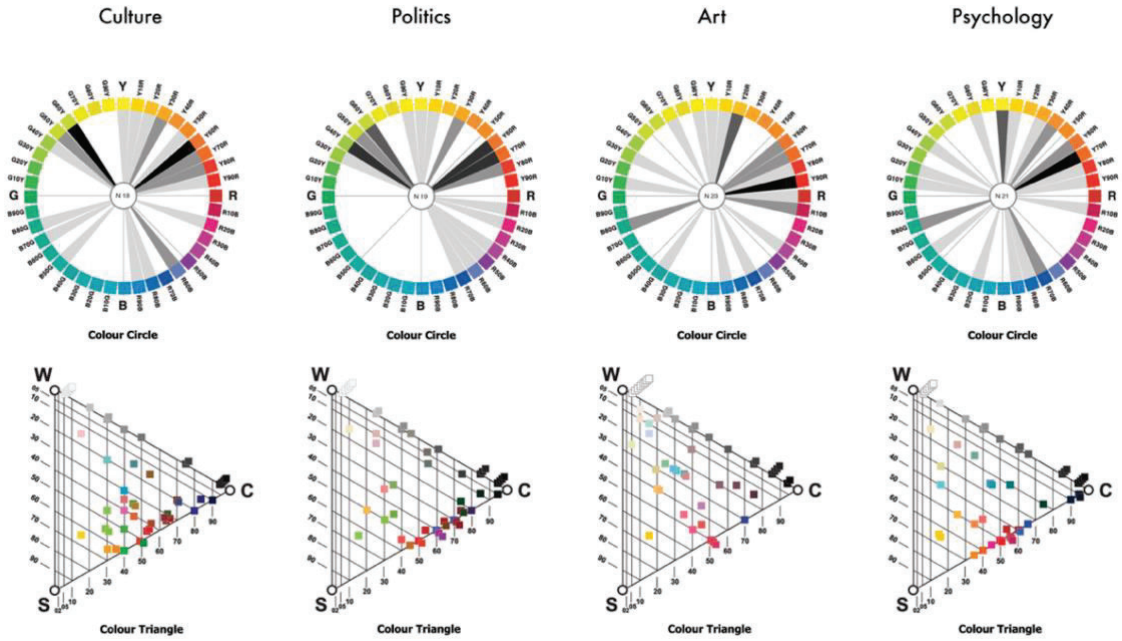

Figure 1: Comparative Color Maps (NCS) for Culture, Politics, Art, and Psychology: W (whiteness), S (blackness), C (chromaticness).

The following part of this paper compares interview-derived rationales and criteria with actual color data from the magazine covers. From each cover, five colors were extracted by the researchers using Adobe Color, converted to NCS codes manually using the NCS color palette swatch, and placed on a color circle and an S-C triangle (Figure 1). This makes it possible to examine how the qualitative criteria - theme fit, legibility, and image harmony from section 2 of the interviews and arising from 'Retrospective Evaluation of Intuitive Color Choices' - appear in actual color selections across four groups (Culture, Politics, Art, and Psychology). Firstly, regarding color choices in the Culture category, participants favored higher Chroma. Mean chroma is the highest (about 24.5), and both warm and cool axes are used. The pattern suggests differentiation while balance is maintained. Secondly, for the Politics category, interviews emphasized salience and hierarchy. The quantitative pattern matches this emphasis: the strongest concentration lies on the Y→R axis. Mean S is high, producing a darker register, while mean chroma is about 19.5. This reads as a high-signal palette with readable contrast. Thirdly, for the Art category, statements about minimalism and consistency are found in the data. Neutrals dominate (N=23/50, 46%). This group shows the lowest mean chroma (about 15.7) and a relatively low mean S (about 38.2), yielding soft contrast. The selection may be perceived as restrained and orderly. Lastly, for the Psychology category, attention to legibility and inclusion aligns with broad exploration. Neutrals are common (N=21/50, 42%), and S-C coverage is the largest (about 74.5%). Many tones are tested while chroma stays around mid-level.

The qualitative findings through the email interviews (theme fit, legibility, and image harmony) align with the quantitative patterns derived from the color circle and the S-C triangle, and the two sets of evidence mutually corroborate one another (Table 3). Salience maps to a Y→R cluster with higher S in Politics. Consistency maps to heavy neutral use and low chroma in Art. Differentiation maps to higher chroma and mixed warm-cool use in Culture. Inclusion and testing map to the widest S-C coverage in Psychology. Pedagogically, it will be effective to respect intuition while making three criteria explicit - theme fit, legibility, and image harmony - and to require students to self-audit with the paired indicators (hue angle and concentration, neutral share, and S-C coverage).

Table 3: Interview themes and NCS evidence

Theme (category)	Quantitative indicator	NCS Evidence
Theme Fit (Politics)	Hue clustering toward warm reds with higher saturation, moderate chroma	Y→R cluster with higher S, described as a high-signal palette consistent with visual salience
Legibility Control (Art)	Higher neutral share, lower S and/or mid chroma, compact S-C footprint	Lowest mean chroma, relatively low S, neutrals dominate
Legibility Control (Psychology)	Broad S-C coverage anchored by neutrals	High neutral share with widest S-C coverage
Image Harmony (Art)	Tight chroma range, low S, limited hue spread	Triangle and circle show restrained, orderly selection consistent with minimalism

CONCLUSION

This study links interview-derived intentions to measurable color behavior in first-year design work. Across findings from email interviews (spread over four sections), four patterns emerge. Motivation splits into form-led and meaning-led profiles, early emphasis on form shifts to audience, hierarchy, and coherence. Immediate color recall is evenly split. Most color choices are retained and judged against three stable criteria: theme fit, legibility control, and image harmony. Color strategy shows no single route. Plan-first, source-led, and layout-first coexisted. Decision quality depended on how evidence was applied. Readability and inclusion were addressed unevenly. Self-reports show strategic fit, intuitive fit, and balanced fit. Future intentions distribute as balanced, intuitive, and

strategic. Two value logics guide choices-justification and message fit versus authenticity and expression-with integration rules that are research-first and intuition-first, and task constraints often prompt compromises.

Five colors were extracted from each participant's magazine cover, converted to NCS codes (n=200), and plotted on a color circle (hue distribution) and an S-C triangle (blackness-chromaticness distribution). Across four categories, the patterns are coherent and interpretable. Culture shows the highest mean chroma and uses both warm and cool axes, indicating differentiation balanced by restraint. Politics concentrates on the Y→R axis with higher S and mid-level chroma. This produces a high-signal palette with readable contrast that aligns with aims of salience and hierarchy. Art is dominated by neutrals and exhibits the lowest mean chroma with relatively low S, yielding soft contrast consistent with minimalism and consistency claims. Psychology combines a high neutral share with the widest S-C coverage, revealing broad exploration under legibility and inclusion concerns while keeping chroma around a mid-range. Taken together, the overlay of qualitative (textual data) and quantitative evidence (color data) indicates alignment. Stated aims map cleanly onto measured indicators: salience to Y→R clustering with higher S, consistency to heavy neutral use and low chroma, differentiation to higher chroma and mixed warm-cool use, inclusion/testing to maximal S-C coverage.

This study provides a standardized, reproducible procedure that maps interview-derived rationales to NCS-based quantitative color metrics and plots in a first-year cohort. Because participants were beginners, the findings establish a baseline for longitudinal work. Future studies could follow the same students to track how color strategies evolve, whether the relative weighting of criteria shifts with experience, and how practice changes under authentic task constraints. Accordingly, the present analysis serves as a foundation for ongoing evaluation of color decision-making in design education.

REFERENCES

[1]. Vallet, F., Eynard, B., Millet, D., Mahut, S.G., Tyl, B. and Bertoluci, G. (2013). Using eco-design tools: an overview of experts' practices. Design Studies. 34(3), 345–377.

[2]. Ozkan, O. and Dogan, F. (2013). Cognitive strategies of analogical reasoning in design: differences between expert and novice designers. Design Studies. 34(2), 161–192.

[3]. Deininger, M., Daly, S.R., Sienko, K.H. and Lee, J.C. (2017). Novice designers' use of prototypes in engineering design. Design Studies. 51, 25–65.

[4]. Ertmer, P.A., Stepich, D.A., York, C.S., Stickman, A., Wu, X., Zurek, S. and Goktas, Y. (2008). How instructional design experts use knowledge and experience to solve ill-structured problems. Performance Improvement Quarterly. 21(1), 7-42.

[5]. Crilly, N. (2015). Fixation and creativity in concept development: the attitudes and practices of expert designers. Design Studies. 38, 54–91.

[6]. Fortney, K.S. and Yamagata-Lynch, L.C. (2013). How instructional designers solve workplace problems. Performance Improvement Quarterly. 25(4), 91–109.

Prediction of Watercolor Mixing L*a*b* Values Based on Kolmogorov–Arnold Networks

Xiang-En Sun, Chen-Yu Yuan, Tzung-Han Lin*

Graduate Institute of Color and Illumination Technology, National Taiwan University of Science and Technology (NTUST), Taiwan

**Corresponding author: thl@mail.ntust.edu.tw*

ABSTRACT

This paper proposes a watercolor mixing prediction model based on Kolmogorov-Arnold Networks (KANs) to assist novice painters in mastering color mixing techniques. Traditional watercolor mixing learning requires substantial time and materials without guaranteeing accurate results. While existing Kubelka-Munk theory and conventional neural networks have been applied to color prediction, they still have limitations in handling the nonlinear characteristics of transparent watercolor pigments.

This research employed Winsor & Newton Cotman series watercolors, using 12 primary colors to generate 594 mixed color samples, measured with an EPSON SD-10 spectrophotometer under D50 illuminant and 2° standard observer conditions. Important findings reveal that $L^*a^*b^*$ values stabilize two days after application due to water evaporation processes. The study identified five key mixing ratios (1:1, 1:2, 1:5, 1:7 and 1:9), and through ratio inversion for data augmentation, expanded the dataset to 1,188 entries. The KANs model adopts an 8-10-3 architecture with a single hidden layer of 10 neurons, using 90% of data for training and 10% for testing.

Comparative analysis shows that the proposed KANs model achieved a test loss (RMSE) of 0.135, comparable to a Multi-Layer Perceptron's 0.16, but with a significantly simplified architecture (8-10-3 versus 8-100-50-3). This confirms that KANs can maintain lower computational complexity while learning nonlinear color mixing patterns, thereby enhancing model work efficiency. This study establishes KANs as an effective tool for watercolor mixing prediction, providing valuable resources for art education and lowering the learning threshold for novice painters.

Keywords: Watercolor Mixing, Color Prediction, Kolmogorov Arnold Networks (KANs).

INTRODUCTION

Watercolor blending presents considerable challenges for novice painters, who frequently encounter difficulties in mastering color mixing techniques and require extensive experiential learning to develop proficiency. Consequently, various educational tools have been developed to facilitate color mixing instruction, including the Itten color wheel, Munsell color system, and Natural Color System, which utilize color charts to assist beginners in comprehending color mixing principles. However, these methodologies are constrained to demonstrating 1:1 mixing ratio results. Numerous investigations have employed Kubelka-Munk theory for color prediction[4; 5], which has been extensively applied to opaque pigments such as paints. Nevertheless, watercolors are transparent pigments, and Kubelka-Munk predictions exhibit discrepancies from actual application outcomes. In recent years, multiple studies have utilized deep learning models for color mixing prediction, such as Chen et al., who employed deep neural networks (DNNs) to predict watercolor mixing results [2], and Moon et al., who applied DNNs for spot ink prediction [7]. However, existing neural networks are fundamentally based on linear weights and fixed

activation functions, which cannot effectively accommodate the nonlinear characteristics of color mixing behaviors. These models typically necessitate deep architectural configurations to capture color mixing patterns, thereby increasing computational complexity and reducing operational efficiency.

Kolmogorov–Arnold Networks (KANs) were introduced by Liu et al. [6], representing a neural network architecture constructed upon the Kolmogorov–Arnold representation theorem. According to the Kolmogorov–Arnold representation theorem, any multivariate continuous function can be decomposed into a mathematical expression comprising one-dimensional continuous functions and additive operations(Eq. 1).

$$\mathrm{f}(x_1, x_2, \ldots, x_n) = \sum_{q=1}^{2n+1} \Phi_q \left(\sum_{p=1}^{n} \phi_{q,p}(x_p) \right) \tag{1}$$

Specifically, the Kolmogorov–Arnold representation theorem comprises inner functions $\phi_{q,p}$: $[0,1]^n \rightarrow \mathrm{R}$ and outer functions Φ_q: $\mathrm{R} \rightarrow \mathrm{R}$. The Kolmogorov–Arnold representation theorem enables the transformation of complex multidimensional functions into combinations of one-dimensional functions. Compared to multidimensional functions, models can more readily execute one-dimensional function computations, facilitating more efficient learning and processing of complex datasets [3].

Furthermore, KANs substitute learnable weights with B-splines positioned on edges, while nodes exclusively perform summation operations. In contrast to conventional neural network architectures such as multilayer perceptrons (MLPs), convolutional neural networks (CNNs), and deep neural networks (DNNs), which utilize fixed activation functions at nodes and position learnable linear weights on edges. This structural distinction enables KANs to demonstrate superior performance in nonlinear data fitting and partial differential equation resolution [6].

METHODOLOGY

Experimental Equipment and Materials

Winsor & Newton Inc. is a renowned British pigment manufacturer whose product line encompasses watercolors, oil paints, acrylic paints, brushes, papers, and other painting materials. Their products are widely utilized by professional artists and in art education. This study employed Winsor & Newton transparent watercolors, utilizing 12 colors commonly used by novice painters. An EPSON SD-10 spectrophotometer was used to measure the L*a*b* values of samples under D50 standard illuminant with a 2° standard observer. All measurement values were utilized as data for subsequently establishing the color mixing prediction model.

Sample Preparation and Data Collection

This study prepared 594 color mixture samples, encompassing all primary color mixing combinations of the 12 pigments. Each combination included five mixing ratios: 1:1, 1:2, 1:5, 1:7, and 1:9. Through ratio inversion, the dataset was augmented to 1,188 samples. All samples were applied using an Edinburgh Realism EAN-030 size 14 nylon watercolor brush, on 300 GSM rough-textured 100% cotton watercolor paper. The color mixing trajectory is shown in Figure 1.

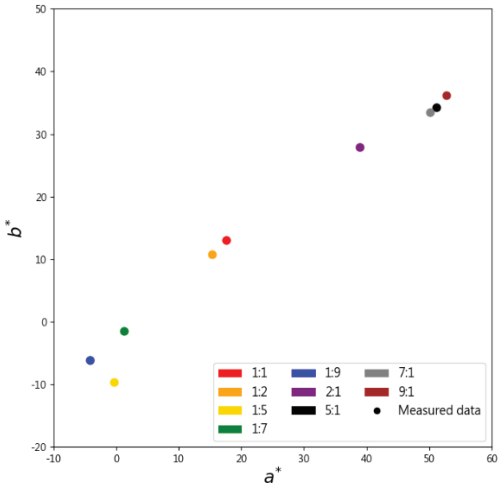

Figure 1: a^*b^* color mixing trajectory of Cadmium Red Hue and Cerulean Blue Hue

To ensure measurement data stability, this study conducted experiments on the temporal stability of L*a*b* values, with the results illustrated in Figure 2. Experiments revealed that darker pigments exhibited larger color differences between measurements taken two days post-application and those taken immediately after application, whereas lighter pigments demonstrated smaller color differences. This phenomenon indicates that immediately after pigment application, the presence of moisture causes the painted area to appear brighter overall. During the process of water absorption by the paper and natural evaporation, the painted area gradually darkens and returns to the pigment's initial color. Therefore, all samples were measured after an identical drying period to ensure L*a*b* value stability.

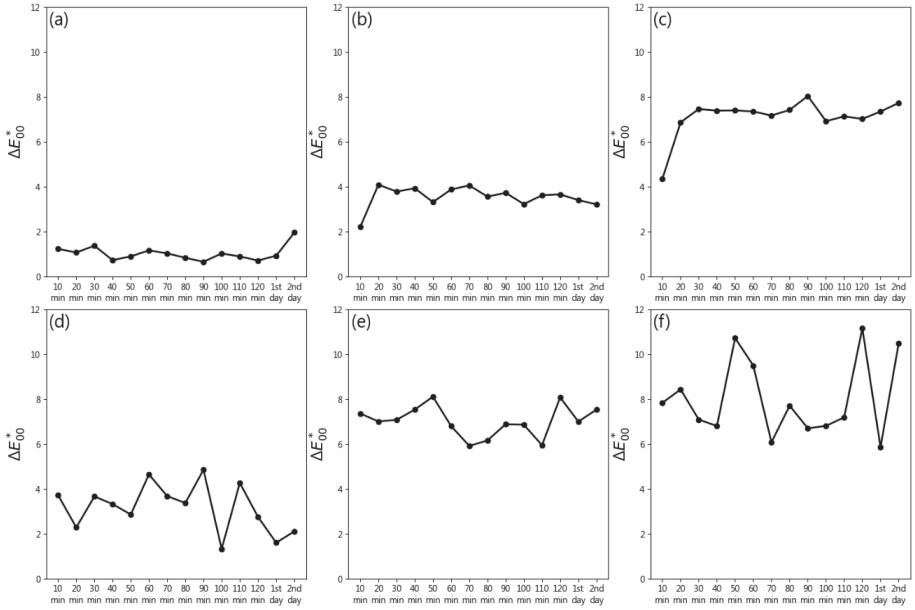

Figure 2: Color difference comparison between initial measurements and measurements at different time intervals for watercolor samples

The color mixture sample preparation process strictly controlled various parameters, including the proportion of mixed pigments during the mixing process, the pigment-to-water ratio, and the number of coating applications during the painting process. Through standardized operational procedures, human factors' influence on measurement results was substantially reduced, ensuring data consistency and reproducibility.

Measurement Data Preprocessing

Prior to establishing the prediction model, this study performed necessary preprocessing on the measurement data. First, all L*a*b* values underwent normalization to ensure numerical ranges were within appropriate intervals, thereby improving model training stability. Second, the distribution characteristics of the data were analyzed to identify potential outliers or measurement errors, which were then appropriately addressed. Finally, the data were partitioned into training and testing sets at a 9:1 ratio to ensure objective model evaluation.

Establishing the KANs Color Mixing Model

This study established a color mixing prediction model based on KANs. The input parameters consisted of the L*a*b* measurements of the first and second pigments and their respective proportions, while the output parameters were the L*a*b* measurements of the mixed color result. The model architecture, as illustrated in Figure 3, comprised one hidden layer with 10 neurons.

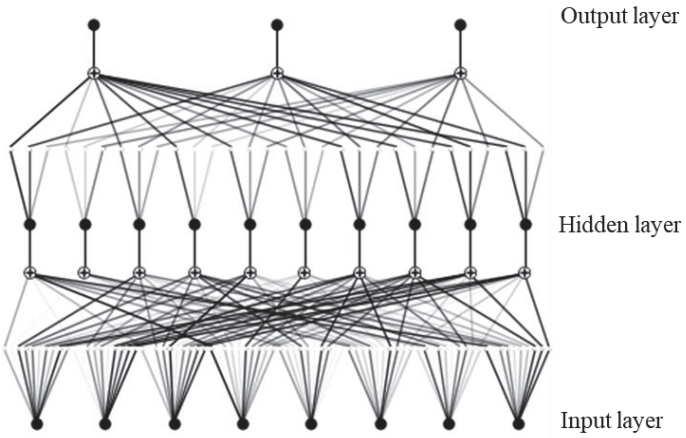

Figure 3: KANs Model Structure

Model Training and Optimization

Model training was conducted in a Python 3.9 environment on a computer equipped with an Intel Core i7-13700 processor, NVIDIA GeForce RTX 3070 graphics card, and 32GB RAM. The training process employed the Adam optimizer with a learning rate set to 0.001. Root Mean Square Error (RMSE) was adopted as the loss function.

RESULTS AND DISCUSSION

Figure 4 illustrates the learning curve of the prediction model in this study. Additionally, this study compared the KANs prediction model with quartic polynomial regression models and multilayer perceptron models, as shown in Table 1.

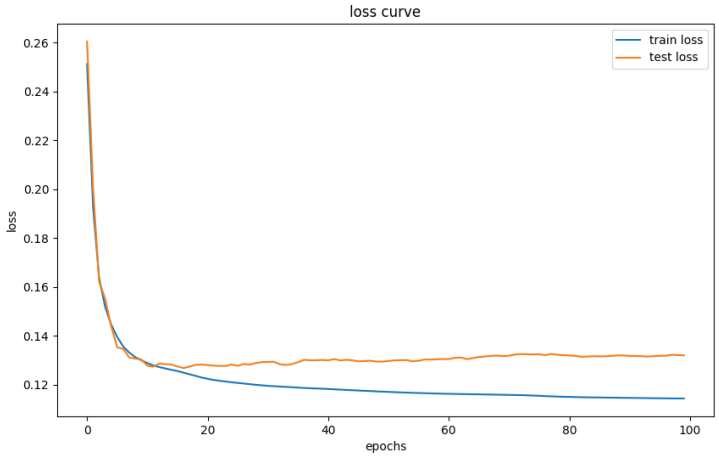

Figure 4: Learning curve of our model

Table 1: All model architectures and training/test loss functions

Model type	Model architecture	Training loss (RMSE)	Test loss (RMSE)
Quartic Polynomial Regression Model	Linear	4.11	6.47
Multi-Layer Perceptron	8-100-50-3	0.11	0.16
Our Method	8-10-3	0.114	0.135

As shown in Table 1, the proposed KANs model in this study achieves comparable loss function values to the multilayer perceptron model, yet the KANs model architecture is significantly smaller than that of the multilayer perceptron. This indicates that KANs exhibit lower computational complexity compared to multilayer perceptron models, whereas the latter's higher computational complexity results in extended training time and reduced overall computational efficiency.

This study successfully developed a watercolor mixing prediction model based on Kolmogorov-Arnold Networks (KANs), providing a practical mixing formula guide for novice painters. The research results confirm the superior performance of KANs in handling nonlinear problems such as watercolor mixing.

Through systematic experimental design, this study collected 594 mixing samples covering various mixing ratios of 12 primary colors from the Winsor & Newton Cotman series. After data augmentation, 1,188 training data entries were obtained, ensuring sufficient model training. Experimental results demonstrate that the KANs model, with its concise 8-10-3 architecture, achieved a test loss (RMSE) of 0.135, comparable to the 0.16 test loss of the Multi-Layer Perceptron (MLP) model with its complex 8-100-50-3 architecture. This fully demonstrates KANs' advantage in significantly reducing computational complexity while maintaining prediction accuracy.

The main contributions of this research include: First, establishing a standardized watercolor mixing sample preparation and measurement protocol, ensuring data consistency and reproducibility. Second, applying KANs to watercolor mixing prediction for the first time, demonstrating its effectiveness in handling nonlinear problems such as pigment mixing.

CONCLUSION

Future research could extend to watercolor pigments from more brands, exploring the effects of different pigment characteristics on mixing results. Furthermore, additional influencing factors such as paper texture and brushstroke techniques could be incorporated to establish a more comprehensive watercolor mixing prediction system. Moreover, developing a user-friendly interface and integrating the prediction model into mobile applications or web-based tools would more directly serve art education and creative practice.

In summary, this study successfully validates the feasibility and superiority of KANs in watercolor mixing prediction, providing a new technical pathway for the development of digital art education tools. This contributes to lowering the barriers to watercolor learning, reducing material waste, and accelerating the process by which beginners master mixing techniques.

ACKNOWLEDGEMENTS

This study was funded by the National Science and Technology Council, Taiwan (NSTC 112-2221-E-011 - 080 -MY2).

REFERENCES

[1]. Alzubaidi, L., Zhang, J., Humaidi, A. J., Al-Dujaili, A., Duan, Y., Al-Shamma, O., Santamaría, J., Fadhel, M. A., Al-Amidie, M., & Farhan, L. (2021). Review of deep learning: concepts, CNN architectures, challenges, applications, future directions. Journal of Big Data, 8(1), 53. https://doi.org/10.1186/s40537-021-00444-8

[2]. Chen, M.-Y., Huang, Y.-B., Chang, S.-P., & Ouhyoung, M. (2019). Prediction model for semitransparent watercolor pigment mixtures using deep learning with a dataset of transmittance and reflectance. arXiv preprint arXiv:1904.00275.

[3]. Granata, F., Zhu, S., & Di Nunno, F. (2024). Advanced streamflow forecasting for Central European Rivers: the cutting-edge Kolmogorov-Arnold networks compared to Transformers. Journal of Hydrology, 645, 132175.

[4]. Kubelka, P. (1948). New contributions to the optics of intensely light-scattering materials. Part I. Journal of the Optical Society of America, 38(5), 448-457.

[5]. Kubelka, P., & Munk, F. (1931). An article on optics of paint layers. Z. Tech. Phys, 12(593-601), 259-274.

[6]. Liu, Z., Wang, Y., Vaidya, S., Ruehle, F., Halverson, J., Soljačić, M., Hou, T. Y., & Tegmark, M. (2024). Kan: Kolmogorov-arnold networks. arXiv preprint arXiv:2404.19756.

[7]. Moon, J., Yang, G., & Tae, H. (2023). A Study on DNN-Based Practical Model for Predicting Spot Color. Applied Sciences,13(24), 13100. https://www.mdpi.com/2076-3417/13/24/13100

Extracting Regional Colors from History: A Case Study on Tsukuba, Kasama, Tsuchiura, and Mito in Japan

Meiqing Xin[a*], Sari Yamamoto[b]

[a]Doctoral Program in Design, University of Tsukuba, JAPAN
[b]Institute of Art and Design, University of Tsukuba, JAPAN
[*] Meiqing XIN: s2230512@u.tsukuba.ac.jp, Sari YAMAMOTO: y-sari@geijutsu.tsukuba.ac.jp

ABSTRACT

This study clarifies a new methodology for extracting regional colors in modern cities based on historical documents. In rapidly developing Asian cities, the transformation of traditional streets into modern urban landscapes has become prevalent. To explore methods for extracting regional colors from modernized streets, Tsukuba City, Tsuchiura City, Kasama City, and Mito City in Ibaraki Prefecture in Japan were selected for the case study. Japan possesses both modern urban landscapes and historical and cultural backgrounds. Literature reviews and field surveys were conducted on these cities. Furthermore, historical documents were chronologically organized, and key events and their associated colors for each era were extracted. Moreover, key historical events and symbolic colors for each region were identified through comparative analyses, and consequently, regional colors were determined. In addition, color palettes were created for each case city. This study proposes a method for discovering and extracting regional colors that is guided by historical context. The findings indicate that when selecting colors that symbolize regional history in Japan, focusing on representative colors from the Edo and Meiji periods is appropriate. Additionally, three key elements are particularly important for extracting regional colors in modern cities: local building materials, cultural symbols, and the characteristics of the natural environment.

Keywords: extraction of historical colors, regional identity, methods for extracting regional colors, culturally symbolic colors, urban landscape and color planning

INTRODUCTION

Previous studies have used various methods to determine regional colors, such as architecture analysis [1], natural materials [2], and watercolor reproductions [3]. According to Lenclos' [4] theory, "All colors belong to a specific culture, identity, and history" [5], a perspective valuable in regional color studies. However, existing research lacks detailed discussions on extracting regional colors from historical contexts. Therefore, this study explores a color extraction method based on historical records to enhance our understanding of regional colors.

This study aims to develop a novel approach to identifying regional colors rooted in local history and culture, applicable even within the context of contemporary urban landscapes. Most previous studies have focused on historical cities and streetscapes in Europe [1,4,6,7], particularly in architectural and urban color research. European cities have preserved many historic buildings, whereas Asian cities have undergone rapid modernization, often leading to the loss of traditional streetscapes. This study provides a methodology for extracting regional colors in modern cities by analyzing historical urban development, organizing data into tables, and identifying representative elements and associated colors.

The study, which focuses on Tsukuba, Kasama, Tsuchiura, and Mito in Japan (Figure 1), organizes their historical timelines and key events into tables to identify representative objects, architecture, and cultural elements from different historical periods. The most significant symbolic objects in each city's

history were extracted by comparing the representative elements across different periods, and their colors were measured and analyzed. The extracted colors from the four cities were then compared to identify each city's representative symbolic color.

Figure 1: Target regions of the study

METHODOLOGY

This study aims to measure and analyze the colors of historically significant elements along historical timelines in order to propose a methodology for extracting regional colors in contemporary urban environments.

First, based on historical records and literature, the histories of Tsukuba, Kasama, Tsuchiura, and Mito were compiled, and key historical events, symbolic colors, and representative images were identified in chronological order. These elements were used to define the historical identity of each region.

Color measurements were then conducted on representative objects. Based on the tables compiled in the first step, objects symbolizing the historical identity of each city were selected, and their colors were measured using the Munsell Color System to determine Munsell Hue, Munsell Value, and Munsell Chroma (Hereafter abbreviated as Hue, Value, and Chroma). To ensure consistency and accuracy, measurements were taken only on clear days, three hours after sunrise and three hours before sunset. The results were recorded on standardized color record sheets (Figure 2).

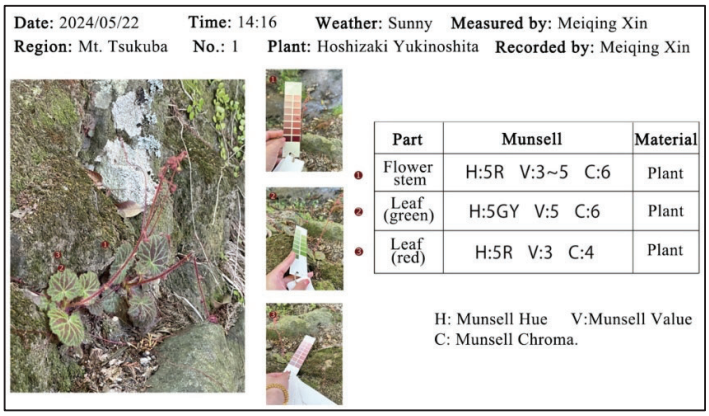

Figure 2: Color Record Sheets

Finally, symbolic colors were extracted through comparison. The measured colors were compiled and compared across the four cities. Elements shared among the regions were excluded to emphasize local distinctiveness, and the final symbolic colors for each city were determined.

RESULTS AND DISCUSSION

This study organizes historical events into chronological order (Table 1) and identifies representative elements that reflect the historical identity of each region (Table 2). The findings revealed that each city

possesses a unique historical and cultural identity, and that its symbolic objects reflect distinctive color characteristics (Table 4).

In Tsukuba City, Mount Tsukuba held spiritual and symbolic significance before the Edo period, and its natural color represented this era. During the Edo period, the area was known for its granite, gamma no abura (toad oil), and wooden clocks, which defined the symbolic colors of the time. In the Meiji period, the Tsukuba Shrine was restored, and the mountains and local granite gained nationwide popularity. The representative colors were those of Mount Tsukuba, Tsukuba Shrine, and granite. In the Taishō–Shōwa period, the development of Tsukuba Science City marked a shift toward modernization. Consequently, modern architectural colors became dominant, and no distinct local colors were identified.

In Kasama City, Buddhism flourished during the Kamakura period, and many Buddhist statues were dedicated. The representative colors included those of Buddhist statues and war-related imagery. Domain governance was established during the Edo period, and both the Kasama Inari Shrine and Kasama ceramics developed significantly. The representative colors are those of Kasama ware and the shrine. During the Meiji period, commerce expanded further, Inada granite gained national recognition, and Kasama entered international markets. Representative colors included those of Inari Shrine, Kasama ware, and Inada granite. In the Taishō–Shōwa period, while modernization advanced, regional identity diminished, and no distinctive symbolic color was identified.

In Tsuchiura City, before the Edo period, the region centered on temples and shōen estates. The representative colors of this period were those related to temples and warfare. During the Edo period, renovations of Tsuchiura Castle and the growth of the soy sauce industry were notable, with corresponding symbolic colors of the castle and soy sauce. From the Meiji to the Shōwa period, modernization progressed with the construction of commercial districts, but distinct local colors faded, leaving modern architecture as the representative, though not unique, color.

In Mito City, before the Edo period, development centered on shrines, temples, and the Naka River. The representative colors of this period were those connected to religious architecture and the Naka River. During the Edo period, Mito experienced cultural prosperity, as exemplified by the tribute of the first-catch salmon, the construction of Tōshōgū Shrine, and the development of Mitogaku. Education and commerce flourished, and representative colors included those of salmon, books and paper, the Naka River, Kōdōkan, and religious architecture. In the Meiji period, modernization progressed, and the compilation of the Dai Nihonshi was completed. Education remained a major focus, and the representative colors were those connected to books and paper. During the Taishō–Shōwa period, urban infrastructure, including the train station and city hall, was built. As in other cities, modern architectural colors became predominant.

Comparative analysis identified a set of symbolic elements reflecting each city's historical identity (Table 2). In Tsukuba, symbolic colors are derived from Mount Tsukuba, Tsukuba Shrine, gama no abura, and granite. In Kasama, the symbolic colors are those of Inada granite, Kasama ware, and Inari Shrine. Symbolic colors in Tsuchiura include the hues of Lake Kasumigaura, traditional soy sauce, and Tsuchiura Castle. In Mito, these include the hues of water, salmon, cotton and paper, Tōshōgū Shrine, historical books, and Kōdōkan.

During this study, the extracted representative elements were subjected to color measurement and classified into natural, social, and cultural environment colors (Table 3). Subsequently, a comparative analysis was conducted to determine the final set of symbolic colors (Table 4) through the elimination of duplications, encompassing cases in which either the representative elements themselves or their colors were identical. When representative elements of a region risked being entirely excluded due to such overlaps, the most extensively applied color was retained. This approach ensured a comprehensive representation of the region's historical and cultural characteristics. For instance, in the case of Tsukuba City, the Tsukubasan Shrine, an important symbol of local history and culture, produced colors that were identical to those of other elements. To preserve its representativeness, the shrine's most widely applied color, 7.5YR 2/4, was ultimately retained in this study. Each city's color palette demonstrates distinctive characteristics. Tsukuba displayed medium to low-Value, medium-Chroma R Hue and low-Chroma, high-Value Y Hue. Kasama exhibited high-Chroma, medium-Value R Hue along with low-Chroma, high-Value

Y Hue. Tsuchiura is characterized by medium-Chroma, medium-Value B Hue and low-Value, low-Chroma YR Hue. Mito showed high-Chroma and medium-Value for YR and PB Hue and low-Chroma and high-Value for 10YR Hue.

Table 1. Historical Events (Kasama City – Selected Examples)

Period	Key Events	Image	Symbolic Color
Pre-Nara ~710	Kasama Inari Shrine was founded in the year 651, etc.	Primitive Society Period Founding of Kasama Inari Shrine	Earthen colors. Colors of Inari Shrines
Nara 710 –794	Kasama Inari Shrine was formally incorporated into the Shikinaisha (State-Recognized Shrines) system	Expansion of shrines	Colors of Shinto shrines
Heian 794 – 1185	The governance structure shifted as local warlords solidified control over their territories.	The region was affected by various wars.	Earthen colors
Kamakura 1185–1333	Kasama Castle was constructed. A standing statue of Miroku Nyorai was donated to Ishidera, etc.	A range of standing Buddhist images were donated to temples and shrines.	Color of wood
Nanboku-chō (Northern and Southern Courts) 1336–1392	The conflict between the Northern and Southern Courts (Nanboku-chō) began, etc.	An era characterized by prolonged military conflict and political unrest.	Earthen colors
Muromachi 1336–1573	Kasama Tsunuhisa reconstructed Sansho Myōjin Shrine and donated banners of the Four Divine Beasts (Shishinki), etc.	Various standing Buddhist statues were donated.	Color of wood
Azuchi–Momoyama 1573–1603	Tamanyu Tadakatsu, a retainer of the Utsunomiya clan, assumed control of the Kasama region, etc.	To be affected by war	Earthen colors
Edo 1603–1868	Kasama Inari Shrine underwent ritual and structural enhancement, reflecting its rising religious prominence, etc.	The cult of Inari gained widespread popularity. The Kasama ceramic tradition flourished.	Colors of Inari Shrines Colors of Kasama Ware (Kasama-yaki)
Meiji 1868–1912	Inari worship became the predominant faith among the general populace. The temple town (monzenmachi) surrounding the shrine experienced substantial growth, etc.	Inari worship underwent significant expansion. The use of Inada stone became increasingly widespread. Kasama ware became increasingly recognized. Modern elements began to appear.	Color of Inada Stone. Colors of Kasama Ware. (Kasama-yaki) Colors of Inari Shrines
Taishō~Shōwa 1912–1989	Buses and trains began operating, Establishment of the Kasama city, etc.	Kasama city entered a modern society	Architectural color

Table 2: Historical Elements Representing Each Region

	Natural Elements	Social Elements	Cultural Elements
Tsukuba	Mt. Tsukuba	Tsukubasan Shrine Granite	Gama no Abura (toad oil)
Kasama	Inada granite	Inari Shrine	Kasama ware (traditional ceramics)
Tsuchiura	Lake Kasumigaura	Tsuchiura Castle	Shihō Shōyu (Shihō Soy Sauce)
Mito	Salmon Naka River	Kodōkan Tōshōgū Shrine	Cotton and Paper Dai Nihonshi (books)

Table 3: Colors of Historically Representative Objects

	Natural Environment Colors	Social Environment Colors	Cultural Environment Colors
Tsukuba	Mt.Tsukuba 5R 3/4* 5R 3/6* 5R 4/6* 5R 5/6* 5GY 5/6*	Tsukubasan Shrine 7.5YR 2/4* 7.5YR 4/4 10G 5/2 Granite 2.5Y 6/2* 2.5Y 7/2 2.5Y 8/2* 2.5Y 9/2*	Gama no Abura 5R 5/6*
Kasama	Inada Granite 5Y 9/1* 2.5Y 8/3*	Inari Shrine 5R 3/10* 7.5R 4/8* 7.5YR 2/4	Kasama ware 10YR 3/2 2.5YR 5/8*
Tsuchiura	Lake Kasumigaura 10B 3/4* 10B 5/6* 2.5PB 6/6*	Tsuchiura Castle 7.5YR 2/4 7.5YR 4/4 N4* N9	Shihō Shōyu 5YR 4/8* 5YR 1/1*
Mito	Salmon 10YR 3/2 10YR 9/2* 10YR 6/10* 2.5Y 8/6* Naka River 5PB 5/8*	Kodōkan 7.5YR 2/2* 2.5Y 9/1* Tōshōgū Shrine 10G 5/2 N1*	Cotton, Paper N9 2.5Y 9/1* Dai Nihonshi 2.5Y 9/1* 2.5Y 7/2 5PB 5/8*

Table 4: Symbolic Color

Tsukuba	5R 3/4	5R 3/6	5R 4/6	5R 5/6	7.5YR 2/4	2.5Y 6/2	2.5Y 8/2	2.5Y 9/2	5GY 5/6
Kasama	5R 3/10	7.5R 4/8	2.5YR 5/8	2.5Y 8/3	5Y 9/1				
Tsuchiura	5YR 4/8	5YR 1/1	10B 3/4	10B 5/6	2.5PB 6/6	N4			
Mito	7.5YR 2/2	10YR 9/2	10YR 6/10	2.5Y 8/6	2.5Y 9/1	5PB 5/8	N1		

The colors of Hoshizaki Yukinoshita, a plant unique to Mount Tsukuba, combined with granite, highlighting the city's natural environment and local building materials; colors of the Inari shrines, Inada stone, and Kasama ware, reflecting Kasama's traditions of faith and craftspersonship; the natural colors of Lake Kasumigaura and soy sauce, symbolizing Tsuchiura's natural resources and industrial characteristics; the combination of salmon colors and book pages, representing Mito's cultural heritage. To visually present these findings, a color palette was also created for each city, summarizing the extracted representative colors and their symbolic meanings.

Although some colors share similar hues, their combinations create distinct urban atmospheres, similar to how Paris and Turin, despite having beige-toned buildings, maintain unique identities through differences in the roof, window frame, and outdoor advertisement colors.

Furthermore, according to the study findings, local industries and cultural characteristics were primarily established in Japan during the Edo and Meiji periods. All four cities developed unique cultural identities during this period. Therefore, when selecting colors that symbolize regional history, focusing on the representative colors of these two periods is most appropriate.

This study proposes a historical method for extracting regional colors using the following steps. First, historical documents must be collected to analyze each city's development. Second, historical timelines

and key events must be recorded systematically. Third, representative elements from different historical periods, including architecture, crafts, and cultural symbols, must be extracted. Fourth, representative objects' colors and characteristics must be recorded. Finally, color data must be analyzed and compared to extract symbolic colors and construct a regional color system.

Additionally, when extracting regional colors in modernized cities, the following three core factors are crucial: (1) Local Materials (The colors of region-specific building materials often serve as symbolic local colors, such as the color of Inada stone in Kasama); (2) Cultural Symbols (The colors of culturally significant objects, such as shrine buildings and historical crafts, reflect the depth of regional traditions and cultural heritage); (3) Natural Environment (The unique colors of local flora, fauna, and landscapes often symbolize a region's historical, industrial, and cultural background).

CONCLUSION

This study demonstrates the effectiveness of a historically grounded method for extracting symbolic regional colors. By organizing historical events, identifying culturally significant objects, and measuring their colors, the research successfully extracted symbolic color palettes for Mito, Kasama, Tsuchiura, and Tsukuba in Japan. The findings highlight the Edo and Meiji periods as historically significant eras in which regional identity in Japanese cities was most strongly expressed. Local building materials, cultural symbols, and natural environments were shown to play a crucial role in shaping regional color characteristics and defining local identity.

The proposed method has broad applicability in contemporary urban design, city branding, and cultural heritage preservation. Future research could extend this approach to a wider geographical scope and explore practical strategies for incorporating regional colors into urban planning to strengthen local identity and cultural distinctiveness.

ACKNOWLEDGEMENTS

This work was supported by the Japan Science and Technology Agency (JST) under the Support for Pioneering Research Initiated by the Next Generation (SPRING) Program (Grant Number JPMJSP2124), and by the Japan Society for the Promotion of Science (JSPS) KAKENHI Grant-in-Aid for Challenging Research (Exploratory), Grant Number 23K17483.

REFERENCES

[1]. Sibillano, L. (2010). The colour space of Zurich: An exemplary research on colour, texture and light in urban space. Proceedings of the AIC 2011 – Interaction of Colour and Lighting in the Arts and Sciences Congress (pp. 7–10).
[2]. Süvari, A., Okuyucu, Ş. E., & Çoban, G. (2022). Color mapping of the building façades in the historical urban fabric: The Ayazini village civil architectural examples. Color Research & Application, 47(4), 966–979. https://doi.org/10.1002/col.22765
[3]. Cordero-Jahr, E., & Cerda-Brintrup, G. (2023). The chromatic atmosphere of Chilean Patagonia: The color of vastness. Color Research & Application, 48(5), 599–611. https://doi.org/10.1002/col.22855
[4]. Lenclos, J.-P., Lenclos, D., & El. (2004). Colors of the world: The geography of color. W. W. Norton & Company.
[5]. Mitsuboshi, M. (2014). Shikisai no kai: Sono shinri to rinri [The pleasure of color: Its psychology and ethics]. Tokyo: Ochanomizu Shobo.
[6]. Ollier, X. (2023). Color coordination project for the historic shipyard site of La Ciotat: A geopoetic approach to urban color design. Color Research & Application, 48(5), 433–444. https://doi.org/10.1002/col.22884
[7]. Pyykkö, S. (2023). Conceptualizing the chromatic experience of environment: Two case studies using the Color Walk method. Color Research & Application, 48(5), 585–598. https://doi.org/10.1002/col.22878

Preference and Emotional Responses to Planterior Design According to The Index of Greenness

SaetByul Kim[a], YounJin Lee[b*]

[a]PhD Candidate, Dept. of Design & Craft, Graduate School, Hongik University, Seoul, South Korea
[b]Professor, Dept. of Color Integrated Design, Graduate School of Industrial Arts, Hongik University, Seoul, South Korea

[*]Corresponding author: YounJin LEE, hacomama@hongik.ac.kr

ABSTRACT

This study investigated the optimal Index of Greenness for interior planterior design, which refers to interior design that incorporates plants into indoor spaces, by analyzing user's visual preferences and emotional responses at varying greenness levels. The "Index of Greenness" refers to the proportion of green plants within a fixed visual field and served as the primary variable for assessing visual and emotional impacts in indoor spaces. Using SketchUp and Enscape 3D software, six visual stimuli depicting office interiors with planterior designs were created, representing greenness levels of 0%, 10%, 20%, 30%, 40%, and 50%. The 0% greenness stimulus was excluded from evaluation and used as a neutral reference to minimize visual aftereffects. The remaining five stimuli, ranging from 10% to 50%, were randomly presented to 20 participants specializing in horticulture and floral design, who rated their preferences and emotional perceptions on a seven-point scale. Participants evaluated visual stimuli based on overall preference and 10 emotional adjectives. Results indicated that a 20% Index of Greenness had the highest preference, followed by 30% and 10%, suggesting moderate greenness enhances visual comfort and emotional satisfaction. In contrast, greenness levels above 40% lowered preference and increased negative perceptions, such as "stuffy". This suggests that increasing greenness beyond a certain threshold does not necessarily improve preference but may instead induce visual congestion and psychological discomfort. Positive descriptors such as "pleasant", "clean", and "lively" tend to increase with higher levels of greenness. Emotional response analysis indicated positive descriptors such as "pleasant", "clean", and "lively" increased with higher levels of greenness. Furthermore, multiple regression analysis identified "balanced", "stuffy", and "lively" as significant variables influencing preference, with "balanced" showing the strongest positive effect and "stuffy" negatively affecting preference. The findings highlight the importance of establishing appropriate greenness levels in planterior design through consideration of visual balance and emotional perceptions, rather than merely increasing the Index of Greenness. This study is expected to contribute to the development of quantitative design guidelines for interior planterior design based on the Index of Greenness.

Keywords: Index of Greenness, Planterior Design, Visual Preference, Emotional Response, Office Interiors

INTRODUCTION

In contemporary society, people spend most of their time indoors, and consequently, the demand for pleasant and healthy indoor environments has been steadily increasing. In particular, planterior design using plants has been widely applied due to its positive effects, such as providing psychological stability, emotional satisfaction, and enhanced spatial utilization [1]. However, previous studies have noted limitations in that an excessive number of plants or monotonous green images may cause spaces to feel stuffy and even lower user satisfaction [2].

Against this backdrop, the concept of the Index of Greenness has gained attention. Originally proposed in Japan, the Index of Greenness was designed to complement the limitations of traditional planar greening ratios. It quantifies the proportion of plant area perceived vertically within the human field of view, thereby more directly reflecting the level of greenery that people actually experience [3][4][5]. Moreover, the Index of Greenness plays a critical role not only in shaping users' psychological stability and comfort but also in influencing landscape preference and satisfaction [4][6].

Nevertheless, most existing research has focused on general discussions of how the Index of Greenness affects spatial perception, while quantitative analyses of user preference and emotional responses across different levels of Index of Greenness remain relatively insufficient. Therefore, this study aims to investigate office spaces under varying Index of Greenness conditions, evaluate visual preference and emotional imagery, and ultimately identify the optimal range most preferred by users.

METHODOLOGY

This study focused on open-plan office spaces where planterior elements are widely visible across the field of view. The Index of Greenness was defined as the proportion of plant area within the total image area, ranging from 0% to 50% in 10% increments [1]. A total of six visual stimuli were produced by modeling and rendering with SketchUp and Enscape 3D software, followed by final adjustments and area calculations using Photoshop (Figure 1).

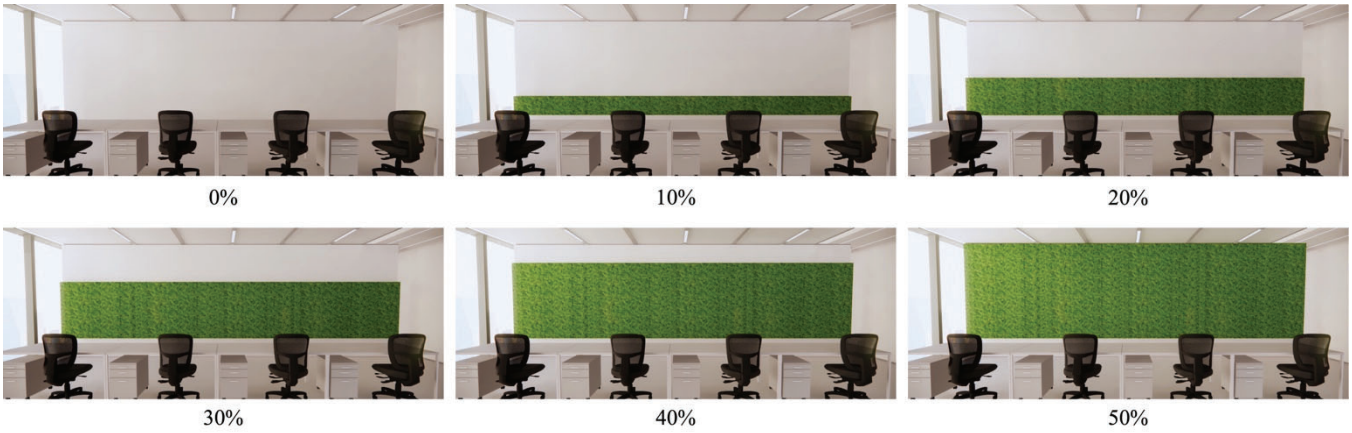

Figure 1: Visual Stimuli by Levels of Index of Greenness (0%, 10%, 20%, 30%, 40%, 50% from left to right, top to bottom)

The participants were 20 students majoring in horticultural and floral design. After excluding one invalid response, data from 19 participants were analyzed. The experiment was conducted from March 8 to 10, 2025, through an online survey (Google Form), with the stimuli presented in random order. To ensure evaluation stability, a 0% greenness stimulus was inserted between each condition to minimize afterimage effects.

Based on previous studies [7][8], a total of 10 emotional adjectives were selected for evaluation (Table 1). These adjectives were categorized into Evaluative (assessing overall satisfaction or dissatisfaction with the space) and Structural (reflecting harmony, balance, and naturalness). Participants assessed both visual preference and emotional imagery for each stimulus, and all items were rated on a 7-point scale.

Table 1: Classification of Emotional Adjectives

Category	Emotional Adjectives
Evaluative	refreshing, pleasant, lively, clean, stuffy, complex, artificial
Structural	balanced, harmonious, natural

RESULTS AND DISCUSSION

The analysis revealed that the Index of Greenness elicited the highest positive responses at moderate levels (20–30%), while negative evaluations became more pronounced at excessive levels (40% or higher). Specifically, the greatest preference was observed at 20%, followed by 30% and 10%. In contrast, preferences declined significantly at 40% and 50%, indicating that higher plant density may lead spaces to be perceived as stuffy or visually overwhelming.

A similar trend was observed in the evaluation of emotional imagery. Positive impressions such as pleasant, clean, and lively increased progressively with higher Index of Greenness, with the most prominent responses emerging in the 20–30% range. This suggests that an appropriate level of greenery imparts vitality and a well-organized impression to the space. Conversely, the perception of stuffy was minimal at lower levels but rose sharply above 40%, demonstrating that excessive greenery can create a closed and heavy atmosphere.

Regression analysis further indicated that the image of balanced exerted the strongest positive influence on preference, while lively acted as an additional reinforcing factor. In contrast, stuffy emerged as a major negative determinant of preference, indicating that excessive levels of the Index of Greenness can substantially diminish spatial satisfaction.

CONCLUSION

This study aimed to examine the effects of different levels of the Index of Greenness on visual preference and emotional evaluation in office planterior design, and to provide baseline data for design applications. Visual stimuli with greenness levels ranging from 0% to 50% were created, and participants majoring in horticultural and floral design evaluated both visual preference and emotional imagery.

The analysis showed that the most positive responses occurred at 20–30% greenness levels. Within this range, preference was highest, with strong evaluations of positive emotional adjectives such as "pleasant", "clean", and "lively". In contrast, when greenness exceeded 40%, preference declined and perceptions of "stuffy" increased, indicating that excessive planting can impose visual burden. Multiple regression analysis further revealed that "balanced" exerted the strongest positive influence on preference, with "lively" serving as an additional positive factor and "stuffy" as a major negative factor. These findings suggest that it is essential not only to secure greenness but also to maintain an appropriate level and visual balance in planterior design.

Unlike previous studies that mainly addressed the general psychological effects of greenness, this study is significant in that it quantitatively analyzed visual preference and emotional responses across varying levels of the Index of Greenness. Future research should incorporate variables such as space type, plant color and species, and arrangement methods to establish more comprehensive design guidelines.

REFERENCES

[1]. Yoo, M., & Lee, E.H. (2014). The impact of modulized interior landscape on office workers' psychological wellbeing: A pilot study focused on the office wall. Journal of the Korean Institute of Interior Design, 23(4), 220–230. https://doi.org/10.14774/jkiid.2014.23.4.220

[2]. Yang, C.W., & Kim, J.H. (2023). From the perspective of space design marketing: A study on the characteristics of complex commercial space planterior design. Journal of the Korea Institute of Spatial Design, 18(5), 325–336. https://doi.org/10.35216/kisd.2023.18.5.325

[3]. Cho, Y.H. (2006). The methods of promoting greenness and the target levels of greenness in streetscape suggested by computer simulation: The case of Seoul. Journal of the Korean Institute of Landscape Architecture, 34(2), 26–35.

[4]. Lee, S.H. (2007). The effects of the index of greenness simulation based on restorative environment model upon emotion improvement. Korean Journal of Health Psychology, 12(2), 439–465.

[5]. Choi, J.K., & Kim, J.Y. (2023). Evaluating visual perception responses for spatial image of greenness index using eye tracking. Journal of the Architectural Institute of Korea, 39(10), 63–74. https://doi.org/10.5659/JAIK.2023.39.10.63

[6]. Yoo, M. (2013). The impact of modulized interior landscape on office workers' psychological wellbeing (Doctoral dissertation, Seoul Women's University, Korea).

[7]. Ro, J.S., & Kim, Y.I. (1998). A study on the visual preference prediction of interiors. Journal of the Korean Institute of Landscape Architecture, 26(2), 269–282.

[8]. Lee, N.H., & Bang, K.J. (1996). The influence of the ratio of greenery on the visual preference in interior landscape. Journal of the Korean Institute of Landscape Architecture, 24(2), 13–24.

Research on The Evaluation of Children's Color Education Effect Based on Cognitive Development Theory

Qian Huang[1*], Anni Li[2], Shang Lan[3]

[1] School of Architecture and Planning, Hunan University
[2] Hunan university secai popularization of science base
[3] School of Architecture and Planning, Hunan University

ABSTRACT

At present, the evaluation system for children's color education in China is not perfect, and there is a gap with the international model that emphasizes process evaluation and interdisciplinary integration. This study is based on cognitive development theory and constructs an evaluation index system from three aspects: emotional development, cognitive development, and skill application. It evaluates the effectiveness of color education for children aged 6-12, provides theoretical support for children's color education, and offers improvement suggestions for practical teaching.

1. INTRODUCTION

1. Research background

The current Chinese children's color education is facing the problem of an imperfect evaluation system, which has led to a lack of systematic development of color art education for Chinese children. There are subjectivity and standard ambiguity issues in the evaluation of children's color education in China. The existing evaluations are mostly attached to art courses, focusing on painting techniques and lacking systematicity. The current methods mainly include grading and personalized comments, which are limited by adult aesthetic perspectives and do not fully reflect the stage specific characteristics of children's cognitive development. The foreign evaluation system emphasizes process evaluation and multiple standards, covering multiple dimensions such as color science, emotional expression, and cultural context, emphasizing practical application and individual differences.

2. The goal of children's color education

Color plays an important role in children's cognitive, emotional, and aesthetic development, and its educational goals cover three dimensions: knowledge, ability, and value.

The knowledge objective emphasizes the mastery of the basic principles and cultural connotations of color, including three stages: (1) understanding the basic color names and their attributes; (2) Understand the historical evolution and cultural symbolism of color; (3) Explore the life applications of color; The ability goal aims to enhance children's observation, creativity, and emotional regulation abilities through color education; The emotional development goal refers to the importance of color education in valuing emotional experiences, promoting positive emotional states, and establishing good interpersonal relationships.

2. THEORETICAL BASIS OF COGNITIVE DEVELOPMENT IN CHILDREN'S COLOR EDUCATION

Color directly affects children's emotional and cognitive development through neuropsychological pathways. Research shows that children are highly sensitive to color stimulation and can stimulate emotional expression and imagination through colors, forming the basis of artistic cognition [2]. Rudolf Steiner pointed out that the

psychological awakening effect of colors can promote children's self-reflection and emotional regulation, and enhance their self-awareness [3].

In cognitive construction, color, as a symbolic intermediary, has three functions: (1)A visual carrier for emotional expression; (2)A mirror tool for self-awareness;(3)A cognitive bridge for social understanding [4]. This multi-dimensional stimulation makes color education an effective way to cultivate children's metacognitive abilities.

V. Lowenfeld's cognitive development theory provides a phased framework for color education: The motor representation stage (7-9 years old) emphasizes operations such as doodling and color mixing, promoting the coordinated development of perception and motor nerves; During the image-based representation stage (aged 9-11), it is necessary to establish psychological images of colors and emotions and strengthen the emotion-memory encoding. The symbolic representation stage (aged 11-13) focuses on the mastery of the color culture coding system, achieving a leap from emotion to social cognition [2].

3. CONSTRUCTION OF TEACHING EVALUATION FOR CHILDREN'S COLOR EDUCATION

3.1 Principles for the Construction of the Evaluation System

Scientific and systematic teaching evaluation is the key to optimizing children's color education. Based on the theory of cognitive development, the evaluation system should follow the three major principles of scientificity, comprehensiveness and operability to ensure that the assessment results are objective, multi-dimensional and easy to implement, thereby effectively guiding teaching practice.

The principle of scientificity requires that the evaluation system be based on solid theoretical grounds and adopt multiple methods to ensure objectivity. Evaluation should set clear goals and standards, and establish a feedback mechanism to optimize teaching. In addition, educators need to continuously update their professional knowledge to ensure the scientific nature and timeliness of the evaluation tools.

The principle of comprehensiveness emphasizes multi-dimensional assessment, covering cognitive, skill, emotional and creative performance. It is necessary to take into account individual differences and combine self-evaluation with external evaluation to comprehensively reflect children's development.

The principle of operability requires that the evaluation system be concise and efficient, and adapt to the current teaching conditions. Clear indicators should be set, easy-to-operate tools should be adopted, and the process should be optimized to reduce teaching interference. Educators should enhance their ability to implement evaluations through training to ensure the synergy between evaluations and teaching.

3.2 Dimensions Associated with Children's Color Education Evaluation

The cognitive dimension is the core indicator for evaluating children's understanding, mastery and application of color knowledge, and it plays an important role in promoting children's cognitive development and aesthetic literacy [5]. This dimension encompasses the abilities of identifying the three attributes of color, color naming, and color emotional expression, emphasizing that children can understand the meaning of the environment and enhance their cognition of social norms through color learning [6]. Teachers need to pay attention to the multi-cognitive performance, combine classroom observation to record children's participation and creativity, and implement personalized guidance to optimize teaching effectiveness.

Emotional dimension evaluates children's emotional attitude and experience towards color, including interest, expression, preference and aesthetic ability development. Studies have shown that color can help children recognize emotions and promote happiness and mental health [5]. With the rapid development of emotional cognition of children aged 6-7, teachers need to guide them to establish the connection between color and emotion, so as to lay the foundation for aesthetic development [3] [9] [10].

A total of 64 valid questionnaires (N = 64, 11 students in the third grade and 53 students in the fourth grade) were collected in a color education survey project in five rural primary schools in China in 2025. The questionnaire

covers the dimensions of color preference, emotional expression and learning willingness, which provides empirical support for the evaluation of emotional dimensions. Based on the questionnaire data, this study systematically evaluated the emotional effects of children's color education from three dimensions: color interest, emotional expression and self-evaluation. In terms of color interest, 60.9% children are keen on color activities, 84.8% agree with the aesthetic feeling of natural scenery color, and 76.1% are willing to continue learning, which reflects the positive influence of environmental color on aesthetic perception. In the dimension of emotional expression, 65.2% agree that color can express emotions, 72.8% feel happy in team creation, and 73.9% tend to use color to record life, reflecting the initial emotion-color connection; In terms of self-evaluation, 67.4% actively tried color matching, but only 43.5% could list three traditional colors (insufficient traditional cultural education); 60.9% think the work is creative, 58.7% are willing to share what they have learned, showing good self-efficacy. These findings echo the existing research, confirm the positive role of color education in promoting children's emotional development and aesthetic ability, and also provide empirical basis for optimizing teaching design. It is suggested that on the basis of maintaining the existing teaching effect, we should strengthen the infiltration education of traditional color culture.

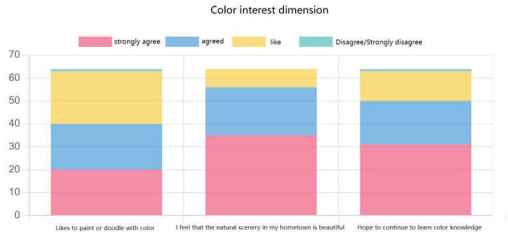

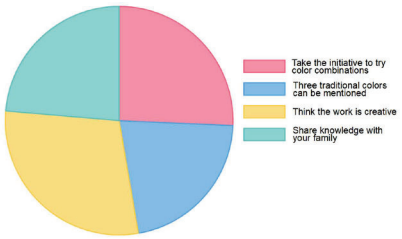

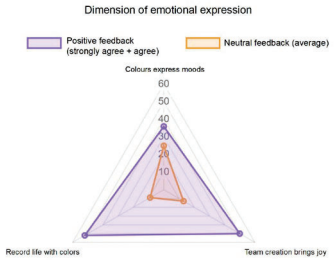

Figure 1 Evaluation of Children's Color Education Interest Dimensions

Figure 2 Self evaluation Dimension Evaluation of Children's Color Education

Figure 3 Evaluation of Emotional Expression Dimensions in Children's Color Education

The skill dimension evaluates children's color use and painting ability, including color matching, mixed color matching, expressiveness, creative practice and completion of works. The use of color examines the mastery of lines, shapes and spatial layout; Mixed color toning and expressiveness focuses on the understanding of color mixing changes; Creative practice measures innovation and problem-solving ability; Completion evaluates detail handling and overall harmony. With the increase of age, children gradually develop from recognizing the natural attributes of color to understanding the relationship of contrast and coordination, and can express it in combination with social content [11].

Innovation dimension is the key to cultivate children's creative thinking, covering color creativity, imagination, experimental exploration, uniqueness of works and problem solving ability. Creativity and imagination examine the ability of scene construction; Problem solving and creative thinking assesses multi-angle associative ability. We can learn from Steiner's art education model and systematically cultivate creativity through free expression and color experience [12].

The process dimension evaluates children's learning attitudes and behavioral performance, including classroom participation, cooperation ability, self-regulation, and reflection ability. Participation focuses on attention and interest; Collaborative ability assessment of peer collaboration; Self regulation and reflection involve emotional management and strategic adjustment. Traditional evaluations are singular, while modern concepts emphasize diverse interactions. For example, Jiang Chengfei (2013) combined MEFOT coloring activities, self-evaluation, and parental feedback to construct a multidimensional system. Jin Zhiyan (2003) enhanced children's interest and participation through practices such as natural object coloring and museum inspections.

3.3 Evaluation Methods for Children's Color Education Teaching

Based on Piaget's cognitive development theory framework, this section systematically constructs a multidimensional dynamic evaluation system, integrating observation method, work analysis method, questionnaire method, interview method, and comprehensive evaluation method to form a methodological matrix that synergizes process and outcome evaluation. The implementation of each method follows the principle of developmental suitability, taking into account the characteristics of children's cognitive stages and the aesthetic creativity of color education.

Observation method is an important method for evaluating children's color learning process. It is a systematic observation that runs through the entire teaching process, focusing on color preferences, combination logic, and emotional expression, combined with quantitative analysis of behavior frequency. It is necessary to deeply analyze student performance based on educational theory, go beyond surface records, and promote teacher professional development.

By systematically analyzing children's color creation works, quantitatively evaluating the color coordination, expressiveness, and cultural connotations of paintings and other works, and combining Piaget's theory of cognitive development stages to explain individual differences, reflecting the level of children's color perception and creativity development.

The questionnaire design should have a concise number of questions, clear expression, avoid privacy issues, and optimize the survey environment. Referring to Huang Renshu's self-evaluation questionnaire, emphasizing the role of teachers in guidance; Gu Yinglan evaluated the effectiveness of traditional art appreciation courses through 15 questionnaires.

The interview method has unique value in the evaluation of children's color education. Through open interaction, it explores children's color cognitive logic, emotional motivation, and teaching barriers, supplementing the lack of quantitative data. The core value lies in revealing psychological mechanisms and teaching adjustment needs, while taking into account the analysis of the impact of family environment.

The comprehensive evaluation method integrates quantitative (questionnaire, work rating) and qualitative data (observation, interview, work interpretation) to construct a multidimensional evaluation system, balancing objectivity and dynamic development analysis, and providing a basis for teaching optimization.

4. CONCLUSION

This study constructs a three-dimensional evaluation index system for children's color education based on cognitive development theory, covering cognitive development, skill application, and emotional development. The evaluation results can provide scientific basis for adjusting teaching strategies, helping students understand learning outcomes, and optimize the learning process. At present, there are still certain limitations in research. In the future, interdisciplinary methods such as artificial intelligence can be used to develop more accurate dynamic evaluation tools, and comparative analysis of cross-cultural samples can be strengthened to promote the comprehensive development of children's color literacy.

REFERENCES

[1] 김지연.한국전통색채의유아교육활동구안.중앙대학교, 2003:71-73.

[2] 최승완.색채학습을통통한아동의미적발달에관한연구——초등미술교육프로그램중심으로.단국대학교, 2006：9.

[3] 이경연.색채교육을통한아동의창의성신장에관한연구.한양대학교, 2010：6.

[4] 이정아.컬러리터러시학습모형에관한연구——대학색채교육의 교과내용을

중심으로.홍익대학교, 2011：2.

[5] Jiang Zhixin Research on Product Design of Color Cognition Education for Preschool Children [D]. East China Normal University, 2023: 27.

[6] Korean Institute of Color Education Children's Color Education [M]. Beijing: Electronic Industry Press, 2009: 8.

[7] Jiang zhixin research on product design of color cognition education for preschool children [d]. East China Normal University, 2023: 27

[8] 이경연.색채교육을통한아동의창의성신장에관한연구.한양대학교, 2010：8.

[9] Korean Institute of Color Education Children's Color Education [M]. Beijing: Electronic Industry Press, 2009: 16-17.

[10] 오현진.창의적아동미술교육에관한연구.세종대학교,55.

[11] Korean Institute of Color Education Children's Color Education [M]. Beijing: Electronic Industry Press, 2009: 18.

[12] 고현주.유아색채교육프로그램이창의성과자기조절능력향상에미치는효과.목포대학교,2016：39.

[13] Korean Institute of Color Education Children's Color Education [M]. Beijing: Electronic Industry Press, 2009: 18.

[14] 강성비.MeFOT기반색채활동이유아의일상적스트레스에미치는효과.동아대학교,2013:50.

[15] 김지연.한국전통색채의유아교육활동구안.중앙대학교, 2003:71-73.

[16] 놀이와관찰을통한효율적색채지도방안에관한구——
초등학교저학년을중심으로.한국교원대학교, 2001：51-52.

[17] 구영란.전통미술의통합적감상을위한프로그램개발연구.중앙대학교, 2004：73.

A Proposal for A Unified Design for Store Signs in Shopping Streets and Its Effects

Nagisa Kishimoto[a*], Shushi Doi[a], and Hideki Sakai[a]

[a]Graduate School of Human Life and Ecology, Osaka Metropolitan University, Osaka, Japan
[*]Corresponding author: Kishimoto, kishimoto.n.106@gmail.com

ABSTRACT

This study focuses on revitalizing a traditional shopping street in Kyoto, Japan, through improved sign design. As many such streets face decline due to competition from large shopping malls and e-commerce, effective store signs can play a key role in attracting foot traffic and sustaining community life. The research targeted a 400-meter-long shopping street with about 30 stores, aiming to create signs that both represent each store's unique offerings and contribute to a cohesive visual identity. Fieldwork was conducted to identify the characteristics of each store and test different sign designs. Three sign size variations were created, and visual clarity was assessed under real-world conditions. Store managers were surveyed for feedback on the designs, desired elements, and store classifications. Most participants approved of the proposed signs, while a few requested revisions, which were accommodated. Stores were grouped into four categories - food service, groceries, retail, and services - with each assigned a distinct color. Colors were selected from traditional Japanese palettes and carefully tested using the Color Simulator app to ensure visibility and differentiation across various types of color vision. The final color choices were tsutsuji (azalea) for food service, kōji (citrus) for groceries, turquoise green for retail, and kikyo (bellflower) for services.

Keywords: shop sign, color coding, shopping street revitalization

INTRODUCTION

Stores put up signs to let people walking by know what type of store it is, and these signs are important for attracting customers. Generally, the signs need to be eye-catching and easy to notice. However, in a shopping district with multiple stores, each store is both a competitor and a community. Therefore, many shopping streets adopt a unified design for their signage. This study attempted to make the shopping district more attractive and revitalize it by proposing a signage design that expresses the characteristics of individual stores and provides a sense of unity.

In recent years, traditional shopping streets composed of small independent retailers have been in decline. This trend is largely due to the rise of large-scale shopping malls and the rapid expansion of e-commerce. However, Jane Jacobs, an American urban theorist, once made an important observation. She argued that human activity on the streets contributes to the maintenance of public safety. Clusters of shops attract people and, in turn, generate "eyes on the street" [1]. In order to sustain community life, the revitalization of shopping streets located near residential areas is therefore essential. This study aims to support such revitalization through the design of shop signage.

The term sign refers to a general category of graphic design intended for information transmission, encompassing a wide variety of forms depending on use and purpose. Signs can be classified into categories such as logos, pictograms, icons, symbol marks, and emblems. A logo represents a proper noun in a distinctive typeface

and, by itself, does not readily convey the nature of a business. A pictogram is a symbol that visualizes an abstract concept, while an icon is a graphic representation designed to enable intuitive understanding of an operation or function. Symbol marks and emblems, on the other hand, serve as symbolic expressions of an organization's philosophy or ideology.

For first-time visitors to a shopping street, signage is required to immediately convey the type of store and what it offers, stimulate interest, and guide them toward entry. From this perspective, signs displaying only the store name or logo are considered insufficient. While existing signage often contains names or logos. For newcomers walking through the street, this information alone is insufficient. It is difficult for them to discern what kind of goods or services a store provides. If pedestrians cannot easily recognize the type of store, they are less likely to feel inclined to enter. Therefore, it is essential to propose forms of signage that allow people to intuitively understand what the store offers. Ideally, displaying actual products outside the store would enable instant recognition. However, this is not always feasible due to legal restrictions or spatial constraints. In such cases, illustrated signage representing the products or services can serve as a substitute.

This study focuses on icon-like designs that effectively convey store information intuitively. This research focuses on an existing shopping street in Kyoto, Japan. It employs fieldwork to identify current issues. Ultimately, it proposes signage designs that can enhance visitor attraction.

METHODOLOGY

Target Shopping Street

The study focuses on a shopping street located in Kyoto Prefecture, Japan (Figure 1). The street extends approximately 400 meters from north to south and consists of about 30 stores. It features a one-sided arcade structure integrated with a housing complex. Each store has a frontage of about 5.7 meters and a height of about 3.6 meters. As shown in Figure 1, Horikawa Shopping Street extends longitudinally from north to south. The streetscape is uniform, with little variation along its length. At present, only signs displaying store names are installed. From the pedestrian's perspective, it is therefore difficult to identify the locations and types of shops. To address this problem, the street was selected as the case study for this research.

Figure 1: Map and photographs of the shopping street

Sign Design

The design direction of the signs was conceived by the lead author and finalized in collaboration with several co-authors. Each sign featured simplified illustrations representing the products or services offered by the respective store. For example, Figure 2 show the signs for a manju café (depicting a manju, a teapot, and a teacup) and for the Kyoto studio of an internet radio broadcasting station (illustrations of a microphone and a DJ).

The illustrated signs were printed in three different sizes and tested in the field for visibility. The dimensions were as follows: a standard version with a width of 400 mm, a height of 520 mm, and illustrations with a diameter of 380 mm; a version with larger illustrations, 470 mm wide, 560 mm high, with a 450 mm diameter for the illustrations; and a vertically elongated version, 400 mm wide, 700 mm high, with illustrations of 380 mm in diameter (Figure 3).

Figure 2: Examples of signs, (Left) Manjū Café and (Right) Radio Broadcasting Station

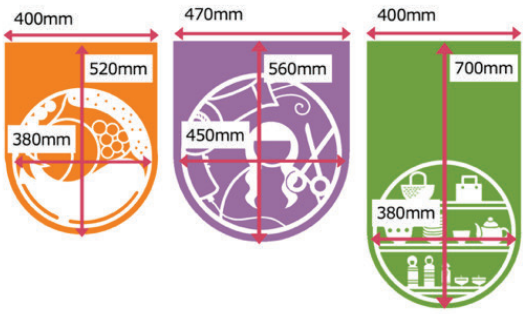

Figure 3: Prototype signs

Questionnaire

A questionnaire survey was conducted with the managers of each store in the shopping street. They were presented with the proposed sign designs and the store category classifications. The questionnaire consisted of four main sections: (1) basic information (store name), (2) evaluation of the store's own sign (multiple-choice format), (3) elements or keywords they wished to incorporate into the design (open-ended), and (4) classification of the store type (multiple-choice format). Representative questions included items such as "How do you feel about the design of your store's sign?" and "Please specify any elements you would like to incorporate into the sign design" based on the existing prototypes. Using the responses from this survey, the sign designs were revised as necessary and finalized with the consent of the store managers.

Color Coding of Categories

All stores in the shopping street were classified into four categories: food service, groceries, retail, and services. To facilitate easy recognition of each store, the signs were color-coded according to these categories. The category colors were selected with reference to DIC colors. Three aspects were considered: color image, cultural associations,

and distinguishability. Warm colors were assigned to food service and groceries, while cool or neutral colors were used for retail and services. Colors were chosen from traditional Japanese colors that suit the atmosphere of the shopping street in Kyoto. White was used as the base color, and illustrations were drawn in the category colors. The colors were selected to have a sufficient contrast with the background and to ensure high distinguishability in accordance with color universal design principles.

In selecting the colors, the CUD Recommended Color Sets (2nd edition, July 2018) were consulted [2]. However, the available examples of color combinations that could be distinguished by people with diverse color vision were limited. Therefore, they could not be directly applied. Combinations of four, five, or six colors were provided. However, most included yellow or light colors. These colors are difficult to distinguish from a white background. Furthermore, it is challenging to differentiate between warm colors; therefore, combining orange, red, and pink in a single palette was not feasible. As a result, no recommended combinations were suitable for including more than one warm color. Based on these considerations, the CUD Recommended Color Sets were not used. Instead, the app Color Simulator [3] was employed in a trial-and-error process. Various color combinations were repeatedly simulated. Their visibility was checked to ensure they could be distinguished by people with diverse types of color vision.

RESULTS AND DISCUSSION

Selection of Sign Designs

Field observations revealed the following findings. First, longer signs, which are closer to pedestrians' line of sight, are more noticeable. Second, thin lines in illustrations make the images difficult to discern. Third, purple appears dark and less visible under the dim arcade lighting. Based on these findings, the signs were adjusted and improved, resulting in the final design proposals.

Questionnaire Results

A questionnaire survey was conducted with the managers of each store regarding the final sign designs developed and the store category classifications. Among the 13 stores that responded, 10 indicated that "the sign design is acceptable as is," while 3 suggested that "the sign design should be modified." Regarding the category classification of stores, 12 stores agreed that the current classification was appropriate. Overall, the proposed designs received general approval from the store managers. For the stores requesting modifications, interviews were conducted and adjustments will be made as necessary.

Validity of Category Color Coding

Colors were selected from traditional Japanese color palettes. This made it possible to create a surprisingly large number of combinations. These combinations could be clearly distinguished by people with various types of color vision. As a result, the following colors were chosen for each category: food service – tsutsuji (azalea) color, groceries – kōji (citrus) color, retail – turquoise green, and services – kikyo (bellflower) color (Figure 4). To ensure that each color could be distinguished by individuals with different types of color vision, the app Color Simulator was used. It confirmed that the category colors were distinguishable not only for individuals with normal color vision (C), but also for those with protanopia (P), deuteranopia (D), and tritanopia (T) (Figure 5).

CONCLUSION

In this study, we adjusted the dimensions, design, color coding, illustrations, etc. of the signs. In the future, we will work with the operators of shopping districts to install the signs in actual shopping districts. The effectiveness of the design will be verified through evaluations from visitors.

Figure 4: Signs color-coded according to the four categories (top left: food service; bottom left: groceries; top right: services; bottom right: retail)

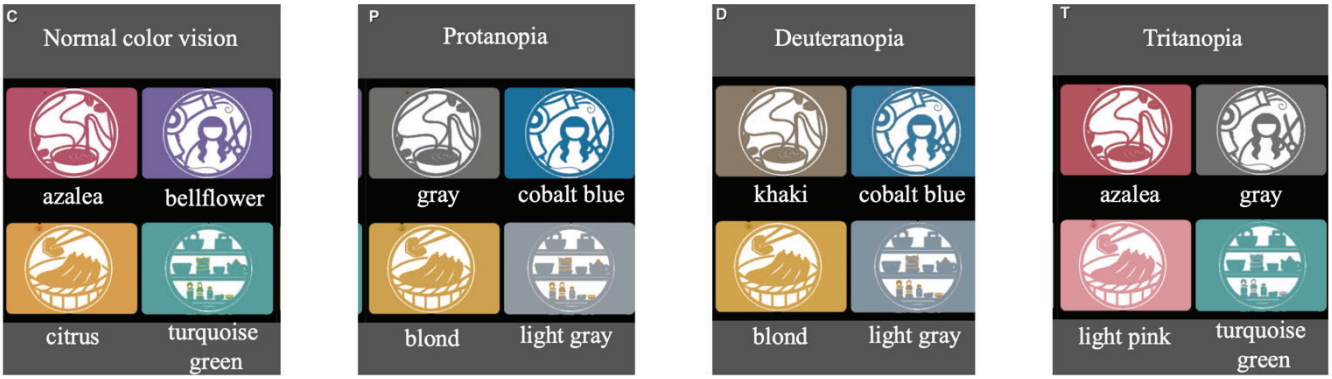

Figure 5: Simulation results showing the color-coded signs from Figure 4 as perceived by individuals with various types of color vision

REFERENCES

[1]. Jacobs, J. (1961) The Death and Life of Great American Cities, New York: Random House, "The Uses of Sidewalks: Safety," 29-54.

[2]. Color Universal Design Recommended Color Set Production Committee (2018) Color Universal Design Recommended Color Set Guidebook, 2nd ed. Tokyo

[3]. Asada, K. (2010) "Iro no Simulator". Version 2.43. Mobile application. iOS, Android. Available via App Store, Google Play.

The Color of Sour and Salty Tastes

Thachapong Ngamsaard[a], Jitlada Longbutsri[a], and Uravis Tangkijviwat[b]

[a]Faculty of Mass Communication Technology, RMUTT, Pathum-Thani, Thailand
[b]Color Research Center, RMUTT, Pathum-Thani, Thailand
*Corresponding author: uravis_t@rmutt.ac.th

ABSTRACT

The interaction between taste and color is a fundamental aspect of human perception, influencing how individuals experience and interpret food. Previous studies showed color can shape taste expectations, affecting taste intensity, sweetness perception, and overall food preference. The relationship between taste and color plays a critical role in food packaging design, as visual cues can significantly impact consumer choices. Packaging color influences how consumers anticipate a product's taste before tasting it, thereby shaping their purchasing decisions. This study aims to investigate the correlation between color and taste, especially sour and salty taste. In the experiment, one hundred and forty-four chromatic color chips varying in hue, chroma, and lightness levels and six achromatic color chips were presented on iPad display as stimuli. One hundred participants were asked to evaluate their sour and salty perception on each color chip. As expected experimental results, a correlation among tastes and color attributes will be explored. An effect of hue, chroma, and lightness on sour and salty tastes will be also analyzed. The findings of this study can be applied for the food and beverage industry, particularly in product development, packaging design, and marketing communication, to enhance the effectiveness of conveying taste through color and to create positive consumer experiences. Additionally, these insights offer valuable guidance for the development of new products that align with cultural contexts and meet consumer expectations in various regions.

Keywords: color and taste, sour color, salty color

INTRODUCTION

Taste perception is one of the primary human senses that significantly influences both food preferences and consumption choices. However, the actual experience of taste does not rely solely on gustatory perception through the taste buds, but rather emerges from the integration of multiple sensory modalities, including vision, olfaction, touch, and even audition [1]. Among these, vision—particularly color—plays a crucial role, as humans often use color as a predictive cue to infer the taste and quality of food before actual tasting occurs [2,3,4]. Consequently, taste expectations are strongly associated with color [5,6]. For instance, sweetness is commonly linked to red and pink hues due to their association with fruits and confectionery, whereas saltiness is connected with blue and yellow, reflecting associations with the ocean and fried potatoes. Similarly, sourness is often related to green and yellow, owing to their association with apples and lemons.

Although numerous studies have confirmed that color can shape taste expectations [1,2], research specifically focusing on sour and salty tastes remains relatively limited, and the findings are sometimes inconsistent. Some studies suggest that green and yellow are typically associated with sourness because of their connection to citrus fruits [7,8], while white, gray, and blue are more frequently linked to saltiness, potentially due to their association with salt or seafood [1,9]. Moreover, previous research has indicated that the relationship between color and taste may vary across cultures and individual consumer experiences [5,10]; however, comprehensive comparative evidence is still lacking.

Therefore, the present study aims to investigate the relationship between color and taste, focusing spe cifically on sourness and saltiness—two taste modalities for which empirical evidence remains inconclusi ve. This study employed the HSL (Hue, Saturation, Lightness) color system to generate one hundred color

samples covering a wide spectrum, thereby providing a robust reference for future research on the use of diverse colors in food packaging design. To this end, a randomized color-order test was developed to exam ine the effects of adjacent color presentation on participants' taste perception.

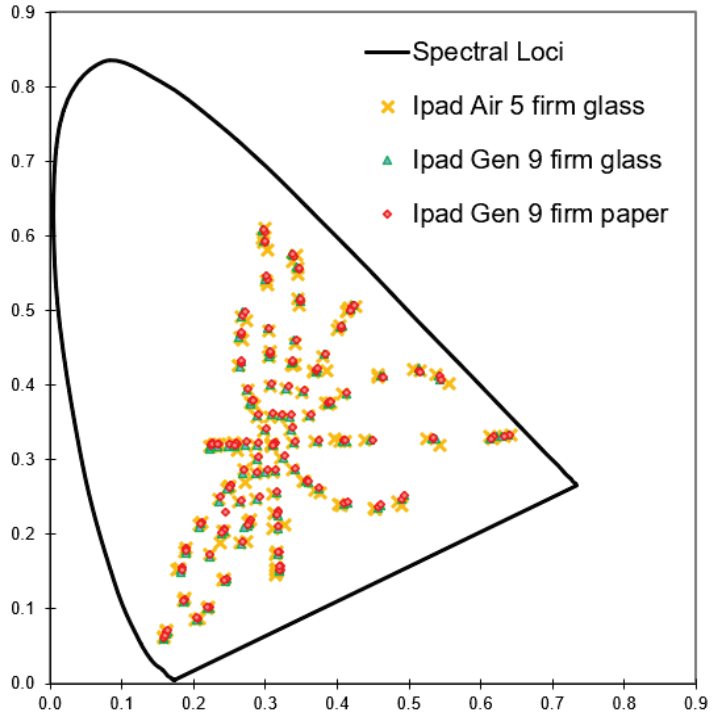

Figure 1. Color gamut of the test displays used in the experiment, comprising three devices: iPad Air 5 (yellow) with glass screen protector, iPad Gen 9 (green) with glass screen protector, and iPad Gen 9 (red) with paper-like screen protector.

METHODOLOGY

Participants

The study included 100 Thai participants, comprising 52 males and 48 females, aged 19–24 years (M = 20.92, SD = 1.28). All participants were screened to ensure normal color vision and normal or corrected-to-normal visual acuity.

Test stimuli

The experiment employed 144 chromatic color samples based on the HSL (Hue, Saturation, Lightness) color system. The hue dimension included 12 levels, varying at 30-degree intervals across the 360-degree color wheel. Saturation was manipulated across 4 levels (25%, 50%, 75%, and 100%), while lightness was varied across 3 levels (25%, 50%, and 75%). In addition, 6 achromatic colors were included, varying in lightness at six levels (0%, 20%, 40%, 60%, 80%, and 100%).

A total of 150 color stimuli were displayed on calibrated iPad screens, each adjusted to ensure comparable color gamuts. Each stimulus subtended 1.27° of visual angle, and the chromaticity coordinates (xy) are presented in Figure 1.

The 150 color stimuli were arranged in two configurations: ordinal color and random color (Figure 2). In the ordinal color arrangement, colors were organized along two axes: horizontally (from left to right), hues varied across 12 levels at 30° intervals on the 360° color wheel; vertically (from top to bottom), saturation increased while lightness decreased. In the four bottom cells, complementary positions were assigned to avoid excessive contrast between adjacent colors. In the random color arrangement, the same set of color stimuli was presented, but the spatial positions were randomized.

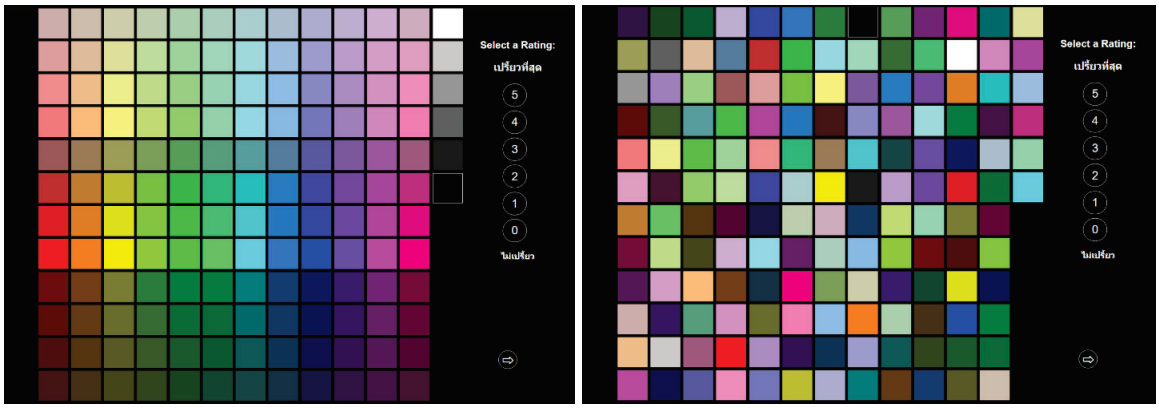

Figure 2. Example of color stimuli: ordinal color (left) and random color (right).

Experimental conditions

As illustrated in Figure 3, the iPad screen was positioned at an angle of approximately 60 degrees, with a viewing distance of about 45 cm. All tasks were performed using an Apple Pencil. The experiment was not restricted to a laboratory setting; however, the ambient illumination was maintained at 300–550 lx, with a correlated color temperature ranging from 5000 to 5500 K.

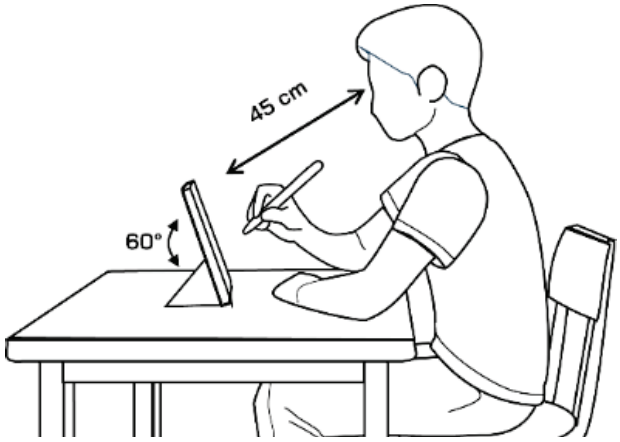

Figure 3. Experimental condition setup.

Experimental procedure

Prior to the experiment, each participant received a detailed explanation of the study and provided written informed consent for voluntary participation, Participants were also asked to provide demographic information, including gender, age, and place of residence. Subsequently, all participants completed the Ishihara Color Vision Test to screen for color vision deficiencies.

Afterward, participants received training on the experimental procedures, including the recording of taste perceptual scores and the sequential steps of the tasks, until all uncertainties were resolved. Once the training was completed, participants were randomly assigned to one of two taste conditions: sour or salty. Once a taste was assigned, the color-ordering task was first presented on the iPad screen. Participants were asked to rate their taste perceived association with the assigned taste by selecting a taste perceptual score for each color sample, ranging from 0 (no perception of that taste) to 5 (strongest perception of that taste).

Upon completion of the color-ordering task, participants proceeded to the randomized-color task under the same taste condition. After finishing both tasks, the procedure was repeated for the remaining taste. Data collection for each participant was considered complete once both taste conditions had been tested.

RESULTS AND DISCUSSION

As shown in Figure 4(a), in the color-ordering condition, sourness was most strongly associated with the color at position D8, corresponding to yellow (H = 90, S = 100, L = 50), with a mean taste perceptual score of 4.51 (SD = 1.155). The next highest taste perceptual score were observed for green at position E8 (H = 120, S = 100, L = 50; M = 4.45, SD = 1.205) and green at position E7 (H = 120, S = 75, L = 50; M = 4.41, SD = 1.023). In the randomized-color condition (Figure 4b), the highest taste perceptual score was obtained for green at position E8 (H = 120, S = 100, L = 50; M = 4.57, SD = 1.153), followed by green at position E7 (H = 120, S = 75, L = 50; M = 4.45, SD = 1.301) and yellow at position D8 (H = 90, S = 100, L = 50; M = 4.33, SD = 1.492). These results suggest that participants consistently rated yellow and green as strongly associated with sourness, though the perceptual strength of yellow decreased in the randomized-color condition, likely due to the influence of surrounding colors.

For saltiness, in the color-ordering condition (Figure 4c), the highest taste perceptual score was observed for brown at position B11 (H = 30, S = 50, L = 25; M = 3.06, SD = 2.145), followed by brown at position B12 (H = 30, S = 25, L = 25; M = 3.05, SD = 2.004) and brown at position B10 (H = 30, S = 75, L = 25; M = 3.04, SD = 2.010). In the randomized-color condition (Figure 4d), the highest taste perceptual score shifted to brown at position A12 (H = 0, S = 25, L = 25; M = 3.61, SD = 2.170), followed by brown at position B11 (H = 30, S = 50, L = 25; M = 3.37, SD = 2.179) and brown at position B10 (H = 30, S = 75, L = 25; M = 3.18, SD = 2.068). Overall, the majority of responses were concentrated on darker hues, with brown emerging as the most salient association for saltiness. Notably, the taste perceptual score for A12 increased in the randomized-color condition, which could be attributed to the influence of surrounding colors, potentially leading participants to associate this hue with fish sauce, a common salty condiment in Thai cuisine.

Follow-up questions revealed that participants often associated sourness with familiar fruits, such as lemon and lime, whereas saltiness was connected to foods and objects related to salty tastes, such as fermented fish, salt, and seawater. Moreover, the randomized condition highlighted the influence of adjacent colors: colors surrounded by highly rated hues tended to receive higher taste perceptual score, while those next to lower-rated hues received lower taste perceptual score. This finding demonstrates that the arrangement of color presentation affects taste-related evaluations.

The results of this study indicate that sourness was most strongly associated with yellow and green hues, while saltiness was linked to orange and brown hues. These findings are consistent with previous research. For example, Velasco et al. [5] demonstrated that American participants exhibited clear crossmodal associations between taste and color. Their results showed that saltiness was associated with blue and yellow, as these resemble the ocean and fried potatoes, whereas sourness was related to green and yellow, reflecting their association with apples and lemons.

When comparing the present findings with those of Velasco et al., it was observed that green was the most dominant hue associated with sourness among Thai participants, followed by yellow. This pattern is broadly consistent with previous work, although the relative salience of the hues differs. Such differences may be attributed to cultural variations in dietary habits. Specifically, Thai participants are more familiar with lemons and limes, which are commonly used in local cuisine, than with green apples or other sour fruits typically referenced in Western contexts.

For saltiness, the range of responses appeared narrower in the present study. Brown remained a salient association, which may reflect cultural familiarity with fried foods, fish sauce, and salt as common culinary elements in Thailand. By contrast, Velasco et al. reported associations with blue, likely reflecting Western participants' familiarity with the ocean as a salient reference point. taken together, these findings suggest that cultural dietary practices exert a clear influence on crossmodal associations between taste and color.

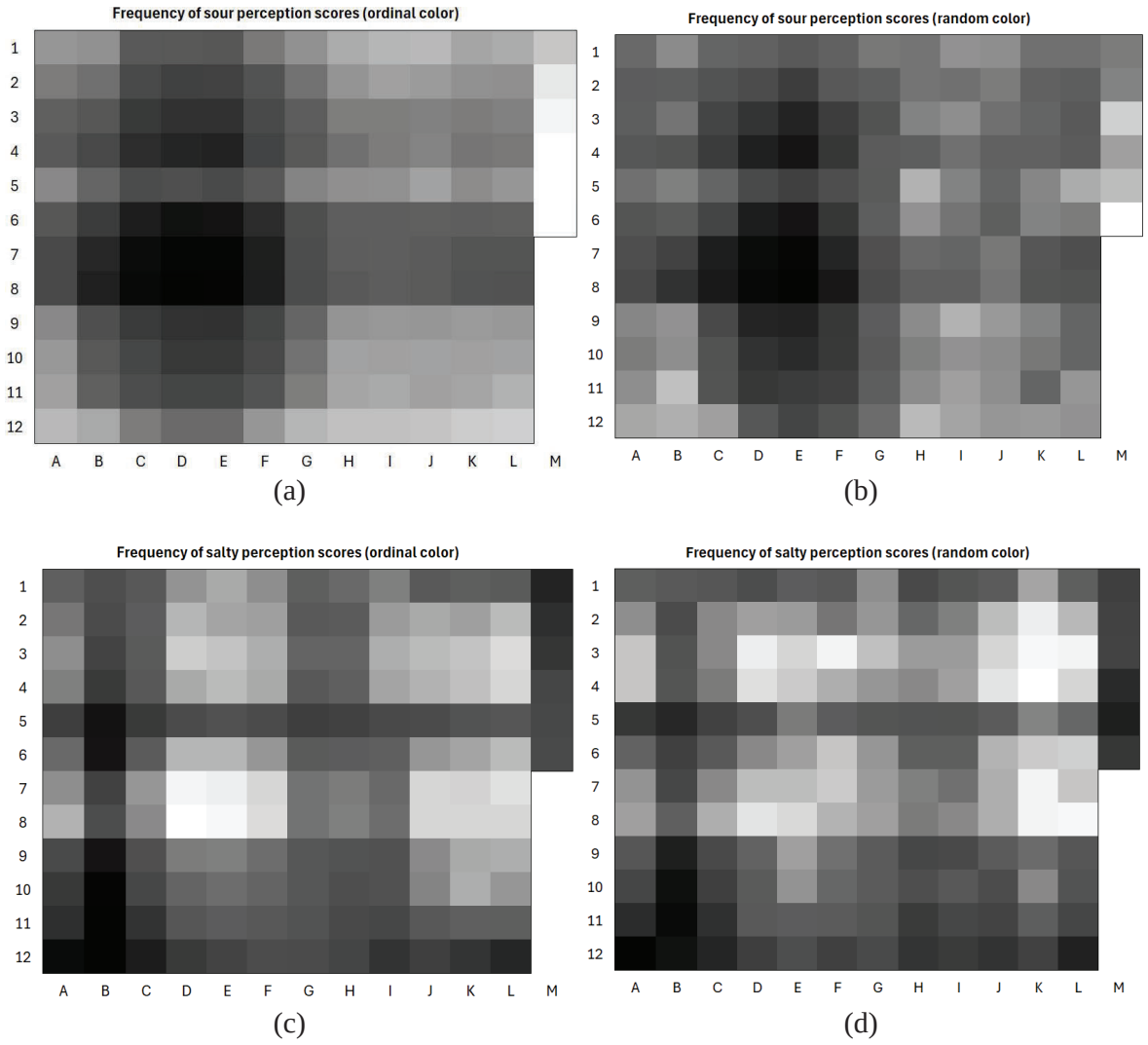

Figure 4. Heatmaps illustrating the distribution of mean taste perceptual score ($\bar{x}$) across different color positions. For clarity, the x-axis was labeled with the letters A–M, and the y-axis with the numbers 1–12. Darker regions represent the higher taste perceptual scores, whereas lighter regions indicate lower taste perceptual score. The upper-left and upper-right heatmaps show sourness perception in the color-ordering and randomized-color conditions, respectively. The lower-left and lower-right heatmaps show saltiness perception in the color-ordering and randomized-color conditions, respectively.

CONCLUSION

This study confirmed that sourness is predominantly associated with green and yellow hues, reflecting the colors of lemon and lime, while saltiness is most often associated with white and dark orange hues, resembling salt and fermented fish. Furthermore, the sequence of color presentation significantly influenced participants' perception ratings, underscoring the contextual effect of adjacent colors. Importantly, the findings also showed that saltiness perception was strongly shaped by participants' personal food experiences: individuals familiar with salt associated it with lighter colors similar to salt, whereas others linked it to darker orange hues reminiscent of fermented fish.

REFERENCES

[1] Spence, C. (2015). Multisensory flavor perception. Cell, 161(1), 24–35. https://doi.org/10.1016/j.cell.2015.03.007

[2] Piqueras-Fiszman, B., & Spence, C. (2015). Sensory expectations based on product-extrinsic food cues: An interdisciplinary review of the empirical evidence and theoretical accounts. Food Quality and Preference, 40, 165–179.

[3] Spence, C. (2019). On the relationship(s) between colour and taste/flavour. Experimental Psychology, 66(2), 99–111. https://doi.org/10.1027/1618-3169/a000439

[4] Spence, C., Wan, X., Woods, A., Velasco, C., Deng, J., Youssef, J., & Deroy, O. (2015). On tasty colours and colourful tastes? Assessing, explaining, and utilising crossmodal correspondences between colours and basic tastes. Flavour, 4(1), Article 23. https://doi.org/10.1186/s13411-015-0033-1

[5] Velasco, C., Escobar, F. B., Spence, C., & Olier, J. S. (2023). The taste of colours. Food Quality and Preference, 112, Article 105009. https://doi.org/10.1016/j.foodqual.2023.105009

[6] Spence, C., & Levitan, C. A. (2021). Explaining crossmodal correspondences between colours and tastes. i-Perception, 12(3), Article 20416695211018223. https://doi.org/10.1177/20416695211018223

[7] Heller, N. G., Levitan, C. A., & Spence, C. (2015). Crossmodal correspondences between colours and tastes: Testing the robustness of the associations. Flavour, 4(1), Article 10. https://doi.org/10.1186/20-44-7248-4-10

[8] Maga, J. A. (1974). Influence of colour on taste thresholds. Chemical Senses, 1(1), 115-119.

[9] Woods, A. T., & Spence, C. (2016). Using single colours and colour pairs to communicate basic tastes. i-Perception, 7(5), 1-14.

[10] Velasco, C., Woods, A., Deroy, O., & Spence, C. (2016). Hedonic mediation of the crossmodal correspondence between taste and shape. Food Quality and Preference, 52, 17-24.

Associative Colors Related to Grief from Pet Loss

YeJee Lim[a *], YounJin Lee[b *]

[a]PhD Candidate, Dept. of Design & Craft, Graduate School Hongik University, Seoul, Korea

[b]Professor, Dept. of Color Integrated Design, Graduate School of Industrial Arts, Hongik University, Seoul, Korea

Corresponding Author: YounJin Lee hacomama@hongik.ac.kr

ABSTRACT

Pet loss induces profound psychological distress in caregivers, yet social support for this experience remains insufficient. This study aims to systematically investigate the emotional experiences of bereaved pet owners suffering from Pet Loss Syndrome and to provide foundational data for the future development of color-based psychological healing programs. The research was conducted in two phases. Study 1 presented 20 negative emotional terms derived from items in the Pet Bereavement Questionnaire (PBQ), the Texas Revised Inventory of Grief (TRIG), and the Prolonged Grief Disorder Scale (PG-13). The analysis identified 'longing', 'sadness', 'upset', 'loneliness', 'depression', 'pain', and 'emptiness' as the primary emotions, and, together with 'guilt' and 'anger' emphasized in previous studies, confirmed nine core emotional terms. Study 2 examined the associative colors of these nine emotions using the Hue & Tone 130 Color Chart. The results revealed two distinct patterns. Longing, upset, loneliness, and guilt showed wide distributions across hue, value, and chroma, forming a dispersive–diffusive group, which reflects the characteristics of mixed emotions in which positive and negative feelings coexist. In contrast, sadness, emptiness, depression, pain, and anger clustered around specific hue groups and tones, forming a concentrated–cohesive group. The significance of this study lies in clarifying the relationship between emotional terms and associative colors in the context of pet loss, and in classifying emotional color tendencies into two distinct groups. Building on these findings, the stepwise development of color-based healing programs may serve as an important basis for evaluating and supporting the emotional states of individuals experiencing pet loss and other forms of bereavement. Furthermore, the color tendencies associated with each emotion are expected to evolve into key indicators for such programs, contributing to the measurement of psychological pain and change, and ultimately facilitating emotional recovery across diverse experiences of loss.

Keywords: Loss, Negative Emotion, Emotional Language, Associative Color, Pet Loss Syndrome

INTRODUCTION

In contemporary society, companion animals are increasingly regarded not merely as pets but as family members. Through affection and care, owners form strong emotional bonds with their animals, while the animals, in turn, provide psychological stability and comfort. However, because companion animals have shorter life spans than humans, their owners inevitably face the experience of loss. During this process, they often experience a wide range of negative emotions such as grief, depression, guilt, and anger, a phenomenon commonly referred to as Pet Loss Syndrome. Although this experience generally lasts for about six months to one year(Mo, 2015), it is not formally recognized as a psychiatric disorder(Cho, 2023, p. 23). Pet loss shares similarities with human bereavement but also exhibits several distinctive features. Hunt and Padilla(2006) identified three key aspects. First, society does not sufficiently encourage mourning after the death of a companion animal, and social support remains

limited (Mo, 2015). Second, because owners often experience unconditional love and acceptance from their pets—forms of emotional support rarely found in human relationships (Sharkin & Knox, 2003; cited in Hunt & Padilla, 2006)—the loss tends to cause deeper psychological shock and long-term effects. Third, unlike the typical stages of grief identified in human bereavement (Brown, Richards, & Wilson, 1996; cited in Hunt & Padilla, 2006), pet loss is often accompanied by particularly intense feelings of guilt (Quackenbush & Graveline, 1985; cited in Hunt & Padilla, 2006). Due to these characteristics, individuals who experience pet loss often endure disenfranchised grief (Mo, 2015), in which their mourning is not socially acknowledged, thereby intensifying their psychological burden. Consequently, the number of owners suffering from Pet Loss Syndrome continues to increase, and their emotional pain often persists over extended periods. Therefore, this study aims to (1) investigate the negative emotional terms experienced by bereaved pet owners, and (2) analyze the associative colors related to these emotions. Such analysis will enable a more concrete understanding of the relationship between negative emotional language and corresponding colors in the context of Pet Loss Syndrome, and will provide essential groundwork for the development of future color-based psychological healing programs.

METHODOLOGY

This study was conducted in two phases. Study 1 derived and selected negative emotional terms related to pet loss, while Study 2 investigated and analyzed the associative colors of the selected emotional terms.

Study 1: Derivation of Negative Emotional Terms

A total of 20 negative emotional terms were collected from the Pet Bereavement Questionnaire (PBQ; Hunt & Padilla, 2006; Jeong, 2019), the Texas Revised Inventory of Grief (TRIG; Faschingbauer, 1987; Ahn, 2006), and the Prolonged Grief Disorder Scale (PG-13; Prigerson & Maciejewski, 2008; Kang & Lee, 2017). These terms were then categorized into four groups: anger, longing, sadness, and others (Table 1).

Table 1: Twenty Negative Emotional Terms

Category	Negative Emotional Terms
Anger	Painful, Unfair, Denial, Shocking, Angry
Longing	Empty, Lonely, Longing, Regretful, Guilt, Yearning
Sadness	Depressed, Avoidant, Upset, Sad, Sorrowful, Embarrassed, Devastated
Others	Numb, Meaningles

A survey was conducted with pet owners who had experienced the loss of a companion animal. The survey items included gender, age, presence of children, duration since the loss, and prior experience of loss. In particular, the item on the presence of children was designed with reference to Mo(2015), which noted that, for couples without children, the loss of a pet may be experienced in ways psychologically similar to the loss of a child. Based on these items, the study examined the tendencies in participants' choices of emotional terms. Participants were asked to select from the presented emotional terms those most closely associated with their own experiences, and they were also given the option to provide additional negative emotional terms. For the analysis, first, the overall frequency was calculated to identify the commonly selected emotional terms. Second, the selection tendencies were compared across each demographic variable.

Study 2: Associative Colors of Negative Emotional Terms

The experimental tool was based on the Munsell color system and the Korean Industrial Standards (KS), and included ten chromatic hues: R(Red), YR(Yellow Red), Y(Yellow), GY(Green Yellow), G(Green), BG(Blue

Green), B(Blue), PB(Purple Blue), P(Purple), and RP Red Purple). According to Han and Na(2021), a single emotional word is influenced not only by hue but also by value and chroma, with tone shown to play a particularly important role in emotional expression. Therefore, 13 tones were employed: s(standard), vv(vivid), dp(deep), dk (dark), dl(dull), sf(soft), lt(light), pl(pale), wh(whitish), ltgy(light grayish), gy(grayish), dkgy(dark grayish), and bk (blackish). The Hue & Tone Color Chart (130 chips) was visualized in tabular form, with each color assigned a number to facilitate participant selection. The background color was set to N5 in order to minimize afterimage effects from surrounding colors(Figure 1). After each emotional term was presented, participants were instructed to select three associative colors.

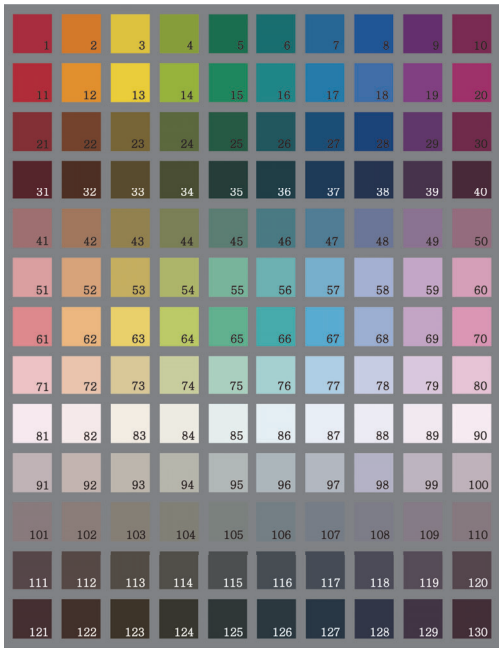

Figure 1: Standardized Hue & Tone Color Chart (130 chips)

RESULTS AND DISCUSSION

In Study 1, a total of 500 participants responded to the online survey. After excluding 36 invalid responses, data from 464 participants were analyzed. First, across all responses, ‘longing’ and ‘sadness’ were reported with the highest frequency, followed by ‘upset’, ‘emptiness’, ‘loneliness’, ‘depression’, and ‘pain’ as major emotional terms. Overall, emotional terms categorized under ‘longing’ and ‘sadness’ were chosen more frequently than those belonging to the ‘anger’ category. Second, in the gender analysis, both men and women commonly selected ‘longing’, ‘sadness’, and ‘loneliness’. However, women more frequently chose ‘emptiness’ and ‘upset’, indicating a tendency toward more nuanced differentiation of emotions. In terms of age, participants in their 20s and 30s selected a wider range of emotional terms, whereas those aged 40 and older showed fewer choices, with ‘pain’ emerging as a distinctive response. Regarding the presence of children, participants without children more frequently reported ‘pain’ and ‘guilt’, consistent with previous findings(Mo, 2015). In the analysis by time since loss, ‘pain’ was most prominent in the early stage (1–3 months), but over time, ‘regret’ and ‘guilt’ became more salient. Furthermore, when comparing groups by prior loss experience, those with prior experience more frequently reported ‘pain’ and ‘guilt’, while those without prior experience more strongly reported ‘depression’. As a result of Study 1, the seven most frequently reported negative emotional terms were ‘longing’, ‘sadness’, ‘upset’, ‘loneliness’, ‘depression’, ‘pain’, and ‘emptiness’. In addition, prior research highlighted ‘guilt’ and ‘anger’ as important emotions that distinguish pet loss from human bereavement. Taken together, nine negative emotional terms were ultimately selected for use in Study 2.

In Study 2, a total of 68 participants responded, and after excluding invalid responses, data from 65 participants were analyzed by mapping each response to the Hue & Tone Color Chart, as shown in Figure 2.

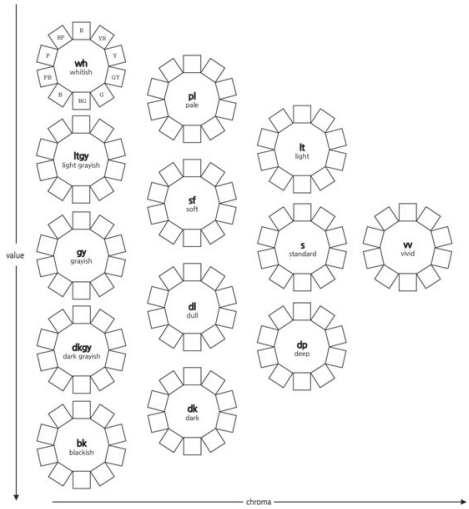

Figure 2: Example of Hue & Tone Color Chart

Figure 3 visualizes the responses according to the nine negative emotional terms, applied to the Hue & Tone color system. Only colors selected by more than 2% of the total participants (at least one respondent) were included. Based on colors chosen by at least 5% of the participants, the analysis revealed the following trends. ‘Longing’ showed a broad distribution across hues and tones, appearing evenly in Y/vv, RP/lt, Y/ltgy, and B/ltgy. ‘Sadness’ was primarily concentrated in the cool hues B and PB, with PB/dk being most representative. ‘Upset’ was prominent in low-chroma areas of medium and low value, with R/dkgy showing the highest selection rate. ‘Emptiness’ appeared across various tones but was particularly high in B/gy (over 14%) and was concentrated in B and PB hues. ‘Loneliness’ was concentrated in low-chroma tones such as ltgy, gy, and dkgy, with B/ltgy as the representative choice. ‘Depression’ was marked in low-chroma and low-value colors of BG, B, and PB hues, with G/gy, B/gy, and BG/dkgy as the main results. ‘Pain’ was concentrated in low-value and low-chroma colors of the R, YR, and RP hues, with R/dk, R/s, and R/vv showing high proportions. ‘Guilt’ was distributed across multiple hues but converged mainly in low-chroma and bk tones, with R/dk, PB/gy, Y/bk, and RP/bk being representative. ‘Anger’ was concentrated in high-chroma areas of the R, YR, P, and RP hues, with R/s, R/vv, and R/dk recording the highest selection rates. Overall, the color tendencies of the emotional terms were divided into two groups. The dispersive–diffusive group included ‘longing’, ‘upset’, ‘loneliness’, and ‘guilt’, which were distributed broadly across a variety of hues and tones. In particular, ‘longing’, as noted by Park and Jeong (2024), can be interpreted as a mixed emotion that simultaneously embodies the negativity of loss and the positive memory of the object, and this duality was reflected in its wide-ranging color selections. Similarly, ‘upset’ has complex meanings that encompass disappointment, resentment, anger, and sadness, allowing for diverse interpretations depending on individual experiences, which in turn produced a dispersed pattern of color choices. ‘Loneliness’, arising from the disruption of social and emotional bonds and persisting across daily life, tended to be associated with a wide range of low- to mid-chroma colors. ‘Guilt’, a self-reflective emotion related to responsibility attribution, was primarily concentrated in low-chroma and bk tones, but also displayed distribution across multiple hues. The concentrated–cohesive group included ‘sadness’, ‘emptiness’, ‘depression’, ‘pain’, and ‘anger’, which converged on specific hue groups and tones. For example, ‘sadness’ and ‘depression’ clustered in low-value, low-chroma regions, while ‘anger’ was concentrated in high-chroma reds. These results indicate that while some negative emotional terms function as mixed emotions and elicit diverse color associations, others reveal clearer emotional directionality and converge on specific color choices.

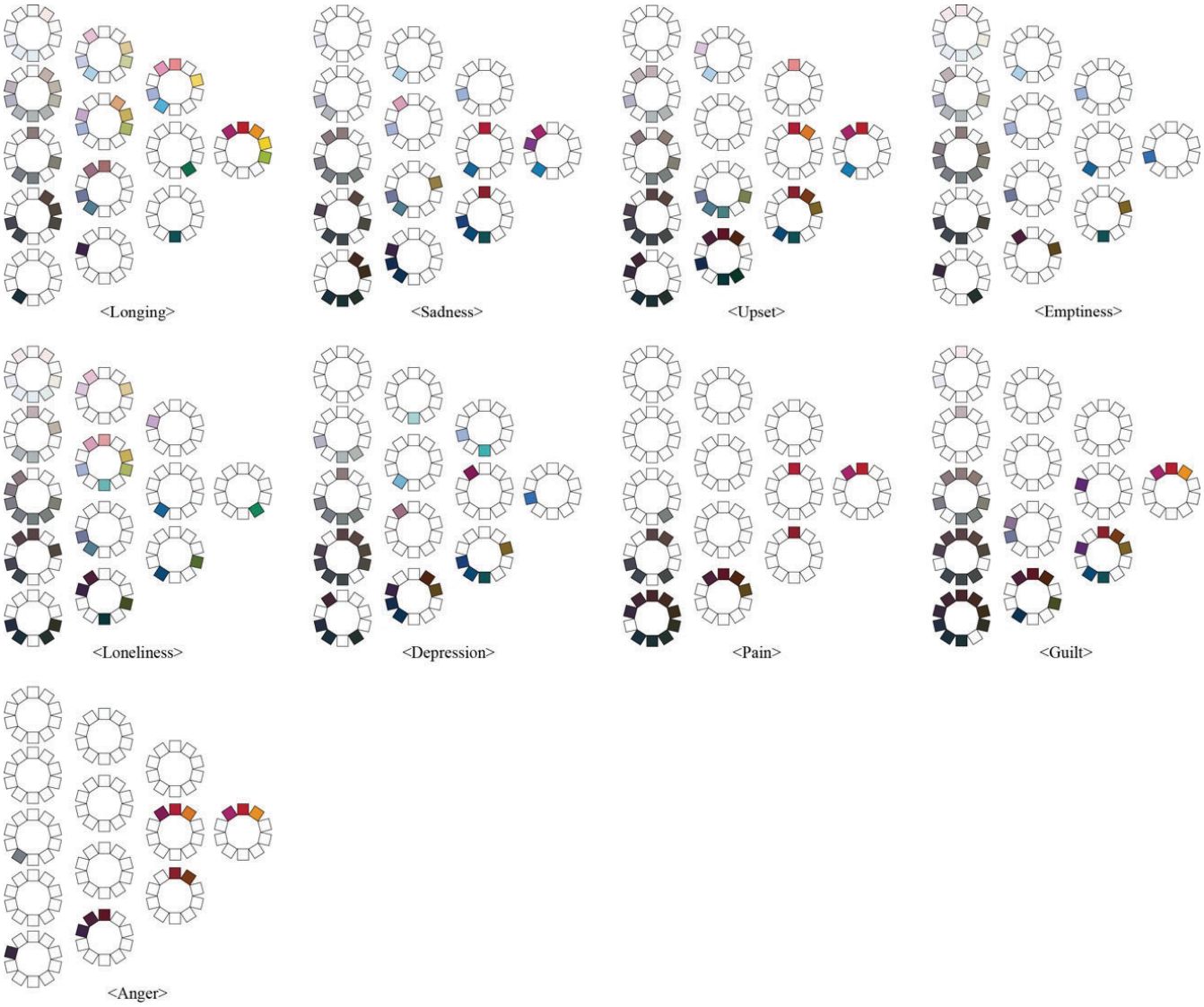

Figure 3: Distribution of Associated Colors for Nine Negative Emotion Words

CONCLUSION

The loss of a companion animal induces profound psychological distress in pet owners, yet social support for such experiences remains insufficient. This study aims to develop color-based healing programs for the emotional recovery of bereaved owners. Focusing on individuals experiencing Pet Loss Syndrome, Study 1 identified negative emotional terms, while Study 2 analyzed the associative colors corresponding to each term. In Study 1, a total of 20 negative emotional terms were derived from items in the Pet Bereavement Questionnaire (PBQ), the Texas Revised Inventory of Grief (TRIG), and the Prolonged Grief Disorder Scale (PG-13). The analysis identified ‘longing’, ‘sadness’, ‘upset’, ‘loneliness’, ‘depression’, ‘pain’, and ‘emptiness’ as major emotions, and, together with ‘guilt’ and ‘anger’ emphasized in previous studies, confirmed nine core emotional terms. In particular, among participants without children, ‘guilt’ and ‘pain’ were prominent, and the longer the period of loss, the more diverse the emotional terms became. In addition, in participants with prior loss experience, ‘guilt’ and ‘pain’ emerged as

significant emotions. Study 2 analyzed the associative colors of the nine emotional terms using the Hue & Tone 130 Color Chart. The results showed that the emotional terms were divided into a dispersive–diffusive group and a concentrated–cohesive group. The dispersive–diffusive group ('longing', 'upset', 'loneliness', and 'guilt') was distributed across a wide range of hues and tones such as Y/vv, RP/lt, B/ltgy, R/dkgy, PB/gy, and Y/bk. In contrast, the concentrated–cohesive group ('sadness', 'emptiness', 'depression', 'pain', and 'anger') tended to converge on specific hues and tones such as PB/dk, B/gy, BG/dkgy, R/dk, R/s, and R/vv. The significance of this study lies in its systematic analysis of pet loss experiences, clarifying the relationship between emotional terms and colors, and categorizing these associations into two distinct types. Notably, the finding that certain emotional terms appear as mixed emotions and are associated with a broad distribution of color selections reveals subtle emotional differences that have been overlooked in previous color studies on bereavement. As a follow-up study, this research suggests that color-based healing programs developed through stepwise investigations may be practically applied to color therapy and counseling for individuals suffering psychological distress due to loss, and further contribute to emotional recovery in various types of bereavement experiences.

REFERENCES

[1]. Ahn, Y. R (2006). Development of Individualized Bereavement Care Program and Its Effects on Widows. Graduate School of Catholic University, Seoul.

[2]. Brown, B. H., Richards, H. C., and Wilson, C. A. (1996). Pet bonding and pet bereavement among adolescents. Journal of counseling and development, 74(5), 505-509.

[3]. Cho, J. H. (2023). Welcome, Petloss Counseling Office. Seoul: Lagom.

[4]. Han, J. W. and Ken, N. (2021). The Characteristics of Colors to the Positive and Negative Emotions of Korean Adults.

[5]. Hunt, M. and Padilla, Y. (2006). Development of the Pet Bereavement Questionnaire. Anthrozoös, 19(4), 308-324.

[6]. Jung, M. J. (2019). Adult's Experience of the Death of a Companion Animal and Complicated Grief. Graduate School of Ewha Womans University, Seoul.

[7]. Kang, H. S. and Lee. D. H. (2017). Korean Version of the Prolonged Grief Disorder Scale (PG-13-K): A Validation Study. Korean Journal Of Counseling And Psychotherapy, 29(4), 1027-1052.

[8]. Mo, H. J. (2015). Grieving after the Loss of Companion Animals - Symptoms of Pet Loss -. Human Beings, Environment and Their Future, (15), 91-120.

[9]. Park J. A, and Jeong Y. H (2024). Analysis of the Meaning of 'Geurium' and Ways to Utilize It in Korean Language Education － Focusing on 'Geurium', 'Geuripda', 'Geuriwohada', and 'Geuriwojida' －. Ratio et Oratio, 17(1), 185-215.

[10]. Quackenbush, J. and Graveline, D. (1985). When Your Pet Dies: How to Cope you're your Feelings. New York: Pocket Books.

[11]. Sharkin, B. S. and Knox, D. (2003). Pet loss: Issues and implications for the psychologist. Professional psychology, research and practice, 34(4), 414-421.

The Influence of Art Material Experience on Basic Color Terms and Color Category Perception

Hyejin Han[a*]

[a]Incheon National University, Incheon, South Korea

[*]Corresponding author: Hyejin Han, hhan@inu.ac.kr

ABSTRACT

Berlin & Kay's theory of the basic color term (BCT) has long influenced the study of color perception across cultures. While earlier studies in Japan and Korea explored emotional and perceptual responses to BCTs (Uchikawa & Boynton; Lee & Ohmi; Kim & Lee), follow-up research in the Korean context remains limited. Most work has centered on the universality of the first eleven terms, with less attention to emerging categories, such as a twelfth term, that may reflect cultural or perceptual distinctions. This study investigates how native Korean speakers with art education backgrounds perceive and categorize BCTs. Fifty-nine participants reported their frequently used art materials and estimated the minimum number of colors required to illustrate a scene. They also freely listed twelve chromatic color terms, defining perceptual boundaries for each. Focal colors and perceptual ranges were derived using the Cascade method based on response frequency. Among the materials, watercolor was identified as the most influential medium on their color knowledge. Furthermore, the estimated minimum number of colors required to construct an image ranged from 6 to 15. The results revealed that while core color terms such as red, blue, yellow, and green exhibited clearly clustered focal areas, peach showed multiple peaks, suggesting interpretive variability. Additional color terms such as navy, yellow-green, and sky blue overlapped with existing categories, indicating limited distinctiveness. These findings suggest that repeated exposure to specific materials can shape how individuals construct and differentiate color categories, and that peach may be emerging as a twelfth basic color term, pending further validation. Moreover, the use of digital displays instead of physical color chips may have subtly influenced focal color selection, highlighting the importance of stimulus modality in color perception research. Ultimately, this study enhances understanding of how linguistic, perceptual, and educational factors shape color categorization, with practical implications for arts education and design.

Keywords: basic color terms, color category, focal color, art materials, art education

INTRODUCTION

Berlin & Kay's theory (1969) of the basic color term (BCT) has long shaped the study of color perception across cultures [1]. Kay & McDaniel (1978) supported Hering's four fundamental hue sensations (red, yellow, green, blue) through neurophysiological evidence of opponent-process mechanisms, and introduced fuzzy set theory to explain the graded structure of basic color categories and focal colors [2]. Uchikawa & Boynton (1987) investigated color category ranges in Japanese based on BCTs [3]. In 2000, Kim & Lee's study on Korean color categories using free classification demonstrated that perceptual grouping aligns with universal basic terms, while Lee & Ohmi's research on Japanese color categories through color chips revealed that emotional responses are closely tied to cognitive color categorization [4], [5]. Webster & Kay (2007) marked a shift by highlighting substantial individual variation in focal color choices within a single language [6]. Lindsey & Brown's research (2014) further revealed that American English speakers use both basic and diverse non-basic color terms, reflecting perceptual subtleties

and cultural variation [7]. The modern Japanese color lexicon (2017) integrates basic, traditional, and loanword terms, illustrating the layered nature of linguistic and cultural influences [8]. Although most studies have focused on the universality of the original eleven BCTs, comparatively little attention has been paid to the potential emergence of additional categories—such as a twelfth term influenced by cultural or perceptual factors. This study investigates how Korean speakers with art education backgrounds perceive and categorize BCTs, focusing on how material experience shapes their perceptual boundaries.

METHODOLOGY

Fifty-nine native Korean-speaking participants (54 women and 4 men; ages 19-26 years) from Incheon National University participated in this study. All were born and raised in South Korea, and had normal or corrected-to-normal color vision, as assessed using Ishihara Pseudoisochromatic plates.

Firstly, participants reported the art materials they commonly use to assess the potential influence of these materials on their perception of color categories. In addition, they were asked to estimate the minimum number of colors required to illustrate a scene. Secondly, participants freely listed BCTs for stimuli based on the Optical Society of America (OSA) Uniform Color Scale, which consisted of 424 color samples. Achromatic terms were excluded from the BCT lists, and supplementary chromatic terms were added to define color boundaries for each category. These additional terms were examined as potential candidates for a twelfth BCT in Korean.

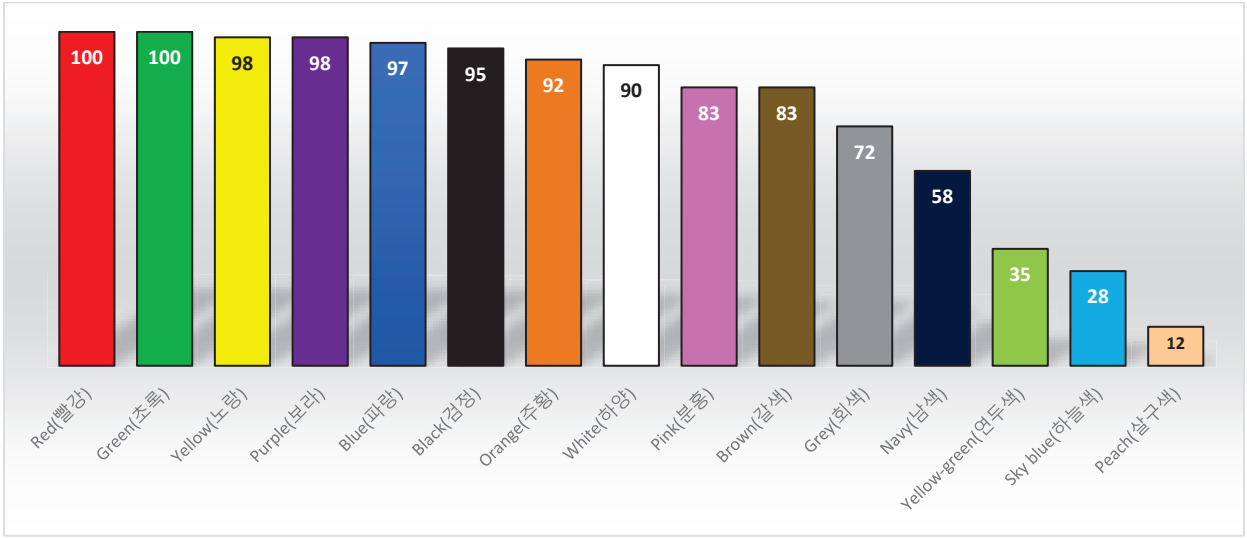

Figure 1: Survey results indicating the potential emergence of a twelfth BCT in Korean (%; N = 60 participants)

Figure 1 presents free listing data from sixty participants (13 men, 47 women; ages 18–26 years). In this graph, color terms that appeared with over 90% agreement, such as red-green and yellow-blue, correspond to Hering's opponent-process theory. Additionally, black-white and purple-orange pairs were also highly represented. When extended to include colors in the 70–89% agreement range, namely pink, brown, and gray, total of eleven BCTs emerge, aligning closely with Berlin & Kay's BCT. Furthermore, colors such as navy, yellow-green, sky blue, and peach appeared as additional candidates, suggesting the possible emergence of a twelfth BCT in a previous study [9]. These terms were also used as Korean color terms in the consensus analysis presented in Figure 4. Participants observed the color chart on a calibrated monitor (Daewoo CND S1-H81BE) using the Spyder X Studio. Focal colors were identified based on frequency of response, and the perceptual ranges of each color category were analyzed. Of the fifty-nine participants, data from three female participants were excluded due to inconsistencies.

RESULTS AND DISCUSSION

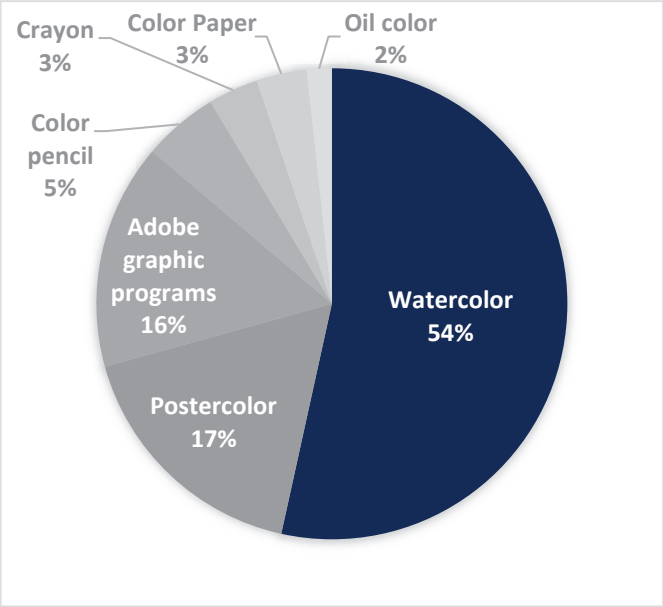

Figure 2: Influence of various color materials on participants' color knowledge

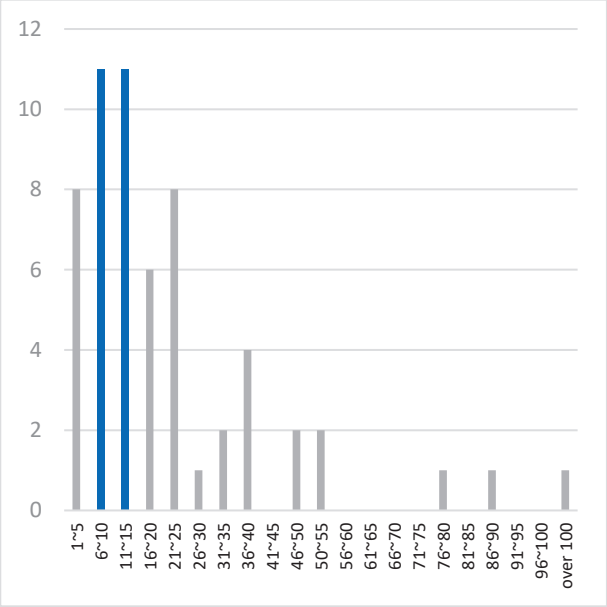

Figure 3: Minimum number of colors required to illustrate a scene

Figure 2 illustrates the influence of various color materials on participants' color knowledge. Among the respondents, watercolor was reported as the most influential medium, accounting for 54% of responses. Figure 3 presents the distribution of responses concerning the minimum number of colors deemed necessary to illustrate a scene. These results suggest that most art students consider 6 to 15 colors sufficient for depicting a scene. This practical range may reflect not only the influence of commonly used art materials but also a cognitive alignment with the eleven BCTs, as proposed by Berlin and Kay.

Participants defined color boundaries for twelve chromatic terms. Based on response frequency, focal colors and perceptual ranges were analyzed. The Cascade method was used to compile and visualize consensus distributions of color selections across participants.

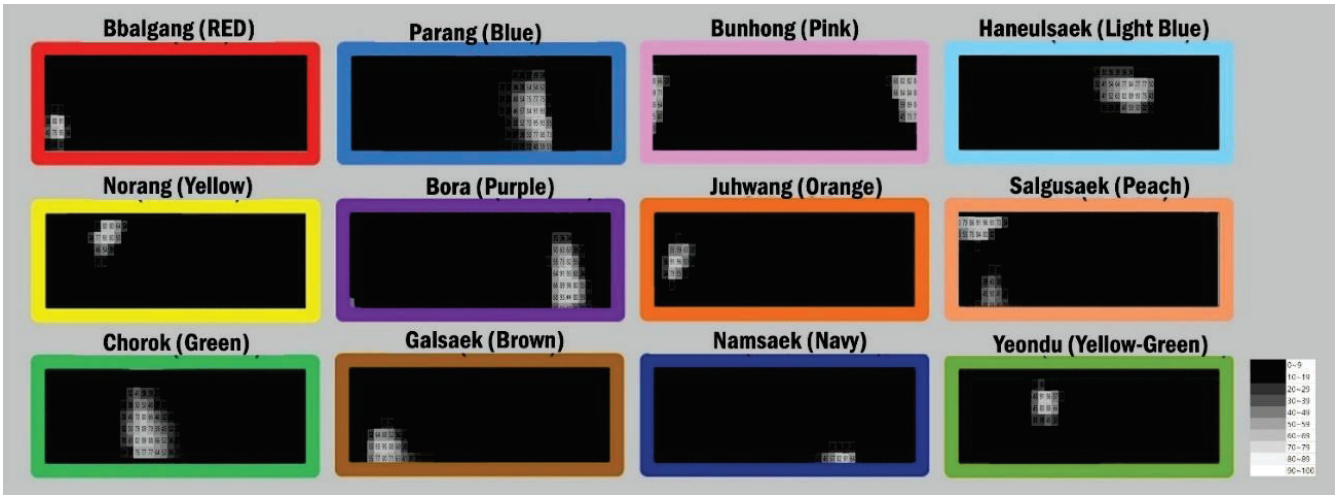

Figure 4: Consensus diagrams of the twelve Korean chromatic color terms by the Cascade method

Figure 4 displays the perceptual ranges of twelve chromatic color terms (excluding achromatic colors) commonly used in Korean. Each colored box represents one color term, with the internal grid displaying participants' selections of corresponding color samples.

The figure reveals that while some color terms (e.g., red, blue, yellow, and green) have clearly clustered focal areas, peach shows multiple peaks, suggesting greater variability in interpretation. Additional color terms such as navy, yellow-green, and sky blue overlapped with existing categories, indicating limited distinctiveness. Clarifying the perceptual boundaries and semantic stability of this potential twelfth term will require more detailed analysis and continued research.

CONCLUSION

The study offers insights into how visual arts and design education affect both the linguistic and perceptual structures of color categorization, with practical implications for color education and design practices in culturally diverse contexts. As digital media become increasingly dominant in art education, understanding how material-based experience shapes perceptual boundaries can inform future curriculum design, interface aesthetics, and intercultural communication.

ACKNOWLEDGEMENTS

The study was inspired and refined through the insightful feedback provided by Prof. Shinomori (Kochi University of Technology, Japan) at the Imaging Society of Japan (ISJ) research meeting. The author sincerely thanks Dr. Sangmyung Lee (Hongik University, South Korea) for her invaluable advice and continuous guidance throughout the course of this research. Special thanks are also extended to Prof. Uchikawa (Tokyo Institute of Technology, Japan), whose theoretical contributions to color categorization have served as a foundation for this study.

REFERENCES

[1]. Berlin, B., & Kay, P. (1969). Basic color terms: Their universality and evolution. Berkeley, CA: University of California Press.

[2]. Kay, P., & McDaniel, C. K. (1978). The linguistic significance of the meanings of basic color terms. Language, 54(3), 610-646.

[3]. Uchikawa, K., & Boynton, R. M. (1987). Categorical color perception of Japanese observers: Comparison with that of Americans. Vision research, 27(10), 1825-1833.

[4]. Kim, Y. S., & Lee, M. Y. (2000, November). Color Category in Free Classification of Color Chips. In AIC MEETING SEOUL, 272-273.

[5]. Lee. S. M., & Ohmi. G. (2000, November). A Relation Between Color-Affection and Color Categories. In AIC MEETING SEOUL, 119-122.

[6]. Webster, M. A., & Kay, P. (2007). Individual and population differences in focal colors. The anthropology of color.

[7]. Lindsey, D. T., & Brown, A. M. (2014). The color lexicon of American English. Journal of vision, 14(2), 1-25.

[8]. Kuriki, I., Lange, R., Muto, Y., Brown, A. M., Fukuda, K., Tokunaga, R., Lindsey, D. T., Uchikawa, K., & Shioiri, S. (2017). The modern Japanese color lexicon. Journal of vision, 17(3), 1-18.

[9]. Han, H. (2019). The Effect of Object Shapes on Color Categories Judgment. Perception, 48, 44.

Contrasting Perceptions of Dark Colours Among Designers and Non-designers: An Empirical Analysis

Qi Xiang[a*], Xu Han[a], Chengliang Ping[a] and Luwen Yu[ab]

[a]The Hong Kong University of Science and Technology (Guangzhou), Guangzhou, China
[b]The Hong Kong University of Science and Technology, Hong Kong, China
[*]Corresponding author: Qi Xiang, qxiang073@connect.hkust-gz.edu.cn

ABSTRACT

Contemporary design increasingly demands nuanced and diversified colour strategies, with particular attention to categories that carry distinctive expressive and functional weight. Among these, dark palettes have become especially prominent, valued for their ability to convey depth, contrast, and atmosphere. Yet despite their ubiquity in branding, product finishes, and interface theming, the very category of dark-colour remains loosely specified and inconsistently interpreted. This study examines how people assign the dark-colour label across hues and what perceptual criteria underlie those assignments. Twenty-nine participants (13 designers and 16 non-designers) completed a two-pass selection task with 1,524 physical Munsell chips: Pass 1 marked dark-colour chips within each hue family; Pass 2 reviewed selections across all hues to refine thresholds and interviews documented decision rules and uncertainties. Analyses in CIELAB indicate that dark-colour is better described as a hue-modulated region in lightness-chroma space: selections cluster at low L*, while admissible chroma (C*ab) varies by hue. Consistent with established findings in colour appearance, warm families (R–Y) can be judged dark at slightly higher L* than cool families (BG–P). Across groups, participants shared baseline cues (low lightness, proximity to black) and reported uncertainty near category boundaries. Designers and non-designers differed mainly in cue weighting (with some emphasizing extreme low L* or, under low L* conditions, extreme saturation as alternative routes to dark-colour, and others relying more on contextual salience), but both provided systematic strategies that converged further after cross-hue review. Methodologically, the study combines dense physical sampling, a two-pass procedure, and interviews to quantify and explain categorical thresholds. Practically, the results offer hue-specific guidance for specifying dark palettes, clarifying when chroma can be retained without losing dark impression. Future work should examine domain-specific contexts such as textiles, fashion, and digital interfaces, where the perception of dark colours may shift with materials and media.

Keywords: Dark-colour Perception, Colour Categorization, Munsell Colour System, CIELAB, Hue Dependence

INTRODUCTION

The strategic deployment of dark palettes has become a hallmark of contemporary design, spanning luxury branding, digital interfaces, and product finishes. Such palettes are valued for durability, luxury, sophistication, or spirituality [1,2]. Advances in dyeing and coating technologies have further expanded the availability of saturated and stable dark shades across materials, making dark-colour an increasingly versatile design resource. Yet this expansion has also magnified a persistent difficulty: the communicative intent behind dark schemes does not always align with user interpretation. While designers may frame dark palettes as minimalistic or focused, lay audiences can perceive them as dull, heavy, or emotionally distancing [3,4].

This tension reflects the complex perceptual and psychological status of dark-colour. Physiologically, dark colours engage the visual system differently from high-brightness or fluorescent hues. Rather than delivering intense

luminance stimulation, they emphasize low-light contrasts and dampened signals, producing an atypical arousal. Psychologically, dark colours carry symbolic and affective weight, connoting formality, intimacy, or melancholy, which amplifies their communicative impact. From a design standpoint, such factors complicate palette specification: what appears suitably dark to a professional may not align with lay viewers, especially when hue and chroma biases shift categorical boundaries. These challenges invite closer examination of how dark-colour is constructed in perception. From a colour science perspective, darkness cannot be reduced to a single luminance threshold (L* in CIELAB) but emerges from interactions among lightness, chroma, and hue [7]. Although this principle is recognized in vision research, far less is known about how different populations apply these dimensions when using the category. Existing studies have typically isolated mechanisms or examined single cohorts, leaving unaddressed the role of expertise in shaping how dark-colour is operationalized.

This study addresses that gap by systematically comparing designers and non-designers. Using a two-pass selection task with physical Munsell samples, complemented by interviews, we investigate (1) how the two groups assign the dark-colour label across hues, and (2) how expertise and contextual evaluation influence their decision criteria. Through this approach, we aim to clarify how dark-colour functions as a multidimensional construct negotiated between perceptual tendencies and professional conventions.

METHODOLOGY

Stimuli comprised 1,524 colour chips from the Munsell Book of Colour (Glossy Edition), spanning ten chromatic hues (R, YR, Y, GY, G, BG, B, PB, P, RP) and one achromatic series (N), covering a broad range of hue-value-chroma combinations. Hue groups followed the Munsell classification and were retained as categorical variables to preserve perceptual groupings and enable tests of hue dependence. Because Munsell Value and Chroma are ordinal, all notations were converted to CIELAB to obtain continuous, approximately interval-scaled coordinates [8]. We analysed L* (lightness) and C*ab (chroma, derived from a and b) as they operationalize the principal dimensions implicated in "dark" judgments and support standard statistical modelling in a uniform metric space. The Munsell atlas provides discrete steps in Value that map to near-regular increments in L*, yielding consistent lightness sampling.

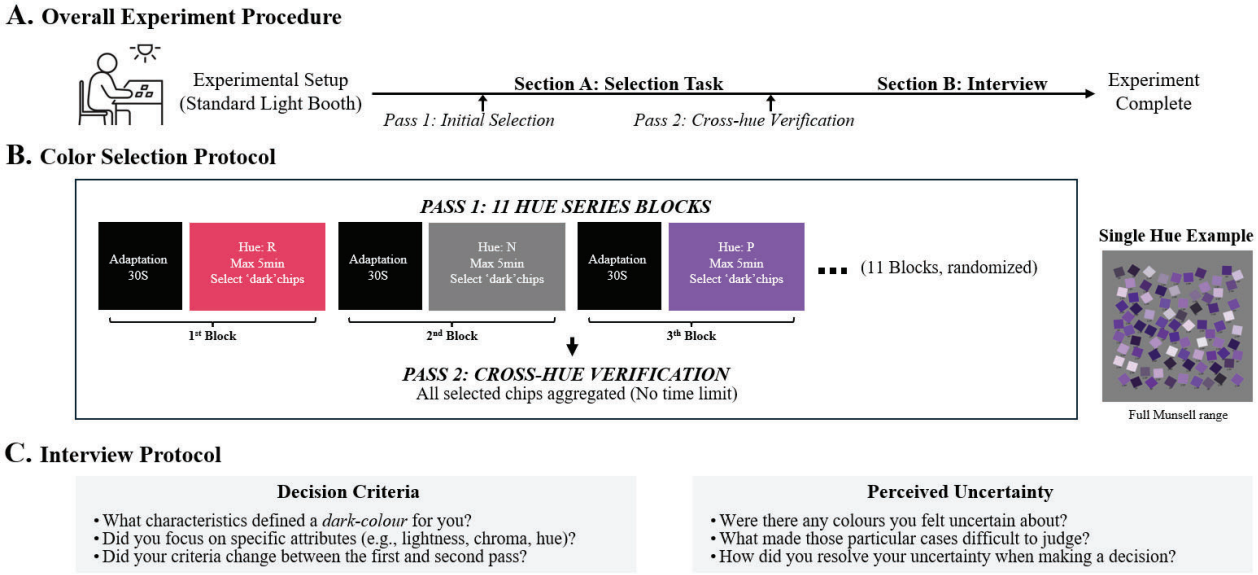

Figure 1: Experimental procedure

A two-pass selection task was implemented, followed immediately by semi-structured interviews (Fig. 1A). The sequential design served to elicit initial, within-hue judgments of dark and subsequently to evaluate cross-hue consistency. In *Pass 1*, participants identified candidate stimuli under controlled viewing conditions, thereby externalizing their preliminary perceptual thresholds; and *Pass 2* re-presented these selections in aggregate, enabling participants to recalibrate and consolidate their judgments across the full set (Fig. 1B). This procedure was intended to minimize inter-hue carryover effects while also capturing intra-participant reliability. The subsequent interviews probed the underlying decision criteria and sources of uncertainty, providing complementary qualitative data to contextualize the behavioural outcomes (Fig. 1C). Twenty-nine adults participated: 13 designers (≥3 years of professional visual or interaction design experience) and 16 non-designers without formal colour training; ages 18–36 years with balanced gender distribution. Normal colour vision was confirmed with Ishihara plates.

RESULTS

Hue-dependent lightness thresholds and chroma allowances

As shown in Figure 2, the distributions of samples judged as dark-colour vary systematically across hue families. Warmer hues (R–Y) include higher lightness levels among accepted darks, with upper quartiles extending above L* ≈ 40, whereas cooler hues (BG–PB) and purples (P, RP) cluster around lower levels, with most selections concentrated near L* ≈ 30. The neutral series (N) spans the widest range, covering nearly the full tested interval, yet its median remains the lowest overall. Across nearly all hues, designers' selections are shifted toward lower L* compared to non-designers, reflecting stricter acceptance of what counts as dark. Non-designers more frequently include higher-lightness samples, particularly in yellow (Y) and purple-blue (PB). Dispersion is also smaller for designers, especially in cool hues, indicating tighter internal criteria (see medians, SD, and ranges in Fig. 2b).

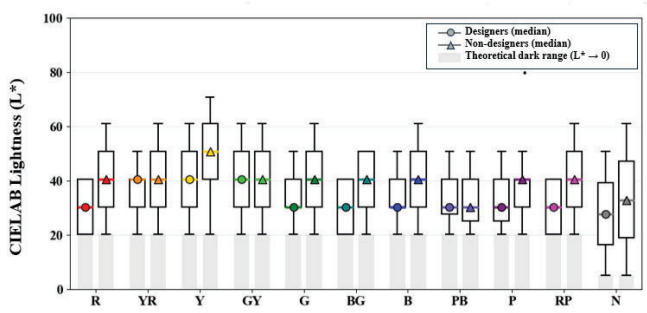

(a)

Hue	Designers Median	SD	Range	Non-designers Median	SD	Range
R	30.38	8.10	20.24–40.74	40.74	11.53	20.24–61.05
YR	40.74	10.37	20.24–51.00	40.74	12.74	20.24–61.05
Y	40.74	11.09	20.24–61.05	51.00	14.30	20.24–70.86
GY	40.74	11.19	20.24–61.05	40.74	11.37	20.24–61.05
G	30.38	9.04	20.24–51.00	40.74	11.28	20.24–61.05
BG	30.38	8.18	20.24–40.74	40.74	11.26	20.24–51.00
B	30.38	9.77	20.24–51.00	40.74	11.61	20.24–61.05
PB	30.38	10.25	20.24–51.00	30.38	9.95	20.24–51.00
P	30.38	9.47	20.24–51.00	40.74	11.70	20.24–80.53
RP	30.38	8.15	20.24–40.74	40.74	11.36	20.24–61.05
N	27.81	14.31	5.12–51.00	32.96	17.26	5.12–61.05

(b)

Figure 2: (a) Distributions of CIELAB lightness (L*) values selected as *dark-colour* across hue families and groups. (b) Summary statistics (median, SD, and range) of selected samples for each hue family and group Boxes show interquartile ranges with medians; outlines show kernel densities. The shaded fill beneath each box extends from the minimum value to L* = 0, visually indicating the theoretical dark region. Values are reported in CIELAB (D65/2°).

Chroma differences are summarised in Figure 3. In warm hues (R–Y), non-designers admit higher chroma values than designers, with median gaps of about +4–6 units. This broader tolerance reflects a greater acceptance of dark-colour, where higher chroma can coexist with the perception of dark. In green-yellow to green (GY–G), the group difference is smaller (≈ +1–2), while in blue to purple-blue (B–PB) it narrows further and can locally reverse. In purples (P, RP), allowances rise again, with non-designers showing medians ≈ +4–5 units above designers. Overall, chroma modulates the dark category in a hue-dependent manner, expanding it into a dark-colour region,

whereas lightness (L*) remains the primary axis. Designers consistently allow lower chroma and show reduced dispersion, especially in cool hues, indicating tighter internal criteria (see medians, SDs, and ranges in Fig. 3b).

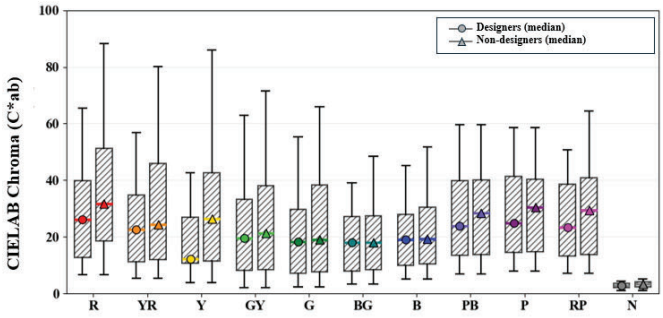

(a)

Hue	Designers Median	SD	Range	Non-designers Median	SD	Range
R	26.23	15.67	6.58–65.42	31.77	21.15	6.58–88.40
YR	22.51	14.03	5.24–56.85	24.41	19.98	5.24–80.09
Y	12.24	15.09	3.76–57.04	26.33	22.87	3.76–85.98
GY	19.64	16.23	2.09–62.83	21.33	19.47	2.09–71.52
G	18.38	14.88	2.28–55.26	19.03	16.59	2.28–65.85
BG	18.06	11	3.42–39.03	18.06	12.04	3.42–48.49
B	19.11	11.55	5.12–45.13	19.28	12.55	5.12–51.82
PB	23.84	14.97	6.87–59.73	28.33	14.92	6.87–59.73
P	24.85	15.34	7.79–58.52	30.35	14.59	7.79–58.52
RP	23.41	12.81	7.22–50.82	29.44	15.69	7.22–64.55
N	2.89	0.98	1.03–4.42	3.23	1.17	1.03–5.08

(b)

Figure 3: (a) Distributions of CIELAB chroma (C*ab) values selected as *dark-colour* across hue families and groups. (b) Summary statistics (median, SD, and range) of selected samples for each hue family and group
Boxes show interquartile ranges with medians; outlines show kernel densities. Chroma was calculated as C*ab = $\sqrt{(a^2 + b^2)}$ in CIELAB(D65/2°).

Figure 5 shows the two-pass comparison of lightness and chroma selections. Designers remain largely consistent between passes, with only minor narrowing of dispersion, whereas non-designers display broader adjustments, especially in warm hues for lightness and in red-purple regions for chroma. These findings indicate that the hue-dependent patterns are stable, but intra-group consistency is higher among designers.

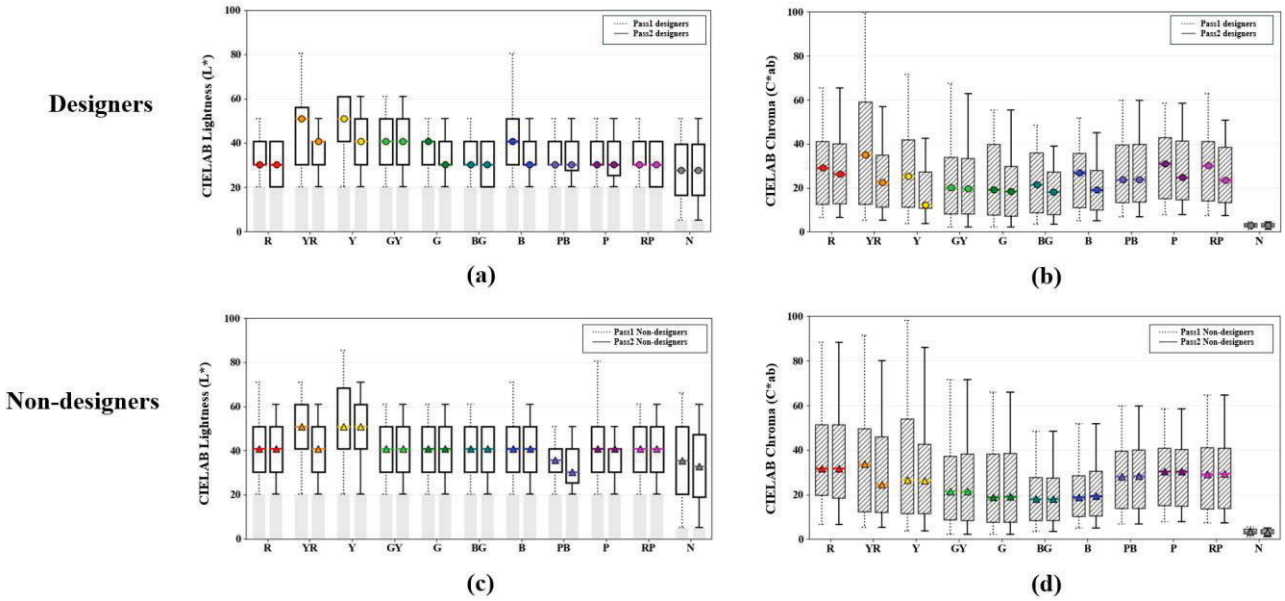

Figure 5: Two-pass comparison of CIELAB lightness (L*, left) and chroma (C*ab, right) values selected as *dark-colour* (a–b) Designers; (c–d) Non-designers
Boxes represent distributions; coloured points indicate medians. Pass *1* ranges are shown as dotted lines, and *Pass 2* ranges as solid lines. The shaded fill beneath each box extends from the minimum value to L* = 0, visually indicating the theoretical dark region.

Qualitative insights

The interview analysis (Fig. 6) suggests that participants relied on different assumed cues when categorizing colours as dark-colour. Designers often described dark-colour in terms of either reduced lightness or increased saturation at low lightness, implying an assumption that these two dimensions could compensate for one another. Non-designers, by contrast, more frequently referred to situational or relational conditions, assuming that contextual contrast or a colour's visual prominence could determine whether it was considered dark-colour. Sources of uncertainty also diverged: designers pointed to the difficulty of reconciling multiple criteria, whereas non-designers almost uniformly assumed that hue exerted a decisive influence. These qualitative patterns indicate how each group constructed working assumptions about what dark-colour entails, shaping the variability reflected in their quantitative selections.

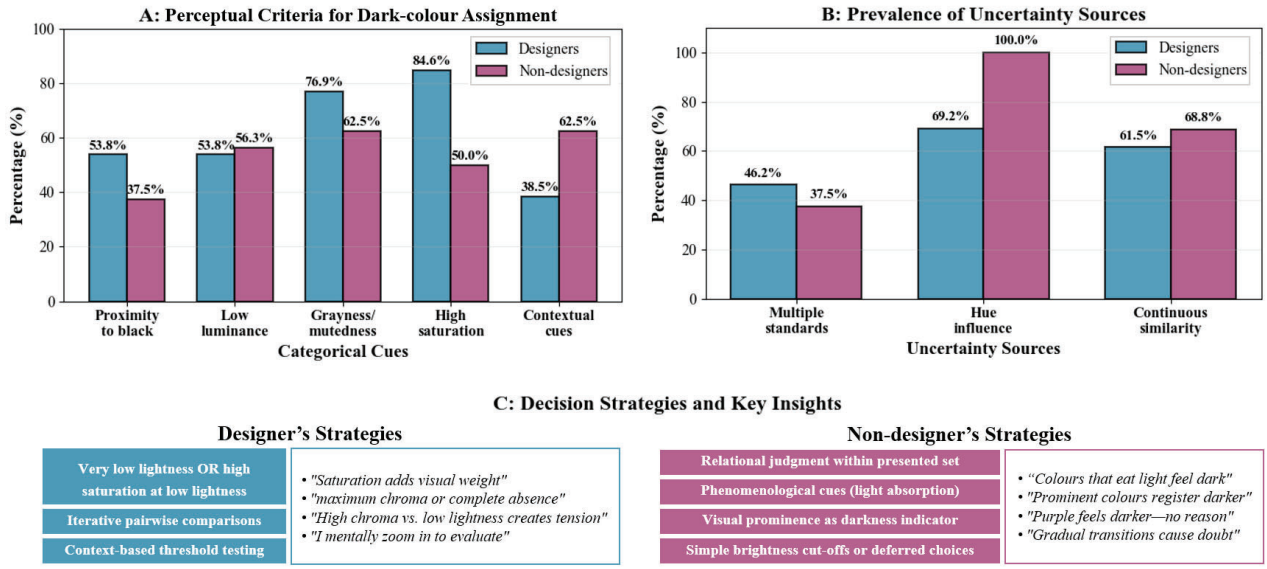

Figure 6: Post-selection interview analysis revealing thematic differences: (A) Perceptual criteria employed, (B) Uncertainty sources encountered, (C) Decision-making strategies utilized by designers (blue) and non-designers (purple)

DISCUSSION

A central outcome of the study is that hue consistently influenced the boundaries of the dark-colour category. Warm hues tended to admit higher L* values, whereas cooler hues required lower thresholds, indicating that perceptual asymmetries shaped judgments across participants. This pattern aligns with the Helmholtz-Kohlrausch effect, where chroma amplifies brightness perception, but it also shows that categorical use of dark remains systematically modulated by hue [9].

Within this hue-dependent structure, expertise introduced further variation. Designers showed a tendency to coordinate lightness and chroma through rule-like criteria, which was associated with relatively stable judgments across contexts. This approach appeared to permit high chroma at low lightness as a legitimate route to dark-colour, a nuance rarely highlighted in prior literature. Non-designers, by contrast, more often relied on relational salience within the presented set, consistent with similarity-based accounts of categorization [10]. These contrasting strategies suggest that expertise moderates how categorical rules are applied rather than replacing perceptual constraints.

Uncertainty was most pronounced when hue-driven tendencies conflicted with absolute thresholds, indicating that judgments of dark are negotiated between sensory input and cognitive strategy. For design communication, this highlights that perceptual categories are contingent on both visual physiology and professional convention. Recognizing such contingencies is critical for bridging the gap between design intent and end-user interpretation, particularly in contexts where dark carries symbolic or affective weight.

CONCLUSION

This study suggests that dark colour perception is better described as a hue-modulated region in lightness-chroma space, shaped by both shared perceptual tendencies and group-specific strategies. Across participants, low lightness emerged as a consistent cue, while the relative influence of chroma and contextual salience varied between designers and non-designers. The two-pass method proved useful for capturing not only approximate thresholds but also the heuristics that informed them, providing a more comprehensive view of how dark-colour is assigned. These findings extend theoretical models of colour categorization by positioning dark-colour as a multidimensional construct in which expertise plays a modulatory role. Practically, the results offer hue-specific guidance for constructing dark palettes and underscore the need to anticipate potential gaps between professional and lay interpretations. Future work could examine how these dynamics unfold across material variation, adaptive viewing environments, and cultural framings of dark.

REFERENCES

[1]. Hagtvedt, H. (2016). The influence of product color on perceived weight and consumer preference. In M. D. Groza & C. B. Ragland (Eds.), Marketing challenges in a turbulent business environment (p. 25). Springer International Publishing.

[2]. Cho, J. Y., & Suh, J. (2020). Spatial color efficacy in perceived luxury and preference to stay: An eye-tracking study of retail interior environment. Frontiers in Psychology, 11, 296.

[3]. Yu, Q., & Nagai, Y. (2020). A new approach to teaching emotional design. Social Sciences, 9(11), 210.

[4]. Wu, F.-G., Chang, E., & Chen, C.-H. (2009). Depressive tendency of design major freshman students explored through the use of color in mosaic creations. The Arts in Psychotherapy, 36(4), 185–190.

[5]. Kremkow, J., Jin, J., Komban, S. J., Wang, Y., Lashgari, R., Li, X., Jansen, M., Zaidi, Q., & Alonso, J.-M. (2014). Neuronal nonlinearity explains greater visual spatial resolution for darks than lights. Proceedings of the National Academy of Sciences, 111(8), 3170–3175.

[6]. Su, Y., Shi, Z., & Wachtler, T. (2024). A Bayesian observer model reveals a prior for natural daylights in hue perception. Vision Research, 220, 108406.

[7]. Divers, E. (2023). Theory to practice: Pleasure-arousal-dominance (PAD) theory for architectural color design. Color Research & Application, 48(5), 445–452.

[8]. Paglierani, P., Liberini, S., Rizzi, A., & Valan, F. (2020). Graphical interpolation of Munsell data. Cultura e Scienza del Colore – Color Culture and Science Journal, 2(12), 21–30.

[9]. Hampton, J. A., Estes, Z., & Simmons, C. L. (2005). Comparison and Contrast in Perceptual Categorization. Journal of Experimental Psychology: Learning, Memory, and Cognition, 31(6), 1459–1476.

[10]. Donofrio, R. L. (2011). Review paper: The Helmholtz-Kohlrausch effect. Journal of the Society for Information Display, 19(10), 658–664.

Color Measurement of Translucent Liquid Materials Using A Noncontact 2D Colorimetric System with Dome Illumination

Hiroyuki Iyota [a*], Mei Higuchi [a], Ayumu Kinugawa[a], Hayato Masuda[a], and Hideki Sakai[b]

[a]Graduate School of Engineering, Osaka Metropolitan University, Osaka, Japan
[b]Graduate School of Human Life and Ecology, Osaka Metropolitan University, Osaka, Japan
[*]Corresponding author: Hiroyuki Iyota, h-iyota@omu.ac.jp

ABSTRACT

Various translucent liquid sauces are commonly used to enhance the flavor and visual appeal of food served in trays. Similarly, translucent paints are widely applied in industrial products. These transparent or semi-transparent layers play a crucial role in determining the visual appearance of objects, whether in culinary or industrial contexts. The color of such liquid materials is typically evaluated by measuring their absorption spectra as light passes through a container. However, conventional contact-type colorimeters cannot perform two-dimensional color measurements of translucent materials, such as sauces coated on food or trays. To address this limitation, we developed a photographic device that integrates an optical trap with dome-shaped illumination, enabling noncontact measurement of two-dimensional color distribution. In this setup, the object is evenly irradiated with diffuse light from the inner wall of the dome. An automatic movable optical trap selectively blocks part of the irradiated light. Images are captured using a digital camera while the trap is moved, and the pixel values with minimum and maximum brightness are combined from all images. This process generates two-dimensional images of the sample that exclude or include specular reflection (specular component excluded (SCE) /specular component included (SCI)) —without physically contacting the liquid surface. The SCE image can then be used to measure the apparent color of the liquid material. In this study, we used a specially designed tray featuring a two-tone (black and white) bottom with four depth levels. A translucent liquid sample was placed in the tray and photographed under dome illumination. Both SCE and SCI images were acquired. The SCE images were then used to quantify the apparent sRGB color values of the liquid, capturing the effect of the tray's bottom color. Using these color values, the characteristic optical properties of the translucent liquid were calculated based on Kubelka–Munk theory. This model assumes a parallel-plate light source, which corresponds to the lighting conditions at the center of the dome illumination system used in this study.

Keywords: noncontact colorimetry, wetted surface, Kubelka–Munk theory, food processing, coating film

INTRODUCTION

Various semi-transparent liquid materials exist, including pre-dried translucent paints, food sauces that enhance both flavor and appearance, and the glossy surfaces of frozen desserts. These transparent layers play a crucial role in determining the visual appeal of objects, from cooked foods to industrial products. Traditionally, the color of such translucent liquids is evaluated by measuring their absorption spectra as light passes through a container. This method requires specialized equipment designed for liquid samples and typically provides only spatially averaged color values. However, accurately measuring the colors of objects coated with translucent liquids remains challenging, as contact-type colorimeters are not suitable for two-dimensional color measurements of semi-transparent materials applied to substrates, such as sauces spread on plates.

To address this limitation, we previously developed a dome-shaped lighting device and demonstrated several of its applications [1]–[5]. This device integrates a movable optical trap within an integrating sphere, allowing a digital camera to capture images of objects placed inside the dome. When the surface of the object

is wet, specular reflections from the dome illumination appear. By combining the lowest-brightness pixels from multiple images, it is possible to generate a two-dimensional image in which specular reflections are effectively eliminated. Additionally, including a color chart within the captured frame enables accurate two-dimensional color acquisition without physical contact.

In this study, we propose a practical application of this device: quantifying the color characteristics of semi-transparent liquids using specially designed containers with varying depths and two different bottom colors (white and black). These containers allow simultaneous acquisition of multiple depth levels and both bottom colors in a single image, greatly simplifying the measurement process. By systematically filling the containers with liquid and capturing images, both specular component-excluded (SCE) and specular component included (SCI) images were obtained. The SCE images were used to evaluate the apparent sRGB color of the semi-transparent liquids, accounting for the combined influence of container depth, liquid color, and bottom color. These effects were then analyzed based on the image data. Furthermore, Kubelka–Munk theory was applied to estimate the scattering and absorption coefficients of the liquids, assuming a parallel-plate light source corresponding to the dome illumination conditions. The influence of liquid depth and color on optical properties was examined, demonstrating the feasibility and practical advantages of this approach.

METHODOLOGY

The imaging device used in this study was a modified version of the previously reported dome-shaped lighting system [5]. Several improvements were made to enhance performance: the light trap was replaced with a real black sheet to achieve near-ideal light absorption, and the LED illumination was upgraded to a high–color-rendering Ra95, 6500 K LED. While the basic structure remained the same as in earlier reports, additional details will be presented by A. Higuchi at the AIC2025 conference [6].

For this study, a new container was designed and fabricated. The outer dimensions were 36 mm × 126 mm, and the inner dimensions were 30 mm × 120 mm, forming a rectangular shape. The container included four depth levels, ranging from approximately 1 mm to 4 mm. At each depth level, white and black resin sheets (15 mm × 30 mm, 0.5 mm thick) were affixed to the bottom surface to serve as contrasting background substrates.

As test samples, four colors of watercolor paint were used: Blue (W292, Ultramarine Lite), green (W067, Permanent Green No. 1), and red (W011, Carmine) — all obtained from Holbein Art Materials Inc., Japan. The paint solutions were prepared to ensure that the effect of the bottom color would be clearly visible when placed in the container.

Under dome illumination, twelve images were captured while moving the light trap [5], enabling the generation of both SCI and SCE images. From each depth region, a central area of approximately 10 mm in diameter (30 × 30 pixels) was selected, and the average sRGB values were calculated separately for the white and black bottom regions.

The apparent sRGB values obtained from the SCE image of the entire container were then converted to CIE XYZ values according to CIE/JIS standards. Using Kubelka–Munk theory [7], which assumes a parallel-plate light source consistent with the dome illumination used in this study, the absorption coefficient (K) and scattering coefficient (S) for each depth level were calculated using equations (1) and (2).

$$\frac{S+K}{S} = a,\ \sqrt{a^2-1} = b \tag{1}$$

$$R_X = \frac{j}{i} = \frac{1 - R_g(a - b\coth bSX)}{a + b\coth bSX - R_g} \tag{2}$$

Where:

i: Light flux passing through an infinitesimal thickness dx in the direction toward the bottom surface.

j: Light flux passing through an infinitesimal thickness dx in the direction toward the liquid surface.

X: Thickness of the liquid layer.Rx: Apparent reflectance of the object, calculated from the sRGB values of the SCE image containing the colored liquid sample.

Rg: Reflectance of the two bottom surfaces (white and black), calculated from the sRGB values of the SCE image with pure water.

Using Eq. (1) and Eq. (2), separate cases for the white and black bottom surfaces were formulated. The absorption coefficient (K) and scattering coefficient (S) were then determined by solving the resulting simultaneous equations, using the measured Rx and Rg data.

RESULTS AND DISCUSSION

Figure 1 shows examples of the captured images. Figure 2 presents the sRGB values extracted from these images, plotted as a function of liquid thickness for both the white and black bottom surfaces.

From the SCE image results, the effect of liquid thickness on the apparent sRGB values was more pronounced for the white bottom surface (Figure 2b) than for the black bottom surface (Figure 2a). For the black bottom (Figure 2a), the R value of the solution color increased with increasing thickness, whereas the G and B values remained low (below 30) and showed minimal change.

In contrast, with the white base (Figure 2b), the R value was relatively high (approximately 225) at a depth of 1 mm and gradually decreased as the thickness increased. The R value remained significantly higher than the G and B values across all depths, indicating a strong contribution from reflection off the white bottom surface.

Furthermore, a comparison of the SCI and SCE images (Figures 2a/2b vs. 2c/2d) revealed that the differences in RGB values were more pronounced for the black bottom surface than for the white bottom surface. This finding suggests that, under dome-shaped lighting, objects with lower reflectance (i.e., darker surfaces) are more influenced by specular reflections, which are captured in the SCI images but effectively removed in the SCE images.

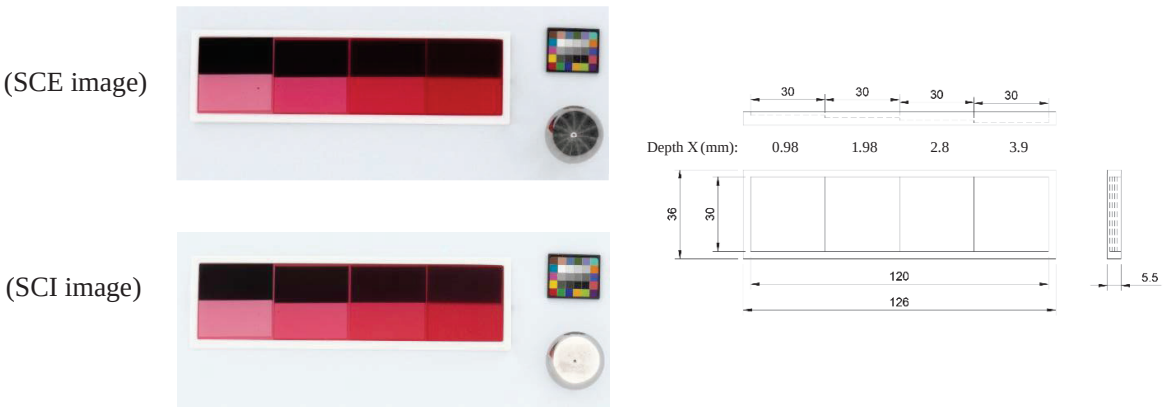

Figure 1: SCE and SCI images of red-colored translucent water prepared with watercolor paint, along with details of the newly developed container

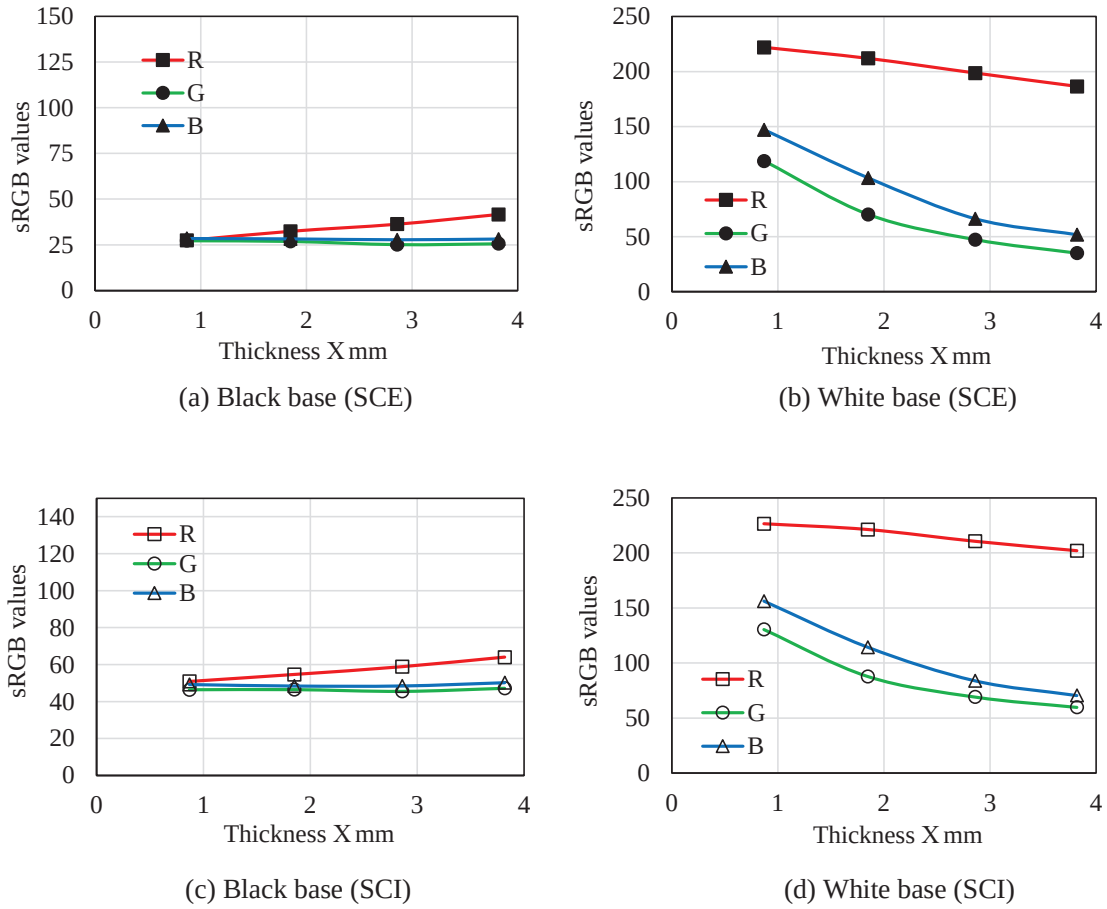

Figure 2: sRGB values obtained from SCE and SCI images for liquid depths of approximately 1–4 mm with white and black bottom surfaces (red-colored solution)

Figures 3(a) and 3(b) show the calculated absorption coefficient (K) and scattering coefficient (S) of the red-colored solution at each depth, based on the tristimulus values (XYZ) converted from the sRGB values obtained from the SCE images.

For the X component, which corresponds to the red channel, the absorption coefficient K was lower than for Y and Z. The scattering coefficients for X, Y, and Z were all relatively low, with the X value being roughly half that of Z and remaining nearly constant regardless of depth.

For Y and Z, both K and S generally decreased with increasing liquid thickness. The differences in K values between 2 mm and 3 mm depths were less than 0.1 for all XYZ components, while thinner layers showed a stronger tendency toward increased K values.

These results suggest that the accuracy of thickness measurement has a relatively greater impact when the liquid layer is thin. This sensitivity may explain some of the observed variations, and additional investigation is needed to validate this effect.

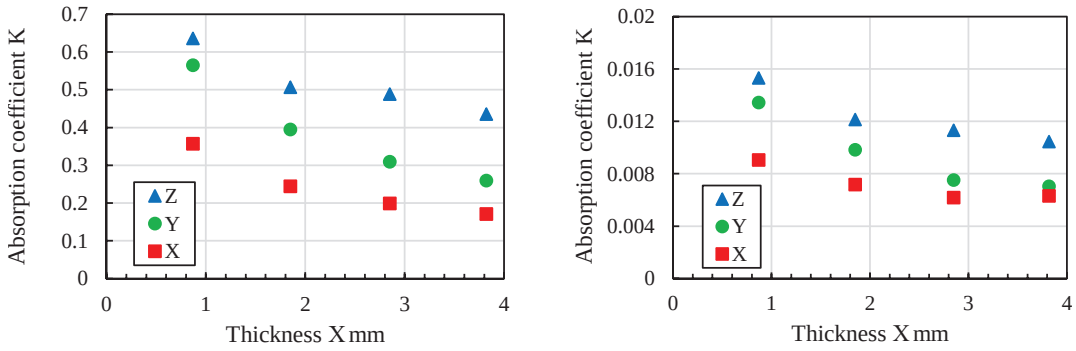

(a) Absorption coefficient K (b) Scattering coefficient S

Figure 3: *K* and *S* calculated using Kubelka–Munk theory (Eqs. 1–2) based on the *X*, *Y*, and *Z* values converted from the sRGB values of the SCE images for liquid depths ranging from 1 to 4 mm (red-colored solution)

CONCLUSION

In this study, we proposed a practical method for acquiring the color characteristics of semi-transparent liquids by combining a dome-shaped imaging device with a specially designed multi-depth container. Using this container, we could quantify the apparent sRGB values of semi-transparent liquids directly from captured images, accounting for both bottom color and liquid depth.

Both SCI and SCE images exhibited similar trends in how liquid depth affected the sRGB values, even though this effect was more pronounced when the bottom surface was white. Additionally, when the bottom surface was black and the liquid layer was shallow, the difference between SCI and SCE values became more significant.

From the SCE images, the apparent sRGB values were converted to CIE XYZ values, and Kubelka–Munk theory was applied to estimate the absorption coefficient (K) and scattering coefficient (S) for each depth. The results showed that the differences in K values between 2 mm and 3 mm depths were less than 0.1 for all XYZ components.

This work demonstrates a simple and efficient method for evaluating the color characteristics of semi-transparent liquids using a dome-shaped imaging system and a specially designed container. Future work will focus on automating the imaging process for improved measurement efficiency and enabling long-term, time-series monitoring of color changes in moisture-containing samples.

REFERENCES

[1]. Iyota, H., Sakai, H., and Mamiya, T. (2013). Color Measurement Methods for Optimization of Oven Operation (Baking of Sliced Bread with Superheated Steam and Hot Air). Food Science and Technology Research, 19(6), 939-947.

[2]. Sakai, H., Isomi, M., and Iyota, H. (2018). Non-Contact Colorimetric Measurement Using Dome Illumination for Complex Shape Objects. Proc. of the 4th Asia Color Association Conference, Chiang Mai, Thailand.

[3]. Hirouchi, A., Iyota, H., Isomi, M., Yamamoto, H., & Sakai, H. (2019). Automatization of 2D-Image Recording System for Analysis of Change in Food Appearance using Dome Illumination with Digital Camera. Proc. of the 5th Asia Color Association Conference, Nagoya, Japan.

[4]. Fukagawa, S., Iyota, H., Sakai, H., & Isomi, M. (2021). Development of color and gloss measurement system with wide range temperature and humidity control unit. AIC 2021 Congress, Milan, Italy.

[5]. Kinugawa, A., Iyota, H., Fukagawa, S., Masuda, H., & Sakai, H. (2021). Observation of color and gloss change during thawing of foods using a non-contact 2D measurement system with a digital camera. Proc. of the 6th Asia Color Association Conference, Yogyakarta, Indonesia.

[6]. Higuchi, M., Yamamoto, S., Kinugawa, A., Iyota, H., Imakoma, H., & Sakai, H. (2025). Observation of Color and Gloss Change during Drying of Particulate Suspension in Polymer Solution Using a Noncontact 2D Colorimetric System with Dome illumination, AIC 2025 Congress, Taipei, Taiwan.

[7]. Kubelka, P., Munk, F.,(1931). Ein Beitrag zur Optik der Farbanstriche. , Z. tech. Physik, 12, 593-601.

Exploring Word–Colour Associations among Koreans and Foreign Residents in Korea

Junglim Lee[a*], and YungKyung Park *

[a] Ewha Womans University, Seoul, Republic of Korea

[*]Corresponding author: YungKyung Park, yungkyung.park@ewha.ac.kr

ABSTRACT

This study examines how Koreans and foreigners living in South Korea associate colours with culturally significant words, offering insight into how meaning-making is shaped by culture and immersion in a globalized context. Using a psychophysical approach to word–colour association, the study focused on the words "Korean traditional" and "Korea." Thirty female participants (15 Koreans and 15 foreigners, aged 20–40, all students at Ewha Womans University) selected three colours per word using an on-screen picker, rated the strength of each association (0–100), and provided short explanations. In total, 180 colours were recorded in RGB, converted to CIELAB values, and analyzed for palette similarity using ΔE_p values. Explanations were categorized into object-based, experience-based, and symbolic/conceptual associations. Results showed strong cross-cultural contrasts: Koreans relied predominantly on symbolic frameworks, linking colours to traditions such as obangsaek, dancheong, and the national flag, while foreigners favoured brighter, more varied palettes, leaning more on experiential associations. Cultural immersion further shaped responses: short-term residents drew more on experience and perceptual cues, whereas long-term residents increasingly adopted symbolic meanings consistent with Koreans. These findings demonstrate that colour associations are culturally mediated rather than universal, with symbolic frameworks gaining strength through immersion. The study contributes to cross-cultural colour research and offers broader implications for design, communication, and cultural studies by showing how colour meanings evolve through cultural contact and adaptation.

Keywords: word-color association, cross-cultural, symbolism, semantics, immersion

INTRODUCTION

Colour functions as more than a visual sensation; it serves as a medium through which meaning, identity, and cultural values are expressed. One of the key ways cultural meaning is communicated is through associations between words and colours. People often connect colours with experiences and memories: a particular hue can evoke a familiar object, material, individual, historical period, or geographic region. This phenomenon, broadly described as colour association, operates in two directions, as colours can trigger concepts just as concepts can call to mind particular colours [1].

Scholars have long emphasized that colour associations are multi-layered, extending beyond immediate perception. Colour experience cannot be reduced to sensory impressions but is structured by the conceptual categories through which individuals interpret the world [2]. In this sense, colours are not only perceived but also understood and classified within broader cultural and cognitive frameworks.

Foundational studies established that colours often carry affective meanings across cultures [3]. Other research

emphasized that preferences and associations are grounded in people's interactions with colour-diagnostic objects in their environment [4]. More recent findings have demonstrated that even abstract and intangible concepts are strongly tied to specific colours [5]. Large-scale psychophysical and cross-cultural investigations have also revealed that while some associations are widely shared, significant variation arises between cultural groups, reflecting the influence of local practices, traditions, and symbolic systems [6,7,8]

In today's globalized world, these issues are particularly relevant in Korea. The spread of Hallyu (the Korean Wave) has made Korean culture highly visible worldwide, and many foreigners are relocating to Korea to study, work, or live. This raises an important question: how do foreigners in Korea associate colours with culturally embedded words compared to local Koreans? The purpose of this study is to explore this question by examining colour associations for the words "Korean traditional" and "Korea." Colour palettes were constructed from the colours selected by the two groups, and visual similarities and differences were analyzed both within and between groups using ΔE_p values. In addition, participants' explanations were categorized into object-based, experience-based, and symbolic/conceptual-based associations. Through this dual quantitative and qualitative approach, the study explores how cultural background and immersion shape the interpretation and transmission of colour meaning in a globalized context.

METHODOLOGY

This study employed the psychophysical approach to word–colour association described by Chen et al [6]. Thirty female students from Ewha Womans University (15 Koreans and 15 foreigners residing in South Korea, aged 20–40) participated. All reported normal colour vision and passed the Ishihara test.

Two stimulus words were chosen: "Korea (한국)" and "Korean Traditional (전통적인)". Korean participants viewed the words in Korean, while foreign participants were presented with English translations. English was used consistently for the foreign group, as all demonstrated adequate academic proficiency.

Two stimulus words "Korea (한국)" and "Korean Traditional (전통적인)" were presented in Korean to Korean participants and in English to foreigners, who demonstrated sufficient English proficiency. Each participant completed the task individually on a laptop. For each word, they selected three colours using an on-screen picker, rated the strength of association (0–100), and provided a brief explanation of their choice. In total, 180 colour responses (30 participants×3 colours×2 words) were collected, recorded in RGB, and converted to CIELAB values for analysis. Palette similarities were analyzed using ΔE_p values following Pan and Westland (2018). Unlike Chen et al. (2018), this study also analyzed participants' textual explanations, which were categorized into object-based, experience-based, and symbolic/conceptual-based associations to provide qualitative insight into cultural and cognitive processes.

RESULTS AND DISCUSSION

The first colours selected by Korean and foreign participants for "Korean traditional" and "Korea" are illustrated in Figure 1. For the word "Korean traditional" (left), two distinct palettes emerge. The Korean palette (left) consists of a wide range of deep, muted, and earthy hues, including greens, blues, browns, yellows, and dark reds. These colours are strongly tied to traditional materials and symbolic frameworks such as "obangs (five cardinal colours)" and natural pigment traditions commonly observed in "dancheong (architectural decoration)." In contrast, the foreigners' palette (right) is narrower but dominated by bright, saturated, and high contrast colours, such as pink, orange, vivid red, yellow, black, and purple. These vivid tones suggest that foreigners perceive "Korean traditional" primarily in terms of visual impact rather than symbolic depth, emphasizing perceptual brightness over cultural meaning. Overall, the comparison highlights how Koreans interpret tradition through culturally embedded symbolic colour systems, while foreigners rely more on surface-level impressions of vibrancy and contrast.

Figure 1: 1st choice colours selected for the words "Korean traditional" (left) and "Korea" (right) by Korean participants (left columns) and foreign participants living in Korea (right columns).

For the word "Korea" (right), two different palettes were again produced by the two groups of participants. However, unlike with "Korean traditional," the palettes for "Korea" show greater resemblance between Koreans and foreigners in their colour choices. Koreans primarily selected strong, saturated reds and blues along with black, resulting in a concentrated palette that strongly reflects the colours of the Korean national flag. In contrast, the palette chosen by foreigners was broader and more varied, incorporating greens, multiple shades of blue (from light cyan to navy), vivid reds, purples, and pinks. These selections highlight perceptual vibrancy and diversity, suggesting that foreigners interpret "Korea" through visually striking impressions and personal experiences in the country, rather than through the symbolic uniformity emphasized by Koreans. Figure 2 presents the full set of colour palettes, showing all three colours selected by participants for each word.

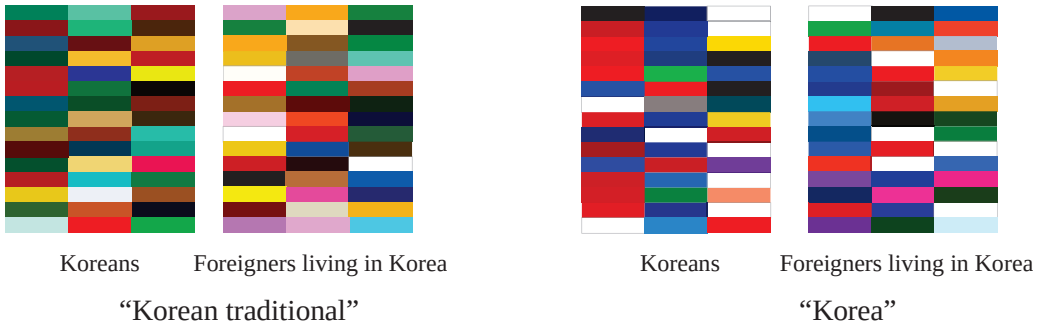

Figure 2: All 3 colours selected for the words "Korean traditional" (left) and "Korea" (right) by Korean participants (left columns) and foreign participants living in Korea (right columns).

Table 1: Visual colour differences ΔE_p within a palette

Word	Koreans	Foreigners living in Korea
Korean traditional	64.4	68.3
Korea	75.8	87.5

Visual colour differences ΔE_p within a palette is analyzed in Table 1 (where smaller value of ΔE_p indicate more similarity between the two palettes). For "Korean traditional," Koreans produced a palette with a slight lower variability (ΔE_p=64.4) compared to foreigners (ΔE_p =68.3), indicating a somewhat stronger consensus among Koreans in their colour choices. For "Korea," the differences were much larger, with Koreans again showing a more cohesive palette (ΔE_p=75.8) than foreigners (ΔE_p=87.5). This suggests that while both groups were less uniform in

their associations for “Korea” than for “Korean traditional,” Koreans still converged more closely on a shared set of colours for the words with Korean cultural values.

Table 2: Visual colour differences ΔE_p between Korean and Foreigner colour palettes

Word	Difference (1st Colour)	Difference (3 colours)
Korean traditional	29.7	14.8
Korea	16.1	10.1

For “Korean traditional,” the difference between Koreans and foreigners was relatively large (ΔE_p = 29.7 for the first colour; 14.8 for all three colours). This reflects the distinctly different palettes observed in Figure 1, with Koreans selecting muted, earthy tones and foreigners preferring bright, high contrast colours. By contrast, for “Korea,” the difference between the two groups was smaller (ΔE_p = 16.1 for the first colour; 10.1 for all three colours), suggesting that their palettes showed more overlap. This indicates that while cultural perspectives diverge sharply in interpreting “Korean traditional,” there is greater convergence in the colours associated with “Korea,” likely due to the strong symbolic influence of the national flag and widely shared visual impressions.

Table 3: Mean strength of association reported by participants

Word	Koreans (1st colour)	Koreans (3 colours)	Foreigners (1st colour)	Foreigners (3 colours)
Korean traditional	71.7	66.4	77.0	68.3
Korea	83.6	78.2	78.1	70.6

For “Korean traditional,” foreigners reported a slightly higher mean strength of association (77.0 for the first colour, 68.3 for all three colours) compared to Koreans (71.7 and 66.4, respectively). This suggests that foreigners expressed more confidence in their selections, despite their palettes being more perceptually vivid and less symbolically grounded, likely reflecting efforts to engage with and learn about the history and culture of a new country. For “Korea,” however, Koreans showed the strongest associations (83.6 for the first colour, 78.2 for all three), exceeding foreigners (78.1 and 70.6). This reflects a clearer symbolic connection for Koreans, as their colour choices aligned with the national flag and other shared cultural markers. Overall, the results suggest that while foreigners felt strong associations with “Korean traditional,” Koreans demonstrated deeper symbolic connections with “Korea.”

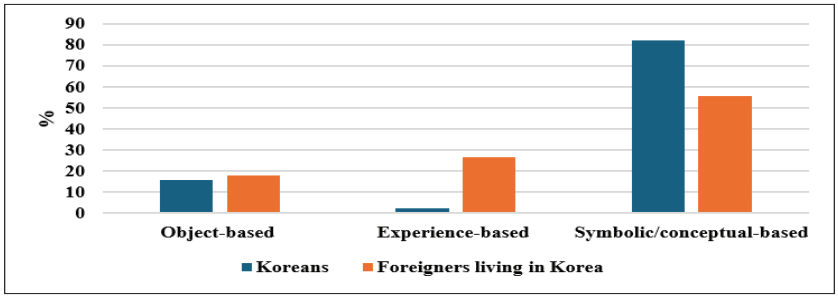

Figure 3: Colour association of Koreans and Foreigners living in Korea to the word "Korea"

Explanations for colour choices were classified into object-based, experience-based, and symbolic/conceptual associations. For “Korea,” Koreans relied predominantly on symbolic/conceptual associations (over 80%), with 92%

of these referencing the national flag. Object-based associations were moderate (about 15%) and experience-based responses were nearly absent, indicating a strong dependence on shared symbolism rather than personal experience. Foreign participants, by contrast, showed a more balanced distribution: symbolic/conceptual associations accounted for around 55%, experience-based for 27%, and object-based for 18%. Their greater use of experience-based reasoning suggests stronger reliance on individual memories and personal encounters with Korea.

Overall, these findings highlight distinct cultural orientations in colour association. Koreans tend to interpret colour predominantly through shared symbolic and conceptual frameworks, while foreigners display a more diversified approach that balances symbolic, experiential, and object-based associations. Interestingly, although Koreans were born and raised in Korea and thus possess extensive lived experience with the country, their colour choices do not primarily reflect personal or experiential associations. Instead, they draw heavily on culturally embedded symbolic systems, suggesting that collective symbolic meanings exert stronger influence than individual experience in shaping colour associations for Koreans.

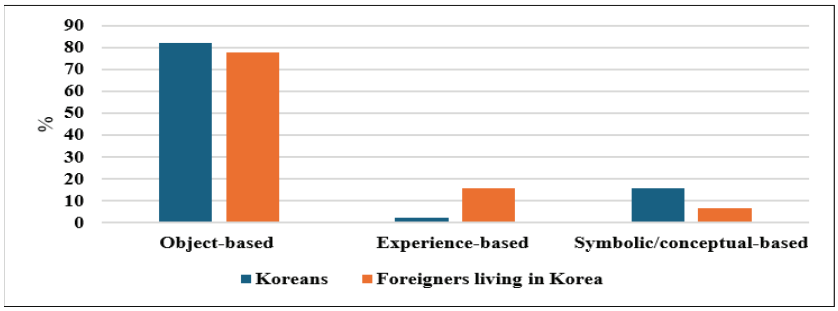

Figure 4: Color association of Koreans and Foreigners living in Korea to the word "Korean traditional"

Figures 4 shows that for “Korean traditional,” both groups showed a strong preference for object-based associations, with Koreans at over 80% and foreigners at about 78%. Koreans relied secondarily on symbolic/conceptual meanings (16%), while foreigners more often drew on personal experiences (16%) and used symbolic associations less frequently (6%). Overall, both groups linked colours mainly to tangible objects, but Koreans leaned more toward symbolic frameworks, whereas foreigners incorporated more experiential reasoning.

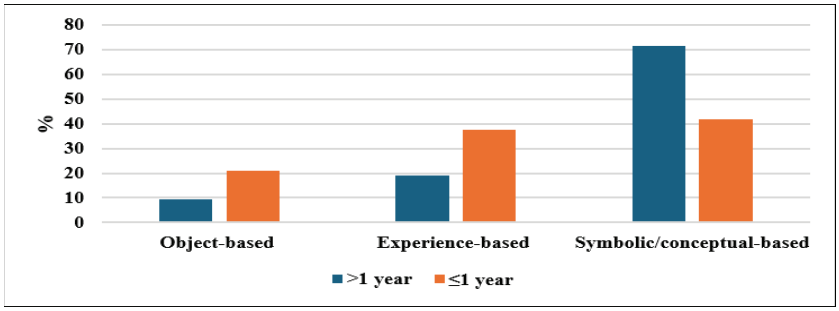

Figure 5: Categories of colour association of foreigners living in Korea to the word "Korea"

Figure 5 shows how foreigners’ colour associations with “Korea” differ by length of residence. Long-term residents (>1 year) relied mainly on symbolic/conceptual associations (over 70%), reflecting deeper integration into Korean symbolic frameworks, while experience-based (18%) and object-based (under 10%) responses were less common. Short-term residents (≤1 year), however, used a more even mix: symbolic (41%), experience-based (38%), and object-based (20%). These results suggest that short-term residents draw more on personal experiences and visible objects, whereas longer-term residents increasingly adopt symbolic meanings similar to those of Koreans.

Overall, the findings highlight that colour associations are shaped by cultural knowledge and exposure, shifting with immersion from experiential and perceptual bases toward culturally shared symbolic frameworks.

Taken together, these findings indicate that color associations are not universal but are shaped by cultural knowledge, exposure, and lived experience. Koreans rely on shared symbolic codes, foreigners initially rely on experience and perception, and with time, foreigners' strategies converge toward the symbolic orientation characteristic of native Koreans. This progression highlights the dynamic interplay between cultural immersion and the construction of meaning in color association.

CONCLUSION

This study demonstrates that colour–word associations are not only perceptual or individual phenomena but are fundamentally shaped by cultural frameworks and the degree of cultural immersion. Koreans predominantly interpret colours symbolically, reflecting long-standing traditions and collective meanings, while foreigners initially rely more on experiential and object-based strategies rooted in personal encounters. With prolonged residence in Korea, however, foreigners gradually shift toward symbolic and conceptual associations, aligning more closely with the interpretive patterns of Koreans. These findings highlight the dynamic and adaptive nature of colour association, showing how cultural exposure fosters the internalization of shared symbolic systems. By combining quantitative palette analysis (ΔEp) with qualitative categorization of explanations, this study also provides a framework for future mixed-method research. Further work could refine these categories and expand the sample to include more diverse demographics, while also exploring more deeply the transition from experiential to symbolic associations. Such research would offer a richer understanding of how colour associations develop in cultural contexts and how they evolve through processes of immersion and adaptation.

REFERENCES

[1]. Kress, G., & Van Leeuwen, T. (2002). Colour as a semiotic mode: Notes for a grammar of colour. Visual communication, 1(3), 343

[2]. Peacocke, C. (1984). Colour concepts and colour experience. Synthese, 58(3), 365-381.

[3]. Adams, F. M., & Osgood, C. E. (1973). A cross-cultural study of the affective meanings of color. Journal of cross-cultural psychology, 4(2), 135-156.

[4]. Palmer, S. E., & Schloss, K. B. (2010). An ecological valence theory of human color preference. Proceedings of the National Academy of Sciences, 107(19), 8877-8882.

[5]. Mohammad, S. M. (2013). Even the abstract have colour: consensus in word-colour associations. arXiv preprint arXiv:1309.5391.

[6]. Chen, Y., Yang, J., Pan, Q., Vazirian, M., & Westland, S. (2020). A method for exploring word-colour associations. Color Research & Application, 45(1), 85-94.

[7]. Tham, D. S. Y., Sowden, P. T., Grandison, A., Franklin, A., Lee, A. K. W., Ng, M., ... & Zhao, J. (2020). A systematic investigation of conceptual color associations. Journal of Experimental Psychology: General, 149(7), 1311.

[8]. Hupka, R. B., Zaleski, Z., Otto, J., Reidl, L., & Tarabrina, N. V. (1997). The colors of anger, envy, fear, and jealousy: A cross-cultural study. Journal of Cross-Cultural Psychology, 28(2), 156–171.

[9]. Pan, Q., & Westland, S. (2018). Comparative evaluation of color differences between color palettes. In Color and Imaging Conference (Vol. 26, pp. 110-115). Society for Imaging Science and Technology.

Reevaluating Brightness Perception: An Empirical Examination of Melanopsin's Influence

Nozomu Mori, Mizuki Takikawa, Marina Saito, Sei-ichi Tsujimura*

Graduate School of Design and Architecture, Nagoya City University, Nagoya, Japan
*Corresponding author: tsujimura@sda.nagoya-cu.ac.jp

ABSTRACT

Brightness perception is a fundamental aspect of human vision. Traditionally, it has been understood through the concept of luminous efficiency, derived from the linear summation of L- and M-cone sensitivities. This model, adopted by the CIE, is derived through flicker photometry and defines luminance using spectral power distributions and the luminous efficiency function. However, such models do not consider the potential contributions of S-cones and melanopsin-expressing intrinsically photosensitive retinal ganglion cells (ipRGCs, hereafter referred to as melanopsin cells), thus potentially oversimplifying the neural basis of brightness perception.

The human retina contains three major types of photoreceptors: rods, cones, and melanopsin cells. Under photopic conditions, rods are largely excluded, while cones and melanopsin cells remain active. Cones are subdivided into L-cones, sensitive to long wavelengths; M-cones, sensitive to middle wavelengths; and S-cones, sensitive to short wavelengths. Melanopsin cells, discovered around 2000, are well known for their roles in non-image-forming functions such as circadian rhythm regulation and the pupillary light reflex. More recently, they have also been shown to contribute to brightness perception.

Given the increasing interest in comprehensive models of brightness perception, this study aims to quantify the contributions of L-, M-, and S-cones, as well as melanopsin photoreceptors, in humans (Fig.1.). We developed a multi-primary stimulation system that enables silent substitution, a technique that allows selective stimulation of one photoreceptor type while keeping the others constant. This method is grounded in the principle of univariance, which ensures that visual responses are determined solely by the level of photoreceptor stimulation rather than the spectral composition of the stimulus. For melanopsin-specific stimuli, metameric pairs were employed to maintain photometric equivalence of cone stimulations across conditions.

In the experiment, we presented a white control stimulus and varied each photoreceptor's stimulation. Ten color-normal observers aged 21–26 participated in a two-interval forced-choice (2IFC) task. Observers indicated which of the two temporally presented lights appeared brighter. The method of constant stimuli was used to measure brightness perception. PSE was obtained by fitting logistic psychometric functions and taking the 50% point. At ±5% contrast, increasing L-cone stimulation and decreasing M-cone stimulation produced robust opponent effects on brightness. At ±5% contrast, neither S-cone nor melanopsin modulation produced a clear change in brightness. Together, these findings refine the photoreceptoral basis of brightness. For small changes in receptor contrast, like those tested in this experiment, L- and M-cones exert strong, opponent influences that dominate S-cone input, whereas melanopsin provides a modest facilitatory component that becomes detectable at higher contrasts. These results highlight limitations of models based solely on L+M additivity and argue for brightness formulations that explicitly incorporate cone opponency and melanopsin pathways. Such models could better account for perceptual phenomena, improve ecological validity under natural viewing conditions, and inform applications in lighting, display design, and clinical assessment.

Keywords: brightness perception, melanopsin, luminous efficiency function, photoreceptor stimulation

INTRODUCTION

Brightness perception is a central aspect of human vision, shaping both theories of visual processing and practical domains such as workplace lighting and display evaluation. Traditionally, it has been operationalized via luminous efficiency functions, most notably the photopic V(λ), derived historically with heterochromatic flicker photometry. These functions form a basis of luminance measurement and many photometric standards.

Flicker photometry, however, relies on high temporal frequency stimuli that selectively stimulate L- and M-cones while largely excluding contributions from other photoreceptors, particularly S-cones. This is likely because S-cones cannot respond to such high-frequency stimuli. This methodological constraint has led to models of brightness perception that may underestimate or entirely ignore the influence of these receptors.

Over the last two decades, a growing body of research has drawn attention to melanopsin, a photopigment discovered in ipRGCs around the year 2000. Initially recognized for its role in non-image-forming processes such as circadian photoentrainment and the pupillary light reflex (Freedman et al., 1999), melanopsin is now increasingly implicated in conscious visual perception, including brightness perception (Brown et al., 2012).

Despite these insights, current luminous efficiency models continue to omit melanopsin, and the exact role of S-cones in brightness remains debated. Furthermore, the majority of evidence supporting melanopsin's role comes from mouse studies, which may not generalize to humans due to interspecies differences in retinal circuitry. As a result, empirical quantification of the contributions of S-cones and melanopsin to human brightness perception remains a critical gap in vision science.

The aim of this study was to quantify the contributions of melanopsin and S-cones to brightness perception, including L- and M-cones, in humans. In addition to its practical applications, brightness perception provides a unique window into how the human visual system integrates signals from multiple receptor classes. By examining brightness, researchers can probe the weighting and interactions of photoreceptors, thereby revealing fundamental neural mechanisms of vision. Understanding these contributions is also crucial for developing lighting guidelines that are not only efficient but also comfortable and supportive of human health.

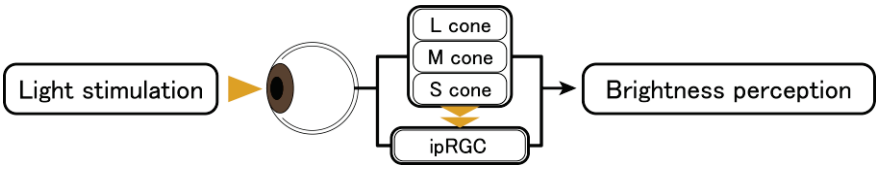

Figure 1 Photoreceptor-based inputs to brightness perception. Light stimulation is detected by L-, M-, and S-cones as well as intrinsically photosensitive retinal ganglion cells (ipRGCs, melanopsin cells), which together contribute to the perception of brightness.

METHODS

To address these questions, we employed a custom-designed multi-primary illumination system, previously developed for photoreceptor-isolating stimulation (Brown et al., 2012). The system used four primaries with peak wavelengths of 633 nm (red), 531 nm (green), 463 nm (blue), and 569 nm (yellow). This arrangement made it possible to modulate the stimulations of L-, M-, and S-cones, as well as melanopsin, independently using the silent substitution technique. The control stimulus was a white light with luminance fixed at 282 cd/m², a level chosen to minimize rod contributions under photopic conditions. This adaptation level was selected to minimize rod contributions under the photopic conditions of the experiment. Cone stimulations were computed using the Stockman & Sharpe cone fundamentals (Stockman & Sharpe, 2000; Stockman, Sharpe, & Fach, 1999), while melanopsin stimulations were estimated from the melanopsin nomogram with a peak of 480 nm.

Participants were ten young adults (aged 21–23 years) with normal color vision. Each participant completed the main experiment in a darkened experimental booth, viewing stimuli monocularly under full-field conditions.

Brightness judgments were measured using a two-interval forced-choice (2IFC) paradigm with the method of constant stimuli. In each trial, participants were sequentially presented with a test stimulus and a reference stimulus and asked to indicate which appeared brighter. In the main experiment, L-, M-, S-cone and melanopsin stimulations were modulated by ±5% (Fig.2).

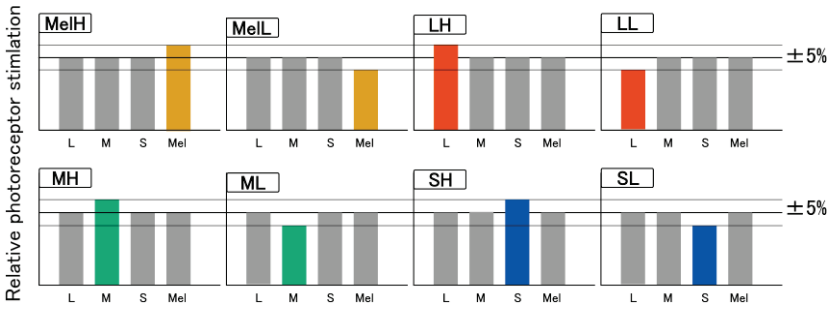

Figure 2 Test stimuli used in the experiment.

Because the effects of S-cone and melanopsin stimulation were small at this modulation level, a supplementary experiment was conducted with a broader range of contrasts (−20%, −10%, −5%, 0, +5%, +10%, +20%). Six participants, again with normal color vision, took part in this additional study. Stimulus presentation was carefully controlled using the calibrated multi-primary system to ensure stable spectral power distributions. The order of trials was counterbalanced across sessions to minimize sequence effects. Each participant underwent a practice session to familiarize themselves with the task before data collection began. Observers were instructed to maintain fixation and to minimize blinking during stimulus presentation, with breaks provided to reduce fatigue.

RESULTS

We first examined perceptual changes in PSE under ±5% modulation of individual cone and melanopsin contrasts (Fig.3). For the L-cone condition, the Wilcoxon signed-rank test revealed a highly significant difference between the ±5% levels ($W = 0$, $p = .002$). A paired-samples t-test confirmed this effect, $t(9) = 9.50$, $p < .001$, Cohen's $dz = 3.00$. Similarly, the M-cone condition showed a robust effect ($W = 0$, $p = .002$; $t(9) = 8.52$, $p < .001$, Cohen's $dz = 2.69$). In contrast, the S-cone condition produced only a weak effect. The Wilcoxon signed-rank test indicated significance ($W = 4.0$, $p = .049$), whereas the paired-samples t-test showed a marginal trend ($t(9) = 2.26$, $p = .051$). Extending the analysis to the full contrast range from −20% to +20% ($N = 6$) did not reveal a significant main effect in repeated-measures ANOVA, $F(6, 30) = 1.89$, $p = .115$ (Fig.4). For melanopsin, no difference was found at ±5% modulation ($W = 8.0$, $p = .688$; $t(5) = -0.58$, $p = .588$, Cohen's $dz = -0.24$). However, when the contrast was varied from −20% to +20% ($N = 6$), a repeated-measures ANOVA revealed a significant main effect, $F(6, 30) = 7.21$, $p < .001$, demonstrating a robust modulation of brightness perception by melanopsin contrast.

Overall, the results indicate that L- and M-cones cause strong opponent effects, melanopsin contributes modestly at higher contrasts, and S-cones show only limited influence under the tested conditions.

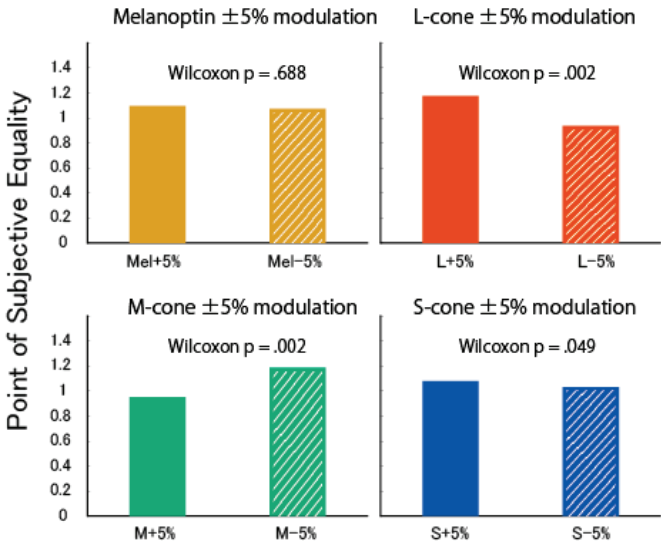

Figure 3. Brightness perception across photoreceptor conditions. Bars show PSEs under high (H) and low (L) stimulation for melanopsin (Mel), L-, M-, and S-cones.

DISCUSSION

The present findings demonstrate that human brightness perception reflects the complementary contributions of multiple photoreceptor classes. L-cones act as strong facilitators of brightness perception, while M-cones exert an inhibitory influence, potentially balancing the visual system's response to spectral variations in natural light. Importantly, melanopsin also contributes positively, although more modestly, reinforcing its role beyond purely non-image-forming functions. The absence of measurable S-cone contributions under these experimental conditions aligns with reports that S-cones have minimal impact on brightness compared to their roles in chromatic processing. Nevertheless, it remains possible that under different lighting regimes, such as mesopic conditions where rods remain partially active, S-cones could interact differently with other photoreceptors to influence brightness. Future studies should therefore extend investigations to mesopic conditions if necessary.

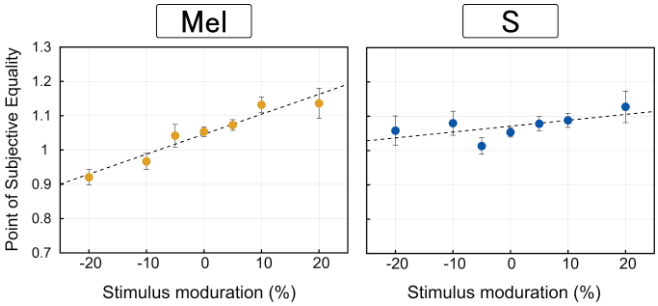

Figure 4. Brightness perception as a function of melanopsin (Mel, left) and S-cone (S, right) stimulation. Error bars show SEM; dashed lines indicate linear fits.

Importantly, the observed facilitatory contribution of melanopsin highlights the limitations of current luminous efficiency models. These models, which are still widely used in applied settings, are incomplete because they ignore melanopsin's role. Integrating melanopsin into brightness models could improve their predictive accuracy, particularly for light environments with strong blue content or unusual spectral distributions. This has practical implications not only for vision science but also for lighting engineering. Future work should systematically explore interactions between cones and melanopsin by varying stimulation simultaneously rather than in isolation.

ACKNOWLEDGEMENTS

This research was supported by the Ministry of Education, Science, Sports and Culture of Japan, Grants-in-Aid for Scientific Research (A) 21H04426 (Prof. Kitaoka) and 20H00614 to ST, the Grant in Aid for Challenging Research (Exploratory) 22K19333 to ST.

REFERENCES

[1]. Brown, T. M., Tsujimura, S., Allen, A. E., Wynne, J., Bedford, R., Vickery, G., . . . Lucas, R. J. (2012). Melanopsin-based brightness discrimination in mice and humans. Curr Biol, 22(12), 1134-1141. doi:10.1016/j.cub.2012.04.039

[2]. Freedman, M. S., Lucas, R. J., Soni, B., Von Schantz, M., Muñoz, M., David-Gray, Z., & Foster, R. (1999). Regulation of mammalian circadian behavior by non-rod, non-cone, ocular photoreceptors. Science, 284(5413), 502-504.

[3]. Stockman, A., & Sharpe, L. T. (2000). The spectral sensitivities of the middle- and long-wavelength-sensitive cones derived from measurements in observers of known genotype. Vision Res, 40(13), 1711-1737. Retrieved from http://www.ncbi.nlm.nih.gov/pubmed/10814758

[4]. Stockman, A., Sharpe, L. T., & Fach, C. (1999). The spectral sensitivity of the human short-wavelength sensitive cones derived from thresholds and color matches. Vision Res, 39(17), 2901-2927. Retrieved from http://www.ncbi.nlm.nih.gov/pubmed/10492818

From Fabric to Fingertips: Nail Polish as A Tool for Personal Colour Analysis

Suchitra Sueeprasan*, and Phithunisara Chaimongkol

Department of Imaging and Printing Technology, Faculty of Science, Chulalongkorn University, Bangkok, Thailand
**Corresponding author: Suchitra Sueeprasan, suchitra.s@chula.ac.th*

ABSTRACT

Personal colour analysis is a valuable tool in fashion, beauty, and personal styling, helping individuals identify colours that enhance their natural features. The draping method is commonly applied in professional image consulting and has been a standard practice for decades. Despite its widespread use, the draping method can be costly and inaccessible to many individuals. Given these limitations, this study explores the use of nail polish colours as an alternative tool for personal colour classification. In this study, the nail polish samples were selected based on the HSV values according to the Angela Wright System, which classifies personal colours into four seasons: spring, summer, autumn, and winter. Each season was represented by three sample colours. The nail polish samples were painted on artificial nails, and three different coloured fake nails from the same season were placed on top of the subjects' nails on three fingers (index, middle, and ring). The images of the subjects' hands were then taken under D65 simulators. This experiment was carried out on 30 female subjects whose personal colour was identified using the draping method. As a result, four images corresponding to different seasons were taken for each subject. An online questionnaire was conducted, where an observer chose the nail polish colours that best complemented the subject's hand. The total of 84 observers participated in the online experiments. It was found that the majority of the subjects had a warm undertone, with 10 classified as spring and 10 as autumn. More than 50% of observers assigned 20 subjects to a certain seasonal type that agreed with the draping method. This revealed that personal colour analysis using the nail polish approach agreed with the draping method by 67%. As a result, it is feasible to classify personal colours using nail polish colours.

Keywords: personal colour analysis, draping method, nail polish, seasonal colour, skin undertone

INTRODUCTION

Personal colour analysis has become an essential tool in personal styling, beauty, and cosmetics, offering individuals a method to discover colour palettes that harmonize with their natural features. By identifying colours that complement one's skin, eyes, and hair, personal colour analysis enhances not only physical appearance but also self-confidence and satisfaction with personal style [1]. One of the most established techniques for determining personal colour type is the draping method, in which fabric swatches of various colours are held up to a person's face to observe which shades make their complexion appear more vibrant or dull [2]. This method is central to the Four Seasons colour analysis model, where individuals are categorized as Spring, Summer, Autumn, or Winter based on skin undertone (warm/cool), clarity or chroma (clear/muted), and value (light/dark) [3]. The draping method is commonly applied in professional image consulting and has been a standard practice for decades. Despite its widespread use, this method suffers from several limitations. It is inherently subjective, reliant on visual judgment, and influenced by inconsistent lighting, fabric quality, and analyst expertise [4]. Additionally,

professional services can be expensive and are not always accessible to the average consumer, limiting the practical application of the method.

Consequently, there is a need for alternative, more accessible tools for personal colour analysis. Kim and Kim [5] demonstrated the use of lipstick colours as an effective classification tool for identifying personal colour types. Their study found that the harmony between lipstick hues and an individual's skin could effectively predict seasonal categories, offering a promising substitute to traditional fabric draping. Angela Wright [6] classified the four seasonal colour palettes based on the three dimensions of colour: hue, saturation and value. The Wright system organizes colours not only by perceptual harmony but also by psychological and aesthetic consistency, offering a quantifiable, replicable foundation for colour grouping and preference prediction. Cassidy [7] measured colour samples from the Wright system and represented them in the HSV (Hue, Saturation, Value) model. The application of HSV metrics allows for systematic classification of colour palettes, removing subjective variability and aligning colour matching with empirical parameters.

This study proposes to investigate nail polish colours as a novel tool for personal colour classification, employing Angela Wright's HSV-based system to inform sample selection and categorization. Nail polish offers several practical benefits: it is readily available, easily tested in direct visual contact with the skin, and capable of being measured and classified using digital colour analysis. By developing a systematic classification method based on nail polish shades, this study aims to provide a more practical and cost-effective solution for personal colour analysis while maintaining scientific accuracy.

METHODOLOGY

The selection of nail polish colour samples was based on the Angela Wright system. First, the samples were painted onto artificial nails, and images were captured under D65 light simulators. The resulting RGB values were extracted and entered into Microsoft Word's colour box feature, which automatically converts them to HSV values. The use of Microsoft Word for HSV conversion follows Cassidy's study [7], which established a connection between the Wright system and the HSV model. Based on these HSV values, the samples were categorised into four seasonal colour palettes (see Table 1). Three colour samples were selected to represent each season.

Table 1: Angela Wright system with HSV values

	Spring	Summer	Autumn	Winter
H	0–118	119–255	0–118	119–255
S	0–255	0–189	190–255	0–189
V	129–255	0–127, 129–255	0–127	128

Thirty female subjects aged 18–25 took part in the personal colour analysis experiments. Each subject's personal colour type was first identified using the fabric draping method. Following this, three artificial nails representing the corresponding seasonal colour palette were applied to the index, middle, and ring fingers. Images of their hands were then captured under D65 light simulators. This procedure was repeated for all seasonal colour samples, resulting in four images per participant.

An online questionnaire featuring images of subjects' hands with artificial nails was conducted to determine which nail colours appeared most aesthetically pleasing. A total of 84 observers, aged 15–30, took part in the online experiment. For each subject, four images—each displaying different seasonal colour samples—were presented simultaneously. Observers were asked to select the nail polish colour that best complemented the subject's skin

tone. This procedure was repeated for all thirty participants. On average, each observer completed the task within five minutes.

RESULTS AND DISCUSSION

Based on the fabric draping method, 10 subjects were identified as Spring, 2 as Summer, 10 as Autumn, and 8 as Winter colour types. For each subject, the number of times observers selected seasonal colour samples was recorded, and the percentages were calculated. A subject was assigned to a seasonal colour type if more than 50% of observers selected the corresponding colour. A 50% threshold was used as the benchmark for an acceptable match, with 60% and 70% representing good and very good agreement, respectively [8]. Table 2 presents the classification results obtained through both the fabric draping method and the nail polish evaluation method.

Table 2: Numbers of subjects classified under each seasonal colour type

Classification Method	Spring	Summer	Autumn	Winter	Total
By the draping method	10	2	10	8	30
By ≥50% of observers	7	1	6	6	20
Agreement (%)	**70%**	**50%**	**60%**	**75%**	**67%**

The results indicate a moderate level of agreement between the fabric draping method and the nail polish colour evaluation conducted via observer responses. Of the 30 subjects, 20 (67%) were classified into the same seasonal colour type by at least 50% of observers. The highest agreement was observed in the Winter group (75%), followed by Spring (70%), Autumn (60%), and Summer (50%). These findings suggest that the nail polish method, based on visual judgment, has potential as a supplementary tool for personal colour analysis, particularly for Winter and Spring types.

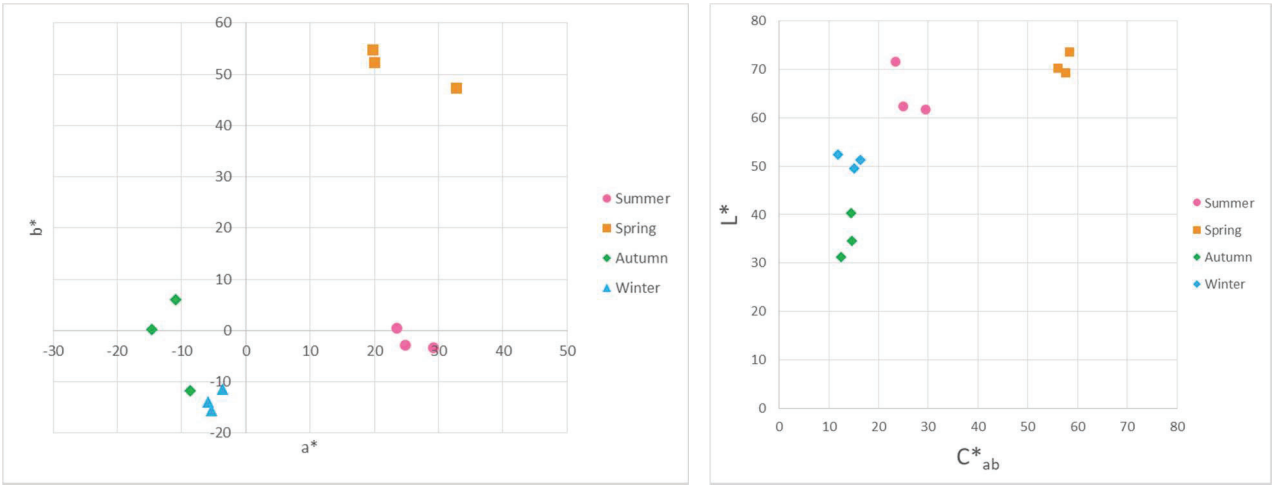

Figure 1: Distributions of nail polish samples in CIELAB

However, closer examination reveals that some Autumn and Winter subjects were classified into the corresponding seasonal types by fewer than 40% of observers, indicating poor agreement in these cases. This may

be attributed to visual similarities between the Autumn and Winter nail polish samples. As illustrated in Figure 1, the CIELAB distribution shows overlapping regions between these two palettes, potentially leading to confusion or misclassification by observers. These results highlight the importance of colour distinctiveness in visual-based methods and suggest that certain seasonal palettes may require further differentiation to improve reliability.

One key limitation of this study lies in the overlap of subjects' skin colour measurements across the four seasonal groups. As shown in Figure 2, the CIELAB values of the skin on the back of the hand revealed substantial overlap among all seasonal categories. This overlap may have contributed to observer misclassifications, particularly when evaluating nail polish compatibility based on skin tone. The lack of clear separation between groups is likely influenced by the limited number of subjects in each seasonal category, particularly in the Summer and Winter groups.

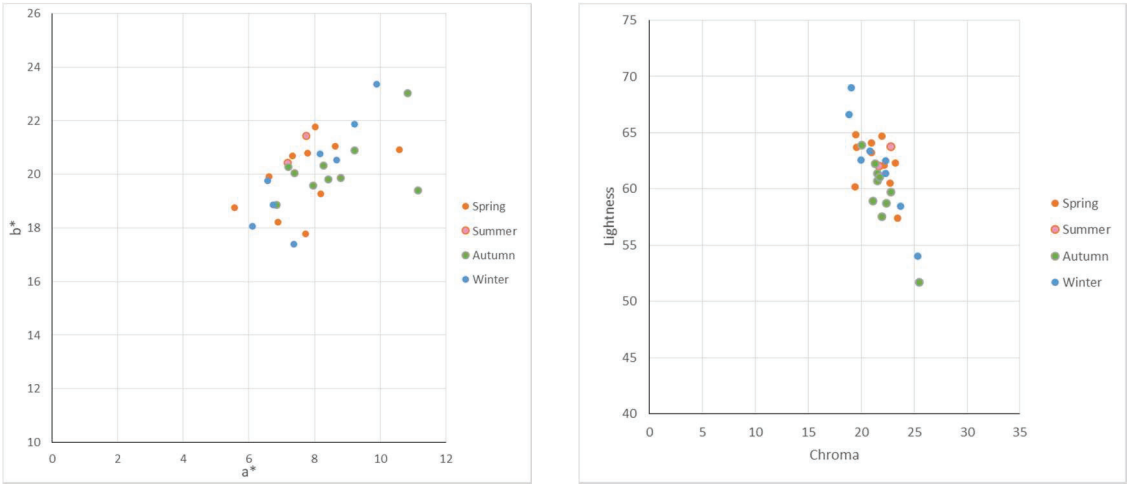

Figure 2: Distributions of skin colours in CIELAB

Furthermore, the subject pool included a higher proportion of individuals with warm undertones, as most were classified into either the Spring or Autumn groups. This imbalance may have skewed the overall results and reduced the generalisability of the findings across all seasonal types. Future research should aim for a more balanced sample across undertones and seasons, and potentially incorporate objective colour-matching algorithms to complement human visual assessment. Expanding the dataset would also allow for more robust statistical analysis and increased reliability of seasonal classification using nail polish colour.

CONCLUSION

This study explored the potential of using nail polish colour as a tool for personal colour analysis, comparing the results with the traditional fabric draping method. The findings revealed a moderate level of agreement between the two methods, with an overall match rate of 67% based on observer evaluations. While the nail polish method showed promising alignment, particularly for Winter and Spring types, challenges were noted in differentiating between Autumn and Winter palettes, as well as in achieving clear skin tone distinctions across seasons.

The study also identified limitations related to sample size and undertone distribution, as the majority of participants had warm skin tones. Despite these constraints, the results suggest that nail polish-based analysis could serve as a supplementary method for seasonal colour typing, especially in contexts where fabric draping is impractical. Future research with a larger and more balanced participant group is recommended to validate and refine this approach.

ACKNOWLEDGEMENTS

The author would like to express sincere gratitude to all the participants who generously contributed their time and involvement in this study. Their participation was essential to the success of this research.

REFERENCES

[1]. Jackson, C. (2011). *Color me beautiful: Discover your natural beauty through the colors that make you look great and feel fabulous*. Ballantine Books.

[2]. Nasr, M. M. (2018). Identifying the role of skin tone in choosing the suitable colors for outfits & fashion accessories, *International Journal of Textile and Fashion Technology*, 8(3), 1-14.

[3]. Kentner, B. (1999). *Color Me A Season: A Complete Guide to Finding Your Best Colors and How to Use Them*. Kenkra Publishers.

[4]. Mathis, C. M., & Connor, H. V. (2009). *The Triumph of Individual Style: A Guide to Dressing Your Body, Your Beauty, Your Self*. Fairchild.

[5]. Kim, D. E., & Kim, Y. S. (2020). Classifying personal colors using lipstick colors, *Asian Journal of Beauty and Cosmetology*, 18(3), 399–412.

[6]. Wright, A. (1998). *The Beginner's Guide to Colour Psychology*. Kyle Cathie Limited.

[7]. Cassidy, T. D. (2007). Personal colour analysis, consumer colour preferences and colour forecasting for the fashion and textile industries, *Colour: Design & Creativity*, 1(1), 6, 1-14.

[8]. Berdie, D. R., Anderson, J. F., & Niebuhr, M. A. (1986). *Questionnaires: Design and Use*. Metuchen, NJ (USA) Scarecrow Press.

A Study on Color Perception on Surfaces Composed of Two Colors
The Effect of Color Difference between Two Colors in A Checkerboard Patternon The Perception of Color Unevenness of One of The Colors

Naoya Hara[a*], Masami Kono[b]

[a] Faculty of Environmental and Urban Engineering, Kansai University, Suita in Osaka, Japan
[b] Faculty of Architecture and Arts, Otemae University, Nishinomiya in Hyogo, Japan
[*]Corresponding author: Naoya Hara, nhara@kansai-u.ac.jp

ABSTRACT

There has been much research into the appearance of individual colors, and color appearance models such as CIECAM02 have been proposed. However, the appearance of individual colors within a surface composed of multiple colors, as well as the appearance of color unevenness and differences of each color, differ from the appearance of individual colors or the appearance of color unevenness and differences of each color. In this paper, about a checkerboard pattern composed of two different colors, a target color and a non-target color we examine the effect of their color differences on the appearance of color unevenness of a target color.

The smaller the standard deviation of the color difference of the target color, the less likely color unevenness is to be perceived. Even if the standard deviation is the same, the greater the color difference between the target color and the non-target color, the less likely color unevenness is to be perceived.

Keywords: large color difference, small color differences, masking, color unevenness, checkerboard pattern

INTRODUCTION

There has been much research into the appearance of individual colors, and color appearance models such as CIECAM02 have been proposed [1]. However, the appearance of individual colors within a surface composed of multiple colors, as well as the appearance of color unevenness and differences of each color, differ from the appearance of individual colors or the appearance of color unevenness and differences of each color.

For example, interior and exterior architectural surfaces are often composed of bricks or blocks of multiple colors. One of the reasons for this is that it is harder to perceive color unevenness of individual bricks or blocks on a surface that is made up of multiple colors than on a surface that is made up of a single color. Large color differences between multiple colors have the effect of masking the perception of small color differences that result in color unevenness of a single color.

In order to quantitatively examine this effect, this study conducts experiments to grasp the effect of the color difference between two colors in a checkerboard pattern on the perception of color unevenness of one of the colors.

METHODOLOGY

One of the colors that make up the checkerboard pattern was given color unevenness consisting only of lightness and chroma differences and was used as the target color to judge its unevenness perception, while the other color was used as the non-target color without color unevenness.

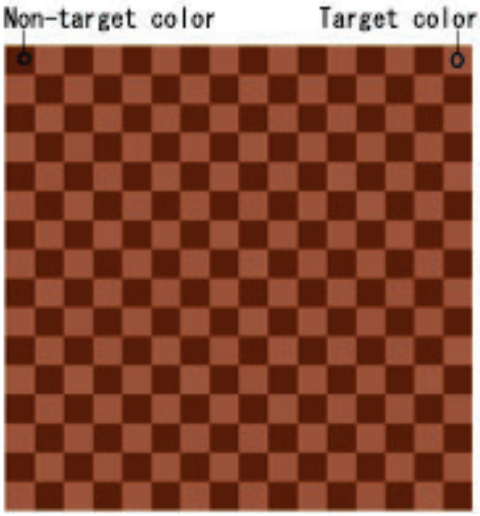

Figure 1. Target color and non-target color in the checkerboard pattern

The checkerboard pattern was displayed at 1024 x 1024 pix in the center of a display which surface was 596.2 x 335.3 mm (3840 x 2160 pix) and color depth of 10 bits, placed 1600 mm away from the viewpoint. The display set on the cubic box which inner surface was black. The subjects observed it through the observation window and the cubic box which inner surface except of one that had observation opening was white. The experimental set up is shown in Figure 1. The white inner surface was illuminated by the 5000K white LED to be uniform and 150 cd/m^2.

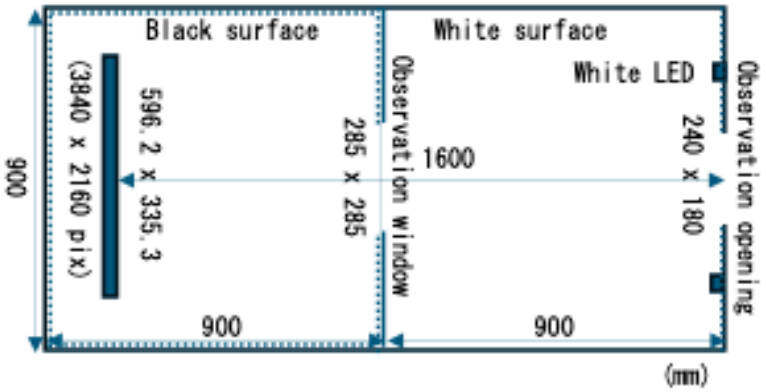

Figure 2. Experimental set up

The background in the display was set to be the same color as the illuminated inner surface color, and assuming a color space in which the CIECAM02 lightness J of this background is 85, the display colors shown below were determined. The target and non-target colors were colors with the same hue component, with the

CIECAM02 hue quadrature (H= 0, 100, 200, and 300). The average color of the target colors for rating color unevenness of each area in the checkerboard pattern was set several of the combinations of four lightness (J=20, 40, 60 and 80) and four chroma (C=0,20,40,60) for each hue quadrature in CIECAM02. The target color for lightness difference had the standard deviation σ_j in the lightness of the target area, which was set to three levels: 0.5, 1.0, and 1.5, and the target color for the chroma difference had the standard deviation σ_c in the chroma of the target area, which was set to four levels: 1.0, 2.0, 3.0 and 4.0. The lightness and chroma of non-target colors were set their lightness difference ΔJ_l or chroma difference ΔC_l from that of target color. There are 11 levels of ΔJ_l and ΔC_l: -20, -10, -5, -2, -1, 0, +1, +2, +5, +10, and +20. However, ΔJ_l was varied independently under $\Delta C_l = 0$, and ΔC_l was varied independently under $\Delta J_l = 0$. All or some of these levels were set according to a combination of lightness and chroma condition of target color.

The number of divisions into the two colors of the checkerboard pattern was set to three levels（P=8,16 and 32, i.e. 8x8, 16x16, and 32x32 divisions respectively）. Of these combinations, the experimental conditions were limited to those that could obtain the relationship between the experimental variables to be examined and the perception of color unevenness, and 883 conditions that could be displayed on the display were used.

The subjects, ten people with normal color vision, observed the checkerboard patterns under each condition and rated whether they could distinguish the target color from the non-target color, that was, whether they could recognize a checkerboard pattern. In the case they distinguish these colors, they rated whether they perceived color unevenness in the target area of checkerboard pattern. In the case they do not distinguish them, they rated whether they perceived color unevenness in the whole area of checkerboard. They rated about the degree of color unevenness in target color area or checkerboard pattern, whether they perceived the color unevenness as 1/16, 1/4, or the entire of them.

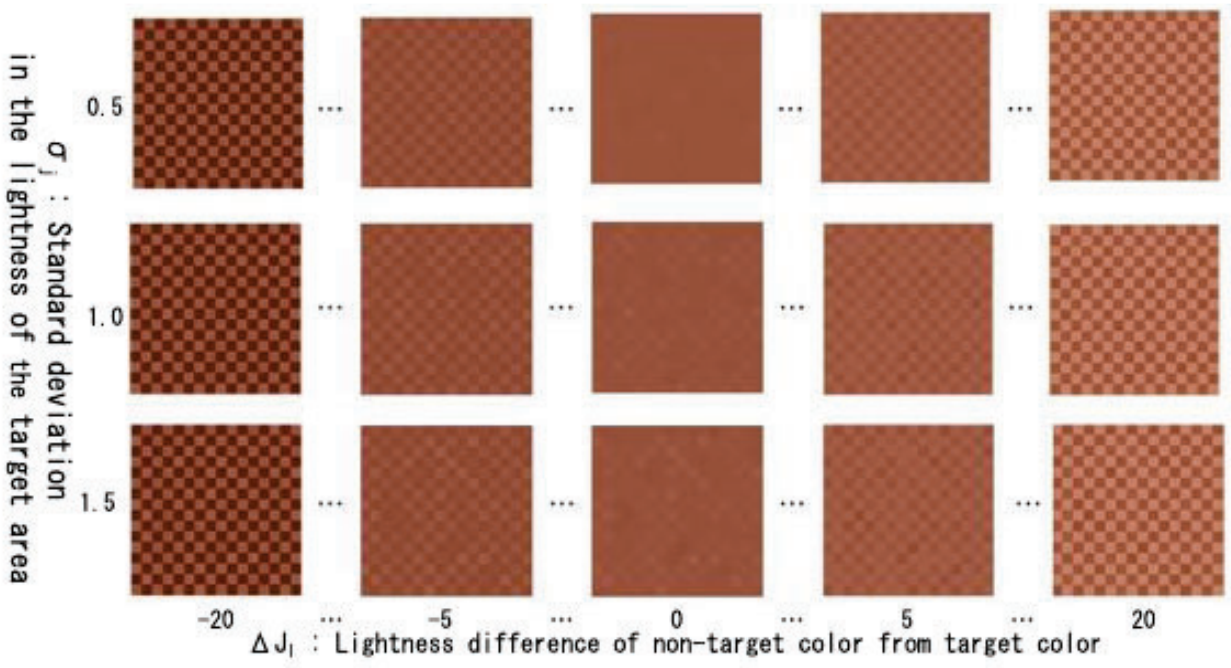

Figure 3. Example of experimental conditions for lightness J difference

RESULTS AND DISCUSSION

As the result of the experiment, cumulative frequency of subjects' ratings for main conditions are shown below. The order of cumulative frequency was as follows: when the checkerboard was not recognized, for whole target and non-target areas color unevenness was not perceived , then perceived in 1/16, then 1/4, and then perceived throughout, and when the checkerboard was recognized, for the target area color unevenness was not perceived, then perceived in 1/16, then 1/4, and then perceived throughout.

Figure 4. shows the relationship between the color difference only in lightness of target ΔJ_l and non-target color and the cumulative frequency of the color unevenness perception ratings with hue quadrature 0 with standard deviation of lightness σ_j 0.5 and 1.5 under average lightness J is 40 and chroma C is 40.

When the absolute value of ΔJ_l is large, a checkerboard pattern is recognized, and the color unevenness of the target is difficult to perceive. In the case σ_j=1.5, the percentage of people who perceive the color unevenness for target area increases compared to σ_j=0.5. As ΔJ_l approaches 0, the percentage who perceive the color unevenness gradually increases in the order of 1/16, 1/4, and the entire target area while still recognizing checkerboard pattern. When ΔJ_l gets close to 0, the percentage of people who are unable to recognize the checkerboard pattern increases. In the case the standard deviation of the lightness of the target color is small, σ_j=0.5, some people do not perceive the color unevenness as a whole and recognize the whole to be a single mixed color. In the case of σ_j=1.5, even when ΔJ_l=0, some people are able to recognize the checkerboard pattern due to the color difference of the target color. While some people did not recognize the checkerboard pattern of larger ΔJ_l compared to the case σ_j=0.5, which is thought to be because when the color difference of the target colors is large, the non-target color blends into target colors.

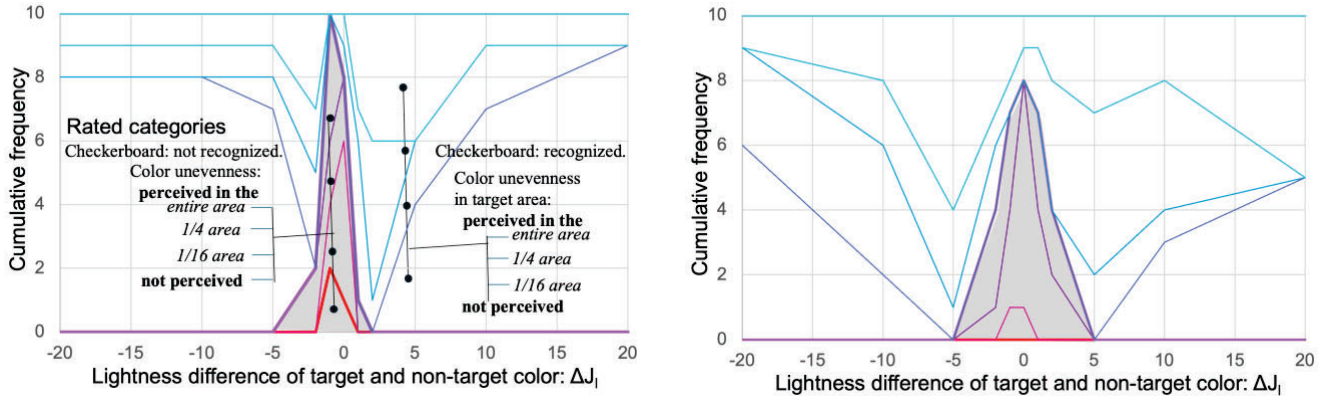

a) Standard deviation of lightness σ_j : 0.5 b) Standard deviation of lightness σ_j: 1.5

Figure 4. The relationship between the color difference only in lightness of target and non-target color and the color unevenness perception (H=0, J=40, C=40)

Figure 5 shows the relationship between the color difference only in chroma of target ΔC_l and non-target color and the cumulative frequency of the color unevenness perception ratings with hue quadrature 0 with standard deviation of lightness σ_c 1.0 and 3.0 under average lightness J is 60 and chroma C is 40. The tendency of the relation shown in Figure 5 is similar to that shown in Figure 4. However, for the chroma difference ΔC_l in Figure 5, the range where the percentage of people who are unable to recognize the checkerboard pattern is large is about twice as wide, even though the standard deviation of chroma is twice as large, σ_c = 1.0, as compared to that range of the lightness difference ΔJ_l in Figure 4, where the standard deviation of lightness is σ_j = 0.5. The percentage of people who do not perceive the color unevenness as a whole and recognize the whole to be a single mixed color is higher

for $\Delta C_l = 0$ in Figure 5 compared to $\Delta J_l = 0$ in Figure 4. This means that even with the same deviation in lightness and chroma difference in CIECAM02, chroma difference is more difficult to perceive than lightness difference. Furthermore, the relationship between the color difference only in lightness of target and non-target color and the color unevenness perception in figure 4, that is, on the target color's H=0, J=40, C=40 is similar that on the target color's H=0, J=60, C=40 in figure 5. Even if the color difference is the same, the effect on the perception of color unevenness seems to be different when it comes to the chroma and lightness of the CIECAM02.

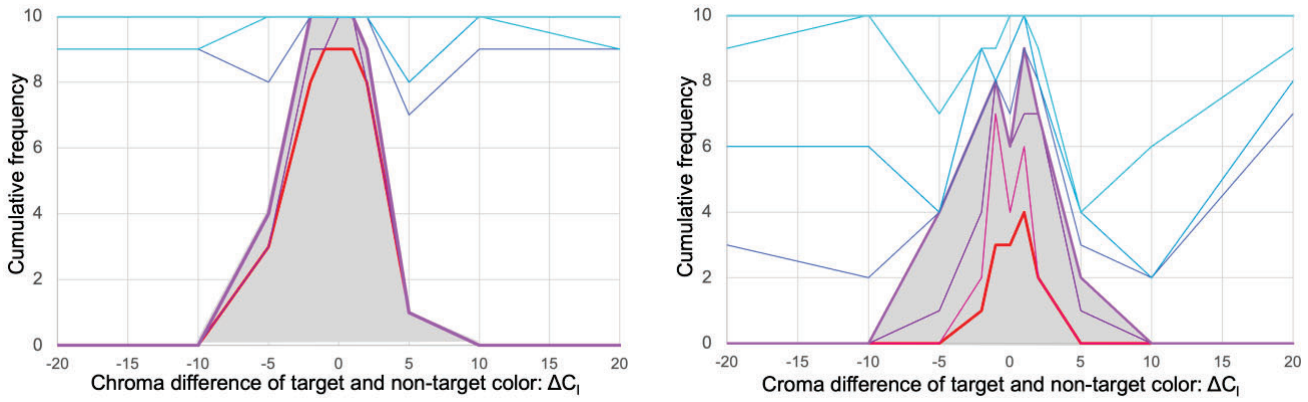

a) Standard deviation of chroma σ_c : 1.0 b) Standard deviation of chroma σ_c: 3.0

Figure 5 The relationship between the color difference only in chroma of target and non-target color and the color

CONCLUSION

The smaller the standard deviation of the color difference of the target color, the less likely color unevenness is to be perceived. Even if the standard deviation is the same, the greater the color difference between the target color and the non-target color, the less likely color unevenness is to be perceived.

ACKNOWLEDGEMENTS

The authors would like to thank Taiga Takiguchi and Zhu Tianming for their contribution to the accomplishment and analysis of the experiments.

REFERENCES

[1]. CIE (2004). A Colour Appearance Model for Colour Management Systems: CIECAM02, CIE Technical Report, 159

Physical Light Field Perception Using Color-Enhanced Photon Flow Visualization

Sho Nakadate[a*], Asuka Momiyama[a], Kazuto Takase[a], Roland Schregle[b], and Nozomu Yosizawa[a]

[a]Tokyo University of Science, Chiba, Japan
[b]RS SciComp, Cologne, Germany
[*]Corresponding author: Sho Nakadate, 7124542@ed.tus.ac.jp

ABSTRACT

This study applies the Photon Flow method, based on volume photon mapping, to visualize colored light fields in architectural spaces by incorporating both light source and surface colors into photons. The reflectance of interior materials and the color of the light source were measured using a spectrophotometer and converted from CIE XYZ to Radiance RGB. A volume photon map (VPM) was generated with mkpmap and exported into a text-based dataset with pmapdump, after which Radiance RGB values were assigned to each photon. Direct photons retained the color of the light source, while reflected photons were modulated by the spectral reflectance of the materials. Photon luminance was then calculated, followed by normalization, scaling, and gamma correction, enabling visualization that matched both human visual perception and the gamma response of the display device. The experiment was conducted under 12 conditions combining light source type (directional/diffuse), interior color (achromatic/chromatic), and evaluation target position (three levels). Sixteen participants predicted the shading of a white sphere in a 3D model that included Photon Flow, using two reference spheres as visual guides. Perceptual accuracy was evaluated with four physical indicators: directionality, intensity, diffuseness, and color difference. The results showed that chromatic conditions exhibited medians closer to zero in intensity error than achromatic conditions, indicating higher predictive accuracy, especially under diffuse light source environments. Regarding diffuseness error, achromatic conditions generally exhibited higher predictive accuracy than chromatic conditions under both diffuse source and directional source environments. Further investigation is required to determine the reasons for this result. No significant differences were found in color difference. In conclusion, the perception of intensity and diffuseness was influenced by whether direct and reflected photons shared the same color (achromatic) or different one (chromatic). Future work will focus on separating the visualization of direct and reflected photons to minimize color-induced bias and enable more consistent evaluation of light fields.

INTRODUCTION

In recent years, the increasing complexity of architectural lighting environments has made it difficult to understand the propagation characteristics of light within space when using conventional two-dimensional evaluations based on illuminance and luminance distribution. To address this issue, a method called “Photon Flow” has been developed, which utilizes volume photon mapping and allows for the description of the physical light field at arbitrary points in space. In this study, we extended the Photon Flow method and evaluated the accuracy of light-field predictions based on Photon Flow, with the aim of establishing a three-dimensional description method rather than the conventional two-dimensional descriptions such as illuminance or luminance distributions. This paper reports the results of an investigation into how differences in floor coloration affect light-field prediction at arbitrary points in the space when the color of photons is assigned to correspond to either the light-source color or the color of interior surface materials.

METHODOLOGY

Visualization of a light field through Photon Flow

In this method, each photon is assigned the color that reflects the reflective properties of real-world materials, thereby enabling the visualization of the colored light field using Photon Flow. To reproduce material colors in the simulation, the reflectance of interior materials was measured in a real-world environment using a spectrophotometer (Konica Minolta CM-700d), and the reflectance spectra were obtained under the standard illuminant CIE A, which closely corresponds to the color temperature (2700K) of the experimental lighting condition. The light source color was derived from the white point coordinates of the 2700K light source on the xy chromaticity diagram (x, y) = (0.45986, 0.41060), and converted to the CIE XYZ color system to obtain the white point values (Xsw, Ysw, Zsw) = (1.0985, 1, 0.35585). In this study, the display monitor for Photon Flow employed the P3 color space with a D65 white point. Therefore, the ratio between the CIE XYZ white point obtained before and the monitor's D65 white point (Xdw, Ydw, Zdw) = (0.95047, 1, 1.08883) was used to convert the material's CIE XYZ values to those in the P3 color space using a transformation matrix (M_D) from CIE XYZ to P3 (Eq. 1). This conversion was carried out in the linear domain ($\gamma = 1$). Gamma-corrected values are non-linear and represent human visual sensitivity rather than physical light intensities. If such values were used directly, additions and color conversions would introduce errors, as the true light strength would not be preserved. Therefore, gamma correction was applied only at the final display stage to match human visual perception and the monitor's response. The resulting XYZ values in the P3 color space were then converted to Radiance RGB. In addition to the material reflectance values, the CIE XYZ values of the light source were measured using a spectrophotometer (Konica Minolta CM-700d) and subsequently converted into Radiance RGB values following the same procedure. These RGB values were subsequently employed in the photon-based calculations described below.

$$\begin{pmatrix} X_{dis} \\ Y_{dis} \\ Z_{dis} \end{pmatrix} = M_D \begin{pmatrix} \frac{X_{dw}}{X_{sw}} & 0 & 0 \\ 0 & \frac{X_{dw}}{X_{sw}} & 0 \\ 0 & 0 & \frac{X_{dw}}{X_{sw}} \end{pmatrix} \begin{pmatrix} X_m \\ Y_m \\ Z_m \end{pmatrix} \tag{1}$$

$$M_D = \begin{pmatrix} 2.493477767 & -0.931555815 & -0.402658221 \\ -0.829620807 & 1.762853645 & 0.023600488 \\ 0.035842416 & -0.076161222 & 0.956926543 \end{pmatrix}$$

Xdw, Ydw, Zdw: D65 white point

Xsw, Ysw, Zsw: White point in the CIE XYZ color space

M_D: A transformation matrix from CIE XYZ to P3

Xm, Ym, Zm: The material's CIE XYZ values

Xdis, Ydis, Zdis: The material's XYZ values in the P3 color space

Before carrying out the subsequent calculations, a volume photon map (VPM) was generated using mkpmap and exported into a text-based photon dataset using pmapdump. Each photon carried color information in the form of Radiance RGB values: direct photons were assigned the Radiance RGB of the light source, whereas reflected photons were computed from the light source RGB values modulated by the spectral reflectance of the encountered materials. The subsequent steps describe how this dataset was processed to obtain normalized RGB values for the visualization of Photon Flow. The process consisted of the following steps: First, the luminance (Y_p) of each photon was calculated from its P3 RGB values. Next, the luminance was normalized by dividing each photon's RGB values by Y_p, which preserved the hue while setting the luminance to 1 (Eq. 3). This procedure ensured that all photons had uniform luminance, thereby enabling direct comparison of color. Then, an A scaling factor was applied to the

normalized RGB values so that the maximum photon radiant flux does not exceed the software limit of 255 for each RGB channel in Rhinoceros. Although a scaling factor can be determined individually for each condition to set the maximum value to 255, differences in photon luminance across conditions would lead to unintended brightness judgments based on variations in lightness and darkness. To avoid this, the same coefficient was applied to all conditions. Specifically, among the scaling factors calculated for each condition, the smallest value was selected, which was 207. This ensured that RGB values did not exceed 255 under any condition, while maintaining equal radiant flux per photon across all conditions. Thus, the introduction of the A scaling factor served to standardize photon luminance among conditions and eliminate the possibility of inappropriate brightness judgments arising from luminance differences. In addition, gamma correction was applied to convert the calculated linear RGB values into non-linear RGB values suitable for display, matching the characteristics of human visual perception and the gamma response of the display device (Eq. 4). Through these steps, the colored light field can be visualized using Photon Flow, as shown in Figure 1.

$$R_{Y207} = {R_{Y1}}^{0.454545} \times 207 \quad G_{Y207} = {G_{Y1}}^{0.454545} \times 207 \quad B_{Y207} = {B_{Y1}}^{0.454545} \times 207 \quad (4)$$

$R_{Y207}, G_{Y207}, B_{Y207}$: Visualization RGB values of each photon in the P3 color space

R_{Y1}, G_{Y1}, B_{Y1} : luminance-normalized RGB values of each photon in the P3 color space

207 : scaling factor ^**0.454545** : Gamma correction (1/2.2 ≈ 0.4545)

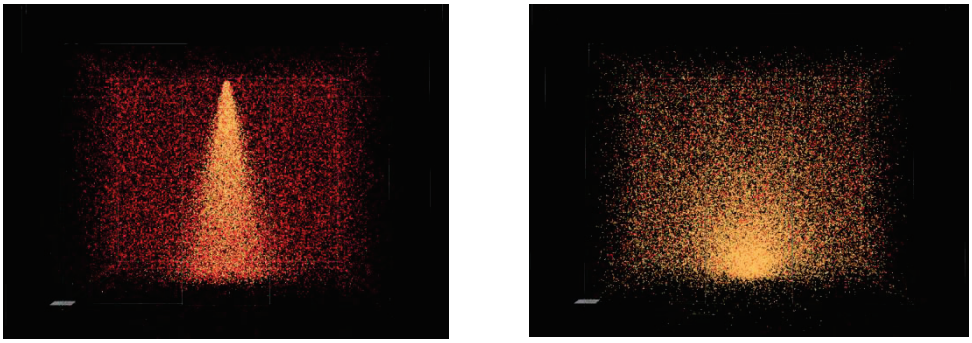

Figure 1: A colored light field through Photon Flow

Experiment-Method Overview

This study employed a white sphere–based evaluation method to capture Light Field perceived by participants [1]. The approach involved predicting the shading that would appear when a white sphere was placed at a designated position in the experimental space, using Photon Flow.

Experiment-Experimental Conditions

The observation conditions consisted of combinations of light source type (directional/diffuse), interior color (achromatic/red), and evaluation target position (three levels with varying degrees of indirect light influence), totaling 12 experimental conditions.

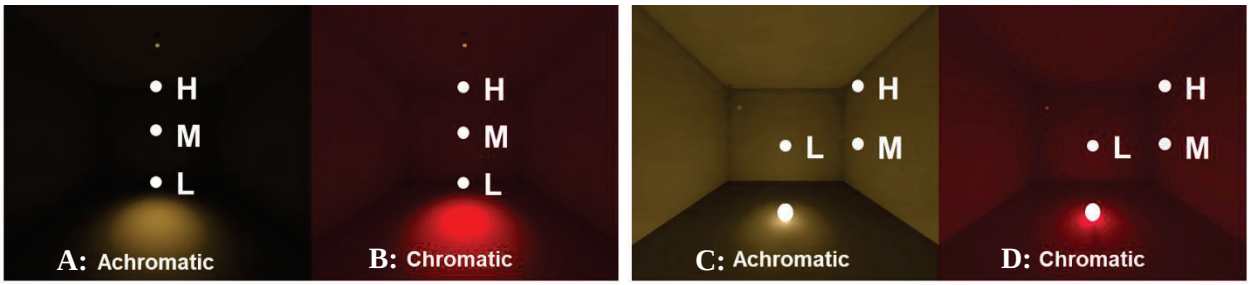

Figure 2: The observation conditions

For the directional light source, a 2700 K LED spotlight with a beam angle of 19° was used, while the diffuse light source was a 2700 K diffused LED. In the chromatic (red) conditions, the areas illuminated directly by the light source were set to red. For example, in spatial condition B, the floor was red, while in condition D, the floor, walls, and ceiling were all red. This design allowed the direct and indirect light coloration to be clearly distinguished in Photon Flow.

The overall luminance of the space was set to a photopic vision level. Two white reference spheres were placed at designated positions within the scene to serve as visual guides for shading prediction at the evaluation target position.

Experiment-Procedure

Each participant underwent a 10-minute adaptation period in the experimental room, during which the experimenter explained the purpose, overview, and evaluation method. Sixteen participants (male and female) in their twenties took part in the experiment. Following adaptation, the participant observed Photon Flow on a monitor using Rhinoceros 3D software. Participants did not observe the actual physical space; instead, they viewed a rendered 3D model that included Photon Flow. Before starting each trial, participants reviewed a floor plan of the experimental space to confirm the viewpoint position, the evaluation target position, and the location of the reference spheres. During the observation, participants referred to the shading of two white reference spheres displayed on the right side of the monitor as a visual guide. They then freely manipulated the 3D model—moving, rotating, and zooming—to inspect light entering the evaluation target position from various directions. The evaluation focused on the appearance of shading when the white sphere at the target position was viewed from the front. After the observation, various rendered images of the white sphere—each depicting different shading appearances—were displayed on the monitor. Participants evaluated whether each white sphere image matched their predicted shading using a three-point scale: “correct,” “unsure,” or “incorrect.” All experimental conditions were presented in random order.

RESULTS AND DISCUSSION

The white sphere exhibits different light-field features at each position, namely directionality, intensity, diffuseness, and chromaticity. For each evaluation position, we computed the absolute difference between the physical light-field features of the white sphere and the light-field features estimated from participants' selections; this absolute difference was used to assess the predictive accuracy of the perceived light field. Equations (1)–(4) present the formulas for directionality error, intensity error, diffuseness error, and color difference, respectively. Smaller values indicate that participants' perceptual representation of the light field more closely matches the physical light field.

$$\theta = cos^{-1}\frac{\overrightarrow{E_v}\cdot\overrightarrow{E_p}}{|\overrightarrow{E_v}||\overrightarrow{E_p}|}\ (1)\quad E_{scalor} = \frac{|\overrightarrow{E_v}|}{4} + {\sim}E\ (2)\quad D = 1 - \frac{|\overrightarrow{E_v}|}{4E_{scalor}}\ (3)\quad RMSE = \sqrt{\frac{1}{n}\sum_1^n(\Delta E)^2}\ (4)$$

$\overrightarrow{E_i}$: Vectors representing the direction of light in the shading image of the white reference sphere at the evaluation target position ($\overrightarrow{E_p}$) and at another position ($\overrightarrow{E_v}$).

θ: The angle between $\overrightarrow{E_p}$ and $\overrightarrow{E_v}$

E_{scalor}: Scalar illuminance [lx] at the position of the white reference sphere shading image selected by the participant

${\sim}E$: Symmetric illuminance [lx] at the position of the white reference sphere shading image selected by the participant.

D: Diffuseness at the position of the white reference sphere shading image selected by the participant.

ΔE: Color difference (CIE DE2000) between the pixels of the white reference sphere shading image at the evaluation target position and those of the shading image selected by the participant.

Directionality: θ [2]

To evaluate the accuracy of perceived light directions, we compared the illumination vector derived from the physical light field (E_p) with that inferred by the participants (E_v). Here, the illumination vector refers to the net directional component of light flow, obtained by comparing illuminance values measured on pairs of opposite faces of a cubic illumination meter. From the geometric definition of the dot product, the angle θ between two illumination vectors is given by Equation (1). This equation follows from the geometric relation that the dot product of two vectors equals the product of their magnitudes and the cosine of the angle between them. Consequently, the measure expresses the pure directional agreement between the illumination vectors, independent of their magnitudes.

Intensity: E_{scalar} [2]

The illumination solid, defined as the three-dimensional distribution of illuminance in space, can be decomposed into two components: a vector (asymmetric) component and a symmetric component. The vector component follows a cosine distribution with its maximum aligned to the illumination vector $|E_v|$, and it represents the directional contribution of the illumination solid. The symmetric component, by contrast, has equal magnitudes in opposite directions, producing a centrally symmetric distribution that corresponds to the diffuse contribution. Regardless of the number of light sources or the complexity of the luminous environment, the illumination solid can always be represented as the sum of these two components. Scalar illuminance (E_{scalar}) is the mean value of the illumination solid, equivalent to the average illuminance on the surface of an ideal white sphere. It is independent of incidence direction and thus serves as an indicator of the potential brightness at a point in space. This reasoning yields the general formulation expressed in Eq. (2).

Diffuseness: D [2]

In Eq. (3), the fraction $|E_v| / (4\ E_{scalar})$ expresses the degree of light directionality. A value close to 1 indicates that the light is highly concentrated in a specific direction, while a value close to 0 indicates that light is uniformly distributed from all directions. Thus, instead of using directionality directly, its complement (subtracted from 1) was defined as diffuseness. Under this definition, D approaches 0 when the light field is completely directional, as in the case of a spotlight, and approaches 1 when it is completely diffuse, as in the case of a cloudy sky.

RMSE of Color difference

The root mean square error (RMSE) was used to evaluate the overall discrepancy in color appearance between the reference shading and the participant's choice. First, for each pixel i on the white reference sphere at the evaluation target position, the color difference ΔE_i (CIEDE2000) between the reference shading image and the shading image selected by the participant was calculated. These pixel-wise differences were then squared and averaged over all n pixels, and finally the square root of this mean value was taken. This measure expresses the average magnitude of the color difference in the same unit as ΔE, independent of the sign of the deviation.

Results

We focused on color difference as well as on intensity and diffuseness, which exhibited clear differences related to floor coloration conditions. For intensity error (Eq. 2), chromatic conditions exhibited medians closer to zero than achromatic conditions, indicating higher predictive accuracy; this trend was more pronounced in diffuse light source environments. Regarding diffuseness error (Eq. 3)), achromatic conditions generally exhibited higher predictive accuracy than chromatic conditions under both diffuse source and directional source environments. This tendency may arise because, in chromatic conditions, direct-component photons and indirect-component photons differ in color; a small number of red-tinted indirect-component photons can cause observers to overestimate the contribution of indirect light, thereby leading to a misperception of diffuseness. However, under diffuse source environments, when the white sphere was placed near the wall at positions H and M, the achromatic conditions showed higher median prediction errors and larger standard deviations, indicating a reduced predictive accuracy for achromatic conditions in these configurations. Further investigation is required to determine the reasons for this

result. Finally, regarding color difference, no substantial differences were observed between chromatic and achromatic conditions, suggesting that floor coloration had little impact on this indicator.

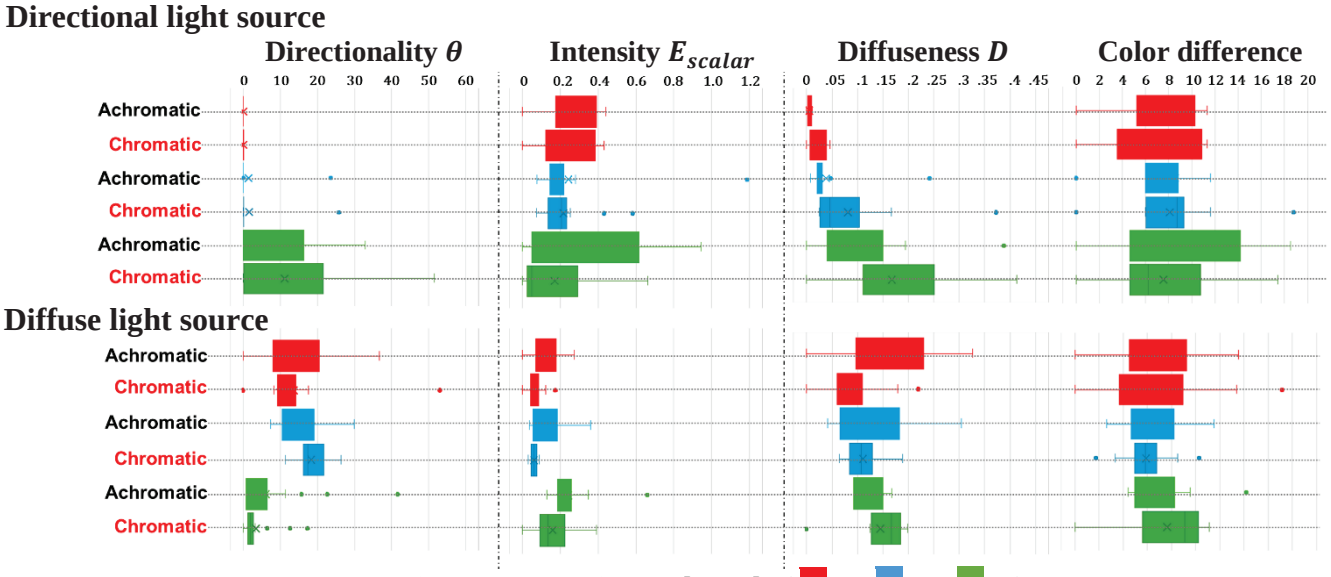

Figure 5: Experimental results(:H :M :L)

CONCLUSION

It was confirmed that the perception of intensity and diffuseness varies depending on the coloration of reflected light. This suggests that the evaluation of intensity and diffuseness was influenced by whether the colors of direct and reflected photons were identical as in achromatic spaces, or different as in chromatic spaces, which provided distinct visual cues. In future work, we aim to reduce or eliminate these perceptual differences between achromatic and chromatic spaces. One possible approach is to separately display direct and reflected photons in the visualization of the light field. By explicitly distinguishing between direct and reflected components, the influence of interior surface colors on participants' judgments may be minimized, enabling more consistent and color-independent evaluation of diffuseness.

REFERENCES

[1]. KARTASHOVA, T. (2016). The Global Structure of the Visual Light Field and Its Relation to the Physical Light Field. Journal of Vision August 2016, Vol.16, 9.

[2]. Cuttle, C. (2003). Lighting by Design. Oxford: Architectural Press

Fashion Color Preferences and Cultural Capital: An Empirical Study Based on Bourdieu's Theory

Jiang Jiani

Tsinghua University, Beijing, China
*Jiang Jiani: jjn20@mails.tsinghua.edu.cn

ABSTRACT

This study, based on Pierre Bourdieu's theory of "taste distinction," explores the role of cultural capital in shaping fashion color preferences. Using a combination of semi-structured interviews and a color preference questionnaire from Shigenobu Kobayashi's Colorist, the research examines a sample of students from various academic disciplines at Tsinghua University. The interviews focused on three key areas: assessing participants' cultural and economic capital, investigating their self-awareness and preferences for color, and analyzing their fashion color choices, including wardrobe colors, acceptance of different colors, and situational preferences.

The findings reveal that cultural capital plays a significant role in influencing fashion color selection and expression. Individuals with higher cultural capital tend to adopt more personalized and innovative color choices, whereas those with middle cultural capital prefer softer, more practical colors with lower saturation, showing a preference for practical, safe color options. Participants from lower social strata demonstrate a "mixed" fashion color taste, characterized by a combination of subtlety and individuality, which aligns with Bourdieu's concepts of "legitimate taste," "middle taste," and "popular taste." Additionally, the way cultural capital is acquired influences color preferences. Students in art-related fields, particularly those studying fashion design, receive greater cultural capital from their education, which provides them with richer color resources and a more professional approach to expressing their color preferences.

Gender and social mobility further moderate fashion color preferences. Male participants' color choices are less strongly influenced by cultural capital, highlighting differences in how gender roles affect fashion and color expression. This study emphasizes the mediating role of cultural capital in shaping fashion color perceptions and decisions, offering new empirical insights into the intersection of color culture and social structure. Given that the sample is predominantly from a high-cultural-capital environment, the findings should be interpreted with consideration of various social contexts when generalized.

Keywords: Color preference; Fashion color; Cultural capital; Distinction of taste; Color culture

INTRODUCTION

The Fashion colors serve as more than mere aesthetic markers; they function as potent symbols of identity and social positioning. Pierre Bourdieu's seminal work, Distinction, argues that aesthetic preferences are socially constructed, reflecting an individual's endowment of "cultural capital"—accumulated through education, family upbringing, and social exposure—and their position within the social space.

While Bourdieu's framework is foundational, its application requires careful contextualization beyond the French context. In contemporary China, the relationship between economic and cultural capital may manifest differently. This study investigates the formation of fashion color tastes among Chinese elite university students, a group situated within a high-cultural-capital field yet internally diverse. It seeks to answer: How does cultural capital stratify color preferences? How do acquisition pathways and social factors like gender moderate this influence?

METHODOLOGY

The study selected a sample of 10 students (5 male, 5 female) from Tsinghua University using purposive sampling to ensure diversity across disciplines (e.g., Law, Social Sciences, Arts, Computer Science).

A mixed-method approach was employed:

Semi-structured Interviews focused on assessing (a) cultural and economic capital (family background, education), (b) self-color cognition, and (c) fashion color choices (wardrobe contents, acceptance, situational preferences).

Questionnaire: The color preference survey from Kobayashi's Colorist was used to map abstract and concrete color inclinations.

Data on participants' profiles were compiled (See Appendix Table 1 for full details). Interviews were transcribed and analyzed thematically to correlate color preferences with capital volume and composition.

RESULTS AND DISCUSSION

Stratification of Color Tastes

The findings reveal a clear homology between cultural capital and color taste.

High Cultural Capital: Participants from affluent or artistically cultivated backgrounds (e.g., Participants C, D, F - See Appendix Table 1) exhibited a "legitimate taste." Their choices were innovative and personalized, featuring bold contrasts and high saturation to signify individuality.

Middle Cultural Capital: This group (e.g., Participants A, B, I) displayed a "middle-brow taste," prioritizing practicality and conformity. Their palettes were dominated by safe, versatile colors like black, white, and navy.

Lower Cultural Capital: Participants from this background (e.g., G, H, J) exhibited a "hybrid" taste. Their everyday wear leaned towards dark, practical tones but was often accented with brighter colors, representing a pragmatic negotiation between constraints and a claim to self-expression.

Pathways of Capital Acquisition

The mode of acquiring cultural capital significantly influenced its expression.

Inherited Capital: Participants from families with high cultural capital (e.g., F, whose parents are professors) internalized discerning color sensibilities from a young age.

Institutionally Acquired Capital: Students in design fields (e.g., H, J) accumulated capital through specialized education. They mastered a professional lexicon to articulate choices (e.g., "saturation," "value gradation"), demonstrating how educational institutions act as sites for reproducing taste.

Moderating Factors: Gender and Social Mobility

Gender: A stark contrast was observed. Male participants' color choices were largely convergent, confined to neutrals and justified as "convenient," showing less variance with cultural capital (See Appendix Table 2 for comparative examples). Female participants demonstrated greater willingness to experiment, using color more consciously as a tool for expression.

Social Mobility: Participants who experienced significant upward mobility (e.g., from tier-4/5 cities to Tsinghua) often displayed a dual consciousness. They adopted muted tones in formal settings to assimilate, while retaining preferences for more expressive colors privately, indicating the ongoing internalization of new cultural codes.

CONCLUSION

This study validates that cultural capital is a primary determinant in the stratification of fashion color tastes, generating distinct patterns from "innovative" to "practical" to "hybrid." It refines Bourdieu ' s theory by highlighting the crucial moderating roles of gender and social mobility, and the importance of acquisition pathways.

Theoretically, it contributes by applying the framework to color culture in a Chinese context. Practically, it reveals that color choices are deeply embedded in social structure, yet also show glimpses of being a tool for identity negotiation (e.g., non-arts students expressing a desire for more aesthetic knowledge).

A key limitation is the sample ' s confinement to an elite institution. Future research should encompass a broader social spectrum. Ultimately, this research bridges color science and sociology, offering a lens to understand how everyday aesthetic choices are woven into the fabric of social reproduction and change.

REFERENCES

[1]. Bourdieu, P. (1984). Distinction: A Social Critique of the Judgement of Taste. Harvard University Press.

[2]. Kobayashi, S. (2006). Color Psychology Analysis (Nankai University Mechanics Color and Public Art Research Center, Trans.). People's Fine Arts Publishing House.

[3]. Xu, B. (2002). The Problem of Cross-Context Transfer in Cultural Critical Theory. Literature & Art Studies, (4), 38–43.

[4]. "2017 China City Tier Classification Complete List". (2017, December 18). Sohu. Retrieved from https://www.sohu.com/a/216473057_351368

APPENDIX

Table 1: Demographic and Socio-Economic Profiles of Participants

Parti-cipant	Highest Education / Field of Study	Family Economic Tier	Hometown Tier (City)	Family Housing Type	Parental Education	Parental Occupation
A	PhD / Law	Middle-class	Tier-2 City	Apartment	Bachelor's Degree	Teacher
B	PhD / Journalism	Middle-class	New Tier-1 City	Apartment	Bachelor's Degree	Engineer
C	Bachelor's / Economics & Management	Affluent	Tier-2 City	Villa	Bachelor's Degree	Director
D	PhD / Painting	Affluent	New Tier-1 City	Apartment	Bachelor's Degree	Professor
E	PhD / Information Design	Mass	Tier-2 City	Apartment	High School Diploma	Engineering Contractor
F	Bachelor's /	Middle-	Tier-1 City	Apartment	PhD	Professor

	Computer Science	class				
G	Master's / Environmental Engineering	Mass	Tier-2 City	Apartment	Bachelor's Degree	Government Clerk (Neighborhood Committee)
H	Master's / Fashion Design	Mass	Tier-5 City	Simple Housing	Junior High School	Worker
I	Master's / Architecture	Middle-class	Tier-4 City	Apartment	Bachelor's Degree	Retired
J	Master's / Fashion Design	Mass	Tier-1 City	Apartment	Bachelor's Degree	Retired

Notes:

Family Economic Tier was self-reported by participants and categorized into three groups: Mass, Middle-class, and Affluent.

Hometown Tier follows the 2017 China City Tier Classification.

Parental Education reflects the highest educational attainment of either parent.

Table 2: Summary of Participant Color Preferences, Influences, and Capital Classification

Parti-cipant	**Gender**	**Cultural Capital Level**	**Kobayashi Color Preference Type**	**Dominant Wardrobe Colors and Descriptive**	**Key Influencing Factors**
A	M	Medium	Sober-Soft	Dark tones / Black / Olive Green	Peer influence
B	M	Medium	Fresh-Soft	Dark tones / Black / Olive Green	Family education (pragmatism)
C	M	High	Multi-preference (Fresh-Soft, Fresh-Sturdy)	Dark tones / Black / Olive Green / Blue	Peer influence
D	F	High	Showy-Soft	Camel tones / Color-blocking	Family education (artistic)
E	F	Low (with High Capital Habitus)	Multi-preference (Fresh-Soft, Gorgeous-Solemn)	Black / High-saturation colors	Trend culture, Overseas

					experience
F	M	High	Multi-preference (Fresh-Soft, Showy-Soft)	Dark tones / Black / Green / Color-blocking	Family education (high-cultural)
G	F	Low	Sober-Dominant 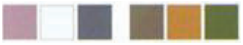	Dark tones	Economic constraints
H	M	Low	Multi-preference (Fresh-Soft, Sober-Dominant)	Grey tones / Bright colors	School education, Peer influence
I	F	Medium	Sober-Sturdy 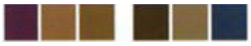	Grey tones / Bright colors	Media, Popular culture
J	F	Low	Sober-Soft	Black / White / Yellow	School education, Economic constraints

Notes:

Cultural Capital Level is a comprehensive assessment based on the volume and composition of economic and cultural capital (derived from data in Appendix Table 1), following Bourdieu's framework.

Kobayashi Color Preference Type is determined using the methodology from Shigenobu Kobayashi's Colorist.

Dominant Wardrobe Colors are based on participant interviews and photographic evidence of their wardrobes.

Key Influencing Factors are the primary reasons cited by participants for their color choices.

Color Appearance of Waterlilies

Chanprapha Phuangsuwan[a]*, Kitirochna Rattanakasamsuk[a], Mitsuo Ikeda[a], and Mikiko Kawasumi[b]

[a]Color Research Center, RMUTT, Pathum Thani, Thailand
[b] Faculty of Information Engineering, Meijo University, Aichi, Japan
*Corresponding author: Chanprapha Phuangsuw an, Phuangsuwan@rmutt.ac.th

ABSTRACT

This study investigates the color appearance of waterlilies using the elementary color naming method, highlighting their natural beauty and biological complexity. It also compares how Thai and Japanese observers perceive these colors. Thirty waterlily specimens were grouped into five dominant color categories; white, yellow, pink, red, and purple and further classified based on their color patterns as either uniform or non-uniform. Observers viewed the images displayed on LCD monitor from a fixed distance, matching the waterlily colors using the Munsell color system book. They then evaluated the color appearance through the elementary color naming method. Next, they identified the hue. Each judgment was repeated three times for consistency. The study successfully captured detailed color appearance data, offering insights into cross-cultural color perception and contributing to the understanding of how people visually interpret the complex coloration of waterlilies.

Keywords: waterlilies, color appearance, elementary color naming, display

INTRODUCTION

The color appearance of waterlilies can be effectively described using basic color terms such as white, yellow, orange, pink, red, blue, and purple. These basic color terms capture how humans perceive the flowers in natural environments without needing complex colorimetric measurements. The way waterlilies display these colors results from a combination of natural pigments, petal structure, environmental conditions, and genetic variation among regular and hybrid species. At the biochemical level, the primary determinants of waterlily coloration are plant pigments, especially anthocyanins, carotenoids, and flavonoids. Anthocyanins are primarily responsible for red, purple, and blue hues, with specific color outcomes influenced by pH levels within the plant cells, co-pigmentation with other molecules, and the presence of metal ions. Carotenoids, by contrast, contribute to yellow and orange tones and are highly stable across environmental conditions. Flavonoids can enhance color brightness and participate in UV protection, adding layers of optical complexity not immediately visible to the human eye but essential for the plant's ecological interactions. In particular, regular and hybrid species selectively accumulate specific pigments in varying concentrations, leading to both subtle and dramatic differences in color across varieties. Environmental factors such as sunlight, water quality, temperature, and soil nutrients can influence the strength and clarity of waterlily colors. For instance, flowers grown in full sunlight often produce more vivid colors, while those in shaded or cooler environments may have paler or slightly different tones. Water with high levels of dissolved minerals can also affect pigment expression, sometimes causing unexpected shifts in color. The surface structure of waterlily petals contributes to their color appearance as well. Petals with rough or cone-shaped (papillate) cells scatter light in a way that makes colors look more vivid and intense. In contrast, petals with smoother surfaces may appear softer and less bright. These microstructures modify how basic colors like pink, red, or blue are perceived by enhancing brightness or creating subtle shimmer effects.

METHODOLOGY

Thirty waterlily specimens were categorized into five color groups: white (WH), yellow (YL), pink (PK), red (RD), and purple (PP), as shown in Fig. 1(a). These dominant color groups define the visual language of waterlilies and were further classified based on their color patterns as either uniform (petals with a plain color) or non-uniform (gradation, texture, or special patterns), as shown in Fig. 1(b). Photographs of the waterlilies were taken and displayed on an EIZO ColorEdge CG2700S 27-inch LCD monitor, calibrated to Gamma 2.2, CCT 6500K, and sRGB mode. The monitor was placed in an experimental room illuminated by white light with a CCT of 6500K and an illuminance of approximately 500 lx. Observers were seated 60 centimeters from the monitor, resulting in a visual angle of approximately 17° × 17°, representing the actual size of a waterlily as seen in a garden. Participants were tasked with matching the color appearance using the Munsell color system book. Following this, they evaluated the color using the elementary color naming method. First, they assessed the elements of color; chromaticness, whiteness, and blackness ensuring the total equaled 100%. Next, they identified the apparent hue using opponent color pairs (red or green, and yellow or blue), selecting no more than two hues according to opponent color theory, again totaling 100%. Each color judgment was repeated three times.

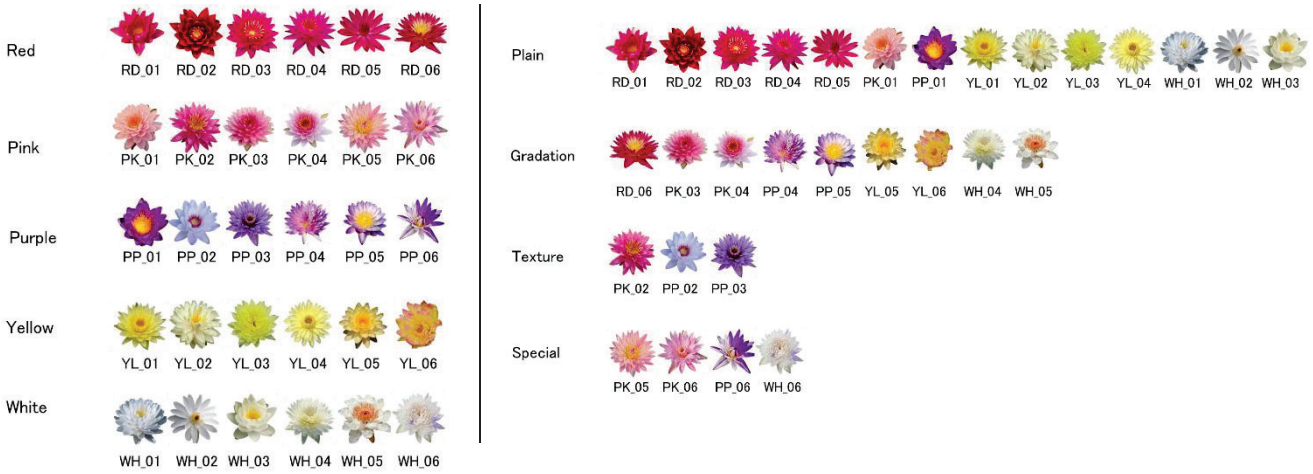

(a) (b)

Figure 1 The picture of thirty waterlilies (a) and the classification into uniform and non-uniform color (b).

The color naming results were calculated hue angle by eq 1 and the color coordinate x and y by eq 2 and 3 respectively. The result was plotted into the polar hue opponency diagram.

$$Hue\ angle = \frac{R \times 0 + Y \times 90 + G \times 180 + B \times 270}{100} \quad (1)$$

$$x = chromaticness \times \cos(hue\ angle) \quad (2)$$

$$y = chromaticness \times \sin(hue\ angle) \quad (3)$$

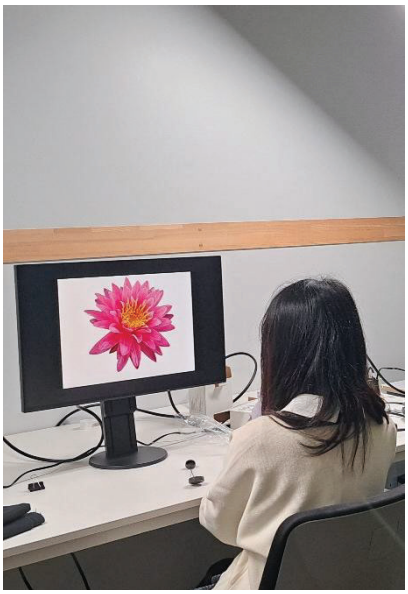

Figure 2 The atmosphere of color naming experiment.

RESULTS AND DISCUSSION

The results from the elementary color naming method are plotted in a polar opponent color diagram, as shown in Fig. 3. Filled symbols represent results from Thai observers, while open symbols represent results from Japanese observers. We found that the waterlilies in the red group did not appear as pure red, but rather as reddish yellow for Japanese observers and reddish blue for Thai observers. A similar trend was observed in the pink group, which appeared reddish blue to Thai participants and reddish yellow to Japanese participants. This difference is intriguing and suggests a potential cultural or perceptual bias that warrants further investigation particularly why Japanese observers tend to perceive more reddish yellow than reddish blue. In the purple group, flowers appeared more bluish to Japanese observers and more reddish to Thai observers. This might be due to differences in experience or familiarity with color naming between the two groups. In contrast, the yellow and white groups did not show significant differences in perceived color.

Overall, waterlilies did not appear as a single, uniform color, even though they are typically categorized into one color tone. This method allows for a more precise specification of hue. However, a higher standard deviation (SD) was observed among Japanese participants, possibly due to a lack of experience with the elementary color naming method. There were no significant differences between the two groups in chromaticness, whiteness, and blackness except in the red color group.

Figure 4 illustrates that our perception can compensate for complex color properties such as gradation and two-tone effects, which are commonly seen in waterlilies. The results suggest that observers tend to judge color appearance based on the most vivid area of the petals, regardless of whether the flower has plain, textured, or gradated coloration. For instance, in specimen PP_06, both Japanese and Thai observers agreed on the purple hue, but not on the presence of white.

The results of color matching using Munsell color chips were generally consistent with the apparent hues identified through the elementary color naming method. In the red group (RD_01 to RD_06), the matched hues were 10RP, 10RP, 2.5R, 7.5RP, 10RP, and 2.5R, respectively. For the yellow group (YL_01 to YL_06), the matched chips were 10Y, N, 10Y, 7.5Y, 5Y, and 7.5Y. For the purple group (PP_01 to PP_06), they were 7.5P, 10PB, 2.5P, 7.5P, 2.5P, and 7.5P. In the pink group (PK_01 to PK_06), they were 5R, 7.5RP, 5RP, 7.5RP, 7.5RP, and 2.5RP.

The white group (WH_01 to WH_06) matched with N9, except for WH_06, which matched with 10PB. Interestingly, WH_06 despite appearing entirely white as shown in Fig. 1(a), it had a small area at the tip of the petal but all observers matched with 10PB, which was also reflected in the color naming results.

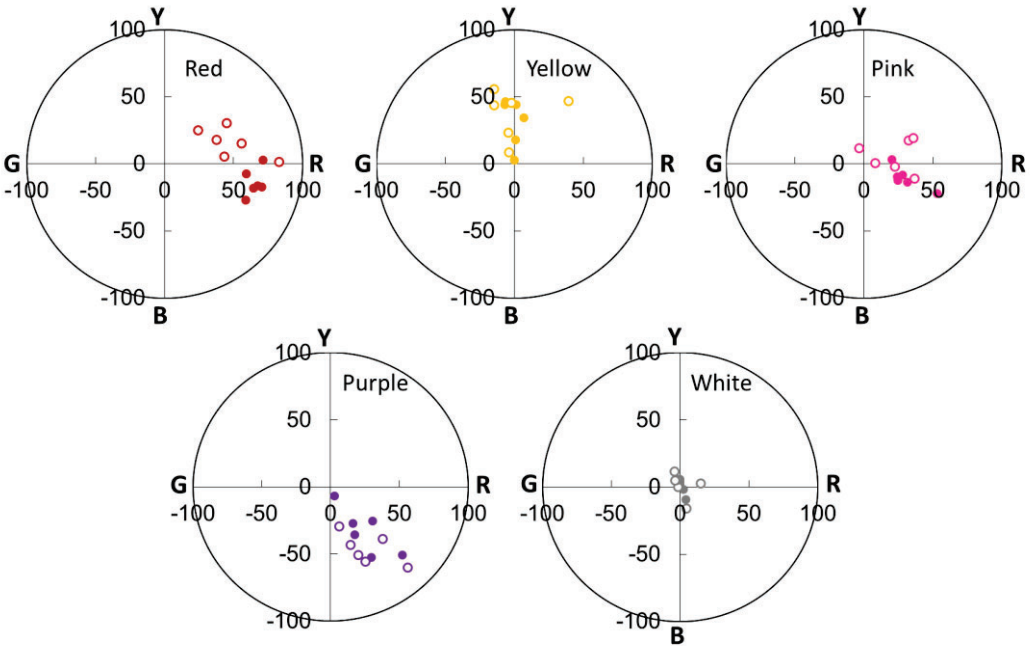

Figure 3 Results of elementary color naming method, filled symbols represent to Thai result and opened symbols represent to Japanese result.

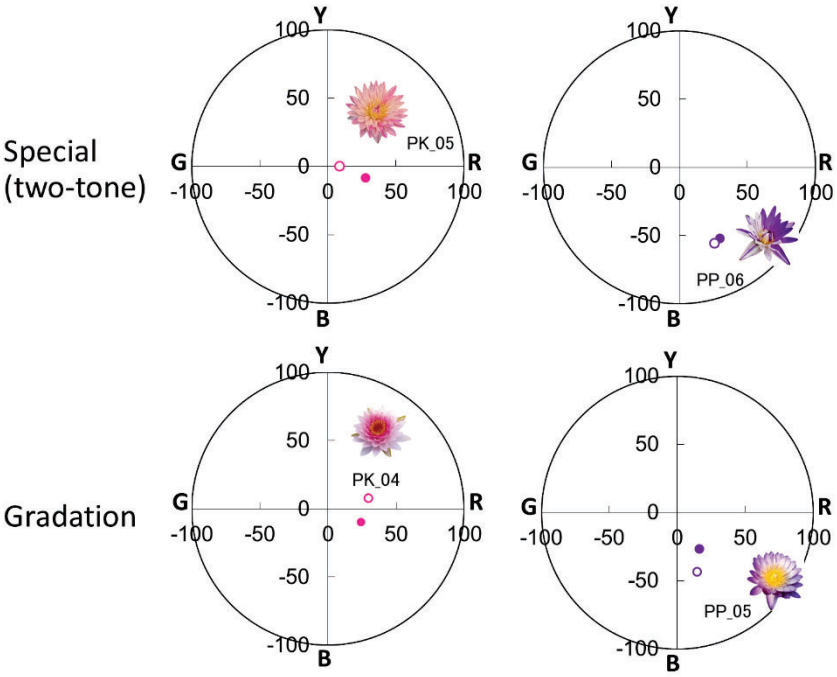

Figure 4 The example of elementary color naming of waterlilies in special and gradation category.

CONCLUSION

We described the color appearance of waterlilies using the elementary color naming method to precisely capture their detailed color characteristics. The color appearance was also confirmed by matching with Munsell color chips, and the results showed good agreement.

ACKNOWLEDGEMENTS

This study was funded from the Meijo university as visiting researcher scholar. We would like to thank all the Kawasumi's laboratory members to participate in the valuable time to complete the experiment sessions.

REFERENCES

[1]. Watana, T. (2004). The Lotus A Symbol of Buddhism, Anurak Thailand Tourism. Retrieved April 5, 2025, from https://www.thailandnow.in.th/life-society/the-lotus-flower-is-everything-everywhere-all-at-once-in-thailand/

[2]. Akarakunthorn, P. (2013). Blooming colors of lotus, how do we develop? Invited talk at ACA2013 conference.

[3]. Phuangsuwan, C., Ikeda, M. and Kawasumi, M. (2025). Color appearance of waterlilies by elementary color naming method. the 56th Annual Meeting of the Color Science Association of Japan to be held on June 6th and 7th in Yonezawa, Japan

Examining The Degrees of Smoke Emissions Using The Calibrated Camera Technology

Chun-Kung Cheng[a], Bao-Jen Pong[b], Yu-Cheng Shih[c], Yu-Zhi Ou[d], and Hung-Shing Chen[e*]

[a] Graduate Institute of Applied Science and Technology, National Taiwan University of Science and Technology, Taipei, 106335, Taiwan
[b] Industrial Technology Research Institute, Taipei, 106335, Taiwan
[c] Graduate Institute of Color and Illumination Technology,
National Taiwan University of Science and Technology, Taipei, 106335, Taiwan
[d] O Know Image Co., Ltd., New Taipei, 106335, Taiwan
[e] Graduate Institute of Electro-Optical Engineering, National Taiwan University of Science and Technology, Taipei, 106335, Taiwan
[*]Corresponding author: Hung-Shing Chen, bridge@mail.ntust.edu.tw

ABSTRACT

The Ministry of Environment (MOENV), Taiwan, has made significant progress in regulating smoke emissions in recent years. Following the completion of the "Simulation and validation of black smoke using image-based smoke detection system" project in 2022–2023, the results demonstrated superiority over traditional visual smoke detection standards (maximum error <15%, average error <7.5%). Building upon the extended outcomes of the aforementioned project (commencing in 2024), this study further develops "Advanced calibration method for intelligent image-based smoke detection system." It expands the opacity levels for black and white smoke and employs color science methodologies to optimize two key tasks. Task 1: "Digital image calibration for smoke"; and Task 2: "Advanced monitor verification of smoke opacity in digital images." Task 1 addresses outdoor smoke image processing. This study incorporates ColorChecker color chart and an improved 9-level Ringelmann smoke chart. Through comprehensive color calibration steps, it ensures the accurate reproduction of smoke image colors captured by digital camera, providing reliable scientific color quality for photographic results. This corresponds to the approximate smoke concentration in each image, serving as an auxiliary tool for training environmental assessment specialists and establishing criteria. Task 2 focuses on verifying darkroom opacity. Using a well-calibrated LCD monitor, it validates brightness measurements of calibrated smoke images. This establishes a standardized workflow for smoke opacity verification systems and produces a high-quality smoke image database. Ultimately, by completing measurements on high-resolution images of black smoke (100 images) and white smoke (101 images), the relationship between the luminance values of the captured images and those on sRGB monitor was analyzed. Results indicate that the correlation coefficient for black smoke images (r= 0.99) exhibits more stable results compared to white smoke images (r= 0.94).

Keywords: smoke detection, opacity estimation, color image processing

INTRODUCTION

Smoke emission intensities are positively correlated with concentrations of air pollutants including PM2.5, PM10, gaseous pollutants, and particulate heavy metals (Chaloulakou et al., 2005; Rose, 1995; California Air Resources Board,1993). Black smoke emission levels are often regarded as a key indicator for identifying pollution sources and assessing air pollution severity (Brink et al., 2021). Research also indicates that white smoke and other colored fumes pose significant threats to the environment and human health (Brunekreef, 2010). Effective regulatory measures to decrease emissions from smoke sources, mitigate air pollution hazards, and improve urban air quality have become critical priorities in environmental policies worldwide.

Visual smoke inspection techniques trace back to the “Ringelmann smoke chart” released in 1888 by Professor Maximilien Ringelmann. This chart measures smoke density across five gray-scale levels, ranging from no smoke (Level 0) to dense smoke (Level 5), requiring observation by comparing smoke against a standard grid pattern. Since outdoor smoke intensities are often influenced by factors such as fuel particle concentration, size, plume thickness, and lighting conditions, observational methods recommend multiple, timed observations and multi-person assistance to enhance accuracy. The fundamental principle is: dark smoke indicates incomplete fuel combustion products, posing health hazards; while white smoke is primarily water vapor condensation. UK and Irish regulations prohibit emissions exceeding Level 2 dark smoke to ensure air quality (Hughes, 2010). The invention of the Ringelmann smoke chart pioneered the technique of visual smoke assessment based on “opacity,” serving as a crucial tool in America's early campaigns to eliminate black smoke emissions (Uekoetter, 2005). Taiwan currently primarily adopts American and British standards for smoke emission assessment, typically conducted by professionally trained smoke inspectors using the Ringelmann smoke scale. Given the scale's long-standing use, significant room for improvement remains in modern air pollution techniques for evaluating increasingly complex dark and white smoke emissions.

The Ministry of the Environment in Taiwan has made progress in regulating smoke emissions in recent years. Following the completion of the “Simulation and validation of black smoke using an image-based smoke detection system” project from 2022 to 2023, the results demonstrated superiority over traditional visual smoke detection standards (maximum error <15%, average error <7.5%). Building upon the outcomes of the aforementioned project (extended from 2024), this study further develops “Advanced calibration method for intelligent image-based smoke detection System.” It expands the smoke opacity levels for black and white smoke and employs color science methodologies to optimize the following two core tasks: Digital image calibration for smoke detection, and Advanced monitor-based verification of smoke images.

Task 1 primarily addresses the processing of outdoor smoke imagery. This study incorporates ColorChecker color chart and an enhanced 9-level Ringelmann smoke chart. Through comprehensive color calibration steps, it ensures the accurate reproduction of smoke imagery's true colors captured by digital cameras, thereby providing reliable, scientifically validated color quality for the photographic results. The enhanced “9-level gray scale chart” is expected to enable automated detection of the closest gray scale value for on-site smoke through programmed operations. This corresponds to the approximate smoke concentration in each image, serving as an auxiliary tool for training environmental assessment specialists and establishing evaluation criteria. Besides, Task 2 focuses on verifying darkroom opacity. Utilizing a well-calibrated LCD display capable of precise configuration conversion and color calibration as the standard display platform, it validates brightness measurements of calibrated smoke images. This establishes a standardized workflow for smoke opacity verification systems, producing a high-quality standard smoke image database. This is expected to serve broader air pollution prevention applications, including training for environmental inspectors, practice test questions for smoke criteria assessment, big data repositories, and machine iterative learning.

METHODOLOGY

Visual smoke assessment traditionally relies on human visual judgment to determine the opacity of black or non-black smoke from exhaust pipes. In Taiwan, assessors are trained using outdoor smoke generators to learn standardized procedures. Actual opacity values are measured via chimney-installed sensors. Beyond routine field training, this study explores the integration of precise digital imaging to advance "intelligent smoke assessment." The first stage, "Digital image calibration for smoke," introduces an enhanced 9-level smoke gauge that refines the original 5-level Ringelmann chart into a realistic 9-level grayscale (Figure 1), improving calibration accuracy for black and white smoke. Subsequent steps—outdoor scene capture, high-resolution color grading, reference image synthesis, file conversion, and screening—enable advanced screen-based verification of digital smoke opacity, as summarized in Figure 2.

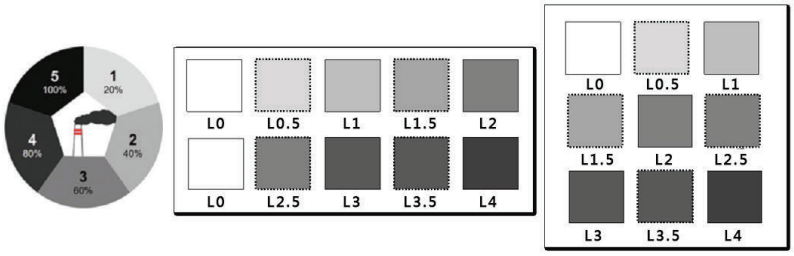

(a) (b) (c)

Figure 1: Schematic of standard gray scale plate generation: (a) Ringelmann chart, (b) and (c) modified smoke charts. (a) Five-level (Levels 1~5) Ringelmannn chart indicating intent. (b) and (c) represent two designed modified nine-level smoke charts. These charts can be served as references for outdoor visual smoke assessment and smoke imaging.

Figure 2: Preparation of three styles of "9-level gray smoke chart". The actual output is a 9-level gray scale chart, designed with three arrangement patterns. The target luminance values (CIE L^*) for the 9-level gray scale are respectively set to correspond to L^* = 45, 55, 60, 65, 75, 80, 85, 90, 95. The produced 9-level gray scale chart was outputted using a high-end inkjet printer on specialized premium paper stock. The color difference values (ΔE_{00}) were all controlled to be less than 1.0.

Outdoor smoke scenes were recorded using three high-end digital cameras, synchronized to simultaneously measure smoke density, ambient illumination, and exposure settings (Canon EOS 5D Mark IV, 30 megapixels, static capture at one frame per second). A 24-color X-Rite ColorChecker® color chart was placed within each smoke scene to enable precise color calibration during post-processing. The standardized brightness measurement procedure consists of the following steps (Figure 3):

1. Image acquisition – Capture outdoor smoke imagery (black and white smoke). The ColorChecker chart is used to generate the camera-specific calibration profile (i.e., ICC color profile).
2. File conversion – Convert the captured RAW image files into Adobe Digital Negative (DNG) format.
3. Profile generation – Use camera calibration softwares, such as X-Rite ColorChecker camera calibration or Lumariver profile designer, to generate the calibration profile and embed the standard image into the DNG file for color-corrected imaging.

4. Reference display calibration – Display the resulting TIFF files on a well-calibrated LCD monitor (EIZO ColorEdge CG2700X), calibrated to sRGB specifications (ambient illuminance of 64 lx; sRGB gamut; 100 cd/m²; 6500 K; γ =2.2). Conduct visual verification of the opacity levels in indoor environmental smoke images under standardized conditions.
5. Photometric measurement – Using a colorimeter (Konica Minolta CS-160), measure the tristimulus values of the selected image area as displayed on the monitor. Report the results as luminance values (Lv, in cd/m²).

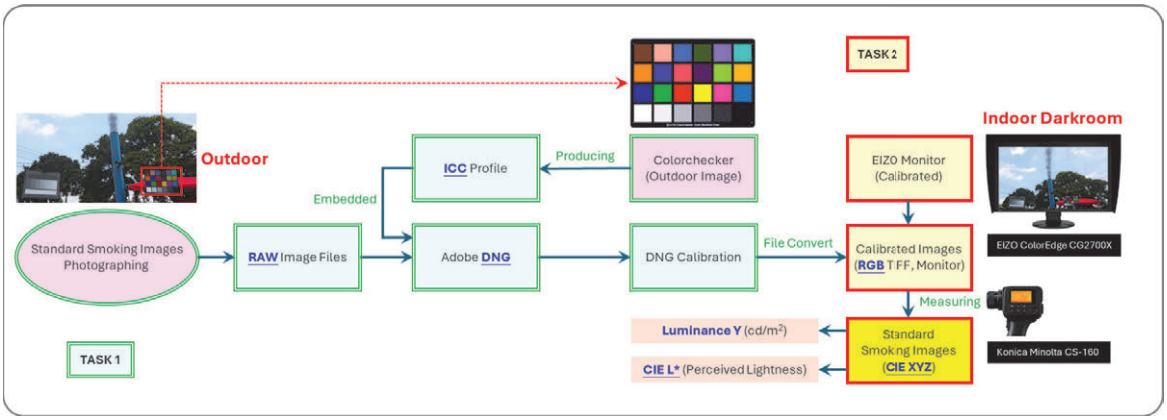

Figure 3. Flowchart for preparation of "Standard smoke emission assessment image".

RESULTS AND DISCUSSION

Through the implementation of the above steps, the key outcomes are as follows:

1. Standard smoke image database: After seven rounds of refined field photography operations (such as the three-scene composite process shown in Figure 4), 847 black smoke images and 431 white smoke images were selected from tens of thousands of field photographs. These smoke images can serve as a future big data standard database.

Figure 4. Scenes from three digital cameras for comparative application, from left to right: smoke machine setting, front-lit shot, side-lit shot.

2. Indoor measurement of standard image opacity: After preparing the standard smoke image dataset, the images were displayed on a well-calibrated LCD monitor. A single-point luminance meter was employed to measure the opacity of the images. For the smoke regions within the selected targets, Figure 5 presents a case in which the opacity of the white smoke generator was set to 75%. The captured image was subsequently displayed on the indoor LCD monitor for measurement and verification.

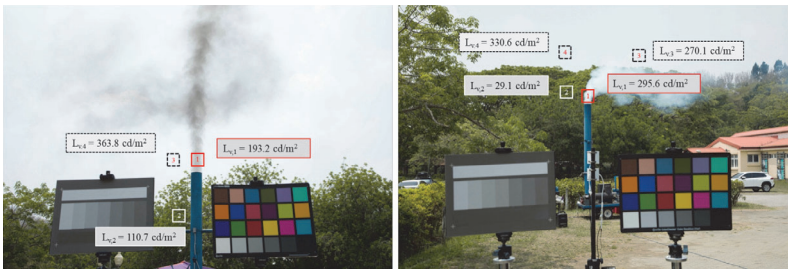

(a) (b)

Figure 5: Schematic diagram of indoor standard display with 75% light transmittance and measurement points: (a) black smoke, (b) white smoke.

3. Standard image measurement and verification: The final standard images of black and white smoke were selected for quantitative evaluation. Figure 6 illustrated the relationship of chromaticity (CIE xy) and luminance (CIE Y) between the sRGB monitor and the captured images for black smoke (n = 100) and white smoke (n = 101). The resulting correlation coefficients were 0.99 for black smoke images and 0.94 for white smoke images, indicating that the captured black smoke images exhibited higher measurement stability.

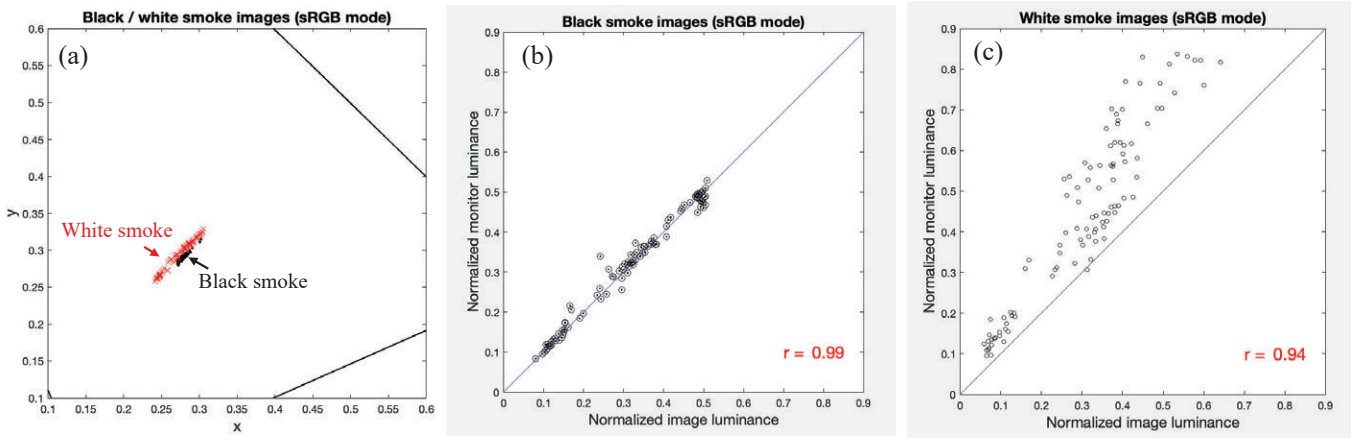

Figure 6: Analytical results of the smoke images: (a) CIE xy distribution, (b) Luminance relation of black smoke images and (c) Luminance relation of white smoke images.

CONCLUSION

The conclusions of this study are arranged as follows: a standardized smoke image database was developed. Seven field campaigns yielded a curated dataset of 847 black-smoke and 431 white-smoke high-resolution images, forming a robust foundation for future big-data training, detection standards, and AI-based interpretation. In addition, a brightness measurement method of image-based smoke detection system was confirmed. An indoor well-calibrated monitor and single-point luminance meter enabled the establishment of a standardized procedure linking scene brightness values to display luminance, ensuring methodological consistency. Finally, the reliabilities of captured black / white smoke image were verified. Correlation analysis demonstrated high reproducibility, with black-smoke images achieving a coefficient of 0.99, outperforming white-smoke images (r=0.94), thus validating their suitability as reference standards for automated smoke monitoring.

ACKNOWLEDGEMENTS

We would like to thank Industrial Technology Research Institute for providing the valuable collaboration opportunity, which enabled our team to successfully complete this fruitful and meaningful research. (Project 2023~2025: Advanced artificial intelligence image-based smoke emissions detection technology enhancement and expansion project)

REFERENCES

Brink, H., Hitzenberger, R., & Keuken, M. (2021). On the Equivalency of Black Smoke / British Smoke and Historic Elemental Carbon. Atmospheric Environment, 244, 117857. https://doi.org/10.1016/j.atmosenv.2020.117857

Brunekreef, B. (2010). The Color of Smoke. Epidemiology, 21(6), 903- 904. https://doi.org/10.1097/ede.0b013e3181f4e1e6

California Air Resources Board. (1993). Visible Emissions Evaluation Handbook. California Environmental Protection Agency, Air Resources Board. From https://fei.psu.edu/dotnetapps/califemissions/

Chaloulakou, A., Kassomenos, P., Grivas, G., & Spyrellis, N. (2005). Particulate Matter and Black Smoke Concentration Levels in Central Athens, Greece. Environment International, 31(5), 651-659. https://doi.org/10.1016/j.envint.2004.11.001

Hughes, G., 2010. Ringelmann Smoke Chart: Assessing Smoke Density, International Initiative for Impact Evaluation. United States of America. Retrieved from https://coilink.org/20.500.12592/dc9fcs on 13 Jan 2024.

Rose, T. H. (1995). Visible Emission Evaluation Procedures Course: Student Manual (Course 325, Final Review Draft). Environmental Institute for Technology Transfer, University of Texas at Arlington. U.S. Environmental Protection Agency. from https://www3.epa.gov/ttnemc01/methods/VECourse.pdf

Yuen, W., Gu, Y., Mao, Y., Koloutsou-Vakakis, S., Rood, M. J., Son, H. K., ... & Du, K. (2017). Performance and uncertainty in measuring atmospheric plume opacity using compact and smartphone digital still cameras. Aerosol and Air Quality Research, 17(5), 1281-1293. https://doi.org/10.4209/aaqr.2016.08.0369

Yuen, W., Gu, Y., Mao, Y., Kozak, P. M., Koloutsou-Vakakis, S., Son, H. K., ... & Rood, M. J. (2018). Daytime atmospheric plume opacity measurement using a camcorder. Environmental technology & innovation, 12, 43-54. https://doi.org/10.1016/j.eti.2018.07.003

Uekoetter, F. (2005). The Strange Career of the Ringelmann Smoke Chart. Environmental Monitoring and Assessment, 106(1-3), 11-26. https://doi.org/10.1007/s10661-005-0756-z

Perceptual Associations Between Classical Music and Colour in Mozart's "Twinkle, Twinkle, Little Star" Variations

Yu Ting Lee [a*], Fei Man Chang[b]

[a]National Taiwan University of Arts, Taipei, Taiwan
[b]National Taiwan University of Arts, Taipei, Taiwan

[*]Corresponding author: YuTing Lee, yuutiing1113@gmail.com

ABSTRACT

This study explores crossmodal correspondences between music and colour, focusing on Mozart's Twelve Variations on "Ah, vous dirai-je, Maman" (K.265/300e), commonly known as the "Twinkle, Twinkle, Little Star" Variations. Forty-six participants with design- or colour-related backgrounds listened to the theme and twelve variations. For each section, they selected the "most congruent" and "least congruent" colours from 27 Munsell-based samples and rated eight pairs of expert-validated semantic differential adjectives on a seven-point scale. The data were analysed using the Preference Index (PI) and Principal Component Analysis (PCA) to examine associations between colour choices and semantic perception.

Results indicated that sections with rapid tempo or rapid note passages were associated with saturated warm colours, while slower or minor sections tended to correspond to cooler or darker colours. Harmonically rich passages were often related to neutral tones. Semantic ratings, mapped onto the Valence–Arousal model, further confirmed that tempo, rhythm, and harmony systematically shaped emotional perception and corresponding colour associations.

By analysing a complete classical work rather than isolated tones or short excerpts, this study provides empirical evidence for structured music–colour correspondences. The findings enhance understanding of auditory–visual interaction and suggest applications in multisensory design, artistic practice, and music education.

Keywords: colour perception, colour semantics, crossmodal correspondence, music–colour association, music visualisation

INTRODUCTION

Crossmodal research has consistently shown associations between music and colour, indicating that colour conveys semantic meaning and shapes musical perception. Yet, most studies have focused on single tones, pitch, or short excerpts, with little systematic analysis across sections of complete classical works. Reymore et al. (2023) further noted that even within a single instrument, changes in pitch range can produce distinct semantic evaluations, emphasising the dynamic nature of musical perception [1].

This study examines Mozart's Twelve Variations on "Ah, vous dirai-je, Maman" (K.265/300e), a composition comprising a theme and twelve variations that, while based on the same melody, presents diverse rhythmic and harmonic treatments. It investigates participants' colour choices and semantic evaluations for each section to explore crossmodal correspondences between music and colour. The aim is to clarify how musical features shape colour associations and to provide an empirical basis for understanding auditory–visual interaction in multisensory design and artistic practice.

METHODOLOGY

Participants were required to be at least 18 years old, without colour vision deficiencies or hearing impairments, and to have a background in design, art, or colour-related fields. These criteria were established to ensure adequate sensitivity to colour and music perception. Previous studies have shown that colour training improves the consistency of semantic judgements [2], that cultural and experiential factors shape colour associations [3], and that artistic training enhances colour discrimination and its link to emotional meaning [4].

The musical stimuli comprised Mozart's Twelve Variations on "Ah, vous dirai-je, Maman", including the theme and twelve variations, yielding thirteen sections in total. Colour samples were constructed based on the Munsell system, covering six primary hues (red, orange, yellow, green, blue, purple), further divided into saturated, light, muted, and dark categories [5]. To supplement the set, black, grey, and white were added as neutral tones, with colour codes following Jonauskaite et al. (2021) [6]. In total, 27 colours were prepared in RGB and HEX formats to ensure consistent on-screen presentation (Figure 1).

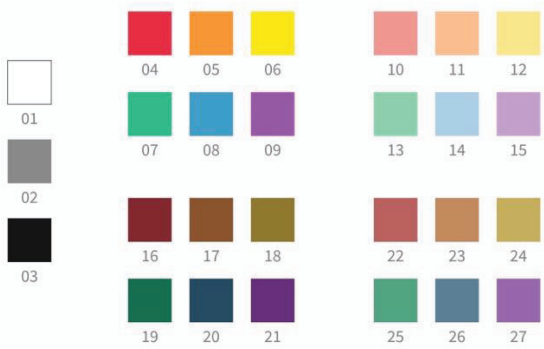

Figure 1: Stimulus set of 27 colours based on the Munsell system

To capture semantic evaluations, 35 pairs of music- and colour-related adjectives were collected from crossmodal and colour semantics studies, together with features of the selected composition. Nine music experts reviewed these items to ensure validity. Based on the Content Validity Ratio (CVR, threshold ≥ 0.78, $N = 9$), 17 pairs were retained, and subsequent evaluation with the Item-Level Content Validity Index (I-CVI) and expert ratings yielded eight final pairs: happy–sad, relaxed–tense, masculine–feminine, bright–dark, warm–cool, light–heavy, soft–hard, and tranquil–hurried.

The experiment was conducted in a quiet, evenly lit environment, with screens set to default brightness and standard colour mode. In the pre-test, participants provided background information, rated their familiarity with the composition, and completed the I-PANAS-SF to exclude extreme emotional states. During the main experiment, they listened sequentially to the thirteen sections while viewing the 27-colour array. After each section, they selected one or more colours judged as the "most congruent" and "least congruent" with the music, then rated the eight adjective pairs on a seven-point Likert scale to assess associations between music, colour, and semantic perception.

RESULTS AND DISCUSSION

The final valid sample comprised 46 participants aged 18–48 years (39 females, 7 males), all with backgrounds in design or colour-related fields. Participants' familiarity with Mozart's Twelve Variations on "Ah, vous dirai-je, Maman" averaged 3.28, indicating a moderate to high level of recognition of the work. To avoid excessive emotional deviation, exclusion criteria based on the I-PANAS-SF (PA < 5 or NA > 20) were applied, and all participants met the inclusion requirements.

Figure 2 presents the heatmap of Preference Index (PI) values for the thirteen sections and 27 colour samples. PI values (−1 to +1) indicate the degree of agreement or disagreement between participants' colour choices and the corresponding music. Results revealed marked differences in colour associations across sections, reflecting crossmodal perception shaped by variations in melody, rhythm, and harmony. The theme was predominantly associated with bright warm colours (yellow, orange), corresponding to positive and clear emotional qualities. Variations I and III, characterised by rapid note passages and ornamentation, were linked with vivid saturated colours (red, orange-red), indicating high dynamism and vitality. Variations II and V, marked by dissonant harmonies, tended towards cooler or darker tones, associated with tension and subtlety. Variations IV and VI, with heightened technical demands, elicited associations with strongly contrasting colours. Variation VII, with its powerful sonority, was associated with golden yellow and deep red, reflecting solemnity and strength. Variation VIII, modulating to C minor, was linked with dark blue and greyish purple, corresponding to tension and lower valence. Variation IX, returning to C major, shifted to bright colours such as pink and yellow-green, contrasting sharply with the preceding minor section. Variation X, with fuller harmonies and chromatic progressions, was associated with neutral tones such as pale yellow and light brown, conveying balance and harmony. Variation XI, performed at a slower tempo, was linked with cool colours such as blue and grey, reflecting a tranquil mood. Finally, Variation XII, characterised by rapid triple metre and a crescendo conclusion, was associated with bright red and orange, reflecting high arousal and an emphatic closure.

In summary, sections with rapid tempo or rapid note passages tended to correspond to saturated warm colours, while slower or minor-mode sections were more frequently associated with cooler or darker tones, and harmonically rich sections with neutral tones. These findings demonstrate that musical features can be consistently mapped onto colour preferences, supporting the existence of structured crossmodal correspondences between music and colour.

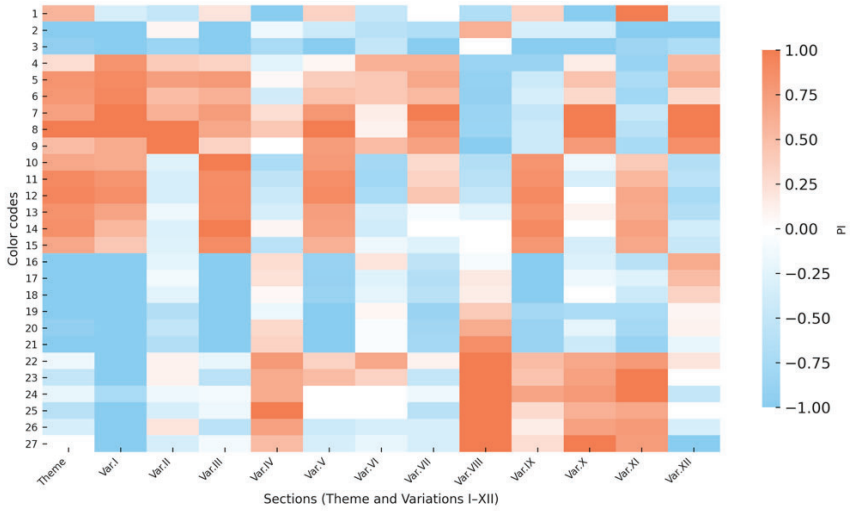

Figure 2: Preference index (PI) heatmap across 27 colour codes and 13 sections

Semantic differential analysis revealed significant differences across the eight adjective pairs between sections. The theme scored positively on "happy–sad", "bright–dark", and "warm–cool", indicating a cheerful atmosphere. Variations I and III were rated towards the "hurried" pole of "tranquil–hurried", consistent with their rapid note passages. Variation VIII received negative ratings on "happy–sad", "bright–dark", and "warm–cool", reflecting associations with sadness and cool colour imagery. By contrast, Variation XI was evaluated towards the relaxed and tranquil poles of "relaxed–tense" and "tranquil–hurried", consistent with its slow-tempo character.

Table 1: Mean scores of the semantic differential scale

	Happy–Sad	Relaxed–Tense	Masculine–Feminine	Bright–Dark	Warm–Cool	Light–Heavy	Soft–Hard	Tranquil–Hurried
Theme	1.89	2.20	-1.00	2.20	1.63	2.28	1.91	1.46
Var.I	2.15	0.09	0.24	2.20	1.20	1.98	0.43	-1.61
Var.II	0.80	-1.11	0.07	0.46	0.61	0.41	-0.02	-1.61
Var.III	1.54	1.13	-0.98	1.35	1.07	1.43	1.39	-0.17
Var.IV	-0.02	-0.59	0.33	-0.57	-0.30	-1.02	-0.37	-0.65
Var.V	1.24	0.96	-0.50	1.46	0.52	1.13	0.54	0.35
Var.VI	0.41	-1.80	1.07	0.15	0.11	-0.80	-1.26	-2.37
Var.VII	1.11	-0.24	0.63	1.24	0.80	0.57	0.35	-1.15
Var.VIII	-1.61	0.11	-1.46	-1.43	-1.39	-1.04	0.98	1.11
Var.IX	-0.07	1.37	-1.24	0.41	0.26	0.65	1.39	1.65
Var.X	0.11	-0.83	0.30	-0.02	-0.24	-0.59	-0.02	-1.24
Var.XI	-0.39	1.74	-1.91	0.24	0.48	0.65	1.80	1.78
Var.XII	0.72	-1.09	0.72	0.50	0.61	-0.20	-0.78	-1.46

Principal Component Analysis (PCA) was further applied to reduce the eight adjective pairs to a two-dimensional Valence–Arousal model. In contemporary music emotion research, the Valence–Arousal (pleasure–arousal) framework has been widely employed. Cui et al. (2022) noted that the Arousal–Valence model has proven effective and reliable in identifying emotions during music listening [7], while Patil et al. (2025) emphasised its role as a core framework for measuring musical emotion [8]. Figure 3 illustrates the distribution of the thirteen sections within this affective space, with the three most frequently selected colours for each section indicated. The X-axis represents Valence, with rightward positions corresponding to perceptions of greater happiness, brightness, warmth, softness, or lightness; the Y-axis represents Arousal, with upward positions corresponding to perceptions of greater tension, hurriedness, or femininity.

Results showed that high-arousal sections (e.g., Variations I, II, VI, VII, XII) were predominantly associated with vivid warm colours; low-valence sections (e.g., Variation VIII) clustered around dark blue and purple; low-arousal sections (e.g., Variation XI) tended towards bluish-grey cool tones; whereas the theme and some more neutral sections were linked with softer shades such as pale yellow, light pink, and light green.

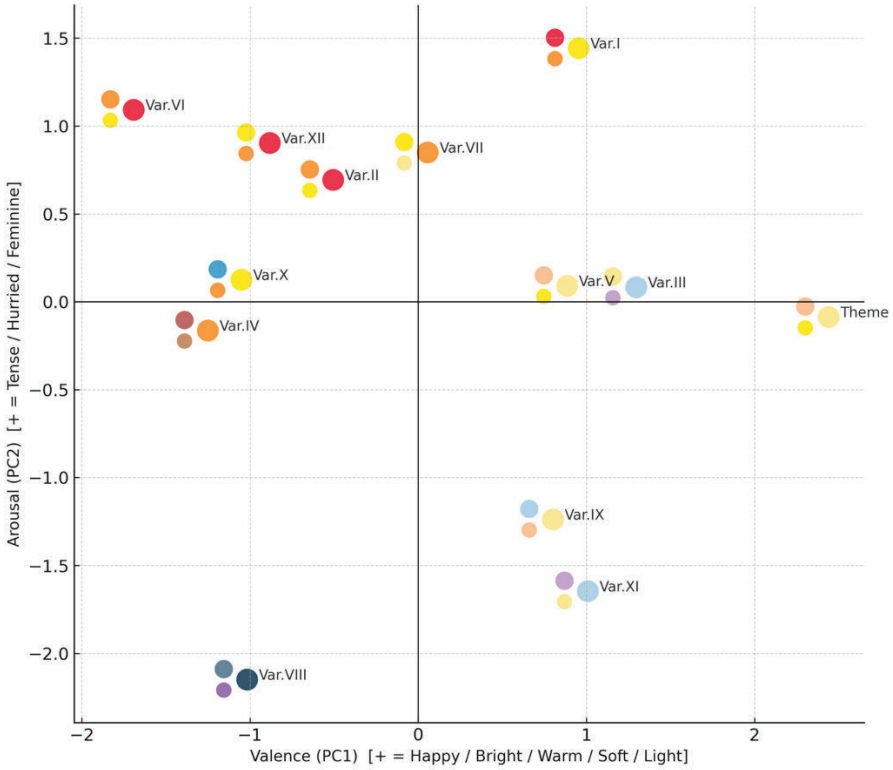

Figure 3: Valence-Arousal Space with Top-3 Colours (Most Agreement Counts)

In summary, this distribution confirms that differences in rhythm, tempo, harmony, and tonality can be mapped onto colour choices through affective semantic evaluations, demonstrating consistent and structured crossmodal correspondences.

CONCLUSION

This study examined crossmodal correspondences between music and colour through colour selection and semantic evaluation, using Mozart's Twelve Variations on "Ah, vous dirai-je, Maman" as the case study. The results showed that rapid sections were predominantly associated with saturated warm colours, slow or minor-mode sections with cooler and darker tones, and harmonically rich sections with neutral shades. The Valence–Arousal analysis further confirmed that variations in rhythm, tempo, and harmony systematically influenced affective perception and were reflected in colour associations.

By addressing an entire classical composition rather than isolated tones or short excerpts, this study fills a gap in previous research and provides empirical evidence for structured music–colour correspondences. The findings offer useful implications for multisensory design and artistic practice. Future work may extend to other musical genres and cultural contexts, broadening the understanding and depth of crossmodal correspondences.

REFERENCES

[1]. Reymore, L., Noble, J., Saitis, C., Traube, C., & Wallmark, Z. (2023). Timbre semantic associations vary both between and within instruments: An empirical study incorporating register and pitch height. Music Perception, 40(3), 253–274. https://doi.org/10.1525/mp.2023.40.3.253

[2]. Ou, L., Luo, M. R., Woodcock, A., & Wright, A. (2004). A Study of Colour Emotion and Colour Preference. Part I: Colour Emotions for Single Colours. Color Research & Application, 29(3), 232-240. https://doi.org/10.1002/col.20010

[3]. Tham, D. S. Y., Sowden, P. T., Grandison, A., Franklin, A., Lee, A. K. W., Ng, M., Park, J., Pang, W., & Zhao, J. (2020). A systematic investigation of conceptual color associations. Journal of Experimental Psychology: General, 149(7), 1311–1332. https://doi.org/10.1037/xge0000703

[4]. Song, L., Zhang, G., Ma, L., Silvennoinen, J., & Cong, F. (2025). Comparative analysis of color emotional perception in art and non-art university students: Hue, saturation, and brightness effects in the Munsell color system. BMC Psychology, 13, Article 650. https://doi.org/10.1186/s40359-025-03034-y

[5]. Schloss, K. B., & Palmer, S. E. (2011). Aesthetic response to color combinations: Preference, harmony, and similarity. Attention, Perception, & Psychophysics, 73(2), 551–571. https://doi.org/10.3758/s13414-010-0027-0

[6]. Jonauskaite, D., Camenzind, L., Parraga, C. A., Diouf, C. N., Mercapide Ducommun, M., Müller, L., Norberg, M., & Mohr, C. (2021). Colour-emotion associations in individuals with red-green colour blindness. PeerJ, 9, e11180. https://doi.org/10.7717/peerj.11180

[7]. Cui, X., Wu, Y., Wu, J., You, Z., Xiahou, J., & Ouyang, M. (2022). A review: Music-emotion recognition and analysis based on EEG signals. Frontiers in Neuroinformatics, 16, 997282. https://doi.org/10.3389/fninf.2022.997282

[8]. Patil, S., Patil, R., Goudar, S., Sangani, S., & Goudar, R. H. (2025). Review on music emotion analysis using machine learning: Technologies, methods, datasets, and challenges. Discover Applied Sciences, 7, 692. https://doi.org/10.1007/s42452-025-07178-9

Gender and Age-Related Differences in The Contributions of Color to The Recognition of Cultural Landscapes

Olga A. Lavrenova[a,b], Yulia A. Griber [a*]

[a]Smolensk State University, Smolensk, Russia
[b]Institute of Scientific Information for Social Sciences of the Russian Academy of Sciences, Moscow, Russia

[*]Corresponding author: Yulia A. Griber, y.griber@gmail.com

ABSTRACT

In this study, we hypothesized that the influence of color on memory and recognition of cultural landscapes would vary according to the age and gender of observers. To address this, we examined whether color plays a broader role in visual recognition by analyzing its contribution to the encoding and retrieval processes involved in pattern recognition. The study sample consisted of 204 participants (70 male), ranging in age from 12 to 66 years. A continuous recognition task was employed to approximate the way individuals perceive and memorize images in real-world contexts. During the encoding phase, participants were presented with a sequence of 36 color and black-and-white photographs depicting various types of cultural landscapes, displayed on a computer monitor. Stimuli were shown in random order with exposure times of 64, 128, 300, or 2000 ms, and the interval between presentations was 7000 ms. During the recognition phase, the same 36 photographs were presented again, along with an equal number of duplicate stimuli. Half of the images were identical to those from the encoding stage, while the other half were modified with respect to color conditions. Participants were asked to determine whether each image had been presented previously or was new. The results revealed that gender- and age-specific patterns of recognition correlated with the key features of cultural landscapes. Recognition differences were observed across landscapes categorized by: compositional structure (open, semi-open, closed), spatial perspective and scale of perception (panoramic, ensemble, intimate), degree of urbanization (urban, rural), scene category (transport facilities; historical sites; parks and recreation areas; industrial and construction sites; residential buildings and gardens; commercial buildings, shops, and markets), genesis and degree of development (intentionally designed, organically evolved, associative). For urban cultural landscapes, gender- and age-related perceptual differences were additionally influenced by the type of ecological framework (mosaic, riverine, peripheral) and by functional purpose (architectural, park, industrial).

Keywords: color vision, recognition, memory, cultural landscape

INTRODUCTION

Color is a significant factor influencing cultural landscape memory, as demonstrated by extensive experimental research (for review, see, e.g. [1]). During the encoding phase, color facilitates rapid segmentation of complex images by the visual system, supports comprehension of compositional structures, delineates object boundaries, and enhances both object identification and semantic labeling [2]. In the recognition phase, color contributes to the representation of complex images in episodic memory and provides cognitive support in the recognition process [3].

In this study, we extended previous research by experimentally examining the influence of color on the recognition of cultural landscapes in people of different gender and age. We hypothesized that the effect of color on memory and recognition of cultural landscapes would vary according to the age and gender of observers.

Accordingly, the primary aim of this study was to identify the key features of cultural landscapes that shape gender- and age-specific recognition patterns.

METHODOLOGY

Participants. A total of 204 participants (70 males), aged between 12 and 66 years participated in the experiment. All had normal or corrected-to-normal visual acuity, and none was color-blind.

Stimuli. We used 72 images in a matched-to-sample task, whereby the image color, original or black-and-white, was manipulated in both learning and recognition phases of the task. The images were sourced from the McGill Calibrated Colour Image Database [4] and other open access databases. Employed were images of different categories of cultural landscapes.

The images were down-sampled to a resolution of 1024 x 768 pixels. For image presentation, a 32-inch Dell S3221QS monitor at 60-Hz vertical refresh rate was used. Participants were seated 80 cm from the monitor.

Experimental procedure and design. A continuous recognition task was used to simulate the process of how people see and recognize images in the real world.

First (at the encoding step), participants were shown a sequence of 36 color and black-and-white photographs of various types of cultural landscapes on a computer monitor. Experimental stimuli followed each other in a random order with an exposure of 64, 128, 300, or 2000 ms; the interval between presentations was 7000 ms. Then (at the recognition step) the same 36 photographs were presented with the equal number of duplicate stimuli.

Half of the stimuli were the same as in the memorization stage; for the second half, the color conditions were changed. Participants had to determine the images that had already been shown in the first stage of the experiment and those they had seen for the first time.

RESULTS AND DISCUSSION

The findings indicate that gender- and age-related patterns of cultural landscape recognition vary according to the types of landscapes, which can be classified on different grounds. These patterns are most strongly shaped by five key properties of the cultural landscape.

(1) (2) (3)

Figure 1: Exemplary images from the cultural landscapes with different compositional structure: (1) open, (2) semi-open, (3) closed

First, the role of color in recognition processes differs across gender and age groups depending on the compositional structure of the landscape: in open landscapes, characterized by wide perspectives; semi-open landscapes, where objects are distributed primarily in the foreground and middle ground; and closed landscapes, in which perspective is absent and only proximate objects are visible (Figure 1).

Since individuals perceive cultural landscapes from within their spatial context, another key factor influencing landscape recognition is viewing distance, which determines the scale of perception. In this regard, three scales of perception, important for the landscape recognition, may be distinguished: panoramic, ensemble, and intimate (Figure 2).

(1) (2) (3)

Figure 2: Exemplary images from the cultural landscapes with different spatial point of view and scale of perception: (1) panoramic, (2) ensemble, (3) intimate

The panoramic scale involves the perception of extensive spatial volumes from a considerable distance, often from elevated vantage points or while moving at high speed, such as along highways. At this scale, there is no direct interaction between the observer and the observed environment; instead, the emphasis falls on large-scale elements that dominate the visual field. Typical examples include river embankments, the linear perspectives of major avenues, or the panoramic views of urban areas observed from mountains or high-rise buildings.

The ensemble scale corresponds to perception at intermediate distances, usually while moving at a slower pace, whether by car or on foot. In this case, specific dominant objects within the composition acquire greater significance, and the process of perception is closely linked to the ability to “read” the spatial and compositional features of the landscape. This mode of perception is characteristic of urban ensembles, such as public squares viewed from adjacent avenues or embankments.

The intimate scale refers to the perception of space by a pedestrian directly “immersed” within the cultural landscape—on a street, in a square, park, or garden. Here, interaction with the environment and its active components, including other people, is direct and immediate. Perception occurs fragmentarily and from specific vantage points, with attention focused on the surrounding details. This scale is typical of historic urban neighborhoods, pedestrian public centers, park ensembles, and garden complexes, where human engagement with the environment is particularly pronounced.

An important factor in gender and age differences in the contribution of color in the recognition of cultural landscapes is also the degree of their urbanization (cf.: [5]) (Figure 3). Rural landscapes are typically characterized by permanent or seasonal settlements integrated with natural environments adapted for agricultural use. These include fields, croplands, meadows, pastures, vineyards, orchards, and vegetable gardens. Such landscapes are inseparably connected to their natural surroundings and reflect both traditional cultural practices and ways of life. By contrast, urban landscapes encompass city silhouettes, street vistas, and residential or commercial blocks

animated by the presence of inhabitants and vehicular movement. In terms of color, urban environments serve as visual records of cultural history. Over time, their chromatic characteristics undergo continuous transformation, often altering to such a degree that their original appearance becomes almost unrecognizable. For urban cultural landscapes, gender and age characteristics of perception also depend on the type of ecological framework (mosaic, riverine, peripheral) and purpose (architectural, park, industrial).

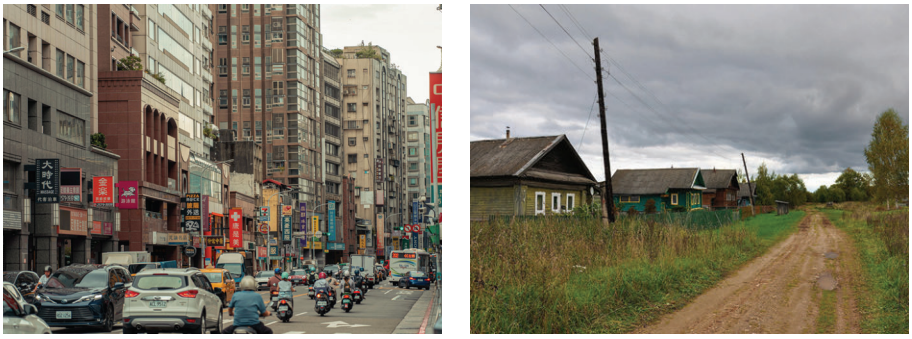

(1) (2)

Figure 3: Exemplary images from the cultural landscapes with different degree of urbanization: (1) urban, (2) rural

Another important dimension of gender- and age-related recognition patterns identified in our analysis is the category of complex scenes (cf.: [6]). Within this category, the role of color demonstrates particularly pronounced variation across different types of environments. These include transport facilities, historical landmarks, parks and recreation areas, industrial and construction sites, residential buildings and gardens, as well as commercial structures such as shops and markets. In each of these contexts, color contributes in distinct ways to the recognition and interpretation of the landscape (Figure 4).

(1) (2) (3)

(4) (5) (6)

Figure 4: Exemplary images from the cultural landscapes with different scene categories: (1) transport facilities, (2) historical landmarks, (3) parks and recreation areas, (4) industrial and construction sites, (5) residential buildings and gardens, (6) commercial buildings, shops, and markets

Regardless of gender and age, the extent of the color impact depends on the genesis mechanisms and the degree of development of the cultural landscape [7]: color affected greater recognition of images of intentionally designed landscapes (e.g., garden and parkland landscapes constructed for aesthetic reasons, modern urban and residential areas, industrial landscapes) and less recognition of organically evolved landscapes, resulting from an initial social, economic or administrative imperative (e.g., cultivated fields, rice terraces, midland and northern villages, historic city panoramas, and historic centres), as well as of associative cultural landscapes (e.g., sites of memory, places of creativity, sacred sites, and battlefields) (Figure 5).

(1) (2) (3)

Figure 5: Exemplary images from the cultural landscapes with different genesis mechanisms and the degree of development: (1) intentionally designed, (2) organically evolved, (3) associative

CONCLUSION

Our experiment confirmed that the mechanism of color contribution to the perception of cultural landscapes varies according to the age and gender of observers and correlates with the key features of cultural landscapes. Recognition differences were observed across landscapes categorized by: compositional structure (open, semi-open, closed), spatial perspective and scale of perception (panoramic, ensemble, intimate), degree of urbanization (urban, rural), scene category (transport facilities; historical sites; parks and recreation areas; industrial and construction sites; residential buildings and gardens; commercial buildings, shops, and markets), genesis and degree of development (intentionally designed, organically evolved, associative). For urban cultural landscapes, gender- and age-related perceptual differences were additionally influenced by the type of ecological framework (mosaic, riverine, peripheral) and by functional purpose (architectural, park, industrial).

ACKNOWLEDGEMENTS

The authors would like to thank Alexey Delov for developing the online platform of the experiment. Support of Karina Zygankova, Alena Nankiewicz, and Grigory Elkind in data collection is gratefully appreciated. The project was supported by the Russian Science Foundation (grant No. 22-18-00407-П; https://rscf.ru/en/project/22-18-00407/).

REFERENCES

[1]. Griber, Y. A. (2023). The influence of color on recognition memory for cultural landscapes. Russian Psychological Journal, 20(3), 157–172. https://doi.org/10.21702/rpj.2023.3.8

[2]. Wichmann, F. A., Sharpe, L. T., & Gegenfurtner, K. R. (2002). The contributions of color to recognition memory for natural scenes. Journal of Experimental Psychology: Learning, Memory, and Cognition, 28(3), 509–520. https://doi.org/10.1037/0278-7393.28.3.509

[3]. Gegenfurtner, K. R., & Rieger, J. (2000). Sensory and cognitive contributions of color to the recognition of natural scenes. Current Biology, 10(13), 805–808. https://doi.org/10.1016/S0960-9822(00)00563-7

[4]. Olmos, A., & Kingdom, F. A. A. (2004). McGill Calibrated Colour Image Database. Retrieved September 1, 2025, from http://tabby.vision.mcgill.ca

[5]. Dupont, L., Ooms, K., Duchowski, A. T., Antrop, M., & Van Eetvelde, V. (2016). Investigating the visual exploration of the rural-urban gradient using eye-tracking. Spatial Cognition & Computation, 17, 1–24. https://doi.org/10.1080/13875868.2016.1226837

[6]. Xiao, J., Ehinger, K. A., Hays, J., Torralba, A., & Oliva, A. (2016). SUN Database: Exploring a Large Collection of Scene Categories. International Journal of Computer Vision, 119(1), 3–22. https://doi.org/10.1007/s11263-014-0748-y

[7]. Operational Guidelines for the Implementation of the World Heritage Convention (2021). Paris: UNESCO. Retrieved September 1, 2025, from https://whc.unesco.org/document/190976

The Effect of Wearing Personal Colors on Attractiveness Rating

Aki Kondo[a*], Mami Ogino[a], Yuto Nonaka[a], Aoi Togasaki[a], and Katsumi Watanabe[a]

[a]Faculty of Science and Engineering, Waseda University, Tokyo, Japan
[*]Corresponding author: Aki Kondo, aki.kondo@aoni.waseda.jp

ABSTRACT

In recent years, the personal color analysis, a method of determining and suggesting clothing colors that harmonize with an individual's skin and hair color, has gained popularity in Japan. However, the extent to which individuals whose colors suggested by professional personal colorists are perceived as more attractive by others remains uncertain. The present study investigated the effect of wearing colors suggested by a personal colorist on attractiveness ratings. The study also investigated whether this effect was due to the colors themselves or to changes in facial expressions caused by wearing the suggested colors. A professional personal colorist and another student with no knowledge of the personal color theory selected colors of clothes that were congruent (or incongruent) with those of six models from a set of 94 color samples. Facial images of the models adorned with these colors served as the stimuli. The results demonstrated that facial images wearing colors selected as congruent (or incongruent) by the professional personal colorist were rated as significantly more attractive (or less attractive) than the chance level. However, these patterns were also observed when only the face images were shown (Experiment 1). Moreover, this effect was not observed when facial expressions were controlled (Experiment 2) and when the combinations of facial expression and clothing colors were swapped (Experiment 3). These results suggest that the effect of wearing the colors suggested by the personal colorist being rated as more attractive was not due to the color congruency themselves, but rather to changes in the facial expressions of the models. Conversely, it was also noted that, when assessing the aesthetic appeal of images generated through diverse color and facial combinations, the impact of these factors alone could not account for the observed variability in attractiveness. These results suggest that the harmony or disharmony between color and facial expression may also influence the attractiveness of people wearing color.

Keywords: personal color, clothing color, attractiveness, facial expression, harmony

INTRODUCTION

The personal color analysis, which has gained popularity in recent years, began attracting attention in Japan around the mid-2010s and is becoming a common concept, particularly in the women's fashion industry. The personal color analysis aims to maximize the wearer's appeal by determining not just which colors suit them, but specifically which hues—in terms of lightness, saturation, and clarity—are most flattering within a given color family.

Previous research on color's influence on attractiveness evaluation has suggested that men significantly prefer brighter colors than women, while women prefer softer colors than men [1]. It has also been suggested that individuals wearing red or black appear more attractive than those wearing other colors [2]. However, the colors used were specific hues with defined brightness and saturation levels. The impact of personally suggested colors on attractiveness ratings has received limited examination.

The present study investigated the impact of wearing colors suggested by a personal colorist on attractiveness ratings (Experiment 1). Furthermore, we also examined whether this effect was due to the color congruency alone or consequential changes in facial expressions caused by wearing the suggested colors (Experiment 2,3).

EXPERIMENT 1

To investigate the impact of wearing colors suggested by a professional personal colorist on perceived attractiveness, Evaluation 1 assessed the attractiveness of images of individuals wearing the suggested colors. Evaluation 2 used cropped images to examine the effect of facial expressions.

METHOD

Stimuli

Facial images of the models adorned with personal colors (and other colors) served as the stimuli. A professional personal colorist selected 2 colors that were congruent and 2 colors that were incongruent with six female models (university students, mean age = 23.3 years, SD = 5.56) from a set of 94 color samples. In order to check the selection was based on the unique professional experience as working a personal colorist, a university student who had no knowledge of the personal color theory also selected 4 colors. For each model, the four colors (best1/best2/worst1/worst2) selected by the personal colorist and those selected by the students were all different, except for one model's best1 color. We took digital photographs of the models against a gray background while wearing eight different colors (Figure 1). The models were aware that the colors had been suggested as congruent (or incongruent) by the professional personal colorist or the student. They were instructed to look directly at the camera during the shoot, but no specific instructions regarding facial expressions were given.

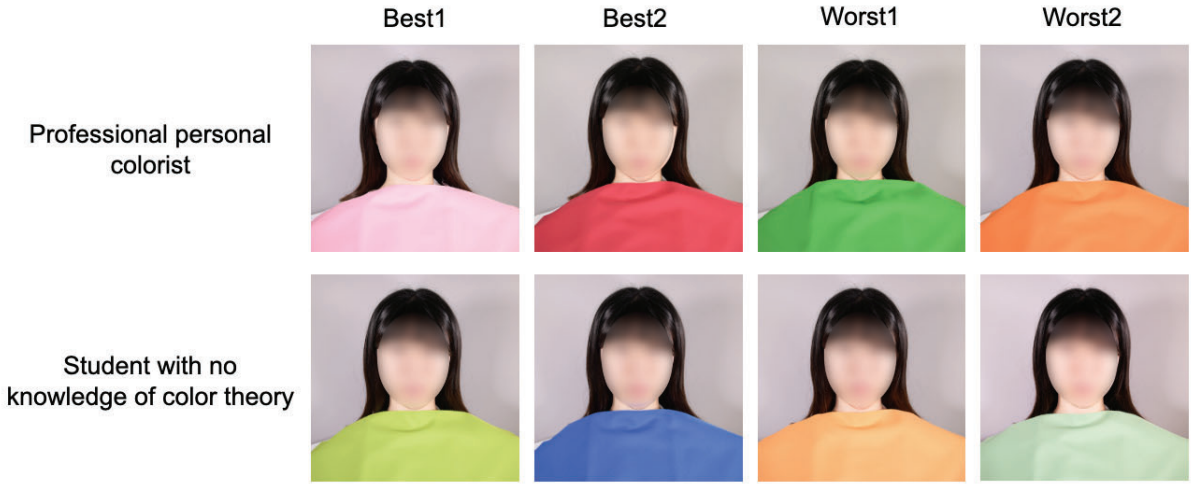

Figure 1: Images of individuals wearing the suggested colors. Faces were not blurred in actual experiments.

Participants

Thirty university students (15 males and 15 females, mean age = 21.1 years, SD = 1.22) participated as paid volunteers. All participants had normal color vision (confirmed with Ishihara plates) and normal or corrected-to-normal visual acuity. Ethical approval for all the experiments in this study was obtained from the Internal Ethics Review Board at Waseda University.

Procedure

Evaluation 1: Images of each model wearing the eight selected colors were presented simultaneously on the computer screen. Participants selected the most attractive image (1st and 2nd) and the least attractive image (1st and 2nd) from among the eight images. For each participant, the order of presentation for the six models and the position of the eight images were randomized.

Evaluation 2: The images used in Evaluation 1 were presented with the face images only (Figure 2). The other procedures were identical to Evaluation 1.

RESULTS AND DISCUSSION

We excluded the data of one model because both the professional personal colorist and the student selected the same color for the model's best1 color. Thus, we analyzed the attractiveness ratings for five models. The frequency of a model being selected as the most attractive (or the least attractive) was counted for each color selected by the professional personal colorist. The Fisher's exact test was used to examine if the probability of a stimulus being selected as the most attractive (or the least attractive) would exceed the chance level.

Table 1 shows the results of calculating the p-value using the Fisher's exact test in Evaluation 1. The results demonstrated that facial images wearing colors that were selected as congruent (or incongruent) by the professional personal colorist were significantly rated more frequently as the most attractive (or the least attractive). However, the pattern was also observed for evaluating the facial images without wearing suggested colors in Evaluation 2 (Table 2). These results suggest that the effect of wearing the colors suggested by the personal colorist being rated as most attractive was not due to the color congruencies based on the personal color theory, but rather to the knowledge that the professional personal colorist selected the colors for the model and (possibly consequential) changes in the facial expressions of the models.

Table 1: Choice frequency and P-value for evaluating facial images wearing colors suggested by the professional personal colorist.

Colors suggested by professional colorists / Participants' attractiveness evaluation	Frequency (Total = 149)	p-value
Best1 color / most attractive	74	<.001***
Best2 color / most attractive	48	.029*
Worst1 color / least attractive	56	<.001***
Worst2 color / least attractive	59	<.001***

Table 2: Choice frequency and P-value for evaluating the facial images only (i.e., without wearing colors suggested by the professional personal colorist).

Colors suggested by professional colorists / Participants' attractiveness evaluation	Frequency (Total = 147)	p-value
Best1 color / most attractive	61	<.001***
Best2 color / most attractive	38	.437
Worst1 color / least attractive	50	.009**
Worst2 color / least attractive	39	.364

EXPERIMENT 2

Experiment 1 showed that an increase in attractiveness ratings was observed even for the facial images only. However, it remains unclear whether this result stems from the effect of the suggested color itself or from the effect of changes in the wearer's facial expressions caused by the analysis as congruent (or incongruent) by the professional personal colorist. Experiment 2 examined these possibilities. To do this, attractiveness ratings were conducted on images of individuals wearing the suggested colors under the condition where facial expressions were controlled.

METHOD

Stimuli

Based on the images in Experiment 1 of the models wearing suggested colors, new stimuli with controlled facial expressions were created. Controlled facial stimuli were selected from images that received the fewest ratings of "most attractive" and "least attractive" in Experiment 1 in order to make them most neutral.

Participants

Thirty university students (15 males and 15 females, mean age = 21.4 years, SD = 2.40) participated in the experiment as paid volunteers. All participants had normal color vision (confirmed with Ishihara plates) and normal or corrected-to-normal visual acuity.

Procedure

The procedures were identical those in Experiment 1.

RESULTS AND DISCUSSION

Table 3 shows the results of calculating the p-value using the Fisher's exact test. When images of individuals wearing the suggested colors were evaluated with facial expression controlled, the best1 colors (worst1 colors) suggested by the professional personal colorist were not significantly rated as most attractive (least attractive). In contrast, the best2 colors (worst2 colors) were significantly rated as most attractive (least attractive). Although the results for best1 (worst1) and best2 (worst2) colors were not consistent, the effect of colors suggested by the professional personal colorist on enhancing attractiveness decreased when facial expressions were controlled. These results also suggest that the effect of wearing the colors suggested by the personal colorist being rated as most attractive was not due to the colors themselves, but rather to changes in the facial expressions of the models.

Table 3: Choice frequency and P-value for evaluating controlled facial images wearing colors suggested by the professional personal colorist

Colors suggested by professional colorists / Participants' attractiveness evaluation	Frequency (Total =150)	p-value
Best1 color / most attractive	39	.419
Best2 color / most attractive	52	.005**
Worst1 color / least attractive	36	.431
Worst2 color / least attractive	49	.021*

EXPERIMENT 3

To further investigate whether the effect of wearing the colors suggested by the personal colorist being rated as most attractive was due to the colors themselves or to changes in facial expressions caused by wearing the suggested colors, we compared ratings of images with swapped combinations of face and clothing colors.

METHOD

Stimuli

We created 12 new images for each model by swapping the combinations of face and clothing colors from the original images used in Experiment 1, where the models wore each of the four colors (best1/ best2/ worst1/ worst2) suggested by the professional personal colorist (Table 4). The combinations of faces and clothing colors in the images were classified into four groups: BB (best face and best color), BW (best face and worst color), WB (worst face and best color), WW (worst face and worst color).

Table 4: Combinations of face and clothing color in Experiment 3.

Clothing color \ Face	Best1	Best2	Worst1	Worst2
Best1	Best1Best1	Best2Best1	Worst1Best1	Worst2Best1
Best2	Best1Best2	Best2Best2	Worst1Best2	Worst2Best2
Worst1	Best1Worst1	Best2Worst1	Worst1Worst1	Worst2Worst1
Worst2	Best1Worst2	Best2Worst2	Worst1Worst2	Worst2Worst2

BB: Best1Best1, Best2Best1, Best1Best2, Best2Best2
WB: Worst1Best1, Worst2Best1, Worst1Best2, Worst2Best2
BW: Best1Worst1, Best2Worst1, Best1Worst2, Best2Worst2
WW: Worst1Worst1, Worst2Worst1, Worst1Worst2, Worst2Worst2

Participants

Thirty graduate and undergraduate students (18 males, 11 females, 1 unknown, mean age = 22.3 years, SD = 1.91) participated in the experiment as paid volunteers. All participants had normal color vision (confirmed with Ishihara plates) and normal or corrected-to-normal visual acuity.

Procedure

For each model, two image pairs from the 16 created images were presented on the left and right sides of the screen. Participants selected the more attractive image in each pair of two images. For each participant, the order of presentation for the six participants and the position of the two images were randomized. Stimuli were presented on a computer monitor. The image pairs for comparison were selected based on four groups of combinations of faces and clothing colors (Table 4).

RESULTS AND DISCUSSION

A chi-square test was performed between the BW, BB, WB, and WW conditions (Table 4). A significant difference was found only in the BW vs. WW comparison ($\chi^2(1) = 3.85$, $p = .049$), indicating that WW was significantly more attractive than BW. However, no significant differences were found in the comparisons BB vs. BW ($\chi^2(1) = 1.33$, $p = .248$), BB vs. WB ($\chi^2(1) = .053$, $p = .817$), and BW vs. WB ($\chi^2(1) = 2.16$, $p = .141$).

When wearing the worst color, the reason the WW was rated as more attractive than the BW may be that WW harmonizes the face and color better than WB, reducing visual discomfort and paradoxically leading evaluators to perceive it as more attractive. It has also been demonstrated that the combination of facial expressions and clothing colors is crucial for evaluations of suitability [3]. This suggests that attractiveness ratings are influenced not only by individual factors like face or color, but also by the harmony or disharmony between facial expression, suggested colors, and the knowledge that a particular color is suggested by the professional personal colorist. However, when wearing the best color, no significant difference was observed in the attractiveness ratings between BB and WB, and the results could not be explained by the harmony between face and color. This asymmetric result suggests that the criteria for evaluating attractiveness may differ between images wearing the worst color and images wearing

the best color. On the other hand, no significant differences in attractiveness ratings were observed between BB vs. BW, BB vs. WB, or BW vs. WB. This indicates that we could not clearly distinguish whether the change in attractiveness stemmed from the effect of the clothing color itself or from the effect of facial expressions resulting from wearing a suggested color. These results also imply that attractiveness ratings may vary not only based on the face or color within an image, but also on the harmony or disharmony between the two.

Table 4: Choice frequency and P-value for evaluating facial images with swapped face and clothing colors

Comparison conditions	Frequency	p-value
BB vs. BW	160, 140	.248
BB vs. WB	152, 148	.817
BW vs. WB	318, 282	.141
BW vs. WW	133, 167	.049*

CONCLUSION

The present study investigated the impact of wearing colors suggested by the personal colorist on attractiveness ratings, and further examined whether this effect stems from the colors themselves or from changes in facial expressions resulting from wearing the suggested colors. The results indicated that wearing colors suggested by the personal colorist significantly improved attractiveness ratings, but suggested that this effect arose not from the colors themselves, but from changes in the models (e.g., facial expressions). Conversely, when evaluating the attractiveness where the combination of face and clothing color was swapped, the observed increase in perceived attractiveness could not be explained by the isolated effects of either factor or facial expression. These results suggest that an individual's attractiveness when wearing different colors may be influenced not only by facial expression or color itself, but also by their harmony or disharmony.

ACKNOWLEDGEMENTS

This research was supported by KAKENHI JP22H00090, JP24K21505, and JP25H01234 from Japan Society for the Promotion of Science.

REFERENCES

[1]. Radeloff, D. J. (1990). Role of color in perception of attractiveness. Perceptual and Motor Skills, 71(1), 151-160.

[2]. Roberts, S. C., Owen, R. C., & Havlicek, J. (2010). Distinguishing between perceiver and wearer effects in clothing color-associated attributions. Evolutionary Psychology, 8(3), 350-364.

[3]. Nakagawa, C., Isoi, K., & Kazama, K. (1990). Influence of the facial expression on the degree of becoming. Sen-i gakkaishi, 46(6), 258-261. [in Japanese]

The Influence of Food Appearance Color Tone on Eating Behavior and Appetite in A Virtual Reality Environment

Tsuyoshi Moriyama[a*], and Aki Matsumoto[a]

[a]*Tokyo Polytechnic University, Kanagawa, Japan*
[*]*Corresponding author: Tsuyoshi Moriyama, moriyama@t-kougei.ac.jp*

ABSTRACT

Conventional nutrition science has targeted the chemical role of food in body, but not about the factors that affect appetite and the quality of diet such as appearance of food. Here we investigated the effect of food color on the taste and the appetite the eaters feel by conducting a subjective experiment where the participants were asked to wear a VR goggle and eat curry with rice. The goggle has a front camera and transmit the image to the computer connected for image processing which detects the food region. The RGB values in the food region, i.e., curry region, are converted to the correspondent L*a*b* values. Subtracting 50 from *a values in the food region made green looking condition and subtracting 50 from *b values blue looking condition. We compared the three conditions of curry color, i.e., original, green, and blue, with respect to eating speed and the subjective evaluation of appetite and how easy to eat. Against our hypothesis, the results demonstrated no significant differences among the conditions, except several participants claimed they have felt different taste under the different color conditions.

Keywords: diet, nutrition science, image processing, augmented reality, illusion

INTRODUCTION

One of the three pillars of daily life—clothing, food, and shelter—eating occupies roughly one-third of a person's daily routine, underscoring its importance. This significance is widely recognized in everyday life. Nevertheless, not everyone is able to enjoy a satisfactory dietary experience. Imbalances in food intake, such as overeating or undereating, can lead to serious health issues and are classified as eating disorders when they reach a clinical level. Current treatments for such disorders include pharmacological interventions by physicians and dietary guidance by specialists, but these approaches have limitations and drawbacks, highlighting the need for new solutions.

The degree of satisfaction derived from eating is influenced not only by the taste and quality of ingredients but also by various sensory and environmental factors, including appearance, aroma, and the dining setting. In previous research, Narumi (2013) and Kobayashi (2009) demonstrated that visual aspects of food—such as plate size, portioning, and lighting color—play a significant role in perceived satiety when using augmented reality to manipulate food appearance. However, the specific effects of each visual factor remain unclear[1][2]. Among these factors, "appetite" is known to be influenced not only by physiological hunger but also by psychological, sensory, and social elements. For example, visually vibrant food or pleasant aromas can stimulate appetite, whereas unpleasant environments or stress can suppress it. Additionally, visual factors such as color and shape may strongly affect interest in food and the quantity consumed.

Based on this context, we hypothesize that it may be possible to modulate appetite through intentional design of food appearance. The aim of this study is to explore the impact of food appearance—specifically changes in color tone—on eating behavior and psychological responses, in order to clarify its potential for appetite control.

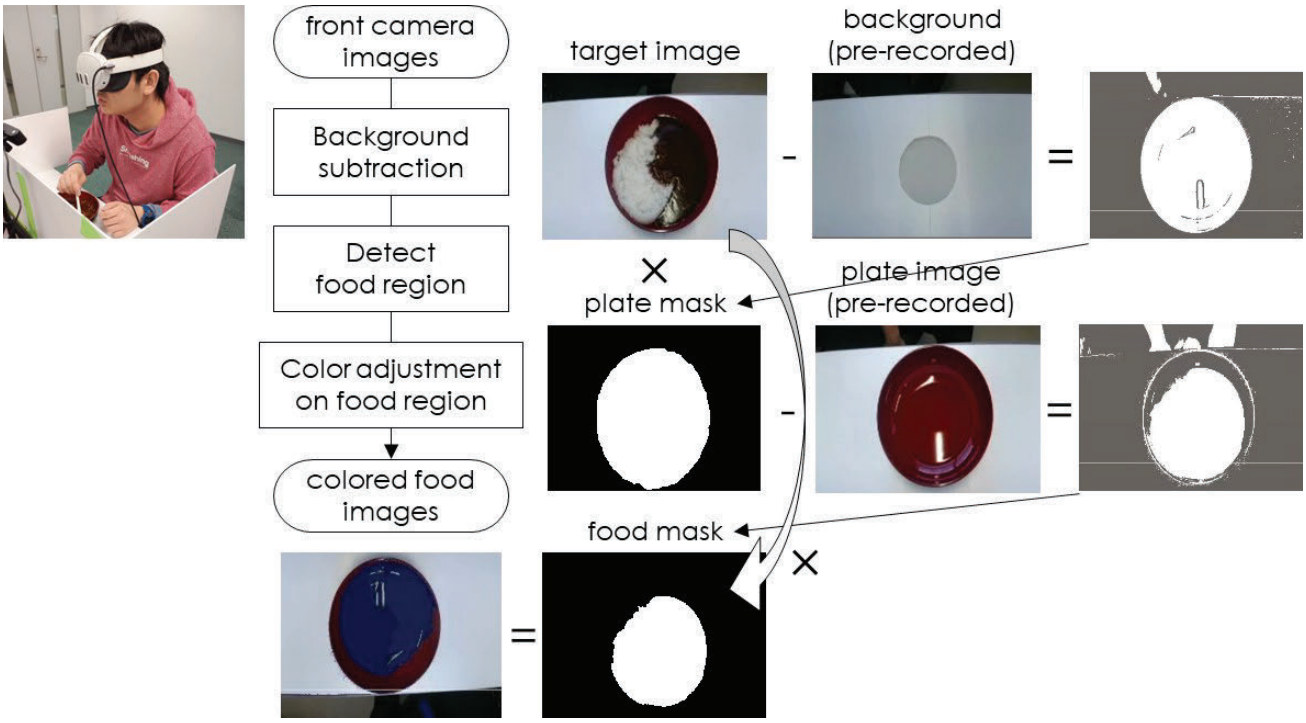

Figure 1: A schematic overview of the method of coloring food region.

THE METHOD OF MANIPULATING APPEARED FOOD COLOR

Detecting Food Region

Figure 1 shows the schematic overview of the method of coloring food region in the input image. The front camera attached to VR goggle captures images in front of a person who attends the experiment in real time during the session. The image of the background behind the food plate and that of food plate with the background were pre-recorded. Firstly, the plate region is obtained by subtracting the background image from the input. The subtraction is processed by morphological filter to eliminate dots and holes then binarized to get the mask image (plate mask in the figure). Secondly, the input image is multiplied by the plate mask and subtracted the plate image to get food region (a plate used has to have different color from food). It is processed by morphological filter and binarized to get the mask image (food mask in the figure) that is multiplied with the input image for limiting the food region for coloring food. This process is applied in each of the input images that come from the VR goggle.

Coloring Food Region

For color adjustment in Figure 1 with a same amount shifted from the original color, RGB color space is not appropriate because it mixes color and brightness in the values. We convert RGB values in the food region into the correspondent CIE L*a*b* values. Then, two additional color conditions are generated: one with the a* value modified by Δa (green condition), and another with the b* value modified by Δb (blue condition) as depicted in Figure 2. Thus, only the food regions are modified in color. The colored food images in Figure 1 are displayed on a VR goggle.

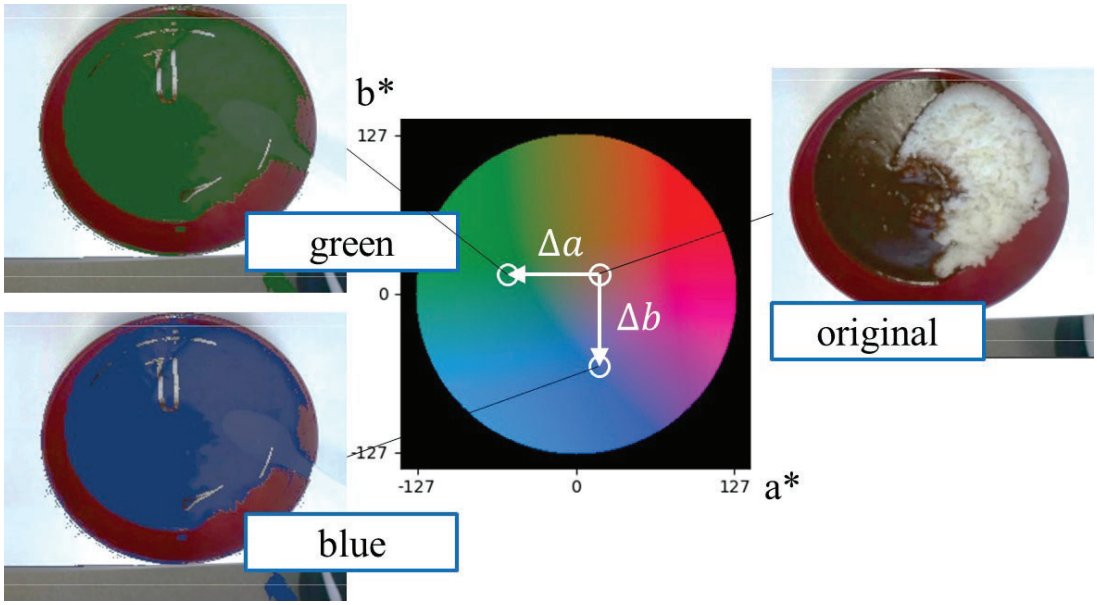

Figure 2: Color modification of food region in the correspondent L*a*b* color space.

AN EXPERIMENT ON THE INFLUENCE OF FOOD COLOR TONE ON APPETITE

Participants wore VR goggles while eating curry and rice, during which the overlaid color on the curry was altered. We then compared eating speed, appetite, and perceived difficulty of eating under the different color conditions.

Instructions to the participants

Six male participants in their 20s were instructed to eat curry while viewing it through a VR headset under three different color conditions (the orders of three conditions were all differed among participants). Participants were asked to refrain from eating for at least five hours prior to each session. Additionally, a minimum interval of 12 hours was maintained between sessions with different color conditions. During the experiment, participants were instructed not to move the curry dish.

System configuration, materials, and experiment room

Meta quest 3 was connected to a host PC that ran a Unity program with Oculus XR Plugin v4.2.0, Meta XR Core SDK v.71.0.0, and XR Plugin Management v.4.5.0[3]. Image processing including color space conversion was conducted using OpenCV[4]. Both Δa and Δb was set to -50 empirically. Professional Quality Beef Curry from House Foods heated in the microwave was put on white rice and provided on the same bowl throughout the experiment. We chose curry and rice because the Japanese participants were all familiar with it since they were small children. The experiment room was shut from the sun light for color control.

Measurements

Regarding eating speed, the time until participants raised hands when finished were recorded. The questionnaire on appetite asked participants to choose from five options in response to the question, "Compared to your usual meals, how has your appetite changed?" The options were: "decreased"(-2), "slightly decreased"(-1), "no change"(0), "slightly increased"(+1), and "increased"(+2) where the numbers in parentheses are the points used to calculate the overall score. The questionnaire on eating difficulty asked participants to select from three options in response to the question, "Compared to your usual meals, did you experience any difficulty eating?" The options

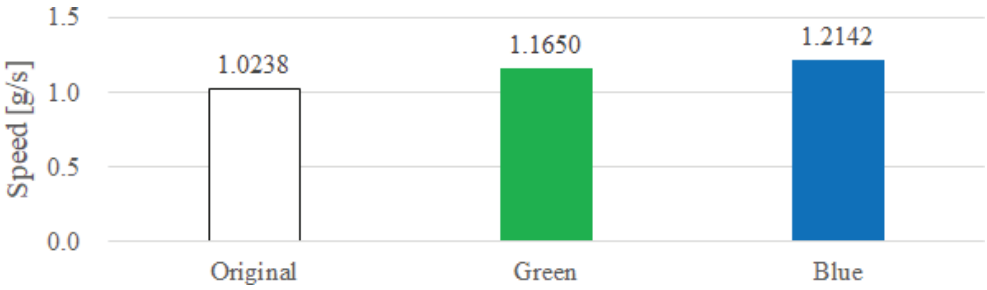

Figure 3: Comparison with respect to eating speed.

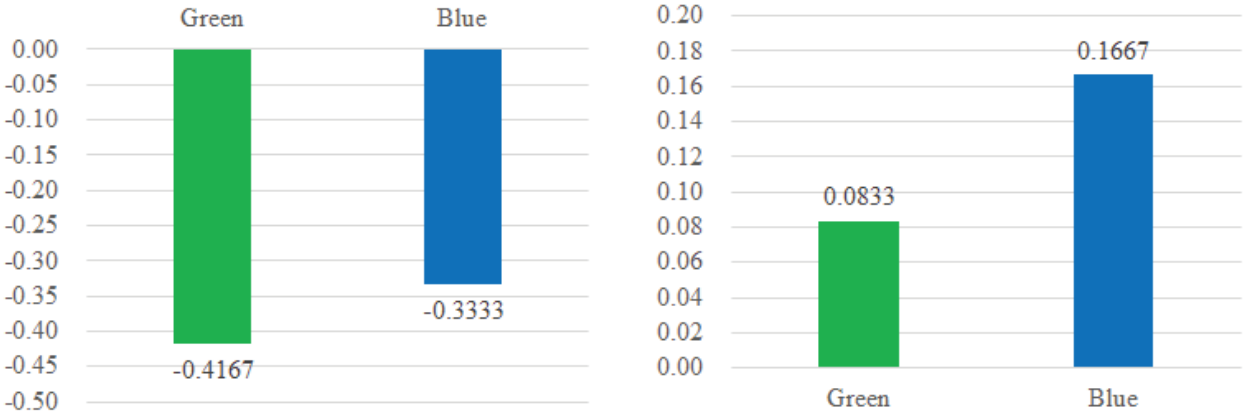

(a) Comparison with respect to appetite (b) Comparison with respect to difficulty

Figure 4: The results of subjective evaluations

were: "yes"(+1.0), "slightly"(+1.5), and "no"(0). In addition, participants were asked to freely describe any thoughts or feelings they had during the experiment.

Results

The average eating speed across participants (Figure 3) was compared among the three conditions. As a result, there was a tendency for eating speed to increase from white to green and from green to blue; however, the Mann–Whitney U test revealed no significant differences between the color conditions.

In the appetite questionnaire, both the green and blue conditions resulted in decreased appetite compared to the white condition. Although the differences were not statistically significant, appetite decreased more under the green condition than under the blue condition (Figure 4(a)).

In the questionnaire on eating difficulty, both the blue and green conditions led to increased difficulty in eating. Although the differences were not statistically significant, the blue condition resulted in greater eating difficulty than the green condition (Figure 4(b)).

Comments from the participants like “I felt more delicious with the original color than the others” and “I felt not so spicy with green and blue conditions compared with the original color” imply color modification may have affected the taste of food. On the other hand, “I felt easier to scoop the food under green and blue conditions than the original because of the higher contract to the plate” sounds consistent with the fact the average eating speed under those conditions was faster than that under the original.

CONCLUSION

In this study, an experiment using VR goggles was conducted to investigate how changes in the visual color tone of food affect eating behavior and appetite. The results showed that while altering the visual color tone of food did not have a statistically significant effect on eating speed, appetite, or eating difficulty, under conditions where the food was colored green or blue, there was a tendency for appetite to decrease, eating difficulty to increase, and eating speed to increase. You may say it is a matter of fact after thinking about cooks always taking care of color coordination of food very carefully. Here, we simulated the possibility that modifying original color of food might be able to control your appetite by changing room illumination. More participants in age, gender, and ethnicities are required in future experiments.

REFERENCES

[1]. Narumi, T. (2013). Modifying Perception of Satiety by Changing Apparent Food Volume with Augmented Reality. *Journal of Information Processing*, 54(4), 1422-1432.

[2]. Kobayashi, S. (2009). Appetite for Food Illuminated with Vivid Color Lights. *Journal of Environ. Eng.*, 74(637), 271-276.

[3]. Develop for Meta Quest workflow. https://docs.unity3d.com/6000.2/Documentation/Manual/xr-meta-quest-develop.html

[4]. OpenCV. https://opencv.org/

Application of Non-Contact Color Measurement Techniques in Heritage Conservation: A Case Study of The Wufeng Lin Family's "Gongbaodi" Residence

Ying-Tsung Lin[a*], Cheng-Min Tsai[b]

[a] *Department of Visual Arts and Design, Nanhua University, Tainan City, Taiwan*
[b] *Department of Visual Communication Design, National Taiwan University of Arts, New Taipei City, Taiwan* [*] *Corresponding author: Ying-Tsung Lin, brian98008@gmail.com*

ABSTRACT

Color is fundamental to cultural heritage preservation, yet restoration often relies on historical imagery and subjective judgment, producing inconsistencies with the original hues. In order to improve restoration accuracy, this study used non-contact colorimetry, establishing standardized recording and analysis procedures. Digital imaging of the Wufeng Lin Family's Gongbaodi residence was performed, calibrated with an X-Rite ColorChecker SG, and ICC profiles were generated using an X-Rite i1Profiler. Non-contact spectrophotometry (X-Rite i1Pro2 with i1Profiler) ensured instrumental repeatability and minimized surface contact damage. Measurements were expressed in CIELab space and collected using randomized 9-, 12-, and 24-point sampling to reduce errors and enhance representativeness. Results identified a representative blue pigment (CIELab L=61, a=−15, b=−16), providing an objective reference for reproduction. A comparative analysis with historical images revealed notable deviations in some restored elements, particularly where prolonged solar exposure and humidity accelerated color shifts. These findings demonstrate that traditional, non-standardized selection practices compromise visual authenticity. Therefore, we propose a practical protocol encompassing stable illumination, instrument calibration, randomized multi-point sampling, and concurrent color-reference swatches. We also recommend creating a comprehensive color database for archival and decision-support purposes. Standardized documentation, including time-stamped records and high-resolution images, augments archival value and enables cross-institutional comparisons. A standardized workflow facilitates reproducible measurements, supports informed restoration choices, and is transferable to other heritage contexts. This protocol supports transparent and verifiable restoration workflows that are suitable for museums and conservation offices. Finally, we advocate the implementation of long-term chromatic monitoring to detect gradual changes and reinforce conservation benchmarks, thereby improving the scientific rigor and sustainability of heritage color management.

Keywords: color technology, non-contact measurement, CIELab color space, heritage restoration, cultural heritage, color data preservation

INTRODUCTION

The motivation for this study was to record CIELab color values and utilize a device-independent color space to preserve the quantitative chromatic data of architectural polychrome decorations through scientific analysis and measurement. These data may serve as valuable reference materials for future conservation and maintenance efforts. Current literature primarily emphasizes digital archiving methods after restoration, which are often limited to photographic documentation and textual descriptions. However, based on the author's review of related studies,

there has been little to no discussion on the preservation of colorimetric data or the establishment of standards or methodologies for archiving color data in cultural heritage and architectural contexts.

Research Objectives

(1) Acquire color data via non-contact measurement.
(2) Record and preserve current color conditions.
(3) Propose post-restoration color measurement procedures.
(4) Provide reference for future architectural color archiving.

METHODOLOGY

The limitations of this study are as follows:

(1) Color data were acquired using non-contact measurement methods.
(2) Measurement focused on the current condition of the blue color at the Gongbaodi Residence.
(3) Color measurement was limited to open spaces.
(4) Readings were restricted to points accessible without climbing equipment.

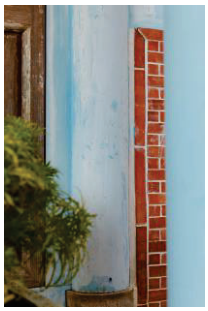

a.Fading

b.Crackinga

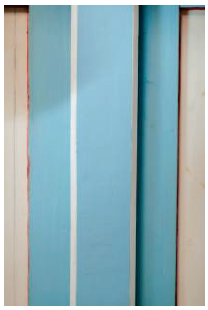

Mean value

This study primarily examined the procedures for color measurement and the comparative analysis of color readings. The objectives of this study were as follows.

a. Analyze current architectural conditions to determine whether sunlight exposure has resulted in pigment or paint fading.

b. Assess whether the polychrome layers in the measured structures display cracking and include such conditions in the study where relevant.

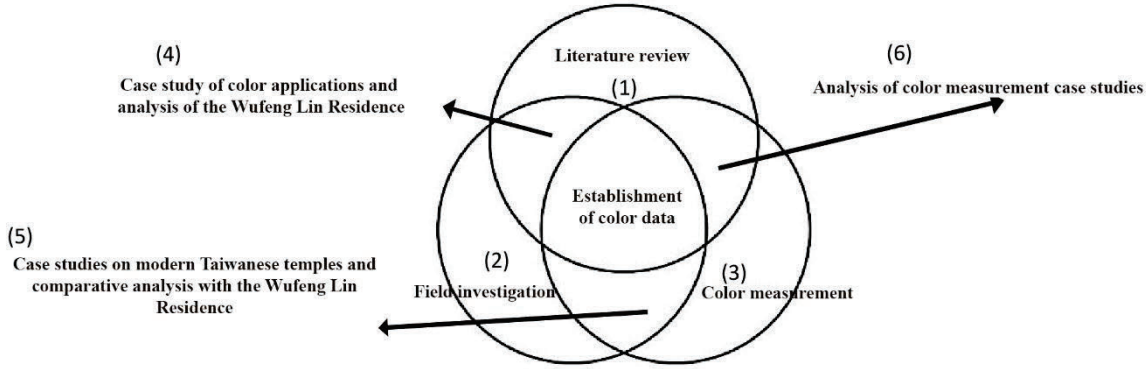

Figure 1: Research Framework

1. Literature Review Method

This study synthesized previous research on the Gongbaodi Residence, including theses, journal articles, and books. Relevant literature was analyzed to extract key concepts, summarize findings, and provide a basis for planning and structuring this research (**Figure 1**).

2. Field Investigation Method

Field visits were conducted at the Wufeng Lin Family's Gongbaodi Residence (Lower House). Data were collected through photography, audio recording, notetaking, and color measurements. These first-hand materials provided the foundation for establishing a color space for subsequent analyses (**Figure 1**).

3. Color Measurement Method

In this study, color measurements were carried out using a noncontact approach implemented in four sequential steps to ensure accuracy and reproducibility (**Figure 1**).

4. Literature Synthesis and Field Investigation

Based on the principles of heritage and artifact conservation, a series of literature syntheses and field investigations were conducted prior to restoration and maintenance. By examining official records, community archives, and oral histories from local residents, a more comprehensive historical context and site development were established (**Figure 1**).

5. Field Investigation and Color Measurements

Field investigations were conducted at the Jingxun Building of the Wufeng Lin Residence. Data were collected through photography, audio recording, notetaking, and color measurement, providing first-hand information essential for establishing the color space (**Figure 1**).

6. Color Measurement and Literature Synthesis

Through literature review and optical inspection, this study highlighted the importance of understanding the internal structure of the building. This approach allowed for the indirect observation and analysis of the polychrome layers during color measurement (**Figure 1**).

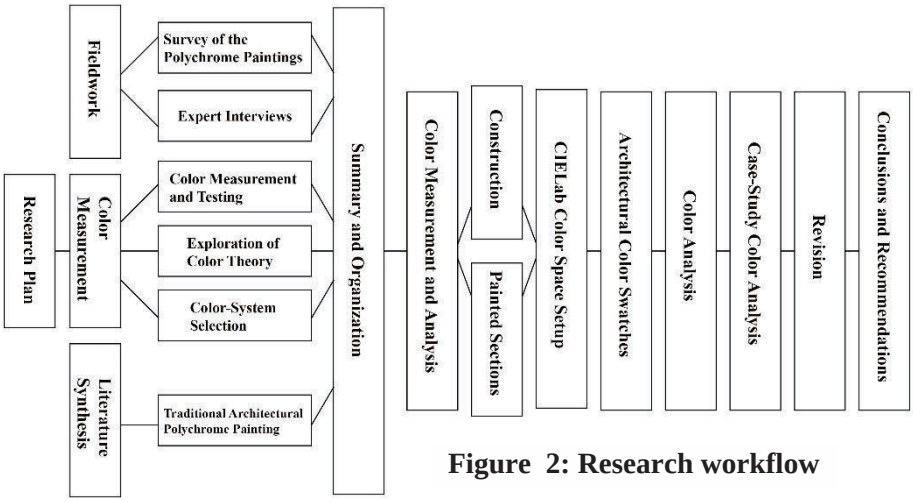

Figure 2: Research workflow

7. Research workflow

This study combined literature review, field investigation, and CIELab-based color measurements of polychrome surfaces in the Jingxun Building to systematically analyze recorded values, establishing procedures and proposing conclusions for heritage color research (**Figure 2**).

8. Color Measurement Procedure

Color measurements were conducted using a non-contact approach in four steps, as described below:

Step 1: A Canon 5D Mark IV camera and an X-Rite ColorChecker SG color reference chart were used for photography. Color data from the beams and columns of the Gongbaodi Residence were analyzed using the X-Rite i1Profiler system to establish a CIELab color space.

Step 2: For the target architectural elements, all blue monochrome beams and columns were divided into three equal sections. Within each section, 24 measurement points were randomly selected to acquire quantitative color data.

Step 3: The measurement data were processed using Adobe Photoshop as the color analysis tool. ICC color profiles generated by the *X-Rite i1Profiler* system were applied to ensure the accurate reproduction of true colors and enable precise color calibration.

Step 4: All measured values were expressed within the CIELAB color space. Conversion to a uniform color space and CIEXYZ coordinates provided a standardized color gamut for design references and effective communication.

RESULTS AND DISCUSSION

1. Number of Color Samples

This study examined the current blue-colored state of the measured architectural components. In total, 249 components were recorded (**Table 1**). Randomized measurements produced 6,723 data points (9-point), 8,964 data points (12-point), and 17,928 data points (24-point), thereby establishing the overall color space condition. (**Table 2**).

Table 1: ***Total Component Count Chart***

Total Count	1 record	2 record	3 record	
1B	4	11	13	28
2B	8	29	8	45
3B	3	21	36	60
4B	5	18	13	36
5B	1	11	9-3	15
5B	1	3	2	6
7B		22	29	51
7B		6	2	8
Total Count	22	121	106	249

Table 2: ***Total Measurement Data Chart***

Total Number of Files	9point data	12point data	24point data
1B	756	1088	2016
2B	1215	1620	3240
3B	1620	2160	4320
4B	972	1296	2592
5B	405	540	1080
5B	162	216	432
7B	1377	1836	3672
7B	216	288	576
Total Count	6723	8964	17928

2. Findings and Conversion of the Architectural Color Scheme of the Gongbaodi Residence (**Table 3**).

Table 3: ***Total Component Count Chart***

Color Analysis Table						
Location:	Gongbao Residence					
Ima ge	Color Space					
	Lab			HSB		
	L	a	b	H	S	B
	61	-15	-16	195	42	69
	Colorimetric Data					
Color Ima ge	最大值(max)	67	-5	-14		
	最小值(min)	50	-16	-20		
	平均值(mean)	59.6666	-12.8333	-16.5		
	中位數(mid)	61	-14.5	-16		
	標準差(sd)	6.497	3.715	2.291		

	L(明度)	a(色相)	b(色相)	色彩
1B	66	-15	-15.5	
2B	66.6	-12.2	-16	
3B	53	-15	-19.7	
4B	64	-16.3	-13.8	
5B	50.2	-5.2	18.5	
7B	58.1	-13.8	-14.2	

CONCLUSION

1. Non-contact color measurement enhances data stability and accuracy

Color measurement was conducted using the X-Rite i1 Pro2 non-contact colorimeter, and data were analyzed using the X-Rite i1Profiler software. CIELAB color values were recorded, and random 9-, 12-, and 24-point measurement methods were applied to reduce variability and improve measurement reliability.

2. Establishment of “Central Blue” color data as a reference for future restoration

The blue color in the Gongbaodi Residence polychrome was highly representative. Data indicated its CIELab values as L: 61, a: -15, b: -16. Through scientific measurements and data recording, this study provided an

accurate reproduction of architectural colors. Corresponding color swatches were also compiled, enabling future restoration projects to achieve precise color adjustments while preserving cultural significance.

3. Recommended standardized color measurement procedures for post-restoration heritage

Results showed that the lack of a standardized workflow led to unstable data and measurement errors. The specific recommendations include the following:

(1) Ensure stable lighting conditions during measurement to avoid interference from sunlight or UV exposure.
(2) Use ICC color profiles for calibration to enhance color accuracy.
(3) Apply a random 24-point measurement method to minimize color deviations caused by point selection errors.
(4) Record color reference charts simultaneously when documenting surface colors to ensure data consistency.

4. Reference value for color archiving methods

The color measurement and recording workflow established in this study serves as a reference model for future archiving of color data in cultural heritage and architectural preservation.

ACKNOWLEDGEMENTS

This research was supported by the National Science and Technology Council, Taiwan (project number NSTC 112-2813-C-343-006-H). The authors gratefully acknowledge this funding, which enabled the successful completion of the study and contributed valuable insights to the preservation and restoration of cultural heritage.

REFERENCES

[1]. Commission Internationale de l'Eclairage (CIE). (1986). *Colorimetry* (CIE Publication No. 15.2). Vienna, Austria: CIE.

[2]. Wang, Hung-Kai. (1988). *The Wufeng Lin Family in Taiwan: Architectural Atlas (Vol. 2).* Taipei, Taiwan: Zili Newspaper Group.

[3]. Lin, Chun-Mei, & Li, Chih-Shang. (2012). *Conservation planning of polychrome wooden decoration and restoration of door gods at the Gongbao Residence of the Wufeng Lin Family (National Monument).* Tainan, Taiwan: Tainan National University of the Arts.

[4]. Shao, Ching-Wang. (2022). *Illustrated dictionary of architectural polychrome terminology: Wooden polychrome.* Taichung, Taiwan: Bureau of Cultural Heritage, Ministry of Culture.

[5]. Shao, Ching-Wang. (2022). *Illustrated dictionary of architectural polychrome terminology: Wooden polychrome.* Taichung, Taiwan: Bureau of Cultural Heritage, Ministry of Culture.

[6]. Hsieh, Jen-Fang. (2016, September). *Modern color science: Color theory, perception, and application.* Taichung, Taiwan: Maoluo Xinzhuang Historical Studio.

[7]. Su, Ling-Hsiang. (1986). *A preliminary study on the polychrome colors of traditional Taiwanese architecture* (Master's thesis, National Cheng Kung University, Graduate Institute of Architecture).

Optimization of Image Colorization for Crime Scene Based on Generative Adversarial Network

Tzu-Ming Liu[a], Ming-Chih Cheng[a], Po-Hsin Yang[a], and Hung-Chung Li[a*]

[a]*Bachelor Program in Intellectual Creativity Engineering, National Chung Hsing University, Taichung, Taiwan*
[*]*Corresponding author: Hung-Chung Li, hcli01@nchu.edu.tw*

ABSTRACT

Color significantly enhances human perception and cognition. Image colorization aims to restore colors to grayscale images by assigning appropriate red, green, and blue values to each pixel. Although recent methods have improved, challenges such as context ambiguity and color bleeding persist. This study proposes a deep learning-based approach to improve colorization, particularly for surveillance footage, aiding criminal investigations. The model is trained and tested on the UCF Crime Dataset, which includes around 1,900 videos totaling over 128 hours of real-life crime scenarios. A Generative Adversarial Network (GAN) is used, combining a U-Net and ResNet18-based generator with a PatchGAN discriminator. The generator outputs A and B color channels from input grayscale (L) images to reconstruct full-color images. PatchGAN evaluates image authenticity through local features. Four activation functions, including ReLU, Leaky ReLU, ELU, and GELU, are tested during training. Model performance is evaluated using three metrics: Peak Signal-to-Noise Ratio (PSNR), Structural Similarity Index (SSIM), and Learned Perceptual Image Patch Similarity (LPIPS). Results show that Leaky ReLU achieves the best image fidelity, with an average PSNR of 35.4 and SSIM of 0.98. GELU performs best in human perceptual similarity, with a low LPIPS score of 0.024. Metric correlation analysis also shows that structural and perceptual similarities are not entirely aligned. Overall, the proposed method offers accurate and visually convincing colorization, with potential applications in surveillance, media restoration, and reducing reliance on color imaging hardware.

Keywords: image colorization, image quality, deep learning, convolutional neural network, generative adversarial network

INTRODUCTION

Color plays a crucial role in human cognition, enhancing visual perception and conveying richer information. Grayscale image colorization aims to add colors to monochrome images in a visually acceptable way by assigning red, green, and blue channel values to each pixel. Since image colorization is inherently multi-modal—meaning a single grayscale image can correspond to multiple plausible color versions—prior knowledge is often required to guide the process for optimal results. To simplify the task, color spaces such as CIELAB and YUV are commonly used, where chrominance channels are predicted based on luminance information [1].

Traditional grayscale colorization methods typically require extensive manual input and are highly sensitive to parameter settings. With the rapid advancement of deep learning technologies, approaches based on deep convolutional neural networks (CNNs) [2–4] or generative adversarial networks (GANs) [5, 6] have become the most common methods in recent years. These approaches have significantly improved both the quality and efficiency of image colorization.

However, despite the growing maturity of image colorization algorithms, challenges remain, such as contextual ambiguity and color bleeding at object edges [7]. Although deep learning-based techniques can colorize images at a lower cost, determining network parameters can be challenging due to insufficient information, and the results are not consistently reliable across different scenarios. Current deep learning methods—whether applied to grayscale or line-art images—still struggle to provide precise control over the colorization output and lack effective interactive mechanisms. Moreover, these methods often produce visually unappealing flaws and color inconsistencies. Given these limitations, further in-depth research on grayscale image colorization is essential.

METHODOLOGY

The study utilizes the UCF Crime Dataset to establish the model and split it into training and testing data. It was collected and organized by the Computer Vision Laboratory at the University of Central Florida. It is a publicly available dataset specifically designed for crime detection and analysis. The dataset comprises approximately 1,900 video clips with a total duration of over 128 hours, encompassing various types of criminal activities that may occur in everyday life. All videos are real surveillance footage and are annotated with specific crime categories, a total of 13 categories, including abuse, arrest, arson, assault, burglary, explosion, fighting, road accidents, robbery, armed assault/shooting, shoplifting, stealing, and vandalism, as illustrated in Figure 1. In this study, 1,378 videos from the dataset are used for training. However, the training data used in this study excluded videos that were initially in grayscale, retaining a total of 604 color videos for model training and 365 for testing. One frame is sampled every 3 seconds from these videos, resulting in a training dataset of approximately 28,000 images and a testing dataset of 10,000 images.

Figure 1: Crime category examples from the dataset

The model adopts a deep learning approach based on GAN to enhance the effectiveness and quality of image colorization. The GAN model architecture includes a generator based on U-Net and ResNet18, capable of generating corresponding red-green (A) and yellow-blue (B) chrominance channels from input grayscale images (L). These are combined with the input grayscale images to produce three-channel color images. The discriminator architecture utilizes PatchGAN, which considers the receptive field, extracts image features, and evaluates the authenticity of the entire image.

The main architecture of the model is illustrated in Figure 2. The input images are resized to 256×256 grayscale images (L channel). The encoder consists of multiple 3×3 convolutional layers integrated with residual blocks to extract multi-level features while progressively reducing resolution through pooling operations. The resolution decreases from 256×256 in the first layer to 128×128 with 64 feature maps, then to 64×64 with 128 feature maps, and finally to 32×32 with 256 feature maps in the third layer. In the bottleneck layer, several 3×3 convolutional layers with residual connections are used. These maintain the spatial resolution while further extracting deep features, resulting in 256 output feature maps. The decoder architecture uses transpose convolutions to upsample the feature maps at each layer. Skip connections are applied by concatenating the corresponding encoder feature

maps with the upsampled outputs. Further 3×3 convolutions are utilized to fuse the features. The final output consists of two 256×256 segmentation maps representing the A and B channels, which carry chromatic contrast information. For feature extraction, four different activation functions are implemented in this study, including ReLU, Leaky ReLU, ELU, and GELU, for comparison.

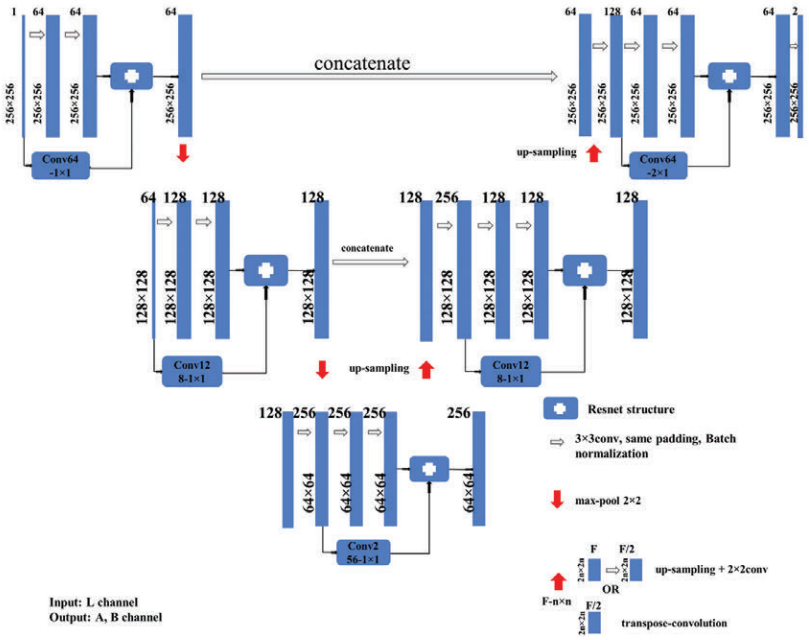

Figure 2: Architecture diagram of U-Net combined with ResNet

The discriminator in this study adopts the PatchGAN architecture and uses the same activation functions as the generator. The input consists of the L, A, and B channels, which are stacked together. The discriminator is composed of four layers, as illustrated in Figure 3. For visualization purposes, the output is later converted back to RGB. The PatchGAN-based discriminator focuses on local image patches. It extracts image features and determines the authenticity of each patch individually.

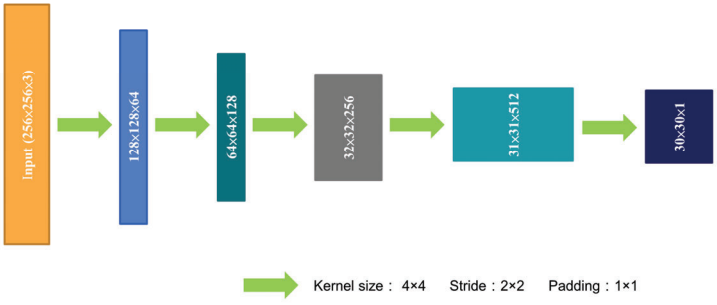

Figure 3: PatchGAN discriminator

The model architecture used in this study is shown in Figure 4. By observing the loss function values, the model training performance can be evaluated. The GAN model includes two loss functions: the generator loss and the discriminator loss. The generator loss indicates how closely the generated images resemble real images; a lower value suggests a stronger capability to produce realistic outputs. The discriminator loss reflects the ability to distinguish between real and fake images, with lower average values indicating better discrimination performance. The model's hyperparameter settings are 20 epochs, a batch size of 16, and the Adam optimizer.

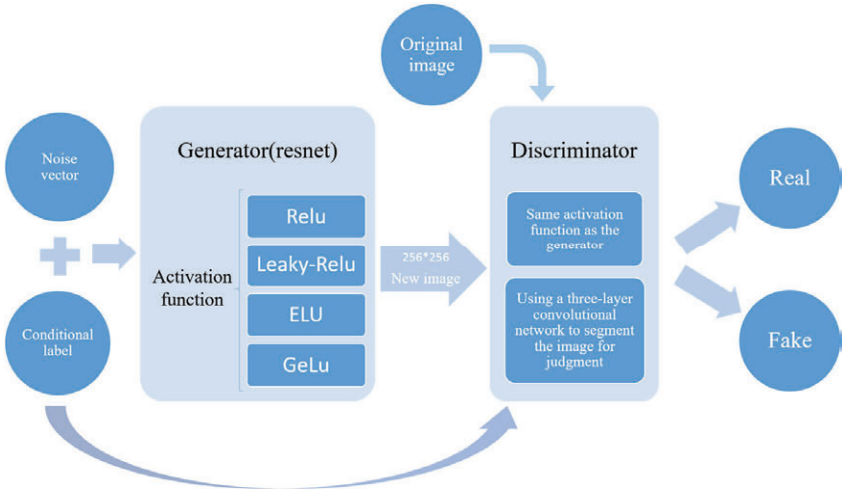

Figure 4: Model architecture

RESULTS AND DISCUSSION

In terms of training time, the ELU activation function required the shortest time among the four activation functions and also achieved the lowest loss. However, relying solely on training time and loss values to evaluate model performance is not entirely reliable, especially for visual tasks such as image colorization. Since the goal of this study is to assess how closely the colorized images resemble the original ones, it is essential to consider not only training efficiency and loss but also multiple image evaluation metrics to comprehensively understand the model's effectiveness in restoring color information.

This study employs three evaluation metrics —PSNR, SSIM, and LPIPS—to compare and assess the similarity between the original and colorized images. PSNR measures the difference between two images in decibels (dB). It evaluates the ratio between the original image and the noise, with higher values indicating better image quality and smaller differences between the two images. SSIM assesses the similarity between images by focusing on structural information. Unlike PSNR, which is based primarily on pixel-wise errors, SSIM emphasizes perceived changes in structural content, luminance, and contrast. SSIM values range from -1 to 1, where 1 indicates identical images, and values closer to 0 or negative suggest greater differences. LPIPS is designed to measure perceptual similarity between images from the perspective of human vision. Lower LPIPS values indicate that the images appear more similar to the human eye.

According to Table 1, the results indicate that the proposed deep learning-based colorization model competes strongly across three evaluation metrics. Regarding signal difference and structural similarity, the color images generated using Leaky ReLU are the most similar to the ground truth, with an average PSNR of 35.4 and SSIM of 0.98. Besides, GELU achieved the best performance for human perceptual similarity, with an LPIPS value of 0.024.

Furthermore, the correlation analysis among the metrics reveals that structural similarity and perceptual similarity are not entirely correlated, as shown in Figure 5.

Table 1: Comparison of the evaluation metrics

Metrics	ReLU	Leaky ReLU	ELU	GELU
PSNR	35.162	35.396	35.181	34.785
SSIM	0.9745	0.9756	0.9745	0.9729
LPIPS	0.0247	0.0243	0.0242	0.0267

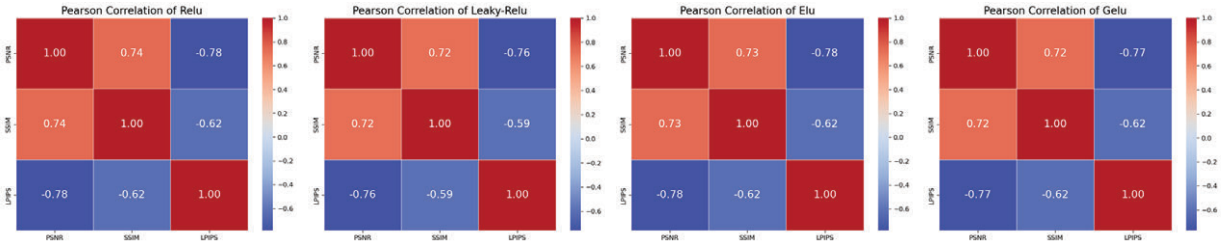

Figure 5: Pearson correlation coefficient matrix of PSNR, SSIM, and LPIPS

Figure 6 presents a comparison of colorization results using different activation functions. The main differences are evident in the skin tone of the man wearing white clothing at the center of the image, where noticeable color inaccuracies appear on the face and hands to varying degrees. Additionally, slight color variations are visible in the shirt of the man on the far left. Based on the comparison results, Leaky ReLU demonstrates superior performance in colorization.

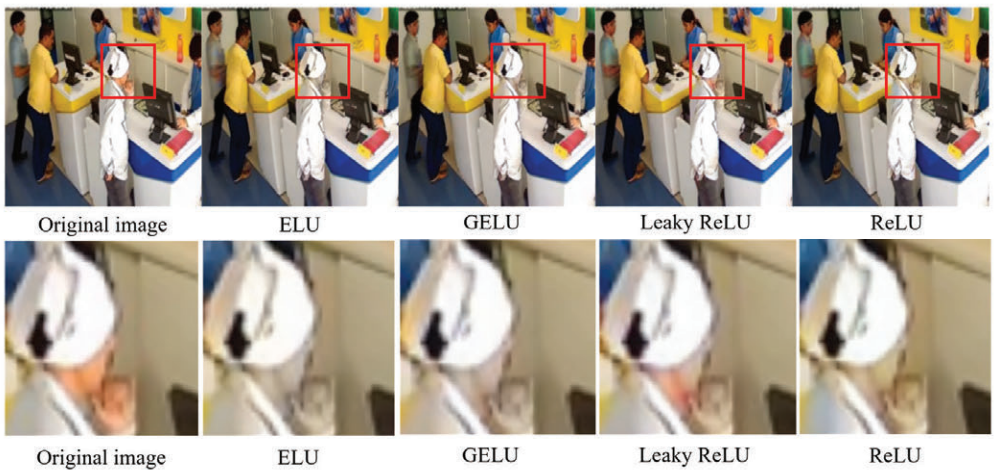

Figure 6: Different colorization results and zoomed-in details

CONCLUSION

The study aims to optimize grayscale image colorization and apply this technique to the analysis of surveillance footage, thereby assisting in criminal investigations. The model is trained using images from the UCF Crime Dataset and adopts a GAN that combines a generator based on U-Net and ResNet18 with a PatchGAN discriminator. The generator produces A and B chrominance channels from the input grayscale (L) image to reconstruct full-color images, while PatchGAN evaluates image authenticity through local features. Besides, the study compares the training performance of four activation functions: ReLU, Leaky ReLU, ELU, and GELU. Three evaluation metrics—PSNR, SSIM, and LPIPS—are used to assess the quality of colorization. The results show that Leaky ReLU performs best in terms of PSNR and SSIM, achieving average values of 35.4 and 0.98, respectively. On the other hand, GELU shows the best performance in LPIPS, indicating that both Leaky ReLU and GELU are recommended. Moreover, the analysis shows that structural similarity and perceptual similarity do not always align closely with each other. The proposed colorization model can effectively address the need for color restoration and colorization in image-related industries, thereby reducing the hardware costs associated with developing color imaging devices. Future research will focus on extending this framework to continuous image colorization, aiming to improve the consistency and naturalness of colorized video sequences.

ACKNOWLEDGEMENTS

This research project is partly supported by the National Science and Technology Council (NSTC-113-2634-F-005-002 and NSTC-114-2221-E-005-024)

REFERENCES

[1]. Cheng, Z., Yang, Q., & Sheng, B. (2015). Deep colorization. In *Proceedings of the IEEE international conference on computer vision* (pp. 415-423).

[2]. Zhang, R., Isola, P., & Efros, A. A. (2016). Colorful image colorization. In *Computer Vision–ECCV 2016: 14th European Conference, Amsterdam, The Netherlands, October 11-14, 2016, Proceedings, Part III 14* (pp. 649-666). Springer International Publishing.

[3]. Zhang, R., Zhu, J. Y., Isola, P., Geng, X., Lin, A. S., Yu, T., & Efros, A. A. (2017). Real-time user-guided image colorization with learned deep priors. *arXiv preprint arXiv:1705.02999*.

[4]. Varga, D., & Szirányi, T. (2016, December). Fully automatic image colorization based on Convolutional Neural Network. In *2016 23rd International Conference on Pattern Recognition (ICPR)* (pp. 3691-3696). IEEE.

[5]. Suárez, P. L., Sappa, A. D., & Vintimilla, B. X. (2017). Infrared image colorization based on a triplet dcgan architecture. In *Proceedings of the IEEE Conference on Computer Vision and Pattern Recognition Workshops* (pp. 18-23).

[6]. Li, B., Lu, Y., Pang, W., & Xu, H. (2023). Image Colorization using CycleGAN with semantic and spatial rationality. *Multimedia Tools and Applications*, 1-15.

[7]. Su, J. W., Chu, H. K., & Huang, J. B. (2020). Instance-aware image colorization. In *Proceedings of the IEEE/CVF Conference on Computer Vision and Pattern Recognition* (pp. 7968-7977).

The Effects of Typeface and Color Combinations on Perceived Trust, Professionalism, Aesthetics, and Usability in Traditional Chinese (Taiwan Standard) and English GUI Design

Fu-Shao Lu[a*], Wen-Yuan Lee[b]

[a] *Postgraduate, Department of Digital Media Design, Tatung University, Taiwan*
[b] *Professor, Department of Digital Media Design, Tatung University, Taiwan*

[*] *Corresponding author:* Fu-Shao Lu g11114011@o365.ttu.edu.tw

ABSTRACT

Literature has indicated a strong positive correlation between usability and visual aesthetics in graphical user interface (GUI) design, challenging the traditional notion that usability and aesthetics are separate concerns and highlighting the need to reconsider how design elements influence both usability and visual aesthetics. Typeface and color are fundamental components of GUI aesthetics, and their impact on visual appeal, readability, and overall user experience is crucial. Effective typeface and color choices can enhance cognitive ease, reducing the mental effort required for users to process information and navigate an interface.

This study aims to comprehensively analyze how optimal typeface and color pairings enhance the perceived quality of GUIs. A psychophysical experiment was conducted. Thirty-six observers were invited to evaluate the impact of typeface and color choices on perceived quality in the GUI. Six typefaces were used in the experimental sample, including four Traditional Chinese (Taiwan Standard) typefaces and two English typefaces: Ming (明體), Hei (黑體), Rounded (圓體), Kai (楷體), Helvetica, and Times New Roman. Nine colors were applied to these six typefaces, including black, gray, red, orange, yellow, green, blue, purple, and brown. A total of 54 experimental samples were produced. All experimental samples were presented on a white background. Each observer was required to evaluate each experimental sample on four perception dimensions: trust, professionalism, aesthetics, and usability.

The results showed that (1) significant differences were found between Traditional Chinese (Taiwan Standard) and English typefaces across all four perceptual dimensions, and (2) the aesthetic–usability effect was evident in both language interfaces, with higher perceived aesthetics enhancing perceptions of trust, professionalism, and usability.

Keywords: Typeface, Color, GUI Design

INTRODUCTION

Recent research has increasingly demonstrated that usability and visual aesthetics in graphical user interface (GUI) design are not separate but closely intertwined. Kurosu and Kashimura (1995) showed that aesthetic impressions strongly influence users' judgments of usability.[2] This finding highlights the significance of design elements, such as typeface and color, in influencing perceptions of interface quality. Similarly, Norman (2004) argued that user experience operates on three interrelated levels—visceral, behavioral, and reflective—underscoring that aesthetics and usability together form the foundation of meaningful interaction.[4]

Color and typography are central to this discussion, as both significantly impact not only visual appeal but also the emotional and cognitive processes that influence user evaluations. Elliot and Maier (2012) emphasized that the psychological impact of color is context-dependent, influencing affect, cognition, and behavior.[1] In parallel, Moshagen and Thielsch (2010) identified four facets of visual aesthetics—simplicity, diversity, color, and craftsmanship—that jointly determine how digital interfaces are perceived.[3] These insights suggest that typeface and color combinations may shape users' judgments not only of aesthetics and usability, but also of more socially grounded perceptions such as trust and professionalism.

Building on these perspectives, the present study examines how typeface and color combinations in Traditional Chinese (Taiwan Standard) and English interfaces affect user perceptions across four evaluative dimensions: trust, professionalism, aesthetics, and usability. To this end, GUI prototypes will be designed using four Traditional Chinese (Taiwan Standard) and two English typefaces, systematically combined with colors, and evaluated through a questionnaire that measures the four perceptual scales.

EXPERIMENTAL PLAN

A psychophysical experiment was conducted to examine how different typefaces and color combinations affect perceived trust, professionalism, aesthetics, and usability in graphical user interface (GUI) design. The study included six typefaces: Traditional Chinese (Taiwan Standard) and English typefaces, specifically Ming, Hei, Rounded, Kai, Times New Roman, and Helvetica (see Figure 1). These typefaces were chosen for their structural contrasts between serif and sans-serif styles.

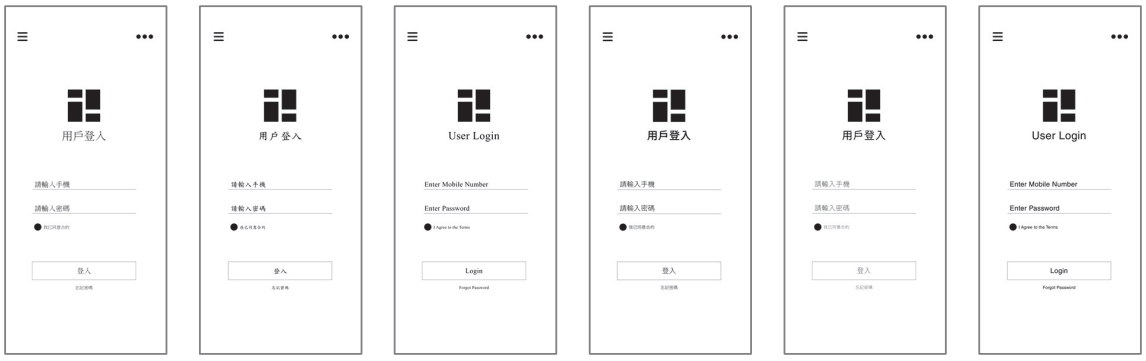

(a) Ming (明體) (b) Kai (楷體) (c)Times New Roman (d) Hei (黑體) (e) Rounded (圓體) (f) Helvetica

Figure 1: Six typefaces used in the experiment

Ten colors were selected from the eleven basic color terms: red, orange, yellow, green, blue, purple, brown, gray, black, and white. White was designated as the background, while pink was excluded due to insufficient visual clarity.

All experiments were conducted on a Samsung Galaxy A54 smartphone, featuring a 6.4-inch OLED display with a resolution of 1080 × 2340 pixels and a 120Hz refresh rate. The display was calibrated using an X-Rite i1 Display Pro colorimeter, achieving a peak luminance of 375 cd/m² and a correlated color temperature of 6389K. To ensure perceptual accuracy, colorimetric measurements and device calibration were performed under CIE standard 10-degree observer conditions. All procedures took place in a controlled indoor environment illuminated by a D65-

standard light source, simulating neutral daylight. The resulting CIELAB color values as displayed on the screen are presented in Table 1.

A total of 36 observers (16 males and 20 females), aged between 18 and 54 years, were recruited for the study. All observers were confirmed to have normal vision using the Ishihara Color Vision Test. Observers were asked to evaluate four perceptual dimensions —trust, professionalism, aesthetics, and usability — on 56 GUI samples, including two duplicate trials to assess response consistency. Ratings were collected using a 5-point categorical judgment (1 = strongly disagree, 5 = strongly agree).

Table 1: Colors used in the experimental samples

color		L	a	b	C_{ab}	h_{ab}
Black(Bk)		0	0	0	0	-
Gray(Gy)		54	0	0	0	-
Red(R)		53	79	43	90	29°
Green(G)		54	-32	11	34	161°
Yellow(Y)		74	13	68	69	79°
Blue(Bl)		54	-11	-33	35	251°
Brown(Br)		31	12	43	45	74°
Orange(O)		64	30	70	77	66°
Purple(P)		53	34	-33	47	316°
background(White)		100	0	0	0	-

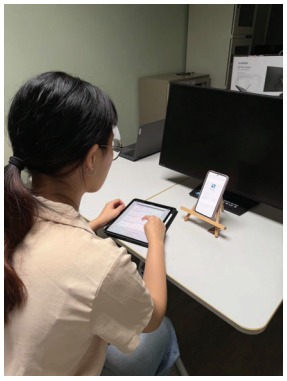

Figure 2: Experimental environment

Each sample was presented using Figma's prototype mode. The presentation order of the sample was randomized for each participant. Each observer completed the experiment in approximately 30 minutes. Observers were seated at a viewing distance of 30 cm, as shown in Figure 2. After each sample was displayed, the screen transitioned to a neutral gray background for 2 seconds. To prevent fatigue, a short break of approximately two minutes was scheduled at the midpoint of the session. Observers were also allowed to pause the session at any time if they experienced discomfort.

INTER- AND INTRA-OBSERVER VARIATION

Before conducting statistical analysis, intra- and inter-observer variations were assessed using the root mean square (RMS). Intra-observer variation was used to see whether observers could consistently repeat their judgments, while inter-observer variation evaluated the agreement between individual observers and the mean results. The RMS equation is given below.

$$RMS = \sqrt{\frac{\sum (x_i - y_i)^2}{n}} \quad (1)$$

For intra-observer variation, X_i and Y_i refer to the initial and replicated judgments, respectively. For inter-observer variation, X_i represents the individual participant's data, while Y_i corresponds to the mean value across all observers. n denotes the number of data points. An RMS value of 0 indicates perfect agreement between the two data arrays, as shown in Figure 3

As illustrated in Figure 3, intra-observer RMS values ranged from 0.00 to 1.73, while inter-observer RMS values ranged from 0.58 to 2.12. One observer (No. 23) exhibited poor consistency, with an inter-observer RMS exceeding 1.75, and was therefore excluded from subsequent analyses.

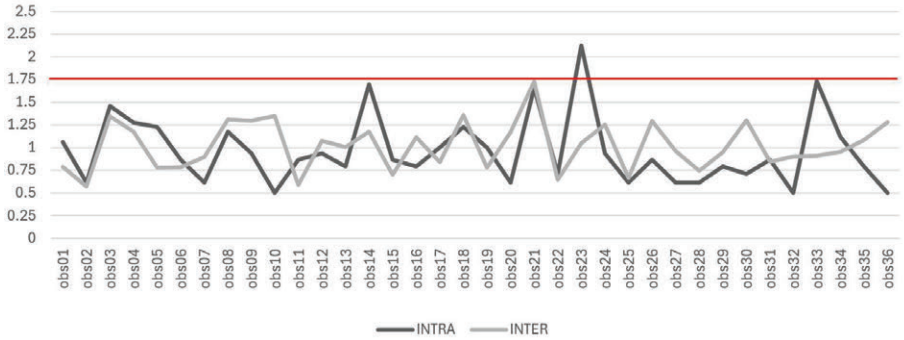

Figure 3 Inter-observer and intra-observer variations

RESULTS

To examine the differences between Traditional Chinese (Taiwan standard) and English typefaces used in graphical user interfaces, independent sample t-tests were conducted to determine if the two language typefaces differ from each other on four perceptual dimensions: trust, professionalism, aesthetics, and usability. The results are summarized in Table 2.

Table 2: Results of independent-sample t-tests comparing Traditional Chinese and English typefaces.

	Interface built with Traditional Chinese (Taiwan Standard) typeface		Interface built with English typeface			
	M	SD	M	SD	t	p
Trust	3.15	1.11	3.45	1.07	-5.6	.000
Professionalism	3.15	1.16	3.62	1.05	-8.9	.000
Aesthetics	2.95	1.15	3.43	1.11	-8.6	.000
Usability	3.56	1.14	3.70	1.10	-2.5	.010

Significant differences were found between Traditional Chinese (Taiwan Standard) and English typefaces on four perceptual dimensions: trust, professionalism, aesthetics, and usability. The interfaces built with the English typeface were found to be higher than those with the Traditional Chinese typeface (Taiwan Standard) on four perception dimensions.

To further explore how typeface and color affect four perception dimensions, a line chart was used, as shown in Figure 4. From left to right, Figure 4 illustrates the perceived trust, professionalism, aesthetics, and usability. The horizontal axis displays color categories, sorted in order of average value. Solid lines represent sans-serif typefaces, while dashed lines represent serif typefaces. The top row of Figure 4 shows Traditional Chinese typefaces (Taiwan Standard), and the bottom row shows English typefaces.

The results showed:

1. An additive effect was observed in perceived trust, professionalism, aesthetics, and usability for interfaces composed of colored Traditional Chinese typefaces, as indicated by the two lines that appear to be ascending, separating, and not crossing in Figures 4(a)~(d).
2. The interfaces built with sans-serif Traditional Chinese typefaces were found to be rated higher than those built with serif typefaces.
3. Compared with the interface built with colored Traditional Chinese typeface, the interfaces built with colored English typeface were found to show that the color category is more influential than the English typeface on perceived professionalism, aesthetics, and usability, as indicated by the two lines appearing overlapped and ascending in Figures 4 (f) ~ (h).
4. On perceived trust, generally speaking, the interface built with serif typefaces was rated higher than those in sans-serif typefaces. However, the interaction effect was found between typefaces and colors, as indicated by the two lines that appear to be ascending and crossing in Figure 4(e). This means that the particular typeface applied to a specific color category can enhance perceived trust, i.e., black color applied to sans-serif fonts increases perceived trust.

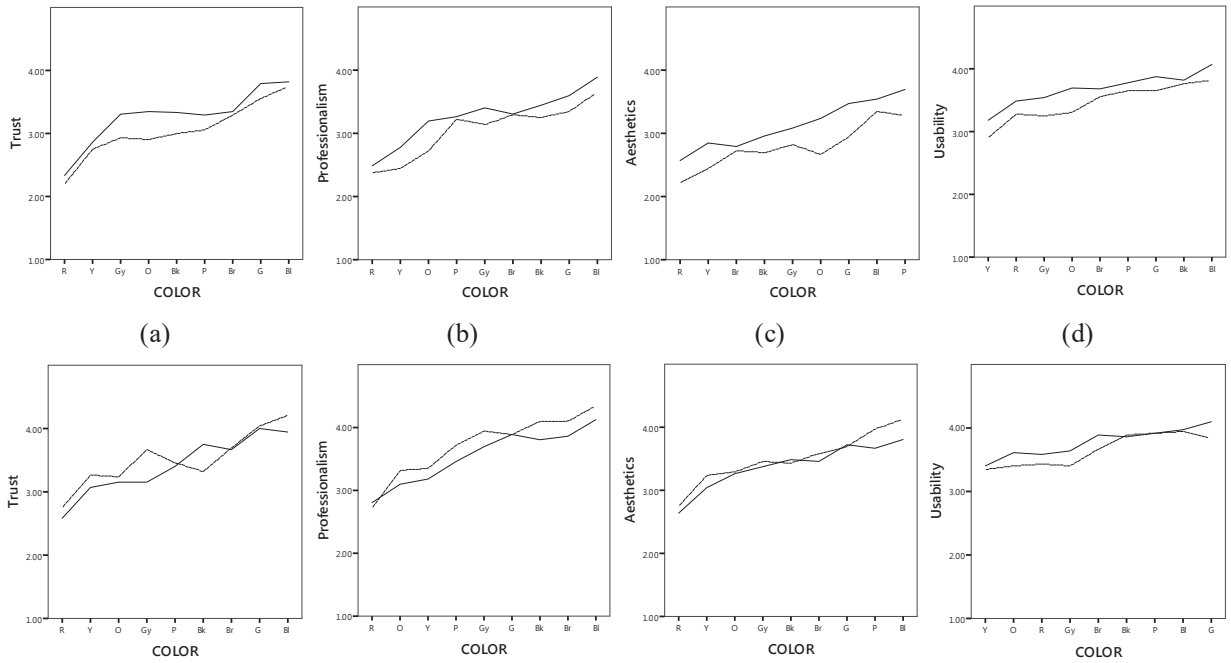

Figure 4: The effect of typeface and color on four perceptual dimensions.

To see how well the correlation between usability and aesthetics in graphical user interfaces, Pearson correlation coefficients were calculated for four perceptual dimensions: trust, professionalism, aesthetics, and usability. The results are summarized in Table 3. In both the interfaces built with Traditional Chinese (Taiwan standard) typefaces and those built with English typefaces, the four perceptual dimensions were positively

correlated. This finding supports the aesthetic–usability effect and reveals that when users perceive an interface as aesthetically pleasing, they also tend to evaluate it as more trusted, professional, and usable. While the correlations between usability and trust, and between usability and professionalism, were positive for the interfaces built in English typeface, they were lower than those for interfaces built in Traditional Chinese (Taiwan standard) typeface.

Table 3: Pearson correlation of four perceptual dimensions

Interface built with Traditional Chinese (Taiwan standard) typeface	Trust	Professionalism	Aesthetics	Usability
Trust	1.00	-	-	-
Professionalism	0.91	1.00	-	-
Aesthetics	0.78	0.78	1.00	-
Usability	0.71	0.83	0.72	1.00
Interface built with English typeface				
Trust	1.00	-	-	-
Professionalism	0.88	1.00	-	-
Aesthetics	0.88	0.85	1.00	-
Usability	0.65	0.63	0.71	1.00

CONCLUSION

This study examined the effects of typeface-color combinations in Traditional Chinese (Taiwan Standard) and English GUI Design. A psychophysical experiment was conducted in which 36 observers evaluated 54 GUI samples in terms of perceived trust, professionalism, aesthetics, and usability. The major results showed that (1) significant differences were found between Traditional Chinese (Taiwan Standard) and English typefaces across all four perceptual dimensions, and (2) the aesthetic–usability effect was evident in both language interfaces, with higher perceived aesthetics enhancing perceptions of trust, professionalism, and usability.

REFERENCES

1. Elliot AJ, Maier MA. Color-in-context theory. Advances in Experimental Social Psychology 2012;45:61–125.
2. Kurosu M, Kashimura K. Apparent usability vs. inherent usability: experimental analysis on the determinants of the apparent usability. Conference Companion on Human Factors in Computing Systems. Denver, Colorado, USA: Association for Computing Machinery; 1995. p 292–293.
3. Moshagen M, Thielsch MT. Facets of visual aesthetics. International journal of human-computer studies 2010;68(10):689-709.
4. Norman DA. Introduction to this special section on beauty, goodness, and usability. Human–Computer Interaction 2004;19(4):311-318.

Perceptual Calibration of Meta Headset: Investigating luminance Accuracy Through 2D and 3D Senses by Unity

Jinbi Jiang*, Stephen Westland, Caroline Hemingray, and Kaida Xiao

University of Leeds, Leeds, UK
**Corresponding author: Jinbi Jiang, sdjj@leeds.ac.uk*

ABSTRACT

Mixed Reality (MR) technologies pose new challenges for accurate colour rendering due to the variability in display characteristics across devices. This study focuses on developing a perception-based calibration method using Meta Quest 3 headsets. The experiment is conducted using a set of custom-built Unity programs, designed to collect data as participants wear a headset and follow guided instructions. This paper will focus on the luminance prediction under two conditions – with and without rendering (corresponding to 3D and 2D perception). Participants adjust the brightness of a target object (a flat square or 3D cube) to match the perceived brightness of background composed of halftone patterns. The goal is to examine whether 2D characterisation models remain valid in 3D contexts and to explore perceptual differences introduced by spatial depth and interaction. Across 21 participants, perceptual matching functions were monotonic and highly similar between no-render (2D) and rendered (3D) conditions. Channel discrepancies with instrument baselines were larger in rendered scenes, most notably at low luminance for red/blue, whereas high-luminance channels (green/mixed) remained close (RMSE = 1.6–4.7 digital counts). In the no-render baseline, interpolation from perceptual data predicts lower luminance than instrument curves at mid–high codes (≈0.4–0.8). Finally, the no-render perceptual mapping can be transported to rendered scenes by scaling with the per-channel bright (or dark) walls luminance; a power-law transport yielded the lowest errors (RMSE 0.006–0.015), outperforming gain-only or multiplicative least-squares scaling. The results indicate that perception-based luminance prediction is stable across scenes and provides a practical basis for MR calibration.

Keywords: Mixed Reality, Display Characterisation, Perceptual MR Adjustment, Computer Graphics, Rendering

INTRODUCTION

Accurate colour representation in virtual and mixed reality (VR/MR) environments is critical for applications in industrial design, medical training, education, and perceptual research. Traditional calibration methods rely on instrument-based measurements, but these approaches often fall short when applied to head-mounted displays (HMDs). Recent work has highlighted the complexity of achieving standardised calibration and stable colour control on such devices [2]. HMDs employ near-eye displays (NEDs) with short focal distances, wide fields of view, and multilayered optical paths which complicate spectroradiometric measurements [3]. Rendering pipelines frequently include automatic tone mapping, exposure control, and post-processing effects, all of which make consistent colour reproduction difficult [4]. Moreover, practical measurement is nontrivial -- MR headsets and spectroradiometers must be precisely aligned with angle and distance controlled. Given these challenges, instrument-based methods, while precise under controlled laboratory conditions, may not be suitable for MR devices. Relatively few studies have examined perceptual calibration in HMDs, especially under mixed rendering conditions where both virtual and real-world elements are combined. This gap highlights the importance of developing user-centred methods that directly measure and model perceptual responses.

This project addresses the limitations of instrument-based calibration by developing a visual method for calibrating MR devices. Rather than claiming higher accuracy than instruments, our goal is to provide a

complementary, user-centred pathway that is more stable and uniform across rendering modes and scenes. We introduce a repeatable perceptual matching method on Meta Quest 3 that pairs rendered and no-rendering conditions to capture how users experience luminance. We also propose a perception-based colour-space conversion routine that links engine input signals to perceived luminance/colour via interpolation. These elements constitute a practical framework that complements instrument-only workflows by improving repeatability and harmonisation in MR colour characterisation.

METHODOLOGY

The experiment was implemented in Unity (URP), selected for its integrated editor and XR runtime support that allow direct control of the rendering pipeline. For all study builds, non-linear camera effects were disabled (tone mapping and automatic exposure off), and channel-isolated stimuli (R, G, B, and mixed) were generated with fixed frame timing. Scene parameters and shaders were held constant across sessions to improve repeatability. Experiments were conducted on a Meta Quest 3 mixed-reality headset which employs two LCD displays, one per eye, with a per-eye resolution of 2064 × 2208 and support for 90 Hz operation. The display uses an RGB-stripe subpixel layout (three subpixels per pixel). The RGB-stripe subpixel structure directly supports subsequent per-channel (R, G, B) and mixed-channel stimulus generation and testing, while the available refresh rate provides sufficient temporal stability for brightness-matching procedures. Throughout data collection, the same unit and system settings were used in rendered and no-rendering conditions.

In general Unity's rendering pipeline, vertex attributes and textures are transformed and rasterised, and per-pixel colour is computed in the fragment stage from material parameters, lighting, and the shading model. To isolate colour formation at the shader level and maintain consistency across conditions, all post-processing stages were disabled so that fragment outputs were written directly to the framebuffer using fixed transfer functions. In the no-rendering condition, the target used an unlit pass that mapped the input code directly to the framebuffer. In the rendered condition, lighting followed a controlled configuration - a "Sunlight" directional light was placed outside the window from the default scene generated, based on default settings but modified to a correlated colour temperature of 6500 K, brightness 2 (Unity units), operating under linear colour space. Shadow parameters for the directional light followed Unity defaults without explicit strength or bias override; the shadow near plane was set to 0.1. To approximate interior illumination, five points lights were positioned inside the room to yield similar average light levels (placement depending on room size). Each point light was set to 6500 K, intensity 1, range 10, under linear colour space. For the point lights, shadow settings used High resolution (512; URP High Fidelity preset), strength 1, bias from the URP asset, and a near plane of 0.1. All other pipeline configurations were held fixed between rendered and no-rendering conditions.

Stimuli consisted of a central adjustable target presented over a background field. In the no-rendering environment, both the target stimulus and the background used Unity UI materials that bypass default rendering calculations and write colour values directly to the framebuffer. The background was implemented as a full screen 2D panel with a spatially uniform halftone pattern. Similarly, in the rendered environment the background was the interior wall of an otherwise empty room (Fig. 1). The wall and the 3D target used default lit material. A button press switched the material's texture (Fig. 1), where each texture simulated an input signal between 1/9 and 8/9 via coverage halftone images. As all halftone images are 3×3, using scripts to set the background with halftone images without stretching and arranging them uniformly, each pixel approximates one-ninth of the image.

Before data collection, participants watched a brief training video include Meta headset usage and the operation of the experimental tasks, and then completed a short practice. Each session began with a short dark-adaptation period inside the headset, with the laboratory lights turned off. During data acquisition, participants were seated and instructed to minimise head motion relative to the fixation region. Participants matched the perceived brightness of the target to the fixed background level by adjusting the target's digital code using the handheld controllers. Fine steps (single count) and accelerated stepping were available to facilitate precise matching. Subsequent analyses were performed on the group mean (N = 21) and standard deviation across participants. For instrumental reference, the same stimuli were reproduced for spectroradiometric measurements under both rendered

and no-rendering conditions. The spectroradiometer was rigidly mounted and aligned to the headset optics; the headset position was fixed, and screen stability had been verified prior to the experiment. Measurements were taken with the laboratory lights off, keeping the spectroradiometer lens as close as practicable to the headset eyepiece and at a constant viewing angle.

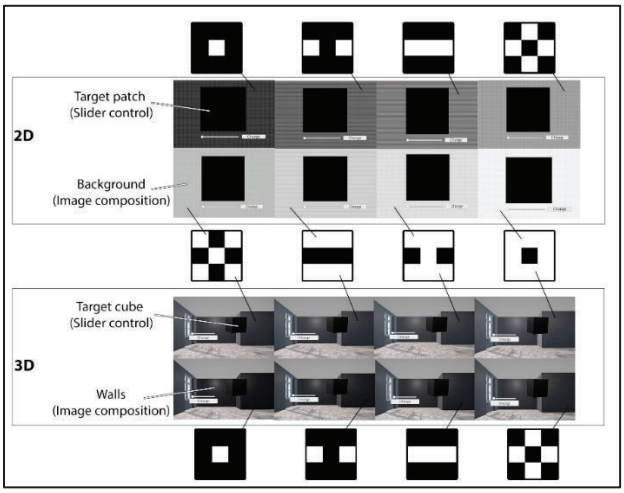

Figure 1: Program interface settings presentation (it does not represent the actual display effect in the headsets)

RESULTS AND DISCUSSION

This section first reports data completeness and quality control (N = 21), then establishes instrument-based luminance baselines alongside perceptual matching curves. We subsequently quantify the effects of rendering (rendered vs no-rendering), geometry (2D vs 3D), and channel (R, G, B, mixed), and conclude with interpolation-based prediction error (RMSE) and agreement analyses.

In Task 1, we preset the background luminance (Y) using a halftone image under unrendered 2D conditions, and the observers achieve perceptual matching by digital counts. Figure 2 (a) shows that for channels (R, G, B, grey), the instrumental results (solid lines) can be compared with the observer data (grey dashed lines) for the 8 halftone patterns. The x-axis is the luminance of the halftone background (dashed - preset luminance 1 bright pixel = 0.11, 2 = 0.22, …, 8 = 0.89, solid line - background halftone luminance Y from CS2000), and the y-axis is the digital count (dashed - participants results, solid line – halftone textures' Unity RGB values). The observer data are monotonic but clearly nonlinear, with strong compression at the dark end - matching the 11% halftone level typically required codes over 90, i.e., ~35% of the display's full-scale grey. Agreement with the instrumental data is channel dependent. Green and grey exhibit close correspondence (RMSE ≈ 1.6–4.7 counts; MaxAE ≤ 7.4 counts), whereas red and blue deviate more strongly in mid–high ranges (RMSE ≈ 17.7–19.4 counts; MaxAE ≈ 25 counts). Figure 3 (a) shows the tone-reproduction curves for the instrumental and visual methods; there is close agreement between the data of instrument result (grey scale from CS2000) and the psychophysical methods. There is a systematic shift upwards of psychophysical with respect to the instrument results which can also be seen in Figure 2 (a). Across participants, dispersion is smallest for green/grey and larger for red/blue, consistent with channel differences in the no-rendering panel's electro-optical response and the halftone integration at low luminance. The observers' data also show relatively high codes to match low-luminance backgrounds, consistent with LCD near-black EOTFs and optical pooling. We calculated the local slope (Δgrey-scale/Δluminance) for R, G, B and grey - sensitivity declines with luminance, shows marked irregularity at the lowest levels, and exhibits a clear dip between 0.11 and 0.22. This pattern accords with LCD channel EOTFs and a near-black/backlight floor that reduce effective contrast, inflating the codes required in the 0.11–0.22 range. Although Task 1 uses unlit UI materials and disables post-processing,

the direction of these nonlinearities anticipates full-pipeline behaviour—global tone mapping (e.g., ACES toe/shoulder), auto-exposure, and colour balance typically further compress extremes and can differentially affect channels.

Figure 4 compares luminance predictions obtained by interpolation (PLCC) from the task 1 perceptual matches with those derived from CS-2000 measurements of the Meta Quest 3 grey-scale (unrendered). Figure 4 (a) – (d) show that the perceptual model systematically predicts lower Y than the instrument model in the mid–high code range (≈0.4–0.8), a pattern summarised in Figure 4 (e) where residuals are predominantly negative across the full range (most around 0.6–0.8). Additionally, errors are channel-dependent -- Blue shows the largest discrepancy, Red the next, whereas Green and Grey are substantially closer, with RMSE < 0.05 (normalised), which is small relative to the dynamic range considered. Moreover, the error magnitude is smallest at low codes and grows towards the highlight, consistent with a gamma/curvature mismatch, others, such as optical pooling, channel EOTFs, may also play a role. These differences are reasonable given blue's lower contribution to photopic luminance and known challenges of HMD optical sampling and centre-spot metrology. Although a post-hoc power-law correction can reduce channel errors (after correction, we got Red RMSE ≈ 0.04, Blue RMSE ≈ 0.02), we favour a calibration strategy that uses the perceptual grey prediction as the primary mapping and derives single-channel luminance via channel luminance weights, prioritising stability and cross-session consistency over device-specific accuracy. This paper provides a stable, rendering-agnostic baseline, may motivating a focus on stability and interpolation-based prediction.

Figure 2 (b) shows that perceptual matching curves in the rendered room retain the same monotonic, nonlinear shape as in Task 1, but the separation from the instrument curves is larger—most clearly at low luminance for R and B. The participant curves are in the same range as the bright wall instrument baseline (especially in the G and Grey channels), but for the backlit wall, the instrument baseline lower perceptual matches approximately 100 counts (0-255 scale). Figure 2 (b) overlays no-rendering and rendered perceptual curves and shows they are highly similar (median absolute deviation = 3.8 counts). That stability implies a practical assumption -- luminance prediction in rendered scenes can reuse in the no-render condition. Figure 3 (b) reconciles the instrument–perception gap that showed, after dividing the bright- and dark-wall luminance (Y) by each channel's maximum, the participant change curve aligns closely with the dark-wall instrument curve. In other words, once dynamic-range differences are factored out, observer's perceptual matching with the dark wall baseline is the similar growth magnitude. Figure 5 (a) – (b) validates how the perceptual mapping obtained in the no-render baseline can be transported to rendered scenes by bidirectionally scaling with the per-channel bright (or dark) walls luminance. In Figure 6 (a) we use multiplicative least squares in the linear domain - given a source curve y_s and a target y_t, we find a gain k that minimises $\|ky_s - y_t\|_2$; this keeps the zero-point fixed and is optimal when the curves mainly differ by scale. Figure 6 (b) implements power-law transport. First fit $y \approx Ax^{\gamma}$ to the source and target, if $\gamma_s \approx \gamma_t$, a gain-only transfer $y' = (A_t/A_s)$ ys suffices; when exponents differ, we use a power map $y' = sy_s^{\alpha}$ with $\alpha = \gamma_t/\gamma_s$ (and s set by the measured bright /dark walls luminance ratio) to match curvature without introducing an offset. The resulting errors are RMSE = 0.006–0.015 (power map), 0.009–0.32 (multiplicative least squares), and 0.014–0.056 (gain only). These results show that scaling by the bright (or dark) walls luminance while preserving the no-render perceptual mapping demonstrates feasibility on our dataset.

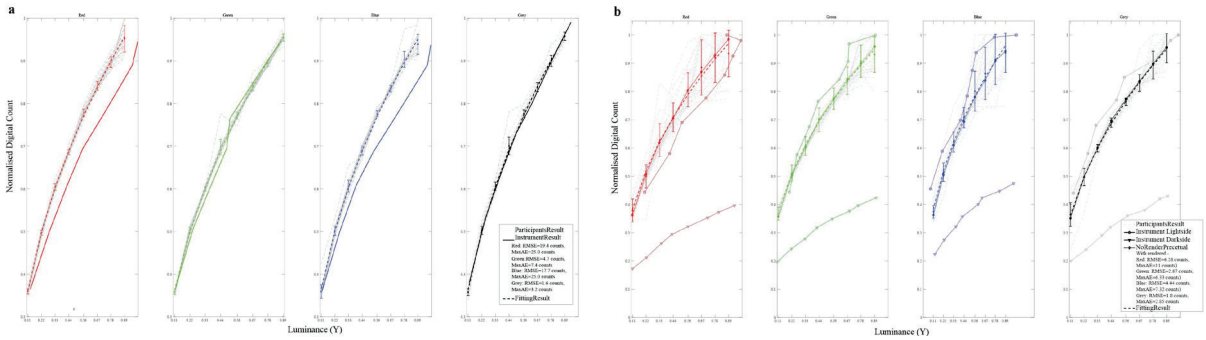

Figure 2: Unrendered (a) and rendered (b) scenes -- Perceived luminance matching results and instrumental results

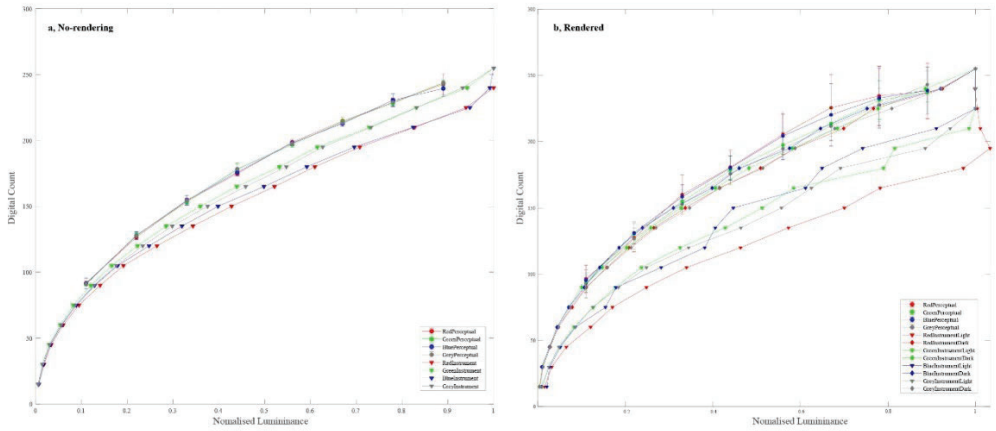

Figure 3: Psychophysical and colorimetric results of no-rendering and rendered sense

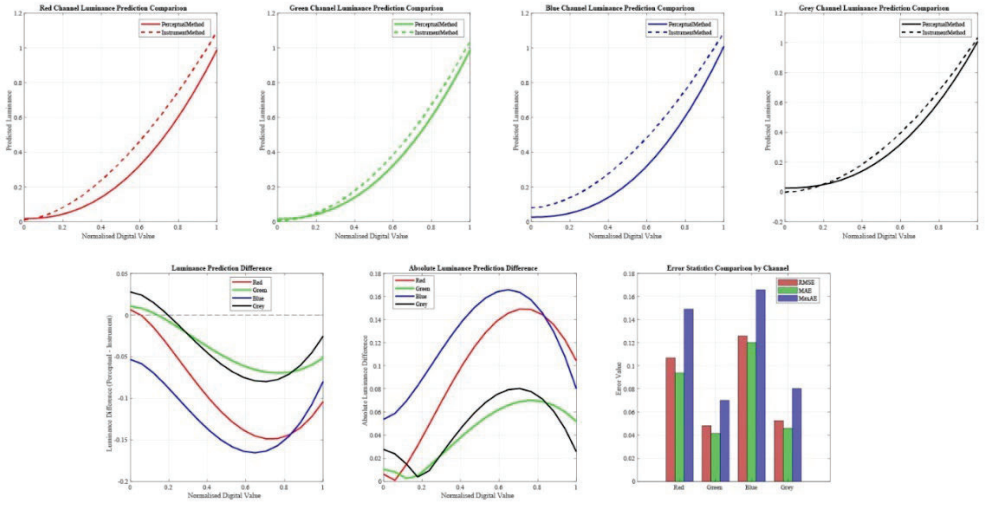

Figure 4: Using PLCC for luminance (Y) prediction comparisons between perceived data and instrument data

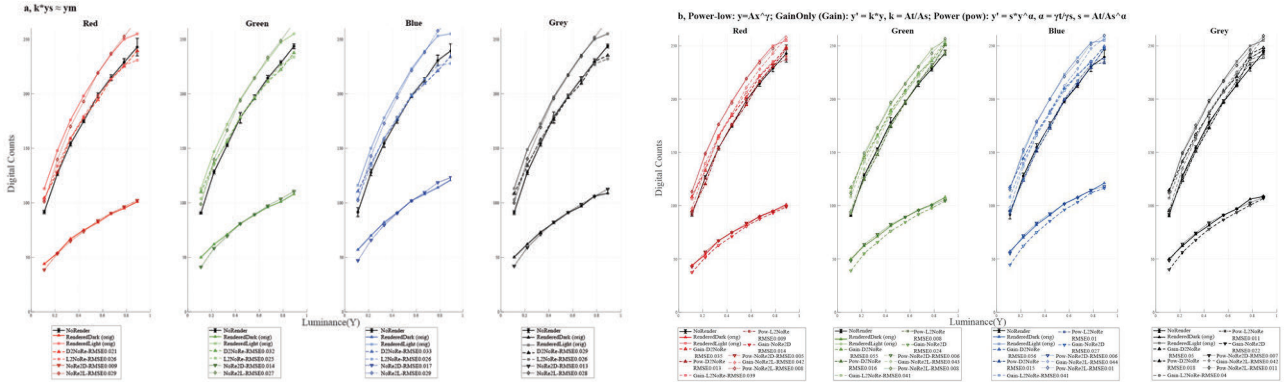

Figure 5: Verification of unrendered and rendered scene luminance predictions

CONCLUSION

Perception-based calibration showed more stable and transferable across scenes, geometries, and channels in MR. A practical route emerges is doing the no-render perceptual mapping first, then transport it to rendered scenes via the per-channel bright (or dark) walls luminance, with a power-law transform providing the lowest errors. These findings support perceptually informed tools (grey-based prediction with channel weighting) as a viable basis for reproducible MR characterisation and calibration.

ACKNOWLEDGEMENTS

We gratefully acknowledge the Society of Dyers and Colourists (SDC) for supporting participant compensation for this study.

REFERENCES

[1]. Xiao, K., Fu, C., Karatzas, D., and Wuerger, S. (2011). Visual gamma correction for LCD displays. *Displays*, *32*(1), 17–23.

[2]. Díaz Barrancas, F., Gil Rodríguez, R., Aizenman, A., Bayer, F. S., and Gegenfurtner, K. R. (2023). Color Calibration in Virtual Reality Using Different Head Mounted Displays. *Journal of Vision*, *23*(9), 5257.

[3]. Gil Rodríguez, R., Hedjar, L., Toscani, M., Guarnera, D., Guarnera, G. C., and Gegenfurtner, K. R. (2024). Color constancy mechanisms in virtual reality environments. *Journal of Vision*, *24*(5), 6.

[4]. Tanuwidjaja, E., Huynh, D., Koa, K., Nguyen, C., Shao, C., Torbett, P., Emmenegger, C., and Weibel, N. (2014). Chroma: A wearable augmented-reality solution for color blindness. 2014 ACM International Joint Conference on Pervasive and Ubiquitous Computing. New York, United States.

Develop The Chinese Hue-Tone Colour System by Utilising The Chinese Adjective Word System (ANCWS)

Wenwen Song[a], Yifei Chen[b] and Shiyang Zhu[c*]

[a]*Colour&Image Institute, Art&Science Research Centre, Tsinghua University, Beijing, China*

[b] *School of Design, University of Leeds, Leeds, China*

[c] *Colour&Image Institute, Art&Science Research Centre, Tsinghua University, Beijing, China**

**Corresponding author: Shiyang Zhu, zhushiyang@mail.tsinghua.edu.cn*

ABSTRACT

This study explores the association between the uniform colour difference model and human nonlinear emotional cognition. Twelve colour tones and sixteen positive-valence adjectives from the Affective Norms for Chinese Words (ANCW) database were evaluated by twenty professional Chinese designers in a psychophysical rating experiment. Results indicate that perceptual similarity among tones is primarily determined by differences in lightness, rather than chroma or overall colour difference. Certain tone pairs—such as strong/vivid and soft/dull—were perceived as emotionally similar, suggesting potential for simplification within the existing system. Based on these findings, a tentative optimisation of the colour tone structure is proposed. The study provides initial evidence for refining colour systems to better align with the affective perception of Chinese users, while highlighting the need for further validation with broader populations and emotional descriptors.

Keywords: *Hue; Emotion; Affective Words; Colour Psychology; Colour in Art and Design*

INTRODUCTION

Colour not only shapes visual experience but also carries rich emotional meanings, which may vary across cultural contexts. While structured colour systems such as The Practical Colour Coordinate System (PCCS) [1], a set of colour reels, which the colours within are selected from certain hue but varies in lightness and chromaticness between each other in order to achieve colour harmony [2], are widely used in design. The PCCS model aligns colour tones with the emotional perception in Japanese culture background, but whether it is adaptive for Chinese designers has not been fully explored. This study investigates how Chinese affective adjectives relate to variations in PCCS tone, aiming to provide preliminary guidance for culturally informed colour system optimisation.

Colour, Emotion, and Cultural Context

While physiological colour perception is relatively universal [3], emotional reactions to colour show substantial cross-cultural differences [4][5]. Early research into colour-emotion associations focused primarily on Western populations, resulting in standard design frameworks such as the Munsell system and the CIE colour space. However, growing evidence suggests that colour preferences and affective responses are not universal, but instead show significant cross-cultural variability[6][7][8]. In particular, studies on Chinese observers indicate a stronger emphasis on **lightness and chroma**—rather than hue—in both preference and emotional discrimination, and a tendency to favour colours described as “clean,” “fresh,” and “modern” [9].

Scaling Affective Meaning in Language

To objectively assess the emotional meaning of language, multi-dimensional affective word databases have been developed, notably the Chinese Affective Words System (CAWS) [10] and, more recently, the Affective Norms for Chinese Words (ANCW) [11]. These resources use dimensions such as valence, arousal, dominance, and concreteness [12] to quantify the affective connotations of thousands of Chinese words, providing a robust psycholinguistic foundation for linking language and emotion.

Recent studies have begun to investigate direct mappings between affective word ratings and colour palettes, suggesting that culturally-specific affective vocabulary may provide a more sensitive probe into local colour–emotion associations than universalist models [13].

Hue–Tone Systems and Their Limitations

The PCCS (Practical Colour Co-ordinate System), widely used in Japanese and Chinese design education, introduced the concept of "tone" as a practical means of grouping colours with similar lightness and chroma, regardless of precise physical similarity. Although inspired by the Munsell system, the PCCS is adapted for perceptual and design utility rather than for strict scientific uniformity.

However, the emotional distinctiveness and practical utility of these tone groupings, especially for Chinese users, remain under-explored. Existing research rarely tests whether such systems align with affective perception as measured by psychophysical or linguistic tools, nor whether tone boundaries are optimal for local cultural contexts.

Research Gap

Despite the rich development of both colour systems and affective word databases, few studies have systematically investigated how the structure of tone-based colour systems (such as PCCS) aligns with the emotional connotations of colour as perceived by Chinese speakers using language-based affective ratings. The degree to which current tone boundaries reflect actual perceptual and emotional similarity is unclear, potentially limiting the utility of these systems in culturally-relevant design.

Aim & Objectives

This study aims to examine the relationship between Chinese affective adjectives and variations in colour tone (i.e., lightness and chroma under a fixed hue), and to evaluate the suitability of existing tone groupings for capturing perceptual and emotional similarity among Chinese designers with separate three objectives:

1. To assess the degree of alignment between PCCS tone groupings and the affective responses of Chinese design professionals, as measured by language-based emotion ratings.

2. To quantify the relationship between affective similarity (based on psychophysical ratings of colour–word pairs) and the colorimetric differences (ΔL, ΔC, ΔE) among PCCS tone groupings.

3. To propose empirically-informed optimisations to the PCCS tone structure based on the findings, aimed at improving emotional discriminability and practical utility for Chinese design contexts.

METHODOLOGY

Colour Stimulus Preparation

A total of 144 colour samples were prepared, comprising 12 PCCS tone categories (pale, light, bright, vivid, strong, deep, soft, dull, dark, light greyish, greyish, dark greyish), each represented by 12 hues. The spectral reflectance of each colour sample was measured using a Konica Minolta CS600-D spectrophotometer at 10 nm intervals from 400 to 700 nm, under D65 standard illuminant and the CIE 1931 10° standard observer. Reflectance spectra were converted to CIE XYZ tristimulus values via the CIE 1931 colour-matching functions. Colour stimuli were accurately reproduced and displayed on a calibrated sRGB monitor in controlled lighting.

Selection of Affective Words

Affective adjectives were selected from the Affective Norms for Chinese Words (ANCW) database, which contains 4,030 Chinese words rated on four affective dimensions: valence, arousal, dominance, and concreteness. Words with mean ratings above the median for each dimension were filtered, irrespective of part of speech. After manual screening for emotional relevance, 16 positive-valence adjectives were chosen as experimental stimuli (快乐 [happy], 魅力 [charm], 使激动 [excite], 广受欢迎的 [popular], 满足 [satisfy], 感激的 [grateful], 欢乐的 [merry], 纪念的 [memorial], 自豪 [pride], 精力充沛的 [lively], 欢呼 [cheer], 高兴 [pleasure], 愉悦 [joy], 希望 [hope], 欣慰 [glad], 爱 [love], 喜爱 [affection], 快乐 [delight]).

Experimental Procedure

Twelve PCCS colour wheels (one per tone), rendered using the calibrated sRGB values, were presented against a mid-grey background (RGB: 128,128,128) on the calibrated monitor. Each colour wheel was randomly paired with an affective adjective (displayed in simplified Chinese). For each pairing, participants were instructed to rate the degree of association between the colour tone and the given emotion using a 7-point Likert scale (−3 = Completely Disagree, 0 = Neutral, +3 = Completely Agree). Twenty Chinese design professionals (mean age 41.8, 50% female) with normal colour vision completed two rounds of tone–emotion association rating in a controlled lab environment.

All responses were recorded electronically. Inter-observer consistency was assessed using Pearson's correlation coefficient and Cronbach's alpha. Statistical significance was determined at $p < 0.05$. Pairs with Pearson correlation coefficients greater than 0.5 were considered to exhibit a strong degree of perceptual similarity, following the criteria proposed by [14] Cohen's d.

RESULTS AND DISCUSSION

Consistency and Data Quality

Responses from the psychophysical experiment demonstrated strong inter-observer reliability (mean Pearson's $r = 0.67$) and high intra-observer consistency (Cronbach's $\alpha = 0.91$), indicating stable and reproducible affective ratings across participants.

Perceptual Similarity among Tones

Tone similarity analysis (Pearson $r > 0.5$) revealed strong emotional overlap for tone pairs such as strong/vivid and soft/dull (see Fig. 1).

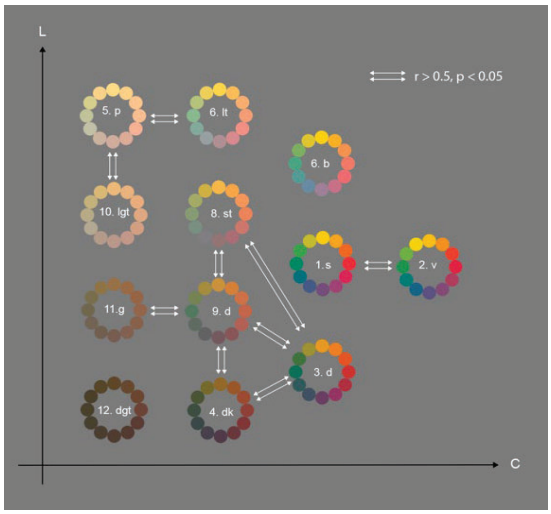

Figure 1: Perceptual similarity among Tones.

Colorimetric Analysis

For each tone pair, differences in lightness (ΔL), chroma (ΔC), and total colour difference (ΔE) were computed using the Hungarian algorithm [15] and CIE1931 colour matching functions. Correlational analyses revealed that perceptual similarity was most strongly associated with differences in lightness ($r_{\Delta L} = -0.28$, $p < 0.01$), whereas chroma ($r_{\Delta C} = -0.19$, $p < 0.05$) and total colour difference ($r_{\Delta E} = -0.03$, ns) were less predictive. Thus, lightness emerged as the principal colorimetric determinant of emotional discrimination among PCCS tones in this sample.

Table 1: Pairs with Significant Perceptual Emotional Similarity

Pair Name	Similarity (r)	Colour Difference		
		Delta E	Delta L	Delta C
1.Strong - 2.Vivid	0.66***	15.57	4.24	7.87
3.Deep - 4.Dark	0.52***	24.70	9.69	21.84
3.Deep - 8.Soft	0.52***	22.58	16.13	9.81
3.Deep - 9. Dull	0.60***	19.49	5.28	16.38
4.Dark - 9.Dull	0.67***	15.76	13.68	6.12
4.Dark - 11.Greyish	0.53***	15.89	8.75	3.94
5.Pale - 6.Light	0.61***	17.69	6.25	11.47
5.Pale - 10.Light Greyish	0.54***	11.27	9.21	4.95
8.Soft - 9.Dull	0.63***	14.67	12.14	6.76
Average	0.59	17.51	9.48	9.91

Implications for Colour Model Optimisation

Feedback from professional designers further corroborated the empirical findings. Tones with minimal lightness differences, such as strong and vivid (ΔL = 4.24), were routinely perceived as emotionally redundant, suggesting they could be merged into a single reel. For high-lightness, low-chroma tones (e.g., pale, light, light greyish), expanding the lightness range within the pale reel may enhance emotional discriminability. Tones with low lightness and moderate chroma (greyish, deep, dark, soft, dull) were found to be affectively indistinguishable by participants, despite substantial colorimetric differences (mean ΔL = 11.38, ΔC = 12.18, ΔE = 19.44, mean r = 0.59). This insensitivity implies that further subdivision in this region is unnecessary.

Proposed Adjusted Model: Chinese Emotional Colour Palette

An optimised Hue–Tone model, **Chinese Emotional Colour Palette (CECP),** was therefore proposed, referencing the Munsell colour system as a perceptual baseline. The four chroma zones of the PCCS were retained, but the strong tone was eliminated from the second-most saturated group. In the second least saturated and darker group, soft and dull tones were merged, reflecting their highest observed emotional similarity (r_soft: dull = 0.63, r_max = 0.67). For the least saturated region (pale, light greyish, greyish, dark greyish), the lightness range was exaggerated, and the reels repositioned to maximise emotional discrimination.

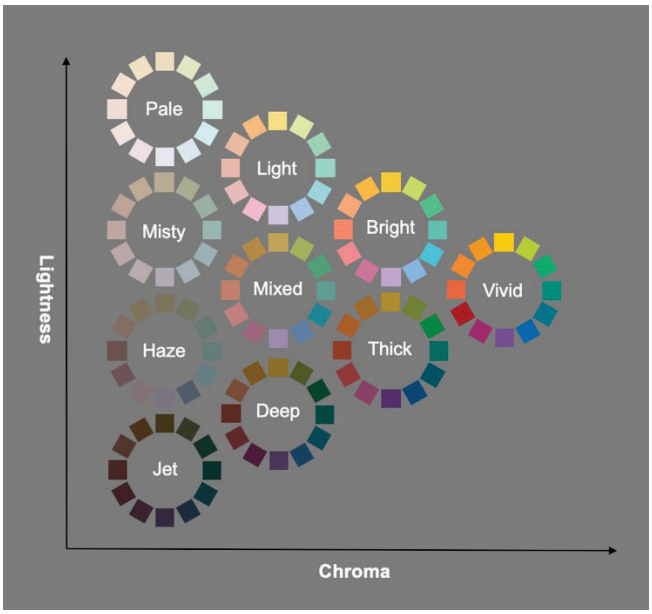

Figure 2: Chinese Emotional Colour Palette.

New colour samples selected from the Munsell Colour Book with PCCS colours mapped within that enhance the perceptual emotional differences according to the correlation between words and colorimetry. The Chinese Emotional Colour Palette is dedicated for practical design application.

CONCLUSION

This study presents an initial exploration of the association between Chinese affective adjectives and variations in colour tone within the PCCS framework, suggesting a new CECP colour model for designers. Results indicate that, for a sample of professional Chinese designers, perceived emotional similarity between tone categories is most

closely related to differences in lightness. Some tone pairs, such as strong/vivid and soft/dull, were found to be affectively similar, suggesting potential for simplification within the current system.

Based on these preliminary findings, we proposed a tentative optimisation of the PCCS colour model, including the merging of emotionally redundant tone pairs and adjustment of lightness intervals in low-chroma regions. Future research is needed to test these proposals with broader populations, a wider range of emotional descriptors, and alternative experimental paradigms. We hope this work can serve as a reference for the ongoing refinement of colour systems to better reflect the perceptual and cultural realities of specific user groups.

REFERENCES

[1]. Wakata, T., & Saito, M. (2013). The impression of hue in practical color co-ordinate system (PCCS).

[2]. Oyama, T. (2001). Color harmony or color-combination effects: From a psychological point of view. *Journal of the color science association of japan*, *25*(4), 283-287.

[3]. Tao, L., Westland, S., & Cheung, V. (2012). Studies of blackness preference and perception. In *Interim Meeting of the International Colour Association International Colour Association* (Vol. 21, pp. 294-297).

[4]. Ou, L. C., Luo, M. R., Woodcock, A., & Wright, A. (2004). A study of colour emotion and colour preference. Part I: Colour emotions for single colours. *Color Research & Application*, *29*(3), 232-240.

[5]. Taylor, C., Clifford, A., & Franklin, A. (2013). Color preferences are not universal. *Journal of Experimental Psychology: General*, *142*(4), 1015.

[6]. Eysenck, H. J. (1941). A critical and experimental study of colour preferences. *The American Journal of Psychology*, *54*(3), 385-394.

[7]. Hogg, J., Goodman, S., Porter, T., Mikellides, B., & Preddy, D. E. (1979). Dimensions and determinants of judgements of colour samples and a simulated interior space by architects and non-architects. *British Journal of Psychology*, *70*(2), 231-242

[8]. Ling, Z., Hurlbert, A., & Robinson, L. (2008). Sex differences in colour preference. In *Progress in colour studies* (pp. 173-188). John Benjamins Publishing Company.

[9]. Ou, L. C., Luo, M. R., Woodcock, A., & Wright, A. (2004). A study of colour emotion and colour preference. part II: colour emotions for two-colour combinations. *Color Research & Application: Endorsed by Inter-Society Color Council, The Colour Group (Great Britain), Canadian Society for Color, Color Science Association of Japan, Dutch Society for the Study of Color, The Swedish Colour Centre Foundation, Colour Society of Australia, Centre Français de la Couleur*, *29*(4), 292-298.

[10]. 王素格, 李德玉, 魏英杰, & 宋晓雷. (2009). *基于同义词的词汇情感倾向判别方法* (Doctoral dissertation).

[11]. Ying, L., Ruyang, Y., Chuanbin, N., Yeqing, W., Qing, L., Yufan, Z., & Fei, G. (2024). ANCW: Affective norms for 4030 Chinese words. *Behavior Research Methods*, *56*(5), 4893-4908.

[12]. Warriner, A. B., Kuperman, V., & Brysbaert, M. (2013). Norms of valence, arousal, and dominance for 13,915 English lemmas. *Behavior research methods*, *45*(4), 1191-1207.

[13]. Dou, Y., Zhang, J., Zhong, Z., Zhu, C., Chen, Z., Zhang, K., & Huang, F. (2024). Layer-by-Layer All-Polymer Solar Cells Approaching 19% with Dual-Donor Modulation of an Interpenetrating Network. *Advanced Energy Materials*, *14*(47), 2402268.

[14]. Diener, M. J. (2010). Cohen's d. *The Corsini encyclopedia of psychology*, 1-1.

[15]. Westland, S., Finlayson, G., Lai, P., Pan, Q., Yang, J., & Chen, Y. (2024). A computational method for predicting color palette discriminability. *Color Research & Application*, *49*(5), 465-473.

The Upper Limit of Lightness to Which The Color Name "Black" Can Be Applied

Ichiro Katayama[a*]

[a]Kindai University, Kinokawa, Japan
[*]Corresponding author: Ichiro Katayama, katayama@waka.kindai.ac.jp

ABSTRACT

A visual evaluation experiment was conducted to investigate the upper limit of lightness to which the color name "black" can be applied. An LCD was used to present test stimuli, with achromatic backgrounds equivalent to N9, N7, and N5. Test stimuli were presented individually at the center of the background, and observers responded with a binary answer indicating whether the appearance of the stimulus corresponded to the color name "black." The experiment was conducted under both lights-off and lights-on conditions in the laboratory. Fourteen university students (male and female) participated as observers, and each evaluated the test stimuli twice. The proportion of "black" responses was calculated for each test stimulus from all observers' responses, and the test stimulus lightness at which this proportion reached 50% was defined as the upper limit of lightness to which the color name "black" can be applied. Results showed minimal effect of laboratory lighting conditions (on/off), with the upper limit of lightness to which the color name "black" can be applied being N4.9, N4.2 (N4.3 under the lights-on condition), and N3.5 for the background of N9, N7, and N5, respectively. These findings indicated that the upper limit of lightness to which the color name "black" can be applied is considerably high. Response times were also longer for test stimuli near the upper limit of lightness.

Keywords: blackness, lightness, color name, response time

INTRODUCTION

Black is commonly used in familiar objects, such as clothing, automobiles, printer ink, and IT equipment, where appearing "blacker" often enhances product value. However, although numerous studies have been conducted on white [1], research on black has been extremely limited [2-4]. As a result, evaluation indices for whiteness and yellowness have existed for a long time, whereas evaluation indices for blackness and grayness have been standardized only very recently [5]. The evaluation indices for blackness and grayness are calculated using identical formulas, with the black evaluation index applied to objects with luminous reflectance generally below 5%. However, the perceptual boundary between black and gray remains unclear. Therefore, in this study, a visual evaluation experiment was conducted to investigate the upper limit of lightness to which the color name "black" can be applied.

VISUAL EVALUATION EXPERIMENT

An LCD (EIZO, CG223W) with its white point adjusted to match the chromaticity of the standard illuminant D65 was used to present test stimuli. Test stimuli were 5 cm squares presented at the center of a 27 cm square background. Observers viewed the test stimuli from a distance of 60 cm, with visual angles of 4.8° and 25.4° for the test stimuli and background, respectively. The background lightness was set to N9, N7, or N5. The area surrounding the background was an achromatic color equivalent to N10, with a luminance of 79.6 cd/m² measured

using a colorimetric luminance meter (Konica Minolta, CS-150). The configuration of the stimulus presentation screen is shown in Figure 1.

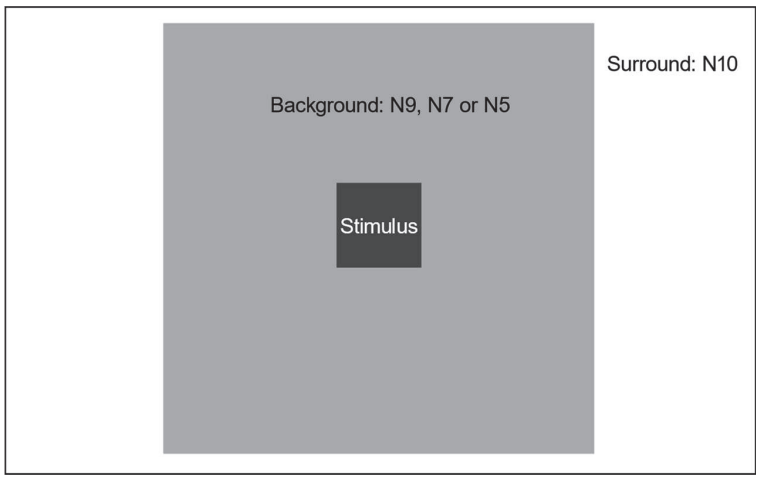

Figure 1: Configuration of the stimulus presentation screen

Test stimuli were achromatic colors set at Munsell Value intervals of 0.2, presented individually at the center of the background in random order starting 1 min after the experiment began. After adapting to the achromatic background for 1 min, observers responded by pressing a button to indicate whether the appearance of the stimulus corresponded to the color name "black." Upon button press, the stimulus disappeared, and another stimulus was presented after 2 s. The time from stimulus presentation to button press was also recorded. Observers evaluated all test stimuli twice.

The visual evaluation experiment was conducted under both lights-off and lights-on conditions in the laboratory. The laboratory lighting consisted of three-band daylight fluorescent lamps, with a correlated color temperature of ~6100K measured using a spectral irradiance meter (Konica Minolta, CL-500A). When the laboratory lighting was on, the illuminance on the desk surface where the LCD was placed was ~400 lx.

Observers were 14 university students (male and female; mean age, 21.1 years) with normal color vision.

RESULTS AND DISCUSSION

For each test stimulus, the proportion of "black" responses was calculated from all observers' responses, and the lightness at which this proportion reached 50% was defined as the upper limit of lightness to which the color name "black" can be applied. The relationship between test stimulus lightness and the proportion of observers responding "black" is shown in Figure 2. The curves represent sigmoid function approximations, with coefficients of determination from 0.976 to 0.995. The relationship between background conditions and the upper limit of lightness to which the color name "black" can be applied is shown in Figure 3. Figures 2 and 3 demonstrate that laboratory lighting conditions (on/off) had minimal effect. The upper limit of lightness to which the color name "black" can be applied was N4.9, N4.2 (N4.3 under the lights-on condition), and N3.5 for the background of N9, N7, and N5, respectively, with corresponding blackness indices M_Y of 73.5, 88.6 (86.3 under the lights-on condition), and 105.6. These results indicated that the upper limit of lightness to which the color name "black" can be applied is considerably high. Furthermore, Figure 3 shows that within the scope of this study, the upper limit of lightness to which the color name "black" can be applied decreases linearly with decreasing background lightness.

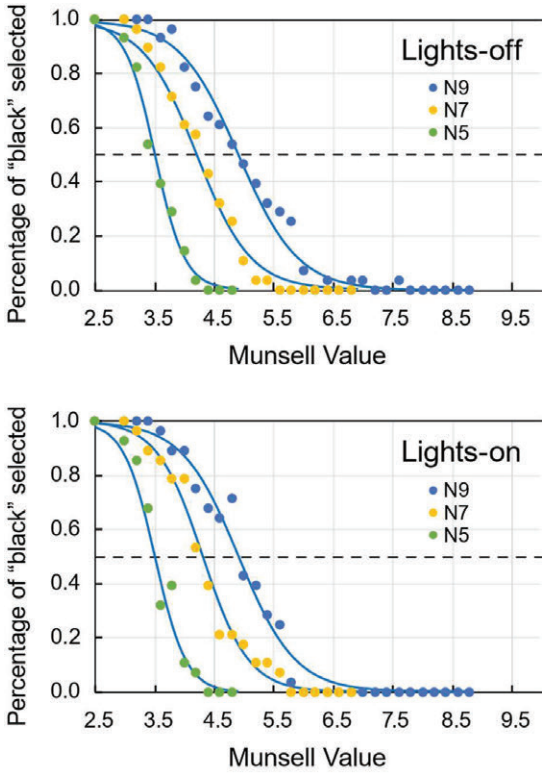

Figure 2: Relationship between test stimulus lightness and the proportion of observers responding "black"

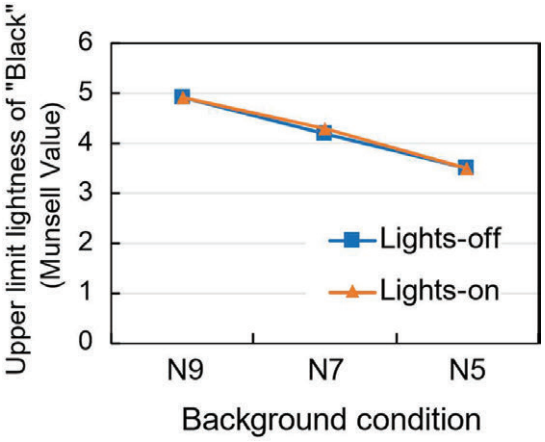

Figure 3: Relationship between background conditions and the upper limit of lightness to which the color name "black" can be applied

Next, the mean response time for observers to answer whether each test stimulus was "black" or not was calculated (Figure 4). The red curves represent cubic function approximations, with coefficients of determination also indicated. The thick vertical lines indicate the background lightness. Figure 4 shows that response times were longer for stimuli at the upper limit of lightness to which the color name "black" can be applied, that is, for stimuli where the judgment of whether something is "black" or not switches.

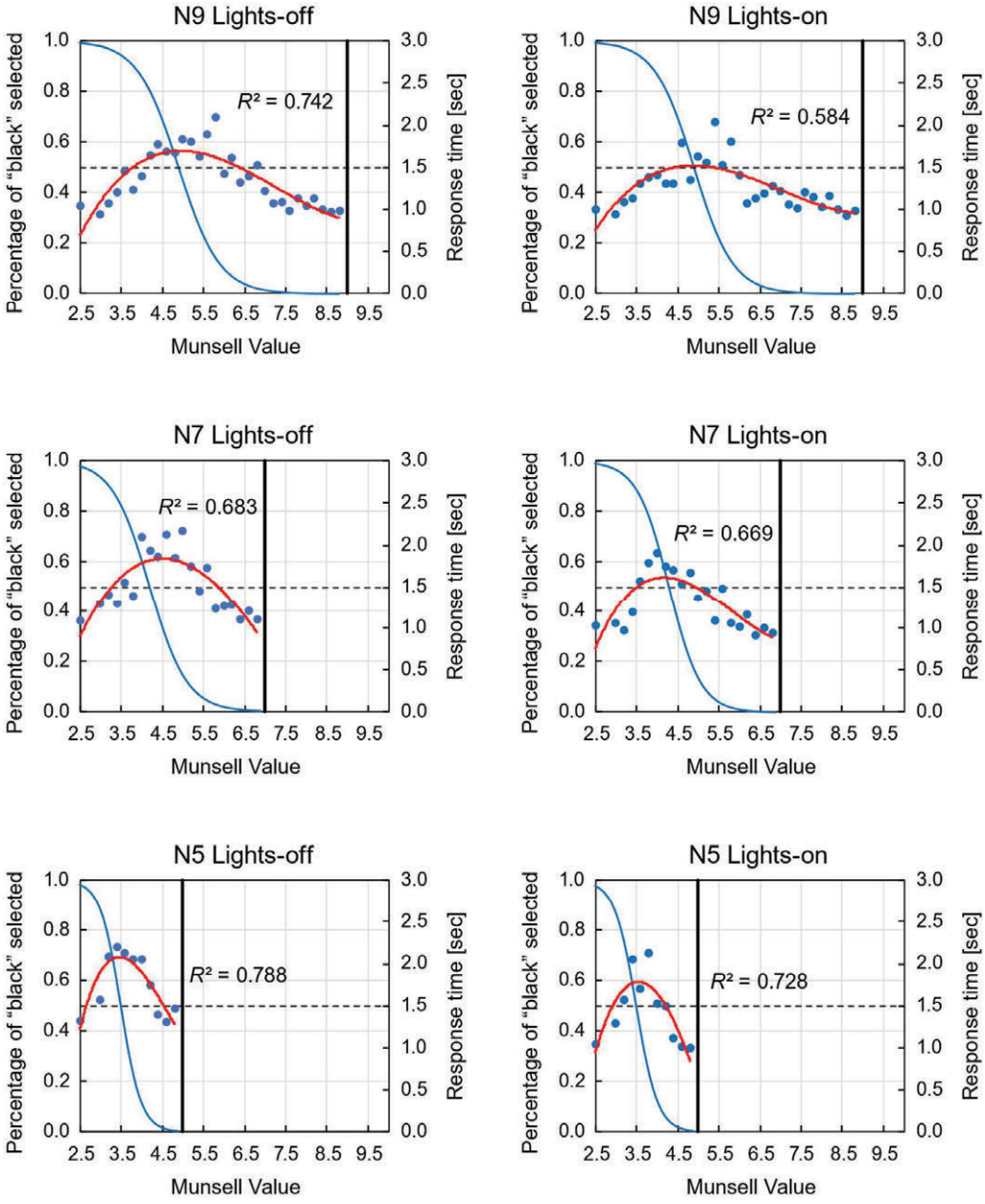

Figure 4: Mean response time for observers to answer whether each test stimulus was "black" or not

CONCLUSION

For achromatic stimuli presented on an LCD, the upper limit of lightness to which the color name "black" can be applied showed minimal effect from laboratory lighting conditions (on/off), with values of N4.9, N4.2 (N4.3 under the lights-on condition), and N3.5 for the background of N9, N7, and N5, respectively, representing considerably high values.

REFERENCES

[1]. Katayama, I. (2019). Performance Comparison of Various Whiteness Formulas Based on Visual Evaluation Experiments. *Journal of Science and Technology in Lighting*, 43, 7-17.

[2]. Westland, S., Cheung, T. L. V., and Lozman, O. R. (2006). A metric for predicting perceptual blackness. *14th Color Imaging Conference Final Program and Proceedings,* 14-17.

[3]. Haslup, J. R. C., Shamey, R., and Hinks, D. (2013). The Effect of Hue on the Perception of Blackness Using Munsell Samples. *Color Research and Application*, 38(6), 423-428.

[4]. Tao, L., Westland, S., and Cheung, V. (2011). Blackness: Preference and Perception. *19th Color Imaging Conference Final Program and Proceedings,* 270-275.

[5]. ISO 18314-3 (2022). Analytical colorimetry- Part 3: Special indices.

Evaluating Perceptual Color Matching Between Different Backlight Displays and Color-Managed Prints

Hong Yu-Kai[a*], Chris Yi-Ho Bai[a]

[a]*Color Technology Lab, BenQ Corp., Taiwan, Taipei.*
[*]*Edward.YK.Hong@BenQ.com*

ABSTRACT

CCFL displays have historically been favored in professional applications for their spectral stability and neutral grayscale performance, while LED technology now dominates the market due to its efficiency and wide color gamut capabilities. However, color-critical workflows still prefer CCFL-like rendering, making it essential to understand the advantages of both technologies. This study investigates the perceptual soft-proofing performance between CCFL-backlight and LED-backlight displays. Two hardware-calibrated displays were measured using a spectrophotometer, and a transformation matrix for LED-backlight displays was derived to simulate CCFL visual output.

This is a continuation study of previous research of generating individual transformation matrix. This experiment involved two separate comparisons in which participants evaluated color similarity, naturalness, and preference between each backlight display and hardcopy printed samples. Eleven test images were used: nine chromatic images (red, green, blue, cyan, magenta, yellow, skin tone, and blended colors) and two grayscale images. Seven professional observers with normal color vision participated in this preliminary study under darkroom conditions with neutral gray surroundings to minimize simultaneous contrast effects.

Both CCFL and LED displays were calibrated to identical targets: Adobe RGB gamut, 150 cd/m² brightness, D50 white point, 0.5 cd/m² black level, and L^* tone response curve. Despite calibration within tolerance limits, participants perceived noticeable differences, attributed to backlight spectral characteristics affecting visual perception. Without transformation, LED displays matched prints more closely for highly saturated reds, yellows, and skin tones, while CCFL displays were rated higher for less saturated colors and grayscale images. Applying the transformation matrix reduced the perceptual differences, with mean ΔE_{00} below 1.0, outperforming CIE 2° Standard Observer-based adjustments.

This research fills a gap in evaluating perceptual color matching performance relative to color-managed print outputs, providing practical value for soft-proofing, digital photography, and color-critical design workflows. The findings highlight LED displays' strengths in saturated color rendering and areas for improvement in neutral and low-chroma reproduction. In addition to the matrix-based approach, the study provides a foundation for future enhancements in backlight-aware display profiling, perceptual color modeling, and cross-media consistency. Future work will explore advanced methods, including chromatic adaptation matrix adjustments, ICC profile tag modifications, 3D LUT-based mapping, spectral compensation algorithms, and integration of updated color appearance models such as CIECAM16, as well as the application of personalized color matching functions in iccMAX, to further reduce perceptual gaps between LED and CCFL displays.

Keywords: CCFL-backlight, LED-backlight, color management, perceptual color evaluation

INTRODUCTION

CCFL displays have long been considered the benchmark in color-critical workflows due to their stable spectral characteristics and neutral grayscale performance [1]. In contrast, LED-backlight displays have become the mainstream choice because of their superior energy efficiency, slim design, and wide color gamut capabilities [2]. However, the spectral differences between these two backlight technologies can lead to noticeable perceptual differences, even when both are calibrated to the same targets [3].

Many color-critical workflows, such as soft proofing, digital photography, and prepress color management, still rely on CCFL-like rendering to ensure accurate color reproduction across media [4]. Previous research has investigated the spectral and colorimetric differences between CCFL and LED displays [2], but limited work has been done to quantify their perceptual soft-proofing performance relative to printed outputs in a structured psychophysical experiment. Given the growing prevalence of LED displays in professional environments, it is important to address their perceptual shortcomings and develop methods to align their output with CCFL reference standards.

Furthermore, studies on individual differences in color matching and observer variability have revealed that standard colorimetric methods may fail to capture the full range of perceptual responses in soft-proofing environments [8][9]. As color perception is highly dependent on viewing context and individual visual physiology, recent ICC standards such as iccMAX provide a more flexible framework for incorporating customized observer models.

In professional color workflows, perceptual accuracy requires more than matching tristimulus values; it demands alignment with the observer's visual response.

The SPD of CCFL and LED backlights differ significantly—CCFL typically has broader, smoother spectral peaks, while LED backlights exhibit narrow-band emissions, particularly in blue and green channels [2]. These spectral differences influence cone responses and, consequently, the perceived color, even when displays are calibrated to the same colorimetric targets. Such metameric mismatches can be especially critical in soft-proofing applications where subtle tonal distinctions are essential.

Standards such as ISO 12646 and ISO 3664 [10] define baseline conditions for visual evaluation, yet real-world perception often deviates due to spectral mismatches. Color appearance models, such as CIECAM02 and the more recent CIECAM16 [6], extend beyond colorimetry by incorporating viewing conditions, adaptation states, and perceptual correlates like brightness and colorfulness.

The objective of this study is threefold: (1) to evaluate the perceptual differences between CCFL and LED-backlight displays when compared against color-managed print samples, (2) to derive a transformation matrix that allows LED displays to simulate the perceptual output of CCFL displays, and (3) to assess the effectiveness of this matrix in reducing perceptual color differences, particularly in the context of soft-proofing workflows.

METHODOLOGY

Experiment 1 Psychophysical Experiment

A controlled psychophysical experiment was conducted to compare the perceptual performance of CCFL-backlight and LED-backlight displays against printed reference samples. Two professional-grade displays—one CCFL and one LED—were hardware-calibrated to identical settings: Adobe RGB color gamut, 150 cd/m² luminance, D50 white point, 0.5 cd/m² black level, and an L^* Gamma Curve [1]. Calibration was performed using a spectrophotometer [7].

The experiment took place in a standardized darkroom with neutral gray surroundings, complying with ISO 3664 viewing conditions. Nine test images were used: six chromatic images (red, green, blue, cyan, magenta, yellow) and three grayscale images. These were prepared in a fully color-managed workflow and printed using a

professional grade inkjet printer configured with an ICC profile conforming to ISO 12647 printing standards [8]. Paper white was also measured.

Seven observers with professional backgrounds in color evaluation and verified normal color vision [9] participated. Each observer evaluated both display types against the printed references separately, providing ratings on three perceptual attributes: color similarity, saturation, and preference. The purpose of this psychophysical experiment was to assess how CCFL and LED displays compared to printed samples in terms of these perceptual attributes.

Figure 1: Psychophysical Experiment

Figure 2: Test images used in Experiment 1

Experiment 2 Validation Experiment

Building on the results of Experiment 1, the spectral measurements of the CCFL display were obtained using a spectrophotometer and used to derive a transformation matrix [10], which was subsequently applied to the LED display. For validation, the ISO-14861 procedure was adopted. Chromaticity coordinates of the ISO-14861 test chart, consisting of 72 color patches including paper white, were measured for both displays and the printed reference samples using a spectrophotometer [7]. The LED display was measured under two conditions—with and without the transformation matrix applied—while the CCFL display was evaluated under its original calibrated settings.

Perceptual differences were quantified by calculating ΔE_{00} values [5] between each display condition and the printed references. Following ISO-14861 thresholds, the validation focused on mean and maximum ΔE_{00} values across all 72 patches and the grayscale subset (mean ≤ 4.0, maximum ≤ 6.5, grayscale ≤ 3.0). Three conditions were compared: (1) CCFL, (2) LED, and (3) LED with the transform matrix, all simulated using Photoshop's soft-proofing function. This ensured that the validation reflected both the ISO-14861 thresholds and the practical workflow commonly used in soft-proofing applications.

Figure 3: ISO-14861 Test Chart

RESULTS AND DISCUSSION

Results confirmed that, despite identical calibration settings, CCFL and LED-backlight displays exhibited distinct perceptual differences when compared to printed samples. As shown in Table 1, CCFL consistently achieved higher similarity scores to the prints than LED display, particularly in grayscale and low-chroma regions. In terms of saturation, LED often appeared more vivid than the prints, while CCFL maintained closer alignment. Preference ratings indicated that observers tended to favor CCFL over LED in most cases, suggesting that its smoother spectral distribution provided a closer perceptual match to printed samples. This overall consistency of CCFL is aligned with its more uniform spectral characteristics [6].

Table 1: Similarity, saturation, and preference ratings of CCFL and LED-backlight displays compared to printed samples (saturation was not evaluated for grayscale samples 7–9).

	Similarity		Saturation		Preference	
Image No.	CCFL	LED	CCFL	LED	CCFL	LED
#1	0	7	7	0	0	7
#2	3	4	3	4	4	3
#3	5	2	7	0	5	2
#4	6	1	7	0	6	1
#5	1	6	6	1	2	5
#6	1	6	7	0	2	5
#7	7	0			7	0
#8	7	0			7	0
#9	7	0			7	0
Total	37	26	37	5	40	23

For all patches (Table 2), CCFL already met ISO-14861 requirements, while LED alone did not. After applying the transformation matrix, the LED Matrix condition showed clear improvements and achieved compliance with ISO-14861.

For grey patches (Table 3), CCFL again showed the smallest deviations, while LED displayed much larger errors, especially in grayscale rendering. With the matrix applied, the LED Matrix condition substantially reduced these deviations and met the ISO-14861 grayscale requirement.

Direct comparisons between CCFL and LED (Tables 4 and 5) further highlight the effectiveness of the matrix. LED showed notable discrepancies relative to CCFL, while LED Matrix consistently reduced these differences to within acceptable limits.

Overall, these results demonstrate that the derived matrix correction effectively reduced perceptual differences across both chromatic and achromatic conditions. Evaluations carried out through Photoshop's soft-proofing function confirm that LED Matrix not only satisfied ISO-14861 requirements but also converged to CCFL in perceptual performance.

These findings are consistent with earlier work suggesting that matrix-based transformations can successfully compensate for spectral mismatches between different backlight technologies. They further reinforce that spectral adaptation is critical for achieving perceptual equivalence in soft-proofing workflows [4]. Nevertheless, residual deviations were observed for highly saturated reds and yellows, indicating that additional refinements, such as LUT-based corrections or spectral compensation algorithms, may be required to achieve uniform improvements across all color regions [6][7].

Table 2: ISO-14861 Validation: Color Differences (All Patches)

	CCFL	LED	LED Matrix
Mean ΔE_{00}	2.72	3.79	3.16
Maximum ΔE_{00}	5.81	6.81	6.46

Table 3: ISO-14861 Validation: Color Differences (Grey Patches)

	CCFL	LED	LED Matrix
Mean ΔE_{00}	1.03	3.22	1.38
Maximum ΔE_{00}	1.98	5.19	2.98

Table 4: ISO-14861 Validation: Color Differences (All Patches, CCFL vs. LED and LED Matrix)

	LED	LED Matrix
Mean ΔE_{00}	3.58	1.69
Maximum ΔE_{00}	8.10	5.74

Table 5: ISO-14861 Validation: Color Differences (Grey Patches, CCFL vs. LED and LED Matrix)

	LED	LED Matrix
Mean ΔE_{00}	3.62	1.50
Maximum ΔE_{00}	5.57	2.58

CONCLUSION

This study demonstrates that applying the ISO-14861 validation method provides a robust framework for evaluating display-to-print consistency. Both the CCFL and the LED Matrix condition fulfilled ISO-14861 thresholds (mean $\Delta E_{00} \leq 4.0$, maximum $\Delta E_{00} \leq 6.5$, grayscale $\Delta E_{00} \leq 3.0$), while the uncorrected LED did not. Through Photoshop's soft-proofing function, the tailored transformation matrix was shown to effectively align LED-backlight display performance with that of the CCFL reference, confirming its ability to reduce perceptual discrepancies and enhance soft-proofing reliability.

These results highlight two key conclusions: (1) CCFL and LED-backlight displays, even under identical calibration, produce different perceptual outcomes due to their spectral characteristics; and (2) matrix-based corrections tailored to backlight type can bring LED displays to a perceptual performance level comparable to CCFL, offering a practical and effective path forward for soft-proofing applications.

ACKNOWLEDGEMENTS

The authors would like to thank the participating observers for their time and expertise in the psychophysical evaluations. Special thanks are extended to the Color Technology Lab at BenQ Corp. for providing the technical resources, calibration equipment, and experimental facilities. The authors also acknowledge the valuable input from colleagues in the display and printing industry, whose feedback helped refine the experimental design and analysis.

The authors would especially like to thank Dr. Chris Bai for his continued guidance and insightful suggestions throughout the development of this research. His leadership and domain expertise greatly contributed to the successful execution and direction of this project.

REFERENCES

[1]. Fairchild, M. D. (1999). Measuring and modeling image quality. Chester F. Carlson Center for Imaging Science.

[2]. Braun, K. M., & Fairchild, M. D. (2000). Psychophysical generation of matching images for cross-media color reproduction. Journal of the Society for Information Display, 8(1), 33–44.

[3]. Engeldrum, P. G. (2000). Psychometric scaling: A toolkit for imaging systems development. Imcotek Press.

[4]. Yendrikhovskij, S. N., Blommaert, F. J. J., & de Ridder, H. (1999). Colour reproduction and the naturalness constraint. Color Research and Application, 24(1), 52–67.

[5]. Ruderman, R. D., Cronin, T. W., & Chiao, C.-C. (1998). Statistics of cone responses to natural images: Implications for visual coding. Journal of the Optical Society of America A, 15(8), 2036–2045.

[6]. Shibata, T., Ohno, Y., & Ito, H. (2013). Visual characteristics of afterimage under dark surround conditions. Journal of the Society of Photographic Science and Technology of Japan, 76(3), 247–252.

[7]. Yano, K., & Ohno, Y. (2020). Spectral optimization of white LED based on mesopic luminance and color gamut volume for dim lighting conditions. Color and Imaging Conference, 28(1), 107–112.

[8]. Calabria, A. J., & Fairchild, M. D. (2003). Empirical modelling of perceived contrast and observer preference data. Journal of Imaging Science and Technology, 47(6), 494–508.

[9]. Evans, R. M. (1959). Eye, film, and camera in color photography. Wiley.

[10]. Hong, Y.K., & Bai, Y.H. (2025). Investigating soft-proofing performance using individual color matching functions. In Proceedings of the 33rd Color and Imaging Conference (CIC33).

Color Reproduction Under Non-Standard Lighting Conditions

Eric Kirchner[a*], Lan Njo[b], Ivo van der Lans[b], Esther Perales[c] and Aurora Navarro Larrosa[c]

[a]College of Optical Science and Engineering, Zhejiang University, *Hangzhou, China*
[b]AkzoNobel Paints & Coatings R&D, *Sassanheim, the Netherlands*
[c]Department of Optics, Pharmacology and Anatomy, University of Alicante, *Alicante, Spain*
[*]*Corresponding author:eric.kirchner9@gmail.com*

ABSTRACT

We investigate color reproduction accuracy on a digital display (iPad Air 2). We matched the light spectrum for five different common lighting situations, not being standardized D65, and reproduced these inside a spectrally tunable light booth. In a visual experiment observers scored the visual color match between physical samples and displayed images calculated by four different methods. The results confirm that when using standardized sRGB color space without accounting for neither the spectrum of ambient light nor chromatic adaptation, poor color reproduction accuracy is obtained. Reproduction accuracy increases by accounting for the illuminant spectrum and for chromatic adaptation using the Von Kries method. The largest improvement in color reproduction accuracy is found when accounting for (1) the spectral power distribution of the ambient lighting, (2) specific display characteristics and (3) the illuminance level of ambient light. This last method achieves color reproduction accuracy similar to experiments under standardized illumination (D65) conditions.

Keywords: color visualization, digital, illumination, adaptation

INTRODUCTION

It is increasingly important that customers can estimate the physical color of products based on images they view on websites. Since most customers have neither the time, tools nor expertise to color calibrate displays, there is a need to improve accuracy of digital color reproduction. Therefore we introduced the Mobile Display Characterization and Illuminance Model (MDCIM) [1]. It accounts for colorimetric properties of specific displays as well as the illuminance level of lighting. So far, we only applied the MDCIM model to lighting conditions with standardized daylight conditions. In the current paper, we extend this to non-standardized illumination spectra.

The goal of this investigation is to optimize digital images such that when shown on a digital display they best match the color of physical samples, when the samples are viewed under non-standardized light conditions. Earlier investigations focused on the role of chromatic adaptation in this optimization process. Chromatic Adaptation Transforms were designed to reproduce appearance as seen by an observer fully adapted to an original viewing condition, after that observer is fully adapted to a second viewing condition [2]. The simplest form of a CAT is the Von Kries transform, which assumes linear scaling of cone responses. More recent CATs such as the Bradford matrix have been shown to perform only slightly better than the Von Kries transform [3][4].

In the present paper we investigate mathematically optimizing the color of a digital image such that when shown on a display it best matches the color of a physical sample viewed under light conditions different from standardized daylight (D65). In visual experiments observers use rapid successive binocular observations to visually compare the physical sample as viewed under particular lighting condition with the digital image on the display.

Earlier research assumed that chromatic adaptation plays a key role. But since in this type of experiment the assumption of full chromatic adaptation to the second viewing conditions (that is made when deriving CATs) is not valid, the concepts of incomplete and mixed adaptation had to be introduced. This involves many adjustable model parameters that critically depend on the details of the observation conditions. It limits the usefulness of applying these models to practical situations, such as general users comparing products that they ordered with their image on a website. The aim of the current paper is to develop a simpler quantitative method that achieves good color reproduction accuracy for non-standard illumination conditions.

METHODOLOGY

We tested four different theoretical approaches:

- **sRGB(D65):** Product images on websites usually assume natural daylight by utilizing standard sRGB color space [5] combined with tristimulus values calculated for standardized daylight D65 illuminant. A standard matrix M is used to convert these tristimulus values to linearized parameters, after which the GOG model with standard parameter values is used to convert to the final nonlinear parameters (R, G, B).
- **sRGB(spectral):** Follows same procedure as for sRGB(D65), but it uses tristimulus values not based on standard D65 spectrum but based on spectral illuminance data measured for particular lighting conditions.
- **Von Kries(D65-to-spectral adaptation)**: Tristimulus values for D65 lighting are transformed with a matrix A to cone responses for D65 lighting. These are scaled to post-adaptation cone signals by linear multiplication factors ($L_{n,adapting}/L_{n,D65}$, $M_{n,adapting}/M_{n,D65}$, $S_{n,adapting}/S_{n,D65}$) where (L_n, M_n, S_n) are the cone responses of a reference white sample under specified illumination conditions as measured. Using the inverse of matrix A we convert back to spectrally adapted tristimulus values, used as for the standard sRGB color space to calculate (R, G, B).
- **MDCIM(spectral)**: Instead of using standardized daylight spectrum (D65) we use measured spectral illuminance data for particular lighting conditions to calculate tristimulus values. These are processed by the normal process of the MDCIM model: convert to linearized parameters by applying a matrix M that depends on specific display properties and on illuminance level of the ambient light [1]. Note that unlike the Von Kries method this method does not take into account adaptation from D65 to specified illumination spectrum, but directly calculates under specified illumination spectrum.

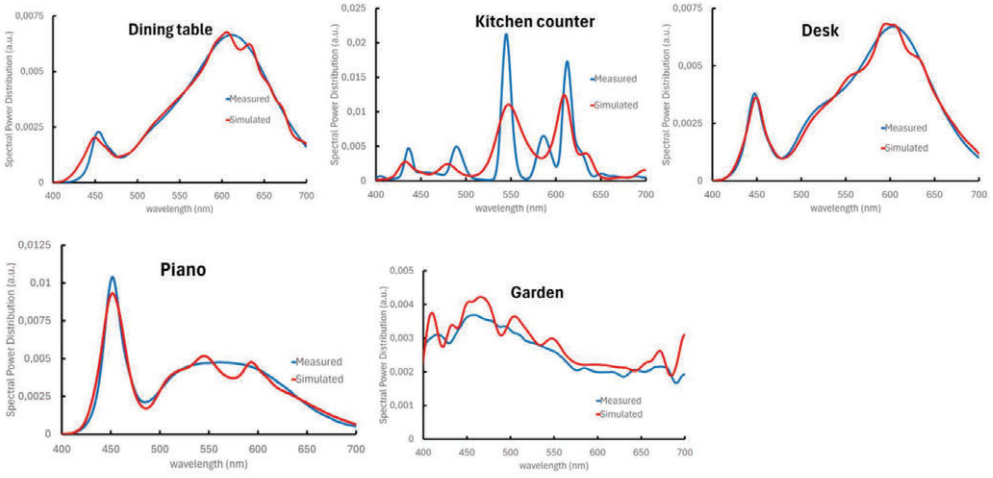

Figure 1: Spectral Power Distributions for five home locations. Blue lines: measurements at the selected locations. Red lines: measurements in light booth after simulating measured spectra with LED lighting.

We used the following experimental methodology. With an illuminance color meter (CL500A, supplier Konica Minolta) we capture the Spectral Power Distribution on five locations in a typical home environment, each with a different type of light source: dining table (warm white LED), kitchen counter (TL fluorescent lighting), desk (a different warm white LED than for dining table), piano lighting (cool white LED) and garden (natural daylight). The measured SPDs are illustrated in Figure 1 (blue lines). We use a spectrally tunable LED light booth to simulate the light spectra measured at the five locations. The LEDView-C23 light booth (Supplier: Thouslite) contains 20 different types of LED in the visible part of the spectrum. We use a least squares fit with software Q_LEDNavigator V3.8.7 (Supplier: Thouslite) to best match measured spectra. The results in Figure 1 (red lines) show good fit quality.

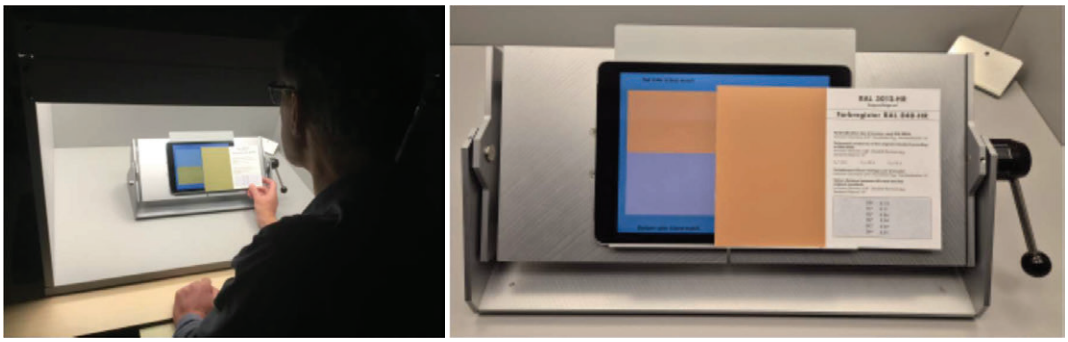

Figure 2: Visual test executed in light booth. The display shows two images calculated using different methods aiming to reproduce the color of the physical RAL sample under specific lighting conditions.

Table 1: Visual scores as used in this test

Visual score	Description
0	No/hardly any difference
1	Small, negligible difference
2	Difference visible, but still reasonable match
3	Difference visible, doubtful match
4	Difference clearly visible, not correct match
5	Large difference, very bad match

Figure 2 shows the visual experiment (for details see [1]). Three observers with normal color vision used a rotation table inside a light booth to ensure physical sample and display are viewed from perpendicular angle. We used the display of an iPad Air 2 with pre-determined model parameters [1]. Observers compared two images (Figure 2b) with the physical sample. Images were calculated using one of the four methods (see Theory section) without the observer knowing which method corresponds to which image. Observers gave a visual score for the quality of the color match with the physical sample, first for the top image, then for the bottom image. Visual scores were quantified using a table (see Table 1) visible to the observers throughout the test.

We collected physical color standard cards for 58 RAL colors roughly covering color space. When representing these colors on a display for given lighting condition and calculation method, in several cases calculated RGB values reached outside the 0-255 range. Since the current investigation aims at optimizing methods to account for different lighting spectra rather than methods to deal with out-of-gamut situations we removed all

out of gamut colors from the visual test. We end up with 27 RAL colors for "dining table" lighting conditions, and 30 (kitchen counter), 32 (desk), 35 (piano) and 41 (garden) for the other lighting conditions.

RESULTS AND DISCUSSION

Average visual scores from all observers and all colors are shown in Table 2. The sRGB(D65) method gives consistently poor results, worse than the values between 3.6 and 4.6 found for the same display when the visual experiment is done under D65 lighting [1]. This is not surprising, since this method does not account for the ambient light spectrum. These results are relevant for practical situations where customers order products on-line using websites with daylight photographs while customers visually assess products under non-daylight conditions.

Table 2: Average visual scores for various lighting conditions and different calculational procedures.

Method	Dining table	Kitchen counter	Desk	Piano	Garden
sRGB(D65)	5.0	5.0	5.0	4.9	4.7
sRGB(spectral)	4.1	3.8	4.2	4.6	4.5
Von Kries (D65-to-spectral)	4.2	4.2	3.6	4.5	4.2
MDCIM(spectral)	2.4	2.0	2.1	2.9	2.6

On average, the Von Kries (D65-to-spectral) and sRGB(spectral) methods give similar reproduction accuracy, both better than sRGB(D65). Best results are found when using the MDCIM(spectrum) method. With the MDCIM(spectral) method the average visual score is between 2.0 and 2.9 depending on light spectrum, similar to earlier results for the MDCIM method for the visual experiment under D65 lighting [1]. This method is therefore well able to discount for non-standard illuminant spectra.

Table 3: Percentage of samples with reasonable or better reproduction accuracy (average visual score < 3).

Method	Dining table	Kitchen counter	Desk	Piano	Garden
sRGB(D65)	0%	0%	0%	0%	0%
sRGB(spectral)	14%	24%	10%	0%	0%
Von Kries (D65-to-spectral)	10%	17%	21%	0%	4%
MDCIM(spectral)	70%	80%	75%	46%	68%

This is further demonstrated by considering cases where the average visual score is equal or worse than a value of 4 ("difference clearly visible; not correct match") as incorrect color matches. The results show that the percentage of incorrectly matching color representations drops from 95-100% to less than 15% when using MDCIM(spectral) instead of sRGB(D65). If we define cases where the average visual score is smaller than 3 ("difference visible, doubtful match") as reasonable (or better) color matches, then Table 3 shows that the percentage of reasonably (or better) matching color representations increases from 0% to 46-80% when using MDCIM(spectral) instead of

sRGB(D65). The results in Table 3 for the MDCIM(spectral) method are similar to earlier results for MDCIM when using D65 lighting [1], again confirming that the MDCIM(spectral) method successfully accounts for the illuminant spectrum.

In all these results the accuracy of the Von Kries (D65-to-spectral) method is better than sRGB(D65), but less good than MDCIM(spectral). This indicates that in the type of experiment chromatic adaptation is not the most important factor when optimizing digital color representations. The best approach to obtain adequate digital color representations is to consistently use ambient spectral power distribution for calculating tristimulus values, as well as accounting for specific display characteristics and illuminance level of ambient light.

CONCLUSION

When using the sRGB(D65) method color reproduction accuracy is very poor for non-standard illumination conditions.

Accuracy increases by choosing one of the following two methods:

(i) accounting for the illuminant spectrum when calculating tristimulus values

(ii) using the Von Kries (D65-to-spectral) method to account for chromatic adaptation (which includes the measured spectrum of the non-standard illumination).

However, we find the largest improvements in color reproduction accuracy by accounting for three factors: (1) the spectral power distribution of ambient lighting, (2) specific display characteristics and (3) the illuminance level of ambient light by using the recently developed MDCIM method. With this last method we achieve a color reproduction accuracy similar to what is found in visual experiments under standardized illumination (D65) conditions.

Future work is needed to quantify the relative importance of the three factors just mentioned, as well as to include more observers.

REFERENCES

[1]. Kirchner, E., van der Lans, I., Martínez-Verdú, F., and Perales E. (2017) Improving color reproduction accuracy of a mobile liquid crystal display, *J Opt Soc Am A* 34, 101-110.

[2]. CIE Technical report (2010) *Chromatic adaptation under mixed illumination condition when comparing softcopy and hardcopy images,* CIE 162:2010.

[3]. Luo, M.R. and Hunt, R.W.G. (1996) *A chromatic adaptation transform and a colour inconstancy index,* Color Res. Appl. 23, 154-158.

[4]. Fairchild, M.D. (2020), *Von Kries 2020: Evolution of degree of chromatic adaptation*, Proceedings of the Color and Imaging Conference 2020, 252-257. https://doi.org/10.2352/issn.2169-2629.2020.28.40

[5]. International Electrotechnical Commission (2003), 100/PT61966(PL) 34 International Standard, *Multimedia systems and equipment– colour measurement and management, part 2.1: default RGB colour space–sRGB* (1999), Amendment 1 (2003).

Influencing Factors of Clothing Colour Preference: A Comparative Study of Beijing and Shanghai Cities

Shuang He[ac*], Vien Cheung[b], Liting Li[c]

[a] *Academy for Advanced interdisciplinary Studies, Beijing Institute of Fashion Technology, Beijing, China*
[b] *School of Design, University of Leeds, Leeds, UK*
[c] *Academy of Arts & Design, Tsinghua University, Beijing, China*
[*] *Corresponding author: Shuang He, sherryhe21@gmail.com*

ABSTRACT

Clothing colour serves as an important reflection of individual aesthetic expression and cultural identity. Preference in clothing colour plays a key role in consumer decision-making, shaped by both internal factors (such as biology and psychology traits) and external influences (including ethnic culture, regional environment, and social background). As two major cultural and economic hubs in China, Beijing and Shanghai offer ideal comparative cases for investigating colour preference given their distinct historical backgrounds, cultural atmospheres, and urban functions. This study adopted a mixed-methods approach, integrating qualitative and quantitative research techniques. Focus group interviews and the Analytic Hierarchy Process (AHP) were used to investigate the factors influencing clothing colour preference among young adults in Beijing and Shanghai. The results showed that young adults in Beijing prioritise practicality and occasion-appropriateness in their clothing colour choices, assigning greater importance to factors such as "colour matching," "special occasions," and "body shape compatibility." In contrast, young adults in Shanghai are more influenced by "educational background," "cultural factors," and "regional environment." Common factors affecting both groups include "personality expression," "weather," and "consumption trends," suggesting cross-regional influences. Overall, this study highlighted the impact of urban and regional differences on clothing colour preferences, offering both theoretical insights and practical implications for clothing brands in colour design and regional market strategies.

Keywords: clothing colour preferences, cultural influence, analytic hierarchy process, influence factor

INTRODUCTION

The values, consumption attitudes, and lifestyles exhibited in the processes of clothing selection, purchase, and use collectively form a cultural phenomenon. Through historical transmission, differentiation, and development, these behaviours reflect the prevailing psychology and lifestyle of a given era [1]. Among the many factors influencing consumer preference in clothing, colour holds particular significance. As one of the most immediate and impactful elements in visual communication [2], colour not only captures attention but also evokes emotional resonance. Colour preference is shaped by a range of influencing factors, including biology [3], ethnic culture [4], historical evolution [5], and age [6], resulting to notable differences among individuals and groups. Therefore, the study of clothing colour preference is not only an exploration of cultural spirit of the present era but also offers insights of individual aesthetic experience and cultural identity.

Beijing and Shanghai, as two of China's most representative cities, are frequently compared in cultural and social research. Beijing, the nation's capital, is geographically located in the north and surrounded by the Yan and

Taihang mountain ranges. It embodies both the solemnity of history legacy and the characteristics of a modern international political centre. However, its deeply politicised history has somewhat overshadowed its identity as a cosmopolitan metropolis. Served as the capital of the Liao, Jin, Yuan, and Qing dynasties, Beijing has long been a multi-ethnic and multi-religious city, embracing Buddhism, Daoism, Islam, and Christianity [7], all of which have contributed to the city's diverse cultural atmosphere. Geographically, Shanghai lies approximately 1,000 kilometres southeast of Beijing. Shanghai, at the confluence of the Yangtze River and the East China Sea, is primarily a flat and coastal city in eastern China. Since the Qing dynasty, Shanghai has become the nation's most prominent intersection of Eastern and Western cultures, cultivating a distinctive Haipai cultural identity that blends Western styles with local traditions [8]. The city's strong commercial orientation and cosmopolitan lifestyle have fostered a unique sense of fashion and cultural character.

In 1983, the China Silk Popular Colour Research Association conducted a survey of 450 Shanghai residents [9], revealing colour preferences at the time favoured dark red (e.g., dark sauce red, purple sauce, wine red), beige-brown (e.g., dark brown, light brown, camel gray, ivory), blue-green, and neutral palette of shades of greys and black-and-white. In 1984, Zeng [10] investigated colour preference among university students in Beijing and identified the order as green, white, blue, red, yellow, orange, purple, black, and grey. Zeng also noted colour preference varies by gender, age, education, and region, and suggested colour preference tend to stabilise after the age of eighteen [10]. More recently, Ji [8] examined cultural differences in clothing consumption across cities such as Beijing and Shanghai. The study found that Beijing consumers most favoured black and red clothing, with green being the least preferred, whereas Shanghai consumers favoured grey, followed by white and black. According to Colour-in-Context Theory [11], the meanings and associations of colours vary depending on cultural and situational contexts, thereby shaping consumer choices. Similarly, Anyanwu and Chiana [12] identified cultural background, social class, family environment, and ethnic identity as four major factors influencing young students' decision making on clothing purchase.

In summary, clothing colour preference serves as an important driver through which young consumers express both self and social identities. As two geographically and culturally distinctive cities, Beijing and Shanghai offer valuable contexts for examining how regional differences and fashion attitudes are reflected in clothing colour choices. Drawing on consumer interviews and the Analytic Hierarchy Process (AHP), this study addresses the following research questions: (1) What are the factors influencing clothing colour preference of young adults in Beijing and Shanghai? (2) What are the similarities and differences in the influencing factors between the two cities? (3) What are the underlying reasons for the similarities or differences?

RESEARCH METHODOLOGY

This study adopted a mixed-methods approach, integrating qualitative and quantitative research techniques. Firstly, high-frequency terms extracted from focus group interview transcripts in Beijing and Shanghai were analysed using the LDA topic model and co-occurrence network analysis to identify key lexical items. The high-frequency terms were then incorporated into the PCS scale [13] to construct primary and secondary factor indicators. Based on these indicators, an AHP matrix was developed. Questionnaires using a nine-point scale were distributed both online and offline to 100 young-adult participants in Beijing and another 100 in Shanghai. Participants were asked to evaluate each pairwise comparison, after which the factor weights were calculated and consistency tests were conducted.

Focus Group Interviews

Participants for the focus groups were recruited through the social networking platform *RED NOTE*. Eligible individuals were either born in Beijing or Shanghai or had resided in the respective city for more than five years. All the participants were between 18 and 30 years old, comprising university students and young professionals, with no restrictions on gender. All of the participants reported normal colour vision and provided informed consent prior to the interviews. The focus group interviews covered three topics:

- **Background information:** education level, family background (parents' occupations), and income level.
- **Lifestyle:** frequented locations, dietary routine, modes of transportation, and leisure activities.
- **Clothing and colour preferences:** preferred clothing styles, brands, colour choices, and perceived factors influencing clothing colour selection.

Figure 1 shows the visual presentation of the focus group scripts using the LDA co-occurrence network analysis. The size of the dots represents the frequency of the keywords, and the thickness of the lines represents the strength of the relationship between the two keywords.

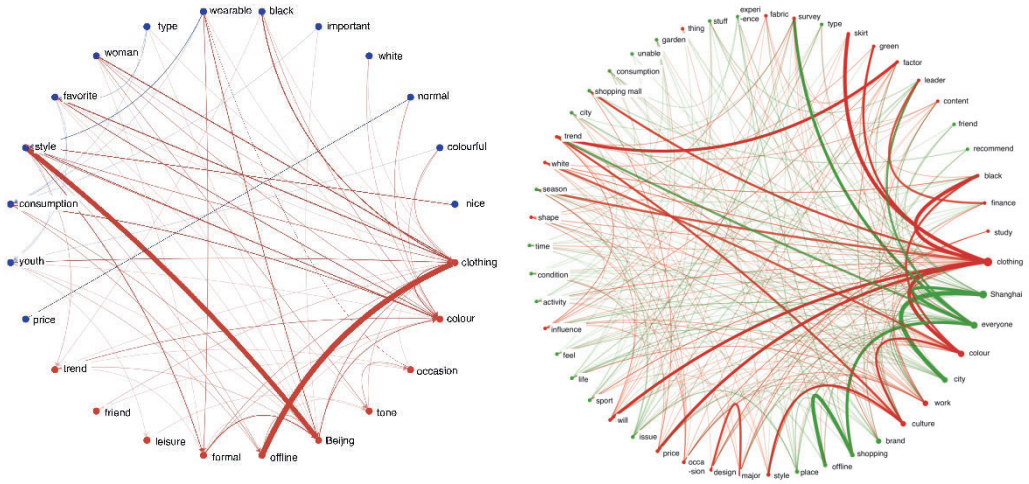

Figure 1: Keyword co-occurrence network of focus group interviews in Beijing (left) and Shanghai (right).

In the Beijing focus group, 7 participants (4 females, 3 males) were included, studying or working in the fields of design, industry, law, and education. LDA analysis showed that female participants played a central role in discussions. Clothing colour consumption among Beijing participants was characterised by a rational approach, often oriented toward professional or social contexts. Consumption was closely linked to formal and leisure activities, with particular emphasis on dress requirements for specific settings. Colour choices were associated with terms such as offline, style, black, white, wearable, and trend. Other terms such as Beijing were frequently co-related with style, formal, colour, and wearable, reflecting a focus on functionality and practicality, while still allowing room for personalised expression. Participants from Beijing showed a preference for *classic* colours that conveyed inclusiveness and diversity. Although offline shopping remained an important channel, clothing choices were centred around activity purposes such as for work, leisure, and formal occasions.

In the Shanghai focus group, 10 participants (8 females, 2 males) were included, studying or working in fields of finance, education, design, game development, and law. Semantic analysis of the transcripts via LDA revealed that their consumption behaviours were highly contextual and diverse. Shanghai consumers emphasised offline shopping, with price, trend, and cultural relevance emerging as key attributes in clothing-related discourse. Their consumption was closely linked to daily routines, sports, cultural activities, and social interactions, thus, indicating their consumption was not only a response to needs but also a reflection of lifestyle practices.

Compared the results from the two cities, the Beijing focus group demonstrated greater stability and situational sensitivity in their clothing colour preference, highlighting practicality and alignment with social roles.

Survey Based on the Proximity of Clothing to Self (PCS) Scale

The Proximity of Clothing to Self (PCS) scale, proposed by Sontag in 1979 [14], is widely used to a individuals' perceptions of the relationship between clothing and self. The PCS scale has been frequently applied in clothing psychology and fashion studies, and its four dimensions include: emotional attachment (the degree of emotional

dependence on clothing), self-expression (the importance of clothing as a tool for self-expression), social recognition (the role of clothing in social identity), and functional value (the practicality and utility of clothing) [15]. In this study, keywords extracted from focus group interviews were integrated into the PCS framework, supplementing its Primary Indicators and Secondary Indicators, and thereby constructing the basis for a questionnaire framework to investigate factors influencing clothing colour preference (see Table 1). The questionnaire was distributed both online and offline to 100 participants in Beijing and 100 in Shanghai, all aged between 18 and 30. A nine-point scale was used, where participants evaluated the relative importance of each primary and secondary indicator in shaping their clothing colour preference. Pairwise comparisons were conducted using scores from 1 to 9, following the AHP approach.

Table 1: Factors Influencing Clothing Colour Preference

Primary Indicators	Secondary Indicators	Secondary Indicators Interpretations
Internal Factors (Self-expression: The importance of clothing as a tool for self-expression)	Body	Skin tone / Hair colour
	Emotion	Sensation / Feeling
	Personality	Identity / Individuality / Confidence / Self-esteem
Colour Attributes (Emotional attachment: The degree of individual dependence on clothing)	Hue	Brightness / Hue / Saturation
	Colour matching	Degree of colour coordination
	Wearing durability	Duration of wearing
External Factors (Functional value: The practicality and utility of clothing)	Weather	Season / Temperature / Climate
	Regional environment	Regional characteristics / Living environment
	Economic income	Personal / Household income
	Educational background	Personal education / Educational environment
Social Dimensions (Social identity: The role of clothing in social identity)	Special occasions	Ceremony / Entertainment / Formal occasions
	Culture	Subculture / Beliefs
	Consumer trends	Consumer trends / Market fashion

RESULTS AND DISCUSSION

Consistency Test

The Eigenvalue of Maximum [16] for the samples from both Beijing and Shanghai was 4.169. The consistency index (CI) values were <0.1 with 0.056 for Beijing and 0.039 for Shanghai. The results indicated that the judgment matrices demonstrated satisfactory consistency and the calculated weights were considered reliable.

Overall Distribution of Weights

At the level of primary indicators, the results showed noticeable differences between the two regions. For participants in Beijing, *Internal Factors* carried a weight of 33.290%, compared with 28.215% in Shanghai (see Table 2). This suggested that young adults in Beijing place greater importance to internal factors—such as body type, emotions, and personality—when making decisions on clothing colour preference, reflecting a stronger reliance on self-perception. In contrast, *Colour Attributes* held a higher weight in Shanghai (34.039%) than in Beijing (30.480%), indicating that young adults in Shanghai are more attuned to the intrinsic properties of colour. The weights of *External Factors* and *Social Dimensions* were similar in both cities, highlighting their shared importance in shaping colour preference.

At the level of secondary indicators, Table 3 shows Beijing participants assigned higher weights on *Colour Matching* (9.102%), *Body* (8.491%), and *Special Occasions* (8.491%). These findings align closely with keywords

identified in the focus group interviews, suggesting a strong orientation towards practicality and situational appropriateness. Conversely, Shanghai participants placed significantly higher emphasis on *Educational Background* (9.450%), *Culture* (9.450%), and *Regional Environment* (8.689%), reflecting the stronger influence of cultural context and educational experience on their clothing colour preference.

When comparing the two cities, both groups assigned similar weights to *Personality*, *Weather*, and *Consumer Trends*, suggesting that these factors function as cross-regional influences within China's metropolitan youth culture. Overall, the findings suggest that young adults in Beijing demonstrated a more pragmatic and occasion-driven approach to clothing colour preference, emphasising functionality and social role alignment. In contrast, young adults in Shanghai showed stronger cultural and educational influences, reflecting the city's international character and multicultural environment. These differences can be attributed to the distinct historical, functional, and cultural contexts of the two cities.

Table 2: Weight Comparison of Primary Indicators between Beijing and Shanghai

Primary Indicators	Weight（Beijing）	Eigenvalue of Maximum	CI Value	Weight（Shanghai）	Eigenvalue of Maximum	CI Value
Internal Factors	33.290%	4.169	0.056	28.215%	4.169	0.039
Colour Attributes	30.480%			34.039%		
External Factors	17.120%			18.892%		
Social Dimension	19.190%			18.854%		

Table 3: Weight Comparison of Secondary Indicators between Beijing and Shanghai

Secondary Indicators	Weight（Beijing）	Weight（Shanghai）	Difference Value
Body	8.491%	6.684%	**1.807%**
Emotion	8.125%	7.464%	0.661%
Personality	7.392%	7.445%	0.053%
Hue	8.369%	6.758%	1.611%
Colour matching	9.102%	6.257%	**2.845%**
Wearing durability	8.002%	7.055%	0.947%
Weather	7.636%	7.909%	0.273%
Regional environment	7.025%	8.689%	1.664%
Economic income	6.414%	7.687%	1.273%
Educational background	5.803%	9.450%	**3.647%**
Special occasions	8.491%	7.427%	1.064%
Culture	7.880%	9.450%	1.570%
Consumer trends	7.269%	7.724%	0.455%

CONCLUSIONS

This study employed focus group interviews and the AHP to investigate the factors influencing clothing colour preference among young adults in Beijing and Shanghai. The main conclusions suggested: (1) Young adults in Beijing prioritise practicality and situational appropriateness. Factors such as colour matching, body fit, and special occasions significantly influence their clothing colour preference. (2) Young adults in Shanghai are more strongly influenced by cultural background and educational experience. Factors such as educational background, cultural orientation, and regional environment play a more prominent role. (3) Mutual factors across both cities include

personality, weather, and consumer trends, reflecting cross-cultural and regional consistencies in fashion psychology among urban Chinese youth. By comparing two representative cities, this study offered both theoretical insights and practical implications for the development of youth-oriented colour planning strategies tailored to different regional markets. However, this study acknowledged the findings are limited by the sample size. Future research will expand the scope with larger sample size and include additional cities with different characteristics to enable broader comparative insights.

ACKNOWLEDGEMENTS

This study was supported by the Interdisciplinary Curriculum Construction Project of Beijing Institute of Fashion Technology (Project Number: NHFZ20250235). The authors would like to express their gratitude to all the participants in this study for their time and input.

REFERENCES

[1] Liu, Y. (2009). Changes in the Consumer Culture of Beijing Clothing. *Textile Journal*, 30(03): 94-98.

[2] Hu, T. (2014). *Principles and Applications of Computer Colour*. Beijing: Tsinghua University Press.

[3] Tong, N., & Kuang, S. B. (2021). Sex differences in the visual system. *Advances in Biochemistry and Biophysics*, (07), 779-787.

[4] Zhang, Z. & Lin, Z. (1993). A study of colour preferences in 3-6 year old Zhuang and Mongolian children. *Psychological Development and Education*, (03), 23-26.

[5] Wang, Y. (1997). An experimental study of colour preferences among Chinese university students. *Psychological Science*, (06), 559-560.

[6] Gong, S-M. & Lee W-Y. (2017). Colour preference model for elder and younger groups. *Journal of the International Colour Association*, (18), 33-42.

[7] Yang Z. (2010). The Urban Character of Beijing. *TongZhouGongJing*, (05), 62-65.

[8] Ji Y. (2013). *Research on the Cultural Differences in Clothing Consumption among Five Major Cities in China*. Shanghai: Donghua University.

[9] Wu Y. (1983). Investigation on the popular colour trends of clothing in Shanghai. *Journal of Textile Research*, (11), 55.

[10] Zeng H. (1986). Characteristics and development of Chinese students' preferences for colours. *Psychological Science Newsletter*, (01), 18-24.

[11] Elliot, A. J., & Maier, M. A. (2012). Colour-in-context theory. *Advances in Experimental Social Psychology*, 45, 61–125.

[12] Anyanwu, E. C., & Chiana, C. A. (2022). Socio-cultural influences on fashion consumption behaviour of university students. *ARRUS Journal of Social Sciences and Humanities*, 2(1), 47-65.

[13] Andrews, F. M., & Withey, S. B. (1976). *Social Indicators of Well-being: Americans' Perceptions of Life Quality*. New York, NY: Plenum Press.

[14] Sontag, M. S. (1979). *Clothing as an indicator of perceived quality of life* (Doctoral dissertation, Michigan State University). Dissertation Abstracts International, (40), 1655B–1656B.

[15] Sontag, M. S., & Lee, J. (2004). Proximity of Clothing to Self Scale. *Clothing and Textiles Research Journal*, 22(4), 161–177.

[16] The SPSSAU project (2024). SPSSAU. (Version 24.0) [Online Application Software]. Retrieved 18th December, 2024, from https://www.spssau.com.

Meanings of Spiritual Experiences Arising from Chromotherapy: A Perspective from Semiotics and Subjectivity as An Alternative Path to Well-Being for The Future

Hernán Felipe Monsalve Ospina

University of Brasilia, Brasilia, Brazil
Casa Arcoíris Foundation NGO, Rionegro, Colombia
hfelipemo@gmail.com

ABSTRACT

This article proposes a conceptual framework for analyzing subjective productions and the meanings of spiritual experiences that arise from the practice of chromotherapy as a well-being alternative for future and as a means of generating reconfigurations in health. A holistic perspective of qualitative research was used, as its integrative approach opens spaces for a new science that constructs new concepts to study the experiences of conscious organisms, including spiritual experiences derived from chromotherapy. The case study is being conducted with 10 individuals who have deeply engaged with chromotherapy, in order to analyze their experiences based on Charles Sanders Peirce's semiotics and Fernando González Rey's Theory of Subjectivity. For this purpose, indicators of subjective meanings have been proposed, grounded in the constructive-interpretative methodology of qualitative epistemology. The research is still ongoing; however, based on document review and the results collected so far, it can be concluded that color generates states of spirituality and altered consciousness that carry meaning for those who experience them, enabling a series of health reconfigurations that range from physical and mental aspects to the ability to relate and to feel that their lives are colorful and purposeful.

Keywords*: chromotherapy, spirituality, semiotics, subjectivity, subjective meanings*

INTRODUCTION

Meanings of spiritual and chromotherapy experiences

Spiritual experiences and integrative or alternative medicine practices, such as chromotherapy, are part of the multiple human experiences through which the subjectivity of the specie is recreated. Human beings, with their capacity to create new realities and intervene in them, naturally and continuously generate various types of phenomena and experiences that go beyond the comprehension of thought. This nourishes the underlying complexity between the subject, their history, and their culture, while also allowing them to generate new subjective meanings about what they live. These meanings are symbolic-emotional units within a historical-cultural perspective (*González Rey, 1996-2019*).

In this line of thought, if we understand that the object of clinical psychology is human experience [1], it can be inferred that spiritual experiences—those that may occur and be generated during and as a result of chromotherapy sessions and the use of color in general—can be studied within the context of clinical psychology

and culture. This approach seeks to identify the meanings, symbols, and significance[1] of these experiences and to deepen their understanding through phenomenological, hermeneutic, and semiotic studies. It is essential that such studies be conducted in an interdisciplinary and holistic manner, as holistic thinking also allows for the appreciation of emotional experience and the recognition that meaning, although a symbolic process, cannot be conceived as the sole concept of analysis. Subjective experience is constructed through semiotic processes involving a wide variety of signs [2].

To understand this variety of signs and meanings, this research is conducted from the semiotic perspective of Peirce and his metaphysical categories, as well as from Fernando González Rey's Theory of Subjectivity. These theoretical approaches allow for the understanding of reality through signs, which may be icons, indices, and symbols in relation to experiences with color.

METHODOLOGY

This study will use a qualitative method and adopt a phenomenological-hermeneutic design with a descriptive-interpretative character, given that "this type of study is highly effective when the goal is to describe a reality in all its main components." [3]. The holistic perspective of qualitative research will also be employed "as its integrative approach opens spaces for a new science that constructs new concepts to study the experiences of conscious organisms. This centrally includes the human spiritual experience." [4]. In this specific case, it allows for the description of the phenomenon of spiritual experiences that may occur during chromotherapy sessions or be generated by chromotherapy itself. A qualitative research method is also chosen because it enables an understanding of both the context and individuals from a holistic perspective, in which people, contexts, or groups are not reduced to variables but are considered as wholes [5].

This research consists of two parts: the first involves a literature review from which a conceptual framework is proposed and presented in this article; the second one, currently in progress, consists of a case study with 10 individuals from Colombia and Brazil (5 from each country) who have had experiences with chromotherapy. Data is being collected through open interviews with the participants and analyzed based on subjective indicators developed using qualitative epistemology and its constructive-interpretative methodology. For the analysis of these indicators, the metaphysical categories proposed by Charles Sanders Peirce (1931–1958) are used as a foundation, since addressing colors across different levels of reality allows for greater scientific rigor and depth in interpretation. The sample has been intentionally selected from individuals who have had chromotherapy experiences, as prior experiences with color serve as the starting point for the theoretical construction intended in this study.

RESULTS AND DISCUSSION

Peirce's Semiotics and Subjective Productions Around Color

Nature itself and everything around us is expressed through color. From the moment we leave the mother's womb, we begin to perceive a wide range of colors from the visible spectrum and to shape our systems of behavior, thought, and understanding of reality. However, reality goes far beyond what is perceptible to the senses and the logic that can be constructed from sensory experience—which, in this case, refers to the experience with colors—

[1] Although in some contexts and depending on the language, 'meaning' is often used with the same sense as 'sense', in this work they will not be treated as synonyms. Meaning will be understood as that which can be attributed by language to an object or phenomenon, whereas sense will be taken to refer to that which belongs to the order of the unsayable and is inscribed within the symbolic universe, where certain traces of sensible and emotional experience may be registered, but which cannot be fully described.

since colors are pure qualities and, at the same time, potentialities. “Color is an example of Firstness; but as a sign, it implies Thirdness, as it conveys a meaning beyond mere sensation.” (C.P 5.424) [6].

Beyond our beliefs and preferences regarding colors, they have the capacity to generate change and significantly impact our lives—from the various sensations evoked by the colors of a sunset, flowers, snow-capped mountains, and the blues of the ocean, to the trance states and altered states of consciousness that can be triggered by different shades of the visible spectrum. The blue of the sky, the red of fire, and the green of the mountains can induce a trance-like state in which notions of time, space, and matter are transformed [7].

Colors: Firstness, Secondness, and Thirdness

According to Peirce, and based on his understanding of reality through signs, it is possible to conceive reality in three distinct realms. The first realm refers to the great variability and diversity of signs present in nature, which relate to the experience of feeling, potentiality, and qualitative aspects—this is known as Firstness. The second realm, or Secondness, refers to individual or concrete phenomena capable of offering resistance to thought, typical of raw events and the capacity to generate effects; these are linked to signs in the form of indices. The third realm, or Thirdness, refers to the universe’s tendency to establish regularities and orders among existing things, allowing for scientific prediction and explanation of phenomena. [8] (as Neubern cited in [7]). This understanding of reality through these categories enables the analysis of the experience of colors not only in the sensory experience of the visible spectrum, but also in the symbolic, emotional, historical, and cultural dimensions.

- Based on the above, beyond the characteristics of each color in the visible spectrum and the wavelengths at which we can perceive them, colors—besides being signs of firstness, that is, of pure quality and potential—also have the capacity to generate countless signs of secondness and thirdness when we interact with their qualities. This includes connecting with emotions such as sadness, euphoria, or fear; expanding our sensations of heat, cold, dryness, or humidity; and even allowing us to understand our sense of life and generate reconfigurations in our health.

- Since experiences with colors are not only inscribed in the bodily dimension, but also in the field of personal subjectivity and the new subjective meanings that can be created from the quality of color—which is fundamentally characterized by its firstness and its ability to generate feelings, images, and reconfigurations in health at the physical, emotional, mental, and spiritual levels—however, “a pure quality, such as the sensation of a color, say red, is something that can be experienced but not defined in terms of something else.” (C.P 5.424) [6].

In this vein, the analysis of subjective production based on the contributions of Professor Mauricio Neubern will be carried out in three stages: In the first stage, focused on the analysis of experiences with chromotherapy and the spiritual experiences that may arise, this will be understood as a moment of firstness, referring to the sensations and feelings that colors can evoke in individuals—this is a stage of sensory experiences; In the second stage, or moment of secondness, references to colors will be taken into account—that is, the effects, impacts, and reactions that people may have in response to them; and he third stage, or moment of thirdness, the meaning and logic that individuals associate with their experiences of color will be explored[2]. For this analysis, the researcher’s constructive and interpretative capacity plays an important role within the framework of subjectivity, since the aim is to identify the vast number of signs that converge in this experience, which will lead to a broader understanding of the phenomenon.

[2] This analysis will be developed based on the teachings and theoretical contributions by Professor Mauricio Neubern, University of Brasília, and his studies on semiotics, complexity, hypnosis, and subjectivity within the CHYS research group (Research Group on Complexity, Hypnosis, and Subjectivity), which he leads and of which I am a member.

Spirituality and the Meaning of Life

Studies on the meanings of spiritual experiences and chromotherapy provide elements to conceive of individuals not only from a productive paradigm, but also from various multidisciplinary approaches that support the preservation of life, well-being, and the holistic health of the human species. This topic opens a wide range of possibilities to counteract discomfort, suffering, and illness, and promotes new areas of action for psychology, integrative practices, and the social and human sciences. Likewise, it represents an alternative path to well-being for both the present and the future—for current generations and those yet to arrive on the planet. For if we understand that "education is the legacy that older generations leave to younger ones", [9], we will recognize that research conducted on color, spirituality, and health will be an advancement and a legacy we can offer to future generations, representing the vast world of possibilities that colors embody, both in their essence and in their generative capacity.

Similarly, the search for meaning in life through spirituality and the contribution of colors enables the construction of community, fosters social well-being, and can help individuals connect with meaningful work, since "human beings, in addition to being rational and emotional, are also spiritual beings in search of meaning and significance in work as a way to develop a communal context" [10]. Thus, understanding these phenomena and their relationship with color could contribute to health recovery processes and provide individuals with tools to understand their illness, rewrite their story, and transform their reality.

To understand the relationship between chromotherapy and spirituality, it is important to first present the conception of spirituality that will be used in this study. Spirituality is understood here as an essential state of connection, a way of life characterized by the feeling of being part of the whole and being connected to all that exists. Through spirituality, one becomes aware of existence itself, experiences transcendence and transpersonality, and finds meaning in life [11]. In this same sense, when spirituality is understood, these experiences are seen as referring to the unique subjective processes related to what the individual considers divine [12] and [13].

Moreover, in this study, spirituality is not understood solely through conceptual definitions mediated by language, but also as human life experiences that cannot always be expressed or described in words. These experiences belong to a suprarational dimension that often escapes rationalist logic—even the context in which these experiences occur. Therefore, it is understood as belonging to the realm of the unspeakable [13], where no single interpretation exists, on the contrary, multiple symbolic interpretations may arise due to the vast variety of signs involved in such experiences.

For example, metaphorically, it is common to hear people say that their life feels gray, that they see no color, that everything is black and white. Conversely, others describe their lives as full of color. Thus, the meanings these experiences hold in our lives not only generate changes in the present but also serve as tools to face daily challenges and adversities. These notions, as expressed by individuals, belong to the emotional and symbolic realms. Therefore, studies in subjectivity will allow for the analysis of these unique references, broaden analytical perspectives, and enable interpretations that value each participant's singular experience. Clinical psychology, in particular, finds in each case study a valuable resource for understanding human complexity.

This interdisciplinary approach represents a highly valuable contribution to the study of the healing properties of colors, which undoubtedly constitute a true treasure for the future and for new scientific approaches in health and human development. It values the singular and subjective experience of individuals in order to understand their logic and meaning—without excluding their history, culture, personal meanings, and spirituality.

Subjective Meanings and Indicators of Color and Spirituality Experiences

Subjective meanings are an inseparable unit of symbolic and emotional processes within a single system, in which the presence of one element evokes the presence of the other, without being absorbed by it [14]. According to *Caires and Patiño* [15], the subjective meanings of a given experience are not limited to that experience alone.

They merge with the subjective meanings of other experiences, which acquire new subjective contours throughout the course of the current experience.

In turn, indicators of subjective meanings are not simply objective or explicit information, and they are not external to either the researcher or the participants in experiences of chromotherapy or spirituality. Instead, they acquire meaning through the researcher's interpretation and have the following characteristics: *1)* They are interpretative and constructive, meaning they are not objective entities but interpretations developed by the researcher based on the information obtained. *2)* They are defined by the relationship between the information, the subject's context, and the researcher's construction-interpretation. *3)* They are dynamic: they evolve and integrate into a continuous process of theoretical construction, feeding new hypotheses and meanings. *4)* They represent connections between different pieces of information, allowing the researcher to uncover hidden or indirect meanings within the empirical material [16].

Table 1: Illustrative Cases of Subjective Meanings in Experiences of Chromotherapy and Spirituality

Subjective Meaning	Semiotics	Subjectivity
* Color and Health Reconfigurations * Spirituality, Colorfulness, and Life Meaning * Color, Relationships, and Social Fabric * Synesthesia and Color Perception * Color, Creativity, and New Possibilities	Stages of Firstness, Secondness, and Thirdness as Related to This Indicator	Assessment of Context, History, and Culture. Identification of Reference Points Based on the Researcher's Constructive-Interpretative Methodology Grounded in the Participant's Experiences.

Source: *developed by the author*

The intention of using qualitative epistemology and a holistic research approach gains greater value and scope when it is understood that "Every clinician, in theory, is a researcher, and that duality of roles has major implications" [7] These implications are of vital importance when analyzing the subjective productions of chromotherapy experiences, since the semiotic analysis and the value attributed to the subject—interwoven with history, context, and culture—enrich the process of constructing interpretations. Indeed, the qualitative research process, like diagnosis or any other type of qualitative construction "is a dynamic process expressed within a progressive continuity that is not exhausted in any of its forms of expression: it involves the very subjects who engage in this process, giving rise to a communicative situation in which relevant indicators may emerge for the construction of knowledge at any given moment of the research process" [17].

CONCLUSIONS

Colors, being pure qualities, have the capacity to generate multiple sensations, emotions, images, and symbols in people's lives. These, in turn, constitute experiences that give rise to new subjective meanings and experiences that go beyond what can be understood through language. Likewise, color—as quality and potential—can induce altered states of consciousness, in which it is common for individuals to encounter spiritual experiences or experiences related to what they perceive as sacred and/or Divine.

Color enables a connection with spirituality and serves as well as a resource for coping with adversity and suffering in human life. The practice of chromotherapy is a possibility-generating practice, rooted in the qualitative richness of colors and their potential to evoke sensory experiences.

In summary, this study delves into everything that color experiences generate in human life, while focusing on the relationship between spirituality and color as a means of fostering well-being and creating new meanings for all that is alive. In this way, the relationship between spirituality and color—along with the qualitative research of

subjectivity based on semiotic analysis—can be approached in the future as a high-potential perspective for generating well-being.

ACKNOWLEDGEMENTS

I would like to thank my husband, Milton David, for being my color co-partner and for the nourishment of his love; Professor Mauricio Neubern for being that good tree whose work guides and inspires us; my friend Bideison Montoya for his loving and detailed collaboration in the translations; Casa Arcoíris Foundation for being our source of inspiration and our banner in this mission; and the Coordenação de Aperfeiçoamento de Pessoal de Nível Superior – Brazil – CAPES No. 23106.000659/2025-40 for funding my doctoral studies.

REFERENCES

[1]. Neubern, M., & Nogueira Gonçalves, H. (2019). Complex hypnosis contributions to Clinical Psychology. En Psicología Clínica e Cultura Contemporânea (págs. 71-90). Brasília: TECHNOPOLITIK

[2]. Colapietro, V. (2014). Peirce e a Abordagem do Self. Uma Perspectiva Semiótica Sobre a Subjetividade Humana. São Paulo: Intermeios.

[3]. Guevara Alban, G., Verdesoto Arguello, A., & Nelly Esther, C. (2020). Metodologías de investigación educativa (descriptivas, experimentales, participativas, y de investigación-acción). RECIMUNDO, 4(3), 163-173. From http://recimundo.com/index.php/es/article/view/860

[4]. Briceño, J., Cañizales, B., Rivas, Y., Lobo, H., Moreno, E., Velásquez, I., & Ruzza, I. (2010). La holística y su articulación con la generación de torías. EDUCERE, 14(48), 73-83.

[5]. Quecedo Lecanda, R., & Castaño Garrido, C. (2003). Introducción a la metodología de investigación cualitativa. PSICODIDÁCTICA(14), 5-40.

[6]. Peirce, C. (1931-1935). Collected Papers of Charles Sanders Peirce. (Vols. 1-6,C). Cambridge, Massachusetts: Harvard University Press (Belknap Press).

[7]. Neubern, M., & Nogueira Gonçalves, H. (2023). 21 Termos para se conceber a pesquisa clínica e qualitativa em hipnose. En Hipnose, Psicoterapia e Pesquisa (págs. 67-89). Curitiba: Juruá.

[8]. Ibri, I. A. (1992). Kósmos Noetós: a Arquitetura Metafísica de Charles S. Peirce. São Paulo: Perspectiva.

[9]. Durkheim, É. (2013). Educación y sociología. Barcelona: Ediciones Península.

[10]. Amorim Silva Filho, A. L., & Ferreira, M. (2015). O Impacto da Espiritualidade no Trabalho Sobre o Bem-Estar Laboral. Psicologia Ciência e Profissão, 35(4), 1171-1187.

[11]. Monsalve Ospina, H., & Orejuela, J. J. (2024). Significados de experiencias espirituales en el mundo organizacional y del trabajo. Teuken Bidikay, 15(24). From https://revistas.elpoli.edu.co/index.php/teu/article/view/2274/2359

[12]. James, W. (1902). The varieties of religious experience: A study in human nature. Nueva York: Longmans, Green & Co. From https://archive.org/details/the-varieties-of-religious-experience_202109

[13]. Neubern, M. (2013). O que significa acolher a espiritualidade do outro? Considerações de uma clínica ethopsy. En Psicologia da religião no mundo ocidental contemporâneo: desafios da interdisciplinaridade (págs. 85-104). Brasília: Universa.

[14]. González Rey, F. (2005). Sujeito e subjetividade: uma aproximação histórico-cultural. São Paulo: Pioneira Thomson Learning.

[15]. Caires de Souza, E., & Patiño Torres, J. (2019). A Teoria da Subjetividade e seus conceitos centrais. Obutchénie. Revista de Didáctica y Psicología Pedagógica, 3(1), 34-57.

[16]. Macedo Pereira, A. B., Gandolfo Conceição, M. I., & Mitjáns Martínez, A. (2016). 13. Epistemología cualitativa de González Rey una forma diferente de análisis de "datos". Revista Tecnia, 1(1).

[17]. González Rey, F. (1997). Epistemología cualitativa y subjetividad. Playa, Cuba: Pueblo y Educación.

Color and Gender in Young Children's Free Drawings: Gender Judgments by Childcare College Students and General College Students

Yukiko Shimada

Department of Child Studies, Faculty of Human Development, Kokugakuin University, Japan
Email address:y-shimada@kokugakuin.ac.jp

ABSTRACT

This study examined the impact of visual elements in young children's free drawings on gender judgments among 1,118 college students, with a particular focus on the differences between students majoring in childcare and those from general college populations. Participants were presented with eight free drawings and asked to identify the gender of the child who created each drawing. The results indicated that the depicted content and objects exerted the strongest influence on gender judgment, whereas color usage was also closely linked to gender stereotypes. Childcare students exhibited greater sensitivity to contextual cues and developmental considerations than did general students. Chi-square analyses revealed significant differences in the reasoning behind gender judgments in Drawings 1 and 7. For Drawing 1, childcare students emphasized the depicted objects and content, whereas general students relied more heavily on the coloring style. For Drawing 7, both groups found it difficult to determine the gender, with a substantial proportion selecting "unknown." These findings suggest that educational background plays a critical role in shaping adults' interpretations of children's creative expression. This study offers novel insights into the intersection of color perception, gender stereotypes, and educational backgrounds, contributing to a deeper understanding of how cultural and developmental contexts influence gender-related interpretations. These results have important implications for promoting inclusive and sex-sensitive practices in early childhood education.

Keywords: young children, color, gender, free drawings, childcare college students, general college students

INTRODUCTION

In Japan, it has traditionally been common for boys to be provided with blue or cool-colored clothing and toys and for girls to be given pink or warm-colored clothing from early childhood. Such color distinctions are deeply rooted in cultural conventions based on children's genders and have been shown to influence the development of gender awareness during early childhood. However, in recent years, there has been a growing tendency to avoid limiting color usage based on gender, and educational settings have begun to explore gender-inclusive approaches to color.

Nevertheless, gender-based color distinctions remain prevalent in kindergartens and nursery schools. For example, some institutions still assign different colors to uniforms depending on the child's gender, such as for art smocks and gymnastic outfits. In art activities, it is also observed that the colors of paints and drawing paper may differ according to gender [1]. These choices may be made intentionally by educators based on the goals and content of the activity, or unconsciously, reflecting ingrained gender-based color stereotypes. A study conducted in Israel revealed that young children identify gender through color and tend to use colors associated with their own gender. In particular, boys showed a strong tendency to avoid colors considered feminine, such as pink [2]. King et al. [3] found that children aged 3–5 years recognize and act according to gender stereotypes, such as boys preferring "masculine" colors and activities. These stereotypes are shaped by cultural and social contexts, particularly the

educational environment. Their study the need for more effective early childhood interventions to promote gender equity [3].

Thus, the use of color in early childhood is strongly shaped by the cultural background, educational practices, and caregiver awareness. Moving forward, it is essential for educators to critically reflect on gender norms and create environments where all children can freely choose and express themselves through color.

METHODOLOGY

A cross-sectional online survey was conducted between July and September 2024 involving 1,118 college students (647 childcare majors and 471 general majors). Participants viewed eight free drawings created using 16-color crayons and judged the gender of the artist who created them. They selected one primary reason for their judgment from seven predefined categories. A chi-square test was used to examine the differences in gender judgment patterns between the two groups. Ethical approval was obtained from the Ethics Committee of Kokugakuin University.

Participants were presented with eight free drawings created by children. For each drawing, participants were asked to identify the gender of the child who created it by selecting one of the following options: “boy,” “girl,” or “unsure.” Participants who selected either “boy” or “girl” were then asked to choose all applicable reasons for their gender judgment from the following options: “Color,” “Depicted objects or content,” “Composition (spatial arrangement),” “Drawing style,” “Coloring method,” “Intuition,” or “Other.”

Eight free drawings with sex-specific characteristics were presented. These drawings exhibit gender-related features in terms of color usage, depicted content, composition, drawing style, and coloring method. This study used eight free-form drawings with concealed gender information（Figure 1)[5].

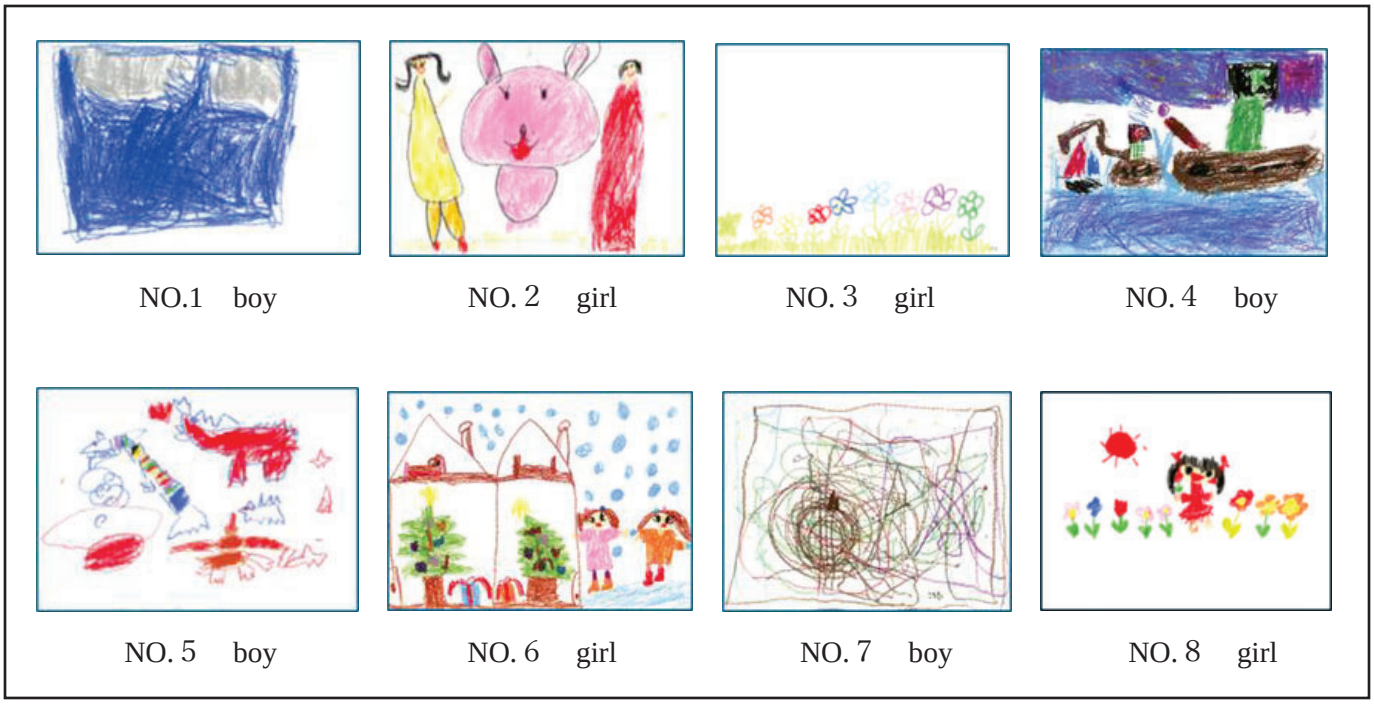

Figure 1: Children's free drawings presented to the college students

RESULTS

Overall, the participants correctly identified the child's gender in seven out of eight drawings, achieving an accuracy rate of over 70%. However, Drawing 7 presents substantial ambiguity, with nearly half of the participants selecting "unknown." (Table 1). A chi-square analysis revealed significant group differences for Drawings 1 (χ^2=22.05, df=4, p<.05) and 7 (χ^2=19.83, df=4, p<.05). Childcare students were more likely to focus on the depicted content. In contrast, general students relied more on the coloring styles. The gender of each child who drew a free drawing was assessed, and the results are shown in Table 1. Over 70% of the participants across all academic disciplines correctly identified the child's gender based on the drawings, except for Drawing 7. Again, except for Drawing 7, students majoring in early childhood education demonstrated a higher rate of accurate gender identification than the general student population (Figure 2).

Table 1: Gender judgments by childcare college students (nursery) and general college students

Major	Judged	No.1	No.2	No.3	No.4	No.5	No.6	No.7	No.8
Nursery	boy	88.6%	1.7%	7.1%	92.0%	81.5%	3.9%	45.4%	1.1%
General		88.3%	1.7%	8.1%	90.0%	81.3%	5.1%	48.6%	1.1%
Nursery	girl	3.4%	95.5%	70.6%	1.5%	5.7%	92.7%	6.3%	95.7%
General		2.3%	94.3%	69.0%	2.1%	3.2%	89.0%	4.7%	92.8%
Nursery	Unknown	8.0%	2.8%	22.3%	6.5%	12.8%	3.4%	48.2%	3.2%
General		9.3%	4.0%	22.9%	7.9%	15.5%	5.9%	46.7%	6.2%

The data point with the higher value between the two is highlighted in yellow.

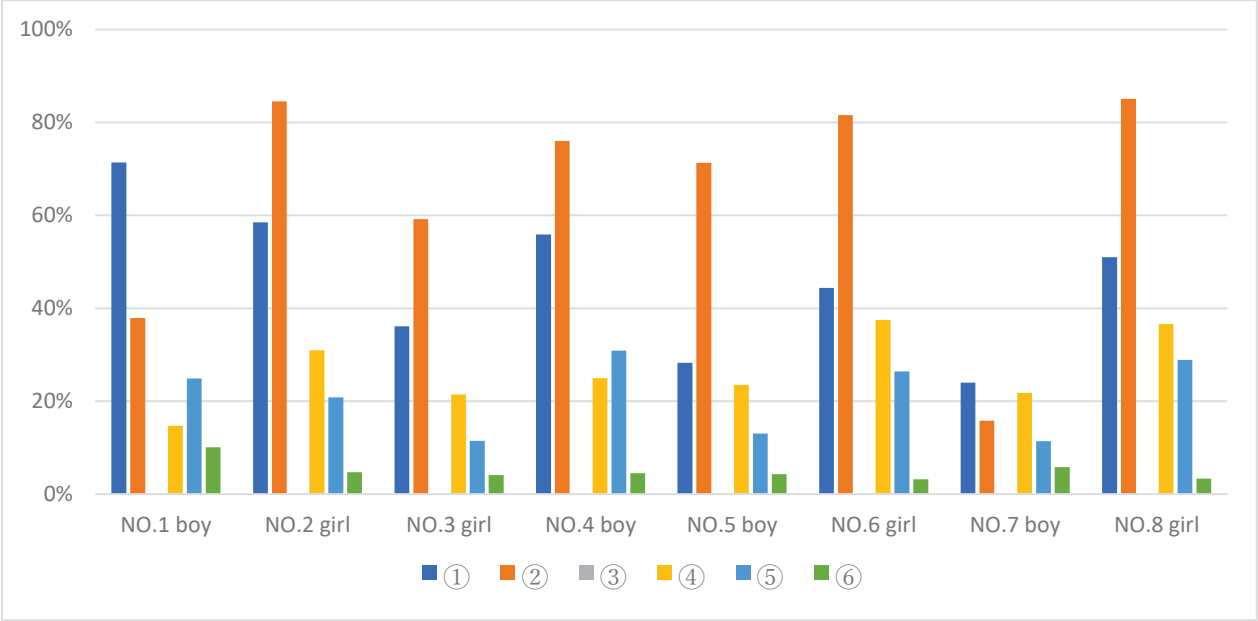

Figure 2: Reasons for gender identification by all participants

DISCUSSION

This study explored how university students perceive gender in their free drawings, focusing on the roles of color and content. In seven of the eight drawings, over 70% of the students correctly identified the child's gender, with early childhood education students showing slightly higher accuracy, likely because of their training and practical experience.

Drawing 7 was notably difficult to interpret, with many students selecting "unknown," suggesting that ambiguous content and color use hindered gender recognition. Differences in reasoning were also observed: Childcare students emphasized drawing content, while general students relied more on color applications, reflecting how educational background shapes interpretation. In early childhood education in Japan, color is closely tied to lived experience [5]. For example, individuals wearing pink associate femininity more strongly than those wearing blue [6]. Cultural traditions such as *Hinamatsuri* and *Tango no Sekku* reinforce gendered color norms [7], and children's experiences of these events may influence both their drawings and how adults interpret them [8]. Additionally, gender differences in emotional language linked to color suggest that color choice may affect gender perception [9]. Biological factors may also play a role in this process. Research in pediatric endocrinology showed that girls with congenital adrenal hyperplasia often prefer the blue color [10], indicating that innate preferences can interact with cultural conditioning. Cross-cultural studies further revealed that children's gendered drawings vary across societies and are shaped by different norms and values (see [4]).

This study highlights the critical role of color, content, and educational background in shaping gender judgments of children's drawings. By clarifying how cultural and developmental factors interact, the findings provide insights into fostering more inclusive early childhood education practices.

CONCLUSION

This study demonstrates that university students rely on both color and drawing content when interpreting the gender of their free drawings. Early childhood education students tended to apply developmental and educational perspectives, whereas general students relied more on visual impressions.

These findings highlight how educational backgrounds and cultural norms influence gender perceptions. They also emphasize the importance of developing art education practices that include gender diversity. Future research should adopt a broader approach that incorporates cultural and biological factors to deepen our understanding of gender expression in children's arts.

Although a deep connection exists between what children choose to depict and the colors they use, accurately assessing the degree of this relationship poses a challenge. This represents a limitation of the current research.

ACKNOWLEDGEMENTS

This study was supported by a grant from the Canon Foundation. I would like to express my sincere gratitude for the generous assistance that made this study possible.

REFERENCES

[1]. Shimada, Y. (2024). Children's plastic expression and caregivers' gender awareness. *Journal of Early Childhood Education and Caregiver Training Studies, 5*, 87-95. https://doi.org/10.60365/jecectet.5.0_87

[2]. Karniol, R. (2011). The color of children's gender stereotypes. *Sex Roles, 65*, 119-132. https://doi.org/10.1007/s11199-011-9989-1

[3]. King, T. L., Scovelle, A. J., Meehl, A., Milner, A. J., & Priest, N. (2021). Gender stereotypes and biases in early childhood: A systematic review. *Australasian Journal of Early Childhood, 46*(2), 112-125. https://doi.org/10.1177/1836939121999849

[4]. Scovelle, A. J., Meehl, A., Milner, A. J., & Priest, N. (2021). Gender stereotypes and biases in early childhood: A systematic review. *Australasian Journal of Early Childhood, 45*(2), 112-125. https://doi.org/10.1177/1836939121999849

[5]. Shimada, Y. (2020). *Characteristics of gender differences in young children's artistic expression* (ID: 10.15068/00160581) [Doctoral dissertation, University of Tsukuba]. https://doi.org/10.15068/00160581

[6]. Farrell, E. (2020). Researching lived experience in education: Misunderstood or missed opportunity? *International Journal of Qualitative Methods, 19*, 1–8. https://doi.org/10.1177/1609406920942066

[7]. Kadoya, A. (2019). Kindergarten practices: Guidance when gender distinctions become overly emphasized. In A. the Gender Equality Committee of Aichi University of Education (Ed.), *Opening the future of gender education* (pp. 18–22). Aichi University of Education Press. https://www.oj.aichi-edu.ac.jp/wp-content/uploads/sites/7/2019/09/4ad9ddf5b33c7a114300a4f8d651337b.pdf

[8]. Hedegaard, M. (2025). Taking children seriously: Their emotional experience, imagination and cognition—A methodological approach. In L. Bøttcher, D. Winther-Lindqvist, M. Hedegaard, & M. Fleer (Eds.), *Sustainability, care, play and the zone of proximal development* (pp. 357–375). Springer. https://doi.org/10.1007/978-3-031-92131-5_17

[9]. Jovanović, V., Adams, S., Aritio-Solana, R., Aryanto, C. B., Avsec, A., Bakhshi, A., Bender, M., Berjot, S., Betancourth Zambrano, S., Brajša-Žganec, A., & Broche-Pérez, Y. (2025). Positive and negative emotional experiences in adolescents across 32 countries: Cross-national and gender differences. *Applied Research in Quality of Life*. https://doi.org/10.1007/s11482-025-10486-2

[10]. Witchel, S. F. (2017). Genetics and pathophysiology of congenital adrenal hyperplasia. In A. Levine (Ed.), *Adrenal disorders* (pp. 109–127). Humana Press. https://doi.org/10.1007/978-3-319-62470-9_5

Towards A New Lighting Method in Museums Considering The Optimal Brightness of Paintings: Practical Classification Process Based on Oil Painting Characteristics

Miyu Aoyama[a]*, Yuki Oe[b], Yoko Mizokami[c], Miho Takashima[d] and Nozomu Yoshizawa[a]

[a]*Tokyo University of Science, Chiba, Japan*
[b]*The University of Shiga Prefecture, Shiga, Japan*
[c]*Chiba University, Chiba, Japan*
[d]*The National Museum of Western Art, Tokyo, Japan*
[*]*Corresponding author: Miyu Aoyama, 7124502@ed.tus.ac.jp*

ABSTRACT

Standards for museum lighting are established to ensure both the visual quality of paintings and the preservation of artworks. Currently, illuminance is commonly used as a metric. However, luminance distribution, which is a physical measure more closely related to perceived brightness, should be considered when determining the appropriate brightness of paintings. Brightness evaluation should involve not only a judgement of 'brightness perception level', but also an assessment of the 'appropriate brightness' for a painting. Our previous research revealed that appropriate brightness has a linear relationship with painting preference, and that the brightness perception level maximising it (optimal brightness) varies with the painting's characteristics. Some paintings were evaluated as more appropriate at higher brightness levels, while others were preferred at lower levels. Previous experiments indicate that the optimal brightness can be predicted from five variables describing oil painting characteristics. Among these, three variables, lightness difference, chroma difference, and maximum edge perception, significantly determine the brightness perception level that yielded the appropriate brightness. To simplify the prediction, we propose a categorical classification method based on multiple regression of qualitative data from these three variables. If these quantities could be predicted from a painting's appearance, determining optimal brightness on site situations would be simpler. Therefore, we tested whether students in a controlled room could judge lightness, chroma, and edge perception from a painting's appearance. A sample sheet was prepared as a reference to evaluate these three attributes. The percentage of correct responses for each painting showed large deviations from painting to painting. Therefore, we focused on paintings with particularly low correct-response rates and found that the rates tended to decrease for abstract works. It is possible that landscape, portrait, and still-life paintings can be predicted from their appearance to some extent. We will continue to revise the sample sheet to enable more accurate predictions. We plan to conduct experiments with curators at an actual museum, with the final goal of using this method in the field.

Keywords: Museum lighting, Oil painting, Brightness perception, Optimal brightness, Painting characteristics

INTRODUCTION

Museum lighting requires sufficient brightness to ensure visual quality and low intensity to protect paintings from light damage. Illuminance is the common metric for museum lighting standards. However, luminance distribution, which reflects the light as perceived by the human eye and is closer to perceived brightness, should be considered when evaluating a painting's appearance from the viewer's perspective.

Our previous research revealed that appropriate brightness is linearly related to painting preference, and that the brightness perception level maximises it (optimal brightness) varies with the painting's characteristics (Figure 1) [1]. That is, some paintings were judged more appropriate at higher brightness levels, whereas others were judged more appropriate at lower levels. Assuming that a painting's brightness perception level can be predicted from its luminance distribution and other factors, this study aims to determine the level that yields optimal brightness for each painting. This approach seeks to preserve visual quality of painting even under low light, thereby contributing to both viewer satisfaction and conservation, and ultimately establishing a new museum lighting method.

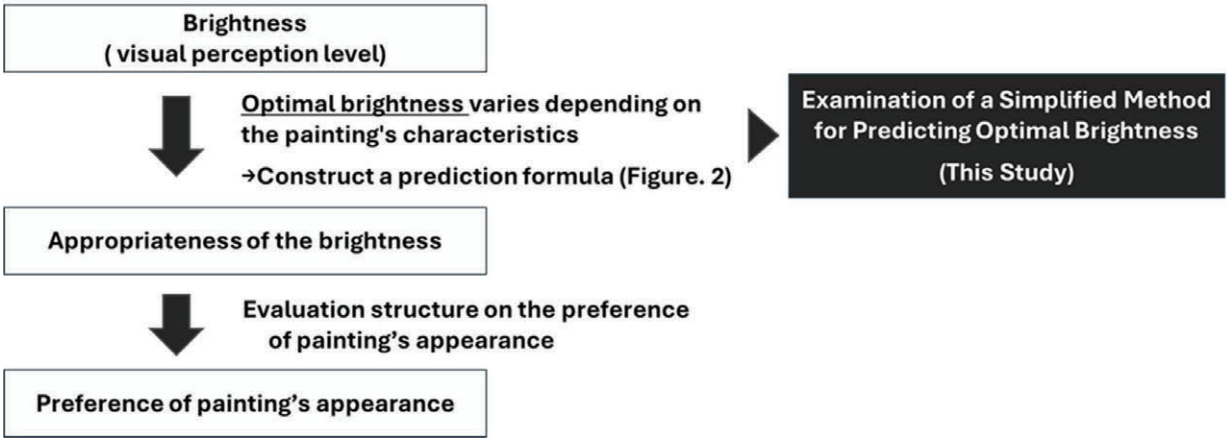

Figure 1: Flowchart for predicting the preference of paintings

The results of previous experiments indicate that the brightness-perception level that maximises appropriate brightness may be predicted from five variables describing oil-painting characteristics: average lightness, lightness difference ('average lightness of the values above the third quartile' – 'average lightness'), average chroma, chroma difference ('average chroma of values above the third quartile' – 'average chroma'), and maximum edge perception (Table 1). Lightness and chroma were computed using the CIECAM16 model, with the J value for lightness and the C value for chroma. Edge perception was obtained using an edge detection algorithm [2]. Among these variables, lightness difference, chroma difference, and maximum edge perception significantly influenced the brightness-perception level yielding optimal brightness. To simplify prediction of optimal brightness, we propose a categorical classification method based on multiple-regression analysis of qualitative data for these three variables. Figure 2 shows the classification flowchart based on painting characteristics and the regression equation derived from the qualitative data, which is used to predict the optimal brightness level. The lower-right graph shows that the regression estimates and the observed values match exactly. If these physical quantities could be predicted from a painting's appearance, determining optimal brightness on site would be simpler. Therefore, we conducted an experiment with university students in a controlled room to verify whether the levels of lightness, chroma, and edge perception could be judged from a painting's appearance. Ultimately, the goal is for curators to apply this method easily in museums.

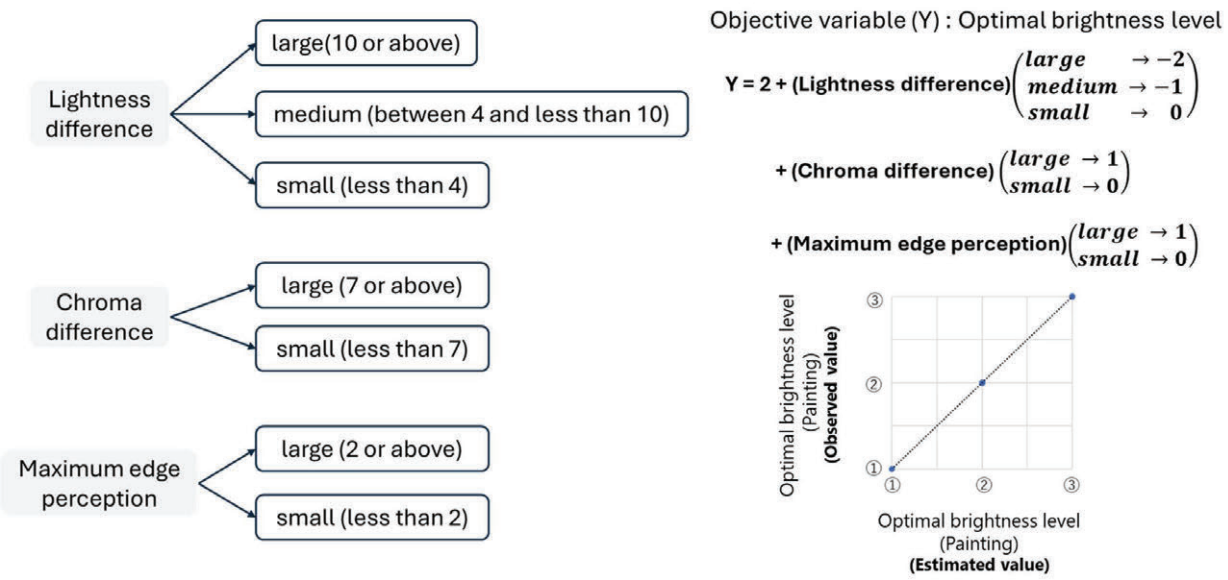

Figure 2: Classification flow and regression equation using categorical data

METHODOLOGY

The experiment was conducted in a full-scale model space (W2900 mm x D5000 mm x H2400 mm), simulating an actual museum. The walls of the experimental space were painted N9.5. The observation point was 830 mm from the background surface, with a viewpoint height of 700 mm. Figure 3 shows the plan and cross-sectional views of the experimental space.

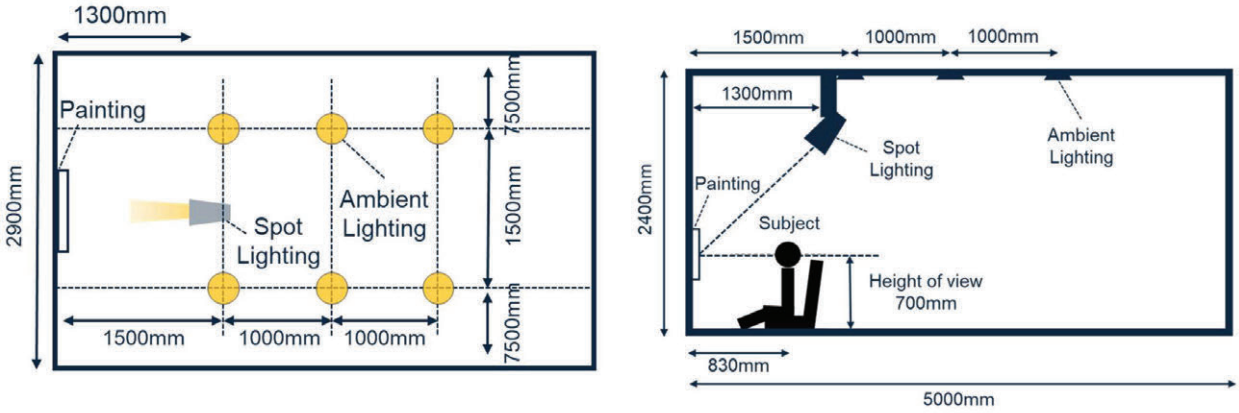

Figure 3: Plan and section of the space

The evaluation items consisted of five variables used to determine the optimal brightness, with the evaluation scales set to two or three levels (Table 1.). The lightness and chroma of the paintings were calculated using 196 points (14 × 14) for Painting A, and 182 points (13 × 14) for the other paintings, after which the averages and quartiles were computed.

Table 1: Evaluation items and Evaluation scale

	Evaluation item	Evalution scale
1	Average lightness	small・medium・large
2	Lightness difference ('Average lightness of the values above the third quartile' – 'Average lightness')	small・large・very large
3	Average chroma	small・medium・large
4	Chroma difference ('Average chroma of the values above the third quartile' – 'Average chroma')	small・large
5	Maximum edge perception	small・large

A total of 15 oil paintings and one lighting condition (painting surface illuminance: 100 lx) were used as the experimental conditions (Table 2.), and each condition was presented randomly. Painting A had the S10 format (530 mm × 530 mm), whereas the other paintings had the F10 format (530 mm × 455 mm). Two types of lighting were used: ambient lighting (LED, Ra = 92, 3000 K) to illuminate the entire space and spot lighting (LED, Ra = 95, 3000 K) to illuminate the painting surface.

Table 2: Oil paintings used in the experiment sand reflectance

	Image	Title	Painter	Reflectance
Painting A		Painting	Joan Miro (Reproduction)	45.3%
Painting B		Number 8, 1951 'Black Flowing'	Jackson Pollock (Reproduction)	30.5%
Painting C		Une allée des rosiers	Claude Monet (Reproduction)	12.6%
Painting D		Sun in the Mist	Claude Monet (Reproduction)	26.1%
Painting E		White Noise	Eishi Sekine (Reproduction)	40.7%
Painting F		No. 5 1948	Jackson Pollock (Reproduction)	9.5%
Painting G		Les Sables d' Olonne	Albert Marquet (Reproduction)	59.2%
Painting H		Church Street EI	Charles Sheeler (Reproduction)	18.4%
Painting I		The Lute Player	Caravaggio (Reproduction)	9.6%
Painting J		Red Fuji	Yasushi Nakao	6.4%
Painting K		La Transfiguration	Peter Paul Rubens(Reproduction)	16.4%
Painting L		Lago di Como	Tadashi Orita	31.3%
Painting M		Northen Alps	Kazuo Hurukawa	41.6%
Painting N		Percian cat	Okartaro Suda (Reproduction)	5.9%
Painting O		Starry Night over the Rhone	Vincent van Gogh (Reproduction)	8.2%

A sample sheet was prepared as an index to determine the magnitude of lightness, chroma, and edge perception in the paintings. Each sample sheet contained approximately 10 printed reference paintings per index, arranged on A4-sized paper. The paintings for the sample-sheets were primarily selected from works exhibited at the National Museum of Western Art, and the calculations were based on measured values. Lightness and chroma were computed using the CIECAM16 model, while edge perception was obtained using an edge detection algorithm based on a neurophysiological model of the human visual system [2]. Finally, the paintings were printed on matte paper with an inkjet printer, and the samples were measured to obtain values for classification. An example sample sheet is shown in Figure 4.

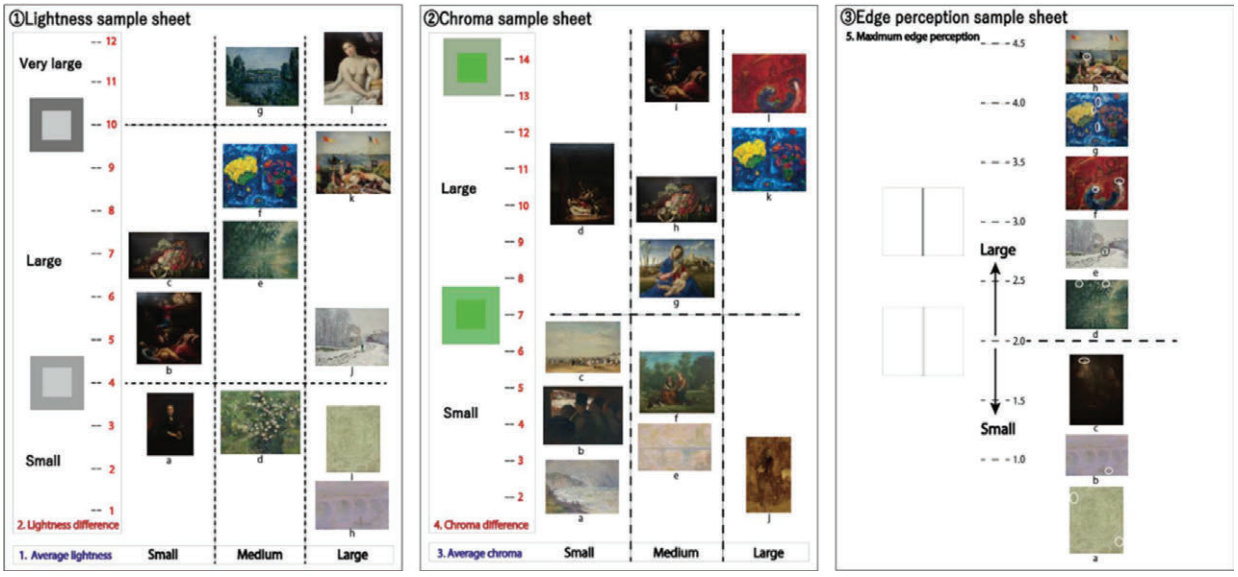

Figure 4: Sample Sheets for Each Evaluation item

RESULTS AND DISCUSSION

The correct response rates for each evaluation item were 57% for ‘lightness difference’, 76% for ‘chroma difference’, and 77% for ‘maximum edge perception’, indicating that ‘lightness difference’ is particularly difficult to judge from a painting’s appearance. In addition, the percentage of correct responses varied greatly from painting to painting (Figure 5).

We focused on paintings with low correct-response rates and found that these rates tended to decrease for abstract paintings. For the six abstract paintings, the correct response rates were 30% (lightness difference), 61% (chroma difference), and 72% (maximum edge perception). For the nine representational paintings, the rates were 75%, 86%, and 81% for lightness, chroma, and maximum edge, respectively. For abstract paintings, where the correct rate for lightness difference was particularly low, the questionnaire results suggested that participants differed in perceiving high-lightness regions, that their understanding of high- and low-lightness colours might be ambiguous, and that hue differences could make lightness judgements more difficult. Landscape, portrait, and still-life paintings can be predicted to some extent from their appearance. However, participants showed greater variability in interpreting abstract paintings, making them more difficult to judge from appearance alone.

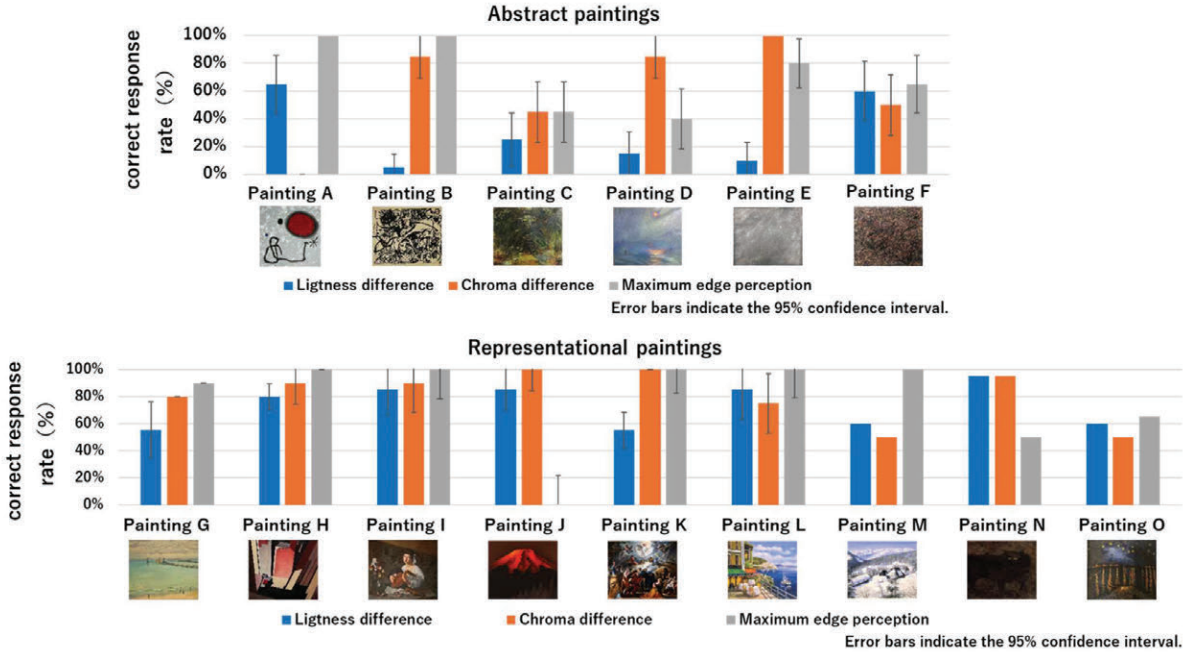

Figure 5: Correct response rate for each painting

CONCLUSION

In this study, we examined whether lightness difference, chroma difference, and maximum edge value—factors influencing the optimal brightness of a painting—can be predicted from visual appearance as a simplified method for estimating optimal brightness. The results suggest that these perceptual attributes can be judged to some extent from the appearance of representational paintings but are more difficult to judge in abstract paintings. Based on the present experimental results, we plan to revise the sample sheet to improve prediction accuracy. In addition, we plan to explore alternative approaches for simplified estimation and conduct experiments with curators in an actual museum, with the ultimate goal of applying this method in the field.

ACKNOWLEDGEMENTS

We express our appreciation to Assistant Professor Takase Kazuto and our lab members for their cooperation.

REFERENCES

[1]. Maeda, A., OE, Y. & Yoshizawa, N. (2021). Evaluation structure on preference of painting's appearance with low reflectance in the museum lighting environment. *Proceedings of CIE Conference* PO45

[2]. Yoshizawa, N., & Shida, H. (2021). A neurophysiology-based model to estimate visibility in actual lighting environment. *Proceedings of CIE Conference*, pp. 380-388.

Differences in The Diversity of Color Names and Evaluation of Darkness and Lightness of Colors in Surface and Aperture Color Modes

Yanan Qiao[a*], Yasuhiro Kawabata[a]

[a]*Hokkaido University, Sapporo, Japan*
[*]*Yanan Qiao, yanan.qiao.x8@elms.hokudai.ac.jp*

ABSTRACT

This study investigated color naming and perceived lightness in surface and aperture color modes using 22 participants. In each mode, participants named and rated the lightness of 100 color chips, providing a direct comparison between the two modes of color observation. Naming was unrestricted, allowing participants to freely use both basic and non-basic color terms, while lightness was evaluated on a continuous 0–10 scale. Results revealed that participants employed a greater variety of color names in the surface mode than in the aperture mode, indicating that surface mode perception affords finer categorical distinctions. Despite this variation, the reliance on basic color terms remained consistently high across both modes. Naming consistency was especially pronounced for orange, green, blue, and purple, reflecting the perceptual salience of these hues. With respect to lightness ratings, chips in the aperture mode generally appeared lighter overall. In both modes, bluish-purple, blue, bluish-green, and purple hues were consistently judged as relatively light, highlighting the perceptual stability of these regions. Taken together, these findings suggest that surface mode perception aligns closely with everyday visual experience, supporting broader categorization and richer naming, whereas aperture mode perception resembles the experience of light sources, with color naming stabilized by basic terms and less influenced by background context.

Keywords: color appearance, color naming, surface color mode, aperture color mode, lightness/darkness

INTRODUCTION

Color is a pervasive feature of daily life, and the ability to perceive and identify it is essential for effective interaction with the environment. Based on variations in hue, lightness, and chroma, humans can distinguish over seven million colors [8]. A study demonstrated that the human visual system does not perceive colors continuously but in discrete categories [14]. Given this vast range, people typically classify them using color names. For instance, "green" encompasses many shades, including light, bright, or dark, yet all are categorized as green to distinguish them from other colors. This phenomenon, known as categorical color perception, reflects the role of linguistic classification in shaping perception [7]. As one of the most salient visual attributes [1], color exemplifies this effect [4].

The concept of color appearance was introduced by David Katz in 1935, who identified two modes of observation: the surface mode, where color is perceived as a property of an object's surface, and the aperture mode, where it is perceived as the color of light itself [10]. In real-world scenes, a surface can appear in either mode depending on conditions. Previous research has focused on basic color naming [12], categorical naming [10], overall lightness under different modes [13], and the triggers of mode shifts [11, 6]. However, few studies have compared the diversity of color names across modes or examined the perceived lightness of individual colors.

Such investigations are important for several reasons. First, analyzing the diversity of color names can reveal subtle variations in perception, offering insight into how the visual system processes complex color information. Second, comparing perceived lightness across modes clarifies how environmental conditions influence perception, providing theoretical guidance for color science, visual cognition, and applications such as design, lighting, and display technologies. Finally, this research can illuminate the mechanisms of categorical color perception, clarifying the interplay between perception and linguistic classification and deepening understanding of visual cognition.

This study had two objectives: (1) to compare color naming across observation modes, and (2) to evaluate perceived lightness of color chips and examine the features associated with each mode.

This study is the first to examine the diversity of color naming across different observation modes and to provide a comprehensive assessment of the perceived lightness of single colors.

METHODOLOGY

Participants

The experiment involved 22 participants (mean age = 29.32 years, SD = 12.76; age range = 19–66 years). Four participants were male. All reported normal or corrected-to-normal vision, with no history of color vision deficiencies. Participants were recruited from psychology courses and speeches. The study was reviewed and approved by the Ethics Committee of Hokkaido University and conducted in accordance with the Declaration of Helsinki (1996). All participants provided informed consent prior to participation.

Device and Stimuli

Tasks were implemented and presented using the PsychoPy software package. The display monitor had a resolution of 2560 × 1664 pixels and a pixel density of 224 ppi. The stimulus on each trial was a 5 × 5 cm square shown at the screen center. In the surface mode condition, the square was surrounded by a white rectangular background (22 × 19 cm; RGB: 255, 255, 255). In the aperture mode, the background was identical in size but black (RGB: 0, 0, 0). To minimize ambient effects, the experiment was conducted in a darkened room, as uncontrolled lighting has been shown to impair color categorization accuracy [5]. The viewing distance between participants and the display was maintained at 88 cm. Illumination levels differed slightly between conditions: 1.448 lux (±0.386) in surface mode and 1.91 lux (±0.535) in aperture mode. The stimuli were drawn from the 100-hue test and consisted of 100 consecutive colors (Figure 1), classified into ten categories: red, orange, yellow, yellowish-green, green, bluish-green, blue, bluish-purple, purple, and reddish-purple. All test caps had a Munsell value of 6, according to the Munsell color system, which numerically represents hue, value, and chroma. This set was chosen because high brightness [6] and high saturation [11] can induce perceptual shifts from surface to aperture mode. The relatively low brightness and chroma of 100-hue test stimuli minimized such transitions and ensured consistency across trials.

Figure 1: Experiment stimuli.

Procedure

Each participant completed two tasks: surface mode followed by aperture mode. Apart from background color, all conditions were identical. Each task included 100 randomly ordered stimuli. A fixation cross appeared for 1000 ms, followed by a blank screen for 1500 ms. The target stimulus was then presented for 1800 ms. After it disappeared, participants freely named the color and rated its lightness/darkness on an 11-point scale (0 =

"extremely dark," 10 = "extremely light"). No time limit was imposed. The next trial began immediately after a response, and the task continued until all 100 stimuli were completed. No restrictions were placed on color vocabulary.

RESULTS

In the surface color mode, participants used an average of 16 color names (± 5.155), whereas in the aperture mode they used 12.41 (±4.261). A paired-sample t-test confirmed that the number of names used was significantly greater in the surface mode ($p < .0001$), indicating wider variability in naming under this condition. Across all 22 participants, 80 distinct names were recorded in the surface mode compared to 54 in the aperture mode, further demonstrating greater diversity in surface color naming. Table 1 lists the 20 most frequently used color names in each mode, showing frequency, proportion, and rank. "Frequency" refers to the number of times a name was applied to the 100 chips by all 22 participants (2,200 namings per mode). "Proportion" is the ratio of that frequency to the total, and "Rank" indicates relative position within each mode. Despite differences in diversity, the four most frequent names in both modes were basic color terms. On average, participants used basic terms in 43.6% (±18.1%) of cases in the surface mode and 54.1% (±19.8%) in the aperture mode, indicating stronger reliance on basic categories in the aperture condition.

Table 1: Statistics of the top 20 most frequently used color names in the two modes

Surface color mode				Aperture color mode			
Color name	Frequency	Proportion	Rank	Color name	Frequency	Proportion	Rank
Green	365	16.591%	1	Green	325	14.773%	1
Purple	278	12.636%	2	Purple	254	11.545%	2
Pink	248	11.273%	3	Yellow	243	11.045%	3
Blue	161	7.318%	4	Pink	230	10.455%	4
Yellow-green	133	6.045%	5	Yellow-green	170	7.727%	5
Orange	107	4.864%	6	Blue	170	7.727%	5
Light blue	97	4.409%	7	Orange	157	7.136%	7
Blue-purple	89	4.045%	8	Light blue	106	4.818%	8
Ochre	76	3.455%	9	Red	78	3.545%	9
Blue-green	75	3.409%	10	Skin color	72	3.273%	10
Red	71	3.227%	11	Blue-green	45	2.045%	11
Yellow	55	2.500%	12	Blue-purple	41	1.864%	12
Lilac	39	1.773%	13	Red-purple	33	1.500%	13
Red-purple	36	1.636%	14	Emerald green	31	1.409%	14
Brown	33	1.500%	15	Golden yellow	23	1.045%	15
Skin color	27	1.227%	16	Lilac	22	1.000%	16
Grass green	27	1.227%	16	Peach color	20	0.909%	17
Beige	22	1.000%	18	Beige	16	0.727%	18
Emerald green	22	1.000%	18	Salmon pink	15	0.682%	19
Sky blue	20	0.909%	20	Fresh grass green	14	0.636%	20

For the 100 stimulus chips spanning 10 hues, naming accuracy, defined as correspondence between participants' labels and the designated hue, was relatively high for four hues: orange (surface: 44.2%; aperture: 39.0%), green (surface: 71.1%; aperture: 64.0%), blue (surface: 38.1%; aperture: 40.9%), and purple (surface: 55.7%; aperture: 38.1%). These results suggest that these hues are perceptually stable and salient across both modes, facilitating more accurate recognition.

Lightness ratings also differed significantly between conditions. Mean lightness was higher in the aperture mode (6.268±2.135) than in the surface mode (5.811±1.81). A two-way repeated-measures ANOVA with sphericity correction showed a significant main effect of mode ($\tilde{A}$ (1, 131) = 12.822, $p < .0001$), indicating that colors appeared lighter in the aperture mode. There was also a main effect of hue ($\tilde{A}$ (6.441, 843.784) = 25.026, $p < .0001$), confirming differences in lightness across hues. Moreover, the interaction between mode and hue was significant ($\tilde{A}$ (6.887, 902.153) = 2.261, $p = .0280$), showing that the effect of mode varied by hue. Simple effect analyses revealed that, in the surface mode, the order of hues from brightest to darkest was blue-purple, blue-green, blue, green, purple, red, red-purple, orange, yellow-green, and yellow. In the aperture mode, the order was: blue-purple, blue, blue-green, purple, orange, green, red, red-purple, yellow-green, and yellow. Across both modes, blue-purple, blue, blue-green, and purple appeared relatively bright. Figure 2 illustrates participants' lightness ratings by hue under the two modes (blue = surface mode, red = aperture mode). The x-axis represents the 10 hues, the y-axis lightness, and error bars indicate standard deviations. The figure shows that blue-purple, blue, blue-green, and purple were consistently rated as relatively bright.

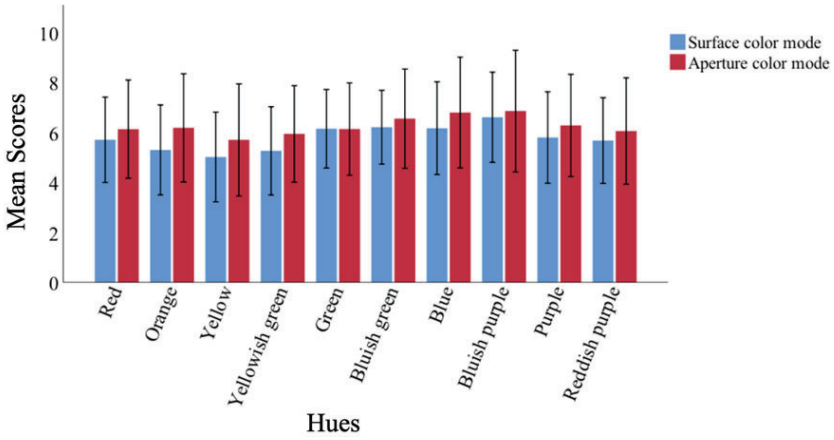

Figure 2: Statistical results of lightness ratings in the two modes.

DISCUSSION

The analysis showed that the four most frequently used color terms in both modes belonged to the category of basic terms. In the surface mode, the proportion of basic term usage exceeded 40% for each participant, while in the aperture mode it exceeded 50%. These results indicate that basic terms exhibit high stability and universality in color naming, maintaining frequent use under different presentation modes. This finding aligns with the theory, which posits that once a color category becomes lexicalized as a basic term, it persists in the language system over time [2]. Consequently, individuals tend to rely on such terms when naming colors. A study further showed that basic terms remain stable across speakers of the same language [3]. This stability may reflect the interaction of memory and semantic networks: a bidirectional relationship exists between color naming and memory, whereby stably named colors are more easily remembered, and easily retrievable categories are more frequently used. This memory–language feedback loop helps preserve the stability of high frequency basic terms.

Participants used more terms in the surface mode than in the aperture mode, indicating stronger color constancy in the surface condition. Because everyday perception predominantly occurs in this mode, individuals can rapidly recognize categories and detect subtle differences, which promotes greater naming diversity. Over time, such experience refines perceptual precision and supports fine-grained representations of color constancy. As the surface mode closely reflects natural environmental color information, the visual and linguistic systems have adapted to allow more elaborate categorization.

High consistency in naming orange, green, blue, and purple can be attributed to perceptual universality. The previous study noted that the human visual system, particularly the retinal L–M and S–(L+M) channels, along with contrast mechanisms, naturally produces perceptually salient color regions that are consistent across individuals [3]. These regions act as anchors for naming, explaining the observed consistency in labeling these hues.

Lightness ratings were higher in the aperture mode than in the surface mode, consistent with the previous study [13]. This effect can be explained by the Mach band phenomenon [9]: when a region is adjacent to a luminance gradient or edge, the visual system exaggerates the lightness or darkness near the edge, making it appear brighter or darker than in reality. In the aperture mode, the black background enhances edge contrast, increasing perceived lightness. In the surface mode, the bright background reduces edge contrast, leading to lower lightness ratings.

With respect to the limitations of this study and directions for future research, first, in the aperture mode naming was largely limited to basic or, occasionally, saturated color terms, suggesting that perceived saturation may shape naming patterns. However, subjective saturation ratings were not collected in this study. As the original participant sample is no longer available, future research will include this measure with a new cohort to clarify the mechanisms underlying these effects. Second, the participants in this study were limited to individuals of Asian descent, and thus potential differences across ethnic groups in color naming under the two observation modes were not addressed. Future research should therefore examine whether people from different ethnic backgrounds exhibit similar or divergent patterns in color categorization.

CONCLUSION

In the surface mode, color perception is closely tied to everyday visual experience, resulting in more diverse categorization and a more refined naming system. In contrast, the higher reliance on basic terms in the aperture mode indicates that perception in this condition is closer to raw sensation. The high frequency and consistency of basic terms highlight their stability and insensitivity to background. Moreover, colors in the aperture mode were perceived as lighter than in the surface mode, suggesting that aperture processing may resemble that of illuminant colors. Across both modes, bluish-purple, blue, blue-green, and purple were consistently perceived as the lightest**,** indicating relative stability of their lightness across backgrounds.

ACKNOWLEDGEMENTS

This research was supported by a Grant-in-Aid for Scientific Research from the Japan Society for the Promotion of Science (Grant Number: 23K28171). The authors thank all participants for their time and cooperation.

REFERENCES

[1]. Amirkhanashvili, A., & Gigilashvili, D. (2020). Color naming and communication of color appearance: Is it different for native Georgian speakers? *Proceedings of the Colour and Visual Computing Symposium (CVCS 2020)*, Tokyo, Japan. https://ceur-ws.org/Vol-2688/paper6.pdf

[2]. Berlin, B., & Kay, P. (1969). *Basic color terms: Their universality and evolution*. University of California Press.

[3]. Dedrick, D. (1998). *Naming the rainbow: Colour language, colour science, and culture.* Kluwer Academic Publishers.

[4]. De Vries, J. P., Akbarinia, A., Flachot, A., & Gegenfurtner, K. R. (2022). Emergent color categorization. in a neural network trained for object recognition. *eLife,* 11, e76472. https://doi.org/10.7554/eLife.76472

[5]. Eguchi, T., Yamada, M., Yeoh, W. L., Okumura, H., Yamaguchi, N., & Fukuda, O. (2024). Extraction and classification of surface color information using selective LED illumination and a statistical neural network. *IEEE Access,* 12, 65606–65614. https://doi.org/10.1109/ACCESS.2024.3398630

[6]. Fukuda, K., Uchikawa, K., & MacLeod, D. I. A. (2011). Influence of surrounding colors in the illuminant-color mode on color constancy. *i-Perception,* 2(4), 375. https://doi.org/10.1068/ic375

[7]. Hanley, J. R. (2015). Color categorical perception. In R. W. Hunt & M. R. Pointer (Eds.), *Encyclopedia of color science and technology* (pp. 1–6). Springer. https://doi.org/10.1007/978-3-642-27851-8_61-11

[8]. Kawabata, M., Kawabata, Y., Sasaki, M., Takahashi, F., Kasai, Y. (2020). The contributions of experience of artistic club activities to color discrimination for undergraduate revealed in 100 hue test evaluation method with reduced time limit [in Japanese]. *Color Science Research*, 44(4), 163-174. https://doi.org/10.15048/jcsaj.44.4_163

[9]. Mach, E. (1865). *Contributions to the analysis of sensations* [German original published 1865]. Leopold Voss.

[10]. Mogi, S., Kamei, M., Sakurai, M., Ishikawa, T., & Ayama, M. (2023). Relationship between color appearance evaluation and categorical color responses of small stimuli in central and near peripheral visual fields. *Color Research & Application,* 48(6), 772-792. https://doi.org/10.1002/col.22890

[11]. Nakano, L., Takeuchi, T., Motoyoshi, I., Li, Y., Adelson, E., & Nishida, S. (2009). The effect of color saturation and luminance contrast on color naturalness. *Journal of Vision,* 9(8), 1040. https://doi.org/10.1167/9.8.1040

[12]. Shinoda, H., Uchikawa, K., & Ikeda, M. (1993). Categorized color space on CRT in the aperture and the surface color mode. *Color Research & Application,* 18(5), 326–333. https://doi.org/10.1002/col.5080180506

[13]. Uchikawa, H., Uchikawa, K., & Boynton, R. M. (1989). Influence of achromatic surrounds on categorical perception of surface colors. *Vision Research,* 29(7), 881–890. https://doi.org/10.1016/0042-6989(89)90099-0

[14]. Uchikawa, K. (1988). Categorical perception of surface color [in Japanese]. *Japanese Journal of Optics: Publication of the Optical Society of Japan,* 17, 661–669.

Investigation of The Colour Design: Follow The User Data or Designer's Intuition to Build A Colour Scheme for The Beer Label

Chunxi Nan[a], Mengmeng Wang[a*], Jinwen Li[a]

[a]*School of Digital Technology and Innovation Design, Jiangnan University, Wuxi, P.R.China*
[*]*Corresponding author: Mengmeng Wang, mm.wang@jiangnan.edu.cn*

ABSTRACT

The colour scheme is crucial for label and package design. Two different approaches, based on user data and relying on the designer's intuition, are currently used in the design industry. These two approaches are also considered to be typical examples of data-driven design and data-aware design, respectively. AI-Generated Content(AIGC) tool shows great potential in graphic design. The procedure of its colour selection was purely data-driven. Some design institutions consider it closer to the trends and reflect consumers' preferences. The designers should follow users' data as the source or their intuition in colour design, which has become an unsorted issue. In this study, these two colour scheme building methods were cross-compared. colour-taste matching was set to be the goal. Two sets of colour schemes were used to design beer labels. One set was gained from a colour-taste association experiment by subjects, and another was gained from designers' intuition. Four types of craft beer labels were generated based on these colour schemes and scored for colour-taste match. The experimental results reveal the difference between the colour schemes based on users' data and designers' intuition regarding hue angles, chroma, and lightness. The colour scheme of the users or the designer showed no strong associations with the description of the professional beer sommelier. Some of the common descriptions, such as the crips of the Pearson, were found to be a good match for both colour scheme approaches. However, the colour scheme of the subjects was found to be a better match to that of the beer sample. Even though the data-driven approach showed higher accuracy in colour-taste match, the branding and market differentiation might need a different approach. AIGC is now embedded with the design industry, and data-driven design seems to be a "reliable" solution for commercial designs. The results showed the strengths of the data-driven design but indicated the limitation of Large Language Models based AIGC.

Keywords: colour-taste association, colour scheme, data-driven design, data-aware design, beer label

INTRODUCTION

Colour is considered a key element in visual design and communication. Research has found that packaging colours not only attract consumers' attention, but can also convey a message about the product to consumers[1]. For the package, colours evoke strong product associations and category images for users[2]. The visual impact of packaging colours was also found to influence consumers' expectations and can bias their experience of the product[3]. Past research has indicated that packaging colour design can convey product information. Therefore, the colour design is generally considered to be a design procedure that can benefit from a broad range of user data.

Colour design is an essential part of the packaging design system. It could fulfil certain expectations, which play a key role in consumption behaviours. To be competitive in the current market, most designers follow two approaches in colour design: data-driven and data-aware strategies. Both methods are based on user data that is widely used in packaging design and has helped drive innovation, improve product success, and enhance user

satisfaction[4]. The AIGC (Artificial Intelligence Generated Content) technology relies on colour preferences data or past design examples to generate colour design, which is considered a typical data-driven design strategy[5].

In contrast, the data-aware approach relies more on designers' sensitivity and intuition towards consumer perception, which allows for creative exploration and contextual adaptation beyond the data content. With the success of many AIGC-generated designs, data-driven strategies have become more widely adopted in packaging colour design. However, the essential differences between data-driven and data-aware approaches in the field of colour design have been limitedly researched.

Craft beer, characterised by its diverse flavours and aromas derived from distinctive brewing techniques, has recently emerged as a growing trend in China. However, it remains relatively unfamiliar to the general public due to its complex manufacturing nature. In this context, packaging colours are not only a matter of aesthetics or brand recognition but also serve as an essential means for delivering flavour-related information to consumers. For this specific design task, the accuracy of providing the flavour information through both colour design strategies is an interesting question to be investigated. This study examines the accuracy of both approaches in craft beer packaging design for delivering flavour information. The accuracy of both colour design strategies was determined through a vision-taste experiment, which provides support for using these two methods for future colour design.

METHODOLOGY

Prior to this experiment, a preliminary study was conducted to investigate the selection of beer flavours and their corresponding colours based on popularity data, and then to evaluate the colour presentation on beer labels. The colour schemes that were chosen through taste for the beer samples were less agreed upon than the ones described. Reflect the tastes perceived by the general public, which can differ from the descriptions provided by professionals. This study aims to focus on the delivery of information to the general public. Therefore, the colour schemes obtained from the beer samples were used to design labels for further investigation.

Stimuli

Based on the colour schemes in the preliminary experiment, labels of craft beers were coloured, and the pattern of the label was set to be identical. The colour scheme for the beer samples was provided to a designer, who had not participated in the preliminary experiment, for colouring the labels. The methods employed in selecting these colours were also offered as a description to this designer. The designer who participated in the taste-colour test was requested to colour the labels according to the colour scheme devised by the previous experimental designers. Two sets of labels were generated, and these labels were used as stimuli in the psychophysical experiment. One set was based on the colours from the colour-taste test (with beer samples), referred as $S_{c\text{-}t}$, while the other set was based on craft beer samples, referred as S_{cb}.

Procedures

Fifty-nine participants, including 43 females and 16 males, aged 21 to 24, voluntarily participated in this experiment. All participants are naive to the preliminary experiment and pass the colour-blind test (using Ishihara colour plates). The labels were simulated on a beer bottle and placed on a 50% neutral background. The participants were asked to rate the level of matches based on the stimulus and the corresponding adjective traits. A professional beer sommelier selected adjectives to describe the unique taste of the target. For Sout, Amber and IPA, two adjective traits were chosen. For Pearson, one adjective trait was chosen. A total of seven adjectives: Sweet, Caramel, Crisp, Citrus, Richness, Smooth, and Mellow. Here, the participant had to score all seven adjective traits according to the stimulus that they observed. Ten levels (-5, -4, -3, -2, -1, 1, 2, 3, 4, 5) were used in this scoring system. The negative score represents a mismatch between the stimulus and the adjective trait. The positive score represents the adjective trait can be perceived from the label. The absolute score refers to the degree of agreement or disagreement between the stimulus and traits, where 1 refers to a just about match/mismatch, and 5 refers to a very strong match/mismatch.

Statistical analysis

The psychophysical experiment results were converted into z-scores by adopting Case V of Thurstone's Law of Categorical Judgements[6]. The z-scores was then used to determine the score of each adjective trait based on the estimation of each category boundary.

RESULTS

The experimental results are shown in Figure 1. In this figure, the features that correlated with the target are marked with black dots. The highest-scoring flavours of each craft beer are marked in red bold. The results show that these two colour schemes do not fully reflect the flavour characteristics of beer. Neither shows a strong association with the traits. $S_{c\text{-}t}$ show good results at Pearson. Sb show good result at the sweet of the Amber; the designer colour scheme got negative at Caramel, Crisp, Citrus. The $S_{c\text{-}t}$ got negative at Smooth.

In this figure, $S_{c\text{-}t}$ referred as the procedure that use the colours from colour-taste test (with beer samples). S_{cb} referred to the procedure that use craft beer samples. Neither showed strong associations with traits. $S_{c\text{-}t}$. Based on the colours from colour-taste test (with beer samples) used to colour the labels showed good results on Pearson in relation to brittleness. Sb showed good results in relation to sweetness of Amber. The designer built colour scheme (S_b) got negative results for Caramel, Crisp and Citrus. $S_{c\text{-}t}$ got negative results for Smooth.

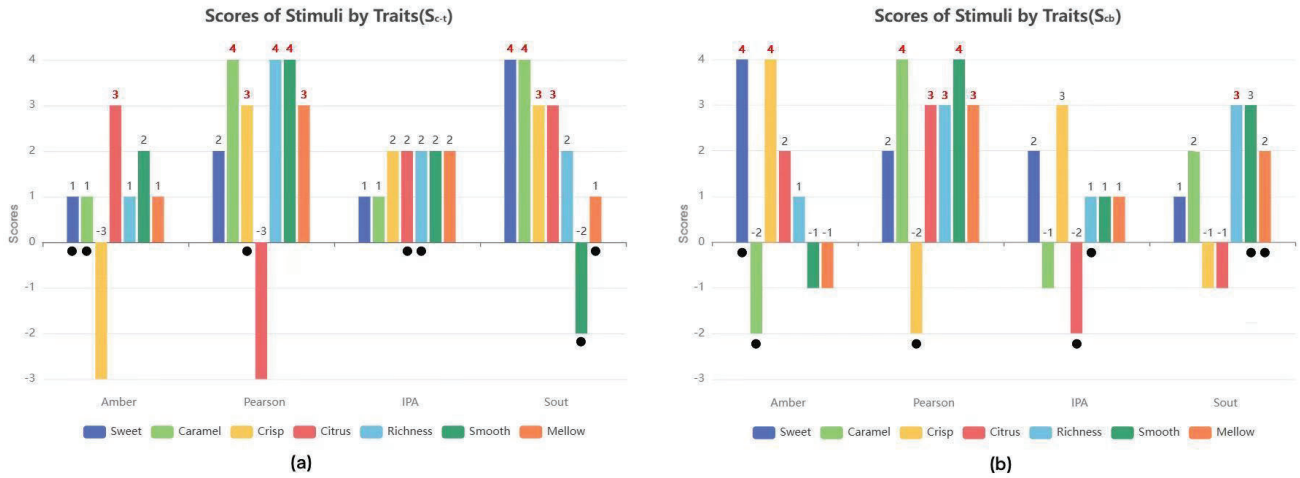

Figure 1: The score of eight stimuli at each adjective trait. (a) Scores of stimuli by traits ($S_{c\text{-}t}$), (b) Scores of stimuli by traits (S_{cb}).

By analysing the degree of matching of the experimental results, the colour scheme $S_{c\text{-}t}$ is a perfect match, while S_{cb} mismatched with Amber and IPA. Both colour schemes received high percentage values in Sout and Pearson, where S_{cb} is higher than the others. The mismatch could be because the designer's instinct does not agree well with the users'. The results show that the colour scheme could provide a valid guide to the designer. Here, the colour scheme based on the user showed a better match. However, in terms of the degree of match, the designer does a better job. These can be due to the designer's process, where flavour information is used to build the colour based on the processed data and her initiative.

The results demonstrate that colour schemes derived from user data performed better in terms of colour–taste matching accuracy, whereas designer-generated schemes showed more inconsistency. These suggest that data-driven design is more effective in delivering clear flavour cues to consumers, which supports its potential as a reliable method in packaging communication. However, the intuitive approach still yielded some meaningful

matches, indicating that intuition may capture certain aesthetic or brand-oriented qualities that are not fully reflected in user data.

Another important observation is that the traits selected by professional beer sommeliers did not align well with either users' perceptions or designers' interpretations. This indicates a possible gap between expert knowledge and general consumer experience. While professional descriptors may offer useful semantic categories, they do not necessarily translate into effective visual cues for colour–taste communication. For practical design, this means that relying solely on expert traits may not be sufficient, and incorporating direct consumer data could be more beneficial.

CONCLUSION

study investigated the accuracy of two colour design strategies, the data-driven design strategy and the data-aware design strategy, in delivering flavour information. The results show that the flavour of craft beer can be delivered through the beer labels matching colour design. The findings highlight two important implications. Data-driven strategy appear to be more reliable in communicating flavour cues through packaging, supporting the growing role of user data in design. Intuition-based design, data-aware strategy, which performed less effectively in accuracy than the data-driven strategy, but it could still contribute to brand differentiation and creative expression.

The role of AIGC in this context becomes particularly relevant. As AIGC systems are built on large datasets of user preferences, they essentially represent an extension of the data-driven approach. As AIGC systems are built on large datasets of user preferences, they essentially represent an extension of the data-driven approach. The results of this study, where user data outperformed intuition in accuracy, suggest that AIGC could be a promising tool for packaging colour design, especially in commercial settings where efficiency and consumer alignment are critical. At the same time, the weaker performance of intuition in this experiment does not imply its redundancy. The limitations of large language models and automated tools indicate that they cannot fully replace the creative insight and contextual judgment of human designers. Future research could therefore explore hybrid approaches, where AIGC-generated schemes are combined with designer intuition to achieve both functional accuracy and creative differentiation in packaging design.

REFERENCES

[1]. Spence, C., & Velasco, C. (2019). Packaging colour and its multiple roles. Multisensory packaging: Designing new product experiences, 21-48.

[2]. Schloss, K. B., Lessard, L., Walmsley, C. S., & Foley, K. (2018). Color inference in visual communication: the meaning of colors in recycling. Cognitive research: principles and implications, 3, 1-17.

[3]. Barnett, A., & Spence, C. (2016). Assessing the effect of changing a bottled beer label on taste ratings. Nutrition and Food Technology: Open Access, 2(4).

[4]. Gan, F., Romainoor, N. H., & Guo, Z. (2022). Research on innovative design of product packaging based on big data technology. Scientific Programming, 2022(1), 4973875.

[5]. You, W.-T., Sun, L.-Y., Yang, Z.-Y., & Yang, C.-Y. (2019). Automatic advertising image color design incorporating a visual color analyser. Journal of Computer Languages, 55, 100910.

[6]. Thurstone, L.L., 1927. Three psychophysical laws. Psychological Review, 34(6), 424–432.

A Study of Lip Color and Social Signalling of Z-Generation

Jinwen Li[a], Mengmeng Wang[a*], Chunxi Nan[a]

[a]*School of Digital Technology and Innovation Design, Jiangnan University, Wuxi, P.R.China*
[*]*Corresponding author: Mengmeng Wang, mm.wang@jiangnan.edu.cn*

ABSTRACT

Lip color is considered as evidence of health and beauty. With the assistance of the cosmetic industry, using lipstick to instantly change the lip color becomes possible. Presently, people not only aim to improve their appearance, but social signalling is also a reason for their lipstick consumption. Since social media has become a mainstream social activity, physical appearance started to have a higher priority than others. This scenario influences how people socially signalling and build their embodied identity.In this research, the social signalling of the Z-generation was studied first. Then, the relationship between the social impression and lip color was investigated. In our questionnaire, 64% of the people will wear lipstick to build a social impression, even if they have no interest in an entire make-up routine. The perceived personalities were found to be more concerned by the Z-generation. Introverted and extroverted were mostly concerted by the subjects. Lip and skin color match was also an important trait and had higher priority than personality. Based on the questionnaire, six adjectives of social impression, which related to the personalities, were further studied. The psychophysical experiment was designed to investigate the relationship between these adjectives and lipstick colors (in terms of hue, lightness and chroma). The results showed that chroma and lightness have a significant influence on the perceived personality. The terms like “Mature and Elegant” and “Enthusiastic and Confident” were found to lay at two extreme sides of lightness and chroma. The research results determine the relationship between lip color and the personality terms that are related to social signalling. They are also reflecting how the online social media influence the Z-generation at social signalling.

Keywords: lip color, social signalling, personality, z-generation

INTRODUCTION

Social signalling provides essential information in human social interactions [1]. It is mainly constructed with non-verbal information, such as profile images, and serves as the earliest perceptual clue during social interaction. This type of information enables individuals to form preliminary judgments and allows observers to predict up to 30% of social outcomes within just five minutes [2]. Accordingly, people often seek to alter visual signals through cosmetics to modify their appearance [3], thereby conveying desired social signals.

Among all cosmetic elements, lipstick color has been proven to hold a particularly significant role [4]. The shades and textures of lipstick are related to different impressions. Studies indicate that variations in lipstick color influence social cognition, with specific shades being favored in contexts where particular situational traits are emphasized [5]. However, the current research is mainly concentrated either on the affective responses elicited by specific colors, or on the impact of lip color on single traits such as sexual attractiveness [6–8].

The Z-generation has grown to be the primary consumption group in the cosmetics market. For females aged from 18 to 24 years old, the proportion reaches 37% [9]. Compared to the millennial generation, who use makeup primarily to improve self-image, the Z-generation considers wearing makeup for personality externalization [10]. Thus, exploring the role of lip color in the social signaling of Z-generation is crucial. This study aims to investigate the relationship between lipstick color and personality of Z-generation. Also, the impact of lip colors on social signaling was studied.

METHODOLOGY

Stimuli

In this study, thirty-six lipstick colors were selected and investigated. These colors were selected based on the CIE LCH system. The hue angle values are 20°, 5°, 0°, 350°, and 330°. The C and L were incremented by 25 each time. These selected colors were then rendering on a female facial image, which skin color is light yellow-toned, with opacity equal to 90%. The display used in this study was a calibrated BenQ SW272U monitor with color mode set as sRGB.

Experimental Procedure

The color experiment involved a total of 20 female participants, all aged between 20 and 23 years, who voluntarily participated in the experiment. The participants had their color vision checked by using Ishihara test. All the participants passed the test. Then the participants were asked to read the experiment information sheet before processed to the dark room for the experiment. During the experiment, a stimulus image is shown on the computer screen with a 50% gray background. Participants were instructed to observe the image and make a A/B judgment between two adjectives, then score the degrees of agreement between the selected adjective and the image with 5 levels. The score 1 referred as not quite conform to the adjectives, score 5 referred as very much conform to the adjectives. All 36 stimuli were displayed in random order to minimize sequence effects. The experiment required about 30 minutes to complete. The personality descriptors were selected as three groups of six words: introverted words, such as "Gentle" and "Reliable"; neutral words, such as "Mature" and "Elegant"; and extroverted words.

RESULTS

The psychophysical experiment results were converted into z-scores by adopting Case V of Thurstone's Law of Categorical Judgements [11]. The z-scores were then used to determine the score of each adjective trait based on the estimation of each category boundary. The results then further analyzed in terms of Lightness, Chroma and hue angle. The results were shown in Figure 1.

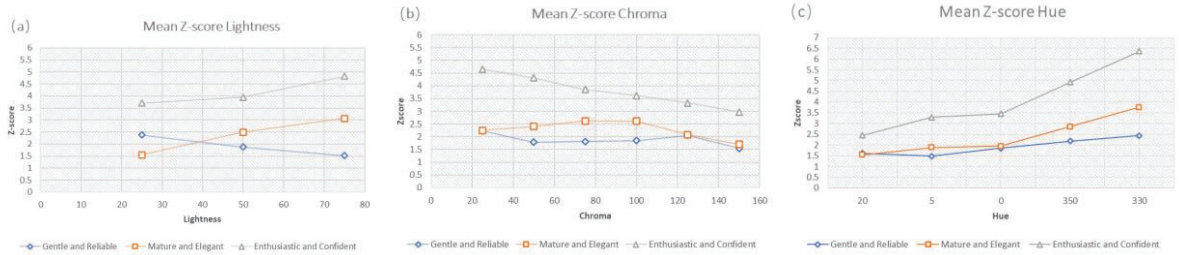

Figure 1: Mean Z-score for different lightness(a), chroma(b) and hue(c)

As the experimental was combine Yes/No experiment and categorical judgement, the 5-level judgement results of both traits were combined. The z-scores between 1 and 5, referred as the results of Gentle, Mature or Enthusiastic. The z-scores between 5 and 10 referred as the results of Reliable, Elegant, or Confident. Figure 1(a) indicated that the z-scores for both Gentle, Reliable and Mature Elegant increase as the lightness of the lip color increases. while the z-score for Enthusiastic and Confident decreases as lightness increases. Chroma value only affects Enthusiastic and Confident, while z-score decreases as chroma increases. Figure 1(c) showed the z-scores of each attribute change along with the hue angle. The attributes, Gentle and Reliable, were found closely related with the hue angle. While hue angle drops to 20°, the z-score of Gentle and Reliable increases, which indicated that the impression of the lip color in terms of Gentle and Reliable appear to be stronger; Conversely, as hue angle rises 330°, the impression of the lip color in terms of Gentle and Reliable decrease. Meanwhile, Elegant and Mature increase as hue rises toward 330°.

Note that the z-score of Enthusiastic and Confident is above 5 while the hue angle equals 20° when lightness is the independent variable. This indicated that z-score only leans toward Confident. Similarly, the z-score of Enthusiastic and Confident is above 5 while the hue angle equals 330° when lightness is the independent variable, which also indicated that z-score only leans toward Confident.

DISCUSSION AND CONCLUSION

The results of the study indicate that social signals exhibit variation in accordance with changes in CIE LCh values. This study explores the impact of lipstick color on social signaling among the Z-generation, offering valuable insights into contemporary identity construction, aesthetic standards and interactional patterns. The findings provide a valid example for understanding the behaviors in socio-cultural dynamics in the digital age.

Based on the analysis and summary above, it can be concluded that colors leaning toward orange with low chroma and high luminance evoke a stronger sense of gentle and reliable, and hue is the most influential factor. Colors with a purple hue, low luminance, and low chroma evoke a stronger sense of elegant and mature. Colors with low luminance and high chroma evoke a stronger sense of Confident and passionate. In this case, luminance is the most influential factor, while hue has little to no effect.

Compared with the previous research, both results showed that colors with high chroma could enhance emotional arousal and elicit feelings of excitement [12]. For the past research that related to the personality perception, colors with high chroma are found to be associated with extroverted personality[13]. These findings also provide valid evidence that high chroma lipstick colors could be used to deliver extroverted social signals. In this study, the lightness was found to be related to the matureness, where the low lightness lipstick color indicated a high matureness. This could because the low lightness colors related to dominance and power [14]. This finding provide a valid example of color in social signalling.

REFERENCES

[1]. Poggi, I., D'Errico, F., & Vinciarelli, A. (2012). Social signals: from theory to applications. Cognitive Processing, 13(2), 189–196.

[2]. Vinciarelli, A., Pantic, M., Bourlard, H., & Pentland, A. (2008). Social signals, their function, and automatic analysis: a survey. Proceedings of the 10th International Conference on Multimodal Interfaces (ICMI'08), 61–68.

[3]. Etcoff, N. L., Stock, S., Haley, L. E., Vickery, S. A., & House, D. M. (2011). Cosmetics as a feature of the extended human phenotype: modulation of the perception of biologically important facial signals. PLoS ONE, 6(10), Available from: https://journals.plos.org

[4]. Kiritani, Y., Ushikubo, M., & Takano, R. (2004). Impressions of color combination of make-up cosmetics in different media. Journal of Japan Society of Kansei Engineering, 5, 27–32.

[5]. Hadiyansyah, D., Bawarti, E., & Ulfa, M. (2023). Lipstick as female students' visual communication strategy. RSF Conference Series: Business, Management and Social Sciences, 3(2), 1–8.

[6]. Tian, B., Gong, H., Chen, Z., Yu, X., Pointer, M. R., Yu, J., Yu, F., & Liu, Q. (2023). Assessment of color preference, purchase intention and sexual attractiveness of lipstick colors under multiple lighting conditions. Frontiers in Neuroscience, 17, from: https://www.frontiersin.org

[7]. Guéguen, N. (2012). Does red lipstick really attract men? An evaluation in a bar. International Journal of Psychological Studies, 4(2), 206–209.

[8]. Zhang, T. (2019). Psychological effects of lipstick colors and the situational nature of their selection. Journal of Nanjing Normal University (Social Science Edition), 2019(6), 71–82.

[9]. Xingshi Anjian. (2022). 2022 Consumer insight analysis report on the lipstick market. [Accessed 9 June 2016]. Available from: https://www.xingshianjian.com

[10]. Melyanita, Y., & Yulianita, N. (2023). The use of makeup as a form of self-image for Generation Z. Bandung Conference Series: Public Relations, 3(2), 634–641.

[11]. Thurstone, L. L. (1927). Three psychophysical laws. Psychological Review, 34(6), 424–432.

[12]. Valdez, P., & Mehrabian, A. (1994). Effects of color on emotions. Journal of Experimental Psychology: General, 123(4), 394–409.

[13]. Adams, F. M., & Osgood, C. E. (1973). A cross-cultural study of the affective meanings of color. Journal of Cross-Cultural Psychology, 4(2), 135–156.

[14]. Pazda, A. D. (2015). Colorful personalities: Investigating the relationship between chroma, person perception, and personality traits. Doctoral thesis, University of Rochester, Available from: https://urresearch.rochester.edu

Effect of Appearance of Damascus Steel Knives on Visual Impression - Comparative Analyses of Observer Nationality -

Rino Nomoto[a*], Mikiko Kawasumi[a], Toshihiko Tsukada[b],
Chanprapha Phuangsuwan[c], Kitirochna Rattanakasamsuk[c], and Uravis Tangkijviwat[c]

[a]*Meijo University, Aichi, Japan*
[b]*Aichi Institute of Technology, Aichi, Japan*
[c]*Rajamangala University of Technology Thanyaburi, Pathumthani, Thailand*
[*]*Corresponding author: Rino Nomoto, 210441110@ccmailg.meijo-u.ac.jp*

ABSTRACT

Damascus-patterned knives, produced through multi-layer clad steel, are globally valued for both their functional quality and distinctive aesthetic appeal. The visual contrast between different cladding metals on the blade surface strongly influences customer preference. This study aims to clarify the variations in the visual impression of Damascus patterns using data science techniques and to explore their application in product development. In a previous study, four prototype knives with distinct Damascus patterns, developed in collaboration with a Japanese steel manufacturer, were presented to 76 participants from Japan and China. Results showed that contrast between layers and mirror-like reflection significantly shaped perceptions of “luxury” and “preference,” with nationality preference trends. Building on these findings, this study engaged approximately 150 observers from Japan, Asia, Europe, and America. Ten Damascus-patterned kitchen knives (65 layers, 18 cm blades) were prototyped and used as visual stimuli. Participants evaluated surface appearance using 16 adjectives on a seven-point scale. Analysis revealed that Thai participants associated “mirror-like” and “visually sharp” attributes with an “elegant” impression, whereas Japanese participants considered more ambiguous patterns to be “elegant.” Principal component analysis identified both shared and divergent impression structures between Japanese and non-Japanese observers, suggesting that cultural familiarity and past exposure to Damascus patterns strongly shape preferences. Future research will aim to refine these analyses, clarifying the relationship between manufacturing conditions and aesthetics to support the development of Damascus products tailored to regional markets.

Keywords: *visual impression, clad steel, Damascus pattern, nationality*

INTRODUCTION

The Damascus pattern, a hallmark of high-end blades, is produced through multi-layer clad steel[1, 2]. Its unique, decorative appearance enjoys strong international popularity. This study seeks to establish new value in Damascus products by identifying visual features most attractive to customers across different regions.

In earlier studies, numerous Damascus-patterned kitchen knives were prototyped through joint collaboration with a steel manufacturer. Surface properties, including color and gloss, were measured using spectrophotometry and gloss meters, while 76 Japanese and Chinese participants evaluated the visual impression of four selected knives. Results indicated that contrast between layers and mirror-like reflection were decisive in shaping impressions of “luxury” and “preference.” Clear differences also emerged across gender and nationality[3]. For example, men generally preferred two-layered high-contrast, high-contrast patterns more strongly than women, while Chinese participants expressed stronger preferences for such designs compared to Japanese participants.

This study expands on this work by assessing impressions of Damascus patterns among participants from a wider range of countries and comparing their responses.

METHODOLOGY

Ten Damascus-patterned kitchen knives (65 layers, 18 cm blades) were specially prototyped in collaboration with a steel manufacturer for these experiments (Figure 1). Each knife featured wood-grain-like striped patterns, with varying reflective properties between steel layers, producing a distinct appearance with diverse texture and contrast. Sixteen adjectives, such as “mirror-like,” “visually sharp,” “elegant,” “beautiful,” and “favorite,” were prepared in Japanese, English, and Thai (Table 1). Each knife was displayed individually in an experimental booth (40 × 40 × 40 cm) under daylight LED lighting (500 lux on the blade surface). Participants viewed each knife from multiple angles and rated their impressions using a seven-point Likert scale (0–6) (Figure 2).

After the evaluation, participants completed a questionnaire on nationality, gender, age, and prior experience with Damascus-patterned knives. The experiment took approximately 30 minutes to conduct per participant. In total, 148 participants to ok part: 63 Thai, 57 Japanese, 8 Chinese, 6 Taiwanese, 4 Korean, 1 Indonesian, 4 Mexican, 2 American, 1 Brazilian, 1 Norwegian, and 1 Bulgarian.

Collected data were analyzed using principal component analysis (PCA) to compare impression structures across observer groups.

Figure 1: Damascus-patterned knives

Table 1: Sixteen adjectives

	Japanese	English	Thai language
1	光沢のある	mirror-like	เงางาม
2	温かい	warm	อบอุ่น
3	シャープな	straight-lined	คม
4	平面的な	flat	แบนราบ, ไม่มีมิติ
5	メリハリのある	visually sharp	ลวดลายชัดเจน
6	強い	strong	แข็งแกร่ง
7	複雑な	complicated	ลวดลายซับซ้อน
8	華やかな	gorgeous	เจิดจรัส
9	先進的な	advanced	ล้ำสมัย
10	上品な	elegant	ประณีต
11	スタイリッシュな	stylish	มีสไตล์
12	独創的な	unique	มีเอกลักษณ์เฉพาะตัว
13	神秘的な	mysterious	ลึกลับ
14	高級な	luxury	หรูหรา
15	美しい	beautiful	สวยงาม
16	好みの	favorite	ชอบ

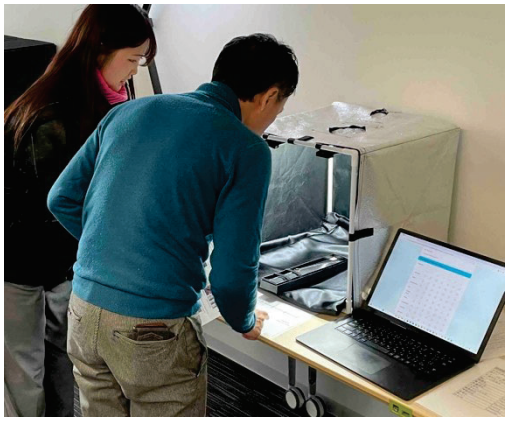

Figure 2: Evaluation scene

RESULTS AND DISCUSSION

Figure 3 presents the Likert-scale scores for "visually sharp" and "elegant" impressions of Damascus patterns A–J, separated by Japanese observers (N = 57) and Thai observers (N = 63). The score differences across patterns were more pronounced for "visually sharp" than for "elegant." This suggests that participants found it easier to evaluate "visually sharp," as it is linked to a more tangible physical attribute. Notably, patterns D, G, H, and J received high scores for both nationalities. Further analysis confirmed that "visually sharp" strongly correlated with impressions of "gorgeous" and "luxury." In contrast, evaluation of "elegant" differed between Japanese and Thai observers for these same patterns. This indicates that the concept of elegance in Damascus knives may vary cross-culturally, reflecting aesthetic frameworks.

Figure 4 compares two subgroups of Japanese observers: those familiar with Damascus knives and those who are encountering them for the first time. Observers with prior experience rated patterns A and B as more "elegant." These two knives have been long available commercially, while the remaining eight patterns were newly prototyped for this experiment. This suggests that familiarity with previously marketed designs contributed to stronger impressions of elegance.

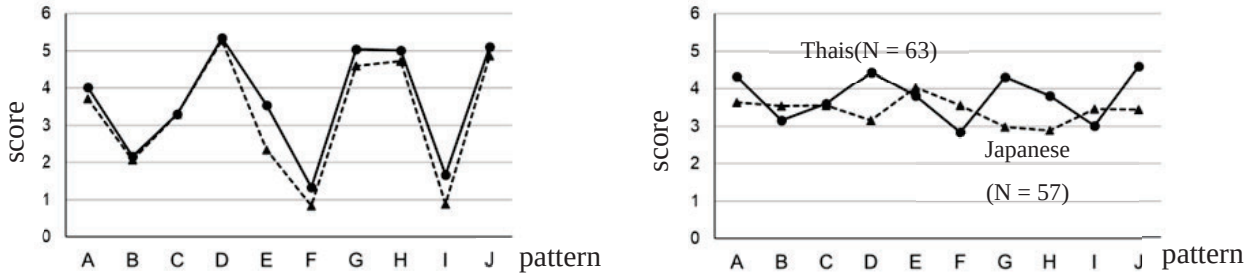

"visually sharp" "elegant"

Figure 3: Comparative scores for "visually sharp" and "elegant" impressions by Japanese and Thai

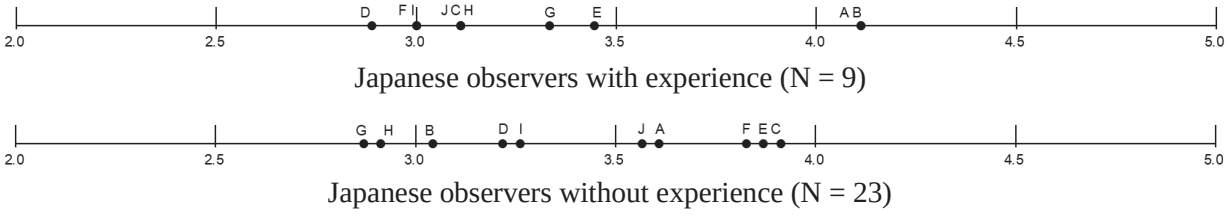

Figure 4: Comparative scores for "elegant" between experienced and first-time observers

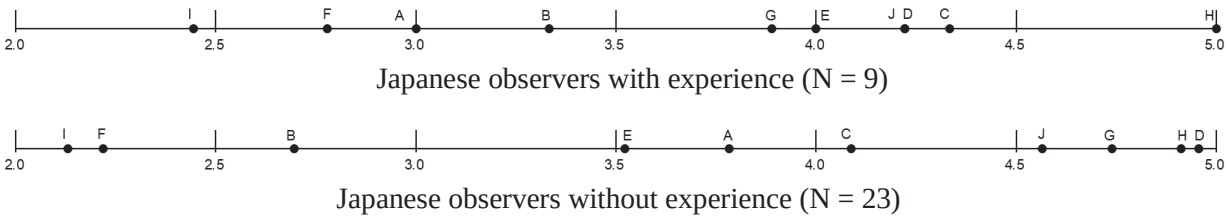

Figure 5: Comparative scores for "unique" between experienced and first-time observers

Scores for "unique" are shown in Figure 5. When compared with the "visually sharp" results in Figure 3, clear differences emerged between experienced and inexperienced observers. First-time observers tended to equate "unique" with high visual sharpness, whereas experienced observers considered unfamiliar or novel designs as more unique, even if they were less sharp in appearance.

Finally, the results of the PCA using selected ten adjectives are summarized in Table 2 and illustrated in Figure 6. Table 2 presents components with a contribution rate of 10% or more, while Figure 6 plots the positioning of ten Damascus patterns in the PCA score space. Both Japanese and Thai groups revealed two main components. However, the distribution differed: Japanese scores spread across four directions in the two-dimensional space, whereas Thai scores clustered more tightly, with patterns D, J, H, and G positioned close, producing three main directions.

Table 2: PCA results for Japanese and Thai participants (components ≥10% contribution)

Japanese participants (N = 57)

Variable name	PC1	PC2
mirror-like	0.975	-0.033
warm	-0.840	0.194
straight-lined	0.957	-0.089
visually sharp	0.957	-0.164
gorgeous	0.958	-0.108
advanced	0.956	-0.015
elegant	-0.515	0.844
stylish	0.972	0.137
beautiful	0.875	0.455
favorite	0.793	0.581
Eigenvalue	7.979	1.361
Contribution rate	0.798	0.136
Cumulative contribution rate	0.798	0.934

Thai participants (N = 63)

Variable name	PC1	PC2
mirror-like	0.865	-0.228
warm	-0.182	0.967
straight-lined	0.915	-0.105
visually sharp	0.901	-0.086
gorgeous	0.974	-0.102
advanced	0.983	0.054
elegant	0.947	0.107
stylish	0.963	0.130
beautiful	0.957	0.239
favorite	0.956	0.144
Eigenvalue	7.999	1.125
Contribution rate	0.800	0.113
Cumulative contribution rate	0.800	0.912

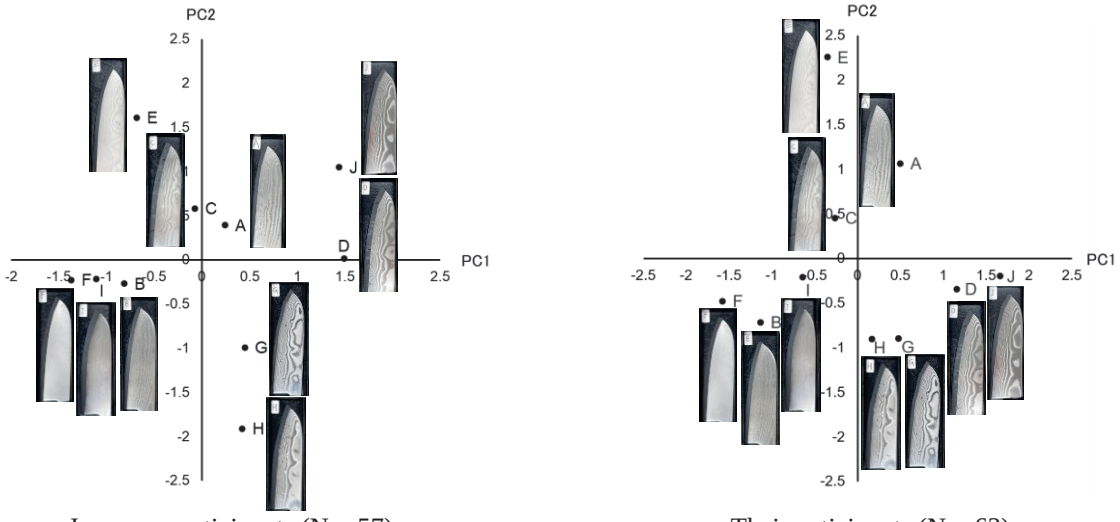

Japanese participants (N = 57) Thai participants (N = 63)

Figure 6: Positioning of ten Damascus pattern on PCA score diagrams

CONCLUSION

This study examined the visual impression of Damascus knife patterns among participants of different nationalities, with particular comparison between Japanese and Thai observers. Results highlighted clear cultural differences: Japanese and Thai participants diverged in their evaluation of “elegant” impressions, while both groups associated “visually sharp” with luxury-related attributes. Prior experience with Damascus knives also influenced perception. Experienced observers tended to associate elegance with familiar commercial patterns, whereas first-time observers linked sharpness directly with uniqueness.

These findings suggest that both cultural background and prior exposure significantly shape aesthetic impressions of Damascus knife patterns. Future research will focus on quantifying the color and reflective properties of the steel surface and linking these measurements to perceptual evaluations, thereby informing the design of Damascus products tailored to diverse regional markets.

ACKNOWLEDGEMENTS

This research was conducted with the support of a joint research manufacturer that provided prototyping of the Damascus-patterned knives. We extend our gratitude to the participating universities, companies, local communities in Japan, and exchange students at Meijo University. We also thank the researchers and staff of Color Research Center at Rajamangala University of Technology Thanyaburi in Thailand for their collaboration in the experiments.

REFERENCES

[1] Yamamoto, T. (2016). Kitchen knife materials: Echizen forged blades. *Chemical Education*, 64(11), pp. 564-565. https://doi.org/10.20665/kakyoshi.64.11_564

[2] Papadatu, C. P., Obreja, D. B., Adam-Papadatu, I. C., & Sandu, I. G. (2023). Learning from the Past: The reconstruction of the original Damascus Steel. *International Journal of Conservation Science*, 14(3), pp. 871-886. https://doi.org/10.36868/IJCS.2023.03.07

[3] Kawasumi, M., & Tsukada, T., (2022). Studies on Improving Kansei Quality for Damascus Patterned Steels. *Proceedings of the 17th Spring Conference of the Japan Society of Kansei Engineering*, 2B01-02.

Observation of Color and Gloss Change during Drying of Particulate Suspension in Polymer Solution Using A Noncontact 2D Colorimetric System with Dome Illumination

Mei Higuchi [a], Shoki Yamamoto[a], Ayumu Kinugawa[a], Hiroyuki Iyota[a],
Hayato Masuda[a], Hironobu Imakoma[a], and Hideki Sakai [b]

[a]*Graduate School of Engineering, Osaka Metropolitan University, Osaka, Japan*
[b]*Graduate School of Human Life and Ecology, Osaka Metropolitan University, Osaka, Japan*
**Corresponding author: Hiroyuki Iyota, h-iyota@omu.ac.jp*

ABSTRACT

Drying is a widely used heat treatment process for industrial products and foodstuffs. Understanding and predicting the effects of drying conditions and the moisture content of the target material on appearance characteristics, such as gloss and color, and controlling the drying process are extremely important for quality control. Diffuse and specular reflections occur when the surface of an object is illuminated. The color of an object is perceived by the diffuse reflected light. Two types of glosses exist: specular and psychological. Specular gloss is perceived through specular reflections. This study aims to clarify the relationship between the drying characteristics of paint films and their visual appearance. We observed the changes in the color and gloss during paint film drying using a color measurement system consisting of an illuminating device modeled on an integrating sphere and a digital camera. This color measurement system allows for noncontact, long-term observation and can obtain images that include specular components as well as those that do not. The sample used was a polyvinyl alcohol aqueous solution with dispersed particles, and silica powder and pigment (chromium oxide) were used as particles. In the samples with dispersed silica powder, as drying progressed, the surface gloss decreased and the brightness increased. In samples with dispersed pigments, changes in color distribution caused by water evaporation were observed. The color measurement system used in this study enables two-dimensional observations during the drying process.

Keywords: noncontact colorimetry, wetted surface, translucent material, food processing, coating film

INTRODUCTION

In industrial products, coatings are used to protect product surfaces and add aesthetic value [1]. During the drying of paint or coating material, the movement of the contained particles, such as pigments and microparticles, within the paint, caused by moisture evaporation and gravitational effects, can cause changes in gloss, color, and color distribution. However, few reports have quantitatively measured the temporal changes in color and gloss associated with the drying of materials containing moisture on their surfaces. This is because of the difficulty in measuring materials with moisture on their surfaces using conventional color measurement methods, and the fact that the surface layer is semi-transparent. Furthermore, mathematical models describing these phenomena have not yet been developed.

This study aims to clarify the relationship between the drying characteristics of paint films and their visual appearance. First, we measured the changes in the color and gloss during the drying of a translucent polymer

aqueous solution (Polyvinyl alcohol (PVA) solution) containing dispersed pigments and silica particles. The color measurement apparatus consisted of a dome-shaped illumination device and digital camera, enabling noncontact color measurement and prolonged temperature and humidity monitoring [2][3]. This report presents a method for observing wet surfaces and describes the coating film model specimens used in the observations and their respective drying procedures.

NONCONTACT 2D COLORIMETRIC SYSTEM WITH DOME ILLUMINATION

Figure 1 shows the color measurement device. The light source used was LED lighting with a color rendering index of 95 and color temperature of 6,500 K, which simulates a D65 light source. A dome with a diameter of 70 cm, designed to mimic an integrating sphere with a white interior, allowed measurements to be obtained in a space in which light was uniformly irradiated. A digital camera was used as a light-receiving unit. Moreover, light traps, which blocked light from a certain direction, were installed at 30° intervals over a 60° range. Twelve photographs were captured while the light traps were rotated in 30° increments. During the measurement, two types of images were captured: one of a 0.2 mm thick white resin plate (TAMIYA PLA-PAPER 0.2 mm B4 SIZE, Shizuoka, Japan) as a reference for shading correction, and another of the object along with a color chart (ColorGauge Pico Target, Image Science Associates, NY, USA) and an iron ball used to confirm the rotation of the light trap on the white resin plate.

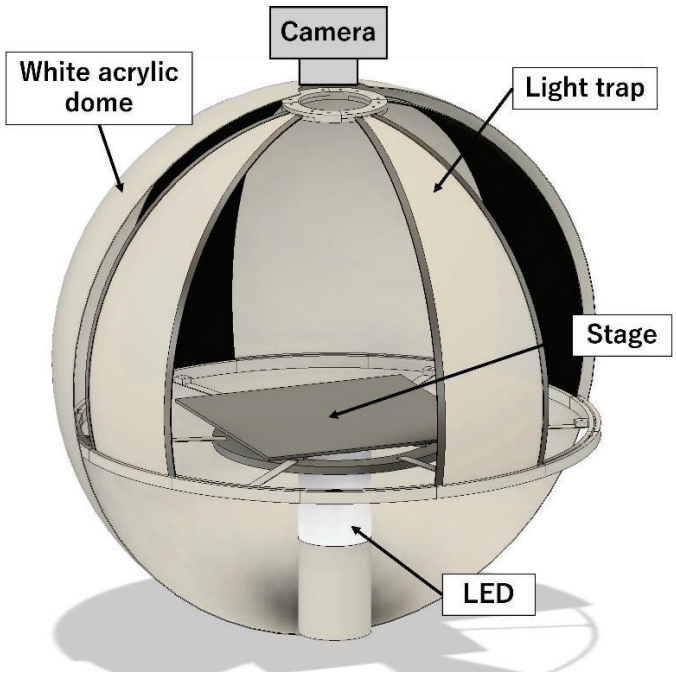

Figure 1: Noncontact 2d colorimetric system with dome illumination

The images of the target object, iron ball, and color chart were corrected for shading correction using only the images of the white resin plate. Color correction was then applied to each pixel based on a color chart. After shading and color corrections, the sRGB values of the images were read and converted into $L^*a^*b^*$ values. Twelve images captured during one rotation of the light trap were compared pixel-by-pixel. A specular component-included (SCI) image was created by collecting pixels with the highest L^* values, that is, the brightest pixels, and a specular component-excluded (SCE) image was created by collecting pixels with the lowest L^* values, that is, the darkest pixels. Subsequently, the two images were combined.

EXPERIMENT

In this study, to investigate the effects of particles on the appearance of the coating film during drying, samples were prepared by coating two types of particle suspensions in polymer solutions onto hydrophilic-treated polyester film. To prepare the sample, distilled water was first placed in a container, and silica powder (TMS-15, Particle size: 15 μm, TAYCA Corp., Osaka, Japan) was gradually added while stirring with a magnetic stirrer. PVA (FUJIFILM Wako Pure Chemical Corp., Osaka, Japan) was then added slowly with continuous stirring, and the mixture was allowed to hydrate for 20–30 min. After hydration, the mixture was heated at 90 °C for 60–90 min in a constant-temperature bath with stirring, and subsequently cooled to below 50 °C while stirring. The mixture was left at room temperature for one day and subsequently degassed. The same procedure was used for the pigment-containing mixture (green matte color: chromium oxide, Mono Co., Ltd., Tokushima, Japan). Before its application to the hydrophilic film, the mixture was stirred to prevent particle sedimentation. A flame-retardant, thermally conductive, double-sided polyester tape was attached to a 50 × 50 mm area on an 80 × 80 mm hydrophilic film substrate, and the mixture was blade-coated onto this area to form a coated sample. The details of the coated samples are listed in Table 1.

Table 1: Details of the coated sample

Object	**Sample 1 slurry paint [Silica Powder-Mixed Coating]**	**Sample 2 color paint [Pigment-Mixed Coating]**
PVA concentration	approx. 10.5 w/w $_{solvent}$ %	approx. 9.1 w/w $_{solvent}$ %
Added substance and concentration	15 μm silica powder	Green matte color pigment
	approx. 1.1 w/w $_{solvent}$ %	approx. 1.0 w/w $_{solvent}$ %
Size [mm]	50 × 50	50 × 50
Thickness [mm]		
(before drying)	approx. 0.75	approx. 0.75
(After drying)	approx. 0.045	approx. 0.040
Substrate film	Hydrophilic-treated polyester film with a thickness of 0.1 mm	
Base color	Black	White

The prepared coating samples were placed on the device stage, photographed hourly, and image processing was performed.

RESULTS AND DISCUSSION

First, we describe the drying process of the slurry coating of sample 1. Figure 2 shows the images captured before and after drying, with the light trap positioned at a fixed location. These images were corrected for shading correction and color. Gloss is determined by the intensity of the specular reflection and the absence of diffuse reflection. On glossy surfaces, the reflected image of an object appears sharply defined. As shown in Figure 2, the sharpness of the light-trap image reflected from the coating film differed before and after drying. Therefore, gloss was evaluated by analyzing the sharpness of the reflected light-trap image. Specifically, the L^* values were extracted along a straight line drawn perpendicular to and crossing the boundary of the reflected image to capture the transition from the inside to the outside of the reflection (the measurement direction is indicated by an arrow in Figure 3). The extracted values were plotted on a graph, and the maximum absolute value of the first derivative was calculated to

quantify the sharpness of the boundary. This procedure was applied to both before and after drying images for comparison. The calculation results and corresponding graphs are shown in Figure 3. The after drying values were lower, indicating a decrease in the clarity of the reflected image and thus, a reduction in gloss compared to the before drying state. This reduction was attributed to the silica particles rising to the coating surface during the drying process, creating surface irregularities that diminish the gloss.

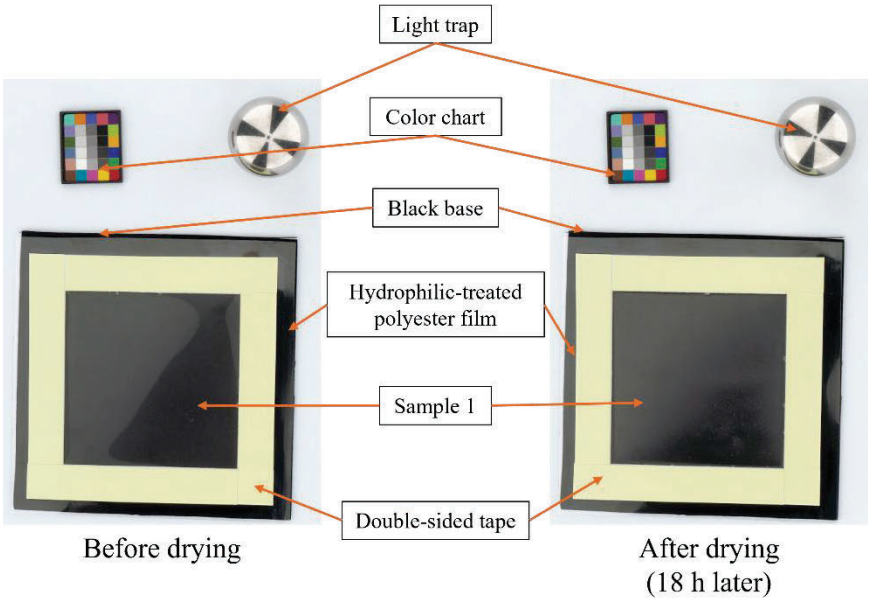

Figure 2: Sample 1 slurry paint before and after drying

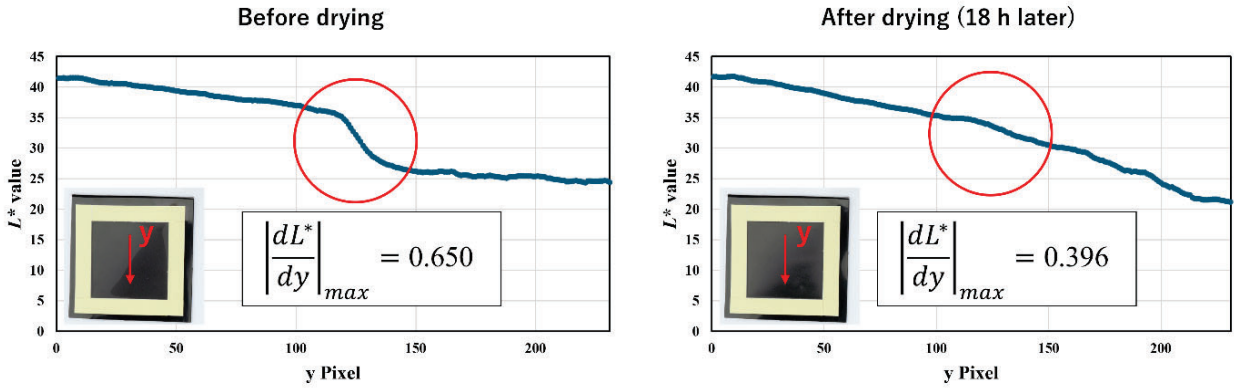

Figure 3: *L profiles and differences along the red arrow crossing the reflection boundary**

Next, we describe the drying process for sample 2. Figure 4 shows the average *L*a*b** values obtained from a 31,396-pixel area (a circular region with a radius of 100 pixels) at the sample center, calculated from the hourly captured SCE images. Color changes were observed in the coated samples due to drying. From the start of drying up to approximately 9 h, the absolute values of *L**, *a**, and *b** increased and then decreased. After approximately 14 h, these values remained almost constant.

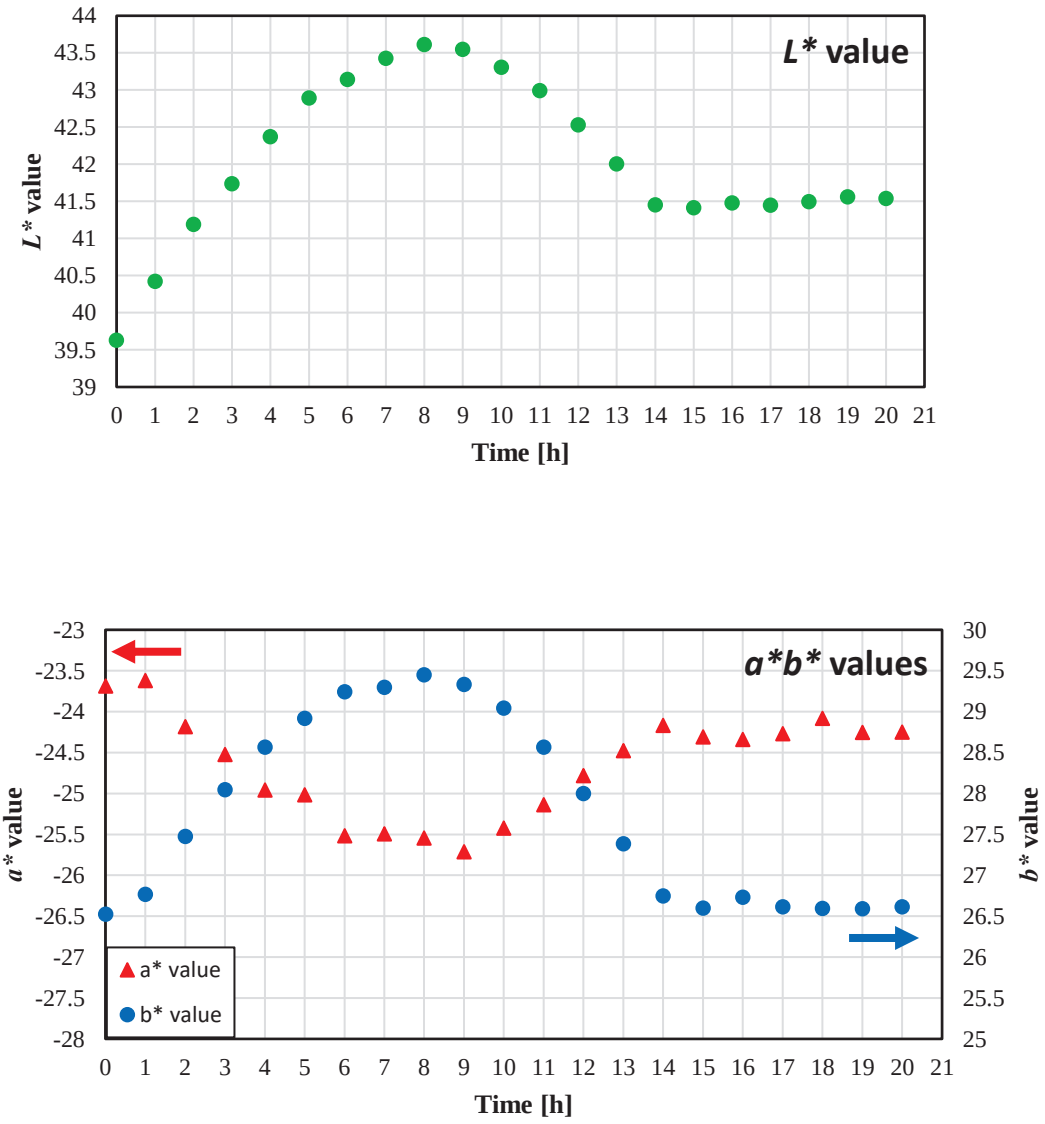

Figure 4: Changes in *L*a*b values of Sample 2 color paint during drying**

CONCLUSION

We investigated the changes in the appearance of the coating films during drying using a noncontact 2D colorimetric system with dome illumination. The appearance of the PVA aqueous solution coatings mixed with silica powder was measured throughout the drying process. The results reveal that the gloss differed before and after drying because of particle exposure on the coating surface during drying. Furthermore, when observing the PVA aqueous solution coatings containing dispersed pigment particles, color changes in the coating samples were observed as moisture evaporated. These results suggest that the color measurement system used in this study enables two-dimensional observations during the drying process.

In future work, we plan to conduct experiments while simultaneously measuring the mass and temperature of the coated samples to elucidate the relationship between drying conditions and visual appearance. Additionally, we attempted to model the motion of the particles within the coating film. Although this study focused on film coatings, we aim to extend our measurements and investigations to food samples and other materials.

REFERENCES

[1]. Curak, M., Saranjam, N., & Chandra, S. (2019). Colour variation in drying paint films. *Progress in Organic Coatings,* 136*,* 105173.

[2]. Fukagawa, S., Iyota, H., Sakai, H., & Isomi, M. (2021). Development of color and gloss measurement system with a wide range of temperature and humidity control unit. AIC 2021 Congress, Milan, Italy.

[3]. Kinugawa, A., Iyota, H., Fukagawa, S., Masuda, H., & Sakai, H. (2021). Observation of color and gloss change during thawing of foods using a non-contact 2D measurement system with a digital camera, Proc. of the 6th Asia Color Association Conference, Yogyakarta, Indonesia.

Effect of ipRGC Response on Contrast Sensitivity in Central Vision

Haruka Matsumoto[a], Masatoshi Ishigane[a], Hiroshi Takahashi[a*], Masahiro Suzuki[b], and Keiji Uchikawa[a]

[a]Kanagawa institute of Technology, Atsugi, Japan

[b]Notre Dame Seishin University, Okayama, Japan

*Corresponding author: htakahashi@ele.kanagawa-it.ac.jp

ABSTRACT

Since the discovery of intrinsically photosensitive retinal ganglion cells (ipRGCs), their roles have been investigated by vision researchers worldwide, particularly regarding their effects on non-image-forming functions such as circadian rhythm and the pupillary light reflex. Recent evidence suggests that ipRGCs may be involved in contrast sensitivity, a fundamental function of the human visual system. Therefore, this study aimed to clarify whether high luminance ipRGC stimulation affects contrast sensitivity in central vision. A silent substitution method was employed using a multichannel variable-wavelength light source to create background stimulus that selectively stimulated ipRGCs. The background stimuli divided into inner and outer regions. The test stimulus was a Gabor stimulus presented on a display. The results showed that greater outer background stimulus of ipRGCs was associated with higher contrast sensitivity, whereas reduced stimulus corresponded to lower contrast sensitivity.

Keywords: ipRGC, contrast sensitivity, central vision, inner background stimuli, outer background stimuli

INTRODUCTION

Until recently, it was believed that only two types of photoreceptors existed in the human retina: rods and cones. However, this theory was overturned with the discovery of intrinsically photosensitive retinal ganglion cells (ipRGCs) as a third type of photoreceptor. Since then, research on the role of ipRGCs has been conducted worldwide, particularly regarding their effects on non-image-forming functions such as circadian rhythm and the pupillary light reflex [1-4]. More recently, it has been shown that ipRGCs may also be involved in visual imaging systems such as color, brightness, and glare perception. Previous studies have suggested that ipRGCs are also involved in contrast sensitivity, a fundamental function of the human visual system. Chien et al. reported that increased melanopsin stimulation enhanced contrast sensitivity in peripheral vision [5], while Takahashi et al. suggested that high-luminance ipRGC stimulation may influence contrast sensitivity in the fovea [6]. However, as Takahashi et al. conducted their experiment under the condition of a uniformly stimulated background, it is unclear which range of the visual field was responsible for the effect. Therefore, in the present study, we aimed to determine which range of ipRGC stimulation affects contrast sensitivity in central vision by dividing the background stimuli into inner and outer regions.

METHODOLOGY

Experimental apparatus

Figure 1 shows the experimental apparatus. The experiment was conducted in a dark room. The heights of a multichannel variable-wavelength light source and a liquid crystal display were adjusted so their centers aligned. The subject's head was fixed on a chin rest and an acrylic-plate window was positioned directly in front of the subject's head for observation with the right eye only. The distance from the front of the subject's eye to the display was 1146 mm. The variable-wavelength light source was also placed at a viewing distance of 1146 mm from the front of the subject's eye, via reflection in a half-mirror. Transmittance and reflectance of the half-mirror were each 50%. An occluder of diameter of 5° was placed at the center of multichannel variable-wavelength light source 1. An additional occluder of diameter of 2° was placed at the center of multichannel variable-wavelength light source 2, along with a shield that blocks light in a range of 5° or more. This arrangement enabled the test stimulus generated by the display to be presented in the central 2° of the visual field while background stimuli generated by the multichannel variable-wavelength light source were presented as an inner background between 2° and 5° and an outer background between 5° and 10°. A non-light-transmitting black board was placed between the light source and the display to prevent mutual interference of these two light sources. Subjects provided their responses via a hand-held keyboard.

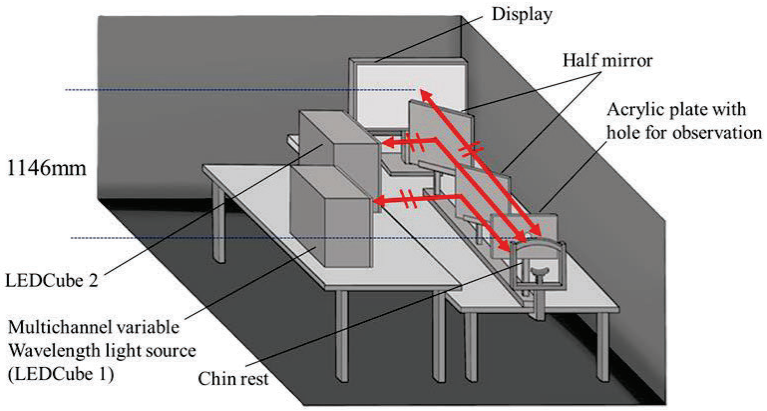

Figure 1: Experimental apparatus

Stimulus

Figure 2 shows an example of the experimental stimuli as observed by the subject. The stimuli were a test (Gabor) stimulus with a 2° center generated by the liquid crystal display, and 2°–5° inner and 5°–10° outer background stimuli generated by the multichannel variable-wavelength light source. The average luminance of the test stimulus was 10 cd/m^2. The spatial frequency of the Gabor stimulus was set to five conditions: 0.5, 1.3, 3.2, 8.0, and 20 cpd. We applied the silent substitution method and used the multichannel variable-wavelength light source to produce three types of light stimuli under high luminance conditions in which the rods are saturated. In the first type, the stimulus intensity of ipRGCs alone was changed, without changing the intensities of L, M, or S cones (ipRGC-variable stimulus; ip-v stimulus). In the second type, the stimulus intensities of L, M, and S cones and ipRGCs were all varied equally (energy-variable stimulus; e-v stimulus. In the third type, luminance and the intensities of L, M, and S cones were varied while ipRGC stimulus intensity was unchanged (luminance-variable stimulus; lum-v stimulus). The spectral distributions of the inner background stimuli are shown in Figures 3–5. The spectral distributions of the outer background stimuli are shown in Figures 6–8. In Figures 3 and 6, M is the reference (middle) stimulus intensity, ip-L indicates low stimulation of ipRGCs alone, and ip-H indicates high stimulation of ip-RGCs alone. In Figures 4 and 7, M is the reference stimulus intensity, e-L indicates reduced values of all stimuli in the photoreceptors, and e-H indicates increased values of all stimuli. In Figures 5 and 8, M is the reference stimulus intensity, lum-L indicates reduced values of stimuli in L, M, and S cones; and lum-H indicates

increased values of stimuli in L, M, and S cones. Two experimental conditions were tested: one in which the inner background stimulus was varied but the outer background stimulus remained constant, and the other in which the inner background stimulus remained constant while the outer background stimulus was varied.

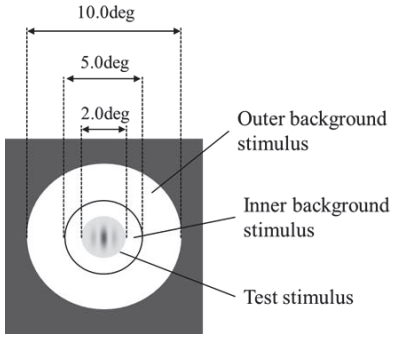

Figure 2: Diagram of experimental stimuli as observed by the subject

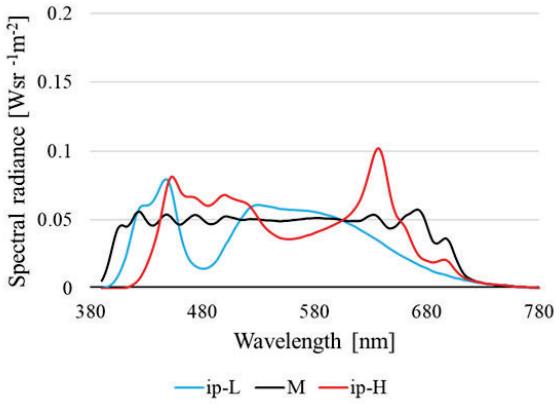

Figure 3: Spectral distributions of ip-v (inner)

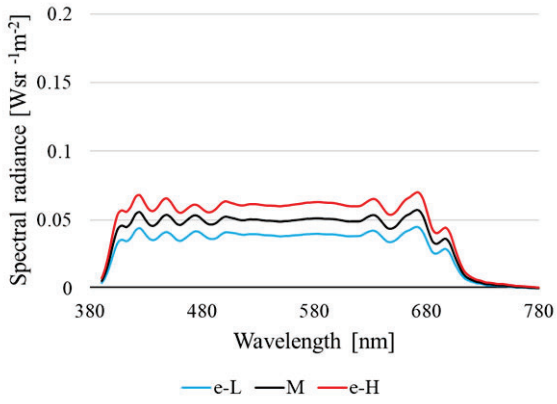

Figure 4: Spectral distributions of e-v (inner)

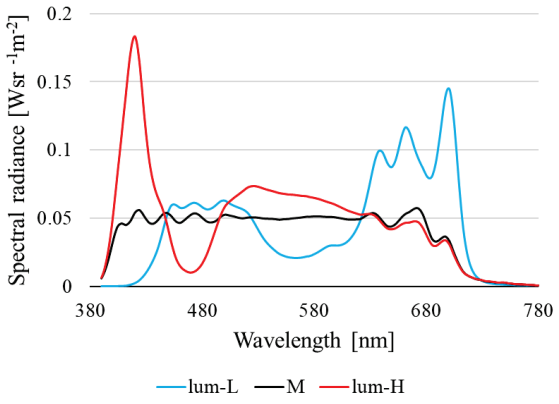

Figure 5: Spectral distributions of lum-v (inner)

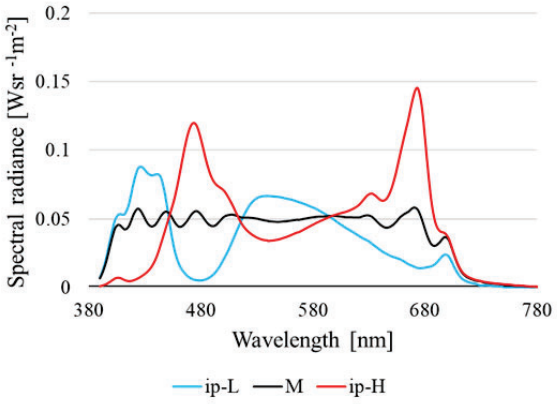

Figure 6: Spectral distributions of ip-v (outer)

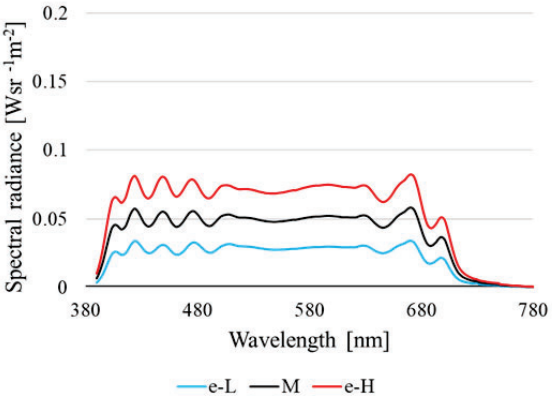

Figure 7: Spectral distributions of e-v (outer)

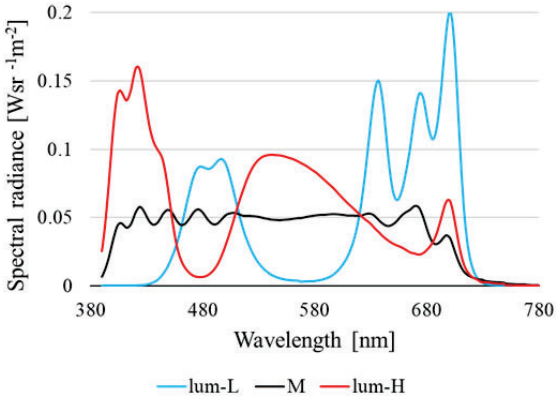

Figure 8: Spectral distributions of lum-v (outer)

Experimental procedure

The double-staircase method was used to measure the contrast sensitivity of the Gabor stimuli in five males in their 20s with normal vision, including corrected vision. After 10 minutes of dark adaptation, subjects were acclimatized to the display luminance for 2 minutes. The experiment was initiated by the subject pressing the enter key on the keyboard. A shutter sound was played at the start of the experiment, and again 1.5 seconds later. The test stimulus was presented for 1 second, to coincide with the onset of either the first shutter sound or the second shutter sound. The subject responded to the timing of the test stimulus using the two-interval forced-choice method, with a key press indicating whether the test stimulus appeared at the first or second shutter sound. The correctness of the response was fed back as a "ping-pong" or "boo" sound for correct and incorrect responses, respectively. After receiving feedback, the subject proceeded to the next trial, initiated by the first shutter sound. The contrast step was adjusted up or down depending on whether the subject's response was correct or incorrect.

The step size varied with spatial frequency, ranging from a maximum of 0.04 to a minimum of 0.02. Double-staircase method comprised 100 trials, and logistic regression analysis was used to determine the contrast threshold corresponding to a 75% correct response rate. Contrast sensitivity was calculated as the inverse of the contrast threshold.

RESULTS AND DISCUSSION

Relationships between the interindividual mean of contrast sensitivity and spatial frequency in the outer background stimulus, results for the ip-v condition, e-v condition, and lum-v condition are shown in Figures 9, 10, and 11, respectively. Spatial frequency (cycles per degree) is shown on the horizontal axis and contrast sensitivity on the vertical axis, with both axes on a logarithmic scale. Figure 9 shows that H had the highest contrast sensitivity at the peak sensitivity of spatial frequency, followed by M and L, in that order. In Figure 10, L had the highest contrast sensitivity in terms of peak spatial frequency sensitivity, followed by H and M, in that order. In addition, there was almost no difference in contrast sensitivity between M and H. In the e-v condition, all energy levels (the amount of stimulus given to each photoreceptor) increased equally from L to H. In the ip-V condition, only the amount of stimulation given to ipRGCs increased from L to H, while cone stimulation remained constant. These results indicate that greater ipRGC stimulation in the outer background stimulus enhances contrast sensitivity in central vision. Figure 11 shows that L has the highest contrast sensitivity in terms of peak sensitivity of spatial frequency, followed by H and M, in that order. In the lum-v condition, stimulus increased from L to H in terms of the amount of stimulation given to L, M, and S cones, whereas ipRGC stimulation remained unchanged.

Furthermore, in lum-L, the amount of stimulation to ipRGCs was relatively higher. This finding suggests that greater ipRGC stimulation in the outer background stimulus is associated with higher contrast sensitivity in central vision. For the inner background stimulus, there was almost no difference in contrast sensitivity among the L, M, and H stimulus levels in each condition.

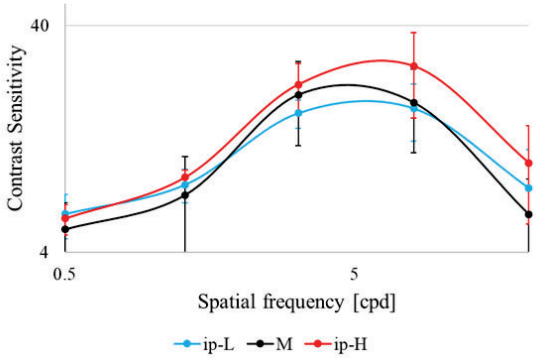

Figure 9: Relationship between the interindividual mean of contrast sensitivity and spatial frequency in the outer background stimulus ip-v condition (left)

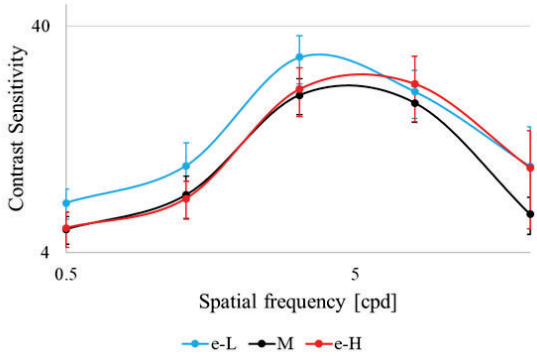

Figure 10: Relationship between the interindividual mean of contrast sensitivity and spatial frequency in the outer background stimulus e-v condition (right)

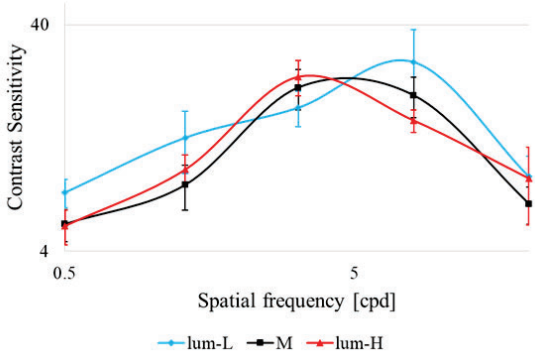

Figure 11: Relationship between the interindividual mean of contrast sensitivity and spatial frequency in the outer background stimulus lum-v condition

CONCLUSION

In this study, we investigated the effects of high luminance ipRGC stimulation on contrast sensitivity in central vision under the condition of fully saturated rods. Contrast sensitivity tended to increase with greater outer background stimulus of ipRGCs. These results suggest that ipRGCs in peripheral vision may influence contrast sensitivity in central vision.

This study was approved by the Ethical Review Board for the use of human subjects of Kanagawa Institute of Technology (No.20240722-02).

ACKNOWLEDGEMENTS

This work was supported by JSPS KAKENHI Grant Number JP24K15154.

REFERENCES

[1]. BERSON, D. M., DUNN, F. A., and TAKAO, M. 2002. Phototransduction by retinal ganglion cells that set the circadian clock. Science, 295(5557), 1070–1073.
[2]. HATTAR, S., LIAO, H. W., TAKAO, M., BERSON, D. M., and YAU, K. W. 2002. Melanopsin-containing retinal ganglion cells: Architecture, projections, and intrinsic photosensitivity. Science, 295(5557), 1065–1070.
[3]. VARTANIAN, G. V., LI, B. Y., CHERVENAK, A. P., WALCH, O. J., PACK, W., ALA-LAURILA, P., and WONG, K. Y. 2015. Melatonin suppression by light in humans is more sensitive than previously reported. Journal of Biological Rhythms, 30(4), 351–354.
[4]. BONMATI-CARRION, M. A., HILD, K., ISHERWOOD, C., SWEENEY, S. J., REVELL, V. L., SKENE, D. J., ROL, M. A., and MADRID, J. A. 2016. Relationship between human pupillary light reflex and circadian system status. PLoS ONE, 11(9), e0162476.
[5]. CHIEN, S., YEH, S., YAMASHITA, W., and TSUJIMURA, S. 2023. Enhanced human contrast sensitivity with increased stimulation of melanopsin in intrinsically photosensitive retina ganglion cells. Vision Research, 209, 108271.
[6]. TAKAHASHI, H., ISHIGANE, M., KURASHIMA, T., SUZUKI, M., and UCHIKAWA, K. 2025. Effect of ipRGC stimulation on contrast sensitivity in central vision. CIE 2025 Proceedings.

Differential Perceptions of Colour and Material in Fashion: A Multisensory Analysis of Designer and Consumer Responses

Xu Han[a*], Liting Li[b], Qi Xiang[a], Kaida Xiao[c], and Luwen Yu[ad]

[a]*The Hong Kong University of Science and Technology (Guangzhou), Guangzhou, China*
[b]*Academy of Arts & Design, Tsinghua University, China*
[c]*School of Design, University of Leeds, United Kingdom*
[d]*The Hong Kong University of Science and Technology, Hong Kong, China*
[*]*Corresponding author: Xu Han, xhan1230@gmail.com*

ABSTRACT

Colour and material are pivotal in fashion design, significantly influencing both consumers purchasing decisions and designers' creative processes. This study aims to delineate perceptual differences between designers and consumers concerning coloured fabrics, enhancing adaptability within the clothing market. Employing a multisensory evaluation approach, this research investigates the emotional impacts of fashion fabric colour and material on these two groups. The experimental setup involved 60 fabric samples across 20 colours and three materials (linen, cotton, silk), with 25 participants (13 professional designers and 12 general consumers) performing psychophysical visual-tactile assessments. Participants rated the samples on 7-point Likert scales measuring emotional dimensions such as coolness, activity, gender association, and likability. Concurrent measurements were taken of colour parameters (L*, a*, b*, C* and h) and tactile properties (resilience, softness, smoothness), and these were examined through correlation studies and multiple linear regression modeling to unearth group-specific cognitive patterns. Quantitative results illustrated material-dependent colour-emotion associations. Consumer fabric preferences correlated strongly with lightness (L*) values, notably in linen ($r = 0.669$) and cotton ($r = 0.470$). In contrast, chroma (C*) and hue (h) values mainly influenced designers' preferences, demonstrating a professional bias towards specific colour attributes. Regression analyses showed that designers' perceptions of coolness incorporated a complex integration of colour and tactile properties (adjusted $R^2 = 0.828$), reflecting a sophisticated, analytical approach to material characteristics. Conversely, consumers' likability was adversely affected by increased resilience and excessive smoothness (adjusted $R^2 = 0.318$), suggesting a preference for practical functionality over aesthetic details. These findings underscore the nuanced interplay between fabric attributes and emotional responses, highlighting the need for a balanced consideration of technical sophistication and utilitarian expectations in fashion development. The study provides empirical support for consumer-oriented textile research and development and establishes a theoretical basis for data-driven colour decision systems in the fashion industry, advancing our understanding of how material-chromatic interactions shape evaluations by professionals versus laypersons.

Keywords: Colour emotion, *Material perception, Visual-tactile evaluation, Fashion design, Consumer-designer di sparity*

INTRODUCTION

Fashion design represents a complex integration of colour and material properties, as designers work together to create garments that are both aesthetically compelling and functionally effective. While existing research has

established the individual importance of fabric colour (evoking emotional responses and cultural symbolism) and material (influencing sensory experience through texture, drape, and temperature regulation) [1], their combined impact on consumer perception remains underexplored. Colour psychology suggests that different hues evoke distinct emotional responses, but these effects are inevitably modulated by the material substrate to which they are applied [2].

Despite advances in understanding colour-emotion relationships and material handfeel properties, a significant gap persists in how these elements interact in multisensory perception, particularly across different evaluator groups. Previous studies have identified notable disparities between designers and consumers in evaluating luxury attributes [3] and tactile qualities [4], suggesting that professional training may fundamentally alter perceptual frameworks. Research further indicates that experts and untrained consumers employ different visual and tactile criteria when assessing fabric aesthetics [5], highlighting the need for comparative studies that account for expertise-based differences in multimodal perception. Moreover, the growing emphasis on customer-centered design approaches underscores the importance of understanding consumer perceptions in the development process [6].

This study aims to address these research needs through two clear objectives: 1) to identify and compare how colour attributes differentially influence emotional responses between professional designers and general consumers; and 2) to investigate how colour-tactile integration strategies vary between these groups across different material contexts.

METHODOLOGY

This study employed a multisensory experimental approach to investigate how colour and tactile properties shape emotional responses to fashion fabrics among professional and non-professional groups, aiming to systematically depict perceptual differences between designers and general consumers in evaluating coloured textiles. A total of 60 fabric samples were selected, comprising 20 prevalent colours widely used in the fashion industry, each rendered in three materials—linen, cotton, and silk—commonly adopted for summer apparel. All samples were plain-woven, solid-coloured, and matte-finished to minimize extraneous variables. Tactile properties (resilience, softness, and smoothness) were quantitatively assessed using a PhabrOmeter fabric evaluation instrument (Table 1), while colour parameters—L*, a*, b*, as well as the derived parameters of C* and h—were measured under D65 illumination using a VeriVide DigiEye system (Table 2).

Table 1: Average and SD of fabric tactile characteristics by PhabrOmeter.

Materials	Resilience (Mean±SD)	Softness (Mean±SD)	Smoothness (Mean±SD)
Linen	25.35±0.79	83.39±0.94	78.78±0.48
Cotton	17.01±2.27	77.05±2.16	83.49±1.84
Silk	12.69±1.14	91.16±0.55	85.40±0.65

Twenty-five participants (13 professional designers and 12 general consumers) took part in the experiment. Evaluations were conducted under combined visual-tactile conditions inside a standardized light booth with a neutral grey background (L* = 50) and a fixed viewing distance of 60 cm. All participants had received formal colour science training prior to the experiment. Each participant rated the samples along four emotional dimensions—warm-cool, calm-active, masculine-feminine, and dislike-like [7, 8]—using a 7-point Likert scale (e.g., -3 = very warm, 3 = very cool). The presentation order of samples was fully randomized to counterbalance order effects.

Emotional response data were converted to Z-scores to facilitate cross-group comparisons. Correlation analyses and multiple regression modeling were employed to examine the effects of colour and tactile attributes on

emotional outcomes, with particular emphasis on identifying differential patterns between designers and consumers. The study protocol was approved by the institutional ethics committee, and written informed consent was obtained from all participants.

Table 2: Colour parameters (L*, a*, b*, C* and h) values- 20 categories of coloured fashion fabric stimuli.

Colour	L*	a*	b*	C*	h	ΔE
Red	39.96	59.62	22.43	63.71	20.62	2.89
Pink	71.64	18.35	3.64	18.72	11.51	4.70
Yellow	72.31	8.92	59.47	60.20	81.78	7.44
Lime	73.07	-12.96	32.28	34.79	111.80	6.55
Orange	68.88	23.05	33.63	40.79	55.70	7.44
Light Yellow	80.61	-5.93	34.16	34.67	99.94	11.03
Nude	72.23	6.18	15.09	16.32	68.04	4.64
Beige	80.97	1.08	7.32	7.40	81.23	5.56
Denim Blue	43.12	-4.23	-17.65	18.32	256.15	4.78
White	84.81	-0.16	0.54	0.81	81.81	5.27
Light Gray	75.38	-0.23	-0.97	1.06	264.21	5.22
Light Blue	73.61	-4.66	-8.92	10.11	243.94	5.67
Cyan	81.73	-7.82	-0.90	7.92	185.72	4.82
Light Purple	74.04	6.39	-7.50	9.86	310.40	5.40
Dark Red	27.20	35.65	17.90	40.12	26.58	5.80
Navy Blue	21.53	1.06	-11.24	11.29	275.43	2.47
Green	41.44	-41.84	22.64	47.58	151.61	5.24
Purple	63.26	14.40	-13.80	20.00	316.68	5.92
Black	13.61	0.60	-0.99	1.87	288.89	4.49
Brown	51.29	9.56	17.20	19.68	61.03	4.19

RESULTS AND DISCUSSION

The results reveal consistent and divergent patterns in how designers and consumers perceive emotional characteristics of colours and materials in fashion fabrics (Figure 1). The most significant agreement was on colour temperature: both groups rated Light Blue and Cyan as the coolest colours, and Red and Dark Red as the warmest, aligning with classic colour theory.

However, notable differences emerged, particularly in neutral and achromatic colours. For beige, designers perceived it as neutral (-0.08) while consumers associated it with femininity (0.12). More notably, regarding preference (dislike-like) for nude tones, consumers showed pronounced aversion to these low-chroma neutral colours (-0.11) compared to designers who were relatively neutral (0.02). The most striking divergence appeared in achromatic colours: designers preferred White (0.63) and Light Gray (0.27), while consumers not very fond of these (White: 0.15, Light Gray: -0.37). For Black, designers perceived it as cool (0.23) with moderate preference (0.32), while consumers categorized it as warm (-0.35) with strong dislike (-1.78).

Beyond colour, significant differences existed in material perception (Figure 2). Both groups consistently rated silk as the most cool, active, feminine, and likable material. Linen was perceived as warmer and less feminine, while cotton occupied an intermediate position. The most striking differences emerged in preference (Dislike-Like dimension), designers showed stronger preference for Light Blue Linen while consumers disliked Black Cotton. In masculinity-femininity perception, designers consistently rated all materials as less feminine than consumers did. This systematic difference indicates designers may assess femininity through more technical lenses rather than

intuitive perception. This emphasizes the need for bridging perceptual gaps in textile design and marketing for summer fashion collections.

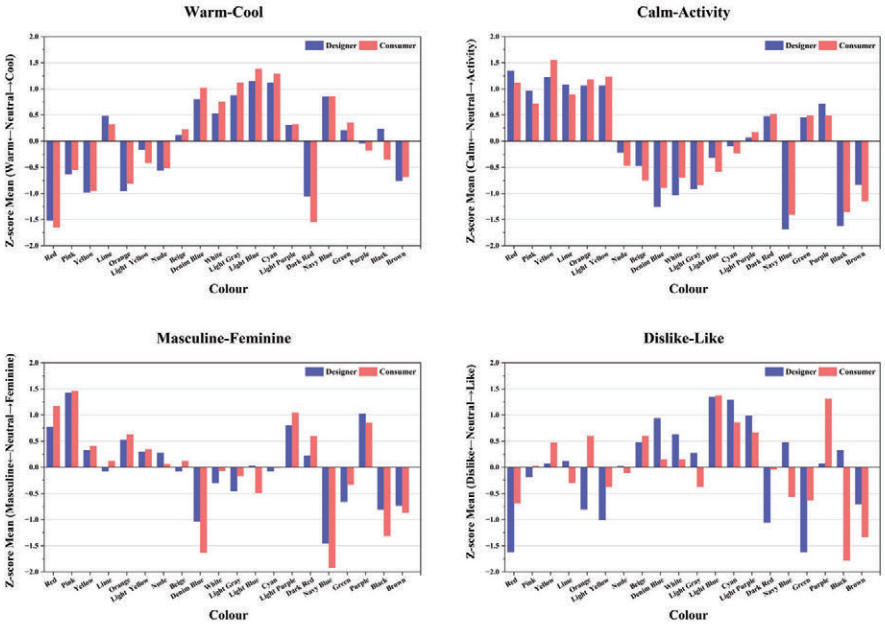

Figure 1: Comparison of Z-score mean for emotional responses to 20 coloured fabrics between designers and consumers

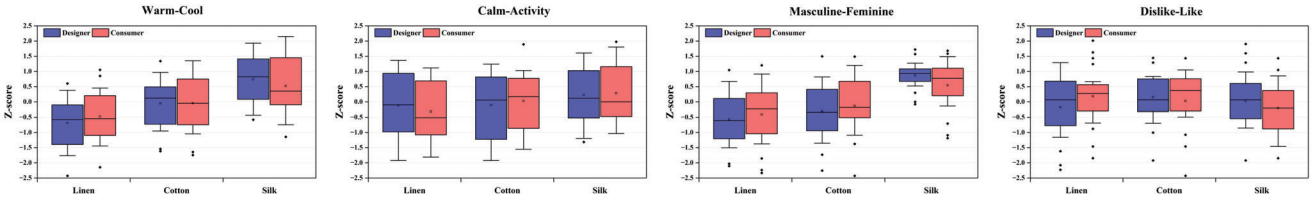

Figure 2: Distribution of Z-score values for emotional assessments by designers and consumers across linen, cotton and silk

These perceptual differences stem from distinct evaluation modes. Based on the correlation coefficients in Table 3, designers consistently demonstrate more complex and colour-driven evaluations: their perception of coolness in linen is more strongly guided by C* (r = -0.739) and h (r = 0.731), whereas consumers rely more on increased brightness (L*) to enhance the activity (r = 0.380) and femininity (r = 0.478) of linen.

This contrast is most evident in preference formation. Table 3 shows that designers display significant negative correlations with C* and b* across all materials, indicating a preference for less saturated and cooler tones. In contrast, consumers' cotton preferences are more influenced by brightness (L*) and improved softness (r = 0.431). Particularly for silk, designers uniquely associate increased resilience (r = 0.489) with greater liking—a relationship absented in consumer responses. These findings highlight the contrast between designers' analytically nuanced, colour-centric evaluation mode and consumers' greater sensitivity to brightness and tactile influences.

Table 3: Significant correlations between colour attributes, tactile properties, and emotional perceptions by material and group. (D: Designer, C: Consumer)

Materials	Component	Warm-Cool	Calm-Activity	Masculine-Feminine	Dislike-Like
Linen	L*		0.380 (C)	0.478* (C)	0.669** (C)
	a*	-0.754** (C)	0.313 (D)	0.461* (D)	-0.354 (D)
	b*	-0.630** (D)	0.602** (D)	0.370 (C)	-0.574** (D)
	C*	-0.739** (D)	0.786** (D)	0.422 (C)	-0.754** (D)
	h	0.731** (D)	-0.521* (D)	-0.434 (C)	0.592** (D)
	Resilience	0.397 (C)	-0.524* (D)	-0.533* (C)	0.312 (D)
Cotton	L*		0.348 (D)	0.461* (D)	0.470* (C)
	a*	-0.765** (D)	0.302 (D)	0.484* (C)	-0.389 (D)
	b*	-0.650** (C)	0.715** (C)	0.324 (C)	-0.395 (D)
	C*	-0.674** (C)	0.811** (C)	0.413 (C)	-0.520* (D)
	h	0.699** (D)	-0.550* (D)	-0.486* (C)	0.590** (D)
	Softness				0.431 (C)
Silk	L*			0.530* (C)	0.309 (C)
	a*	-0.650** (C)	0.373 (C)	0.557* (D)	
	b*	-0.697** (D)	0.761** (C)	0.326 (C)	-0.538* (D)
	C*	-0.735** (D)	0.833** (C)		-0.600** (D)
	h	0.583** (D)	-0.497* (C)	-0.370 (C)	
	Resilience				0.489*(D)
	Smoothness	0.337 (C)			

Table 4: Comparative regression model performance of emotional responses to colour and material properties between designers and consumers. (D: Designer, C: Consumer)

Emotion	Designer (Sig., Predictors, B)	Consumer (Sig., Predictors, B)	Adjusted R^2 (D/C)
Warm-Cool	a* (−0.023), b* (−0.024), Softness (0.032), Smoothness (0.131)	L* (0.011), a* (−0.025), b* (−0.026), Softness (0.030)	0.828 / 0.796
Calm-Activity	L* (0.013), a* (0.014), b* (0.029)	L* (0.010), a* (0.012), b* (0.030)	0.525 / 0.526
Masculine-Feminine	L* (0.018), a* (0.021), Resilience (−0.066), Softness (0.068)	L* (0.023), a* (0.025), b* (0.009), Resilience (−0.076), Softness (0.043)	0.630 / 0.604
Dislike-Like	L* (0.016), b* (−0.028)	L* (0.026), b* (−0.012), Resilience (−0.081), Smoothness (−0.166)	0.361 / 0.318

Regression analysis confirms distinct cognitive models underlying designers' and consumers' fabric evaluations (Table 4). Designers exhibit a systematic, multi-sensory integration of colour and tactile attributes,

forming a highly predictive model for coolness perception (Adj.R^2 = 0.828) that incorporates chromatic parameters (a, b) and textural nuances (softness, smoothness). In contrast, consumers rely more heavily on brightness (L*) and tactile comfort, showing pronounced aversion to excessive resilience and smoothness in preference formation. While both groups align closely in colour-driven activity assessment, they diverge significantly in femininity perception and likability. These results highlight designers' expert multi-attribute synthesis against consumers' pragmatic tactile sensitivity, underscoring the value of integrating both professional and end-user perspectives in textile development and marketing.

CONCLUSION

This study systematically reveals the fundamental differences between designers and consumers in multisensory fabric perception. While designers employ analytical, colour-centric models integrating complex tactile-colour interactions, consumers prioritize practical brightness and tactile comfort. These distinct cognitive frameworks—professional expertise versus intuitive sensitivity—highlight the critical need for bridging perceptual gaps in fashion design. The findings provide empirical foundation for developing consumer-oriented textile products that balance aesthetic sophistication with wearable functionality, ultimately enhancing emotional engagement in fashion experiences.

REFERENCES

[1]. Li Q, Liang J, Lu Y, et al. (2021) Quantification of the effect of colour appearance and materials on the visual-tactile properties of fabrics. *Proceedings of the AIC 14th Congress 2021*, 167-172.

[2]. Han X, Yu L, Li L, et al. (2023) The effects of colour in human fabric perceptions. *Proceedings of the 15th Congress of the International Colour Association 2023*, 354-359.

[3]. Bahn S, Lee C, Nam C S, et al. (2009). Incorporating affective customer needs for luxuriousness into product design attributes. *Human Factors and Ergonomics in Manufacturing & Service Industries*, 19(2), 105-127. https://doi.org/10.1002/hfm.20140

[4]. Kim W, Lee Y, Lee J H, et al. (2018). A comparative study on designer and customer preference models of leather for vehicle. *International Journal of Industrial Ergonomics*, 65, 110-121. https://doi.org/10.1016/j.ergon.2017.07.009

[5]. Kanai H, Morishima M, Nasu K, et al. (2011) Identification of principal factors of fabric aesthetics by the evaluation from experts on textiles and from untrained consumers. *Textile research journal*, 81(12), 1216-1225. https://doi.org/10.1177/0040517511399960

[6]. Liu W, Moultrie J, & Ye S. (2019) The customer-dominated innovation process: involving customers as designers and decision-makers in developing new product. *The Design Journal*, 22(3), 299-324. https://doi.org/10.1080/14606925.2019.1592324

[7]. Ou, L. C., Luo, M. R., Woodcock, A., & Wright, A. (2004). A study of colour emotion and colour preference. Part I: Colour emotions for single colours. *Color Research & Application*, *29*(3), 232-240. https://doi.org/10.1002/col.20010

[8]. Lamb J M, & Kallal M J (1992). A conceptual framework for apparel design. *Clothing and Textiles Research Journal*, 10(2), 42-47. https://doi.org/10.1177/0887302X9201000207

Effects of Mixed Color Temperatures on Spatial Perception in Office Lighting Environments

Mika Kato[a*], Kokoro Kikuchi[b]

[a] Nihon University, Narashino, Japan
[b] Formerly Nihon University, Narashino, Japan
[*]Corresponding author: Mika Kato, kato.mika@nihon-u.ac.jp

ABSTRACT

In recent years, the impact of COVID-19 and work style reforms has led to the widespread adoption of telework, free address systems, and hybrid work, resulting in increasing diversification of office spaces. These changes have necessitated a reevaluation of the role and design of office environments, particularly regarding lighting. Traditional Japanese offices have employed unified high color temperature lighting, typically around 5000K. However, in contemporary offices where different functional zones for concentrated work, meetings, and communication coexist within the same space, lighting needs have become more complex. This study focuses on spatial impressions and psychological comfort in office environments when ceiling lighting with different color temperatures is introduced. A preliminary online survey of 105 participants investigated discomfort and spatial impressions when observing simulated office images under various lighting conditions. Based on these findings, a main experiment was conducted using virtual reality (VR) environments with 24 participants in their twenties. Results showed that high color temperature environments maintained high ratings for concentration and task-oriented impressions. However, mixed color temperature environments with intentional zoning were rated more highly for collaborative work, emotional diversity, and visual warmth.

Keywords: Office Lighting, Color Temperature, Spatial Perception, Mixed Lighting Environment, Well-being and Productivity

INTRODUCTION

Contemporary workplaces have undergone significant transformation in recent years due to technological advances, changes in work styles, and global events such as the COVID-19 pandemic. These changes have fundamentally altered how office spaces are designed, utilized, and perceived by occupants. The proliferation of telework, hybrid work, and free-address office systems has challenged conventional assumptions about office lighting design and its impact on worker productivity and health.

Historically, Japanese office environments have been characterized by uniform lighting conditions, typically using fluorescent lights with color temperatures of approximately 5000K. However, as office functions have diversified to accommodate multiple activities within the same space—including individual concentrated work, collaborative meetings, informal communication, and relaxation—the appropriateness of uniform lighting has come into question.

The emergence of free-address office systems, where employees do not have fixed desks and can work from various locations within the office, has created spaces with multiple functional zones. These environments require

lighting solutions that can support different types of activities while maintaining overall spatial coherence. Furthermore, the increasing emphasis on employee well-being and the introduction of circadian lighting systems have made office lighting design considerations more complex.

This study investigates the effects of mixed color temperature lighting on spatial impressions in office environments. Specifically, it examines whether the strategic use of different color temperatures within a single office space can enhance user experience while maintaining acceptable levels of visual comfort and spatial unity. To investigate this issue, we first conducted a preliminary online survey to examine initial impressions of mixed color temperature lighting in office environments. From July 15, 2024, over a two-month period, 105 participants ranging from teenagers to those in their 50s (48 males, 57 females) observed computer-generated images of office spaces with different color temperature configurations and evaluated their impressions using a 5-point scale.

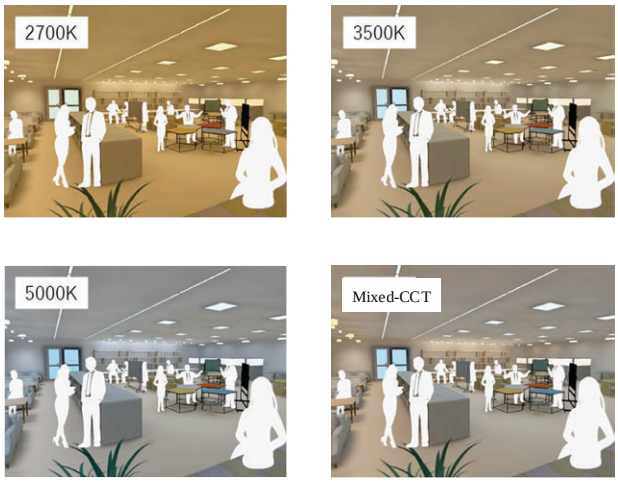

Figure 1: Example images with different color temperatures presented in the online survey

The preliminary survey quantitatively revealed that participants experienced significant discomfort when a single luminaire had a different color temperature within a unified lighting environment. Among the 105 participants, 93 respondents (88.6%) reported such conditions as "bothersome" (63 participants, 60.0%) or "somewhat bothersome" (30 participants, 28.6%), while 94 respondents (89.5%) expressed a desire for color temperature uniformity, either "wanting uniformity" (77 participants, 73.3%) or "somewhat wanting uniformity" (17 participants, 16.2%). However, when color temperature variations were systematically distributed across different functional zones, 52 out of 105 participants (49.5%) selected the mixed color temperature environment as the "space they would most like to work in," showing a preference rate more than twice as high as single color temperature conditions. Based on these preliminary findings, a VR experiment was designed for more detailed verification.

METHODOLOGY

To clarify the acceptable boundaries for mixed color temperature in office spaces, base lighting was installed in a tenant office, and only the color temperature of the lighting was varied to investigate how changes in color temperature affect spatial impressions. Lighting with different color temperatures was arranged in three ways: divided by area within the office according to ratios, arranged regularly, and arranged irregularly, to determine their acceptability as ceiling lighting for offices.

A free-address tenant office was designed using 3D modeling, and participants observed the VR space through VR headsets before conducting evaluations. Ideally, participants should experience spaces with actual mixed color temperature in real environments for investigation. However, using VR allows participants to easily experience

consistent conditions and obtain stable evaluations. Furthermore, conducting experiments with VR minimizes participant burden, which is why VR headsets were used.

The VR headset used was Meta Quest 2 (Meta 899-00183-02, 1832×1920 pixels per eye, 90Hz refresh rate). Among the ceiling lighting, color temperatures were varied by dividing them by area within the office according to ratios, arranging them regularly, and arranging them irregularly, to investigate their acceptability as office ceiling lighting. During this process, office dimensions, reflectance, furniture, and lighting fixture positions were kept constant, with only the lighting color temperature being varied. The evaluation criteria focused on whether combinations of ceiling lighting colors are acceptable and how these combinations affect spatial impressions.

Experimental Space

The physical space dimensions were W: 2832mm × D: 3300mm × H: 2700mm. Three base lighting fixtures (ENDO ERK1043W) were installed. The interior surface reflectance values were 75.44% for the ceiling, 59.04% for the walls, and 28.91% for the floor. The average luminance of the experimental space (21.34 cd/m²) was adjusted to match that of the VR space (21.37 cd/m²) to ensure consistent visual conditions between the physical and virtual environments. As shown in Figure 2, a desk and chair were positioned at the center of the space so that the participant's eye level would be 1200mm when seated. Additionally, a chair without a backrest was used to allow participants to observe the VR space through 360°.

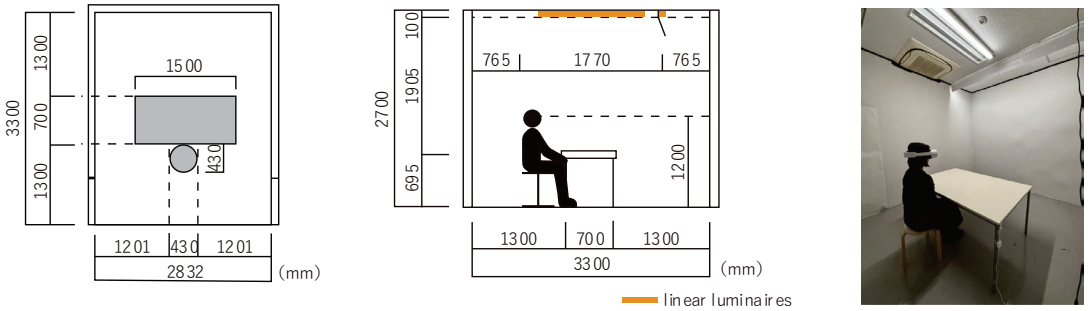

Figure 2: Experimental room dimensions and interior views

VR Spatial Conditions

The VR headset brightness was set to maximum to ensure correct color recognition. The VR space was created using BIM software Revit (Autodesk) to simulate a free-address tenant office, with office dimensions (W: 24000mm × D: 20000mm × H: 2600mm), reflectance values (ceiling: 50%, walls: 30%, floor: 10%), furniture, and lighting fixture positions kept constant. Achromatic furniture was installed to avoid influencing spatial impressions.

Lighting fixtures were arranged using the lighting design application software Luminous Planner (Panasonic), with a total of 81 fixtures positioned to achieve an average illuminance of 750lx on the desk surface. The lighting fixtures used in the VR space were public facility lighting as shown in Table 8. To make color temperature mixing more distinct, the color temperature of XLX460TELT LR9 was adjusted to 2000K using the lighting simulation tool Lightning Flow (Panasonic). Additionally, to maintain consistent lighting placement, the luminous flux of XLX460TEDT LR9 was adjusted to match XLX460TELT LR9 using Luminous Planner.

The color temperature and arrangement methods for each VR condition are shown in Table 1. The floor plan of the VR office space and the participants' observation positions are indicated by the star marks in Figure 3. An example of the 360° images actually used in the experiment is shown in Figure 3. Furthermore, to prevent presentation order from affecting evaluations, conditions were presented randomly.

Table 1: VR conditions (CCT ratios and arrangements)

1. All 2000 K	2. All 6500K	3. 2000 K: 6500 K = 8.9: 1.1, Area-zoned	4. 2000K : 6500K =8.9 : 1.1 Regular pattern	5. 2000K: 6500K= 8.9: 1.1 Irregular pattern	6. 2000 K : 6500 K =6.7 : 3.3 , Area-zoned
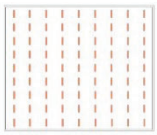	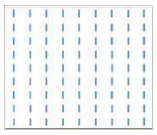	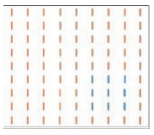	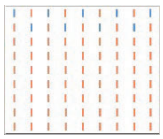	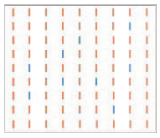	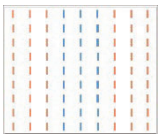
7. 2000 K : 6500 K =6.7 : 3.3 Regular pattern	8. 2000 K : 6500 K =6.7 : 3.3 Irregular pattern	9. 2000K: 6500K =5.6 : 4.4 Area-zoned	10. 2000K: 6500K =5.6 : 4.4 Regular pattern	11. 2000K: 6500K =5.6 : 4.4 Irregular pattern	12. 2000K: 6500K =3.3 : 6.7 Area-zoned
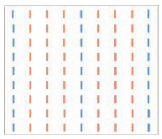	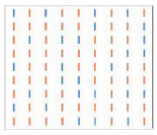	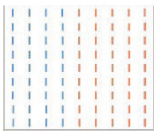	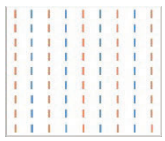	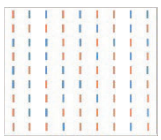	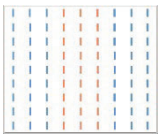
13. 2000K: 6500K =3.3 : 6.7 Regular pattern	14. 2000K: 6500K =3.3 : 6.7 Irregular pattern	15. 2000K: 6500K =1.1 : 8.9 Area-zoned	16. 2000K: 6500K =1.1 : 8.9 Regular pattern	17. 2000K: 6500K =1.1 : 8.9 Irregular pattern	
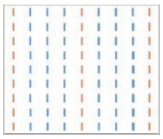	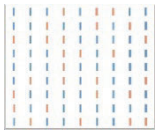	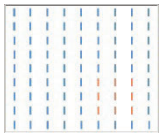	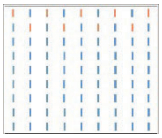	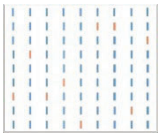	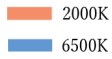 2000K 6500K

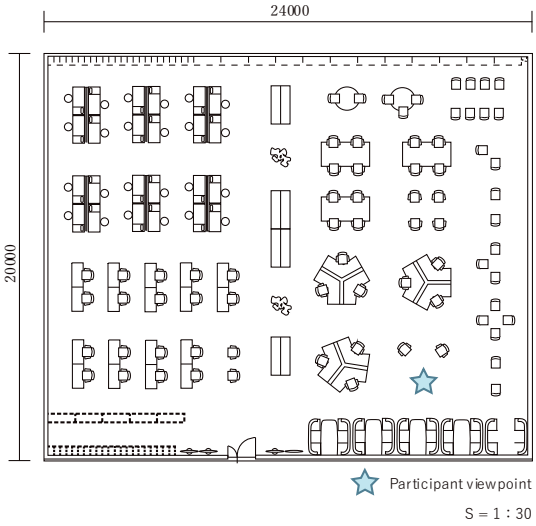

Figure 3: Floor plan of the VR space and participant viewpoint; example VR scene

Evaluation Criteria

Participants sat in the central chair in the physical space and evaluated the VR space after wearing the VR headset. The questionnaire items are shown in Table 2, investigating the appropriateness of ceiling lighting for tenant offices. Participants first evaluated whether the lighting was suitable as office ceiling lighting, then assessed

detailed spatial impressions using a 3-point scale (positive-negative). All participants were 24 individuals in their twenties (12 males and 12 females), all with normal color vision and no history of eye surgery.

The experiment began with visual acuity testing (50cm distance) and color vision testing to assess participants' vision and color perception. After the tests, a 10-minute initial adaptation period was conducted. Subsequently, the following steps ① to ④ were repeated for each condition. ① Put on the VR headset and adapt to the VR space for 30 seconds. ② Observe the VR space. ③ Conduct evaluation. ④ Remove the VR headset.

Table 2 List of Evaluation Items

No.	Question Content
1	In an open-plan office space, is the color temperature combination of the ceiling lighting appropriate?
2	Do you feel a sense of unity in the space?
3	Do you feel a sense of calm in the space?
4	Do you feel you could concentrate and work in this space?
5	Do you feel communication would be easy in this space?
6	Do you feel collaborative work would be easy in this space?
7	Do you feel it would be easy to refresh your mood in this space?
8	Do you feel warmth from the space?
9	Do you feel vibrancy in the space?
10	Do you feel sophistication in the space?
11	Would you actually like to work in this space?

RESULTS AND DISCUSSION

For Question 1, the unified 6500K environment received the highest evaluation, indicating that many people are accustomed to high color temperature unified office spaces. Even in mixed color temperature conditions, approximately 60% or more of participants responded "appropriate" for many conditions, with particularly high evaluations for conditions 13 and 15 (mixed conditions with high cool color ratios). In contrast, the unified 2000K environment received the lowest evaluation as office space lighting.

For Question 4 shown in Figure 4, the unified 6500K condition achieved the highest evaluation, reflecting that conventional offices have prioritized concentrated work in their lighting design. In mixed conditions, evaluations improved as the number of high color temperature fixtures increased, with conditions 7 and 10 receiving high evaluations. Conversely, for Question 6 shown in Figure 5, condition 10 received the highest evaluation, and overall, mixed conditions received higher evaluations than unified conditions.

For Question 7 shown in Figure 6, condition 9 recorded the highest evaluation, with mixed conditions receiving higher evaluations than unified conditions. Regarding arrangement methods, area-based placement tended to receive high evaluations regardless of color temperature ratios. For Question 11 shown in Figure 7, condition 3 received the highest evaluation, with mixed spaces receiving high evaluations similar to other items. An important finding was that while conventional high color temperature unified spaces received high evaluations for "appropriateness for office spaces," many participants preferred mixed environments when asked if they would "actually like to work" in the space.

Statistical analysis quantitatively confirmed the relationship between work type and color temperature preferences. High color temperature lighting was preferred for individual work, while low color temperature mixed spaces were preferred for collaborative work and breaks. Regarding arrangement methods (regular, irregular, area-based), no significant differences were observed between conditions, suggesting the need for more detailed investigation.

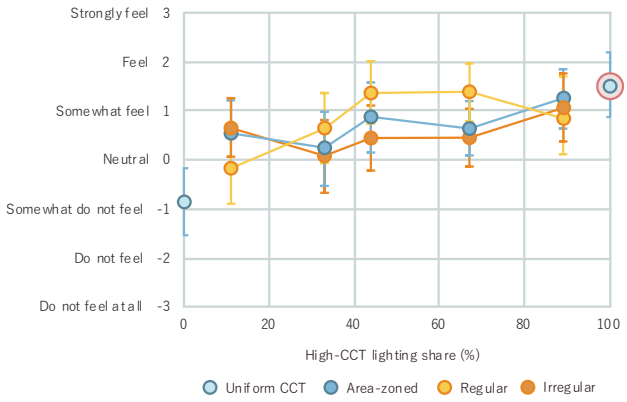

Figure 4: Q4 Results (Focus)

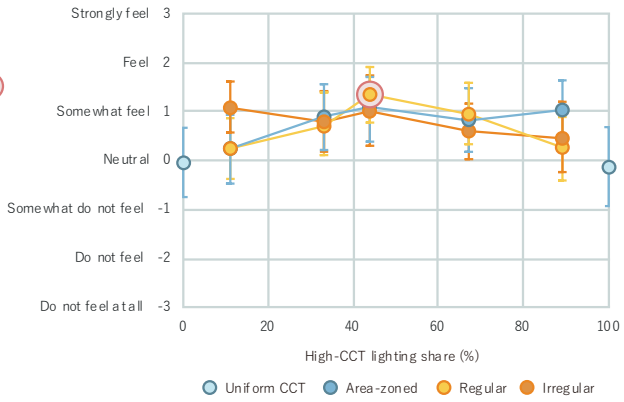

Figure 5: Q6 Results (Collaboration)

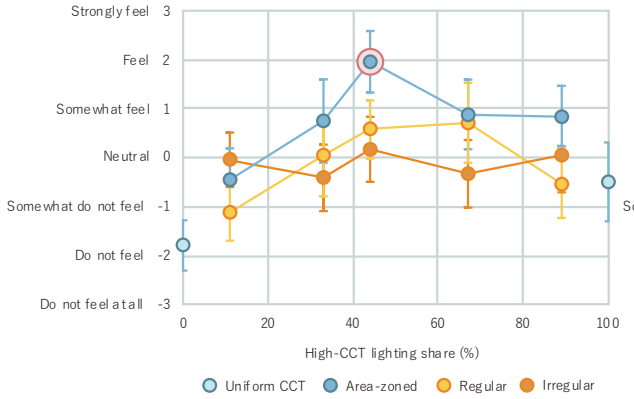

Figure 6: Q7 Results (Refreshability)

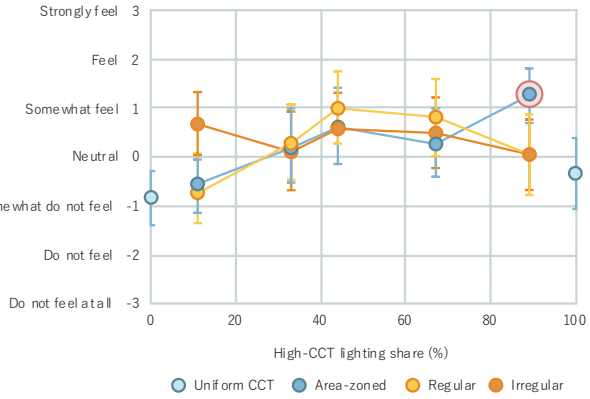

Figure 7: Q11 Results (Willingness to work)

CONCLUSION

This study demonstrated that mixed color temperature lighting in office environments can outperform unified lighting in specific functions when systematically implemented. While unified 6500K lighting maintained advantages for concentration tasks, area-based mixed environments achieved superior evaluations for collaborative work and mood refreshing. The key finding revealed a discrepancy between "appropriateness" perceptions and actual work preferences, with participants favoring mixed environments despite rating unified conditions as more "appropriate". Future research should address several important areas to further develop these findings. First, verification across broader age groups beyond the current 24 participants in their twenties is essential to establish generalizability. Second, long-term studies in actual office environments are needed to validate the short-term VR-based observations. Third, more detailed investigation of arrangement methods is required, as no significant differences were observed between regular, irregular, and area-based placements in this study. Finally, cross-cultural validation in diverse office environments beyond Japan would strengthen the international applicability of these guidelines.

ACKNOWLEDGEMENTS

We thank Mr. Naohiro Toda (Panasonic Corporation) for guidance on using Lighting Flow and for providing photometric data.

A Study of Fluorescent Effect on Ink Jet Paper by Spectral Analysis

M. James Shyu

Chinese Culture University, Taipei, Taiwan
mjshyu@faculty.pccu.edu.tw

ABSTRACT

Conventional color printing process by ink and paper relies on the spectral absorption of the inks to modulate the spectral reflectance of the printing paper to produce a wide range of colors. Nowadays, printing paper may contain optical brightening agents (OBAs) to enhance the printing quality by producing a whiter appearance. The whiter appearance is due to the fluorescent effect of the OBAs that would absorb UV light and emit blue visible light to compensate the natural yellowness of the paper. This extra blue visible light can significantly influence the total appearance of the color reproduction, and yet it is not directly relate to the spectral absorption characteristics of the printed inks. Therefore when OBAs is present, color management process must account for not only the variation of the ink amounts but also the influence from the fluorescent effect by the OBAs. This study aims to provide a better understanding of the role of the fluorescent effect during the inkjet printing process on paper containing OBAs. The M1 and M2 measurement conditions are utilized to gather the spectral reflectance values with and without UV light. By comparing the spectral differences between these two measurement conditions on paper with and without OBAs, the influence of the fluorescent effect can be revealed. Test charts with various ink dot areas of C, M, Y and K inks were printed on two types of ink jet paper with-and-without OBAs. Principal component analysis (PCA) was then performed to investigate the relationship between the variations in ink dot areas and fluorescent effect. The experimental results indicate that two principal components are necessary to more comprehensively explain the fluorescent characteristics observed in this study.

Keywords: fluorescent effect, spectral analysis, color management, optical brightening agents

INTRODUCTION

It is very common to add optical brightening agents (OBAs) to paper for improving the whiteness and brightness to create a more pleasing look on the paper. The OBAs absorb ultraviolet light and emits visible blue light to increase the surface radiant power in the blue region so as to compensate the yellowness in the paper. This phenomenon that the OBAs absorb ultraviolet power and then emits visible light is commonly known as the fluorescent effect. When combing with the regular surface reflected radiant power, these fluorescent characteristics of the OBAs not only would influence the spectral reflectance measurement on the pure flat white paper area, but also can impact the total color appearance of the inks printed on the paper with OBAs.

Theoretically, when color inks are printed on paper, it is the spectral absorption of the ink that makes the spectral-selective variation of the reflectance off the base paper for the color changes. Yule studied the penetration of light into paper and pointed out that multiple internal reflections occur so that simple equation relating dot area to density is not accurate [1]. At that time, the computation of density is by the logarithm of integrated wide-band

reflectance values. Now that similarly related to the ink dot area coverage to the paper to modulate the reflectance, however more than simple reflectance, this fluorescent effect is stimulated by UV energy reaching to the OBAs and being converted to visible light, then emitting out from the paper but partially blocked by the inks, and along with the regular reflectance on the paper surface simultaneously. How the fluorescent effect interacts with plain ink jet paper as well as ink dot area variation is explored in this study.

ISO standard 13655 specifies spectral measurement conditions for graphic arts. There are M0, M1, M2 and M3 measurement conditions. The M1 condition uses CIE illuminant D50, which includes the UV-content. The M2 condition is UV-free. It is assumed that the spectral difference between M1 and M2 measurements on the same color sample would reveal this fluorescent effect here. Figure 1 illustrates a typical M1 and M2 measurement results of an ink jet paper having OBAs and the difference between these two measurements in spectral manner. It is further assumed that when changing the ink dot area settings, these spectral difference values between M1 and M2 measurements can give a good indication for the influence of dot areas to the fluorescent effect. By spectrally analyzing the relation between ink dot area variation and consequent variation of the M1-M2 difference, this fluorescent effect can be understood better.

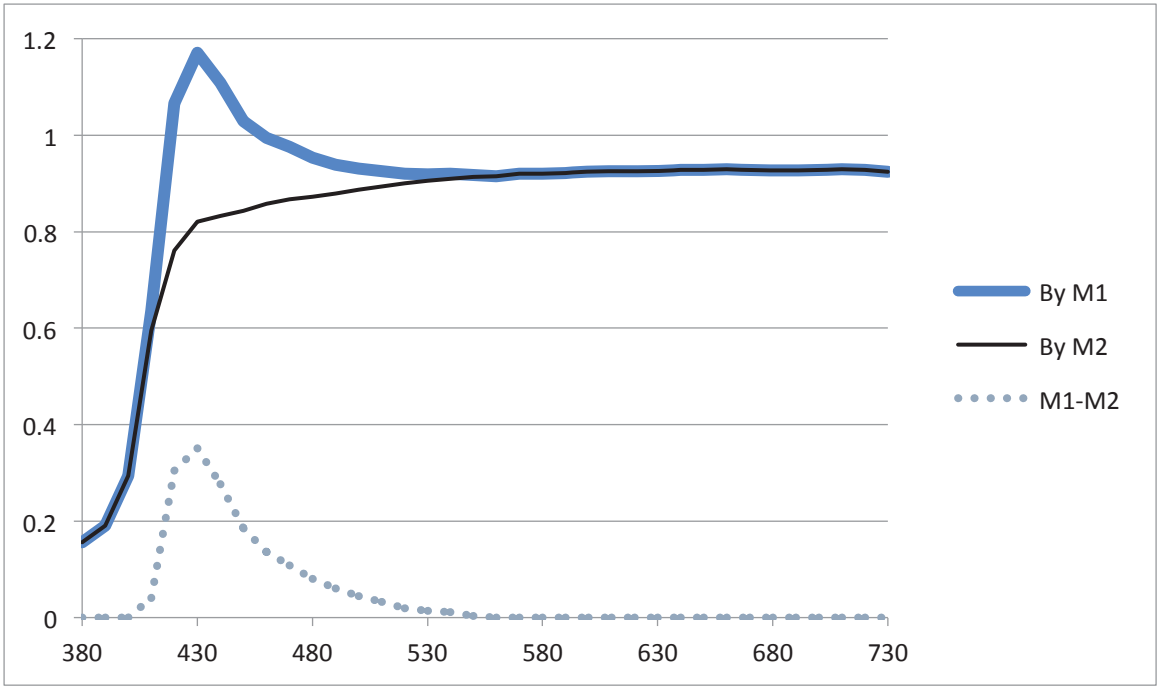

Figure 1: Example of measured spectral reflectance curves for plain ink jet paper with OBAs (wider blue line is by M1, narrow black line is by M2, dotted line is the difference)

Principal component analysis is used to decipher the ink dot area variation to the spectral variation introduced by the OBAs. Estimated spectral reflectance curves can be reconstructed from the linear combination of the component vectors and corresponding loadings [3]. The color differences between the original spectral reflectance values and its reconstructed spectral values from the principal components are used to assess the goodness of the reconstruction. The influence from the fluorescent effect to the color characteristics for ink jet paper with OBSs is analyzed accordingly.

METHODOLOGY

Two types of ink jet papers were used for testing. One paper (Hahnemuhle FineArt ink jet paper, Photo Rag Pearl, 320 gsm) is without OBAs. Another paper (Epson Photo Quality Glossy Paper) is with OBAs. Color test charts were printed on these two types of ink jet paper by a Mimaki UJF-3042 UV ink jet printer. An X-rite iOne Pro 2 spectro-colorimeter with i1iO automatic reader in M1 and M2 measurement modes was used. Spectral reflectance factors were collected through iOne profiler software in .txt file format. Figure 2 shows the tested color chart. The test chart was created in CMYK color mode with ink dot area set as 5%, 0%, 10%, 20% …100%. The position of 0% is deliberately swapped with the 5%, so that the boundary can be identified more precisely when positioning the i1iO measurement set.

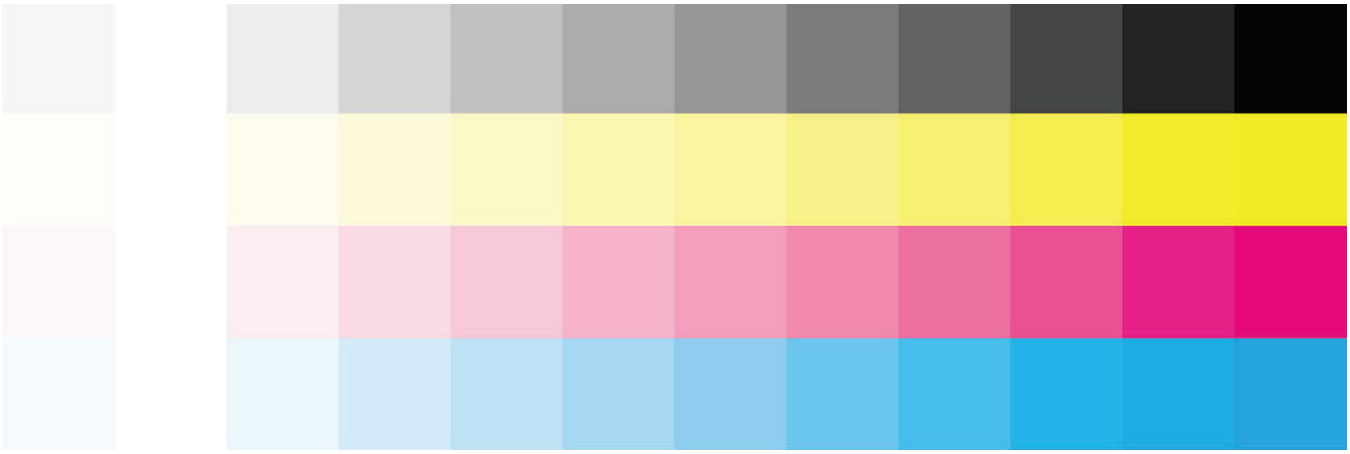

Figure 2: Example of the test chart in C, M, Y and K dot area variations

The comparison and analysis are performed both in colorimetric values as well as spectral values in visible region. Two indexes are used to look into the difference between M1 measurements and M2 measurements from the same color sample. One index is the CIELAB 1976 color difference between M1 measurement and M2 measurement so that the difference can be comprehended in visual scale. Another is the difference between the spectral reflectance values. Principal component analysis is further used to reveal the primary components found in the spectral variations.

RESULTS AND DISCUSSION

It is assumed that the difference between the M1 and the M2 measurement readings simultaneously on the color sample is due to the difference triggered by with-or-without the UV component in the M1/M2 measurements respectively. According to the experimental results, this M1-M2 difference is fairly small for non-OBA paper. However, the M1-M2 difference on paper with OBAs reveals significant influence from the fluorescent effect related to the printed ink dot area.

The measured spectral reflectance curves were used to compute the CIELAB values with D50 light source and D50 reference white. The CIELAB 1976 color difference between M1 and M2 measurements on the color test chart were calculated and the averaged, maximum and minimum values for both types of paper are listed in Table 1. For non-OBAs paper, the averaged difference between M1-M2 is 0.31. This serves as a baseline reference for color variation that might be introduced by the unevenness on the paper texture and inks or repeatability of the instrument. For paper with OBAs, the averaged difference between M1 and M2 measurements is 6.58, to a degree quite visible. Further spectral analysis was then performed.

Table 1: CIELAB Color difference between the M1 and M2 measurements on the test samples

CIELAB Color Difference	Paper without OBAs	Paper with OBAs
Average	0.31	6.58
Maximum	0.52	11.72
Minimum	0.13	1.44

The spectral reflectance differences between M1 and M2 measurements are shown in Figure 3. It demonstrates the variation contributed directly due to the interaction between UV illumination and OBAs. Principal component analysis was used in different combinations of test color ramps. The percentages of accumulated variance explained by the numbers of component for all colors and respectively C, M, Y and K color inks are listed in Table 2. It is noticed that the first component can explain 99% of the variance for all 5 test cases. The relationship between the ink dot area percentage and the first component's loadings including four all test color samples is showing in Figure 4. It can be seen that the fluorescent effect decreases as ink dot areas increases.

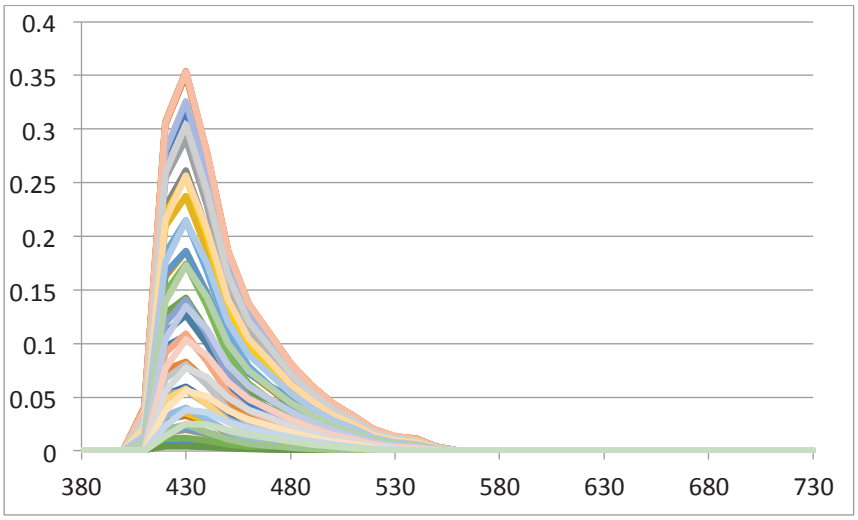

Figure 3: Spectral difference between M1 and M2 measurements for all colors from paper with OBAs

Table 2: Accumulated variance explained by principal component analysis for different colors of ink (OBA)

Test colors	1st Component	2nd Component	3rd Component
C, M, Y, K all	99.8540%	99.9346%	99.9877%
C	99.8001%	99.9959%	99.9999%
M	99.9388%	99.9988%	99.9996%
Y	99.8879%	99.9993%	99.9997%
K	99.9988%	99.9997%	99.9999%

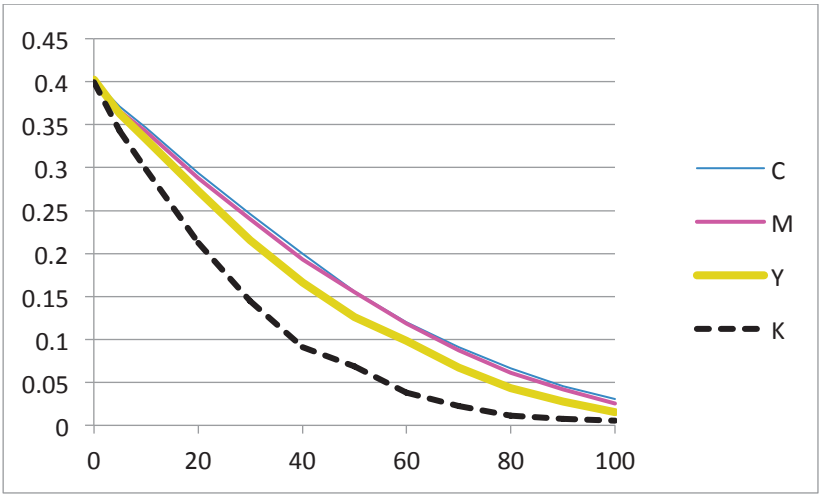

Figure 4: The loading (Y-axis) of the first component from principal component analysis on the spectral difference between M1 and M2 measurements for all 4 colors with OBAs paper vs. ink dot area (X-axis)

Further analysis in colorimetric difference was performed to understand how well the reconstruction of the spectral difference curves is from the principal components analysis. Table 3 lists all the CIELAB 1976 color difference values between the calculated M1-M2 spectral difference and the reconstructed spectral difference curves for each of the 5 sets of test samples when using one component and two components from the principal component analysis.

Table 3: Average CIELAB Color difference between the measured and reconstructed spectral reflectance difference curves from the principal component analysis for 5 color test sets with OBA paper

Test colors	1 Component	2 Components
CMYK All	2.22	1.04
C	1.00	0.14
M	1.78	0.26
Y	4.16	0.16
K	0.09	0.08

These color differences can also indicate the quality of the reconstruction with the number of components is used while explaining the variations among the test sets. When taking all colors together into one group, reconstruction with just one component can only result in 2.22 color difference even though the accumulated variance explained is 99.8540%. Adding one more component can increase the accumulated variance explained, however the color difference is still higher than the base line reference (0.31 from the non-OBAs paper). Individual tests were performed for each color of the ink and results are also shown in Table 3. For K ink, one component is sufficient to reconstruct the spectral curve that meets the base line reference. For each C, M and Y inks, just one component is not sufficient to predict all the difference between M1-M2 variations. However by using the same second component, the difference still counts for 1.04 color difference, which is not within the

range of the base line reference. It seems that each C, M and Y ink requires a separate second component to explain the spectral difference between M1 and M2 measurements for color inks printed on paper with OBAs.

It is assumed that the fluorescent effect is reduced when the ink dots cover more area on the paper to prevent the amount of UV radiant power to reach OBAs. This trend is explained in these experimental results by the relationship between the first component and the corresponding loadings. However, different second components seem to be needed for more precise explanation for C, M and Y inks in this case. Will that be some sort of internal reflections mentioned by Yule from OBAs this time? Or, there is some other spectral interaction due to the fluorescent effect? In comparison with the accuracy achieved in Dhote's study, this second component might be the key to resolve the uncertainty when OBAs are involved for color reproduction by inks on paper [4]. Currently, this finding is based on an UV ink jet printer. It will be an interesting topic to look into further with other types of ink jet printer as well.

CONCLUSION

This study explores the spectral characteristics of ink jet paper both with and without optical brightening agents (OBAs). Color samples in various cyan, magenta, yellow and black ink dot percentages respectively are the test objects. The primary data used to explore the fluorescent effect were the spectral differences between M1 and M2 measurements. Based on principal component analysis and corresponding color difference evaluation on paper with OBAs, the findings indicate that as the ink dot area increases, the influence of fluorescent decreases proportionally. However, a second component was found to be involved in this case, which can improve the prediction of this fluorescent effect to within the base line reference at 0.3 CIELAB color difference. This factor (component) might be spectrally selective to the inks and deserves further study.

ACKNOWLEDGEMENTS

The author would like to thank Eva Lin and Alton Mao for the assistance in processing the spectral data with Python program.

REFERENCES

[1]. Yule, J. A. C., and Neilsen, W. J. (1951). The penetration of light into paper and its effect on halftone reproduction. *Proc. TAGA 1951*.

[2]. ISO 13655:2017, Graphic technology – Spectral measurement and colorimetric computation for graphic arts images.

[3]. Tzeng, D. –Y., & Berns, R. S. (2005). A review of principal component analysis and its applications to color technology. *Color Research and Application*, 30, 84-98.

[4]. Dhote, Y. , Altay, B. N., Myers, B. L., Telhan, R. (2024). Impact of optical brightening agents on alkali-based inks in packaging: a comparative study on color accuracy. *Color Research and Application*, 49, 258-271. https://doi.org/10.1002/col.22914

Improving RGB Camera-Based Spectral Reflectance Estimation Through A Machine-Learning Approach

Shogo Nishi[a*]

[a] *Department of Engineering Informatics, Osaka Electro-Communication University, Neyagawa, Osaka, Japan*

[*] *Corresponding author: Shogo Nishi, s-nishi@osakac.ac.jp*

ABSTRACT

In this study, we propose a new calibration framework that improves the accuracy of spectral reflectance estimation from RGB images by integrating a physical model and machine learning. The proposed method consists of two main components: estimation by Linear Minimum Mean Square Error (LMMSE) and correction by Gaussian Process Regression (GPR). First, based on the output of an RGB camera, we estimate an initial spectral reflectance by LMMSE. Although LMMSE yields a physically consistent initial estimate, errors due to nonlinearities and real-world conditions remain. To correct these residuals, we introduce GPR as a flexible nonparametric regression method that maps the LMMSE output to the true reflectance. For training the GPR model, we first simulate LMMSE outputs from a large spectral reflectance database and perform pre-training using pseudo data. We then carry out fine-tuning with measured data to bridge the domain gap between simulation and real data. In the experiments, we used an iPhone 7 as the RGB camera and captured an X-Rite ColorChecker Passport as the evaluation target. The reflectance estimated by LMMSE was applied to the trained GPR model to perform calibration. As a result, the estimation accuracy on the absolute scale was greatly improved compared with the uncorrected LMMSE. These results show that the proposed method is effective for improving spectral reflectance estimation from RGB images.

Keywords: spectral reflectance estimation, absolute spectral calibration, LMMSE estimation, Gaussian Process R egression, smartphone RGB imaging

INTRODUCTION

Advances in digital image processing and colorimetry have led to a growing demand for accurate estimation of spectral information from images. Spectral reflectance, in particular, represents fundamental information that characterizes the intrinsic properties of object surfaces. Its precise estimation is essential not only for color measurement but also for a wide range of applications such as object recognition, material classification, color constancy, and photorealistic image reproduction. Estimating spectral reflectance from images has also become an important technique in diverse fields including medical diagnosis, food quality inspection, remote sensing, and environmental monitoring [1-2].

Conventional approaches have often relied on multiband imaging systems using gelatin filters or tunable filters, where spectral information is reconstructed from multiple captured images [3-5]. However, these methods face practical limitations such as optical axis misalignment, illumination variations, and procedural complexity due to filter exchange, which hinder their application in dynamic scenes and in-field measurements. To overcome these issues, there is a need for a one-shot approach based on standard RGB imaging that enables reliable recovery of absolute spectral reflectance without mechanical filter replacement.

In our previous work, we proposed a calibration method that combined Linear Minimum Mean Square Error (LMMSE) estimation with a radial basis function (RBF) network [6]. The RBF network was trained using both measured and estimated reflectance values of 904 colors from the Munsell chart, consisting of 20 hues and 18 intermediate tones. However, when trained with all colors simultaneously, the estimation accuracy tended to deteriorate, while restricting the training to colors similar to the target improved performance. This revealed a strong dependence on the selection of training data, making it difficult to achieve generalization and stability simultaneously.

Building on these findings, the present study proposes a new calibration framework that integrates physical modeling and machine learning for high-accuracy estimation of spectral reflectance from RGB images. The proposed method consists of two stages. First, an initial physically consistent estimate is obtained using LMMSE estimation, which incorporates the camera's spectral sensitivity, noise characteristics, and prior distribution of reflectance. Second, Gaussian Process Regression (GPR) is employed to learn the residual mapping from the LMMSE output to the ground-truth reflectance, thereby correcting nonlinear errors and wavelength-dependent distortions observed under real-world conditions. GPR is well suited to this task due to its ability to model nonlinear relationships and quantify predictive uncertainty. Through this framework, we aim to achieve absolute spectral reflectance estimation from a single RGB image without the need for reference targets such as a white standard.

METHODOLOGY

LMMSE-based Spectral Reflectance Estimation

We model the camera observation for each RGB channel $c \in \{R, G, B\}$ as

$$y_c = g\int_{400}^{700} x(\lambda)e(\lambda)r_c(\lambda)\mathrm{d}\lambda + n_c, \tag{1}$$

where $x(\lambda)$ is the surface spectral reflectance, $e(\lambda)$ is the illuminant spectral power distribution, $r_c(\lambda)$ is the camera's spectral sensitivity for channel c, $g > 0$ is a scene-dependent gain (geometry and illumination), and n_c is additive noise (zero-mean, uncorrelated with x) [7]. Discretizing the visible range yields the linear model

$$\mathbf{y} = g\mathbf{A}\mathbf{x} + \mathbf{n}, \tag{2}$$

with $\mathbf{y} \in \mathbb{R}^3$, $\mathbf{x} \in \mathbb{R}^K$ (reflectance sampled at K wavelengths), and $\mathbf{A} \in \mathbb{R}^{3\times K}$ whose rows are given by $e(\lambda)r_c(\lambda)$ over the sampled wavelengths. The noise $\mathbf{n}$ is modeled with covariance $\mathbf{\Sigma}_n = \sigma^2\mathbf{I}$. When necessary, we adopt a channel-wise diagonal form for $\mathbf{\Sigma}_n$ (e.g., $\mathrm{diag}(\sigma_R^2, \sigma_G^2, \sigma_B^2)$). Assuming a Gaussian prior $\mathbf{x} \sim \mathcal{N}(\bar{\mathbf{x}}, \mathbf{P})$ with mean $\bar{\mathbf{x}}$ and covariance $\mathbf{P}$, the LMMSE estimator of $\mathbf{x}$ is

$$\hat{\mathbf{x}} = \bar{\mathbf{x}} + g\mathbf{P}\mathbf{A}^t\left(g^2\mathbf{A}\mathbf{P}\mathbf{A}^t + \mathbf{\Sigma}_n\right)^{-1}(\mathbf{y} - g\mathbf{A}\bar{\mathbf{x}}). \tag{3}$$

Here, $\bar{\mathbf{x}}$ and $\mathbf{P}$ summarize the reflectance statistics, $\mathbf{A}$ is determined by the illuminant spectral power distribution and the camera spectral sensitivities, and $\mathbf{\Sigma}_n$ encodes the sensor noise levels. Keeping g explicit preserves the absolute scale of reflectance; in practice, g and $\mathbf{\Sigma}_n$ are set from imaging conditions and noise characterization, respectively. This linear-Gaussian formulation yields the LMMSE-optimal linear estimate and serves as the physically consistent first stage before subsequent machine-learning-based calibration.

GPR-Based Nonlinear Calibration

Following the LMMSE first stage, we employ GPR to learn a nonlinear correction for the remaining error [8]. The LMMSE output is converted into a feature vector, and the difference between the ground-truth reflectance and the LMMSE estimate is expressed on a low-dimensional PCA basis. Each basis coefficient is then regressed by an

independent Gaussian process. This design limits the model's degrees of freedom and promotes smooth, robust spectra.

We use a Matérn kernel with an added white-noise term. Hyperparameters are estimated by maximizing the marginal likelihood with multi-start numerical optimization. At inference, the GPR predicts the low-dimensional coefficients from the LMMSE features; the residual spectrum is reconstructed by the inverse basis transform and added to the LMMSE estimate. The final spectrum is constrained to the physical range [0,1] to preserve consistency.

The GPR also provides a per-sample uncertainty. We use this quantity to attenuate corrections in regions that are outside the support of the training data and to blend the GPR output with the LMMSE estimate, thereby avoiding over-correction. Training follows a two-stage schedule: pre-training on synthetic pairs generated from camera sensitivities, illuminants, noise models, and reflectance statistics, followed by fine-tuning on measured pairs to reduce domain gap. Prior work has explored kernel-based spectral reconstruction on consumer devices without using device spectral priors and often with multi-illumination capture [9]. In contrast, we first obtain an absolute-scale estimate via LMMSE that explicitly uses camera sensitivities, illuminant spectral power distribution, and noise statistics, and then perform GP-based residual calibration with uncertainty-aware blending and [0,1] range compliance from a single-shot RGB. This calibration stage preserves the absolute scale established by LMMSE while flexibly absorbing residual nonlinearity and wavelength-dependent distortion.

RESULTS AND DISCUSSIO

We used an iPhone 7 mounted on a tripod and capture X-Rite ColorChecker Passport charts under CIE Illuminant A. In the first stage, we reconstructed spectral reflectance from RGB images using the LMMSE estimator. The scalar gain g in Eq. (1) was fixed to $g = 1$ after shading correction and exposure normalization. Camera noise variance was estimated per RGB channel from flat-field images: after the same shading correction, we computed the pixel variance within a region of interest and used the resulting values as the diagonal entries of the observation-noise covariance. As an absolute-scale metric, we used RMSE averaged over the 24 ColorChecker patches with 61 wavelengths (400–700 nm at 5 nm steps). The blue line in Figure 1 shows the estimated results. With LMMSE alone, the mean RMSE was 0.553. While several patches were accurate, others retained errors due to excessive gain and wavelength-dependent distortions.

In the second stage, we applied GPR for nonlinear calibration of the LMMSE output. Training followed a two-stage schedule: we pre-trained on 1,284 synthetic spectrum pairs generated from camera spectral sensitivities, illuminants, noise models, and reflectance statistics, and we fine-tuned on 904 measured pairs acquired with a Konica Minolta CM-2600d spectrophotometer. The evaluation set is the same 24 ColorChecker patches used in the first stage. Given the LMMSE estimates, the trained GPR predicts a low-dimensional residual that is inverse-transformed and added to obtain the calibrated spectrum. This reduces the mean RMSE to 0.193, eliminates out-of-bounds values (<0 or >1) across all 24×61 samples, and maintains smoothness as indicated by a low second-order-difference RMS. The relative-shape metric SAM (Spectral Angle Mapper) increases for some patches, indicating a trade-off when prioritizing absolute-scale consistency.

Figure 1 illustrates representative outcomes before and after calibration. The top row shows cases where GPR markedly reduces error relative to LMMSE, whereas the bottom row shows cases with limited improvement in more extrapolative regions. Overall, these results indicate that a two-stage framework combining physically consistent LMMSE with GPR-based nonlinear correction improves absolute spectral accuracy without relying on in-scene reference targets.

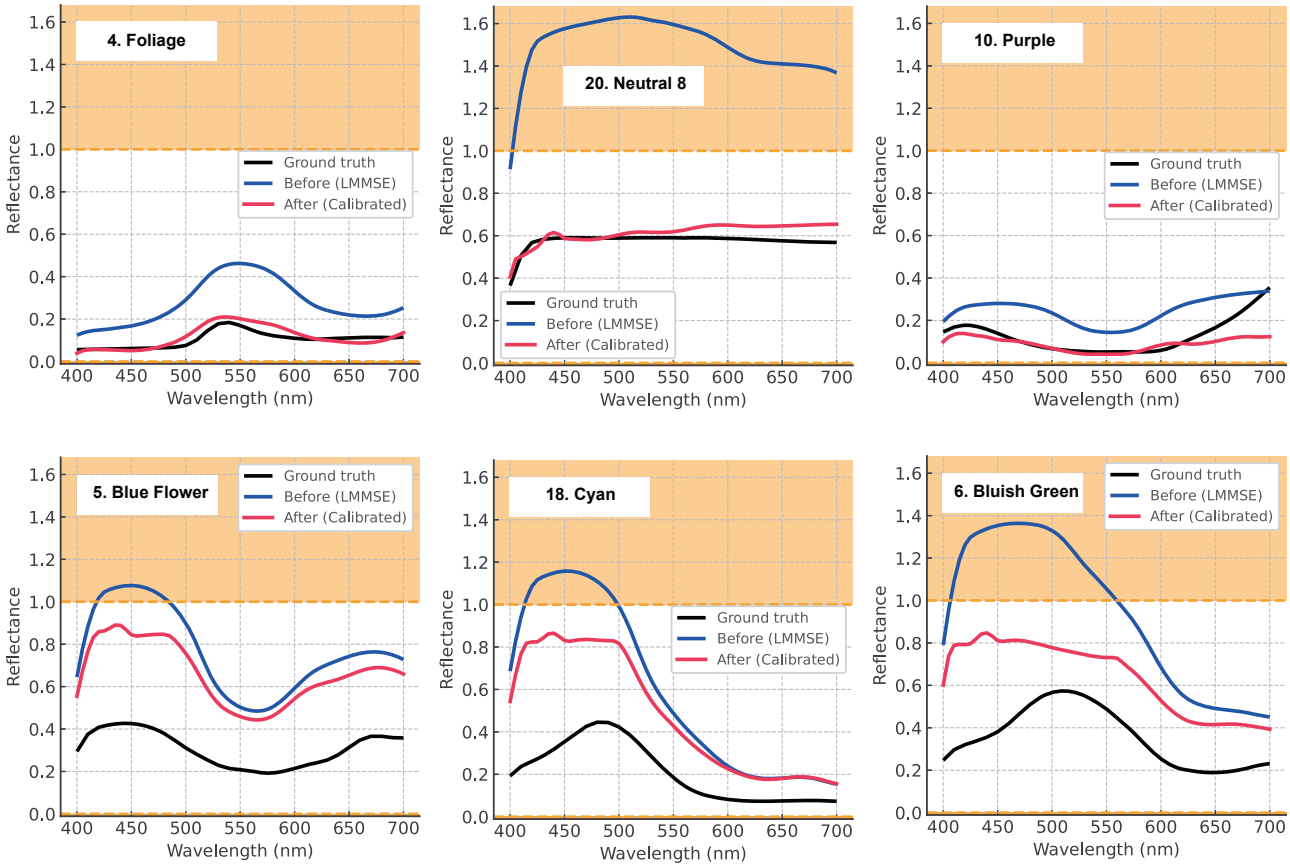

Figure 1: GPR-Based Correction Improves LMMSE Spectral Estimates

CONCLUSION

In this paper, we have proposed a two-stage framework that estimates and calibrates spectral reflectance from smartphone RGB images with an emphasis on absolute accuracy. In the first stage, a physically consistent initial estimate is obtained via an LMMSE estimator that incorporates camera spectral sensitivities, the illuminant, and noise statistics. In the second stage, the difference (residual) between the LMMSE output and the ground truth is expressed in a low-dimensional basis, and GPR is applied for nonlinear correction. The proposed method reduces the mean RMSE while preserving smooth spectral shapes, although a trade-off in relative-shape metrics is observed for some patches. These results suggest that integrating physical modeling with machine learning is effective for improving absolute spectral accuracy even under target-independent conditions. In particular, we confirm that the method calibrates spectral reflectance on an absolute scale without any scalar normalization to ground truth. Future work will broaden the evaluation, verify generalization across devices and illuminants, and pursue further gains in accuracy.

REFERENCES

[1]. McGonigle, A. J. S., Wilkes, T. C., Pering, T. D., Willmott, J. R., Cook, J. M., Mims, F. M., & Parisi, A. V. (2018). Smartphone spectrometers. *Sensors*, 18(1), Article 223.

[2]. Rateni, G., Dario, P., & Cavallo, F. (2017). Smartphone-based food diagnostic technologies: A review. *Sensors*, 17(6), Article 1453.

[3]. Imai, F. H., & Berns, R. S. (1999). Spectral estimation using trichromatic digital cameras. In *Proceedings of the International Symposium on Multispectral Imaging for Digital Archives*, 42–49.

[4]. Tominaga, S., & Tanaka, N. (2008). Spectral image acquisition, analysis, and rendering for art paintings. *Journal of Electronic Imaging*, 17(4), 043022.

[5]. Nishi, S., Kimachi, A., Doi, M., & Tominaga, S. (2017). Image registration for a multispectral imaging system using interference filters and application to digital archiving of art paintings. *Cultura e Scienza del Colore – Color Culture and Science*, 7, 59–68.

[6]. Nishi, S. (2024). Estimation of spectral reflectance using a smartphone camera and its calibration method. In *Proceedings of the 8th Asia Color Association Conference*, 182–185.

[7]. Tominaga, S., Nishi, S., Ohtera, R., & Sakai, H. (2022). Improved method for spectral reflectance estimation and application to mobile phone cameras. *Journal of the Optical Society of America A*, 39(3), 494–508.

[8]. Rasmussen, C. E., & Williams, C. K. I. (2006). *Gaussian processes for machine learning*. MIT Press.

[9]. Heikkinen, V., Cámara, C., Hirvonen, T., & Penttinen, N. (2016). Spectral imaging using consumer-level devices and kernel-based regression. *Journal of the Optical Society of America A*, 33(6), 1095–1110.

Research on The Colors and Color Temperatures Unpopular in Home Kitchen Cabinets

Chia-Hua Tsai*, Cheng-Min Tsai

Department of Visual Communication Design, National Taiwan University of Arts, New Taipei City, Taiwan, R.O.C.
**Corresponding author: Chia-Hua Tsai, j5282356@yahoo.com.tw*

ABSTRACT

In modern residential interior design, kitchen have become a core area of family life. As such, the rationality and aesthetic appeal of kitchen cabinets color design are receiving increasing attention. From the perspective of the production costs for colored kitchen panels, mass-producing colors that are less favored by consumers are not cost-effective. Therefore, it is essential to understand which kitchen cabinet colors are less preferred from the perspective of kitchen manufacturers. This insight not only helps optimize production strategies, but also assists interior designers in avoiding the use of less popular colors, thereby reducing communication time and cost when working with clients. Previous studies on color preferences in kitchen cabinets are limited, a gap that motivated this study. The objectives of this study are (1) to identify the colors and color tones of kitchen panels that are perceived as undesirable by users, and (2) to explore the correlation between disliked colors and their associated color tones in the context of kitchen panel design. This study employed a questionnaire survey to investigate individuals' least preferred colors for kitchen panels and their preferences regarding the color temperature of kitchen lighting. The research design involved six color options combined with three different kitchen ambient light color temperatures. A series of kitchen space configurations were presented using 3D-rendered color simulations, showcasing various combinations of panel colors and lighting environments. A total of 119 questionnaires were collected. Descriptive statistical analysis revealed that green and blue were the least preferred kitchen panel colors among the respondents. Additionally, warm yellow lighting was found to be the least favored kitchen ambient light color. The researchers hope that these findings will serve as valuable references for kitchen panel designers and manufacturers, highlighting the importance of avoiding color and lighting combinations that are generally disliked by consumers.

Keywords: Kitchen Cabinetry, Color Preference, Ambient Lighting, Interior Design, NCS Natural Color System.

INTRODUCTION

1.The Importance of Kitchen Color Schemes and the Application of the NCS Color System

core space in family life, the kitchen plays a vital role in daily activities. The color scheme of kitchen environments has a profound impact on users' psychological responses, as well as the efficiency and comfort of their operations within the space. In terms of color selection, the Natural Color System (NCS) was adopted, as it is a comprehensive and internationally standardized color system. It offers a high degree of consistency and standardization, making it a reliable tool for achieving systematic and user-centered color designs in kitchen interiors.

Ou and Hui-Yi (2000) proposed that interior design preferences are influenced by residents' cultures, lifestyles, and aesthetic literacy. In turn, these factors affect individual preferences for spatial color schemes. To a certain extent, the coordination and application of colors influence the overall aesthetics of interior spaces. Colors play an essential

role in daily life by evoking various emotional and perceptual responses. The surrounding environmental colors in a given space can have a strong impact on human perception because spatial color schemes create distinct atmospheres and impressions. After years of rapid growth, the kitchen cabinet industry has entered a steady development phase. As new kitchen elements become integrated into modern households, kitchen cabinets are no longer valued solely for their functionality but are also expected to be aesthetically pleasing and design-oriented. In response to this shift, companies in the kitchenware industry have begun to reassess their internal competitiveness from both short- and mid-to long-term perspectives. To remain competitive, businesses must identify and develop their unique strengths and core capabilities (Tseng, Chun-Yuan, 2013).

2. Research Motivation and Objectives

Research on kitchen cabinet color schemes and the application of the Natural Color System (NCS) remains relatively limited in Taiwan. This study aims to fill this gap by conducting an in-depth investigation of NCS color combinations that are unsuitable for kitchen cabinets. This study aims to provide innovative theoretical support for future kitchen cabinet designs and production. The findings of this study can serve as a valuable reference for future kitchen-space design, helping designers understand and respond to the psychological needs of consumers more objectively and effectively. The specific objectives of this research were as follows: (1) To identify the colors and lighting conditions that people find undesirable in kitchen cabinets. (2) To explore the correlations between disliked colors and lighting conditions in kitchen cabinets.

LITERATURE REVIEW

1. Key factors of kitchenware color matching

Multiple factors influence the color-selection process in kitchenware design, ranging from aesthetic trends to functional requirements and user-centered considerations. In contemporary minimalist kitchens, designers often favor clean and neutral tones such as white and gray to establish a sense of simplicity and freshness. In contrast, classical kitchen interiors typically incorporate warmer hues—such as beige and yellow—to create a more traditional and elegant atmosphere. From a functional perspective, color also plays a critical role in enhancing safety and usability. For instance, heating elements and stovetop controls often feature vivid red indicators to signal heat or danger, ensuring that users can quickly and intuitively recognize the operational functions. Color has the inherent ability to shape the "atmosphere" of a space. As society moves into a more emotionally driven era, the demand for personalized and sensory-rich environments has increased the role of color as a critical criterion in design evaluation. According to Cheng and Lin (1989), personal traits such as personality, mood, and past experiences can significantly affect an individual’s perception of and preference for color. User preferences for kitchenware colors are also shaped by demographic differences such as age, culture, and lifestyle. Research in color psychology has demonstrated that different hues can elicit varying emotional responses; warm colors are typically associated with comfort and energy, whereas cool colors convey calmness and clarity. Therefore, to meet diverse user expectations, kitchenware color designs must carefully consider both psychological impacts and sociocultural contexts.

2. The effect of different color lights on kitchen space.

IIn the early stages of lighting development in Taiwan, only two main color temperatures were commonly used: cool white light (6000 K) and warm yellow light (3000 K), leaving little room for variation in lighting design. With technological advancements, natural white light (4000 K) was introduced and has gradually replaced both 6000 K and 3000 K as the most commonly used lighting options. The increasing adoption of LED lighting has further advanced the field, allowing for flexible adjustment of color temperature. Modern LED fixtures now offer a wide range of selectable color temperatures, often exceeding 20 different settings, overcoming the limitations of traditional fixed-temperature lighting (Lin, Kuo-Hua, 2019). Such developments have enabled research on how

adjustable lighting affects user behavior and psychological states. Different lighting conditions can significantly influence visual perception and emotional responses in various spaces. For instance, restaurants often use warm yellow light (3000 K) to create a cozy atmosphere and stimulate appetite, whereas offices typically use cool white light (6000 K) to enhance brightness and reduce visual fatigue.

RESEARCH METHOD

1. Research design

1.1 Build sample model

Modeling and Sample Design. Before constructing the 3D kitchen models, we selected a commonly used single-line kitchen layout (also known as one-wall or straight kitchen) as the basis for spatial planning. The surface material of the kitchen panels (hereafter referred to as "kitchen cabinets") was set to have a low-reflection finish to avoid light interference during the evaluation. (1) Color Selection: Six fundamental colors were chosen from the Natural Color System (NCS) based on 90-degree intervals on the NCS color circle. These include the main hues: R (Red), Y (Yellow), G (Green), B (Blue), W (Black), and S (White). (2) Model Configuration: The kitchen model was designed using a single-line layout to maintain consistency and control the spatial composition. The models were constructed using SketchUp and rendered using 3ds Max to generate high-quality photorealistic samples for the experimental phase.

1.2 Questionnaire method.

After constructing and categorizing the 3D kitchen model samples, a questionnaire was designed and distributed to investigate the least preferred color and lighting combinations in the kitchen cabinet designs. This study employed a questionnaire survey method to collect data, which were then subjected to statistical analyses. The 3D kitchen configuration models used in the questionnaire are shown in Figure 1.

2. Questionnaire design

To ensure color consistency across visual samples, the Natural Color System (NCS) was adopted as the standard for color selection. Basic hues were selected from the NCS color circle to serve as primary color variables. A home kitchen space was modeled using 3D rendering software, with color schemes applied based on the selected NCS hues. To assess the participants' subjective preferences for different color and lighting combinations, a Google Forms questionnaire was distributed because of its accessibility, efficiency, and ease of data collection. Respondents were asked to rate their level of preference for each kitchen design on a 5-point Likert scale, where 1 indicated "strongly like" and 5 indicated "strongly dislike." Due to time and human resource limitations, this study employed a convenience sampling method to gather responses.

3. Home kitchen space design sample

In terms of spatial samples, this study focused on the 3D modeling of kitchen space design, selecting the commonly used single-line kitchen layout as the base configuration. Three lighting conditions were applied to the models, forming the core spatial planning framework for this study. Using six fundamental NCS colors, 18 different kitchen model samples were created by combining each color with three lighting scenarios. The rendered models were incorporated into a questionnaire for data collection and analysis.

RESULTS AND DISCUSSION

In total, 129 questionnaires were collected, 119 of which were valid. Through Pearson's correlation analysis along with evaluations of means and standard deviations, the results indicated that the least preferred combination was green and blue kitchen panel colors paired with warm yellow lighting. This combination of color and lighting was consistently identified as the most commonly rejected by respondents across the sample.

Table 1: Mean and standard deviation analysis

Light source	Color	Mean	S.D.	Light source	Color	Mean	S.D.
3000k	Green	4.07	1.125	4000k	Blue	3.85	1.154
3000k	Blue	4.04	1.100	3000k	Yellow	3.80	1.239
6000k	Green	3.93	1.133	6000k	Blue	3.76	1.221
4000k	Green	3.93	1.155	6000k	Red	3.73	1.260
3000k	Red	3.88	1.121				

According to the results of the descriptive statistical analysis, the combination of green and blue kitchen cabinets paired with 3000 K lighting received the highest mean scores of 4.07 and 4.04, respectively, indicating that these two combinations were the most widely disliked among all tested color and lighting pairings. Across all lighting conditions (6000 K, 4000 K, and 3000 K), green and blue consistently emerged as the least preferred colors, regardless of the color temperature used. Further analysis using Pearson's correlation revealed several statistically significant and highly positive correlations between specific color-lighting combinations and users' dislike levels. The correlation coefficient was greater than 0.7 in Table 2. These findings indicate strong and consistent patterns of negative perceptions of blue and green color schemes, particularly when paired with warmer lighting temperatures.

Table 2: Correlation coefficient and significance

Light source	color	Average value	Standard deviation	Correlation coefficient	significance
6000k	Blue/Green	3.76/3.93	1.221/1.133	.760	<.001
4000k/6000k	Green	3.93/3.93	1.155/1.133	.754	<.001
4000k/3000k	Green/ Blue	3.93/4.04	1.155/1.100	.709	<.001
4000k	Red/ Blue	3.54/3.85	1.227/1.154	.722	<.001
4000k	Blue/Green	3.85/3.93	1.154/1.155	.882	<.001
4000k/3000k	Blue	3.85/4.04	1.154/1.100	.759	<.001
4000k/3000k	Green	3.93/4.07	1.155/1.125	.753	<.001
3000k	Blue/Green	4.04/4.07	1.100/1.125	.853	<.001

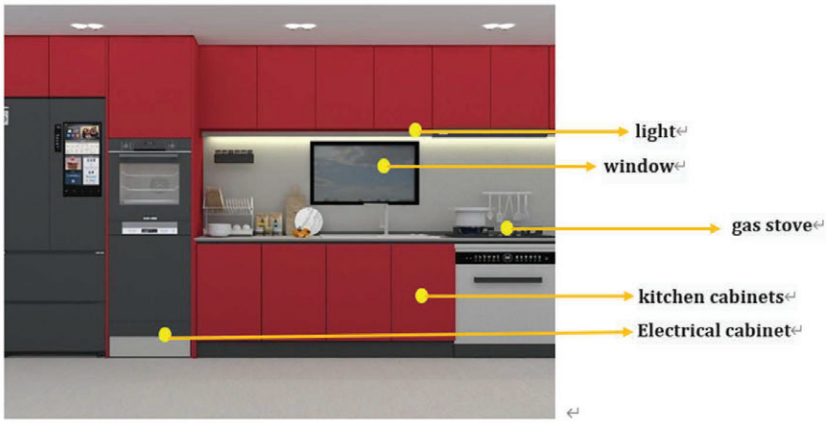

Figure 1: 3D Example of a figure

Figure 2: 3D Example of a figure

CONCLUSION

Research Objectives and Methodology. The main objectives of this study are to (1) identify the colors and lighting conditions that people find undesirable in kitchen cabinets and (2) explore the correlation between disliked colors and lighting types. A series of 3D kitchen utensil models was designed using a Natural Color System (NCS) in combination with three different correlated color temperatures (CCTs). The study was conducted using a

questionnaire survey method, collecting a total of 119 valid responses. Statistical analyses including means, standard deviations, and Pearson's correlation coefficients were used to examine the results. The findings revealed that blue and green were the most commonly disliked colors for kitchen utensils, regardless of lighting conditions. These two colors showed a significant and strong positive correlation ($r > 0.07$, $p < .001$). Furthermore, when paired with a 3000 K color temperature, the disparity became even more pronounced ($r > 0.08$, $p < .001$). These results suggest that blue and green lights, particularly under warm white lighting (3000 K), are the least preferred combinations for kitchen utensil designs. The insights gained from this study may serve as valuable references for future kitchen interior and product design considerations.

REFERENCES

[1]. Ou, Hui-yi (1999). *Research on the Application of Spatial Color Imagery in Design. Graduate School of Industrial Design,* National Cheng Kung University. Master's Thesis

[2]. Tseng, J. Y. (2013). *A Study on the Competitive Strategy of Taiwan's Kitchenware Industry - A Case Study of Company O.* National Kaohsiung University Executive MBA Program

[3]. Lin, Guo-hua (2019)*The Effect of Color Temperature and Behavior Patterns on Workers' Emotions under General Illumination: A Case Study of 5001x Illuminance.* Department of Architecture, Chung Yuan Christian University. Master's Thesis.

[4]. Liu, Ren-hao (1999). *A Study on Color Preference and Imagery in Home Spaces. Graduate School of Information and Communication,* Chinese Culture University. Master's thesis.

Electrochemical Polymerization of Conductive Polymer Thin Films to Obtain Metallic Luster with High Reflectance

Katsumi Yamada[a*],Shota Tsuneyasu[a], and Fukuro Koshiji[a]

[a]*Tokyo Polytechnic University, Atsugi, Japan*
[*] *Katsumi Yamada, kyamada@t-kougei.ac.jp*

ABSTRACT

As a new electropolymerization method for conductive polymers, multi-step potetiostatic (MS-PS) polymerization was carried out in which alternately applies a constant potential (potential A) for the oxidation of the monomer and a constant potential (potential B) for the reduction of the resulting polymer. The polymer films with a metallic luster were obtained in short time by MS-PS polymerization of 3-methoxythiophene. This is expected to be due to the continuous application of potential B, which sufficiently reduces the polymer on the electrode and forms a higher-order structure. The color of metallic luster changed from green (or gold) to red upon electrochemical oxidation, this indicates that reflective electrochromism occurs in the system. The green metallic luster in the reduced state was changed to golden one with decreasing the number of MS-PS polymerization cycles. This is expected to be due not only to a decrease in the polymer film thickness but also to the flattening of the film surface condition. On the other hand, the MS-PS polymerization of 3,4-ethylenedioxythiophene were also carried out in the study. When the resulting polymer film was peeled off from the electrode, its surface exhibited a metallic luster that was golden color in the reduced state and reddish-purple color in the oxidized state. This is the first time that a golden metallic luster has been achieved with a single layer of PEDOT film, rather than a multilayer film with other polymers.

Keywords: Poly(3-methoxythiophene), Poly(3,4-ethylenedioxythiophene), Golden Metallic luster, Multi-step Potentiostatic Polymerization, Reflective electrochromism

INTRODUCTION

Color enriches our lives. Among these, colors with a metallic luster are particularly appealing. In most cases, items with a metallic luster are made from materials that contain metallic elements. These metal products exist several problems and challenges. These include difficulty in processing molding, allergies to the human body, radio interference, lightweight, and disposal after use. Other options for materials that can achieve a metallic luster are required to realize a sustainable society. For this reason, research into metallic luster from materials that do not contain metallic elements has become active in recent years. [1-7]

In these studies, studies into conductive polymers that exhibit a golden metallic luster has been attracting particular attention. [8-12] Hoshino et al. at Chiba University reported that a gold metallic luster could be obtained from a thiophene derivative polymer [8]. In their works, they obtained polymer films with a metallic luster by chemical and electrochemical polymerization. In the electrochemical method, they reported that the formation of polymer lamellae is necessary to form highly reflective polymer films, and that a slow cyclic potential scan of 10 mV/s is required [9]. The slow scan rate increases the overall synthesis time. Furthermore, the applied potential is continuously changed, which can result in polymer products with non-uniform properties, especially due to variations in the oxidation potential of the monomers. A polymer with as much uniformity as possible is required

to achieve high reflectivity. To address these issues, we have proposed a new method, the multi-stage potentiostatic polymerization (MS-PS) method, in which a constant potential for the oxidation of the monomer and a constant potential for the reduction of the resulting polymer are alternately applied [13]. This method allows for the continuous application of a constant potential, resulting in the formation of uniform polymers in a short time. Furthermore, this method allows for the film thickness, reflectivity, and color to be selected arbitrarily by changing the applied potential, the application time, and number of cycle repetitions.

It was revealed that MS-PS polymerization for 3-methoxythiophene (MT) results in the polymer (PMT) film with a green metallic luster in the reduced state and a red luster in the oxidized state. Here, we report on the results of controlling the color tone of the PMT luster by the conditions of MS-PS polymerization, and on the appearance of a golden luster from a 3,4-ethylenedioxythiophene (EDOT) polymer film obtained by MS-PS polymerization.

METHODOLOGY

An electrolyte solution was prepared by dissolving 3-methoxythiophene (MT) of 50 mM, lithium perchlorate of 0.1 M, and sodium dodecyl sulfate of 0.1 M in a mixture of ultrapure water and 1-butanol (volume ratio 96:4). An electrolyte solution was prepared by dissolving 3,4-ethylenedioxythiophene (EDOT) of 8 mM and tetra-n-butylammonium perchlorate of 0.1 M in acetonitrile. Multi-step potentiostatic (MS-PS) polymerization was carried out using a cleaned ITO glass plate as the working electrode, a silver-silver chloride as the reference electrode, and a platinum wire as the counter electrode. For the electrochemical polymerization of MT, a constant potential of +1.2 V was applied for 15 s in the first step (oxidation process) to oxidize the monomer, and a constant potential of −1.0 V was applied for 35 s in the second step (reduction process) to reduce the resulting polymer. In the electrochemical polymerization of EDOT, a constant potential of +1.3 V was applied for 15 seconds in the first step (oxidation process) to oxidize the monomer, and a constant potential of -1.0 V was applied for 25 seconds in the second step (reduction process) to reduce the resulting polymer. Reflectance measurements of the resulting polymer film were carried out using a Konica Minolta CM-26dG as the spectrophotometer. Transmission spectra were measured using an Ocean Optics OP-TR/RF-GONIO-MN as the diffuse transmittance/diffuse reflectance measurement system.

RESULTS AND DISCUSSION

1. Poly(3-methoxythiophene) [PMT]

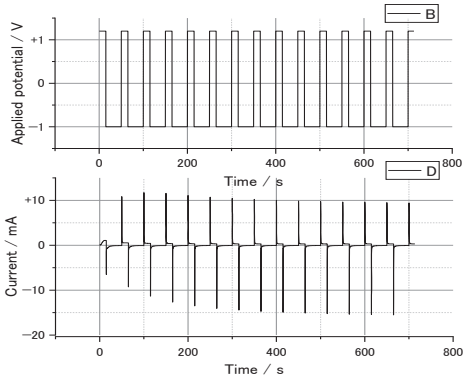

Figure 1: Time dependence of applied potential and reaction current during MS-PS polymerization of MT.

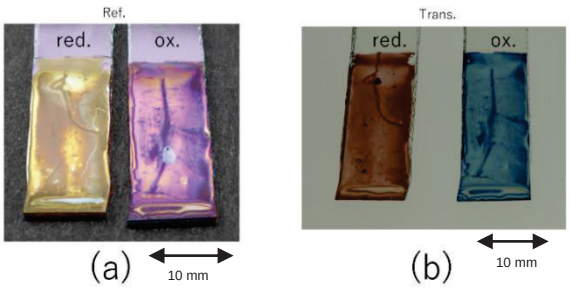

Figure 2: Photographs of the obtained PMT film in the reduced state (red.) and the oxidative state (ox.). These photo.s were taken with top illumination (a) and back illumination (b).

A constant potential of +1.2 V was applied for 15 seconds to oxidize MT, followed by a constant potential of -1.0 V for 35 seconds to reduce the polymer formed on the electrode. One cycle of MS-PS polymerization consists of the first step of monomer oxidation and the second step of polymer reduction. Figure 1 shows the time course

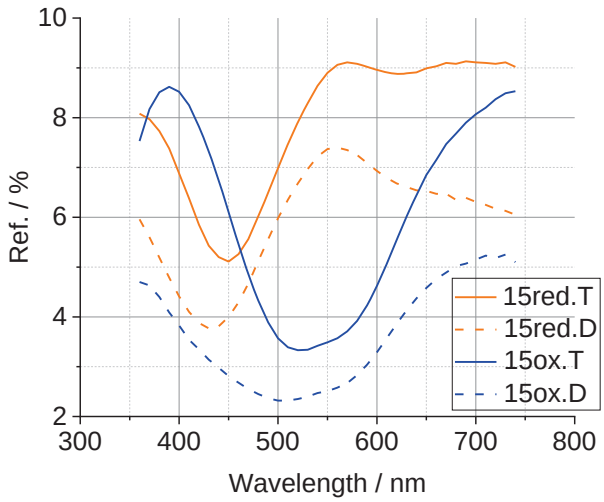

Figure 3: Total reflectance (T) and diffuse reflectance (D) spectra of the PMT films.

of the applied potential and current during MS-PS polymerization. The reduction current increased with increasing cycles, confirming the formation of an MT polymer (PMT) film on the electrode. Figure 2a shows a photograph illuminated with a white light source from the PMT film side on a black substrate. The surface of the PMT film formed on an ITO electrode after 15 cycles of MS-PS polymerization exhibited a gold metallic luster in the reduced

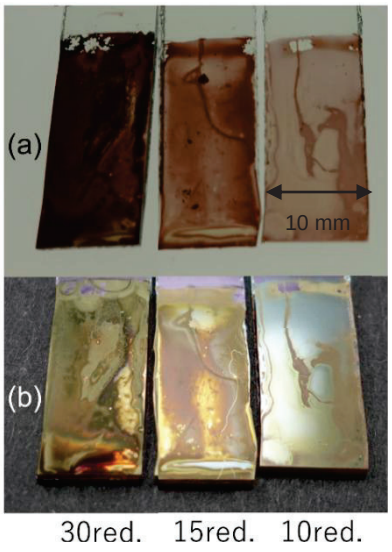

Figure 4: Photographs of the obtained PMT films (10-30 cycles for MS-PS polymerization) in the reduced state (red.). These photo.s were taken with top illumination (a) and back illumination (b).

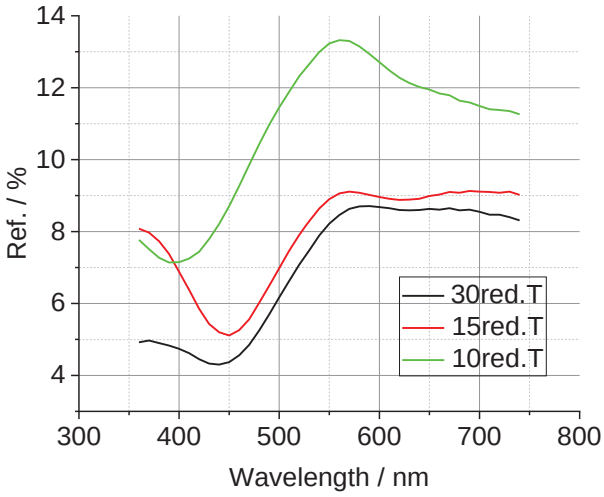

Figure 5: Total reflectance (T) spectra of the PMT films (10-30 cycles for MS-PS polymerization).

state and a reddish-purple metallic luster in the oxidized state. Figure 2b shows a photograph illuminated with a white light source from the back of the PMT film. These images show the transmitted color of the PMT, which was red color in the reduced state and blue color in the oxidized state. Figure 3 shows the total and diffuse reflectance spectra of the PMT film formed on an ITO electrode after 15 cycles of MS-PS polymerization. In this case, the specular reflectance is calculated by subtracting the diffuse reflectance (abbreviated as D) from the total reflectance (abbreviated as T). As the higher the specular reflectance, the stronger the metallic luster. In Figure 3, 15red.T and 15ox.T represent the total reflectance spectra for the reduced and oxidized states, respectively. In the reduced state, the total reflectance at 570 nm was approximately 9%. The reduced state exhibited a golden color, but the specular component accounted for more than 20% of the total, resulting in a week metallic luster. In contrast, in the oxidized state, a maximum reflectance was observed at 390 nm (8.6% reflectance), with reflections observed at wavelengths longer than 600 nm. Figure 4 shows photographs of PMT films obtained after each cycle of MS-PS polymerization. Figure 4a was obtained by illumination with the transmitted light, and figure 4b was obtained by the reflected light. The transmitted light weakened as polymerization progressed, indicating an increase in film thickness. The color of the luster was observed to change from gold to green as the number of polymerization cycles increased. Figure 5 shows the total reflectance spectra for each cycle of MS-PS polymerization. It was found that the PMT films obtained after each polymerization cycle also exhibited a maximum reflectance at approximately 570 nm. The reflectance decreases as the number of MS-PS polymerization cycles increases. The film with the 10 cycles, is significantly more reflective than the other films and has a distinct golden color. This film's surface is expected to have a very smooth surface, resulting in strong specular reflection.

2. Poly(3,4-ethylenedioxythiophene) [PEDOT]

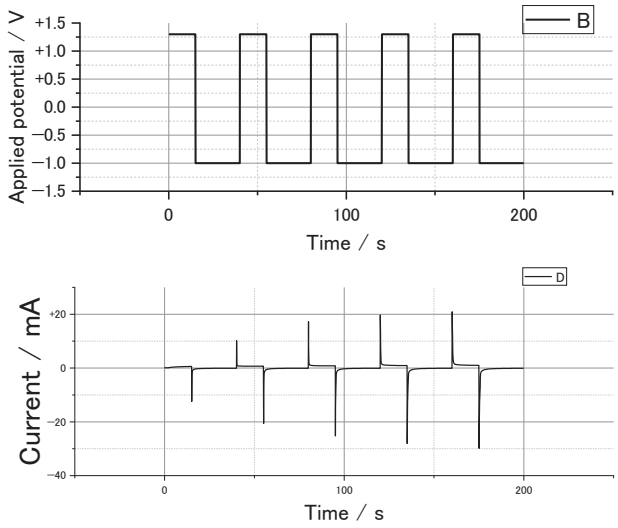

Figure 6: Time dependence of applied potential and reaction current during MS-PS polymerization of EDOT.

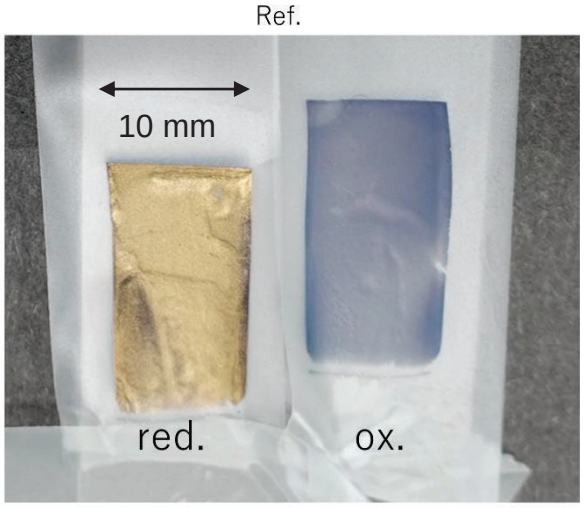

Figure 7: Photographs of the obtained PEDOT films in the reduced state (red.) and the oxidative state (ox.).

A constant potential of +1.3 V was applied for 15 seconds to oxidize EDOT, followed by a constant potential of -1.0 V for 25 seconds to reduce the polymer formed on the electrode. Figure 6 shows the time course of the applied potential and current during MS-PS polymerization. The oxidation and reduction currents increased with increasing cycle count, confirming the formation of a PEDOT film on the electrode. The PEDOT film surface formed on the ITO electrode was dark blue in the reduced state and light blue in the oxidized state. Then, peeling the polymer film off with adhesive tape exposed the film surface in electrode side. Figure 7 shows a photograph of PEDOT film on the tape. Under a white light source, a golden metallic luster was observed in the reduced state. A blue luster was observed in the oxidized state. Figure 8 shows the total and diffuse reflectance spectra of PEDOT formed on the tape (after five cycles of MS-PS polymerization). A maximum reflection was observed at a wavelength of 650 nm, with a reflectance of 12.3%. Figure 9 shows the relationship between the number of cycles and the total reflectance at the maximum reflection wavelength. The reflectance decreased with an increase in the number of cycles. This decrease in reflectance is also influenced in the difference in the surface condition, with a tendency for the surface to become rougher with an increase in the number of cycles.

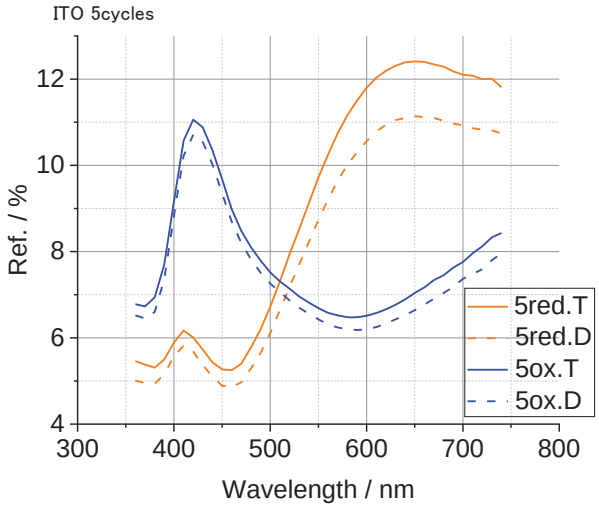

Figure 8: Total reflectance (T) and diffuse reflectance (D) spectra of the PEDOT films.

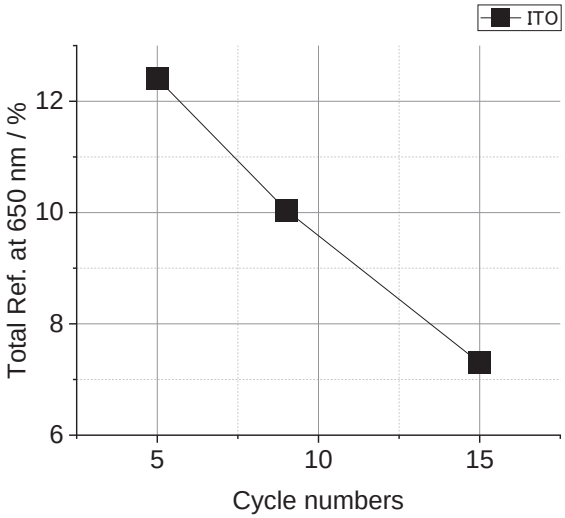

Figure 9: Relationship between the cycle number of MS-PS polymerization and the reflectance at the reflection maximum of the PEDOT film.

CONCLUSION

A golden metallic luster was observed from the PMT film formed on an ITO electrode by MS-PS polymerization. It was revealed that the reflectance and color tone of the luster changed depending on the number of MS-PS polymerization cycles. A golden metallic luster was observed from the PEDOT film in a reduced state by MS-PS polymerization. While golden metallic luster has previously been observed from bilayer films of polyaniline and PEDOT [10], this is the first time that golden metallic luster has been observed from a PEDOT single layer film .

REFERENCES

[1]. Ogura, K., Zhao, R., Yanai, H., Maeda, K., Tozawa, R., Matsumoto, S., and Akazome, M. (2002). Facile formation of stable crystals with gold-like metallic luster from organic molecules: 1-Aryl-2-(2-thienyl)-5-[5-(tricyanoethenyl)-2-thienyl] pyrroles: *Bull. Chem. Soc. Jpn.*, 75(11), 2359-2370.

[2]. Pradel, T., Climent-Font, A., Molera, J., Zucchiatti, A., Ynsa, M. D., Roura, P., and Crespo, D. (2007). Metallic and nonmetallic shine in luster: an elastic ion backscattering study: *J. Appl. Phys.,* 101, 103518.

[3]. Goto, H. (2013). Crystal–liquid crystal ordered double layer electroactive polymer prepared with phase transition sequential polymerization, showing metallic electrochromism–bronze, silver, and gold: *J. Polym. Sci. Part A,* 51(15), 3097-3102.

[4]. Kondo, Y., Matsumoto, A., Fukuyasu, K., Nakajima, K., and Takahashi, Y. (2014). Gold-Colored organic crystals formed from an azobenzene derivative: *Langmuir,* 30(15), 4422-4426.

[5]. Yazima, H., Sasaki, M., Takahashi, K., Hiraoka, K., Oshima, M., and Yamada, K. (2018). Green metallic luster on the film of safflower red pigment extracted by a traditional method -Approach with optical measurements-: *J. Soc. Photogr. Imaging. Jpn.,* 81, 65-69.

[6]. Yajima, H., Sasaki, M., Takahashi, K., Oshima, M., Hiraoka, K., Yashiro, M, and Yamada, K. (2018). Influence of photo-illumination on greenish metallic luster of safflower red pigment film: *Bull. Soc. Photogr. Imaging. Jpn.*, 28(2),18-22.

[7]. Kaki, T., and Yamada, K. (2021). Metallic luster from materials without metallic elements -Relationship between molecular orientation by stretching and polarization reflection -: *Bull. Soc. Photogr. Imaging. Jpn.*,31(2), 5-8.

[8]. Tagawa, R., Masu, H., Itoh, T., and Hoshino, K. (2014). Solution-cast selfassembled films of perchlorate-doped oligo(3-methoxythiophene) showing a gold-like luster: *RSC Adv.,* 4, 24053-24058.

[9]. Tokuda, T., and Hoshino, K. (2016). Electropolymerized films of 3-methoxythiophene with a potential sweep-induced gold like luster: *Polym. J.,* 48, 1141-1149.

[10]. Takada, H., Ochiai, T., and Nagata, M. (2019). Color-changeable gold luster film based on polyaniline and poly(3,4-ethylenedioxythiophene): *Thin Solid Films*, 677, 33-38.

[11]. Tsukada, S., Saito, R, and Hoshino, K. (2023). Color control of metal-like lustrous films of 3-alkoxythiophene oligomer dyes by changing subnanometer-scale interlamellar distance: *ACS Appl. Opt. Mater.,* 1, 1847-1855.

[12]. Goto, H. (2025). Preparation of golden polyaniline and interpretation with a Lorentz model: *Next Materials*, 8, 100582100582.

[13]. Yamada, K. (2024). A new method for preparing metallic luster of 3-methoxythiophene polymers: *Bull. Soc. Photogr. Imag. Japan.*, 34(2), 31-33.

The Impact of Dynamic Lighting Conditions on The Color Perception and Texture Impression of Fabric

Shuilan He[a*]

[a] *Osaka Seikei University, Osaka, Japan*

ABSTRACT

This study aims to clarify the impact of dynamic lighting conditions on the color perception and texture impression of fabrics. Subjective evaluation experiments were conducted using various types of fabrics differing in material and structure, under environments where lighting parameters—such as color temperature, illuminance, and angle of incidence—were varied over time. In addition to participants' subjective evaluations, objective indicators were extracted through image analysis to investigate the correlation between perceived color and texture attributes (e.g., glossiness, roughness, and softness). The results revealed that, for certain materials, changes in lighting significantly altered the perceived hue and depth, with glossy fabrics in particular showing pronounced shifts in texture impression. Furthermore, it was found that dynamic lighting induced greater changes in the visual impression of fabrics compared to static lighting, suggesting potential applications in design strategies for online retail and lighting-based presentation.

Keywords: Dynamic Lighting, Color Perception, Texture Impression, Fabrics

INTRODUCTION

Global Apparel Industry Statistics reports that 79% of fashion sales happened in stores, and only 21% came from online sales. It is also reported that online sales are growing rapidly [1]. Based on this trend, many researchers have begun to study how to reduce the cognitive gap between color perception and texture impression in online images and actual products, in order to lower the return rate in online sales. Ko et al. [2] attempted to simulate store environments on computers to investigate the relationship between lighting, color, and texture. Ishikawa et al. [3] examined image presentation methods in online shopping environments by dynamically altering fabric textures. In my previous studies [4,5], I investigated the relationship between lighting conditions—specifically illuminance and spectral distribution—and fabric color perception and texture impression.

In this study, I attempt to create a new and more cost-effective approach by using animated images to reduce the cognitive gap between color perception and texture impression in online images and actual products.

METHODOLOGY

(1) Experimental Method

In the experiment, the Semantic Differential (SD) method was applied using eight adjective pairs to assess the perceived color and texture impressions of the fabric samples (see Table 1). To conduct absolute evaluations of images or animated images.

(2) Lighting Conditions

An observation booth was employed for the experiment (Figure 1), with light sources positioned at three angles: overhead (90°), lateral (60°), left-up (30°) and left-side (0°). Three types of commercial LED lamps served

as the light sources: LDA12D-G-E26 (LED-D65), LDA12L-G-E26 (3000K), and DiCUNO ProOE (HighRa). The specifications of each lighting condition applied in the experiment are summarized in Table 2. The camera (Nikon D7500) was set to fixed shooting parameters (Av f5.6, iso 300, EV ±0, 4928×3264 Pixel) and used to capture digital photographs of the fabric stimuli from a fixed angle.

Table 1: Adjective pairs

(-4	0	4)
Muted	—	Vivid
Dark	—	Bright
Heavy	—	Light
Polished	—	Unpolished
Matte	—	Glossy
Soft	—	Hard
Rough	—	Smooth
Thick	—	Thin

Table 2: Adjective pairs

	LED-D65	LED-HighRa	LED-3000
CCT	6470	5116	2912
duv	0.00818	0.00194	-0.00127
Ra	83.2	97.5	82.7
R9	5	85	6
R10	69	97	83
R11	84	97	82
R12	63	96	76

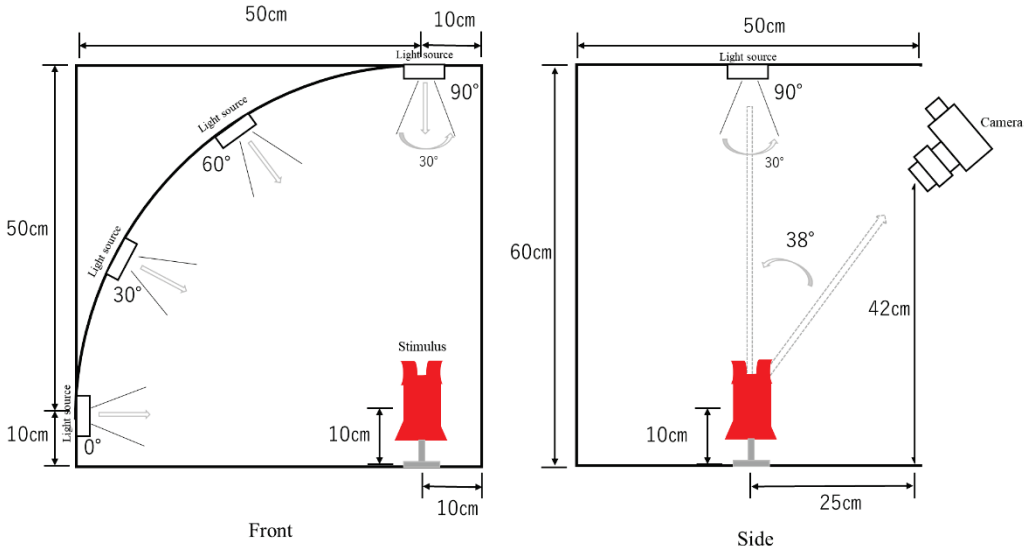

Figure 1. Lighting booth

(3) Evaluation Samples

The evaluation samples (Figure 2) were as follows:

Fabric Types: Broadcloth (moonfarm, 100% cotton, 120g/m², thread count: CD40×CD40), Silk Satin (Toray, 100% polyester, 120g/m², thread count: CD80×CD80)

Color: Red (Figure 3)

Surface Characteristics: Glossy, Matte

Sizes: Standing size: 9.6cm x 4.8cm, flat lay: 4.8cm x 5.8cm (1/100 of the actual size of the garment).

The image data was converted to a resolution of 150 dpi using Photoshop 2020 (Adobe), and the hue and saturation of the background area of the original image were changed.

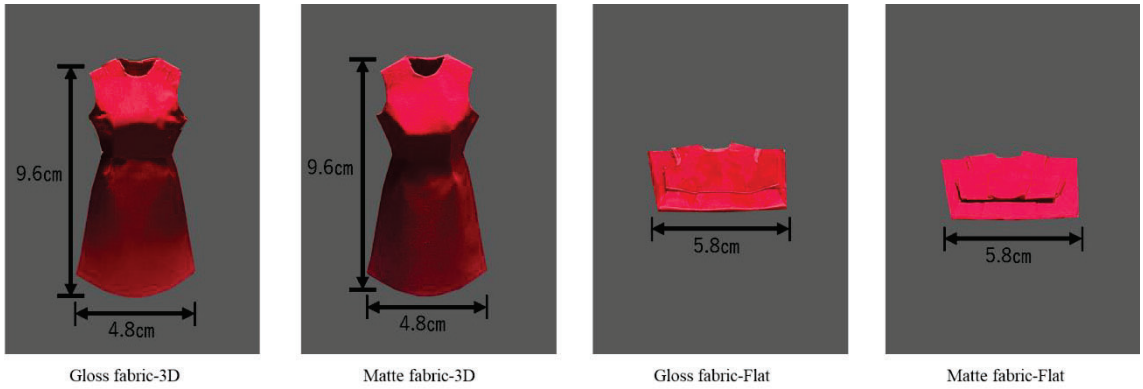

Figure 2. The evaluation samples

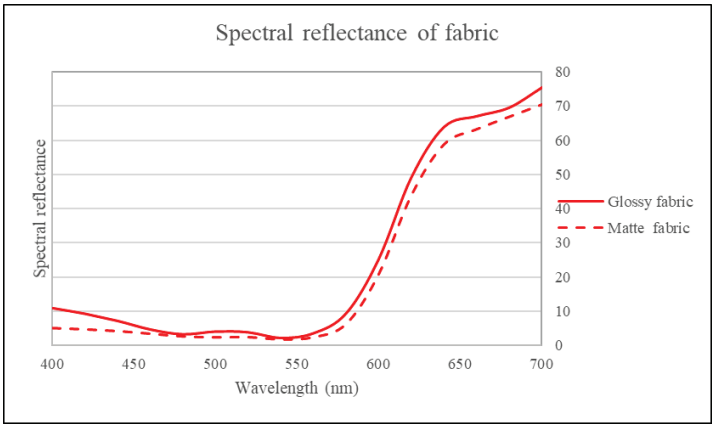

Figure 3. Spectral reflectance (SCE) of evaluation samples

(Gloss: solid line, matte: dotted line)

(4) Experimental stimuli

Two types of stimuli were prepared. The first type consisted of static photographs (JPEG format) of four fabric samples—Gloss fabric-3D (G-3D), Matte fabric-3D (M-3D), Gloss fabric-Flat (G-Flat), and Matte fabric-Flat (M-Flat)—captured under three lighting conditions (LED-D65, 3000K, and HighRa) at a fixed illumination angle of

60°. The second type consisted of dynamic images (GIF format) created by combining photographs of the same four fabric samples taken under the three lighting conditions at three illumination angles (0°, 30°, 60°and 90°). Each dynamic image sequentially presented the photographs of a given sample under the same lighting condition at 0°, 30°, 60°and 90° illumination angles, with each frame displayed for 0.5 seconds in a continuous loop.

(5) Experimental Procedure

The experiment was carried out in a darkroom (Figure 4) using an LCD display (EIZO Color Management Monitor, ColorEdge CG277; pixel density: 109 ppi, pixel pitch: 0.233 × 0.233 mm, gradation: 1024 levels, color depth: 10 bits per channel). The monitor was calibrated colorimetrically to the CIE XYZ system, with a white point set at 5000 K and a maximum white luminance of 80 cd/m².

Participants were given a 3-minute period of dark adaptation prior to the experiment. Subsequently, participants adapted for one minute to a gray screen (equivalent to N7) presented on the monitor. Following this adaptation phase, image stimuli (6 cm wide × 9 cm high) were displayed at the center of the screen, and participants recorded their evaluations of color appearance and texture impression on the response sheet. Once the evaluation was completed, the participant pressed the confirmation key on the keyboard to proceed to the next image pair. To minimize the influence of afterimages between trials, an achromatic random-dot pattern was presented for 2 seconds, thereby reducing the carryover effects of the preceding stimulus.

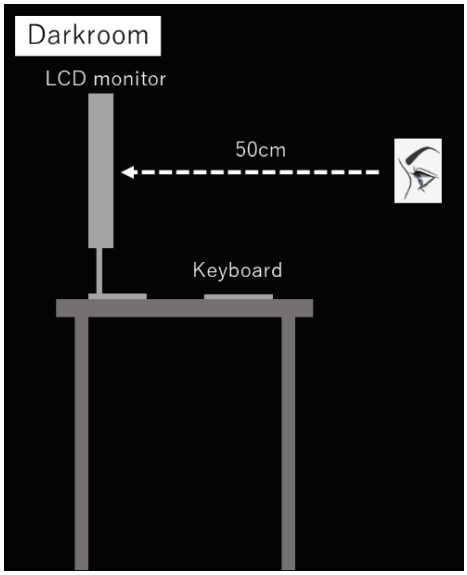

Figure 4. Experimental environment

(6) Participants

The experiment involved six participants with normal color vision, aged 19 to 41, some of whom wore corrective glasses or contact lenses.

RESULTS AND DISCUSSION

(1) The result of Principal Component Analysis

The subjective evaluation results for all participants under each stimulus were analyzed using Principal Component Analysis (IBM SPSS). As shown in Table 3, the first principal component was associated with fabric surface properties, the second with brightness perception, and the third with softness perception.

Table 3: The result of Principal Component Analysis

Evaluative adjective pairs / Principal Component			(Ⅰ)Fabric surface properties	(Ⅱ)Brightness perception	(Ⅲ)Softness perception
Polished	—	Unpolished	-0.94	0.12	0.09
Muted	—	Vivid	-0.89	-0.11	-0.09
Matte	—	Glossy	-0.89	0.35	0.07
Rough	—	Smooth	-0.87	0.33	0.06
Dark	—	Bright	-0.58	-0.62	-0.20
Heavy	—	Light	-0.34	-0.83	0.26
Thick	—	Thin	-0.53	-0.5391	0.43
Soft	—	Hard	0.54	-0.44	-0.57

(2) Subjective Evaluation Results

For the first principal component, representing fabric surface impressions, the analysis considered adjective pairs including ‘Polished–Unpolished, ’Muted–Vivid,’ ‘Matte–Glossy,’ and ‘Rough–Smooth.’ These were examined in relation to the participants’ subjective evaluation results.

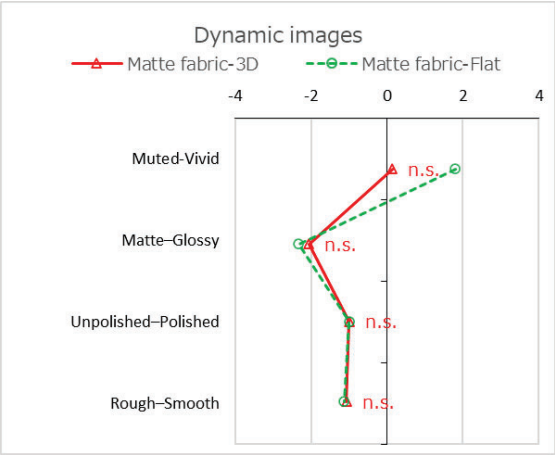

Figure 5. The relationship between Matte fabric-3D and Matte fabric-Flat in dynamic images

The subjective evaluation results for fabric surface impressions of the dynamic images, specifically Matte fabric-3D and Matte fabric-Flat, are shown in Figure 5. No significant difference was found in subjective evaluations between Matte fabric-3D and Matte fabric-Flat°.

As shown in Figure 6, for matte fabric samples, subjective evaluations related to lighting angle, corresponding to the first principal component, varied significantly depending on the angle of the light source. T-tests revealed significant differences between Matte fabric-3D and Matte fabric-Flat at the 0° lighting angle ($t(4) = 14.39$, $p < 0.001$). For the flat-shaped samples, subjective evaluations were more frequently associated with descriptors such as ‘Muted,’ ‘Matte,’ ‘Unpolished,’ and ‘Rough.’

As with the author’s previous experiment, the results of the other experiments also revealed that the subjective evaluations of the perceived color and texture impressions of the fabric samples varied significantly depending on the angle of the lighting source.

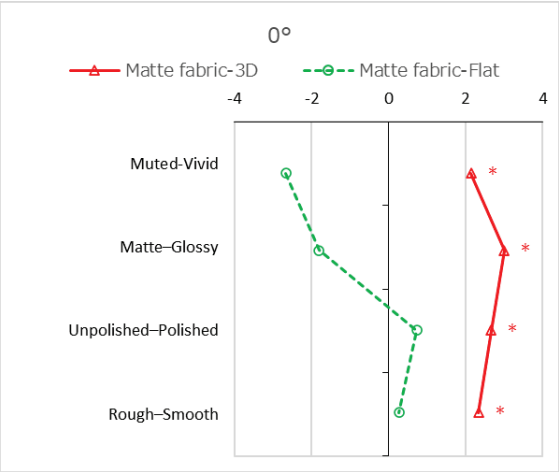

Figure 6. The relationship between Matte fabric-3D and Matte fabric-Flat in Lighting angle 0°

CONCLUSION

The present findings highlight the significant role of lighting conditions in shaping the perceptual evaluation of fabrics. The comparison between static and dynamic lighting conditions revealed that dynamic illumination produced greater variations in perceived color and texture. This suggests that the continuous shifts in lighting angle may enhance the observer's perceptual sensitivity, leading to more pronounced alterations in visual impressions.

These results extend previous research on color and texture perception by demonstrating that lighting dynamics, in addition to spectral composition, serve as critical variables in fabric evaluation. From an applied perspective, this has important implications for the field of online retail and digital presentation of fashion products. Since one of the major challenges in e-commerce is the discrepancy between digital representations and the actual experience of fabrics, the findings suggest that employing dynamic lighting techniques in digital imagery may provide consumers with richer, more realistic cues of fabric qualities. Consequently, this approach could reduce the perceptual gap between online images and physical products, thereby addressing one of the primary causes of product returns.

REFERENCES

[1]. Nancy Cardona. (2025). Global Apparel Industry Statistics. National Sales | Uniform Market. Retrieved March 8, 2025, from https://www.uniformmarket.com/statistics/global-apparel-industry-statistics

[2]. T.K. Ko, et al. (2016). Simulation and perceptual evaluation of fashion shop lighting design with application of exhibition lighting techniques. SungBuilding Simulation. 9(6). pp.641–658.

[3]. Ishikawa, T., Tsuji, R., Sasaki, K., Miyatake, K., Ayama. M. (2016). Investigation of Fabric Texture Expression through Dynamic Alteration of Drapes- Image Presentation Method in Online Shopping Environments -. International Journal of Affective Engineering. Vol.15No.2 pp.45-50.

[4]. He, S., & Nakajima, Y., (Eds.). (2020). Effect of Spectral Distribution of Illumination on Color Appearance and Texture Impression of the Fabric with Different Surface Properties. J. Illum. Engng. Inst. Jpn. 104 (2020), pp. 3–10.

[5]. He, S., & Nakajima, Y., (Eds.). (2019). The Influence of Spectral Distribution of Illumination on the Color and Texture Appearance of Glossy Fabric. Journal of Japan Society of Kansei Engineering. Vol.18No.5 pp.407-416.

Elderly Users' Color Emotions and Preferences Toward The Appearance of Differently Designed Care Robots

Ching-Chih Liao[a*], Shi-Min Gong[b], Ya-Han Hsu[c]

[a b c] *Ming Chuan University, Taoyuan, Taiwan*

**Corresponding author: Ching-Chih Liao, ccliao@mail.mcu.edu.tw*

ABSTRACT

Taiwan has entered an aging society, and AI caregiving robots are considered essential for future care. This study aimed to investigate emotional associations with appearance and color preferences for caregiving robots among 60 older adults (mean age 72.6), and to examine gender differences. The study used preliminary surveys and a two-stage experiment; data were analyzed using ANOVA, Friedman, and Mann–Whitney tests. Results showed that the older adults preferred a "wheeled robot" for caregiving. Regarding color–emotion associations, warm colors were more likely to evoke feelings of friendliness, comfort, safety, softness, and liveliness; cool colors (blue-green, blue) tended to convey impressions of rationality and calmness. For both robot appearances, the most prominent color–emotion associations were rationality and friendliness, followed by comfort, safety, and softness, with liveliness rated lowest. There were no significant gender differences in overall color preference, although females showed a greater preference for purple and males for white. Overall, both men and women preferred warm, bright, and vivid colors and were less likely to choose Black, Gray, and Cyan. The study also indicated that robot form moderately influences color preference.

Keywords: Color-emotion, Color preference, Care robot, Elderly, Appearance design

INTRODUCTION

Taiwan entered an aged society in 2018, with over 14% of the population aged 65 or above; by 2025, this proportion is expected to surpass 20%, reaching a super-aged society [1]. With declining birth rates and a shortage of caregivers, care robots are anticipated to play an increasingly vital role.

Most care robots are currently designed in white or silver. As these products mature, it is essential to examine whether their colors meet users' emotional and aesthetic needs. Product color not only influences psychological identification but also affects cognitive and behavioral responses [2]. Since colors carry multiple meanings and perceptions vary across age, gender, and life experience [3, 4], this study investigates elderly adults' emotional associations and preferences toward robot colors, as well as gender differences in responses. The findings aim to inform the aesthetic design of future care robots.

Care robots are defined as autonomous or semi-autonomous systems performing physical or emotional caregiving tasks [5]—can be categorized as "professional-use" or "personal/home service" robots [6]. This study focuses on the latter, specifically "humanoid" and "wheeled" designs [6]. Prior research suggests that elderly adults often prefer less human-like robots [7, 8, 9]. Although white dominates current robot design, Bartneck et al. [10] questioned this prevalence, noting that color diversity can reduce bias and influence perception. Warm hues, such as yellow, are often perceived as more approachable than darker colors [2].

Color symbolism has long been shown to affect psychological responses, marketing communication, and consumer behavior [11, 12]. Meanings vary across cultures and contexts—for instance, yellow represents happiness,

red conveys anger or love, and gray suggests sadness [13, 14, 15]. Such associations are further shaped by memory, culture, and lived experience [16, 17, 18].

Color preference—people's tendency to favor certain hues—is influenced by demographic factors and object type [19, 20]. For example, red and blue are popular for clothing, while orange and yellow are less favored [21, 22]. Studies show that blue and red are consistently accepted across age groups [23]. However, gender differences are evident: female university students least preferred pink, while males least favored gray, brown, and white [24]. Hallock [25] further reported that 57% of men and 35% of women preferred blue, while men disliked brown and women disliked orange. These findings underscore the importance of considering demographic factors when applying color to robot design.

METHODOLOGY

Experimental Design- Two hypotheses were proposed: 1. Gender influences emotional associations with robot colors. 2. Gender influences color preferences for different robot forms. Three independent variables were used: gender (n = 2, between-subjects), hue, and emotional semantic (n = 12, n = 6, within-subjects, respectively). Dependent variables were color–emotion associations and color preferences. Emotional associations were measured using the semantic differential (SD) method with a seven-point scale and analyzed via repeated-measures ANOVA; preferences were analyzed using Friedman and Mann–Whitney tests. Sixty Taiwanese adults aged 65+ (M = 72.6, SD = 6.77), equally split by gender, participated after signing informed consent.

Stimuli Design- Following Berlin and Kay [26], twelve colors were selected (white, gray, black, red, orange, yellow, green, blue, purple, pink, brown, cyan), and their CIELAB values were measured using an X-Rite i1 device (**Table 1**). Based on the author's prior findings, the most preferred commercially available wheeled (non-humanoid) robot and the relatively less preferred humanoid robot were redesigned. Both models were constructed in 3D using Rhino, rendered in Keyshot at a standardized height of 62 cm, and each was assigned the twelve colors. This procedure produced 24 color–robot combinations (S1–S12 for non-humanoid robots, S13–S24 for humanoid robots) (**Figure 1**). For the preference ranking task, pairs of robots were displayed side by side on the same screen, yielding 26 images.

Table 1: **12 color samples**

	W	Gy	Bk	R	O	Y	G	B	P	Pk	Br	C
L*	100	58	11	56	66	85	47	52	53	86	57	45
a*	0	-1	0	63	35	-2	-46	-16	23	14	23	-41
b*	0	-2	-1	37	59	79	24	-36	-33	-2	13	-15
C*	0	2	1	73	69	79	52	40	40	14	26	43
h	360	241	279	30	59	92	152	246	305	354	29	200

	S1	S2	S3	S4	S5	S6	S7	S8	S9	S10	S11	S12
L*	95.59	61.68	25.96	55.29	64.99	77.2	45.85	60.89	55.04	84.47	60.78	50.29
a*	9.93	6.67	4.63	30.71	21.56	5.44	-16.01	2.08	18.09	14.64	14.11	-5.02
b*	-7.37	-8.47	-6.31	13.66	25.98	58.36	13.4	-28.12	-29.33	-8.12	0.72	-13.54
C*	12.38	10.78	7.82	33.75	33.87	58.62	20.59	28.21	34.46	16.74	14.13	14.7
h	323.33	308.33	306.33	21.67	49.67	84.67	140.33	274.33	301.67	330.67	3	252

S13	S14	S15	S16	S17	S18	S19	S20	S21	S22	S23	S24

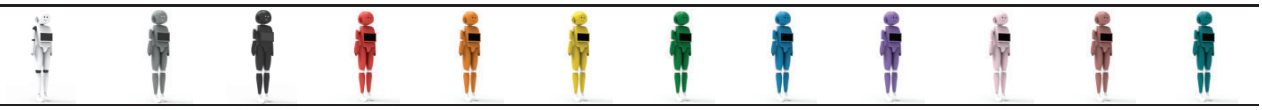

L*	92	59.52	25.16	54.33	64.75	74.9	43.18	52.1	54.86	81.08	57.14	46.41
a*	9.68	6.54	4.49	30.47	18.69	5.48	-16.12	-6.77	17.03	14.45	17.92	-6.71
b*	-6.46	-5.61	-5.28	12.16	18.67	44.14	12.78	-14.15	-26.7	-6.97	2.25	-14.15
C*	11.75	8.79	6.94	32.94	26.45	44.52	20.58	15.69	31.67	16.05	18.1	15.7
h	327.33	319.67	310.33	20.33	44.67	82	142	271.67	302.67	334.33	7	244.67

Figure 1: 12 Non-Humanoid & Humanoid Robot Samples

Measurement Instruments-Stimuli were displayed on a 15.6-inch screen, calibrated with the X-Rite i1 device. Questionnaires were administered via SurveyCake hosted on iPay. Six adjectives representing emotional semantics were selected based on pretests with 91 participants aged 50 – 70: friendly, comfortable, reassuring, rational, gentle, and lively. A 7-point Likert scale (1 = low, 7 = high) was used to measure emotional associations.

Procedure- Experiments were conducted individually. Participants were randomly assigned the order of robot forms: some started with humanoid robots, others with non-humanoid robots. Within each form, stimuli were presented in random order. Participants first rated emotional associations for each robot-color combination. Subsequently, they selected and ranked their top three preferred colors from the paired images (13th stimulus), providing reasons for their choices. Each experiment concluded with presenting a small gift to the participant to express appreciation for their participation.

RESULTS AND DISCUSSION

Color–emotion Associations- A repeated measures ANOVA was conducted to examine participants' emotional associations with robot colors. No significant gender main effect was found for either non-humanoid robots, F (1,58) = 0.408, p = .526, η^2p = .007, or humanoid robots, F (1,58) = 0.691, p = .409, η^2p = .012, indicating that gender did not influence color–emotion associations.

For the main effect of emotional semantics, significant effects were observed for both non-humanoid robots, F (5,290) = 17.032, p = .001, η^2p = .227, and humanoid robots, F (5,290) = 16.450, p = .001, η^2p = .221. Scheffé post-hoc tests showed that participants most strongly associated both robot types with rationality (M = 4.578/4.607) and friendliness (M = 4.503/4.451), while liveliness received the lowest ratings (M = 3.933/3.924).

Further analysis of emotional–color associations for non-humanoid robots (**Table 2**) showed that yellow, white, pink, orange, and red were most strongly linked with positive emotions such as friendliness, comfort, and liveliness. In contrast, black, gray, and cyan conveyed distance and seriousness. For "rational," warm hues like orange, pink, and red ranked lowest, suggesting they were less aligned with cognitive impressions.

For non-humanoid robots, a significant main effect of color emerged, F (11,638) = 36.038, p = .001, η^2p = .383. Scheffé post-hoc analysis ranked colors as: yellow > white > orange, pink, red, brown, green > blue, purple > cyan > gray > black (**Table 2**).

Table 2: Non-Humanoid Robot Color-Emotion Rankings

Friendly Code/*M*	Comfortable Code/*M*	reassuring Code/*M*	rational Code/*M*	gentle Code/*M*	lively Code/*M*
S6/ 6.03	S6/ 5.78	S6/ 5.75	S1/ 5.41	S10/ 5.6	S6/ 6.21
S1/ 5.36	S1/ 5.33	S10/ 5.3	S8/ 5.28	S6/ 5.51	S5/ 5.71
S5/ 5.31	S10/ 5.3	S1/ 5.16	S6/ 4.78	S1/ 5.26	S4/ 5.33
S4/ 5.3	S5/ 5.1	S5/ 5.03	S11/ 4.7	S11/ 4.98	S1/ 4.28
S10/ 5.25	S4/ 5.03	S11/ 4.96	S7/ 4.68	S7/ 4.68	S7/ 4.2
S11/ 4.98	S11/ 4.93	S4/ 4.95	S12/ 4.65	S5/ 4.66	S10/ 3.9
S7/ 4.81	S7/ 4.8	S7/ 4.8	S9/ 4.63	S4/ 4.51	S11/ 3.85
S8/ 4.36	S8/ 4.4	S8/ 4.45	S2/ 4.55	S8/ 4.43	S9/ 3.55
S9/ 4.26	S9/ 4.13	S9/ 4.31	S3/ 4.23	S9/ 4.26	S8/ 3.43

S12/ 3.61	S12/ 3.83	S12/ 3.75	S4/ 4.15	S2/ 3.6	S12/3.05
S2/ 3	S2/ 3.16	S2/ 3.26	S10/ 3.93	S12/ 3.55	S2/ 2.06
S3/ 1.71	S3/ 1.86	S3/ 1.96	S5/ 3.91	S3/ 1.93	S3/ 1.5

Further analysis of emotional–color associations (**Table 3**) for humanoid robots showed that white, blue, and green ranked highest for rationality, while yellow and pink were most strongly linked with positive emotions (friendly, comfortable, reassuring, gentle). Darker or muted colors like black, gray, and cyan were least associated with positive feelings. In contrast, warm colors like pink, orange, and red were least associated with rationality, indicating that brightness and warmth do not always align with cognitive perceptions.

Bright warm hues (yellow, pink, orange, white) elicited the strongest positive responses in older adults, while darker tones reduced affective engagement. Gender had no significant effect, suggesting that color choice is more important than demographic factors in designing care robots.

A significant main effect of color was observed for humanoid robots, $F(11,638) = 26.322$, $p = .001$, $\eta^2p = .312$, indicating apparent differences among the 12 colors. Scheffé post-hoc analysis ranked them as: yellow > white, pink, orange, brown > red, purple, blue, green, cyan > gray > black, confirming that bright, warm colors were most strongly associated with positive emotional responses (**Table 3**).

Table 3: Humanoid Robot Color-Emotion Rankings

Friendly Code/*M*	Comfortable Code/*M*	Reassuring Code/*M*	Rational Code/*M*	Gentle Code/*M*	Lively Code/*M*
S6/ 5.76	S6/5.50	S6/ 5.35	S1/ 5.63	S10/ 5.53	S6/ 6.21
S10/ 5.31	S10/ 5.28	S10/ 5.31	S8/ 5.21	S6/ 5.25	S5/ 5.48
S5/ 5.25	S1/ 5.06	S11/ 5.18	S12/ 5.05	S1/ 5.23	S4/ 4.78
S11/ 4.91	S11/ 5.06	S1/ 4.93	S11/ 5.00	S11/ 4.83	S9/ 4.75
S1/ 4.91	S5/ 4.93	S5/ 4.91	S6/ 4.81	S5/ 4.65	S1/ 4.11
S4/ 4.83	S4/ 4.73	S4/ 4.71	S7/ 4.55	S9/ 4.41	S10/ 4.00
S9/ 4.78	S7/ 4.45	S7/ 4.46	S2/ 4.55	S4/ 4.15	S11/ 3.68
S7/ 4.60	S9/ 4.45	S9/ 4.35	S9/ 4.23	S8/ 4.05	S7/ 3.58
S8/ 4.26	S8/ 4.40	S8/ 4.30	S3/ 4.21	S12/3.80	S8/ 3.40
S12/ 4.16	S12/ 4.06	S12/ 3.75	S10/ 4.05	S7/ 3.65	S12/3.23
S2/ 2.83	S2/ 2.80	S2/ 3.26	S5/ 4.00	S2/ 3.41	S2/ 2.15
S3/ 1.76	S3/ 1.88	S3/ 1.96	S4/ 3.96	S3/ 1.88	S3/ 1.68

Color Preference Rankings for Non-Humanoid and Humanoid Robots- Participants' color preferences were analyzed using the Friedman test. For non-humanoid robots, results showed a significant difference among the 12 colors, $\chi^2(60) = 122.308$, $p = .001$. Based on mean ranks, the top four colors were red, white, green, and yellow, while the least preferred were black, gray, and cyan (**Figure 2**-(a)). Wilcoxon signed-rank tests between the top and bottom colors showed no significant pairwise differences.

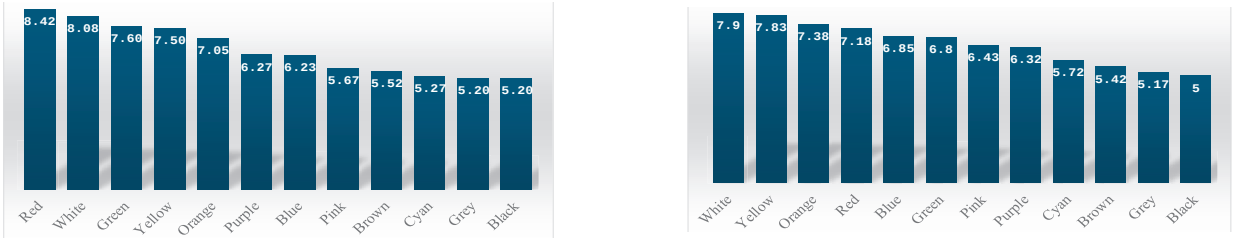

(a) Non-Humanoid Robots / The values in the bar chart represent the Mean Rank.

(b) Humanoid Robots / The values in the bar chart represent the Mean Rank.

Figure 2: The color preference ranking of two types of care robot appearances

A significant difference was also observed for humanoid robots, χ^2 (60) = 87.872, p = .001. The top four colors were white, yellow, orange, and red, and the least preferred were black, gray, brown, and cyan (**Figure 2**-(b)). Consistent with non-humanoid robots, participants generally favored bright, warm colors and showed lower preference for dark or muted tones.

Gender Differences in Color Preference for Non-Humanoid and Humanoid Robots- Mann–Whitney tests revealed gender differences in color preferences: males favored white (Z = -2.790, p = .005), whereas females favored purple (Z = -2.209, p = .027). Other colors showed no significant differences; black was rarely chosen, while pink and red were similar across genders. As shown in **Table 4**, which presents the most frequent reasons for selection, both genders preferred bright, high-saturation warm colors, associated with friendliness, liveliness, comfort, and warmth.

For humanoid robots, a gender difference appeared only for purple (Z = 2.105, p = .040), with females showing a greater preference. Other colors showed no significant differences, and black was seldom selected. **Table 4** indicates that both genders preferred white, red, yellow, and orange, which are linked to comfort, simplicity, brightness, and warmth. While the first-choice colors were consistent across genders, second- and third-choice preferences varied slightly by gender and robot type.

Table 4: Gender-based color preferences and selection reasons for two robot types

Non-humanoid robots				humanoid robots			
Preference Rank	Gender	Color	Reasons / Frequency	Preference Rank	Gender	Color	Reasons / Frequency
1st	Male	White	Comfortable (7)	1st	Male	White	Comfortable (8)
	Female	Red	Vivid (9)		Female	Red	Vivid (6)
2nd	Male	Red	Obvious (5)	2nd	Male	Yellow	Bright (6)
	Female	Yellow	Lively (4)		Female	Yellow	Bright (7)
3rd	Male	Green	Comfortable (9)	3rd	Male	Orange	Warm (6)
	Female	Orange	Bright (5)		Female	Purple	Personal preference (5)

Discussion- Consistent with prior surveys, both genders preferred wheeled over humanoid robots, supporting Dario et al. (1999) [7], Arras & Cerqui (2005) [8]. This suggests Taiwanese older adults prioritize approachability and safety over human-likeness.

Warm colors (yellow, pink, orange, red) elicited stronger positive associations across five of six emotional dimensions, with yellow rated highest, perceived as vivid, lively, warm, and friendly (Louine, 2018 [2]; Fugate & Franco, 2019 [14]; Jonauskaite et al., 2020 [15]). Pink was moderately accepted, showing culture, age, and context influence color preference (Jonauskaite et al., 2016 [21]; Manav, 2007 [22]).

For non-humanoid robots, white ranked among the top three colors in most emotional dimensions except "lively," with similar trends for humanoid robots. Brightness variations of white merit future study (Myers, 2020)—males associated white with environmental compatibility, suggesting marketing potential.

Overall, gender differences were minor: males preferred white, females preferred purple; other preferences were similar. Males slightly favored mid-tone or cooler colors but liked red, challenging assumptions about older male color preferences. Blue, generally favored by adults, was not especially preferred for care robots, highlighting that color preference depends on object type.

CONCLUSION

Warm colors are strongly associated with friendly, comfortable, reassuring, gentle, and lively emotions, while cool colors like white and blue are more associated with rationality. Color preferences concentrate on warm and neutral hues, including red, white, green, yellow, and orange. It is recommended that care robots adopt wheeled forms that appear cute, approachable, and safe, with color schemes favoring warm, cheerful, friendly, and pleasant tones. Future research could explore different robot types and interactive elements to enrich the understanding of care robot design further.

REFERENCES

[1] National Development Council. (2014). *Population projections of the Republic of China*. National Development Council.

[2] Louine, J., May, D. C., Carruth, D. W., Bethel, C. L., Strawderman, L., & Usher, J. M. (2018). Are black robots like black people? Examining how negative stigmas about race are applied to colored robots. *Sociological Inquiry, 88*(4), 626–648.

[3] Kaya, N., & Epps, H. H. (2004). Relationship between color and emotion: A study of college students. *College Student Journal, 38*(3), 396–405.

[4] Horvath, R. (2015). The color differences between men and women. *Three Digital.* Retrieved Sep. 14, 2025, from https://bit.ly/2YhAVoR

[5] Goeldner, M., Herstatt, C., & Tietze, F. (2015). The emergence of care robotics—A patent and publication analysis. *Technological Forecasting and Social Change, 92*, 115–131.

[6] Allego. (2017). [Robotics lecture] Many types of robots: How should they be classified? Retrieved Sep. 14, 2025, from https://bit.ly/3ci5yme

[7] Dario, P., Guglielmelli, E., Laschi, C., & Teti, G. (1999). MOVAID: a personal robot in everyday life of disabled and elderly people. *Technology and Disability, 10*(2), 77–93.

[8] Arras, K. O., & Cerqui, D. (2005). *Do we want to share our lives and bodies with robots? A 2000-person survey*. Technical Report No. 605.

[9] Wu, Y.-H., Fassert, C., & Rigaud, A.-S. (2012). Designing robots for the elderly: Appearance issue and beyond. *Archives of Gerontology and Geriatrics, 54*(1), 121–126.

[10] Bartneck, C., Yogeeswaran, K., Ser, Q. M., et al. (2018). Robots and racism. In *Proceedings of the 2018 ACM/IEEE International Conference on Human-Robot Interaction* (pp. 196–204).

[11] Simonson, A., & Schmitt, B. H. (1997). *Marketing aesthetics: The strategic management of brands, identity, and image.* Free Press.

[12] WebFX. (2020). *Psychology of color.* Retrieved from https://www.webfx.com/tools/color-guide/

[13] Lundberg, A. (2020). Color meanings and the art of using color symbolism. *99designs.* Retrieved Sep. 14, 2025, from https://99designs.com/blog/tips/color-meanings/

[14] Fugate, J. M. B., & Franco, C. L. (2019). What color is your anger? Assessing color–emotion pairings in English speakers. *Frontiers in Psychology, 10*, 206.

[15] Jonauskaite, D., Abu-Akel, A., Dael, N., et al. (2020). Universal patterns in color–emotion associations are further shaped by linguistic and geographic proximity. *Psychological Science, 31*(10), 1245–1260.

[16] Wilms, L., & Oberfeld, D. (2018). Color and emotion: Effects of hue, saturation, and brightness. *Psychological Research, 82*(5), 896–914.

[17] Lane, R. (1991). Does orange mean cheap? *Forbes, 148*(14), 144–147.

[18] Madden, T. J., Hewett, K., & Roth, M. S. (2000). Managing images in different cultures: A cross-national study of color meanings and preferences. *Journal of International Marketing, 8*(4), 90–107.

[19] Fortmann-Roe, S. (2013). Effects of hue, saturation, and brightness on color preference in social networks: Gender-based color preference on the social networking site Twitter. *Color Research & Application, 38*(3), 196–202.

[20] Taylor, C., Clifford, A., & Franklin, A. (2013). Color preferences are not universal. *Journal of Experimental Psychology: General, 142*(4), 1015–1027.

[21] Jonauskaite, D., Mohr, C., Antonietti, J.-P., et al. (2016). Most and least preferred colours differ according to object context: New insights from an unrestricted colour range. *PLOS ONE, 11*(3), e0152194.

[22] Manav, B. (2007). Color–emotion associations and color preferences: A case study for residences. *Color Research & Application, 32*(2), 144–150.

[23] Birren, F. (2016). *Color psychology and color therapy: A factual study of the influence of color on human life.* Pickle Partners Publishing.

[24] Baniani, M. (2022). The association between colors, color preferences, and emotions among Japanese students: From elementary school to university. *Color Research & Application, 47*(4), 992–1004.

[25] Hallock, J. (2003). *Colour assignment.* Retrieved from http://www.joehallock.com/edu/COM498/

[26] Berlin, B., & Kay, P. (1969). *Basic color terms: Their universality and evolution.* University of California Press.

Colours For The Future : Achrome Photographs In Archaeology Maraghiannis Of Candie Publishing House

Annie-Dominique Denhez[*]

[a]*Université Paris-Nanterre, Nanterre, France*
[*]*Corresponding author: Denhez, anniedo.denhez@gmail.com*

Abstract

Archaeological excavations at the end of the 19th century, need photographs. But without colors photographs, how rendering colours is possible ? We show the work by a Greek photographer, Georgios Maraghiannis, publishing the Minoan colours from recent excavations in Crete, from 1906 to 1915: *Cretan Antiquities* in three phototype albums. The black-and-white technique- sepia plates for landscapes, terracottas and gold jewellery, and grey plates for bronzes- let see the shades and tons. We shall compare these plates using sepia and black for phototypic emulsions.

Photography, Archaeology, Polychromy, Achromy, Colours

Introduction

Archaeological excavations intensified at the end of the 19th century, when photography became indispensable on excavation sites. Beautiful photographs were also used as propaganda to attract financial backers for these works. Since the birth of photography, people had been waiting for the possibility of reproducing colours. The Lumière brothers' autochrome plate (1904) was marketed in 1907, but it proved disappointing: it produced a single, non-reproducible image that was also difficult to use. Archaeologists used chromolithography to try to reproduce colours, but the flat colours were dull, lacking in nuance and without brilliance. However, recent discoveries of Minoan colours in Crete have caused astonishment and surprise: Gilliéron's watercolours prove it. How can these tones be reproduced using reproducible processes?

TEXT

It was at this time that a Greek photographer, Georgios Maraghiannis, published the Minoan colours from recent excavations in Crete, from 1906 to 1915: *Cretan Antiquities* in three phototype albums. (Fig. 1.) Through subtle achromaticity, he paradoxically spread ancient polychromy to a European audience. He continued this contemporary venture, for a decade. Although he patented his work in 1904, when when the Lumière brothers filed their industrial patent, this did not deter him from setting up his own phototype company in Candie for the second volume, whereas the first volume had been a collaboration with Victor Angerer's company in Vienna. He also chose the achromatic technique, known as black and white. He used two tools: emulsion, i.e. the choice between sepia and black, and the background contrasting with the objects: light or dark.

Thus, sepia plates were used for landscapes, terracotta, gold jewellery and paintings, and black plates for bronzes (tools and sculptures), stone (vases and sculptures) and soapstone. For these sites, which were highly

surprising to the world at the beginning of the 20th century, fidelity to polychromy is built on this paradox: achromaticity for polychromy.

It is certainly through the high quality of the achromatic edition that ancient polychromy becomes visible. This is why the photographer chooses to control the edition: his attentive eye seeks to ensure that the gradations are rendered faithfully, which he considers to be a major challenge (Fig. 2 & Fig. 3). It is his t*echné* that is at stake.

These are art photographs. Before looking at these plates, it should be noted that not everyone (including archaeologists) shares an interest in colour, and that the trained eye of the photographer and of the archaeologist can discern the range of colours in the tones presented, where an untrained eye might see only contrasts.

CONCLUSION

But is this ancient polychromy visible to everyone? Is it only restored for the trained eye?

These views suggest this colourful ancient world: the early Minoan period in relation to Egypt: Hagia Triada, Gortyna, Mochlos, Vasiliki, Chamaizi, Pseira, Palaikastro, Phaistos, Gournia, Knossos... because at the time, some people still struggled to recognise Greek polychromy. However, photography, with its autoscopic view but without reproduced colours, has undoubtedly and unfortunately also contributed to the belief in a « white Greece ».

REFERENCES :

[1] Jockey Ph., (2015), *Le Mythe de la Grèce blanche.*
[2] Maraghiannis, G., (1911), *Antiquités crétoises*, deuxième série.

ILLUSTRATIONS

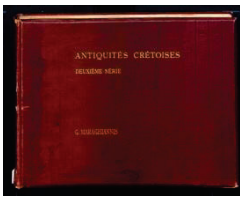

fig. 1: « G. Maraghiannis, *Antiquités crétoises*, deuxième série, 1911 ».

Sepia plates: for landscapes, Fig. 2 : in Maraghiannis, G. (1911) : « Mochlos, constructions sur la côte »earth and stones, buildings.

for terracotta, Fig. 3 : in Maraghiannis, G. (1911) : « Pl. XXII, Vases de Pseira, (M. M.) »

for stone vases, Fig. 3bis : in Maraghiannis, G. (1911) : « Pl. XXVI, Lampe et plat en pierre de Gournia (L. M. II-III) »

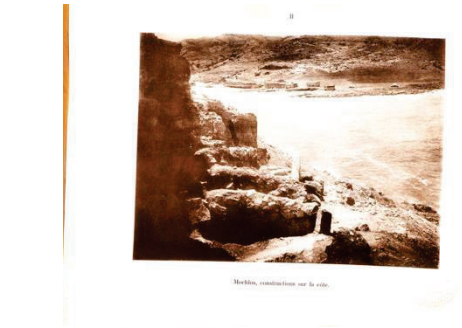

for terracotta, Fig. 4 : in Maraghiannis, G. (1911) : « Gournià, rhyton en forme de femme nue »

for paintings: Fig. 5 : in Maraghiannis, G. (1911) : « Pl. XLV : Sarcophage de H. Triada (L. M. III)
Fig. 5 bis : in Maraghiannis, G. (1911) : « Pl. XXXVIII Sarcophage de Palaikastro (L M. II-III)
for fresco Fig. 6 : in Maraghiannis, G. (1911) : « Pl. XLIII Fresque de H. Triada L M II »

for gold Fig. 7 : in Maraghiannis, G. (1911) : « Pl. V : Bijoux de Mochlos »

They manage to convey the colours and brilliance, playing with cropping and dark or light backgrounds

Black plates

for bronzes, Fig. 8 : in Maraghiannis, G. (1911) : « XLI Bouclier de bronze de l'Antre Idée MJ ».

for bronze tools, Fig. 9 : in Maraghiannis, G. (1911) : « Pl. XXXIII, Armes et outils en bronze de Gournià, (L M. III)

For stone vases, Fig. 10 : in Maraghiannis, G. (1911) : « Pl. XIX, Vases en pierre de Pseira (L. M. II) »

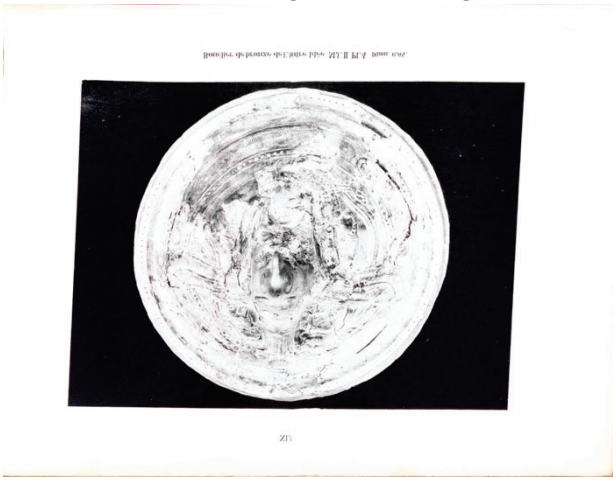

©photo. Annie Dominique Denhez after the Marighiannis's book, in the library of École Française d'Athènes, Greece.

https://cmt3.research.microsoft.com/AIC2025/Submission/Index.

The Effects of Positive and Negative Emotional States on Memory Colors

MinSeon Yun[a], YounJin Lee[b*]

[a]*Master, Dept. of Color Integrated Design, Graduate School of Industrial Arts, Hongik University, Seoul, South Korea*

[b]*Professor, Dept. of Color Integrated Design, Graduate School of Industrial Arts, Hongik University, Seoul, South Korea*

**Corresponding author: YounJin LEE, hacomama@hongik.ac.kr*

ABSTRACT

Emotions influence human color perception, and memory color can be reconstructed through cognitive processes even in the absence of physical stimuli. This study aimed to empirically analyze the effects of four emotional states (relaxation, joy, sadness, fear) on the visual attributes of memory color, focusing on emotional valence, arousal level, and the emotional context of stimuli. Based on the Geneva Emotion Wheel, the four emotions were categorized along the dimensions of positive-negative valence and high-low arousal and were induced using black-and-white film clips. The study measured ten linguistic stimuli—neutral (apple, banana, sprout, sea), positive (sunlight, baby's cheek, chick), and negative (storm, blood, drought)—in the CIE L*a*b* color space with a sample of 31 women in their 20s to 30s. Memory color changed depending on emotional state, with emotional valence emerging as a stronger influencing factor than arousal level. Under positive emotions, hue variation increased along with lightness and saturation, whereas under negative emotions, lightness variation was greater, and both lightness and saturation decreased. The findings confirm that memory color is modulated by the interaction of emotion and cognition, with emotional valence playing a particularly key role. These results offer practical implications for fields such as color design and visual communication.

Keywords: Memory Color, Emotional States, Valence, Color Perception, Chroma

INTRODUCTION

Emotion is a psychological factor that closely influences human cognition and perception, and prior studies have shown that color also varies with emotional states [1],[2]. This suggests that color perception involves not only bottom-up processing driven by physical stimuli but also top-down processing shaped by an individual's past experiences and current psychological state. In particular, memory color refers to the canonical color imprinted in memory for a specific object or scene, and it is reconstructed through cognitive processes even in the absence of physical stimulation [3]. This indicates that emotion and memory interact in the color perception process, and that memory color is a cognitive product that goes beyond mere reproduction of visual information.

However, existing research on the relationship between color perception and emotion has largely been confined to color preference or affective associations, and there is a lack of systematic investigation into how specific emotional states influence the visual attributes of memory color. Therefore, this study aims to empirically analyze changes in memory color when valence (positive/negative), arousal (high/low), and the emotional context of stimuli (neutral/positive/negative) interact across four emotional states—relaxation, joy, sadness, and fear. The hypotheses to be tested are as follows. First, memory color will differ according to emotional state. Second, there will be differences in memory color by valence. Third, memory color will vary with arousal level.

METHODOLOGY

Experimental Stimuli

The classification of emotions was based on the Geneva Emotion Wheel (GEW), which categorizes emotions along two dimensions: valence (positive vs. negative) and arousal (high vs. low). Based on this model, four emotional states were selected as experimental conditions: relaxation (positive–low arousal), joy (positive–high arousal), sadness (negative–low arousal), and fear (negative–high arousal). Emotional induction stimuli consisted of video clips, each edited to under one minute, based on previous studies. To eliminate the influence of color stimuli, all videos were converted to black and white. The relaxation condition featured scenes of everyday interactions, joy included scenes of celebration after victory, sadness involved farewell scenes, and fear used scenes in which a ghost appears (see Table 1). The memory color stimuli consisted of ten verbal stimuli categorized into three emotional contexts: neutral (apple, banana, sprout, sea), positive (sunlight, baby's cheek, chick), and negative (storm, blood, drought) (see Table 2).

Table 1: Emotion-specific film clips

Emotion	Relaxation	Joy	Sadness	Fear
Film Title	Little Forest	Bunt	1987: When the Day Comes	A Tale of Two Sisters
Clip Duration	0:57:40-0:58:37 (57s)	1:27:56-1:28:50 (54s)	0:41:03-0:41:02 (59s)	1:45:21-1:46:12 (51s)
Still Image				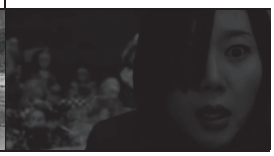

Table 2: Experimental stimuli categorized by emotional contexts

Stimuli	Apple	Banana	Sprout	Sea	Sunlight	Baby's Cheek	Chick	Storm	Blood	Drought
Emotional Contexts	Neutral				Positive			Negative		

Participants

A total of 31 women in their 20s and 30s with normal color vision participated in this study. The average age was 28.7 years (31 participants in their 20s and 8 in their 30s). The participant pool was limited to women in this age range based on prior findings indicating that women tend to have greater sensitivity in color perception and more accurate color memory [4], and that individuals aged 25 to 39 demonstrate the most stable color memory abilities [5].

Emotion Assessment

To verify whether the emotional induction stimuli effectively elicited the intended emotional states, a unipolar 5-point Likert scale was administered immediately after the presentation of each video. For the evaluation of the "relaxation" emotion, a score of 1 indicated "not relaxation at all," while a score of 5 indicated

"very relaxed." This scale was used consistently to assess emotional states—including neutral, relaxation, joy, sadness, and fear. Participants' memory color selections were quantified using the L*, a*, b* values in the CIE L*a*b* color space. These values served as evaluation metrics to measure quantitative changes in hue, lightness, and chroma.

Experimental Procedure

The experiment was conducted through one-on-one, in-person sessions. Participants first selected memory colors in a neutral emotional state. Then, emotions were induced in the following order: relaxation, joy, sadness, and fear, with repeated measurements using the same stimuli under each condition. A one-minute break was provided after each emotional induction to minimize the effects of visual afterimages and chromatic adaptation [6], [7].

RESULTS AND DISCUSSION

Results According to Emotional Induction Stimuli

As shown in Table 3, the average scores for each targeted emotion were as follows: Relaxation (M = 4.32) when relaxation was induced, joy (M = 3.94) when joy was induced, sadness (M = 3.97) when sadness was induced, and fear (M = 3.97) when fear was induced. Each emotional induction stimulus received the highest average score for its corresponding target emotion, indicating that the stimuli effectively elicited the intended emotional states.

Table 3: Mean emotional by emotion induction stimuli

Emotion	Neutral emotion induction	Relaxation induction	Joy induction	Sadness induction	Fear induction
Relaxation	3.61	4.32	3.58	2.77	1.87
Joy	3.16	3.68	3.94	1.94	1.84
Sadness	2.13	1.68	1.48	3.97	2.03
Fear	1.81	1.26	1.55	2.48	3.97
Mean	2.68	2.73	3.00	2.50	2.50

Memory Color According to Emotional State

Memory color tended to shift depending on the emotional state (see Table 4). In the Relaxation condition, there was minimal change in hue, but most stimuli showed an increase in lightness. Changes in chroma (saturation) did not follow a consistent pattern. In the joy condition, both lightness and chroma significantly increased, particularly for stimuli associated with negative emotional contexts. In the sadness condition, both lightness and chroma generally decreased, with notable changes observed in neutral-context stimuli such as sprout and sea. The fear condition showed the most significant changes in both lightness and chroma. Neutral stimuli—apple, banana, sprout, and sea—exhibited the greatest variation depending on emotional state, indicating that these stimuli are most sensitive to emotional shifts.

Table 4: Memory Color Variations Across Emotional States: Changes in Hue, Lightness and Chroma

Hue

Relaxation	Joy	Sadness	Fear
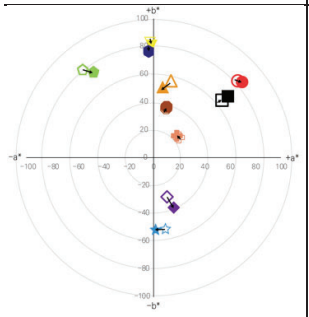	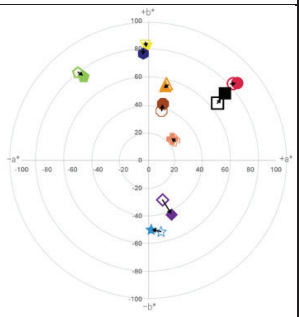	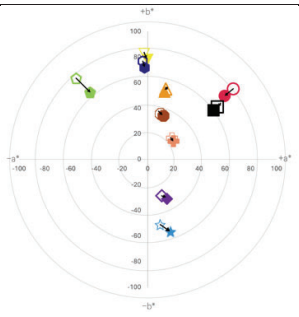	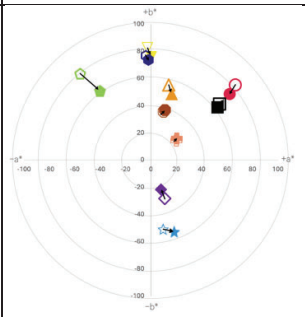

Lightness and Chroma

Relaxation	Joy	Sadness	Fear
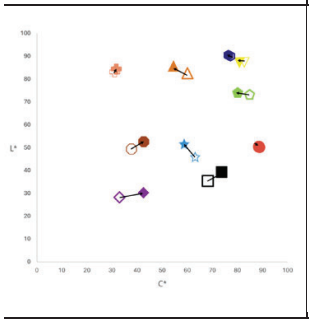	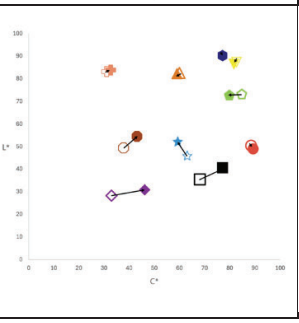	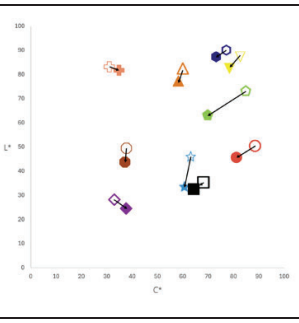	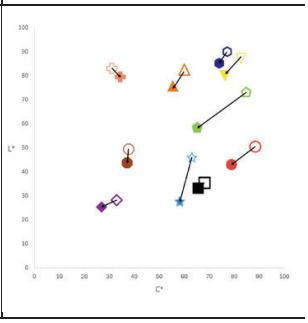

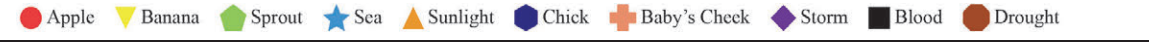

Color According to Emotional Valence

A comparison between positive emotions (Relaxation, joy) and negative emotions (sadness, fear) revealed that the greatest color difference was observed in chroma (C*), as shown in Table 5. Hue shifts were more pronounced under positive emotional states (ΔH* = 9.71) compared to negative ones (ΔH* = 9.04), while lightness shifts were greater under negative emotions (ΔL* = 9.66) than positive emotions (ΔL* = 7.16). In general, positive emotions were associated with brighter lightness and higher chroma, whereas negative emotions showed a tendency toward darker lightness and lower chroma (see Figure 1). These results suggest that emotional valence is a major factor influencing changes in memory color.

Table 5: Color differences between positive and negative emotions

Mean values	ΔE*	ΔL*	ΔC*	ΔH*
Positive	19.64	7.16	11.95	9.71
Negative	22.58	9.66	14.88	9.04

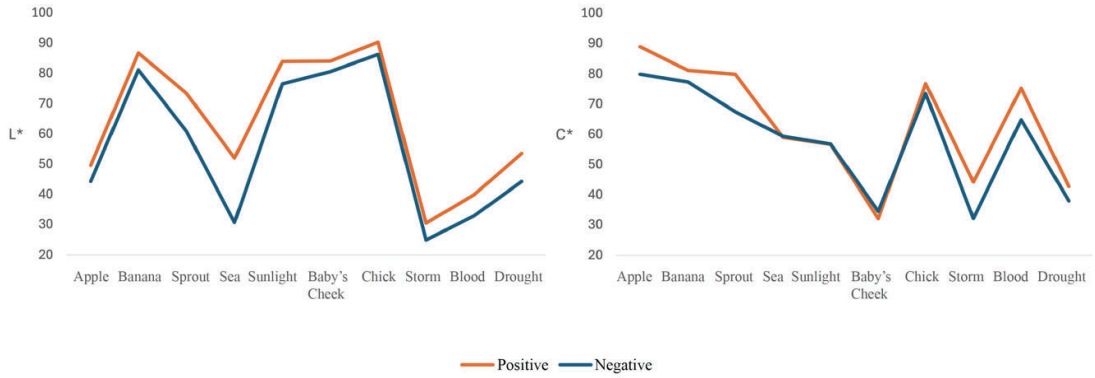

Figure 1: Comparison of lightness and chroma between positive and negative emotions across stimuli

Color differences were found to be greater under negative emotions than under positive emotions (see Figure 2). Among the stimuli, "sea" and "storm" showed large color differences in both positive and negative emotional states, indicating that they were most sensitive to emotional changes. In contrast, stimuli such as "banana" and "chick" showed relatively small color differences, even when emotional states changed, suggesting they were less affected by emotional context.

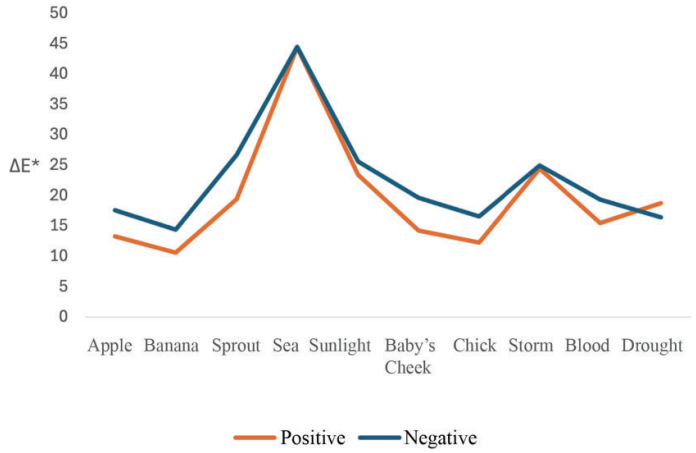

Figure 2: Color Difference Between Positive and Negative Emotions

The effect of arousal level was minimal compared to that of emotional valence, suggesting that emotional valence is a stronger influencing factor than arousal in memory color changes.

CONCLUSION

This study empirically examined the effects of emotional states on memory color and yielded the following key findings: First, memory colors varied distinctly depending on the emotional state. Second, there were clear differences based on emotional valence (positive vs. negative). Under positive emotions, greater changes were observed in hue, while negative emotions led to more significant changes in lightness. Furthermore, as emotional valence became more positive, both lightness and chroma increased; under negative emotions, memory colors tended to become darker and less saturated. The stimuli "sea" and "storm" showed the largest color differences, indicating high sensitivity to emotional changes, whereas "banana" and "chick" showed

the smallest differences. This suggests that the inherent emotional symbolism and typical color associations of objects may influence their responsiveness to emotional states. Third, the effect of arousal level was minimal, indicating that emotional valence plays a more significant role than arousal in memory color changes. These findings support the idea that memory color is shaped by the interaction between emotion and cognition, offering practical implications for a wide range of fields, including color design, visual communication, user experience (UX), and color therapy. However, the study has certain limitations: the participants were restricted to women in their 20s and 30s, and the stimuli were limited to 10 verbal items. Future research should aim to explore the relationship between memory color and emotion more comprehensively by including diverse age groups and genders.

REFERENCES

[1]. Wilms, L., & Oberfeld, D. (2018). Color and emotion: effects of hue, saturation, and brightness. *Psychological research*, *82*(5), 896-914.

[2]. Jonauskaite, D., Althaus, B., Dael, N., Dan-Glauser, E., & Mohr, C. (2019). What color do you feel? Color choices are driven by mood. *Color Research & Application*, *44*(2), 272-284.

[3]. McKeefry, D. J., & Zeki, S. E. M. I. R. (1997). The position and topography of the human colour centre as revealed by functional magnetic resonance imaging. *Brain*, *120*(12), 2229-2242.

[4]. Pérez-Carpinell, J., De Fez, M. D., Baldoví, R., & Soriano, J. C. (1998). Familiar objects and memory color. *Color Research & Application*, *23*(6), 416-427.

[5]. Choi, W. J. (2015). A Study on Focal Colors and Color Names as a Factor Forming Memory Colors. *Unpublished PhD Dissertation. Ewha womans University, Seoul, Republic of Korea*.

[6]. Fairchild, M. D., & Reniff, L. (1995). Time course of chromatic adaptation for color-appearance judgments. *Journal of the Optical Society of America A*, *12*(5), 824-833.

[7]. Wyszecki, G., & Stiles, W. S. (2000). *Color science: concepts and methods, quantitative data and formulae*. John wiley & sons.

Color Embodiment in Semantics of Abstract Concepts: Correlating Semantic Similarities with Visual Color Proximity in Metaphorical Lexemes Derived from the Chinese Color Term *Huáng*, 黄 'Yellow'

Yufeng Wu[a*]

[a] *City University of Hong Kong, Hong Kong, China*
[*] *Corresponding author: Yufeng WU, yufenwu2-c@my.cityu.edu.hk*

ABSTRACT

This study investigates the perceptual grounding of 18 metaphorical lexemes derived from the Chinese basic color term *huáng* 黄 'yellow' by integrating linguistic and visual analyses. Building on debates between symbolic and embodied cognition, it examines whether abstract metaphorical meanings of *huáng* are systematically associated with perceptual color features. A multimodal dataset was compiled consisting of 1,800 textual instances and 1,800 images representing 18 metaphorical lexemes. The linguistic component was annotated for 130 semantic and morphosyntactic features, while the visual component was characterized by 15 JzAzBz-based color metrics, including brightness, hue, entropy, and contrast. Lexeme-level similarity matrices were constructed for both modalities separately, and cross-modal correlations were evaluated using Pearson and Spearman tests alongside Mantel permutation procedures. Results reveal two entrenched clusters, pornography-related and royalty-related lexemes, that display strong internal cohesion across both semantic and visual domains. Peripheral categories, such as *huángle* 黄了 'failure' and *jiǎohuáng* 搅黄 'ruin', exhibited weaker cross-modal alignment. The findings indicate that while symbolic associations account for part of the variation, perceptual embodiment significantly contributes to the organization of *huáng* metaphors. Methodologically, this study demonstrates the utility of combining corpus annotation with perceptual color metrics, and conceptually, it highlights the partial but systematic role of sensory grounding in abstract lexical meaning.

Keywords: metaphor, embodiment, color semantics, perceptual grounding, Chinese lexemes

INTRODUCTION

Understanding how abstract concepts are mentally represented and linguistically expressed is a central concern in cognitive science and lexical semantics. Traditional symbolic theories argue that word meanings, particularly abstract ones, are processed through amodal, arbitrary symbols independent of sensory experience [1]. By contrast, embodied cognition proposes that meaning arises from perceptual and bodily interactions with the world, suggesting that even abstract meanings are grounded in sensorimotor systems [2][3]. One compelling domain for testing these competing accounts is metaphor, which often maps abstract ideas onto concrete experiences. Colors, as perceptually salient categories, have long provided rich sources of metaphorical extension, encoding emotions, judgments, and social constructs across languages.

Within this domain, the Chinese basic color term *huáng* exhibits particularly diverse metaphorical meanings. Historically associated with imperial authority and the color of gold, *huáng* has also developed modern associations with pornography, vulgarity, failure, and taboo [4]. These meanings appear in highly conventionalized expressions,

such as *huáng*páo 黄袍 ‘imperial robe’ and sǎo*huáng* 扫黄 ‘clear pornography’. Yet it remains uncertain whether such metaphorical extensions are merely symbolic conventions, or whether they are systematically related to perceptual attributes such as brightness, hue, entropy, and contrast. Previous research in embodied cognition has shown that perceptual features, including color, often underlie metaphorical and evaluative mappings [5][6]. Cross-cultural work further demonstrates that color metaphors simultaneously reflect universal perceptual tendencies and culture-specific traditions [7][8]. These findings highlight the need for an integrative analysis of color metaphors that consider both linguistic and visual data.

Under this background, the present study investigates whether the metaphorical lexemes of *huáng* are symbolically arbitrary or perceptually grounded. Specifically, it examines whether semantic and syntactic similarities among *huáng* metaphors correlate with similarities in visual features derived from associated images. By integrating corpus-based semantic annotation with computational color analysis, the study evaluates the embodiment hypothesis in the domain of Chinese color metaphors. The objectives of this research are threefold: (1) to investigate in what way lexemes are semantically and visually like each other? (2) whether the similarity shows cross modal consistency? In doing so, this work aims to advance debates on the grounding of abstract meaning and provide empirical evidence for the embodied dimensions of Chinese color metaphors.

METHODOLOGY

Data and Lexeme Selection

The data for this study were drawn from large contemporary Chinese corpora, including zhTenTen17, Chinese GigaWord 2, and the Chinese Trends corpus (2023-present). From these resources, a stratified random sampling procedure was used to identify metaphorical expressions containing the color morpheme *huáng* 黄 ‘yellow’. Based on frequency thresholds and prior literature, a total of 18 metaphorical lexemes were selected for analysis. Each lexeme was represented by one hundred example instances, yielding 1,800 textual instances in total. Parallel to the linguistic data, 1,800 images were collected to capture the visual representations associated with the same set of lexemes. Lexemes with fewer than one hundred instances in the corpora were excluded to ensure reliability in both semantic and visual analyses.

Semantic Feature Representation

The textual dataset was enriched through a comprehensive annotation scheme covering 130 features across lexical, morphosyntactic, semantic, discourse, and topical categories. Because the annotated variables were categorical in nature, they were transformed into a one-hot representation, whereby each possible feature category was encoded as a binary indicator. To produce lexeme-level profiles that were directly comparable across items, the binary values were aggregated as proportions: for example, if 70% percent of the tokens of a lexeme occurred in subject position, the lexeme received a value of 0.70 for that feature. This procedure yields a continuous vector for each lexeme that captures the probabilistic distribution of its semantic and syntactic properties.

Visual Feature Representation

The visual dimension was quantified through color analysis of the 1,800 collected images. Each image was characterized by 15 features derived from the JzAzBz perceptually uniform color space, including average values along the Jz (lightness), Az (red-green), and Bz (blue-yellow) axes, measures of variability for each dimension, entropy-based indices of distributional complexity, as well as composite descriptors such as hue angle, colorfulness, and contrast. To minimize the influence of outliers and ensure robust lexeme-level summaries, feature values were aggregated across all images for each lexeme using the median. The result is a stable visual profile that reflects the typical perceptual characteristics associated with each metaphorical expression of *huáng*.

Similarity Analysis

Semantic and visual profiles were then used to construct pairwise similarity matrices. For the semantic features, similarity between lexeme distributions was computed using a mixed approach: Jensen-Shannon divergence was applied to nominal features, while ordered features such as syntactic position were compared using the Wasserstein-1 distance. These measures were transformed into similarity scores on a 0-1 scale and averaged across features to generate a lexeme × lexeme semantic similarity matrix. For the visual features, Wasserstein-1 distances were computed on the numeric distributions of each feature and normalized by their global ranges, again yielding similarity scores between 0 and 1. Both matrices were inspected through heatmaps and subsequently used for clustering analyses, which revealed coherent groupings of lexemes reported in the results section.

Cross-modal Correlation

To assess whether semantic similarity among lexemes corresponded to visual similarity, cross-modal correlations were conducted between the two matrices. Vector correlations were first calculated by flattening the upper triangles of the matrices and applying Pearson's r and Spearman's ρ. In addition, Mantel tests with 9,999 permutations were employed to provide permutation-based significance levels that are more appropriate for structured similarity data. This combined approach allowed us to determine both the strength and robustness of cross-modal associations. Residual analysis was further conducted to identify lexeme pairs that either aligned or deviated from the global correlation pattern.

RESULTS AND DISCUSSION

Semantic similarity

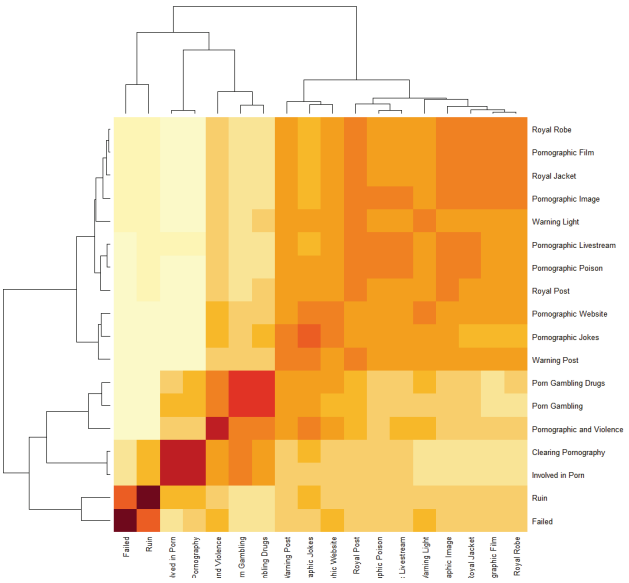

Figure 1. Semantic similarity of paired lexemes

The semantic similarity analysis revealed clear clustering patterns among the *huáng*-derived lexemes. Lexemes associated with pornography (e.g., Pornographic Film, Pornographic Image, Pornographic Livestream, Pornographic Poison) formed a dense group with extremely high similarity values, often exceeding 0.98. Likewise, lexemes tied to royalty and imperial symbolism (e.g., Royal Robe, Royal Jacket, Royal Post) also exhibited high internal similarity, with Royal Jacket and Royal Robe reaching a near-perfect score of 0.99. In addition, expressions linked to anti-pornographic actions, such as Clearing Pornography and Involved in Porn, clustered tightly with a similarity of 0.97, underscoring their close semantic association.

By contrast, lexemes such as Failed and Ruin occupied peripheral positions in the similarity map. Their pairwise similarities with either pornography-related or royal lexemes were consistently low (often below 0.25), suggesting that these metaphorical uses of *huáng* are less entrenched and more context-dependent.

These results point to two entrenched semantic poles: pornography and royalty, both deeply rooted in Chinese socio-cultural contexts. The pornography pole reflects the strong conventionalization of *huáng* as an index of sexually explicit content, reinforced by widespread collocational use. The royalty pole, by contrast, stems from traditional associations with imperial power, especially the imperial robe, which remains a stable semantic domain. Meanwhile, peripheral meanings such as 'failure' or 'ruin' demonstrate ongoing semantic diversification, yet their weak grouping indicates that these newer metaphorical senses are less integrated within the overall semantic structure.

To conclude, the findings suggest that *huáng* lexemes exhibit a structured semantic organization with two dominant, cohesive groups (pornography and royalty) and a set of marginals, emergent meanings. This pattern captures both the diachronic layering of *huáng* (from imperial robe to pornography) and its synchronic extension into novel, but less conventionalized, metaphorical domains.

Color similarity

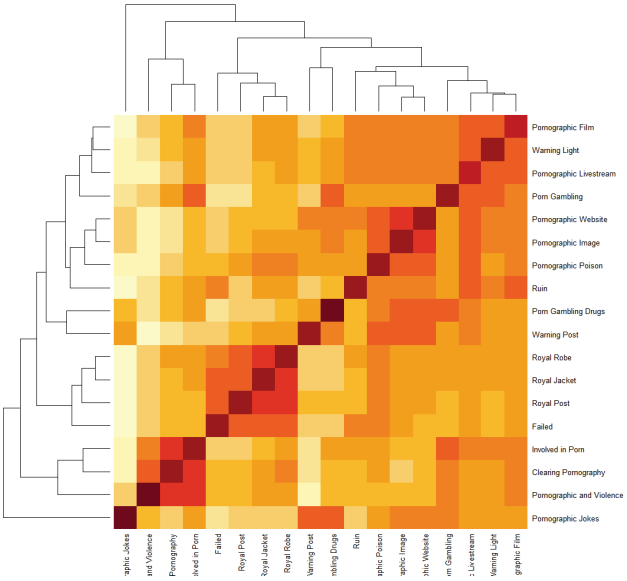

Figure 2. Visual similarity of paired lexemes

The visual similarity analysis revealed two prominent clusters. First, lexemes denoting pornographic content (e.g., Pornographic Film, Pornographic Livestream, Pornographic Image, Pornographic Website) demonstrated consistently high similarity values (>0.96), reflecting their shared perceptual features such as imagery, color cues, and visual framing. Second, lexemes tied to royal symbolism (Royal Jacket, Royal Robe) also clustered closely, indicating stable and recognizable visual associations with imperial attire.

In contrast, lexemes referring to failure or ruin showed very low similarity to either pornography or royalty groups, confirming their peripheral status in the visual domain. Interestingly, terms such as Clearing Pornography and Involved in Porn were visually cohesive, suggesting that both are embedded in a shared discourse space centered on pornographic imagery.

Overall, the findings suggest that *huáng* lexemes exhibit visual clustering parallel to semantic clustering: pornography and royalty serve as the two visually entrenched poles, while peripheral metaphorical extensions such as failure/ruin remain visually divergent.

Correlation between Semantic and Visual Similarities

To examine the relationship between semantic and visual similarity structures of *huáng*-derived lexemes, we conducted both conventional correlation analyses (Pearson and Spearman) and Mantel tests based on permutation procedures. The results are summarized in Table 1.

Table 1. Correlation and Mantel test results

Test	r / ρ	correlation p-value	Mantel p-value	Permutations
Pearson correlation	0.25	0.0018	0.0633	9999
Spearman correlation	0.29	0.00028	0.0284	9999

The Pearson correlation revealed a modest but significant positive association ($r = 0.25$, $p = 0.0018$), while the Spearman correlation produced a slightly stronger coefficient ($\rho = 0.29$, $p < 0.001$). These findings indicate that lexemes showing higher semantic similarity also tend to display higher visual similarity, although the effect is not strong.

The Mantel tests, which provide permutation-based significance estimates more appropriate for matrix data, yielded the same correlation coefficients (Pearson = 0.25; Spearman = 0.29). However, the significance levels differed: the Mantel Pearson test was marginally non-significant ($p = 0.0633$), while the Mantel Spearman test reached significance ($p = 0.0284$). This contrast suggests that rank-based associations between semantic and visual structures are more robust than purely linear ones.

Table 2. Residual analysis of semantic-visual similarity alignment for *huáng*-derived lexeme pairs

lexeme_i	lexeme_j	Semantic similarity	Visual similarity	predicted	residual	std_resid
aligned						
Pornographic Website	Royal Jacket	0.91	0.92	0.92	0.00	-0.01
Involved in Porn	Pornographic Image	0.32	0.90	0.90	0.00	-0.02
Pornographic Image	Royal Jacket	0.83	0.91	0.91	0.00	0.02
Involved in Porn	Pornographic Film	0.37	0.90	0.90	0.00	0.04
Pornographic Image	Pornographic Jokes	0.98	0.92	0.92	0.00	-0.05
deviant						
Royal Jacket	Warning Light	0.70	0.81	0.91	-0.10	-2.93
Pornographic and Violence	Warning Post	0.86	0.82	0.92	-0.10	-2.87
Failed	Royal Robe	0.34	0.81	0.90	-0.09	-2.74
Porn Gambling Drugs	Warning Post	0.79	0.83	0.91	-0.08	-2.43
Pornographic Image	Pornographic Livestream	0.77	0.83	0.91	-0.08	-2.43

Residual analysis revealed that some lexeme pairs were well aligned, with semantic and visual similarities closely matching. For example, *Pornographic Website–Royal Jacket* and *Pornographic Image–Pornographic Jokes* showed near-zero residuals, while *Involved in Porn–Pornographic Image* demonstrated how visual cues can compensate for weaker semantic ties. In contrast, deviant pairs such as *Royal Jacket–Warning Light* and *Pornographic and Violence–Warning Post* produced large negative residuals, indicating visual divergence despite semantic proximity. Cases like *Failed–Royal Robe* and *Pornographic Image–Pornographic Livestream* further illustrate metaphorical extensions of *huáng* that are less visually grounded and less predictable from semantic similarity.

These findings point to a gradient model of embodiment: entrenched domains such as pornography and royalty show strong cross-modal alignment, while emergent or context-dependent meanings (e.g., failure, ruin, warning) display weaker or inconsistent links. This suggests that the semantic evolution of *huáng* is not uniformly mirrored in visual representation but instead reflects selective reinforcement across domains.

CONCLUSION

This study demonstrates that metaphorical lexemes derived from *huáng* 黄 'yellow' show systematic yet partial convergence between semantic organization and visual color properties. Entrenched domains such as pornography and royalty exhibit strong cross-modal reinforcement, whereas more peripheral extensions remain less visually aligned. The moderate correlations observed across modalities suggest that embodied grounding is not uniform but gradient, shaped by cultural salience and perceptual distinctiveness.

Methodologically, the integration of corpus-based annotation, perceptually grounded color metrics, similarity matrices, clustering, and permutation-based correlation tests offers a replicable framework for exploring the interface between linguistic and perceptual systems. Conceptually, the findings challenge strictly symbolic accounts by showing that abstract lexical meanings are variably anchored in perceptual experience depending on semantic domain.

Future research should extend this analysis to additional color terms and across languages to evaluate whether partial embodiment is a universal tendency or a culture-specific phenomenon. By linking lexical semantics with perceptual properties of color, this study advances our understanding of how abstract meaning is grounded in cognition and underscores the potential of multimodal evidence for debates on metaphor, embodiment, and conceptual representation.

REFERENCES

[1]. Mahon, B. Z., & Caramazza, A. (2008). A critical look at the embodied cognition hypothesis and a new proposal for grounding conceptual content. Journal of Physiology-Paris, 102(1-3), 59-70.

[2]. Barsalou, L. W. (1999). Perceptual symbol systems. Behavioral and Brain Sciences, 22(4), 577-660.

[3]. Lakoff, G., Johnson, M., & Sowa, J. F. (1999). Review of Philosophy in the Flesh: The embodied mind and its challenge to Western thought. Computational Linguistics, 25(4), 631-634.

[4]. Xing, J. Z. (2009). Semantics and pragmatics of color terms in Chinese. Studies of Chinese Linguistics: Functional Approaches, 1, 87.

[5]. Hamilton, R. L. (2016). Colour in English: From Metonymy to Metaphor,

[6]. Meier, B. P., & Robinson, M. D. (2005). The metaphorical representation of affect. Metaphor and Symbol, 20(4), 239-257.

[7]. Jonauskaite, D., Parraga, C. A., Quiblier, M., & Mohr, C. (2020). Feeling blue or seeing red? Similar patterns of emotion associations with colour patches and colour terms. I-Perception, 11(1), 2041669520902484.

[8]. Yang, H., Zhang, S., & Lin, D. (2025). Green and black: the implicit color metaphor of environmental concepts and its impact on pro-environmental behavior. Humanities and Social Sciences Communications, (12), 1099.

A Suggestion on Local Colour Guidelines to Build Inner Mongolia's City Brand

Huang Jing[a*], Yoosun Kim[b], and Yoomi Kim[c]

[a]*Sahmyook University, Seoul, Korea*
[b]*Sahmyook University, Seoul, Korea*
[c]*Hankuk University of Foreign Studies, Seoul, Korea*
[*]*Corresponding author: Yoomi Kim, 02ymkim@gmail.com*

ABSTRACT

This study aims to suggest local guidelines for branding and sustainable development in Inner Mongolia's cities. To examine regional colour for city branding, this study extracted colour based on the cultural colour theory with an iterative refinement approach. The results of finding shows the 12-colour regional palette (Grassland Red, Sky Blue, Grassland Green, Lucky White, Lama Kim, Blue brick gray, chilehuang, Coral Red, Amber Brown, Liuli Qing, Snowfield Siver, Twilight Purple) for urban design guidelines regarding historical context and cultural heritage such as Dazhao, Chilechuan Grassland, Zhaojun Tomb, Wuta Temple, Zhaojun'stomb, Nadam Assembly clothing, Haoniuwan landform, Landscape of Mazui Mountain Ski Resort, Holy Water Beam Landscape. This study expects to strengthen Innter Mongolia's identity and brand appeal by following this regional color guideline.

Keywords: Inner Mongolia, city brand, regional colour, local colour guidelines, regional palette

INTRODUCTION

Against the backdrop of China's accelerated urbanization process, the national level has proposed the strategic goal of new urbanization, emphasizing that cities should combine regional characteristics by highlighting the cultural connotations and brand building of the city. The Inner Mongolia Autonomous Region is facing new opportunities to build a distinctive urban brand through its international influence and ethnic minorities. In art, colour has long influenced human consciousness, with its meanings evolving over time due to factors like religion, cultural traditions, and geographical location (Dimcheva, 2021). The hypothesis of this study is that the regional colour in Inner Mongolia entails the incorporation of regional cultural characteristics into the urban landscape, thereby engendering a distinctive and appealing city image (Zhang et al., 2024). In this context, the objective of this study is to suggest a local colour for creating a unique image and identity for a city, with the aim of attracting tourists, investors, and residents while promoting sustainable development.

METHODOLOGY

This study is based on the cultural colour theory as a unifying framework and the intermediary function of colour between culture and brand. Studies show that while there are universal sensory processes in colour perception (Adams & Osgood, 1973; Yokosawa et al., 2016), cultural factors significantly influence how colour are categorized (Lindsey et al., 2020; Jameson, 2005). For this reason, the choice of colour in branding should consider cultural values and associations (Aslam, 2006). The extraction of regional colour should consider the city's historical context, physical geography, and cultural heritage. Jean-Philippe Lenclos's "geography of colour" theory (2004) provides a framework for understanding the intricate relationship between colour, geographical environment, and cultural background. This approach helps maintain the city's identity while accommodating

modern developments (Lu & Pei, 2016). Based on these previous studies, the methodology of this study is as follows:

To ensure comprehensive seasonal coverage, field research and sampling procedures were conducted over a 12-month period from February 2024 to February 2025. These included on-site spectrophotometer measurements, standardized photography procedures, drone panoramic photography, and systematic colour data recording in multiple formats (RGB, LAB, Munsell, NCS). The colour extraction in city of inner Mongolia was executed through an iterative refinement approach, whereby the initial 80 extracted colour were systematically reduced to 50, then to 30, and ultimately to 12 core representative colour. RAW images are processed using X-Rite colour Checker camera calibration software, and white balance is uniformly adjusted to the D65 standard light source. Then, colour card patches are verified against standard values (Delta-E < 2.0 is required). To translate visually identified colour, this research standardized colour coordinates within established colour systems (e.g., Munsell, CIE Lab*, RGB). The colour matching function of colour Brewer 2.0 was utilized to demonstrate regional colour guidelines.

RESULTS AND DISCUSSION

The fieldwork documented that in several cities, iconic traditional colour schemes in historic districts or cultural sites are surrounded by new developments that adopt globalized or trendy aesthetics with little regard for local colour palettes. For example, a city that identifies itself with earth tones and traditional Mongolian patterns might see a new high-rise business complex clad in mirrored glass and cool grays appear on its skyline. In addition, Inner Mongolian cities face how to honor cultural heritage while projecting a modern image. Traditional heritage calls for the use of culturally symbolic colour-for example, the deep blues and whites associated with Mongolian identity, or the reds and golds found in local religious and historic architecture. It points to the need for more integrated planning, stakeholder collaboration, and perhaps flexible guidelines that can adapt to new developments while still protecting the essence of the city's colour brand.

It is recommended that Hohhot and other Inner Mongolian cities formally incorporate the 12-colour regional palette into urban design guidelines (Table 1). Key public spaces (squares, parks, street facades) and architectural projects should use the palette to create a coherent visual identity. In particular, important tourist directional signs could use Mongolian red as an accent colour that not only attracts attention but also evokes the local festive heritage and hospitality. Likewise, neighborhood entrance signs or community bulletin boards might use mysterious purple or earthy yellow (if they were on the palette) to reflect local stories (purple perhaps associated with mystery or legend, yellow with grassland soil or wheat fields). Such use of colour in signage should be done in consultation with graphic designers to ensure legibility and contrast - e.g., white or black text overlaid on a coloured background for clarity. In this way, the city's functional infrastructure doubles as a branding canvas, subtly embedding the brand identity into everyday life. However, officials should be mindful of the need to balance tradition with modernity - meaning that while traditional colour form the core, designers can still incorporate modern accents or materials.

Table 1: Regional Colour 12 Representative Colour

colour name	Origin and symbolism	Typical application scenarios	Representative	Representative colour

Grassland Red	Originating from the red walls of Dazhao Temple and traditional Mongolian clothing, it symbolizes passion, power, and religious sacredness.	Dazhao Temple red walls, Mongolian yurt decorations, festival costumes.	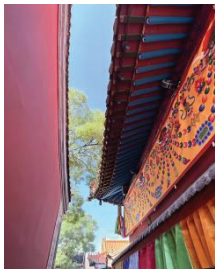	PANTONE® P 55-16 U
Sky Blue	Taken from the grassland sky and the Mongolian belief in "Changsheng Tian,", symbolizing vastness, freedom, and sacredness.	Chilechuan grassland landscape, Hada patterns, religious murals.		PANTONE® P 112-8 U
Grassland Green	Representing the grassland ecological base colour, symbolizing vitality and harmony with nature.	Chilechuan Grassland, Usu Tu Natural Landscape, Urban Greening.	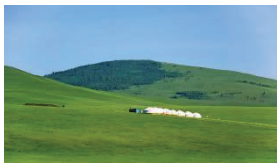	PANTONE® P 162-8 C
Lucky White	Associated with Hada, Aoba sacrifice, and Tibetan Buddhist White Pagoda, symbolizing purity, auspiciousness, and sacredness.	Zhaojun Tomb Qingzhong, Baita Temple, Sacrifice Ceremony.		PANTONE® P 1-1 C
Lama Kim	Originating from the gilded decoration of Tibetan Buddhist temples, it symbolizes brightness, wisdom, and religious authority.	Wuta Temple relief, Dazhao Temple golden roof, Thangka painting.	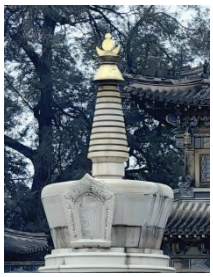	PANTONE® P 8-6 C

Blue brick gray	Taken from historical buildings such as the Zhaojun Tomb and the General's Office, it reflects the integration of historical weight and Central Plains architectural culture.	The wall of Zhaojun's tomb and the courtyard on the old street.		PANTONE® P 173-8 C
Chilehuang	Originating from the autumn grassland and Loess Plateau of Chilechuan, it symbolizes harvest and regional ecological characteristics.	Grassland autumn scenery, traditional pottery, folk festival decorations.	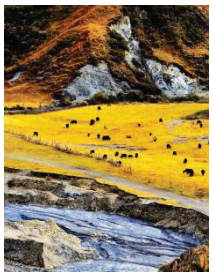	PANTONE® P 7-8 C
Coral Red	From Mongolian clothing and saddle decoration, symbolizing passion and national artistic aesthetics.	Nadam Assembly clothing, Mongolian yurt interior.		PANTONE® P 55-8 U
Amber Brown	Taken from the rock walls of the Yellow River Canyon in Laoniuwan and Mongolian leather craftsmanship, it symbolizes the texture of the earth and traditional handicrafts.	Laoniuwan landform, leather goods, wood carving art.		PANTONE® P 13-12 U
Liuli Qing	Originating from the dome of a mosque and Mongolian blue and white porcelain, it blends Islamic culture with grassland art.	Halal temple architecture, traditional porcelain patterns.		PANTONE® P 113-1 U

Snowfield Silver	Symbolizes the winter snow scenery of Daqing Mountain and the Mongolian silver jewelry culture, reflecting purity and ethnic craftsmanship.	Landscape of Mazui Mountain Ski Resort, Mongolian silverware.		
Twilight Purple	Taken from the mountain colour at sunset on the holy water beam, symbolizing mystery and natural poetry.	Holy Water Beam Landscape, Modern Art Installation.		

This research proposes a structured application of the extracted regional palette across multiple urban dimensions, including architecture, public space, and wayfinding systems. For example, urban planners could strategically incorporate historical and cultural landmarks such as "Grassland Green" and complementary tones such as "Earth Ochre" into street furniture, architectural facades, and public artworks to reinforce a visually unified urban identity (Figure 1).

Figure 1: Design Sketch - Color Scheme

CONCLUSION

In conclusion, the practical color guidelines for Inner Mongolian cities extracted 12 regional palettes from historical heritage. Embedding the culturally derived colour palette into the fabric of the city has significant implications for its branding and promotion of the city in Inner Mogolia. By following this regional color guideline, all cities in Innter Mogolia can strengthen their place identity and enhance their brand appeal. For further studies related to regional color guidelines, subsequent studies could examine whether cities that adopt

these recommendations experience tangible gains in tourism, business attraction, or citizen satisfaction compared to.

REFERENCES

[1]. Adams, F.,& Osgood, C. (1973). A Cross-Cultural research of the Affective Meanings of Colour. *Journal of Cross-Cultural Psycholog*y, 4: 135 - 156.

[2]. Aslam, M. (2006). Are You Selling the Right Colour? A Cross-cultural Review of Colour as a Marketing Cue. *Journal of Marketing Communications*, 12: 15 - 30.

[3]. Dimcheva, M. (2021). The Symbolism of colour in Art – Traditions and Modernity. *Visual Studies*.

[4]. Lenclos, Jean-Philippe. (2004). *Colors of the world : the geography of color*. New York : W.W. Norton & Co.

[5]. Lu, W., & Pei, H. (2016). Research on colour Planning of Yantai Based on Regional Culture.

[6]. Yokosawa, K., Schloss, K., Asano, M.,& Palmer, S. (2016). Ecological Effects of Cross-Cultural Differences Between U.S. and Japanese Colour Preferences. *Cognitive science*, 40 7, 1590-1616.

[7]. Zhang, W., Zhang, R.,& Zou, Y. (2024). Urbanization and Cultural Industry Correlation: An Empirical Analysis from China. *Sustainability*

The Power of Nature in Art: Exploring Biomorphic Abstraction with Colour and Design

Diana Sena Avoke[*]

[1]*University of Education, Winneba, Winneba, Ghana*
[2]*Takoradi Technical University, Takoradi, Ghana*
[*]*Corresponding author: Diana S. Avoke, avokesena97@gmail.com*

ABSTRACT

This article explores how colour, design and various elements of design can be used to create abstract works of art, drawing on biomorphic styles and patterns found in the natural environment. Objects of nature such as leaves and flowers will be explored for their complex, rich and aesthetic values and structures, as inspiration for artistic production. Biomorphic or nature-centric styles have played a major role in art, design and architecture throughout history. Its powerful and profound influence in the visual arts not only enhances the aesthetic appeal of artworks but also deepens our connection and understanding of the natural world. Artists, student artists and art practitioners, especially in the field of visual arts, design and fashion, need to know how such elements of nature can fuel and stimulate imaginative or unique ideas when seeking inspiration to produce dynamic and diverse works. The findings in this paper demonstrate how the appearance of biomorphic forms influences artistic styles and techniques by being an insightful source of reference with its range of colours, patterns and textures, when directing the artistic practice. From the aesthetic qualities found in leaves and flowers, the outcome of the study would also highlight the impact and relevance of artistic techniques and elements used in understanding the natural environment with art.

Keywords: abstract art, colour theory, nature-centric designs, elements of art, digital painting

INTRODUCTION

Throughout history, many artists have sourced inspiration, concepts and references from nature and the environment due to its complexity, beauty and phenomenon. Most artists in the field of art and education have extended this practice by bridging representations of nature in art with global, political or ecological issues and ideologies, as pillars in creating awareness and establishing communication.

Nature has a complex way of inspiring artists. This has been the case where art movements dating back from the 18th century to the 20th century, indicated various ways of representing natural scenes and objects. Art movements such as realism, naturalism and even the radical shift to art forms like abstract expressionism, were able to recognise and reflect the aesthetic values of art in many ways and aspects. The various forms and modes of art are mostly known to take huge inspiration from nature-centered (representational) or abstract (non-representational) ideas.

Abstract art-forms and styles generally fall under the category of non-representational art, due to its trend of not having a detailed reference to the natural world (Smith, 2023). This makes it unique and fluid for artists to express their ideas and inspirations when seeking to not confine or restrict themselves to a specified object or mode of expression. With that, artists have the liberty to transform or manipulate, distort, exaggerate and extract various elements in art through the process of abstraction. The movement's unique aesthetic qualities and its striking use of colour and form, have inspired not only generations of visual artists and designers, but also the many educationists in the field as well. Today, abstract art finds new ways of influencing the digital field, AI and in the contemporary arts, due to the advancements of technology (Magnusson, 2024).

For the purpose of this paper, abstract art will be limited to the natural objects in the environment, its aesthetics qualities and how it serves as a source of inspiration and reference in design and other modes of artistic expression, for artists and students in the field of visual arts to gain some insight in creating unique and dynamic forms of art. Due to the multitude of nature-centric designs and biomorphic styles and elements found in the environment, the familiarity and accessibility of leaves and flowers that was derived from the neighbouring surroundings of the Takoradi Technical University campus in Ghana, will serve as the main source of inspiration for the study.

Aim and Scope

Nature-centric or biomorphic forms and styles in art has generally not been fully used for its potential by most visual artists, students and practitioners in the field. Abstract art is a great mode of expression when seeking inspiration and understanding of nature, as it creates the opportunity for artists to have the liberty to express themselves and their ideas creatively, with the use of various visual art elements and techniques. Since most artists generally find abstraction to be somewhat difficult by how imaginatively involving and spontaneous it can be, the natural environment can serve as a source of inspiration when transforming ideas or realistic references in unique and distinct ways.

This article intends to create such awareness for artists to explore and utilise the elements of nature, by observing the intricate designs and colours of leaves and flowers within their immediate surroundings to create two-dimensional imagery with various artistic techniques, mediums and the elements of design. It will also enhance our need as artists and learners to advocate and take initiative in protecting the natural environment and ecosystem, while also being inspired by it.

Abstract Art

According to Wallace (2024), abstract art is generally known for its non-representational way of creatively arranging, simplifying or complicating various artistic elements of lines, shapes, and colours, to convey meaning and emotion. As it does not aim to represent visual references directly from the outside world in the broader sense (Tate, 2024), its characteristics of deconstructing an image can extend beyond to the purest geometric element. Encyclopaedia Britannica (2025) states that, abstract art is generally thought to have much commonality with design due to both approaches usage of the foundational artistic elements.

When it comes to the topic of abstract art and its misconceptions of the practitioners of the field, it is relevant to generally note that, abstract artists do not create art merely for the sake of it. But rather, as a form of expression that could not simply be defined by mimetic forms of representation, due to its known historical foundation of breaking away from the traditional ways by finding meaning within the unconventional (Jose Art Gallery, 2024). Abstract art is therefore important as it frees artists from objective reality and allows them to experiment with various forms, by giving more reign to the artist's imaginative self (Gaugy, 2016), and the freedom to grow imaginative thoughts to create compositions in their own unique way (Heily, 2024).

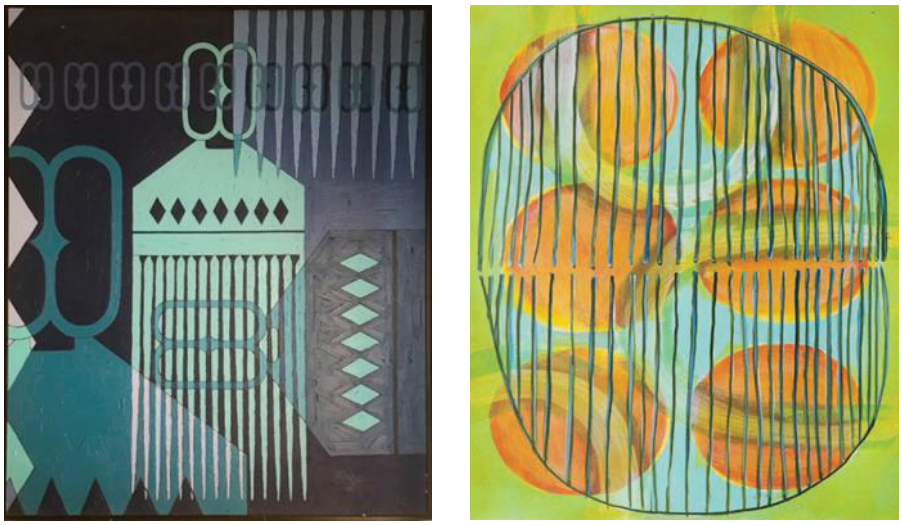

Figure 1: Image (left) of the Blue Symphony 2003, by Rikki Wemega-Kwawu, acrylic on canvas, located at Aicon Gallery, New York. Image (right) titled as Summer Temple 2020, by Nicky Marais, acrylic & ink on paper, Artsy.net.

"Abstract art celebrates the freedom of expression, allowing artists to experiment with shapes, colours, lines, and textures to create visually compelling compositions." (Berj Gallery, 2023)

LINKING NATURE TO ABSTRACT ART AND DESIGN

Abstract art aids in intensifying the awareness of natures impact, by providing a great source of inspiration to both artists and viewers of the art. While abstract art does not directly replicate the natural world, many artists draw upon its properties of form, colour, and pattern, as accessible elements of art and design which is also seen in the environment around us. According to Dikrse (2025), the elements in nature directs artists by offering them a fresh perspective on art through its provision of organic shapes and forms, diverse colour palettes, as well as textures and patterns, to aid artists in relaying subjective forms of emotions, feelings and movements through their work. To elaborate further, the main elements of art that is predominant with abstract art, such as; line, colour, texture and form, are easily identifiable in nature.

Line

Line is a path created between two points that vary in shape, length and width (Anthony, 2022). Berj Gallery (2023) states that, the use of lines in its form and direction to create movement, rhythm and structure is essential in deriving the unique qualities of objects in nature when creating an abstract composition or art work in general. With each type of line bringing various interpretations of fluidity, rigidity or dynamism, artists are able to manipulate and transform whatever they take from the natural world, to provide intensity, depth or directed mood to the viewer through their abstract representations.

Texture

The overall appearance and structure of a leaf is a perfect example of how texture can be seen in nature. Haupt (1953), describes a leaf to be a vascular plant, which is structurally composed of various veins that vary considerably from species to species of a plant (James & Bell, 2000; Mauseth, 2010). Texture in nature shows distinct forms of structure, illusion, depth and definition, mostly through the human senses of sight and touch. Although some of these elements that are identified in nature are somewhat subjectively complex, texture can still be explored and understood with various elements, techniques and mediums in art, or even with just the use of colour. The idea of texture can be represented in abstract as a smooth or rough, tactile surface or impression, as adding another layer of sensory experience to the artwork (Berj Gallery, 2023).

Colour

There have been questions highlighting why humans find flowers and nature in general, pleasing to the human eye. According to Gottesman (2017), Physicist David Deutsch suggested it to be attributed to how the blossoms contain a type of objective beauty with its appearance of harmonious colours, soft curves and symmetrical forms, which aesthetically and naturally tends to attract not only insects, but humans as well.

The ideology, application and subjective perception of colour, plays a major role when highlighting nature's power and influence in art. Overtime, artists have used colours to create interpretations, depictions and experimentations of objects, ideas and scenes, as forms of artistic expression and meaning-making. In abstract art, colour is generally seen to be the main element of the work, since many prominent abstract artists have made the genre popular through their approach and manipulation of it with the emphasis of colour. According to the Berj Gallery (2023), colour is one of the main ways artists can express and represent harmony, tension, contrast or other principles of art, from their perceptions of emotions, or other sensory and visual experiences into a composition.

Depending on its context or use in relation to the elements elaborated above and abstract art, a flower or leaf can represent and symbolise many things to an individual or a society. Throughout history, the representation of flowers has been strongly used by artists as the forefront and subject of visual expression. From ancient history to the contemporary era of artistic evolution, the prevalence of leaf patterns, blossoms, floral-inspired styles and other biomorphic styles or forms have been found in many prominent art movements and decorative pieces (Richman-Abdou, 2018). These designs are creatively arranged by artists through the organic elements they poses from its natural state and appearance.

Historical Context of Biomorphic Themes in Art

Meyer (2024), describes biomorphic art as a creative approach which allows artists and designers to use abstract organic forms and styles or nature-centric elements to direct their artistic practice. Biomorphic shapes are mostly abstract in nature since they evoke living forms in the environments, like plants and other living organisms (Jović et al., 2024). As the forms and styles relate to the natural elements of nature, artists are able to easily explore the natural world uniquely, without representing it directly.

In history, nature has had a leading role by being a powerful source of inspiration in art, design and architecture. This dates back to the ancient drawings found of animals, plants and other natural objects in caves and on pottery, which were mostly the driving force of inspiring ideas of sympathetic magic and other aspects of their livelihood (Wolverton, 2019; Meyer, 2024). According to Mason (2016), before the idea of nature-centric design and art, biomorphic forms in the period of the nineteenth century were mainly used for studying medicines in natural history and science, as findings were recorded and drawn in botanical books which focused on living organisms. The research focus from these biologists and scientists at the time were centred on form, function and transformation of appearances and constituent functions of plant life, as well as its flexible and dynamic structures (Abdelsabour, 2019; Ramzan, 2022). This transitioned itself as an influence in the art world around the early 20th century, were artists sought to move away from the rigidity of geometry forms, to the organic shapes and flows found in living organisms, which demonstrated the mysteries and marvel of the natural world (Meyer, 2024).

In Europe and other parts of the world, most biomorphic inspired art and decorative illustrations of interior or exterior spaces were of mostly plants, leafs and flowers. Later on, artistic thought at the turn of the century became strongly influenced by the popularization of the aesthetic qualities and elements that were found from the previous discoveries made on plant forms, botanical patterns and structures of minute organisms (Momaa, 2024). Thus introducing nature as a universal model for artistic creation and a guideline for the fine and decorative arts. The Art Story (2008) noted that, many biomorphic forms were usually seen to be abstract derivations of nature, due to their fluidity and spontaneity. Modern artists who mainly explored abstraction, used the elements of nature as an opportunity to investigate the hidden and intricate structures and artistic methods of visual exploration, representation and expression (Crowther & Wunsche, 2012).

With the evolution of nature-centric and biomorphic styles of the contemporary era, artistic modes of expression and representation were able to inspire more artist to incorporate certain organic and unique themes into their work. This revolutionised the concept of art, design and architecture. When creating biomorphic inspired images and forms, artists' utilise various innovative techniques which are executed two-dimensionally or in three-dimensional form. These artistic or decorative techniques may comprise of painting, mosaic, sculpture, architecture, digital design, printing-making, engraving, amongst others as exemplified in the images below.

(a) (b) (c) (d)

Figure 3: Yellena James Weightless, 2023, mixed media (a). Rainbow mandala, 2021 via @murderandrose on Instagram (b). Inside the Revelry Divine Painting, 2011, by Tiffany Davis-Rustam, oil on canvas (c) and White Iris, 1930, by Georgia O'Keeffe, London, oil on canvas, Located at Tate Modern (d)

Chapman's 1978 Lists of the Four Sources of Inspiration

Generally, abstract painters are inspired by particular colours and textures found in objects or scenery primarily of the environment. As artists are known for critical observation, their creative practice also entails exploring nature and describing it by way of photography, drawing, painting, etc. There is also some form of appreciation or fulfilment when viewing and capturing the moment of what nature reveals and its impact in creating inspiration. Chapman (1978), listed the four major sources of inspiration for an artwork. These consist of ordinary experience, natural and constructed environment, inner feelings and imagination, as well as the quest for order (Chapman, 1978; Bartel, 1999).

The four sources of inspiration as stated by Laura H. Chapman, were used as the benchmark for creating most of the nature inspired works of art for this study:

1. Ordinary experiences are the spontaneous drawings, with some aspects of a person's inner feeling and imagination.

2. Inner feelings and imagination deals with an artist's way or approach to artistic expression.

3. Quest for order are the careful and deliberate used of the elements or principles of art.

4. The natural and constructed environment are mainly observational work, from actions and processes that take place in the environment.

METHODOLOGY

This art-based research graphically explores the various procedures and outcomes used in executing this project. It therefore took into consideration critical observations of the physical and aesthetic qualities of the leaves and flowers within the Takoradi Technical University environs, before creating abstract works out of them.

The following are the general procedures highlighted in the study, which includes tools, material and preparatory drawing procedures.

Tools and Materials: Brushes, Acrylic paint, Paper, Pallet, Pallet knife, Pencil, Prepared canvas, Oil pastels, Photoshop software tool, Camera, Cardboard.

(a) (b) (c) (d) (e)

Figure 5: Actual images of the Aegopodium pdagraria leaf (a), Canna flower (b), Vipers bowstring hemp plant (c), Plantain leaf (d) and the Croton Zanzibar plant (e), as natural objects taken with the use of a phone camera.

(a)

Figure 6: Example of the preparatory and preliminary drawings derived from patterns and designs of the Aegopodium podagraria leaf (a).

Procedure (Colour Selection, Technique and Medium):

(a) (b) (c) (d) (e)

Figure 7: An illustration (above) of the main colours taken from each of the leaves and flowers used in the following paintings highlighted below.

RESULTS AND DISCUSSION

Figure 8: Example of a Papier Collé artwork of the Canna flower (b).

Collage is great technique that can be used in creating abstract works. Figure 8 of the image above, demonstrates such artistic use of paper which varies in shape, size and colour. The arrangements and layering of the paper as a college or mixed-media work, takes reference from the elements and vibrant play of colours, referenced from its original image (left), as it is able to be transformed into an entirely unique art piece of a flower. The representation also exemplifies how impressions of an object rendered in two-dimensional form can still have some similarities to the original. Collage allows artists to use various materials such as recycled paper, fabrics or found objects, to create an image or composition through the processes of combining, layering, juxtaposition or pasting (Theartofmann, 2023).

Mixed media as another technique also allows artists to expand their ideas to make something new. Aside collage or the use of acrylic paints, other mediums can be explored to create abstract images of leaves and flowers due to the unique qualities and distinct visual elements they possess. Such alternative mediums such as oil pastels and digital media have been used to bring such ideas and inspirations from nature to art in this study.

Figure 9: A colouring of the Aegopodium pdagraria leaf (a) with oil pastels.

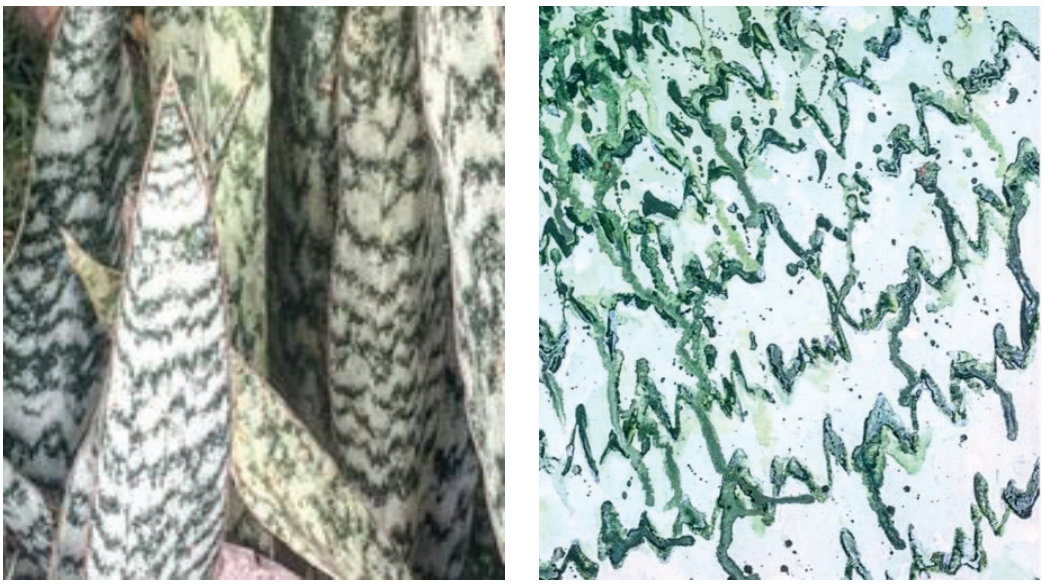

Figure 10: Acrylic painting of the Viper bowstring hemp plant (c).

(a)

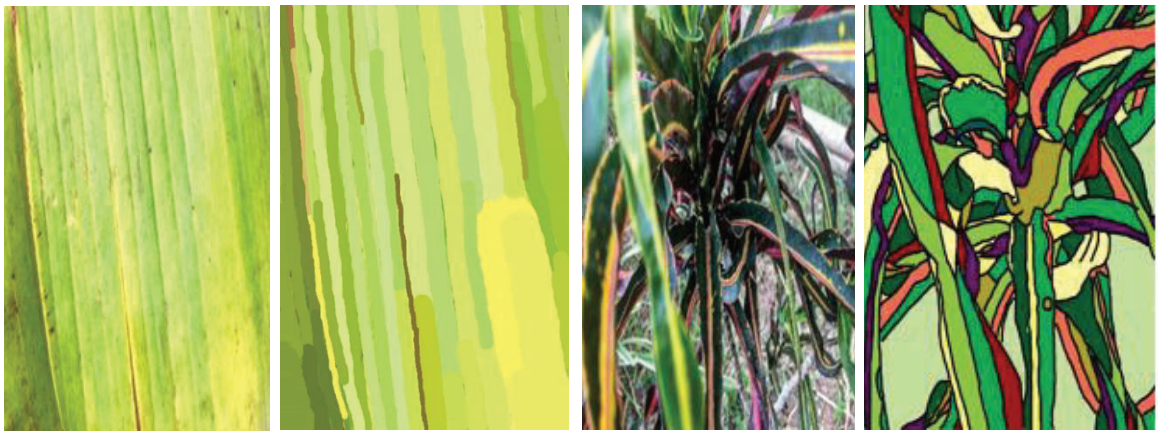

(d) (e)

Figure 11: Images of the Aegopodium pdagraria leaf (a), Plantain leaf (d) and the Croton Zanzibar plant (e), rendered as abstract paintings through digital media on the Photoshop software.

CONCLUSION

This article explores and highlights the visual impact of nature on various artistic approaches, techniques and styles through its array of vibrant colours, textures, patterns, form and design, which all constitutes as aesthetic qualities. In general, the idea of nature-centric or biomorphic forms and styles have existed as decorative and artistic inspirations throughout history to the present contemporary genre. Both viewers and artists' have uniquely gravitated towards their attraction for the natural environment physically, emotionally and artistically, due to its special qualities. When we view objects in the environment, it gives us ideas on how to appreciate them through practices like art. Biomorphic forms and styles thus becomes a powerful source of inspiration and reference for artistic creation and expression in areas such as the visual arts. This is why ideas and objects of nature with distinct and vibrant aesthetic qualities have pushed the boundaries of art, design and architecture.

In view of this, the findings exemplifies various components of a leaf or flower taken from the environment to produce numerous abstract designs from its form, pattern and colour. And as abstract art strengthens artists'

convictions of the absoluteness of aesthetics and provides them discipline in pure design through the elements and principles of art (Shapiro, 2014), more focus should be centered on the diverse aspects of biomorphic styles and its influence in contemporary art, design and painting. .

REFERENCES

[1]. Abdelsabour, I. (2019). Investigating Bio-morphism Approach to Enhance Structures Creativity and Efficiency. *Journal of Engineering and Applied Science, Faculty of Engineering, Cairo University (JEAS), 66*, 491-513. https://www.researchgate.net/publication/339043001

[2]. Anthony, J. (2022). *Line in Art – Take a Look at Different Examples of Line in Art*. https://artfilemagazine.com/line-in-art/

[3]. Bartel, M. (1999). *The Innate Quest for Order and Design*. https://www.goshen.edu/art/ed/quest4o.htm

[4]. Berj Gallery. (2023). *The Captivating Realm of Abstract African Art*. https://www.berjartgallery.com/news/the-captivating-realm-of-abstract-african-art/

[5]. Chapman, L. (1978). Approaches to Art in Education. 46-52.

[6]. Crowther, P., & Wunsche, I. (2012). Life into Art. In I. Wunsche, *Meaning of Abstract Art: Between Nature and Theory* (p. 11). New York: Routledge.

[7]. Encyclopaedia Britannica. (2025). *Abstract Art*. (G. Lotha, Editor). https://www.britannica.com/art/abstract-art

[8]. Gaugy, M. (2016). *Quora*. https://www.quora.com/what-is-the-significance-of-abstract-art

[9]. Gottesman, S. (2017). *A Brief History of Flowers in Western Art*. https://www.artsy.net/article/artsy-editorial-van-gogh-okeeffe-art-historys-famous-flowers

[10]. Haupt, A. W. (1953). *Plant Morphology.* University of Michigan, USA: McGraw-Hill.

[11]. Heily, L. (2024). *The Power of Abstract and Controversial Art: Unlocking Imagination and Creativity*. https://arabelart.com/blogs/articles/the-power-of-abstract-and-controversial-art-unlocking-imagination-and-creativity

[12]. James, S. A., & Bell, D. T. (2000). Influence of light availability on leaf structure and growth of two Eucalyptus globulus ssp. globulus provenances. *Tree Physiology*, 1007-1018. DOI:10.1093/treephys/20.15.1007

[13]. Jose Art Gallery. (2024). *What is Abstract Art: The Journey from Vision to Expression*. https://joseartgallery.com/articles/what-is-abstract-art-the-journey-from-vision-to-expression

[14]. Jović, B., Zdimalova, M., & Chemarum, B. (2024). Biomorphic Design in Landscape Architecture: An Overview and Application Via Experimental Design Inspired bySpecies, Carica papaya L. *Bulletin od the Faculty of Forestry*, 39-58. https://DOI.org/10.2298/GSF2430039J

[15]. Magnusson , A. (2024). *Abstract Art Reimagined: The Digital Renaissance of the 21st Century*. https://www.rockandart.org/abstract-art-digital-renaissance-21st-century/

[16]. Mason, M. (2016). *Introduction to Botany*. https://www.environmentalscience.org/botany

[17]. Mauseth, J. D. (2010). Botany. An introduction to plant biology. *Annals of Botany, 105*(5), 672. https://DOI.org/10.1093/aob/mcq055

[18]. Meyer, I. (2024). *Biomorphism – The Artistic Expression of Organic Patterns*. https://artincontext.org/biomorphism/

[19]. Momaa. (2024). *Biomorphic Forms: Nature-Inspired Aesthetics in Art and Design*. https://momaa.org/biomorphic-forms/google_vignette

[20]. Paul Dikrse. (2025). *The Influence of Nature on Abstract Art*. https://pauldirkse.nl/nl/blogs/news/the-influence-of-nature-on-abstract-art

[21]. Ramzan, M. (2022). *History of Botany – Biology History*. https://biologyteach.com/history-of-botany/

[22]. Richman-Abdou, K. (2018). *my modern met*. https://mymodernmet.com/flower-art-history/

[23]. Smith, E. (2023). *Representational vs Nonrepresentational Art: Difference and Comparison*. https://askanydifference.com/difference-between-representational-and-nonrepresentational-art-with-table/

[24]. Tate. (2024). *Abstract art*. https://www.tate.org.uk/art/art-terms/a/abstract-art

[25]. The Art Story. (2008). *Summary of Biomorphism*. https://www.theartstory.org/movement/biomorphism/

[26]. Theartofmann. (2023). *Exploring the Boundless Possibilities of Collage: Techniques, Materials & Inspiration*. https://www.theartofmann.com/blog

[27]. Wallace, A. (2024). *21 Abstract Art Compositions with Examples*. https://www.culturefrontier.com/abstract-art-composition-examples/

[28]. Wolverton, B. (2019). *Why Nature Inspires Art*. https://www.eaglesnestoutfittersinc.com/why -nature-inspires-art/

Relationship between Stability of Color Preference and Personality Traits

Shinji Nakamura[a*]

[a] *Faculty of Education and Psycholgy, Nihon Fukushi University, Aichi, Japan*

[*] *Corresponding author: Shinji Nakamura, shinji@n-fukushi.ac.jp*

ABSTRACT

Abstract

This study examined the stability of individual color preferences and their relation to personality traits. Participants (N = 500; ages 20–60) completed two web-based surveys one month apart; 471 responded in the second, and 345 valid datasets were analyzed. Preferences for eight colors (red, blue, yellow, green, brown, purple, pink, orange) were measured using three methods: pairwise comparison, 7-point Likert scale, and ranking. Personality traits were assessed with the Color Cognitive Attitudes Scale, the Self-Consciousness Scale, and the Personal Attitude Stability Scale. Stability of color preference was indexed by rank correlations across the two surveys. Results revealed relatively high stability: pairwise comparison and ranking revealed strong correlations (≈0.75), while the Likert scale was slightly lower (≈0.67). Convergent validity among the three methods was also high (≥0.7), suggesting robustness across measurement approaches. Analyses of personality traits revealed a weak but significant negative correlation between color consciousness and preference stability, particularly among women. These findings suggest that individuals with higher sensitivity to daily color usage tend to experience greater fluctuation in preferences. In contrast, personal attitude stability revealed no significant association with color preference stability. These findings indicate that while color preference demonstrates considerable temporal robustness, its stability might be influenced by individual differences in color-related awareness, and it might differ fundamentally from general psychological attitudes. Further research is required to elucidate these distinctions.

Keywords: color preference, attitude, personality trait, stability

INTRODUCTION

Typically, each of us has an individual color preference which can be internally represented and externally expressed without a specific effort. Color preference has been one of the major topics in color sciences for long years, and many researchers have tried to accumulate wider knowledge about color preference in a various way. Color preference researches have revealed wider variations of preferred/hated colors as a function of genders, ages, countries and related factors, by collecting data from massive group of survey participants. In these researches, it has been revealed that color preference has a certain range of robustness against a passage of time, and colors selected as preferred or hated color did not show a huge variation within a specific participant's group. Similarly, color preference also shows a certain range of stability within an individual person on average. These findings suggest that individual color preference might stem from a stable characteristic of the participant's personality, not affected by transient feelings varied from day by day.

Nevertheless, it has been also revealed that the intrapersonal stability/consistency of color preference might be subject to relatively large individual differences, and well established that there might be some persons with very

high stability in their color preferences, while other persons did not show a stable preference. The purpose of this investigation was to elucidate factors underlying the individual differences in the stability of color preference. Questionnaire surveys were executed in order to examine relationship between participants' personality characteristics and their intrapersonal consistency (or stability) of expressed color preference.

METHODOLOGY

The color preferences and personality traits of survey participants were measured using a web-based questionnaire survey. Regarding color preferences, eight colors—red, blue, yellow, green, brown, orange, pink, and purple—were evaluated using color names. The survey employed three methods: (1) a paired comparison method (participants were asked to choose which of two colors they preferred) In this study, participants were asked to rate their preference for each color on a 7-point scale), (2) a Likert scale method (asking participants to rate the degree of preference for each color on a 10-point Likert scale), and (3) a ranking method (asking participants to rank the colors in order of preference from 1st to 8th).

Regarding personality trait measurement, three scales were used: (1) Cognitive Attitude toward Colors Scale (Hanari & Takahashi, 2009 [1]), (2) Shortened Self-Awareness Scale (Gosling, Rentfrow, & Swann, 2003 [2]), and (3) Personal Attitude Stability Scale (Xu et al, 2020 [3]). The Cognitive Attitude toward Colors Scale consisted of questions about attitudes toward color and was composed of two sub-scales: color consciousness, which indicates the degree of sensitivity/particularity on color, and color stereotypes, which indicate typical attitudes toward color (e.g., color consciousness: "I always concern about the colors of clothes or belongings"; color stereotypes: "I believe that there are colors appropriate for spring and colors appropriate for autumn"). The self-consciousness scale consisted of public self-consciousness, which refers to the parts of oneself that are visible to others, such as gestures and behavior (e.g., "When doing something in front of others, I am concerned about my gestures and appearance"), and private self-consciousness, which refers to the parts of oneself that are not visible to others, such as one's emotions and inner thoughts (e.g., "I often try to understand my own feelings"). The personal attitude stability scale measures the degree to which one's attitude remains stable over the long term, even if there are no objections in daily life (e.g., I rarely change my opinion even after a discussion). Due to the nature of the survey, the number of questions in each scale was limited to the 10 items with the highest factor loadings, and participants were asked to respond using a 7-point scale.

Participants were recruited using the crowdsourcing service Freeasy (https://freeasy-survey.com/), and responses were obtained using the web survey system provided by the same service. The web survey was repeated twice at approximately four-week intervals. In Survey 1, color preference measurements using three methods and cognitive attitude toward colors measurements were conducted. In Survey 2, color preference measurements similar to those in Survey 1 and measurements using self-awareness and attitude stability scales were conducted.

Survey 1 involved 500 participants aged 20 to 60, including both men and women. For Survey 2, participants who had participated in Survey 1 were asked to participate again, and responses were obtained from 471 participants.

RESULTS AND DISCUSSION

Data Analysis

Considering that this survey was conducted via the web, participants who provided inappropriate responses were excluded from the data analysis. Specifically, those who (1) had a deviation of 0 for their responses in each section of the questionnaire and (2) provided different responses to two intentionally repeated questions in the same

survey were excluded from the analysis. Ultimately, 345 survey participants were included in the analysis (approximately 70% of those who participated in Survey 1, 172 men and 172 women).

In color preference measurement using the paired comparison method, since there are eight evaluation colors, seven judgments are made for each evaluation color. The average of these evaluation values was calculated and used as the color preference score for each evaluation color using the paired comparison method. This score was treated as an ordinal scale, along with the results obtained using the Likert scale and ranking method. Regarding the personality scale, the scale scores were calculated based on the original paper, including the sub-scales.

Stability of Color Preference

The rank correlation between color preference scores based on the three measurement methods in Surveys 1 and 2 was calculated for each survey participant and used as an indicator of color preference stability. Table 1 shows the average color preference stability between surveys for each measurement, and Table 2 shows the average color preference stability between measurements in each survey.

While stability between surveys was slightly lower in the Likert scale, the paired comparison method and ranking method yielded high correlations of approximately 0.75, indicating that color preference tendencies measured repeatedly over a period of about one month maintained relatively high stability. Additionally, with respect to stability between measurement methods, a high correlation of 0.7 or higher was obtained for all combinations, confirming that color preference tendencies measured using different methods revealed relatively high consistency among participants.

Table 1 Color Preference Stability across the Surveys

Paired Comparison	Likert Scale	Ranking
0.75(0.33)	0.67(0.38)	0.74(0.33)

Stability scores were provided by
averaged rank correlations (and SDs)

Table 2 Color Preference Stability between the Measurements

	Paired Comparison-Likert Scale	Likert Scale-Ranking	Ranking-Paried Comparison
Survey1	0.73(0.37)	0.73(0.36)	0.76(0.34)
Survey2	0.72(0.40)	0.73(0.36)	0.75(0.37)

Differences in Color Preference Stability by Age and Gender

The survey participants were divided into three age groups: 20s and 30s (n=76), 40s (n=110), and 50s and above (n=156). Differences in color preference stability were examined in combination with gender. Figure 1 shows color preference stability across surveys for each age group and gender. The ANOVA revealed that the main effect of age was significant in the Likert scale and the ranking method ($F(2.341)=6.52, 5.42$, $p<.001$, respectively). In summary, color preference stability was low in the 20s and 30s, and high in the 40s and 50s or above.

Relationship between Color Preference Stability and Personality Trait

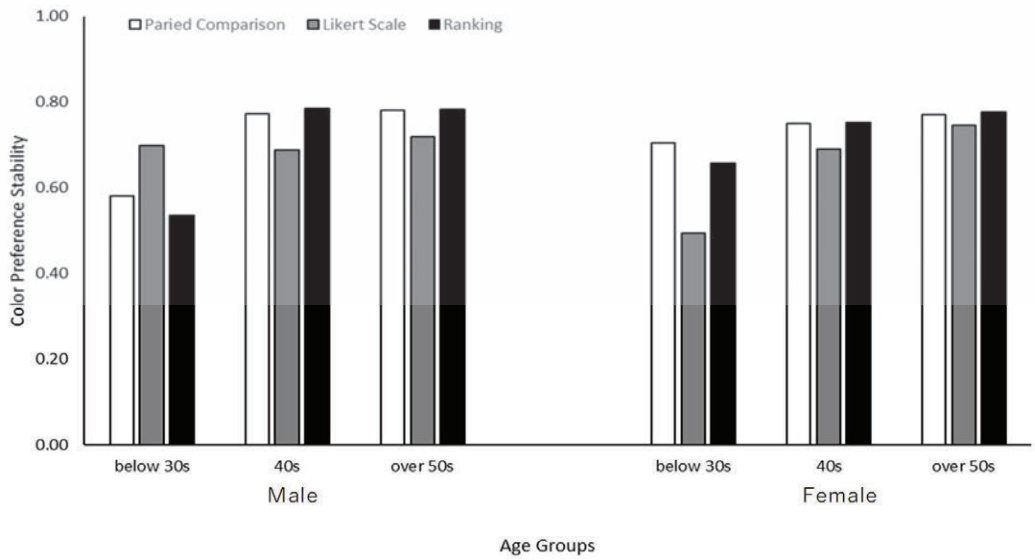

Figure 1 Color Prefefence Stability acorss Participant's age Groups

Examination of the relationship between color preference stability across surveys and the personality traits of survey participants revealed that a weak but significant negative correlation existed between color consciousness scores and color preference stability. When examining the correlation by gender, a significant correlation was found only among female participants (Table 3). This result suggests that women who have a higher consciousness/sensitivity for colors tend to have lower color preference stability. Individuals with high color consciousness are likely to frequently experience changes in their perception and evaluation of color based on daily experiences, compared to those with lower color consciousness. The negative correlation between color consciousness and color preference stability observed in this study is presumed to reflect this phenomenon.

In this study, self-awareness and personal attitude stability were found to have no particular association with color preference stability among the participants. Since color preference can be considered as an individual attitude in liking or disliking colors, it is important to note that color preference stability was not associated with personal attitude stability in this study. Further investigation is needed to determine whether color preference has characteristics that differ from other general psychological attitudes.

Table 3 Correlation between Color Preference Stability and Color Consciousness

Participants	Paired Comparison	Likert Scale	Ranking
Total	-.153**	-.176**	-.139**
Male	-.0834	-.0346	-.0173
Female	-.208**	-.246**	-.221**

$^{**}p<.01$

CONCLUSION

This study revealed that the color preferences of survey participants, measured using three different methods at intervals of approximately one month, revealed a high degree of stability. These findings suggest that abstract color preferences measured by psychological surveys reflect stable internal characteristics of participants and have psychological validity. Additionally, it was found that the degree of color preference stability among participants can be partially explained by their personality traits, specifically the strength of their sensitivity on color. Future investigations, we aim to conduct repeated measurements on an annual basis to determine whether color preference stability persists over longer time intervals and to explore whether other personal characteristics exist that better explain individual color preference stability.

.

REFERENCES

[1]. Hanari, T. and Takahashi, S. (2009). Color preference style for multi colors and individual characteristics in color cognition. Journal of the Color Science Association of Japan, 33, 319-326 (In Japanese with English Abstract).

[2]. Gosling, S. D., Rentfrow, P. J., and Swann, W. B., Jr. （2003）. A very brief measure of the Big-Five personality domains. Journal of Research in Personality, 37, 504- 528.

[3]. Xu, M., Briñol, P., Gretton, J. D., Tormala, Z. L., Rucker, D. D., and Petty, R. E. (2020). Individual differences in attitude consistency over time: The personal attitude stability scale. Personality and Social Psychology Bulletin, 46, 1507–1519.

The Effect of Chroma Contrast in Infographic Color Design on The Viewer's Reading Experience

Chen Pang Tsan [a*], Chun Po Wang[b]

[a] *Tamkang University Department of Information and Communication Assistant Professor, New Taipei City, Taiwan*
[b] *Ming Chuan University Department of Commercial Design lecturer, Taoyuan City, Taiwan*
[*] *Corresponding author: Chen Pang Tsan, deardeal.d@gmail.com*

ABSTRACT

In today's era of information overload, infographics have emerged as a vital tool for efficiently conveying complex content. With the rise of flat design and minimalist aesthetics, simplifying the visual complexity of infographics has become increasingly significant. Among the various design elements, color is the first visual cue processed by the human brain. This study focuses on chroma contrast—a form of contrast in color combinations—as the entry point to investigate how varying levels of chroma contrast affect the reading experience of infographic viewers.

The study examines three levels of chroma contrast as comparative variables: low chroma contrast, original chroma contrast, and high chroma contrast. After expert-based categorization and sampling of infographic stimuli, a questionnaire was designed to assess five key dimensions: visual saliency, comprehension of content, image recognizability, reading comfort, and reading fatigue. Statistical analysis was performed using the Chi-square test or Fisher's exact test, depending on the distribution of the data. Based on the collected results, patterns of how chroma contrast influences the infographic reading experience were identified. The study concludes with three key findings, which may provide valuable references for future visual design applications:

1. The original chroma configuration effectively balances visual appeal and reading comfort, making it suitable for most chart design scenarios.
2. High-chroma designs can significantly enhance chart prominence, but should be adjusted according to the audience's age and the thematic nature of the chart.
3. Chroma contrast is not a sole determining factor; it should be considered alongside hue and tonal structure to achieve optimal visual communication.

Keywords: Infographic, Chroma Contrast, Color Harmony, Color Scheme, Reading Experience

INTRODUCTION

In visual communication design, color is the primary element through which viewers receive information. Appropriate color configurations can enhance the readability and comprehensibility of infographics. With the evolution of design theories, the Munsell color system, known for its three-dimensional structure describing hue, value (lightness), and chroma, serves as the foundation for color application in this study. Although value and hue are often considered the most influential, this research focuses on chroma contrast to explore its role in infographic design.

The development of infographics has progressed from mixed text-image formats to highly visualized representations, and has been categorized into types such as diagrams, charts, and maps. Infographics emphasize visual representation and rapid information delivery, yet the impact of color usage varies significantly across audiences of different ages and backgrounds. Therefore, this study manipulates dual-toned chroma contrast as an experimental variable and conducts a reading experience survey based on factors including gender, age, occupation, education level, and prior exposure to infographics. The objectives of this research are:

1. To identify chroma configurations suitable for different audiences.
2. To analyze the effects of chroma on reading comprehension and comfort.
3. To explore the influence of chroma on visual attention.

LITERATURE DISCUSSION AND METHODOLOGY

The Munsell Color System

Albert H. Munsell (1858–1918) established a three-dimensional color system in 1898, quantifying color characteristics through three dimensions: hue, value (lightness), and chroma (saturation). The hue circle is composed of five principal hues and five intermediate hues, each subdivided into 10 steps, resulting in 100 hue variations. A 20-step version is commonly used. Value is represented along the Z-axis, ranging from black to white, while chroma extends radially outward along the XY-plane—higher values indicate greater saturation. This model facilitates the scientific manipulation of color contrast and harmony strategies.

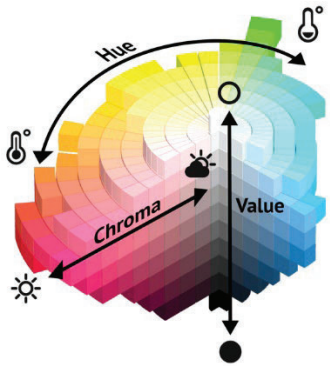

Figure 1: Munsell Color Solid

Application of Contrasting Colors

Color contrast plays a significant role in visual perception studies. Numerous studies have shown that background brightness, hue combinations, and chroma variations influence perceived color depth and recognition sequence (e.g., Dengler, Lotto). Theories by Chevreul and Birren emphasize the advantages of contrasting colors in communication and recognition. Physiological and psychological research also indicates that high-chroma colors significantly affect stimulus intensity, visual attention, and recognition accuracy (e.g., Shinomori, Mizokami).

Trends in Infographic Color Application

From observing popular infographics on Behance, common color trends include hue simplification and the use of chroma contrast. Design styles vary depending on content tone—some works use high-chroma colors to enhance attention, while others employ low-chroma schemes to maintain visual harmony—revealing a lack of standardized rules. As such, "the impact of chroma contrast on information comprehension and visual experience" has become the central focus of this study.

Research Hypotheses

Based on literature and observations, this study proposes the following hypotheses:

H1: Increasing chroma contrast improves information comprehension.

H2: Increasing chroma contrast enhances visual attention.

In addition, while visual comfort is a subjective perceptual factor and no hypothesis is established for it, it is still included in the scope of subsequent observation and discussion. To eliminate the influence of extraneous variables, this study focuses specifically on the impact of chroma contrast levels on chart reading performance, centering on the following three key research questions:

1. To what extent do viewers understand the content of infographics designed with contrasting color tones?
2. Does the degree of chroma contrast significantly affect viewers' visual comfort?
3. Under consistent chart structure, does chroma contrast significantly influence visual attention?

Chart Sample Selection and Processing Procedure

The samples used in this study were collected from four international design annuals (2016–2022) and two international design websites, encompassing a variety of cultural and stylistic approaches. The selection process was conducted in two stages using the KJ method, carried out by five senior infographic designers and professors in related fields.

1. Based on the infographic classification system proposed by Chen-Pang Tsan (2017).

From the categories of "diagram + chart + data visualization," three representative works were selected for their rich hues, visual complexity, and ease of reconstruction: Global Localization of Portugal, Hydrogen Society, and Japan’s Economic Growth.

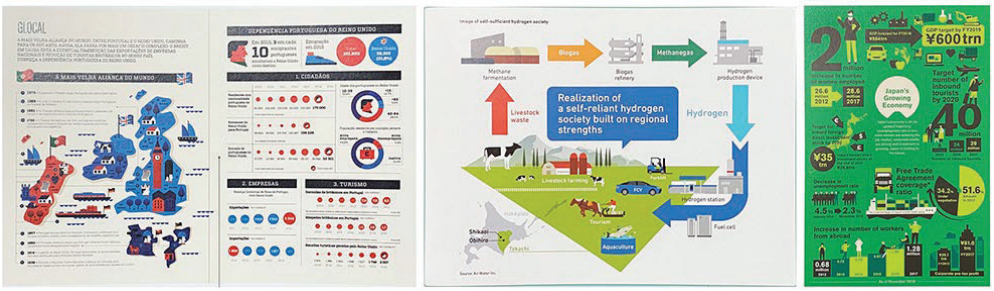

Figure 2: The reinterpreted works selected through the KJ method are, from left to right：(a) Global Localization of Portugal (b) A Self-Sufficient Hydrogen Society Enabled by Regional Capabilities (c) Analysis of Japan’s Economic Growth

Chart Reconstruction and Color Standardization

After completing the sample selection, the study proceeded with digital reconstruction and duotone processing of the charts to meet the design requirements for chroma contrast experimentation. All text was translated into Chinese, and RGB color values were standardized. The color strategy adopted a duotone design, using the two most frequently occurring primary colors from the original chart. These two primary colors were then adjusted according to the Munsell system to create three chroma variations (high / original / low) for experimental comparison.

Figure 3: Global Localization of Portugal

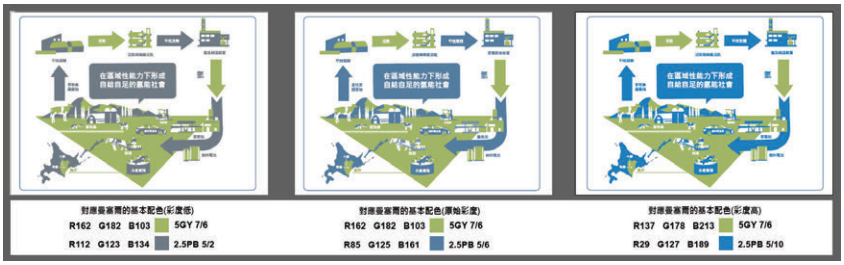

Figure 4: A Self-Sufficient Hydrogen Society Enabled by Regional Capabilities

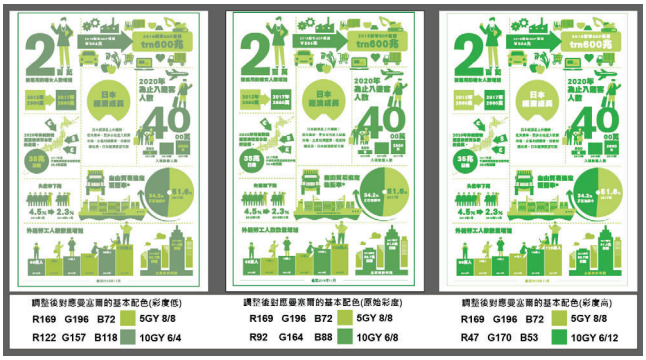

Figure 5: Analysis of Japan's Economic Growth

Theoretical Basis of Questionnaire Design

The questionnaire is grounded in the concepts of the "attention economy" and the three core functions of infographics: attracting attention, facilitating understanding, and enhancing memory. Based on expert discussions, the questionnaire was designed around six key dimensions: attention level, comprehensibility, reading comfort, visual fatigue, information clarity, and color preference.

Chart Sample Selection and Processing Procedure

1. A total of 249 participants were recruited, including students from Tamkang University (118) and members of the general public (131).
2. Both paper-based and online questionnaires were administered on campus, collecting background information such as gender, age, education level, occupation, and experience with infographics.
3. Each participant was randomly shown the same three sets of duotone charts (original, high chroma, low chroma) and asked to evaluate their directional preference based on six questions.

4. Chi-square tests or Fisher's exact tests were used for categorical variables, Z-tests were applied to percentage comparisons, and Cronbach's α was used to assess internal consistency. The significance level was set at $P < 0.05$, and analysis was conducted using SPSS V25.

RESULTS AND DISCUSSION

This study aims to explore the impact of varying chroma contrast in infographics on the reading experience, with a further analysis of how age differences moderate chart perception. A total of 249 valid participants were sampled for a visual experiment involving three chroma conditions (low contrast, original color scheme, and high contrast). Participants were divided into two age groups—young adults and middle-aged or older—for cross-group comparison.

Results show that, overall, high chroma contrast significantly enhanced chart attention and recognition; however, it was less favorable than the original color scheme in terms of reading comfort and visual fatigue. Comparatively, the younger group was more sensitive to high-chroma charts, indicating a greater tendency toward visual fatigue when viewing high-chroma designs. In contrast, the middle-aged and older group performed better under high-chroma conditions, possibly reflecting a higher need for strong visual stimuli.

Each chart responded differently to hue combinations and chroma manipulation. In the Global Localization chart, the original color scheme had advantages in comfort and fatigue metrics. In Hydrogen Society, the high-chroma version achieved the best results across attention, comprehension, and recognition. The Japan's Economic Growth Analysis chart reflected greater reading stability with mid-tone hues at original chroma levels.

This study applied Cronbach's alpha to analyze the internal consistency of six evaluation indicators for each of the three charts (Global Localization, Hydrogen Society, and Japan's Economic Growth Analysis), with results of 0.85, 0.87, and 0.90 respectively. All three chart groups demonstrated good internal consistency reliability ($\alpha > 0.80$), indicating that participants' response trends were consistent across the chart conditions.

CONCLUSION

General Discussion

This study used infographics with three different chroma contrast conditions—original color scheme, low chroma contrast, and high chroma contrast—as experimental materials to investigate the impact of age-based differences on viewers' information comprehension. The results show that, in the comparison between "low chroma contrast vs. original color scheme," the original scheme outperformed the low-contrast version across all six evaluation items. This suggests that, without intentionally reducing chroma contrast, the original color scheme offers a better cognitive experience during reading.

This study proposes a set of principles for applying chroma contrast in duotone chart design and suggests that future research could further explore the interaction between color strategies and thematic semantics to deepen both the theoretical and practical foundations of information visualization design.

Conclusion

The findings of this study can be summarized into three key conclusions, providing practical references for design applications:

1. The original chroma configuration effectively balances visual appeal and reading comfort, making it suitable for most chart design scenarios.

2. High-chroma designs can significantly enhance chart attention but should be adapted based on the audience's age and the thematic nature of the chart.
3. Chroma contrast is not a sole determining factor; it must be considered alongside hue and tonal structure to achieve optimal visual communication.

In summary, the contribution of this study lies in establishing an operational definition and evaluation framework for the role of chroma contrast in infographic reading experiences, as well as proposing chroma control guidelines applicable to duotone chart design. The results offer valuable references for future applications in color strategy within information design and visual data communication.

Research Limitations

This study applied color manipulation based on the Munsell color system. Although every effort was made to select colors closely matching the originals, slight discrepancies in color reproduction may still exist. Additionally, national flags included in the charts were not recolored due to their strong symbolic meaning, in order to avoid potential cognitive confusion. Questionnaire responses indicated that no participants reported being visually disturbed by the flag colors, suggesting that this handling did not have a substantial impact on the research results.

ACKNOWLEDGEMENTS

I would like to thank all the participants who contributed to the questionnaire and visual testing—your input provided valuable empirical data for this study. Special thanks go to the experts in the fields of design and color studies whose feedback helped enhance the completeness of this research. I also gratefully acknowledge the original infographic designers whose works served as reference material for the visual reconstructions in this study. Finally, sincere thanks to the AIC and the conference organizers for providing a professional and inspiring academic platform that made it possible to present and discuss this research.

REFERENCES

[1]. Birren, F. (2006). Color dimensions: Creating new principles of color harmony and a practical equation in color definition. Whitefish, *MO: Kessinger Publishing.*

[2]. Chevreul, M. E. (1987). *The principles of harmony and contrast of colors and their application to the arts. Atglen* PA: Schiffer.

[3]. Keizo Shinomori, Ippei Negishi. (2021). Suppression of Luminance Contrast Sensitivity by Weak Color Presentation, *Frontiers in Neuroscience, Sec. Perception Science, Volume 15.USA.*

[4]. M. Dengler, W. Nitschke. (1993). Color stereopsis: A model for depth reversals based on border contrast. Attention, *Perception, & Psychophysics 53,* pp.150–156. USA.

[5]. R. Beau Lotto, Dale Purves. (2020). *An empirical explanation of color contrast, PNAS 97*(23), USA.

[6]. Yoko Mizokami, Carrie Paras, Michael A. Webster. (2004). Chromatic and contrast selectivity in color contrast adaptation, *Visual Neuroscience, 3*, pp.359-363. UK.

Color Standards in City Planning and Store Facade Design Changes Relationship between The Content of The Landscape Formation Standards and The Adopted Design Change Methods

Toshiharu Terashima[a*], Masayuki Harada[b], and Takashi Hanari[c]

[a]*Aichi Sangyo University, Okazaki, Japan*
[b]*Nagoya City University, Nagoya, Japan*
[c]*Sugiyama Jogakuen University, Nagoya, Japan*
[*] *Toshiharu Terashima: ttera@asu.ac.jp*

ABSTRACT

This paper clarifies the relationship between the content of the landscape formation standards in the landscap e plan and the adopted design change methods and to clarify the effects of incorporating content related to the met hods of design change in landscape formation standards. Via analysis of five cities and seven districts, including Osaka and Kyoto, we confirmed regulations' details and their extent of adoption using the 15 design change meth ods summarized in a previous paper. Results of analysis showed that "recommendation of cut lettering design" an d "prohibition of protruding signboards" and "low color chroma" were effective, On the other hand, it was not pos sible to determine whether the "relaxing chroma restrictions for indoor advertisements" would indirectly lead to "r eplacing signs from outdoor to indoor."

Keywords: Landscape Law, Landscape Regulation, Landscape Formation Standards (LFS), Field survey, Corporate Identity (CI)

INTRODUCTION

Since enactment of the 2004 Landscape Law, Japan's landscaping policy has undergone a major shift. As of March 2025, more than 660 local governments have developed landscape plans. Many local governments with landscape plans establish priority districts, setting LFS with respect to colors and other aspects to guide and restrict landscaping. However, many chain stores already have standardized facades that maintain corporate identity (CI), thus challenging store operators to balance public welfare (in landscaping) with CI. This study aims to determine how facade design-change methods can contribute to balancing public welfare (in landscaping) with preservation of CI. In a previous paper [1], the authors discussed the relationship between LFS and design modification methods for stores in Osaka and Kyoto. In this paper, we increased the number of districts analyzed and aimed to gain detailed understanding of the effects of incorporating change methods into LFS.

METHODOLOGY

Landscape Formation Standards in the survey area

The study examined seven central urban districts lined with medium- and high-rise buildings in five cities (two in Osaka, two in Kyoto, and one each in Kanazawa, Okayama, and Tokyo). Table1 shows the regulations concerning store facade design for each districts, with the content extracted and organized. All districts had LFS and regulations for exterior advertising materials, detailed below, but their regulation and enforcement methods differed.

First, looking at buildings. For example, to create a lively atmosphere, two Osaka districts and one Tokyo district allow a certain freedom in color choices. Conversely, the other four districts limit color choices to ensure a calm urban landscape.

Next, for advertising materials, two Osaka districts and Tokyo's Aoyama Street districts require low-chroma colors, but the Aoyama Street districts and Midosuji Guideline districts allow any colors for low-rise areas of buildings. Additionally, two Kyoto districts and the Kanazawa, and Okayama districts regulate color chroma using the Munsell color system. Despite this, Kyoto has slightly relaxed its chroma restrictions for advertisements on glass surfaces, on the other hand the Kanazawa and Tokyo districts limit the number of colors to a minimum. Regarding form, the five districts outside Kyoto recommend using cutout letters for signs. Finally, the two Kyoto districts prohibit signs that protrude above the road.

Field Survey Overview

Field surveys were conducted on both sunny and cloudy days from May 2023 to February 2024, from 3 hours after sunrise to 3 hours before sunset. Targets were all chain stores with standard designs, including individual ground-floor entrances. Standard store designs were determined by drawing on several recently opened stores in unregulated areas. Survey items were all CI elements of store facades, which were photographed and colors measured visually. Finally, based on survey results, the research team determined which stores to analyze.

Classification of facade design-changes methods for facades

We classified the 15 design change methods observed in the field survey into 3 categories (upper section of Table 2). Sign color's A-Change/Omission is color-change organized into eight methods—a range from changing to low chroma and low value to reducing high-chroma colors' area. Sign element's B-Change/Omission is organized into five methods involving change in form, such as omitting part of a sign. Sign position's C-Change/Omission is organized into two methods. Although we have classified these methods into 15 types, in practice, they are often used with some other methods. The 15 change methods can be broadly divided into two categories: methods that change the corporate color ([A1], [A2], [A4]) and methods that maintain the corporate color (the other 12 methods). In addition, some chain stores adopted methods such as [B1] Changing to cutout letters as their standard design. This classification of change methods is a slight revision of the change methods in our previous paper [2].

RESULTS AND DISCUSSION

1. Hypotheses that can be read from the regulations

To clarify the extent to which regulations have been reflected in the change methods, Table 2 summarizes each store's changes. Due to space limitations, however, only three districts are listed. Furthermore, based on each region's regulations (Table 1), we hypothesized that clearly-specified methods are more likely to be adopted (see summary in Table 3). For example, cut lettering design are recommended in five areas outside Kyoto, so possibly, use of [B1] will increase. In the next section, we conduct a detailed analysis for each hypothesis.

Table3: Hypothesis on regulation's effects

Hypothesis Design-change methods expected to increase in adoption	**Regulatory content** to verify effectiveness	**Expressions** in Table 1	Regulated district (Restricted districts marked by black circles)						
			Osaka		Kyoto		Kanazawa	Okayama	Tokyo
			Midosuji Dist.	Midosuji Guideline Dist.	Karasuma Street Dist.	Oike Street Dist.	Musashi to Korinbo Dist.	Momotaro Boulevard Dist.	Aoyama Street Dist.
[B1] Cut lettering design	Recommending "cut lettering design"	Red text	●	●			●	●	●
[B5] Omission of protruding signs	Prohibition of protruding onto the road	Green text			●	●			
[C1] Replace signs position from outdoor to indoor	Deregulation of indoor advertising	Blue text			●	●			
Changing color hue [A1] [A2] [A4]	Limiting high-chroma colors	Orange text			●	●	●	●	
	Use fewer number of colors	Purple text					●		●
Reduces the area of use without changing the color hue [A5] to [A9]	Limiting high-chroma colors	Orange text			●	●	●	●	
	Use fewer number of colors	Purple text					●		●

2.The effect of recommending “Cut lettering design”

Table 4 shows the number and percentage of stores that have adopted [B1] cut lettering design; the highlighted districts have recommended cut lettering designs due to landscape regulations. Additionally, the highlighted percentages of stores using [B1] Cut lettering design are higher than in other districts..

Among the five districts recommending cut lettering designs, adoption rates in the Midosuji Guideline, Okayama, and Tokyo districts are high, especially Tokyo is quite high. However, in the Midosuji and Kanazawa districts, the adoption percentage is low, as in the two Kyoto areas without regulations. Although two districts show low adoption rates, the remaining three districts clearly exhibit higher adoption rates, suggesting the regulations are having an effect. The reason for the extremely high adoption percentage in the Aoyama Street area (Figure 1) is thought to be that there are many glass-walled buildings, making it difficult to install board-type signs. Furthermore, while the reason for the low adoption rate on Midosuji remains unclear at this time, the low adoption rate in Kanazawa is thought to be due to the use of a different methodology, as described later in Section 5 of this chapter.

Table4: Stores that have adopted the [B1] Cut lettering design

	Osaka		Kyoto		Kanazawa	Okayama	Tokyo
	Midosuji Dist.	Midosuji Guideline Dist.	Karasuma Street Dist.	Oike Street Dist.	Musashi to Korinbo Dist.	Momotaro Boulevard Dist.	Aoyama Street Dist.
Number of stores	39	35	53	28	20	23	35
Number of stores without standard Cut lettering design	37	30	40	25	20	21	30
Number and percentage of stores adopted [B1]	4	10	6	3	2	6	15
	10%	29%	11%	11%	10%	26%	43%

Fig1: Example of B1

3.The effect of prohibiting “Protruding onto the road”

Protruding signs increase visibility from the street, but Kyoto prohibits them. However, signs within the premises may be installed. Table 5 shows that the two Kyoto districts have a high percentage of adoption [B5] (omission of protruding signs) indicating highly effective regulations (Fig. 2). Although Osaka and Tokyo also use [B5], Kanazawa’s percentage of adoption [B5] (omission of protruding signs) is very low, perhaps because sidewalks and roadways there are narrower than in other districts.

Table5: Stores that have adopting [B5] Omission of protruding signs

	Osaka		Kyoto		Kanazawa	Okayama	Tokyo
	Midosuji Dist.	Midosuji Guideline Dist.	Karasuma Street Dist.	Oike Street Dist.	Musashi to Korinbo Dist.	Momotaro Boulevard Dist.	Aoyama Street Dist.
Number of stores	39	35	53	28	20	23	35
Number and percentage of stores adopting [B5]	12	13	22	19	2	6	11
	31%	37%	42%	68%	10%	26%	31%

Fig2: Example of B5

4. The effect of relaxing chroma restrictions for indoor advertisements

In two districts of Kyoto, regulations on indoor advertisements’ chroma have been relaxed, so many chain stores can adopt CC as is by adopting [C1]; possibly they are being indirectly encouraged to do so. However, Table 6 shows the adoption rate of [C1] is highest in the Oike district, while the other district, Karasuma, has the lowest rate. Therefore, it is impossible to determine whether deregulation had any effect.

Table6: Stores adopting [C1] Replace signs’ positions from outdoor to indoor

	Osaka		Kyoto		Kanazawa	Okayama	Tokyo
	Midosuji Dist.	Midosuji Guideline Dist.	Karasuma Street Dist.	Oike Street Dist.	Musashi to Korinbo Dist.	Momotaro Boulevard Dist.	Aoyama Street Dist.
Number of stores	39	35	53	28	20	23	35
Number and percentage of stores adopted [C1]	2	3	0	0	0	0	5
	5%	9%	0%	0%	0%	0%	14%
Number and percentage of stores combined using [C1].	6	9	5	8	2	3	5
	15%	26%	9%	29%	10%	13%	14%

Fig3: Example of C1

5. The effect of limiting “High-chroma colors”

Compared to the Osaka and Tokyo where free use of color is permitted in low-rise buildings, the two Kyoto districts show nearly identical rates of “modification methods to low chroma (A1, A2, A4)”, while Kanazawa and Okayama (especially Kanazawa) have significantly higher adoption rates. The requirement that all newly installed advertisements in Kanazawa undergo individual review is thought to be related to its high adoption rate. We also analyzed the adoption rate of methods to reduce the amount of high-chroma colors (A5 to A9). Table 7 shows that adoption is high in the regulated Kyoto, Kanazawa, and Okayama.

Therefore, considering both the adoption rate of “modification methods to low chroma” and the adoption rate of “methods reducing the amount of high-chroma colors” together, the combined rate is significantly higher than in the three unregulated districts. Regarding high-chroma color regulations, although increasing the use of “modification methods to low chroma” presents high hurdles in some districts, it is thought to be effective, considering the increasing number of methods to reduce the amount of high-chroma colors.

Table7: Stores adopting [A1], [A2], and [A4] Low chroma and [A5] to [A9] Reduce high chroma

	Osaka		Kyoto		Kanazawa	Okayama	Tokyo
	Midosuji Dist.	Midosuji Guideline Dist.	Karasuma Street Dist.	Oike Street Dist.	Musashi to Korinbo Dist.	Momotaro Boulevard Dist.	Aoyama Street Dist.
Number of stores	39	35	53	28	20	23	35
Number and percentage of stores adopted [A1], [A2], [A4]	3	6	9	5	10	7	2
	8%	17%	17%	18%	50%	30%	6%
Number and percentage of stores adopted [A5] to [A9]	5	5	14	11	4	6	4
	13%	14%	26%	39%	20%	26%	11%

Fig4: Example of A1（left）, A7(right)

CONCLUSION

This paper analyzes current conditions in seven districts across five cities to determine the feasibility of promoting design-change methods by incorporating them into Landscape Formation Standard. Results showed that the Direct regulatory expressions such as “recommendation of cut lettering design” “prohibition of protruding signs” and “low color chroma” appear to have a guiding effect. However, “low color chroma” present a high adoption hurdle and may only lead to the adoption of method that reduce high-chroma colors. On the other hand, it was impossible to determine whether “relaxing chroma restrictions for indoor advertisements” would indirectly lead to “replacing signs from outdoor to indoor.”

ACKNOWLEDGEMENTS

This study was supported by JSPS KAKENHI (23H03682 / 23K28371).

REFERENCES

[1]. Harada, M., Terashima, T., & Hanari, T. (2025). Color Standards in City Planning and Store Facade Design Changes: Part 8 Relationship between the content of the landscape formation standards and the adopted design change methods. *The Color Science Association of Japan, Proceedings of the 56th Annual Meeting*,.

[2]. Shibahara, K., Ono, T., Terashima, T., Harada, M., Takeuchi, A. Hanari, T., & Mukaiguchi, T. (2024). C Color Standards in City Planning and Shore Facade Design Changes: Part 2 Field Survey on Priority Landscape Districts in Osaka City, Kyoto City, and Kanazawa City and Classification of Methods for Changing CI Elements of Stores. *AIJ Journal Architectural Institute of Japan Tokai Branch Research Paper*, Volume 62, .429-432.

Table 1: Landscape Formation Standards for Priority Areas (Excerpt)

City		Osaka City		Kyoto City		Kanazawa City	Okayama City	Minato Ward, Tokyo
District		Midosuji District	Midosuji Guideline District	Karasuma Street District	Oike Street District	Musashi to Korinbo District	Momotaro Boulevard District	Aoyama Street District
Architecture	Common matters	Strive to blend in with the surrounding cityscape.		The goal is to preserve and create a harmonious roadside cityscape.		Design a cityscape that exudes elegance and tranquility.	The façade should blend in with the cityscape and have a sophisticated and calm appearance.	Creating an elegant and lively cityscape.
	Form	The design of the first floor is intended to bring liveliness to the area.		Ensure a calm walking space by using natural materials, such as stone, in low-rise areas.		Strive to adopt a traditional form and design.	The form should be unified and harmonious with the surrounding cityscape.	The form should harmonize with surrounding buildings.
	Color	・Low-rise areas may use any color they wish. However, in the mid- and high-rise areas, brightness and saturation should be regulated, and colors should be more subdued. ・Avoid using high chroma colors. ・The chroma shall be 6 or less. ・If colors with a chroma greater than 6 are used, they should serve as accent colors and cover less than one-fifth of each surface's apparent area.		・Except for the roof, colors shall be as follows to harmonize with the roadside cityscape. ① Hue should be YR, Y, P, PB, or N series. ② Value should be medium or high brightness. ③ The chroma should be low. ・The following colors may not be used on major exterior walls. However, this rule does not apply to natural materials that have not been colored. ① In the hue YR, colors with chroma greater than 6 ② In the hue Y, colors with chroma greater than 4. ③ In the hue PB and P, colors with chroma greater than 2. Note that the Munsell system value is not specified.		・The exterior wall color should harmonize with the traditional urbanscape and be a subdued shade of brown, beige, or gray. ・Roof colors should be shades of black, gray, or brown with low chroma. ・Don't use the following prohibited colors as the main color for exterior walls and roof. Prohibited colors: ① In the hues R, and YR, colors with chroma greater than 6 ② In the hue Y, colors with chroma greater than 4. ③ In hues other than ① and ②, colors with chroma greater than 2. ④ Fluorescent color	・Use subdued colors instead of garish ones. ・Colors must conform to the following standards. ① Hues in the R, YR, and Y series must have a value of at least 3 and a chroma of no >6. However, the R series should not have a value greater than 8 and a chroma greater than 4. ② Other hues must have a value of at least 3 and a chroma of no >2. ・This does not apply to colors of natural materials, traditional techniques, or accent colors used on <10% of the surface area.	Colors must conform to the standards specified by the Munsell system and harmonize with the surrounding cityscape in color hue, value, and chroma. ・Exterior walls should be a medium chroma color that blends with the surrounding cityscape and promotes serenity. ・Other colors may be used on exterior walls to create liveliness and moisture. However, their use should be limited to no more than one-fifth of each exterior wall.
		The colors should match the town and buildings, and be appropriate for Midosuji Boulevard.	The low-rise part of the building can be any color but must match Midosuji Boulevard.					
Outdoor advertisements	Common matters	・The advertising material should blend in with the calm, harmonious atmosphere of Midosuji Boulevard.	Advertising materials should blend in with the surrounding cityscape and buildings along Midosuji Avenue.	In the central area of Kyoto, which is the city's commercial and business center, outdoor advertising material in commercial and business districts shall be permitted if they are in harmony with the cityscape in height, area, form, and design.		The design and colors should be appropriate to the surrounding cityscape without detracting from the city's aesthetics.	Promote a clean cityscape by integrating the design, colors, and installation methods with the buildings.	Advertising materials should blend with the surrounding cityscape and be integrated into the building.
	Form and Color	・The design and color of advertising material shall comply with the following regulations ①The lettering should be **cut lettering design or box letters**. ②The ground color should match the color of the wall. ③ **Reduce the use of high chroma.**		・Prohibition of Rooftop Outdoor advertising material ・Flashing or moving lights are prohibited. ・**Prohibition of road protrusions (partial restriction of protruded advertising material).** **【Regulated color】 Any colors whose Munsell chroma exceeds the values listed below shall be regulated.** ① In the hue R, colors with chroma greater than 6 ② In the other hue, colors with chroma greater than 8.		・**Avoid using garish colors for the ground color.** ・**Use fewer number of colors.** ・**Avoid using high-chroma colors in large areas.** ・The store's name and logo on the wall should be made of **cut lettering design or boxed letters**. ・**Only use R and Y hues and high-chroma colors as accent colors on a limited basis.** ・Prohibited colors (see above) are not used. ・All new advertising materials are individually reviewed.	・**The main color of advertising material should not be garish (chroma of 8 or more) or dark (value of <3).** ・**Do not use garish colors that cover more than half of the display area in advertising materials.** ・ As much as possible, display in **cut lettering design or box letters.**.	・Advertising materials should enhance the town's attractiveness and value. ・**In the higher part of the building**, advertising material should be integrated into the wall surface using **cut lettering design or box letters**. In the lower part of the building, advertising material should be used to create a lively atmosphere. ・**Avoid using high-chroma colors and color combinations. Limit the number of colors** used so as not to stand out from the cityscape.
			However, advertising material and signage will be permitted in low-rise areas.					
	Others	Each district has individual regulations regarding the size and installation height of each type of advertising material.						
Advertisements inside glass surface		・Similar regulations to those for outdoor advertising material. ・Only advertising materials designed for integration with the exterior of buildings and installation at heights of <10 meters may be installed.	・Consider the harmony of the building by aligning shapes and positions. ・The display method should use **cut lettering design** and be concise. Consideration should be given to color and size.	・It is regulated as a specific type of indoor advertising material. ・The chroma of the grand color of advertisements must not exceed the following values. Additionally, no advertising material may be displayed that are inconsistent with the appearance of buildings and the surrounding cityscape may be displayed. ① Y and YR hues should have a chroma of 10 or less. ② Other hues should have a chroma of 8 or less.		・It is regulated as a specific type of indoor advertising material. ・These are regulations similar to those for outdoor advertising material, except for restrictions on the display ratio. ・The limit on the percentage of display per window is no >50% for the ground floor. ・Grand color should **avoid garish hues** and **use as few number of colors as possible.**	Prohibited in principle	Similar regulations to those for outdoor advertising material.

Note: Indoor advertising material are subject to less stringent chroma rules than outdoor ones.

Table 2: Adopted Change Methods by Each Store: (Excerpts from the "Midosuji Guideline District" and "Oike Street District"and "Momotaro Boulevard District").

City	Disrict	Industry (Major category)	Industry (subcategory)	chain store name	Standard Design	Methods for Changing CC			Methods for maintaining colors (CC)											
						A. Change/Omission of sign color								B. Change/Omission of sign elements					C. Change/Omission of sign position	
						[A1] Achromatization	[A2] Material colorization	[A4]Low chroma and Low lightness	[A5] Color number reduction	[A6] Color inversion of figure-ground	[A7] Reduction in regulated color area ratio	[A8] Use CC as a line	[A9]Signboard background whitening	[B1] Cut lettering design	[B2] Abbreviation of store name	[B3] Abbreviation of symbol mark	[B4] Sign Size Reduction	[B5] Omission of protruding signs	[C1] Replace signs position from outdoor to indoor	[C2] Replace signs position on outdoor
Kyoto city	Oike Street District	Food and Beverage	fast food	Mos Burger										●				●		
			Other	Miyamoto Munashi	●													●		
				Marugame Udon										●				●		●
				YAYOI KEN		●												●		
		Retail industry	Convenience store	7-Eleven							●									
											●							●		
				family mart							●							●		
											●						●	●		
				LAWSON						○				●		●	●	●		
			General store	welcia dacs				●										●		
				Sugi Pharmacy													●	●	○	
			Other	vision-megane		●											●	●		
				falco Pharmacy	●													●		
				YAMAYA				●									●	●		
		Service industry	banking and securities	Aizawa Securities	●														○	
				KYOTO SHINKIN BANK	●		○							○					○	
				KYOTO CHUO SHINKIN BANK	●		○							○						
					●		○							○				●	○	
			Mobile phone	au						●		●								
				docomo									●					●		
			Real Estate	UR Rental Housing	●													●	○	
				Mitsubishi Jisho House Net									●					●	○	
			Other service industries	Curves	●													●		
				NIPPON RENT-A-CAR						●									○	
Osaka City	Midosuji Guideline District	Food and Beverage	Café	Starbucks Coffee	●									○					○	
					●									○						
				Doutor Coffee										●						
														●				●	●	
			to go	krispykreme		●								●						
		Retail industry	Convenience store	7-Eleven		●								●				●		
														●			●	●		
				Daily Yamazaki	●													●		
				family mart										●						
														●				●	●	
			General store	KOHYO										●				●		
				daikokudrug	●															
		Service industry	banking and securities	Iyo Bank	●		○			○				○				●	○	
				Kiyo Bank	●		○							○					○	
				Nomura Securities	●					○								●	○	
				Mizuho Securities	●	○				○				○						
				SUMITOMO MITSUI BANK			●												○	
							○			○										
				MUFG BANK			●											●	○	
				MUFG Trust and BANK			●											●	○	
			Mobile phone	au						●		●								
				docomo	●													●		
			Real Estate	Mitsui rehouse										●				●	○	
				minimini	●															
				Post office						○				●					○	
							●													
Okayama City	Momotaro Boulevard District	Food and Beverage	Café	Mister Donut	●													●		
			fast food	Matsuya	●							○	○							
				YOSHINOYA	●															
			to go	Hotto Motto						●								●		
		Retail industry	Convenience store	family mart	●															
				LAWSON	●													●		
			General store	BICCAMERA										●						
				Matsumotokiyoshi										●						
		Service industry	banking and securities	Mizuho Securities	●		○												○	
				MUFG BANK						○				○					○	
				Sumitomo Mitsui Bank	●		○													
				Chugoku Bank	●		○													
				HIROSHIMA BANK	●		○													
			Real Estate	Daikyo Anabuki Real Estate						○			○						○	
				Apamanshop	●					○										
				ABLE						○				●				●		
			Other service industries	ACCEA	●													●		
				Post office	●	○								○						
				YAMATO TRANSPORT													●	●		

Among the advertising regulations shown in Table 1, the regulation "②The ground color should match the color of the wall" in the two Osaka districts could indirectly encourage modification method A6, but it has been excluded from the analysis in this paper.

Colorimetric Characterization of Transparent OLED Displays under Various Backlighting Conditions

Chun-Ting Shen[a], Chao-Hua Wen[a*], Bao-Jen Pong[b]

[a]*National Taiwan University of Science and Technology, Taipei, Taiwan, R.O.C.*
[b] *Industrial Technology Research Institute, Hsinchu, Taiwan, R.O.C.*

**Corresponding author: chwen@mail.ntust.edu.tw*

ABSTRACT

This study presents a comprehensive spectral-based colorimetric characterization methodology for transparent OLED displays, addressing the critical challenge of background illumination effects on color reproduction accuracy. Using the International Display Metrology Standard (IDMS) Color Gamut Envelope protocol, we systematically evaluated a 30" transparent OLED under six controlled backlighting conditions combining three correlated color temperatures (CCTs: 2800K, 3900K, 5500K) at two illuminance levels (35-73 lx and 280-583 lx). Results of comparisons between 602-color and 98-color sampling methods revealed that the denser sampling significantly improved measurement accuracy, with relative errors increasing from 11.4% to 33.9% when using sparse sampling under extreme illumination. Spectral measurements demonstrated severe gamut volume degradation from 1,430,529 ΔE^3 under dark conditions to 46,937 ΔE^3 at maximum illumination, representing a 96.7% reduction. Even modest ambient lighting of 35-37 lx caused 65-75% gamut reduction. These findings establish a standardized characterization framework essential for developing adaptive color management systems and quality assessment protocols for transparent display applications in automotive, retail, and augmented reality environments.

Keywords: Colorimetric characterization, transparent display, color modelling, OLED display

INTRODUCTION

Transparent organic light-emitting diode (OLED) displays represent a transformative technology enabling simultaneous viewing of digital content and real-world environments. Their unique see-through properties make them invaluable for automotive head-up displays (HUDs), retail showcases, and augmented reality applications. However, this transparency introduces fundamental colorimetric challenges absent in conventional opaque displays.

Unlike traditional displays where the black state is determined solely by the display technology, transparent OLEDs experience additive mixing between self-emitted light and transmitted background illumination. This phenomenon causes dynamic color shifts, reduced contrast ratios, and gamut compression over varies ambient lighting conditions. In automotive applications, these variations can compromise critical safety information legibility, while retail environments face challenges maintaining brand color consistency.

Despite growing commercial deployment, systematic characterization methodologies for transparent displays remain underdeveloped. Previous studies have noted ambient light effects qualitatively, but comprehensive quantification using standardized protocols across diverse illumination conditions has not been established. The varying combinations of correlated color temperature and illuminance levels encountered in real-world applications require thorough investigation.

This study addresses these critical gaps through three primary objectives. First, we establish a standardized colorimetric characterization methodology based on IDMS protocols specifically adapted for transparent displays. Second, we quantify gamut degradation across systematically varied illumination conditions representative of real-

world applications. Third, we compare sampling density requirements to determine optimal measurement protocols for quality assessment and certification procedures.

METHODOLOGY

All measurements were performed under strictly controlled environmental conditions to accurately assess background illumination impact.

Experimental Setup

All measurements were conducted in a controlled darkroom environment with ambient illuminance maintained below 5 lx. The temperature was controlled at 24±3°C with relative humidity between 25% and 80% to ensure stable display performance and measurement consistency. A custom-designed light box measuring 77 cm × 48 cm × 50 cm was constructed to simulate uniform background illumination. The interior surfaces were coated with matte white paint achieving greater than 90% reflectance uniformity to eliminate potential artifacts from non-uniform backgrounds. Adjustable LED modules with variable CCT and intensity capabilities provided controllable illumination conditions.

The device under test was a commercial 30" transparent OLED display with 1920×1080 pixels resolution. A TOPCON SR-UL1R spectroradiometer, was positioned perpendicular to the display center at a distance of 1 meter. The instrument captured spectral power distributions from 380 to 780 nm. The measurement spot size was adjusted to cover a 2-degree field of view, ensuring adequate spatial averaging while maintaining positional precision.

Test Color Sets and Procedures

Three color temperature conditions were systematically evaluated: warm white (~2800K), neutral white (~3900K), and cool white (~5500K). Each CCT was tested at two distinct illuminance levels: low illuminance (35-73 lx) and high illuminance (280-583 lx). The illuminance variations within each level resulted from different luminous outputs of the LED modules at different CCT settings. This design yielded six illuminated test conditions plus a dark baseline reference.

Two sampling densities were evaluated following IDMS guidelines [1]. The test stimuli consisted of color points distributed uniformly on the surface of the RGB cube using the formula:

$$n = 6m^2 - 12m + 8$$

where m represents the grid dimension per cube face. The 602-color method employed m=11 (yielding n=602 unique color points), while the 98-color method used m=5 (yielding n=98 points). This approach samples the gamut boundary surface for maximum color range evaluation. Automated Python scripts controlled the sequential display of color patches and synchronized spectroradiometer data acquisition.

Data Analysis

The measured spectral power distribution data were converted to CIE 1931 XYZ tristimulus values and subsequently transformed into the CIE 1976 L*a*b* (CIELAB) color space for analysis using CIE standard illuminant D65 as the reference white [2] in order to compare the effects of the variable CCT settings. The primary metric was the CIELAB Gamut Volume (CGV), measured in ΔE^3 units. CGV was calculated using the convex hull algorithm [3] with an empirical correction factor of 0.85. Coverage of the standard color gamuts, sRGB and DCI-P3, was determined using Monte Carlo sampling within the convex hulls of the measured gamut and reference gamut, calculating the intersection ratio based on the proportion of random points falling within both volumes [4].

RESULTS

Validation of Sampling Methods

Figure 1 illustrates the comparisons between the 98-color and 602-color sampling approaches under dark conditions. Table 1 lists the quantitative comparisons for both dark and extreme illumination conditions.

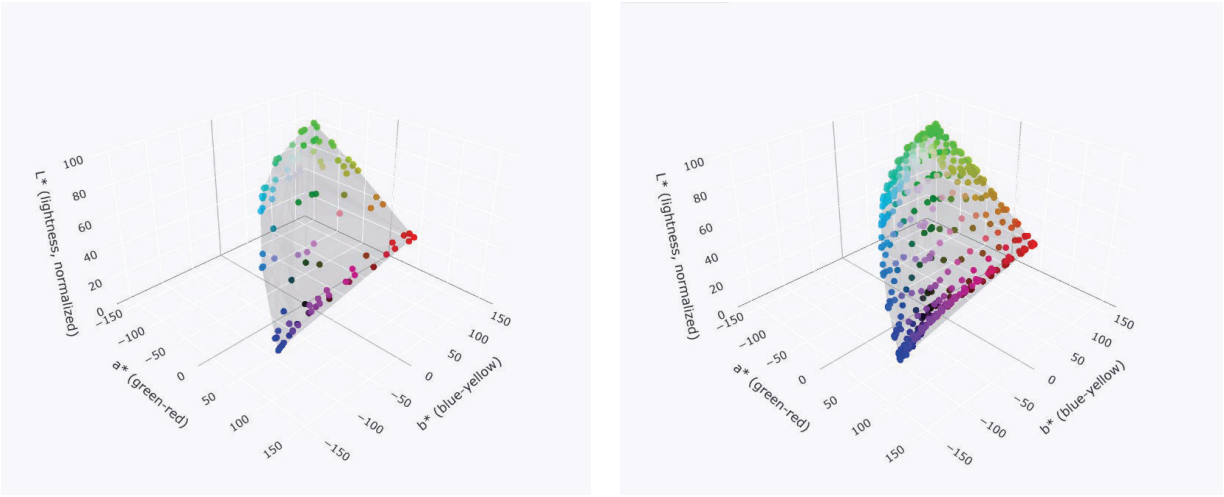

(a) 98-color 3D CIELAB gamut **(b) 602-color 3D CIELAB gamut**

Figure 1: Comparison of 98-color vs 602-color sampling methods under dark condition.

Table 1: Comparison Between 98-color and 602-color Sampling Methods

Condition	Metric	98-color	602-color	Difference (%)
Dark (backlit off)	Gamut Volume (ΔE^3)	1,267,675	1,430,529	11.4
	sRGB Coverage (%)	76.2	78.8	-
	DCI-P3 Coverage (%)	78.6	70.8	-
3900K, 583.3 lx	Gamut Volume (ΔE^3)	31,039	46,937	33.9
	sRGB Coverage (%)	2.8	4.2	-
	DCI-P3 Coverage (%)	2.0	3.0	-

The method of the 98-color set shows 11.4% lower gamut volume under dark conditions compared to the 602-color method. This difference increases to 33.9% under extreme illumination (3900K, 583.3 lx), demonstrating that sampling density becomes increasingly critical as background illumination degrades the gamut. Coverage percentages for both sRGB and DCI-P3 also differ between methods, though direct comparison is less meaningful due to the different calculation bases.

Comprehensive Characterization Using 602-Color set

Figure 2 presents the 3D CIELAB gamut visualizations for all six illuminated conditions. Table 2 summarizes the quantitative metrics.

Analysis of Illuminance and CCT Dependencies

Figure 3 illustrates the relationship between background illuminance and gamut volume degradation. The transparent OLED's gamut volume decreased from 1,430,529 ΔE^3 under dark conditions to 46,937 ΔE^3 under the brightest condition (3900K, 583.3 lx), representing a 96.7% reduction. Figure 4 presents 2D projections on the CIELAB a*-b* plane for four representative conditions.

Table 2: Gamut Performance for Three CCT Conditions at Low and High Illuminance Levels (602-color method)

Condition	Gamut Volume, ΔE^3	sRGB Coverage (%)	DCI-P3 Coverage (%)
Dark(backlit off)	1,430,529	78.8	70.8
2800K, 35.3 lx	501,561	44.9	32.5
5500K, 36.8 lx	351,506	31.5	22.8
3900K, 73.2 lx	243,308	21.8	15.8
2800K, 280.4 lx	94,027	8.4	6.1
5500K, 298.1 lx	53,340	4.8	3.5
3900K, 583.3 lx	46,937	4.2	3.0

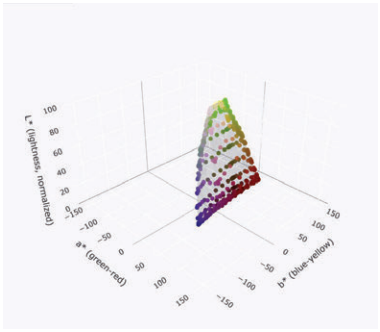

(a) 2800K, 35.3 lx

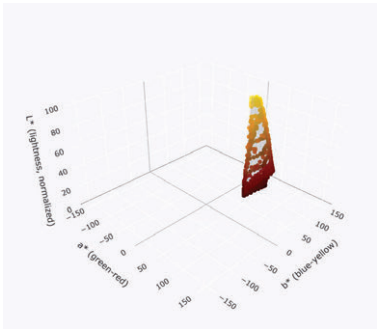

(b) 2800K, 280.4 lx

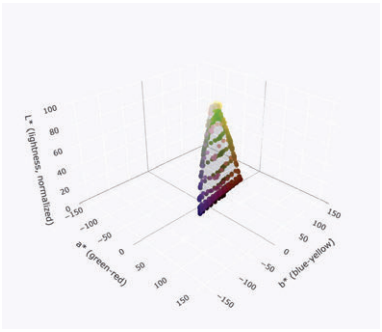

(c) 3900K, 73.2 lx

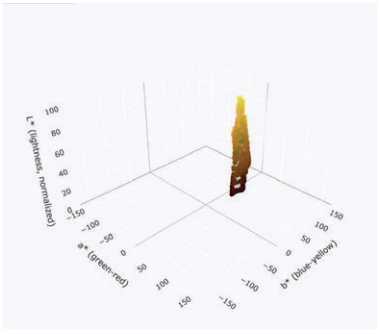

(d) 3900K, 583.3 lx

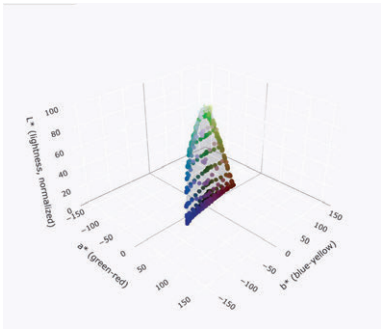

(e) 5500K,36.8 lx

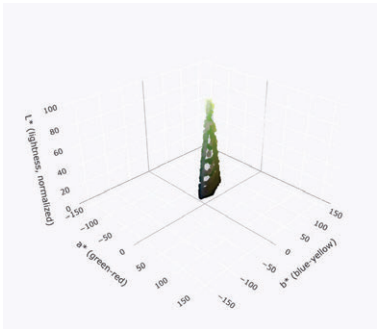

5500K 298.1 lx

Figure 2: Complete 602-color gamut characterization under six illuminated conditions.

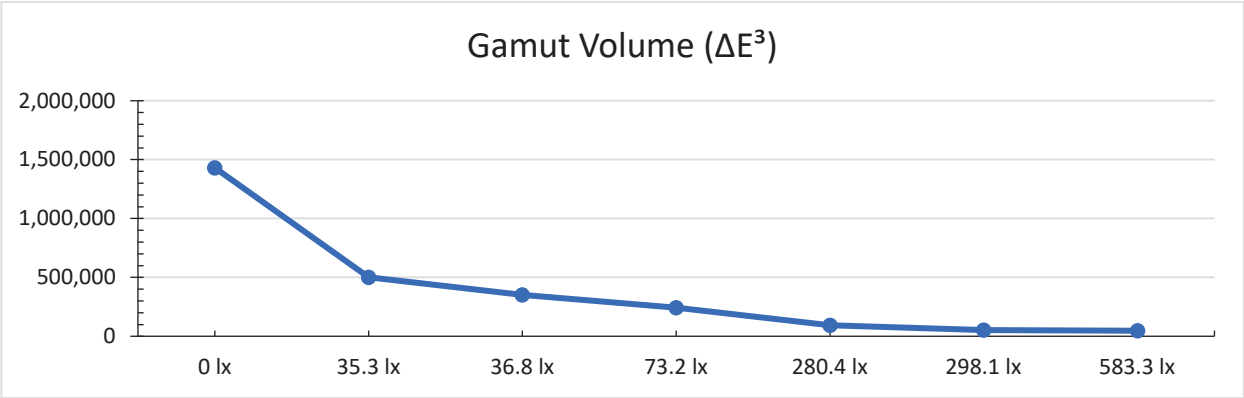

Figure 3: Relationship between background illuminance and measured gamut volume for the 602-color method.

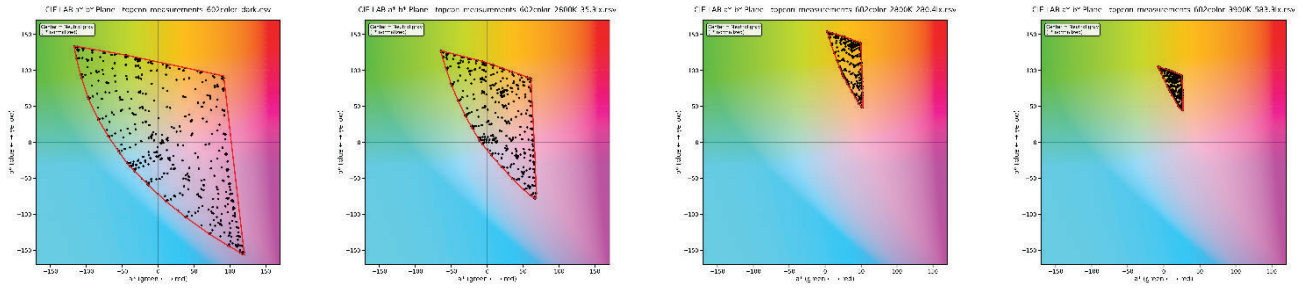

(a) Dark (0 lx) **(b) Low illuminance (2800K, 35.3 lx)** **(c) Medium illuminance (2800K, 280.4 lx)** **(d) High illuminance (3900K, 583.3 lx)**

Figure 4: 2D a-b plane projections showing progressive gamut compression with increasing illuminance:

DISCUSSION

The characterization revealed that background illuminance is the dominant factor affecting transparent OLED gamut performance. At low illuminance levels (35-73 lx), gamut volumes ranged from 243,308 to 501,561 ΔE^3, representing 65-83% reduction from the dark condition baseline of 1,430,529 ΔE^3. At high illuminance levels (280-583 lx), the degradation became severe with volumes dropping to 46,937-94,027 ΔE^3, a 93-97% reduction.

The mechanism underlying this degradation involves additive mixing of transmitted background light with OLED self-emission, raising the effective black level and compressing dynamic range. CCT variations produce additional chromaticity shifts—different color temperatures create distinct biases in the displayed colors, indicating that compensation algorithms must account for both intensity and spectral composition of ambient light.

The comparison between 98-color and 602-color sampling methods revealed significant practical implications. The 11.4% error under dark conditions increases to 33.9% under extreme illumination, demonstrating that higher sampling density is necessary for accurate characterization under variable lighting conditions. This finding suggests that measurement protocols should specify sampling requirements based on intended use conditions.

For practical applications, transparent OLEDs in retail environments require either controlled ambient conditions or compensation systems. Automotive HUD applications need adaptive color management to maintain contrast across varying daylight conditions. The validated 602-color methodology provides a standardized approach for transparent display characterization suitable for quality control and certification protocols.

CONCLUSIONS

This study established a comprehensive methodology for transparent OLED characterization under various backlighting conditions. The IDMS-based 602-color sampling method proved essential for accurate measurement, with relative errors increasing from 11.4% to 33.9% when compared to the 98-color method under extreme conditions. Systematic characterization revealed severe gamut degradation—from 1,430,529 ΔE^3 (dark) to 46,937 ΔE^3 (3900K, 583.3 lx), representing a 96.7% reduction. Low illuminance conditions (35-73 lx) reduced gamut volume by 65-83%, while high illuminance (280-583 lx) caused 93-97% degradation.

The framework provides standardized protocols and baseline data for developing adaptive color management systems. Future research should extend this single-sample study to multiple units, investigate complex non-uniform backgrounds, and evaluate dynamic content effects. Extension to other transparent display technologies and perceptual factors also warrant investigation. These findings establish foundations for transparent display deployment in applications requiring consistent color performance under dynamic lighting.

ACKNOWLEDGMENTS

The authors would like to express their gratitude to the Graduate Institute of Color and Illumination Technology at National Taiwan University of Science and Technology for providing the research facilities and resources that made this study possible.

REFERENCES

[1]. International Committee for Display Metrology. (2025). International Display Metrology Standard (IDMS) Version 1.3, Section 5.32 "Color Gamut Envelope-Color Capability". Society for Information Display.

[2]. International Commission on Illumination (CIE). (2018). CIE 015:2018 Colorimetry (4th ed.). CIE Central Bureau, Vienna, Austria.

[3]. Barber, C. B., Dobkin, D. P., and Huhdanpaa, H. (1996). The Quickhull algorithm for convex hulls. ACM Transactions on Mathematical Software, 22(4), 469-483.

[4]. Smith, E., Heckaman, R. L., Lang, K., Penczek, J., and Bergquist, J. (2020). Measuring the color capability of modern display systems. Journal of the Society for Information Display, 28(6), 548-556.

Application of Kubelka-Munk Theory in Jadeite Colour Evaluation

Jinbi Jiang, Qinxin He*, and Stephen Westland

University of Leeds, Leeds, United Kingdom
**Corresponding author: Qinxin He, ml20q2h@leeds.ac.uk*

ABSTRACT

This study evaluates a physics-based workflow for jadeite colour assessment by combining reflectance measurements with the Kubelka–Munk (K–M) theory. Four polished jadeite samples (≈1 cm thick) were measured on black and white backgrounds to allow the K/S spectra for the jadeite to be derived. Across samples, the K/S spectra exhibit characteristic peak–trough structure -- peak/trough positions align with perceived hue, fluctuation amplitude relates to colour contrast/saturation, and the overlap between black- and white-background K/S curves offers a practical proxy for transparency. In colorimetric comparisons, daylight-simulating D-series and U-series illuminants produced more consistent appearance than incandescent conditions (A10, HOR 10 (SPL)) in this dataset. The results indicate that K–M-based analysis is a promising basis for jadeite identification and for selecting viewing/lighting conditions.

Keywords: Jadeite, Kubelka-Munk Theory, Colour Evaluation, Colour and Lighting

INTRODUCTION

Jadeite, one of the most valuable gemstones, holds significant importance in the Southeast Asian market, particularly in China. Jadeite exhibits complex optical properties that influence its appearance under different lighting conditions. Assessing jadeite quality is a critical aspect of both gemmological research and commercial grading. While traditional evaluation methods consider factors such as translucency and colour, they often rely on experiential judgment. This study introduces Kubelka-Munk theory as a potential evaluation standard for selecting optimal lighting conditions for different types of jadeites. Additionally, it explores the feasibility of using Kubelka-Munk theory as a new standard for jadeite identification. This study focuses on establishing the experimental conditions for measuring jadeite, initially assessing the applicability of Kubelka-Munk theory, and using CIELAB values to predict more practical lighting conditions. The valuation criteria for jadeite primarily depend on colour, clarity, translucency (diaphaneity), and texture [1].

The colour of jadeite is due to Cr^{3+} and Fe^{3+} taking the place of aluminium ions (Al^{3+}) in the crystal structure of jadeite (NaAlSi2O6) [2]. Cr^{3+} strongly absorbs blue and red light, so that the residual greenish light dominates the visual perception of the human eye, and jadeite takes on a greenish hue. Fe^{3+} strongly absorbs ultraviolet and blue light, so that residual yellow-green light is reflected and jadeite may take on a yellow-green hue [2]. Jadeite with higher transparency is typically characterised by lower internal impurities, well-developed crystal grains, and a uniform structure. Additionally, a more even distribution of Cr^{3+} and Fe^{3+}, as opposed to concentrated clustering, enhances both the uniformity of colour and the overall transparency. High-quality jadeite, particularly the highly valued pure green variety, requires a balanced Cr^{3+} concentration, avoiding excessive amounts that yield dark green tones or insufficient amounts that result in light green coloration. Simultaneously, a low Fe^{3+} content is desirable to prevent undesired yellowish-green or greyish-green hues.

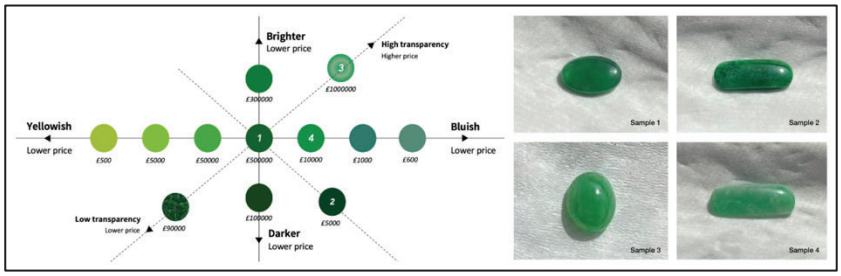

Figure 1: (a) Jadeite Price and Colour & Transparency; (b) the four samples selected for this study

METHODOLOGY

Given the very high market value of jadeite, only four samples were selected for this study (see Figure 2). Samples 1 and 2 exhibit similar pure green tones but differ in transparency, whereas Samples 3 and 4 are randomly selected jadeite with other green hues; in terms of transparency, the order is Sample 1 > Sample 3 > Sample 4 > Sample 2. All samples have a similar thickness of 1 cm (d = 0.01 m). As publicly recognised "jadeite" is typically in a polished state and raw, unpolished material exhibits significant colour differences and holds little commercial value, all samples used in this study are polished. The MetaVue VS3200 spectrophotometer was used to measure the reflectance factors of the jadeite samples, and to ensure accuracy the experiment was performed in a dark room, eliminating any external light interference so that the instrument served as the sole light source. The samples were measured on black and white panels, and measurements were consistently taken from the same point with the same viewing angle on each sample. The measurement of reflectance data over two differently coloured backgrounds is one way to allow the Kubelka-Munk absorption K and scattering S values to be derived from the reflectance data. However, to satisfy the assumptions required by the subsequent Kubelka–Munk analysis, a colourless and transparent oil layer was introduced between the sample and the background tile to reduce the influence of inter-reflections caused by changes in refractive index at the air gap between the jade and the tile; the use of oil in this way ensures that the jade and the oil are in optical contact. Reflectance data (between 400nm and 700nm at intervals of 10nm) were recorded under four scenarios: white background and black background.

Kubelka-Munk Theory

The optical properties of the jade samples are characterised using the Kubelka-Munk (K-M) theory which utilises absorption (K) and scattering (S) coefficients. The two-flux K-M model as shown in Figure 2 [3].

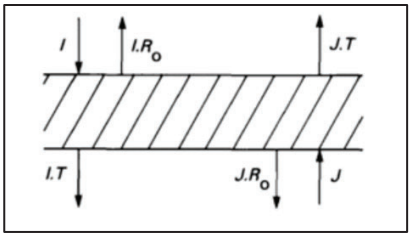

Figure 2: The Kubelka-Munk two-flux model's simplified light path

The model relies on several assumptions such as that the sample is spatially unform and that the sample is sufficiently large so that any light lost from the edges (travelling horizontally in Figure 2) is negligible and can be ignored. In Figure 2, R_o and T are the reflectance and transmittance respectively of the layer (in this case the jadeite sample) when it is illuminated from above diffusely and imagined to be suspended freely in air. If we introduce a background of reflectance R_g then we can derive an equation that calculates the reflectance R of the layer over the background from the reflectance of the background and the reflectance and transmittance of the freely suspended layer thus:

$$R = R_o + \frac{T^2 R_g}{1 - R_g R_o} \tag{1}$$

Eq. (1) is known as Stokes equation [4]. The idea behind this analysis is that if we measure R for two different values of R_g (for example, over a white and a black background) then we have two equations and two variables (R_o and T) and the reflectance and transmittance of the freely suspended layer can be found using simple mathematics. Once R_o and T are known it is possible to calculate K and S using Eq. (2) – (4), where d is the thickness of the layer and in this study can be set to 1 and ignored and where R∞ is the reflectance of an infinitely thick later of the jadeite The reason that K and S are calculated in most applications is that it allows predictions to be made about how different colorants subtractively mix. This is because K and S are assumed to be linearly related to colorant concentration. However, in this study, K and S are calculated to characterise the jade samples in a way that is meaningful and intuitive.

$$a = \frac{1+{R_o}^2-T^2}{2R_o}, \quad b = \sqrt{a^2 - 1} \tag{2}$$

$$\frac{K}{S} = a - 1, \; Sd = \frac{\text{arosh}(\frac{1-aRo}{T})}{b}, \; arosh(x) = In(x + \sqrt{ax^2 - 1}) \tag{3}$$

$$F(R_\infty) = \frac{(1-R\infty)^2}{2R\infty} = \frac{K}{S} \tag{4}$$

RESULTS AND DISCUSSION

Figure 3 presents the reflectance factors for the samples under different background conditions. Figure 4 analyses the relationship between the K/S values and jadeite samples which exhibit a characteristic pattern of two peaks and one trough. In the K/S curve, peaks correspond to wavelengths where the material exhibits strong absorption, the troughs indicate regions with higher reflection or transmission. The colour of jadeite is primarily determined by the chromophore elements absorption, such as Cr^{3+} and Fe^{2+}/Fe^{3+}. Cr^{3+} typically exhibits strong absorption around 550 nm, resulting in the characteristic green colour of jadeite. And Fe^{3+} may absorb light in the blue-violet region (e.g., around 450 nm) or in the red region. For all samples, the first peak, observed at approximately 430-450 nm, corresponds to the blue-green wavelength region, where absorption (*K*) is relatively high or scattering (*S*) is relatively low which is consistent with the electronic transitions of chromium ions. Also, it may be cause by the charge transfer band of Fe^{3+}, inhibiting the reflection of blue-violet light and leading to an increase in *K* and consequently a higher K/S value. Specifically, Sample 1 on a white background and Sample 4 (their first peak at 430 nm) are consistent with stronger strong Fe^{3+} related absorption, which could suppression of violet light. This may be due to a yellowish colour shift, as the complementary colour of absorbed violet light is yellow. However, the difference in absorption peak positions (430–450 nm) may reflect variations in Fe^{3+} content or coordination environment, could affect the degree of blue tone suppression, which in turn influences the brightness and hue of the green colour. The second peak, located near 640 nm, corresponds to the orange-red wavelength region. This region represents the complementary colour of jadeite green, and the electronic transitions of Fe^{2+} transitions could contribute to an orange-red response, increasing *K* and thus the K/S value. The trough, situated near 520-540 nm, corresponds to the green wavelength region, where absorption (*K*) is lower and scattering (*S*) is higher. The troughs often aligns with the perceived green region that is the reasons samples 1 and 2 is consistent with that Cr^{3+} predominantly contributes to the green colour (as its characteristic absorption band is at 550 nm). However, the slight shift in the trough position suggests weaker absorption, possibly indicating a lower Cr content. The trough at 520 nm (Samples 3 and 4) may suggest that Cr^{3+} and Fe^{3+} jointly influence the colour, or that other elements (such as V^{3+}) are interfering, causing a blue shift in the absorption band.

The feasibility of the Kubelka-Munk theory in jadeite identification can be discussed by analysing relative changes in K/S values. According to the physical definition, higher K/S values indicate stronger absorption (or

weaker scattering), resulting in deeper and higher saturated colours, vice versa. Comparing the K/S curves in Figure 4, samples 1 and 2 exhibit the most pronounced fluctuations between peaks and troughs, particularly sample 1 on a black background. This suggests that these two samples have higher colour contrast and greater saturation, likely appearing as purer green. In contrast, samples 3 and 4 show smaller variations in their K/S curves, indicating lower colour contrast and less saturated colour.

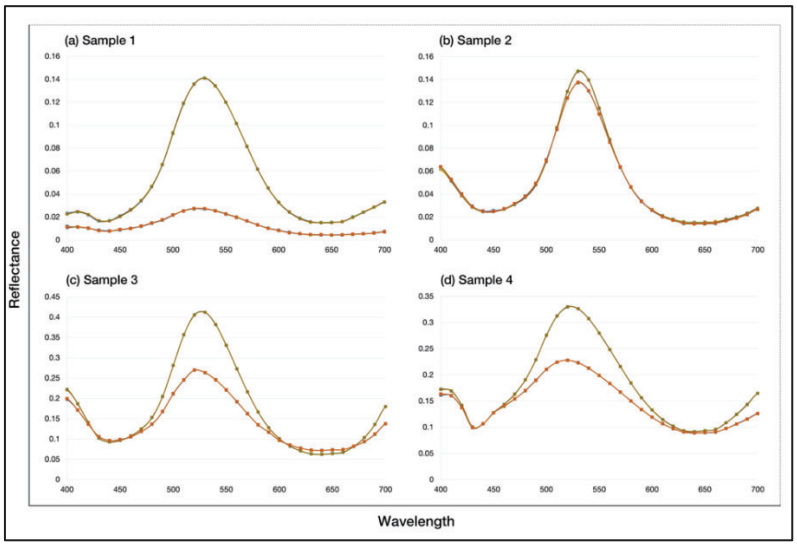

Figure 3: Reflectance factors of the four samples for white and black background conditions

In addition, for transparency, the K/S curves reveals that sample 1 has almost no overlap between the black and white background curves, followed by sample 3, sample 4, and finally sample 2. For highly transparent samples, light has a stronger reflection on a white background, while reflected light is significantly reduced on a black background which is observed in Sample 1 (Figure 4 (a)). This further validates the sample properties - the K/S curves for sample 1 show minimal overlap on both black and white backgrounds, while sample 2 exhibits the greatest overlap range. It also supports that K/S curves of high-transparency samples are more influenced by the high-scattering properties of a white background and the high-absorption characteristics of a black background. Using the overlap percentage of K/S curves on black and white backgrounds seem to a reasonable for evaluating jadeite as general standard.

Based on the analysis in Figure 4, the identification of the samples according to the K/S curves is as follows:

- Sample 1, after the absorption in the blue-violet and red regions, shows an enhancement in reflectance around 540 nm. The K/S value difference is significant, and the overlap between the black and white background curves is low. It is predicted that Sample 1 predominantly exhibits a high-saturation green with yellowish, characterised by vivid green hues. And it may appear slightly darker due to stronger absorption in the red region.

- Sample 2's reflectance is concentrated in the yellow-green range, but due to stronger absorption in the blue region, it overall presents a deeper, bluish green. The K/S value difference is moderate, the colour is vibrant but not as bright as Sample 1.

- Sample 3 shows a reflectance peak shifted towards the shorter wavelength (520-530 nm), indicating weaker Cr^{3+} absorption. It may contain other impurities (such as V^{3+}) that cause interference. The K/S value difference is small, and the colour appears light and soft, tending towards a bright blue-green.

- Sample 4 has a small K/S value difference. The trough near 520 nm corresponds to the edge of the Cr^{3+} absorption band, with reflectance concentrated in the blue-green region. However, due to the combined absorption

from the violet and red regions, the colour is pale and less vivid, overall exhibiting a low brightness green or bluish hue.

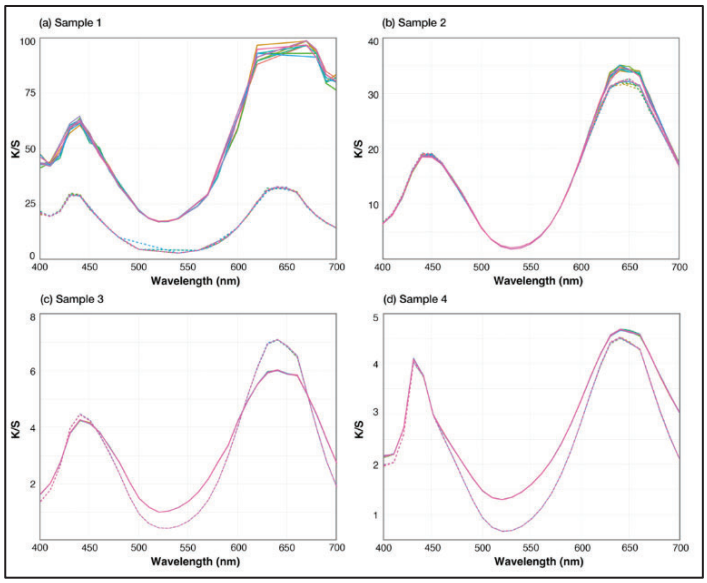

Figure 4: K/S of samples 1, 2, 3 and 4 under different background conditions

The instrument employs a fixed physical light source to measure spectral reflectance factors $R(\lambda)$. In this study, colorimetric (CIELAB) values were also computed under different illuminants. Regardless of transparency, the colour difference of jadeite under different illuminants is greater on a white background than on a black background (Figure 5). Additionally, the correlated colour temperature (CCT) affects jadeite colour appearance. Across all tested conditions, warm yellow temperature (despite A10 showing notable inconsistencies) exhibit higher colour consistency than cool artificial illuminants. Daylight-simulating sources (D-series) and U-series temperature demonstrate greater colour stability, whereas incandescent (A10, HOR 10 (SPL)), LED B1 (10), and fluorescent (F02 (CWF)) show more pronounced variations in colour, with incandescent illuminants exhibiting the most significant differences.

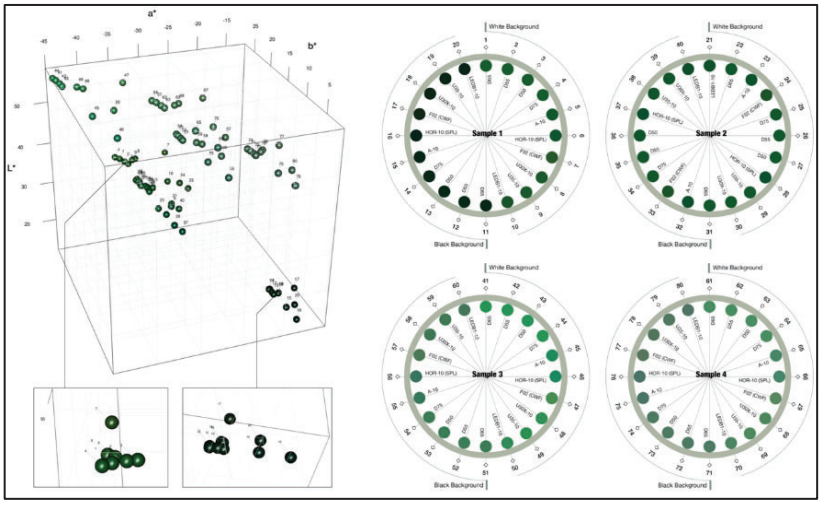

Figure 5: Lab (D65/2 °) values for 4 samples under different illumination conditions

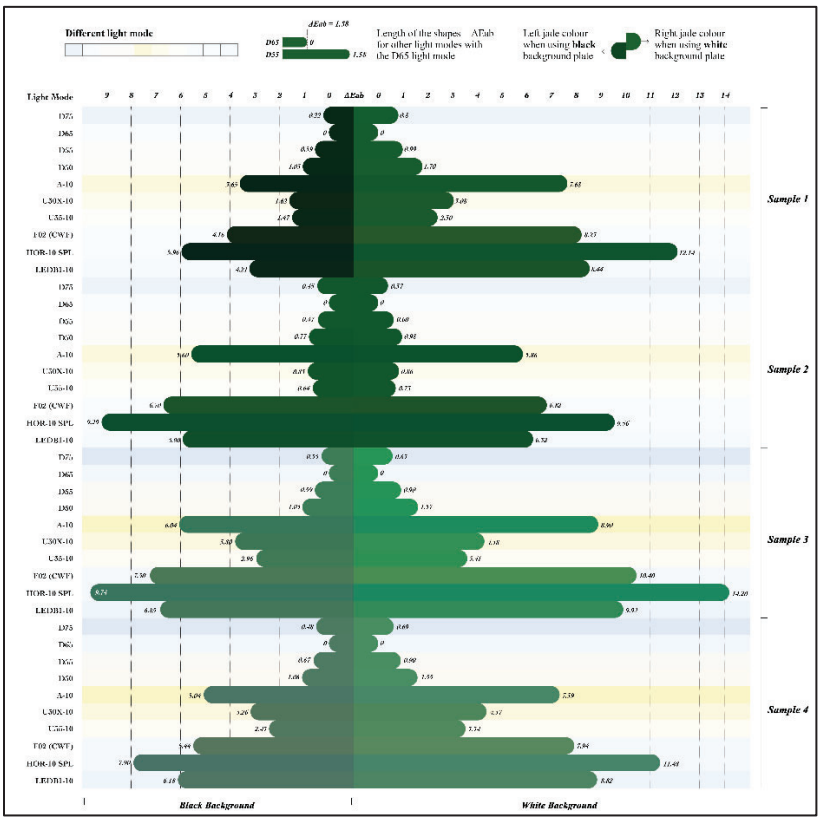

Figure 6: Lab difference and ΔE_{ab} of 4 samples in different illumination

CONCLUSION

This paper measured the reflectance of four polished jadeite samples under controlled conditions to evaluate experimental factors and assess the applicability of the Kubelka–Munk (K–M) framework for jadeite analysis. The K–M approach shows promise for identification: peak/trough positions in the K/S spectrum relate to perceived colour, fluctuation amplitude reflects colour contrast and saturation, and the overlap of black–white background K/S curves serves as a practical proxy for transparency. In colorimetric comparisons, daylight-simulating D-series and U-series illuminants yielded more consistent appearance, whereas incandescent sources (A10, HOR 10 (SPL)) produced larger, more noticeable variations.

REFERENCES

[1]. Ou Yang, C. M. (1999). How to make an appraisal of jadeite. *Australian Gemmologist*, 20(5), 188–192.

[2]. Prewitt, C. T., and Burnham, C. W. (1966). The crystal structure of jadeite, NaAlSi2O6. *American Mineralogist*, 51(7), 956–975.

[3]. Džimbeg-Malčić V, Barbarić-Mikočević Ž & Itrić K. (2011), Kubelka-Munk theory in describing optical properties of paper (I), *Tehnicki Vjesnik*, 19(1), 191-196.

[4]. Nobbs, J.H. (1985), Kubelka-Munk theory and the prediction of reflectance. *Review of Progress in Coloration and Related Topics*, 15 (1), 66-75.

Beyond Averages: Individual Differences in How Wall Colour Influences Affective Responses and Room Impressions

Arsaika Widasati*, Stephen Westland, Caroline Hemingray, Soojin Lee

University of Leeds, Leeds, United Kingdom
**Corresponding author: Arsaika Widasati, sdaw@leeds.ac.uk*

ABSTRACT

Existing research on wall colour effects in interior spaces has predominantly focused on generalised trends. This study investigates individual variability in how each of 12 different room impressions (e.g. pleasantness, complexity) relates to positive (PA) and negative (NA) affect. Five paint colours (blue, green, red, yellow, and grey) were chosen and standardised by adjusting their lightness and chroma to isolate hue as the independent variable. Virtual Reality (VR) was used to create immersive living room environments with systematically varied wall colours. The affective responses of 30 participants were measured using the Positive and Negative Affect Schedule (PANAS), and the room impressions were also rated. An exploratory factor analysis was then conducted to reduce the 12-room impressions into two latent factors: aesthetic and emotional appeal, and the spatial and structural qualities. Subsequently, colour comparisons were analysed in pairs (e.g. blue vs green, red vs grey). For each pairing, participants were grouped based on their ratings of a specific room impression dimension. They were grouped into three categories: those who rated Colour 1 higher than Colour 2 (C1 > C2), those who rated Colour 1 lower than Colour 2 (C1 < C2), and those who rated them equally (C1 = C2). Group differences in affective responses across the two factors were then assessed using percentage differences and effect sizes. Participants who rated a room impression higher in one dimension tended to report higher levels of PA. NA responses showed more variability, such that a higher room impression rating did not necessarily lead to lower NA.

Keywords: individual differences, affective responses, room impressions, colour psychology, PANAS

INTRODUCTION

The experience of interior spaces extends beyond physical boundaries. The built environment shapes not only how a room looks but also how it feels and supports individuals' daily activities. Colour is an important feature of environmental design. It can alter the ambience of a space, influence people's evaluations of it, and influence well-being and performance in subtle yet consequential ways. For this reason, colour has long attracted interest across interior architecture, design and psychology.

A large body of research has documented general links between colour and emotion. As such, blue is often associated with calmness, or red with heightened arousal [1-3]. Another example of these generalisations is that cool colours are linked to low arousal, restful and spacious, while warm colours are linked to high arousal, exciting and stimulating [4]. However, those findings usually reflect averaged responses across participants. While valuable, such an approach obscures that affective reactions to colour vary considerably between individuals, shaped by context, culture or personal experience. A given colour may elicit positive responses in one group but negative responses in another. This perhaps makes it difficult to generalise from "colour X produces emotion Y" to everyday interior settings.

Moreover, studies connecting colour specifically to room impressions remain limited. Much of the literature has examined coloured light or lighting temperature, whereas fewer have focused on wall colour as a spatial variable on its own. Research on wall colour has more often reported general emotional reactions, rather than systematically addressing the structured room impression construct. Within environmental psychology, however, affective states and room impressions are typically regarded as related, yet distinct domains, often captured with different measures (e.g. affect scales versus SMB-based impression items). Although Kuller et. al and Veitch and Newsham dealt with lighting rather than wall colour, their work is cited here to illustrate this conceptual distinction [5,6]. Building on that separation, the present study concentrates on wall colour and asks how variations in affective response correspond with structured room impressions, moving beyond the assumption of uniform colour–emotion effects. By linking affective responses directly to subjective evaluations, the study extends colour–emotion research into interior perception.

METHODOLOGY

Stimuli

This study utilised a virtual living room in five different wall colour conditions: blue, green, red, yellow and grey, as stimuli. The stimuli were presented through a virtual reality (VR) headset (HTC Vive Pro) to ensure participants were immersed in the room and experienced spatial conditions, with scale perception closely resembling real spaces. VR allows control over various environmental variables that might be challenging to achieve in physical settings. Prior studies suggested no significant difference between perceived virtual and the physical environments [7-8]. Additionally, VR creates a comparable impression of a room, including its spaciousness and depth [9].

The living room model was selected due to its simple spatial layout, straightforward furniture and interior elements, and, most importantly, its neutral colour scheme. The model was created using SketchUp and rendered with Enscape to generate a mono 360° panorama. Layout, spatial proportions, and lighting were kept constant across all conditions, so that wall colour was the only manipulated variable.

Previous studies have often used highly vivid primary colours, which may not reflect realistic interior settings [4,11, 12]. However, the present study used colours selected from design websites featuring the most popular living room colours of 2023. The colours were converted from RGB to LCH colour space to find similar lightness and chroma values. Four colours (red, green, blue, and yellow) were chosen and adjusted to have the same level of lightness and chroma to focus on the hue attribute. A neutral colour (grey) with a similar lightness level was added to the stimuli. These colours were applied to the walls of the VR living room. To verify colour fidelity in the VR headset, the applied colours were measured using a Konica Minolta CS-2000 spectroradiometer (Table 1).

Table 1: Colour stimuli measurements from the VR headset

Hue	R	G	B	L*	a*	b*	C*
Blue	143	205	252	89.84	23.13	9.09	24.85
Green	194	204	147	89.94	-9.81	20.02	22.29
Red	254	180	172	88.70	-8.14	-18.78	20.47
Yellow	220	196	143	90.67	1.38	22.97	23.01
Grey	198	199	190	89.99	0.57	-0.21	0.61

Experimental Procedures

Thirty individuals participated in this study. The group had a balanced gender distribution, with participants aged 24 to 34. All individuals had normal colour vision. The experiment received approval from the University of

Leeds Ethics Committee (AHC FREC 1220). Before the study began, all participants provided written informed consent.

Participants visited the laboratory individually for five sessions, each focusing on one of the coloured virtual living rooms per week (Figure 1). Each session lasted 20 to 25 minutes, allowing all participants to experience each of the five virtual living rooms over five weeks. There was a one-week gap between visits to prevent any carry-over effects from previous visits. Each participant experienced the environments in a different random order to eliminate potential order effects. Participants spent around 8 minutes seated in the virtual reality environment, following pre-recorded audio instructions. They then verbally completed two assessments on a 7-point Likert scale:

- Affective responses. Participant reported their positive and negative affect using the Positive and Negative Affect Schedule (PANAS).
- Room impressions questionnaire [12]. Participants rated 12 impression dimensions: pleasantness, complexity, coherence, openness, strength, lavishness, timelessness, specialness, spaciousness, brightness, preference and attractiveness.

Afterwards, they removed the VR headset and took a break before completing a written motion sickness self-assessment.

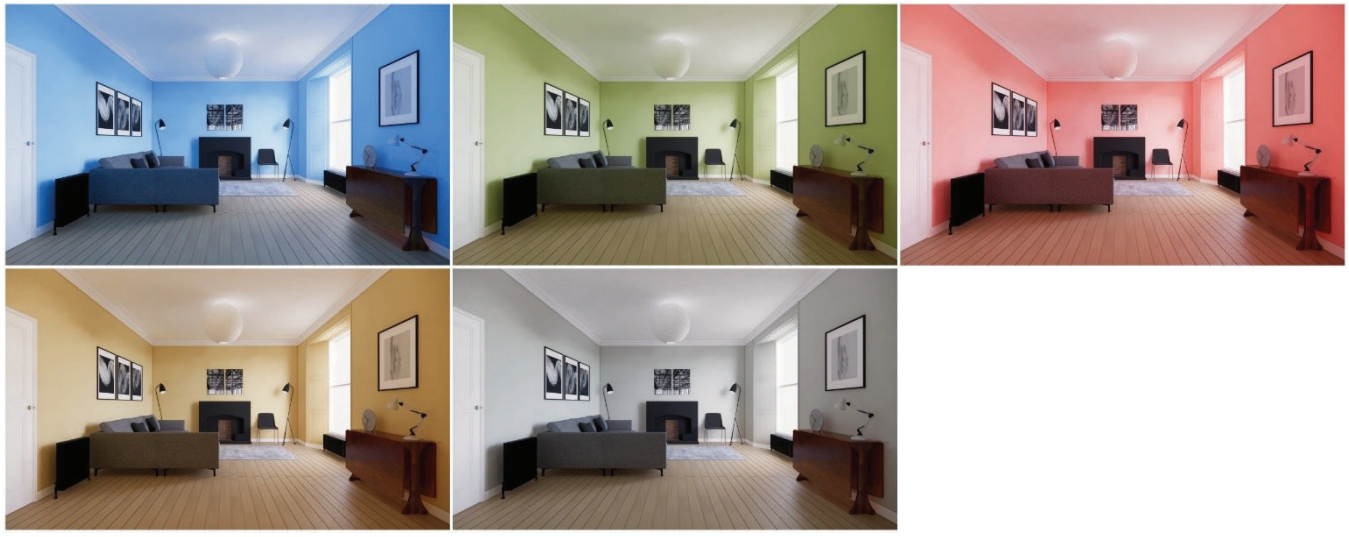

Figure 1: Virtual living room stimuli in the five wall colour conditions.

RESULTS AND DISCUSSION

An exploratory factor analysis (EFA) was conducted on the 12 room impressions to reduce dimensionality. Two latent factors with eigenvalues > 1 emerged, accounting for 70.42% of the total variance. The first factor, Aesthetic and Emotional Appeal, includes pleasantness, complexity, coherence, strength, lavishness, timelessness, specialness, preference and attractiveness. The second factor, the Spatial and Structural Qualities, includes openness, spaciousness and brightness. Colour pairings were then analysed (e.g., blue vs green, red vs grey). For each colour pairing, participants were categorised as either C1 > C2 (those rating Colour 1 higher than Colour 2), C1 < C2 (those rating Colour 1 lower than Colour 2) or C1 = C2 (those rating the colours equally). Note that group 3 (C1 = C2) was excluded from further analysis since it showed no directionality. For each comparison, mean differences in Positive Affect (PA) and Negative Affect (NA) scores from group 1 (C1 > C2) and group 2 (C1 < C2) were examined relative to the two latent factors. Results were expressed as percentage differences (see Figures 2 and 3) and effect sizes (Cohen's d) to capture both magnitude and direction of the effects.

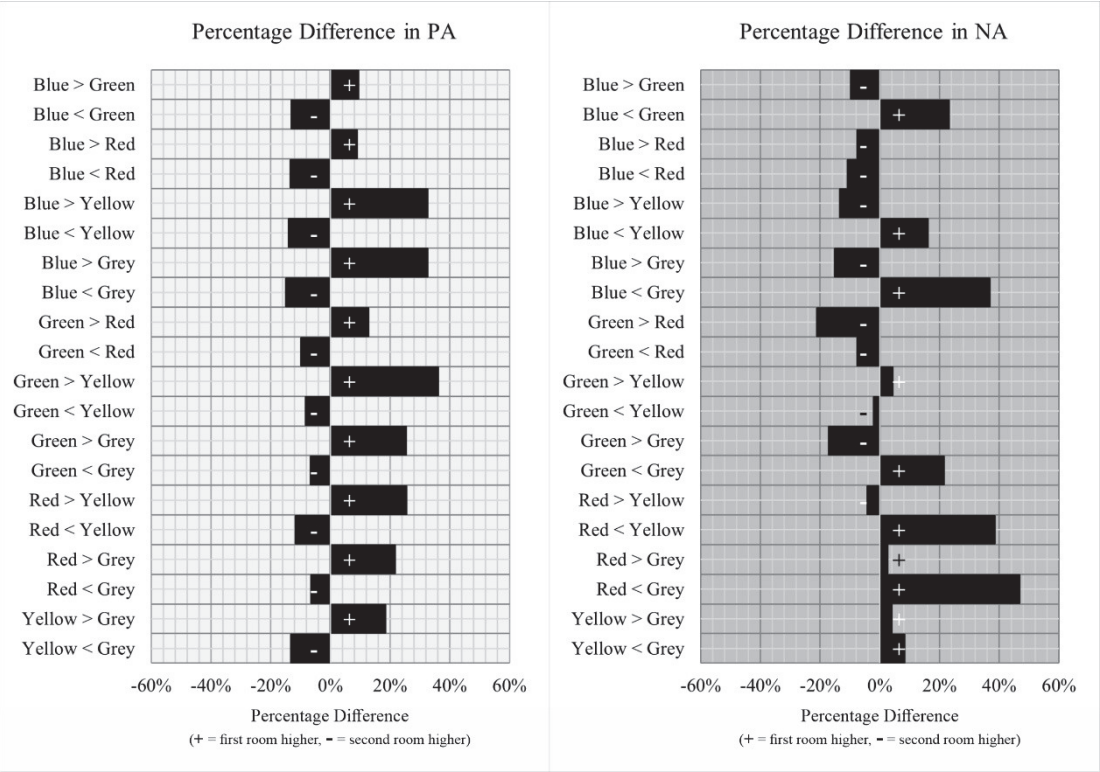

Figure 2: Percentage differences in Positive Affect (PA) and Negative Affect (NA) scores for the Aesthetic and Emotional Appeal factor between room colours. Positive percentages indicate that the first room in a pair was rated higher (for PA: stronger positive affect; for NA: stronger negative affect) than the second, while negative percentages indicate the opposites.

In Figure 2, examples help illustrate how to interpret the percentages. +9.4% PA for blue > green indicates that the blue room was rated 9.4% higher on the Aesthetic and Emotional Appeal factor than the green room. On the other hand, -13.1% PA for blue < green shows that the green room was rated higher on this factor than the blue room. For NA, the same calculation applies but reflects negative affect. For NA, the same calculation applies but reflects negative affect. -9.9% NA for blue > green means the blue room evoked less negative affect on this factor than the green room, while +23.2% NA for blue < green shows that the green room was rated as evoking less negative affect than the blue room.

PA differences consistently showed higher scores for the Aesthetic and Emotional Appeal factor (Figure 2), indicating that participants' higher rated room colours generally elicited higher PA. The largest effect was observed for green > yellow (d = 1.44), and the smallest for red < grey (d = 0.24). This demonstrated that PA reliably reflects the aesthetic and emotional appeal of the room colours. In terms of NA, the results showed a less consistent pattern. Some NA percentage differences appeared large in the graphs (e.g. red < grey and blue < grey), but the effect sizes were relatively small (0.04 – 0.72) compared to PA. Some comparisons even went in the opposite direction (e.g. blue < red, green < red). This indicates that NA responses were inconsistent and less predictive than PA.

For the Spatial and Structural Qualities factor (Figure 3), the interpretation of the percentages is the same as in Figure 2. PA again exhibited consistently higher scores for the higher-rated room, with the most substantial effect in red > yellow (d = 1.11) and the smallest in blue > red (d = 0.12). These findings suggest that PA consistently reflects participants' perceptions of spatial and structural qualities. The NA results showed more varied outcomes, with two pairings (green < red, yellow > grey) going in the opposite direction. Some percentage differences appear large (e.g. red > grey and red < grey), but Cohen's d remained relatively small (0.01 – 0.95), indicating that average

differences appear notable, but individual responses were highly varied. This shows that NA is less stable as a predictor of spatial and structural qualities.

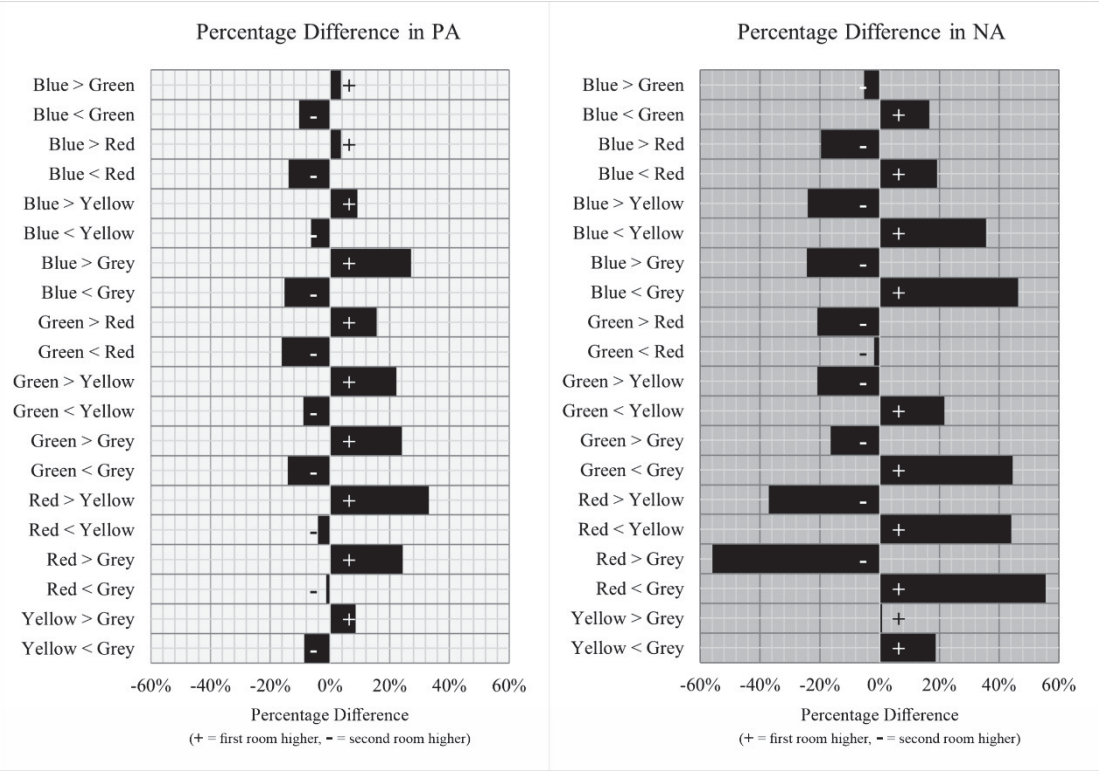

Figure 3: Percentage differences in Positive Affect (PA) and Negative Affect (NA) scores for the Spatial and Structural Qualities factor between room colours. Positive percentages indicate that the first room in a pair was rated higher (for PA: stronger positive affect; for NA: stronger negative affect) than the second, while negative percentages indicate the opposites.

The comparison between PA and NA in both latent factors indicates that PA is a more reliable predictor of subjective room impression than NA. In cases where PA had greater effect sizes, participants indicated a more positive rate of room impression, as opposed to NA having inconsistent and weaker effect sizes. These results extend prior colour-emotion studies on wall colour [3,4,11], focusing mainly on average level effects. An analysis of the pairwise grouping (C1 > C2 vs C1 < C2) approach shows a clear connection between affective responses and subjective room impression. The results also relate to broader models of affective influence in the built environment [2], reiterating that environmental cues (such as colour) can shape emotional experience in interior space.

CONCLUSION

This study shows that Positive Affect (PA) has a stronger and more consistent correlation to subjective room impressions than the Negative Affect (NA) responses. PA response patterns generally matched participants' favourable room impressions rating, with most reporting high in PA and low in NA. NA response patterns were generally far more variable, and therefore less predictive of subjective room impressions.

The current study has a limitation: while the percentage differences observed in the visualisations may appear large, most effect sizes (Cohen's d) were in the very small to medium range, with some being large effects. This

would suggest that the associations we observed, while present, are rather subtle and perhaps need more robust samples to observe consistent differences. Despite its limitations, this study highlights that designing with colour enhances positive affect and can meaningfully shape the overall subjective impressions of interior spaces. While NA may provide additional context, PA offers the most reliable guidance for design decisions to promote favourable user experiences.

REFERENCES

[1]. Valdez, P., & Mehrabian, A. (1994). Effects of color on emotions. *Journal of Experimental Psychology: General*, 123(4), 394–409. https://doi.org/10.1037/0096-3445.123.4.394Elliot & Maier (2014)

[2]. Elliot, A. J., & Maier, M. A. (2014). Color psychology: Effects of perceiving color on psychological functioning in humans. *Annual Review of Psychology*, 65, 95–120. https://doi.org/10.1146/annurev-psych-010213-115035

[3]. AL-Ayash, A., Kane, R.T., Smith, D. and Green-Armytage, P. (2016), The influence of color on student emotion, heart rate, and performance in learning environments. *Color Research and Application*, 41: 196-205. https://doi.org/10.1002/col.21949

[4]. Yildirim, K., Hidayetoglu, M. L., & Capanoglu, A. (2011). Effects of Interior Colors on Mood and Preference: Comparisons of Two Living Rooms. *Perceptual and Motor Skills*, 112(2), 509-524. https://doi.org/10.2466/24.27.PMS.112.2.509-524

[5]. Küller, R., Ballal, S., Laike, T., Mikellides, B., & Tonello, G. (2006). The impact of light and colour on psychological mood: a cross-cultural study of indoor work environments. *Ergonomics*, 49(14), 1496–1507. https://doi.org/10.1080/00140130600858142

[6]. Veitch, J.A. & Newsham, G.R. (1998) Determinants of Lighting Quality I: State of the Science, *Journal of the Illuminating Engineering Society*, 27:1, 92-106. https://doi.org/10.1080/00994480.1998.10748215

[7]. Heydarian, A., Carneiro, J. P., Gerber, D., Becerik-Gerber, B., Hayes, T., & Wood, W. (2015). Immersive virtual environments versus physical built environments: A benchmarking study for building design and user-built environment explorations. *Automation in Construction*, 54, 116–126. https://doi.org/10.1016/j.autcon.2015.03.020

[8]. Latini, A., Di Giuseppe, E., D'Orazio, M., & Di Perna, C. (2021). Exploring the use of immersive virtual reality to assess occupants' productivity and comfort in workplaces: An experimental study on the role of walls colour. *Energy and Buildings*, 253, 111508. https://doi.org/10.1016/j.enbuild.2021.111508

[9]. Jin, X., Meneely, J., & Park, N. (2022). *Virtual reality versus real–world space: Comparing perceptions of brightness, glare, spaciousness, and visual acuity.* Journal of Interior Design, 47(2), 31–50. https://doi.org/10.1111/joid.12209

[10]. Kwallek, N., Woodson, H., Lewis, C.M. and Sales, C. (1997), Impact of three interior color schemes on worker mood and performance relative to individual environmental sensitivity. *Color Research and Application*, 22: 121-132. https://doi.org/10.1002/(SICI)1520-6378(199704)22:2<121::AID-COL7>3.0.CO;2-V

[11]. Cha, S. H., Zhang, S., & Kim, T. W. (2020). Effects of Interior Color Schemes on Emotion, Task Performance, and Heart Rate in Immersive Virtual Environments. *Journal of Interior Design*, 45(4), 51-65. https://doi.org/10.1111/joid.12179

[12]. Küller, R. (1972). A Semantic Model for Describing Perceived Environment (Document D12). National Swedish Institute for Building Research. https://lup.lub.lu.se/record/4359745

Linked Hybrid: Color, Light and Perception in The Architecture of Steven Holl

Camila Pinheiro Consani [a*], and João Carlos de Oliveira Cesar [b]

[a, b] *Faculty of Architecture, Urbanism and Design, University of São Paulo (FAU USP), São Paulo, Brazil*

[*] *camila.consani@usp.br*

ABSTRACT

This article develops a study of the Linked Hybrid, a project conceived by Steven Holl in Beijing, from the perspective of architectural atmosphere, with an emphasis on the role of color in the configuration of multisensory experiences. Positioned between the scales of the building and the city, the complex is composed of towers interconnected by elevated walkways and organized around a public ground floor with a reflecting pool. By creating fluid connections between interior and exterior, public and private spheres, the project stands out not only for its innovative urban solution but also for its immersive and phenomenological character. The methodological approach is based on a theoretical framework anchored in the phenomenology of architecture, highlighting the works of Peter Zumthor, Gernot Böhme, and Juhani Pallasmaa. Architectural atmosphere is understood as an immediate and affective mode of perception - an enveloping spatial quality that resonates with the body, the senses, and the emotional state of the user. In this context, the study introduces the concept of architectural atmosphere as a perceptual condition mediated by color in interaction with light, materiality, texture, and movement. In the Linked Hybrid, the use of translucent glass and the chromatic palette applied to the façades stand out, producing mutable visual effects according to the incidence of light and the point of view. Color is not limited to a decorative function but acts as an active agent in the creation of atmospheres, articulating sensory and symbolic dimensions. The study argues that color, light, and materiality play an essential agency in mediating between body and space, expanding the understanding of color in architecture as a structuring element of experience.

Keywords: architectural atmosphere, color in architecture, phenomenology, spatial perception, Steven Holl

1. INTRODUCTION

This article presents a study of the Linked Hybrid, a project by Steven Holl completed in 2009 in Beijing, from the perspective of architectural atmosphere. It is based on the understanding that contemporary architecture has sought to intensify the sensory dimensions of space, integrating body, perception, and environment. From this perspective, color and light cease to be mere visual complements and instead assume the function of active agents in the constitution of atmospheres, influencing the user's experience and reinforcing the identity of places.

The office Steven Holl Architects, founded in 1977 and headquartered in New York, Hudson Valley, and Beijing, stands out for its sensitivity to context, mastery of light and space, and the creation of projects of various scales that integrate sustainable technology and innovative vision [1]. With a sustainable focus and phenomenological foundation, the office demonstrates a commitment to the future of the built environment, and Holl is internationally recognized as one of the leading architects, with award-winning works in several countries.

Contemporary projects tend to work with high densities, organized into multifunctional complexes that bring together housing, work, and leisure in the same space, the so-called “hybrid spaces”, aiming at energy optimization, green and permeable areas, accessibility, and sustainable technologies [2]. The Linked Hybrid is an example of this concept: an integrated complex with a density of over 1.000 inhabitants per hectare and around 2.500 residents, representing contemporary architecture and the complexity of today’s megacities.

By articulating urban and architectural scales, the Linked Hybrid proposes a spatial solution that emphasizes the integration between building and city, public and private space, interior and exterior. The choice of this project as the object of study is justified by the fact that color, in association with light and materiality, constitutes an essential dimension of architectural experience. Unlike other works by Holl, in the Linked Hybrid color is not confined to a symbolic language but asserts itself as a perceptual, urban, and phenomenological resource on a large scale. Therefore, the aim of this study is to understand how color, in dialogue with light and materiality, contributes to the configuration of multisensory experiences, situating itself within the contemporary debate on color and atmosphere through an established theoretical framework.

Figures 1 and 2: Linked Hybrid during the day. Source: (1) https://iwan.com/ and (2) https://www.stevenholl.com/

2. METHODOLOGY

2.1 Approach

The research adopts a qualitative, exploratory, and interpretative approach, structured around a single case study. The Linked Hybrid was selected as it is an emblematic project that integrates color, light, and materiality as central elements of the architectural experience.

2.2 Procedures

The investigation was conducted in four main stages. Initially, a documentary survey was carried out, including plans, sections, photographs, videos, and critical texts. Next, a detailed description and analysis of the object were undertaken, systematizing aspects such as site plan, volumetry, spatial organization, materials, and chromatic solutions. The third stage consisted of analyzing the project from four perspectives: architectural atmosphere as a sensory experience; color as a spatial language in dialogue with light and materiality; the formal and chromatic solutions applied to façades and walkways; and the way in which the moving body apprehends and constructs the perception of space.

Finally, a phenomenological interpretation was developed, relating the data obtained to the theoretical framework, with special attention to the external and semi-public spaces, where color, light, and materiality are manifested most clearly. It should be noted that no technical or chromatic measurements were carried out, since the study maintained an interpretative and qualitative character, treating color as an agent of atmosphere rather than merely a visual attribute.

2.3 Architectural Atmosphere: Theoretical Perspectives

The reflections of Peter Zumthor, Gernot Böhme, and Juhani Pallasmaa offer important paths for understanding architectural atmosphere, each author contributing in a unique way to the comprehension of the sensitive experience of space. Inserted within a phenomenological perspective, this analysis considers space as a multisensory experience. In this approach, Zumthor [3] understands atmosphere as a sensitive quality, Böhme [4] discusses the aesthetics of presence, and Pallasmaa [5] emphasizes corporeality and the senses in architecture. These references make it possible to interpret the architectural work beyond its formal aspects, highlighting its perceptive, affective, and symbolic dimensions.

For Zumthor [3], architectural atmosphere is a sensitive quality perceived immediately by our emotional sensibility. It is a rapid, intuitive perception that precedes conscious reflection and provokes instant affective responses of acceptance or rejection, differing from linear and rational thought by directly mobilizing body and emotions. Complementarily, the author [3] notes that what moves him in a space is not a single isolated element, but the joint presence of people, sounds, noises, colors, materials, textures, and forms. These aspects, experienced in an integrated manner, awaken emotions and expectations, revealing that the architectural experience is constituted in the sensitive interaction between body, environment, and perceptive qualities.

The philosopher Böhme [4], broadens this perspective by stating that atmosphere is the true object of architecture, as it goes beyond form and function to focus on how spaces are perceived and felt. Architecture, more than the construction of buildings, creates spatial situations that guide the body, establish directions and perspectives, and, by radiating qualities, directly affect emotions and states of mind. In this context, the author [4] emphasizes that qualities such as color should not be understood as fixed properties restricted to objects, but as something that expands and radiates presence in space. Color, for example, is not confined merely to the material surface, it projects into the surroundings, diffusing through them and transforming environmental perception, acting as a phenomenological quality that affects the body and the senses.

For Pallasmaa [5], the authenticity of the architectural experience is grounded in corporeality. Space is not reduced to visual contemplation but involves the whole body in its tactile, kinesthetic, and perceptive dimension. Architecture acquires meaning when it guides gestures, movements, and postures, establishing a direct dialogue between body and environment. Furthermore, the author [5] reinforces that the architectural experience is multisensory, lived by the body in its entirety. Space is not only seen but also felt through touch, hearing, memory, and emotion. In this lived experience, light, shadow, color, texture, and sound are not reduced to visual or formal aspects but are configured as qualities that directly affect the senses and intensify the subject’s presence in space.

Thus, it can be affirmed that every architectural space generates a perceptive quality that goes beyond the physical: atmosphere. For Zumthor [3], it is an immediate impression that moves us before reflection; for Böhme [4], it is something that radiates from things, like color, and affects the environment; and for Pallasmaa [5], it is fully realized only when lived by the body in its entirety, involving all the senses and not only vision. Taken together, these perspectives reveal that architectural atmosphere is not an isolated attribute, but an existential condition, constructed in the relationship between space, body, and sensibility.

3. RESULTS AND DISCUSSION

3.1 Characterization of the Linked Hybrid

Conceived as an urban microcosm in the center of Beijing, the Linked Hybrid integrates housing, leisure, commerce, and services. The complex is composed of nine towers interconnected by elevated walkways, which promote circulation on multiple levels and connect different functions. At ground level, a large public space, marked by a central reflecting pool, reinforces integration with the city and creates an inviting and permeable environment.

Built between 2003 and 2009, with a total area of 221.563 m², the project proposes a porous, open, and welcoming urban space, configuring an “open city within the city” [6]. From the earliest conception sketches, four main circulation routes stand out, reinforcing this urban porosity, as well as the intentional use of color as an atmospheric resource, particularly striking at night.

In the Linked Hybrid, the ground floor accommodates open passages for residents and visitors, articulated by shops, a large reflecting pool, and public functions such as a restaurant, hotel, Montessori school, kindergarten, and cinematheque, all connected to green spaces. Public gardens occupy the roofs of the lower buildings, while private gardens are located at the top of the residential towers. Between the 12th and 18th floors, elevated walkways containing a swimming pool, gym, cafés, gallery, auditorium, and lounge connect the towers and offer views of the city [6].

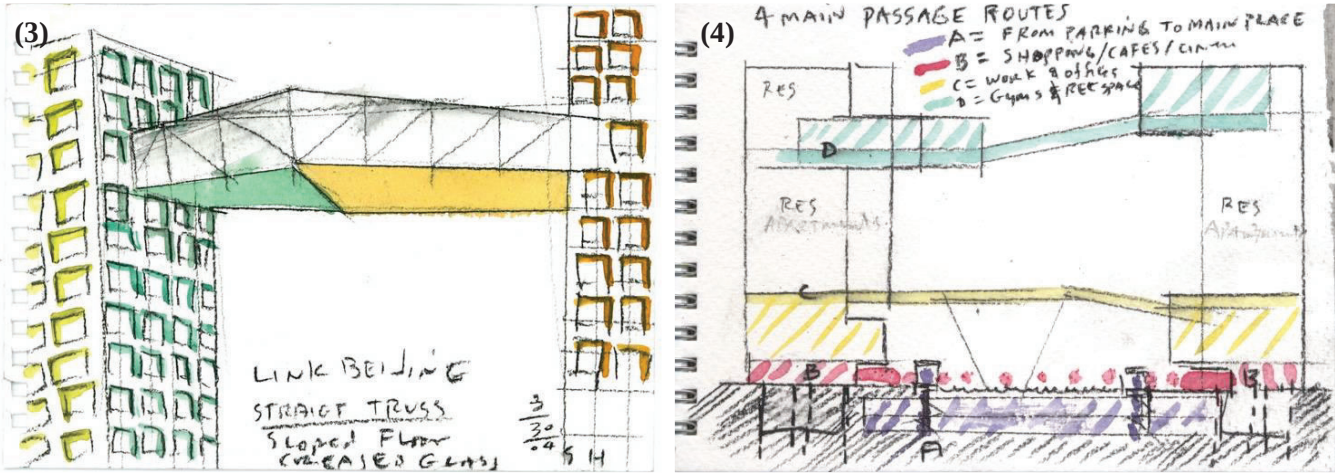

Figures 3 and 4: Conceptual sketches of the Linked Hybrid. Source: https://archello.com/

3.2 Chromatic and Material Solutions

The materiality of the complex is characterized by the use of translucent glass, which allows for different degrees of transparency, and metallic panels, capable of reflecting light and varying in tone according to environmental conditions. The most striking element, however, is the presence of multicolored window frames, arranged in a mosaic across the façades, providing visual identity, dynamism, and chromatic effects in constant transformation throughout the day.

The polychromatic architecture of ancient China inspires the Linked Hybrid in the creation of a new spatial dimension, referred to as “nocturnal spatiality”. Beneath the cantilevers, colored membranes glow at night like illuminated clouds, intensifying the atmospheric experience of the complex [7]. The window frames, in turn, were colored based on chinese tradition, defined randomly according to the principles of the *I Ching* [8]. The chromatic

palette combines shades of red, orange, yellow, blue, violet, and green and, through its diversity, reinforces the expressive character of the complex.

In the same way that the areas under the cantilevers glow at night, water fountains fed by the reservoir activate nighttime illumination, creating colorful clouds. Furthermore, on the base of the floating structure that houses the cinematheque, images of the films being shown are projected, reflected in the central reflecting pool, and creating a unique visual experience [7].

Figures 5 and 6: Linked Hybrid at night. Source: https://iwan.com/

3.3 Color as an Active Agent of Experience

In the Linked Hybrid, color is not limited to a decorative function: it operates as an essential design component. In dialogue with daylighting and the translucency of materials, the hues configure mutable compositions that respond to environmental variations and the movement of the user. In this way, color acquires a perceptive and symbolic dimension, enriching the sensory experience and qualifying spatiality.

In the book *Questions of Perception: Phenomenology of Architecture*, Steven Holl [9] describes that architecture, by integrating different planes and perspectives, harmonizes materiality, space, and details, providing a complex sensory experience that involves touch, light, aromas, sounds, and proportions. For the author [9], this perceptual experience is inextricably linked to architectural intention, since only when intention is clear does the work transcend mere scientific phenomenology, articulating itself in the tension between preexisting concepts and the uniqueness of experience.

A relevant aspect is that color in the Linked Hybrid transforms over time: during the day, the multicolored window frames appear more discreet in contrast with the sheen of metal and glass; at night, however, they become protagonists, radiating colored lights that expand the perception of space and activate its expressive dimension.

3.4 Body, Space, and Perception

The spatial organization encourages exploration and discovery. The elevated walkways allow for multiple perspectives, while the open ground level fosters interaction and circulation. In this context, color intensifies the perception of planes, volumes, and depth, generating emotional responses and reinforcing the active presence of the body in space.

This experience confirms Pallasmaa's [5] view that space only acquires meaning when lived by the body in its entirety. Through movement, touch, and memory, the subject actively participates in the construction of spatial

perception. In this sense, the Linked Hybrid demonstrates how color, light, materiality, and spatial organization are articulated in the constitution of sensitive and meaningful experiences.

4. CONCLUSION

The study of the Linked Hybrid shows that color assumes a central function in mediating between body and space, acting in dialogue with light and materiality to create immersive and meaningful atmospheres. More than a visual attribute, color is presented as a structuring element of experience, capable of reinforcing identities, qualifying spaces, and enriching the perception of the environment.

The analysis contributes to broadening the understanding of color as a phenomenological and symbolic agent, while also providing support for design practices that seek to integrate color and atmosphere in a conscious and creative manner. In this sense, it reinforces the relevance of methodological approaches that combine theory and case study to investigate the sensory and perceptual dimensions of contemporary architecture.

Finally, by revealing the potential of color in the Linked Hybrid, this work highlights the importance of considering the multisensory dimension in design processes, pointing to pathways for an architecture that articulates perception, identity, and aesthetic experience as essential foundations of lived space.

ACKNOWLEDGMENTS

This work was carried out with the support of the Coordenação de Aperfeiçoamento de Pessoal de Nível Superior - Brazil (CAPES) - Financing Code 001.

REFERENCES

[1]. Steven Holl Architects. (2023). *About*. https://www.stevenholl.com/about/

[2]. Silva, G. J. A. da, Silva, S. E., & Nome, C. A. (2016, February). Densidade, dispersão e forma urbana: Dimensões e limites da sustentabilidade habitacional. *Arquitextos, 16*(189.07). Vitruvius. https://vitruvius.com.br/revistas/read/arquitextos/16.189/5957

[3]. Zumthor, P. (2006). *Atmospheres: Architectural environments, surrounding objects*. Birkhäuser.

[4]. Böhme, G. (2017). *The aesthetics of atmospheres*. Routledge, Taylor & Francis Group.

[5]. Pallasmaa, J. (2024). *The eyes of the skin: Architecture and the senses*. John Wiley & Sons Ltd.

[6]. Steven Holl Architects. (2009). *Linked Hybrid*. https://www.stevenholl.com/project/beijing-linked-hybrid/

[7]. *El Croquis*. (2008). *Steven Holl 2004-2008* (141).

[8]. Holl, S. (2009). *Urbanisms: Working with doubt*. Princeton Architectural Press.

[9]. Holl, S., Pallasmaa, J., & Pérez-Gómez, A. (2006). *Questions of perception: Phenomenology of architecture*. William Stout Publishers.

Color Yoga: A Semiotic and Subjective Perspective on Wellbeing for The Future

Milton David Henao Jiménez[a*] and Hernán Felipe Monsalve Ospina[b]

[a]*Casa Arcoíris Foundation, NGO, Rionegro, Colombia*
[b]*University of Brasilia, Brasilia, Brazil*
[*] *Miton Henao, miltonhenaojimenez@gmail.com*

ABSTRACT

This study explores the subjective meanings and contributions of the integrative practice known as the Color Yoga from a semiotic perspective that combines yoga and chromotherapy as a well-being proposal for future. The research is grounded in the conceptual references of Charles Sanders Peirce's semiotic theory and the contributions of Fernando González Rey's theory of subjectivity, aiming to deeply understand this practice in which multiple signs converge from the symbolic, emotional, historical, and cultural dimensions of human life. This proposal presents the methodology of the Color Yoga developed and implemented by the researchers in Colombia and Brazil, consisting of a series of practical exercises called color kriyas, which are made up of seven routines associated with the chromatic scale, starting with red and ending with violet. In the first phase of the research, a documentary analysis was conducted to establish the theoretical and conceptual foundation. In the second phase, a descriptive-interpretative approach will be used, based on qualitative epistemology, as it allows for the construction of subjective indicators and the integration of both researchers and participants. The research is still ongoing; however, preliminary results have led to the conclusion that, from a semiotic and subjective perspective, Color Yoga impacts various dimensions—physical, mental, emotional, spiritual, and social—generating effects on well-being and human development. Furthermore, it expands the use of color in the health field and enables new reconfigurations in the subjective life of those who experience the combination of these integrative practices.

Keywords: color yoga, integrative practices, semiotics, subjectivity, well-being

INTRODUCTION

The Color Yoga proposal is based on the combination of yoga and chromotherapy, understood as integrative and complementary health practices. This proposal originates from the experience of these practices in two South American countries. In Brazil, the practices are part of the public health system, and in Colombia, they are offered as a wellness service by Casa Arcoíris Foundation NGO, which promotes integrative practices, primarily chromotherapy. The CY (Color Yoga[1]) emphasizes its importance mainly in two aspects: first, the use of color for therapeutic purposes, expanding its applications beyond its common associations with paint production, makeup, toys, graphic design, architecture, among others; and second, as an innovative proposal for the future in the health field through various chromotherapy technologies, which offer countless contributions to well-being experiences. In this regard, we will begin by addressing the general concepts of health and well-being, and then present the theoretical contributions of Peirce's semiotics and González Rey's theory of subjectivity.

[1] From this point forward, the acronym CY will be used to refer to Color Yoga.

The World Health Organization (WHO) is a global reference and clarifies that the concept of health not only refers to the absence of disease, but also encompasses a complete state of well-being in the individual. This involves a holistic view of the human being, in which its constitutive systems and dimensions operate in an interconnected manner, referring to the physical, mental (understood as the psychic and all its mental processes), emotional, and social dimensions, as well as the relationship with the environment. Moreover, the notions of health and illness are strongly influenced by the worldview and cultural framework in which the individual is immersed [1], enabling a study approach from alternative perspectives that address, for example, the interaction between individual and culture—a central aspect of subjectivity—as well as the signs associated with health and well-being described through semiotic analysis. In this same vein, the theory of subjectivity and qualitative epistemology allow for an understanding of the mind as inseparable from history, culture, and current contexts of human social life, as well as the spectrum of emotional and symbolic dimensions. This is because it conceives the subjective dimension as emerging "when emotion becomes sensitive to symbolic registers, allowing humans to produce the world in which they live, rather than simply adapt to it" [2].

In relation to the notions of yoga and chromotherapy, and with the aim of achieving greater conceptual precision, we will refer to the definitions provided by Brazil's public health policies [3]:

> ***Yoga****: an Eastern body–mind practice used as a technique to control both, combined with meditation. It includes specific techniques such as Hatha Yoga, Mantra Yoga, and Laya Yoga, which refer to specialized traditions. It works on the physical, mental, emotional, energetic, and spiritual aspects of the practitioner, aiming for the unification of the human being.*
>
> ***Chromotherapy****: Therapeutic practice that uses the colors of the solar spectrum—red, orange, yellow, green, blue, indigo, and violet—to restore the body's physical and energetic balance.*

Another reference that broadens the meaning of chromotherapy states that this practice "is the interaction of the human species with the energy and the implicit and explicit properties of light and the different shades of color; it is a form of knowledge that allows for the harmonization, healing, and enhancement of inner energy, intellectual capacities, and the various gifts and talents a person possesses" [4]. In this sense, the previous definitions show that both yoga and chromotherapy act upon the sensory systems and the dimensions through which the human being expresses itself, namely: the physical body, emotions, mind, and spirit or transpersonal dimension, as proposed by Roberto Assagioli in Psychosynthesis [5].

The complexity and subjective richness of this type of study requires a multidisciplinary and interdisciplinary approach, allowing the descriptions and interpretations emerging from the research to not only explore new forms and tools for human well-being, but also to integrate different sciences, bodies of knowledge, and integrative practices. It also contributes to the expansion and enrichment of various qualitative and quantitative research projects related to health, well-being, and human development. Therefore, establishing connections with different areas of knowledge could generate new research methods and techniques of great scientific, academic, and social value. For this reason, we consider that the constructive-interpretative methodology of the theory of subjectivity is a scientific approach that enables an understanding of the subject from a new ontological conception—beyond the psyche and traditional views of psychology—in order to grasp the complexity of the universe of human signs and the conception of the mind "as inseparable from history, culture, and the contexts of human social life." (*González, R., 1995-2019*).

This particular study requires a scientific research perspective that evaluates the phenomenon as a whole and enables an integrative study of colors and the practice of yoga within the framework of well-being and human development, in order to address the research questions derived from the objectives we have set out to explore: 1. How can color be applied in the field of well-being and health? 2. Which theoretical paradigms allow for the study of CY and its contribution to well-being? 3. What is the subjective production derived from color?

METHODOLOGY

To carry out this work, a qualitative research approach was used, consistent with the literature review and theoretical frameworks related to the study. A descriptive-interpretative approach was chosen, as this type of study is highly effective for describing a reality in all its main components [6]. The approach is based on qualitative epistemology, as it allows for the construction of subjective indicators and the integration of both researchers and participants. A qualitative research method was selected because it "understands the context and people from a holistic perspective, in which individuals, contexts, or groups are not reduced to variables, but are considered as a whole".

The research will be carried out in two phases: the first, of a theoretical-methodological nature, based on the review of selected literature relevant to this article. This phase presents a general theoretical framework that supports the use of color as a therapeutic tool within what is proposed as CY. The second phase, currently in progress, involves a case study with a group of 12 individuals (children and adults) from Colombia and Brazil, in collaboration with the Institute of Clinical Psychology and Culture at the University of Brasília and the Colombian NGO Casa Arcoíris. The criterion for selecting the sample is that these individuals have had integrative experiences combining yoga and chromotherapy. For this purpose, different yoga and color classes are proposed, called Color Kriyas, which consist of the use of various color elements combined with yoga postures and breathing exercises, grouped into seven segments associated with the chromatic scale and the different organs and energy centers of the human body.

RESULTS AND DISCUSSION

Conceptual References for the Analysis of Color Kriyas

From Peirce's semiotics, we will analyze how CY (Color Yoga) can become a sign of well-being, and we will base our analysis on his three metaphysical categories of reality to understand the phenomenon. According to this theory, reality can be understood through signs of Firstness, Secondness, and Thirdness [8]. Firstness represents pure possibility—the quality itself. Secondness is defined by the act, the interaction between action and reaction, and refers to concrete existence. Thirdness represents generality—the rule or principle that connects Firstness and Secondness and also refers to concrete existence [9]. In our own words, and with a heuristic approach, we propose that under the triadic scheme of semiotics, CY is configured as a sign, representing our object of study—well-being and health—and completing the tripartite scheme with the interpretant, which arises from the individual's lived experience. Furthermore, the three essential categories can be described as follows: Firstness as the potential of color as pure quality (regardless of its field of applicability); Secondness as the reaction on the individual's dimensions in the context of CY application; and Thirdness as the logical effect produced by the sign—in our case, CY—which enables the representation and interpretation of the practice.

From González Rey's theory of subjectivity (1995–2019), the emotional component of human life becomes perceptible and understandable within the subject's symbolic universe, valuing their history and culture, as well as their capacity to generate new subjective meanings and reconfigurations. This theory understands that it "allows for the integration of cognitive and affective aspects as a functional unit" [10]. Within this framework, one concept of great value for the development of this study is the notion of units of subjective meaning, understood as instantaneous emotional-symbolic units that characterize the flow of human experience as life is subjectively lived. The subjective meanings of a given experience are not limited to that experience alone; rather, they merge with the subjective meanings of other experiences, acquiring new subjective contours throughout the course of the current experience. This is because they "represent new productions in relation to lived experiences that are inseparable from the subjective organization of individuals and the multiple contexts in which their social life unfolds" [11]. In this sense, meanings and subjective senses highlight the uniqueness and complexity of an experience that, theoretically, breaks with the standardization and universalization of the dominant understanding of psychological

phenomena [12]. It is also important to note that subjective meanings cannot be known a priori, nor defined by a positivist logic; that is, they are generated within the pragmatic dimension of experience and go beyond Cartesian or purely rational explanations, as they unfold in subtle and intangible dimensions beyond the physical body, where subjectivity operates.

Another important reference within Qualitative Epistemology relates to the indicators associated with subjective meanings, which serve as a central input in the process of constructing and analyzing information. Unlike traditional "data", indicators are not simply objective or explicit information; rather, they acquire meaning through the researcher's interpretation [13]. Indicators have the following characteristics: 1) They are interpretative and constructive, meaning they are not objective entities, but interpretations developed by the researcher based on the information obtained. 2) They are defined by the relationship between the information, the subject's context, and the researcher's construction-interpretation. 3) They are dynamic, evolving and integrating into a continuous process of theoretical construction, feeding new hypotheses and meanings. 4) They represent connections between different pieces of information, allowing the researcher to uncover hidden or indirect meanings in the empirical material [13], that is, the essential information produced from subjective meanings. The constructive-interpretative methodology used refers to a conversational system, as both the researcher and the participant engage through their reflections [14]. This methodology links the production of indicators, which are grounded in subjective meanings.

Color Kriyas

The concept kriya[2] will be understood as the practical space and structural elements of yoga practice, characterized by having a defined sequence and purpose. This structure has effects on the different dimensions of the human being: physical, emotional, mental, and transpersonal, through the application of yoga's practical resources: physical postures (*asanas*), breathing techniques (*pranayama*), recitation of syllables and words (*mantras*), meditations, and relaxation techniques. Color Kriya refers to the proposal of incorporating chromotherapy and the color spectrum into the practice, giving rise to the applied methodology of CY (Color Yoga).

The following table summarizes the seven Color Kriyas that combine chromotherapy and yoga, which have been practiced at Casa Arcoíris Foundation since 2017. These experiences, along with the invaluable subjective richness shared by the participants, have motivated us to seek scientific research methods that allow us to understand the scope of CY (Color Yoga) in generating subjective reconfigurations in health and well-being. For this reason, we previously presented the conceptual framework through which we have been analyzing the experiences with Color Kriyas from both semiotic and subjective perspectives.

Table 1: Color Kriyas

Kriya and color	Dimensions and approach	Series and resources
RED	Structure, Roots, and Self-sufficiency – Root Chakra (*Muladhara*)	Physical Space (PS): Lights, objects, and garments in red tones. *Asanas* (ASN): butterfly pose (*Baddha Konasana*), Standing postures (windmill-archer-lateral bends-leg lifts), Sun Salutation (*Surya Namaskara*). Relaxation (RLX): Mental bath with red color or with red rose petals. Meditations (MDT): Focused on grounding, stability, and connection to the earth. *Mantra* (MNT): *EK*. Lock (BH): *mulbandh*.

[2] *Kriya* is a Sanskrit word meaning action, deed, or complete effort. The root "*kri*" means to do or to create. In the context of Kundalini Yoga, kriya refers to a specific set of yogic exercises—either individual or structured sequences—designed to produce a predictable effect on consciousness [15].

Kriya and color	Dimensions and approach	Series and resources
ORANGE	Dynamism, Creativity, and Self-Recognition – Sacral Chakra (*Svadhisthana*)	PS: Lights, objects, and garments in orange tones. ASN: Sufi circles, Spinal twists and bends, Dynamic forward bend (*Paschimottanasana*), Equestrian pose (*Ashwa Sanchalanasana)*, Cobra pose (*Bhujangasana*), *Sat kriya*. RLX: Mental bath with bright orange light. MDT: Visualization of the orange hues of sunrise or sunset. MNT: *ONG* en *Buddhi mudra*.
YELLOW	Confidence and Self-Acceptance – Solar Plexus Chakra (*Manipura*)	PS: Lights, objects, and garments in yellow tones. ASN: Alternating leg lifts, Dynamic bridge pose (*Setu Bandhasana*), Cat-Cow flow, Bicycle movement, Camel pose (*ustrasana*), Breath of Fire (*agni pran*). RLX: Mental bath with bright yellow flower petals. MDT: Visualization of bright sunflowers or sun rays. MNT: *KAR* o *JAR* Performed with navel pumping in *Surya Mudra*. BH: *uddiyana bandh*.
GREEN	Expansion, Balance, and Self-Esteem – Heart Chakra (*Anahata*)	PS: Lights, objects, and garments in green tones. ASN: Easy pose (*sukhasana*), Arms extended at 60 degrees, Heart center stretch, Arm rotations. RLX: Mental bath with radiant green leaves. MDT: In *prana mudra* Visualization of deep green light, Focus on love, compassion. MNT: *SAT* in *Shuni mudra.*
BLUE	Communication, Affiliation, and Self-Expression – Throat Chakra (*Vishuddha*)	PS: Lights, objects, and garments in blue tones ASN: Neck rotations, Chair pose variation (*Utkatasana*), Bridge pose with head tilt (*Setu Bandhasana*), Fish pose (*Matsyasana*). RLX: Mental bath within the ocean. MDT: *cithali pranaya* en *gyan mudra.* MNT: NAM en *gyan mudra.* BH: *jalandhar bandh*.
INDIGO	Introspection, Projection, and Self-Communication – Third Eye Chakra (*Ajna*)	PS: Lights, objects, and garments in indigo tones. ASN: Standing forward bends, Standing ego eradicator, Downward-facing dog (*Adho Mukha Svanasana*), *uttanasana*, Head rotations, Shoulder stand (*sarvangasana*), Plow pose (*jalasana*), Child's pose (*balasana*). RLX: Mental bath with bright indigo light. MDT: *nadi shodhana pranayama* in *gyan mudra*. MNT: *SIRI* in *gyan mudra.*
VIOLET	Expansion, Transcendence, and Self-Connection – Crown Chakra (*Sahasrara*)	PS: Lights, objects, and garments in violet tones. ASN: Head rotations, *uttanasana*, Shoulder stand (*sarvangasana*), Headstand (*sirsasana*). RLX: Mental immersion in lavender fields MDT: Visualization in an amethyst cave, Breath retentions (after inhale and exhale), Application of bandhas, Silent meditation. MNT: *WAHE GURÚ* or silence in Gyan Mudra

Source: *Self-developed work created at Fundación Casa Arcoíris, based on personal experiences, training in chromotherapy and yoga, and the book Fuerza Multicolor*

CONCLUSION

The core concepts of semiotics and subjectivity contribute to the studies on the subjective meanings generated by the practice of CY, as they value the emotional and symbolic within the broader framework of human experiences. This perspective allows for an analysis of the human being in their entirety, because 'the individual, as mentioned, is a whole that cannot be separated into dimensions, since it is not easy to determine how much one influences the others or how much they depend on each other' [16].

The experimentation involved in the practice expands the generative nature of human experience and enables an understanding of the subject within their culture, history, and role as a creator of new possibilities and realities. This research opens the door to future studies and applications of color in fields beyond traditional ones, such as health, and paves the way for new developments in psychology and healing technologies.

ACKNOWLEDGEMENTS

We extend our gratitude to the institutions that have supported the development of the color-based experiences, to Casa Arcoíris Foundation NGO for being the epicenter and pioneering institution in chromotherapy and integrative practices, as well as the laboratory for practice, training, and learning for the researchers. We also thank the faculty members of the Institute of Psychology at the University of Brasília who are aligned with this line of work and have helped to broaden the understanding and study presented in this article

REFERENCES

[1]. Sarudiansky, M., & Saizar, M. (2007). El yoga como terapia complementaria en pacientes con estrés en Buenos Aires (Argentina). Mitológicas, 69-83

[2]. . González Rey, F., & Torres Patiño, J. F. (2017, 04 01). La epistemología cualitativa y el estudio de la subjetividad em una perspectiva cultural-histórica. Conversación com Fernando González Rey. From https://doi.org/10.7440/res60.2017.10.

[3]. Brasil, G. F. (n.d.). Práticas Integrativas e Complementares em Saúde (PICS). (Ministerio da Saúde do Brasil) From https://www.gov.br/saude/pt-br/composicao/saps/pics

[4]. Monsalve Ospina, H. F. (2022). Fuerza Multicolor. Guía de Cromoterapia y sanación. Medellín: Fundación Casa Arcoíris

[5]. Assagioli, R. (2000). Psicosínteisis: Ser Transpersonal.

[6]. Guevara Alban, G., Verdesoto Arguello, A., & Castro Molina, N. (2020). Metodologías de investigación educativa (descriptivas, experimentales, participativas, y de investigación-acción). RECIMUNDO, 4(3), 163-173.

[7]. Quecedo Lecanda, R., & Castaño Garrido, C. (2002). Introducción a la metodología de investigación cualitativa. Revista de Psicodidáctica, 14, 5-39.

[8]. Peirce, C. (1931-1935). Collected Papers of Charles Sanders Peirce. (Vols. 1-6,C). Cambridge, Massachusetts: Harvard University Press (Belknap Press).

[9]. Restrepo J., M. (1990). La Semiótica de Charles S. Peirce. Signo y Pensamiento., 9(16), 27-46.

[10]. González Rey, F. (1997). Epistemología cualitativa y Subjetividad. São Paulo: Educ.

[11]. González Rey, F. (2010). Las categorías de sentido, sentido personal y sentido subjetivo en una perspectiva histórico-cultural: un camino hacia una nueva definición de subjetividad. Universitas Psychologica, 9(1), 241-253.

[12]. Caires de Souza, E., & Patiño Torres, J. (2019). A Teoria da Subjetividade e seus conceitos centrais. Obutchénie. Revista de Didáctica y Psicología Pedagógica, 3(1), 34-57. From https://pdfs.semanticscholar.org/a1f6/98458c3cbaf91b56e6138b872b0071bd48a3.pdf

[13]. Alciane Barbosa, M., Gandolfo Conceição, M., & Mitjáns Martínez, A. (2016). Epistemología cualitativa de González Rey: una forma diferente de análisis de “datos”. Revista Tecnia, 1(1). From https://periodicos.ifg.edu.br/tecnia/article/view/379

[14]. González Rey, F., & Mitjáns Martínez, A. (2016). Una epistemología para el estudio de la subjetividad: Sus implicaciones metodológicas. PSicoperspectivas. Individuo y Sociedad, 15(1), 5-16.

[15]. 3HO International. (2024, 5 17). What is kriya? Retrieved 9 1, 2025 from https://shorturl.at/TTpbH

[16]. Alonso Palacio, L. M., & Escorcia de Vásquez, I. (2003). El ser humano como una totalidad. Salud Uninorte (17), 3-8.

Analysis of The Color and Object Characteristics of Seasonal Natural Landscape Images in Japan

Hanui Yu[a*], Takeshi Akita[b], Kotaroh Hirate[a], and Risa Fujii[c]

[a]*The University of Tokyo, Tokyo, Japan*
[b]*Tokyo Denki University, Tokyo, Japan*
[c]*Kogakuin University, Tokyo, Japan*
**Corresponding author: hnwind@arch1.t.u-tokyo.ac.jp*

ABSTRACT

This study analyzed color and object characteristics of seasonal landscape images to understand how they evoke seasonal impressions. Using paired comparison and laddering techniques, cherry blossoms, sunflowers, autumn foliage, and snow were identified as key objects for spring, summer, autumn, and winter, respectively. Color attributes such as bright yellows and vivid greens in spring, deep blues in summer, warm reds and oranges in autumn, and dominant whites in winter strongly influenced perception. These findings support the use of seasonally appropriate colors and natural objects in architectural design to enhance psychological comfort and well-being.

Keywords: Seasonality, Natural Landscape Images, Color Characteristics, Object Features, Psychological Recov ery, Spatial Design

INTRODUCTION

Previous studies have shown that viewing seasonal natural landscapes can reduce stress, enhance well-being, improve concentration, and promote psychological recovery [1], [2]. These psychological benefits highlight the importance of integrating seasonal visual objects into architectural and spatial design. In order to effectively incorporate such seasonal imagery, it is essential to clarify the visual characteristics—particularly colors and natural objects—that contribute to the perception of each season. This study aims to identify the natural features that evoke seasonal impressions and analyze the color and object characteristics of natural landscape images representing spring, summer, autumn, and winter in Japan.

METHODOLOGY

Preliminary Survey: Selection of Natural Objects Evoking Seasonal Impressions

To extract natural objects that evoke a sense of each season, an online questionnaire was conducted using Google Forms. Participants were asked, for each season, to "list as many natural landscapes and objects as possible that make you feel the season." The survey targeted 25 university students in their early twenties (mean age: 21.3, SD: 0.5; 11 males, 14 females).

The aggregated results identified the top four objects for each season as follows. For spring, flower-related items such as cherry blossoms and dandelions were frequently mentioned. The objects evoking summer were diverse and not confined to specific categories compared to other seasons. Autumn impressions were mostly associated with leaf-related objects. In contrast, winter had the fewest mentions of natural objects compared to the other seasons.

Participants

Twenty university students in their early twenties (mean age = 21.4, SD = 0.6; 10 males, 10 females) with normal vision participated in the study. The survey was conducted remotely using a web conferencing tool on participants' personal computers.

Study Procedure

Based on the preliminary survey identifying natural objects evoking seasonal impressions, a total of 16 images were selected—four per season:

- **Spring:** Cherry blossoms, Rapeseed flowers, Cherry blossom avenue, Dandelion
- **Summer:** Sea, Cumulonimbus cloud, Sunflower, River
- **Autumn:** Autumn leaves, Fallen leaves, Ginkgo, Sunset/dusk
- **Winter:** Snow, Withered tree, Withered leaves, Frozen lake

The main survey first employed a paired comparison method using the images for each season. For spring, pairs of two images out of the four spring images were presented to participants, who were then asked, "Q1: Which image evokes a stronger sense of spring?" Participants selected one image from each pair.

Following the paired comparison, laddering **(*Note 1*)** interviews were conducted focusing on the selected images (objects). Participants were asked, "Q2: Why do you feel this image evokes spring more strongly?" The participant would respond, "A2: Because of ○○." Then, using a ladder-up approach, repeated questions such as "Q3: You said you feel more spring because of ○○, but why does ○○ evoke spring more strongly?" were asked until no further reasons were provided. Subsequently, a ladder-down approach was applied by asking, "Q4: Specifically, what conditions or states make ○○?" to elicit more concrete details, repeated until no additional answers were given.

For spring images, the paired comparison was repeated six times. After completing the paired comparison and laddering interviews for spring, the same procedure was applied to the four images of summer, autumn, and winter respectively.

RESULTS AND DISCUSSION

Results of the Paired Comparison

The results of the paired comparison were standardized using a mean of 0 and a standard deviation of 1, and these standardized values were used as scale scores. Figures 1 through 4 present the distribution of these scale scores by season.

According to **Figure 1**, cherry blossoms were the most frequently selected object for spring. This aligns with the findings from the preliminary survey, in which respondents provided answers in descriptive form (without images), and cherry blossoms were again the most frequently mentioned. These results suggest that cherry blossoms are the natural object most strongly associated with the feeling of spring. According to **Figure 2**, sunflowers were most frequently selected for summer. However, in the preliminary survey, the sea was mentioned most often, followed by cumulonimbus clouds, and then sunflowers. This discrepancy indicates that there may be a difference between what people imagine when thinking of a season and how they react when viewing actual images. According to **Figure 3**, autumn leaves were the most frequently selected object for autumn, both in the preliminary survey and in the paired comparison. However, images featuring multi-colored autumn foliage were selected more often than those showing ginkgo trees, suggesting that color variety, in addition to the presence of autumn leaves, also influenced the perception of the season. According to **Figure 4**, for winter, images were more likely to be selected based on the degree to which snow was present. This trend was also observed in the preliminary survey, in which snow-related objects were frequently mentioned. These results suggest that the presence of snow, rather than specific types of plants or other features, plays a more decisive role in evoking the feeling of winter in an image.

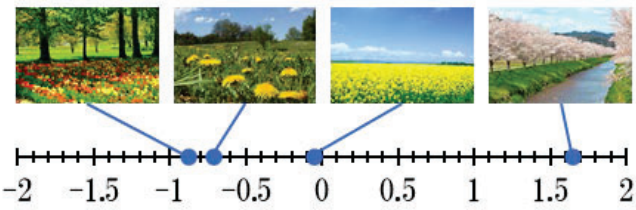

Figure 1: Scale distribution results for spring

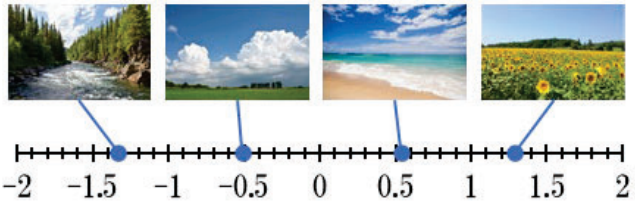

Figure 2: Scale distribution results for summer

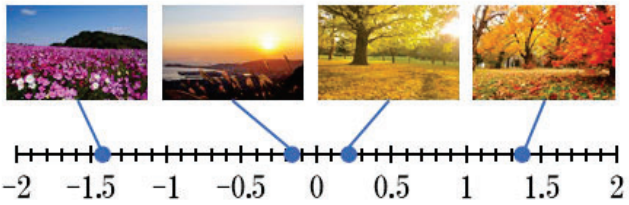

Figure 3: Scale distribution results for autumn

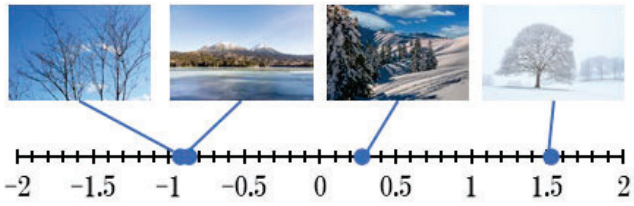

Figure 4: Scale distribution results for winter

Results of the Laddering Analysis

The information obtained from the laddering interviews was organized into evaluation structure diagrams, presented in Figures 5 through 8. In each diagram, the number of respondents who mentioned each item is indicated in parentheses. The borders of the boxes are drawn with a medium-thick line for responses with 5 or more votes, and a thick line for responses with 10 or more votes. Responses that were mentioned only once were omitted from the diagrams.

The evaluation structure was constructed as follows: responses to Q2 in **Figure 5-8** were defined as the original evaluation items, responses to Q3 (ladder-up) were categorized as higher-level items, and responses to Q4 (ladder-down) were categorized as lower-level items. In this analysis, particular attention was paid to the lower-level items, as they provide insight into the specific visual conditions and natural objects that contribute to the perception of each season—aligning with the overall objective of the study. Across all four seasons, responses frequently referenced color attributes and the appearance of seasonal objects depicted in the images.

According to **Figure 5** (Spring), items related to color appeared relatively frequently, though no strong bias was observed overall. Among these color-related responses, many referred to brightness and vividness, such as “bright yellow” and “vivid green.” In particular, brightness was identified as a spring-specific feature, not observed in responses for other seasons. Regarding the appearance of objects, many responses focused on flowers and the sky, with expressions such as “in full bloom” and “few clouds.” Taking these results together with those from the paired comparison task, it can be inferred that in addition to the prominent object of cherry blossoms, variations in blooming degree, brightness, and color intensity contributed to a stronger seasonal impression of spring. Moreover, lower-level items such as “high density” and “spread across the entire field” frequently appeared in responses about flowers, suggesting that images showing a larger quantity of flowers tended to evoke a stronger sense of spring. According to **Figure 6** (Summer), many responses were related to the appearance of objects, such as “flowers in full bloom” and “exposed to sunlight.” Compared to other seasons, a greater number of responses also referred to the sky. This suggests that while the mere presence of natural objects contributes to the perception of summer, their specific condition—along with the appearance of the background sky—plays a significant role in shaping seasonal impressions. Regarding color, most responses referred to strong and distinct hues, such as “deep blue” and “vivid blue.” According to **Figure 7** (Autumn), many of the original evaluation items referred to objects depicted in the image, such as “colored leaves” and “fallen leaves.” These findings indicate that the presence of objects symbolizing autumn had a greater influence on seasonal perception than the overall color tone or brightness of the image. Among the lower-level items, many responses were concerned with the color attributes of autumn-related objects.

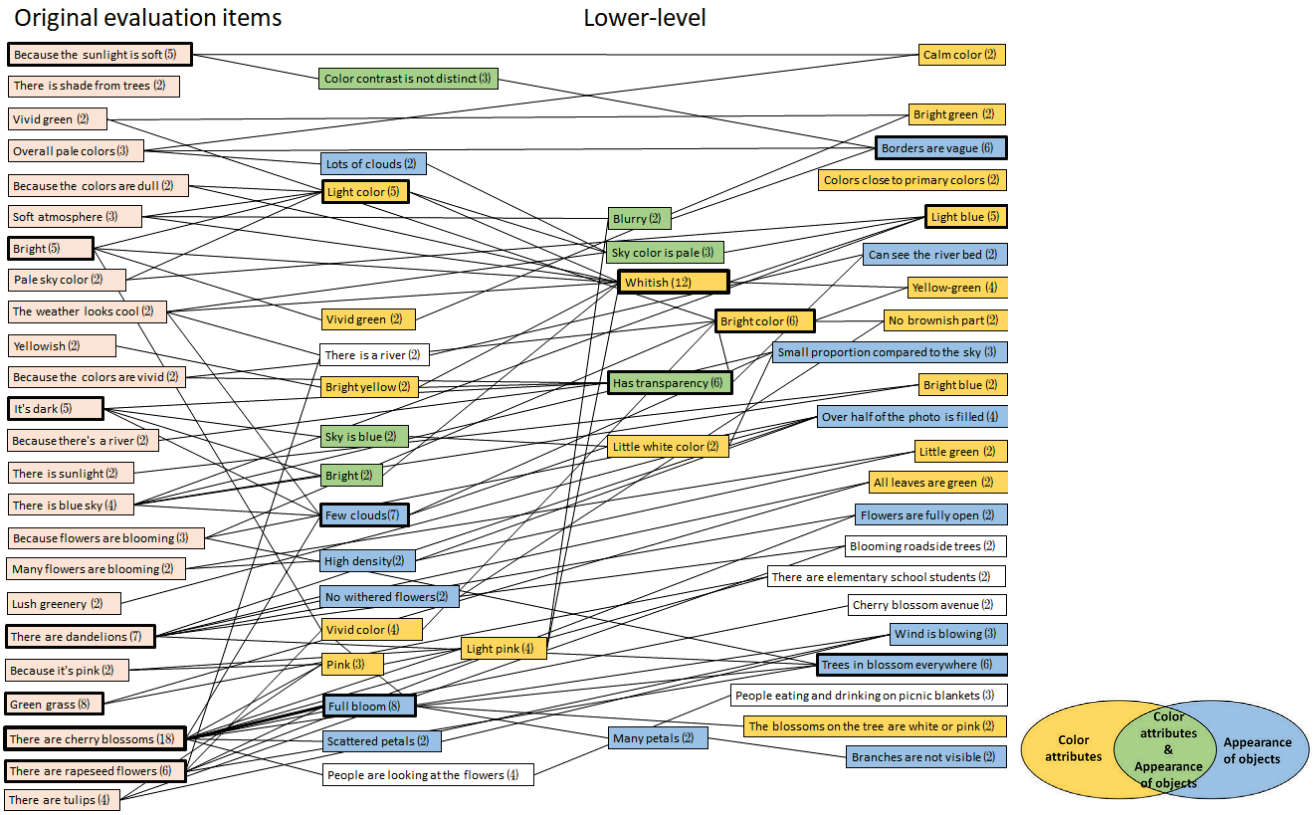

Figure 5: Evaluation structure diagram of objects evoking spring (2 or more votes)

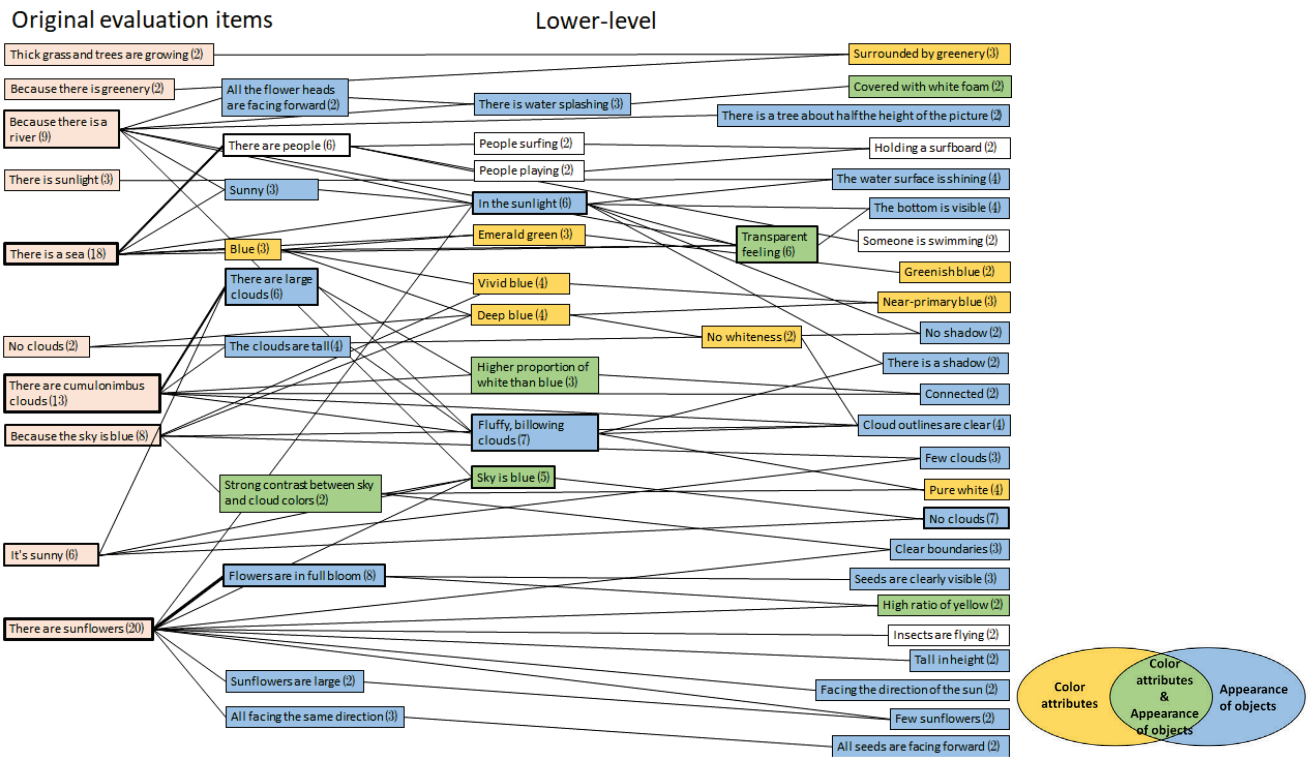

Figure 6: Evaluation structure diagram of objects evoking summer (2 or more votes)

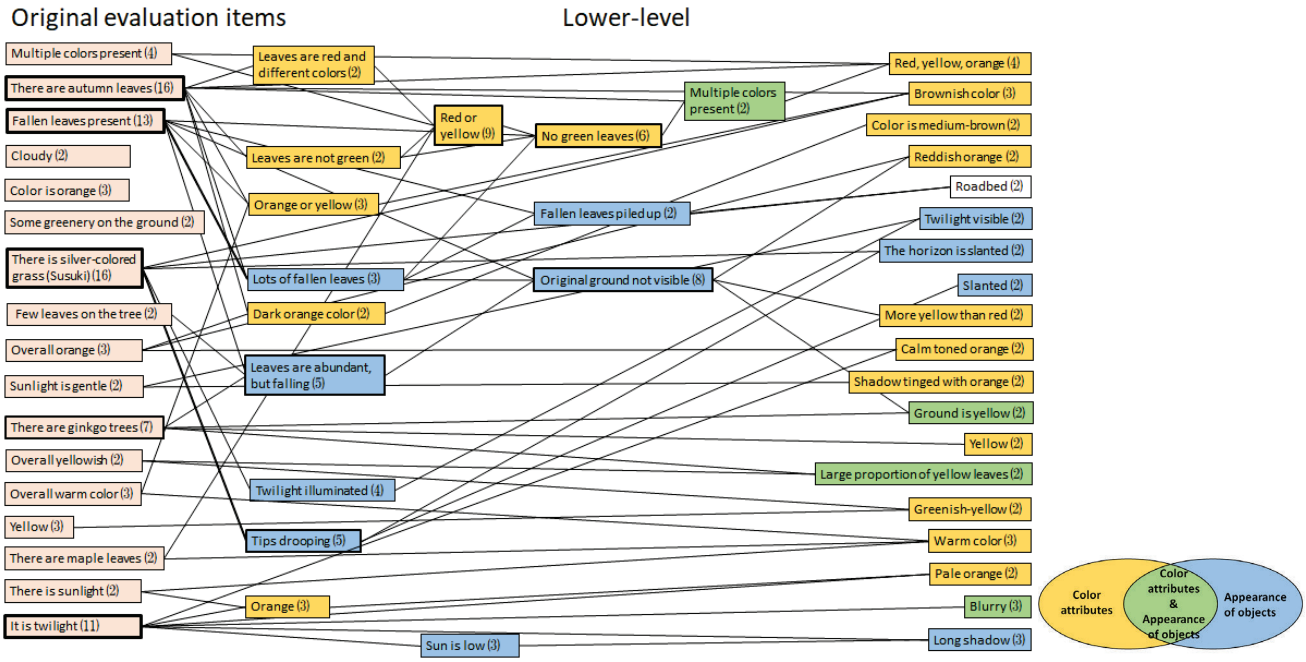

Figure 7: Evaluation structure diagram of objects evoking autumn (2 or more votes)

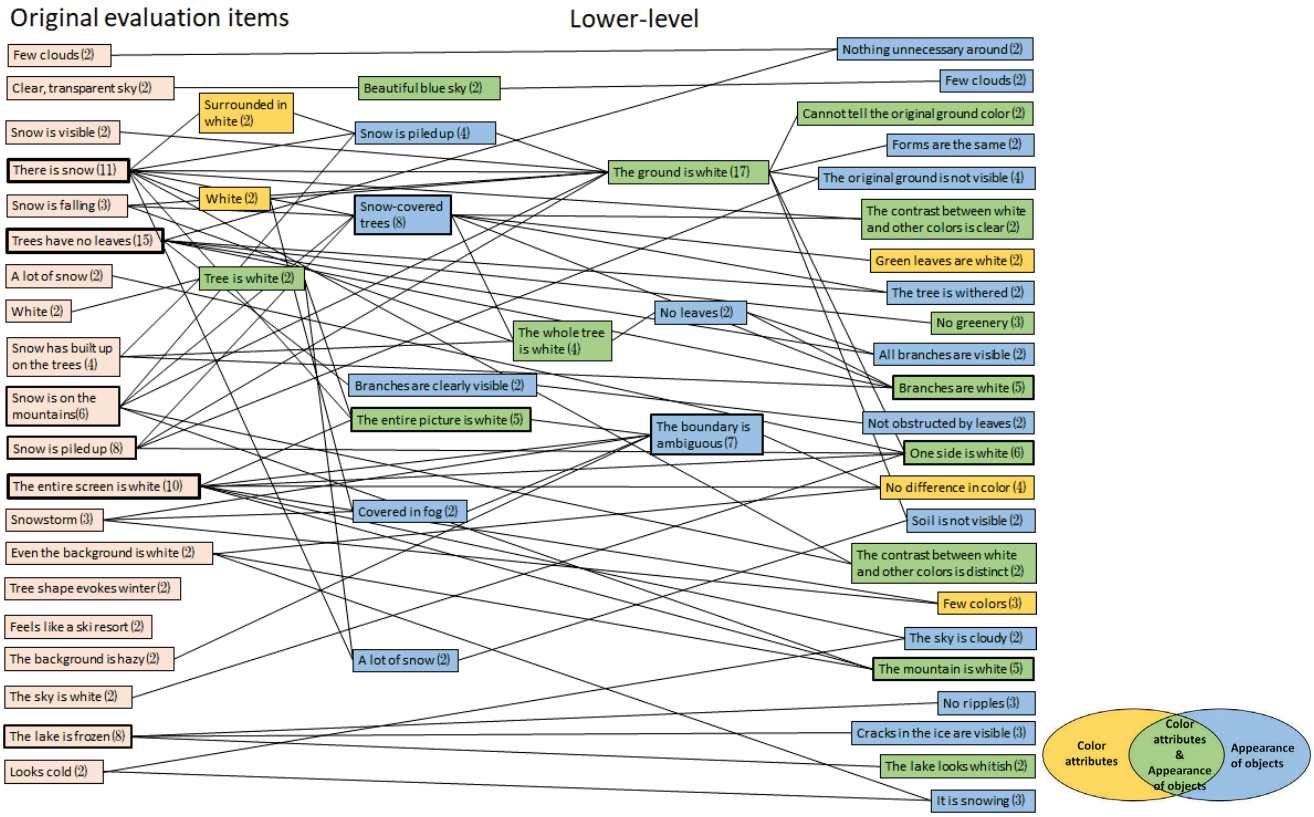

Figure 8: Evaluation structure diagram of objects evoking winter (2 or more votes)

For instance, colored leaves and fallen leaves were often associated with warm colors such as red, yellow, and orange, and the clearer or more saturated these colors were, the stronger the impression of autumn was. In contrast, sunset responses such as “muted orange” and “light orange” were more common, suggesting that less saturated orange tones better conveyed the atmosphere of autumn. According to **Figure 8** (Winter), responses were more frequently related to the appearance of objects than to color. Both original evaluation items and lower-level items often referred to snow, and accordingly, most of the color-related responses concerned white. For example, among the lower-level responses to “presence of snow,” items like “snow is accumulated” and “snow on the trees” were common, indicating that accumulated snow—rather than falling snow—made the image feel more wintry. Additionally, the high frequency of responses such as “the whole screen is white,” “the entire area is white,” and “a lot of snow” suggests that a greater amount of visible snow led to a stronger impression of winter. Furthermore, regarding the state of plants, images showing leafless or withered vegetation were perceived as more representative of winter.

CONCLUSION

This study explored how seasonal impressions are formed through the analysis of color and object characteristics in natural landscape images representing the four seasons in Japan. Using a paired comparison method combined with laddering interviews, key natural objects and their visual attributes were identified that significantly influence the perception of seasonality. The paired comparison confirmed that cherry blossoms, sunflowers, autumn foliage, and snow serve as the most representative natural objects for spring, summer, autumn, and winter, respectively. The laddering analysis further highlighted two main factors shaping seasonal perception: color-related attributes and the appearance of seasonal objects. In particular, color played a pivotal role: spring was characterized by bright and highly saturated hues such as vivid greens and bright yellows; summer was distinguished by intense sunlight and deep, clear blue skies; autumn featured warm, rich colors like red, orange, and yellow; and winter’s seasonal feeling was conveyed primarily through white snow and the visual state of snow-covered landscapes. These findings emphasize the importance of incorporating seasonally appropriate colors and natural objects in architectural and environmental design to foster comfort, psychological stability, and well-being. This research shows how certain colors and objects create a seasonal feeling, offering useful ideas for designing spaces that use color effectively to improve people’s experience in built environments.

ACKNOWLEDGEMENTS

We sincerely thank Ayaka Natsui and Aoi Yubune for their invaluable assistance and support throughout the experiment. We also thank all participants for taking the time to join the experiment.

REFERENCES

[1]. Berman, M. G., Jonides, J., & Kaplan, S. (2008). The cognitive benefits of interacting with nature. *Psychological Science, 19*(12), 1207–1212.

[2]. Ulrich, R. S., Simons, R. F., Losito, B. D., Fiorito, E., Miles, M. A., & Zelson, M. (1991). Stress recovery during exposure to natural and urban environments. *Journal of Environmental Psychology, 11*(3), 201–230.

[3]. Architectural Institute of Japan. (2011). Designing Surveys for Homes and Communities: A Guide to Interviews, Questionnaires, and Psychological Experiments. Ohmsha.

Note 1: Laddering is a questioning technique used to elicit higher- and lower-level evaluation criteria. The hierarchical structure derived from this method is referred to as the “evaluation structure” in the Evaluation Grid Method. Typically, higher-level items reflect psychological values, while lower-level items indicate physical conditions.[3]

Study on 3D Digital Preservation of Orchids Using Photogrammetry Method

Tzu-Hsuan Liu[1], Chen-Yu Yuan[2], Chi-Pin Tsai[2], Shih-Chen Chang[2], and Tzung-Han Lin[2*]

[1]*National Taiwan Normal University, Taipei, Taiwan*
[2]*National Taiwan University of Science and Technology, Taipei, Taiwan*
[*]*corresponding author: thl@mail.ntust.edu.tw*

ABSTRACT

Taiwan is a global leader in orchid cultivation, and phalaenopsis dominates national exports. However, conventional 2D images cannot totally retain the 3D shapes and nuanced color appearance of blossoms after bloom, leading to limited documentation and reuse. This study establishes a reproducible 360-degree photogrammetry workflow for phalaenopsis using an automated dual-camera orbit around the stationary flower, and examines how three single factors, including the size of targets, petal textures, and numbers of images, affect reconstruction quality. Utilizing the opensource of OpenCV, a python script program was developed to obtain the images with 4K resolutions and able to control the properties of focusing, exposure value, shutter speed, and capturing frequency. 3D Reconstruction process was carried out by Meshroom software and manipulated in the Blender software. Findings show that single-flower yields near-continuous meshes, whereas whole-plant models preserve overall geometry but are locally limited by self-occlusion and shadows. Texture contrast is the primary factor for successful reconstruction: patterned petals reconstruct more completely than gradient, which in turn exceeds solid, reflecting differences in feature density and match stability. For the numbers. of images, around 30 images were the most compromising for single blossoms; for whole plants, about 60 images performs best. Simply adding frames to 90 per camera without inducing more details of texturing while increasing computation time. These results consolidate clear design principles—align rig geometry with target scale, favor viewpoint diversity over raw frame count, and keep backgrounds simple—and provide actionable guidance for preservation, documentation, exhibition, and cultivar identification across orchid collections.

Keywords: Orchids, Photogrammetry, 3D reconstruction, Digital Preservation, 3D image.

INTRODUCTION

Taiwan holds a significant position in the global orchid industry, supported by favorable geography and advanced cultivation techniques. Among commercial species, phalaenopsis accounts for nearly 70% market share of Taiwan's orchid exports and is thus the most representative variety in both economic and cultural terms. Given this prominence, phalaenopsis is adopted as the focal subject of this study.

Despite Taiwan's success in cultivation, current digital preservations—primarily two-dimensional color images such as photography or pressed specimens—are insufficient to preserve the intricate three-dimensional architecture and nuanced color patterns of orchids. Once the bloom period ends, even award-winning cultivars often lack faithful, reproducible documentation of their true appearance. This gap limits long-term archiving, public dissemination, and research reuse of high-value specimens.

Recent work in flower-focused photogrammetry shows that close-range, multi-view acquisition can reconstruct research-grade 3D flower models from 2D images while preserving visible color and morphology [1]. At the same time, compact plant-phenotyping studies emphasize that viewpoint diversity and sufficient overlap—

rather than merely adding near-duplicate frames—are the primary drivers of pose stability and dense-reconstruction quality [2]. Building on these insights, this study evaluates whether a controlled 360° photogrammetry workflow can accurately recover the three-dimensional form and visible color texture of phalaenopsis. To have valuable and speed up the process, we systematically examine three factors—capture scope (single flower vs. whole plant), petal texture (solid, gradient, patterned), and numbers of images per orbit (30, 60, 90 per camera)—with the objective of consolidating a streamlined and reproducible workflow that supports long-term preservation, data sharing, digital exhibition, academic research, species identification, and related applications.

METHODOLOGY

Materials and Equipment

Because orchid inflorescence stems are slender, rotating the specimen itself often induced wobble and motion blur; we therefore adopted moving-cameras and static-specimen orbit. Two high resolution webcams—one mounted above and pitched 30° downward, the other mounted below and kept level—were placed to widen vertical coverage and reduce occlusions. The orchid was set at the center of a customized and motorized platform, and the camera rig orbited at a fixed angular velocity through 360° (Figure 1). This dual-view configuration complements a single viewpoint and recovers petal details that are otherwise difficult to capture. Images were recorded at a resolution of 2160 × 3840 pixels as the portrait format.

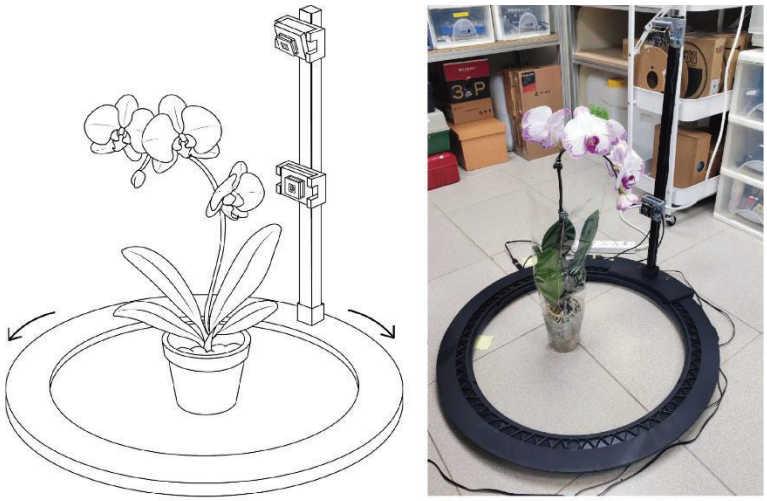

Figure 1. The proposed 360-degree orchid scanning framework: (a) schematic drawing and (b) photograph

Software

During image acquisition, cameras were connected to a computer and driven by a python script program with the OpenCV library developed in Visual Studio Code. The script program locked exposure value and focus, shutter speed and capturing frame rate once it started. And it also kept white balance on auto, and automatically saved images into specific folders with sequential filenames during taking photos. 3D reconstruction was then performed in Meshroom software, which was the version of 2023.3. The output mesh and texture was inspected and manipulated in another opensource named Blender.

Reconstruction Pipeline (key nodes settings of Meshroom software)

3D Reconstruction was carried out by Meshroom software following its standard node graph which consists of feature extraction, guided image/feature matching with geometric verification, incremental SfM, GPU-accelerated depth maps, meshing, and LSCM plus multi-band texturing [3] (as shown in Figure 2). Its modular and

cacheable design aligns with the goal of this research to establish a standardized orchid modeling process, and it can also be smoothly applied in the context of single flowers and whole plants. In “camera initialization and feature extraction” step, EXIF intrinsics were read when available; local features were extracted using AliceVision (which was a SIFT-based algorithm). In “image and feature matching” step, neighbor proposals and guided matching emphasized adjacent views along the orbit, and geometric verification pruned inconsistent matches. In “structure from motion (SfM)” step, incremental pose estimation and sparse point-cloud triangulation were performed, with outliers removed by reprojection error and track length. During “dense preparation, depth-map estimation, and filtering” procedure, all views were undistorted and normalized; dense per-view depths were computed using a cost-volume with SGM-style aggregation and then cross-checked for multi-view consistency before fusion [4], producing a consistent point set. In “meshing and mesh filtering”, a watertight surface was reconstructed and lightly filtered, avoiding aggressive smoothing to preserve petal rims/veins. And in the final step as well as “texturing”, UVs were unwrapped and color projected, and a single high-resolution atlas (e.g., 4K or more) with standard padding was used. As a result, a color 3D model using wavefront object format was exported..

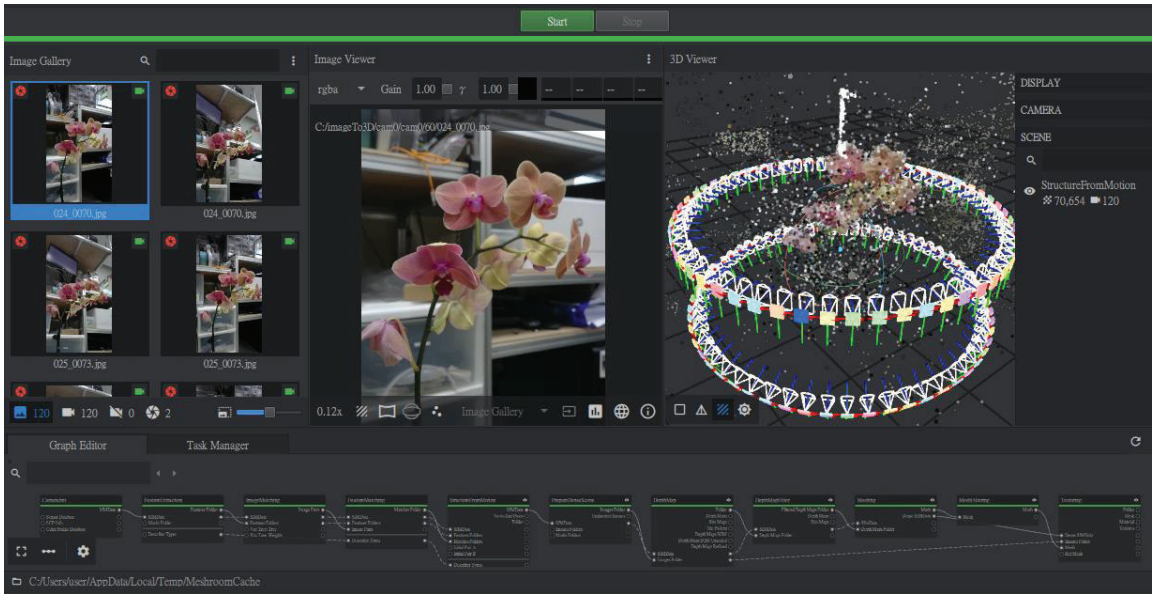

Figure 2. A snapshot for the pipeline, node settings and reconstrued 3D points of Meshroom software

Experimental Design

Three factors with several conditions were evaluated: (i) capture scope: single-flower vs. whole-plant; (ii) color/pattern: solid, gradient, patterned; (iii) image count per 360°: 30, 60, 90. In all experiments, the viewing distance, orbit radius, rotation speed and resolution were kept constant. The target blossom was centered in all views. All experiments were executed in a well-controlled environment, therefore all factors were run once.

RESULTS AND DISCUSSION

- Capture scope — single flower vs. whole plant

Since the rig was originally designed around whole-plant imaging, the two scopes behave differently. Whole-plant reconstructions remain globally coherent and preserve the overall geometry of the inflorescence, but local breakage and small floating fragments appear where blossoms self-occlude or fall into deep shadow; this points to view obstruction rather than the pipeline as the main limitation, as shown in Figure 3. By contrast, when the target is a single blossom, the mesh is nearly continuous and petal rims and labellum details are clearer. Because the scene

is simpler, mutual occlusion and shadow contrast are reduced, which stabilizes track formation and texturing, as shown in Figure 4.

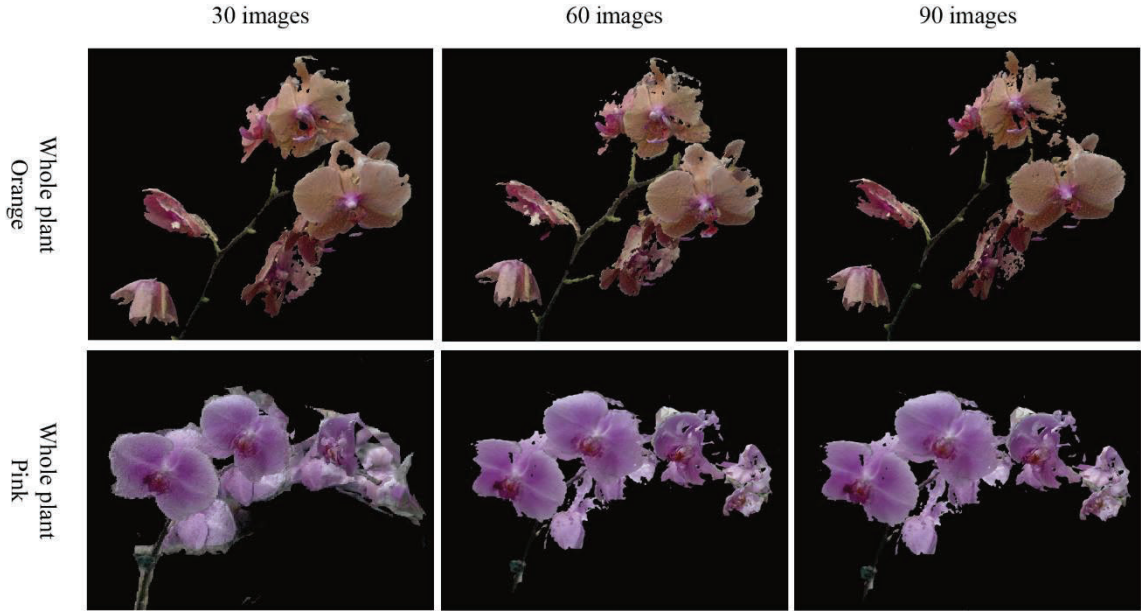

Figure 3. Effect of numbers of images and capture scope on 3D reconstruction quality (Whole plant)

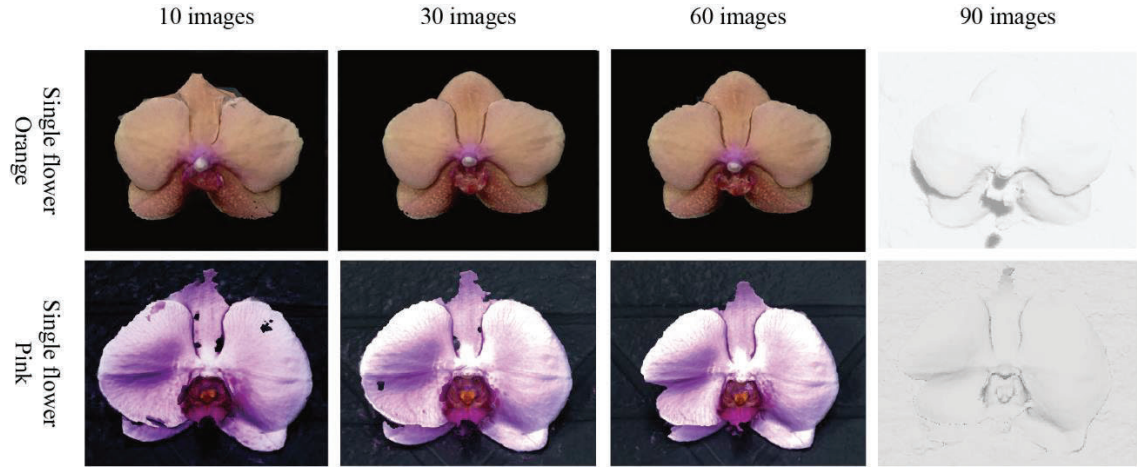

Figure 4. Effect of numbers of images and capture scope on 3D reconstruction quality (Single flower)

- Images per 360° orbit

With the dual cameras operating simultaneously, each camera acquires N images per orbit, yielding $2N$ frames in total for reconstruction. Under the single-flower condition using10 per camera under-samples the subject: edges show holes and jagged rims (the first column of Figure 1). 30 per camera already produces a continuous, complete mesh. 60 per camera is similar to 30, with no clear improvement. 90 per camera usually completes geometry but fails at texturing. Under the whole-plant condition, 60 per camera gives the best completeness; 30 shows regions that blend into the background; 90 is less clean on petal surfaces than 60. Computation time grows roughly with total frame count, so for single-flower capture we recommend about 30 images per camera; when more detail is

required, prefer a short oblique micro-orbit to introduce new viewpoints rather than simply adding frames within the same orbit.

- Petal texture

Under the single-flower condition, patterned petals reconstruct most completely, gradient is second, and solid is most prone to holes or fragments. This follows the dependence of photogrammetry on feature density and match stability. Higher texture contrast and more distinct local features yield more robust multi-view matches and support a continuous mesh, as illustrated in Figure 5. This observation aligns with quantitative evidence that insufficient surface texture elevates noise and degrades SfM accuracy, whereas stronger contrast improves correspondence stability [5]

Figure 5. Effect of petal texture complexity on 3D reconstruction quality

- Overall observations

Improving quality is driven more by viewpoint diversity than by indiscriminate frame increases within a single orbit. For single-flower capture, around 30 images per camera balances quality and time; for whole-plant, around 60 per camera performs best. If the project goal shifts toward single-flower priority, reduce the orbit radius, increase the downward pitch, and lower the camera height so the blossom occupies more of the frame and thin edges are better covered.

CONCLUSION

This study establishes a reproducible 360° photogrammetry framework for phalaenopsis using an automated dual-camera photographing and provides systematic observations on three single factors: capture scope, petal texture, and images per orbit. The results show that single-flower reconstructions typically achieve a near-continuous mesh, whereas whole-plant models preserve overall geometry but remain limited in regions affected by self-occlusion and shadows. Texture contrast is the primary driver of quality—patterned, gradient and then solid—consistent with higher feature density and more stable matches. For image count, single-flower capture reaches the best quality–time balance at about 30 images per camera, while whole-plant capture performs best at about 60 per camera; when no new viewpoints are introduced, merely adding frames tends to destabilize texturing. Overall, viewpoint diversity matters more than raw frame count. In practice, single-flower capture benefits from a smaller orbit radius, a stronger downward pitch, and a lower camera height; whole-plant completeness improves with targeted micro-orbits and a simplified background with high-contrast fiducials.

ACKNOWLEDGEMENTS

This work was supported by the National Science and Technology Council (NSTC), Taiwan, under the Undergraduate Student Research Project Grant No. 114-2813-C-011-014-B. We gratefully acknowledge Taida Horticultural Co., Ltd. for providing the orchid specimens used in this study.

REFERENCES

[1]. Leménager, M., Burkiewicz, J., Schoen, D. J., & Joly, S. (2023), "Studying flowers in 3D using photogrammetry.," New Phytologist, 237(5), 1922–1933. https://doi.org/10.1111/nph.18553

[2]. Wu, S., Wen, W., Gou, W., Lu, X., Zhang, W., Zheng, C., Xiang, Z., Chen, L., & Guo, X. (2022), "A miniaturized phenotyping platform for individual plants using multi-view stereo 3D reconstruction," Frontiers in Plant Science, 13, 897746. https://doi.org/10.3389/fpls.2022.897746

[3]. Griwodz, C., Gasparini, S., Calvet, L., Gurdjos, P., Castan, F., Maujean, B., De Lillo, G., & Lanthony, Y. (2021), "AliceVision Meshroom: An open-source 3D reconstruction pipeline," Proceedings of ACM Multimedia Systems Conference (MMSys '21), 241–247. ACM. https://doi.org/10.1145/3458305.3478443

[4]. Stathopoulou, E. K., & Remondino, F. (2023), "A survey on conventional and learning-based methods for multi-view stereo," The Photogrammetric Record, 38(183), 374–407. https://doi.org/10.1111/phor.12456

[5]. Nielsen, M. S., Nikolov, I., Kruse, E. K., et al. (2023), "Quantifying the Influence of Surface Texture and Shape on Structure from Motion 3D Reconstructions," Sensors, 23(1), 178. https://doi.org/10.3390/s23010178

On The Narrative Function of Costume Color in Chinese Cinema

Peitong Li[a],Dan Han[b]

[a]Northeast Normal University, Changchun, China
[b]Northeast Normal University, Changchun, China

ABSTRACT

In the realm of Chinese cinematic art, color serves as a vital visual language. The diversity of color enhances the narrative function of films. As a key prop in cinema, the color of costumes, through subjective artistic interpretation, can vividly portray individualized characters and convey deeper narrative messages. This thesis analyzes the classic Chinese films 'Raise the Red Lantern' and 'In the Mood for Love' as case studies, seeking to explore the distinctive role of costume color in the narrative function of Chinese cinema. Methodologically, this study analyzes relevant literatures to sort out the colors of characters' costumes in these films mentioned above, with a particular focus on the characteristics of costume color across various narrative scenes. Additionally, a questionnaire survey of 40 viewers was conducted to assess their psychological responses to the different costume colors presented in the films. Through comparative reflection on cinematic imagery, this thesis reveals that the narrative function of costume color in Chinese cinema is a multi-dimensional expression. Costume color in Chinese films functions as a precise encoding within the cinematic language, enabling audiences to intuitively grasp the deeper meanings conveyed through visual impact. Even if viewers remain unaware of the deliberate design behind the color choices, their emotions and attention are subconsciously guided, thereby amplifying the transmission of the Chinese aesthetics and artistic value embedded in the films. This encapsulates the allure of the art of costume color in cinema.

Keywords: Chinese cinema, costume color, narrative function

INTRODUCTION

With the advancement of Chinese film technology, the transition from black-and-white to color imagery has become an indispensable component of the film narrative system. Among various elements, costumes, as a crucial carrier of information, often draw the audience's attention first. Chinese cinema excels at employing the costume colors of characters-a significant visual symbol-to convey a "silent narrative language." When analyzing the narrative function of costume colors in Chinese films, it is essential to distinguish them from Western color theories based on optics and physics. In Chinese cinema, costume colors not only serve as the visible external "image" of characters but also embody a deeper symbolic "meaning." Chinese film costume colors often start from the "image" and culminate in the "meaning". In different narrative scenes, they not only have symbolic narrative functions, but also have certain emotional narrative functions, which can depict the characters' psychology and convey their emotions.

The two classic Chinese films selected for this study, Raise the Red Lantern and In the Mood for Love, are renowned both domestically and internationally. These works are crafted by the renowned directors Zhang Yimou and Wong Kar-wai, respectively, and have received high acclaim at top international film festivals, sparking extensive academic discussions that transcend East and West to this day. The reason for choosing these two films as case studies lies not only in their status as landmark works that have propelled Chinese film aesthetics onto the global stage but also in the fact that the costume colors in both films are far from mere background decorations.

Instead, they are highly stylized visual elements that serve as the core narrative impetus. Both films embody national identity while possessing universally appealing aesthetic values.

METHODOLOGY

This study conducts a systematic investigation into the narrative function of costume colors in Raise the Red Lantern and In the Mood for Love based on theories of chromatics, visual communication, and aesthetics. Employing methodologies of close reading and comparative analysis, key scenes featuring the female protagonists were selected from both films. Color extraction tools were utilized to perform quantitative analysis of the various hues present in the characters' attire. To examine the alignment between theoretical interpretation and audience perception, a structured questionnaire was designed, incorporating free association exercises and multiple-choice questions on narrative function recognition to collect data. By using visual analysis methods such as line charts, the intensity and cognitive differences of audience emotional reactions to different colors are presented, reflecting the narrative of "macro symbolism of social power" and "micro externalization of individual emotions" achieved by directors Zhang Yimou and Wong Kar wai through the use of different clothing color strategies, which deeply reveals the operational mechanisms and rich connotations of costume color as a powerful visual discourse in Chinese cinematic narration.

RESULTS AND DISCUSSION

Due to space constraints, we focus our analysis on the costume colors of the female protagonists in the two films. In Raise the Red Lantern, we explore the intertextual relationship between the symbolic function of Songlian's costume colors and her fate trajectory. She was dressed in a simple light blue shirt when she first entered the Chen household, a feudal mansion. . The pale blue symbolizes both the purity and free will characteristic of her identity as a female student. However, as she becomes increasingly embroiled in the household's power struggles, her attire is gradually engulfed by intense red hues—red jackets and skirts that represent both passive submission to the power structure and external projection of her inner desires. This red does not embody the traditional Chinese concepts of celebration and vitality but rather symbolizes Songlian's assimilation and discipline under the feudal system, hinting at her gradual loss of self. As the lie of Songlian's false pregnancy is exposed, she was permanently "sealed off", and the vibrant red is stripped from her. Clading in worn-out garments of dark blue everyday, she abandoned all self-regard, ultimately descending into madness—a complete erosion of her individuality.

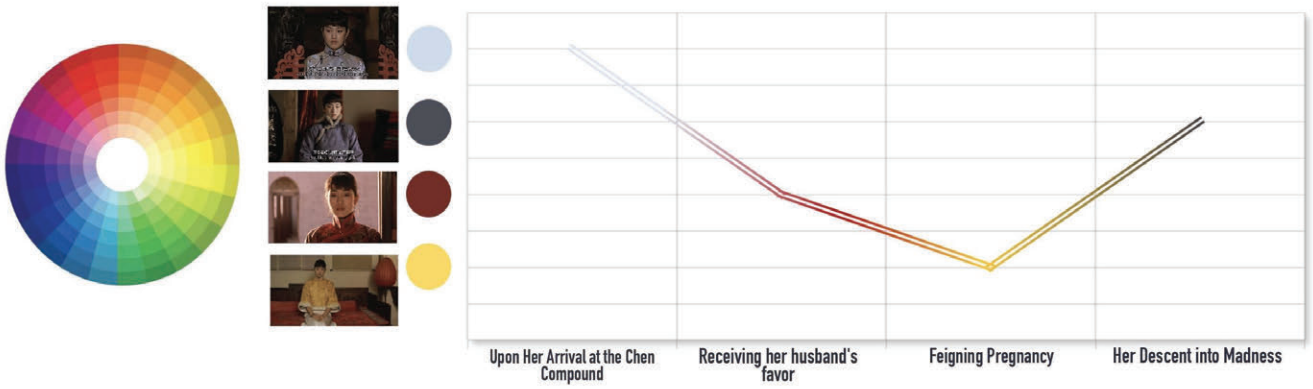

Figure 1:Songlian's Fate and Costume Color Trajectory by the authors

We have identified and arranged the important costume colors from the film in a clockwise order according to the color wheel, and use a clear timeline to sort out the fate twists and clothing colors of Song Lian in different plot points of the movie , also supplemented by movie images for a clearer presentation. This trajectory of costume colors, from light to dark, from cool to warm, and ultimately into silence,has become a symbolic representation of Songlian’s tragic journey from resistance to downfall.

In contrast, the cheongsam colors of Su Lizhen in In the Mood for Love exhibit a more complex and subtle emotional narrative function. The more than twenty cheongsams featured in the film not only replicate the urban aesthetics of 1960s Hong Kong but also serve as a delicate externalization of Su Lizhen’s inner world. Unlike the symbolic function of Songlian’s costume colors in indicating her fate, Su Lizhen’s costume colors naturally reveal her inner emotions: when she hides her feelings for Chow Mo-wan, she wears low-saturation colors such as dark red, forest green, and navy blue, paired with exquisite patterns, which align with her social identity as a secretary ,but also metaphorically expressing her repressed emotional stirrings. As her feelings for Chow Mo-wan intensify, vibrant warm tones appear in her cheongsam colors, while cool colors like dark purple dominate when she restrains her emotions. The following figure illustrates the changes in Su Lizhen’s costume colors and her corresponding psychological and emotional states in different scenes of In the Mood for Love. These subtle changes convey emotional narratives through color without the need for dialogue. It is noteworthy that Su Lizhen’s cheongsam colors are always set against dim lighting, rainy streets, and narrow corridors, creating a hazy and oppressive atmosphere that aptly conveys the reserved and repressed emotional aesthetics in the Chinese context.

Cinematic Imagery	Costume Color	Emotional Narrative
	PANTONE 4060 C (C30M91Y71K0) PANTONE 318 C (C50M0Y20K0)	The apprehension and anti cipation upon first arriving in Hong Kong
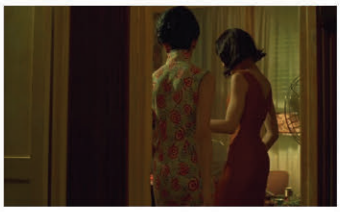	PANTONE 172 C (C0M85Y90K0) PANTONE 304 C (C44M1Y12K0)	The ease and relaxation af ter assimilating into life in Hong Kong
	PANTONE 4145 C (C89M85Y54K26) PANTONE 4241 C (C33M33Y48K0) PANTONE 3523 C (C53M89Y77K27) PANTONE 4224 C (C77M64Y78K34)	The inner conflict, restrain t, and forbearance felt as romantic feelings for Mr. Chow developed

	PANTONE 2271 C (C78M0Y99K0)	The palpitations and quiet elation in Mr. Chow's company
	PANTONE 2272 C (C81M21Y100K0) PANTONE 225 C (C13M92Y0K0) PANTONE 2070 C (C56M96Y0K0)	The ambiguous tension and tentative exploration teetering on the verge of infidelity between them
	PANTONE 697 C (C50M86Y68K13) PANTONE 6104 C (C96M87Y18K0)	The anguished struggle and profound resignation upon realizing the relationship was futile
	PANTONE 177 C (C0M63Y32K0)	The liberating sense of release upon overcoming adversity in the finale

Figure 2:Emotional and Costume Color Evolution in In the Mood for Lovey by the authors

The viewing experience of audiences also provides strong evidence for our research. The author selected 40 film enthusiasts who had watched both films to participate in the survey. Schurian once stated that the perceptual structure of a film is similar to that of the visual perception in daily life environments, but the perception and grasp of a film's meaning may differ from daily life environment due to the viewer's possible lack of active involvement in the film's storyline. Therefore, five foreign viewers were included in the survey to provide us withmore comprehensive information on the perception of costume colors in Chinese films. According to the survey summary below, the data clearly reveals two distinct color narrative modes and their psychological effects on the audience. Chinese viewers have a strong personal perception of the symbolic narrative of costume colors in Raise the Red Lantern. A staggering 95% of Chinese viewers reported feeling intense "oppression" and "suffocation" when watching scenes where Songlian is forced to wear red attire, rather than associating the color red with traditional celebrations and good fortune. However, among the five foreign viewers, three believed that red is a traditional Chinese wedding attire color and did not have strong perceptions or feelings about the

costume colors. The starkly different perceptions of the same color symbol (red) between Chinese and foreign viewers stem from differences in their underlying cultural systems and historical collective memories. For Chinese viewers, their "oppressive" interpretation of red in Raise the Red Lantern is not solely derived from the visual image itself but from a deep cultural context. This result fully demonstrates that the costume color narrative in Zhang Yimou's films is deeply rooted in his national cultural soil. Through the external imposition and forced use of costume colors, the narrative function focuses on symbolizing social critique and power relations, allowing most viewers to clearly perceive the tragic fate of Songlian. In stark contrast, the subtle emotional narrative of Su Lizhen's costume colors in In the Mood for Love is reflected in the questionnaire data, which shows that over 85% of Chinese viewers can perceive her "restraint and forbearance" through her cool-toned cheongsams, while their perceptions shift to "ambiguity and excitement" when warm-toned cheongsams appear. The perception of Su Lizhen's cheongsam colors is more nuanced and subconscious. For this film, the five foreign viewers shared a consistent emotional narrative resonance. Unlike the "red" symbol in Raise the Red Lantern, which relies on a specific cultural context, Wong Kar-wai constructs a more universal emotional grammar in In the Mood for Love. Although Su Lizhen wears traditional Chinese cheongsams, the core of the resonance lies deeper in a shared emotional narrative structure. The film's central theme revolves around memory, time, and missed emotions, which are universal themes that global audiences can understand and feel. This is why In the Mood for Love successfully resonates with cross-cultural audience in its costume color narrative.

CONCLUSION

The use of costume colors in the two films embodies two distinct narrative strategies: Raise the Red Lantern uses strong contrast as a symbolic narrative, with Songlian serving as a visual metaphor for oppression in feudal society; while In the Mood for Love presents emotional narratives through color, using costume colors to reflect the complex emotions naturally overflowing from Su Lizhen's inner world. Together, they reveal the multifaceted functions of costume colors in Chinese film narratives—they serve as both carriers of symbolic meaning and extensions of characters' emotions.

REFERENCES

[1]. Academy of Arts & Design, Chinese National Academy of Arts. (2016). Proceedings of the symposium on traditional Chinese color theory 2016. Culture and Art Publishing House.

[2]. Schurian, W., & Luo, D. (1998). Film psychology. Sichuan People's Publishing House.

[3]. Wu, X. (2023). Research on film color models and applications based on mathematical analysis. Guangming Daily Press.

Address: Dan Han,Northeast Normal University,

Academy of Fine Arts,ChangChun , China

E-mails:hd3256138@gmail.com

From Tang Sancai to Ink Painting: Cheng Shifa's Reinterpretation of Ceramic Glaze Aesthetics in Modern Chinese Art

Shan-shan Wang[a*], Keqiang Wang[b], andYinghe Xue[c]

[a]*Shanghai Business School, Shanghai, China*
[b.c]*Shanghai Hooyi, Shanghai, China*
[*]*Corresponding author: Shan-shan Wang, hooyix@qq.com*

ABSTRACT

Cheng Shifa, a renowned Chinese painter, holds an important position in the history of Chinese painting thanks to his unique artistic style. His works integrate traditional and modern elements, boasting distinctive personal traits, and stand out for their unique innovations particularly in color application.Tang Sancai, a representative of Tang Dynasty ceramic art, has exerted a significant influence on Cheng Shifa's artistic creation through its color elements. Cheng introduced the color expression of Tang Sancai into Chinese ink wash painting: he translated the colors of ceramics, the fluidity and sense of layering of ceramic forms, and the randomness of kiln transformation into visual expressions through the techniques of Chinese painting. This practice enabled him to achieve a cross-media color translation—from a material form (ceramics) to a two-dimensional form (ink wash painting)—reconstruct the traditional artistic language, and drive the innovation of color expression in Chinese painting.Against the backdrop of globalization, Cheng Shifa's color translation strategy not only expanded new directions for the application of colors in Chinese painting and reshaped the value of traditional aesthetics, but also accomplished the identity reconstruction of Chinese painting in the new context through cross-cultural dialogue and exchange. Ultimately, this exploration provides new insights for the contemporary transformation of traditional Chinese art.

Keywords:Cheng Shifa; Tang Sancai; Color Translation; Ink Wash Painting

INTRODUCTION

Tang Sancai (tri-color glazed pottery of the Tang Dynasty) is one of the representatives of ceramic art in the Tang Dynasty. It is not only beloved in China but also spread to all parts of the world via the Silk Road, exerting a profound influence on global ceramic art. Traditional Tang Sancai features yellow, green, and white as its main tones, and is divided into two types: porcelain body and pottery body [1] . Produced using low-temperature lead-glazed technology, it can present flowing color layers and rich visual effects.

Cheng Shifa's works cover a wide range of themes, including figures, landscapes, flowers, and birds. With his distinctive artistic style and unique color language, he has become one of the outstanding representatives in the field of Chinese painting.

Cheng Shifa's creations absorbed a variety of Chinese and foreign artistic styles, influenced by traditional art forms such as Shanghai School painting, folk art, and Tang Sancai, as well as Western painting. He emphasized that traditional art should be understood from a modern perspective and that simply "copying antiques" should be avoided. This way of thinking enabled him to maintain uniqueness in the innovation of Chinese painting and adhere to the modernity of artistic innovation. He also pointed out that the aesthetics of innovative art should avoid absolutism and maintain sensitivity to the balance between tradition and modernity. Since the 1950s, he has studied the characteristics of Tang Sancai's colors and applied them to the creation of Chinese ink wash painting, promoting the innovation of the color language of Chinese painting. He once mentioned that he was full of interest in Tang Sancai, and in his creation, he not only regarded it as a heritage of ancient art but also considered

how to transform it into a modern artistic expression. He made full use of the color system of Tang Sancai in his creations, producing works that not only embody the essence of traditional Chinese art but also integrate modern aesthetics [2] .

RESEARCH MOTIVATION AND SIGNIFICANCE

This study aims to explore the evolution of the cultural context behind Cheng Shifa's color practice, as well as the way in which the ceramic properties and glaze color language of Tang Sancai are translated into the system of Chinese painting. His color translation is not only a technological innovation but also the outcome of an in-depth dialogue between traditional Chinese art and modern artistic language. Against different historical backdrops, the application of Tang Sancai techniques to Chinese painting has endowed Chinese painting with new visual expressions, demonstrating the transformation and adaptability of traditional art in modern society.

The significance of this study lies in revealing the uniqueness of Cheng Shifa ' s color translation and exploring how this translation goes beyond simple formal imitation to exhibit its profound cultural and historical significance. In terms of color selection, Cheng Shifa not only inherits the tradition of Tang Sancai but also develops innovative expressions based on this tradition, promoting the artistic development of Chinese painting against the backdrop of globalization. This study helps to understand the development path of Chinese painting in modern society, as well as the transformation and innovation of traditional art in the contemporary cultural context.

RESEARCH OBJECTIVES

The objective of this study is to systematically analyze, from three dimensions—historical, technical, and aesthetic communication—how Cheng Shifa translated the color language of Tang Sancai into the expressive system of ink wash painting.

Cultural Context of Color Translation: This part analyzes how Cheng Shifa, against the social backdrop of China in the 20th century, responded to the construction of national cultural identity and the innovative needs of artistic ontology as well as individual artists through color translation. In particular, it explores how he developed innovative color expressions within the dual framework of political influence and national discourse.

Painting Techniques and Color Translation: This section examines how Cheng Shifa drew on the ceramic glaze color characteristics of Tang Sancai in his works, carried out innovations through appropriate painting techniques, and translated these characteristics into the color language of ink wash painting.

How Color Translation Promotes the Global Development of Chinese Painting: This part studies how Cheng Shifa, through the innovative application of Tang Sancai's color system, promoted the display and dissemination of Chinese painting on the global art stage and established new cross-cultural artistic dialogue.

Through this study, we will gain a comprehensive understanding of how Cheng Shifa, by virtue of Tang Sancai's color system, enabled his ink wash painting language to not only inherit traditional Chinese art but also find innovation and breakthroughs in the context of modern art—thereby providing new paths and perspectives for the future development of Chinese painting.

RESEARCH METHOD

1. Research Object and Data Source

The main object of the study is Cheng Shifa's works of art, especially his ink and wash paintings created from the 1950s to the early 21st century. The materials used include his original works, Tang Sancai ceramics, relevant documents, his own comments and the comments of art critics. These data provide a basis for the study of how he translated the glaze language of the Tang Tri Color into the color system of Chinese ink painting.

The original work was provided by Cheng Shifa Art Museum and collector Wang Keqiang, and the materials were from the works and papers about Cheng Shifa. The works of the tri colored pottery of the Tang Dynasty are mainly from the Shanghai Museum and the Chinese Archaeological Museum.

2. Research Methods:

Through specific painting cases, this study analyzes how Cheng Shifa translated the colors, flowing glaze characteristics, and contingency of kiln transformation of Tang Sancai into the color language of ink wash painting. Regarding color contrast, color data from his works will be extracted using color software for statistical analysis.

(1) Literature Collection and Work Analysis:

Collect materials on Cheng Shifa’s artistic creation background, the color characteristics of Tang Sancai, and relevant art reviews to provide a theoretical framework for subsequent research. In particular, organize and summarize his own views on Tang Sancai and color translation.

Analyze the colors in Cheng Shifa ’ s works, with a focus on studying how he reproduced the color characteristics of Tang Sancai through techniques that mimic flowing glaze and kiln transformation.

(2) Interviews and Expert Analysis:

By interviewing academic researchers of Cheng Shifa, art critics, and color science experts, this study gains in-depth insights into his creative intentions in color application and the cultural context of his time, so as to further verify the research findings.

Key Interviewees:

Cheng Duoduo (*Painter, Son of Mr. Cheng Shifa, Honorary Director of the Cheng Shifa Art Museum*)

Zhao Peisheng (*Professor, Vice President of the Shanghai Chinese Ceramic Artists Association*)

Chen Hao (*Deputy Director of the Cheng Shifa Art Museum*)

Zhou Xian (*Chinese painter*)

RESEARCH CONTENTS

1. The Cultural Context of Cheng Shifa’s Color Translation

Cheng Shifa’s translation of Tang Sancai’s colors was not a mere imitation of form, but was deeply rooted in the specific social and cultural context of China in the 20th century. During this period, the development of Chinese art was simultaneously influenced by both the political environment and national culture. Artists needed to respond to the ideological requirements of the state while exploring ways to integrate tradition and modernity, in order to open up new artistic spaces. He chose Tang Sancai as the object of translation precisely because it not only represents the glorious memory of the prosperous Tang Dynasty civilization, but also exhibits a high degree

of visual expressiveness through its unique glaze color language—thus serving as a bridge between national cultural symbols and modern artistic innovation.

(1) Expression in the Context of the Times:

In the mid-20th century, the cultural and artistic policies of New China emphasized that artistic creation should serve society, and followed guiding principles for cultural and artistic work such as "Let a hundred flowers bloom and a hundred schools of thought contend" and "Make the past serve the present and foreign things serve China." These policies advocated inheriting and absorbing all beneficial knowledge and culture at home and abroad, and emphasized the use of modern science and culture to organize China's excellent cultural heritage, so as to "create a socialist national new culture." In this political context, artists were inevitably influenced by ideology. As a typical example of Tang Dynasty art, Tang Sancai became one of the most important material carriers for understanding the great Tang Dynasty and interpreting its prosperous era. Regarded as a symbol of national glory, it possesses a strong cultural identity attribute. By introducing the glaze color language of Tang Sancai into the system of Chinese painting in his creations, Cheng Shifa not only complied with the state's advocacy for nationalized art, but also injected into traditional painting the sense of historical depth and cultural continuity expected by the political context [3].

(2) The Construction of National Cultural Identity:

In the process of constructing national cultural identity, how to achieve innovation while inheriting tradition was a key issue facing artists. Due to its harmonious color system and the magnificent momentum of the prosperous Tang civilization, the color language of Tang Sancai was endowed with the significance of symbolizing the spirit of Chinese aesthetics. Cheng Shifa did not rigidly adhere to archaeological reproduction; instead, through techniques such as splash-color, color collision, and washing, he translated the contingency and fluidity of Tang Sancai into ink wash painting, thereby creating a painting style that combines traditional spirit with modern flair. This color strategy not only continued the cultural foundation of national art, but also, through modern visual transformation, responded to the need for cultural identity reconstruction in 20th-century Chinese society.

(3) The Needs of Artistic Ontology and Individual Artistic Innovation:

The cultural diversity brought about by the reform and opening-up policy allowed art to gradually break away from its single attribute as a political instrument, and artists gained greater space for personal exploration. Against this background, Cheng Shifa elevated the color language of Tang Sancai to the level of artistic ontological innovation. Through cross-media color translation, he transformed the harmony, fluidity, and contingency of Tang Sancai's glaze colors into expressive means for ink wash painting. This translation broke through the traditional limitations of Chinese painting in terms of color, enabling his works to maintain a unique tension between figuration and abstraction, and exhibit a high degree of experimentality and modernity. His exploration was not only an inheritance of Tang Sancai, but also a re-creation of its color system—turning the traditional color system into a new type of visual symbol in the context of contemporary art, and bringing his artistic creation to its peak.

Cheng Shifa's translation of Tang Sancai's colors was driven by threefold forces: political influence, the construction of national culture, and the innovation of artistic ontology. At the political level, he used Tang Sancai to respond to the state's call to "organize China's excellent cultural heritage"; at the cultural level, he strengthened national identity and cultural confidence through the re-creation of Tang Sancai's colors; at the artistic level, he broke through the color limitations of ink wash painting by means of techniques such as splash-color and fluidity, forming a painting system that integrates Oriental aesthetics with modern experimental spirit. It can be seen that His color translation is not only a technical experiment, but also a manifestation of cultural strategy. It not only promoted the modernization process of Chinese painting, but also established new visual symbols and discourse power for Chinese art in the context of globalization.

2. Painting Techniques and Color Translation

In his creations, Cheng Shifa paid special attention to the harmony of colors, flowing glaze, and kiln transformation characteristics of Tang Sancai, translating these features into the color expression of ink wash painting. Through in-depth research on the glaze colors of Tang Sancai, he demonstrated unique artistic charm in the selection and application of colors.

(1) Color Contrast Analysis

This study selects the Tang Sancai ceramic work *Camel Carrying Musicians Figurine* and Cheng Shifa's *Mulan Joins the Army* for color comparison, focusing on the analysis of their main colors. The Tang Sancai *Camel Carrying Musicians* Figurine takes ochre, yellow glaze, and green glaze as its main tones, supplemented by a small amount of black and off-white. It features high color saturation, creating a strong visual impact.

Figure 1:Color Comparison(Camel Carrying Musicians Figurine and Cheng's Mulan Joins the Army)

In *Mulan Joins the Army*, while retaining the unique gray-scale layers of ink wash painting, he consciously incorporated the color composition of Tang Sancai: the reddish-brown of the horse echoes the ochre tone of the Tang Sancai camel; the pale green of Mulan's battle robe and the cyan-gray of the flying birds reflect the green glaze commonly seen in Tang Sancai; and the yellow and earthy tones dotted in the painting maintain a corresponding relationship with the yellow glaze of Tang Sancai.

The contrast between reddish-brown and ink black highlights the characters' martial demeanor, while the combination of green and yellow balances the cold-warm tones of the composition. This makes the overall painting not only possess the sense of profundity of Tang Sancai, but also retain the fresh and moist atmosphere of ink wash painting. Such compatibility in color application established a new aesthetic connection in his works between tradition and modernity, as well as between craftsmanship and painting.

(2) Flowing Glaze Characteristics and Color Layering

Cheng Shifa drew inspiration from the flowing glaze of Tang Sancai, and recreated its artistic charm through the fluidity and layering of colors. In depicting figures and landscapes, he excelled at applying an effect similar to the natural flow of Tang Sancai's glaze surface, allowing colors to present a sense of gradation and transition on rice paper. Particularly in the creation of large-scale paintings, Cheng further tilted the painting board to let ink

flow freely—a technique that shares a similar artistic effect to the natural seepage and superposition of Tang Sancai's glaze colors.

Figure 2:Tang Sancai

Figure 3:Cheng Shifa Painting

In his *Deer Garden in Eternal Spring* , he used extensive color washing on the deer's bodies and the clothing folds of court ladies, making colors flow downward in large areas and endowing the painting with a warm and smooth textural flowing rhythm. This technique not only avoids the rigid division of colors but also enhances the sense of space and layering in the work.

On the deer's tails, he applied large-area ink washing and subtle gradational blurring, creating an effect as if glaze was slowly flowing on the pottery surface, forming natural stacking and fusion. Meanwhile, the color superposition on the folds and belts of the court ladies' costumes echoes the blending effect of Tang Sancai's glazes in green, yellow, brown, and other colors—revealing an aesthetic style that combines Oriental classical beauty with the free spirit of modern brushwork. This is an artistic translation of Tang Sancai's glaze characteristic of "flowing without disorder."

Figure 4: Deer Garden in Eternal Spring

Figure 5: Cai Wenji

This experiment of using paper as a substitute for pottery transformed the fluidity of Tang Sancai from a three-dimensional artifact into a two-dimensional painting language. He employed the same technique in his work Cai Wenji: although the figure's dress uses only a limited number of colors, the flowing and dissolving of colors creates a rich visual effect [4].

Figure 6: Flowers in a Vase

Transplanting the "flowing" artistic language of Tang Sancai into rice paper painting not only broke through the flattened pattern of traditional meticulous heavy-color painting but also transcended the model of relying solely on line outlining. Through this method of "color and ink merging, flowing into form," the painting presents an artistic tension that lies between figuration and abstraction.

(3) The Accidental Aesthetics of Kiln Transformation

The kiln transformation effect of Tang Sancai is a crucial component of its unique charm. Cheng Shifa skillfully drew on this effect in his creations, employing techniques such as splash-color and stain-dyeing to simulate the contingency and irregularity of glaze colors generated during the kiln transformation process. In his *Flowers in a Vase*, Cheng recreated the accidental aesthetics of Tang Sancai's glaze colors through the layering and natural flow of colors, transforming traditional colors into an artistic language with a modern feel.

During the high-temperature firing of Tang Sancai, factors such as temperature variations, glaze thickness, and reactions of mineral components often result in natural and integrated color textures that flow and overlap on the pottery surface. This contingency involves irreproducible random changes, embodying unique aesthetic value. In *Flowers in a Vase*, Cheng translated this "contingency" into the free seepage and diffusion of brushwork, ink, and water-based colors: the large areas of ink green, dark cyan, and ochre on the lotus leaves seep into and blend with each other, while the blurring at the edges creates a texture with rich layers — resembling the natural formation of glaze colors in a kiln fire; the overlapping transition of pink, yellow, and cyan on the lotus petals is precisely a painterly reproduction of the colorful, flowing, and blending hues of Tang Sancai's kiln transformation.

This simulation is not a mere imitation but an artistic refinement. By leveraging the absorbency and permeability of rice paper and ink wash, Cheng Shifa reconstructed the accidental spectacle of Tang Sancai's "color formation in fire," thereby presenting an accidental beauty on the two-dimensional canvas that is comparable to the kiln transformation of ceramics. Like Tang Sancai, his works emphasize unpredictable aesthetic generation, endowing the paintings with an irreproducible uniqueness. This translation of the contingency of kiln transformation allowed his paintings to break free from the linear arrangement of colors and embody the aesthetic spirit of "coloring according to category" in Oriental art [5]

Research Dimension	Expression of Tang Sancai	Translated by Cheng Shifa	Academic Significance
Color Contrast	It takes yellow, green, and brown as the dominant color palette, featuring high color saturation and overall harmony.	Cheng incorporates reddish-brown, green, and yellow, and integrates with ink black, creating echoes between cold and warm tones.	Cheng reorganizes the traditional color system and achieves the modern transformation of traditional colors.
Fluidity	The glaze colors flow naturally, with gradational transitions between layers, embodying the effect of "flowing without disorder".	Cheng creates color gradation by means of techniques such as splash-ink, washing, and tilting the painting board.	Cheng achieves cross-media transformation and enhances the sense of space and layering in the painting.
The Contingency of Kiln Transformation	During high-temperature firing, unpredictable glaze color changes occur due to temperature differences and glaze reactions, forming the "kiln transformation aesthetics".	Cheng employs splash-color and stain-dyeing to create natural seepage and accidental textures.	Cheng embodies the Oriental aesthetic spirit of "being formed spontaneously" and transforms contingency into creative value.

3. Cheng Shifa's Color Translation and the Global Development of Chinese Painting

Cheng Shifa once stated: "Chinese painting must possess nationality and contemporaneity" and "We must assimilate and integrate these outside elements, not be assimilated or lose our essence to them." This assertion not only emphasizes the importance of Chinese painting preserving its cultural roots in the process of modernization but also reveals his in-depth understanding of the relationship between tradition and modernity in artistic practice. He also emphasized: "What matters for artists is to bring beauty to humanity, collectively envision a better life, and thereby expand this into humanity's overall pursuit of the realm of beauty." [6]

Spreading the art of Chinese painting to the world was a pursuit shared by Cheng Shifa and many other artists. In choosing forms of dissemination, he leveraged the influence of Tang Sancai elements to enhance the global readability of his works, providing a crucial direction for researching the modern innovation and cross-cultural communication of Chinese painting.

(1) Tang Sancai as a Cross-Cultural Visual Symbol

Before the Tang Dynasty, only monochromatic glazes were generally used in pottery-making techniques, and it was already rare to use two types of glazes on a single artifact. By the Tang Dynasty, frequent foreign trade and cultural exchanges in China led to growing inclusiveness toward foreign cultures in Tang society, and people's aesthetic perspectives also underwent significant changes accordingly. [7]

Since the Tang Dynasty, Tang Sancai has spread to Central Asia, Western Asia, and even Europe via the Silk Road, becoming one of the most recognizable Chinese artistic images worldwide. The Tang Sancai of the prosperous Tang Dynasty, characterized by distinct glaze color layers and high fluidity, to a certain extent also reflects the vibrant, passionate temporal vibe of the flourishing Tang era, and is highly romantic. [8] Its color system, dominated by yellow, green, and brown, along with the flowing effect of its glazes, not only embodies the unique aesthetics of Oriental art but also has formed a lasting visual memory in cross-cultural exchanges. By

introducing this traditional color system into Chinese painting, Cheng Shifa endowed his works with an inherent "cross-cultural symbol" attribute, thus laying a visual and semantic foundation for the dissemination of Chinese painting in the context of globalization.

(2) From Traditional Material Memory to Modern Color Language

Cheng Shifa's absorption and re-creation of Tang Sancai were not mere imitation, but an innovative practice based on the linguistic system of Chinese painting. In works such as *Deer Garden in Eternal Spring, Flowers in a Vase, and Mulan Joins the Army*, he integrated the contingency of Tang Sancai's glaze colors and the aesthetics of kiln transformation into ink wash creation, forming a visual style of "color and ink merging, flowing into form." This method broke through the limitation of traditional Chinese painting's emphasis on ink tones, expanded the space for color expression, and endowed his works with stronger visual impact and modernity—allowing them to engage in dialogue with the aesthetic system of international modern art.

(3) Cross-Cultural Artistic Dialogue and Exchange

In the process of Chinese art "going global" in the 20th century, Cheng Shifa's color translation provided an effective model of "cultural translation." He had visited Japan, the United States, Singapore, Australia, and other countries, where he gave lectures and held art exhibitions, enabling his artistic practice to be directly presented and exchanged in multicultural environments. Through the re-combination and artistic processing of Tang Sancai's colors, the visual language of Chinese painting became more accessible and understandable to international audiences. As a globally shared cultural symbol, Tang Sancai endowed Cheng Shifa's works with cross-cultural readability, while the uniqueness of ink wash techniques preserved the local identity of Chinese art. This dual attribute allowed his works to embody both "Chineseness" and "modernity," thereby gaining recognition in the global art context.

(4) The Identity Reconstruction of Chinese Painting in the Context of Globalization

The significance of Cheng Shifa's color translation lies not only in expanding techniques and expressiveness but also in promoting the identity reconstruction of Chinese painting on the global art stage. By combining Tang Sancai with ink wash, he constructed a color system that integrates the depth of Oriental aesthetics and universal international visual traits—transforming Chinese painting from a mere continuation of Oriental classical art into a modern visual expression that can stand alongside global art. His experience of giving lectures and holding exhibitions overseas not only allowed international audiences to intuitively perceive the unique charm of Chinese painting but also provided a practical platform for cross-cultural artistic dialogue, demonstrating the adaptability and openness of Chinese painting in the context of globalization.

In summary, through the translation of Tang Sancai's colors and his academic and exhibition practices on the international stage, Cheng Shifa achieved innovations in the form, technique, and global communication strategy of Chinese painting. His practice used Tang Sancai as a bridge to connect traditional Chinese art with the modern international context, highlighting the important role of cultural translation in the globalization of art and enhancing the discourse power of Chinese painting in global art.

CONCLUSION

This study demonstrates that through the systematic translation of Tang Sancai's colors, Cheng Shifa achieved innovation and expansion of Chinese painting across three dimensions: technique, visual effect, and cultural expression.

In terms of technique, by translating the colors, flowing glaze characteristics, and contingency of kiln transformation of Tang Sancai, he reconstructed the color system of ink wash painting, endowing his works with both a sense of historical depth and modern tension.

In terms of visual effect, he employed a variety of painting techniques to transform traditional material colors into two-dimensional, cross-culturally intelligible symbols, enhancing the international communicability of Chinese painting.

In terms of cultural expression, he integrated the artistic memory of Tang Sancai with modern aesthetics, realizing the organic integration of traditional aesthetics and modern spirit.

Cheng Shifa's practice not only promoted the modernization process of Chinese painting in the context of globalization but also serves as a model for the contemporary transformation of traditional art, cross-cultural communication, and cultural identity construction. This study reveals the multi-dimensional value of color translation as an artistic innovation strategy, and provides a new theoretical perspective and practical paradigm for understanding the development path of Chinese painting in the modern and global context.

REFERENCES

(1) Li,H.X.and Qin,D.S.（2022）. Review and Discussion on the Research of Tang Sancai Wares .A Collection of Studies on Archaeology,14(02),174

(2) Cheng Shifa Art Museum.(2011)Cheng Shifa's Talks on Painting,1nd. Ed.,Shanghai People's Fine Arts Publishing House. 68-69

(3) Li,M.Q.and Li,Y.J.（2021）. The Party's Literary and Artistic Guidelines and a Century of Literary and Artistic Innovation Practices. Retrieved July 3, 2025, from https://www.artsc.gov.cn/portal/article/index/id/8096.

(4) Chen,H.（2017）. The Artistic Conception of Brush and Ink and the Pursuit of the Times in Cheng Shifa's Chinese Freehand Figure Painting in Ink and Wash .The World of Chinese Painting & Calligraphy,2017(02),29.

(5) Chi,K.（1979）. On the Art of Painting by Cheng Shifa.Literature & Art Studies,1979(03),87

(6) Cheng Shifa Art Museum.(2011)Cheng Shifa's Talks on Painting,1nd. Ed.,Shanghai People's Fine Arts Publishing House.92

(7) Zhou,H.D.（2013）. Art of Tri-Coloured Glazed Pottery of the Tang Dynasty.Hundred Schools in Arts,2013(7),228

(8) Zhao,D.（2019）. Review and Discussion on the Research of Tang Sancai Wares .Identification and Appreciation to Cultural Relics,2019(23),66

The Influence of Similarity on Color Harmony and Preference

Hyemi Rho, YungKyung Park*

Ewha Womans University , Seoul, Republic of Korea
**Corresponding author: yungkyung.park@ewha.ac.kr*

ABSTRACT

This study investigates how chroma similarity shapes color harmony and preference in multicolor combinations. Forty pairs of color stimuli were systematically generated within the CIELAB color space, and participants judged harmony and preference using a forced choice paradigm. Results indicate that lower chroma levels generally yield combinations that are both more harmonious and more preferred, although the two judgments do not always coincide. Low chroma pairs consistently received higher harmony ratings, underscoring the pivotal role of chroma similarity in achieving harmony. By contrast, higher chroma reduced interobserver rating consistency and lowered subjective preference. Taken together, these findings provide clear evidence that calibrating chroma is critical for enhancing visual satisfaction in color design.

Keywords: Color Harmony, Color Preference, Color Attributes, Similarity, Visual Perception

INTRODUCTION

The human visual system inherently seeks equilibrium, making color harmony a central theme in perception and design. Historical and modern theories—from Goethe's symmetry, Munsell's balance of brightness and saturation, Ostwald's proportional model, to Moon and Spencer's (1944) mathematical approach, Itten's contrast theory, and Nemcsics' Coloroid system—show that harmony arises from hue, lightness, chroma, spatial relations, and contextual interaction. Among these, chroma plays a pivotal role in perceptual quality and emotion. Studies demonstrate that increasing chroma enhances vividness, arousal, and pleasantness (Fedorovskaya et al., 1996; Wilms & Oberfeld, 2017; Gao & Xin, 2006), though excessive saturation reduces naturalness and harmony. While most research has focused on single colors, real environments involve multicolor contexts where harmony depends on chroma similarity, hue proximity, and lightness differences (Ou et al., 2010). Cultural and psychological influences further shape perception and preference (Elliot & Maier, 2009; Schloss et al., 2012). Building on this foundation, the present study examines how chroma similarity influences harmony and preference in multicolor combinations, aiming to deepen theoretical understanding and provide practical guidelines for design, marketing, and psychology.

METHODOLOGY

This study examined how chroma similarity in multicolor pairs influences judgments of harmony and preference. Stimuli consisted of forty pairs of three adjacent color squares, parametrically varied in C* within the CIELAB space. LCh coordinates were obtained from monitor-rendered colors and are reported in Table 1. All stimuli were displayed on a mid-gray background (L* = 50). Eight graduate students in color design at Ewha Womans University participated. A forced-choice paradigm was employed: on each trial, two color pairs were shown and participants selected the more harmonious or preferred pair, even when differences were subtle. Harmony and preference were assessed in separate sessions, with an additional combined session to compare judgments directly. An example stimulus screen is shown in Figure 1. This design enabled systematic testing of

chroma similarity effects, providing empirical evidence and practical implications for multicolor design applications.

Figure 1: Experimental Stimuli

Table 1: Color Stimulus Values of 40 Color Pairs in CIELAB

Numbers	L	C	h	L	C	h	L	C	h
1	54	28	277	72	33	122	64	30	65
2	38	47	11	65	47	70	54	46	163
3	38	11	236	41	11	141	74	11	71
4	44	55	32	42	54	284	66	54	115
5	35	36	282	83	34	95	60	33	27
6	84	13	172	30	14	40	34	16	265
7	87	27	86	43	27	232	32	28	28
8	57	23	11	38	24	217	57	23	75
9	39	31	171	58	30	77	70	29	21
10	69	41	40	53	42	99	32	42	296
11	81	20	13	52	20	209	64	21	80
12	65	2	115	91	3	150	86	3	47
13	73	8	152	40	9	85	46	10	47
14	81	20	13	54	22	243	64	21	80
15	79	36	154	39	37	346	35	36	282
16	70	53	153	67	52	102	45	52	29
17	32	42	296	43	42	337	53	42	99
18	30	20	315	48	22	251	57	23	75

19	54	53	2	42	54	284	66	54	115
20	59	12	190	74	11	71	28	11	264
21	69	18	220	55	18	156	50	19	48
22	61	38	271	39	37	436	79	36	154
23	47	51	309	53	51	355	67	52	102
24	87	27	86	43	27	232	70	29	21
25	53	50	26	47	51	309	70	53	153
26	74	39	135	46	40	52	43	42	337
27	33	23	294	57	23	11	57	23	75
28	79	36	154	39	37	346	35	36	282
29	32	12	191	82	11	118	74	11	71
30	69	18	220	55	18	156	30	18	10
31	69	41	40	32	42	296	43	42	337
32	83	34	95	62	34	188	60	33	27
33	39	31	171	58	30	77	43	31	34
34	30	20	315	81	20	13	64	21	80
35	42	54	284	54	53	2	59	54	22
36	66	14	153	34	16	265	30	14	40
37	34	16	265	30	14	40	46	16	136
38	52	29	136	87	27	86	70	29	21
39	79	36	154	83	34	95	35	36	282
40	51	39	147	46	40	52	61	38	271

RESULTS AND DISCUSSION

Figure 2 shows that color harmony was consistently higher at lower chroma levels, while average harmony scores decreased as chroma increased. Low-chroma ranges displayed smaller variance and greater consistency, whereas higher chroma levels resulted in less consistent evaluations with larger standard deviations. These patterns persisted across both harmony-only and combined evaluation conditions, although harmony scores were slightly lower when harmony and preference were judged simultaneously.

Figure 3 illustrates that color preference also decreased with increasing chroma, demonstrating a negative correlation. The decline in preference was steeper when harmony and preference were judged simultaneously, suggesting contextual influence on evaluation. Again, low-chroma ranges showed greater consistency, whereas high-chroma conditions produced higher variability.

Figures 4 and 5 further demonstrate that both harmony and preference declined with chroma. Preference decreased more sharply, while harmony declined more gradually. At low chroma, both harmony and preference

were rated high with stable judgments, whereas at high chroma, both measures declined and evaluations became less consistent.

This study confirms chroma as a critical determinant of harmony and preference in multicolor combinations. While high chroma enhances vividness and arousal (Wilms & Oberfeld, 2017; Gao & Xin, 2006), excessive saturation reduces naturalness and induces disharmony (Fedorovskaya et al., 1996). By contrast, low-chroma combinations foster visual balance and coherence. Prior research highlights the importance of balance: Moon and Spencer (1944) noted equilibrium from large low-chroma areas with smaller high-chroma accents; Gong and Lee (2019) found that moderate sums of lightness and chroma maximize harmony; Ou et al. (2018) confirmed that harmony depends on chroma, hue, and lightness similarity. Cultural contexts further complicate evaluation: low-chroma colors are preferred in Japan and Korea (Saito, 1996), while higher chroma is favored in China and Malaysia. Moreover, Schloss and Palmer (2010) showed that harmony and preference diverge, with preference shaped by subjective and contextual factors. Overall, the findings underscore the need to distinguish between harmony and preference in design practice. Adjusting chroma to moderate, balanced ranges can enhance harmony, but preference requires consideration of cultural and situational contexts.

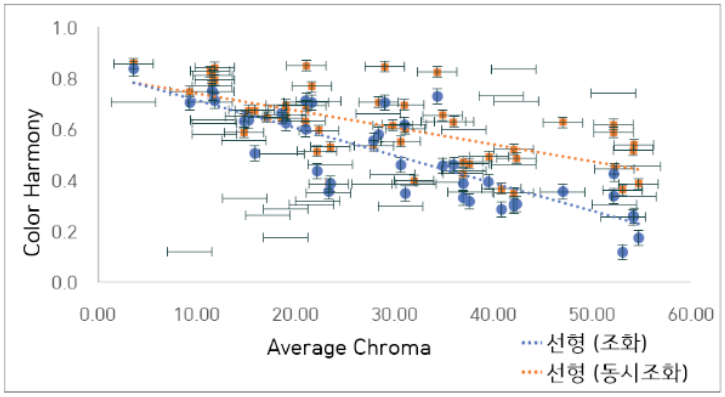

Figure 2 : The Relationship Between Average Chroma and Color Harmony

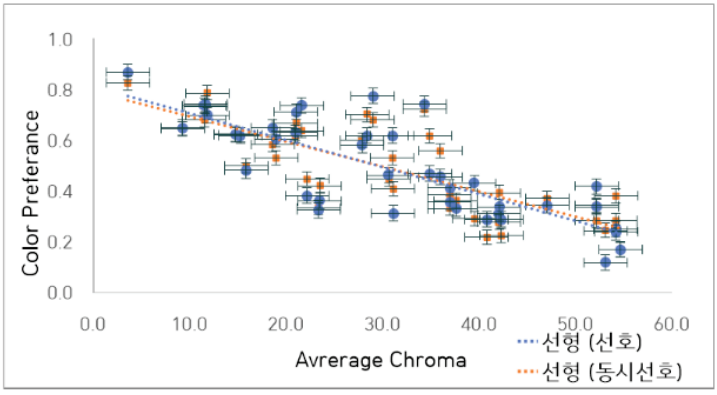

Figure 3 : The Relationship Between Average Chroma and Color Preference

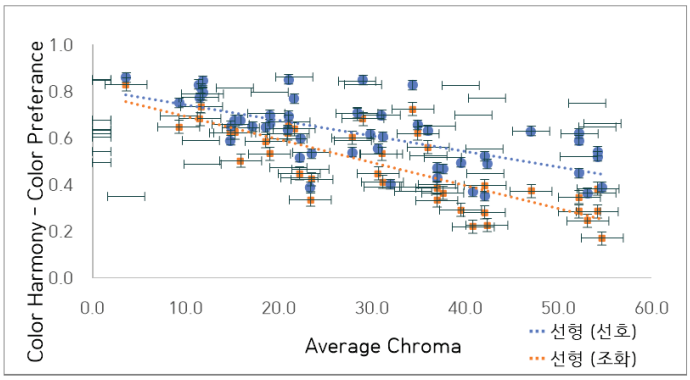

Figure 4 : The Relationship Between Average Chroma and Color Harmony - Color Preference

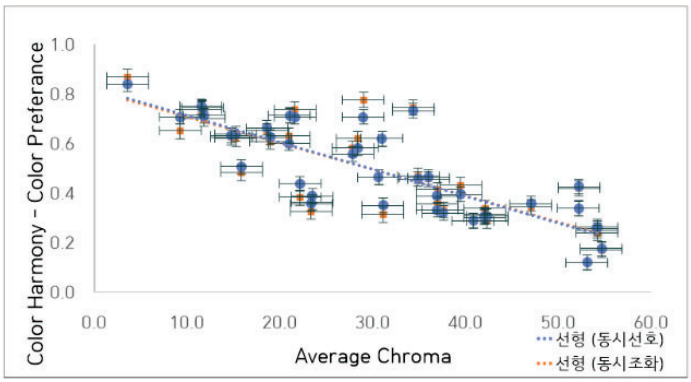

Figure 5 : The Relationship Between Average Chroma and Color Harmony - Color Preference

CONCLUSION

This study demonstrates that chroma similarity plays a decisive role in shaping color harmony and preference in multi-color combinations. Lower chroma levels generally produced more harmonious and preferred combinations, whereas high chroma reduced consistency and preference. Importantly, harmony and preference judgments did not always align, confirming that these are related but distinct dimensions. The findings highlight the necessity of chroma adjustment in multi-color design and provide empirical evidence to guide applications in design, marketing, and psychology.

REFERENCES

[1]. Wilms, L., & Oberfeld, D. (2017). Color and emotion: Effects of hue, saturation, and brightness. *Psychological Research, 82*(5), 896–914.

[2]. Gao, X.-P., & Xin, J. H. (2006). Investigation of human's emotional responses on colors. *Color Research and Application, 31*(5), 411–417.

[3]. Fedorovskaya, E. A., de Ridder, H., & Blommaert, F. J. J. (1996). Naturalness and image quality: Chroma and hue variation in color images of natural scenes. Proceedings of the SPIE, 2411, 170–176.

[4]. Moon, P., & Spencer, D. E. (1944). Area in color harmony. *Journal of the Optical Society of America, 34*(2), 93–103.

[5]. Gong, S.-M., & Lee, W.-Y. (2019). Colour harmony of two-colour combinations using a 3D colour configuration. *Coloration Technology, 135*(4), 292–304.

[6]. Ou, L.-C., Chong, P., Luo, M. R., & Minchew, C. (2010). Additivity of colour harmony. *Color Research & Application, 36*(5), 355–372.

[7]. Ou, L.-C., Yuan, Y., Sato, T., Lee, W.-Y., Szabó, F., Sueeprasan, S., & Huertas, R. (2018). Universal models of colour emotion and colour harmony. *Color Research & Application, 43*(5), 736–748.

[8]. Elliot, A. J., & Maier, M. A. (2012). Color-in-context theory. In P. Devine & A. Plant (Eds.), *Advances in experimental social psychology*(Vol. 45, pp. 61–125). Elsevier.

[9]. Saito, M. (1996). Comparative studies on color preference in Japan and other Asian regions, with special emphasis on the preference for white. *Color Research & Application, 21*(1), 35–49.

[10]. Ou, L.-C., & Luo, M. R. (2006). A colour harmony model for two-colour combinations. Color Research & Application, 31(3), 191–204.

[11]. Burchett, K. E. (2002). Color harmony. Color Research & Application, 27(1), 28–31.

[12]. Schloss, K. B., & Palmer, S. E. (2011). Aesthetic response to color combinations: Preference, harmony, and similarity. Attention, Perception, & Psychophysics, 73(3), 551-571.

[13]. Ou, L.-C., Luo, M. R., Sun, P.-L., Hu, N.-C., & Chen, H.-S. (2010). Age effects on colour emotion, preference, and harmony. Color Research & Application, 37(2), 92-105.

[14]. Schloss, K. B., Strauss, E. D., & Palmer, S. E. (2012). Object color preferences. Color Research and Application, 38(6), 393–411.

Color as Ingredients: A Material-Driven Design Approach to Natural Pigments in Sustainable Baked Goods

Tzu-Jung Wang[1], Tsuei-Ju Hsieh[2]

[1]Department of Arts & Design, National Tsing Hua University, Hsinchu, Taiwan
[2]Department of Arts & Design, National Tsing Hua University, Hsinchu, Taiwan
emily040422@gapp.nthu.edu.tw
hsiehtj@mx.nthu.edu.tw

ABSTRACT

This study employs a Material-Driven Design (MDD) approach to integrate natural pigments into 3D-printed okara cookies and to quantify how color appearance modulates consumer expectations. Ten pigments were tested at three concentrations (0.5/1/2 g per 100 g dough) and baked at two oven setpoints (120 °C vs. 190 °C). Under D50 viewing, instrumental color was measured with a 45°/0° spectrophotometer (CIELAB; ΔE00), complemented by standardized image capture. An affective study (N=85) rated samples on perceived naturalness, healthiness, expected sweetness, and attractiveness (7-point scales), and performed five paired comparisons between 120 °C and 190 °C (excluding "no-difference" responses for inference). Across 30 pigment–concentration pairs, baking at 190 °C produced ΔE00=2.24 (SD=1.77; 95% CI [1.60, 2.87]) relative to 120 °C, with mean component shifts of ΔL=+0.50, Δa*=+0.58, Δb*=+2.65 and ΔC*=+2.33, indicating a tendency toward more yellowish/reddish, slightly higher-chroma appearances rather than uniformly darker luminance. In paired comparisons, 190 °C samples were more often judged natural (62.8% vs. 37.2%), healthy (60.2% vs. 39.8%), and appetizing (72.3% vs. 27.7%) than 120 °C (binomial p<.001; Cohen's h=.41–.92), whereas expected sweetness did not differ (52.5% vs. 47.5%; p=.42; h=.10). The results yield a color-as-ingredient playbook for food design: to enhance perceived healthiness/naturalness, designers can steer toward "baking-golden" vectors (b↑, a*↑, C*↑) via thermal parameters rather than relying on synthetic dyes. For food-and-health education, the workflow scaffolds hands-on modules in which students valorize okara while learning how instrumental color shifts shape cross modal expectations. In innovative dessert experience services, 3D printing enables mass personalization of color-form-texture; coupling our appearance targets with menu-level previews and simple ΔE00 control bands can standardize kitchen workflows and communicate sustainability cues without sacrificing visual appeal. Together, these contributions position natural pigments as active design materials that bridge sustainable ingredients, measurable appearance control, and consumer-centric experiences in future food systems.

KeyWords: material-driven design, natural food colorants, color-taste congruency, 3d food printing, sustainable food innovation

INTRODUCTION

Color appearance is a primary visual cue in food that shapes flavor expectations, palatability, and purchase intent (Spence, Levitan, Shankar, & Zampini, 2010) [1]. To design and compare such effects rigorously, standardized colorimetry—CIELAB (CIE L*a*b*) and ΔE_{00} under controlled viewing—provides a reproducible basis for measurement and reporting (CIE, 2018; Sharma, Wu, & Dalal, 2005) [2] [10]. In parallel, sustainability and digitalization are reshaping food innovation: valorizing okara (the fiber- and protein-rich

by-product of tofu) addresses waste while offering a functional matrix for baked goods (O'Toole, 1999) [3]; industry digital transformation and 3D food printing enable scalable mass customization of form and appearance (Demartini et al., 2018; Sun, Peng, Yan, Fuh, & Hong, 2015) [4] [5]. Although the global bakery sector continues to expand and consumer discourse emphasizes sustainability, health orientation, convenience, and experience design (BBM Magazine, 2025; Price, 2025) [6] [7], adopting natural colorants in place of synthetic dyes raises a well-known stability–perception trade-off because many plant pigments are sensitive to pH and thermal processing (Sigurdson, Tang, & Giusti, 2017) [8]. Accordingly, this study focuses on integrating natural colorants into 3D-printed okara cookies by: (i) applying a Material-Driven Design (MDD) methodology to operationalize natural pigments as functional design materials in cookie dough (Karana, Barati, Rognoli, & van der Laan, 2015) [9]; (ii) quantifying how color modulates expectations of naturalness, healthiness, expected sweetness, and attractiveness; and (iii) examining how baking temperature interacts with color reproduction (CIELAB; ΔE_{00}) to shape preference.

METHODOLOGY

2.1 Materials preparation

All ingredients were food-grade. Butter: Anchor fermented unsalted butter. Okara powder: Shangyeo Okara Powder (lot recorded per batch). Egg yolk: separated from whole eggs (PX Mart). Soy milk: Uni-President "Yang Guang" high-fiber unsweetened soy milk. Sweetener: erythritol. Natural colorants (10 types, Caihong Natural Food Colorants): red yeast rice; gardenia red; gardenia red (A); anthocyanin-carrot; gardenia purple; anthocyanin-purple sweet potato; gardenia yellow; gardenia black; gardenia green; gardenia blue. Brand names are reported for traceability only.

A base okara cookie dough was prepared as follows: butter 20 g, erythritol 10 g, egg yolk 10 g, okara powder 50 g, plus soy milk q.s. to workable consistency. Butter and erythritol were creamed until homogeneous; egg yolk was incorporated in two additions; okara powder was folded in; soy milk was added gradually. For each condition the dough mass was normalized to 100 g. Natural colorants were dosed at 0.5 / 1.0 / 2.0 g per 100 g dough and mixed to uniformity (≥60 s at low speed), with bowl-scraping to eliminate streaks. The dough was rested 10–15 min at 4 °C to reduce spread, sheeted to 3.00 ± 0.05 mm (digital caliper), and cut into 50.0 ± 0.2 mm discs. Per pigment × concentration × temperature, n = 3 discs were reserved for instrumental colorimetry/imaging; additional discs were prepared for the perceptual study. Each disc received a randomized code for blind handling. Baking was performed in a preheated electric convection oven (setpoint accuracy ±2 °C), middle rack, on an anodized aluminum tray lined with parchment. Two setpoints were tested: 120 °C and 190 °C. To minimize confounding from unequal drying, batches were baked to a mass-loss endpoint of 11–13% (tray + specimen weighed before/after on a 0.01 g balance). Typical dwell times were shorter at 190 °C than 120 °C; exact times per batch were logged. After baking, samples cooled 30 min on a wire rack to ambient (22–25 °C) before measurements.

2.2 Color measurement and reproduction

Visual matching was conducted in a D50 viewing booth compliant with ISO 3664:2009 (neutral surround Munsell N5/N7, luminance uniformity ≤10%). Observers adapted for ≥2 min before assessments. PANTONE swatch matching was recorded as a supplementary descriptor; the primary analyses relied on instrumental colorimetry (ISO, 2009). Instrumental color was measured using an X-Rite i1Pro 45°/0° spectrophotometer with 2° standard observer and illuminant D50 (i1Profiler). The device was calibrated against the manufacturer's white tile before each session. For each disc, 3 non-overlapping locations avoiding pores/edges were measured through a black aperture mask (effective aperture ≈ 4.5 mm) and averaged to obtain CIELAB (L*, a*, b*). From these, C* and h were derived. Cross-temperature differences (190 °C vs. 120 °C) were summarized by component shifts (ΔL*, Δa*, Δb*, ΔC*) and ΔEcomputed per CIEDE2000 (CIE, 2018; Sharma, Wu, & Dalal, 2005) [10]. Images were captured in RAW format using a DSLR on a fixed tripod, lens axis normal (90°) to the specimen plane, under a

D50-simulated LED light source (CRI ≥ 95; symmetric 45°/45° arrangement to minimize specular). An X-Rite Color Checker Classic was included in every frame. Post-processing was performed in Adobe Camera Raw/Photoshop with: (i) camera-specific DNG/ICC profile generated from the chart; (ii) mid-gray patch used for white balance (rather than the white patch to avoid clipping); and (iii) identical tone/color transforms across images. This pipeline enabled calibrated menu-level previews and documentation while keeping instrumental colorimetry as the ground truth (ISO, 2009) [11].The Left part of Figure 1. shows Scatter of CIELAB a*–b* coordinates for all baked cookie samples (N = 60 pigment × concentration × temperature conditions). Each dot represents the meaning of three spot readings per disc, averaged across n = 3 discs per condition (D50, 2° observer; 45°/0° geometry). Right: Representative D50-calibrated photographs of cookies corresponding to selected points in the scatter (captured with the imaging pipeline in § 2.4.3). (Background hue wheel shown for orientation; L* not encoded.)

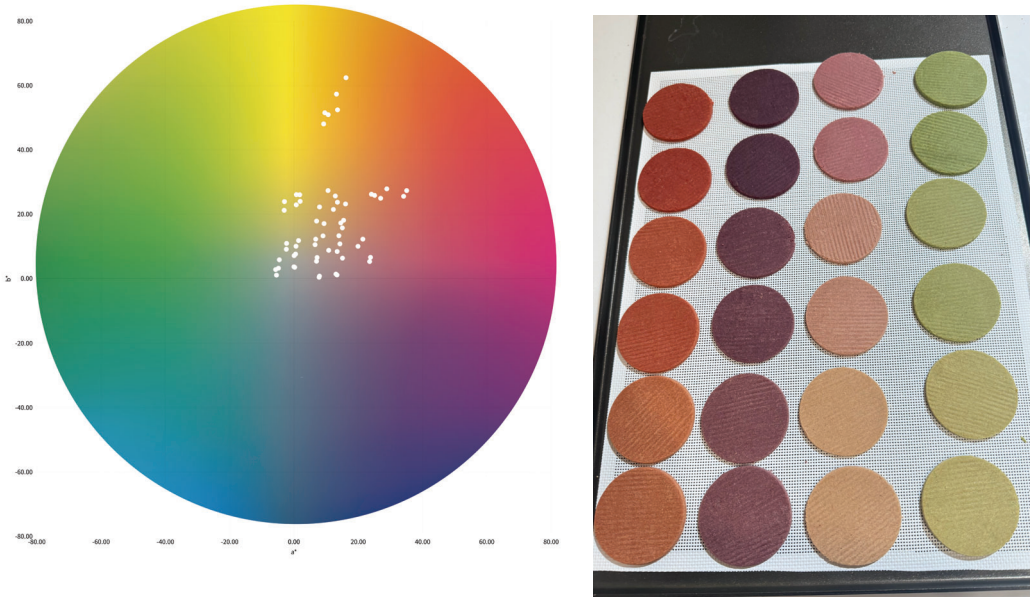

Figure 1: Scatter of CIELAB a*–b* coordinates for all baked cookie samples$\bar{A}$

2.3Assessment with affective questionnaire

There were 85 adult participants (campus/community), naive to the study aims, provided informed consent. Only visual judgments of cookie appearance were collected. Responses were anonymous and de-identified. Two stimulus sets were used: Single-temperature set: 10 cookies at 120 °C, 1.0 g/100 g pigment concentration (one per pigment). Paired-temperature set: 10 paired cookies at 1.0 g/100 g, each pair showing 120 °C vs. 190 °C for the same pigment. All stimuli were presented under the same D50 booth. Presentation order was randomized within blocks; left–right positions in paired trials were counterbalanced. In the single-temperature block, participants rated each cookie on four attributes—naturalness, healthiness, expected sweetness, attractiveness—using 7-point Likert scales (1 = very low; 7 = very high). In the paired-temperature block, for each attribute participants indicated which cookie (120 °C vs. 190 °C) better fit the descriptor; a "no difference" option was allowed and recorded.

To investigate affective responses toward cookie colors, a consumer survey was conducted with 85 participants. Participants were instructed that no tasting was required; instead, they were asked to evaluate cookies solely based on visual color appearance. The questionnaire consisted of two sections:

(a) Perception of single-temperature cookies were prepared with a standardized formulation (natural pigment concentration of 1 g per 100 g dough, baked at 120 °C). Using a 7-point Likert scale, participants rated each cookie's

color on four perceptual attributes:
1. Healthiness (How healthy does this cookie appear?)
2. Naturalness (How natural does this cookie appear?)
3. Expected Sweetness (How sweet do you expect this cookie to taste?)
4. Attractiveness (How visually appealing is this cookie?)

(b) Comparative Evaluation Across Baking Temperatures Paired cookies were prepared with the same pigment concentration (1 g/100 g) but baked at 120 °C vs. 190 °C, and presented side by side. Participants were asked to indicate which cookie appeared:
1. Healthier (Which cookie looks healthier?)
2. More natural (Which cookie looks more natural?)
3. Sweeter (Which cookie looks sweeter?)
4. More appetizing (Which cookie looks more appetizing?)

This design enabled both absolute evaluations of color attributes under standardized conditions and comparative judgments of how baking temperature influenced consumer perception of natural pigment appearance.

RESULTS

3.1 Single-temperature rating results

Participants (N = 85) rated cookies colored with ten natural pigments on naturalness, healthiness, expected sweetness, and attractiveness using 7-point Likert scales (1 = very low, 7 = very high). Table 1 reports the means (M) and standard deviations (SD) for the 120 °C; 1.0 g/100 g set. Anthocyanin-based hues—carrot and purple sweet potato—showed the highest average ratings on naturalness (M=5.48±0.85; M=5.07±1.20) and healthiness (M=4.99±0.98; M=4.85±0.97), whereas red yeast rice and gardenia blue ranked lower across these attributes (naturalness M≈3.18 and 2.73; healthiness M≈3.02 and 2.73). Expected sweetness tended to be higher for reddish hues (e.g., red yeast rice M=5.02±1.17; gardenia red (A) M=4.67±1.16). Attractiveness broadly mirrored the naturalness/healthiness pattern, with anthocyanin-carrot (M=4.71±1.04) and anthocyanin-purple sweet potato (M=4.47±1.28) leading. Fig. 1 visualizes the a*–b* distribution of all measured samples (warm-quadrant clustering), with calibrated photographic exemplars for ecological reference.

	Red Yeast Rice	Gardenia Red	Gardenia Red (A)	Anthocyanin Carrot	Gardenia Purple	Anthocyanin Purple Sweet Potato	Gardenia Yellow	Gardenia Black	Gardenia Green	Gardenia Blue
Naturalness (M)	3.18	3.79	3.81	5.48	4.36	5.07	4.16	3.93	4.62	2.73
Naturalness (SD)	1.51	1.46	1.33	0.85	1.28	1.20	1.50	1.62	1.22	1.60
Healthiness (M)	3.02	3.41	3.53	4.99	4.15	4.85	3.86	3.75	4.45	2.73
Healthiness (SD)	1.26	1.21	1.08	0.98	1.19	0.97	1.45	1.38	1.16	1.38
Expected sweetness (M)	5.02	4.52	4.67	3.86	3.92	3.79	4.35	3.64	3.78	3.88
Expected sweetness (SD)	1.17	1.19	1.16	1.08	1.27	0.95	1.30	1.52	1.20	1.52
Attractiveness (M)	3.11	3.45	3.55	4.71	4.19	4.47	3.75	3.74	4.46	2.94
Attractiveness (SD)	1.41	1.36	1.37	1.04	1.44	1.28	1.59	1.57	1.42	1.54

Table 1: Mean (M) and standard deviation (SD) of consumer evaluations (7-point Likert scale) of cookies colored with ten natural pigments at 120 °C.

To test whether pigment type affected the four attributes at 120 °C (1.0 g/100 g), we ran Friedman tests with repeated measures across the ten pigments. All attributes showed significant overall effects (χ^2 with df=9; p<.001):

- Naturalness: χ^2=275.03, p<.001, Kendall's W=.036
- Healthiness: χ^2=300.24, p<.001, W=.039
- Expected sweetness: χ^2=123.50, p<.001, W=.016
- Attractiveness: χ^2=157.01, p<.001, W=.021

Planned post-hoc rank summaries indicated anthocyanin-carrot and anthocyanin-purple sweet potato among the top-ranked pigments on naturalness/healthiness/attractiveness, while gardenia blue and red yeast rice trailed.

3.2 Paired comparisons across baking temperatures

Preference analyses excluded "no-difference" responses as pre-registered. 190 °C samples were more often chosen as:

- More natural: 62.8% (95% Wilson CI [0.573, 0.680]), vs. 37.2% for 120 °C; binomial $p=6.9\times10^{-6}$; Cohen's h=0.52.
- Healthier: 60.2% [0.548, 0.654], vs. 39.8% for 120 °C; $p=2.8\times10^{-4}$; h=0.41.
- More appetizing: 72.3% [0.671, 0.769], vs. 27.7% for 120 °C; $p=7.5\times10^{-16}$; h=0.92.
- Sweeter (expected): 52.5% [0.469, 0.581], vs. 47.5% for 120 °C; p=.42; h=0.10.

Thus, higher-temperature baking shifts visual judgments toward naturalness/healthiness/appetite, while expected sweetness is temperature-insensitive in purely visual appraisal. The direction of these preferences aligns with instrumental color shifts reported below.

3.3 Color shifts between temperatures

Across 30 pigment–concentration pairs, baking at 190 °C relative to 120 °C produced a mean ΔE=2.24 (SD=1.77; 95% CI [1.60, 2.87]), with component shifts ΔL*=+0.50, Δa*=+0.58, Δb*=+2.65, ΔC*=+2.33. In other words, the higher-temperature condition tended to yield more yellowish/reddish and slightly higher-chroma appearances rather than uniformly darker luminance; indeed, 63% of pairs showed L* increases. Taken together, the psychophysical results (Friedman/paired-comparison tests) and instrumental findings (ΔE and component vectors) converge. Anthocyanin-based hues perform best on naturalness/healthiness/attractiveness at 120 °C, and thermal parameters can be used as a practical lever to steer okara cookies toward preferred "golden-baked" appearances without inflating sweetness expectations.

CONCLUSION AND DISCUSSION

This study demonstrates that the visual appearance of naturally pigmented cookies significantly affects consumer perceptions of healthiness, naturalness, sweetness expectations, and appetizing appeal. While cookies baked at higher temperatures (190 °C) were generally perceived as healthier, more natural, and more appetizing compared to those baked at lower temperatures (120 °C), sweetness judgments remained relatively balanced. Moreover, qualitative associative tests revealed that color alone was sufficient to trigger strong flavor, ingredient, and emotional associations, underscoring the role of color as both a sensory and symbolic cue in food perception. Building upon these findings, the use of okara (soy pulp) in 3D food printing offers promising opportunities to merge sustainability with design-driven personalization. While this study provides a foundational understanding, it also opens several avenues for future research and development. First, sensory studies should go beyond visual evaluation to include actual tasting experiments, verifying whether the color-induced expectations observed here correspond to perceptible differences in flavor experience. For example, do participants find the purple-pigmented cookies taste as "healthy" or as pleasantly fruity as they anticipate, or do red-hued cookies actually seem sweeter when eaten? Investigating such flavor–color congruency would shed light on how visual cues interact with taste

and aroma in naturally pigmented foods. Second, further research is recommended on the stability and shelf-life of natural colorants in baked products. Anthocyanins and other plant pigments can be sensitive to pH, light, and heat, leading to fading or color shifts over time (Ghazal et al., 2019) [12]. Evaluating how the cookies' appearance holds up during storage (and developing strategies to preserve vibrancy, such as encapsulating pigments or optimizing packaging) will be crucial for real-world applications. Third, on the technological front, exploration of real-time pigment modulation in 3D printing would be highly beneficial.

REFERENCES

[1]. Spence, C., Levitan, C. A., Shankar, M. U., & Zampini, M. (2010). Does food color influence taste and flavor perception in humans? Chemosensory Perception, 3(1), 68–84. https://doi.org/10.1007/s12078-010-9067-z

[2]. Sharma, G., Wu, W., & Dalal, E. N. (2005). The CIEDE2000 color-difference formula: Implementation notes, supplementary test data, and mathematical observations. Color Research & Application, 30(1), 21–30. https://doi.org/10.1002/col.20070 search.r-project.org

[3]. O'Toole, D. K. (1999). Characteristics and use of okara, the soybean residue from soy milk production: A review. *Journal of Agricultural and Food Chemistry, 47*(2), 363–371. https://doi.org/10.1021/jf980754l

[4]. Demartini, M., Pinna, C., Tonelli, F., Terzi, S., Sansone, C., & Testa, C. (2018). Food industry digitalization: From challenges and trends to opportunities and solutions. IFAC-PapersOnLine, 51(11), 1371–1378. https://doi.org/10.1016/j.ifacol.2018.08.337

[5]. Sun, J., Peng, Z., Yan, L., Fuh, J. Y. H., & Hong, G. S. (2015). 3D food printing—An innovative way of mass customization in food fabrication. International Journal of Bioprinting, 1(1), 27–38. https://doi.org/10.18063/IJB.2015.01.006

[6]. BBM Magazine. (2025, January 22). The 8 major bakery products trends for 2025. https://magazinebbm.com/blog/the-8-major-bakery-products-trends-for-2025-3661

[7]. Price, C. (2025, January 15). Top bakery industry trends and statistics in 2025. Toast. https://pos.toasttab.com/blog/on-the-line/bakery-industry-trends-and-statistics

[8]. Sigurdson, G. T., Tang, P., & Giusti, M. M. (2017). Natural colorants: Food colorants from natural sources. *Annual Review of Food Science and Technology, 8,* 261–280. https://doi.org/10.1146/annurev-food-030216-025923

[9]. Karana, E., Barati, B., Rognoli, V., & van der Laan, A. Z. (2015). Material driven design (MDD): A method to design for material experiences. International Journal of Design, 9(2), 35–54.

[10]. International Commission on Illumination (CIE). (2018). Colorimetry (4th ed., CIE 015:2018). Vienna, Austria: Authoronlinelibrary.wiley.com

[11]. International Organization for Standardization (ISO). (2009). Graphic technology and photography — Viewing conditions (ISO 3664:2009). Geneva, Switzerland: Author. iso.org

[12]. Ghazal, A. F., Zhang, M., & Liu, Z. (2019). Spontaneous color change of 3D printed healthy food product over time after printing as a novel application for 4D food printing. Food and Bioprocess Technology, 12(10), 1627–1645. https://doi.org/10.1007/s11947-019-02327-6

Color System Conversion from RGB to L*a*b* Using Four-Layer Neural Network for A Novel Colorimeter Independent of Light Sources

Kaito Miyazawa[a*], and Masashi Ohkawa[b]

[a]*Graduate School of Science and Technology, Niigata University, Niigata, Japan*
[b]*Faculty of Engineering, Niigata University, Niigata, Japan*
[*]*Corresponding author: Kaito Miyazawa, f24l009a@mail.cc.niigata-u.ac.jp*

ABSTRACT

Color measurement is important in various industries, such as fashion, printing, food, cosmetics, and medical care. Colorimeters are typically useful in a measurement range of a few mm² to a few cm². However, wide-range and non-contact color measurement would be helpful in two-dimensional measurements. To realize such color measurement, a novel colorimeter based on RGB-to-L*a*b* conversion using an imaging device is proposed. Moreover, the proposed colorimeter can measure color, independent of the lighting illuminant, using an artificial neural network. In this study, datasets were prepared by calculating the RGB and L*a*b* values for 1577 color samples of the JIS standard color chart. Also, standard/supplementary illuminants (A, B, C, D50, D55, D65, D75) and LED light sources with color temperatures ranging from 2900 K to 6000 K were chosen as illuminants. The input layer of the neural network has six units for RGB values of the target and reference colors, and the output layer has three units for L*a*b* values. The hidden layers varied in size (256 to 2048 units), and training was conducted using the Adam optimizer with the ReLU activation function over 10,000 epochs. Cross-validation was performed by dividing the datasets according to the illuminants. Color difference was used as an evaluation index, divided into six categories. Using the trained model, excellent generalization performance in RGB-to-L*a*b* conversion could be successfully demonstrated.

*Keywords: Color measurement, Neural network, Colorimeter, RGB, L*a*b**

INTRODUCTION

Color measurement is important in various industries, such as fashion, printing, food, cosmetics, and medical care [1-3]. Colorimeters are typically useful in a measurement range of a few mm² to a few cm². However, wide-area and non-contact color measurement would be helpful for agricultural products, face and skin diagnosis. etc. To realize such color measurement, this group has proposed a novel colorimeter based on RGB-to-L*a*b* conversion using an imaging device. Color representation by digital cameras is generally RGB, whereas in color management, uniform color spaces, such as, L*u*v* and L*a*b* are usually used. Therefore, it is often necessary to convert the RGB values into the L*a*b* values. Incidentally, RGB values obtained by the imaging devices vary depending on the illuminant, lighting conditions, shooting conditions, etc [4]. Thus, implementing a color system conversion which is independent of the above conditions is necessary. However, preparing a linear or nonlinear transformation formula for each condition is not practical. Consequently, this group is developing an RGB-to-L*a*b* conversion system, independent of the lighting illuminant, using an artificial neural network. In order to avoid variation due to characteristics of the imaging device, RGB values were calculated using the spectral distributions of the standard/supplementary illuminants and LED light sources, and the spectral reflectances of JIS standard color

samples. The calculated RGB and $L^*a^*b^*$ values were used to train and test the neural network. Using the trained neural network, accuracy of the RGB-to-$L^*a^*b^*$ conversion system was examined.

CONFIGURATION OF NEURAL NETWORK AND CONDITIONS OF TRAINING AND TEST

The configuration of the neural network for the RGB-to-$L^*a^*b^*$ conversion system is illustrated in Fig. 1. To make ensure independence from any illuminants, the RGB values of a white reference (N9) were introduced as additional input information to represent the lighting source. The input layer thus comprised six units: three for the RGB values to be converted to $L^*a^*b^*$ and three for the RGB values of N9. The hidden layers consisted of three layers with a same number of units. In this study, these were set to 256, 512, 1024, or 2048. The output layer has three units for the $L^*a^*b^*$ values.

The dataset used to train the neural network consisted of RGB and $L^*a^*b^*$ values. In the experiment, these values were calculated instead of directly obtaining them from imaging devices in order to eliminate influence from imaging device characteristics. As illuminants, the standard and supplementary standard illuminants (A, B, C, D50, D55, D65, D75) with spectral distributions as shown in Fig. 2(a) and LEDs with various color temperatures (2900 K–6000 K) as shown in Fig. 2(b), were chosen. In the calculation of RGB and $L^*a^*b^*$ values, spectral reflectance of the JIS standard color samples of 1,577 and the CIE XYZ color matching functions were employed [5]. Moreover, $L^*a^*b^*$ values were calculated using the standard illuminant D65 as the white point.

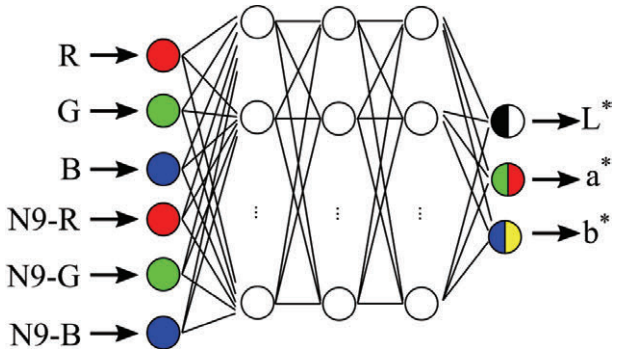

Figure 1: Configuration of a neural network for RGB- $L^*a^*b^*$ conversion

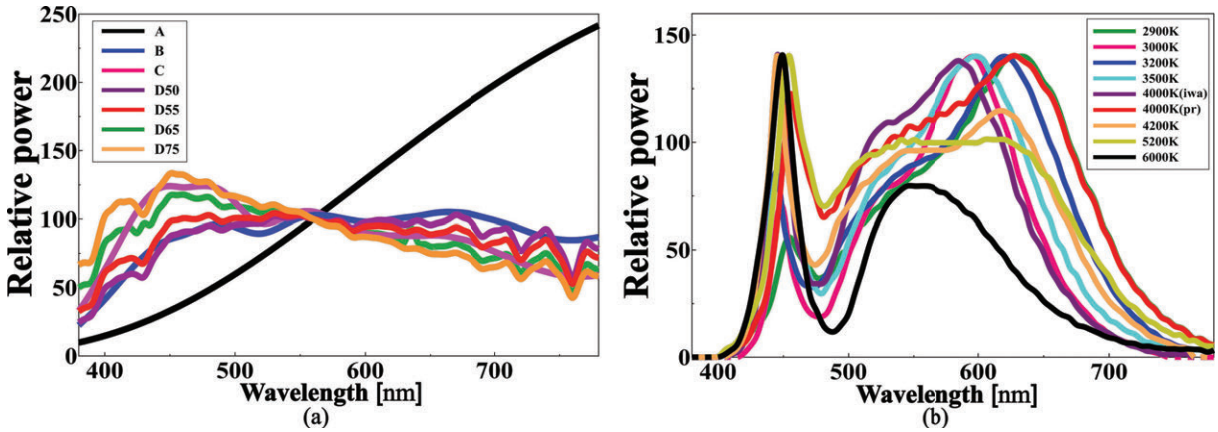

Figure 2: Spectral distributions of (a) the CIE standard and supplementary standard illuminants, and (b) LED light sources

Training conditions are shown in Table 1. The neural network had three hidden layers, and each hidden layer had units of 256, 512, 1024 or 2048. As the activation functions, ReLU for the hidden layer and Linear for the output layer were used [6-8]. For the optimization method, Adam was used. Moreover, the learning rate, epochs, and batch size were set at 0.001, 10000 and 512, respectively. Three kinds of datasets were employed for training and evaluation: (1) dataset #1 for standard/supplementary standard illuminants, (2) dataset #2 for LED illuminants, and (3) dataset #3, a combined dataset of #1 and #2. Each dataset was divided into subsets by light source, and cross-validation was conducted. One subset was used as the test data while the remaining subsets served as training data. This process was repeated until all subsets had been used as test data. For the test, weights and biases in the epoch, at which validation loss reached its minimum during training, were saved and used for evaluation. From the output values of $L^*a^*b^*$, color differences were calculated using the expected values, and divided into six categories: (i) 0 - 1.2, (ii) 1.2 - 2.5, (iii) 2.5 - 5.0, (iv) 5.0 - 10.0, (v) 10.0 - 20.0, and (vi) 20.0 or more. Performance of the RGB-to-$L^*a^*b^*$ conversion was evaluated based on the relative frequency for every category.

Table 1: Experimental settings for training

Hidden layers	3
Units of hidden layers	256, 512, 1024, 2048
Activation function	ReLU(hidden layer), Linear(output layer)
Optimization method	Adam
Learning rate	0.001
Epochs	10,000
Batch size	512

RESULTS AND DISCUSSION

Results of training and validation using dataset #1 based on the standard/supplementary standard illuminants, while varying the number of units in each hidden layer, are shown in Fig. 3. The horizontal axis indicates the test subset used in cross-validation, and the vertical axis indicates the proportion of color differences for the predicted $L^*a^*b^*$ values (out of 1577 samples) based on the color difference categories. Except for illuminant A, all other light sources as test data showed greater conversion accuracy as the number of the units in each hidden layer increased, and more than 70% had a color difference of less than 1.2. In contrast, illuminant A had a unique spectral distribution among the standard/supplementary standard illuminants as shown in Fig. 2(a), and the color difference for illuminant A was quite large.

Results for dataset #2, based on LED light sources, are shown in Fig. 4. The horizontal axis indicates the test subsets, and the vertical axis indicates the proportion of each color difference category. Except for several LED light sources, 50% at most had a color difference of less than 1.2. The results for dataset #2 were worse than that for dataset #1. Since the spectral distributions of LEDs, as shown in Fig. 2(b), vary greatly, a lack of similarity in the dataset may cause poor performance. Moreover, increasing the number of units did not improve results.

Results for dataset #3, which consisted of standard/supplementary standard illuminants and the LED light sources, with a varying number of units in each hidden layer, are shown in Fig. 5. The horizontal axis indicates the test subsets, and the vertical axis indicates the proportion of each color difference category. The combined dataset #3 showed significant improvement in performance compared to the results using dataset #2 which consisted only of the LED dataset. In particular, for 2900 K and 5200 K, more than 90% of the test data showed a color difference of less than 1.2.

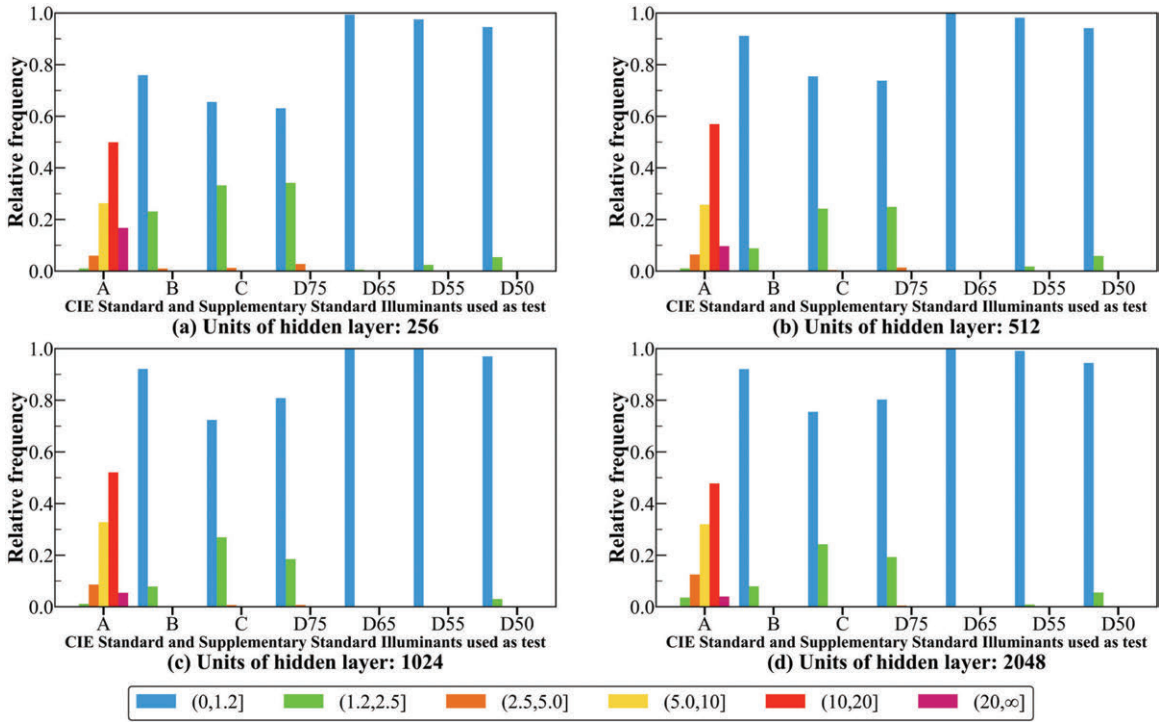

Figure 3: Results of training for dataset #1 based on the standard/supplementary standard illuminants, with a varying number of units in each hidden layer

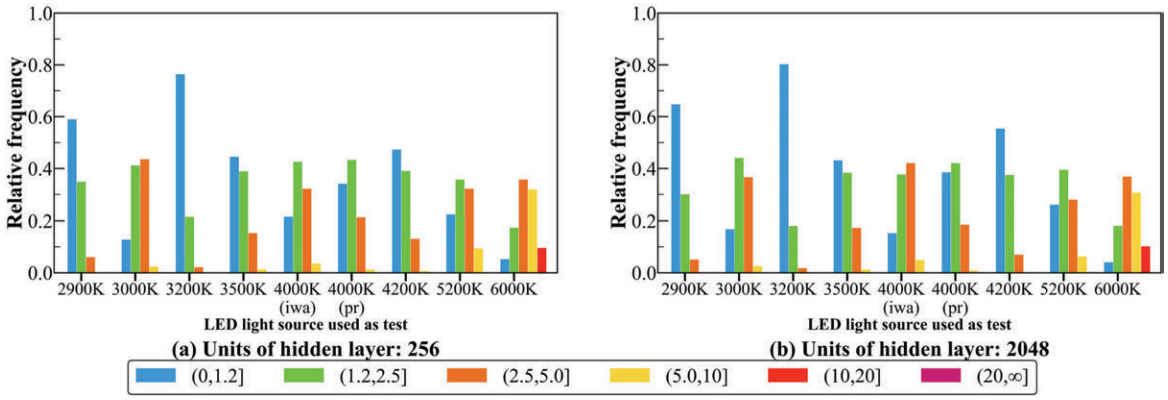

Figure 4: Results of training for dataset #2 based on LED light sources, with a varying number of units in each hidden layer

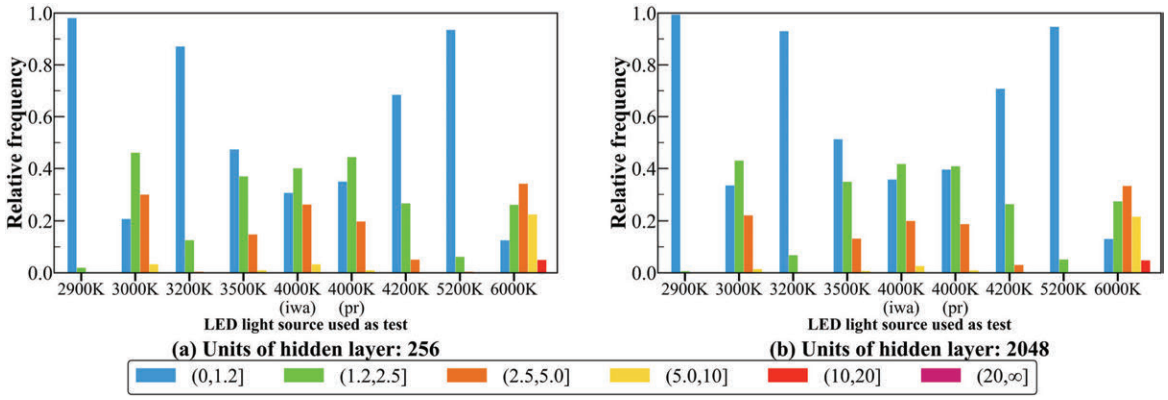

Figure 5: Results of training for the combined dataset #3 using the standard/supplementary standard illuminants and LED light sources, with a varying number of units in each hidden layer

CONCLUSION

In this study, an RGB-to-L*a*b* conversion system, independent of lighting sources, using a four-layer neural network was examined. When dataset #1 based on the standard/supplementary illuminants was used, more than 70% of the test data had a color difference of less than 1.2, except for illuminant A. Moreover, for dataset #2 based on only LED lamps, 60% or less of test samples had a color difference of less than 1.2, except for 3200 K. This was considerably worse than the results using dataset #1 based on the standard/supplementary standard illuminants. Incidentally, when the combined dataset #3 consisting of datasets #1 and #2, conversion accuracy remarkably improved for 2900 K and 5200 K, compared to that using dataset #2. The number of units in the hidden layers, which was more than 512, did not significantly contribute to an improvement in performance since the number of data used to train the network was relatively small. Excellent conversion accuracy was achieved for the standard/supplementary standard illuminants, suggesting good feasibility in the realization of a RGB-L*a*b* conversion system independent of the light source. However, obtaining excellent conversion accuracy for LED light sources was somewhat difficult due to the wide range of spectral distributions of LEDs. Therefore, a large amount of data is considered necessary to train the network.

REFERENCES

[1]. Makiguchi, A., Moriya, T., Tashiro, K., Ohkawa, M. (2019). Color system transform from RGB to L*a*b* using neural network - consideration in hues of PB, P and RP -. 5th ACA 2019. Aichi, Japan.

[2]. Minz, P. S., Saini, C. S. (2021). RGB camera-based image technique for color measurement of flavored milk. *Measurement:Food*, 4(3), 100012.

[3]. León, K., Mery, D., Pedreschi, F., León, J. (2006). Color measurement in L*a*b* units from RGB digital images. *Food Research International*, 39(10), 1084–1091.

[4]. Horta-Velazquez, A., Ramos-Ortiz, G., Morales-Narvaez, E. (2025). The optimal color space enables advantageous smartphone-based colorimetric sensing. *Biosensors and Bioelectronics*, 273(1), 117089.

[5]. Fairman. H. S., Brill, M. H., Hemmendinger, H. (1997). How the CIE 1931 Color-Matching Functions Were Derived from Wright–Guild Data. *Color Research and Application*, 22(1), 11-23.

[6]. LeCun, Y., Bengio, Y., Hinton, G. (2015). Deep Learning. *Nature*, 521(7553), 436–444.

[7]. Schmidhuber, J. (2015). Deep Learning in Neural Networks: An Overview. *Neural Networks*, 61(3), 85-117.

[8]. Dubey, S. R., Singh, S. K., Chaudhuri, B. B. (2022). Activation Functions in Deep Learning: A Comprehensive Survey and Benchmark. Neurocomputing, 503(11), 92-108.

Survey on The Empowerment Initiatives for Students with Color Vision Deficiencies

Shion Maruyama[a*], Tsukasa Muraya[b], Shoji Sunaga[c]

[a]*Graduate School of Design, Kyushu University, Japan*

[b]*Faculty of Contemporary Social Studies, Chikushi Jogakuen University, Japan*

[c]*Faculty of Design, Kyushu University, Japan*

**Corresponding author: maruyama.shion.785@s.kyushu-u.ac.jp*

ABSTRACT

Color vision is a mechanism that yields color sensation in the human brain. It is known that there is diversity in the mechanism. Although human color vision is generally trichromacy, there are some individuals with a minority of color vision types called color vision deficiency in the medical field. Due to differences in color perception, people with color deficiency have faced various limitations. Understanding of color vision diversity has progressed over the recent years, but students with color vision deficiency still face many problems and/or unfair treatment in schools in Japan. To solve these problems, this study focused on the perspective of empowerment for color-deficient students. From this perspective, we conducted an interview and a questionnaire survey to understand color deficiency, the support that has been received, and the support that would have been appreciated in developing an educational program for color-deficient students in elementary schools. Based on the analysis results, we conducted a workshop to discuss methods for supporting and assisting students with color vision deficiency and fostering an understanding of color vision diversity. Additionally, at the end of the workshop, we administered a survey to parents and teachers to explore areas for future improvement.

Keywords: color vision deficiencies, color vision diversity, empowerment

INTRODUCTION

Color vision is a sensation that occurs in the human brain, and it is known that there is diversity in its mechanisms. The medical field refers to a minority type of color vision that differs from the majority's color vision as “color vision deficiency.”

While understanding of “color vision deficiency” has advanced to some extent, some challenges remain in educational settings. For example, “Episodes Related to Color Vision” reported by Miyaura et al. in 2012[1] highlights numerous instances of disadvantages and unfair treatment stemming from color vision deficiencies in school life. Furthermore, a certain number of people continue to regret not learning because they didn’t learn the correct knowledge about color vision or how to cope with their color vision characteristics during their school years [2].

This suggests that appropriate support was needed during the school years, when many people become aware of their color vision characteristics [3], to empower children and students with color vision deficiency. The term 'empowerment' we use here refers to the concept of helping socially disadvantaged and discriminated individuals become aware of the discriminatory structures and oppressive factors that affect them, and to recover and improve

their self-confidence, self-determination, and overall situation. Although several papers and books discussing self-empowerment about color vision deficiency have been published in Japan, they are all highly specialized and difficult for elementary school students to comprehend.

This study focused on developing a learning support program to empower elementary school students. We conducted interviews and surveys on their understanding of color vision deficiency and the support they had received or desired. Based on the analysis of these results, we conducted a workshop to help students understand the diversity of color vision.

INTERVIEW AND QUESTIONNAIRE SURVEY

Interview Survey

We conducted interviews with six undergraduate and graduate students at Kyushu University, aged 20 to 24, who have color vision deficiency. The interviewees had been confirmed to have severe color vision deficiencies through preliminary experiments.

The interviews were conducted either face-to-face or remotely via Zoom, with an average interview time of approximately one hour. The interview format was semi-structured. The interviews were conducted from November 21 to November 27, 2024. The pre-determined questions asked of the six participants are shown in Table 1.

Table 1: Pre-determined questions and the number of questions

Questions	Number of questions
When you noticed your color vision deficiency, and the person you consulted	5
Challenges in drawing and crafts classes	2
Challenges in school life	1
Care you received at school	1
About future path	3
Current awareness of color vision deficiency and social position	9

Questionnaire Survey

The survey participants consisted of 9 undergraduate and graduate students from Kyushu University and 23 individuals registered as Color Universal Design verification collaborators with the Color Universal Design Organization (CUDO), totaling 32 participants. All subjects had been confirmed to have color vision deficiency through prior experiments or diagnoses.

The questionnaire survey was conducted using Google Forms in an anonymous self-response format. The questions are shown in Table 2. The survey period was from December 15 to December 31, 2024, for Kyushu University students, and from December 15, 2024, to January 7, 2025, for the CUDO cooperators.

Table 2: Questionnaire questions and the number of questions

Section	Questions	Number of questions
1	About profile	3
2	About awareness and understanding of color vision dificiency	9
3	About art, drawing, and art classes	12
4	About school life and education in general	12
5	About career choices	6
6	About awareness and understanding of color vision deficiency	20

Results of the interview survey

The qualitative analysis was applied to the interview data. The procedure is shown below.

1. Transcribe the interview content.
2. Extract labels from the conversation based on the transcribed interview content.
3. Assign categories to similar labels and group them.

From the interviews, we extracted labels and categories related to the difficulty of distinguishing colors, unique coping methods, reactions received from other persons, and recognition of color vision deficiency and changes in the recognition. Note that the interview results were described in colloquial language.

The followings show examples of the obtained answers. Extracted labels are enclosed in ＜＞, and categories are enclosed in 《》.

《Personal coping methods》

- When I was drawing, I had painted human skin color with a light green, so I wondered what to do. Then, I became to use eyedropper tools picking up colors from a color palette. ＜Coping methods when drawing＞

《Difficulty in distinguishing colors》

- When a teacher wrote on the blackboard with a yellow or an orange chalk, I couldn't distinguish between them. ＜Indistinguishing between chalk colors＞

Results of the questionnaire survey

A simple tabulation was applied to each question, and a cross-tabulation was applied to several selected questions. The followings show examples of the questionnaire results.

(Question #4-7) Do you think the support provided at school for color vision deficiency is sufficient?

No responses were sufficient. While 16% answered 'somewhat sufficient,' 37% answered 'somewhat insufficient,' and 31% answered 'insufficient,' indicating that a total of 68% felt the support was inadequate.

(Question #4-8) For those who answered "somewhat insufficient" or "insufficient" in Question #4-7, what kind of support do you think would be helpful?

Twenty-five answers were obtained. Some of them are shown below.

<Answers >

- Explain that color vision deficiency is not rare and create an environment where it is easy to disclose this to others. Until junior high school, I felt embarrassed about my color vision and hid it from others, which made it difficult for me to receive support.
- It is necessary to identify people with color vision deficiencies in advance.
- I dislike and feel embarrassed about other students knowing that I have color vision deficiency. Therefore, I would like people with color vision deficiency to be able to live without telling others.

As shown above, the desired support covers a wide range of issues, including acquiring accurate knowledge about color, protecting human rights, including privacy, and addressing color usage issues related to color universal design.

Discussion on the interview survey and the questionnaire survey

The survey results revealed that many people have difficulties distinguishing colors in their daily lives and feel embarrassed about their color vision deficiency. Some people have found ways to cope on their own. The support that such people seek is primarily knowledge. By acquiring basic knowledge, we can understand that students with color vision deficiency see colors differently, which will enable us to provide support from their perspective. Additionally, there is currently a lack of clarity regarding what the term color vision diversity refers to. Therefore, it is essential to not only convey knowledge but also to promote proper understanding through education.

WORKSHOP FOR LEARNING THE DIVERSITY OF COLOR VISION

Workshop "What color is this paint?"

Based on the results of interviews and questionnaires, we designed and conducted workshops, titled "What color is this paint?", to promote an understanding of color vision diversity among elementary school students. The aim and design of this workshop have been reported by Muraya et al [5].

This workshop was held twice on July 29 and August 22, 2025. Twenty teachers participated in the first workshop, and eighteen elementary school students participated in the second workshop. In the second workshop, the parents of the participating students observed it. The procedure of the workshop is the following.

1. Lecture on color vision and color vision diversity
   Elementary school students learn that colors do not actually exist on objects but instead are recognized through the processing of light reflection by the eyes and brain.

2. Dividing into two teams, the members of each team wore one of four different colored goggles.
   The colored goggles used are shown in Figure 1. Four types of colored goggles were prepared for each team to reproduce a variety of color perceptions.

Figure 1: The color goggles

3. Each team drew a painting on a large canvas.
   The team members painted a 5m x 1.4m canvas together. First, they used a roller to paint the background (Figure 2), and after the background was completed, they switched to brushes to draw the picture (Figure 3). To prevent the elementary school students from wondering what to draw, we provided sample photos and motif images as references.

Figure 2: Scene of drawing a picture using a roller

Figure 3: Scene of drawing a picture using a brush

4. Viewing the painted artwork
   The artwork was viewed in three steps. First, the artwork was viewed while wearing the color goggles. Next, participants removed their own color goggles and viewed the artwork. Finally, the participants exchanged their own color goggles with those worn by others and viewed the artwork.
   These three steps were performed for both their own team's artwork and the artwork of the other team.

5. Summary on color vision and color vision diversity

We summarized the following three points: 1) objects don't have color; each person perceives colors differently, 2) we have no direct way to know what color others perceive, and 3) therefore, there's no right or wrong color, even if others perceive different colors.

After the workshop, we conducted a survey targeting the teachers and the parents of the participating students. A total of 20 responses were received from teachers and 10 from parents. The contents of the questionnaire for teachers are shown in Table 3, and the contents of the questionnaire for parents are shown in Table 4.

Table 3: Questionnaire for teachers

Section	Questions	Number of questions
1	About profile	5
2	What teachers knew about "color vision diversity" before attending the workshop	3
3	Impressions after experiencing the workshop (from the perspective of teachers)	15
4	What to expect when children experience the workshop	7
5	Children's learning the concept of "color vision diversity" through the workshop	2
6	Elementary school "Guidelines for Learning" and "Teaching Materials on Color Vision"	5

Table4: Questionnaire for parents

Section	Questions	Number of questions
1	About profile	2
2	What partents knew about "color vision diversity" before attending the workshop	3
3	Impressions after experiencing the workshop (from the perspective of parents)	13
4	What to expect when children experience the workshop	7
5	Children's learning the concept of "color vision diversity" through the workshop	2
6	Empowerment of children with "color dificiencies"	2

Results of the workshop and the questionnaire

As examples of the answers, the answers to the common questions between the teacher questionnaire and the parent questionnaire, Questions #3-9 and #5-1, are summarized in Tables 5 and 6.

(Question #3-9) Do you agree or disagree with implementing this workshop in elementary school classes (targeted at third graders and above, with no subject limitation)?

The answers to Question #3-9 are shown in Table 5. The numbers in parentheses in the table indicate the percentage of answers from the teachers and the parents. Both the teachers and the parents had positive responses, with high percentages indicating satisfaction with the workshop.

(Question #5-1) Do you think this workshop contributes to teaching elementary school students in the middle grades (third and fourth graders) about color vision diversity, that color perception may differ from person to person?

The answers to Question #5-1 are shown in Table 6. As in Table 5, the numbers in parentheses in the table show the percentage of answers from the teachers and the parents. All respondents answered, "strongly agree" or "agree." One of the parents did not answer.

Table 5: The result of Question #3-9

	Agree	Neutral	Disagree
teachers	18 (90%)	1(5%)	1 (5%)
parents	9 (90%)	0	1 (10%)

Table6: The result of Question #5-1

	Strongly agree	Agree	Neutral	Disagree	Strongly disagree
teachers	18 (90%)	2 (10%)	0	0	0
parents	5 (50%)	4 (40%)	0	0	0

Discussion on the workshop and the questionnaire

The survey results showed that both teachers and parents were positive about integrating the workshop into conventional classes. The workshops could also help elementary school students learn about the diversity of color vision. However, there were also opinions that the learning content was difficult for third- and fourth-grade students. While the act of drawing a picture itself can be easily performed by even younger elementary school students, there is a need for improvement in terms of helping them understand the learning content. As the survey was conducted

with teachers and parents, collecting the opinions of children who experienced the workshop could lead to the development of a workshop that is easier for children to learn from.

CONCLUSION

In this study, we conducted a survey to identify the needs of children with color vision deficiency, such as the support they received during their early childhood and the support they desired and held workshop in order to develop an educational program to empower children and students with color vision deficiency.

Prospects include matching the workshop with previous surveys and collecting opinions from elementary school students who participated in the workshop. We are also considering creating supplementary materials that will help participants better understand the purpose and content of the workshops. Finally, we hope to create an educational program that clarifies the knowledge and needs related to color vision that school teachers and children require.

ACKNOWLEDEMENTS

This work was supported by JSPS KAKENHI Grant Numbers JP 21H04342 and JP 24H00167

REFERENCES

[1] Miyaura, T., Utumi, Y., Sakai, M., Yamagishi, N., Takano, S. (2012). Survey on Individuals with Congenital Color Deficiencies Who Received Medical Care in Fiscal Years 2010 and 2011 (Follow-up Report), The Journal of the Japan Ophthalmologists Association, 83(10), 1421-1438. (in Japanese)

[2] Kouyou (2017). Color Vision Diversity??? Don't be ridiculous! Retrieved August 22, 2025, from https://ameblo.jp/kouyou1126/entry-12308737658.html (in Japanese)

[3] Miyaura, T., Utumi, Y., Sakai, M., Yamagishi, N., Takano, S. (2012) . Survey on Individuals with Congenital Color Deficiencies Who Received Medical Care in Fiscal Years 2010 and 2011, The Journal of the Japan Ophthalmologists Association, 83(10), 1421-1438. (in Japanese)

[4] The Asahi Shimbun Cross Research's Modern Terminology, Retrieved August 22, 2025, from https://xsearch.asahi.com/help/jpn/qa_login.html (in Japanese)

[5] Muraya, T., Hamasaki, H., Nagatomi, M., Chikara, R., Inoshita, T., Harada, T., Sunaga, S., (2022). Design of Color Education Programs for Understanding the Diversity of Color Vision, Proceedings of the ACA 2022 Conference – Color for Future, 175-180.

Creation of Educational Materials Designed for A Game about Color Vision Diversity Education

Toshiki Fujii[a*], Tsukasa Muraya[b], Shoji Sunaga[c]

[a]*Graduate School of Design, Kyushu University, Japan*
[b]*Faculty of Contemporary Social Studies, Chikushi Jogakuen University, Japan*
[c]*Faculty of Design, Kyushu University, Japan*
[*]*Corresponding author: Toshiki Fujii, fujii.toshiki.393@s.kyushu-u.ac.jp*

ABSTRACT

Color is a subjective sensation caused by the response of photoreceptor cells to light reaching the retina and the processing of this information by the brain. This sensation mechanism is called color vision, and it is well known that there are individual differences and diversity. However, color education in Japanese schools targets only trichromats, and no clear educational policies exist for students with color vision deficiencies. As a result, children with color vision deficiencies may struggle with using color due to the discrepancy between how colors are perceived and how they are taught. To address this issue, it is necessary for not only those with color vision deficiency, but also teachers and other students, to have a correct understanding of color vision. As a way to assist such understanding, we developed an educational game designed to teach about color vision diversity and its significance. In this game, players form teams, and each member wears a colored goggle out of five colors. The difference in color perception through color filters is a crucial factor, and players progress through the game by sharing distinct visual information. For developing the game, two types of educational materials —papers and digital devices —were created based on the CAM16 color appearance model, and a digital version was adopted. The game was tested by Japanese high school students, and it was found to be effective for learning color vision diversity and its significance.

Keywords: color vision diversity, color education, educational game

INTRODUCTION

Color is a subjective sensation caused by the response of photoreceptor cells to light reaching the retina and the processing of this information by the brain. Therefore, even if the same light reaches the eye, it is not necessarily the case that we see the same. Additionally, this sense of perceiving color is known as color vision, and it is recognized that there are individual differences and diversity.

Although it is known that there is diversity in color vision, color education in Japanese schools targets only trichromats, and no clear educational policies exist for students with color vision deficiencies. As a result, children with color vision deficiencies may struggle with using color due to the difference between the colors they perceive and the colors that are taught. To address this issue, it is necessary for not only those with color vision deficiency, but for everyone, to understand that color is a subjective experience created in the brain. We are all part of the diversity of color vision, and this diversity is something positive. We have been developing an educational game that utilizes color filters to aid children in learning about color vision in schools [1]. As an educational work to promote awareness of color vision diversity among children, there are picture books designed to help children appreciate the variety of color perception [2]. Their approach focuses on facilitating understanding of color vision

diversity through the content and interactive mechanisms of the books. In contrast, our educational game aims to foster a deeper understanding of the meaning and significance of color vision diversity by not only allowing children to experience perceptual changes using color filters, but also by emphasizing collaborative activities with peers using different types of filters.

In this study, we utilized predictions based on the CAM16 color appearance model [3]. Using this model, we created two types of educational materials: paper and digital. We then developed a digital learning game focused on color vision diversity and evaluated its educational effectiveness through a study conducted with high school students.

METHODOLOGY

Creation of educational materials

The educational materials were patterns in which different digits could be observed depending on the color of the color filters. Two versions of the materials were created: a paper version using color chips, and a digital device version designed for display on an iPad Air (Apple). Color filters were prepared in a total of 104 colors: 73 colors of POLYCOLOUR (TOKYO BUTAI SHOWMEI), 12 colors of gel filters (AMBITFUL), and 19 colors of color correction gel filters (CAMNOON). The spectral transmittances of all color filters were measured by a spectroradiometer (CS-2000, Konica Minolta). Five colors were chosen and used for each educational material. Both materials were created using the following procedure: 1) selection of color filters, 2) color scheme design, and 3) creation of patterns.

Paper version

1) Selection of color filters

The material of the paper version was constituted of the color chips out of DIC Color Guide 1 to 6 (DIC Graphics Corporation) of 1,196 colors. We used the CAM16 color appearance model to predict the colors that the color chips would appear as when viewed through each of the color filters. Based on these predictions, we chose a total of five filters: red, blue, bluish purple, orange, and green. The spectral reflectance of all color chips as measured using a spectrophotometer (CM-2600d, Konica Minolta). In the CAM16 color appearance model, the measured spectral distribution of a D65 LED lamp was used as the illuminant, the viewing condition was set to "average," and the background and adapting luminance were defined based on the spectral reflectance of N6.7 gray paper. Figure 1 shows the spectral transmittance of the five chosen color filters, and Figure 2 shows color chips through these filters in CAM16-UCS. The distribution of color chips varied significantly depending on the filter, indicating

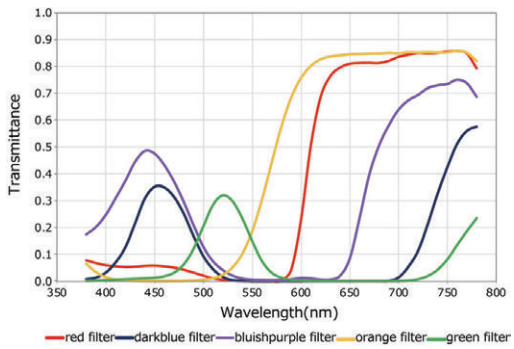

Figure 1: Spectral transmittance of color filters

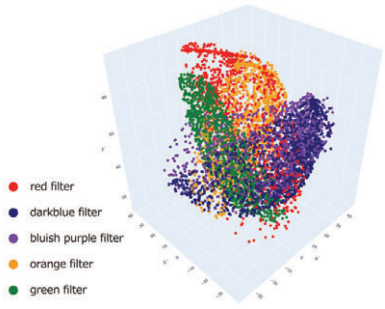

Figure 2: Color chips through each color filter in CAM16-UCS

that the color appearance of the color chips changes markedly with different color filters.

2) Color scheme design

Figure 3 illustrates an example of the pattern structure and color scheme for each part: a figure and its ground. The color scheme was designed based on color differences in CAM16-UCS, in which the color differences are defined as the Euclidean distance. By setting an arbitrary target color chip for each filter and assigning color chips close to the target to the digit figures of the pattern, the specific digit figure became visible when viewed through each corresponding color filter. The figure area was composed using color chips whose color differences from a designated target were less than 5. For the ground area, color chips with color differences of 5 or more from the target were used. The target color chips were set as DIC-542 for the red filter, DIC-172 for the dark blue filter, DIC-431 for the bluish-purple filter, DIC-258 for the orange filter, and DIC-2525 for the green filter, respectively.

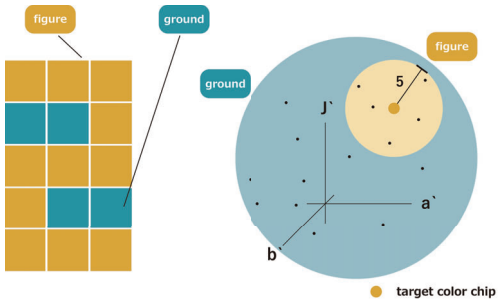

Figure 3: Pattern structure and color scheme

3) Creation of the pattern and its validation

The created pattern is shown in Figure 4. The pattern was made by cutting the color chips into 13mm squares and pasting them onto the gray paper. The digit pattern for each filter was connected horizontally to form the 5-digit pattern. The validation experiment, in which participants were asked to report the digit they saw while wearing color-filtered goggles, revealed that the expected digit could not be identified for some filters, or in some cases, multiple digits were reported. These results suggest that improvements to the pattern design are necessary.

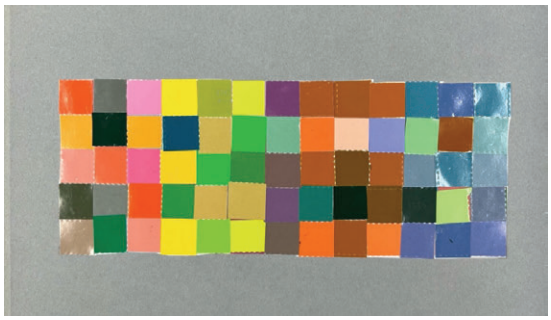

Figure 4: Educational material: paper

Digital device version

1) Selection of color filters

The digital device version was created using a tablet device (iPad Air 4th generation, Apple). The color gamut was Display P3. The spectral radiance distribution of each primary color was measured. The measured spectral distributions are shown in Figure 5. Summing these scaled spectra across the three primaries, a spectral distribution set comprising 52 × 52 × 52 = 140,608 colors was generated. In the calculations, the luminance of each color was normalized by the maximum luminance of 500 cd/m². Based on the prediction of the color appearance of each color in CAM16, five color filters were chosen: red, dark blue, blue, orange, and green. The four of them, except for the blue, were the same as those used in the paper version. In the CAM16 calculations, "average" was used as the surrounding condition, the background was the peak white, and an absolute luminance of 20 percent of the peak white was used as the adaptation luminance. Figure 6 shows the

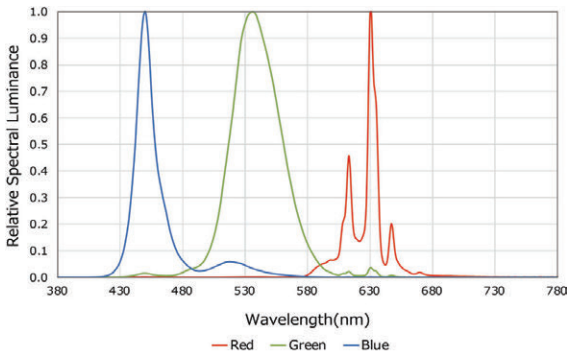

Figure 5: Spectral distribution of primary colors

spectral transmittances of the five chosen color filters, and Figure 7 shows the colors through them in CAM16-UCS.

2) Color scheme design

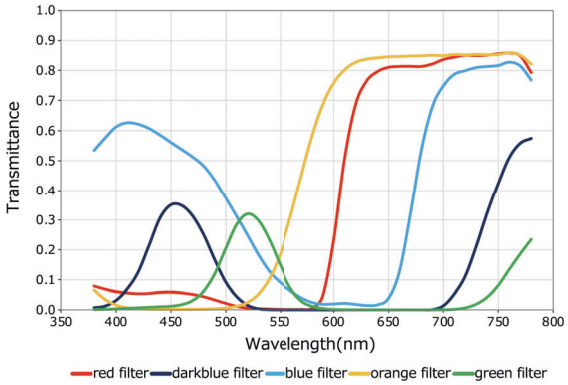

Figure 6: Spectral transmittance of color filters

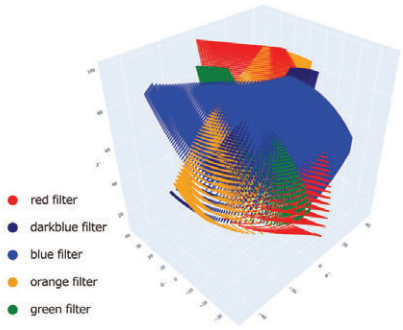

Figure 7: Colors through each color filter in CAM16-UCS

The color scheme was designed based on color differences in CAM16-UCS. The idea behind the color scheme was to replace the color chips in the paper version with colors on the tablet device; however, there were two significant changes. First, the target color was incorporated into the ground area, which was constituted from similar colors. Second, the color difference between the target color and the colors assigned to the figure was changed from 5 to 2. The target color of each filter was listed in Table 1. An asterisk (*) shows that the color scheme in that part incorporates colors that obscure the figure when viewed through another filter. Further details will be provided later. Because of the nonlinear relationship between the computer's output and input values, gamma correction is necessary to derive DisplayP3 RGB values from the generated spectral distribution. A gamma value of 2.2 was applied in the calculation.

3) Creation of patterns

Figure 8 shows the digit patterns of the digital device version, which was created in Xcode using the Swift UI library. The color shown in bold indicates the filter color necessary for viewing the pattern. Each pattern consisted of 5 × 5 squares, which were 14 pixels on a side, with the devised color scheme applied to each square. Although all patterns shown in Figure 8 denote the digit 1, the patterns indicating the digits 2 to 8 were also created. A color name marked with an asterisk (*) at the bottom right of the pattern shows that colors which obscure the figure when viewed through the marked color filter have been added to the ground. In other words, colors whose color difference from the target in the figure is less than 2 when viewed through the marked color filter are incorporated into parts of the ground. This adjustment was made because, without the added colors, the figure was clearly recognizable even when viewed through the marked color filter.

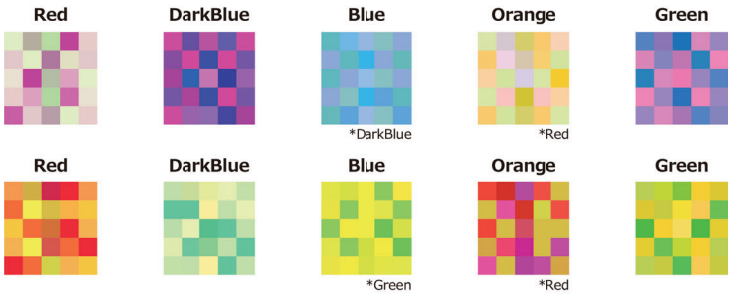

Figure 8: Color scheme of digit patterns in digital device version

Table 1: Filter color and target color

Filter color	Figure P3(R,G,B)	Ground P3(R,G,B)
Red	180,205,166	229,190,199
	219,055,067	254,055,067
DarkBlue	095,037,254	067,078,199
	146,232,154	193,243,173
Blue	087,190,246	087,193,199 *
	252,250,037	252,236,055 *
Orange	216,205,162	254,205,173 *
	219,055,067	254,055,067 *
Green	170,121,202	177,136,202
	184,224,037	187,208,037

Development of an educational game

An educational game was developed using materials for the digital device version. It was designed for multiple players to participate in teams, each wearing one of the five colored goggles on their own choice: red, dark blue, blue, orange, or green.

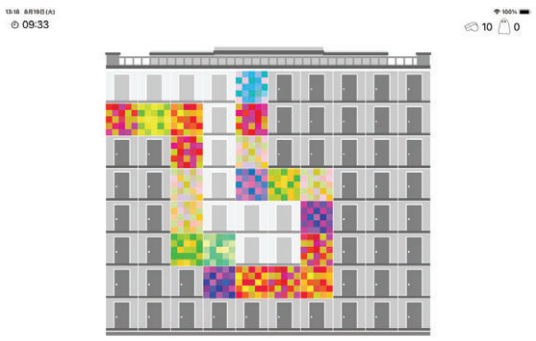

Figure 9: Game play screen

The Minesweeper algorithm was implemented in the game. Ghosts were adopted instead of mines. In this game, the team that finds the most ghosts in the building wins. There are $8 \times 10 = 80$ rooms on the display, and ghosts are randomly hidden in these rooms. The digit patterns are used to indicate the number of ghosts in the adjacent eight rooms. The player's task is to identify the rooms where ghosts exist based on the digit numbers. The displayed color scheme is chosen randomly. Therefore, the digit can be visible only to the player wearing the color goggles corresponding to its color scheme. To find all the ghosts, they will need to work with others wearing the different color goggles. Since the patterns displayed in the game are created to match the five color filters, the number of colors of the goggles in each team is critical. The more colors there are, the greater the advantage.

The rooms can be opened by tapping on them. If the players open a room where a ghost is, the game will end. By tapping and holding a room, the players can use the "Use the mysterious whistle" command. If a ghost is in the room, it will appear. The number of ghosts you have found will increase by one. If no ghost in the room, the door will open as it would with a standard tap. This command has a limited number of uses, equal to the number of hidden ghosts. Therefore, even if a team has few colors of goggles and cannot determine which rooms contain ghosts, they can still progress in the game by using this command, but the total number of ghosts they can finally find will be reduced. The game also has a time limit, and players must communicate actively with one another to avoid running out of time.

The developed game was tested with 19 Japanese high school students on August 20, 2025, at Kyushu University. One of them was found to have color vision deficiency by the questionnaire after playing the game. Test participants were divided into four groups and played the game. After playing the game, they learned color vision diversity and its significance through explanations tailored to their gaming experience. The explanations emphasized three points. The first point is that color is a subjective sensation in the brain; it is explained in relation to the change in color perception depending on the color filter. The second point is diversity in color vision, which was explained by the variation in the number of color filters. The third point is that diversity in color vision can provide strength to teams or groups. It was explained by the concept that the more types of color filters in the team, the greater the advantage. At the end of the test, they answered a questionnaire about the game and its educational effects.

RESULTS AND DISCUSSION

Figure 10 shows the scene of playing the game. As soon as the game began, the participants seemed somewhat confused about the game rules and how to play. However, as the game progressed, they immediately came to understand the controls and rules, and they were observed cooperating and enjoying the activity together. Table 2 shows the questionnaire results. In the questionnaire, 19 participants were asked to select the option that best applied to them on a five-point scale. The table presents each question along with the number of participants who chose each option. According to the results, all participants found the game enjoyable and valued the relationship between the game and the learning content. Also, almost all participants answered that they would like to share the learning content. These results suggest that this educational game is effective in enjoyable learning about color vision

diversity, and that by actively sharing what they have learned with others, it may contribute to the broader dissemination of social knowledge regarding color vision diversity.

While the questionnaire results showed the positive aspects of the game, several points still require revision. One of them is whether students with color vision deficiencies can fully enjoy the game. In the game, since many people see colors differently through color filters, they are less likely to feel negative about seeing colors differently from others. However, patterns created using the prediction CAM16 color appearance model, which is based on the perception of a standard observer, are used. Therefore, the patterns created may not consistently be recognized as intended. Even in this case, they can still participate in the game by guessing the rooms that contain ghosts based on numbers that other players see. However, it is essential to examine how they recognize patterns and form impressions of the game.

Figure 10: Scene of playing the game

Table 2: Questionnaire results

Question	Strongly agree	Somewhat agree	Neutral	Somewhat disagree	Strongly disagree
The game was enjoyable	18	1	0	0	0
The difficulty of the game was appropriate	11	7	0	1	0
Game controls were easy to use	11	6	2	0	0
I was able to understand the learning content	17	2	0	0	0
The learning content was difficult to understand	1	0	5	8	5
The game was suitable for the learning content	17	2	0	0	0
I want to share the learning content with people close to me	15	1	1	2	0

CONCLUSION

This study revealed that the developed game, which utilizes a color filter, is effective in understanding the concept of color vision diversity and its significance. In the future, we plan to investigate how individuals recognize these patterns and further enhance the game.

ACKNOWLEDEMENTS

This work was supported by JSPS KAKENHI Grant Numbers JP 21H04342, JP 24H00167

REFERENCES

[1]. Fujii, T., Muraya, T., and Sunaga, S. (2024). Creation of Educational Materials for an Educational Program for Learning Color Vision Diversity and Subjectivity. *Bulletin of the color science association of Japan*, 3(2), 93.

[2]. Yoshikawa, A., Akai, A. (2023). “irotoridori”, a series of picture books let you enjoy the various ways of seeing colors together. Proceedings of the 70th Annual Conference of JSSD, 278-279.

[3]. Li, C., Li, Z., Wang, Z., Xu, Y., Luo, M. R., Cui, G., Melgosa, M., Brill, M. H., and Pointer, M. (2017). Comprehensive color solutions: CAM16, CAT16, and CAM16-UCS. *Color Research and Application*, 42(6), 703-718.

Colour Accuracy of Low-Cost Spectrophotometers

Anders Nilsson[a*], Eric Kirchner[b], and John Seymuor[c]

[a]NCS Colour AB, Stockholm, Sweden
[b]College of Optical Science and Engineering, Zhejiang University, Hangzhou, China
[c]John the Math Guy, LLC, Greenville, South Carolina, USA
[*]Corresponding author: Anders Nilsson, anders.nilsson@ncscolour.com

ABSTRACT

Low-cost pocket-size spectrophotometers are today available on the market. These devices often have measurement specifications which appear good enough for most colour control tasks, even if they are not as good as the much more expensive, traditional benchtop spectrophotometers. For this reason, it can be hard for a user to judge if the low-cost instrument really is as good as the specification indicates. In both quality control and colour matching, instruments with di:8° geometry are regarded as the most accurate. Five pocket-size spectrophotometers were selected where the manufacturers specify spectral measurement in agreement with measuring geometry di:8°. Three high-end benchtop spectrophotometers, having the same measurement geometry, were included as reference and for comparisons. The following parameters were compared, the short time repeatability, the reproducibility, the inter-instrument agreement, inter-model agreement and accuracy. Apart from these standard tests, the calibration process and measurement of anisotropic samples were investigated. The test samples were selections of colour samples from different NCS, Munsell and RAL colour cards. All samples were selected as pairs, having the same notations but differing in production batch and gloss to give examples of small to medium colour differences and metamerism. The colour samples were selected to cover different hues, different chromaticness and different lightness. All CIELAB coordinates and ΔE values were calculated from the spectral data using the same weighting functions and algorithms in Excel to avoid differences coming from the different manufacturers' software.

Keywords: spectrophotometer, colour measurement, colour accuracy

INTRODUCTION

Today a new type of colour measurement instrument is available, the low-cost, pocket-size spectrophotometers ($150-650). Traditionally, accurate spectrophotometers are costly benchtop instruments for lab usage ($5000-20000). Handheld, portable instruments have also been available for more than 30 years, but the price tag for these instruments is still high ($3000-15000). The di:8° instruments are of most interest as this geometry is regarded as the most accurate in both quality control and colour matching.

The end users of these instruments are mostly professionals in architecture and design, production industry, painters and paint resellers. The usage in architecture and design is to analyze and document surface colours. For industry the use is to check production tolerances. Painters use these instruments to analyze and check colours. Paint resellers analyze colours for customers to find closest paint formulations and to do colour corrections.

To analyze and document colours, absolute accuracy is of importance but the true value in CIELAB coordinates of a surface colour is not well defined. All manufacturers of spectrophotometers on the market, both high-end and low-cost instruments, only report short-term repeatability and inter-instrument agreement between

instruments of the same model. No specifications for the absolute accuracy of instruments are published. A user expects that different instruments give the same CIELAB value from measurements on the same surface, but this is in general not true. For quality control purpose, the instruments' ability to accurately measure a colour difference between two samples is of importance. A user will expect their instrument to give the same ΔE as other instruments when comparing the same samples. For spectrophotometers also the measured metamerism between two samples is expected to be the same.

The new pocket-size instruments often have specifications for repeatability and inter-instrument agreement good enough for most colour control tasks and not far behind the much more expensive, traditional benchtop spectrophotometers. For this reason, it can be hard for a user to judge if the low-cost instrument really is as capable for the task as the specification indicates. There are different use-cases for instrumental colour control where measurement accuracy plays different roles:

1. Measure the colour difference between a standard and a sample having the same gloss and texture, measured in sequence, in the same instrument without calibration in between.
2. The standard and the sample have different gloss and/or texture.
3. The standard is measured in the same instrument but months or years earlier
4. The standard is measured in another instrument of the same model
5. The standard is measured in another instrument of another model

In cases 1 and 2 the repeatability and the measurement geometry are of importance. In case 3, the reproducibility and long-time stability add to the demands. In case 4 the inter-instrument agreement (IIA) is vital. In case 5 the accuracy is of importance. In all cases, the inter-model agreement is important, as the measured ΔE values and metameric indexes normally are compared to a specification from other instruments.

The objective of this study is to compare the specifications and the actual performance of pocket-size spectrophotometers to the traditional high-end spectrophotometers to evaluate if the new pocket-size instruments fulfill the requirements in the use-cases.

METHODOLOGY

Instruments

Five pocket-size spectrophotometers with measuring geometry di:8°[1] were tested. Three high-end benchtop spectrophotometers with the same geometry were included as reference and for comparisons. All instruments reported reflectance data from 400 to 700 nm in 10 nm steps. Four pocket-size instruments models have an integrating sphere, one has 45:0 measurement geometry but approximates the di:8° values based on the user-supplied gloss level.

Table 1 lists the low-cost pocket-size spectrophotometers used for this study. The instruments are of five different models, for three of the models, two instruments were included also for IIA comparisons. Table 2 lists the three benchtop spectrophotometers of two different models. All instruments have a label that is used for identification in the following tables. The instrument CM3700_1 in Table 2 was used as the main reference. For some investigation, the average value from instrument CM3700_1 and CM3700_2 were used. Instrument DC700 was included to illustrate the differences a user must expect also between high end benchtop instruments of different brands and models. The aperture for the benchtop instrument was selected to match the pocket-size instruments.

Table 1. The eight investigated pocket-size spectrophotometers with data from the manufacturer

No	Label	Producer	Model	Geometry	Aperture	Repeatability	IIA
1	CR3_1	3nh	ColorReader CR3	di:8	8 mm	0.05 ΔE*	0.01 DP[1]
2	CR3_2	3nh	ColorReader CR3	di:8	8 mm	0.05 ΔE*	0.01 DP
3	CCP_1	FRU	Color Cat Pro	di:8	8 mm	0.05 ΔE*	0.01 DP
4	CCP_2	FRU	Color Cat Pro	di:8	8 mm	0.05 ΔE*	0.01 DP
5	CMM_1	CHNSpec	ColorMeter Max	di:8	8 mm	0.05 ΔE_{00}	0.2 ΔE_{00}
6	CMM_2	CHNSpec	ColorMeter Max	di:8	8 mm	0.05 ΔE_{00}	0.2 ΔE_{00}
7	S1P	Variable	Spectro 1 Pro	d/0 (SCI)	8 mm	0.05 ΔE_{00}	0.2 ΔE_{00}
8	CRS	Datacolor	ColorReader Spectro	45/0 (SCI)	6 mm	0.03 SD[2]	0.4 ΔE_{00}

Table 2. Three benchtop spectrophotometers used as reference with data from the producer

No	Label	Producer	Model	Geometry	Aperture	Repeatability	IIA
9	CM3700_1	Konica-Minolta	CM-3700A	di:8	11/8 mm	0.005 SD	0.08 ΔE*
10	CM3700_2	Konica-Minolta	CM-3700A	di:8	11/8 mm	0.005 SD	0.08 ΔE*
11	DC700	Datacolor	Spectro 700	di:8	9/5 mm	0.03 ΔE*	0.15 ΔE*

Test samples

Table 3 list the notations for the NCS, Munsell and RAL samples pairs, together with the ΔE_{00} and gloss values, used for the comparisons. For the short-term repeatability investigation, a white ceramic tile was used.

Thirty NCS notations, representing greyscale and high chromatic colours with different hues and lightness were selected. For each notation, a pair of samples from two different production batches of the NCS Index, having a small colour difference, was used. The samples have a gloss of 17.5 ± 2.5 60° GU [2]. For comparison of colour differences between glossy and matte surfaces, nine high chromatic Munsell notations and ten RAL notations were selected with hues spread out around the hue circle. The Munsell samples from the glossy and matte edition, having the same notations, were used. RAL samples with the same number from three different collections; K5 semi matt, K5 Gloss and K7 (Gloss) was used. None of the samples were fluorescent.

[1] Display Precision, the number of decimals shown in the instruments built in display. This is the only accuracy/IIA figures given by the producer.

[2] Standard Deviation, It is unclear how this is determined. This is presumably the standard deviation of reflectance measurements at a specific wavelength.

Table 3. Test samples.

30 NCS sample pairs

NCS	ΔE00	NCS	ΔE00	NCS	ΔE00
S 0580-Y10R	0.49	S 3060-R70B	0.17	S 0570-G60Y	0.39
S 0580-Y30R	0.36	S 2565-R80B	0.34	S 0575-G90Y	0.41
S 0580-Y50R	0.48	S 2065-R90B	0.20	S 0500-N	0.43
S 0580-Y70R	0.39	S 1565-B	0.24	S 4500-N	0.15
S 0580-Y90R	0.21	S 2555-B20G	0.17	S 9000-N	0.61
S 1080-R	0.24	S 2060-B50G	0.16	S 6020-Y10R	0.13
S 2060-R20B	0.45	S 2555-B80G	0.05	S 6020-Y80R	0.09
S 2060-R40B	0.07	S 1565-G	0.23	S 6020-R20B	0.14
S 3055-R50B	0.16	S 0570-G20Y	0.31	S 6020-R90B	0.15
S 3555-R60B	0.19	S 0570-G40Y	0.52	S 6020-B50G	0.16
Average	0.33				

9 Munsell sample pairs

Munsell	Matte	Glossy	ΔE00
5Y 8/12	2	79	1.8
5YR 7/12	3	73	3.3
5R 5/14	2	64	3.3
2.5RP 6/12	2	65	1.4
2.5P 5/10	1	52	2.6
10B 6/10	2	68	2.3
10G 7/8	2	77	1.6
7.5GY 7/10	2	67	2.4
10Y 8/12	2	77	1.9
Average	2	69	2.3

10 RAL sample triplet's

	Gloss			ΔE00	
RAL	K5_1	K5_2	K7	K5_1-K5_2	K5_2-K7
1018	25	63	59	0.93	0.28
1033	25	60	51	1.20	0.47
2012	28	58	56	0.77	0.33
3003	26	60	61	0.59	0.63
3013	26	58	56	0.77	1.07
4008	26	58	61	0.25	0.02
5005	22	59	52	0.67	1.31
5018	24	58	64	0.88	0.37
5024	28	59	59	0.45	0.69
6017	27	62	59	0.64	0.16
Average	26	60	58	0.71	0.53

Colour calculations

To focus on the practical use of the instruments, this investigation limits colour system and colour coordinates to using CIELAB coordinates, CIEDE2000(ΔE_{00}) and CIELAB ΔE^* (ΔE^*) colour differences [1], all instruments can give these values. All measurement data was exported as spectral data. The CIELAB coordinates and colour difference values were then calculated in accordance with CIE publ. 15 [1].

Illuminations

All specifications from manufacturers are given under CIE Standard daylight, D65 [1]. In this investigation, we also include values for CIE illuminant F11 as a worst-case scenario. F11 represents a fluorescent tube commonly used in shops to illuminate products. In many parts of the world, LED sources are now replacing fluorescent tubes, hopefully with some better spectral properties then F11.

Measurements

All measurements were done in a lab with a controlled temperature of 23 ± 0.5°C and the samples were acclimatised at least one hour before measurements. Measurements were taken as single measurements except for measurements in the two CM-3700A instruments, see discussion under "Anisotropy effects" below.

RESULTS AND DISCUSSION

Repeatability

Repeatability is the random error of a measurement, without moving the instrument between measurements [3]. Normally, the repeatability reported from the manufacturer is on the instrument white calibration tile. This was not possible for some of the instruments, since these instruments detect the presence of their calibration tile and automatically perform a calibration, i.e. always returning the stored values. Instead, a white ceramic calibration tile from Datacolor was used. The tile was measured 20 times at 10 seconds intervals. The procedure to measure repeatability varies slightly between manufacturers and standards, having 20 or 30 measurements. To give best possible values, the lowest common delimiter, 20 was chosen. For instrument S1P a variable interval between 10 and 30 seconds was used due to demands in this instrument's software, the LED's needs longer cooling time the more they are used. It is not clear from the manufacturers specifications how the repeatability is calculated, here we take the difference from the first measurement to detect drift. Table 4 lists the resulting repeatability values in ΔE00 and Table 5 show the ΔE^* values. All instruments, except CRS, CCP_1 and CCP_2 meet their specifications. Table

6 shows in diagrams how each of the three CIELAB colour coordinates L*, a* and b* change during a measurement series. Clear trends can be seen for the instruments CRS, CCP_1 and CCP_2. The first measurements have the largest change; the deviation then stabilise some after five to ten measurements. The other instruments show more consistent results with an expected random pattern.

Table 4. Short term repeatability, values for D65 in ΔE_{00}

Instr.	CM3700_1	CM3700_2	DC700	CR3_1	CR3_2	CCP_1	CCP_2	CMM_1	CMM_2	S1P	CRS
Av	0.005	0.004	0.012	0.018	0.030	0.062	0.035	0.033	0.050	0.021	0.058
Sdev	0.002	0.001	0.006	0.009	0.005	0.031	0.021	0.019	0.021	0.008	0.014
RMS	0.005	0.004	0.013	0.020	0.031	0.070	0.041	0.038	0.054	0.022	0.060
Max	0.010	0.006	0.022	0.043	0.039	0.124	0.090	0.078	0.097	0.034	0.075

Table 5. Short term repeatability, values for D65 in ΔE*

Instr.	CM3700_1	CM3700_2	DC700	CR3_1	CR3_2	CCP_1	CCP_2	CMM_1	CMM_2	S1P	CRS
Av	0.005	0.005	0.011	0.015	0.028	0.061	0.037	0.027	0.039	0.019	0.054
Sdev	0.002	0.001	0.005	0.008	0.005	0.031	0.019	0.011	0.015	0.006	0.013
RMS	0.006	0.005	0.012	0.017	0.028	0.069	0.041	0.029	0.041	0.020	0.056
Max	0.010	0.007	0.020	0.039	0.036	0.114	0.091	0.054	0.072	0.030	0.070

Table 6. Short term repeatability, L*a*b* coordinate change during measurement series.

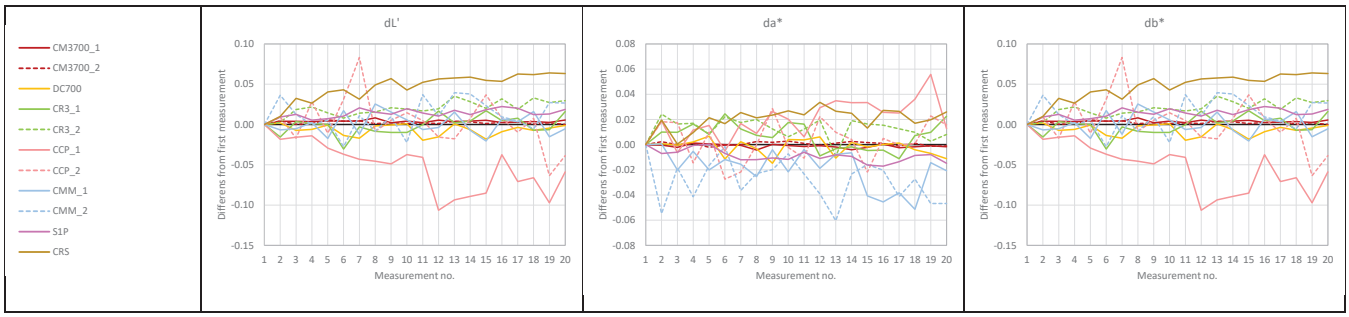

Reproducibility

Reproducibility for on instrument can be defined in different ways [3], but is generally a broader test than repeatability, with at least one condition changing between measurements. This may involve, for example, repositioning the instrument on the sample or having a different operator. Here we calculate the reproducibility as the differences between two measurements of the same sample set in the same instrument, the same measurement conditions are used, and the instrument is calibrated before each measurement of the set. All samples from NCS, Munsell and RAL was measured. None of the samples were fluorescent.

Table 3 was used. Table 7 and Table 8 show the results. The samples with different gloss levels are shown separately. The reproducibility for the samples with lowest gloss is slightly worse compared to the mid and high gloss sets in the three benchtop instruments, the surface of low gloss samples is often not 100% homogenous and easy to be damaged during measurement. There is no specification of the reproducibility from any instrument manufacturer. The reproducibility is between 2 and 4 times worse for the pocket-size instruments compared to the benchtop instruments.

Table 7 Reproducibility in ΔE00

	Sample no.	CM3700_1	CM3700_2	DC700	CR3_1	CR3_2	CCP_1	CCP_2	CMM_1	CMM_2	S1P	CRS
Matt	9	0.05	0.03	0.04	0.05	0.05	0.11	0.09	0.05	0.05	0.05	0.1
Semi matt	70	0.02	0.02	0.03	0.05	0.05	0.09	0.08	0.10	0.10	0.11	0.1
Gloss	29	0.03	0.03	0.03	0.05	0.05	0.14	0.16	0.08	0.07	0.09	0.0
All	108	0.02	0.02	0.03	0.05	0.05	0.10	0.10	0.09	0.09	0.10	0.0
RMS	108	0.04	0.03	0.04	0.06	0.06	0.12	0.13	0.11	0.12	0.12	0.1

Table 8 Reproducibility in ΔE*

	Sample no.	CM3700_1	CM3700_2	DC700	CR3_1	CR3_2	CCP_1	CCP_2	CMM_1	CMM_2	S1P	CRS
Matt	9	0.07	0.09	0.09	0.11	0.10	0.19	0.21	0.09	0.09	0.11	0.1
Semi matt	70	0.04	0.04	0.05	0.08	0.07	0.15	0.14	0.15	0.17	0.18	0.2
Gloss	29	0.05	0.06	0.08	0.09	0.09	0.25	0.27	0.14	0.12	0.16	0.1
All	108	0.04	0.05	0.06	0.09	0.08	0.18	0.18	0.14	0.15	0.17	0.2
RMS	108	0.06	0.07	0.08	0.11	0.10	0.22	0.22	0.16	0.18	0.20	0.2

Anisotropy effects

Most samples are isotropic, meaning that rotating an instrument around the surface normal will not appreciably change the measurements. But some coloured surfaces or combinations of surfaces and instrument give rise to anisotropy effects. Earlier investigations have shown that this can be due to polarisation effects from a visible or microscopic surface structure. This also could be due to non-polarizing structures such as preferred orientation of paper fibres or striations in metal that has been stretched. To investigate this, all samples were measured two times with 90-degree rotation in between in one instrument of each model, and the average ΔE_{00} between these measurements was calculated. Table 9 shows the reproducibility compared to the sample rotation. For all pocket-size instruments, the difference from rotation is smaller than the reproducibility. For the instrument CM-3700A this effect can be large, as indicated in Table 9, for highest accuracy, the average of two measurements with 90-degree rotation in between is then needed. Table 10 show this effect on the two worst colours in the test sets.

Table 9 Reproducibility compared to 90-degree sample rotation in average ΔE_{00}

	CM3700_1	CM3700_2	DC700	CR3_1	CCP_1	CMM_1	S1P	CRS
Reproducibility	0.03	0.03	0.03	0.05	0.11	0.08	0.09	0.09
Rotation	0.06	0.07	0.05	0.04	0.06	0.06	0.06	0.04

Table 10 Reproducibility compared sample rotation for two worst colours

Color	Comparison	CM3700_1	CM3700_2	DC700	CR3_1	CCP_1	CMM_1	S1P	CRS
5YR 7/12	Rotation	0.51	0.50	0.19	0.08	0.10	0.17	0.08	0.04
5YR 7/12	Reproducibility	0.10	0.03	0.02	0.09	0.12	0.04	0.08	0.03
S 6020-Y10R	Rotation	0.56	0.54	0.05	0.01	0.04	0.14	0.16	0.05
S 6020-Y10R	Reproducibility	0.03	0.02	0.03	0.06	0.06	0.13	0.20	0.08
Average		0.24	0.25	0.07	0.03	0.03	0.05	0.05	0.02

Calibration stability

The reproducibility tests indicated some unexpected offset between the first and the second measurement of the samples. This led to the suspicion that the calibration procedure was not stable on some instruments. The

benchtop instruments have a green ceramic tile that is measured in the calibration process to check the calibration. None of the pocket-size instruments have this feature. To test the calibration stability the process of calibrating and measuring the same sample 21 times in a row was performed. The glossy Munsell 5Y 8/12 was selected for the test. Diagram 1 shows the ΔE_{00} difference between the first and the following 20 measurements, with calibration in between each. The average difference is around 0.06 ΔE_{00} for all instruments. The measurement with instrument CR3_2 indicates larger errors in the calibration. This was the first instrument to be tested; it also has a special white standard holder that needs to be manually pressed against the instrument. The improvement for this instrument after measurement 14 and for the other instrument of the same model, CR3_1, indicates that a learning period was necessary for users using this instrument.

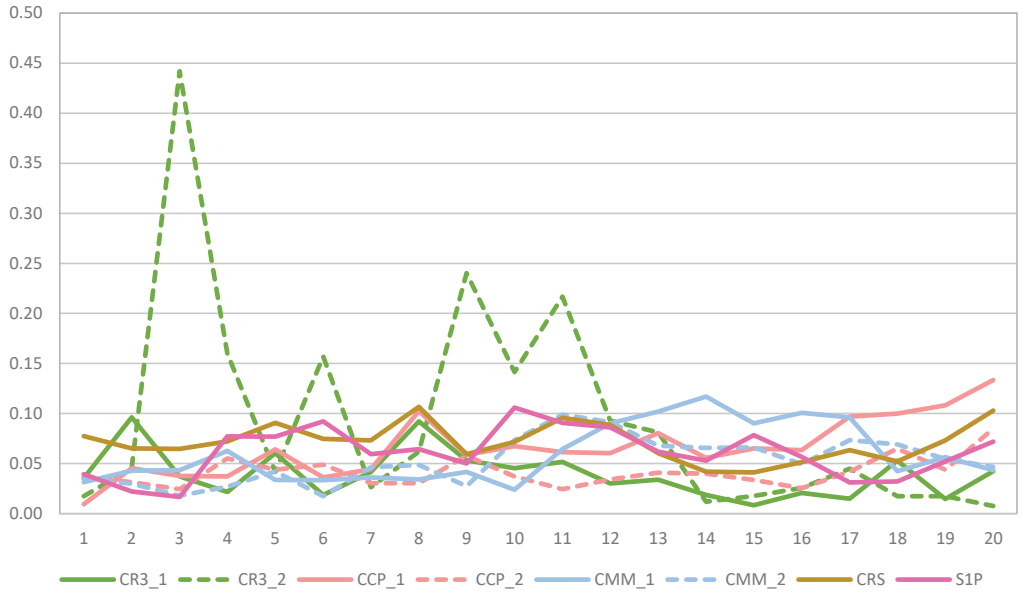

Diagram 1 Calibration stability in ΔE00

Inter-instrument agreement (IIA)

IIA is defined as the reproducibility between two instruments of the same model [3]. IIA is normally given as the average difference in CIELAB values for the 12 BCRA tiles [4] between an individual instrument and the "Master Body" for the model. Theoretically the difference between two individual instruments can then be up to twice the specified value. IIA was calculated for the four instrument models having two instruments in this investigation. The difference between the measured CIELAB and ΔE values for each model was calculated and compared to the manufacturer's specifications if this was given in Table 1 or Table 2. The agreement of measured colour difference was calculated as the absolute difference in ΔE for all sample pairs. This is probably the most important use case in practice but is never included in any specification from the manufacturers. The IIA for CIELAB values for all colour samples together with available specification is given in Table 11. The absolute difference for the ΔE value for all sample pairs is also listed in Table 11.

The benchtop instrument, CM3700, is probably within the manufacturer's specification for the CIELAB values, the pocket-size instruments are 15 to 20 times higher and probably outside expected IIA. The agreement between measured colour difference, ΔE is better, as seen in Table 11 and is close to the reproducibility for each instrument but the RMS value is higher, close to double, compared to the reproducibility for the pocket-size instruments. The instrument model CR3 is notably better compared to the other two pocket-size instrument.

Table 11 IIA for CIELAB and ΔE values

IIA for CIELAB values

	CM3700	CR3	CCP	CMM
ΔE00	0.05	0.79	1.19	0.74
ΔE*	0.11	1.31	1.74	1.27
Specified	0.08 ΔE*	-	-	0.2 ΔE00

IIA for ΔE values

		CM3700	CR3	CCP	CMM
ΔE00	Average	0.02	0.04	0.10	0.10
	RMS	0.03	0.06	0.15	0.15
ΔE*	Average	0.04	0.09	0.19	0.21
	RMS	0.06	0.14	0.30	0.31

Inter-model agreement (IMA)

IMA is defined as the reproducibility between two instruments of different model 12[3]. We only investigate the reproducibility for ΔE values here, as the CIELAB values is described under accuracy below. To investigate the spectral qualities of the instruments we compare the metameric index using CIE standard light source F11 (M_{F11}) [5]. The average value from the benchtop instrument's CM3700_1 and CM3700_2 are used as the true value for both ΔE and metameric index.

Table 12 and Table 13 show the absolute difference between the measured ΔE value for each instrument compared to the benchtop model, CM3700, for ΔE_{00} and ΔE*. For the two sample set with small gloss and/or small ΔE difference, NCS and RAL Gloss, the differences in measured ΔE are comparable to the instrument's reproducibility. For the sample-sets with higher gloss difference the differences in measured ΔE increase. For the other benchtop model, DC700, the values are close to the reproducibility for all sets. For the low-cost pocket-size instruments the measured ΔE values are significantly different from values measured by the benchtop instruments, with the largest differences found for instrument S1P.

Table 14 and Table 15 show the absolute difference in metameric index between the CM3700 (labelled M_{F11}) and the other instruments. The NCS sample set have low metamerism between the two batches, and here all instruments have reasonable agreement. For the RAL sample set with much higher metamerism, the difference is much higher. This indicates that inadequate spectral resolution is the main cause for the differences in IMA for the low-cost pocket-size instruments.

Table 12. Difference in ΔE00 compared to CM3700

Instrument		DC700	CR3_1	CR3_2	CCP_1	CCP_2	CMM_1	CMM_2	S1P	CRS
NCS Semi matt	Average	0.02	0.12	0.12	0.08	0.09	0.10	0.09	0.17	0.13
	RMS	0.03	0.23	0.24	0.10	0.13	0.16	0.14	0.29	0.20
RAL Gloss	Average	0.03	0.10	0.08	0.13	0.17	0.07	0.09	0.40	0.12
	RMS	0.04	0.13	0.10	0.17	0.23	0.08	0.13	0.52	0.16
RAL Semi matt - Gloss	Average	0.03	0.25	0.25	0.29	0.24	0.18	0.23	0.39	0.29
	RMS	0.04	0.33	0.33	0.39	0.31	0.24	0.32	0.52	0.37
Munsell Matt - Gloss	Average	0.06	0.15	0.12	0.51	0.58	0.54	0.57	0.74	0.40
	RMS	0.07	0.19	0.17	0.53	0.61	0.62	0.61	0.96	0.48
ALL	Average	0.03	0.16	0.15	0.20	0.21	0.18	0.19	0.34	0.21
	RMS	0.04	0.25	0.25	0.30	0.30	0.28	0.30	0.53	0.30

Table 13. Difference in ΔE* compared to CM3700

Instrument		DC700	CR3_1	CR3_2	CCP_1	CCP_2	CMM_1	CMM_2	S1P	CRS
NCS Semi matt	Average	0.03	0.16	0.16	0.10	0.11	0.18	0.16	0.23	0.18
	RMS	0.03	0.24	0.24	0.14	0.14	0.36	0.32	0.34	0.23
RAL Gloss	Average	0.04	0.20	0.26	0.25	0.25	0.16	0.20	0.51	0.26
	RMS	0.04	0.27	0.35	0.37	0.33	0.24	0.28	0.63	0.40
RAL Semi matt - Gloss	Average	0.07	0.52	0.58	0.60	0.70	0.60	0.58	0.65	0.48
	RMS	0.09	0.82	0.86	0.84	0.89	0.87	0.84	0.92	0.63
Munsell Matt - Gloss	Average	0.06	0.24	0.21	0.50	0.58	0.56	0.57	1.02	0.54
	RMS	0.08	0.37	0.32	0.55	0.63	0.67	0.66	1.38	0.78
ALL	Average	0.04	0.28	0.31	0.32	0.36	0.35	0.34	0.50	0.33
	RMS	0.06	0.50	0.52	0.52	0.55	0.59	0.56	0.78	0.49

Table 14. Difference in M_{F11} compared to CM3700 in ΔE00

	ΔGL	ΔE00	M_{F11}		DC700	CR3_1	CR3_2	CCP_1	CCP_2	CMM_1	CMM_2	S1P	CRS
NCS	0	0.3	0.16	Average	0.02	0.11	0.12	0.11	0.10	0.12	0.11	0.09	0.08
				RMS	0.04	0.17	0.17	0.14	0.13	0.21	0.20	0.13	0.13
RAL Gloss	0	0.5	0.43	Average	0.03	0.22	0.22	0.24	0.22	0.17	0.24	0.31	0.25
				RMS	0.06	0.68	0.69	0.67	0.54	0.63	0.61	0.59	0.62
RAL Semi matt - Gloss	33	0.8	1.18	Average	0.06	0.61	0.59	0.62	0.59	0.58	0.51	0.61	0.51
				RMS	0.08	0.86	0.85	0.87	0.83	0.79	0.69	0.88	0.78
Munsell Matt - Gloss	67	2.3	0.81	Average	0.03	0.41	0.40	0.46	0.43	0.32	0.30	0.42	0.24
				RMS	0.04	0.55	0.54	0.60	0.55	0.40	0.37	0.63	0.34
All	-	1	0.58	Average	0.04	0.31	0.31	0.32	0.30	0.29	0.27	0.32	0.25
				RMS	0.06	0.54	0.53	0.55	0.51	0.48	0.44	0.55	0.47

Table 15. Difference in M_{F11} compared to CM3700 in ΔE*

	ΔGL	ΔE00	M_{F11}		DC700	CR3_1	CR3_2	CCP_1	CCP_2	CMM_1	CMM_2	S1P	CRS
NCS	0	0.4	0.26	Average	0.03	0.15	0.16	0.14	0.13	0.13	0.11	0.16	0.13
				RMS	0.06	0.20	0.20	0.18	0.18	0.19	0.18	0.21	0.18
RAL Gloss	0	1.1	0.77	Average	0.06	0.35	0.37	0.41	0.34	0.33	0.42	0.52	0.39
				RMS	0.13	1.30	1.30	1.28	1.06	1.22	1.16	1.10	1.13
RAL Semi matt - Gloss	33	1.4	2.17	Average	0.12	1.01	0.98	1.12	0.99	0.89	0.82	1.02	0.87
				RMS	0.16	1.50	1.47	1.54	1.44	1.32	1.22	1.46	1.31
Munsell Matt - Gloss	67	4.5	1.66	Average	0.06	0.82	0.76	0.92	0.79	0.61	0.57	0.87	0.50
				RMS	0.08	1.06	1.02	1.21	1.04	0.81	0.76	1.31	0.70
All	-	1	1.22	Average	0.07	0.52	0.51	0.56	0.49	0.44	0.42	0.56	0.43
				RMS	0.10	0.93	0.91	0.97	0.89	0.80	0.75	0.96	0.79

Accuracy

An instrument accuracy is defined by ISO and ASTM as the conformance of a series of readings to the accepted or true value [3]. If two different instruments are accurate, the measurement values of a standard in the first instrument can be used to calculate an accurate colour difference to the measurement values of a sample in the second instrument. This is a demand for accurate, digital colour communication. For CIELAB values, there are no generally accepted true values as the measured reflectance depends on the instrument construction and the resulting colour values often differ much more than the visible acceptable difference. In this investigation we use the average value from the benchtop instrument's CM3700_1 and CM3700_2 as the true value. Table 16 list the average ΔE values between the "true value" and the measured value in each instrument for all test samples.

Table 16. Accuracy compared to CM3700 instruments in ΔE00 and ΔE*

	DC700	CR3_1	CR3_2	CCP_1	CCP_2	CMM_1	CMM_2	S1P	CRS
ΔE00	0.22	0.95	1.18	1.69	1.63	1.02	1.01	1.03	0.54
ΔE*	0.31	1.72	2.07	3.02	3.39	1.73	1.94	2.23	1.11

CONCLUSION

The aim of this investigation was to compare low-cost pocket-size spectrophotometers to the high-end instruments. Spectrophotometers are used to check if a colour is within a specified tolerance. The reproducibility of the instrument should then be significantly smaller than the tolerance. For colour measurement the demand is normally a reproducibility of 1/3 to 1/5 of the tolerance. The smallest visible colour difference is around 0.3 ΔE. Production tolerances vary between products and industries; automotive on 0.3-0.6, coatings 0.6-1.0, textile 1.0-2.0 and printing 2.0. Also, the colour difference equation differs, here we only use ΔE00.

Repeatability is significantly lower than any tolerance for all tested instruments. For some of the pocket size instruments a small drift is noted especially for instrument CCP_1 and CRS.

Reproducibility for the benchtop instrument is lower than 1/5 of the lowest tolerance for all tested gloss levels of samples. For the pocket-size instruments, the CR3 shows good values, the other instruments can't manage tolerances below 1.0 ΔE00.

Anisotropy effects are only a problem for the CM3700 benchtop instrument in this test. If each sample is measured as the average of two measurements with 90 degrees rotation in between, this effect disappears. This effect should be investigated further in the future.

Calibration stability gives a random error up to 0.1 DE00 for all instruments. For instrument CR3, this can be larger due to its complicated calibration procedure and special care need to be taken for this instrument model.

The inter instrument agreement (IIA) for measuring absolute CIELAB values is bad for all pocket-size instruments compared to the benchtop instrument. This is a concern when using low-cost pocket-size instruments, but it does not make these instruments useless for many user scenarios. For example, a common situation in industry is to share a physical colour standard between producer and customer. Then the difference in measured ΔE value is of importance instead of the absolute CIELAB values; for the pocket-size instruments this difference is smaller and comparable to the reproducibility. Therefore, such a scenario is well supported by the low-cost pocket-size instruments.

The inter model agreement (IMA) between CM3700 and the other instruments show good agreement for the benchtop model, DC700. For the pocket-size instruments the difference not only varies with the magnitude of the ΔE but also with the gloss difference. The average difference for all samples is more than twice compared to the IIA for each model. The comparison of metameric index shows a large dependency on the metamerism in the samples. The NCS sample set, with low metamerism, gives small differences for all instruments. But for sample sets with large metamerism, the differences increase way over reproducibility except for the desktop instrument DC700. This indicates a bad spectral accuracy in the pocket-size instruments. The instrument S1P give the largest errors, especially for the sample set with gloss difference. This may be influenced by the d/0 like design in this instrument.

The accuracy of the pocket-size instrument is low in terms of comparisons to CIELAB values from a reference (benchtop) instrument. The CIELAB values from these instruments will only allow useful user applications for user scenarios where tolerances in the range of 4-5 ΔE00 is acceptable. Even for the high-end benchtop instruments the accuracy is not good enough for tolerances beneath 1.5 DE00. For measuring colour differences, in which both samples are measured by the same instrument (either benchtop or low-cost instrument), the low-cost instruments perform quite well. If the same model of the low-cost pocket-size instruments is used with shared accurate physical standards, colour tolerances of around 1.0 DE00 can reliably be checked. If colour differences are measured with respect to measurements from a benchtop instrument, then benchtop instruments are needed.

Since for the low-cost instruments investigated here the inter instrument agreement is much better than the inter model agreement, it may be possible to strongly improve the accuracy of these instruments by deriving instrument-specific conversion algorithms. An example of such a derivation for a low-cost instrument was published before [6]

COMMENT

This paper is, in part, about colour accuracy. Unfortunately, this word has many uses. In the eyes of the purchaser of a product with colour, accuracy may mean that the results agree with what their own eyes see. For a colour scientist writing standards, accuracy means the ability for an instrument to provide measurements that agree with an instrument which is deemed to be correct. In the best of all worlds, testing the accuracy of a spectrophotometer would require sending representative samples to a national standards laboratory -- a proposition which is expensive, may take months, and is suspect if the representative samples have any possibility of degrading. Instead, a high-end spectrophotometer is often designated the master instrument and accuracy is assessed as agreement with the master. Since many users of spectrophotometers do not have a high-end instrument, their effective master instrument may be an instrument with lower accuracy.

Instrument manufacturers thus have a difficulty when developing their specifications. Their customers tacitly expect that a newly purchased instrument will agree with whatever instrument they have on whatever samples they have. One side of the equation is completely out of the control of the instrument manufacturer. As a result, instrument manufacturers generally only provide specifications for those things that they have control over. Two specifications are commonly found: repeatability, which is the extent that an instrument agrees with itself over a short time span without changing the positioning on the sample, and inter-instrument agreement (IIA), which is the extent that an instrument agrees with instruments of the same make and model. Since customers of spectrophotometers expect some loosely defined idea of accuracy, when they are presented with a specification with jargon that sounds like accuracy, they assume a third definition of accuracy: having a small number for repeatability and IIA. But while good repeatability and good IIA are both necessary for accuracy, they are not sufficient. One of the goals of this paper is to provide an objective assessment of the accuracy of these low cost spectrophotometers.

REFERENCES

[1]. CIE 015:2018, Colorimetry, CIE 2018, Vienna

[2]. ISO 2813:2014, Determination of gloss value at 20°, 60° and 85°

[3]. ASTM E2214, Standard Practice for Specifying and Verifying the Performance of Color Measuring Instruments. ASTM International, Philadelphia 2019.

[4]. www.lucideon.com

[5]. ISO 18314-4, Analytical colorimetry — Part 4: Metamerism index for pairs of samples at change of illuminant, Geneva 2024.

[6]. E. Kirchner, P. Koeckhoven, K. Sivakumar, "Improving Color Accuracy of Colorimetric Sensors", Sensors 2018;18:1252; https://doi.org/10.3390/s18041252

Colour Heritage of Chinese Painting Through Dynastic and Stylistic Change

Wenan Li[a*], Ming-Xuan Chen[a], Xingkai Wang[a], David ip[a,b], and Luwen Yu[a,b]

[a]*The Hong Kong University of Science and Technology (Guangzhou), Guangzhou, China*
[b]*The Hong Kong University of Science and Technology, Hong Kong, China*
[*]*Corresponding author: Wenan LI, wli103@connect.hkust-gz.edu.cn*

ABSTRACT

The analysis reveals consistent, low-chroma earth palettes in landscape painting, broader saturation and hue coverage in bird-and-flower painting, and the widest chromatic range in figure painting, with a gradual diversification from the Song/Yuan to the Ming/Qing periods. These trajectories are coherent with documented shifts in materials and aesthetics, and they align with genre conventions that modulate hue range, chroma, and background lightness. Together, the findings provide a quantitative basis for comparing chromatic signatures across dynasties and genres. Beyond historical interpretation, several application pathways emerge. For heritage analysis and conservation, quantified palettes can assist curators and conservators in detecting anachronistic colour regions, prioritising areas for pigment testing, and informing palette reconstruction during restoration. For exhibition design and lighting, dynasty- and genre-specific chromatic profiles can guide background, mount, and light-spectrum choices to enhance legibility while respecting historical appearance, including the trend to lighter grounds in later dynasties. For collection search and education, chromatic fingerprints can power visual query tools that retrieve works by palette, supporting public engagement and teaching modules on materials, technology, and style. For computational creativity and design transfer, the profiles can serve as constraints in colour-transfer or generative systems, enabling designers to create contemporary artefacts that echo historical chroma–hue balances without direct copying. Several limitations should be noted. The current pipeline relies on digitised RGB images, so results inevitably reflect capture conditions, colour management, and the ageing of substrates. Future work should incorporate spectral imaging and calibrated profiles, and, where feasible, link clusters to pigment identifications. Area-based proportions conflate figure and ground; semantic segmentation (e.g., separating sky, foliage, garment, flesh) would enable motif-level comparisons across dynasties. Fixed-k clustering supports comparability but may underfit highly variegated works; adaptive models and mixture-based representations could better capture local nuance. In summary, the study establishes reproducible, comparable descriptors of chromatic structure across four dynasties and three genres, providing a bridge between connoisseurship and computation. The immediate value lies in heritage analysis, curatorial decision-making, exhibition design, and education; the forward trajectory points to heritage-aware, context-adaptive colour systems for creative industries and immersive media. By turning quantification into tools and guidelines, historical palettes can inform future colour—not as static templates, but as living constraints that steer sustainable, intelligible, and culturally grounded colour practice.

Keywords: Chinese Painting, Colour Analysis, Digital Image Processing, Cultural Heritage, Computational Art History

INTRODUCTION

Colours in traditional Chinese painting form a vital component of cultural heritage, reflecting aesthetic traditions, symbolic meanings, and material practices [1]. Within digital humanities [2], computational analysis complements connoisseurship by providing objective, reproducible measurements of palette structure that are

difficult to perceive by eye. Techniques such as digital image processing and *k*-means clustering [3] enable fine-grained description and cross-collection comparison of colour distributions.

Palettes evolved over time in response to artistic ideals, cultural exchange, and material innovation [4]. In the Song dynasty, the organic blue colourant indigo appeared in portable painting; in the Yuan dynasty, gamboge and lac dye saw broader use [5]. During the Qing dynasty, synthetic pigments such as Paris green and synthetic ultramarine blue were introduced and adopted in the practice of painting [6-8]. These developments mirror advances in pigment technology and shifts toward more vivid, varied aesthetics.

Colour usage also varies systematically by genre. Landscape painting often employs muted greens and blues, accompanied by black line work, to convey harmony and natural balance [9]. Bird-and-flower painting favours saturated reds and yellows to emphasise vitality and beauty [10]. Figure painting typically combines warm, earthy tones for flesh and ground with an accent hue for garments and ornament. Such conventions suggest that both genre and period shape chromatic choices.

This study employs computational analysis on 436 paintings spanning four dynasties (Song, Yuan, Ming, and Qing) and three genres (landscape, bird-and-flower, and figure painting) [10]. Painting images were collected from the National Palace Museum (Taipei) and the Palace Museum (Beijing). After removing extraneous elements (borders, seals, and surrounding text), pixel data were extracted and mapped to CIE L*C*h° (LCH) for analysis and display. Dominant colour groups were identified using *k*-means clustering with a fixed number of clusters to ensure comparability. Cluster proportions were summarised with treemaps, and cluster centres were visualised in polar (Hue–Chroma) and 3D (Lightness–Chroma–Hue) spaces. These representations facilitate systematic comparison of chromatic signatures across dynasties and genres.

By quantifying palette structure and proportion, the study provides an empirical baseline for discussing stylistic change, material adoption, and genre convention in Chinese painting. The results highlight historically grounded differences in hue range, chroma, and lightness, and illustrate how computational methods can support research in cultural heritage and art history.

METHODOLOGY

To characterise colour usage across dynasties and genres, a standardised pipeline was employed comprising dataset assembly, inclusion/exclusion control, pre-processing, colour extraction and clustering, and visualisation. The workflow was designed to maximise comparability of area-based colour proportions and to support reproducible large-scale analysis.

Data sources and scope. A dataset of 436 digitised paintings was compiled from the National Palace Museum (Taipei) and the Palace Museum (Beijing), covering four dynasties (Song, Yuan, Ming, Qing) and three genres (landscape, bird-and-flower, figure).

Figure 1: Exclusion criteria with examples *(a) Unclear dynastic attribution (reason: attribution ambiguity); (b) Monochrome ink-only work (reason: no chromatic palette except seals/substrate); (c) Non-rectangular format—fan/round/leaf (reason: area-based proportion bias)*.

Inclusion and exclusion. To ensure like-for-like comparison, works with unclear dynastic attribution, monochrome ink-only rendering (aside from seals and substrate tone), and non-rectangular formats (e.g., fan, round, leaf) were excluded (Figure 1). These criteria prevent bias in proportion estimates arising from attribution ambiguity, limited chromatic content, or irregular image area.

Pre-processing. Only the main painted area was retained by cropping out borders, seals, and surrounding text, thereby avoiding paratextual colour contamination prior to pixel-level analysis (see pipeline in Figure 2b).

Colour extraction and clustering. Pixel colours were extracted using OpenCV and mapped to CIE L*C*h° (LCH) for analysis and display. Dominant colour groups were identified via *k*-means clustering (k = 25), with a fixed k to enable consistent comparison across images.

Visualisation. Cluster proportions were summarised with treemaps, while cluster centres were plotted in polar (Hue–Chroma) and 3D (Lightness–Chroma–Hue) spaces. All procedures were implemented in Python (OpenCV, scikit-learn, Matplotlib). Figure 2 provides an overview of dataset composition (Figure 2a) and the end-to-end pipeline (Figure 2b).

a. Sample examples and counts across dynasties and genres

Dynasties	Genres	Sample Examples	Sample Counts
Song	Landscape		11
	Bird-and-Flower		20
	Figure		31
Yuan	Landscape		14
	Bird-and-Flower		4
	Figure		49
Ming	Landscape		62
	Bird-and-Flower		14
	Figure		77
Qing	Landscape		47
	Bird-and-Flower		60
	Figure		47

b. Sample processing and colour analysis

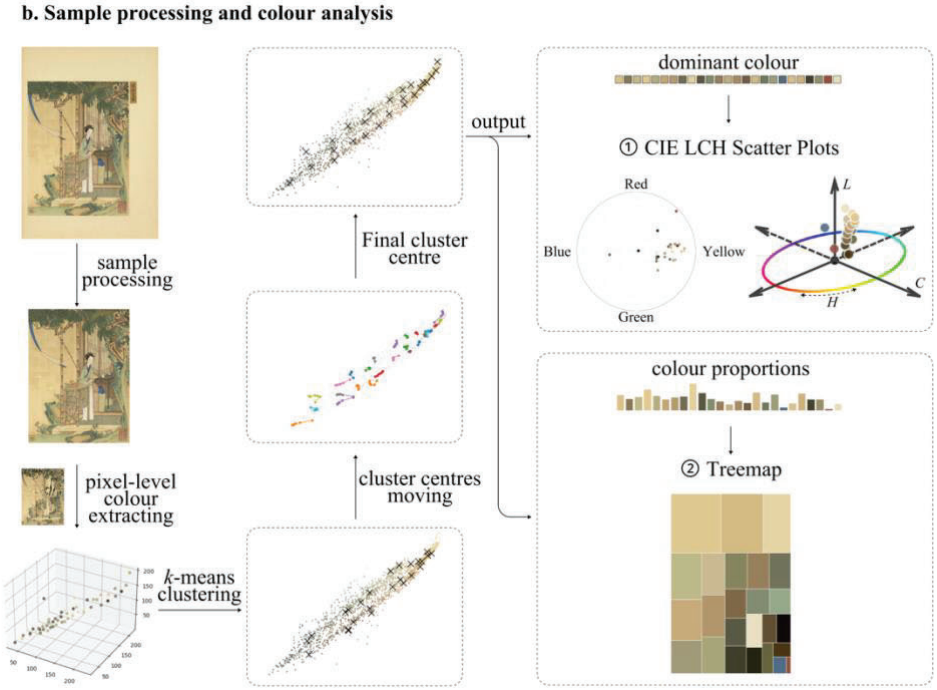

Figure 2: Dataset composition and analysis pipeline *(a) Dataset by dynasty × genre with thumbnail examples and counts; (b) Pipeline: image acquisition → crop paratext (borders/seals/text) → pixel extraction → k-means (k = 25) → L*C*h° mapping → outputs (treemap; polar and 3D plots)*.

RESULTS

Chromatic structure is summarised using two complementary visualisations. Figure 3 plots the distribution of cluster centres in CIE L*C*h° (polar Hue–Chroma and, where shown, 3D Lightness–Chroma–Hue), indicating the range and typical concentration of hues and chroma across dynasties and genres. Figure 4 presents treemaps of cluster proportions, revealing the area-based dominance of colours within paintings and changes in background lightness and accent saturation.

Across dynasties, *landscape painting* is characterised by low-chroma, earth-toned palettes with hues concentrated in the yellow–red–green sectors. In Figure 3, the Song and Yuan dynasties show tightly clustered distributions, consistent with restrained colour choices; in Figure 4, darker earth tones occupy larger areas. The Ming and Qing dynasties display a modest increase in chroma and lighter grounds, visible as broader radial spread in Figure 3 and as larger beige or light-yellow blocks in Figure 4.

Bird-and-flower painting exhibits a broader chromatic span than landscape. Song and Yuan remain relatively balanced yet subdued, whereas the Ming and Qing periods introduce more saturated reds and blue-greens. In Figure 3, this appears as expanded coverage across hue angles and greater chroma radii; in Figure 4, high-saturation blocks increase in area alongside lighter background fields, aligning with more decorative compositions in later dynasties.

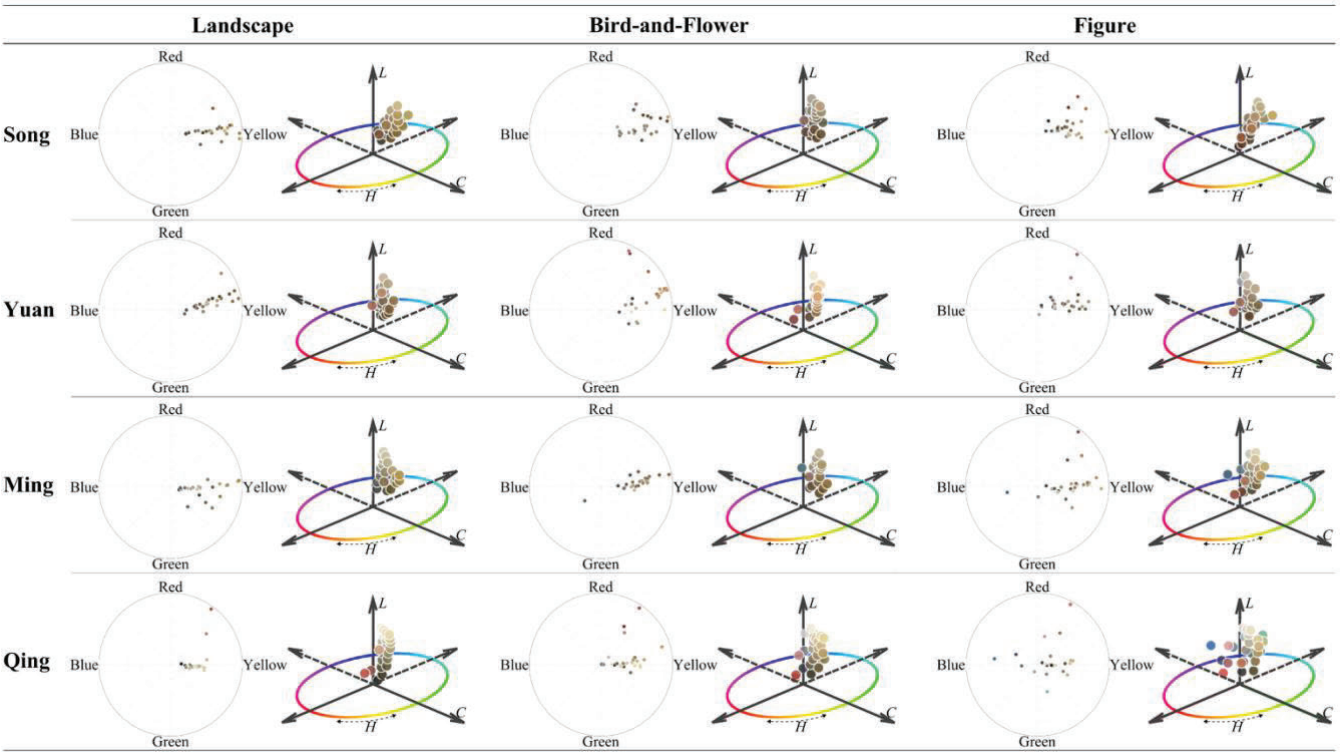

Figure 3: Chromatic distributions by dynasty and genre in CIE L*C*h° *(Points denote k-means cluster centres (k = 25 per image) mapped to polar Hue–Chroma (and 3D Lightness–Chroma–Hue, if shown). Angle = hue (0–360°); radius = chroma. Denser point concentrations indicate more frequently occurring palette regions. Panel layout follows dynasty × genre for direct comparison)*.

Figure painting shows the widest hue range among the three genres. Warm, earthy tones remain foundational across all periods, yet the Qing dynasty introduces marked chromatic diversity, including vivid reds, greens, and blues. Figure 3 registers dispersion into cooler sectors at moderate-to-high chroma, and Figure 4 shows greater shares of saturated accent colours while the warm base persists.

Overall, restrained palettes dominate the Song and Yuan dynasties, with incremental diversification in the Ming and Qing periods. Genre conventions modulate this trajectory: landscapes retain the most restraint, bird-and-flower increases saturation to convey vitality, and figure painting achieves the broadest chromatic envelope while maintaining warm bases.

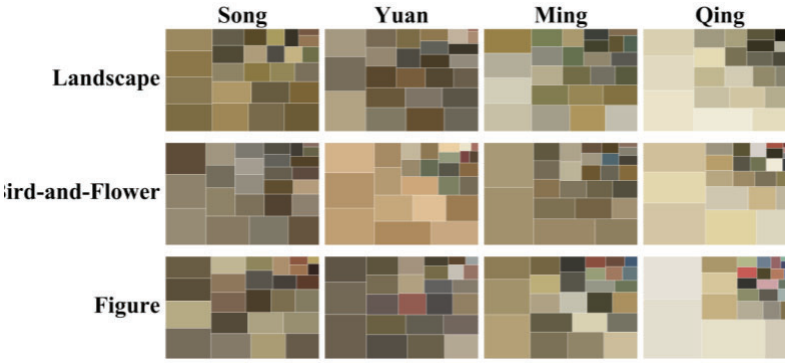

Figure 4: Treemap of colour proportions by dynasty and genre *(Block area encodes the proportion of pixels assigned to each cluster. Panels are grouped by dynasty × genre. Larger light-background blocks in later dynasties indicate lightening palettes; larger saturated red/green blocks denote increasing chroma in bird-and-flower and figure painting)***.**

DISCUSSION AND CONCLUSION

The results reveal coherent chromatic trajectories across dynasties and genres. Landscape painting remains anchored in low-chroma, earth-toned palettes in the Song and Yuan periods, with modest lightening and diversification in the Ming and Qing. These patterns align with historical contexts: Song ideals of scholarly restraint and interreligious cultivation encouraged harmonious, subdued palettes [11]; the Yuan era's cosmopolitan networks under Khubilai Khan fostered broader stylistic exchange [12]; and the Ming–Qing expansion of handicrafts and material innovation supported richer colour deployments [13]. Genre conventions further mediate these shifts, with colour relationships carrying aesthetic and symbolic functions across subjects [14].

Interpretively, shifts in chroma and hue range align with historical evidence for pigment availability and adoption, from indigo and natural dyes to later synthetic pigments such as Paris green and synthetic ultramarine blue. At the same time, genre functions appear to regulate palette choices: landscapes prioritise harmony and restraint; bird-and-flower emphasises vitality; figure painting balances naturalistic flesh tones with decorative garments and ornaments. In this sense, material innovation operates within stable pictorial aims, producing gradual, genre-modulated change rather than abrupt transformation. Pragmatically, the quantified palette descriptors provide a baseline for heritage studies. Curatorial and conservation work can draw on chromatic profiles to screen for anachronisms, inform non-destructive testing priorities, and support historically plausible palette reconstruction. Exhibition and communication design can reference dynasty- and genre-typical lightness and chroma balances to select backgrounds and lighting that enhance legibility without overstating saturation. For public engagement and education, palette signatures enable colour-based retrieval and comparative viewing across collections. These uses connect computation with connoisseurship and help document colour heritage at scale.

Several limitations temper interpretation. Analyses rely on digitised RGB images and area-based clustering, which reflect capture conditions and conflate figure and ground. Future work could incorporate calibrated or spectral imaging, device-independent rendering, and semantic segmentation of motifs (e.g., sky, foliage, garment, flesh). Fixed-k clustering supports comparability but may under-represent highly variegated works; adaptive or mixture models could capture local nuance.

In summary, the study establishes reproducible, comparable descriptors of chromatic structure for four dynasties and three genres. The contribution lies in providing an empirical bridge between historical interpretation and computational analysis while supporting digital preservation. Looking ahead to *future colour*, heritage-aware, context-adaptive applications—grounded in measured hue–chroma–lightness relationships—can inform conservation, exhibition, and design without departing from the cultural logic embedded in historical palettes.

REFERENCES

[1]. Haoran, X., Shuyao, C., & Zhang, Y. (2023). Magical Brush: A Symbol-Based Modern Chinese Painting System for Novices. *Proceedings of the 2023 CHI Conference on Human Factors in Computing Systems*, 1–14. https://doi.org/10.1145/3544548.3581429

[2]. Flueckiger, B., & Halter, G. (2020). Methods and Advanced Tools for the Analysis of Film Colors in Digital Humanities. *DHQ: Digital Humanities Quarterly*, *14*(4).

[3]. Basar, S., Ali, M., Ochoa-Ruiz, G., Zareei, M., Waheed, A., & Adnan, A. (2020). Unsupervised color image segmentation: A case of RGB histogram based K-means clustering initialization. *PLOS ONE*, *15*(10), e0240015. https://doi.org/10.1371/journal.pone.0240015

[4]. Haber, J., Lynch, S., & Carpendale, S. (2011). ColourVis: Exploring colour usage in paintings over time. *Proceedings of the International Symposium on Computational Aesthetics in Graphics, Visualization, and Imaging*, 105–112. https://doi.org/10.1145/2030441.2030464

[5]. McCarthy, B., & Giaccai, J. (n.d.). The Introduction of Nontraditional Pigments and Dyes into the Chinese Palette. *Scientific Studies of Pigments in Chinese Paintings*, 79.

[6]. Bell, I. M., Clark, R. J. H., & Gibbs, P. J. (1997). Raman spectroscopic library of natural and synthetic pigments (pre- ≈ 1850 AD). *Spectrochimica Acta Part A: Molecular and Biomolecular Spectroscopy*, *53*(12), 2159–2179. https://doi.org/10.1016/S1386-1425(97)00140-6

[7]. Burgio, L., Melessanaki, K., Doulgeridis, M., Clark, R. J. H., & Anglos, D. (2001). Pigment identification in paintings employing laser induced breakdown spectroscopy and Raman microscopy. *Spectrochimica Acta Part B: Atomic Spectroscopy*, *56*(6), 905–913. https://doi.org/10.1016/S0584-8547(01)00215-4

[8]. Liu, Z., Zhang, H., Zhou, W., Hao, S., Zhou, Z., Qi, X., & Shi, J. (2019). Pigment identification on an undated Chinese painting by non-destructive analysis. *Vibrational Spectroscopy*, *101*, 28–33. https://doi.org/10.1016/j.vibspec.2018.08.009

[9]. Chen, X., Liu, Q., Chen, Y., Wang, R., You, Y., Deng, W., Chen, W., & Wang, X. (2024). ColorNetVis: An Interactive Color Network Analysis System for Exploring the Color Composition of Traditional Chinese Painting. *IEEE Transactions on Visualization and Computer Graphics*, *30*(6), 2916–2928. IEEE Transactions on Visualization and Computer Graphics. https://doi.org/10.1109/TVCG.2024.3388520

[10]. Choy, M. C., Tang, W., Eric. (2018). *Essential Terms of Chinese Painting*. City University of HK Press.

[11]. Liu, P. (2024). Su Shi: A Paragon of Interreligious Harmony in Song Dynasty China. *Religions*, *15*(8), 979. https://doi.org/10.3390/rel15080979

[12]. Watt, J. C. Y. (2010). *The World of Khubilai Khan: Chinese Art in the Yuan Dynasty*. Metropolitan Museum of Art.

[13]. Chen, J. (2025). A Study on the Relationship between the Development of Handicrafts and the Innovation of Painting Art in the Ming and Qing Dynasties. *Art Horizons*, *1*(1), 43–49. https://doi.org/10.63313/ah.9005

[14]. Li, J., & Zhang, M. (2025). Expressing the aesthetic of Chinese painting through color relationships. *Cambridge Arts and Humanities Research*, *2025*(2), 6–13. https://doi.org/10.62852/cahr/2025/138

From Cobalt Blue to Iron Brown: Color Semiotics in Joseon

Wona Lhi[1*], YungKyung Park[2]

[1] PhD Candidate, Color Design, Ewha Womans University, Seoul, Republic of Korea
[2]Professor, Color Design, Ewha Womans University, Seoul, Republic of Korea

*Corresponding author: YungKyung Park, yungkyung.park@ewha.ac.kr

ABSTRACT

This study interprets the transition from blue-and-white to iron-painted porcelain in the Joseon dynasty not as a simple replacement of pigments but as a symbolic transformation shaped by changing historical and cultural conditions. In the fifteenth century, blue-and-white porcelain imported from China was adopted as ritual ware, symbolizing royal authority, elite culture, and Confucian virtues, and the vivid cobalt blue distinguished it from the traditional East Asian spectrum of blue while functioning as a visual marker of political legitimacy and prestige. After the Imjin War (1592–1598) and the Manchu invasions, the supply of cobalt pigments became unstable, and domestically available iron oxides were introduced as substitutes. Initially a practical response, iron-painted porcelain gradually evolved into an aesthetic medium reflecting Confucian ideal of restraint and frugality. By the seventeenth and eighteenth centuries, iron-painted porcelain had established itself as a significant stylistic tradition. It continued to be produced even during the later revival of blue-and-white porcelain, preserving its distinctive symbolic role. Blue-and-white and iron-painted porcelains are visually distinct: while blue-and-white porcelain symbolized authority and international prestige, the warm reddish-brown of iron-painted porcelain embodied the aesthetics of modesty and restraint. Physical measurements numerically demonstrated this chromatic contrast, revealing the shift of Joseon's symbolic colors from an imported blue to a domestically sourced reddish-brown. Ultimately, this transformation shows that in Joseon, color expanded from signifying external authority to also expressing indigenous morality and the aesthetics of frugality. It implies that color functioned not merely as a visual attribute but as a sign through which social meaning was articulated.

Keywords: blue-and-white porcelain, iron-painted porcelain, Joseon dynasty, color symbolism, frugality

1. INTRODUCTION

From its foundation, the Joseon dynasty sought to implement Confucian political ideals by reforming its culture and institutions. Standardizing ceremonial objects that visually affirmed the legitimacy of royal authority was a central state undertaking. In this process, blue-and-white porcelain decorated with deep cobalt pigment replaced gold and silver vessels. It was adopted as the official ritual ware for the royal court and government offices. Initially dependent on imported pigments and production techniques from China, Joseon gradually pursued independent production, leading to the emergence of a distinctively local style. However, the Imjin War (Japanese Invasions of Korea, 1592–1598) and the Manchu invasions (1627, 1636) severely disrupted the official kiln system and the infrastructure of porcelain production. In the postwar period, porcelain demand rose sharply while the supply of costly cobalt pigments diminished, prompting the use of iron-based pigments as an alternative. What began as an unavoidable choice gradually evolved into a visual language embodying the Confucian aesthetic of *simplicity and modesty*. Even after the resurgence of blue-and-white porcelain in the late Joseon period, iron-painted ware persisted and adapted to shifting aesthetic, political, and cultural conditions.

Despite extensive research on the history of Joseon porcelain production, little attention has been paid to how the color symbols of blue-and-white and iron-painted porcelain were reinterpreted and sustained. This transition

can be understood not merely as a substitution of pigments but as a transformation of cultural signs reconstituted within historical conditions. Eco (2023, pp. 178–180) conceptualized the sign system as a dynamic structure continually reshaped by historical and social experience, while Curtin (2009) regarded color as a visual sign that acquires meaning within the codes assigned by society. From this perspective, the cobalt-blue pigment of Joseon blue-and-white porcelain was not merely a dye; rather, it functioned as a sign symbolizing international trade networks, elite culture, and political authority. The costly Persian cobalt was reserved for the royal court and upper classes, while the chromatic expression of blue-and-white porcelain served as a visual medium through which authority and identity were articulated. Such pigment use represented a symbolic choice that embodied the hierarchical order and cultural ideals of the time (Zhang et al., 2022).

Accordingly, this study examines and compares the semiotic meanings of blue-and-white and iron-painted porcelain as they were shaped and transformed under different historical and socio-cultural conditions, to elucidate how color signs were reinterpreted, sustained, and transformed within the same porcelain medium.

2. THEORITICAL BACKGROUND

2.1 . Blue and white porcelain in Joseon

2.1.1. Confucian political ideology and the institutionalization of blue and white porcelain

In the early Joseon period (15th century), the state reorganized its ritual system in accordance with Confucian ideology and sought to standardize ceremonial and court utensils. In the 29th year of King Sejong's reign (1447), when the supply of gold and silver vessels became difficult, porcelain was officially adopted as the material for state ritual ware. Blue-and-white porcelain had already been introduced to Korea through exchanges with China since the late Goryeo and early Joseon periods. During the Xuande era (1426–1435), the quantity of imperial gifts and tribute goods brought by Chinese envoys greatly expanded, and thereafter, blue-and-white porcelain became firmly established as ritual ware for the royal court in Joseon. Subsequently, Joseon initiated independent production centered on the official kilns. While early production closely imitated Yuan and Ming models, distinctively Joseon motifs and forms gradually emerged. The adoption and production of blue-and-white porcelain, therefore, represented both a symbolic and practical choice that embodied state institutions and Confucian ideology (Yoon, 2006).

2.1.2. From substitute to traditional style: the spread of iron-painted porcelain

During the mid-Joseon period, following the Imjin War and the Manchu invasions of the late 16th and early 17th centuries, the government kiln system suffered a significant setback, and the production base for porcelain intended for the royal family and government offices was severely disrupted. At the same time, socio-structural changes, including post-war recovery, population growth, improved agricultural productivity, and the expansion of commerce and industry—led to a substantial increase in demand for ceramics. At this time, the import of Persian cobalt, the principal pigment for blue-and-white porcelain, became increasingly complex, prompting the adoption of iron-based pigments as an alternative and resulting in the broader production of iron-painted porcelain.

This type of ware was characterized by patterns painted on the white porcelain surface using a reddish-brown pigment derived from iron oxide. As it could be mined and processed domestically, it represented a practical and economical choice. By the seventeenth century, the pigment—a stable and familiar traditional material—was actively employed even in official kilns. By the eighteenth century, it had come to embody the aesthetic principles of Confucian restraint and continued to be used for official vessels, including royal ritual wares. In this way, it transcended its initial role as a mere substitute and established itself as a significant style within the ceramic culture of the late Joseon period (Song, 2010).

2.1.3. The revival of blue-and-white porcelain and the coexistence of iron-painted porcelain

In the eighteenth century, economic recovery, growth in the yangban class (the hereditary Confucian elite of Joseon Korea), and the influence of Silhak (Practical Learning) and Bukhak (Northern Learning) stimulated an increased demand for high-quality porcelain. At the same time, wealthy farmers and merchants emerged as a new consumer class. They valued aesthetic refinement and dignity over mere utility, which stimulated a renewed interest in blue-and-white porcelain. With the relocation and eventual privatization of the royal kilns, the center of production and distribution shifted to the private sector, and it came to be used widely as a high-quality ware not only within the royal court but also among the literati and the public (Jang, 2021).

From the latter half of the eighteenth century, the decorative tendencies of porcelain underwent significant transformation. With the importation of foreign porcelains and the spread of luxury culture, elaborate designs and the combined use of cobalt, copper, and iron pigments became widespread. Iron oxide pigments were employed in conjunction with cobalt as secondary coloring agents, and their use expanded. This development reflected the prevailing aesthetic consciousness and decorative demands of the period, and its modes of expression became increasingly diversified and complex across different ceramic forms. Despite the renewed popularity of blue-and-white porcelain, iron-painted porcelain persisted in coexistence, sustaining its unique semiotic significance within the multilayered aesthetic sensibilities and cultural transformations of the time (Woo, 2011).

3. METHODOLOGY

This study was conducted with a limited sample consisting of five blue-and-white porcelains and two iron-painted porcelains. Nevertheless, the chromatic differences between the two types were pronounced enough to be distinctly separated within the CIELAB color space. For this reason, the research design emphasized comparative characteristics and semiotic interpretation over statistical generalization (Figure 1). All samples were obtained from high-resolution images provided by the official archive of the National Museum of Korea and the Museum of Oriental Ceramics, Osaka, whose standardized protocols for photography and color correction guarantee the reliability of the dataset. Because the measurements were based on digital images rather than on-site examination of physical objects, potential discrepancies arising from lighting conditions, white balance, and display calibration could not be excluded entirely. To mitigate these limitations, the analysis relied exclusively on images taken under uniform conditions.

3.1 Sample Selection and Sources

Figure 1. Porcelain. Images courtesy of the National Museum of Korea (Type 1 Public Domain) and the Museum of Oriental Ceramics, Osaka. They can be freely downloaded from the official websites (https://www.museum.go.kr, https://www.emuseum.go.kr, https://www.moco.or.jp/ko/)

3.2 Color Measurement Procedure and Analytical Framework

Measurements were taken using a Konica Minolta CA-210 colorimeter from digital image data. Each sample was measured three times, and the mean value was used. The resulting data were then converted into the CIELAB color space using a conversion program to obtain L*C*a*b* values.

4. RESULTS

As shown in Figure 2, blue-and-white and iron-painted porcelains exhibited a clear contrast in their CIELAB values. Blue-and-white samples, including Joseon as well as Ming and Qing porcelains, were in the negative coordinates of both a* and b* (e.g., a* –10.9 to –0.2, b* –26.7 to –36.8), forming a cool bluish range. In contrast, iron-painted samples appeared in the positive coordinates (a* 31.2–42.3, b* 12.1–26.6), reflecting a warm reddish-brown tone. The chroma (C*) values of iron-painted ware (33.5–50.0) were also higher than those of blue-and-white (17.5–38.4), producing a more saturated and vivid appearance. In terms of hue angle (h), blue-and-white porcelain was distributed within the blue region of 237°–270°, whereas iron-painted ware fell within the reddish-yellow range of 21°–32°, indicating a divergence of more than 200° and occupying entirely distinct color coordinates. Joseon blue-and-white porcelains overlapped considerably with Ming and Qing samples, suggesting a broadly similar chromatic range, but iron-painted ware established a clearly distinct and independent color domain.

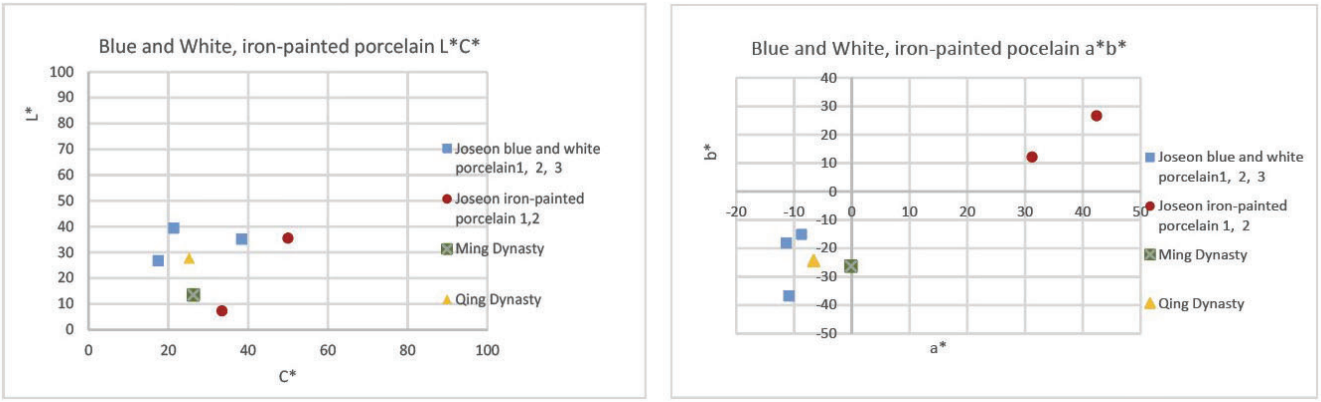

Figure 2 L*C*a*b* graph

5. DISCUSSION

The CIELAB analysis indicates that Joseon blue-and-white and iron-painted porcelains occupied distinct chromatic domains. Blue-and-white porcelains clustered in the negative a* and b* region, forming a bluish palette that symbolizes royal authority and international prestige. This cobalt hue stood in marked contrast to traditional East Asian blue tones and functioned as a visible marker of legitimacy and external prestige (Zhang et al., 2022). By contrast, iron-painted porcelain was concentrated in the positive a* and b* region, producing warm reddish-brown tones. Initially adopted as a pragmatic substitute during periods of cobalt scarcity following the Imjin War and the Manchu invasions, iron pigments gradually accrued new cultural significance. Their chromatic qualities came to embody Confucian ideals of frugality and restraint, illustrating that color acquires meaning not from inherent properties but from the cultural codes in which it is embedded (Curtin, 2009). The transition from blue-and-white to iron-painted porcelain was therefore not a simple material substitution but a symbolic reconfiguration reflecting shifts in social order and aesthetic values. Whereas blue-and-white porcelains signified the external authority of imported prestige, iron-painted porcelains articulated an indigenous ethic of modesty and restraint. This transformation illustrates Eco's (2023) view that symbols are not fixed but are continually reconstituted through

historical practice, and the coexistence of blue-and-white and iron-painted porcelain underscores the multiplicity of symbolic orders within Joseon society.

6. CONCLUSION

This study has shown that the transition from cobalt to iron pigments in Joseon porcelain was not a technical substitution, but a semiotic transformation shaped by changing historical and cultural conditions. Blue-and-white porcelains, produced with imported cobalt, embodied royal authority and foreign prestige, while iron-painted porcelains, based on domestic iron oxides, came to symbolize the Confucian values of modesty and restraint. Their coexistence after the eighteenth century reveals that Joseon's symbolic order was not monolithic but continuously reconfigured, with color functioning as a cultural code through which social values were expressed and redefined. Comparable shortages and substitution strategies also appeared in Ming–Qing China and Japan, yet their aesthetic receptions diverged. Future comparative studies will investigate these differences more fully to clarify the distinctiveness of Joseon's choices within the broader East Asian context.

[1] Curtin, B. (2009). *Semiotics and visual representation*. Semantic Scholar. https://www.semanticscholar.org/paper/Semiotics-and-visual-representation-Curtin/

[2] Eco, U. (2023). *Signs: Concept and history* (B.-H. Kim, Trans.). Moonye Publishing. (Original work published 1975)

[3] Song, I.-h. (2010). The characteristics of Joseon white porcelains painted in underglaze iron-brown of the 17th–18th century: The case of porcelains discovered at ancient kiln sites. *Korean Journal of Art History (Formerly Art and Archaeology), (267),* 77–110.

[4] Woo, M. (2011). Changes in the characteristics of white porcelain in underglaze iron-brown produced in Joseon official kilns. *Misulsa Yeongu: Journal of Art History, (25),* 241–273.

[5] Yoon, H. (2006). The production and usage of blue-and-white porcelains of the 15th and 16th centuries of the Joseon dynasty. *Korean Journal of Art History (Formerly Art and Archaeology), (0),* 315–360.

[6] Zhang, Y., & Pollard, A. M. (2022). The archaeological and scientific analysis of blue-decorated ceramics in the Tang and Song dynasties. *Archaeometry, 64*(6), 1394–1410. https://doi.org/10.1111/arcm.12791

A Study on Prompting The In-Depth Exploration of Environmental Color Imagery Using Generative AI

Yuh-Chang Wei[1], Monica Kuo[2], Ya-Ping Kuo[3], Zhe Liu[4]

[1,2,3,4] *Chinese Culture University, Taipei, Taiwan R.O.C.*

**Corresponding author：Yuh-Chang Wei, ycwei@ulive.pccu.edu.tw*

ABSTRACT

This study investigates the ability of generative AI to produce semantic color representations that align with human perception and measured environmental chromatic data. Using the Kobayashi Color Image Scale (CIS) coordinate plane, we mapped and compared three datasets: (1) environmental color survey chromatograms, (2) observer semantic color measurements, and (3) AI-generated color swatches based on semantic prompts. Results show partial alignment between AI-generated outputs and both human perception and measured chromatic data, particularly in the “Beautiful & Romantic” imagery zone. However, significant discrepancies remain in zones characterized by high-chroma and high-brightness color swatches—most notably in the “Dynamic & Gorgeous” zone, where AI produced no distinct color representation. These findings highlight the need for further refinement of AI models to capture subtle semantic variations and produce contextually accurate colors for environmental color planning.

Keywords: Environmental Color Imagery, AI Generated Chromatogram, Kobayashi Color Image Scale, Semantic Color Mapping

INTRODUCTION

Environmental color planning plays a critical role in shaping urban aesthetics, influencing human emotion, and promoting cultural identity. The Kobayashi Color Image Scale (CIS) offers a systematic framework for mapping color semantics along axes of lightness, chroma, and imagery association. However, translating complex human color perception into actionable design palettes remains a challenge.

Generative AI models have recently been introduced into color design workflows, capable of producing color palettes based on textual or semantic prompts. Yet, it remains unclear how well these AI-generated outputs align with either measured environmental chromatic data or human intuitive color perception. This study seeks to address this gap by systematically comparing AI-generated semantic colors, human observer responses, and environmental image-derived color measurements using the CIS coordinate plane.

METHODOLOGY

A three-layer comparative framework has been adopted:

1. Environmental color survey chromatograms derived from high-resolution images of the study site.
2. Semantic color measurements collected from a group of participants, using structured questionnaires and a 7-point semantic differential scale.
3. AI-generated color swatches produced via a text-to-color generation model, prompted with semantic descriptors corresponding to each imagery zone.

Environmental Color Survey

The environment color investigation is through NCS color survey process [11] using photography, color measurement, sampling, coding, and classification. The selected color images (see Fig.1) are analyzed, classified, and presented by means of chromatography chart.

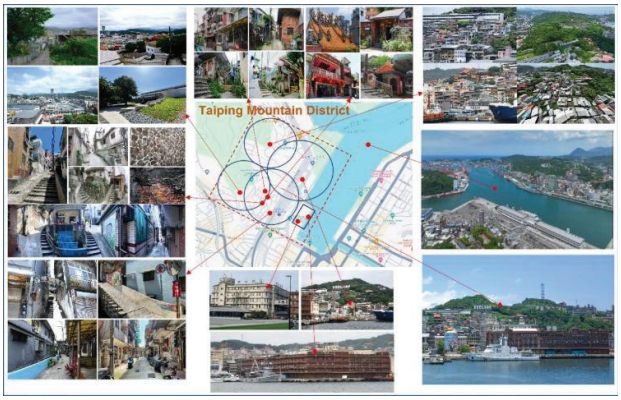

Figure 1. Selected images of Taiping Mountain District of Keelung City harbor region.

Environmental Color Chromatograms

Environment color collected from both the macro (sky, sea, mountain, harbor, urban landscape, etc.) and micro (architecture, street, façade, etc.) levels based on the characteristics of regional landscape colors including main color, auxiliary color and embellishment color are respectively marked on the local cultural color image space. Photoshop software is used for auxiliary analysis to establish the Taiping Mountain District environment color database (see Fig.2).

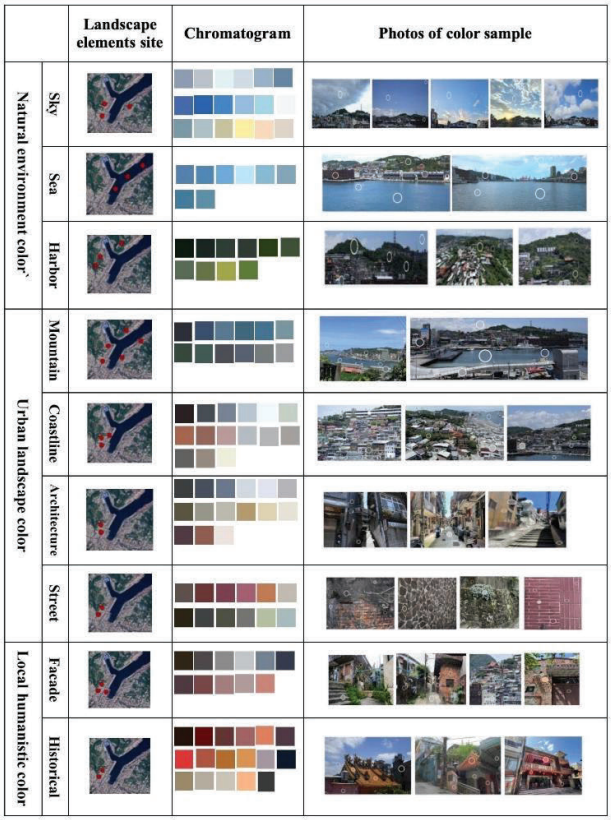

Figure 2. Chromatograms were categorized by NCS color system to represent the environment colors in this region of Taiping Mountain District.

Psychophysical Experiment

Environmental Color Imagery Survey

A Semantic Differential Scale (SDS) was developed based on the Kobayashi Color Image Scale [5] to evaluate the observers' perception of environmental color imagery. A color psychophysical approach was employed to measure each participant's semantic perception of the landscape colors. Each participant completed a single experimental session consisting of **30 trials**, yielding a sufficient dataset for subsequent statistical analysis.

Utilizing Generative AI to Generate Color Chromatograms

Generative AI was employed to create semantic color chromatograms corresponding to each imagery zone. Text-based prompts describing the targeted semantic attributes were used as input, and the resulting AI-generated color swatches were extracted and subsequently mapped onto the Kobayashi coordinate plane for comparison with both measured environmental colors and observer SDS results.

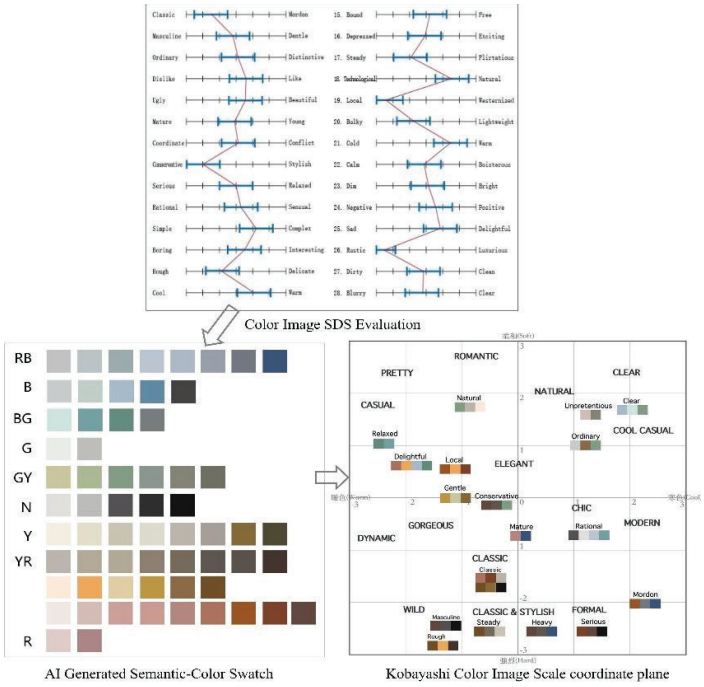

Figure 3. Input the text prompts of color semantics into AI to generate color swatches and map them to the Kobayashi coordinate plane.

RESULTS AND DISCUSSION

Environmental Colors Imagery and Semantic Differential Analysis

After conducting statistical analysis, the spatial distribution of the local color image was plotted using the Kobayashi Color Image Scale coordinate plane as follows:

1. The collected natural environment color image sample chromatograms were mapped to the Kobayashi color image coordinate plane. Semantic color image zones were created to present the natural environment landscape color imagery of Taiping Mountain District. Four zones were plotted as: 1. Clear–Natural-Cool Casual, 2. Natural-Casual-Domestic, 3. Casual-Dynamic, 4. Modern-Classic-Stylish-Wild (See Fig. 4)

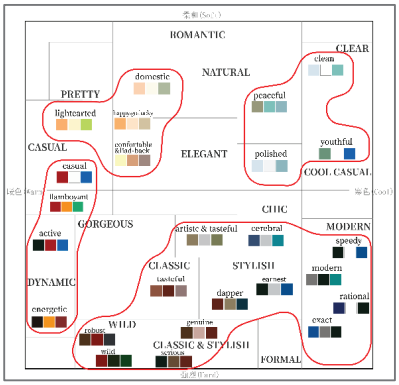

Figure 4. N**atural environment color image zones plotted on Kobayashi color image scale coordinate plane.**

2. The environmental landscape color image obtained through the SD evaluation experiment were mapped to the Kobayashi color image coordinate plane. Semantic color image zones were created to present the perceived landscape color image of Taiping Mountain District. Four zones were plotted: 1. Pretty-Romantic-Casual, 2. Natural- Cool Casual-Elegant 3. Dynamic, 4. Classic-Stylish-Wild (see Fig. 5)

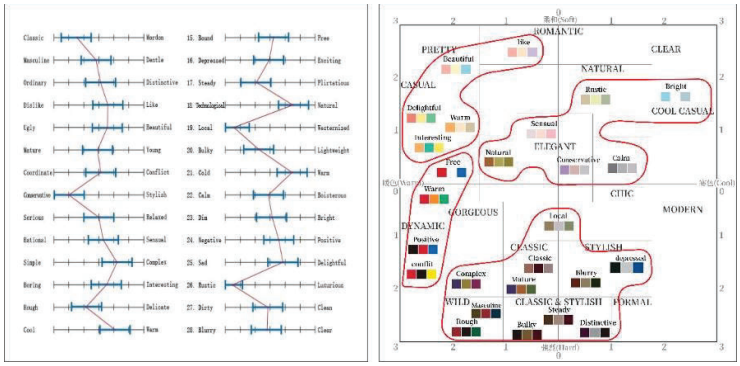

Figure 5. Ccolor image SD evaluation results (left). Perceived semantic color image zones plotted on Kobayashi color image scale coordinate plane (right).

3. AI-generated semantic color swatches mapped on the Kobayashi Color Image Coordinate Scale. Semantic color image zones were created to present the perceived landscape color image of Taiping Mountain District. Three zones were plotted: 1. Pretty-Romantic-Casual, 2. Natural- Clear-Cool Casual 3. Dynamic-Gorgeous, 4. Classic-Stylish-Wild-Modern (see Fig. 6)

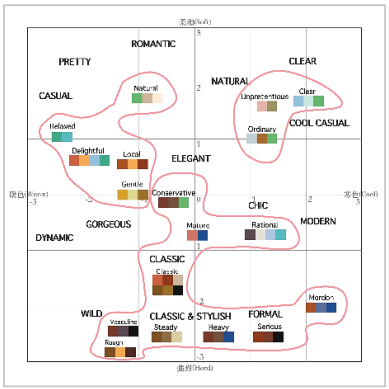

Figure 6. AI-generated semantic color image zones plotted on Kobayashi color image scale coordinate plane.

Discussions

The experimental results suggest that AI-generated semantic color swatches show a general correspondence with the color–semantic relationships inferred from scientific instruments and the Kobayashi Color Image Scale. Nevertheless, there remain significant discrepancies between AI-generated distributions and both the natural environmental color imagery and human perceptual responses. These differences underscore the need for further investigation into how AI can more accurately capture subtle semantic variations and produce color outputs that better reflect both environmental context and human color perception—ultimately enabling AI to serve as a more reliable tool for environmental color planning.

Using the Kobayashi Color Image Scale coordinate plane, we mapped three sets of data: the environmental color survey chromatogram, the semantic color measurements provided by observers, and the color swatches generated by AI based on semantic prompts (see figure 7). We then compared these across the defined environmental color imagery zones and analyzed the similarities and differences between AI-generated semantic colors and the observers' perceptual color semantics.

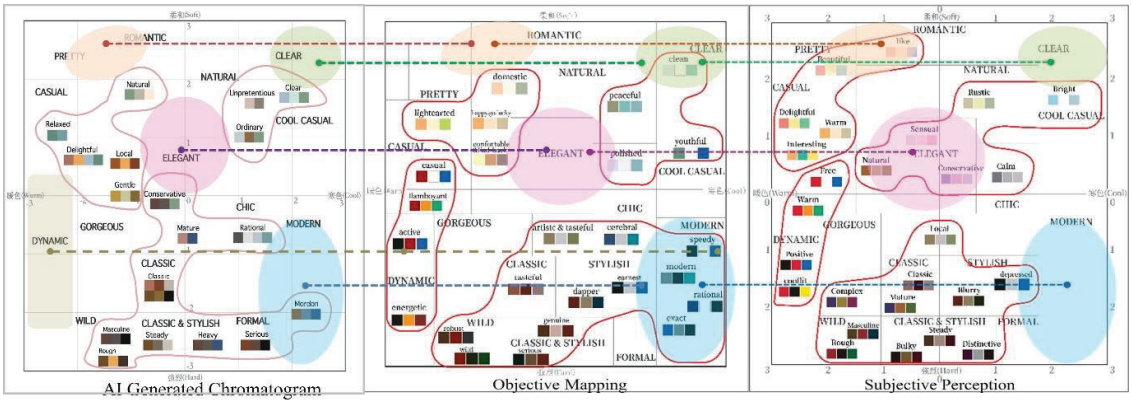

Figure 7. Comparative Analysis of Environmental, Perceptual, and AI-Generated Color Imagery

The discussion is summarized as follows:

1. **Natural, Clear, and Elegant Zone**
   AI-generated color swatches derived from semantic intensity were characterized by medium-to-low lightness and chroma, closely matching the colors measured from natural environmental images. However, AI failed to reproduce the medium-to-high lightness and chroma colors, particularly soft purples, that were strongly present in the observers' responses.

2. **Modern and Stylish Zone**
   AI produced only partial modern-style colors, represented by light blues and browns with medium-to-low lightness and chroma. Observer responses in this zone were nearly blank, suggesting minimal color association, while the natural image measurements revealed a rich and saturated palette of medium-to-high chroma blues, blacks, and grays—highlighting a major divergence between AI output and the photographic data.

3. **Pretty and Romantic Zone**
   AI-generated colors were relatively saturated, showing medium lightness and high chroma, including green, orange, red-ochre, pale gray-blue, and pink. These results were largely consistent with both the

observers' color impressions and the environmental image measurements, indicating strong correspondence between AI, human perception, and real-world chromatic data in this zone.

4. **Dynamic and Gorgeous Zone**
   AI failed to produce any color swatches for this zone. In contrast, observers' perceived colors aligned closely with natural image measurements, which were dominated by high-chroma colors such as blue, white, red, green, black, and orange.

This visualization shows the spatial distribution of three data layers—environmental imagery colors, human-perceived semantic colors, and AI-generated colors—across the four defined imagery zones. The mapping allows direct comparison of AI semantic color outputs with both human perception and real-world chromatic measurements. (see Table 1)

Table 1：Mapping of environmental color survey chromatogram, observer semantic color measurements, and AI-generated semantic color swatches using the Kobayashi Color Image Scale coordinate plane.

Imagery Zone	AI-Generated Colors	Observer Perception	Natural Image Measurements	Key Insights
1. Natural, Clear & Elegant	Medium-to-low lightness & chroma; lacks medium-to-high tones (esp. soft purples)	Medium-to-high lightness and brighter tones; strong preference for soft purples	Medium-to-low lightness & chroma; close to AI results	AI matches photo data well but fails to capture the brighter, higher-chroma colors that observers favor.
2. Modern & Stylish	Partial representation (light blues, browns, medium-to-low lightness & chroma)	Nearly blank responses; weak color association	Rich palette of medium-to-high chroma blues, blacks, grays	AI underrepresents the chromatic richness captured in environmental imagery, diverging from both photo data and observers.
3. Pretty & Romantic	Medium lightness, high chroma (green, orange, red-ochre, pale gray-blue, pink)	Similar color impressions; good alignment with AI	Similar distribution of bright, saturated colors	Strongest correspondence between AI, human perception, and measured data; AI performs best in this zone.
4. Dynamic & Gorgeous	No distinct color output	Strong perception of high-chroma blue, white, red, green, black, orange	Clear presence of high-chroma colors	AI completely fails to represent this zone; human perception and imagery are strongly aligned.

CONCLUSIONS

AI-generated semantic color swatches demonstrate a partial alignment with both human perception and real-world chromatic data, particularly in the Pretty & Romantic zone. However, significant gaps remain in zones requiring high-chroma or high-brightness representations - especially in the Dynamic & Gorgeous zone, where AI output was absent. These findings underscore the need to refine AI models to better capture subtle semantic variations and generate more accurate, contextually relevant color palettes for environmental color planning.

ACKNOWLEDGEMENT

The research project (NSTC113-2410-H-034-012) was funded by National Science and Technology Council. It is to express our sincere gratitude to NSTC in support of this research.

REFERENCES

[1]. Bergen, N. & Huang, A. (2023). "A Brief History of Generative AI" . *Dichotomies: Generative AI: Navigating Towards a Better Future* (2): 4.

[2]. Hård, A.; Sivik, L. & Tonnquist, G. (1996). "NCS Natural Color System - from Concepts to Research and Applications. Part I". *Color Research and Application*. Vol. 21, p.180–220. Toronto, Canada: John Wiley & Sons

[3]. Hård, A.; Sivik, L. & Tonnquist, G. (1996). "NCS Natural Color System - from Concepts to Research and Applications. Part II". *Color Research and Application*. Vol. 21, p. 206-220. Toronto, Canada: John Wiley & Sons

[4]. Guan SS & Hung PS (2010), 'Influences of Psychological Factors on Image Colour Preferences Evaluation', *Colour Research and Application*, 35 (6), 213-232.

[5]. Kita N and Miyata K (2016), 'Aesthetic Rating and Colour Suggestion for Colour Palettes", *Computer Graphics Forum*, 35 (7), 127-136.

[6]. Kobayashi, S. (1981). "The Aim and Method of the Color Image Scale", *Color Research & Application*, 6, 93-106. Toronto, Canada: John Wiley & Sons

[7]. Lee, L.S., Chien, C.C. & Lee, C.Y. (2012). 'The Harbor Environment Color Assessment and Planning Research", Proceedings of the 34th Ocean Engineering Conference in Taiwan National Cheng Kung University. P.625~630. Kaohsiung: Taiwan.

[8]. Sato T, Kajiwara K, Hoshino H and Nakamura T (2000), "Quantitative Evaluation and Categorizing of Human Emotion Induced by Colour', Advances in Colour Science and Technology, 3, 53-59.

[9]. Tseng YC & Wei YC (2019), "A Systematic Process in Developing a Colour Scheme based on Landscape and Urban Environmental Colour Analysis", Proceedings of the 5th Asia Colour Association Conference, 453-458, Nagoya (Japan).

Film Color Grading Model Based on Computer Vision: Construction of Personalized Color Libraries

Ming-Xuan Chen[a*], Shijunyan Luo[b]

[a]*The Hong Kong University of Science and Technology (Guangzhou), Guangzhou, China*

[b]*Macau University of Science and Technology, Macau, China*

**Corresponding author: mchen837@connect.hkust-gz.edu.cn*

ABSTRACT

Over the course of a century in the evolution of film art, color has played a pivotal role in shaping and revolutionizing visual storytelling. From the early experiments like "A Visit to the Seaside" in 1908, to the iconic "The Wizard of Oz" in 1939, and potentially a reference to "Gone with the Wind" in 1939, the debate continues in academic circles about the origins of the first color film. Nevertheless, color has become an essential expressive symbol in film art, enriching the narrative and emotional depth of films within each frame.

In today's film industry, the advent of digital color correction systems, grounded in color spaces such as RGB and HSV, has vastly expanded the creative possibilities. However, the pursuit of personalized color grading encounters three primary challenges: achieving the precise artistic vision of the director, adhering to the established color conventions of specific film genres, and seamlessly integrating the unique style of the colorist.

The research examines the top ten Chinese mainland box office films from 2014 to 2024 (N=100) and constructs a comprehensive classification system within a typological framework. Utilizing computer vision technology, the samples are preprocessed, including the removal of black and white images and the reduction of noise in subtitle areas. A detailed analysis is conducted to build a film color database and data model. Based on the developed data model, we aim to create a resource library that catalogs film colors according to directors, genres, themes, and regional characteristics. Furthermore, we explore the potential for developing a personalized color library that caters to individual colorists' preferences and styles. This study seeks to streamline the color grading process, enabling creators to efficiently find the right colors to enhance their storytelling and emphasize their unique artistic vision, all while reducing production costs and time constraints.

Keywords: Color Analysis, Film Art, Film Color Grading, Cinematic Color Theory, Computer Vision Applications

INTRODUCTION

In the development history of film art, color has transcended its original status as a visual or technical element, gradually evolving into a highly expressive symbolic language system [1]. It not only strengthens the perceptual connection between the image and reality, but also, through the precise regulation of visual parameters such as hue, Lightness, and saturation, conveys more abundant and distinct narrative information within a limited time. Color has become one of the core media for communicating emotions between the screen and the audience, making film not only an art of light and shadow, but also a color spectrum carrier that can directly trigger psychological and emotional responses. From an academic perspective, film color has long been regarded as an important artistic expression means, with its functions covering narrative advancement, space construction, emotion guidance, and cultural symbolism, among others [2]. For instance, the use of warm and cool tones often not only serves visual

aesthetics, but also deeply participates in the creation of emotional atmosphere and the transmission of cultural meaning, reflecting the aesthetic deliberation and intention control of the film's author.

With the continuous advancement of digital technology and the increasingly refined processes of the film industry, the focus of color creation has gradually shifted from traditional techniques to a more individualized and artistically expressive style pursuit [3]. Contemporary film creators are facing new challenges in color grading: how to explore visual strategies that conform to specific film genres and personal aesthetic visions while adhering to the common industry norms? Color not only needs to serve narrative consistency but is also increasingly required to reflect the unique perspective of the director or cinematographer. At the same time, color grading, as a key step in post-production, no longer merely focuses on technical corrections but has gradually evolved into an important means of shaping the overall visual style of the film. This transformation places higher demands on professional colorists - they need to strike a balance between standardized processes and artistic innovation, using color to help the work establish a distinct identity and effectively guide the audience's emotions and cognitive responses [4]. As numerous studies have pointed out, the manifestation of color on the screen is both science and art, and its effect stems from both objective technical configuration and subjective perception and cultural context. Therefore, it urgently requires more systematic and adaptable theoretical support and practical frameworks.

Therefore, this study aims to establish a systematic film color resource library. By classifying and analyzing the application of colors in various film genres, it will provide detailed visual data and style references, with the expectation of promoting the development of personalized color grading tools. This resource library will integrate color usage cases from different types of films, and clearly label information such as color palettes, color emotional effects, and cultural symbolic meanings. Based on this, the research will further explore color configuration schemes that meet the personalized needs of professional colorists, enabling them to expand creative boundaries within existing industrial standards and develop more authorial color languages. The ultimate goal is to provide an open resource that combines theory and practice for film color creation, promoting the transformation of color from technical parameters to the core dimension of narrative and emotional expression, and empowering the production of more innovative and compelling visual narrative works.

METHODOLOGY

A film color analysis method based on the golden section principle is used to systematically extract and analyze the main color features in the film images. As the intersection of mathematics, aesthetics and natural laws, golden section is widely used in the abstract expression of natural optimization structure [5]. In the practice of film composition, except for special artistic design, most film creators tend to place important visual information near the golden section point. According to Zettl's (2017) theory of visual media composition, more than 80% of the key visual elements in the picture are distributed in the golden section area [6]. Based on this consensus, this study selects the top 10 domestic films in the Chinese mainland from 2014 to 2024, a total of 100 films as the sample library, so as to ensure the commercial representation and market recognition of the sample.

In terms of data processing method, frame sampling technique is used in this study, where only the first frame of each film is extracted per second, and key pixels are further located by golden section points in each frame. Specifically, according to the golden ratio (0.382 and 0.618), four segmentation lines (two vertical lines and two horizontal lines) in the width and height direction of the screen are determined. The grid points formed by the intersection of these segmentation lines are the color sampling area. This method not only ensures the sampling efficiency, but also effectively captures the core visual elements in the picture.

The MiniBatchKMeans algorithm is used for color clustering analysis, which is a variant of the standard K-Means algorithm and greatly improves the computational efficiency on large data sets by processing in small batches. The number of clusters is set to 20, and a second merging of similar colors is performed using a color merging threshold (default 30.0). The merging process is based on Euclidean distance calculation. If the distance between the centers of two color clusters is less than a threshold, they will be merged into the same color category.

When d<30 (the threshold), similar color clusters are merged. The threshold is set according to CIE76 color difference formula [7], which corresponds to 6 times tolerance of the minimum color difference critical value (about 5 CIE units) that can be recognized by human eyes, so as to adapt to the dynamic change characteristics of film pictures. This double clustering strategy not only ensures the diversity of color features, but also avoids the analysis complexity caused by excessive subdivision.

In the aspect of color space conversion, the RGB color value is converted to HSV (Hue, saturation, lightness) space, which is realized by color-sys library. According to the visual perception research of Smith & van den Berg (2018), the three-dimensional characteristics of HSV (Hue: 0-360° color type; Saturation: 0-100% color purity; lightness Value: 0-100% Lightness) are closer to the human color cognition mechanism [7].

In the design of sample classification system, a three-level index classification system is established. The first level distinguishes between live action and animated films, based on whether the film is generated by live action or special effects animation. The second level refers to the classification of drama in Aristotle's Poetics, including tragedy, comedy and drama (serious drama) [8]. The third-level indicators are divided into five categories, ancient, modern, modern, future and fictional, according to the historical era classification standard of China. These classification indicators together constitute the test contrast coding table of 100 films, which provides a structured framework for the subsequent comparative analysis of color features.

RESULTS AND DISCUSSION

Compared with other live-action films, the color distribution of animated films is more scattered, and the overall trend of Lightness is bright. The span of RGB values is also large, especially in the red and blue spectral range, which shows a jump fluctuation, reflecting the high contrast and strong conflict color matching tendency in animation creation. In terms of lightness, the difference between animation and live-action film is still obvious. The lightness of animated film is about 8 values higher than that of live-action film by the simple average calculation method, and the lightness of animated film is also about 5 values higher than that of live-action film by the weighted average algorithm. It can be seen that both live-action and animated films have similar visual comfort adjustment logic, that is, in the case of significant difference in color concentration, it is necessary to maintain the sense of hierarchy through the balance of Lightness. This combination mode of "high saturation + wide color gamut + Lightness" not only reflects the aesthetic advantages of animated films breaking through the constraints of reality, but also reveals its narrative strategy of stimulating audience's emotional resonance through exaggerated colors.

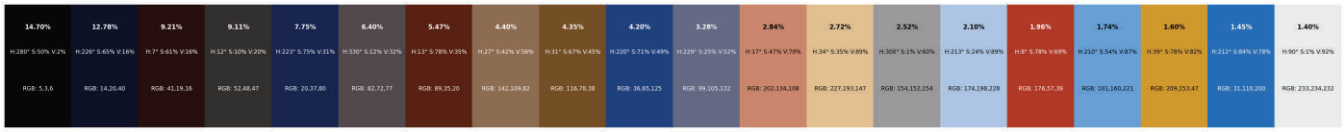

Figure 1: animated film clustering chromatogram

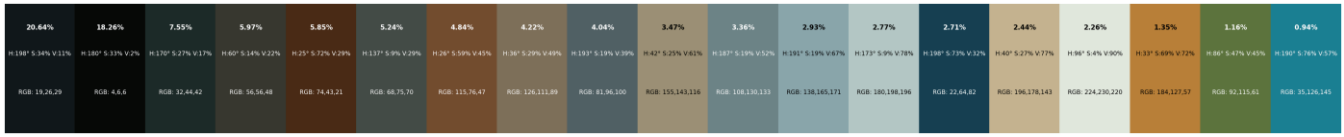

Figure 2: Live-action film clustering chromatogram

From the perspective of color saturation and lightness, the saturation and lightness characteristics of the three dramas are relatively moderate, without obvious characteristics, in line with the standard paradigm of color adjustment in film color production.

According to the data analyzed by the system, due to the heavy theme and emotional depression, tragedy films show a cold color tendency of low saturation and low Lightness. The RGB value clustering focuses on brown gray (RGB: 47,48,38), dark blue gray (RGB: 17,37,42) and dark cyan gray (RGB: 54,67,62). Tragic films are used to show gloomy, scary, depressed and other emotions, and are accustomed to using gray and black tones to strengthen the suspense and despair of crime, misfortune and misery in the film plot.

Figure 3: Tragic film clustering chromatogram

Among the 100 experimental films, most of the drama films are based on history and war themes. Besides the environmental colors such as black and gray, the hue results are close to reality and logical red and yellow are also clustered before the test. A closer look at the color characteristics displayed by the system shows that the moderately saturated warm color of the drama not only retains the historical reality, but also weakens the entertainment attribute of the drama film by appropriately reducing the saturation compared with the comedy film, which better balances the conflict between the realistic demand of the film genre and the artistic expression of the film. The medium Lightness balances the picture level. Among the 33 drama films, the story background takes place after modern times, which not only conforms to the audience's understanding of the time background, but also maintains the visual solemnness.

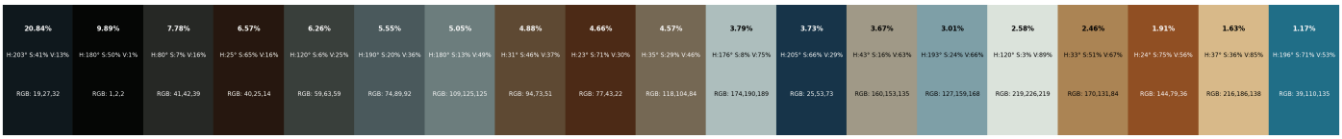

Figure 4: Drama film clustering chromatogram

Comedy films occupy the majority of the test data. According to the data given by the system, without discussing the proportion, more than half of the colors with more than 50% Lightness occupy more than half when clustering and segmentation are performed 28-30 times, showing the characteristics of excellent phase rich, high saturation and high Lightness as a whole. Of course, there is still a significant gap compared with animated films. From the perspective of hue, compared with the extreme performance of animated films, comedy films are slightly restrained by the restriction of real-life comedies. The hue contrast is not too obvious, and the intermediate cohesion color is more abundant, which plays the role of excessive hue. In terms of saturation, comedy films often do not give a gloomy story background, so there are more daytime dramas than night dramas and more colorful scenes than single color scenes. Therefore, the saturation needs to be relatively improved to achieve the effect of directly stimulating the audience's dopamine secretion and fit the decompression demand brought by the overall plot to the audience. Compared with tragedy and drama, lightness has a significant improvement. The principle of lightness basically follows the subconscious association of "Lightness is joy".

Figure 5: Comedy film clustering chromatogram

According to the background age of the film's core story as the basis for division, according to the perspective of The Times extending from far to near to the future, it can be seen that the background films of ancient films are limited by historical authenticity and material aesthetic logic, and the overall characteristics are excellent and monotonous. The color clustered by the largest proportion is the cold color blue (RGB: 5,37,56) and other colors

construct a visual system with low hue richness. This is in line with the color psychology, the audience's understanding of ancient dye technology is often oxidized and limited by the problems of ancient technology. Most of the historical objects watched by the audience in museums, books, videos and other channels have lost the original color part, which forms the audience's collective cognition of ancient color. In the background films of modern films and contemporary films, the hue is obviously richer than that of ancient times, which is mostly due to the popularity of modern industrial pigments and the iteration of modern digital color matching technology, thus showing the expansion of color dimensions. However, the color dimension of future background films is reversed, which is rooted in the symbolic expression of science fiction visual narration of "scientific and technological rationality". The use of single colors such as silver gray and cold blue is in line with the audience's imagination of future rational and dehumanized colors. This color strategy, to a certain extent, shows the common expression of film art creators to express the deprivation of human senses by technology.

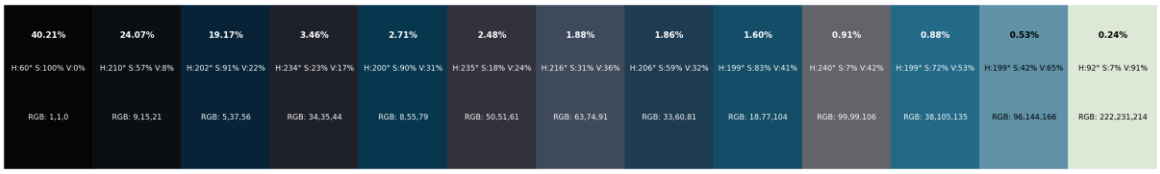

Figure 6: Ancient film clustering chromatogram

Figure 7: Recent background film clustering chromatogram

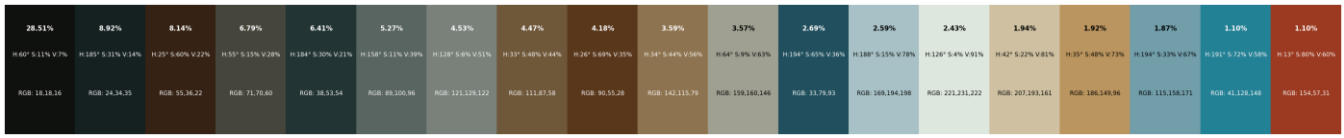

Figure 8: Contemporary background film clustering chromatogram

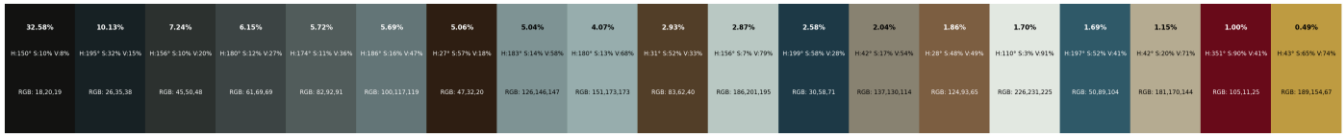

Figure 9: Future background film clustering chromatogram

CONCLUSION

Based on computer vision technology, this paper constructs a film color grading model to establish a personalized color database. This paper takes the top 10 100 films in the Chinese mainland from 2014 to 2024 as samples, extracts key pixels through frame sampling and golden section point positioning, uses MiniBatchKMeans

algorithm for color clustering, and combines CIE76 color difference formula to merge similar colors. Perceptual consistency is analyzed in HSV color space. A three-level classification system was established according to actual shooting/animation, tragedy/comedy/drama, and time background (ancient/modern/contemporary/future). The results show that the color distribution of animated films is more scattered, the Lightness and saturation are higher, and the RGB values change greatly. The overall tone of the tragedy film is cold, and the saturation and Lightness are low. The saturation of drama films should be appropriately reduced on the basis of maintaining historical authenticity. Comedy films are rich in color, high Lightness and saturation; Ancient and future themes are limited by historical or technological imagery, and the color performance is relatively monotonous. In addition, this study explored the potential of developing personalized color libraries to meet the preferences and styles of individual colorists. Based on the principles of color psychology, design, and film color theory, we invited 150 industry professionals to test the personalized color library. From the feedback, it can be seen that more than 80% of the respondents are confident in selecting a color grading template that conforms to the historical style of the director, the nature of the film and television work, and their own working practice. The study aims to streamline the color grading process, enabling creators to efficiently find the right colors to enhance their storytelling and emphasize their unique artistic voice, while reducing production costs and time constraints. This study creates a structured resource library for film color, which helps to support color grading and stylization in production, and improve the personalization level of visual narrative while reducing production costs.

REFERENCES

[1]. Thompson, K., & Bordwell, D. (2018). Film history: An introduction (4th ed.). McGraw-Hill Higher Education.

[2]. Magrin-Chagnolleau, I. (2013, July). The use of color in theater and film. 12th International AIC Congress, Newcastle upon Tyne, United Kingdom. https://hal.science/hal-03328903

[3]. Flueckiger, B., Halter, G., et al. (2021). Methods and advanced tools for the analysis of film colors in digital humanities. Digital Humanities Quarterly, 14(4). http://www.digitalhumanities.org/dhq/vol/14/4/000533/000533.html

[4]. Lin, J. (2021, Feb 28). Deep integration of Chinese modern natural painting color and film ecological art. Journal of Arts and Culture. 66-72.

[5]. Livio, M. (2002). The golden ratio: The story of phi, the world's most astonishing number. Broadway Books.

[6]. Zettl, H. (2017). Sight sound motion: Applied media aesthetics(8th ed.). Cengage Learning.

[7]. Sharma, G. (Ed.). (2003). Digital color imaging handbook. CRC Press.

[8]. Butcher, S. H. (Trans.). (1902). Aristotle's poetics. Macmillan and Co.

[9]. Bellantoni, P. (2005). If it's purple, someone's gonna die: The power of color in visual storytelling. Focal Press.

[10]. Flueckiger, B., et al. (2019). Digital tools for film color analysis. Proceedings of the 12th International Symposium on Visual Computing.

From Glaze Color to Perception: A Study on The Color Changes of Opaque Glaze and Human Perceptual Associations

Hsuan-Hsuan, Su[a*], Yan-Jun, Lin[b], Fu-Chi, Shin[c] , Tsuei-Ju, Hsieh[d]

[a]*Tsing Hua University, Hsinchu, Taiwan*
[b]*Tsing Hua University, Hsinchu, Taiwan*
[c]*Tsing Hua University, Hsinchu, Taiwan*
[d]*Tsing Hua University, Hsinchu, Taiwan*
**Corresponding author: Hsuan-Hsuan, Su, chris2540@gapp.nthu.edu.tw*

ABSTRACT

Rigorous colorimetric measurement of traditional craft materials whose appearance depends on subsurface scattering, gloss, and viewing geometry remains underrepresented in the literature. This motivates our study, which quantifies how nickel oxide (NiO) dosage and clay body jointly shape opaque glaze appearance and human preference, and translates the results into actionable CMF rules for ceramics. A constant base glaze was applied to three clay bodies (yellow earthenware, white earthenware, Japanese No. 26 porcelain) while varying NiO from 0.2–10%. Instrumental colorimetry used an X-Rite i1 Pro 3 (D50, 2°); a preference study with n = 21 participants (aged 18–26) covered 75 specimens. Two-way ANCOVA shows a strong main effect of NiO on L*, a*, b*, c*, and h° (e.g., L* model $R^2 = 0.836$, $p < 2\times10^{-40}$), whereas the clay main effect is smaller (significant only for L*, $p \approx 0.043$), and interactions are generally non-significant. Adjacent-step differences reveal a high-sensitivity regime at ≤ 5% NiO (mean ΔE*76 per step ≈ 1.74/1.46/1.28 for 26-porcelain/white/yellow) and a fine-tuning regime at > 5% (≈ 1.23/1.05/0.86). Preference peaks around J-1.20 (with W-4.00 also in the top set) while Y-0.40 ranks lowest; linear models explain little variance ($R^2 \approx 0.07$–0.09), indicating that liking is not a simple function of colorimetric proximity. Applications: we provide ceramic CMF guidelines—use 0.2–5% for series-level palette spacing, > 5% for batch-level correction and tolerance setting (with ΔE-based QC), and apply cross-clay dosage slopes as substrate-aware transfer functions for design, brand palette planning, and waste-reducing production control.

Keywords: ceramics; 0paque glaze; nickel oxide (NiO);cielab ;color preference;cmf design

INTRODUCTION

1.1 Research Background

Glaze appearance arises from the interplay of colorant concentration, clay-body composition, and optical/mesostructured factors (e.g., sub-surface scattering in opacified glazes, gloss cues, geometry-dependent highlights). In practice, transition-metal oxides—including NiO—tune hue, chroma, and lightness; yet broad dosage sweeps can mask perceptually salient micro-step changes and offer limited guidance for production-level series spacing or batch correction

On the measurement side, rigorous colorimetric protocols for traditional craft materials are still underrepresented; most reports focus on printed samples or displays rather than on real, strongly scattering materials such as opaque glazes. This leaves a gap between instrumental colorimetry and design-relevant perceptual outcomes (preference, semantic associations) that CMF teams must ultimately manage

1.2 Research Purpose

This study addresses that gap by (i) parameterizing the mapping from NiO dosage and clay body to CIELAB coordinates (L*, a*, b*, c*, h°) under controlled conditions (X-Rite i1 Pro 3, D50, 2°), and (ii) linking those mappings to human preference. A two-way ANCOVA (Color ~ NiO × Clay) on our dataset confirms a strong NiO main effect across coordinates (e.g., the L* model attains $R^2 \approx 0.836$), while the clay main effect is modest (significant only for L*), and interactions are generally non-significant. Adjacent-step analyses further reveal a high-sensitivity regime at ≤ 5% NiO (larger mean ΔE*76 per step) and a fine-tuning regime at > 5% (ΔE near JND), which directly informs CMF decision rules for palette spacing and tolerance setting.

The purpose is to produce design-operational knowledge that connects materials control to perceptual response in opaque glazes. Concretely, we pursue four questions:

RQ1 (Color mapping): How do NiO dosage and clay body jointly affect L*, a*, b*, c*, and h°? (Tested via two-way ANCOVA; NiO shows strong main effects.)

RQ2 (Step separability): How do adjacent-step color differences (ΔE*76 / ΔE00) distribute below vs. above 5% NiO? (Result: ≤5% forms a high-sensitivity range, >5% a fine-tuning range.)

RQ3 (Preference linkage): To what extent do colorimetric predictors explain liking? (Linear models explain little variance—indicating preference is not a simple distance function.)

RQ4 (Design translation): How can these findings be turned into CMF rules for series-level palette spacing, batch-level correction, and substrate-aware transfer across clay bodies?

1.3Limitations of the Study

We isolate the NiO dosage factor using a single base-glaze recipe and a fixed firing schedule, applying the same overglaze to three commercially available clay bodies (yellow earthenware, white earthenware, Japanese No. 26 porcelain). Thickness and surface finish are kept within practical tolerances but are not systematically manipulated; alternative colorants, kiln atmosphere, and temperature variants are outside scope. Colorimetry uses X-Rite i1 Pro 3 under D50/2°; results are reported in CIELAB with ΔE*76 (ΔE00 available). The preference study involves n = 21 participants (ages 18–26); thus, generalization beyond this demographic and beyond the tested glaze system should be made cautiously. These constraints allow clean identification of NiO-and-clay effects and support design-relevant inference, while motivating future work that adds gloss/roughness, thickness, and use-context semantics as explicit factors.

LITERATURE REVIEW

2.1 Linking Glazes to the Contemporary Color Lexicon

Glaze color is jointly determined by chromophore concentration (e.g., Ni, Co, Fe), opacification (zircon $ZrSiO_4$), and microstructure-dependent light transport (sub-surface/particle scattering), and is further influenced by the clay-body composition. Zircon-opacified systems show how pigment–opacifier–glaze interactions govern absorption and scattering; when pigment and zircon fractions vary, simplified Kubelka–Munk predicts the reflectance and color of opaque glazes.[1] Zircon clustering during densification alters optical properties and whiteness/opacity, underscoring that “glaze color” is inseparable from glaze physics.[2] In addition, opacifier particle size and dispersion, nucleation/crystallization (e.g., Ti-bearing phases), and firing profiles shape structural whiteness and colorimetry, providing a basis for repeatable appearance under process constraints.[1] [2]

For color specification and evaluation, contemporary practice typically reports CIELAB coordinates with ΔE metrics; CIEDE2000 improves perceptual uniformity over earlier formulae and is widely recommended for appearance QA in industry.[3] For cross-context predictions (e.g., different surrounds/illuminants), CAM16/CAM16-UCS offers an updated color-appearance framework and near-uniform space superseding CIECAM02-UCS.[4] These models provide the quantitative backbone for linking glaze formulation to design-relevant, perceptual color targets.

2.2 Color as a Marketing Language

Color functions as a high-bandwidth semantic cue in branding and product communication. Classic experiments show that brand–color appropriateness depends on product category and positioning, shaping judgments of logo fit and meaning.[5] Large-sample evidence maps specific hues (and their saturation/value) onto brand-personality dimensions (e.g., "exciting red," "competent blue"), with downstream effects on purchase intent and brand familiarity/likability.[6] At a broader psychological level, the Ecological Valence Theory (EVT) explains color preference via affective associations to color-diagnostic objects (e.g., blues with clear skies/water), aligning with modern findings that color influences affect, cognition, and behavior beyond low-level vision.[7] For CMF work in ceramics, these strands justify connecting instrumental colorimetry to affect/usage semantics and market-sensitive palettes.

2.3 Material Appearance & Measurement for Craft Materials (new)

Unlike printed or emissive samples, craft materials (e.g., opaque glazes) exhibit geometry- and illumination-dependent appearance due to gloss, mesostructure, and sub-surface scattering. Vision science shows that gloss, translucency, and material category judgments rely on highlight structure and image statistics, not just pointwise color.[8] [9] Large-scale psychophysics confirms humans are sensitive to optical-material changes across conditions, reinforcing that "equal colorimetry" ≠ "equal appearance" when geometric cues differ (e.g., specular layout, microscopic texture) (Wiebel-style large-scale materials study; see review corpus). Thus, studies on ceramic CMF benefit from standardized viewing and measurement (e.g., ISO 3664 D50 viewing conditions; ISO 13655 M-series spectral modes) to ensure that reported CIELAB/ΔE are interpretable and reproducible. For perceptual scaling beyond JNDs, MLDS offers a principled way to recover suprathreshold difference scales from observer choices, complementing ΔE metrics when relating micro-formulation steps to perceived separation.[10] [11] [12]

METHOD

We pursued two goals: (i) to parameterize how NiO dosage and clay body jointly determine opaque-glaze color in CIELAB coordinates; (ii) to assess whether those variations map onto human preference and associative meanings, thereby yielding CMF rules usable in design and production.

3.1 Materials preparation

A constant base-glaze recipe was applied to three commercially available clay bodies: yellow earthenware (Y), white earthenware (W), and Japanese No. 26 porcelain (J). Nickel oxide (NiO) served as the sole chromophore; all other glaze constituents and firing conditions were held constant. NiO dosage covered 0.2–10.0 wt%. Consistent with our pilot and the final dataset, the ≤5% range followed an equal-step schedule of 0.2% increments (0.2, 0.4, …, 5.0), and the >5% range used 0.5% increments (5.5, 6.0, …, 10.0). Each specimen was coded as *Clay-NiO* (e.g., J-1.20, W-4.00, Y-0.40) and fired under the same schedule (see Figure. 1). Glaze thickness and surface finish were not systematically manipulated and remained within practical process tolerances.

Figure 1: Glaze producing procedure experiment material

3.2 Colorimetric Measurements

Instrumental measurements were conducted with an X-Rite i1 Pro 3 spectrophotometer under D50 illumination and the CIE 2° standard observer. Device spectral sampling (≈10 nm, 380–730 nm) was used to compute CIELAB values (L*, a*, b*), from which chroma ($c^* = \sqrt{(a^{*2}+b^{*2})}$) and hue angle ($h^\circ = \text{atan2}(b^*,a^*)$) were derived(see Figure 2). For appearance separability we report ΔE*76 for adjacent dosage steps within each clay; ΔE00 (CIEDE2000) was also computed for consistency checks using the implementation notes of Sharma, Wu, and Dalal

(2005). Viewing/measurement conditions follow graphic-arts practice for D50 standardization to enhance reproducibility across laboratories (cf. ISO 3664).

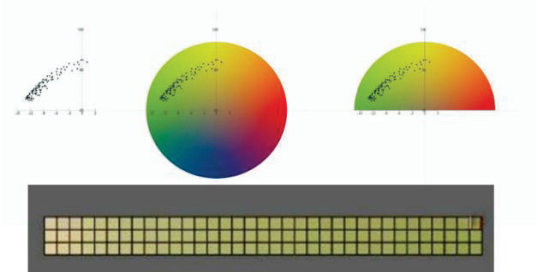

Figure 2: CIELAB Color Distribution Plot

3.3 Preference and associative judgments

Participants. n = 21 university students/graduate students (18–26 years). All provided informed consent. Stimuli & tasks. Participants viewed the fired specimens and provided single stimulus liking judgments for 75 coded glaze samples (randomized order). To probe usage semantics, we additionally administered a single forced-choice categorization: for selected items (stratified by prior liking into "high-preference" and "low-preference" sets), participants chose one life-domain label (food, clothing, housing, mobility, education, recreation, utility) that best matched their first impression. Environment & order. Sessions used consistent ambient conditions approximating D50 with a neutral background; trial order was randomized per participant.

All analyses used $\alpha = .05$ (two-tailed). For color coordinates (L*, a*, b*, c*, h°), we fit OLS two-way ANCOVA models of the form Color ~ NiO (continuous) × Clay (Y/W/J, categorical) with Type-II sums of squares, reporting F, p, and R^2; residual Q–Q and residual-vs-fitted diagnostics were inspected and HC3 robust SEs checked where heteroskedasticity was suspected. From the interaction model we extracted per-clay marginal slopes (dL*/dNiO, da*/dNiO, db*/dNiO, dc*/dNiO, dh°/dNiO). Step separability was assessed by computing adjacent-step ΔE*76 (and ΔE00) within each clay and summarizing by ≤5% vs >5% NiO to test the high-sensitivity versus fine-tuning hypothesis. For preference, we first averaged ratings per specimen, then fit linear mixed-effects models with random intercepts for participants (and, as a sensitivity check, random slopes for NiO), and compared piecewise (knot at 5%) and quadratic specifications by AIC; we report pseudo-R^2 as the squared correlation between fitted and observed ratings. Finally, we examined the association between |Δpreference| and ΔE for adjacent steps. Reporting includes coefficients, p-values, Top/Bottom specimen rankings, clay-wise means, and life-domain association counts (by gender when available).

RESULTS

4.1 Main effect

Figure 3 shows representative specimens across dosage and clay bodies. NiO dosage exerted a strong, monotonic influence on CIELAB coordinates across the three clay bodies. Two-way ANCOVA (Color ~ NiO × Clay) showed a significant NiO main effect for all coordinates, with high model fit for L* ($R^2 = 0.836$; $p = 1.96\times10^{-40}$), a* ($R^2 = 0.697$; $p = 4.15\times10^{-27}$), b* ($R^2 = 0.790$; $p = 6.01\times10^{-35}$), c* ($R^2 = 0.786$; $p = 1.55\times10^{-34}$), and a smaller but reliable effect for h° ($R^2 = 0.353$; $p = 1.65\times10^{-10}$). The clay main effect was modest—significant only for L* ($p = 0.043$)—and NiO × Clay interactions were not significant ($p \approx 0.27$–0.70). Marginal dosage slopes (per 1% NiO) from the interaction model were consistent across substrates. Adjacent-step separability (ΔE*76) within each clay confirmed two practical regimes. Mean ΔE per step declined from ≤5% NiO to >5% NiO as follows: J 1.74→1.23, W 1.46→1.05, Y 1.28→0.86. Thus, ≤5% operates as a high-sensitivity range for creating visible series spacing, while >5% serves as a fine-tuning range near JND levels.

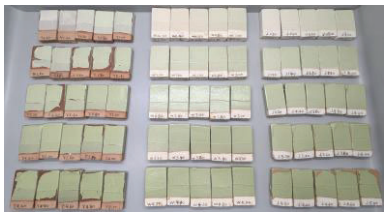

Figure 3: Coloration of Glaze Test Pieces (NiO)

4.2 Color Preference Distribution

Across n = 21 participants (ages 18–26) and 75 specimens, the distribution of mean liking scores had M = 0.42, SD = 0.89. The Top-5 specimens were J-1.20 (2.85), Y-1.20 (2.20), Y-0.80 (2.17), J-2.20 (2.02), W-4.00 (1.94); the Bottom-5 were Y-0.40 (−1.51), Y-3.80 (−1.31), Y-2.40 (−1.00), Y-0.20 (−0.96), J-2.00 (−0.95). Mean liking by clay was J = 0.579, W = 0.513, Y = 0.168; a one-way ANOVA for clay was not significant (p = 0.220).Linear models explained little variance in preference: an ANCOVA of Preference ~ NiO × Clay yielded $R^2 \approx 0.066$, and mixed-effects models with random intercepts for participants produced pseudo-$R^2 \leq 0.10$ with no reliable fixed-effect slopes. Moreover, color difference does not predict preference change: for adjacent steps, preference was uncorrelated with ΔE (Spearman r = −0.028; Pearson r = −0.039; n = 72 pairs). Figure 4 visualizes specimen-wise preference scores and highlights the top/bottom sets.

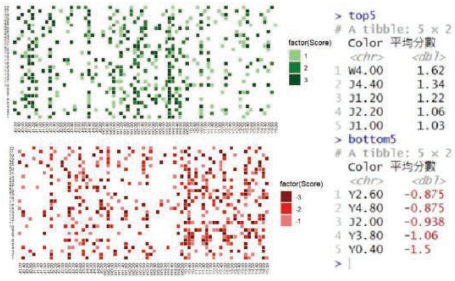

Figure 4. Pecimen-wise preference scores and highlights the top/bottom sets

4.3 Perceptual Associations

In a restricted single-choice categorization targeting everyday life-domain semantics, the highest-rated glaze in each set most often evoked “food” contexts. For the top specimen W-4.00, the association distribution was Food 50%, Utility 33.3%, Housing 8.3%, Mobility 8.3% (n = 12 responses), indicating a stronger propensity to elicit food-related imagery.

DISCUSSION AND CONCLUSIONS

This study shows that NiO dosage dominates opaque-glaze color across coordinates, while clay adds a small baseline shift and their interaction is negligible. Consequently, regardless of substrate, higher NiO yields darker, greener–yellower, more chromatic glazes. Stepwise results reveal two usable regimes: ≤5% NiO is a high-sensitivity band (large visible spacing), while >5% is a near-JND fine-tuning band—turning formulation into levers for palette spacing and batch correction. Preference did not follow simple CIELAB distance; instead, semantic/usage cues (e.g., “clean/edible/modern”) mediate liking beyond colorimetric proximity—color control is necessary for quality, but meaning drives desirability.

1. Use 0.2–5% NiO to build visibly tiered series; reserve >5% for micro-adjustment and define ΔE-based QC bands there.
2. Apply cross-clay dosage slopes to transfer targets between substrates during scaling and vendor changes.

3. Pair instrumental control with semantic validation (short preference/association checks) when curating product lines—especially for tableware, where "food" connotations matter.

In current study, we isolated NiO under a single base glaze and firing schedule with pragmatic control of thickness and finish. Future work should: (i) systematically vary gloss/roughness and thickness, and include multi-geometry / multi-illuminant measurements; (ii) expand and diversify the participant pool; and (iii) directly compare real glazes vs. print/screen matches to quantify where "equal colorimetry" still fails to reproduce material appearance and preference.

Overall, the study converts studio intuition into concise, transferable rules for ceramic CMF: predictable dose-to-color behavior, a two-regime planning strategy for palettes.

REFERENCES

[1]. Sharma, G., Wu, W., & Dalal, E. N. (2005). The CIEDE2000 color-difference formula: Implementation notes, supplementary test data, and mathematical observations. Color Research & Application, 30(1), 21–30. https://doi.org/10.1002/col.20070

[2]. Wang, S., Peng, C., Huang, Z., Zhou, J., Lü, M., & Wu, J. (2014). Clustering of zircon in raw glaze and its influence on optical properties of opaque glaze. Journal of the European Ceramic Society, 34(2), 541–547. https://doi.org/10.1016/j.jeurceramsoc.2013.08.018

[3]. Sharma, G., Wu, W., & Dalal, E. N. (2005). The CIEDE2000 color-difference formula: Implementation notes, supplementary test data, and mathematical observations. Color Research & Application, 30(1), 21–30. https://doi.org/10.1002/col.20070

[4]. Li, C., Li, Z., Wang, Z., Xu, Y., Luo, M. R., Cui, G., Melgosa, M., Brill, M. H., & Pointer, M. (2017). Comprehensive color solutions: CAM16, CAT16, and CAM16-UCS. Color Research & Application, 42(6), 703–718. https://doi.org/10.1002/col.22131

[5]. Bottomley, P. A., & Doyle, J. R. (2006). The interactive effects of colors and products on perceptions of brand logo appropriateness. Marketing Theory, 6(1), 63–83. https://doi.org/10.1177/1470593106061263 ORCA

[6]. Labrecque, L. I., & Milne, G. R. (2012). Exciting red and competent blue: The importance of color in marketing. Journal of the Academy of Marketing Science, 40(5), 711–727. https://doi.org/10.1007/s11747-010-0245-y

[7]. Elliot, A. J., & Maier, M. A. (2014). Color psychology: Effects of perceiving color on psychological functioning in humans. Annual Review of Psychology, 65, 95–120. https://doi.org/10.1146/annurev-psych-010213-115035

[8]. Fleming, R. W. (2014). Visual perception of materials and their properties. Vision Research, 94, 62–75. https://doi.org/10.1016/j.visres.2014.01.001

[9]. • Nishida, S. (2019). Image statistics for material perception. Current Opinion in Behavioral Sciences, 30, 94–99. https://doi.org/10.1016/j.cobeha.2019.07.003

[10]. International Organization for Standardization. (2009). ISO 3664:2009—Graphic technology and photography—Viewing conditions. (D50 viewing conditions; P1/P2 levels).

[11]. International Organization for Standardization. (2009). ISO 13655:2009—Graphic technology—Spectral measurement and colorimetric computation for graphic arts images. (M0–M3 measurement conditions; M1≈D50).

[12]. Maloney, L. T., & Yang, J. N. (2003). Maximum likelihood difference scaling. Journal of Vision, 3(8), 5, 573–585. https://doi.org/10.1167/3.8.5

The Use of Color on The Expiatory Temple of The Sagrada Família by Antoni Gaudi: Nature, Life and Symbolism

Leonardo Pestana Collalto Toni[a*], João Carlos de Oliveira Cesar[a]

a Faculty of Architecture, Urbanism, and Design of the University of São Paulo – FAUUSP, São Paulo, Brazil
[*]Corresponding author: Leonardo Pestana Collalto Toni, leocollalto@usp.br

ABSTRACT

Conceived by Antoni Gaudí i Cornet as a Bible in stone, the Expiatory Temple of the Sagrada Família in Barcelona employs various tools to convey the Christian philosophy through its architecture. In this way, each element - color, façade, ornament, or even structural component - was intentionally designed to symbolically express religious passages and concepts, using references drawn from nature. Gaudí's use of natural references in both the design process and architectural representation is rooted in his perception of the natural world as the ultimate expression of divine creation - viewed by him as a master from whom one must observe and draw lessons. Thus, his symbolic representations aimed to transform the religious edifice into a space he believed to be the closest possible to the divine: nature itself. In pursuit of this objective, light and color - fundamental elements in shaping spatial perception and, by extension, our experience of nature and its settings - were likewise employed as central design strategies in Gaudí's effort to evoke a naturalistic ambiance within the interiors of the Sagrada Família and on important symbolic elements of its exterior. The inseparable relationship between light and color, for Gaudí, also held symbolic significance: the idea that color is the device through which nature reveals the presence of life. Consequently, architecture, too, should be abundant in color. This belief led the architect to propose a polychromatic treatment of the temple's elements and spaces, either to emphasize the presence of life or to communicate particular symbolic messages within the Christian iconography. For instance, Porphyry - a reddish stone - was used at temple's central tower and main altar, both dedicated to Christ, while Blue Bahia stone, in bluish hues, was chosen for the tower dedicated to Mary. The Gaudí's project for the Sagrada Família Basilica demonstrates a wide variety of uses and applications of chromaticism in architecture, as well as its associated meanings - established through the building's relationship with both nature and religion through its symbolism. These aspects offer new perspectives on the symbolic and practical role of color in architectural design. This article therefore aims to analyze the concept, application and significance of chromaticism in the work of Antoni Gaudí, investigating his design processes through the study of his magnum opus, the Expiatory Temple of the Sagrada Família.

Keywords: chromatic design, biomimicry, expiatory temple of the sagrada familia, symbolism

INTRODUCTION

Under construction since 1882, the Expiatory Temple of the Sagrada Família is the masterpiece of Antoni Gaudí i Cornet, the Catalan architect born in 1852, who lived for 74 years, forty of which were devoted to the design of this monumental work. The Sagrada Família represents the culmination of a unique style created by Gaudí, crystallizing a set of references and approaches never before employed in architecture, whose stylistic classification continues to challenge critics to this day. Antoni Gaudí developed his personal style through careful observation of nature and the rationalization of its features into formal, structural, and symbolic syntheses, which were translated

into architecture through extensive practical experimentation throughout his career [1]. The resulting biomimetic architecture incorporates a variety of natural characteristics into his buildings, including forms, structures, spatial configurations, cultural symbolism, and colors.

During the development of his master's dissertation, Toni [2] identified that, although Gaudí's work has been the subject of extensive scholarly literature, little attention has been devoted to its chromaticity, a fundamental aspect in the construction of Gaudí's oeuvre.

In light of this, it became evident that further investigation into this rich characteristic of Antoni Gaudí's work is necessary, seeking to expand the technical framework and deepen the understanding of his concepts, creative processes, and the ways in which he employed color in his architecture. To this end, his magnum opus, the Expiatory Temple of the Sagrada Família, will serve as the case study.

METHODOLOGY

For the development of this investigation, the adopted methodology consisted of a critical review of selected literature, based on studies of Gaudí's work, on the reports of his collaborators and disciples, such as Cesar Martinell Brunet and Isidre Puig Boada, as well as on texts by the current chief architect responsible for the construction of the temple, Jordi Faulli i Oller. This research focuses on the manner in which the architect conceived and applied colors in his most significant work, comparing the concepts identified in the bibliographic review with personal experience within the analyzed environments.

RESULTS AND DISCUSSION

Conceived by Gaudí as a physical representation of the Bible, the sacred text of Christianity, the Expiatory Temple of the Sagrada Família consolidates forty years of design development undertaken across his prolific career as an architect, between 1883—when he assumed responsibility for the temple's project—and 1926, when he died after being struck by a tram in Barcelona [3]. Gaudí's vision for the temple was that the building should, through its structures, spaces, façades, and elements, narrate the life of Christ, from his birth to his death and resurrection. To achieve this, he employed a variety of creative references to translate his concept into architecture, the foremost of which—and the one that unified all others—was nature.

Gaudí grew up closely observing the natural world, as from childhood he suffered from rheumatic pain that prevented him from living actively like other children his age, forcing him to experience life activities more as an observer than as a participant [3]. During his childhood and youth, he studied the peculiarities and phenomena of nature, establishing with it a philosophical and spiritual bond, regarding it as the closest representative of the divine and a source of knowledge meant to guide humanity. As Ramis i Juan affirms [4, p. 68]:

> "Nature is conceived as a total work of art, as something sublime that man cannot surpass. […] In Gaudí this concept persists. The architect sees in this nature the source of all knowledge: 'The great book, always open and which one must strive to read, is that of Nature; the other books are made from it, and in them there are mistakes and interpretations of man. There are two revelations: one doctrinal, of Morality and Religion, and another leading to facts, which is that of the great book of Nature.'"

This relationship with nature led the architect to imprint in his works natural characteristics and references that endowed his architecture with a singular aspect, as though they were marine living beings—such as Casa Batlló—or geological formations—such as Casa Mila. In this way, Gaudí brought into his creations visions of nature as both a source of knowledge and an exemplar of divine creation. A crucial element in this natural referencing, and in his effort to evoke atmospheres reminiscent of natural environments, was his intelligent and creative use of color, stemming from his particular vision of its importance in nature.

For Gaudí, architecture had to be polychromatic, since color is nature's primary instrument for signaling the presence of life [5]. This belief is recorded in two statements compiled by Isidre Puig Boada, Gaudí's personal friend and collaborator in the development of the Sagrada Família: "In art there must be life, and this manifests itself mainly through color" [5, p. 107]; and "People are not mistaken when, upon seeing a colorless person, they say he looks like a walking corpse; and when they see a cadaver with rosy cheeks, it looks as if it were still alive!" [5, p. 158].

This conviction led the architect to conceive the temple's polychromatic treatment as a whole, particularly in elements intended to convey the impression of living presence [2]. On the exterior, Gaudí reserved the most elaborate use of color for the temple's eastern façade, the Nativity Façade, dedicated to communicating the events of Christ's birth and early life, as well as his relationship with his parents, Mary and Saint Joseph. His project envisioned the complete polychromatic treatment of this stone façade, with colors corresponding to the natural decorative motifs framing this moment of Christ's life.

The façade is composed of three porticos ornamented with innumerable plant and animal species sculpted in stone, giving its entire surface an almost living aspect, as if a dynamic natural scene had been suddenly petrified by Medusa, the Greek monster. Above the porticos, a monumental cypress tree symbolizes the eternal life of the Christ, flanked by four pinnacles, two on each side. Cesar Martinell Brunet, Gaudí's disciple and friend, recorded the architect's reflections on the polychromatic treatment of the portals of this façade, expressed during one of their conversations:

> "He reveals that this door will also be polychromatic, he says that color is life, and the lack of color is the most visible manifestation of death. The roses that adorn this door, carved in stone (very well crafted), are not yet roses, for the most beautiful and characteristic thing about these flowers is their color, which these portals still lack" [6, p. 62].

In 1889, Gaudí created a polychrome model of this façade (Figure 1) to be presented at the Paris Universal Exposition of the same year. This became one of the few surviving records of his chromatic project for the temple, since, in addition to many of his documents and drawings having been destroyed during the Spanish Civil War in 1936, financial limitations at his time prevented the full execution of the chromatic treatment he envisioned.

Figure 1: Section of a polychrome plaster model of the Nativity Façade, created by Gaudí for the 1889 Paris Universal Exposition. Source: Leonardo Toni, 2023.

Gaudí's vision of the vitality of color is also expressed in his reflections on the chromatic quality of Mediterranean sunlight, and on how it could be applied to architecture in order to endow it with life:

> "In the Sagrada Família we shall polychrome only the lower parts and those not touched by the sun. The upper parts will be polychromed naturally, since the sun is a great painter, which in our regions paints with very beautiful colors: the walls of Tarragona with a copper hue and the cathedral as well, with colors as lovely as those here (in Barcelona). The buildings in the North have dark green or black colors. This is explained by the agents that produce them. In the Sagrada Família, the centuries will take care of this painting" [6, p. 107].

For Gaudí, color was not determined solely by the materials applied to his architecture by him and his craftsmen, but also by the passage of time, which would transform it through natural patinas and the chromatic variations of the constructive materials themselves. His conception of a living architecture was not limited to forms and colors; it extended to the very idea of the building as an organism that ages and, through environmental effects, changes in appearance and tone. Consequently, large portions of the building display on their façades the inherent color of their construction materials, primarily sandstones originally quarried from Montjuïc mountain in Catalonia. Nonetheless, Gaudí introduced chromatic accents in specific architectural or symbolic elements, such as the temple doors, the edges of the six central towers—dedicated to Jesus, Mary, and the four biblical Evangelists—and the sculptural compositions crowning the numerous pinnacles that adorn the façades. Brunet describes this chromatic treatment:

> "Decoration was, is, and will be colored," Gaudí declared. He based his assertion on the example of Nature, which in none of its realms falls into the monotony of a single hue. Therefore, he added, we must polychrome architectural elements, either wholly or partially. The sun is the great painter of Mediterranean lands, he exclaimed, relying on the patina that light, air, and microorganisms bestow upon noble construction materials. Thus, he logically reserved polychromy for parts less accessible to patina and more protected from rain. He also used colored stones and polychrome stained glass to cover walls built with ordinary materials" [6, pp. 158–189].

These elements serve as symbolic representations of religious and cultural references to moments in the life of Christ or to regional celebrations of his story. For instance, on the tower dedicated to Christ and the four surrounding towers, porphyry—a red-colored stone symbolizing the blood of Christ—was used on their edges. On the tower dedicated to Mary, instead, Bahia Blue stone was employed, with its bluish tone evoking the Catholic association of the Virgin with purity [7].

Figure 2: Sculptural compositions of fruit baskets crowning the pinnacles above the large stained-glass windows of the Nativity and Passion lateral façades. Source: Leonardo Toni, 2023.

Similarly, the pinnacles crowning the large lateral stained-glass windows (Figure 2) consist of sculptural compositions of fruit baskets, referencing the festivities of Christmas (Christ's birth), represented by chestnuts, and Easter (Christ's death and resurrection), represented by figs—each placed on the façade corresponding to these episodes [7]. Also, at the crowning of the eight lateral bell towers, there are polychromatic geometric compositions inspired by crystals, representing the episcopal insignia: the miter, the ring, and the crozier.

These highly chromatic elements are, significantly, located at the highest points of the temple, where the building "touches the sky" and connects with the divine. This vision is reinforced by Alsina as part of the symbolic interpretation expressed by Gaudí: "We can observe the most spectacular geometric compositions in the highest part of the works, which is not without a metaphorical significance: the increasing complexity towards the sky" [8, p. 188]. These sculptural elements have their chromaticism applied through the technique known as Trencadís, created by Gaudí, consisting of the application of small, broken ceramic or glass pieces onto irregular surfaces, forming a kind of mosaic.

This Gaudí's polychromatic vision also manifests itself in the interior of the temple, where he once again employs sunlight as a transformative element of architectural chromaticism and as a generator of a naturalistic atmosphere. The interior is flooded with multicolored light projected by the sun through the large polychrome stained-glass windows that flank its naves, producing a symphony of colors designed to convey the tonal qualities of sunlight at different times of the day. These colors range from cool tones such as blue and green to warm ones such as orange and red, orchestrated in such a way that their intensity and distribution follow the rhythm of the sun's rays.

On the eastern façade, oriented toward the rising sun and representing the birth of Christ, cooler tones predominate, intended to reproduce the chromatic nuances of dawn light (figure 3). Conversely, on the western façade, facing the setting sun and symbolizing Christ's Passion and death, warmer tones are applied, imitating the spectrum of colors found in the sunset, the daily "death" of the sun (figure 4).

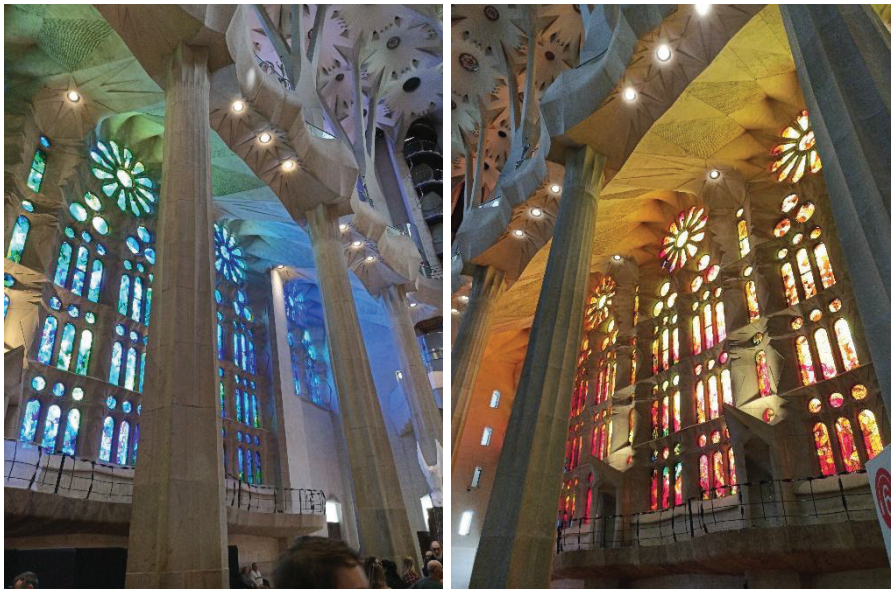

Figures 3 and 4: Multicolored stained-glass windows on the eastern and western façades, respectively. Source: Leonardo Toni, 2023.

This strategy creates within the temple an atmosphere that transports visitors—together with the tree-like structures formed by its columns—into a forest, a place Gaudí believed to be the closest to God [6]. The only location where Gaudí conceived light entering the temple as colorless was in the stained-glass windows placed at

the highest section of the central nave, motivated by the symbolism of white light in Christian cosmology, as explained by Faulí i Oller:

> "The upper stained-glass windows of the aisles explain Jesus' parables "I am the fountain of living water, the vine, the good sower, the good shepherd..." Those of the central nave, as envisaged by Gaudí, are colorless so as to be conducive to the entry of light at the vaults, and so that any light that enters does not mask the color of the ceramic vaults; the artist created leaded stained glass windows made of translucent glass of different kinds and textures." [7, pp. 157–158].

CONCLUSION

In Gaudí's Sagrada Família, color emerges as the tool through which the architect endowed his architecture with a vital presence, serving not only as a medium of symbolic communication but also as the element that unites the earthly and the sacred. This naturalistic and delicate chromatic treatment does not disregard the passage of time, which Gaudí from the outset considered as a collaborator in composing the chromatic surfaces of his magnum opus, with its surfaces gradually transformed by sunlight, rain, and microorganisms in the years to come.

> "It is important to emphasize, however, that ornamentation for Gaudí is ephemeral, something ultimately replaced by the imprint of time. To regard time as an element intervening in the work is to confer upon the edifice a transcendental value, for it is thereby endowed with life of its own" [4, p. 64].

REFERENCES

[1]. Cirlot, J.-E., Vivas, P., & Pla, R. (2014). *Gaudí: Introducción a su arquitectura*. Barcelona: Triangle Postals,

[2]. Toni, L. P. C. (2024). *Processos biomiméticos aplicados ao desenvolvimento do projeto arquitetônico: Dois estudos de caso* [Masters dissertation, Universidade de São Paulo], São Paulo.

[3]. Castellar-Gassol, J. (1999). *Gaudí. The life of a visionary* (P. Martin, Trans.). Barcelona: Edicions de 1984.

[4]. Ramis i Juan, R. (2016). Gaudí para além de Gaudí (E. Flavian, J. Norman, & J. Lima, Trans.). In I. T. Ohtake (Ed.), *Gaudí. Barcelona 1900* (pp. 58–89). São Paulo: Instituto Tomie Ohtake.

[5]. Boada, I. P. (2015). *El pensamiento de Gaudí: Complicación de textos y comentarios*. Barcelona: Dux Editorial

[6]. Brunet, C. M. (2007). *Conversas com Gaudi* (1ª edition). São Paulo: Perspectiva.

[7]. Faulí i Oller, J. (2021). *The Basilica of the Sagrada Familia*. Barcelona: ALDEASA.

[8]. Alsina, C. (2004). *Macla de Geometrias* (E. B. Etcheverry, M. C. R. Ardoy, M. B. Colapietro, & M. A. C. Ribeiro, Trans.). In Instituto Tomie Ohtake (Ed.), *Gaudí: A Procura da Forma*. São Paulo: Instituto Tomie Ohtake.

Exploring The Emotional Impact of Color Design in Children's Picture Book Covers

Yixuan Wang[a*], Wenfei Geng[b]

[a]*Nanjing University of Science and Technology, Nanjing, China*

[b]*Nanjing University of Science and Technology, Nanjing, China*

**Yixuan Wang:wangy433@coventry.ac.uk*

ABSTRACT

As a primary visual interface between children and literature, picture book covers serve as a decisive factor in stimulating reading interest and driving purchasing behavior. The strategic use of color in cover design assumes particular significance as it must simultaneously fulfill educational objectives while maintaining strong market appeal. Existing research has primarily focused on textual and illustrative elements of cover design, while studies on how color coordination reconciles designers' personal preferences with market demands remain insufficient. Adopting a cross-cultural perspective, this study investigates the design principles of picture book cover colors by systematically analyzing the color characteristics of 60 best-selling picture books from four major markets: Europe, Japan, Taiwan (China), and Mainland China. The research aims to uncover culturally preferred color-matching patterns and provide data-driven design references for practitioners.

The study employs a quantitative analytical approach: Using Photoshop and MATLAB tools, five dominant colors are extracted from each cover based on the CMYK printing model, resulting in 300 colors and 60 palettes. The Color Thresholder App is then applied to segment cover images, extract dominant colors, and process the data via the k-means clustering algorithm. A quantitative analysis of each market's color palette is conducted, constructing color distribution axes for the four regions. Finally, this study, in combination with the theory of color emotion, establishing a "Cross-Cultural Quantification of Color Emotion" analytical framework. This allows for a comparative analysis of the most favored color schemes across markets, revealing similarities and differences in color selection under varying cultural contexts.

The empirical findings provide data-supported insights for picture book cover design, particularly in balancing educational attributes and commercial appeal. Academically, the study advances methodological approaches to visual communication analysis and establishes a replicable model for cross-cultural design research. The framework's applications extend beyond children's literature to inform visual design strategies in diverse cultural contexts.

Keywords: Picture book design,Color preference,Color design, Cover, Color Psychology

INTRODUCTION

Picture books, as a literary form deeply loved by children, have always represented a perfect integration of design and art throughout history [1]. The cover serves as the first visual point of contact between a child and a picture book, and the visual impact of its colors significantly influences children's preferences and level of interest [1]. Among various design elements of picture books, color is recognized as a key factor affecting consumers' purchasing decisions and is considered one of the most critical elements in visual marketing [2][3], accounting for 62%–90% of purchase choices [4].

Although color plays a decisive role in the market performance of children's picture books, a significant gap exists between design practice and theoretical expectations. This contradiction is reflected in the fact that designers' color preferences heavily influence picture book design, yet most designers rely on experiential intuition when creating color schemes [5]. Research shows that designers consistently consider color throughout the design process [6], and many face challenges in color selection [7]. Thus, there remains a lack of research on how to reconcile conflicts between designers' personal aesthetics and market demands.

Studies in color psychology indicate that colors can evoke specific emotional responses [10][11]. The Ecological Valence Theory (EVT) proposed by Palmer and Schloss [12] attributes color preferences to emotional responses associated with color-related objects, although this theory primarily explains color preferences in industrialized cultures [13]. Research consistently shows that blue is the most preferred color, yellow the least preferred, while a universal preference for white exists; people tend to prefer brighter and more saturated colors [14], and overall, light colors are favored when considering lightness [15]. However, most of these studies are confined to Western cultural contexts and lack cross-cultural comparative analysis.

Color influences market performance by eliciting consumers' emotional responses and shaping color preferences, a principle that also applies to the cover design of children's picture books. Studies have found that saturated and bright colors are more effective in arousing emotions [16]. Gao et al. [17] suggest that hue and cultural background have limited impact on color emotions, yet preferences in color associations still exhibit both similarities and differences across cultures in terms of market demand. The meaning of color is inherently social and cultural [18], and color preferences are learned [19].

In addition to the perspective of market demand, the personal color preferences of designers also warrant in-depth investigation. Existing research indicates distinct color tendencies among designers: Bonn [20] suggested that designers show the strongest preference for the three primary colors—red, yellow, and blue, while Bonnardel et al. [21] found that designers tend to favor combinations with lower chroma and more similar hues compared to non-designers. As this study focuses on the influence of market demand on color selection in picture books, the role of designers' individual preferences will be explored in future research.

Therefore, this study employs a quantitative analysis approach, integrating the CMYK printing model, the k-means clustering algorithm, and color emotion theory to construct a "cross-cultural color emotion quantification" framework. This framework aims to uncover the patterns of color matching and dominant color preferences in picture book covers, examining both similarities and differences across various cultural markets. The research seeks to compare and analyze the most popular color schemes in different cultural contexts, revealing the commonalities and variations in color choices influenced by cultural background. Not only does this study address the gap in how color coordination can reconcile designers' preferences with market demands from a market-oriented perspective, but it also provides data-supported decision-making guidance for visual design in the children's picture book publishing industry.

METHODOLOGY

This study adopts a quantitative research approach, focusing on the color design of children's picture book co vers. A total of 60 picture book covers were selected, comprising 15 samples each from the Mainland China, Japa n, Taiwan (China), and United Kingdom markets. The samples were obtained through authoritative commercial d ata platforms:Mainland China samples were sourced from Dangdang (http://bang.dangdang.com/books/bestsellers /01.41.70.00.00.00-year-2024-0-1-1), Taobao (https://s.taobao.com/search?page=1&q=%E7%BB%98%E6%9C% AC&spm=a21bo.tmall%2Fa.201867-main.d11_7.6614c3d5zRK2Dh&tab=mall), and Douban's Top 100 Picture B ooks (https://m.douban.com/subject_collection/EC644XZ7I); Japanese samples were obtained from Nippan Bests eller Rankings (https://www.nippan.co.jp/ranking/annual/?post_id=&ranking_cat=101#single), Amazon Japan Pic ture Book Bestsellers (https://www.amazon.co.jp/-/zh/gp/bestsellers/nonfeatured/4852974051/ref=zg_bs_pg_1_u ndefined?ie=UTF8&pg=1), and Rakuten Books Picture Book Bestsellers (https://books.rakuten.co.jp/search?g=00

1003&s=1&o=0&l-id=search-c-pager); Taiwan (China) samples were collected from Books.com.tw Bestsellers (https://www.books.com.tw/web/sys_storecatt/children_fbooks_06/?loc=P_greenbar_th_2_030), Eslite Bookstore Bestsellers (https://www.eslite.com/best-sellers/online/42637/42649), and Momo Shopping Network Children's Books Ranking (https://www.momoshop.com.tw/category/DgrpCategory.jsp?d_code=4002800985&p_orderType=6&showType=chessboardType); UK samples were sourced from Amazon UK Children's Books Bestsellers (https://www.amazon.co.uk/best-sellers-books-Amazon/zgbs/books/69/ref=zg_bs_pg_1_books?_encoding=UTF8&pg=1) and Waterstones Picture Books Bestsellers (https://www.waterstones.com/category/childrens-teenage/picture-books/sortmode/bestselling/page/1#p_11104856). Regional classification follows WTO publication trade statistical standards.

Figure 1 **Figure 2** **Figure 3** **Figure 4**

Researchers obtained high-quality samples through official channels. Initially, Adobe Photoshop was used to extract five dominant colors from each book cover based on the CMYK color model, resulting in 60 initial palettes (Figures 1-4). The CMYK model was selected for its alignment with printed materials, ensuring closer resemblance to physical book colors. To enhance color fidelity and methodological rigor, MATLAB was subsequently employed to re-extract the color data, yielding 300 colors in CMYK format (organized into 60 palettes).

After obtaining the color palettes, the k-means clustering algorithm was applied for color quantization analysis. As an efficient and widely used method for color reduction, k-means clustering effectively simplifies and reduces the dimensionality of color data.

To facilitate cross-cultural color analysis, the 300 colors were categorized by market to construct four regional palettes and four color distribution axes (Figures 5-8). This approach enabled visual comparison of the most popular color schemes across different cultural markets, revealing similarities and differences in color choices for picture book covers under diverse cultural contexts. By integrating k-means clustering analysis with color psychology theories—such as ecological valence theory—a "cross-cultural color emotion quantification" framework was established. This framework provides a replicable research model for cross-cultural color-emotion design.

RESULTS AND DISCUSSION

This study conducted dominant color extraction and K-means clustering analysis on a total of 60 picture book cover samples from four cultural markets (Mainland China, Taiwan China, Japan, and the United Kingdom), yielding 300 colors and 60 color palettes. Based on the CMYK printing model and HSV color space, and further incorporating color emotion theory, we quantitatively compared the color preferences across these four cultural markets, ultimately constructing an "intercultural color emotion quantification" analytical framework.

Analysis of Dominant Color Clustering Results

Figures 5 to 8 present the color distributions and clustering results of the dominant colors on picture book covers from Mainland China, Japan, Taiwan (China), and the United Kingdom. Each regional palette consists of five cluster center colors, reflecting the most common color combinations in local design.

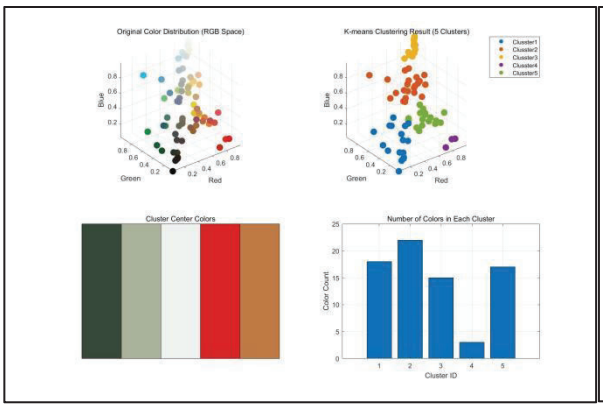

Figure 5. Mainland China samples

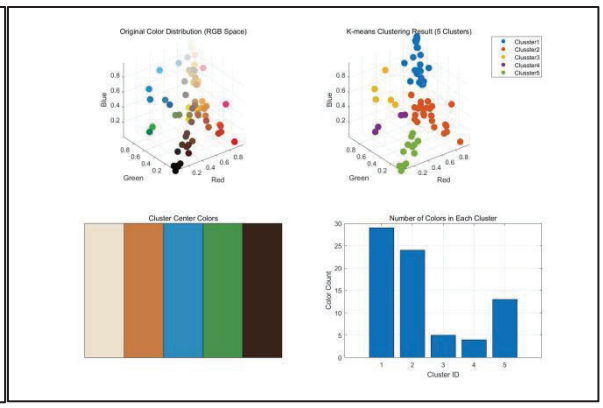

Figure 6. Japan samples

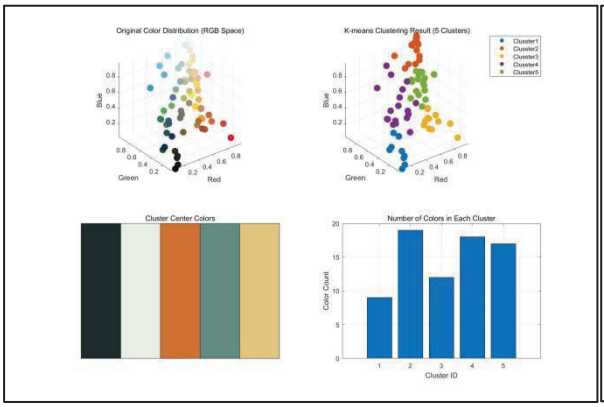

Figure 7. Taiwan, China samples

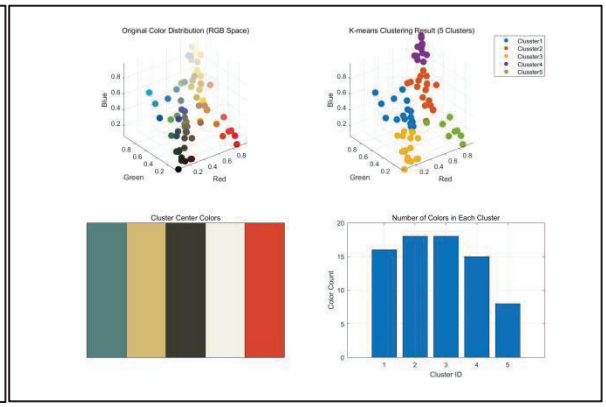

Figure 8. UK samples

In the Mainland China samples (Figure 5), the red cluster is most prominent, demonstrating a distinct prefere nce that differentiates it from other markets and aligns with traditional Chinese cultural inclinations toward festive colors. The remaining colors show the most uniform distribution among all regions.

The Japanese samples (Figure 6) are characterized by a significant proportion of cool tones (blue and green), with moderate saturation and low brightness, conveying a calm and restrained aesthetic consistent with "wabi-sab i" philosophy. Among dark colors, black is uniquely preferred, while light colors with low saturation and warm to nes with medium saturation are also favored.

The Taiwan (China) samples (Figure 7) exhibit an overall high brightness, frequently featuring light yellow a nd light blue, resulting in a soft and warm style. There is a clear preference for light colors with high brightness an d low saturation. The distribution across clusters is relatively balanced, with the white cluster comprising the large st proportion, showing a vertically concentrated distribution.

The UK samples (Figure 8) display strong color contrasts, often combining deep green, crimson, and bright y ellow. Saturation and brightness values span a wide range, reflecting a direct and vivid expressive style typical of Western culture. The clusters are concentrated both horizontally and vertically.

Comprehensive analysis reveals that all four markets share a common preference for colors with low brightn ess and low saturation, while also showing a consistent tendency toward using a larger proportion of light and pal e colors.

The Correlation between Color Emotion and Market Performance

Drawing upon color psychology theories (such as the ecological valence theory), this study finds that warm c olors (red, yellow, orange) are universally associated with positive emotions across cultures and are particularly fa vored in the Mainland China and UK markets. Cool colors (blue, green) dominate the Japanese market, aligning with the cultural emphasis on calmness and natural emotional experiences. The color usage in the Taiwan China r egion reflects a "neutralized" aesthetic—neither overly stimulating nor excessively subdued—consistent with the cultural values of inclusiveness and gentleness.

These findings confirm a significant correlation between color emotion and market performance, while also highlighting the need for designers to adapt color strategies according to the cultural background of target audienc es in cross-cultural markets.

CONCLUSION

This experiment primarily utilized Adobe Photoshop for color extraction and MATLAB for data analysis, e mploying K-means clustering to address the complex color schemes of book covers. The study revealed a univers al market preference for a greater proportion of light and muted colors. The Mainland China market showed a pref erence for color combinations associated with positive emotions and demonstrated the most balanced distribution of preferences across various color families. The Japanese market exhibited a cultural inclination towards calmnes s and restraint through its preference for cool color tones. The Taiwan China market favored soft color palettes, w hile the UK market preferred designs with strong color contrasts.

However, the study acknowledges certain limitations and areas requiring further validation. The limited sam ple size may be influenced by sales variations within the specific data collection period, and the selected covers m ay not fully represent all color design cases that could impact market performance across these regions. Future res earch will expand the sample size and systematically analyze color preferences in picture book covers across diffe rent cultural markets through the three dimensions of hue , saturation, and value.

REFERENCES

[1] Xu, W., Xu, H., & Guo, X. (2022). Modelling Design of Color Graphics Books Using Visual Vocabulary Based on Children's Color Language Preferences. *CMES-Computer Modeling in Engineering & Sciences*, 130(2).

[2] Shagal, S., Shagal, G., & Sharma, A. (2016). Visual merchandising: A key element in retail industry. *Management*, *2*, 115–120.

[3] Javed, S. A., & Javed, S. (2015). The impact of product’s packaging color on customers’ buying preferences under time pressure. *Market Branding Research*, *2*(1), 4.

[4] Singh, S. (2006). Impact of color on marketing. *Management Decision*, *44*(6), 783–789.

[5] Deng, L., Zhou, F., & Zhang, Z. (2022). Interactive genetic color matching design of cultural and creative products considering color image and visual aesthetics. *Heliyon*, 8(9).

[6] Attiah, D. Y., Cheung, V., Bromilow, D., & Westland, S. (2014, October). Colour planning in the interior design process. Paper presented at the Proceedings of the Second Conference of Asia Color Association, Seoul, South Korea. (pp. 187-191).

[7] hen, Y., Yu, L., Westland, S., & Cheung, V. (2021). Investigation of designers' colour selection process. *Color Research and Application*, *46*(3), 557–565.

[8] Abbott, M., Holland, R., Giacomin, J., Shackleton, J., & Management, B. (2009). Changing affective content in brand and product attributes. *Journal of Product & Brand Management*, *18*(1), 17–26.

[9] Rocchi, B., & Stefani, G. J. (2006). Consumers' perception of wine packaging: A case study. *International Journal of Wine Marketing*, *18*(1), 33–44.

[10] Bagchi, R., & Cheema, A. (2012). The effect of red background color on willingness-to-pay: The moderating role of selling mechanism. *Journal of Consumer Research*, *39*(5), 947–960.

[11] Schnurr, B., Brunner-Sperdin, A., & Stokburger-Sauer, N. E. (2017). The effect of context attractiveness on product attractiveness and product quality: The moderating role of product familiarity. *Marketing Letters*, *28*(2), 241–253.

[12] Palmer, S. E., & Schloss, K. B. (2010). An ecological valence theory of human color preference. *Proceedings ofthe National Academy of Sciences*, 107, 8877–8882. doi:10.1073/pnas.0906172107

[13] Taylor, C., Clifford, A., & Franklin, A. (2013). Color preferences are not universal. *Journal of Experimental Psychology: General*, 142(4), 1015.

[14] Schloss, K. B., & Palmer, S. E. (2023). Color Preference. In Encyclopedia of *Color Science and Technology* (pp. 456-462). Cham: Springer International Publishing.

[15] Zhang, Y., Liu, P., Han, B., Xiang, Y., & Li, L. (2019). Hue, chroma, and lightness preference in Chinese adults: Age and gender differences. *Color Research and Application*, *44*(6), 967–980.

[16] Wilms, L., & Oberfeld, D. (2018). Color and emotion: effects of hue, saturation, and brightness. *Psychological research*, 82(5), 896-914.

[17] Gao, X. P., Xin, J. H., Sato, T., Hansuebsai, A., Scalzo, M., Kajiwara, K., . . . & Billger, M. (2007). Analysis of cross-cultural color emotion. *Color Research & Application*, *32*(3), 223–229.

[18] Konker, C. S. (1985). Human color perception: An examination of biological and cultural aspects of affective responsiveness. In L. Miller (Ed.), *CreatingMeaning*. (pp. 22-28). Tacoma Park, MD: IVLA.

[19] Franklin, A., Bevis, L., Ling, Y., & Hurlbert, A. (2010). Biological components of colour preference in infancy. *Developmental Science*, *13*(2), 346–354.

[20] Bonn, T. L. (1982). Under cover: An illustrated history of American mass. *Penguin*.

[21] Bonnardel, V., Beniwal, S., Dubey, N., Pande, M., & Bimler, D. (2018). Gender difference in color preference across cultures: An archetypal pattern modulated by a female cultural stereotype. *Color Research and Application*, *43*(2), 209–223.

A Cost-Effective Method for Measuring and Simulating The Color Appearance of Transparent Plastic Samples

Yung-Chen Hsu and Pei-Li Sun*

National Taiwan University of Science and Technology, Taipei, Taiwan
**Corresponding author: plsun@mail.ntust.edu.tw*

ABSTRACT

Accurately assessing the color appearance of transparent plastic samples is essential in various industries such as packaging, coatings, and product design. However, conventional methods often rely on expensive measuring equipment or complex computational models, limiting their accessibility and scalability. This study proposes a cost-effective approach that uses webcam-based reflective color measurements to estimate both reflective and transmitted colorimetric data.

The proposed method consists of four main components: image acquisition, data extraction, model prediction, and visual simulation. In the image acquisition stage, the transparent sample is imaged against both black and white backings under a ring-shaped white LED light source. During data extraction, the ColorChecker patches placed beside the sample are automatically extracted to quantify and characterize the webcam's color response. Reflective and transmitted colorimetric measurements of two sets of plastic chips—transparent and opaque—are obtained using a spectrophotometer. Each plastic chip contains three thickness regions (1 mm, 2 mm, and 3 mm). Finally, a multi-layer perceptron (MLP) model is trained to predict these measurements. Two modeling approaches were investigated. In the Thickness-Independent Model, six image-derived XYZ values were used as input features, while the output targets were nine measured LAB values obtained under three background conditions (white, black, and white LED) across three sample thicknesses. In contrast, the Thickness-Dependent Model incorporated the sample thickness as an additional input feature, along with the six image-derived XYZ values extracted from 2 mm-thick samples. The output targets remained the same as in the Thickness-Independent Model, consisting of nine measured LAB values across the three lighting conditions and thicknesses. The experiment results indicate that the Thickness-Dependent Models preforms better.

To simulate the color appearance of the transparent objects in free 3D visualization platforms such as Web3D and Blender, a simple color rendering approach is introduced to improve color accuracy using basic rendering setup.

Keywords: color measurement, transparent plastics, image-based measurement, color appearance simulation, MLP regression, Blender rendering

INTRODUCTION

Transparent plastics are widely used in packaging, coating, and consumer products, where accurate color appearance is critical to visual quality and brand consistency. However, conventional methods [1,2] often rely on expensive measuring equipment or complex computational models, limiting their accessibility and scalability. Additionally, the time required for device setup and data acquisition remains a practical challenge, especially in workflows that prioritize efficiency and rapid iteration.

To acquire colorimetric data more affordably, this study utilizes a consumer-grade webcam operated via Python program developed ourselves to automate image capture of PANTONE plastic and opaque color samples under controlled lighting environment. Each sample was placed on a X-Rite ColorChecker Grayscale Card with a ColorChecker Mini chart for color characterization of the webcam. A circular light source at a 45-degree angle simulated the CIE 45a:0 measuring geometry [3] of the i1 Pro2 spectrophotometer.

Captured images were processed using OpenCV, with a modified SIFT algorithm [4] applied to identify the 24 color patches of the ColorChecker. The RGB values of six key points on a plastic sample were extracted to predict XYZ tristimulus values across three thickness levels and two background colors (black and white). Spectral radiance, measured under a uniform white LED panel with and without the plastic sample, was recorded using an X-Rite i1 Pro 2 spectrophotometer to estimate the sample's spectral transmittance. The resulting spectral transmittance data were then converted into transmitted CIELAB values under a D50 illuminant.

A multi-layer perceptron (MLP) regression model was employed to predict transmitted LAB values based on thickness and reflective XYZ values of the sample under black and white backgrounds, as estimated by the webcam. Both transmissive and opaque samples were modeled together to capture transmissive behavior by comparing XYZ values under the two backgrounds. When the values were approximately equal, the sample was classified as optically opaque.

Using 3D modeling software to simulate transparent plastic samples is useful. However, most rendering models do not support color transmittance settings. To reduce color errors in the simulation, this study proposes a method to determine diffuse RGB values and a single transmittance value for visualizing plastic samples.

METHODOLOGY

The overall framework of the proposed method is illustrated in Figure 1. It consists of four main components: image acquisition, data extraction, model prediction, and visual simulation. The details of each component are introduced in the following section.

Figure 1. Overview of the four-stage pipeline.

Image Acquisition

To facilitate accurate colorimetric measurement of transparent samples, a controlled photographic setup was constructed. A backing plate, composed of horizontally aligned white patch and black frame from the ColorChecker Gray Scale Card, was positioned beneath the transparent color sample. A ring-shaped white LED light source (D50, Ra=86) with a radius of 42 cm was mounted 21 cm above the samples to provide uniform and gloss-free illumination. A high-end 4K webcam was mounted at the center of the ring light, establishing a CIE 45a:0 measurement geometry relative to the color sample. To ensure accurate color characterization without interference from the webcam's auto-exposure and auto-white-balance features, a ColorChecker Mini chart was positioned adjacent to the transparent samples. In addition, a mirror was placed on the opposite side of the samples to allow the camera to capture surface gloss characteristics through reflected highlights. The color difference between the direct sample and its mirrored reflection, can be used to infer the approximate surface glossiness of the sample. Furthermore, the degree of blurring at the boundary between the black and white backgrounds serves as an indicator of the sample's scattering characteristics.

Data Extraction

To accurately detect the 24 color patches of the ColorChecker Mini for single-photo color characterization, the Scale-Invariant Feature Transform (SIFT) algorithm [4] was modified to extract feature points from each RGB channel individually. Matching feature points across the three color channels enhances the robustness of feature point matching between the ColorChecker reference template and the test image.

For each image, RGB values were quantitatively extracted from six predefined regions of interest (ROIs): three sample areas with nominal thicknesses of 1 mm, 2 mm, and 3 mm, and two background reference regions

corresponding to white and black. The RGB values were transformed into CIE XYZ tristimulus values under the D50 illuminant using second-order polynomial regression [5] to ensure device-independent color representation. The regression coefficient matrix was estimated by using BabelColor's averaged ColorChecker measurements (CIEXYZ with illuminant D50) as the training targets.

Figure 2. Left: Photographic setup. Right: Central region of the webcam-captured image. The six red points mark predefined regions of interest used for color extraction of an orange plastic sample.

Transmissive Colorimetric Measurement

To estimate the true transmissive colorimetric values (CIELAB under illuminant D50) from webcam-derived reflective measurements, a uniformly diffused white LED backlight was positioned beneath the plastic samples. Two comprehensive sets of PANTONE Plastics Selector Chips, varying in color, transparency, and thickness, were spectrally measured using the Emission-Reader mode of BabelColor PatchTool 7 in combination with an X-Rite i1 Pro2 spectrophotometer. The spectral transmittance of each plastic sample was determined by calculating the ratio of spectral radiances measured with the sample in place to those measured without the sample. The transmitted CIE XYZ and CIELAB values under the D50 illuminant were then derived by combining the sample's spectral transmittance with the spectral power distribution of the D50 illuminant.

The dataset comprised 628 transparent clips and 405 opaque clips. Each color chip measures 27 mm × 33 mm and is available in three thicknesses: 1 mm, 2 mm, and 3 mm. Transparent chips feature a glossy finish on both sides, while opaque chips have a glossy finish on the front and a matte finish on the reverse side.

Model for Predicting Colorimetric Values

A multi-layer perceptron (MLP) regression model was developed using the Scikit-learn machine learning library to predict the CIE LAB values of plastic samples under opaque white, black, and LED transmission conditions. The MLP architecture was chosen for its ability to capture nonlinear relationships between image-derived features and colorimetric measurements. Two modeling approaches were investigated:

- **Thickness-independent Model:** Input features consisted of six image-derived XYZ values, while the output targets included nine measured LAB values corresponding to three background conditions (white, black, and white LED) across three sample thicknesses.
- **Thickness-dependent model:** Input features included the sample thickness along with six image-derived XYZ values obtained from 2 mm-thick samples. The output targets were the same as in the thickness-independent model, i.e., nine measured LAB values across the three lighting conditions and thicknesses.

The model architecture comprised two hidden layers with 15 neurons each, using ReLU activation. The dataset consisted of N samples, split into training and validation sets using an 80/20 ratio. Training was conducted with the Adam optimizer and mean squared error (MSE) loss function.

Simulate the Color Appearance using Blender

Blender and Three.js are popular tools for VR simulation of 3D objects. Both provide a variety of built-in 3D rendering models with key parameters for color rendering, such as diffuse color, transmission, roughness, clearcoat, and refractive index. However, these tools do not support wavelength-dependent transmittance for simulating the color appearance of transparent objects. For example, a red transparent filter should exhibit high transmittance at long wavelengths and low transmittance at medium and short wavelengths. Most rendering models, however, apply a single uniform transmission value across all color channels, leading to inaccurate simulations of transparent colors, especially for highly saturated samples.

Consider a red filter: if the diffuse color is set to pure red, the filter should appear red when placed in front of white, yellow, or red opaque objects. Yet if transmission is set to 100% (maximum value of the RGB transmittance), the filter becomes invisible, and the background colors dominate. Conversely, if transmission is set to 0% (minimum value of the RGB transmittance), the background objects are completely obscured, making the filter behave like an opaque surface rather than a transparent one.

To break the limitation, we proposed a simple solution consisting of the following steps:

(1) Predict the transmitted and white-backing CIELAB values of the sample using the proposed webcam color characterization and MLP models.
(2) Convert the predicted D50 LAB values to the D65 sRGB color space.
(3) Perform 3D color rendering of the scene using the white-backing RGB as the diffuse component and the transmitted R as the transmission value; extract only the red channel from the rendering result.
(4) Perform 3D color rendering using the same white-backing RGB as the diffuse component and the transmitted G as the transmission value; extract only the green channel from the result.
(5) Perform 3D color rendering again with the white-backing RGB as the diffuse component and the transmitted B as the transmission value; extract only the blue channel from the result.
(6) Combine the red, green, and blue channels obtained in steps 3–5 to generate the final output image.

RESULTS AND DISCUSSION

The color accuracy of the proposed cost-effective method depends not only on the method itself, but also on the stability and characteristics (i.e., image enhancement) of the webcam, the accuracy of the color measuring instrument, and the limitations of the commonly used 3D rendering model. The section will report the performance of the single-photo color characterization of the webcam, the accuracy of the MLP model's colorimetric prediction, and an demonstration of 3D color simulation using Blender as an example.

Color Characterization of the Webcam

Image acquisition was performed using an AVerMedia PW515 4K webcam. The mean CIEDE2000 color differences [6] from the ColorChecker pattern in the photos were 1.76, 1.73, and 3.82 ΔE_{00} for the mean, median, and 95th percentile, respectively, averaged across images. These results are acceptable for color characterization of a webcam when using the 8-bit image format with auto exposure and auto white balance. It is worth noting that if the background lightness is too low (e.g., use a black platform), the ColorChecker and color samples may become overexposed, thereby reducing the accuracy of color characterization.

Model Performance

Table 1 summarizes the color accuracy of the MLP model predictions. Four models were trained, varying by approach (Thickness-Independent vs. Thickness-Dependent) and training set (transparent only vs. mixed with opaque samples). The results indicate that Thickness-Dependent Models outperformed Thickness-Independent Models. Between the two training sets, the "transparent only" set yielded better accuracy than the mixed set. However, the "transparent only" models cannot be used to predict the colorimetric values of opaque samples. In contrast, the mixed-sample models can predict opaque samples, though with reduced overall accuracy.

Table 1: Color accuracy of the MLP colorimetric prediction models (unit: ΔE_{00})

Modeling approach	Backing	Transparent samples only			Transparent and opaque samples		
		median	stdev.	95th perc.	median	stdev.	95th perc.
Thickness Independent	White	2.49	2.70	9.07	2.58	2.54	7.59
	Black	2.86	2.08	7.15	3.39	4.40	10.77
	White LED	2.35	2.47	7.91	2.64	3.70	11.51
Thickness Dependent	White	2.44	2.45	7.84	3.64	3.45	11.40
	Black	2.31	1.92	6.71	2.62	1.94	6.26
	White LED	1.26	1.55	3.54	2.35	2.79	7.40

Color Appearance Simulation

The left photo of Figure 3 shows three chips from the PANTONE Plastics Transparent Selector (T-505-1-3, T-505-1-5, and T-505-6-1), used for webcam-based transparent color estimation. Using the previously described Thickness-Dependent model, we estimated the LAB values of nine plastic patches with 3 different thicknesses and 3 different colors on white and LED backings. In Blender, the patches were rendered using the simplest Principled BSDF model. In the color rendering setting, since this model only provide a cross-channel transmission value for each color patch, we employed the method described in the previous section: the transmission LAB values estimated from the LED backing were converted into per-channel transmission rates in the sRGB color space. These per-channel transmission rates were then used to set the transmission values for each color patch. Finally, separate renderings were obtained for the R, G, and B channels, which were then combined to produce the image shown on the right in Figure 3. The simulation image demonstrates realistic transparent colors, showing a significant improvement over results obtained by assigning a single cross-channel transmission value to each color patch.

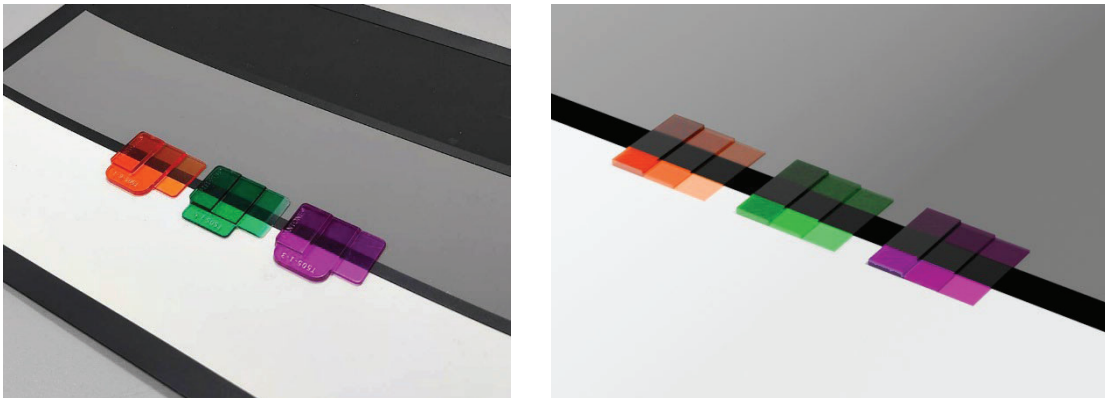

Figure 3. Left: Three transparent plastic chips with three different thicknesses (photography), and Right: Simulated color appearance using Blender with the proposed method.

CONCLUSION

The study introduces a cost-effective webcam-based method for assessing the color appearance of transparent plastics, offering an alternative to expensive equipment and complex models. The approach involves four stages: image acquisition (samples photographed against black and white backings with LED lighting), data extraction (using ColorChecker patches to calibrate the webcam's response), model prediction (training an MLP model with spectrophotometer-measured colorimetric data), and visual simulation (rendering in platforms like Blender). Two modeling approaches were tested: a Thickness-Independent Model (image-derived color inputs only) and a Thickness-Dependent Model (inputs plus sample thickness). Results showed the Thickness-Dependent Model provided superior predictions. For "transparent-only samples", the median errors were 2.44, 2.31 and 1.36 ΔE_{00} for predicting transparent colors with white, black and white LED backings. However, for "transparent and opaque samples", the errors increase significantly.

Finally, a simple rendering approach was introduced to improve the color accuracy of transparent objects in 3D visualization, using a basic rendering setup in Blender.

REFERENCES

[1] ASTM D 1003 (2003). *Standard test method for haze and luminous transmittance of transparent plastics*. West Conshohocken, PA: American Society for Testing and Materials.

[2] Gigilashvili, D. and homas, J. B. (2023). Chapter 14: Appearance beyond colour - Gloss and translucency perception, Fundamentals and applicaitons of color engineering, Green, P. editor, Wiley.

[3] CIE 15:2018. (2018). *Colorimetry*, 4th Edition, International Commission on Illumination.

[4] Szeliski, R. (2021). Chapter 7: Feature detection and matching, *Computer vision: Algorithms and applications*, Springer.

[5] Hong, G., Luo, M. R. and Rhodes, P. A. (2001). A study of digital camera colorimetric characterization based on polynomial modeling, *Color Research and Applications*, 26, 79-86.

[6] Luo, M. R., Gui, G. and Rhodes, P. A. (2001). The development of the CIE 2000 colour-difference formula: CIEDE2000, *Color Research and Applications*, 26, 340–350.

A Corpus-Linguistic Study of Context-Dependent Color Naming in Japanese

Hiromasa Mita[a*]

[a]*University of Tokyo, Tokyo, Japan*
[*]*mita-hiromasa299@g.ecc.u-tokyo.ac.jp / hiromasa.mita@gmail.com*

ABSTRACT

This study investigates how colors are communicated through language compositionally, focusing on Japanese simile-based constructions such as *NOUN noyoona iro* and *NOUN mitaina iro* (*NOUN-like color*). While previous research on color and language has concentrated mainly on lexicalized color terms, these compositional strategies also play an important role in everyday communication, where speakers often describe colors by reference to familiar objects rather than utilizing conventional vocabulary. To examine this phenomenon, a large-scale Japanese web corpus was analyzed with the concordance tool Sketch Engine, yielding 3,693 instances of the target patterns. These examples were then classified according to the conceptual properties of their Source nouns. The analysis revealed that simile-based expressions strongly favor shapeless Sources such as liquids and granular substances, in contrast to lexicalized color terms, which tend to be associated with shaped entities. Furthermore, nearly half of the shaped cases involved resemblance not only in color but also in shape, indicating that simile-based color naming frequently draws upon broader visual analogies. Taken together, these results point to systematic differences between simile-based and lexicalized color terms, and they suggest an aspect of the underlying principle by which speakers and writers extend the expressive resources of the language beyond the limits of the conventional lexicon.

Keywords: color naming, compositional vs. lexicalized expressions, simile, Japanese, corpus linguistics

INTRODUCTION

Research on the relationship between color and language has initially concentrated on so-called basic color terms, and over the past several decades, scholars in philology, anthropology, psychology, and linguistics have built up a substantial body of knowledge on these terms from multiple perspectives. Yet if we treat color naming as part of a community's cultural heritage, a focus on basic terms alone offers only a limited picture. Consequently, many studies have broadened their scope to include traditional or specialist naming systems, with the aim of documenting and analyzing the full range of color expressions that exist—or once existed—in a given language.

From the standpoint of natural language use and communication, however, important gaps remain. Most prior studies have focused on conventionalized, lexicalized items—terms that can be listed in dictionaries as nouns or adjectives. Moreover, as often pointed out, such terms have typically been examined in a decontextualized way, apart from the actual contexts in which they are used [1][2]. This raises the need to describe when, about what kinds of objects, and through what linguistic strategies speakers actually verbalize color. In everyday communication, unless speakers are specialists in color or color terminology, they often adopt more ad hoc and compositional strategies. Rather than relying on established names, they frequently describe a target's color by referring to familiar objects as reference points. Here, metaphor and simile play a central role. For example, speakers may describe colors with phrases such as *as red as a pomegranate, honey-colored*, or *like the color of sapphire*. In general, similes explicitly state a perceived similarity between two entities, consisting of the Target (the entity being described), the Source (the object used for comparison), and the Ground (the aspect of similarity). For instance, in the sentence *The*

lake reflected a jade-like color at sunset, the Target is the lake water, the Source is jade, and the Ground is color. This kind of expression is, of course, not limited to color: more broadly, linguistic strategies that describe perceptual properties through reference to concrete objects are discussed under notions such as image metaphor or source-based language, which have recently attracted growing attention in cognitive linguistics and psycholinguistics [3][4].

Against this background, the present study investigates how compositional color expressions are used in Japanese, drawing on corpus-linguistic methods. Specifically, it examines two simile-based constructions: *NOUN noyoona iro* and *NOUN mitaina iro* (literally, *NOUN-like color* in English), and addresses the following questions:

1.What kinds of entities tend to be selected as Sources in Japanese compositional color naming?

2. What principles or tendencies underlie the language users' choice of one Source over potential alternatives?

3. In what respects do these compositional expressions differ from conventional, lexicalized color terms?

Addressing such semantic and cognitive questions is still relatively challenging within corpus linguistics, a field that has often prioritized structural patterns. In this sense, the present study's contribution lies not only in its findings but also in the methodological perspective it introduces.

METHODOLOGY

Step 1. Data Preparation

Using the concordance function of Sketch Engine (http://www.sketchengine.eu), a corpus query tool, all instances matching the target patterns were retrieved together with their surrounding context from the Japanese web corpus jaTenTen11 (approximately 8 billion words). The searches were conducted using Corpus Query Language (CQL), specified as follows:

NOUN noyoona iro: [tag="N.*"][word="の"][word="よう"][word="な"][word="色"]

NOUN mitaina iro: [tag="N.*"][word="みたい"][word="な"][word="色"].

The *noyoona* type yielded 3,416 concordance lines, and the *mitaina* type yielded 2,218 lines. In the CQL queries above, the NOUN slot ([tag="N.*"]) specifies a single word; however, in actual data it may be preceded by additional modifier words, and the entire phrase can function as the Source. For this reason, all instances were manually examined in order to identify the Source correctly. It should also be noted that in cases such as *suika noyoona iro* (*watermelon-like color*), the description may refer either to the rind (green-and-black) or to the flesh (red) depending on which part of the object is foregrounded, or in semantic terms, which Active Zone is evoked in the context in question [5]. Speakers would not normally say *the-rind-of-a-watermelon-like color* nor *the-flesh-of-a-watermelon-like color*. In determining the Sources, the relevant Active Zone was always taken into account, and the omitted constituents were supplied on the basis of contextual cues.

Then the following patterns were excluded as noise:

1. Syntactic violations: cases where *NOUN noyoona* syntactically modifies something other than *iro*. For example, *oorora noyoona iro no henka* (*aurora-like color change*), where *aurora-like* modifies *henka* (*change*), not *iro* (*color*).
2. Semantic violations: cases where the expression figuratively describes emotions, sounds, or other non-color properties. For example, *kanasimi noyoona iro* (*sadness-like color*) meaning a sorrowful face.
3. Multiple Grounds: cases where the Ground involves more than color. For example, *choko noyoona iro to aji* (*chocolate-like* [*color and taste*]).

4. Color terms as Sources: cases where the Source is already a conventional color term. This applies both to basic color terms and to nouns used exclusively as color names (e.g. *neibii*, which means only navy blue in Japanese, not navy in the military sense).
5. Deictic or pronominal Sources: cases where the description depends on discourse participants and cannot be interpreted independently. For example, *anata no booshi noyoona iro* (*your hat-like color*).
6. Uninterpretable data: cases where the corpus line was malformed or too fragmentary to interpret.

After excluding such cases, 2,116 instances of the *noyoona* type and 1,577 instances of the *mitaina* type remained. The total dataset subjected to analysis therefore consisted of 3,693 examples.

Step 2. Shaped vs Shapeless Test

A rough observation of the data suggested that the Source often consisted of liquids or substances with similar properties. For instance, coffee and blood frequently appeared as Sources. To examine this tendency in detail, all 3,693 examples of the Sources were classified into two categories—*shaped entities* and *shapeless entities*—by means of a linguistic test. Here, a linguistic test refers to the procedure of using possible linguistic forms (whether attested or created) in a controlled context and judging, by introspection, whether they are grammatically or semantically acceptable. Such tests are widely employed in linguistic observation and argumentation to determine whether a given linguistic form exhibits certain properties.

The classification here builds on a well-known observation in linguistics: in English, the *count vs. mass* distinction is correlated with whether the referent is conceptualized as having a well-defined shape or boundary [6]. In Japanese, which essentially lacks grammatical countability, numeral classifiers (e.g., *chaku* for garment, *dai* for vehicle, *ri/nin* for person) are said to display a parallel behavior. Thus, the presence or absence of an appropriate classifier can serve as a diagnostic for whether an entity is conceived as having shape. In light of this, the following linguistic test was applied: if a Source noun can occur with an appropriate numeral classifier, the Source was classified as a shaped entity. If no suitable classifier exists, the Source was classified as shapeless. Note, however, that if attaching such a classifier yields an interpretation referring to containers of the object, processed products made of it, or subtypes rather than the object itself, the Source was treated as shapeless. To give some typical examples, in *kaeru noyoona iro* (*frog-like color*), the Source noun *kaeru* (*frog*) can be counted as *ippiki no kaeru* (*one* + classifier *hiki* + *frog*), and was therefore classified as shaped. In contrast, in *koohii noyoona iro* (*coffee-like color*), the noun *koohii* (coffee) cannot naturally occur with a classifier in the sense of a single unit. *Ikko no koohii* (*one* + classifier *ko* + *coffee*) would instead refer to one cup of coffee or one variety of coffee beans. Accordingly, the Source *koohii* (*coffee*) was classified as shapeless. In short, this principle parallels the distinction in English whereby *frog* is typically countable, whereas *coffee* is uncountable.

Step 3-1. Subclassification of Shapeless Sources

In Step 3, different procedures were applied to shapeless and shaped entities. Shapeless Sources were further subdivided into ten categories: Liquid, Gas, Mineral/Metal/Wood, Meat/Flesh, Light/Fire, Skin/Hair, Space (two-dimensional and three-dimensional), Fabric, Mass (e.g. powders and granules), and Others. This classification is not intended as an absolute or physically-defined taxonomy of physical reality, but rather as a heuristic scheme. Nevertheless, it partly overlaps with typical subgroups of uncountable (and thus shapeless) nouns in English and with classificatory schemes that have traditionally been employed in studies of color terminology. Most importantly, given the aim of this study, what matters is to capture the general tendencies in the choice of Sources; as long as the criteria are applied consistently, such a classification can be justified.

English translations of typical examples are presented below. In each case, the underlined portion corresponds to an instance of simile-based compositional color naming in the original Japanese text:

1. Liquid: *The rivers here look <u>the color of whisky</u>* (*uisukii noyoona iro*) *because the land is full of peat.*

2. Gas: *These colored varieties are thought to result from impurities or radiation damage to the crystal, such as yellow to brown citrine, smoky quartz* (*kemuri noyoona iro*), *and black morion*.

3. Mineral/Metal/Wood: *A lake with that leaden color* (*namari noyoona iro*) *really gives you a sense of nature.*

4. Meat/Flesh: *When I say red, I mean the color of raw meat* (*namaniku mitaina iro*).

5. Light/Fire: *Its moonlight-like hue* (*tsukinohikari noyoona iro*) *gives it an untouchable elegance.*

6. Skin/Hair: *The floor and walls were the color of a dead woman's skin* (*shinda onnano hada noyoona iro*).

7. Space: *The stage had a desert-like floor* (*sabaku noyoona iro*) *with a few stone-like objects, and a catwalk encircling it above.*

8. Fabric: *The kitten, the color of unbleached cloth* (*kinari noyoona iro*)*, was officially recorded as born at the end of September.*

9. Mass/Granules: *The honey has the color of brown sugar* (*kurozatoo noyoona iro*)*, with a unique flavor.*

Step 3-2. Subclassification of Shaped Sources

For shaped Sources, rather than classifying them into subcategories as in Step 3-1, a different procedure was applied to examine the relationship between the Source and the Target. This was motivated by the observation that in many instances classified as shaped Sources, the Source and the Target appeared to resemble each other not only in color but also in shape. In one case, for example, the simile *gurinpiisu noyoona iro* (*green pea-like color*) is used to describe the appearance of the eggs of a beetle species known as the Tarandus stag beetle. Here, the Target is the eggs of the beetle, and the Source is green peas. What is important here is that, although not explicitly stated, the beetle's eggs and green peas are comparable not only in color but also in shape and size. Indeed, if the Ground of the simile is changed from color to shape, producing a form such as *gurinpiisu noyoona katachi* (*green pea-like shape*), the comparison remains fully interpretable.

This observation suggests a possible linguistic test: replacing the Ground of the simile from color to shape makes it possible to determine whether the Target and Source resemble each other not only in color but also in shape. Based on this color-to-shape substitution test, each example was classified into one of three categories:

1. Resemblance in shape

2. No resemblance in shape

3. Indeterminate (cases where the Target could not be clearly identified)

Step 4 Sources in Color Term Dictionaries

Finally, how do these compositional color naming strategies differ from lexicalized color terms? To address this question, two color dictionaries intended for a general readership were examined [7][8]. From the entries in these dictionaries, the 279 object names appearing within color terms were classified according to the same criteria as in Step 2 and Step 3-1—that is, into shapeless versus shaped categories and, for shapeless entities, into the relevant subtypes. A previous pioneering study examined historical and traditional Japanese color terms using a specialized dictionary in order to identify the kinds of objects that serve as Sources [9]. However, the dictionaries used in the present study mainly include contemporary color terms including loanwords, and the classification scheme adopted here differs from that of the earlier study.

RESULTS AND DISCUSSION

Table 1 summarizes the distribution of Sources across the *noyoona* type, the *mitaina* type, and lexicalized color terms from the two dictionaries, classified into shaped and shapeless categories.

	NOUN noyoona iro		*NOUN mitaina iro*		Lexicalized terms	
Total	2116	100.00%	1577	100.00%	279	100.00%
Shapeless	1363	64.41%	876	55.55%	99	35.48%
Shaped	753	35.59%	701	44.45%	180	64.52%

Table 1. Distribution of shaped and shapeless Sources in simile-based and lexicalized expressions

First, the two compositional simile-based expressions show a predominance of shapeless Sources: 64.41% for *noyoona* and 55.55% for *mitaina*, whereas lexicalized color terms display the opposite pattern, with 64.52% shaped. This indicates a systematic difference: context-dependent compositional color naming tends to draw on substances without fixed boundaries, while lexicalized terms are linked to objects with stable shapes. Notably, *mitaina* contains a somewhat higher proportion of shaped Sources (44.45%) than *noyoona* (35.59%). A chi-square test confirmed that the group differences were highly significant ($\chi^2(2) = 97.06$, $p < 0.0001$), and standardized residuals showed that shapeless Sources were overrepresented in *noyoona*, while shaped Sources were strongly overrepresented in lexicalized terms.

Table 2 presents the subclassification of shapeless Sources into ten categories.

	NOUN noyoona iro		*NOUN mitaina iro*		Lexicalized terms	
Total	1363	100.00%	876	100.00%	99	100.00%
Liquid	673	49.38%	506	57.76%	32	32.32%
Gas	3	0.22%	3	0.34%	0	0.00%
Mineral+	165	12.11%	64	7.31%	35	35.35%
Meat+	19	1.39%	23	2.63%	2	2.02%
Light+	49	3.60%	17	1.94%	0	0.00%
Skin+	36	2.64%	27	3.08%	0	0.00%
Space	160	11.74%	47	5.37%	6	6.06%
Fabric	23	1.69%	4	0.46%	4	4.04%
Mass+	86	6.31%	51	5.82%	9	9.09%
Others	149	10.93%	134	15.30%	11	11.11%

Table 2. Subclassification of shapeless Sources in simile-based and lexicalized expressions

Liquids were the dominant category among shapeless Sources: 49.38% of *noyoona* and 57.76% of *mitaina*. By contrast, lexicalized terms relied less on liquids (32.32%) but heavily on mineral/metal/wood (35.35%). Space-related items were relatively frequent in *noyoona* (11.74%), while categories such as light, skin, and meat appeared only in simile-based forms and were virtually absent from lexicalized terms. The chi-square test showed highly significant differences ($\chi^2(18) = 141.31$, $p < .0001$). Standardized residuals indicated that liquids were overrepresented in *mitaina*, while minerals were strongly overrepresented in lexicalized terms. In addition, space-related items were frequent in *noyoona*, and fabric terms were somewhat overrepresented in lexicalized terms.

Why, then, do compositional color expressions so often draw on shapeless Sources, particularly liquids? One possible explanation is that such substances, by their very physical nature, tend to display visually homogeneous colors and can expand or contract freely. In this sense, they function as a kind of "convenient paint," readily lending themselves to use as reference points for ad hoc color descriptions.

Turning to the shaped Sources, Table 3 presents the distribution of shape similarity between Source and Target.

	NOUN noyoona iro		*NOUN mitaina iro*	
Total	753	100.00%	701	100.00%
Resemblance in shape	330	43.82%	325	46.36%
No resemblance in shape	378	50.20%	325	46.36%
Indeterminate	45	5.98%	51	7.28%

Table 3. Distribution of shape similarity between Source and Target

As Table 3 shows, nearly half of the examples in both *noyoona* (43.82%) and *mitaina* (46.36%) involve Sources that resemble the Target not only in color but also in shape. This indicates that simile-based color expressions often rely on a broader perceptual similarity than color alone. Rather than being confined to hue, the choice of Source is frequently influenced by shape resemblance as well.

CONCLUSION

This study has demonstrated that Japanese simile-based color expressions differ systematically from lexicalized color terms. Whereas simile-based forms favor shapeless Sources such as liquids, lexicalized terms are more often associated with shaped objects. In addition, nearly half of the shaped cases involved resemblance not only in color but also in shape. Taken together, these findings suggest that visual homogeneity in shapeless entities and combined color–shape similarity in shaped entities play a key role in how colors are conceptualized and expressed in actual contexts.

This study also has clear limitations. The results presented here capture only overall tendencies in context-dependent color naming, and in actual communication speakers' choices are undoubtedly shaped by a wider range of contextual and individual factors. Moreover, the analysis inevitably relied heavily on the researcher's interpretation of corpus data. Nevertheless, designing and proposing a framework for classifying such expressions is itself an important aim of this study, and future work should complement this approach with methods such as questionnaires to ensure greater objectivity.

REFERENCES

[1]. Lucy, J. A. (1997). The linguistics of 'color.' In C. Hardin & L. Maffi (Eds.), *Color categories in thought and language* (pp. 320–346). Cambridge University Press.

[2]. Biggam, C. P. (2012). *The semantics of colour: A historical approach*. Cambridge University Press.

[3]. Kövecses, Z. (2010). *Metaphor: A practical introduction.* Oxford University Press.

[4]. Winter, B. (2019). *Sensory linguistics: Language, perception and metaphor*. John Benjamins.

[5]. Langacker, R. W. (1990). *Concept, image, and symbol: The cognitive basis of grammar*. Walter de Gruyter.

[6]. Murphy, M. L. (2010). *Lexical meaning*. Cambridge University Press

[7]. Arai M. (2018). *Iro no jiten* (A dictionary of colors). Raicho-Sya.

[8]. Nagasawa Y. (2020). *Chiisana iro no hon* (The little book of colors). Liberal-Sha.

[9]. Toratani, K. (2023). Metonymy in the nomenclature of Japanese traditional colors. *Cognitive linguistic studies*, 10(1), 57–84.

An Investigation about The Influence of Color Contrast on Binocular Fusion

Chia-Chun Liu[a*], Vincent C. Sun[b], Ming-Chuan Fu[a]

[a]*Department of Visual Communication Design, National Taiwan University of Art, Taipei, Taiwan*
[b]*Department of Mass Communication, Chinese Culture University, Taipei, Taiwan*
**Corresponding author: sealfamily0299@gmail.com*

ABSTRACT

Binocular vision, arising from retinal disparity, is essential for accurately perceiving depth and spatial relationships. In recent years, virtual reality (VR) technologies have rapidly expanded globally and continue to grow in popularity among consumers. This study aims to determine the minimum retinal disparities required for effective depth perception and further enhance individual user experiences within virtual environments. Additionally, the study explores whether color contrast significantly affects depth perception and the overall visual experience. In the experiment, participants viewed pairs of line cube patterns simultaneously displayed on a monitor, with each image intended separately for the left and right eyes. A haploscope was employed to ensure proper visual separation and binocular fusion, guiding each participant to direct the left image to their left eye and the right image to their right eye. The study included two experimental conditions: one with a white background featuring black-lined cubes and another with a black background featuring white-lined cubes. Each condition comprised 11 image pairs with varying levels of retinal disparity. Participants with normal or corrected-to-normal vision were recruited for the study. During the experiment, each participant was instructed to observe the stimuli and select one cube from four positioned at the top, bottom, left, and right that appeared visually distinct. Stereo depth thresholds derived from retinal disparities were calculated based on accuracy rates from a four-alternative forced-choice (4AFC) task. The effect of color contrast was analyzed by comparing detection thresholds across the two background conditions. Statistical analyses of the collected data were conducted to determine if contrast significantly influences sensitivity to visual disparity. The outcomes of this research may aid in developing enhanced VR content and user interface designs, optimizing depth cues, and improving user comfort and immersion within virtual environments.

Keywords: Binocular, Stereoscope, Virtual Reality, Visual Psychology

INTRODUCTION

Vision, as one of the most essential human senses, enables humans to interact with a physical world composed of three-dimensional spaces and objects. Consequently, binocular vision plays a vital role in perceiving depth, judging distance, and maintaining spatial orientation in everyday life. In binocular vision, the left and right eyes receive slightly different images of the same object. This occurs because, when fixating on a point, we turn or converge the optical axes, resulting in non-identical projections of the object onto the two retinas (Brewster, 1856/2023). When a distant point falls on different retinal locations of the two eyes, it is still perceived as the same point. This phenomenon of combining the two images into one is called fusion (Hershenson, 1998). These differences form the basis of binocular disparity, which enables depth perception. From the stereoscopic photographs of the 19th century to today's virtual reality (VR) technologies, the underlying principle has consistently relied on visual disparity, a primary cue that enables binocular vision and depth perception. These foundations make the study of binocular vision not only crucial for understanding basic human perception but also highly relevant for applications in emerging digital environments.

Most relevant research has focused on distance, shape, and size (Brenner & van Damme, 1999), as well as on motion parallax (Hartle & Wilcox, 2021; Brenner & Landy, 1999), while comparatively fewer studies have investigated variations in visual disparity and the role of color contrast. Yet, visual disparity is the primary cue that drives stereoscopic depth perception, determining both its clarity and salience. Importantly, depth perception is not solely determined by disparity; it can also be modulated by visual attributes such as color contrast. With advances in technology, from the stereoscope of the 19th century to contemporary virtual reality (VR) systems, disparity-driven depth perception—particularly as influenced by color contrast—has become increasingly critical in shaping viewers' cognitive and perceptual experiences.

The purpose of this research is to determine the minimum retinal disparities required for reliable stereoscopic depth perception and to examine how color contrast modulates this perception. Specifically, the study aims to (a) establish stereoacuity thresholds based on disparity, (b) assess the influence of color contrast on these thresholds, and (c) discuss the implications of these findings for optimizing depth cues in virtual reality (VR) environments.

METHODOLOGY

Five participants with normal or corrected-to-normal vision were recruited. None reported a history of visual disorders. All participants signed informed consent forms prior to the experiment. Stimuli were presented on an ROG Strix XG49WCR LCD display (5120 × 1440 pixels, 165 Hz refresh rate). Participants viewed the display through a stereoscope at a distance of 1.1M, with head position stabilized by a chin rest (Figure 1). The experiment was programmed and controlled using SuperLab (Cedrus Corporation).

The experiment consisted of two contrast conditions: (1) white background with black-lined cubes (Figure 2), and (2) black background with white-lined cubes (Figure 2). For each condition, 15 stereoscopic stimuli were generated using Cinema 4D (C4D) software by simulating two virtual cameras aligned to replicate the positions of the left and right eyes. Binocular disparity was defined in pixel units on the display, with each pixel corresponding to 0.01213° of arc. The 15 disparity levels were 0, 0.01213, 0.02426, 0.03639, 0.04852, 0.06065, 0.08491, 0.10917, 0.13343, 0.15769, 0.18195, 0.20621, 0.2426, 0.25473, and 0.29112 degrees of arc.

Prior to the main experiment, participants completed a visual calibration procedure. The calibration image consisted of concentric circles formed by orange and blue lines, superimposed with a red–green cross (Figure 3), to ensure proper fusion through the stereoscope and eliminate potential double images. Following calibration, instructions were displayed to inform participants about the purpose of the experiment and the required response procedure. After receiving the instructions, participants completed a set of practice trials to familiarize themselves with the experimental task, after which they proceeded to the main experiment (Figure 4).

Each trial began with a countdown sequence displaying the numbers "2" and "1" for one second each, followed by a central fixation point and the presentation of the stereoscopic stimuli. After the stimulus display, a noise mask was shown for 1000 ms to eliminate potential afterimages(Figure 5). In each trial, four cubes were presented simultaneously around the fixation point, one in each of the four cardinal positions (above, below, left, and right), with each cube located 65 mm from the fixation point. A 4AFC paradigm was employed, in which only one cube contained the target disparity while the others served as distractors. The stimuli remained visible until participants responded or until 15 seconds had elapsed, at which point the trial was automatically terminated. Participants were instructed to respond within 10 seconds; if they were unable to detect the target disparity, they were still required to make a forced choice among the four alternatives. Responses were collected using a response box, where participants pressed the key corresponding (Figure 6) to the cube that appeared visually different from the others.

Each of the 15 disparity levels was tested with the target appearing equally often in the upper, lower, left, and right positions, yielding 15 × 4 unique stimulus configurations. These configurations were presented three times in randomized order. The two stereoscopic conditions were tested in separate experimental sessions, scheduled at least

one day apart to minimize fatigue and carryover effects. The entire experiment was conducted in a darkened room to eliminate external light interference and ensure consistent visual conditions.

Accuracy data were analyzed by fitting psychometric functions to the proportion of correct responses at each disparity level. A logistic function was used to fit the relationship between retinal disparity and performance. For the 4AFC task, the threshold was defined as the disparity level corresponding to 62.5% correct (i.e., midway between chance level at 25% and perfect performance at 100%). Thresholds were estimated separately for each participant and experimental condition, and then compared at the group level between the two contrast conditions (white background with black-lined cubes vs. black background with white-lined cubes).

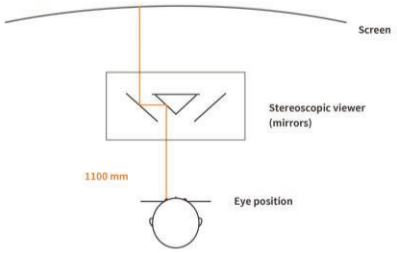

Figure 1: Schematic illustration of the apparatus and viewing distance used in the experiment.

Figure 2: Stereoscopic stimuli: white background with black-lined cubes (left); black background with white-lined cubes (right).

Figure 3: Stereoscopic stimulus: black background with white-lined cubes.

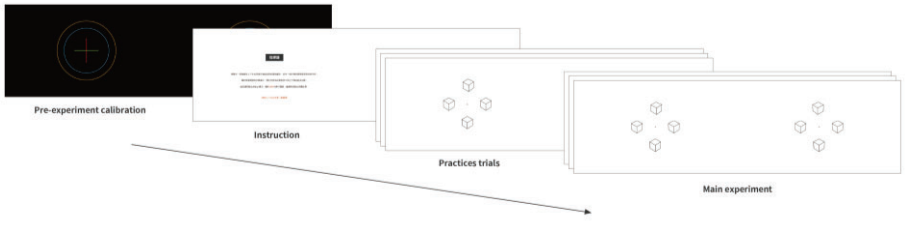

Figure 4: Flowchart illustrating the experimental procedure.

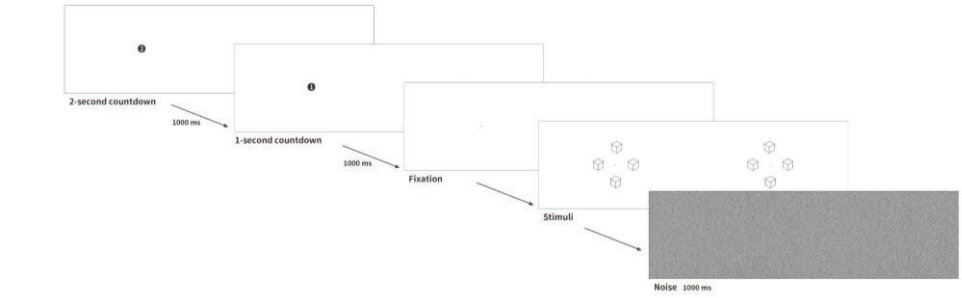

Figure 5: Trial sequence of the experiment.

Figure 6: Illustration of the correspondence between the stimuli and the response box positions.

RESULTS AND DISCUSSION

Data collected from each participant were fitted with a psychometric function logistic under the two contrast conditions, and thresholds for detecting the stereoscopic stimuli were estimated from the fittings. For Participant A, the estimated thresholds were approximately 0.027° in the white-background condition and 0.017° in the black-background condition (Figure 7). For Participant B, thresholds were 0.011° and 0.012° for the white- and black-background conditions, respectively (Figure 7). For Participant C, thresholds were 0.024° and 0.048° under the white- and black-background conditions, respectively (Figure 7). For Participant D, thresholds were 0.022° and 0.020° for the white- and black-background conditions, respectively (Figure 7). For Participant E, thresholds were 0.024° and 0.011° in the white- and black-background conditions, respectively (Figure 7).

In conclusion, this study demonstrated that binocular disparity thresholds vary not only across individuals but are also influenced by the color-contrast conditions of the stereoscopic stimuli. Although individual thresholds differed, accuracy consistently increased as disparity ranged from 0° to 0.29°. Some participants exhibited lower thresholds under the white-background condition, whereas others showed greater sensitivity with black-background stimuli (Table 1). These findings highlight that both disparity and color contrast are critical factors shaping stereoscopic vision, and they provide valuable implications for optimizing stereoscopic design in contemporary virtual reality applications. Future work may benefit from increasing the number of participants and incorporating sufficient pre-experiment practice to enhance the robustness of the findings.

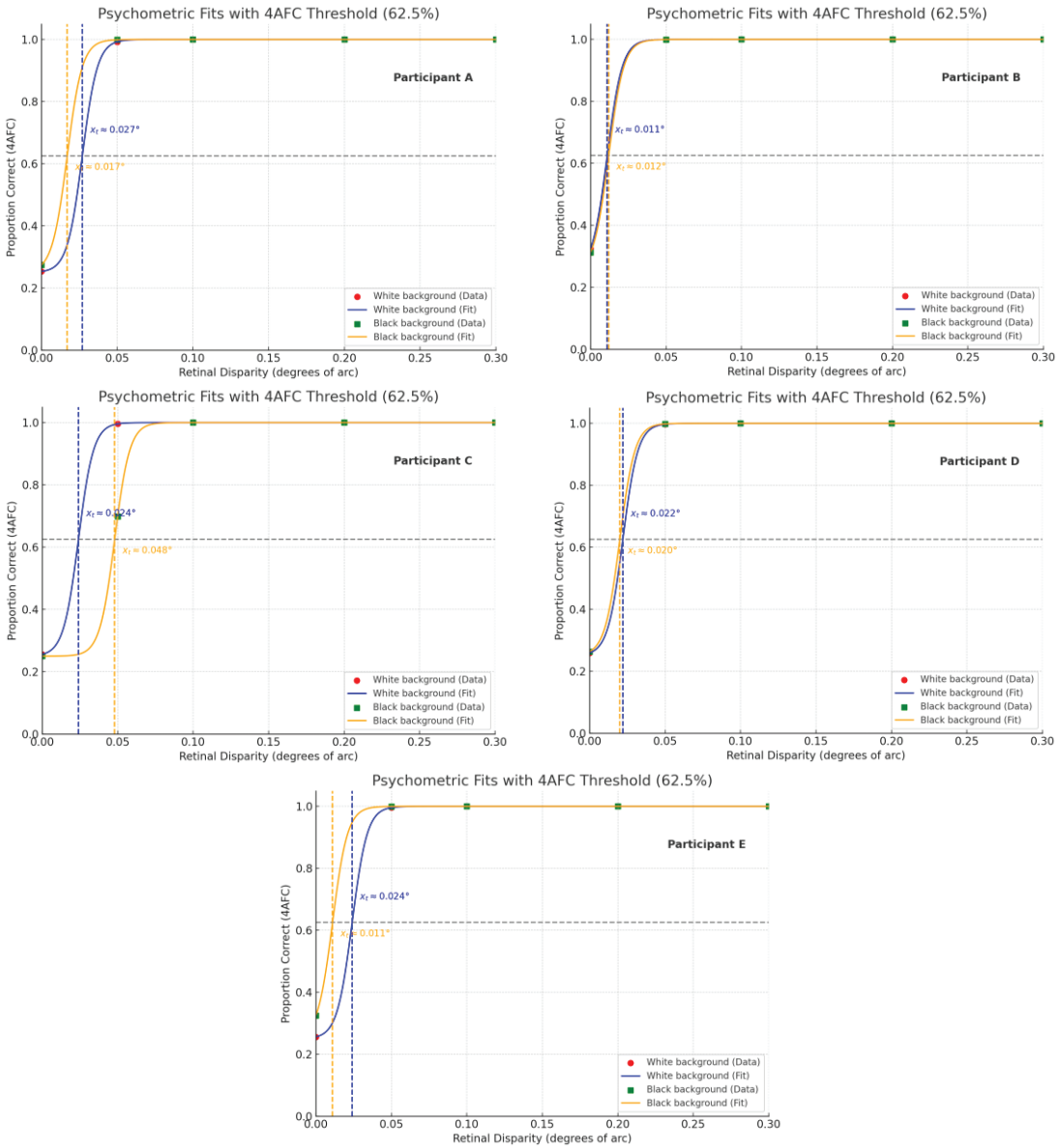

Figure 7: Logistic function fits for the five participants. The top row shows Participants A and B, the middle row shows Participants C and D, and the bottom row shows Participant E. Blue curves represent the white-background condition, and orange curves represent the black-background condition. The dashed line indicates the 62.5% threshold for the 4AFC task.

Table 1: The disparity threshold in each condition (degrees of arc)

	White-background condition	Black-background condition
Participant A	.027	.017
Participant B	.011	.012
Participant C	.024	.048

Participant D	.022	.020
Participant E	.024	.011

CONCLUSION

In conclusion, the present study demonstrated that binocular disparity thresholds are influenced both by individual variability and by the contrast polarity of stereoscopic stimuli. Although accuracy consistently increased with greater disparities, participants differed in whether they showed lower thresholds under white-background or black-background conditions. These findings suggest that both disparity magnitude and contrast polarity are critical in shaping binocular fusion. Beyond providing insight into fundamental aspects of stereoscopic vision, the results carry implications for the optimization of stereoscopic displays in contemporary virtual reality applications. Future research with larger samples and extended training may further validate and refine these observations.

REFERENCES

[1]. Brewster, D. (1856/2023). *The stereoscope: Its history, theory, and construction, with its application to the fine and useful arts and to education*. London: John Murray.

[2]. Hershenson, M. (1998). *Visual space perception*. Cambridge, MA: MIT Press.

[3]. Brenner, E., & van Damme, W. J. M. (1999). Perceived distance, shape and size. *Vision Research*, 39(5), 975–986. https://doi.org/10.1016/S0042-6989(98)00162-X

[4]. Hartle, B., & Wilcox, L. M. (2021). Cue vetoing in depth estimation: Physical and virtual stimuli. *Vision Research*, 188, 51–64. https://doi.org/10.1016/j.visres.2021.07.003

Individual Cone Spectral Sensitivities and Colour Matching Functions

Andrew Stockman[a], Ming Ronnier Luo[b], Siyuan Song[b], Keyu Shi[b], Andrew Rider[a]

[a] UCL Institute of Opthalmology, [b] Zhejiang University

ABSTRACT

Cone spectral sensitivities (CSSs) and their linear transforms, the colour matching functions (CMFs), vary between observers because of individual differences. These differences, which can be substantial, arise because of shifts in the spectral positions of the L- and M-cone photopigments, and differences in the optical densities of the macular pigment, lens pigment and the three cone photopigments. Consequently, people often see colors reproduced by projectors, displays and on printed or dyed material as different, even though according to colour standards such as CIE 1931 they should appear the same. Such disagreements are known as failures of observer metamerism and are becoming a more pressing concern with the development of displays with narrowband primary lights (e.g., Mini-LED, QD-OLED) that accentuate the effects of individual differences.

One way of correcting failures in observer metamerisms is to use individual CSSs or CMFs rather than mean or standard functions. To that end, we, in collaboration with Thouslite, have developed an LED-based visual trichromator, called LEDMax. This trichromator presents two half-fields to the observer, each illuminated by a multispectral light made up of 18 LEDs of different wavelengths from 400 to 700 nm. One half-field is illuminated by LEDs that combine to produce a fixed white standard light, and the other is illuminated by a series of triplets of lights of different wavelengths. For each triplet, the observer's task was to adjust the three lights to match the white. Both 2° and 10° fields of view (FOV) were used. The spectral power distribution (SPD) of each match was measured. Grassmann's laws mean that excitations in the three cone types should be the same for all matched triplets, since they all appear identical. Thus, we can use the measured SPDs and a model of how cone spectral sensitivities vary between individuals to estimate the individual cone spectral sensitivities for each observer. The model we used was the CIE 2006 LMS standard defined by Stockman & Sharpe (2000) and reformatted as continuous functions of wavelength by Stockman & Rider (2023).

So far, we have obtained estimates of the eleven parameters that vary between individuals (the L- and M-cone spectral shifts, 2° and 10° macular density, lens density and 2° and 10° L-, M- and S-cone photopigment optical densities) from the colour matches of 120 colour normal observers of varying age. The individual differences that we find are consistent with the CIE 2006 observer except for small shifts in the M- and L-cone photopigments and a slightly denser 2° macular pigment density, and as expected changes in lens density with age. We are continuing this work and now measuring CSSs in 30+ red-green colour vision deficient observers and comparing their CSSs with standard tests for colour vision deficiency. The results are promising and consistently distinguish between protanopes and deuteranopes. In addition, we are refining our methods. The initial analysis was based on color matches made between the white standard and 11 triplets for both 2° and 10° FOVs that each differed by one LED from a standard triplet (of 445, 530 and 445 nm). First, thanks to an upgrade of LEDMax, we have added 405 and 415 nm LEDs to the sequence of triplets, which allows a better definition of the lens and macular densities. Second, we have analyzed the effects of varying the 11 parameters on the matches for all possible matching triplets, and selected those that best define each parameter. This has enabled us to reduce the number of matches required and thus the time to reliably estimate the individual CSS.

Our research enables the estimation and generation of CSSs and CMFs for individual normal and colour deficient human observers, thus allowing display devices and colour reproduction to be individually optimized.

Keywords:Cone spectral sensitivities, Colour matching functions, Individual differences, Observer metamerism failures

Perception−Language Conflict in Color Vision Minorities: A Study of Miscommunication in Naming and Color Term Usage in Japan and China

Meiyan Lei[a*], Tsukasa Muraya[b], Shoji Sunaga[c]

[a]*Graduate School of Design, Kyushu University, Japan*
[b]*Faculty of Contemporary Social Studies, Chikushi Jogakuen University, Japan*
[c]*Faculty of Design, Kyushu University, Japan*
[*]*Corresponding author: lei.meiyan.878@s.kyushu-u.ac.jp*

ABSTRACT

This study aims to elucidate how conflicts between perception and language emerge within the linguistic environment surrounding individuals with color vision diversity, by comparing the situations in Japan and China with respect to terminology and the use of color terms. Specifically, the analysis focuses on the actual use and perception of terminology referring to color vision minorities, as well as on the relationship between color term usage and the color perception of these individuals. Through this research, I aim to clarify the structure of miscommunication that arises from discrepancies between perception and language within the linguistic environment of individuals with minority characteristics of color vision (color vision deficiency). Furthermore, by examining issues of terminology and color naming within a unified framework, the study explores the potential of linguistic approaches to improve the linguistic environment for color vision minorities. In addition, by conducting a Sino-Japanese comparison, the research aims to reveal how language influences perceptions of color vision minorities, thereby contributing to broader discussions on the acceptance of color vision diversity and addressing the question of whether “new terminology” or “distinctive color terms” are necessary.

Keywords: Color Vision Minority, Naming Conventions, Color Terminology

INTRODUCTION

Since the discovery of color blindness, both the phenomenon itself and the appropriate terminology for referring to individuals with this color vision characteristic have been a constant subject of scholarly debate. In the nineteenth-century English-speaking world, various terms were proposed, some of which were regarded as problematic; ultimately, however, the term “colour blindness” became established within the academic community. This constitutes the origin of the Japanese term 色盲(*shiokimo in Japanese, sèmáng in Chinese*) corresponding to “colour blindness.” In China, with the advent of the modern era, ophthalmological terminology from Japanese entered the Chinese language under the influence of the Ishihara test charts invented by Shinobu Ishihara. It is considered that the term 色盲 was among those introduced in this process.

However, these terms cannot be said to reflect the actual perceptual characteristics accurately. The term 色盲 contains the meaning of “blindness,” yet in reality, individuals with this condition are not entirely unable to perceive colors. Similarly, the terms 色覚異常(*shikikaku-ijyo in Japanese*, color vision abnormality in literal translation) and 色覚障害(*shikikaku-shogai in Japanese*, color vision disorder in literal translation) describe the characteristics of a minority whose way of seeing colors is simply different, by framing them as 異常 or 障害. Thus, their appropriateness remains open to debate. Even among specialists, although the problematic aspects of

such terminology are recognized, the conventional terms are still frequently employed out of intuitive habit. In everyday communication as well, there are cases where these terms are deliberately used. Against this backdrop, the question arises as to whether distinctive terminology is necessary.

Furthermore, in color communication, even when the same color terms are used, the actual colors perceived differ between trichromats and individuals with color vision deficiency. Attention should be paid to the fact that people with color vision diversity possess their own "color dictionaries," recognizing colors through sensitivity and imagination. This study examines how perceptual differences influence miscommunication in the use of color terms and discusses whether distinctive color terms are necessary.

From a linguistic perspective, there exists the hypothesis that language draws boundaries upon the world, and how these boundaries are drawn differ across languages. That human thought is shaped by the particular segmentation of the world encoded in one's language—the Sapir–Whorf hypothesis. Viewed from this hypothesis in relation to color vision and language, one may propose that the use of language, such as terminology for referring to color vision minorities and the use of color terms, influences our perceptions of color vision minorities. In other words, the miscommunication that arises in color communication with color vision minorities can be described, at a hypothetical level, as a structure originating in the linguistic environment.

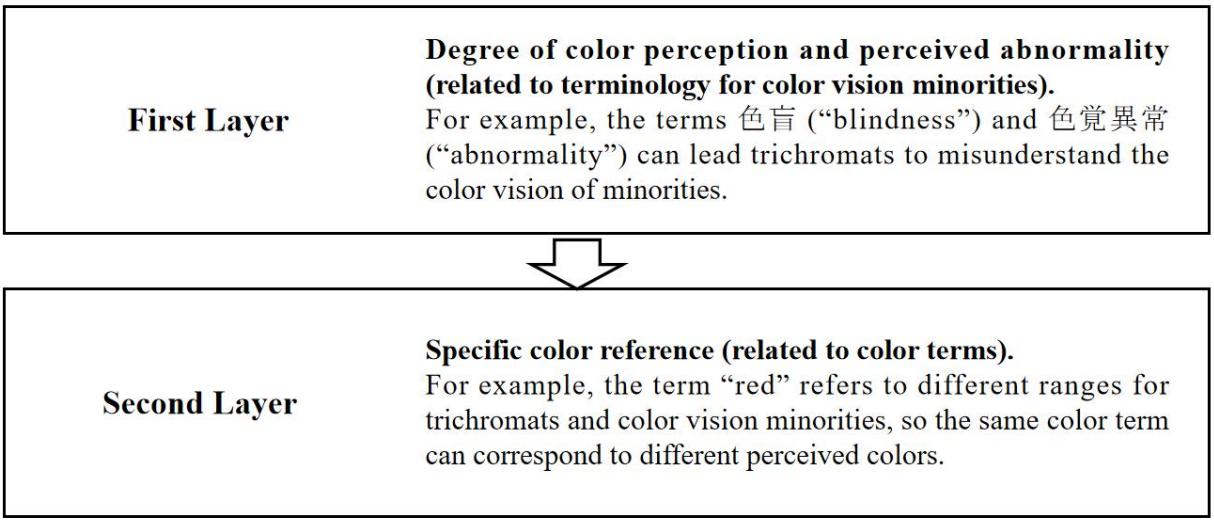

Figure 1: The Structure of Miscommunication with Color Vision Minorities in Color Communication

METHODOLOGY

Regarding the investigation of terminology use, in light of recent reconsiderations of terminology, this study first analyzed Japanese and Chinese linguistic data to understand the current use of terms in both written and spoken language. In addition, questionnaires were conducted targeting both the general public and specialists to examine awareness of and tendencies in the use of terminology. Furthermore, an image survey was carried out to clarify impressions and associations with each term. On the other hand, the discussion on the use of color terms focused on theoretical considerations, based on analyses of existing studies and the experiences of individuals with color vision deficiency.

RESULTS AND DISCUSSION

First Layer： Terminology Surrounding Color Vision Minorities

In Japan, a reconsideration of terminology occurred around the 2010s. Accordingly, this study first examines the frequency of term usage from two perspectives−written and spoken language since 2010, and the viewpoints of both specialists (e.g., medical doctors, color researchers, art teachers, and school nurses) and the general public−to identify the terms actually in use. For written language, sources such as Google Trends, newspaper databases (Yomiuri, Asahi, Mainichi), and academic papers were investigated. For spoken language, questionnaires targeting both the general public and specialists were conducted to examine usage trends. The results of these investigations are presented below.

Results of the Investigation on Written Language

Table 1: Results of the Investigation on Written Language

Genre	Japanese	Chinese
Outside of academic publications	among the general public, the term 色盲 appears most frequently. In the newspaper industry, however, the frequency of 色盲 has decreased significantly, and usage patterns vary among different newspapers. Overall, based on frequency of occurrence, the terms rank as follows: 色覚障害, 色弱, 色覚異常, and 色盲.	The term 色盲 appears most frequently, and the frequency of each term ranks as follows: 色盲, 色弱, 色覚異常, and 色覚障碍.
Academic publications	The term 色覚異常 appears most frequently, followed by 色弱 and 色覚障害; in addition, the use of new terminology can also be observed.	The term 色盲 has gradually decreased in frequency, while 色覚異常 has become mainstream in its place. Overall, a tendency is observed in which the terms most frequently occurring appear in the following order: 色覚異常, 色盲, and 色覚障碍.

Results of the Investigation on Spoken Language

In a workshop titled “What color is this paint?” held on June 15, 2024, as part of the 12th Kyushu University Open Campus “Experience of Wonders in Design” at the Faculty of Design, Kyushu University, questionnaires were distributed to Japanese participants, yielding 18 valid responses. And in May 2025, a questionnaire was distributed via a dedicated online survey platform to a general pool of Chinese respondents, yielding 18 valid responses. The aggregated results of these responses were shown in Figure 1.

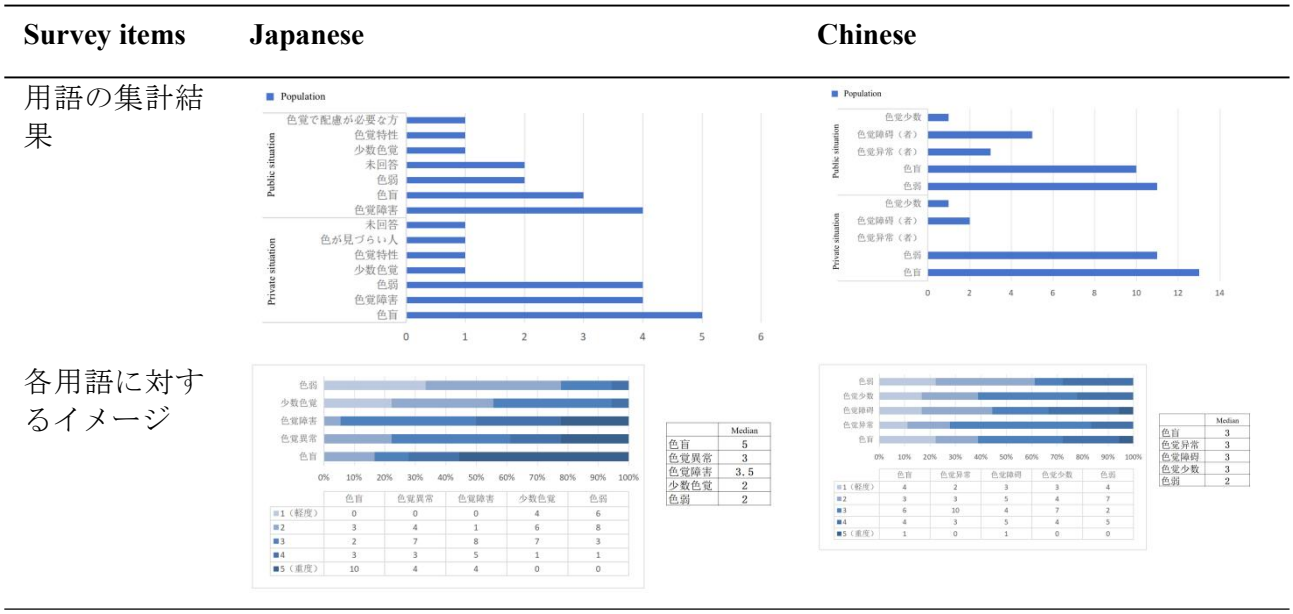

Figure 1 : Results of the Questionnaire on Spoken Language

Analysis

According to the results, with respect to Japanese, the term 色盲 is the most frequently used overall. However, in public conversations and written texts, the terms 色覚異常 and 色覚障害 are used more frequently than 色盲. Among all the terms, 色盲 is perceived most negatively. By contrast, in Chinese, the results indicate that 色盲 is the most frequently used term overall, and the differences in perception across terms are relatively small. This is likely due to differences in the semantic range of the character 盲 in Japanese and Chinese.

To examine its traditional meaning, dictionaries published prior to the 2010 reconsideration of terminology were consulted. In the *Nihon Kokugo Daijiten*, the meaning of 盲(*mou*) is given as "being unable to see" or "lacking the ability to discern the essence of things." In contrast, in the *Xiandai Hanyu Cidian*, the meaning of 盲–particularly in the compound 色盲–is described metaphorically as "being unable, or hardly able, to distinguish something." Furthermore, in the open-ended responses of the questionnaire distributed to Chinese speakers, some non-specialist respondents noted that they use the term 色盲 not in the sense of "being unable to see colors," but instead in the sense of "being unable to distinguish colors."

Second Layer: color terms from the perspective of color vision minorities

According to Ito, whenever we attempt to understand the world, mediation is inevitably involved [6]. The most universal form of such mediation is language. With regard to color, language has functioned to articulate perceptual experience and connect it to a socially shared system of knowledge. Among the most well-known frameworks in this regard is the Sapir – Whorf hypothesis. This hypothesis posits that language divides the continuous world into categories, that the manner of such division varies across languages, and that these linguistic structures influence human thought and perception. The oft-cited example of how many colors are distinguished in a rainbow illustrates that color perception cannot be separated from the structure of language.

When this framework is applied to color vision minorities, intriguing issues emerge. Color vision minorities also use everyday color terms such as "red" and "green." Yet the "red" or "green" they articulate is frequently perceived as deviating from the chromatic world of the majority. Typical expressions include assertions such as "red-blind individuals cannot see red" or the outright denial, "that is not green." Such instances of

miscommunication arise insofar as the linguistic structure of the majority is presupposed to be the sole legitimate standard.

Color terms are not labels that directly affix an individual's sensory qualia; instead, they are signs constituted within the practices of a community. From a semiotic perspective, color terms simultaneously possess a Saussurean signifier–signified relation and function as indexical resources in social practice, signaling other norms, roles, and ideologies. While color terms exist as discrete lexical categories, their referents occupy a continuous color space. This tension is resolved on two levels: (i) the prototypical exemplars of the community and (ii) the boundaries that delimit categorical extension. In the case of the majority (trichromats), these prototypes and boundaries are socially standardized and reproduced as norms through repetition in education, industrial standards, and media representations.

A central question concerns the meaning of color terms for color vision minorities, such as dichromats. Color terms function not only as instruments of communication but also as signs mediating one's perceptual world. In dichromatic vision, the use of color terms constitutes a semiotic strategy to "align" with the prototypical exemplars of the community, functioning as a multi-cue index that integrates non-hue information such as luminance, saturation, contextual cues, and object identity. For color vision minorities, even when colors cannot be perceived directly, color terms remain indispensable for navigating social life, being acquired through linguistic and cultural channels beyond direct visual experience. However, when color vision minorities and trichromats employ the same color term, the perceptual regions to which they refer may differ, making direct equivalence impossible.

Would the creation of color terms unique to dichromats, directly visualizing their perceptual experiences, resolve the problem of miscommunication? As long as their experiences are interpreted according to the majority's system, they always carry the risk of being regarded as "incorrect." Moreover, inventing unique color terms entails the risk of losing communicative compatibility with the majority. The present study adopts the stance that color terms should not function as a normative apparatus of "correctness/incorrectness," but rather be redesigned as a translation infrastructure bridging different perceptual spaces.

A "translation infrastructure" refers to the institutional, linguistic, and technological mechanisms that enable individuals with differing perceptual bases to coordinate social action. To relativize normative judgments, color terms must be treated not as "absolutely correct labels" but as resources premised on mutual translation. For example, when a dichromat says "red," it should not be evaluated as "incorrect," but understood as an expression that maintains a translational relationship to red within the speaker's perceptual system. In this framework, color terms become translatable signs. By reorganizing color terms as translatable resources rather than normative standards, silence and exclusion can be mitigated, thereby providing a pathway toward the social inclusion of color vision minorities.

CONCLUSION

These linguistic factors, together with social ones, contribute to the structure of miscommunication involving color vision minorities and influence both the reconsideration of terminology and the acceleration of social inclusion. This analysis demonstrates that, in defining discriminatory language, one must consider not only the negative connotations inherent in a word itself, but also the awareness and context of its users. Consequently, before proposing new terminology, it is essential to understand why the term 色盲 was abolished; otherwise, one risks falling into tautology−claiming that the word is unacceptable merely because it has been prohibited.

Furthermore, this study has examined color terms for color vision minorities from a linguistic perspective, addressing two central questions: what color terms mean for dichromats, and whether dichromats require their own unique color terms. As a future direction, the study aims to propose the linguistic mechanisms of translation between different perceptual spaces from a linguistic standpoint.

ACKNOWLEDGEMENTS

This work was supported by JSPS KAKENHI Grant Number JP 24H00167. My sincere thanks go to all participants who generously shared their time and experiences.

REFERENCES

[1]. Nishijima, Yutaro (2022). The Wonders of Chinese Characters Related to Medicine. Taishukan Shoten.(in Japanese)

[2]. Baba, Yasuto (2020).“Color Blindness” and Modernity: The Reorganization of the Color Order in the Nineteenth Century. Seikyusha. (in Japanese)

[3]. Kawabata, Hiroto. (Accessed March 8, 2025). “A Column between the Preparatory Chapter [Part 1] and [Part 2]: Organizing Terms Related to Color Vision.” https://gakugei.shueisha.co.jp/mori/serial/iroiro/008.html(in Japanese)

[4]. Yasukawa, Yuki. (2008). A Study on the Psychological Changes in People with Color Vision Deficiency. Master's thesis of the Graduate School of Education, Hyogo University of Teacher Education., p.4. (in Japanese)

[5]. Uemura, Kentaro. (2014). A Study of Change in Use of New Words and Vogue Words : In using Google Trends and Newspaper Article Databases. *Meikai New Japanese Language*, 19, 11–20. (in Japanese)

[6]. Itō, Jun’ichirō(2024). Color Qualia and Testimony.*the Bulletin of the Color Science Association of Japan*, 3(4), 179–182. (in Japanese)

[7]. Zhou, Xinhua (1999). Chinese and Western Medical Understandings of “Color Blindness.” *Journal of Jiangxi College of Traditional Chinese Medicine*, 11(3), 8. (in Chinese)

[8]. Xia, Yuanyuan (2023). Yu Ziping and the Birth of the Most Influential “Color Blindness Test Chart” in China. *Journal of Nanjing Medical University (Social Sciences Edition)*, 117(4), 356–359. (in Chinese)

Celebrating NCS Colour
80 years of colour research.
The global colour standard built on human perception.

NCS S 4020-B70G
Inspired by colours of the skyscraper Taipei 101. Defined by NCS+.

NCS

The NCS System is a scientifically based colour system that reflects how we perceive colour. It's a universal language for precise and confident colour communication worldwide.

Our design tools and Academy courses provide a strong foundation for working with colour in both design and research.

Visit ncscolour.com to learn more.

Create Your Color Brand

Customize. Visualize. Materialize.

Turn color into the language of your brand.

- **Spectrophotometer** – Precision color measurement tools
- **Color Tree** – Visualizing your color universe
- **Color Cards** – Bringing your palette to life
  (All customizable to your brand's needs.)

Our Strengths

- The most advanced color solid technology
  — translating color data into tangible accuracy.
- A library of over 20,000 colors
  — the largest and most versatile color database in the industry.
- Comprehensive color hardware lineup
  — from spectrophotometers to color trees and cards.
- Fully customizable solutions
  — build your brand's unique color identity with precision and confidence.
- Cost-effective and globally scalable
  — enabling large-scale applications and international partnerships.

CONTACT US

Website: www.dchcolor.com
Email: Rumia.Xu@dchcolor.com

Taiwan Headquarters
YPRAINBOW CO., LTD. (TAIWAN)
1F., NO.1, ALY. 13, LN. 40 XINXING ST. GUISHAN.,
TAOYUAN CITY 33379, TAIWAN(R.O.C.)

Shanghai R&D Center
DONGHUA UNIVERSITY YP COLOR RESEARCH CENTER
1/F, Building 3, No. 2399, Guangfulin Road, Songjiang District, Shanghai, China (Donghua University, Songjiang Campus, Rooms 1089–1096)

DCHcolor | YP

THOUSLITE

Learn More

The World's Leading

MULTI-CHANNEL LED LIGHTING SOLUTIONS

High-Precision Lighting Environments

Advanced Spectral Tuning

Accurate Color Calibration

Thouslite is a global leader in multi-channel LED lighting technology and light quality management. We are dedicated to providing high-efficiency, energy-saving, and superior lighting solutions across diverse industries, including medical, commercial, and scientific research. As an active participant in international technical conferences and standardization organizations, Thouslite sets global standards and drives innovation in LED lighting technology.

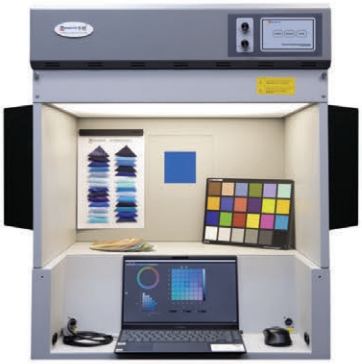

LEDCube

Any SPD Simulator

LEDCube is an illuminator that simply and accurately simulates any lighting environment, covering a wide range of CCTs and a high dynamic range of luminance. There are 48 channels available for assessing camera quality.

LEDSimulator

Total Appearance Reproduction System

LEDSimulator is a powerful tool for communicating Total Appearance throughout the supply chain. It supports design creativity, allowing color to be 1) visualized on a wide range of textures and 2) matched between the virtual and real samples. LEDSimulator can also be used to build a color-texture database for testing camera quality.

LEDView

Lighting Cabinet

LEDView products are sophisticated lighting cabinets utilizing multi-channel LED technology, engineered to provide consistent color assessment and quality control across industries such as textiles, coatings, and printing. Equipped with high-power LEDs and the LEDNavigator-LV software, they ensure precise matching to any SPD, including daylight.

www.thouslite.com +86-0519-85289860 sales@thouslite.com Building 32A, No.28 Panyang Road, Xinbei District, Changzhou City, Jiangsu Province, China , 213031

跨屏色彩 精準一致

提供最直覺**色彩同步**和**色彩管理步驟**
實現跨顯示器的色彩一致性

Palette Master Ultimate
獨家校色參數複製功能

Display ColorTalk
手動同步對色，無需校色器

無反光面板
Nano Matte Panels
反射率<3，降低色彩誤判

PANTONE® Validated
PANTONE™ SkinTone™ Validated
calman

In. Licht Product Series

In. Licht Pro
Lighting Fact Sensor

Accurate. EML Capable. Portable.

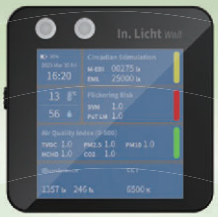

In. Licht Well
Light and Air Quality Guardian

Make sense for WELL

In. Licht Ultra
Spectrum/WELL Meter

Full Spectrum. Human-Centric Lighting. Flicker Safe.

5 Key Metrics at Your Fingertips
Instantly access Illuminance, CCT, EML, visual contrast, and uniformity.

12 EML Scenario Presets
Evaluate and interpret human-centric lighting instantly.

Instant Response. Smarter Light Monitoring
Real-time updates for efficient mobile monitoring.

Lightweight and Long-Lasting
Only 40g — extended battery life with replaceable batteries for nonstop on-site monitoring.

Upgradeable to Full-Space Monitoring
Pair with In. Licht Well for smart, whole-space management.

Whole-Space Health Protection
Light Quality, Circadian, Flicker Health, and Air Quality — real-time monitoring and instant alerts.

Monitor Light, Air, and Thermal Comfort — All in One
Tracks 19 key indicators:
Illuminance, CCT, SDCM, CRI, Duv, EML, M-EDI, flicker frequency/index/percent, SVM, Pst LM, temperature, humidity, TVOC, PM2.5, PM10, HCHO, and CO_2.

Designed for All Spaces
Adapts to homes and commercial spaces — built for wellbeing anywhere

Wellness Anywhere. One Device Fits All
Fixed or portable — effortless monitoring, anytime, anywhere, with flexible power.

Easily pairs with Pro as needed

All-in-One Lab-Grade Spectrometer
Measure 23+ lighting metrics — full spectrum, illuminance, CCT, CRI, TM-30, SDCM, flicker, and more.

Human-Centric Lighting Indicators
CAF, EML, M-EDI, S/P ratio, Blue Light Hazard, and CS — complete circadian metrics. Use with the tripod for accurate and easy measurements.

Flicker Risk Assessment
Real-time visualization of percent flicker, flicker index, frequency, and SVM — with clear visual indicators.

Spectral Comparison & Multi-Point Measurement
Instant design validation with light quality reports and spectral data — fully aligned with WELL standards.

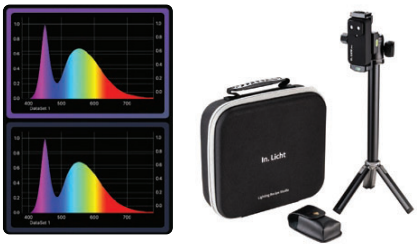

Applicable Scenarios	In. Licht Pro	In. Licht Well	In. Licht Ultra
Human-Centric Lighting	✓	✓	✓
WELL Inspection	✓	✓	✓
Commercial Spaces	✓	✓	✓
Residential Spaces	✓	✓	
Spectrum Analysis			✓
Continuous Data Monitoring	✓	✓	
Lighting Equipment Manufacture	✓		✓
Laboratory / Quality Control	✓		✓
Spatial / Lighting Design	✓	✓	✓
Plant and Animal Grow Light			✓

Works with WELL™ Certification — Enhancing Wellbeing

All In. Licht products have earned the Works with WELL™ mark, meeting WELL Building Standard requirements to support healthier indoor spaces and improved user wellbeing.

Aligned with the WELL Building Standard and grounded in human-centered design, the In. Licht series follows WELL lighting concepts, offering real-time data verification and one-click report export to streamline WELL project tracking and management.

*For full details on alignment and approvals, please visit our official website.

Complete Indoor Coverage

In. Licht Ultra provides full spectrum & human-centric lighting data. **Pro** scans multiple areas. **Well** monitors long-term. From design to real-time monitoring, export professional reports with one click.

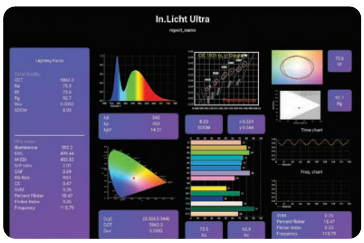

About Lighting Recipe Studio

Human-centered and grounded in the science of light, we build light for life. Together with IWBI and other ecosystem partners, we create life-friendly lighting environments, illuminating the path toward smart and healthy lighting for the industry.

Official Brand Store

Authorized Retailers

Lighting Recipe Studio
www.LightingRecipe.com

Organizers

AIC International Colour Association
Internationale Vereinigung für die Farbe
Association Internationale de la Couleur

NSTC 國家科學及技術委員會
National Science and Technology Council

中華色彩學會
Color Association of Taiwan

華梵大學
Huafan University

Gold Sponsors

NCS

DCHcolor | YP

Silver Sponsors

BenQ

THOUSLITE

Lighting Recipe Studio
Light for Life

Supporting Partners

CIE Taiwan
台灣照明委員會

TACA
TAIWAN Association of
Color Applications
台灣色彩應用協會

財團法人
紡織產業綜合研究所
Taiwan Textile Research Institute

PTRI
印刷創新科技研究發展中心
Printing Technology Research Institute

臻印藝術
CONSUMMATE ARTWORK GALLERY

THE COLOUR GROUP (GB)

國立臺灣科技大學

國立清華大學
NATIONAL TSING HUA UNIVERSITY

國立臺灣藝術大學
National Taiwan University of Arts

大同大學
TATUNG UNIVERSITY

中國文化大學
CHINESE CULTURE UNIVERSITY

TAIPEI 觀光傳播局
Department of Information and Tourism